British Journal of Pharmacology

July 1992

Volume 106 Number 3 pages 503–756

Br. J. Pharmacol. (1992), **106**, 505–506

SPECIAL REPORT

Human brain contains a metalloprotease that converts big endothelin-1 to endothelin-1 and is inhibited by phosphoramidon and EDTA

[1,2]Timothy D. Warner, Harald H.H.W. Schmidt, *Jane Kuk, [1]Jane A. Mitchell & *Ferid Murad

Northwestern University Medical School, Chicago, IL 60611, U.S.A. and *Abbott Laboratories, Abbott Park, IL 60064, U.S.A.

Incubation of big endothelin-1 (bET-1) with protein derived from the detergent-extracted 100,000 *g* pellet prepared from human brain tissue resulted in the formation of endothelin-1 (ET-1) at a rate of 90 fmol mg^{-1} protein min^{-1}. This formation was inhibited in a concentration-dependent manner by either phosphoramidon or EDTA, with half-maximal inhibitory concentrations of 2 and 20 μM, respectively. No conversion of big endothelin-3 (bET-3) to endothelin-3 (ET-3) was detected under the same conditions. These results show the presence in the human brain of a metalloprotease-like enzymatic activity which selectively converts bET-1 and ET-1. Together with earlier reports of mRNA for ET-1 this suggests the presence of the entire synthetic pathway for ET-1 in human brain.

Keywords: Endothelin-1; big endothelin-1; endothelin-3; big endothelin-3; buman brain; endothelin-converting enzyme; phosphoramidon; EDTA.

Introduction Endothelin-1 (ET-1) was first discovered as a potent vasoconstrictor peptide synthesized and released from porcine endothelial cells (Yanagisawa *et al.*, 1988). It is believed that the synthesis of ET-1 involves the cleavage of its precursor big ET-1 (bET-1) by a specific endothelin-converting enzyme (ECE) (Ohnaka *et al.*, 1990). This enzyme is most probably a metalloprotease which is inhibited by phosphoramidon, or the metal ion chelator, EDTA. It is present in endothelial (Ohnaka *et al.*, 1990; Okada *et al.*, 1990; Warner *et al.*, 1992) and smooth muscle cells (Matsumura *et al.*, 1991), and we have found it also in rat brain (Warner *et al.*, 1992). Here we show that human brain contains ECE activity.

Methods *Preparation of subcellular fractions* Human cerebellum was obtained during a normal autopsy procedure, and frozen and stored at − 80°C. After thawing the tissue was homogenized in buffer A (HEPES 50 mM; NaCl 100 mM; pH 7.4) and centrifuged (100,000 *g*, 1 h). The particulate fraction was resuspended in buffer A and treated with the detergent CHAPS (20 mM, for 30 min) to remove membrane-associated and solubilizable particulate proteins. After centrifugation (100,000 *g*, 1 h) the remaining pellet containing the cytoskeletal fraction was resuspended in buffer A and assayed for ECE activity. This fraction was used because the cytoskeleton from rat brain contains the most clearly distinguishable metalloprotease-ECE (Warner *et al.*, 1992).

Determination of ECE activity Protein (22.5 μg) from the cytoskeletal fraction was incubated (37°C, 60 min), at pH 7.4 with bET-1 (human) or bET-3 (human) (135 pmol) and sometimes test inhibitors, in a total volume of 52.5 μl. All samples were incubated in duplicate in the absence and presence of phosphoramidon (100 μM). The reaction was stopped by the addition of a mixture of protease/peptidase inhibitors (phenylmethylsulphonyl fluoride, 1 mM; leupeptin, 2 μM; pepstatin A, 1 μM) and EDTA (1 mM), to a total volume of 62.5 μl. The incubates were then rapidly frozen in liquid N_2 and stored (max. 2 h) at − 20°C. After rapid thawing the amounts of ET-1/3 in each sample were assessed by bioassay and ELISA (enzyme-linked immunosorbent assay). Each ECE/bET-1/3 combination was assayed in triplicate in each experiment. For ET-1/3 bioassay aliquots (12.5 μl) of each sample were added to single wells of porcine kidney epithelial (PK_1) cells, grown to confluency in 12-well plates, bathed in Locke buffer. After 4 min the incubation buffer was removed and the reactions stopped by addition of 1 ml ice-cold sodium acetate buffer (50 mM, pH 4.0). The samples were quickly frozen with liquid N_2 (Ishii *et al.*, 1991). The amount of ET-1 or ET-3 present in the sample was then calculated from the levels of guanosine 3′:5′-cyclic monophosphate (cyclic GMP) produced in the PK_1 cells by known amounts of ET-1 or ET-3 (Warner *et al.*, 1992). In these cells bET-1, at concentrations up to 100 nM, does not produce significant elevations in cyclic GMP levels (Warner *et al.*, 1992). The ELISA for ET-1/3 used antibody directed against the C-terminal fragment of ET-1/3 ($ET\text{-}1/3_{(17-21)}$) with approximately 0.01% cross reactivity with bET-1 or bET-3. Binding was detected by peroxidase-labelled goat anti-rabbit IgG antibody using *o*-phenylenediamine-2HCl as a substrate. The optical density of each well was measured at 490 nm with a microplate reader (Bio-Tek model EL 311). The amount of ET-1 or ET-3 formed in each incubation mixture by metalloprotease enzyme-activity was calculated as the difference between paired samples incubated with and without phosphoramidon (100 μM).

Results The cytoskeletal fraction converted bET-1 to ET-1 as detected by either PK_1-bioassay or ELISA. The rate of conversion was 90 fmol mg^{-1} protein min^{-1} (mean of 3 ELISA and 2 bioassay determinations, each in triplicate). This conversion was inhibited in a concentration-dependent manner by either the metalloprotease inhibitor, phosphoramidon (10 nM - 1 mM, Figure 1a), or the metal ion chelator, EDTA (300 nM - 10 mM, Figure 1b), with half-maximal inhibitory concentrations of 2 and 20 μM, respectively. The maximum inhibition caused by phosphoramidon was 88 ± 2%, at a concentration of 1 mM, and by EDTA 60 ± 4% at a concentration of 10 mM. In experiments with bET-3 as a substrate in the same assay conditions no formation of ET-3 was detected by PK_1-bioassay or ELISA ($n = 3$ for each).

[1] Present address: The William Harvey Research Institute, St. Bartholomew's Hospital Medical College, Charterhouse Square, London, EC1M 6BQ, U.K.
[2] Author for correspondence.

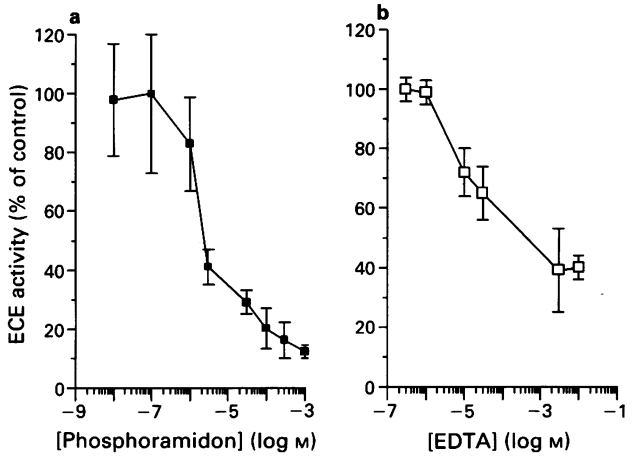

Figure 1 Phosphoramidon and EDTA inhibit in a concentration-dependent manner the conversion of big endothelin-1 (bET-1) to endothelin-1 (ET-1) by the cytoskeletal fraction prepared from human brain. When incubated with protein (22.5 μg) from the cytoskeletal fraction of human brain and bET-1 (135 pmol) in a total volume of 52.5 μl the metalloprotease-inhibitor, phosphoramidon (10 nM–1 mM, a), or the metal ion-chelator, EDTA (300 nM–10 mM, b) inhibited the formation of ET-1 with half-maximal inhibitory concentrations of 2 and 20 μM, respectively. Data shown were derived by bioassay (a) and by ELISA (b). Similar results were obtained when samples were tested in the alternate assay.

Discussion Our results show the presence of an enzyme in human brain which selectively converts bET-1 to ET-1, and which resembles other mammalian ECE activities previously described in rat, bovine and porcine cells. The formation of ET-1 was detected by both bioassay and ELISA, demonstrating that our biochemical assay was not detecting inactive ET-1 fragments, but biologically active ET-1. The ET-1 production was due to the activity of a metalloprotease similar to that present in endothelial cells, for it was inhibited in a concentration-dependent manner by both phosphoramidon and EDTA. This is the first report of metalloprotease-like ECE activity in human nervous tissue.

Interestingly, although brain tissue from other species contains more ET-3 than ET-1 (Takahashi *et al.*, 1991) we were not able to detect the conversion of bET-3 to ET-3, as has been reported previously in bovine endothelial cells (Okada *et al.*, 1990). This may be because the fraction we employed does not contain the appropriate enzyme activity, or alternatively that it is not active under our assay conditions. It is not due to a lack of sensitivity of our assays as these are equally sensitive to ET-3 and ET-1 (Ishii *et al.*, 1991; Warner *et al.*, 1992). This result does suggest however, that the metalloprotease within human brain that converts bET-1 to ET-1 has a highly selective substrate requirement. The activity we detected in human brain tissue is considerably lower than that present in rat whole brain (Warner *et al.*, 1992). This may be explained by the time delay between the excision of the tissue and its use in the assay, and also by the variability of ECE activity in different brain regions (unpublished observations). Thus the tissue that was available may well be from a brain area which does not contain a high ECE activity.

Together with the previous observations of mRNA for ET-1 in human brain (Lee *et al.*, 1990) it is clear that this tissue contains the synthetic pathway for ET-1. ET-1 may have roles in brain functions from neurosecretion (Yoshizawa *et al.*, 1990) to control of motor activity (Lecci *et al.*, 1990). Our data support the conclusion that endogenous ET-1, and perhaps other members of the endothelin family of peptides, are produced in the human central nervous system and presumably have important central and peripheral effects.

References

ISHII, K., WARNER, T.D., SHENG, H. & MURAD, F. (1991). Endothelin-1 stimulates cyclic GMP formation in porcine kidney epithelial cells via activation of the L-arginine-dependent soluble guanylate cyclase pathway. *J. Cardiovasc. Pharmacol.*, **17**, Suppl. 7, S246–S250.

LECCI, A., MAGGI, C.-A., ROVERO, P., GIACHETTI, A. & MELI, A. (1990). Effect of endothelin-1, endothelin-3 and C-terminal hexapeptide, endothelin (16-21) on motor activity in rats. *Neuropeptides*, **16**, 21–24.

LEE, M.-E., DE LA MONTE, S., NG, S.-C., BLOCK, K.D. & QUERTERMOUS, T. (1990). Expression of the potent vasoconstrictor endothelin in the human central nervous system. *J. Clin. Invest.*, **86**, 141–147.

MATSUMARA, Y., IKEGAWA, R., TSUKAHARA, Y., TAKAOKA, M. & MORIMOTO, S. (1991). Conversion of big endothelin-1 to endothelin-1 by two-types of metalloproteinases of cultured porcine vascular smooth muscle cells. *Biochem. Biophys. Res. Commun.*, **178**, 899–905.

OHNAKA, K., TAKAYANAGI, R., YAMAUCHI, T., OKAZAKI, H., OHASHI, M., UMEDA, F. & NAWATA, H. (1990). Identification and characterization of endothelin converting activity in cultured bovine endothelial cells. *Biochem. Biophys. Res. Commun.*, **168**, 1128–1136.

OKADA, K., MIYAZAKI, Y., TAKADA, J., MATSUYAMA, K., YAMAKI, T. & YANO, M. (1990). Conversion of big endothelin-1 by membrane-bound metalloendopeptidase in cultured bovine endothelial cells. *Biochem. Biophys. Res. Commun.*, **171**, 1192–1198.

TAKAHASHI, K., GHATEI, M.A., JONES, P.M., MURPHY, J.K., LAM, H.-C., O'HALLORAN, D.J. & BLOOM, S.R. (1991). Endothelin in human brain and pituitary gland: comparison with rat. *J. Cardiovasc. Pharmacol.*, **17** Suppl. 7, S101–S103.

WARNER, T.D., MITCHELL, J.A., D'ORLEANS-JUSTE, P., ISHII, K., FÖRSTERMANN, U. & MURAD, F. (1992). Characterization of endothelin-converting enzyme from endothelial cells and rat brain: detection of the formation of biologically active endothelin-1 by rapid bioassay. *Mol. Pharmacol.*, **41**, 399–403.

YANAGISAWA, M., KURIHARA, H., KIMURA, S., TOMOBE, Y., KOBAYISHI, M., MITSUI, Y., YAZAKI, Y., GOTO, K. & MASAKI, T. (1988). A novel potent vasoconstrictor peptide produced by vascular endothelial cells. *Nature*, **332**, 411–415.

YOSHIZAWA, T., SHINMI, O., GAID, A., YANAGISAWA, M., GIBSON, S.J., KIMURA, S., UCHIYAMA, Y., POLAK, J.M., MASAKI, M. & KANAZAWA, I. (1990). Endothelin: a novel peptide in the posterior pituitary system. *Science*, **247**, 462–464.

(Received March 29, 1992
Accepted April 3, 1992)

Br. J. Pharmacol. (1992), **106**, 507–508

SPECIAL REPORT

Dependence of the metabolism of nitric oxide (NO) in healthy human whole blood on the oxygenation of its red cell haemoglobin

[1]Å. Wennmalm, G. Benthin & A.-S. Petersson

Department of Clinical Physiology, Gothenburg University, Sahlgrenska Hospital, S-413 45 Gothenburg, Sweden

Plasma or whole venous or arterialized blood from healthy human donors was incubated with NO (50–300 μM), and the resulting formation of methaemoglobin (MetHb), nitrosyl haemoglobin (HbNO), and plasma nitrite and nitrate were measured. In plasma, NO was converted to nitrite and nitrate in a ratio of 5:1. In arterial blood (O_2 sat. 94–99%) NO was almost quantitatively converted to nitrate and MetHb. No nitrite was detected and HbNO formation was low. In venous blood (O_2 sat. 36–85%) more HbNO and less nitrate was formed, in comparison to arterialized blood. We propose that NO liberated from endothelium of conductance and resistance vessels is taken up by red blood cells and inactivated by HbO_2 via stoichiometric conversion to MetHb and nitrate.

Keywords: Blood; EDRF; endothelium; erythrocytes; haemoglobin; methaemoglobin; nitrate; nitric oxide; nitrite

Introduction

NO has potent biological activities as a vasoactive, cytotoxic, platelet regulatory, and neurotransmitter agent (Furchgott & Zawadzki, 1980; see Moncada *et al.*, 1991 for references). Accumulating data also indicate a significant role for NO in several settings of cardiovascular disease (Gordon *et al.*, 1989; Drexler *et al.*, 1991). We assumed that quantitative methods to estimate NO formation might facilitate further evaluation of some of its physiological and pathophysiological roles. The development of such methods relies upon proper knowledge about the inactivation and elimination of NO from the intact organism. In this paper we describe a route by which NO in human blood is converted to nitrate, i.e. a metabolite that is readily eliminated via the kidneys.

Methods Portions of venous blood from healthy donors were incubated with NO (AGA Special Gas, final conc. 50–200 mM) with or without previous oxygenation. O_2 saturation was estimated with a standard method. The incubation was interrupted by separation of the blood into cells and plasma followed by freezing of the cell fraction at 70 K in electron paramagnetic resonance (EPR) tubes. Plasma was kept at −20°C until analysis. Other plasma fractions were separated before incubation with NO as above. The EPR spectra of the blood cell fraction were recorded for MetHb and HbNO at a microwave frequency of 9.22 GHz and a power of 20 mW from about 500 to 3500 gauss with a modulation amplitiude of 20 gauss. Plasma levels of nitrite and nitrate were analyzed with liquid chromatography/uv detection at 214 nm after separation of proteins with ultrafiltration, and verified with gas chromatography/mass spectrometry (stable isotope dilution with $^{15}NO_3^-$, conversion to nitrotuluene, negative ion-chemical ionization, selective monitoring of m/e 136 for endogenous nitrate and m/e 137 for the ^{15}N-labelled internal standard).

Results Basal plasma nitrate was 44 ± 3.8 μM (mean ± s.e., $n = 20$). Basal plasma nitrite was below 1 μM; often no nitrite could be detected. The basal levels of MetHb and HbNO were 19 ± 2.0 ($n = 20$) and 1.2 ± 0.3 ($n = 20$) units, respectively. Incubation of arterialized blood (O_2 sat. 96 ± 0.8%) with NO for 2 min resulted in dose-dependent increases in the formation of nitrate and MetHb (Figure 1). At the highest NO concentration (200 μM) nitrate in plasma reached a level of 203 μM, suggesting almost quantitative conversion of NO to nitrate. In parallel, MetHb was elevated to about 140 units. HbNO increased very little, to about 11 units at 200 μM NO. Prolongation of incubation time to 15 min revealed mainly the same pattern: plasma nitrate was 237 μM, and MetHb and HbNO were 151 and 10 units, respectively (Figure 1). Incubation of venous blood (O_2 sat. 61 ± 8.5%) with NO for 2 min revealed a different pattern. Nitrate and MetHb levels increased in parallel, but to lower concentrations (130 μM and 135 units, respectively) than when NO was incubated with arterialized blood (Figure 1). In contrast, the formation of HbNO was markedly enhanced, to 92 units at a NO concentration in the incubate of 200 μM (Figure 1). When the incubations of venous blood with NO were prolonged to 15 min, the products formed were more similar to those obtained in arterialized blood. Plasma nitrate and MetHb increased, to 260 μM and 260 units, respectively. HbNO was mainly unaffected after 15 compared to after 2 min of incubation (Figure 1). Incubation of plasma with NO (200 μM, $n = 3$) for 15 min resulted in semiquantitative conversion to nitrite and nitrate, in a ratio of about 5:1. These levels of nitrite and nitrate were stable.

Discussion Plasma, in comparison to whole blood, was rather inefficient in converting NO to nitrite in the present experiments, highlighting the activity of the blood cell fraction in the inactivation of NO. Since the red cells are the most abundant, and the conversion of NO to nitrate was found to involve haemoglobin, it appears that the conversion occurred in the erythrocytes. Furthermore, the conversion of NO to nitrate was more rapid in blood with high compared to low oxygen saturation of the haemoglobin. This strongly suggests that HbO_2 acted as oxygen donor to the NO molecule in its conversion to nitrate. Conversion of NO to nitrate by oxygen also involves a one electron transfer to the resulting NO_3^- molecule. Our data indicate that the ferrous haeme of the haemoglobin acted as electron donor, to be converted to

[1] Author for correspondence.

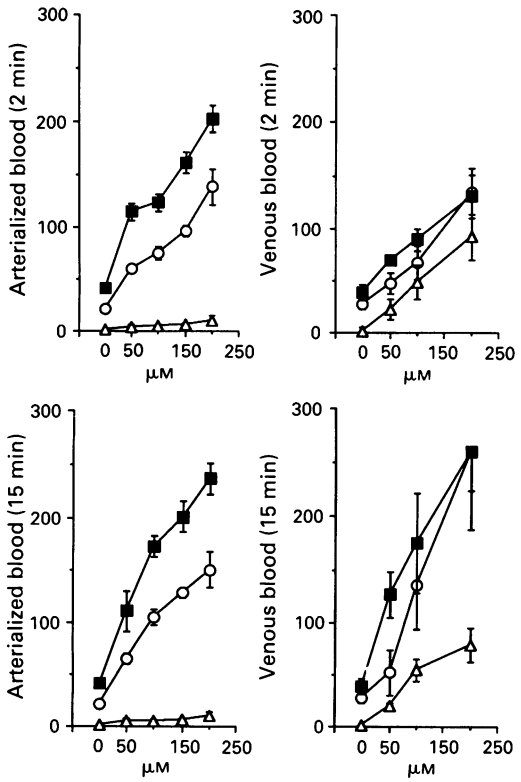

Figure 1 Dose-response curves demonstrating the formation of nitrate (■), methaemoglobin (○), and nitrosyl haemoglobin (△) in whole arterialized (O_2 saturation 94–99%) or venous (O_2 sat. 36–85%) blood incubated with nitric oxide (NO, 50–200 μM is indicated on the horizontal axis) for 2 or 15 min. Symbols indicate mean of 4–6 observations with s.e. shown by vertical bars. Concentrations on vertical axis: nitrate in μM, methaemoglobin and nitrosyl haemoglobin in EPR units. One EPR unit corresponds to about 1 μM of methaemoglobin and 0.1 μM of nitrosyl haemoglobin.

ferric haeme, inasmuch as the amount of methaemoglobin formed increased in parallel to the formation of nitrate. These data consequently suggest that NO is converted to nitrate according to the formula

$$Hb^{(Fe^{2+})}O_2 + NO \rightarrow Hb^{(Fe^{3+})} + NO_3^-$$

The equilibrium of this conversion appeared shifted to the right, inasmuch as incubation with NO yielded virtually quantitative formation of nitrate. Thus, when NO (200 μM) was incubated with arterialized blood for 15 min, plasma nitrate increased from the basal average level of 41 μM to a final average concentration of 237 μM. In the incubations of venous blood with NO a significant formation of nitrosylated Hb was also obtained. It seems that NO, when entering the red blood cell, may either form nitrate and methaemoglobin stoichiometrically together with HbO_2 or nitrosylate non-oxygenatad Hb. Consequently, haemoglobin may inactivate NO along either of two different routes, i.e. by conversion to nitrate or by nitrosylation. The fraction of NO inactivated along either of these routes seems to be determined by the HbO_2/Hb ratio in the red cells.

Although NO is formed in several different cell types (see Introduction) it may be assumed that the vascular endothelium is the source of a considerable part of the total body production of NO. Some considerations on how NO may be inactivated in the circulation are therefore warranted. Endothelial NO seems to play the most important role as a physiological vasodilator in conductance and possibly also resistance vessels (see Moncada *et al.*, 1991 for references), being of less significance in capillaries and on the venous side of the systemic circulation. Hence, a substantial proportion of NO released luminally from the endothelial cells will enter blood with a high O_2 saturation. The present data demonstrate that such NO is readily converted to nitrate, with parallel formation of MetHb, These products may then be either eliminated via renal excretion (nitrate) or reversed with known endogenous mechanisms (conversion of methaemoglobin to haemoglobin, Tomoda *et al.*, 1979). If small amounts of HbNO are formed, this complex can also be disintegrated successively by a high oxygen tension, as in the alveolar capillaries in the lungs (Chiodi & Mohler, 1985). The process for inactivation and elimination of NO proposed here thereby seem to fulfill the criteria of providing a physiologically reasonable elimination route that also conforms to present and previously known data concerning plasma (Kelm *et al.*, 1991) and urine (Green *et al.*, 1982) levels of nitrite and nitrate.

This study was supported by The Swedish Medical Research Council, and by The Swedish Heart Lung Foundation.

References

CHIODI, H. & MOHLER, J.G. (1985). Effects of exposure of blood hemoglobin to nitric oxide. *Environ. Res.*, **37**, 355–363.

DREXLER, H., ZEIHER, A.M., MEINZER, K. & JUST, H. (1991). Correction of endothelial dysfunction in coronary microcirculation of hypercholesterolaemic patients by L-arginine. *Lancet*, **338**, 1546–1550.

FURCHGOTT, R.F. & ZAWADZKI, J.V. (1980). The obligatory role of endothelial cells in the relaxation of arterial smooth muscle by acetylcholine. *Nature*, **288**, 373–376.

GORDON, J.B., GANZ, P., NABEL, E.G., FISH, R.D., ZEBEDE, J., MUDGE, G.H., ALEXANDER, R.W. & SELWYN, A.P. (1989). Atherosclerosis influences the vasomotor response of epicardial coronary arteries to exercise. *J. Clin. Invest.*, **83**, 1946–1952.

GREEN, L.C., WAGNER, D.A., GLOGOWSKI, J., SKIPPER, P.L., WISHNOK, J.S. & TANNENBAUM, S.R. (1982). Analysis of nitrate, nitrite, and [^{15}N]nitrate in biological fluids. *Anal. Biochem.*, **126**, 131–138.

KELM, M., FEELISH, M., GRUBE, R., MOTZ, W. & STRAUER, B.E. (1991). Metabolism of endothelium-derived nitric oxide in human blood. *Second. int. Meeting. Biology of Nitric Oxide*, London, 30th September/2nd October 1991 (Abstract).

MONCADA, S., PALMER, R.M.J. & HIGGS, E.A. (1991). Nitric oxide: physiology, pathophysiology, and pharmacology. *Pharmacol. Rev.*, **43**, 109–142.

TOMODA, A., YUBISUI, T., TSUJI, A. & YONEYAMA, Y. (1979). Kinetic studies on methemoglobin reduction by human red cell NADH cytochrome b_5 reductase. *J. Biol. Chem.*, **254**, 3119–3123.

(Received March 30, 1992
Accepted April 19, 1992)

Br. J. Pharmacol. (1992), **106**, 509–510

SPECIAL REPORT

(S)-homoquisqualate: a potent agonist at the glutamate metabotropic receptor

Richard H.P. Porter, [1]Peter J. Roberts, *David E. Jane & *Jeffrey C. Watkins

Department of Physiology & Pharmacology, Biomedical Sciences Building, University of Southampton, Southampton, SO9 3TU and *Department of Pharmacology, School of Medical Sciences, University of Bristol, Bristol, BS8 1TD

The synthetic quisqualate analogue, (S)-homoquisqualate was examined for activity at the glutamate metabotropic receptor, in relation to its ability to stimulate phosphoinositide hydrolysis in rat pup cerebro-cortical slices. The compound produced a robust increase in hydrolysis ($EC_{50} = 50.2 \pm 1.6\ \mu M$), which, in common with responses to quisqualate and (1S,3R)-1-aminocyclopentane-1,3-dicarboxylate ((1S,3R)-ACPD), was antagonized uncompetitively by L-2-amino-3-phosphonopropionate (L-AP3). In contrast to quisqualate which exhibits low efficacy, (S)-homoquisqualate behaves as a full agonist at the metabotropic receptor.

Keywords: Homoquisqualate; quisqualate; (1S,3R)-ACPD; glutamate metabotropic receptor

Introduction The glutamate metabotropic receptor is coupled via a guanine nucleotide binding protein to mediate phosphoinositide (PI) hydrolysis in the CNS (Nicoletti *et al.*, 1986). The pharmacology of this receptor is poorly characterized and, although quisqualate, ibotenate and glutamate are effective agonists, to date, only two selective agents have been reported, viz (1S,3R)-1-aminocyclopentane-1,3-dicarboxylate ((1S,3R)-ACPD) (Palmer *et al.*, 1989) and (2S,3S,4S)-α-(carboxycyclopropyl)glycine (L-CCG-I) (Nakagawa *et al.*, 1990). Quisqualate frequently is found to produce a much weaker effect than ibotenate. Reported inhibitors of excitatory amino acid-stimulated phosphoinositide hydrolysis include L-2-amino-3-phosphonopropionate (L-AP3) (Schoepp *et al.*, 1990b) and L-aspartate-β-hydroxamate (Ormandy, 1992). Both compounds appear to act non-competitively and irreversibly; however, antagonism of metabotropic responses has not been consistently reported (Schoepp *et al.*, 1990a).

The development of new compounds active at glutamate metabotropic receptors is of considerable importance for elucidating the increasing range of its hypothesized physiological functions, particularly in view of the proposal of receptor heterogeneity based on pharmacological evidence (Raulli & Wroblewski, 1991; Tanabe *et al.*, 1991) and the recent isolation of four cDNA clones encoding a family of metabotropic receptors (Tanabe *et al.*, 1992).

Methods Wistar rat pups (postnatal day 6) were decapitated and the brains rapidly removed. The cerebral cortices were dissected free, washed in ice-cold Krebs-bicarbonate buffer (composition, mM: NaCl 120, KCl 3.1, $MgSO_4$ 1.2, KH_2PO_4 1.2, $CaCl_2$ 2.6, glucose 10, $NaHCO_3$ 25, pH 7.4), continuously gassed with 95% O_2/5% CO_2. Slices (0.3 × 0.3 mm) were prepared on a McIlwain tissue chopper and immediately suspended in 250 ml buffer at room temperature, followed by 3 subsequent changes of buffer.

After a 90 min incubation at 37°C in 20 ml fresh buffer containing 75 μCi D-myo-[^{3}H]-inositol (Amersham), the slices were washed 5 times to remove unincorporated label and allowed to settle. Fifty microlitre aliquots of gravity-packed slices were transferred to 5 ml polypropylene tubes containing a final volume of 250 μl buffer and 10 mM LiCl. The antagonist L-AP3, if present, was added at this stage. Tubes were gassed, capped and incubated at 37°C for 20 min prior to addition of agonists. The assay was terminated by addition of 1 ml $CHCl_3/CH_3OH$ (1:2 v/v), 0.3 ml deionised water and 0.3 ml $CHCl_3$. After vortexing and centrifugation, 750 μl of the upper aqueous phase was removed, added to 2 ml water and applied to minicolumns containing Dowex-1X8-200 (formate form) columns. A further 5 ml water followed by 5 ml 25 mM ammonium formate eluted residual free [^{3}H]-inositol, inositol glycerophosphates and cyclic inositol phosphates. Addition of 10 ml 0.2 M ammonium formate eluted [^{3}H]-inositol monophosphate and 1 ml aliquots were added to 4 ml Optiphase Hisafe scintillation fluid (LKB) and counted for tritium on an LKB Rackbeta scintillation spectrometer.

(S)-homoquisqualic acid was synthesized in our laboratory from (S)-4-amino-2-(benzyloxycarbonylamino)butanoic acid. Purification was by resin chromatography. Care was taken throughout the synthesis to avoid reaction conditions which might cause racemisation.

Of the other substances used in the experiments, L-AP3, ibotenic acid, quisqualic acid and (1S,3R)-ACPD were obtained from Tocris Neuramin Ltd (Bristol, UK).

Results Quisqualate was found to be the most potent agonist at the glutamate metabotropic receptor in rat pup cerebral cortical slices, with an EC_{50} of $0.92 \pm 0.4\ \mu M$. However, in agreement with other studies, the dose-response curve was shallow and non-parallel with those generated upon exposure to (1S,3R)-ACPD and ibotenate, which exhibited high efficacy and EC_{50}s of 18.6 ± 1.0 and $23.9 \pm 1.1\ \mu M$, respectively. In contrast to quisqualate, (S)-homoquisqualate behaved as a potent full agonist ($EC_{50} = 50.2 \pm 1.6\ \mu M$), displaying a dose-response curve parallel to that for (1S,3R)-ACPD and ibotenate (Figure 1). L-AP3 produced a concentration-dependent uncompetitive antagonism of the (S)-homoquisqualate response with an $IC_{50} = 127\ \mu M$ (Figure 2a), analogous to that found with quisqualate ($IC_{50} = 129\ \mu M$) and (1S,3R)-ACPD ($IC_{50} = 120\ \mu M$) (Figure 2b).

Discussion The results described here demonstrate that (S)-homoquisqualate, which differs from natural quisqualate (also (S) configuration) only by an additional CH_2 in the side chain, is a full agonist at the rat cerebro-cortical metabotropic receptor, although with somewhat less than half the potency of the highly selective agonist (1S,3R)-ACPD. The selectivity of (S)-homoquisqualate for the metabotropic

[1] Author for correspondence.

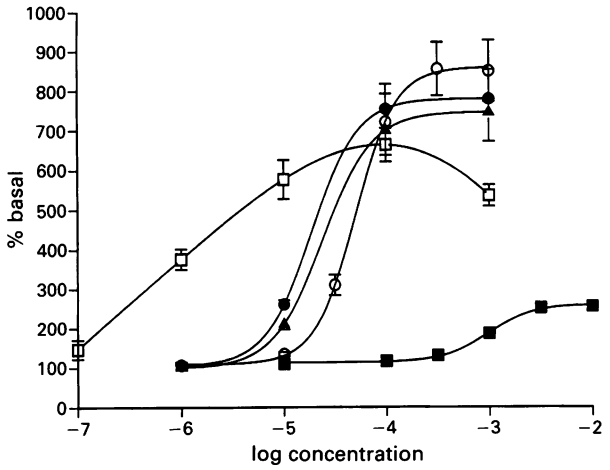

Figure 1 Concentration-dependent accumulation of [^{3}H]-inositol monophosphate in 6 day old rat cerebral cortex slices in response to quisqualate (□), (1S,3R)-ACPD (●), ibotenate (▲), (S)-homoquisqualate (○) and L-AP3 (■) in the presence of 10 mM Li^+. The data points represent the means and s.e.mean (vertical bars) of 4 independent experiments performed in triplicate. EC_{50} values were determined from the logistic sigmoid plots fitted to the equation: y = min + (max-min)/(1 + exp(-k*(X-X50))). For abbreviations, see text.

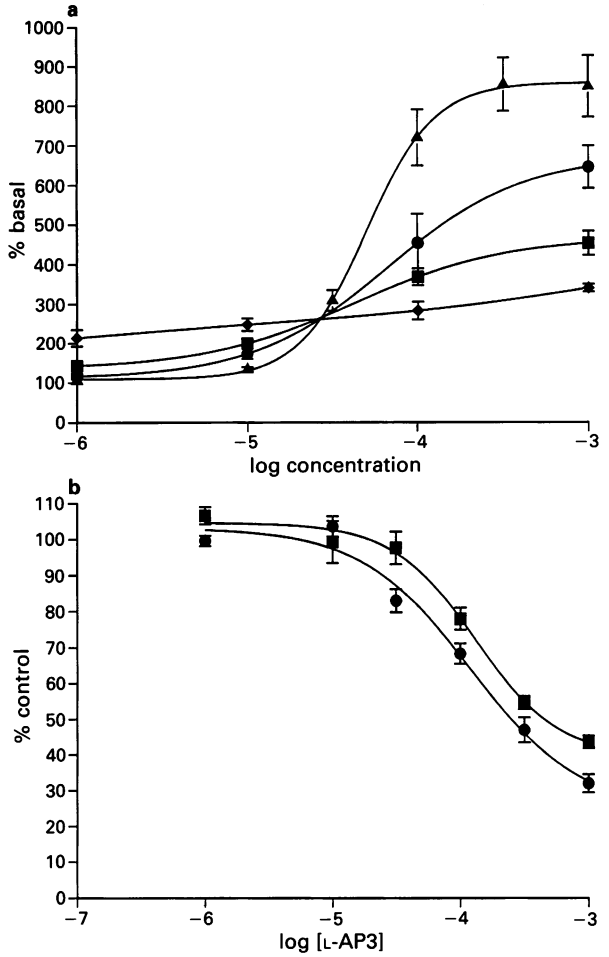

Figure 2 (a) (S)-homoquisqualate-stimulated accumulation of [^{3}H]-inositol monophosphate (▲) and its antagonism by L-AP3, 100 μM (●); 300 μM (■) and 1 mM (◆). Data points are mean with s.e.mean (vertical bars) of 4 independent experiments. (b) Antagonism of 100 μM (1S,3R)-ACPD (●) and 10 μM quisqualate (■)-stimulated accumulation of [^{3}H]-inositol monophosphate by L-AP3. Data points represent the mean of 3 independent experiments. For abbreviations, see text.

receptor has not yet been defined. However, this compound has been synthesized previously and, although lacking N-methyl-D-aspartate (NMDA) receptor activity, was reported to possess weaker agonist activity than quisqualate at the locust muscle 'quisqualate receptor' (Bycroft *et al.*, 1991).

The explanation of the much smaller stimulation of PI hydrolysis by quisqualate than with (S)-homoquisqualate, ibotenate and (1S,3R)-ACPD is unclear. The observation raises the possibility of the presence of two metabotropic receptor subtypes in the immature cortex, both mediating the same cellular response. However, when agonists were tested together at maximally effective concentrations, no additive effects were observed (data not shown). This suggests that a single excitatory amino acid receptor subtype is involved. Regarding the alternative possibility that quisqualate is a partial agonist, we have not been able to verify this by demonstrating an ability of quisqualate to antagonize responses to the full agonist, (1S,3R)-ACPD. Nevertheless, quisqualate displays a strikingly different quantitative activity from the other agonists tested. (S)-homoquisqualate and newer analogues should provide useful tools for investigating the structure-activity profile of excitatory amino acid metabotropic receptors.

R.P. is supported by Research into Ageing; D.J. and J.W. by the Medical Research Council.

References

BYCROFT, B.W., CHHABRA, S.R., HONE, N. & USHERWOOD, P.N.R. (1991). Stereoselective synthesis of chain extended analogues of quisqualic acid: potential agonists and antagonists for excitatory amino acid receptors. *Amino Acids*, **1**, 164.

NAKAGAWA, Y., SAITOH, K., ISHIHARA, T., ISHIDA, M. & SHINOZAKI, H. (1990). (2S,3S,4S)-α-(carboxycyclopropyl)glycine is a novel agonist of metabotropic glutamate receptors. *Eur. J. Pharmacol.*, **184**, 205–206.

NICOLETTI, F., WROBLEWSKI, J.T., NOVELLI, A., ALHO, H., GUIDOTTI, A. & COSTA, E. (1986). The activation of inositol phospholipid metabolism as a signal-transducing system for excitatory amino acids in primary cultures of cerebellar granule cells. *J. Neurosci.*, **6**, 1905–1911.

ORMANDY, G.C. (1992). Inhibition of excitatory amino acid-stimulated phosphoinositide hydrolysis in rat hippocampus by L-aspartate-β-hydroxamate. *Brain Res.*, **572**, 103–107.

PALMER, E., MONAGHAN, D.T. & COTMAN, C.W. (1989). Trans-ACPD, a selective agonist of the phosphoinositide-coupled excitatory amino acid receptor. *Eur. J. Pharmacol.*, **166**, 585–587.

RAULLI, R. & WROBLEWSKI, J.T. (1991). Stimulation of phosphoinositide hydrolysis by ibotenic acid in cerebellar neurons via two glutamate receptor subtypes. *Drug Dev. Res.*, **24**, 375–384.

SCHOEPP, D.D., BOCKAERT, J. & SLADECZEK, F. 1990a). Pharmacological and functional characteristics of metabotropic excitatory amino acid receptors. *Trends Pharmacol. Sci.*, **11**, 508–515.

SCHOEPP, D.D., JOHNSON, B.G., SMITH, E.C.R. & MCQUAID, L.A. (1990b). Stereoselectivity and mode of inhibition of phosphoinositide-coupled excitatory amino acid receptors by 2-amino-3-phosphonopropionic acid. *Mol. Pharmacol.*, **38**, 222–228.

TANABE, S., ITO, I. & SUGIYAMA, H. (1991). Possible heterogeneity of metabotropic glutamate receptors induced in *Xenopus* oocytes by rat brain mRNA. *Neurosci. Res.*, **10**, 71–77.

TANABE, Y., MASU, M., ISHII, T., SHIGEMOTO, R. & NAKANISHI, S. (1992). A family of metabotropic receptors. *Neuron*, **8**, 169–179.

(Received April 1, 1992
Accepted April 14, 1992)

Br. J. Pharmacol. (1992), **106**, 511–516

Differential inotropic effects of flosequinan in ventricular muscle from normal ferrets versus patients with end-stage heart failure

Cynthia L. Perreault, Nancy L. Hague, Evan Loh, Ian M. Hunneyball, Malcolm F. Sim & [1]James P. Morgan

Harvard-Thorndike Laboratory and Department of Medicine (Cardiovascular Division), Beth Israel Hospital, Harvard Medical School, 330 Brookline Avenue, Cardiovascular Division, Brigham and Women's Hospital, Boston, MA, U.S.A., and Research Department, Boots Pharmaceuticals, Nottingham, U.K.

1 In right ventricular papillary muscles from control ferrets, flosequinan (10^{-7}–10^{-4} M) produced a concentration-dependent positive inotropic effect (10^{-5} M = 153 ± 24, 10^{-4} M = 198 ± 44% increase in isometric tension; control tension = 100%; $n = 11$) associated with a corresponding increase in amplitude of the intracellular Ca^{2+} ($[Ca^{2+}]_i$) transient recorded with aequorin (10^{-5} M = 133 ± 11, 10^{-4} M = 187 ± 36% increase in $[Ca^{2+}]_i$ transient; $n = 11$).

2 The positive inotropic effect of flosequinan in control ferret ventricular muscle was neither blocked by propranolol (6×10^{-7} M), nor associated with the abbreviation of the $[Ca^{2+}]_i$ transient and contraction that is typical of catecholamines.

3 Neither flosequinan ($n = 12$) nor BTS 53 554, its sulphone metabolite ($n = 6$) produced a positive inotropic effect or altered the time course of contraction in myocardium from the hearts of patients with end-stage failure.

4 In contrast to milrinone, which produces a positive inotropic effect via phosphodiesterase inhibition, the unresponsiveness of myopathic human myocardium to flosequinan was not restored after intracellular adenosine 3':5'-cyclic monophosphate (cyclic AMP) levels were increased by prior treatment with forskolin ($n = 13$).

5 Taken together, these data indicate that flosequinan has a direct positive inotropic effect that is Ca^{2+}-dependent, but independent of changes in intracellular cyclic AMP concentrations.

6 The positive inotropic effect may be species-dependent or altered by the presence of hypertrophy and/or heart failure. However, when used therapeutically in patients with severe heart failure, our data suggest that flosequinan should not adversely affect myocardial oxygen consumption through direct or catecholamine-mediated actions on the heart.

Keywords: Flosequinan; vasodilator; calcium; aequorin; heart failure; inotropic drugs; myocardium; milrinone; sulphone metabolites

Introduction

Flosequinan is a mixed arteriovenous vasodilator that is currently being investigated in the clinic as an afterload/preload reducing agent in patients with congestive heart failure (Cohn, 1991). Flosequinan has been shown to produce positive inotropic effects on mammalian myocardium under certain conditions. For example, in ferret papillary muscle preparations studied *in vitro*, flosequinan has been reported to produce a positive inotropic effect over the range of concentrations from 1–100 μM (Falotico *et al.*, 1989; Greenberg & Touhey, 1990). In guinea-pig isolated atria, positive inotropic effects were observed with flosequinan over the concentration-range of 10^{-6} M–10^{-3} M (Yates & Hicks, 1988). Under these conditions, flosequinan appeared to be similar in potency to theophylline, but less potent than the positive inotropic agents, milrinone and sulmazole (Yates, 1991). We investigated the positive inotropic effects of flosequinan and their relationship to changes in intracellular calcium (Ca^{2+}_i) in ferret papillary muscles isolated *in vitro*, a frequently used experimental preparation for assessment of the cardiotonic activity of cardiovascular drugs. We also examined the effects of flosequinan on intracellular calcium handling in these tissues in order to delineate further the mechanism of the positive inotropic actions of the drug.

The responsiveness of failing human myocardium to cardiostimulatory drugs differs from that of normal myocardium. In this respect, the inotropic activity of β-adrenoceptor agonists such as isoprenaline, and phosphodiesterase inhibitors such as milrinone, are markedly reduced in muscles from patients with heart failure (Feldman *et al.*, 1987; Erdmann & Bohm, 1989). However, in the presence of forskolin, which elevates adenosine 3':5'-cyclic monophosphate (cyclic AMP) levels via direct adenylate cyclase stimulation, the inotropic responsiveness of myocardium from failing human hearts is markedly potentiated. These sorts of data suggest that an abnormality in cyclic AMP production may be a fundamental defect present in patients with end-stage heart failure. A defect of this type could diminish the effectiveness of agents that depend upon intracellular generation of cyclic AMP to exert their cardiotonic effects. Therefore, a second purpose of this present study was to investigate whether flosequinan, or BTS 53 554 its long-acting sulphone metabolite (Wynne *et al.*, 1985; Yates, 1991), would produce any inotropic effect on human myocardium in either the presence or absence of forskolin. These experiments with human muscle are of interest in light of evidence suggesting that drugs producing positive inotropic effects via increasing myocardial concentrations of cyclic AMP may adversely affect morbidity and survival in patients with heart failure (Packer, 1988; 1989).

[1] Author for correspondence at: Cardiovascular Division, Beth Israel Hospital, 330 Brookline Avenue, Boston, MA 02215, U.S.A.

Methods

Acquisition of ferret tissue and initial preparation

Papillary muscles of 1.0 mm or less in diameter were excised from the right ventricles of hearts removed from adult male ferrets, 12–14 weeks of age, under chloroform anaesthesia. Acquisition of human tissues is described below. The methods of preparation and instrumentation used in these studies have been described in detail (Gwathmey & Morgan, 1985; Blinks & Endoh, 1986; MacKinnon *et al.*, 1988; Perreault *et al.*, 1990). After removal from the hearts, muscles were placed in baths containing bicarbonate-buffered physiological salt solution bubbled with a gas mixture of 95% O_2 and 5% CO_2 to pH 7.4 and $[Ca^{2+}]_o$ of 1 or 2.5 mM. All human and ferret ventricular aequorin experiments were performed at 30°C. A subset of ferret right ventricular experiments were performed at 38°C. Muscles were stimulated to contract at 3 s intervals with pulses of 5 ms duration. Threshold voltage (i.e., $\leqslant 10\%$ above threshold) delivered via a punctate electrode was used to stimulate the muscles in order to minimize catecholamine release from the adrenergic nerve endings (Blinks, 1966). An initial 2 h equilibration period was allowed during which muscles were gradually stretched to the length where maximal isometric force developed. Since it was possible to obtain up to four papillary muscles per ferret, our n refers to the number of papillary muscles, not the number of ferrets.

Acquisition of human muscle

Myopathic human hearts were obtained from transplant recipients following the guidelines of a protocol approved by the Committee for the Protection of Human Subjects at Brigham and Women's Hospital, Boston. Muscles were obtained from the right and left ventricles of patients with either idiopathic cardiomyopathy or ischaemic cardiomyopathy undergoing cardiac transplantation for end-stage heart failure. In general, our muscle selection involved avoidance of areas of dense necrosis or fibrosis which tended to be more pronounced in the left ventricle. At the time of excision, the hearts were placed in an oxygenated physiological salt solution at room temperature. Cardiac samples were rapidly transported to the laboratory where suitable trabeculae carneae of $\leqslant 1.0$ mm in diameter were selected for study. From this point on, human trabecular preparations were handled exactly as described for ferret papillary muscles (Feldman *et al.*, 1987; Gwathmey *et al.*, 1987).

Aequorin studies

A subset of muscles from both the ferret ($n = 11$) and human ($n = 3$) groups were macroinjected with aequorin, a bioluminescent calcium indicator. The solution, purification and loading of aequorin are described in detail elsewhere (Blinks, 1982; 1986; Kihara *et al.*, 1989; Kihara & Morgan, 1989). Light signals were recorded with a photomultiplier by means of a specially-designed light collecting apparatus (Blinks & Endoh, 1986). In order to obtain a satisfactory signal-to-noise-ratio, it was usually necessary to average successive signals (from 16 to several hundred depending on the light intensity). Signal averaging was performed only after responses had reached the steady state. The light and tension responses and stimulus artifact were recorded simultaneously both on magnetic tape and on chart strip recording paper; light signals were passed through a filter with a 10 ms time constant. The light signal was measured in nanoamperes of anode current. The amplitude and time course of the aequorin light signals were analyzed in the same manner described above for tension.

It is possible for drugs to interact directly with aequorin and modify the luminescent reaction or the sensitivity of aequorin to Ca^{2+} (Kamaya *et al.*, 1977; Baker & Schapira, 1980). Therefore, the potential for interaction of flosequinan and aequorin was tested *in vitro* by use of the basic method and calibration device described by Blinks and Endoh (1986). Briefly, aequorin was added to a solution containing free $[Ca^{2+}]$ between 10^{-7} and 10^{-6} M; under these conditions a low level of luminescence persists for several minutes until the aequorin is gradually consumed. After initiating the luminescence reaction, flosequinan dissolved in dimethylsulphoxide (DMSO) was added to the reaction pipette. We found that neither the drug, nor DMSO without drug, affected the luminescence response measured at the concentrations used in these experiments.

Statistical analysis

All data were compared by unpaired or paired (when appropriate) Student's t test and by a Wilcoxon signed rank test. Statistical significance was set at $P<0.05$.

Drugs

The aequorin used in these experiments was obtained from the laboratory of Dr J.R. Blinks of Seattle, Washington, U.S.A.; propranolol was purchased from Sigma Chemical Company, St. Louis, Missouri, U.S.A.; milrinone was a generous gift of Sterling-Winthrop, Inc., Rensselaer, New York, U.S.A., and forskolin was purchased from Cal-Biochem, San Diego, California, U.S.A. The flosequinan (7-fluoro-1-methyl-3-methylsulfinylquinolin-4-one) and its principal sulphone metabolite BTS 53 554 (7-fluoro-1-methyl-3-methylsulphonylquinolin-4-one) used in these studies were prepared by Boots Pharmaceuticals, Nottingham, U.K. Stock solutions were prepared with distilled water except for milrinone, flosequinan and the sulphone metabolite of flosequinan. The milrinone stock solution was acidified by addition of a small amount of HCl, in the quantities used in these experiments, the diluent did not affect the pH of our bicarbonate buffer or muscle function. Flosequinan and its metabolite were dissolved in DMSO. In the amounts added in these experiments, DMSO did not significantly affect muscle function.

Results

Ferret papillary muscles

Figure 1 and Table 2 show that the peak isometric tension and peak of the calcium transient were increased in a dose-dependent fashion by flosequinan over the range of concentrations from 10^{-7} M–10^{-4} M. A subset of ferret papillary muscle experiments ($n = 5$) was performed at 38°C to com-

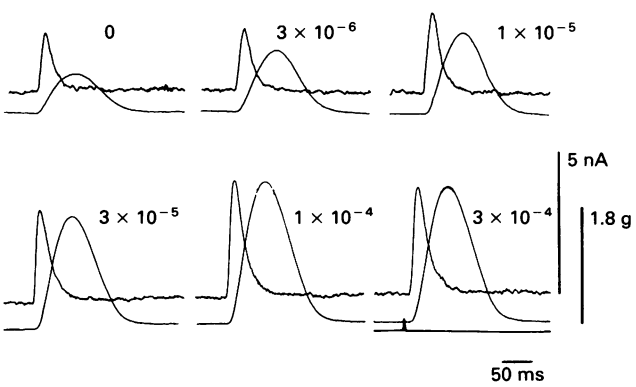

Figure 1 The effect of flosequinan (M concentrations) on the aequorin light signal (noisy tracing) and isometric tension response (smooth tracing) recorded from a right ventricular ferret papillary muscle. $[Ca^{2+}]_o = 2.5$ mM; stimulation frequency = 0.33 Hz; pulse duration = 5 ms; 30°C.

pare the inotropic effectiveness of flosequinan at 38°C to 30°C. At 38°C, flosequinan produced a 108 ± 6% increase at 10^{-6} M, a 120 ± 5% increase at 10^{-5} M ($P<0.05$) and a 168 ± 21% increase at 10^{-4} M ($P<0.05$). This was similar to the maximum increase in peak tension at 30°C of 198 ± 44% ($P<0.05$). Therefore, 30°C was selected for subsequent experiments because of the greater stability of these preparations at lower temperatures (i.e., slower mechanical run down; lower rate of aequorin consumption). Intracellular Ca^{2+} simultaneously increased with tension; a maximum response of 187 ± 36% ($P<0.05$) at the 10^{-4} M concentration of flosequinan was noted (Figure 1). As shown in Table 1 and Figure 2, the time courses of both tension and light remained unchanged in the presence of all concentrations of flosequinan studied. The presence of 6×10^{-7} M propranolol did not affect the positive inotropic action of flosequinan ($n = 5$; 255 ± 91% increase at 10^{-5} M, $P<0.05$, 336 ± 132 increase at 10^{-4} M, $P<0.05$). As shown in Figure 3, higher concentrations of flosequinan (10^{-4} M and greater) were associated with toxicity as shown by after-glimmers in the aequorin light signals and after-contractions in the isometric tension responses.

Human muscle studies

Table 2 shows that peak isometric tension was not significantly increased with either flosequinan or BTS 53 554 over the dose range from 10^{-6} M–10^{-4} M, reaching a peak response of 109 ± 6% at 10^{-4} M flosequinan and a peak response to BTS 53 554 of 103 ± 4% ($P<0.05$). The time course measurements of the twitch were not affected by any concentration of flosequinan tested (see Table 2). Figure 4 shows an aequorin-loaded myopathic human muscle in which no significant response to flosequinan occurred either in the isometric tension response or the $[Ca^{2+}]_i$ transient even at the highest dose. The dose-response relationships of flosequinan and BTS 53 554 to isometric tension are depicted in Figure 5.

The effects of flosequinan were tested on myopathic human trabeculae before and after the addition of a minimally effective concentration of forskolin (Figure 5b). Sufficient forskolin was added to produce a 5–15% increase in developed tension. Flosequinan was ineffective in producing a positive inotropic effect even under conditions of forskolin pre-stimulation. Forskolin also did not restore the inotropic effectiveness of BTS 53 554 (Figure 5c). These data are in contrast to our results with milrinone in human myopathic myocardium where forskolin pretreatment restored the inotropic effectiveness of this phosphodiesterase inhibitor (Figure 5a).

Discussion

Mechanism of inotropic effect

Most of the inotropic agents available for experimental or clinical use predominantly act to increase the availability of

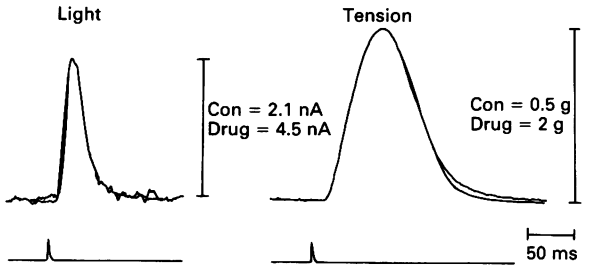

Figure 2 Aequorin light and isometric tension responses electronically adjusted to equal amplitudes and superimposed to demonstrate that flosequinan (3×10^{-5} M) does not alter the time course of either the light or tension responses in this aequorin-loaded ferret right ventricular papillary muscle. Absolute tension and light calibration scales are shown to the right of both traces. $[Ca^{2+}]_o = 2.5$ mM; stimulation frequency = 0.33 Hz; pulse duration = 5 ms; 30°C.

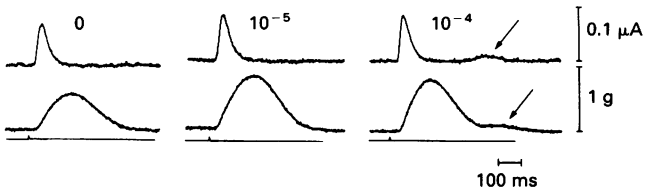

Figure 3 Toxicity of 10^{-4} M flosequinan in an aequorin-loaded ferret right ventricular papillary muscle as shown by after-glimmers and after-contractions (indicated by arrows). $[Ca^{2+}]_o = 1$ mM; stimulation frequency = 0.33 Hz; pulse duration = 5 ms; 30°C.

Table 2 The effects of flosequinan and its major metabolite, BTS 53 554, on peak tension and the time course of the isometric contraction in myopathic human myocardium.

A	*Flosequinan*			
	0	10^{-6} M	10^{-5} M	10^{-4} M
PT (%)	100 ± 0	105 ± 5	106 ± 5	109 ± 6
TPT (ms)	349 ± 45	394 ± 57	367 ± 36	268 ± 45
T5T (ms)	246 ± 20	268 ± 21	264 ± 19	237 ± 16
B	*BTS 53 554*			
	0	10^{-6} M	10^{-5} M	10^{-4} M
PT (%)	100 ± 0	102 ± 6	102 ± 3	103 ± 4
TPT (ms)	338 ± 26	323 ± 46	318 ± 46	344 ± 27
T5T (ms)	245 ± 31	270 ± 46	252 ± 41	225 ± 31

Flosequinan was tested in 12 human myopathic muscles (**A**) and the effect of its major metabolite, BTS 53 554, on 6 human myopathic muscles (**B**). PT = peak tension; TPT = time to peak tension; T5T = time to 50% relaxation; $[Ca^{2+}]_o = 2.5$ mM; values are means ± s.e.mean.

Table 1 Peak tension, peak light and the time courses of light and tension responses to flosequinan in 11 aequorin-loaded right ventricular papillary muscles

	Flosequinan				
	0	10^{-7} M	10^{-6} M	10^{-5} M	10^{-4} M
PT (%)	100 ± 0	112 ± 7*	119 ± 10*	153 ± 24*	198 ± 44*
PL (%)	100 ± 0	104 ± 2*	117 ± 6*	133 ± 11*	187 ± 36*
TPT (ms)	170 ± 17	195 ± 12	185 ± 12	197 ± 11	176 ± 4
T5T (ms)	123 ± 13	119 ± 11	123 ± 10	116 ± 11	112 ± 11
TPL (ms)	59 ± 7	50 ± 5	57 ± 5	60 ± 5	55 ± 5
T5L (ms)	47 ± 3	53 ± 8	46 ± 4	47 ± 4	48 ± 6

The effect of flosequinan on the peak tension (PT); peak light (PL); time to peak tension (TPT), time to peak light (TPL), time to 50% relaxation of the tension (T5T), time to 50% decline from the peak light (T5L); $[Ca^{2+}]_i = 1$ mM, 30°C, stimulation frequency = 0.33 Hz; pulse duration = 5 ms; values are means ± s.e.mean; ($n = 11$); *$P<0.05$ versus control.

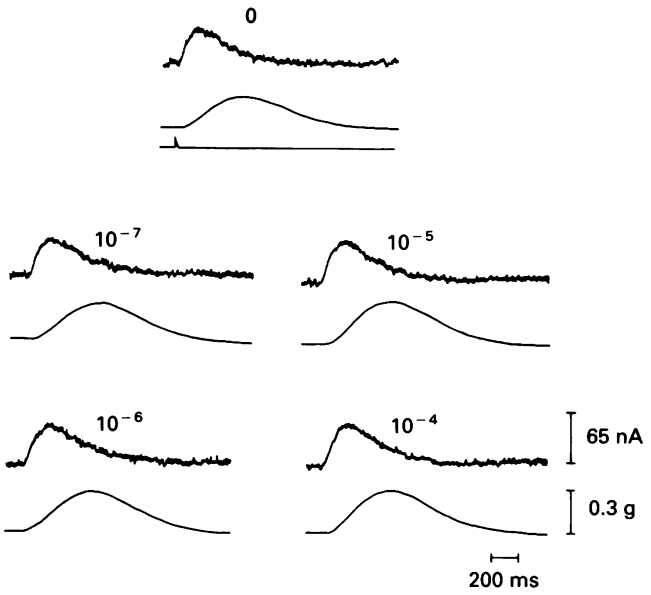

Figure 4 The effect of flosequinan (M concentrations) on an aequorin-loaded trabeculae carneae from a patient with end-stage heart failure. Aequorin light signals are the noisy tracings and the isometric tension responses are the smooth tracings. $[Ca^{2+}]_o = 2.5$ mM; 30°C; stimulation frequency = 0.33 Hz; pulse duration = 5 ms.

activator $[Ca^{2+}]_i$. Alternatively, a small number of experimental agents may increase myofilament Ca^{2+} responsiveness and increase contractility by mechanisms that are largely independent of changes in $[Ca^{2+}]_i$ (Morgan, 1988; Morgan & Morgan, 1989). Our results indicate that the positive inotropic effect of flosequinan, when present, is associated with an increase in $[Ca^{2+}]_i$.

There are several mechanisms by which inotropic drugs may increase $[Ca^{2+}]_i$ availability. In general, this occurs by one or a combination of four main effects: (1) increased transsarcolemmal Ca^{2+} entry; (2) decreased transarcolemmal Ca^{2+} efflux; (3) increased release of Ca^{2+} from the sarcoplasmic reticulum; or (4) decrease re-uptake of Ca^{2+} by the sarcoplasmic reticulum. Most of the agents now available for clinical use produce the first effect by increasing intracellular concentrations of cyclic AMP. This in turn leads to increased Ca^{2+} influx via the voltage-dependent, L-type sarcolemmal calcium channels, an effect that is mediated by cyclic AMP-dependent phosphorylation. Available evidence suggests that flosequinan does not affect the β-adrenoceptors or histamine receptors, which are coupled to adenylate cyclase, nor inhibit phosphodiesterase isoenzymes except at concentrations much higher than the usual therapeutic range (Allcock *et al.*, 1988; Packer *et al.*, 1988; Frodsham *et al.*, 1989; Frodsham *et al.*, 1990; Yates, 1991). Along with an increase in contractility, a corresponding abbreviation of the time course of the Ca^{2+} transient and isometric twitch also typically occurs with cyclic AMP-dependent agents due to phosphorylation of phospholamban in the sarcoplasmic reticulum. Since no abbreviation of these parameters occurred with positive inotropic doses of flosequinan in our experiments with ferret papillary muscles, cyclic AMP-mediation of this effect appears unlikely (Gwathmey & Morgan, 1985). Moreover, since the adenylate cyclase activator, forskolin, restored the inotropic effectiveness of milrinone but not flosequinan in myopathic human myocardium (Figure 5), it appears that the latter drug does not have functionally significant phosphodiesterase inhibitor properties, at least in the concentrations used in these experiments. Along these same lines, it is important to note that some drugs (i.e., metaraminol, amphetamine, and cocaine) may produce an increase in cyclic AMP through release of catecholamines from the sympathetic nerve endings

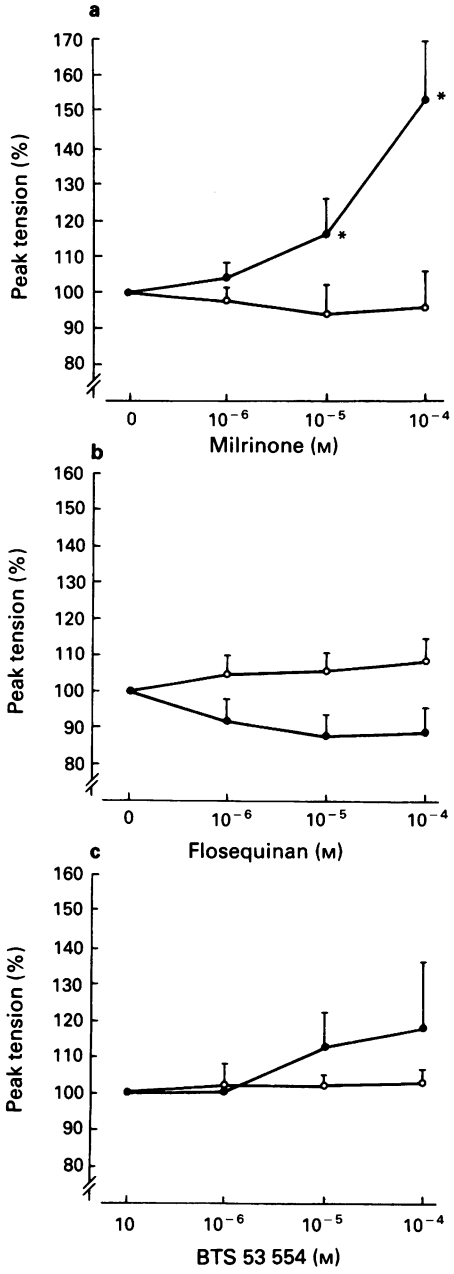

Figure 5 (a) The dose-response relationship of milrinone (○) before the addition of forskolin ($n = 10$) and after the addition of forskolin (●, $n = 10$); (b) flosequinan (○) before forskolin ($n = 12$) and after forskolin (●, $n = 13$) and (c) BTS 53 554 (○) before forskolin ($n = 6$) and after forskolin (●, $n = 6$) in myopathic human myocardium.

(for example, see Perreault *et al.*, 1990). The inability of propranolol to block the inotropic response to flosequinan in our experiments argues against this possibility with regard to flosequinan.

The above results indicate that flosequinan does not enhance transsarcolemmal Ca^{2+} influx by increasing cellular cyclic AMP concentrations. However, an effect mediated by some other second messenger, such as IP_3 or diacylglycerol (Yates & Holmes, 1988; Yates *et al.*, 1989) or a direct effect on the Ca^{2+} channels is not ruled out by our results, although none of the available evidence on this drug supports such a mechanism (Yates, 1991) except in smooth muscle (Richards *et al.*, 1989; Resnick *et al.*, 1990).

In addition to effects on the L-type Ca^{2+} channels, drugs and intervention can produce a positive inotropic effect by enhancing influx of Ca^{2+} via Na^+/Ca^{2+} exchange (Morgan &

Morgan, 1989; Wier, 1990). For example, the cardiotonic steroids, like dogoxin, or Na^+ channel agonists, like DPI 201-106, may produce NA^+ loading of the myocyte and facilitate Ca^{2+} entry for Na^+ extrusion at the exchange site (Kihara *et al.*, 1989). None of the available evidence suggests that flosequinan affects Na^+/K^+ ATPase activity or Na^+/Ca^{2+} exchanger function (Yates, 1991). However, the possibility of cellular loading of Na^+ under the influence of flosequinan was not directly tested in the present series of experiments.

Inhibition of Ca^{2+} re-sequestration by the sarcoplasmic reticulum would be expected to prolong activation time and produce a positive inotropic effect. This action is in part responsible for the positive inotropic actions of caffeine and DPI 201-106 in the myocardium of some species. Moreover, drugs with this action typically prolong the Ca^{2+} transient and markedly increase the duration of isometric relaxation. The observation in the present study that inotropic doses of flosequinan do not change the time course of the $[Ca^{2+}]_i$ transient or twitch provides evidence against this possible effect.

In summary, the positive inotropic action of flosequinan, when present, appears to be caused by increased availability of activator Ca^{2+}. Although the precise mechanisms responsible for this increase remain unknown, our data indicate it does not appear to be caused by an increase in cyclic AMP concentrations, although some other second messenger system may be involved. Therefore, on the basis of available evidence, we feel that the most likely mechanism appears to be an increase in transsarcolemmal Ca^{2+} entry either via the voltage-dependent L-type channels or Na^+/Ca^{2+} exchanger or by decreased transsarcolemmal Ca^{2+} efflux at the site of the exchanger. Delineation of the precise mechanism by which flosequinan increases $[Ca^{2+}]_i$ and contractile force awaits further studies.

Toxicity mediated by intracellular Ca^{2+} overload

The toxicity of positive inotropic drugs is often associated with spontaneous oscillatory Ca^{2+} release and in experimental, aequorin-loaded muscles, is shown by after-contractions in the isometric tension response and after-glimmers in the aequorin light signals (Morgan & Morgan, 1984). As shown in Figure 3, flosequinan at higher concentrations, can produce toxicity resulting in after-glimmers and after-contractions in ferret ventricular papillary muscles. This was not seen in the myopathic human myocardium in which flosequinan failed to produce a positive inotropic response or dysrhythmias. It is of interest that flosequinan has been reported not to affect ischaemic arrhythmias in anaesthetized rats (Jones & Sim, 1990).

Therapeutic implications

The observation that flosequinan does not have a significant inotropic effect on muscle from patients with end-stage failure has potentially important therapeutic implications. In recent years, considerable interest has developed in a broad class of drugs generally referred to as inodilators (Opie, 1986). These agents possess both vasodilator and positive inotropic properties and have been proposed as useful agents in patients with heart failure in whom both afterload reduction and increased contractility are therapeutic goals. Examples of this class include phosphodiesterase inhibitors, such as amrinone and milrinone, and partial β-adrenoceptor agonists such as xamoterol (Packer, 1988). However, this combination of effects may be undesirable in patients with heart failure who have impaired myocardial energy reserves and therefore may not tolerate the increased demands imposed by enhanced contractility. Patients with ischaemic cardiomyopathy, in particular, might be expected to tolerate poorly agents with this combination of effects, although recent studies have questioned the wisdom of using agents directed at increasing contractility in any patient with heart failure. Preliminary results from the recent multicentre Promise Trial of milrinone therapy for heart failure raise the possibility that increased contractility may be associated with decreased survival despite symptomatic improvement, although this point is far from completely settled (Packer, 1989).

Some (Burstein *et al.*, 1990; 1991; Corin *et al.*, 1991), but not all (Fisher *et al.*, 1990) clinical studies have reported evidence to suggest that flosequinan or its metabolite may produce a positive inotropic effect in patients that is not explained on the basis of changes in pre-load or serum catecholamine levels. Moreover, in view of the current questions about the value of positive inotropic therapy, it is important to note that our results suggest that neither flosequinan nor its major sulphone metabolite directly affect the contractile state of the heart, at least in patients with more severe degrees of failure. The range of concentrations tested (10^{-6}–10^{-4} M) correlated with clinically effective serum concentrations of flosequinan plus its metabolite, which are around 10^{-5}–3×10^{-5} M (Packer, 1988). Therefore, it should be possible to use flosequinan safely as a mixed vasodilator in these patients to produce afterload reduction without enhancing metabolic demands on the heart.

It is of interest that some positive inotropic agents like DPI 201-106 (Hajjar *et al.*, 1988) can differentially affect normal versus myopathic human myocardium or may lose their effectiveness as the severity of heart failure progresses (Wilsmhurst *et al.*, 1984; Erdmann & Bohm, 1989). Additional studies are warranted to determine if inotropic responsiveness to flosequinan is species-dependent, and/or affected by the presence of cardiac hypertrophy or failure. Flosequinan appears to have a greater inotropic effect on myocardium from ferrets than from guinea-pigs or dogs based on currently available literature (Yates, 1991).

Partial support was provided by NIH grant HL-31117, and a Grant-In-Aid from the American Heart Association. The authors express their appreciation to Mr Jason Kravitz for his assistance in the preparation of this manuscript and to Dr Frederick Schoen, and the Division of Cardiac Pathology, Division of Pathology at Brigham and Women's Hospital for their help in obtaining the human hearts.

References

ALLCOCK, A.A., FRODSHAM, G. & SIM, M.F. (1988). Effects of flosequinan, a novel arteriovenous dilating agent, on cGMP levels in rat isolated aortic strips. *Br. J. Pharmacol.*, **94**, 430P.

BAKER, P.F. & SCHAPIRA, A.H.V. (1980). Anesthetics increase light emission from aequorin at constant ionized calcium. *Nature*, **284**, 168–169.

BLINKS, J.R. (1966). Field stimulation as a means of effecting the graded release of autonomic transmitters in isolated heart muscle. *J. Pharmacol. Exp. Ther.*, **151**, 221–235.

BLINKS, J.R. (1982). The use of photoproteins as Ca^{2+} indicators in cellular physiology. In *Techniques in Cellular Physiology* ed. Baker, P.F. pp. 1–38. Amsterdam: Elsevier.

BLINKS, J.R. (1986). Intracellular $[Ca^{2+}]$ measurements. In *The Heart and Cardiovascular System*. ed. Fozzard, H.A., Haber, E. & Jennings, R.B. pp. 671–701. New York: Scientific Foundations.

BLINKS, J.R. & ENDOH, M. (1986). Modification of myofibrillar responsiveness to Ca^{2++} as an inotropic mechanism. *Circulation*, **73** (Suppl III), 85–96.

BURSTEIN, S., SEMIGRAN, M.J., DEC, G.W., BOUCHER, C.A. & FIFER, M.A. (1990). Positive inotropic effect of flosequinan in patients with heart failure: demonstration by left ventricular end-systolic pressure volume-analysis. *Circulation*, **82**, 1530 (Abstract).

BURSTEIN, S., SEMIGRAN, M.J., DEC, C.W., BOUCHER, C.A. & FIFER, M.A. (1991). Flosequinan improves left ventricular relaxation in patients with heart failure. *J. Am. Coll. Cardiol.*, **17**, 142A (Abstract).

COHN, J.N. (1991). Future directions in vasodilator therapy for heart failure. *Am. Heart J.*, **121**, 969–974.

CORIN, W.J., MONRAD, E.S., STROM, J.A., GIUSTINO, S., SONNENBLICK, E.H. & LEJEMTEL, T. (1991). Flosequinan: a vasodilator with positive inotropic activity. *Am. Heart J.*, **121**, 537–540.

ERDMANN, E., & BOHM, M. (1989). Positive inotropic stimulation in normal and insufficient human myocardium. *Basic Res. Cardiol.*, **84** (Suppl. 1), 125–133.

FALOTICO, R., HAERTLEIN, B.J., LAKAS-WEISS, C.S., SALATA, J.J. & TOBIA, A.J. (1989). Positive inotropic and hemodynamic properties of flosequinan, a new vasodilator, and a sulfone metabolite. *J. Cardiovasc. Pharmacol.*, **14**, 412–418.

FELDMAN, M., COPELAS, L., GWATHMEY, J.K., PHILLIPS, P., WARREN, S.E., SCHOEN, F.J., GROSSMAN, W. & MORGAN, J.P. (1987). Deficient production of cyclic AMP: pharmacologic evidence of an important cause of contractile dysfunction in patients with end-stage heart failure. *Circulation*, **75**, 331–339.

FISHER, E.A., PORDER, J.B., KUKIN, M.L., SCHEIN, I.D., KLAPPER, A.S., PACKER, M. & GOLDMAN, M.E. (1990). How do vasodilators improve cardiac performance in chronic heart failure? Insights gained from two-dimensional color flow doppler echocardiography. *J. Am. Coll. Cardiol.*, **15**, 150A (Abstract).

FRODSHAM, G., JONES, R.B. & SIM, M.F. (1989). Effects of flosequinan, a novel arteriovenous dilating agent, and its metabolite on bovine heart phosphodiesterase activity. *Br. J. Pharmacol.*, **98**, 733P.

FRODSHAM, G., JONES, R.B. & SIM, M.F. (1990). Effect of flosequinan and its major metabolite BTS 53 554, on phosphodiesterase (PDE) isoenzyme types I, II and III from guinea-pig ventricle. *Br. J. Pharmacol.*, **100**, 441P.

GREENBERG, G. & TOUHEY, B. (1990). Positive inotropy contributes to the hemodynamic mechanism of action of flosequinan (BTS 49 465) in the intact dog. *J. Cardiovasc. Pharmacol.*, **15**, 900–910.

GWATHMEY, J.K., COPELAS, L., MACKINNON, R., SCHOEN, F.J., FELDMAN, M.D., GROSSMAN, W. & MORGAN, J.P. (1987). Abnormal intracellular calcium handling in myocardium from patients with end-stage heart failure. *Circ. Res.*, **61**, 70–76.

GWATHMEY, J.K. & MORGAN, J.P. (1985). The effect of milrinone and piroximone on intracellular Ca^{2+} handling in working myocardium from the ferret. *Br. J. Pharmacol.*, **85**, 97–108.

HAJJAR, R.J., GWATHMEY, J.K., BRIGGS, G.M. & MORGAN, J.P. (1988). Differential effects of DPI 201-106 on the sensitivity of myofilaments to Ca^{2+} in intact and skinned trabeculae from control and myopathic human hearts. *J. Clin. Invest.*, **82**, 1578–1584.

JONES, R.B. & SIM, M.F. (1990). Effect of flosequinan on ischemic arrhythmias in anaesthetized rats. *Br. J. Pharmacol.*, **100**, 440P.

KAMAYA, H., VEDA, I. & EYRING, H. (1977). Reversible and irreversible inhibition by anesthetics of the calcium-induced luminescence of aequorin. *Proc. Natl. Acad. Sci. U.S.A.*, **74**, 5534–5537.

KIHARA, Y., GROSSMAN, W. & MORGAN, J.P. (1989). Direct measurements of changes in intracellular calcium transients during hypoxia, ischemia, and reperfusion of the intact mammalian heart. *Circ. Res.*, **65**, 1029–1044.

KIHARA, Y., GWATHMEY, J.K., GROSSMAN, W. & MORGAN, J.P. (1989). Mechanisms of positive inotropic effects and delayed relaxation produced by DPI 201-106 in mammalian working myocardium: effects on intracellular calcium handling. *Br. J. Pharmacol.*, **96**, 927–939.

KIHARA, Y. & MORGAN, J.P. (1989). A comparative study of three methods for intracellular loading of the calcium indicator aequorin in ferret papillary muscle. *Biochem. Biophys. Res. Commun.*, **162**, 402–407.

MACKINNON, R., GWATHMEY, J.K., ALLEN, P.D., BRIGGS, G.M. & MORGAN, J.P. (1988). Modulation by the thyroid state of intracellular calcium and contractility in ferret ventricular muscle. *Circ. Res.*, **63**, 1080–1089.

MORGAN, J.P. (1988). Intracellular calcium in heart failure. *Cardiovasc. Drugs Ther.*, **1**, 621–624.

MORGAN, J.P. & MORGAN, K.G. (1984). Calcium and cardiovascular function: Intracellular calcium levels during contraction and relaxation of mammalian cardiac and vascular smooth muscle as detected with aequorin. *Am. J. Med.*, **77** (Suppl 5A), 33–46.

MORGAN, J.P. & MORGAN, K.G. (1989). Intracellular calcium and cardiovascular function in heart failure: effects of pharmacologic agents. *Cardiovasc. Drugs Ther.*, **3** (Suppl. 3), 959–970.

OPIE, L. (1986). Inodilators. *Lancet*, **i**, 1336.

PACKER, M. (1988). Vasodilator and inotropic drugs for the treatment of chronic heart failure: distinguishing hype from hope. *J. Am. Coll. Cardiol.*, **12**, 1299–1317.

PACKER, M. (1989). Effect of phosphodiesterase inhibitors on survival of patients with chronic congestive heart failure. *Am. J. Cardiol.*, **63**, 41A–45A.

PACKER, M., KESSLER, P.D., PORTER, R.S., MEDINA, N., YUSHAK, M. & GOTTLEIB, S.S. (1988). Do plasma levels of flosequinan correlate with its hemodynamic effects in severe chronic heart failure? *J. Am. Coll. Cardiol.*, **11**, 42A.

PERREAULT, C.L., HAGUE, N.L., RANSIL, B.J. & MORGAN, J.P. (1990). The effects of cocaine on intracellular Ca^{2+} handling and myofilament Ca^{2+} responsiveness of ferret ventricular myocardium. *Br. J. Pharmacol.*, **101**, 679–685.

RESNICK, M.S., MAITLAND, L.A. & MORGAN, K.G. (1991). Flosequinan, a vasodilator with a novel mechanism of action. *Br. J. Pharmacol.*, **102**, 974–978.

RICHARDS, N.T., POSTON, L. & HILTON, P.J. (1989). Flosequinan-induced vasodilatation of human resistance vessels is associated with decreased calcium sensitivity. *Br. J. Pharmacol.*, **98**, 734P.

WIER, W.G. (1990). Cytoplasmic $[Ca^{2+}]$ in mammalian ventricle: dynamic control by cellular processes. *Ann. Rev. Physiol.*, **52**, 467–485.

WILMSHURST, P.T., WALKER, J.M., FRY, C.H., MOUNSEY, J.P., TWORT, C.H.C., WILLIAMS, B.T., DAVIES, M.J. & WEBB-PEPLOE, M.M. (1984). Inotropic and vasodilator effects of amrinone on isolated human tissue. *Cardiovasc. Res.*, **18**, 302–309.

WYNNE, R.D., CRAMPTON, E.L. & HIND, I.D. (1985). The pharmacokinetics and haemodynamics of BTS 49 465 and its major metabolite in healthy volunteers. *Eur. J. Clin. Pharmacol.*, **28**, 659–664.

YATES, D.B. (1991). Pharmacology of flosequinan. *Am. Heart J.*, **121**, 974–983.

YATES, D.B. & HICKS, G.R. (1988). Effects of flosequinan on guinea-pig atria and on cardiac variables in the anesthetized dog. *Br. J. Pharmacol.*, **95**, 711P.

YATES, D.B., HICKS, G. & SIM, M.F. (1989). The effects of vasorelaxants which increase cyclic nucleotides on phosphoinositide metabolism. *Br. J. Pharmacol.*, **96**, 112P.

YATES, D.B. & HOLMES, J.R (1988). Effect of flosequinan and other vasorelaxants on rat aortic contractions stimulated by noradrenaline and phorbol ester. *Br. J. Pharmacol.*, **95**, 819P.

(Received August 19, 1991
Revised December 18, 1991
Accepted February 17, 1992)

Br. J. Pharmacol. (1992), **106**, 517–523

Ionic mechanisms responsible for the antiarrhythmic action of dehydroevodiamine in guinea-pig isolated cardiomyocytes

*Shih-Hurng Loh, **An-Rong Lee, **Wen-Hsin Huang & [1],*†Cheng-I Lin

*Institute of Pharmacology and **School of Pharmacy, National Defence Medical Centre, Taipei and †National Research Institute of Chinese Medicine, Taiwan

1 Dehydroevodiamine alkaloid (DeHE), an active ingredient of a Chinese herbal medicine Wu-Chu-Yu (*Evodiae frutus*), has been shown to decrease aterial blood pressure in experimental animals and prolong action potential duration in cardiac cells. The aim of the present study was to explore the ionic basis of its possible antiarrhythmic effects.

2 Guinea-pig atrial and ventricular myocytes were isolated enzymatically and the ionic currents were recorded under whole-cell patch-clamp with single suction pipettes.

3 DeHE at a concentration of 0.1 μM inhibited reversibly the time-dependent outward K current (delayed rectifier, I_k) and the Na-dependent inward current (I_{Na}).

4 In low-K (1 mM) and high-Ca (9 mM) solution, DeHE also depressed the delayed afterdepolarizations (DAD) and the transient inward current (I_{ti}) induced by 2 μM strophanthidin. On the other hand, DeHE occasionally induced early afterdepolarizations and slow response action potentials at a depolarized level.

5 At higher concentrations (1 μM and above), the L-type Ca current ($I_{Ca,L}$) was moderately inhibited.

6 The present findings indicate that DeHE may depress triggered arrhythmias in Ca-overloaded guinea-pig cardiac myocytes through its inhibitory actions on I_{Na}, I_{ti} and, to a smaller extent, I_{Ca}. DeHE may also exert class III antiarrhythmic effect through a reduction of outward K currents (I_k) across the sarcolemma.

Keywords: Dehydroevodiamine; action potential; ionic currents; myocytes; atrium; ventricle; triggered activity; whole-cell patch-clamp

Introduction

Dehydroevodiamine (DeHE), a quinazolinocarboline alkaloid isolated from a Chinese folk medicine Wu-Chu-Yu (*Evodiae frutus*) (Chen *et al.*, 1981), has been shown to induce hypotension and bradycardia in rats (Yang *et al.*, 1988; 1990). Recent studies on rabbit sinoatrial tissues in our laboratory (Lin *et al.*, 1990) have shown that the negative chronotropic effect of this compound was associated with a prolongation of action potential duration (APD) and a reduction of maximum diastolic potential and diastolic slope. In ventricular papillary muscles, DeHE at higher concentrations ($\geqslant$ 0.3 μM) induced a development of early afterdepolarization (EAD) but consistently decreased force of contraction only at concentrations higher than 3 μM (Lin *et al.*, 1990). The aims of the present experiments were to investigate the ionic mechanisms responsible for the APD prolongation and to explore the possible antiarrhythmic effect induced by DeHE on guinea-pig cardiac cells with whole-cell voltage-clamp techniques.

Methods

Single atrial and ventricular myocytes of the guinea-pig, weighing 300–500 g, were used. The methods described by Mitra & Morad (1985) and Tytgat *et al.* (1990a) for cell dissociation, whole-cell patch-clamp recording, and superfusion and internal perfusion of the cells were used in the present study. In brief, guinea-pigs were killed by a blow on the neck and the heart was quickly removed and mounted on a Langendorff perfusion column. The aorta was cannulated and the heart was perfused with a solution containing collagenase and protease at 37°C. After isolation, the cardiomyocytes were bathed at room temperature (20–25°C) in a superfusate containing (in mM): NaCl 137.6, KCl 5.4, $CaCl_2$ 1.8, $MgCl_2$ 0.5, HEPES 11.5 and glucose 22. The pipette solution contained KCl 120, $MgCl_2$ 6, Na_2ATP 5, HEPES 10, EGTA 5, and $CaCl_2$ 0.15, adjusted to pH 7.2 with 1 N KOH. To record action potential, the myocytes were occasionally paced through a recording micropipette by use of suprathreshold depolarizing stimuli of 2 ms duration provided by a Grass S88 stimulator.

For measurement of ionic currents, single-electrode chopped clamp technique was used by means of an Axoclamp 2-A amplifier (Axon Instruments, Calif, U.S.A.). Data acquisition and analysis were controlled by pCLAMP software (Axon Instruments). The cells were allowed to stabilize in the bath at room temperature for at least 30 min before experiments. The time-dependent outward K currents (I_k) of atrial and ventricular cells were activated by pulses from a holding potential of −70 mV to a conditioning potential of +20 mV of varying duration (0.3–1.8 s), and outward tail currents were measured at −30 mV (see Roden *et al.*, 1989).

For determination of L-type calcium current ($I_{Ca,L}$) of the ventricular cell, a holding potential (V_h) of −50 mV was used to inactivate T-type calcium current ($I_{Ca,T}$) (Tytgat *et al.*, 1990a). Currents were produced at clamped potentials from −40 to +60 mV in 10 mV steps for 250 ms every 2 s. To measure accurately $I_{Ca,L}$ with no contamination of other ionic currents, the cells were bathed in K- and Na-free Tris solution containing (in mM): tris (hydroxymethyl) aminomethane 137.6, $MgCl_2$ 1, CsCl 20, $CaCl_2$ 5.5 and glucose 27.5. The standard internal solution in the micropipette (2–5 MOhm

[1] Author for correspondence at: Department of Pharmacology, National Defence Medical Centre, P.O. Box 90048-504, Taipei, Taiwan.

resistance) contained (in mM) CsCl 125, MgATP 5, EGTA 15, tetraethylammonium Cl 20, and HEPES 10, adjusted to pH 7.2 with 1 N CsOH. $I_{Ca,L}$ was measured as the difference between peak inward current and the current at the end of the 250 ms pulse. There was almost invariably a run-down of the $I_{Ca,L}$ (Belles *et al.*, 1988), especially during the initial 15 min of internal cell perfusion. Thus experiments were started after a 15 min period of internal perfusion when a further decline of $I_{Ca,L}$ with time had become about 10% for a 30–60 min period. To determine the effects of DeHE, the drug was added to the Tris bath solution at concentrations ranging from 0.1 to 3 μM. For measurement of the Na-dependent inward current (I_{Na}), the experiments were performed in a very low $[Na]_o$ (2 or 12 mM) in K-free Tris solution following the method of Tytgat *et al.* (1990b).

To evaluate the depressant effects of DeHE on triggered activity, the cells were bathed in low-K (1 mM), high-Ca (9 mM) HEPES solution plus 2 μM strophanthidin. The cells were dialysed with a pipette solution containing (in mM): KCl 120, Na_2ATP 5, HEPES 10, EGTA 0.5, $MgCl_2$ 1, $CaCl_2$ 0.01 and pH 7.2 (see Enous *et al.*, 1990). The holding potential was set to −44 mV. A 1.2 s depolarizing pulse to +20 mV was applied every 6 s for 10 steps. Each depolarizing step elicited a time-dependent I_{Ca}. On returning to V_h, a series of transient inward currents (I_{ti}, see Kass *et al.*, 1978) were observed. After eliciting the I_{ti} for 10–15 min, DeHE (0.1– 1 μM) was added to the superfusate and changes in amplitudes of the first I_{ti} on repolarization were measured from the first to the tenth step.

The dehydroevodiamine chloride (DeHE) was synthesized chemically following the methods described in the literature (Shapiro & Abramvitch, 1955; Abramovitch & Shapiro, 1956; Pachter & Suld, 1960; Pachter *et al.*, 1960). Other chemicals were obtained from Sigma Chemicals (U.S.A.).

Values are expressed as mean ± s.e.mean. Student's *t* test was used to compare test and control values. The values obtained before, during, and after DeHE exposure were evaluated by one way analysis of variance (ANOVA). *P* values less than 0.05 were regarded as being statistically significant.

Results

Effects on action potential duration

DeHE prolonged the action potential duration (APD) in both atrial and ventricular myocytes as illustrated in Figure 1. At a constant driving frequency of 1 Hz, 0.1 and 0.3 μM DeHE increased APD at 50% repolarization (APD_{50}) of an atrial myocyte by 22 and 41%, respectively (Figure 1a and b). In ventricular myocytes (Figure 1c and d), the percentage increases in APD_{50} induced by DeHE were relatively smaller (22 and 26% by 0.3 and 1 μM DeHE, respectively). The APD returned to control value within 10 min of washout. Results obtained from 7 atrial and 12 ventricular myocytes are summarized in Table 1.

Effects on time-dependent outward K current

To investigate the role of delayed rectifier (I_k) in the DeHE-induced prolongation of action potential, depressant effects of DeHE on I_k were determined. Figure 2b shows an example in an atrial myocyte. DeHE (0.1 μM) reduced the outward current tail, measured at −30 mV after varying duration (0.3–1.8 s) depolarizing pulses, by about 50% in 8 min (right upper section of Figure 2b). Increasing the concentration of DeHE to 0.3 μM reduced further the I_k tail to about 25% of the control value (left lower section of Figure 2b). I_k returned to 60% of the control value after washout in DeHE-free perfusate for 20 min (right lower Figure 2b). In ventricular myocyte (Figure 2c, right upper and left lower panels), 0.1 and 1 μM DeHE reduced the I_k tail to a similar extent (50% and 20%, respectively, of the control value) as that observed in atrial myocyte. However, the I_k tail returned to near control value after 20 min washout (right lower Figure 2c). Figure 2d and e summarize the results of 9 experiments in atrial myocytes and 13 experiments in ventricular myocytes, respectively.

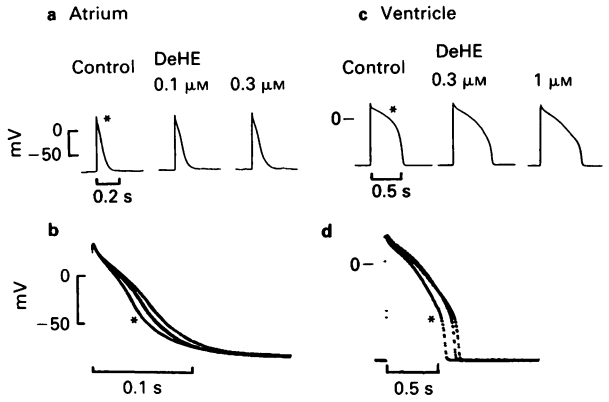

Figure 1 Prolongation of action potential duration induced by dehydroevodiamine (DeHE) in guinea-pig atrial (a and b) and ventricular myocytes (c and d). Upper panels (a and c) show the chart recordings of action potential before (Control, asterisk) and during 10th min superfusion with DeHE (0.1 and 0.3 μM in a, 0.3 and 1 μM in c). The oscillascope traces of action potential before (asterisk) and during DeHE exposure were superimposed in (b) and (d). Duration of each drug exposure was 10 min. The myocytes were paced through a recording micropipette by use of 2 ms duration depolarizing stimulus at 1 Hz in left panels and at 0.3 Hz in right panels.

Table 1 Prolongation of action potential duration (APD) induced by dehydroevodiamine (DeHE) in guinea-pig cardiomyocytes

	Atrium (change in %)			*Ventricle* (change in %)		
Condition	n	APD_{50}	APD_{90}	n	APD_{50}	APD_{90}
DeHE 0.1 μM	5	13 ± 4	31 ± 11*	7	9 ± 3	9 ± 3
DeHE 0.3 μM	4	23 ± 6*	40 ± 8*	6	14 ± 3*	12 ± 3*
Wash	4	5 ± 5	13 ± 6	3	4 ± 4	14 ± 14
DeHE 1 μM	6	28 ± 5*	54 ± 11*	9	20 ± 6*	24 ± 10*
Wash	5	21 ± 10*	35 ± 18*	7	14 ± 12	11 ± 11

The atrial and ventricular cells were superfused in normal HEPES-Tyrode solution. APD_{50} and APD_{90}, action potential duration measured at 50% and 90% repolarization, respectively. Values are means ± s.e. of the percentage changes in APD as compared with the control values before drug exposure. *$P < 0.05$, significantly different from control by one way ANOVA. The control absolute values of APD_{50} and APD_{90} before drug exposure were 100 ± 10 and 169 ± 27 ms, respectively, for 7 atrial myocytes. Those values for 12 ventricular myocytes were 475 ± 44 and 547 ± 51 ms, respectively.

Effects on inwardly rectifying K current

To study whether DeHE also blocked the inward rectifier I_{k1}, the effects of DeHE on steady state K current seen at potentials negative to −60 mV were analyzed. A series of hyperpolarizing voltage clamp pulses in 10 mV steps were applied from a V_h of −50 mV. Results showed that 0.1–1 μM DeHE reduced I_{k1} in three myocytes, but increased it slightly in another three cells and did not change it in the remaining two cells. Thus DeHE may serve as a tool for the pharmacological separation of the delayed rectifier and the inward rectifier.

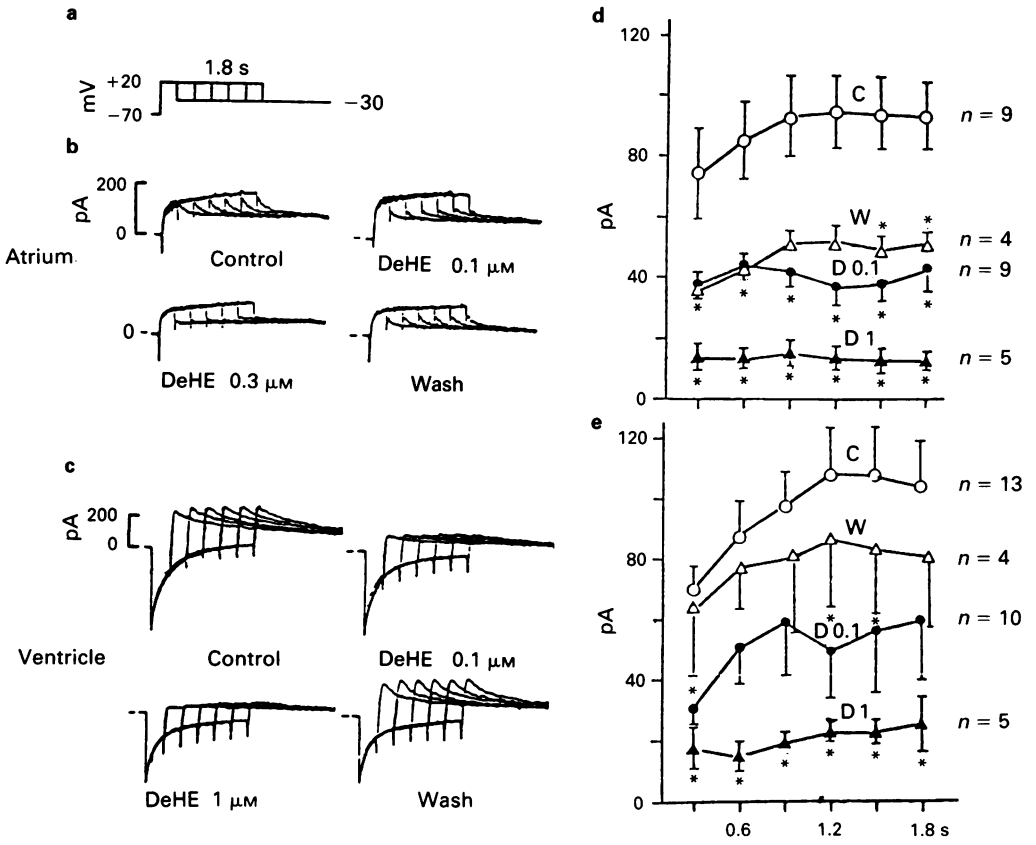

Figure 2 Depressant effect of dehydroevodiamine (DeHE) on delayed rectified (I_k) in guinea-pig atrial (b and d) and ventricular myocytes (c and e). The membrane was held at −70 mV and was conditioned to +20 mV for various durations (0.3, 0.6, 0.9, 1.2, 1.5 and 1.8 s) and then repolarized to −30 mV as indicated in (a). Upper (b) panels show the current traces of a single atrial myocyte before (control) and during 8th min of DeHE (0.1 μM) superfusion. Lower (b) panels show the current traces during 0.3 μM DeHE exposure and after washout of DeHE for 20 min (Wash). Note changes in the amplitude of tail of I_k on repolarization after each conditioning step. In (c) traces obtained from a single ventricular myocyte before (Control) and during 5th min of DeHE (0.1 μM) superfusion are shown in upper panels. The lower panels show traces during 1 μM DeHE exposure and after washout in DeHE-free superfusate for 20 min (Wash). Panels (d) and (e) summarize the time-dependent depressant effect of DeHe on I_k in atrial and ventricular myocytes, respectively. *n* indicates number of cells. $^*P<0.05$, significantly different from control value (C) before drug exposure by one way ANOVA. D 0.1 and D 1, exposure to 0.1 and 1 μM DeHE, respectively, for 10 min. W, washout in DeHE-free superfusate for 20–30 min.

Effects on inward Ca current

The prolongation of APD_{50} induced by DeHE could also be due to an enhanced Ca influx, in addition to an inhibited outward K current. Therefore, the effect of DeHE on the L-type Ca current ($I_{Ca,L}$) was also determined in K- and Na-free Tris solution in the presence of CsCl. As shown in Figure 3, I_{Ca} were elicited in the ventricular myocyte by a series of depolarizations from a holding potential of −50 mV. The peak I_{Ca} was elicited by a clamp step to 0 mV and its amplitude was reduced by 13% and 24% after exposure to 1 and 3 μM DeHE, respectively, for 10 min. The depressant effect of DeHE on I_{Ca} was not reversible after 20 min washout. Lower concentrations of DeHE did not induce a consistent effect on I_{Ca}. Table 2 summarizes results obtained from 18 experiments with 0.1–1 μM DeHE.

Effect on Na-dependent inward current

Separation of the inward Na current (I_{Na}) and T-type Ca current ($I_{Ca,T}$) was obtained by the different current method of Tytgat *et al.* (1990b) in the presence and absence of 2 or 12 mM $[Na]_o$. As shown in Figure 4a (column 1), step depolarizations were applied from a holding potential of −90 or −50 mV and the different current obtained in the absence of Na_o (Figure 4b, column 1) is assumed to be $I_{Ca,T}$. The difference current in the presence of Na_o contains a Na

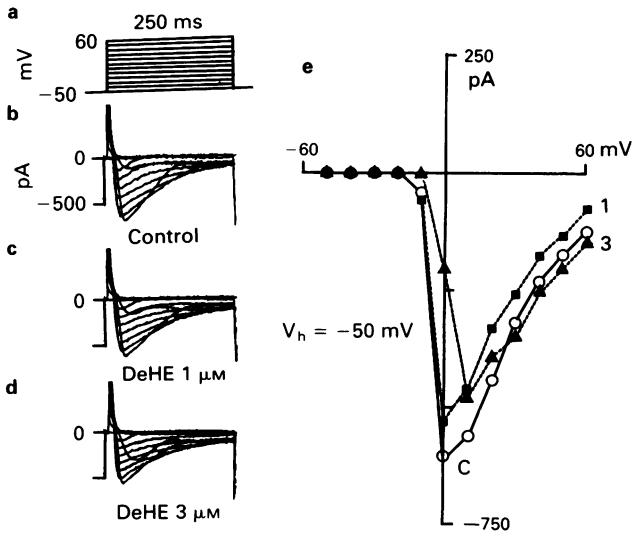

Figure 3 Ca currents recorded from a single ventricular cell in the absence (Control, b) and presence of 1 and 3 μM dehydroevodiamine (DeHE) (c and d, respectively). Currents were recorded in K- and Na-free external and internal solutions. Holding potential (V_h) was −50 mV and voltage step potentials were from −40 to +60 mV in 10 mV steps as indicated in (a). In (c) is shown the current-voltage relationship of peak inward Ca currents before (C, ○), during 1 μM (■) and 3 μM DeHE (▲) exposure for 10 min.

Table 2 Inhibition of L-type Ca current ($I_{Ca,L}$) induced by dehydroevodiamine (DeHE)

Condition	n	$I_{Ca,L}$ (change in %)
DeHE 0.1 μM	9	−8 ± 4
DeHE 0.3 μM	6	−18 ± 5
DeHE 1 μM	18	−19 ± 4*
Wash 10 min	13	−27 ± 7*
Wash 30 min	13	−32 ± 7*

The guinea-pig ventricular myocytes were superfused in Tris solution. All experiments were started after 15 min period of internal perfusion. Values are means ± s.e. of the percentage reduction of $I_{Ca,L}$ as compared with the control values before drug exposure. *$P<0.05$, significantly different from control by one way ANOVA. In the absence of DeHE, the decline of $I_{Ca,L}$ with time (run-down) was about 10% for 30–60 min.

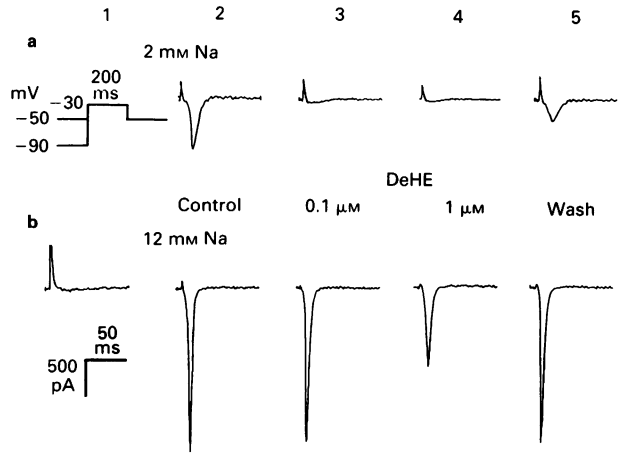

Figure 4 Depressant effect of dehydroevodiamine (DeHE) on Na-dependent inward current. Column 1 in (a) illustrates the experimental protocol for separation of T-type and L-type Ca current in Na-free, tris (hydroxymethyl)-aminomethane. Step depolarizations from a holding potential of either −90 or −50 mV to −30 mV were applied. The difference current in Na-free Tris (T-type Ca current) is displayed in column 1 (b). The difference current (fast inward Na current) in 2 mM Na Tris (a panels) or 12 mM Na Tris (b panels) before (Control, column 2), during 0.1 μM (column 3) and 1 μM DeHE exposure (column 4), and after washout (column 5) for 20 min (a) or 4 min (b) are illustrated. Traces in (a) and (b) were obtained from two different myocytes.

current in addition to $I_{Ca,T}$. Subtracting the difference current in the absence of Na from that in the presence of Na gives the Na-dependent component of the current (Figure 4, column 2). In the presence of 2 mM $[Na]_o$ (Figure 4a), 0.1 and 0.3 μM DeHE induced a strong depressant effect on I_{Na} to 10% and 8%, respectively, of control value. Also the I_{Na} remained depressed (36% of control value) after 20 min washout in DeHE-free superfusate. In the presence of 12 mM $[Na]_o$ (Figure 4b), however, 0.1 μM DeHE reduced only slightly the I_{Na} and 1 μM DeHE reduced it to 48% of the control value. The I_{Na} recovered to 90% of control value after 4 min washout. Table 3 summarizes results obtained from 5 experiments with 2 mM $[Na]_o$ and another 5 experiments with 12 mM $[Na]_o$.

Effects on afterpotentials

Since DeHE reduces both the I_{Na} and the I_{Ca}, it should be able to depress the delayed afterdepolarization (DAD) and the triggered activity (Cranefield, 1977; Kass *et al.*, 1978)

Table 3 Percentage inhibition of dehydroevodiamine (DeHE) on Na-dependent current (I_{Na})

Condition	*2 mM $[Na]_o$* I_{Na} (Δ%)	*12 mM $[Na]_o$* I_{Na} (Δ%)
DeHE 0.1 μM	−41 ± 12*	−10 ± 3
DeHE 0.3 μM	−54 ± 11*	−32 ± 8*
DeHE 1 μM	−68 ± 12*	−48 ± 16*
Wash	−41 ± 7*	−28 ± 10*

The guinea-pig ventricular myocytes were superfused in 2 or 12 mM $[Na]_o$ Tris solution. Values are means ± s.e. of the percentage inhibition of I_{Na} as compared with the control values before drug exposure. Number of preparations = 5. *$P<0.05$, significantly different from control by one way ANOVA.

developed in myocytes overloaded with calcium ion. Figure 5 illustrated the generation of DADs in a ventricular myocyte paced by a train of depolarizing stimuli at 0.67 Hz (left panels) or 1.25 Hz (right panels) in a low-K and high-Ca superfusate containing 2 μM strophanthidin. At a pacing frequency of 0.67 Hz, 0.1 μM DeHE suppressed completely the DADs within 10 min (Figure 5b, left panel), while APD was reduced presumably due to opening of a Na-activated K channel in the presence of Na pump blockade (Luk & Carmeliet, 1990) induced by strophanthidin. These effects remained after 22 min washout in DeHE-free superfusate. At the higher pacing frequency (1.25 Hz), the DADs were larger in amplitude and shorter in cycle length. The depressant effect of DeHE was weaker even at a concentration of 0.3 μM.

In 6 myocytes, the average resting potential was −111 ± 2 mV before pacing. At ending of pacing (0.67–1.25 Hz) for 10–30 beats, the MDP and the amplitude of DAD were −107 ± 2 mV and 13 ± 4 mV, respectively. DeHE (0.1 μM) barely changed the MDP (−106 ± 2 mV) but reduced the amplitude of DAD to 5 ± 1 mV. In another myocyte (Figure 6), two triggered action potentials were generated after termination of electrical drive (Figure 6a). Exposure to 0.1 μM DeHE reduced the number of triggered action potentials by half (Figure 6b). After washout in DeHE-free superfusate, the number of triggered action potentials increased to four as

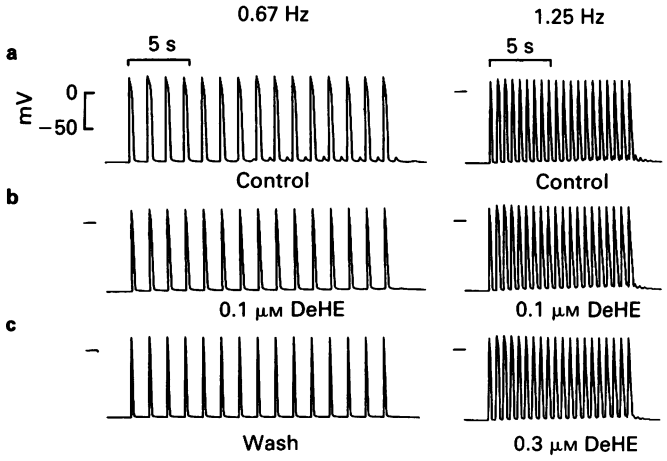

Figure 5 Depressant effect of dehydroevodiamine (DeHE) on delayed afterdepolarizations induced by a train of electrical stimulations with different pacing frequency (0.67 Hz in left panels and 1.25 Hz in right panels). The myocytes were superfused in low-K (1 mM) and high-Ca (9 mM) solution plus 2 μM strophanthidin. Traces of action potential in (a) and (b) were recorded before (Control) and during superfusion with 0.1 μM DeHE for 10 min, respectively. The left panel (c) was recorded after washout in DeHE-free superfusate for 22 min and the right panel (c) during 0.3 μM DeHE superfusion.

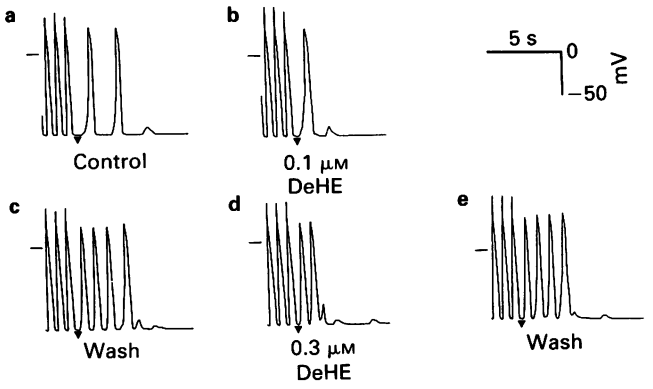

Figure 6 Depressant effect of dehydroevodiamine (DeHE) on triggered action potentials induced by superfusing the ventricular myocyte in low-K and high-Ca solution plus 2 μM strophanthidin. In each panel, a train of 30 depolarizing stimuli was applied but only the last 3 driven action potentials are illustrated. Electrical stimulation was terminated at (▼). Panels (a) and (b) show the traces before (Control) and during superfusion with 0.1 μM DeHE for 10 min. After washout in DeHE-free superfusate (c), the myocyte was exposed to 0.3 μM DeHE for 10 min (d). Panel (e) shows that, after washout of 0.3 μM DeHE for 5 min, the driven action potentials were followed by 4 triggered action potentials and 2 delayed afterdepolarizations.

the effects of strophanthidin progressed (Figure 6c). Exposure to 0.3 μM DeHE depressed the triggered activity again (Figure 6d).

In contrast to the depressant effect on DAD and triggered activity, DeHE should be able to potentiate the development of early afterdepolarization (EAD) through its inhibitory action on outward K current as quinidine did (Roden & Hoffman, 1985). Figure 7 shows a ventricular myocyte paced by a train of depolarizing stimuli at 2 Hz in the low-K and high-Ca superfusate. The repolarization process was inhibited and action potential duration was increased in the presence of 0.1 μM DeHE (Figure 7b). When the concentration of DeHE was increased to 0.3 μM, the myocyte failed to repolarize completely and, after termination of electrical drive, a series of slow response action potentials (EADs) were induced at a depolarized level (near −60 mV) (Figure 7c). The

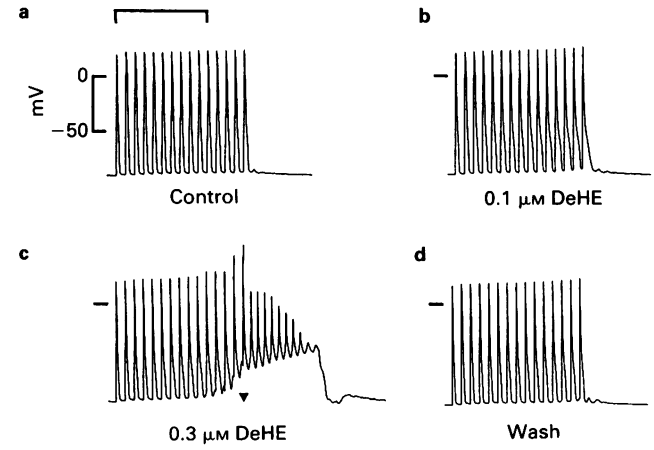

Figure 7 Inhibition of repolarization process and induction of early afterdepolarizations in ventricular myocyte superfused in low-K and high-Ca solution plus 2 μM strophanthidin. The myocyte was paced with a train of 15 depolarizing stimuli at 2 Hz. Panel (a) was recorded before (Control) and (b) during the 10th min of superfusion with to 0.1 μM dehydroevodiamine (DeHE). Panel (c) shows that, during the 6th min of superfusion with 0.3 μM DeHE, a series of slow responses and EADs were induced at a depolarized level after termination of electrical drive (at ▼). Panel (d) was recorded after washout in DeHE-free solution for 15 min.

effect was reversible after 15 min washout (Figure 7d). It is important to note that the same myocyte had been paced at 1 Hz and generated DADs of about 8 mV in amplitude. DeHE (0.1 μM) suppressed the DAD but did not reduce the MDP or induce EAD (traces not shown).

In 4 myocytes, the resting potential before pacing was −110 ± 2 mV and the MDP at end of pacing (1–2 Hz) for 20–30 beats was −106 ± 2 mV. In the presence of 0.1–1 μM DeHE, the resting potential before pacing was about the same (−112 ± 2 mV) but during pacing the MDP was reduced gradually to a level of −79 ± 4 mV at end of the 11–30th beat and was followed by EADs which lasted for 9 ± 4 s.

Effect on transient inward current

It has been demonstrated that generation of transient inward currents (I_{ti}) is responsible for the development of DAD and the subsequent triggered action potentials (Kass *et al.*, 1978). Thus effects of DeHE on I_{ti} were investigated in ventricular myocytes superfused with low-K and high-Ca solution containing 2 μM strophanthidin. As shown in Figure 8a, a 1200 ms depolarizing pulse from a V_h of −44 mV to +20 mV was applied every 6 s for 10 steps. Each depolarizing step induced a slow inward Ca current (I_{si}) and on repolarization to V_h a series of I_{ti}. Only traces obtained from the first and tenth step (arrow) were superimposed in Figure 8b. Figure 8c shows the time-dependent reduction in I_{ti} induced by 0.1 μM DeHE in all ten steps. It is evident that 0.1 μM DeHE reduced significantly the amplitude of I_{ti} after 2 min of DeHE exposure and more so after a longer period of exposure. On the other hand, I_{si} was only slightly inhibited after 10 min exposure. The inhibition on both currents was not reversible even after washout in DeHE-free superfusate for 30 min. The time course of changes in I_{si} and I_{ti} induced by 0.1 μM DeHE in this preparation are illustrated in Figure 8d. Table 4 summarizes results obtained from 8 experiments.

Discussion and conclusions

The present findings in guinea-pig myocytes provide evidence for the depressant actions of DeHE on the Na-dependent inward current (I_{Na}) and the transient inward current (I_{ti}) generated under conditions of Ca overloading induced by a cardiotonic steroid in low-K and high-Ca superfusate. The changes in ionic currents are correlated with depression of arrhythmogenic delayed afterdepolarization (DAD) and triggered action potential. Thus in addition to the hypotensive effect reported in the literature (Yang *et al.*, 1988; 1990), DeHE may exert an antiarrhythmic action on triggered activity.

It has been well documented that DADs, aftercontractions and triggered action potentials (Cranefield, 1977) could be induced by cardiotonic agents such as digitalis (Vassalle, 1986), catecholamines and methylxanthines (Lin *et al.*, 1985; Hou *et al.*, 1989; Satoh & Vassalle, 1989), especially in the presence of high-Ca and/or low-K (Lin & Vassalle, 1980). These electromechanical activities were indications of intracellular Ca overload and could be depressed by either Ca or Na channel blockers. The I_{ti} (or I_{os}) is the underlying ionic mechanism responsible for the DAD and the subsequent triggered action potentials (Kass *et al.*, 1978; Lin *et al.*, 1986). The fact that 0.1–0.3 μM DeHE induced significant inhibitory actions on I_{ti} but not on I_{Ca} suggests that DeHE has a selective effect on transport of Na across sarcolemma. This concept is supported by our findings that 0.1–0.3 μM DeHE reduced markedly the I_{Na} measured by using the difference current method (Tytgat *et al.*, 1990b) in the absence and presence of 2 mM or 12 mM $[Na]_o$. Also the depressant effect of DeHE was greater and lasted longer in the presence of 2 mM $[Na]_o$ than in 12 mM $[Na]_o$ (Figure 6 and Table 3), in agreement with the antagonistic action of DeHE on Na transport. A decrease in Na influx should

result in a decrease in intracellular Na ion activity (Vassalle & Lee, 1984). The fall in intracellular Na would in turn decrease cellular Ca through the Na-Ca exchange mechanism (Mullins, 1979; Kimura *et al.*, 1987; Beuckelmann *et al.*, 1989) and, as a consequence, suppress the I_{ti} and DAD induced by the cardiotonic steroid (Kass *et al.*, 1978). How-

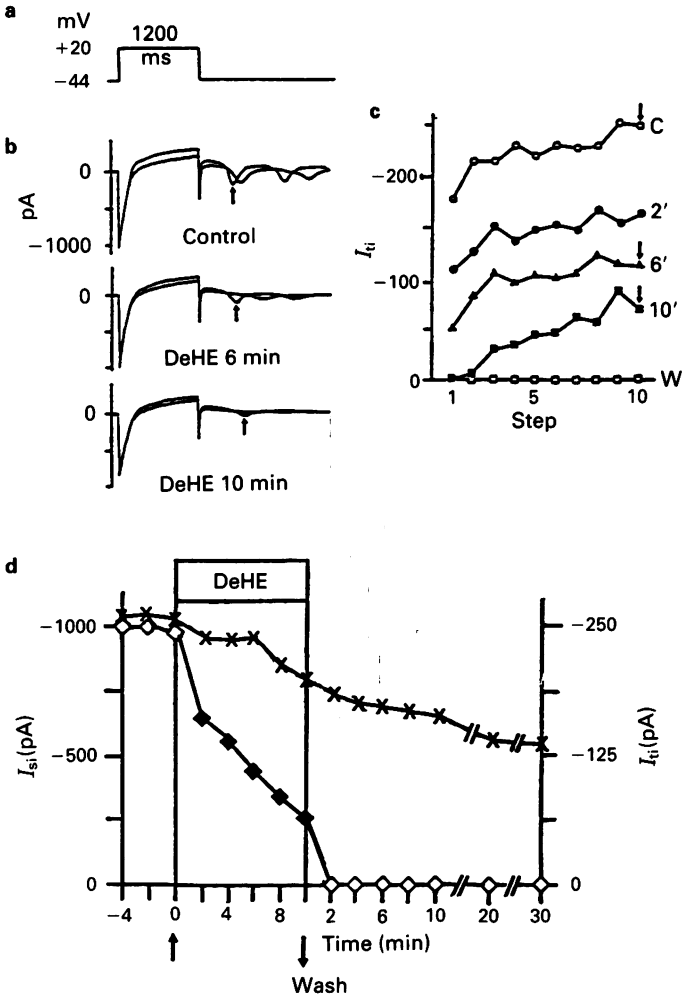

Figure 8 Depressant effect of dehydroevodiamine (DeHE, 0.1 μM) on transient inward current (I_{ti}) of a single ventricular myocyte induced by 2 μM strophanthidin in low-K and high-Ca superfusate. Panel (a) shows the experimental protocol. The holding potential was −44 mV. A 1200 ms depolarizing pulse to +20 mV was applied every 6 s for 10 steps. In (b), I_{ti} induced by the first and the tenth step (arrow) were superimposed before (Control) and during exposure to DeHE for 6 min (middle panel b) and 10 min (lower panel b). Panel (c) shows the amplitudes of the first I_{ti} on repolarization from first to the tenth steps. Curve C (open (○) circles) indicates the values before DeHE exposure; (●) (2'), (▲) (6') and (■) (10') indicate time-dependent reduction in I_{ti} during DeHE superfusion. W indicates that the value of I_{ti} decreased to baseline after washout of DeHE for 2 min. Panel (d) shows time course of changes induced by 0.1 μM DeHE in slow inward Ca current (I_{si}) on depolarization and transient inward current (I_{ti}) on repolarization. Left ordinate scale gives amplitudes of I_{si} (X) and right ordinate values of I_{ti} (◆) in pA. DeHE was added between the two vertical lines. Abscissa scale gives time in min. Upward arrow (time 0) indicates beginning of DeHE exposure while downward arrow shows washout of DeHE.

Table 4 Percentage inhibition of slow inward Ca current (I_{si}) and transient inward current (I_{ti}) induced by dehydroevodiamine (DeHE)

		Step 1		*Step 5*		*Step 10*	
Condition	n	I_{si} (Δ%)	I_{ti} (Δ%)	I_{si} (Δ%)	I_{ti} (Δ%)	I_{si} (Δ%)	I_{ti} (Δ%)
DeHE							
2 min	8	−6 ± 2	−29 ± 13*	−12 ± 7	−24 ± 5*	−7 ± 1	−33 ± 7*
5 min	8	−14 ± 5	−56 ± 10*	−10 ± 4	−57 ± 7*	−12 ± 3*	−55 ± 8*
10 min	8	−27 ± 9*	−78 ± 10*	−15 ± 5*	−77 ± 7*	−17 ± 4*	−78 ± 7*
Wash							
10 min	6	−37 ± 11*	−86 ± 13*	−25 ± 8*	−86 ± 6*	−24 ± 8*	−71 ± 10*
20 min	4	−34 ± 9*	−100 ± 0*	−33 ± 11*	−100 ± 0*	−39 ± 9*	−87 ± 11*
30 min	4	−41 ± 8*	−100 ± 0*	−41 ± 10*	−100 ± 0*	−41 ± 8*	−100 ± 0*

The ventricular myocytes were superfused in high-Ca and low-K solution containing 2 μM strophanthidin. Values are means ± s.e. of the percentage reduction in I_{si} or I_{ti} as compared with control values before DeHE (0.1 μM) exposure. *$P<0.05$, significantly different from control by one way ANOVA.

ever, as indicated by the findings of our previous experiments on rabbit sinoatrial tissues and high-K depolarized guinea-pig ventricular tissues (Lin *et al.*, 1990), the inhibitory action on transmembrane Ca current is also important for the depressant effect of DeHE. In human multicellular atrial preparations, DeHE (0.1–0.3 μM) also depressed the Ca-dependent automatic rhythm and the slow response action potential generated at a depolarized level (MDP near −40 mV). Thus a reduction of Ca influx may be involved in the depression of DAD and aftercontraction induced by 2.5 μM adrenaline in human atrial tissues (unpublished observations). Further experiments using human atrial myocytes are required to clarify this point.

In multicellular guinea-pig and rabbit ventricular muscle fibres (Lin *et al.*, 1990), DeHE at low concentrations (0.1–0.3 μM) has been shown to increase the APD. The prolongation of APD could be due to either an enhanced Ca influx or an inhibited K conductance. The marked depressant effect of I_k and the lack of enhancement of I_{Ca} observed in the present experiments suggest that the depressed K conductance was responsible for the increase in APD. An increase in APD and refractory period could exert a protective effect against cardiac tachyarrhythmias as class III antiarrhythmic drugs did (Singh & Nademanee, 1985). On the other hand, DeHE at concentrations of 1 μM and above consistently induced arrhythmogenic EAD in rabbit ventricular tissues as reported in our previous study (Lin *et al.*, 1990). In the guinea-pig myocytes, 0.1–1 μM DeHE also could induce EAD in the presence of low-K. This effect was correlated to an inhibition of I_k and similar to that induced by quinidine in canine Purkinje fibres (Roden & Hoffman, 1985).

In conclusion, DeHE at low concentrations (0.1–0.3 μM) inhibited markedly the I_{Na} and depressed the arrhythmogenic DADs and I_{ti} induced by cardiotonic steroid in low-K and high-Ca superfusate. DeHE also may exert class III antiarrhythmic effect through a reduction of the time-dependent outward K current (Figure 2) and the subsequent prolongation of APD (Figure 1) and effective refractory period.

The authors wish to thank Mr T.H. Cheng and Miss S.F. Huang for technical assistance. The present work was supported in part by grants from National Research Institute of Chinese Medicine and National Science Council (NSC80-0412-B016-90), Taipei.

References

ABRAMOVITCH, R.A. & SHAPIRO, D. (1956). Tryptamines, carbolines, and related compounds. Part II. A convenient synthesis of tryptamines and beta-carbolines. *J. Chem. Soc.*, 4589–4592.

BEUCKELMANN, D.J. & WIER, W.G. (1989). Sodium-calcium exchange in guinea-pig cardiac cells: exchange current and changes in intracellular Ca^{2+}. *J. Physiol.*, **414**, 499–520.

BELLES, B., MALECOT, C.O., HESCHELER, J. & TRAUTWEIN, W. (1988). "Run-down" of the Ca current during long whole-cell recordings in guinea pig heart cells: role of phsophorylation and intracellular calcium. *Pflügers Arch.*, **411**, 353–360.

CHEN, C.F., CHEN, S.M., LIN, M.T. & CHOW, S.Y. (1981). In vivo and in vitro studies on the mechanism of cardiovascular effect of Wu-Chu-Yu (Evodiae Fructus). *Am. J. Chin. Med.*, **9**, 39–47.

CRANEFIELD, P.F. (1977). Action potentials, afterpotentials, and arrhythmias. *Circ. Res.*, **41**, 415–423.

ENOUS, R., COETZEE, W.A. & OPIE, L.H. (1990). Effect of angiotensin II on the transient inward current in single isolated guinea-pig ventricular myocytes. In *Ionic Currents and Ischaemia.* ed. Vereecke, J. van Bogaert, P.P. & Verdonck, F. pp. 243–245. Leuven: Leuven University Press.

HOU, Z.Y., LIN, C.I., VASSALLE, M., CHIANG, B.N. & CHENG, K.K. (1989). Role of acetylcholine in induction of repetitive activity in human atrial fibers. *Am. J. Physiol.*, **256**, H74–H84.

KASS, R.S., LEDERER, W.J., TSIEN, R.W. & WEINGART, R. (1978). Role of calcium ions in transient inward currents and aftercontractions induced by strophanthidin in cardiac Purkinje fibres. *J. Physiol.*, **281**, 187–208.

KIMURA, J., MIYAMAE, S. & NOMA, A. (1987). Identification of sodium-calcium exchange current in single ventricular cells of guinea pig. *J. Physiol.*, **384**, 199–222.

LIN, C.I., CHIU, T.H., CHIANG, B.N. & CHENG, K.K. (1985). Electromechanical effects of caffeine in isolated human atrial fibres. *Cardiovasc. Res.*, **19**, 727–733.

LIN, C.I., KOTAKE, H. & VASSALLE, M. (1986). On the mechanism underlying the oscillatory current in cardiac Purkinje fibers. *J. Cardiovasc. Pharmacol.*, **8**, 906–914.

LIN, C.I., LOH, S.H., LUK, H.N., LUE, W.M. & CHEN, C.F. (1990). Electropharmacological effects of dehydroevodiamine on mammalian hearts. *J. Chin. Med.*, **1**, 84–93.

LIN, C.I. & VASSALLE, M. (1980). The antiarrhythmic effect of potassium and rubidium in strophanthidin toxicity. *Eur. J. Pharmacol.*, **62**, 1–15.

LUK, H.N. & CARMELIET, E. (1990). Na^+-activated K^+ current in cardiac cells: rectification, open probability, block and role in digitalis toxicity. *Pflügers Arch.*, **416**, 766–768.

MITRA, R. & MORAD, M. (1985). A uniform enzymatic method for dissociation of myocytes from hearts and stomachs of vertebrates. *Am. J. Physiol.*, **249**, H1056–H1060.

MULLINS, L.J. (1979). The generation of electric currents in cardiac fibers by Na/Ca exchange. *Am. J. Physiol.*, **236**, C103–C110.

PACHTER, I.J., RAFFAUF, R.F., ULLYOT, G.E. & RIBEIRO, O. (1960). The alkaloids of *Hortia arborea* Engl. *J. Am. Chem. Soc.*, **82**, 5187–5193.

PACHTER, I.J. & SULD, G. (1960). The structure and synthesis of rhetsinine (hydroxyevodiamine). *J. Org. Chem.*, **25**, 1680–1682.

RODEN, D.M., BENNETT, P.B., SNYDERS, D.J., BALSER, J.R. & HONDEGHEM, L.H. (1989). Quinidine delays I_k activation in guinea pig ventricular myocytes. *Circ. Res.*, **62**, 1055–1058.

RODEN, D.M. & HOFFMAN, B.F. (1985). Action potential prolongation and induction of abnormal automaticity by low quinidine concentrations in canine Purkinje fibers: relationship to potassium and cycle length. *Circ. Res.*, **56**, 857–867.

SATOH, H. & VASSALLE, M. (1989). Role of calcium in caffeine-norepinephrine interactions in cardiac Purkinje fibers. *Am. J. Physiol.*, **257**, H226–H237.

SHAPIRO, D. & ABRAMOVITCH, R.A. (1955). Application of the Japp-Klingemann reaction. A new synthesis of ornithine. *J. Am. Chem. Soc.*, **77**, 6690–6691.

SINGH, B.N. & NADEMANEE, K. (1985). Control of cardiac arrhythmias by selective lengthening of repolarization: theoretic considerations and clinical observations. *Am. Heart J.*, **109**, 421–430.

TYTGAT, J., VEREECKE, J. & CARMELIET, E. (1990a). Mechanism of cardiac T-type Ca channel blockade by amiloride. *J. Pharmacol. Exp. Ther.*, **254**, 546–551.

TYTGAT, J., VEREECKE, J. & CARMELIET, E. (1990b). A combined study of sodium current and T-type calcium current in isolated cardiac cells. *Pflügers Arch.*, **417**, 142–148.

VASSALLE, M. (1986). Cardiac glycosides: regulation of force and rhythm. In *Cardiac Muscle: The Regulation of Excitation and Contraction.* ed. Nathan, R.D. pp. 237–267. New York: Academic Press.

VASSALLE, M. & LEE, C.O. (1984). The relationship among intracellular sodium activity, calcium and strophanthidin inotrophy in canine cardiac Purkinje fibers. *J. Gen. Physiol.*, **83**, 297–307.

YANG, H.Y., LI, S.Y. & CHEN, C.F. (1988). Hypotensive effects of dehydroevodiamine, a quinazolinocarboline alkaloid isolated from Evodiae rutaecarpa. *Asia Pacific J. Pharmacol.*, **3**, 191–196.

YANG, M.C.M., WU, S.L., KUO, J.S. & CHEN, C.F. (1990). The hypotensive and negative chronotropic effects of dehydroevodiamine. *Eur. J. Pharmacol.*, **182**, 537–542.

(Received July 12, 1991
Revised December 19, 1991
Accepted February 17, 1992)

Br. J. Pharmacol. (1992), **106**, 524–532

Pharmacological characteristics of 5-hydroxytryptamine autoreceptors in rat brain slices incorporating the dorsal raphe or the suprachiasmatic nucleus

[1]J.J. O'Connor & [2]Z.L. Kruk

Department of Pharmacology, Queen Mary & Westfield College, Mile End Road, London E1 4NS

1 Changes in extracellular concentrations of 5-hydroxytryptamine elicited by electrical stimulation in rat brain slices containing the dorsal raphe nucleus and the suprachiasmatic nucleus were monitored with fast cyclic voltammetry.

2 Using pseudo single pulse stimulation (5 pulses applied at 100 Hz) we have shown that the release of 5-hydroxytryptamine in the dorsal raphe and the suprachiasmatic nucleus can be regulated by autoreceptors in both brain regions.

3 In the suprachiasmatic nucleus, 5-carboxamidotryptamine, RU24969, 1-(*m*-trifluoromethylphenyl) piperazine and sumatriptan caused a concentration-dependent inhibition of stimulated 5-hydroxytryptamine overflow in the range 1×10^{-9} M to 3×10^{-6} M. The actions of 5-carboxamidotryptamine and RU24969 were reversed competitively by methiothepin (10^{-8} M to 10^{-6} M); Schild plots revealed pK_B values of 7.9 and 8.1. By contrast, ipsaparone and 8-hydroxy-2(di-n-propylamino)tetralin (8-OH-DPAT) are not effective 5-hydroxytryptamine autoreceptor agonists in the suprachiasmatic nucleus.

4 Isamoltane (10^{-6} M), the putative 5-HT_{1B} receptor antagonist, blocked the responses to RU24969 (10^{-6} M) and 1-(*m*-trifluoromethylphenyl)piperazine (10^{-6} M) in the suprachiasmatic nucleus.

5 In the dorsal raphe nucleus, 8-OH-DPAT, ipsapirone, RU24969, 5-carboxamidotryptamine, and sumatriptan (all 1×10^{-8} M to 3×10^{-6} M) produced a concentration-dependent reduction in the stimulated release of 5-hydroxytryptamine. The maximum effect observed was less than that seen in the suprachiasmatic nucleus.

6 Methiothepin (1×10^{-7} M) blocked the effect of 5-carboxyamidotryptamine (10^{-8} M to 10^{-6} M) in the dorsal raphe nucleus while propranolol (10^{-6} M) and NAN-190 (10^{-6} M) but not isamoltane (10^{-6} M) were found to block significantly the effect of ipsapirone (10^{-6} M).

7 We conclude, that drugs with 5-HT_{1A} binding activity act as agonists in the dorsal raphe nucleus while drugs showing some activity for 5-HT_{1B} and 5-HT_{1D} binding sites, act as agonists in the suprachiasmatic nucleus. Our results confirm predictions from binding studies, that functional 5-HT autoreceptors regulating release of endogenous 5-HT have different drug specificity in the dorsal raphe and suprachiasmatic nucleus.

Keywords: 5-HT autoreceptors; 5-HT_{1A} agonists; 5-HT_{1B} agonists; methiothepin; dorsal raphe nucleus; suprachiasmatic nucleus; fast cyclic voltammetry

Introduction

Ligand binding studies *in vitro*, and autoradiographic studies in brain slices, indicate a heterogeneity of 5-hydroxytryptamine (5-HT) receptors in the rat brain (Peroutka & Synder, 1979; Bradley *et al.*, 1986; Hoyer *et al.*, 1986a,b; Peroutka, 1988a,b). Three types of 5-HT receptor (designated 5-$HT_{1,2,3}$) have been described on the basis of work with ligands, which have subsequently been shown to be either agonists or competitive antagonists of 5-HT receptors in functional studies (see Bradley *et al.*, 1986; and Peroutka, 1988a for reviews); there is speculation about the existence of 5-HT_4 receptors (Schenker *et al.*, 1987; Dumuis *et al.*, 1989).

5-HT_1 receptors were originally characterized as having selective affinity for 5-HT, and differentiated from 5-HT_2 receptors which had selective affinity for spiperone (Peroutka & Snyder, 1979). Subsequent studies divided 5-HT_1 receptors into four subtypes, based on affinity of agonists, brain distribution and species. 8-Hydroxy-2(di-n-propylamino)tetralin (8-OH-DPAT) (Middlemiss & Fozard, 1983) and ipsapirone (Dompert *et al.*, 1985) were shown to be selective agonists at 5-HT_{1A} receptors. They were found postsynaptically in cortex of all species examined (Hoyer *et al.*, 1986a), and presynaptically in the dorsal raphe nucleus of the rat (De Montigny *et al.*, 1984; Sprouse & Aghajanian, 1986) where they serve as 5-HT autoreceptors. It has been suggested (Sills *et al.*, 1984) that RU24969, and TFMPP are selective ligands for 5-HT_{1B} receptors on 5-HT axon terminals in the rat (Pazos & Palacios, 1985), and that 5-HT_{1B} receptors serve as autoreceptors at these sites (Middlemiss, 1984; Engel *et al.*, 1986). In species other than rat (including man, calf, pig and guinea-pig), it has been generally accepted that axon terminal 5-HT autoreceptors constitute a separate class designated 5-HT_{1D} (Heuring & Peroutka, 1987; Waeber *et al.*, 1988), although Herrick-Davis & Titeler (1988) and Limberger *et al.* (1991) suggest that both 5-HT_{1B} and 5-HT_{1D} receptors may coexist in the rat. Sumatriptan (GR 43175; Humphrey *et al.*, 1988) has been shown to be a selective agonist at 5-HT_{1D} receptors. 5-HT_{1C} receptors have been found in all mammalian species examined, present on the choroid plexus only (Pazos *et al.*, 1984; Hoyer *et al.*, 1989); they have not been associated with 5-HT autoreceptor function.

No selective competitive antagonists have been described for 5-HT_1 receptor subtypes (Peroutka, 1988a,b). Methiothepin can competitively block all 5-HT_1 receptor subtypes as well as 5-HT_2 receptors; propranolol has antagonistic actions at 5-HT_{1A} and 5-HT_{1B} receptor types as well as at β-adrenoceptors (Göthert, 1990). NAN-190 has antagonistic activity at

[1] Present address: Department of Pharmacology, University of Dublin, Trinity College, Dublin 2, Ireland.
[2] Author for correspondence.

5-HT_{1A} receptor subtypes (Glennon *et al.*, 1988) and isamoltane (Schoeffter & Hoyer, 1989) has weak selectivity for 5-HT_{1B} receptors.

Among the mechanisms regulating 5-HT release at both somatodendritic and axon terminal sites, are 5-HT autoreceptors (reviewed by Starke *et al.*, 1989; Kalsner & Westfall, 1990). Electrophysiological and behavioural studies *in vivo*, have shown that 5-HT_{1A} receptor agonists applied to the dorsal raphe nucleus, act on 5-HT autoreceptors which regulate firing of 5-HT neurones (De Montigny *et al.*, 1984; Dourish *et al.*, 1986; Vander Maelen *et al.*, 1986; Sprouse & Aghajanian, 1986; Haj-Dahmane *et al.*, 1991). The consequences of changes in the electrical activity of 5-HT nerve cells on release of 5-HT at axon terminals has been investigated *in vivo* by voltammetry and dialysis. When 5-HT_{1A} selective agonists were applied either systemically or into the dorsal raphe nucleus (Marsden & Martin, 1986; Sharp *et al.*, 1989) activation of 5-HT_{1A} receptors in the raphe nuclei lead to decreased 5-HT metabolism and release at axon terminals. At 5-HT axon terminals, 5-HT_{1B} agonists have been shown to decrease 5-HT release and metabolism by acting at terminal 5-HT autoreceptors (Middlemiss, 1985; Martin & Marsden, 1986; Limberger *et al.*, 1991).

The involvement of 5-HT in many neurological, psychiatric and neuroendocrine disorders means that there is a real prospect of novel therapies for a wide range of clinical disorders, if drugs acting selectively and specifically at 5-HT receptors can be developed (Meltzer, 1990). Discovery of such agents depends on qualitative and quantitative characterization of 5-HT receptors in the central nervous system. While electrophysiological studies have good anatomical precision, quantitative characterization of the receptors involved can be difficult *in vivo*, as the concentration of drugs can be difficult to measure. By contrast, in biochemical studies *in vitro* where the concentration of ligands can readily be determined, the site of action of the drug may be difficult to determine in either brain slices or broken cell preparations.

We have shown that fast cyclic voltammetry can monitor changes in the extracellular concentration of 5-HT following electrical stimulation in either the dorsal raphe nucleus (DRN) or the suprachiasmatic nucleus (SCN; O'Connor & Kruk, 1991a,b). This method is anatomically precise, as the electrodes are small (being an exposed carbon cylinder measuring 7 μm by 30 μm). Quantitative pharmacological characterization of dopamine autoreceptors is possible, when fast cyclic voltammetry is applied in suitably prepared brain slices (Bull *et al.*, 1990; Bull & Sheehan, 1991; Palij *et al.*, 1990). In order to study pulse to pulse regulation of release of 5-HT and to measure effects of agonists at 5-HT autoreceptors, it is necessary to work under conditions when the endogenously released 5-HT does not act to modulate its own release (Singer, 1988). We have shown (O'Connor & Kruk, 1991b) that single pulse electrical stimulation does not release sufficient 5-HT for it to be measurable reliably above the background. To overcome this, we have used a short burst of stimuli (pseudo single pulse stimulation; Singer, 1988; Cejna *et al.*, 1990; Limberger *et al.*, 1991) which we have shown causes 5-HT release which is unaffected by the presence of methiothepin, indicating that such short periods of stimulation do not activate 5-HT autoreceptors.

Here, we describe results of qualitative and quantitative experiments in which we have studied the effects of 5-HT_1 ligands on their ability to modify release of endogenous 5-HT in an axon terminal region (SCN) or at a somatodendritic site (DRN). A preliminary account of some of these findings has been given previously (O'Connor & Kruk, 1990; 1991c).

Methods

All experiments were carried out on rat brain slices prepared and treated as has been described in detail previously (O'Connor & Kruk, 1991a); only a brief outline is presented here.

Preparation of brain slices

Male Wistar rats (150–250 g) were killed and the brain gently and rapidly removed into ice cold oxygenated artificial cerebrospinal fluid (ACSF; composition in mM: NaCl 125, KCl 2.0, KH_2PO_4 1.25, $MgSO_4.7H_2O$ 2.0, $NaHCO_3$ 25.0, D-glucose 11.0, $CaCl_2$ 2.0) and saturated with 5% CO_2 in oxygen. Blocks of tissue, 3 mm thick containing either DRN or SCN were dissected with a razor blade, and a single slice (350 μm) containing either DRN or SCN was prepared with an Oxford vibratome. The slice was transferred to a full immersion incubation chamber (Richards & Tegg, 1977) perfused at a rate of 1.1 ml min^{-1} with artificial oxygenated ACSF maintained at 32°C, and allowed to equilibrate for 1 h.

Fast cyclic voltammetry

Following a 1 h equilibration period, a single carbon fibre microelectrode (8 μm diameter and 30–50 μm exposed tip) was located 80 μm below the surface of the brain slice in either brain region, and a bipolar stimulating tungsten microelectrode (tip separation 200 μm) was implanted at the same depth about 100–200 μm away from the carbon fibre electrode. Fast cyclic voltammetry was applied twice a second, and the oxidation peak of 5-HT (+ 600 mV) was monitored with a sample and hold device, and displayed on a chart recorder. Variations in the height of the peak at +600 mV were used to monitor changes in the extracellular concentration of 5-HT during electrical stimulation. A triphasic W shaped voltage wave form was applied, and the applied potential as well as the resulting current waveform were monitored on a digital storage oscilloscope (Nicolet 310; Figure 1a and b). Fast cyclic voltammetry was performed with a Millar voltammeter (PD Systems, West Molsley, Surrey) and voltammetric current signals were applied to a CED 1401 interface for digitalization and storage of wave forms on hard disk using CED signal averaging (Sigavg) software. Electrodes were calibrated in solutions of 5-HT before and after each experiment; concentrations in brain slices were determined by interpolation of calibration curves (see O'Connor & Kruk, 1991a).

Electrical stimulation

In the DRN or SCN single pulse (0.1 ms width, 20 V amplitude; 1P), 5 single pulses applied at 100 Hz (5P/100 Hz) or repeated stimulation was controlled by a Neurolog system incorporating a DS2 constant voltage stimulator.

Experimental procedure

All drugs were dissolved in ACSF and applied at increasing concentration in a cumulative manner. Each agonist concentration was superfused until the response achieved a plateau (less than 30 min). In the studies using methiothepin and 5-CT or RU24969, a concentration-response curve was carried out with the agonist and the slice was then washed with drug free ACSF. The slice was then equilibrated with a single concentration of methiothepin (10^{-8}, 10^{-7} or 10^{-6} M) for 1 h before a second agonist concentration-response curve was performed. Concentration-ratios were calculated at the EC_{50} level and used to construct Schild plots (Arunlakshana & Schild, 1959; Kennakin, 1984) in order to derive pK_B values. The maximum % inhibition of 5-HT overflow (E_{max}) caused by each agonist was calculated. On occasion (for example see Figure 6) a single concentration (10^{-6} M) of agonist was perfused into the slice chamber for 30 min. The slice was then equilibrated with antagonist alone for 1 h before the same concentration of agonist was perfused in the presence

of the antagonist. Maximum changes in stimulated 5-HT overflow were then calculated for the agonist in the absence and in the presence of the antagonist.

Drugs and solutions

Drugs were obtained from the following sources: 5-hydroxytryptamine (5-HT) HCl (Sigma); TFMPP (1-(*m*-trifluoromethylphenyl)piperazine; Research Biochemicals Incorporated), 8-OH-DPAT (8-hydroxy-2(di-n-propylamino)tetralin; Research Biochemicals Incorporated). The following were generous gifts from the sources indicated: methiothepin maleate (Hofmann La Roche), RU24969 (5-methyoxy-3(1,2,3,6,-tetrahydro-4-pyridinyl)-1H-indole; Russel Uclaf), ipsapirone (TVX Q 7821; Troponwerke, Koln, Germany), NAN-190 (1-(2-methoxyphenyl)-4- [4-2 (phtalimmido) butyl] -8-azaspiro (4,5) decane-7,9-dione; Dr Richard Glennon, Medical College of Virginia, Richmond, VA, U.S.A.), isamoltane (Ciba Geigy) and buspirone HCl (Bristol-Myers Company). We thank Glaxo Group Research for the following drugs: 5-carboxamidotryptamine (5-CT) and sumatriptan (GR43175; 3-(2-dimethylamino)ethyl-N-methyl-1H-5-methane sulphonamide).

Statistical analysis

Examples of raw data are shown where appropriate. Means and standard deviations were determined from pooled data and levels of statistical significance were determined by paired or unpaired Student's *t* test as appropriate. Slopes and intercepts in Schild plots were determined from linear regression programmes available on an Apple Macintosh computer (Cricket Graph and Statsview 512).

Results

Voltammetric identification of release substance

The applied potential waveform and the charging current flowing in the carbon fibre microelectrode are shown in Figure 1a and b respectively. The upper trace in Figure 1b represents the faradaic current superimposed on the charging current obtained in the SCN of the rat during a train of 50 pulses applied at 100 Hz. Digital subtraction of the charging current (oscilloscope or computer) reveals the faradaic current (Figure 1c). A single oxidation peak (O) is seen at +600 mV and two reduction peaks (r_1 and r_2) are observed at 0 and −200 mV respectively. Figure 1d shows the faradaic current obtained in the DRN during a train of 25 pulses applied at 100 Hz. Figure 1e shows the faradaic current in the presence of 1×10^{-7} M 5-HT *in vitro*.

Effect of 5-HT receptor agonists on stimulated 5-HT overflow evoked by 25 pulses in the DRN and SCN

Figure 2 shows the results from a typical experiment in which changes in stimulated 5-HT overflow evoked by trains of 25 pulses were monitored for about 2 h in either the DRN (Figure 2a) or the SCN (Figure 2b) in the presence of 5-CT. A concentration-dependent decrease in stimulated 5-HT overflow was seen and a maximal response of 64% inhibition was observed in the SCN. In a series of studies summarized in Figure 3, the effects of 5-CT, buspirone, 8-OH-DPAT and RU24969 were shown to decrease electrically stimulated 5-HT overflow in the DRN (Figure 3a) and SCN (Figure 3b) in a concentration-dependent manner. EC_{50} values and maximum inhibition of release (E_{max}) in both regions are summarized in Table 1 (columns 1/2 and 5/6). Evidence from experiments using low concentrations of methiothepin (results not shown; for full details see O'Connor & Kruk, 1991b) indicated that 25 pulses at 50 Hz released endogenous 5-HT which could activate 5-HT autoreceptors in both brain regions, 5 pulse stimulation (see Introduction) was used in all subsequent experiments to avoid this potentially confounding effect.

Effects of 5-HT$_1$ receptor agonists on changes in stimulated 5-HT overflow evoked by 5 pulse stimulation in the SCN

Five pulses at 100 Hz stimulation applied once every 5 min for up to 6 h in either DRN or SCN resulted in reproducible

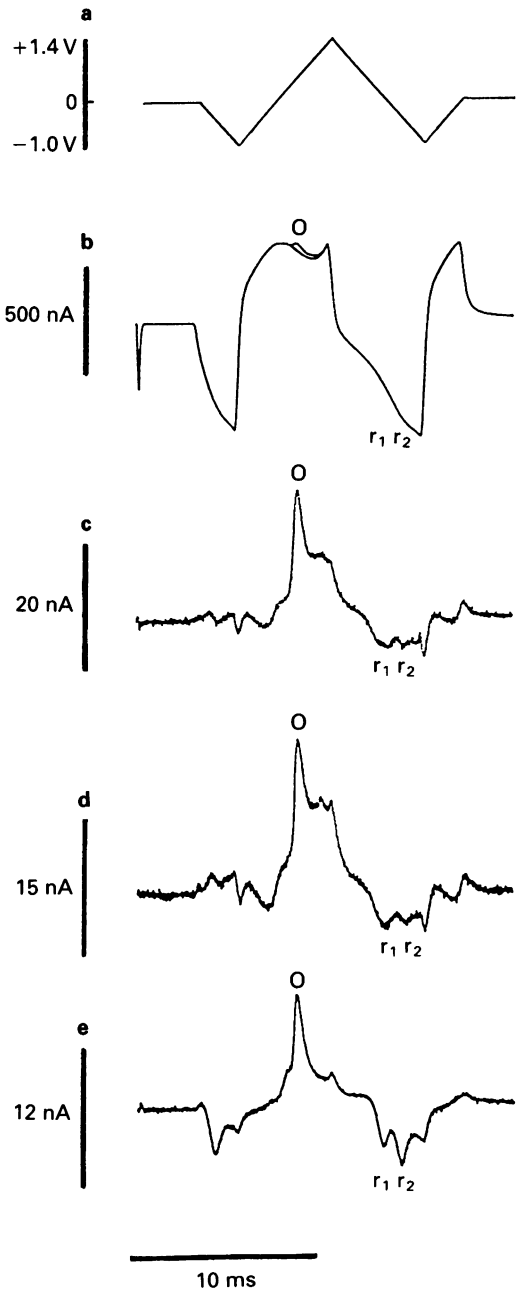

Figure 1 Voltammetric driving ramp and currents. The bar at the foot of the figure denotes time and applies to all traces. (a) Driving voltage ramp applied to the carbon fibre electrode. (b) Charging and charging plus faradaic currents flowing in the carbonfibre electrode in a rat brain slice containing the suprachiasmatic nucleus (SCN) before and following a 50 pulse/100 Hz stimulation. (c) Faradaic current produced after digital subtraction of the charging currents (shown in b) following the 50 pulse/100 Hz stimulation in the SCN. (d) Faradaic current produced after digital subtraction of the charging currents following a 25 pulse/100 Hz stimulation in the dorsal raphe nucleus (DRN). (e) Faradaic current produced due to the presence of 0.1 μM 5-hydroxytryptamine (5-HT, following digital subtraction of the charging current). The peak oxidation and reduction potentials are indistinguishable in (c), (d) and (e).

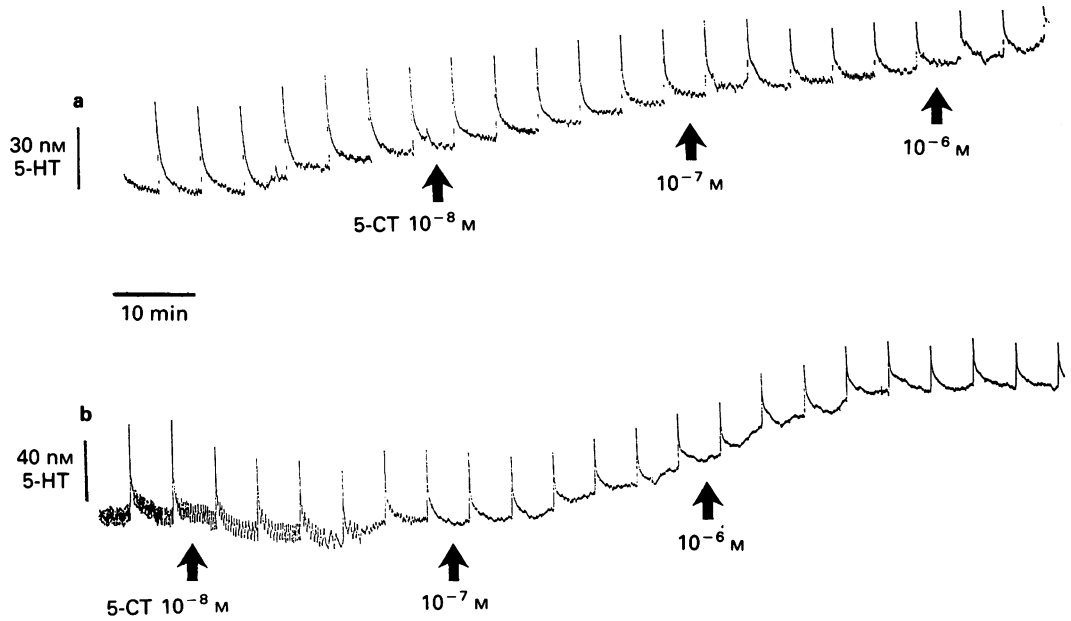

Figure 2 Sample and hold output traces showing the effects of 5-carboxamidotryptamine (5-CT) at the concentrations indicated upon the height of the peak 5-hydroxytryptamine (5-HT) oxidation signal (+600 mV). Electrical stimulation was applied once every 5 min in either (a) the suprachiasmatic nucleus or (b) dorsal raphe nucleus. After experiments the electrodes were calibrated in exogenous 5-HT at the concentrations indicated by the scale bar.

Table 1 Effect of 5-HT_1 receptor ligands on stimulated 5-hydroxytryptamine (5-HT) overflow evoked by trains of 25 pulses delivered at 50 Hz (25P/50 Hz) and trains of 5 pulses delivered at 100 Hz (5P/100 Hz)

	DRN				*SCN*			
	25P/50 Hz		*5P/100 Hz*		*25P/50 Hz*		*5P/100 Hz*	
Agonist	EC_{50}	E_{max}	EC_{50}	E_{max}	EC_{50}	E_{max}	EC_{50}	E_{max}
5-CT	21 ± 3	47.2 ± 7.8	25 ± 11	48 ± 7	67 ± 16	64.4 ± 6.5	5.6 ± 3.1	86 ± 6
RU24969	39 ± 19	29 ± 5.8	23 ± 13	51 ± 7.5	14 ± 2	50.7 ± 6	3.8(2.5)	89 ± 5
8-OH-DPAT	25 ± 6	44.2 ± 4.3	35 ± 19	43 ± 9	36 ± 18	24.2 ± 3.2	—	12 ± 4
Buspirone	65 ± 35	42.7 ± 7.8	NC	NC	140 ± 85	24 ± 9.5	NC	NC
Ipsapirone	NC	NC	12 ± 10	50 ± 6	NC	NC	—	−4 ± 5
Sumatriptan	NC	NC	180 ± 80	36 ± 8	NC	NC	42 ± 29	70 ± 6
TFMPP	NC	NC	NC	NC	NC	NC	5.0 ± 3.4	90 ± 5

EC_{50}: concentration of agonist (nM) required to reduce 5-HT to 50% control values. E_{max}: maximum inhibitory effect (%) of agonists. NC: experiments not carried out. $n = 3-7$ for each value (± s.e.mean). For abbreviations, see text.

and stable release of 5-HT (O'Connor & Kruk, 1991b). The effects of RU24969 at 3 different concentrations on 5 pulse stimulated 5-HT overflow in the SCN are shown in Figure 4a. Pooled results for RU24969, TFMPP, 8-OH-DPAT, ipsapirone, sumatriptan, and 5-CT are shown in Figure 4b. In the SCN, RU24969, 5-CT, and sumatriptan (3×10^{-9} to 1×10^{-6} M) caused a concentration-dependent decrease in 5 pulse stimulated 5-HT overflow. By contrast, ipsapirone and 8-OH-DPAT did not decrease stimulated 5-HT overflow significantly following 5 pulse stimulation.

The order of potency of the agonists, and comparison of the concentration needed to produce a 50% decrease in the maximum response, and the maximum effect obtainable with each agonist in both brain regions is summarized in Table 1 (columns 7 and 8).

Effect of methiothepin and isamoltane on the response to 5-HT_1 receptor agonist in the SCN

Addition of the non selective 5-HT_1/5-HT_2 receptor antagonist, methiothepin, had no significant effect on 5 pulse stimulation on its own (see above). However, methiothepin caused a concentration-dependent parallel shift to the right of the concentration-response curves to RU24969, 5-CT or sumatriptan in the SCN (Figure 5a,b and c, respectively). The same maximum response was obtained to bath-applied RU24969, 5-CT and sumatriptan in the presence of the antagonist. In Figures 5d and 5e, Schild plots are drawn for RU24969 and 5-CT respectively. Simple linear regression analysis showed that the slope in each case was not significantly different from unity (0.83 and 1.18 respectively), and the pK_B for methiothepin with RU24969 was 7.9 and with 5-CT was 8.1.

Isamoltane (10^{-6} M), the putative 5-HT_{1B} receptor antagonist was found to attenuate significantly the maximum response to RU24696 (10^{-6} M; $P<0.01$; $n = 4$, compared to controls) and TFMPP (10^{-6} M; $P<0.01$; $n = 4-5$, compared to controls) in the SCN (Figure 6a and b).

Effects of 5-HT_1 receptor agonists on stimulated 5-HT overflow evoked by 5 pulse stimulation in the DRN

The effects of 8-OH-DPAT at two different concentrations on 5 pulse stimulated 5-HT overflow in the DRN is shown in Figure 7a. Ipsapirone, RU24969, 5-CT and sumatriptan decreased 5-HT release in a concentration-dependent manner in response to 5 pulse stimulation in the concentration-range 10^{-9} M to 10^{-6} M (Figure 7b). These compounds proved to

be less potent in the DRN than in the SCN, and even when the concentration of agonists was increased above 10^{-6} M in no case was it possible to obtain a complete inhibition of 5-HT release. Table 1 (columns 3 and 4) summarizes the ED_{50} and maximum effect of each agonist on 5 pulse stimulated 5-HT overflow in the DRN.

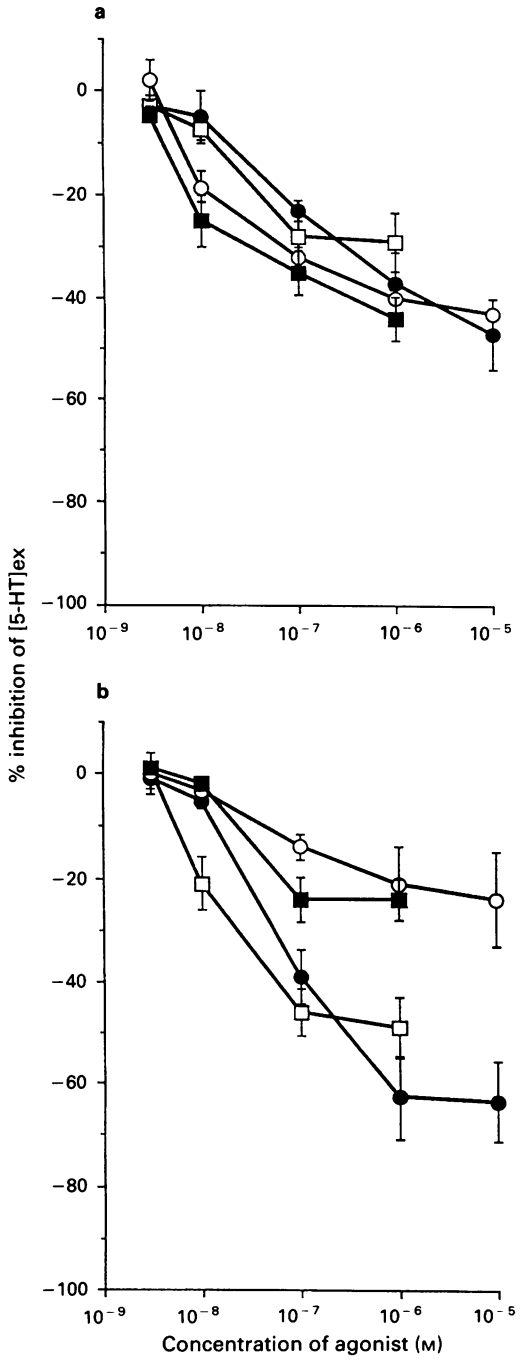

Figure 3 The effects of 5-HT_1 receptor ligands on stimulated 5-hydroxytryptamine overflow ([5-HT]ex) evoked by trains of 25 pulse/50 Hz in (a) the dorsal raphe nucleus or (b) the suprachiasmatic nucleus. The effects of 5-carboxamidotryptamine (●), RU24969 (□), buspirone (○) and 8-hydroxy-2(di-n-propylamino)tetralin (■) at the concentrations indicated are shown for both regions. Results are expressed as percentage inhibition of release when compared to predrug controls (mean with s.e.mean shown by vertical bars; $n = 4-5$) at each observation point. This figure is derived from data such as that shown in Figure 2 for a single experiment.

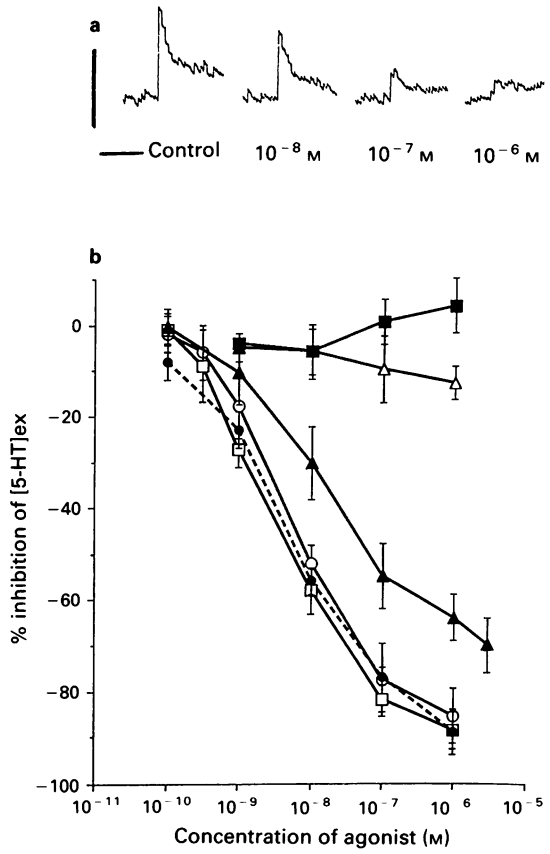

Figure 4 The effects of 5-HT_1 receptor ligands on stimulated 5-hydroxytryptamine overflow ([5-HT]ex) evoked by 5 pulse 100 Hz stimulation in the suprachiasmatic nucleus (SCN). (a) Sample and hold output, set at the peak oxidation potential for 5-HT (+600 mV), for a single experiment during application of RU24969 at the concentrations indicated. Vertical bar: 10 nM 5-HT; horizontal bar: 10 s. (b) The effects of 5-carboxamidotryptamine (●), RU24969 (□), sumatriptan (▲), TFMPP (○), ipsapirone (■) and 8-hydroxy-2(di-n-propylamino)tetralin (△) on electrically evoked endogenous 5-HT overflow in brain slices containing the SCN. The drugs were applied at the concentrations indicated and percentage inhibition was calculated by comparison in each case with pre-drug control release. Electrical stimulation consisted of 5 × 0.1 ms pulses; 100 Hz; 20 V; applied every 5 min. Each point shows the mean with s.e.mean indicated by vertical bars; $n = 4-5$.

Effect of 5-HT receptor antagonists on the response to 5-HT_1 receptor agonists in the DRN

Figure 7c shows the concentration-response curve for 5-CT in the absence and presence of methiothepin in the DRN. There was a significant reduction in the inhibition of stimulated 5-HT overflow produced by 5-CT in the presence of methiothepin ($P<0.05$ for 10^{-7} M and 10^{-6} M 5-CT; $n = 4-5$).

Isamoltane the putative 5-HT_{1B} receptor antagonist did not significantly attenuate the response to ipsapirone in the DRN (results not shown; $P<0.73$; $n = 4-5$, maximum inhibition in controls versus maximum inhibition in the presence of isomoltane).

NAN-190 (1×10^{-6} M) the putative 5-HT_{1A} antagonist when perfused in the presence of ipsapirone (10^{-6} M) significantly antagonized its effect in the DRN (results not shown; $P<0.01$; $n = 4$; compared to controls).

Propranolol in the range 1×10^{-8} M to 1×10^{-5} M had no effect on stimulated 5-HT overflow in the DRN on its own ($n = 4$). However, the response to ipsapirone (10^{-6} M) was attenuated after pretreatment with 10^{-6} M propranolol (results not shown; $P<0.5$; $n = 4$, compared to controls).

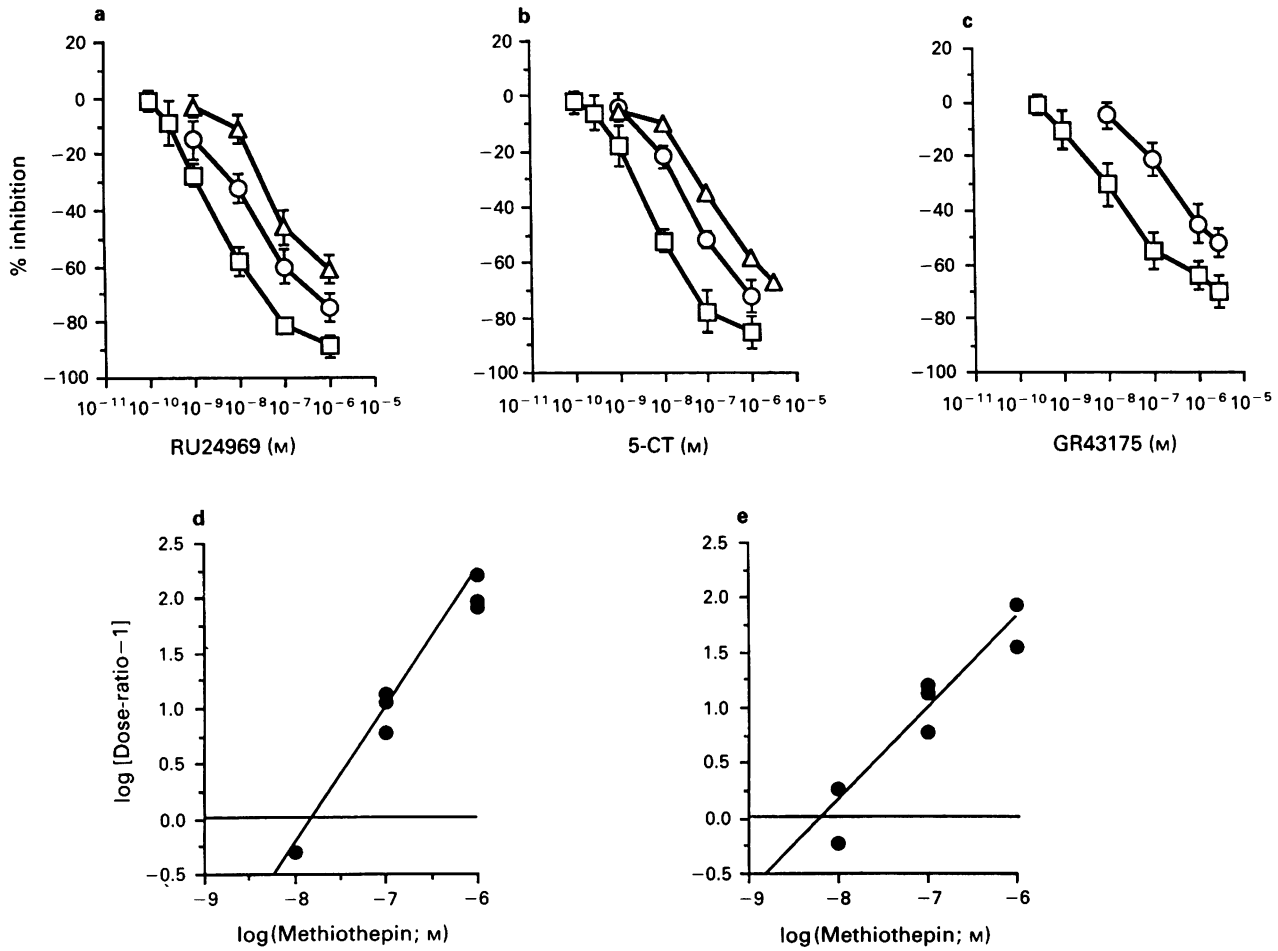

Figure 5 The effects of methiothepin applied at different concentrations on the concentration-response curves to (a) RU24969, (b) 5-carboxyamidotryptamine (5-CT) and (c) sumatriptan in the suprachiasmatic nucleus. Agonists were applied at the concentrations indicated either on their own (□) or in the presence of 0.1 μM methiothepin (○) or 1.0 μM methiothepin (△). Each point shows the mean with s.e.mean indicated by vertical bars; $n = 4-5$. (d) and (e) show the Schild plots derived from the data shown in (a) and (b) respectively. The slopes of the calculated regression line did not differ from unity in either case (0.81 (d) and 1.2 (e)). The effect of 0.01 μM methiothepin on the concentration-response curves to RU24969 and 5-CT is not shown in (a) or (b) for clarity.

Discussion

The use of a brain slice (where axon terminals and somatodendritic sites are separated), is advantageous for receptor characterization studies. While the use of brain slices had its limitations in that afferent inputs may be removed, for pharmacological experiments where the characteristics of autoreceptors are studied both qualitatively and quantitatively, this can be regarded as an advantage. In this study, we were able to study the pharmacology of the axon terminal autoreceptor in the absence of influences from the nerve cell body. The suprachiasmatic nucleus was chosen as a representative axon terminal site, as it possesses one of the highest concentrations of 5-HT located in axon terminals in the brain (Saavedra *et al.*, 1974b). The dorsal raphe nucleus was used as a representative somatodendritic structure which has been extensively studied.

In vivo voltammetric studies in which either 5-hydroxyindoleacetic acid was used as an index of 5-HT release (Marsden & Martin 1985; 1986) or measurement of endogenous 5-HT in dialysates (Sharp *et al.*, 1990) have produced qualitative information about 5-HT receptor subtypes, but such studies do not allow quantitative characterization of autoreceptors at either nerve cell bodies or axon terminals. Systemic administration of drugs in these studies makes it difficult to identify a particular anatomical target for action, although local application of the drug helps. When drugs are applied systemically, the influence of changes in the firing rate of 5-HT nerve cell bodies makes interpretation of the measurement of 5-HT concentrations at axon terminals difficult, especially if an inhibitor of 5-HT uptake is routinely added to the dialysis fluid (Sharp *et al.*, 1989; 1990).

We have shown in other studies (O'Connor & Kruk, 1991a,b) that fast cyclic voltammetry can be used to measure rapid (less than 500 ms) changes in the extracellular concentration of 5-HT in the dorsal raphe nucleus or in the suprachiasmatic nucleus of the rat. In the present study we have shown that the voltammetric signal observed following electrical stimulation is indistinguishable from the signal obtained with exogenous 5-HT. In contrast to dopamine systems, we have found that it is not possible to obtain reproducible release of 5-HT following single pulse stimulation. Bull *et al.* (1990) were able to demonstrate dopamine release in response to single electrical pulse stimulation in the caudate putamen and nucleus accumbens; this may reflect the higher concentration of dopamine found at these sites. Our inability to demonstrate 5-HT release following single pulse stimulation may reflect relatively lower concentrations of 5-HT in the DRN and SCN (Saavedra *et al.*, 1974a,b). Five pulse stimulation at 100 Hz (a stimulus resulting in release of endogenous transmitter sufficiently brief to avoid activation of autoreceptors) has been shown to be an effective tool to study regulation of [^{3}H]-noradrenaline (Valenta *et al.*, 1988; Singer, 1988), [^{3}H]-dopamine (Mayer *et al.*, 1988), endogenous dopamine (Trout & Kruk, 1991) and [^{3}H]-5-HT (Singer, 1988; Fischer *et al.*, 1990; Limberger *et al.*, 1990; 1991).

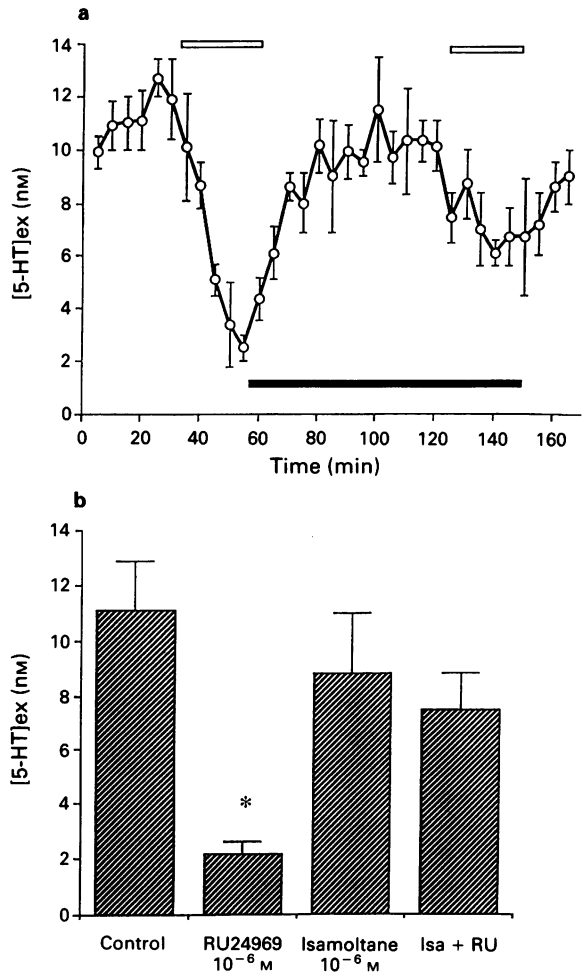

Figure 6 The effects of 5-hydroxytryptamine (5-HT) receptor antagonists on stimulated 5-HT overflow ([5-HT]ex) in the suprachiasmatic nucleus (SCN). (a) The time course of effect of isamoltane (1 μM) on inhibition of 5 pulse at 100 Hz stimulated endogenous 5-HT overflow by TFMPP (1 μM) in slices containing the SCN. Each point shows the mean with s.e.mean indicated by vertical bars; $n = 4$. The open bar shows the time course while TFMPP was perfused; the black bar shows the time course of perfusion of isamoltane. (b) The effects of isamoltane (1 μM) on RU24969 (1 μM)-induced inhibition of 5-HT overflow is shown in the form of histograms. Each column shows the mean (s.e.mean indicated by vertical bars) ($n = 4$; $^*P < 0.01$; Isa: isamoltane; RU: RU24969).

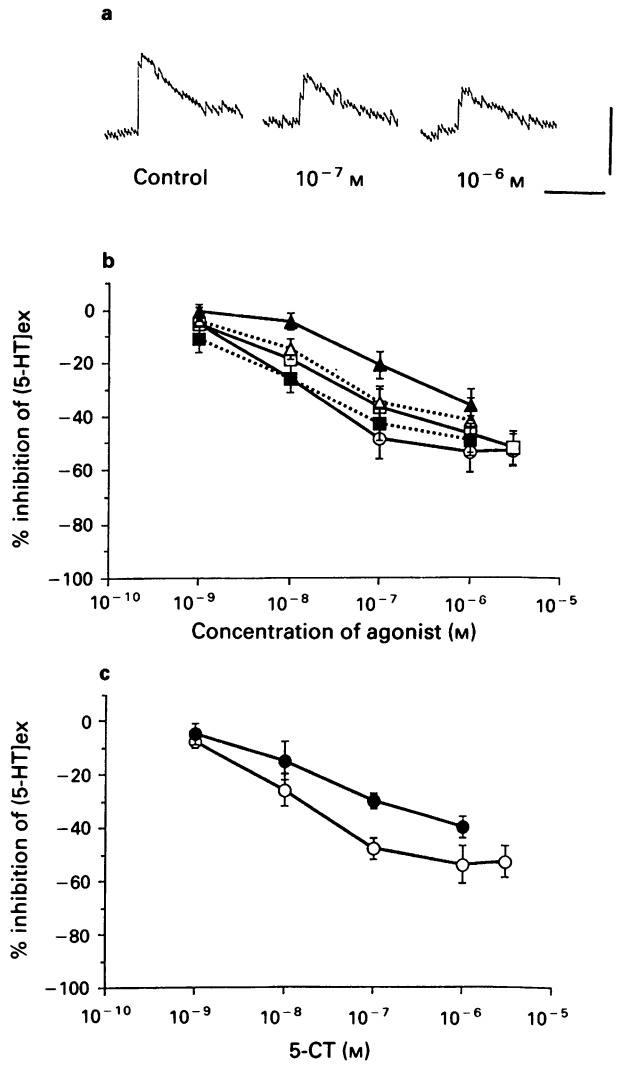

Figure 7 The effect of 5-HT_1 receptor ligands on stimulated 5-hydroxytryptamine overflow ([5-HT]ex) evoked by 5 pulses at 100 Hz in the dorsal raphe nucleus (DRN). (a) Sample and hold outputs showing traces from a single experiment in which 8-hydroxy-2(di-n-propylamino)tetralin (8-OH-DPAT) was applied at the concentrations indicated. Horizontal bar: 10 S; vertical bar: 10 nM 5-HT. (b), The effects of 5-HT_1 ligands present at the concentrations indicated upon inhibition of overflow of endogenous 5-HT evoked by 5 pulses at 100 Hz in brain slices containing the DRN (8-OH-DPAT ■), 5-carboxamidotryptamine (5-CT, ○), ipsapirone (△), sumatriptan (▲) and RU24969 (□); each point shows the mean (s.e.mean shown by vertical bars; $n = 4-7$). (c) The effect of 0.1 μM methiothepin (●) on the concentration-response curve to 5-CT (○) in the DRN; each point shows the mean with s.e.mean indicated by vertical bars; $n = 4-7$.

Initially we examined the ability of 5-HT receptor agonists to inhibit endogenous 5-HT release elicited by trains of 25 pulses applied at 50 Hz (500 ms duration of stimulation). While 5-CT and RU24969 were more potent than ipsapirone or 8-OH-DPAT at inhibiting endogenous 5-HT release in the SCN, the same four agonists were approximately equipotent when their ability to inhibit release of 5-HT was examined in the DRN. In neither region did any of the drugs cause a full inhibition of stimulated 5-HT overflow. Experiments using methiothepin (0.1 μM; O'Connor & Kruk, 1991b) indicated that stimulations with 25 pulses at 50 Hz released endogenous 5-HT which activated 5-HT autoreceptors in both brain regions. It is likely that the perfused exogenous agonist competes with the released endogenous 5-HT when these stimulation parameters are used. This may account for the high EC_{50} values observed in the SCN when compared to the EC_{50} values obtained with stimulations of 5 pulses at 100 Hz (Table 1 columns 5 and 7).

Five pulse stimulation was used in all subsequent experiments to avoid the potentially confounding effects of the endogenous 5-HT inhibiting its own release or preventing access of exogenously applied drug to the autoreceptors under study. Using this stimulus, we have shown (O'Connor & Kruk, 1991b) that release of endogenous 5-HT is unaffected by the presence of 1 μM methiothepin, thus indicating that this stimulus is not susceptible to autoreceptor regulation. Therefore by using 5 pulses at 100 Hz stimulation in both regions, we were able to study the effects of agonists and antagonists in the absence of autoinhibition by endogenous 5-HT.

Using the agonists and 5 pulses at 100 Hz stimulation, it was possible to establish an agonist potency series in the SCN. RU24969, TFMPP and 5-CT were virtually equipotent, more potent than sumatriptan, much more potent than 8-OH-DPAT and ipsapirone. The order of potency of agonists in this study is in accord with that described by

Limberger *et al.* (1991) who measured the ability of 8-OH-DPAT, 5-CT and RU24969 to inhibit [^{3}H]-5-HT release in slices of rat cortex. It is interesting to note, that in common with Limberger *et al.* (1991), we find that perfused exogenous 5-HT (in the presence of 1×10^{-6} M fluvoxamine to block 5-HT uptake) inhibited in a concentration-dependent manner, 5 pulse stimulated 5-HT overflow in the SCN, and had a potency intermediate between that of RU24969, 5-CT, TFMPP and 8-OH-DPAT (EC_{50} 110 nM; E_{max} 82%; O'Connor & Kruk, unpublished observations). 5-HT applied to the perfusion medium in the absence of uptake inhibitor had very little effect on stimulated 5-HT overflow, even when concentrations as high as 1 μM 5-HT were used.

None of the agonists studied caused complete inhibition of stimulated 5-HT overflow in the dorsal raphe nucleus. This does not imply that these drugs were acting as partial agonists, since 5-HT (in the presence of fluvoxamine; 1 μM) caused a similar degree of inhibition as that exerted by the more selective agonists used (O'Connor & Kruk, unpublished observations). We conclude that either a full agonist for 5-HT_{1A} autoreceptors has yet to be discovered, or electrically stimulated 5-HT release cannot be completely inhibited by activation of 5-HT autoreceptors at this site.

Methiothepin was found to act as a competitive antagonist to RU24969, 5-CT and sumatriptan in the SCN. Detailed concentration-response studies showed that the pK_B for methiothepin appears constant when measured against 5-CT or RU24969 in the SCN with values of 7.9 and 8.1 respectively; this is in excellent agreement with the value of 7.9 in rat cerebral cortex determined by Limberger *et al.* (1991), and a K_d value of 7.3 in ligand binding studies in rat brain (Hoyer & Middlemiss, 1989). Isamoltane, the putative 5-HT_{1B} antagonist (Schoeffter & Hoyer, 1989) was able to antagonize the effects of TFMPP and RU24969 in the SCN, but it was not established whether this antagonism was competitive.

It is interesting that agonists of the 5-HT_{1B} receptor with distinct potency and differing efficacy in the SCN, appear to be approximately equipotent and equally efficacious in the dorsal raphe nucleus. In the DRN, antagonist studies could only at best be qualitative, because full agonist action could not be obtained. Methiothepin blocked the effect of 5-CT in the DRN, and this is in accord with it having affinity for 5-HT_{1A} receptors (Hoyer & Middlemiss, 1989). Isamoltane (see above), was not an antagonist of the effect of ipsapirone in the DRN, while NAN 190 (Glennon *et al.*, 1988), a putatively selective 5-HT_{1A} antagonist, did antagonize the inhibitory effect of ipsapirone on stimulated 5-HT overflow. Sprouse & Aghajanian (1986) reported that (−)-propranolol could antagonize the inhibition of spontaneous firing in the DRN caused by 5-HT. In this study, (−)-propranolol while having no effect on stimulated 5-HT overflow on its own, could block the effect of ipsapirone in preventing release of endogenous 5-HT. Further characterization of the 5-HT_{1A} receptor may require the development of more selective antagonists of 5-HT receptor subtypes.

Conclusions

We have shown that 5-HT autoreceptors in the SCN can be characterized by measuring agonist potency and antagonist affinity, at an anatomically precise location in slices prepared from rat brain. Our results are in good agreement with quantitative studies with radiolabelled 5-HT when these are made in the absence of reuptake inhibitors. Our results confirm that a wide range of agonists is available for characterization of 5-HT_{1B} receptors on axon terminals, but we conclude that characterization of somatodendritic 5-HT autoreceptors in the rat requires further study.

We thank Glaxo Group Research for financial support.

References

ARUNLAKSHANA, O. & SCHILD, H.O. (1959). Some quantitative uses of drug antagonists. *Br. J. Pharmacol. Chemother.*, **14**, 48–58.

BRADLEY, P.B., ENGEL, G., FENIUK, W., FOZARD, J.R., HUMPHREY, P.P.A., MIDDLEMISS, D.N., MYLECHARANE, E.J., RICHARDSON, B.P. & SAXENA, P.R. (1986). Proposals for the classification and nomenclature of functional receptors for 5-hydroxytryptamine. *Neuropharmacol.*, **25**, 563–576.

BULL, D.R., PALIJ, P., SHEEHAN, M.J., MILLAR, J., STAMFORD, J.A., KRUK, Z.L. & HUMPHREY, P.P.A. (1990). Application of fast cyclic voltammetry to measurement of electrically evoked dopamine overflow from brain slices in vitro. *J. Neurosci. Methods*, **32**, 37–44.

BULL, D.R. & SHEEHAN, M.J. (1991). Presynaptic regulation of electrically evoked dopamine overflow in nucleus accumbens: a pharmacological study using fast cyclic voltammetry in vitro. *Naunyn-Scheimdebergs Arch. Pharmacol.*, **343**, 260–265.

CEJNA, M., AGNETER, E., DROBNY, H., VALENTA, B. & SINGER, E.A. (1990). Pulse to pulse modulation of transmitter release in the central nervous system: basic and pharmacological aspects. In: Presynaptic receptors and the question of autoregulation of neurotransmitter release, Edited by S. Kalsner. *Ann N.Y. Acad. Sci.*, **604**, 211–221.

DE MONTIGNY, C., BLIER, P. & CHAPUT, Y. (1984). Electrophysiologically-identified serotonin receptors in the rat CNS: effect of antidepressant treatment. *Neuropharmacol.*, **23**, 1511–1520.

DOMPERT, W.U., GLASER, T.R. & TRABER, J. (1985). ^{3}H-TVX Q 7821: Identification of 5-HT_1 binding sites as target for a novel putative anxiolytic. *Naunyn-Schmeidebergs Arch. Pharmacol.*, **328**, 467–470.

DOURISH, C.T., HUTSON, P.H. & CURZON, G. (1986). Putative anxiolytics 8-OH-DPAT, buspirone and TVX Q 7821 are agonists at 5-HT_{1A} autoreceptors in the raphe nuclei. *Trends Pharmacol. Sci.*, **7**, 212–215.

DUMUIS, A., SEBBEN, M. & BOCKAERT, J. (1989). A non-classical 5-hydroxytryptamine receptor positively coupled with adenylate cyclase in the central nervous system. *Mol. Pharmacol.*, **34**, 880–887.

ENGEL, G., GOTHERT, M., HOYER, D., SCHLICKER, E. & HILLENBRAND, K. (1986). Identity of inhibitory presynaptic 5-hydroxytryptamine (5-HT) autoreceptors in the rat brain cortex with 5-HT_{1B} binding sites. *Naunyn-Schmeidebergs Arch. Pharmacol.*, **332**, 1–7.

FISCHER, M.R.G., LIMBERGER, N. & STARKE, K. (1990). The transmitter release pattern of serotonin axons in rabbit brain cortex slices during short pulse trains. *Neurochem. Int.*, **17**, 129–137.

GLENNON, R.A., NAIMAN, N.A., PIERSON, M.E., TITELER, M., LYON, R.A. & WEISBERG, E. (1988). NAN-190: an arylpiperazine analog that antagonises the stimulus effects of the 5-HT_{1A} agonist 8-hydroxy-2-(di-n-propylamino)tetralin (8-OH-DPAT). *Eur. J. Pharmacol.*, **154**, 339–341.

GÖTHERT, M. (1990). Presynaptic serotonin receptors in the central nervous system. In: Presynaptic receptors and the question of autoregulation of neurotransmitter release. Edited by S. Kalsner. *Ann N.Y. Acad. Sci.*, **604**, 102–112.

HAJ-DAHMANE, S., HAMON, M. & LANFUMEY, L. (1991). K+ channel and 5-hydroxytryptamine1A autoreceptor interactions in the rat dorsal raphe nucleus: an in vitro electrophysiological study. *Neuroscience*, **41**, 495–505.

HERRICK-DAVID, K. & TITELER, M. (1988). Detection and characterization of the serotonin 5-HT_{1D} receptor in rat and human brain. *J. Neurochem.*, **50**, 1624–1631.

HEURING, R.E. & PEROUTKA, S.J. (1987). Characterization of a novel ^{3}H-5-hydroxytryptamine binding site subtype in bovine brain membranes. *J. Neurosci.*, **7**, 894–903.

HOYER, D., PAZOS, A., PROBST, A. & PALACIOS, J.M. (1986a). Serotonin receptors in the human brain. I. Characterization and autoradiographic localization of 5-HT_{1A} recognition sites. Apparent absence of 5-HT_{1B} recognition sites. *Brain Res.*, **376**, 85–96.

HOYER, D., PAZOS, A., PROBST, A. & PALACIOS, J.M. (1986b). Serotonin receptors in the human brain. II. Characterization and autoradiographic localization of 5-HT_{1C} and 5-HT_2 recognition sites. *Brain Res.*, **376**, 97–107.

HOYER, D. & MIDDLEMISS, D.N. (1989). Species differences in the pharmacology of terminal 5-HT autoreceptors in mammalian brain. *Trends Pharmacol. Sci.*, **10**, 130–132.

HOYER, D., WAEBER, C., SCHOEFFTER, P., PALACIOS, J.M. & DRAVID, A. (1989). 5-HT_{1C} receptor-mediated stimulation of inositol phosphate production in pig choroid plexus; a pharmacological characterization. *Naunyn-Schmeidebergs Arch. Pharmacol.*, **339**, 252–258.

HUMPHREY, P.P.A., FENIUK, W., PERREN, M.J., CONNOR, H.E., OXFORD, A.W., COATES, I.H. & BUTINA, D. (1988). GR 43175 – a selective agonist for the 5-HT_1-like receptor in dog saphenous vein. *Br. J. Pharmacol.*, **94**, 1123–1132.

KALSNER, S. & WESTFALL, T.C. (Editors; 1990). Presynaptic receptors and the question of autoregulation of neurotransmitter release. *Ann. N.Y. Acad. Sci.*, **604**, 1–647.

KENNAKIN, T.P. (1984). The classification of drugs and drug receptors in isolated tissues. *Pharmacol. Rev.*, **36**, 165–222.

LIMBERGER, N., DEICHER, R. & STARKE, K. (1991). Species differences in presynaptic serotonin autoreceptors: mainly 5-HT_{1B} but possibly in addition 5-HT_{1D} in the rat, 5-HT_{1D} in the rabbit and guinea-pig brain cortex. *Naunyn-Schmeidebergs Arch. Pharmacol.*, **343**, 353–364.

LIMBERGER, N., STARKE, K. & SINGER, E.A. (1990). Serotinin uptake blockers influence serotonin autoreceptors by increasing the biophase concentration of serotonin and not through a "molecular link". *Naunyn-Schmeidebergs Arch. Pharmacol.*, **342**, 363–370.

MARSDEN, C.A. & MARTIN, K.F. (1985). *In vivo* voltammetric evidence that the 5-HT autoreceptor is not of the 5-HT_{1A} sub-type. *Br. J. Pharmacol.*, **86**, 445P.

MARSDEN, C.A. & MARTIN, K.F. (1986). Involvement of 5-HT_{1A} and α_2-receptors in the decreased 5-hydroxytryptamine release and metabolism in rat suprachiasmatic nucleus after intravenous 8-hydroxy-2-(di-n-propylamino)tetralin. *Br. J. Pharmacol.*, **89**, 277–286.

MARTIN, K.R. & MARSDEN, C.A. (1986). In vivo voltammetry in the suprachiasmatic nucleus of the rat: effects of RU24969, methiothepin and ketaserin. *Eur. J. Pharmacol.*, **121**, 135–139.

MAYER, A., LIMBERGER, N. & STARKE, K. (1988). Transmitter release patterns of noradrenergic, dopaminergic and cholinergic axons in rabbit brain slices during short pulse trains and the operation of presynaptic autoreceptors. *Naunyn-Schmeidebergs Arch. Pharmacol.*, **338**, 632–643.

MELTZER, H.Y. (1990). Role of serotonin in depression. In *Neuropharmacology of Serotonin*. ed. Whitaker-Azmitia, P.M. & Peroutka, S.J. *Ann. N.Y. Acad. Sci.*, **600**, 486–500.

MIDDLEMISS, D.N. (1984). 8-Hydroxy-2-(di-n-propylamino)tetralin is devoid of activity at the 5-hydroxytryptamine autoreceptor in rat brain. Implications for the proposed link between the autoreceptor and the [^{3}H]5-HT recognition site. *Naunyn-Schmeidebergs Arch. Pharmacol.*, **327**, 18–22.

MIDDLEMISS, D.N. (1985). The putative 5-HT_1 receptor agonist, RU 24969, inhibits the efflux of 5-hydroxytryptamine from rat frontal cortex slices in stimulation of the 5-HT autoreceptor. *J. Pharm. Pharmacol.*, **37**, 434–437.

MIDDLEMISS, D.N. & FOZARD, J.R. (1983). 8-Hydroxy-2-(di-n-propyl-amino)-tetralin discriminates between subtypes of the 5-HT_1 recognition site. *Eur. J. Pharmacol.*, **90**, 151–153.

O'CONNOR, J.J. & KRUK, Z.L. (1990). Effects of 5-HT_1 receptor agonists on stimulated endogenous 5-HT overflow studied using fast cyclic voltammetry. *Br. J. Pharmacol.*, **100**, 552P.

O'CONNOR, J.J. & KRUK, Z.L. (1991a). Fast cyclic voltammetry can be used to measure stimulated endogenous 5-hydroxytryptamine release in rat brain slices. *J. Neurosci. Methods*, **38**, 25–33.

O'CONNOR, J.J. & KRUK, Z.L. (1991b). Frequency dependence of 5-HT autoreceptor function in rat dorsal raphe and suprachiasmatic nucleus studied using fast cyclic voltammetry. *Brain Res.*, (in press).

O'CONNOR, J.J. & KRUK, Z.L. (1991c). 5-HT_1 like and 5-HT_{1B} ligands but not 5-HT_{1A} ligands modulate 5-HT release in the suprachiasmatic nucleus of the rat. *Br. J. Pharmacol.*, **104**, 64P.

PALIJ, P., BULL, D.R., SHEEHAN, M.J., MILLAR, J., STAMFORD, J.A., KRUK, Z.L. & HUMPHREY, P.P.A. (1990). Presynaptic regulation of dopamine release in corpus striatum monitored in vitro in real time by fast cyclic voltammetry. *Brain Res.*, **509**, 172–174.

PAZOS, A., HOYER, D. & PALACIOS, M. (1984). The binding of serotonergic ligands to the porcine choroid plexus: characterization of a new type of serotonin recognition site. *Eur. J. Pharmacol.*, **106**, 539–546.

PAZOS, A. & PALACOIS, J.M. (1985). Quantitative autoradiographic mapping of serotonin receptors in the rat brain. I. Serotonin-1 receptors. *Brain. Res.*, **346**, 205–230.

PEROUTKA, S.J. (1988a). 5-Hydroxytryptamine receptor subtypes. *Annu. Rev. Neurosci.*, **11**, 45–60.

PEROUTKA, S.J. (1988b). 5-Hydroxytryptamine receptor subtypes: molecular, biochemical and physiological characterization. *Trends Neuro. Sci.*, **11**, 496–500.

PEROUTKA, S.J. & SNYDER, S.H. (1979). Multiple serotonin receptors: differential binding of ^{3}H-serotonin, ^{3}H-lysergic acid diethylamide and ^{3}H-spiroperidol. *Mol. Pharmacol.*, **16**, 687–699.

RICHARDS, C.D. & TEGG, W.J.B. (1977). A superfusion chamber suitable for maintaining mammalian brain tissue for electrical recording. *Br. J. Pharmacol.*, **59**, 526P.

SAAVEDRA, J.M., BROWNSTEIN, M. & PALKOVITS, M. (1974a). Serotonin distribution in the limbic system of the rat. *Brain Res.*, **79**, 437–441.

SAAVEDRA, J.M., PALKOVITS, M., BROWNSTEIN, M. & AXELROD, J. (1974b). Serotonin distribution in the rat hypothalamus and preoptic region. *Brain Res.*, **77**, 157–165.

SCHOEFFTER, P. & HOYER, D. (1989). Interactions of arylpiperazines with 5-HT1A, 5-HT1B, 5-HT1C and 5-HT1D receptors: do discriminatory 5-HT1B receptor ligands exist? *Naunyn-Schmeidebergs Arch. Pharmacol.*, **339**, 675–683.

SHARP, T., BRAMWELL, S.R. & GRAHAME-SMITH, D.G. (1989). 5-HT_1 agonists reduce 5-hydroxytryptamine release in rat hippocampus in vivo as determined by brain microdialysis. *Br. J. Pharmacol.*, **96**, 283–290.

SHARP, T., BRAMWELL, S.R. & GRAHAME-SMITH, D.G. (1990). Release of endogenous 5-hydroxytryptamine in rat ventral hippocampus evoked by electrical stimulation of the dorsal raphe nucleus as detected by microdialysis: sensitivity to tetrodotoxin, calcium and calcium antagonists. *Neuroscience*, **39**, 629–637.

SHENKER, A., MAAYANI, S., WEINSTEIN, H. & GREEN, J.P. (1987). Pharmacological characterization of two 5-hydroxytryptamine receptors coupled to adenylate cyclase in guinea pig hippocampal membranes. *Mol. Pharmacol.*, **31**, 357–367.

SILLS, M.A., WOLFE, B.B. & FRAZER, A. (1984). Determination of selective and non-selective compounds for the 5-HT_{1A} and 5-HT_{1B} receptor subtypes in the rat frontal cortex. *J. Pharmacol. Exp. Ther.*, **231**, 480–487.

SINGER, E.A. (1988). Transmitter release from brain slices elicited by single pulses: a powerful method to study presynaptic mechanisms. *Trends Pharmacol. Sci.*, **9**, 274–276.

SPROUSE, J.S. & AGHAJANIAN, G.K. (1986). (−)-Propranolol blocks the inhibition of serotonergic dorsal raphe cell firing by 5-HT_{1A} selective agonists. *Eur. J. Pharmacol.*, **128**, 295–299.

SPROUSE, J.S. & AGHAJANIAN, G.K. (1987). Electrophysiological responses of serotoninergic dorsal raphe neurons to 5-HT_{1A} and 5-HT_{1B} agonists. *Synapse*, **1**, 3–9.

STARKE, K., GOTHERT, M. & KILBINGER, H. (1989). Modulation of neurotransmitter release by presynaptic autoreceptors. *Physiol. Rev.*, **69**, 865–989.

TROUT, S.J. & KRUK, Z.L. (1991). Characteristics of autoreceptor control of dopamine release in olfactory tubercle in the absence of uptake inhibition. *Br. J. Pharmacol.*, **102**, 9P.

VALENTA, B., DROBNY, H. & SINGER, E.A. (1988). Presynaptic autoinhibition of central noradrenaline release in vivo: operational characteristics and effects of drugs acting at alpha-2 adrenoceptors in the presence of uptake inhibition. *J. Pharmacol. Exp. Ther.*, **245**, 944–949.

VANDER MAELEN, C.P., MATHESON, G.K., WILDERMAN, R.C. & PATTERSON, L.A. (1986). Inhibition of serotonergic dorsal raphe neurons by systemic and iontophoretic administration of buspirone, a non-benzodiazepine anxiolytic drug. *Eur. J. Pharmacol.*, **129**, 123–130.

WAEBER, C., SCHOEFFTER, P., PALACIOS, J.M. & HOYER, D. (1988). Molecular pharmacology of 5-HT_{1D} recognition sites: radioligand binding studies in human, pig and calf brain membranes. *Naunyn-Schmeidebergs Arch. Pharmacol.*, **337**, 595–601.

(Received October 14, 1991
Revised February 4, 1992
Accepted February 28, 1992)

Br. J. Pharmacol. (1992), **106**, 533–538

Effects of vapiprost, a novel thromboxane receptor antagonist, on thrombus formation and vascular patency after thrombolysis by tissue-type plasminogen activator

[1]Hiroyuki Matsuno, Toshihiko Uematsu, Kazuo Umemura, Yoshiharu Takiguchi, Kouichirou Wada & Mitsuyoshi Nakashima

Department of Pharmacology, Hamamatsu University, School of Medicine, Hamamatsu 431-31, Japan

1 A thrombus was induced in the rat femoral artery by endothelial damage due to the photochemical reaction between systemically-injected Rose Bengal and transillumination with green light (wavelength: 540 nm). The artery of the control rat was completely occluded in 302.8 ± 27.0 s after the initiation of the reaction.

2 Pretreatment with vapiprost (0.1, 0.3 and 1.0 mg kg^{-1}, i.v., 5 min before the reaction) prolonged the time required to occlude the femoral artery in a dose-dependent manner. The efficacy of vapiprost on the time required for occlusion was over 10 times higher than that of aspirin which was administered 30 min before the reaction.

3 The thrombolytic effects of tissue-type plasminogen activator (tPA) on the established arterial thrombus in the presence and absence of vapiprost were also studied in the same model. When vapiprost (0.3 mg kg^{-1}, i.v.) was administered just before tPA infusion (100 $\mu g\ kg^{-1}\ min^{-1}$ for 30 min), the time required to reperfuse the occluded artery was reduced, the incidence of the reperfusion was increased and the arterial blood flow after reperfusion was improved.

4 When vapiprost (1.0 mg kg^{-1} daily p.o.) was administered for 1 week after the establishment of reperfusion by tPA combined with vapiprost, the patency of the reperfused artery was improved and the femoral arterial blood flow was better preserved than after treatment with only tPA.

5 These findings suggest that this thromboxane receptor antagonist may be a useful adjunct to anti-thrombotic therapy. The combination therapy with tPA may be more effective than treatment with tPA alone and provides greater protection against reocculsion after reperfusion.

Keywords: Vapiprost; thromboxane receptor antagonist; antithrombotic effect; tissue-type plasminogen activator; reperfusion; patency of reperfused vessel

Introduction

Platelets play an important role in thrombus formation associated with various ischaemic vascular events. Recently, the so-called 'arachidonic cascade', which liberates various prostaglandins from the vascular wall and platelets, was fully elucidated. It has been suggested that deterioration of the balance between thromboxane A_2 (TXA_2) production by platelets and prostaglandin I_2 (PGI_2) production by endothelial cells may be a trigger to ischaemic disease because TXA_2 subsequently causes powerful platelet aggregation and contraction of blood vessels, while PGI_2 counteracts TXA_2 (Aiken *et al.*, 1980). Anti-platelet drugs which inhibit platelet aggregation and possess a relatively low risk of general bleeding, are frequently prescribed for the treatment of ischaemic disease and thrombosis. On the other hand, thrombolytic therapy with tissue-type plasminogen activator (tPA) is highly effective for recanalization of the coronary artery obstructed by intraluminal thrombi (Collen *et al.*, 1984; Williams *et al.*, 1986). However, the thrombolytic therapy is not necessarily free from spontaneous reocclusion of the reperfused vessel, especially in the vessel with a residual stenosis of 80% or more (Gold *et al.*, 1986). Recent data suggest that TXA_2 may play a role in reocclusion following tPA-induced thrombolysis (Shebski *et al.*, 1988). We have established a model of arterial thrombosis in the rat femoral artery (Matsuno *et al.*, 1991). This thrombus is platelet-rich and quite representative of that observed clinically (Friedman *et al.*, 1966). It has been suggested that platelet-rich regions are more resistant to antithrombotic or thrombolytic interventions than erythrocyte-rich ones (Ik-Kyung *et al.*, 1989). In the present study, we have therefore examined the efficacy of the novel thromboxane receptor antagonist, vapiprost, on the prevention of platelet-rich thrombus formation in the rat femoral artery induced by a photochemical reaction, in comparison with a well-known cyclo-oxygenase inhibitor, aspirin and inhibition of reocclusion of the femoral artery reperfused with tPA.

[1] Author for correspondence.

Methods

Male Wistar rats (weighing from 240 to 260 g) were used. These rats were anaesthetized by intraperitoneal injection of 50 mg kg^{-1} of sodium pentobarbitone. Animals were allowed to breathe spontaneously. Body temperature of the rats was maintained at 37.5°C with a heating-pad (American Pharmaseal Company, K-module Model K-20).

Induction of thrombus in the femoral artery

The experimental procedure to induce a thrombus in the rat femoral artery has been described elsewhere (Matsuno *et al.*, 1991) in detail. In brief, a short incision was made in the skin and subcutaneous tissue on the right groin region and the femoral neurovascular sheath was gently exposed. A 5 mm-long portion of the right femoral artery distal to the inguinal ligament was isolated by rubbing it against the blade of a forceps, and a pulsed doppler flow probe (Model PDV-20 Crystal Biotech, U.S.A.) positioned for monitoring blood

flow. The contralateral femoral artery and vein were cannulated for monitoring blood pressure and pulse rate and for drug delivery by intravenous injection, respectively. Transillumination with green light was achieved by use of a xenon lamp with a heat absorbing filter and a green filter (a band width of 54 nm centered at 540 nm; Hamamatsu Photonics Inc., Japan). The light was directed by an optic fibre mounted on a micromanipulator so that the head would be approximately 5 mm away from the intact right femoral artery, proximal to the flow probe. About 10 min after establishing the baseline blood flow, the irradiation with green light was started, and after 10 min, Rose Bengal (10 mg kg^{-1}) was injected. The arterial blood flow, blood pressure and pulse rate were continuously monitored on a multi-channel thermo-pen writing oscillograph (WS-681G, Nihon Kohden, Japan). The femoral artery was judged to be occluded when the blood flow fell almost to zero.

Experimental protocol

Aspirin (3 and 10 mg kg^{-1}) and vapiprost (0.1, 0.3 and 1.0 mg kg^{-1}) were administered intravenously 30 min and 5 min before the injection of Rose Bengal, respectively. The transillumination with green light was continued until the artery was occluded. The observation was continued for 1 h after the injection of Rose Bengal. Because both agents were dissolved in different solvents, i.e. aspirin was dissolved in saline and vapiprost was dissolved in 50 mM phosphate buffer (pH 7.4), control experiments were performed separately for each of the agents using the appropriate solvent.

In the thrombolytic study with tPA, the i.v. infusion of which with an infusion pump (Model 22, Harvard, U.S.A.) was started immediately after the establishment of occlusion of the femoral artery and continued for 30 min at a rate of 100 $\mu g\ kg^{-1}\ min^{-1}$, observation was continued for 1.5 h after the cessation of tPA infusion. Just before starting the infusion with tPA, care was taken to flush out any heparin solution (about 100 u kg^{-1}) remaining in the catheter. The patency of the reperfused artery was assessed at 24 h and at 1 week after the above procedures. Control values were obtained by infusion of saline instead of tPA. The effects of co-administration of vapiprost were assessed when vapiprost (0.3 mg kg^{-1}, i.v.) was injected once just before the infusion of tPA and when oral administration of vapiprost (1.0 mg kg^{-1}) was subsequently continued for 1 week following the acute i.v. bolus injection. The artery was defined as reperfused when the blood flow was restored to more than 25% of the baseline value.

Ex vivo *whole blood aggregation*

In a separate experiment using 10 rats, the time-profiles of plasma concentration and suppression of whole blood aggregation *ex vivo* were investigated after i.v. injection of vapiprost (1.0 mg kg^{-1}). Blood samples (5 ml each) were collected into plastic tubes containing 300 μl of 50 u ml^{-1} heparin from the descending aorta under anaesthesia with sodium pentobarbitone (50 mg kg^{-1}, i.p.) after either 5, 30 or 60 min after the injection and, then, the rat was killed. An impedance aggregometer (C550S, Chrono-log Corp., U.S.A.) was used. Collagen was used and the increase in electrical impedance was observed until the tracing reached a plateau.

Histopathological observation

At the end of some experiments using tPA only or in combination with vapiprost, whether the occluded artery ($n = 4$) was reperfused or not, the rats were killed with an overdose of pentobarbitone and the irradiated segments of femoral arteries were excised. These segments were immediately fixed with 2.0% glutaraldehyde in 0.1 M sodium phosphate buffer for 1 h. Each segment was cut open longitudinally to allow visual inspection, and these sections were processed for routine scanning with an electron microscope (SEM).

Agents

Aspirin and heparin were purchased from Sigma and Nobo-industry, Denmark, respectively; vapiprost and tPA (TD-2061) were a gift from Glaxo Group Research Ltd, England and Daiichi C.L., Japan, respectively.

Statistical analysis

All data are expressed as the mean ± standard deviation (s.d.). Comparisons of femoral blood flow and the time to reperfusion were performed with unpaired Student's t test. Comparison among groups was carried out by use of Wilcoxon's test for the time to occlusion and χ^2 test for the reperfusion rate and the reocclusion rate.

Results

Antithrombotic effects of vapiprost and aspirin in the in vivo *study*

Animals from all groups studied had similar body weights and haemodynamic conditions before induction of thrombosis. Typical changes in arterial blood pressure, pulse rate and femoral arterial blood flow from a control animal are illustrated in Figure 1a. Vapiprost-treated groups are also shown in Figure 2. The lowest dose of vapiprost had only a slight effect on the occlusion time (681.28 ± 58.61 s). However, 0.3 mg kg^{-1} of vapiprost was significantly effective in preventing a femoral arterial thrombus ($P < 0.01$ vs control). In six of the nine rats, occlusive thrombi did not develop within 60 min. The times required for occlusion in the three rats in this group in which the femoral arteries had become occluded by the formation of thrombi (11, 18 and 21 min, respectively), were much more prolonged than those with aspirin. At the highest dose of vapiprost studied (1.0 mg kg^{-1}), complete cessation of femoral arterial blood flow could not be obtained in the first 60 min of observation, although the blood flow itself was diminished as compared with the control value. Figure 1b and c shows the effects of vapiprost, i.e., the dose-dependent prolongation of time required to occlude the artery and cyclic flow variations (CFVs) in the femoral arterial blood flow. The result of aspirin treatment is illustrated in Figure 2. Occlusive femoral arterial thrombi occurred in all 7 rats of the aspirin vehicle-treated groups in a mean time of 326.6 ± 26.9 s. In the group of rats receiving aspirin at a dose of 3.0 mg kg^{-1}, the time required to occlude the artery was only slightly prolonged (341.5 ± 32.6 s). At 10.0 mg kg^{-1} the time to occlusion was further prolonged (417.0 ± 103.4 s), but with either dose level the thrombus was finally established within 12 min in all animals.

Ex vivo *study*

When platelet aggregation was induced with 1.0 μM collagen, extensive inhibition by vapiprost was observed as compared with that of non-treated rats. Vapiprost was very effective in blocking collagen-induced platelet aggregation *ex vivo* in this experiment, inhibition rates of aggregation at 5, 30 and 60 min after administration of vapiprost being 90.6 ± 8.2%, 75.7 ± 13.3% and 81.9 ± 8.9%, respectively. In this case, plasma concentrations of vapiprost at 5, 30 and 60 min were 1675.5 ± 69.3, 869.7 ± 43.3 and 560.5 ± 17.9 ng ml^{-1}, respectively.

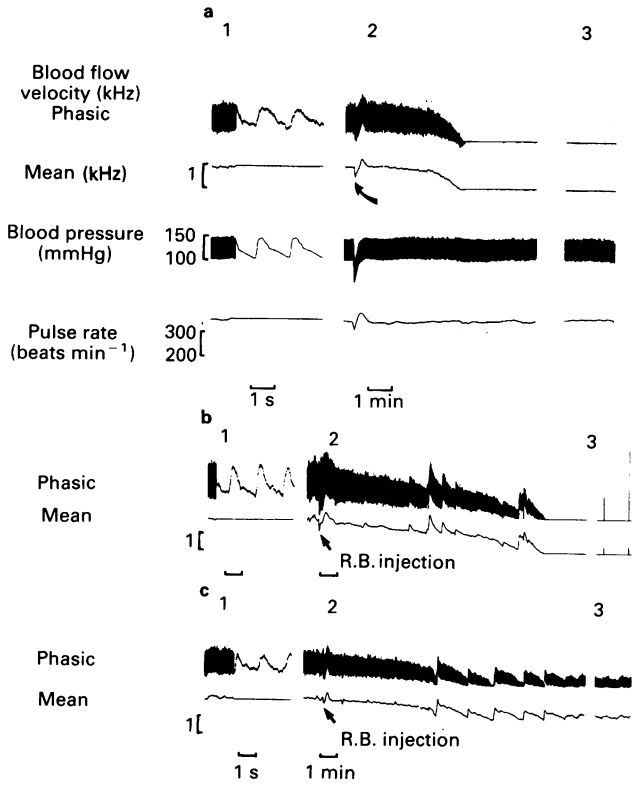

Figure 1 (a) Simultaneous records of typical changes in blood velocity of the irradiated femoral artery and, pulse rate and blood pressure from the contralateral femoral artery. (1) Baseline measurements; (2) change before and after the i.v. injection of Rose Bengal (RB, 10 mg kg^{-1}); (3) 30 min after thrombus formation. Continuous records of femoral blood flow from two animals receiving vapiprost at a dose of 0.3 mg kg^{-1} (b) and 1.0 mg kg^{-1} (c). Thrombosis was induced by the photochemical reaction between xenon light and Rose Bengal injection.

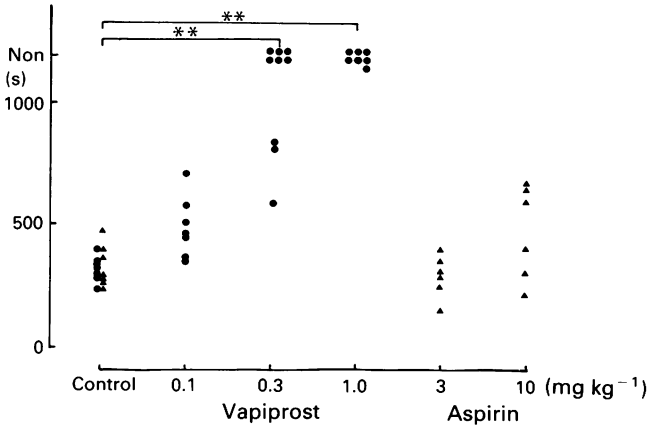

Figure 2 Time to occlusive femoral arterial thrombosis in the individual experiments. The solvent group was divided into 2 groups of animals receiving the vehicle of either vapiprost (●) or aspirin (▲). $^{**}P<0.01$ versus control group.

Thrombolytic effects of tPA alone and vapiprost on tPA

The control resting flows before the formation of thrombus did not differ significantly between these groups of rats or any groups tested. The incidence of reperfusion within the 1.5 h observation period was 38.5% for tPA (100 μg kg^{-1} min^{-1}) and the time to reperfusion was 70.8 ± 11.6 min (Table 1). Following reperfusion the femoral arterial blood flow was much decreased as compared with that before thrombosis. Animals given either saline or vapiprost (1.0 mg kg^{-1}) alone failed to reperfuse in all cases without tPA (Table 1). tPA was much more effective in restoring femoral arterial blood flow in the presence of vapiprost (0.3 mg kg^{-1}) than in the absence of thromboxane inhibition. tPA at 100 μg kg^{-1} min^{-1} alone produced reperfusion in 5 of 12 rats whereas in the presence of vapiprost, 11 of 13 rats reperfused. Likewise, femoral arterial blood flow of reperfusion (Figure 3) and the time to reperfusion (Table 1) also indicate the greater effectiveness of tPA in the presence of vapiprost.

Inhibition of reocclusion with vapiprost

The incidence of reocclusion with animals reperfused ($n = 5$) was 60% during the 1 week of observation and the femoral arterial blood flow of the group treated with tPA alone was much decreased. In rats receiving i.v. injection of vapiprost just before the infusion of tPA, reocculsion incidence after 1 week was unchanged; however, reocclusion incidence after 24 h was improved as well as the blood flow (Figure 3). Additionally, after receiving vapiprost for 1 week (1.0 mg kg^{-1} daily, p.o.), reocclusion incidence and femoral arterial blood flow were improved in comparison with the other groups (Table 1, Figure 3).

Histopathological observations

Scanning electron microscopy of femoral arteries collected after the interruption of blood flow showed that mural thrombi were present in the lumen of the arteries. The luminal thrombi were composed of aggregates of platelets which had entrapped red blood cells within them, and the central portions of the mural thrombi were rich in fibrin (Figure 4). Following reperfusion with tPA, platelets remained anchored to the disrupted arterial wall in spite of restoration of femoral arterial blood flow. However, red blood cells were lost (Figure 5a). Figure 5b shows a femoral artery after reperfusion with vapiprost and tPA. When vapiprost (0.3 mg kg^{-1}) was injected before infusion of tPA, platelet aggregates

Table 1 Frequency of femoral artery reperfusion and reocclusion in the photochemical induced thrombosis model in the rat

Groups	n	*Reperfusion incidence*	*Reperfusion time* (min)	*Reocclusion incidence* 90 min	24 h	1 week
tPA alone	12	5/12	70.8 ± 11.6	2/5	1/3	0/2
Group I	13	11/13*	55.7 ± 8.7*	1/11	2/10	4/8
Group II	6	5/6	52.8 ± 11.2*	0/5	1/5	0/4

Data are expressed in means ± s.d. $^{*}P<0.05$ versus tPA-only treated group. Group I was treated with tPA in combination with i.v. injection of vapiprost just before the start of tPA infusion. Group II: vapiprost (p.o.) was administered for 7 days in addition to single i.v. administration. Denominators of reocclusion incidence express the number of animals maintaining the reperfusion state at that time.

were also observed but in general, aggregates were less prevalent in the vapiprost-treated rats than in the tPA-only treated group, and reocclusion state was similar to the control without tPa treatment. The arterial endothelia were repaired after 1 week, however, examination over a longer period was not carried out. In the case of the arterial segments in which blood flow decreased after 1 week, many platelets adhered to the repaired endothelial surface and the reocclusion state was observed (Figure 6a). These adherent platelets were also decreased by administration of vapiprost (0.3 mg kg^{-1} daily) for 1 week (Figure 6b).

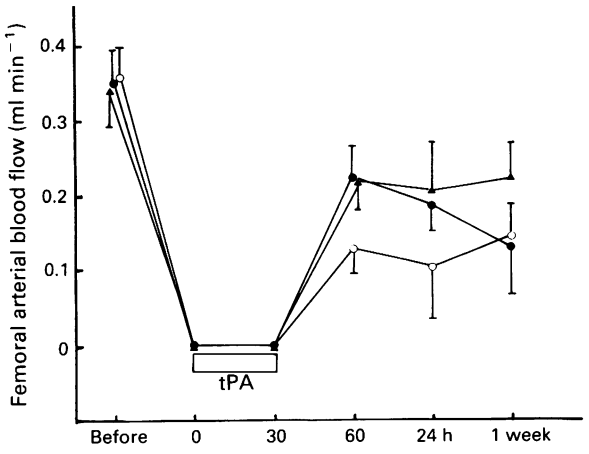

Figure 3 Femoral blood flow during the continuous administration of vapiprost after reperfusion was more increased than that after tPA alone. The effect of chronic treatment with vapiprost upon tPA-induced reperfusion and maintenance of blood flow. Infusion of tPA (100 μg kg^{-1}) was started 30 min after the complete cessation of blood flow and continued for 30 min (indicated by horizontal bar). Group I was treated with tPA in combination with i.v. injection of vapiprost just before the start of tPA infusion. Group II was treated with vapiprost (1 mg kg^{-1} daily, p.o.) which was administered for 7 days in addition to a single i.v. administration. $*P<0.05$ versus tPA-only treated group. Symbols: tPA only (○); Group I (●); Group II (▲). Values are mean with s.d. shown by vertical bars.

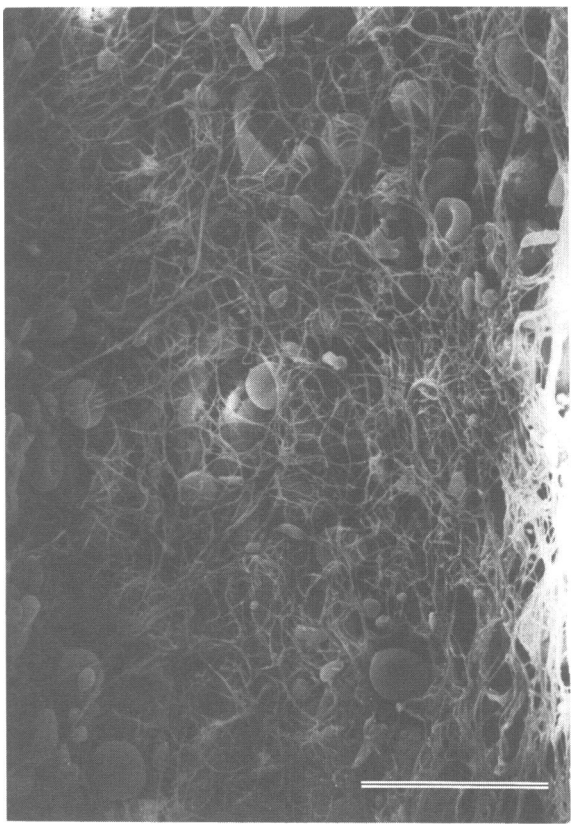

Figure 4 Electronmicrograph of femoral artery showing complete interruption of blood flow. The lumen of the irradiated arterial segment is packed with red blood cells; many platelets with pseudopods and fibrin nets on the swollen endothelial cells are shown. The bar in the photograph denotes 20 μm.

Discussion

The present study has shown vapiprost to be an effective and potent antithrombotic drug *in vivo* in a photochemically induced thrombosis (PIT) model in the rat. The thrombus produced subsequent to the injury to the vascular endothelium, is platelet-rich and resembles clinically observed thrombi (Matsuno *et al.*, 1991). TXA_2, although relatively labile, is synthesized in large quantities by platelets in response to a variety of stimuli (Best *et al.*, 1980; Ambler *et al.*, 1985). Thromboxane receptor antagonists (TRAs) such as vapiprost (Lumley *et al.*, 1989), sulotoroban (Shebuski *et al.*, 1988; Fujita *et al.*, 1988) and Ah-23848 (Brezinski *et al.*, 1988) have been shown to interfer with platelet function through specific competitive inhibition of the platelet membrane receptor that binds either TXA_2 or the cyclic endoperoxides intermediate, PGH_2. By preventing the recruitment of platelets and the secondary release reaction, TRAs may effect a moderate reduction in TXA_2 levels (Ashton *et al.*, 1986), but their mechanism of action is almost entirely through their antagonism of the TXA_2-PGH_2 receptor (Ogletree *et al.*, 1985; Hanasaki *et al.*, 1988). Vapiprost (GR32191) prevents stimulation of platelet aggregation both by TXA_2 and its less potent but longer-lived precursor, PGH_2, in a dose-dependent manner and has been shown to inhibit partially platelet deposition on damaged arteries and artificial surfaces (McCabe *et al.*, 1987). In our study of its antithrombotic effect, vapiprost (1.0 mg kg^{-1}) proved to be effective in preventing the formation of occlusive femoral thrombi. Indeed, occlusion did not occur in any animals during the 60 min observation period. However cyclic flow variations (CFVs) were observed after administration of a single bolus injection of vapiprost as was observed in dogs (Shebski *et al.*, 1988). The animals which received the lower dose of vapiprost or the vehicle all had occlusive thrombi at times similar to those in the control group (Matsuno *et al.*, 1991), despite the platelet aggregation response to collagen being inhibited in *ex vivo*. These results are supported by the findings of Hornby *et al.* (1989). The above investigations suggest that TXA_2 is an important element in the thrombus formation on the vascular wall. Schmitz *et al.* (1985) have reported that the increased production of thromboxane at the site of the damaged arterial wall is a very potent trigger for irreversible platelet aggregation and thrombus formation. Therefore, TRAs, like vapiprost, may be very effective antithrombotic agents in clinical conditions of arterial damage and platelet deposition. The doses of vapiprost used in this experiment did not influence systemic haemodynamic parameters. Aspirin, acetylsalicylic acid (ASA), reduces platelet aggregation by irreversibly inhibiting cyclo-oxygenase and thereby preventing platelet PGH_2 and TXA_2 synthesis (Folts *et al.*, 1988). Although concurrent inhibition of endothelial cell PGI_2 production is potentially detrimental, this does not appear to have been a problem in models in which high-dose ASA has resulted in a striking improvement (Kelton *et al.*, 1978; Wu *et al.*, 1981; Zammit *et al.*, 1984).

The results of the thrombolytic study demonstrated that the administration of vapiprost increased the incidence of reperfusion, shortened the time to tPA-induced arterial thrombolysis and increased the femoral arterial blood flow after reperfusion. These results suggest that inhibition of

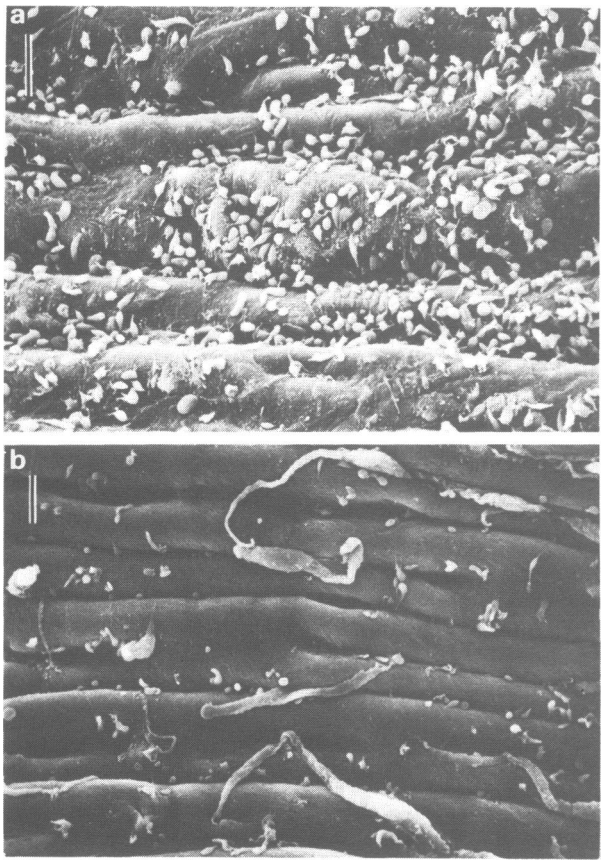

Figure 5 The luminal surface of a femoral artery after successful thrombolysis. Note the presence of platelets with pseudopods adherent to the surface of the vessel in spite of the restoration of blood flow (a). After combination thrombolytic therapy with tPA and vapiprost (0.3 mg kg^{-1} i.v.), platelets on the surface of the vessel decreased as compared with the tPA only treatment (b). The bars in both photographs denote 5 μm.

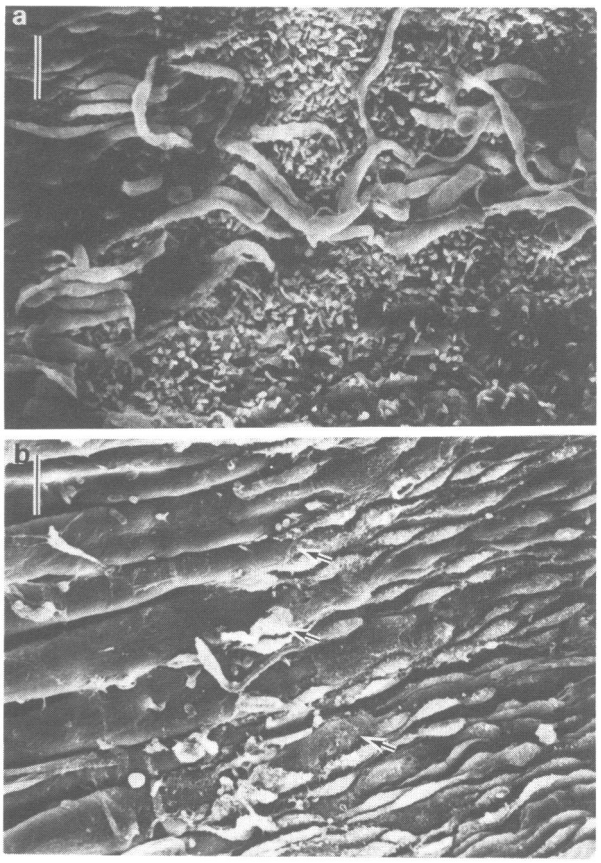

Figure 6 The luminal surface of a femoral artery fixed 1 week after successful thrombolysis with tPA alone. There are few blood cells, however, more platelets remain on the repaired endothelial cells (a). Following vapiprost treatment for 1 week, blood elements are scarcely present on the luminal surface. Arrows indicate the border line between the repaired surface of endothelial cells after injury by photochemical reaction and non-damaged surface (b). The bars in both photographs denote 5 μm.

TXA_2-mediated platelet aggregation may be beneficial in the therapeutic effectiveness of a fiblinolytic agent such as tPA. The effect may be related to platelet activation and an increase in TXA_2 that occurs as a consequence of fibrinolytic administration in experimental animals (Fitzgerald & Fitzgerald, 1989). Platelet activation may slow the rate at which thrombolysis proceeds and may play an important role in acute rethrombosis. Furthermore, scanning electron microscopy has confirmed that platelet aggregation is involved in spontaneous reocclusion in this study.

Reocclusion after reperfusion has been recognized as one of the major limitations of thrombolytic therapy. For example, the benefit of establishing coronary reperfusion is significantly offset by an acute spontaneous reocculsion rate of 20.0% to 45.0%, despite full heparinization (Collen *et al.*, 1984; Williams *et al.*, 1986; Sheehan *et al.*, 1987). In patients with myocardial infarction, coronary reocclusion can be prevented by a maintenance infusion of low doses of rtPA for up to 4 h (Gold *et al.*, 1986). However, these prolonged infusions caused a significant depletion of circulating fibrinogen of up to 50% of the initial values. In contrast, our findings have demonstrated that prevention of reocculsion by the use of combination therapy of tPA and low-dose vapiprost has been successful without prolonged tPA infusion. This supports the concept that residual platelets are one of the causes of the reocclusion. In the present study, the combination of vapiprost and tPA produced a depression of platelet reactivity and increase of blood flow after reperfusion. However, in the case of once only treatment with vapiprost, arterial blood flow was not maintained after 1 week. Scanning electron microscopy of arteries collected in animals with decreased blood flow after 1 week showed that mural thrombi were present in the lumen of the arteries. However, the depression of blood flow was prevented by continous therapy of vapiprost (1.0 mg kg^{-1} daily, p.o.) for 1 week. These examinations strongly suggest that platelet aggregation plays an important role in spontaneous and cyclical reocclusion after successful thrombolysis. The results also suggest that TXA_2 generation may be activated limiting the response to fibrinolysis as TXA_2-mediated platelet activation occurs simultaneously with clot dissolution. The inhibition of TXA_2-mediated platelet activation, as with a combination therapy between tPA and vapiprost, may provide benefit to thrombolytic therapy.

In conclusion, the results of the present study indicate that vapiprost is capable of preventing experimentally induced artery thrombosis. A combination of vapiprost and tPA may be more effective than tPA alone in enhancing the outcome of thrombolytic therapy. Continuous therapy with vapiprost after reperfusion would prevent the acute reocculsion after reperfusion.

This study was supported by Grant-in-Aid for Scientific Research 03671097 from the Ministry of Education, Science and Culture in Japan. We are grateful for the critical reading of the manuscript and helpful suggestions provided by Dr P. Lumley.

References

AIKEN, J.W., SHEBUSKI, R.J. & GORMAN, R.R. (1980). Blockage of partially obstructed coronary arteries with platelet thrombi: Comparison between its prevention with cyclooxygenase inhibitors versus prostacyclin. *Adv. Prostaglandin Thromboxane Res.*, **7**, 635–639.

AMBLER, J., BIRCH, J., MAGUIRE, E.D. & WALLIS, R.B. (1985). Role of thrombaxane A2. *Adv. Exp. Med. Biol.*, **192**, 293–308.

ASHTON, J.H., SCHMITZ, J.M., CAMPBELL, W.B., OGLETREE, M.L., RAHEJA, S., TAYLOR, A.L., FITZGERALD, C., BUJA, L.M. & WILLERSON, J.T. (1986). Inhibition of cyclic flow variations in stenosed canine coronary arteries by thromboxane A2/prostaglandin H2 receptor antagonists. *Circ. Res.*, **59**, 568–578.

BEST, L.C., HOLLAND, T.K., JONES, P.B. & RUSSELL, R.G. (1980). The interrelationship between thromboxane biosynthesis, aggregation and 5-hydroxyptamine secretion in human plates in vitro. *Thromb. Haemost.*, **43**, 38–40.

BREZINSKI, M.E., OSBORNE, J.A., YANAGISAWA, A. & LEFER, A.M. (1987). Beneficial action of the thromboxane receptor antagonist, AH-23,848, in acute myocardial ischemia. *Methods Find. Exp. Clin. Pharmacol.*, **9**, 703–709.

COLLEN, D., TOPOL, E.J., TIEFENBRUN, A.J., GOLD, H.K., WEISFELDT, M.L., SOBEL, B.E., LEINBACH, R.C., BRINKER, J.A., LUDBROOK, P.A., YASUDA, T., BULKLEY, B.H., ROBINSON, A.K., HUTTER, J.A., BELL, W.R., SPADARO, J.J., KHAW, B.A. & GROSSBARD, E.B. (1984). Coronary thrombolysis with recombinant human tissue-type plasminogenc activator: a prospective, randomized placebo-control trial. *Circulation*, **70**, 1012–1017.

FITZGERALD, D.J. & FITZGERALD, G.A. (1989). Role of thrombin and thromboxane A2 in reocclusion following coronary thrombosis with tissue-type plasminogen activator. *Proc. Natl. Acad. Sci. U.S.A.*, **86**, 7585–7589.

FOLTS, J.D. & ROWE, G.G. (1988). Epinephrine potentiation of in vivo stimuli reverses aspirin inhibition of platelet thrombus formation in stenosed canine coronary arteries. *Thromb Res.*, **50**, 507–516.

FRIEDMAN, M. & VAN DER BOVERKAMP, G.J. (1966). The pathogenesis of a coronary thrombus. *Am. J. Pathol.*, **48**, 19–44.

FUJITA, T., HASAN, S., STORER, B.L. & SHEBUSKI, R.J. (1989). Effect of selective endoperoxide/thromboxane A2 receptor antagonism with sulotroban on tPA-induced thrombolysis in a rabbit model of femoral artery thrombosis. *Fundam. Clin. Pharmacol.*, **3**, 643–653.

GOLD, H.K., LEINBACH, R.C., GARABEDIAN, H.D., YASUDA, T., JOHNS, J.A., GROSSBARD, E.B., PALACIOS, I. & COLLEN, D. (1986). Acute coronary reocculsion after thrombolysis with recombinant human tissue-type plasminogen activator: preventation by a maintenance infusion. *Circulation*, **73**, 347–352.

HANASAKI, K. & ARITA, H. (1988). Characterization of a new compound, S-145, as a specific TXA2 receptor antagonist in platelets. *Thromb. Res.*, **50**, 365–376.

HORNBY, E.J., FOSTER, M.R., McCABE, P.J. & STRATTON, L.E. (1989). The inhibitory effect of GR32191, a thromboxane receptor blocking drug, on human platelet aggregation, adhesion and secretion. *Thromb Haemost.*, **61**, 429–436.

IK-KYUNG, J., HERMAN, K.G., ANDREW, A.Z., JOHN, T.F., ROBERT, E.H., ROBERT, C.L., JAMES, W.M. & DESIRE, C. (1989). Differential sensitivity of erythrocyte-rich and platelet-rich arterial thrombi to lysis with recombinant tissue-type plasminogen activator. *Circulation*, **79**, 920–928.

KELTON, J.G., HIRSH, J., CARTER, C.J. & BUCHANAN, M.R. (1978). Thrombogenic effect of high-dose aspirin in rabbits. *J. Clin. Invest.*, **62**, 892–895.

WU, K.K., CHEN, Y.C., FORDHANS, E., TS'AO, C.H. & MATAYOSHI, D. (1981). Differential effects of two doses of aspirin on platelet-vessel wall interaction in vivo. *J. Clin. Invest.*, **68**, 382–387.

LUMLEY, P., WHITE, B.P. & HUMPHREY, P.P.A. (1989). GR32191, a highly potent and specific thromboxane A_2 receptor blocking drug on platelet and vascular and airway smooth muscle *in vitro*. *Br. J. Pharmacol.*, **97**, 783–794.

MATSUNO, H., UEMATSU, T., NAGASHIMA, S. & NAKASHIMA, M. (1991). Photochemically induced thrombosis model in rat femoral artery and evaluation of effects of heparin and tissue-type plasminogen activator with use of this model. *J. Pharmacol. Method*, **25**, 303–318.

McCABE, P.J., STRATTON, L.E., HORMBY, E.J. & FOSTER, M. (1987). Inhibition of guinea-pig platelet function in vivo and using the thromboxane A2 antagonist AH23848 and GR32191. *Thromb. Haemostas.*, **58**, 182 (Abstr 669).

OGLETREE, M.L., HARRIS, D.N., GREENBERG, R., HASLANGER, M.F. & NAKANE, M. (1985). Pharmacological action of SQ29548, a novel selective thromboxane antagonist. *J. Pharmacol. Exp. Ther.*, **234**, 435–441.

SHEBSKI, R.J., SMITH, J.M. Jr, STORER, B.L., GRANETT, J.R. & BUGELSKI, P.J. (1988). Influence of selective endoperoxide thromboxane A2 receptor antagonism with sulotroban on lysis time and reocclusion rate after tissue plasminogen activator-induced coronary thrombolysis in the dog. *J. Pharmacol. Exp. Ther.*, **246**, 790–796.

SCHMITZ, J.M., APPRILL, P.G., BUJA, L.M., WILLERSON, J.T. & CAMPBELL, W.B. (1985). Vascular prostaglandin and thromboxane production in a cainine model of myocardial ischemia. *Circ. Res.*, **57**, 223–231.

SHEEHAN, F.H., BRAUNWALD, E., CANNER, P., DODGE, H.T., GORE, J., VAN NATTA, P., PASSAMANI, E.R. & CO-INVESTIGATORS (1987). The effect of intravenous thrombolytic therapy on left ventricular function: a report on tissue-type plasminogen activator and streptokinase from the thrombolysis in myocardial infarction (TIMI Phase I) trial. *Circulation*, **75**, 817–829.

WILLIAMS, D.O., BORER, L., BRAUNWALD, E. & CO-INVESTIGATORS (1986). Intravenous recombinant tissue-type plasminogen activator in patients with acute myocardial infarction: a report from the NHLBI Thrombosis in Myocardial Infarction Trial. *Circulation*, **73**, 338–346.

ZAMMIT, M., KAPLAN, S., SAUVAGE, L.R., MARCOE, K.F. & WU, H.D. (1984). Aspirin therapy in small-caliber arterial prostheses: long-term experimental observations. *J. Vasc. Surg.*, **1**, 839–851.

(Received November 26, 1991
Revised January 21, 1992
Accepted February 27, 1992)

Br. J. Pharmacol. (1992), **106**, 539–543

Receptor-coupled shortening of α-toxin-permeabilized single smooth muscle cells from the guinea-pig stomach

Teruaki Ono, ‡Mitsuo Mita, Osamu Suga, ‡Takao Hashimoto, [1]Kazuhiko Oishi & Masaatsu K. Uchida

Department of Molecular Pharmacology and ‡Department of Pharmacology, Meiji College of Pharmacy, 1-35-23 Nozawa, Setagaya-ku, Tokyo 154, Japan

1 Isolated single smooth muscle cells from the fundus of the guinea-pig stomach were permeabilized by use of *Staphylococcus aureus* α-toxin. Receptor-coupled shortening of individual cells was monitored under phase contrast microscopy.

2 Most of the isolated cells responded to 0.6 μM Ca^{2+}, but not to 0.3 μM Ca^{2+}, with a resulting maximal shortening to approximately 65% of the resting cell length. The contractile activity of these permeabilized cells lasted for several hours and repeated shortening was readily achieved after washing out.

3 Addition of acetylcholine (ACh) at a maximal concentration (10 μM) resulted in a marked decrease in the concentration of Ca^{2+} required to trigger a threshold response from 0.6 μM to 0.2 μM, and 1 mM guanosine 5′-diphosphate (GDP) blocked this decrease. Moreover, treatment with 100 μM guanosine 5′-triphosphate (GTP) mimicked the action of ACh.

4 Addition of 100 μM inositol 1,4,5-trisphosphate ($InsP_3$) with 0.2 μM Ca^{2+} did not cause cell shortening, whereas 10 μM ACh with 0.2 μM Ca^{2+} did, suggesting that $InsP_3$-induced Ca^{2+} release is not involved in ACh-operated cell shortening.

5 The present study demonstrates an α-toxin-permeabilized single smooth muscle cell preparation which retains its receptor function and also provides an insight into mechanisms leading to augmentation of Ca^{2+} sensitivity by stimulation of muscarinic receptors or GTP-binding proteins.

Keywords: Ca^{2+} sensitivity; permeabilization; smooth muscle cells; muscarinic receptor; GTP-binding protein

Introduction

One approach to elucidate the intracellular mechanisms underlying smooth muscle contraction involves permeabilization of the plasma membrane, which permits manipulation of the intracellular environment. α-Toxin, a cytolytic exotoxin secreted by *Staphylococcus aureus* that forms pores of 2–3 nm diameter in the plasma membrane, has been used as a tool for selectively permeabilizing the plasma membrane of, for example, secretory cells to small molecules with molecular weights up to a thousand daltons (Füssle *et al.*, 1981; Ahnert-Hilger *et al.*, 1985; Hohman, 1988). This technique has been applied to whole smooth muscles and preparations where intact receptors and signal transduction systems were retained (Nishimura *et al.*, 1988; Kitazawa *et al.*, 1989; 1991). It thus provides a valuable new means of investigating the mechanisms of stimulus-contraction coupling. One of the main shortcomings when applying this technique to intact smooth muscle preparations is the difficulty of ensuring homogeneous permeabilization of all the cells. In order to overcome this problem, we have extended the method to isolated single smooth muscle cells. We have shown for the first time that α-toxin-permeabilized single muscle cells retain their receptor function. Moreover, these permeabilized single cells from the fundus of the stomach are suitable for studying the increase in Ca^{2+}-sensitivity induced by stimulation of muscarinic receptors or guanosine 5′-triphosphate (GTP)-binding proteins.

Methods

Preparation of α-toxin

α-Toxin was purified from the culture supernatant of *Staphylococcus aureus* strain Wood 46 by the method of Hohman (1988). The haemolytic activity of α-toxin was checked with rabbit erythrocytes. Purified α-toxin was 80–85% pure as judged by sodium dodecyl sulphate polyacrylamide gel electrophoresis. The purified toxin permeabilized rat basophilic leukaemia (RBL-2H3) cells to [^{3}H]-adenine but did not permit release of lactate dehydrogenase. Protein was determined according to Lowry *et al.* (1951) with bovine serum albumin used as standard.

Cell isolation

Smooth muscle cells were isolated from the fundus of the guinea-pig stomach by a modification of the method of Mita & Uchida (1987). Guinea-pigs (400–800 g) were killed by a blow on the neck and exsanguinated. The stomach was removed immediately and the fundus was resected. The serosa and mucosa were dissected from the muscle layer of the fundus. Strips of fundic muscle were suspended in normal N-2-hydroxyethylpiperazine-N′-2-ethanesulphonic acid (HEPES)-Tyrode solution bubbled with air at 37°C for 90 min and then transferred to Ca^{2+}-free HEPES-Tyrode solution (Ca^{2+}-free solution) bubbled with air at 37°C for 75 min. The normal solution had the following composition (mM): NaCl 137, KCl 2.7, $CaCl_2$ 1.8, $MgCl_2$ 1.0, glucose 5.6 and HEPES 4.2 (pH 7.4 at 37°C). The Ca^{2+}-free solution had the same composition as normal HEPES-Tyrode solution except that $CaCl_2$ was omitted. The tissue was then minced and incubated with 0.5 mg ml^{-1} collagenase (127.5 unit ml^{-1}), 0.125 mg ml^{-1} elastase and 0.1 mg ml^{-1} trypsin inhibitor in 2 ml of Ca^{2+}-free solution containing 4% bovine serum albumin at 37°C for 80 min with gentle stirring. The suspension was diluted with 8 ml of Ca^{2+}-free solution containing 4% bovine serum albumin and was centrifuged at 120 *g*. This washing procedure was repeated once more. The cells were suspended in 4 ml of Ca^{2+}-free solution and dispersed with a wide-bore pipette. The viability of isolated single cells,

[1] Author for correspondence.

measured by trypan blue exclusion, was more than 90%. The mean length of intact single cells obtained by this method was 112 ± 3 μm (mean ± s.e.mean, $n = 21$). Approximately 50% of the intact smooth muscle cells retained the ability to contract in response to acetylcholine (ACh); these cells were spindle shaped and bright, and their surface was smooth.

Measurement of shortening of single cells

Shortening of individual isolated smooth muscle cells was measured by the method of Mita & Uchida (1987). In brief, the cell suspension was placed on a silicon-coated glass slide with a cover slip. The cells were perfused continuously with Ca^{2+}-free solution at 30°C. The perfusion fluid was introduced from one side of the slide and blotted off with filter paper from the other side. The silicon-coated glass slide was placed on the temperature-controlled stage (30°C) of a phase contrast microscope. The shortening of individual cells observed by phase contrast microscopy was recorded on a video tape and the cell length was measured with the ARUGUS-10 Image Analyzer (Hamamatsu Photonics K.K., Japan).

Cell permeabilization

In order to ensure that intact isolated cells did not respond to extracellular Ca^{2+}, individual cells were perfused before permeabilization with the cytosolic substitution solution containing an ascending concentration of free Ca^{2+} buffered at 10 nM to 30 μM. The cytosolic substitution solution had the following composition (mM): potassium propionate 114, glycoletherdiamine-N,N,N',N'-tetraacetic acid (EGTA) 1, $MgCl_2$ 4, ATP 4, creatine phosphate 10, and piperazine-*N,N'-bis* (2-ethanesulphonic acid) (PIPES) 20 (pH 7.1 at 30°C). Free Ca^{2+} concentrations were determined according to the method of Harafuji & Ogawa (1980). After washing the cells with the Ca^{2+}-free cytosolic substitution solution (the free Ca^{2+} concentration was estimated to be 2.5 nM), permeabilization was achieved by perfusing with the solution containing 10 μg ml^{-1} α-toxin and 0.1 μM Ca^{2+} for 3 min. α-Toxin was then washed out by perfusing with the Ca^{2+}-free cytosolic substitution solution, and the effectiveness of permeabilization was checked by exposing the cells to the cytosolic substitution solution containing an ascending concentration of free Ca^{2+} buffered at 10 nM to 3 μM, and observing shortening. After extensive washing with the Ca^{2+}-free cytosolic substitution solution for 20 min, responding cells were isolated and used for experimentation. Since the contractile response occurred within 90 s in all cases, the time of exposure at each concentration of Ca^{2+} was 120 s. The first shortening was evoked by perfusion with the cytosolic substitution solution containing an ascending concentration of free Ca^{2+} buffered at 10 nM to 3 μM. After extensive washing with the Ca^{2+}-free cytosolic substitution solution for 20 min, a second shortening was evoked with an ascending concentration of Ca^{2+} in the presence or absence of ACh, GTP, or guanosine 5'-diphosphate (GDP).

Drugs used

Collagenase (type 1), bovine serum albumin (fraction V), creatine phosphate and adenosine 5'-triphosphate dipotassium salt (ATP) were purchased from Sigma Chemical Co. (St. Louis, MO, U.S.A.); elastase, guanosine 5'-diphosphate dilithium salt (GDP), and guanosine 5'-triphosphate disodium salt (GTP) were from Boehringer; acetylcholine (ACh, Ovisot) was from Daiichi Pharmaceutical Co., Ltd. (Tokyo, Japan); inositol 1,4,5-trisphosphate ($InsP_3$) was from Wako Pure Chemical Industries (Osaka, Japan); N-2-hydroxyethylpiperazine-N'-2-ethanesulphonic acid (HEPES), piperazine-N,N'-*bis* (2-ethanesulphonic acid) (PIPES), and glycoletherdiamine-N,N,N',N'-tetraacetic acid (EGTA) were from Dojindo Laboratories (Kumamoto, Japan); potassium propionate was from Nakarai Tesque (Kyoto, Japan). All other chemicals were of reagent grade.

Results

Figure 1 shows a typical shortening of an α-toxin-permeabilized isolated smooth muscle cell from the fundus of the guinea-pig stomach induced by increasing free Ca^{2+} in the cytosolic substitution solution. In most cases, 0.6 μM Ca^{2+} caused maximal shortening although 0.3 μM or lower Ca^{2+} did not. In all experiments, the contractile response occurred within 90 s and reached a steady state within 60 s. The cells were relaxed again by washing with the Ca^{2+}-free cytosolic substitution solution. In a control study in which the same procedure was carried out without α-toxin, Ca^{2+} in concentrations up to 30 μM did not cause cell shortening. The contractile activity was abolished by removal of ATP and creatine phosphate from the cytosolic substitution solution.

Shortening could be repeatedly evoked by the same threshold concentration of Ca^{2+} for a period of 3 h, but incomplete relaxation in the presence of the Ca^{2+}-free cytosolic substitution solution resulted in a reduction in the absolute magnitude of subsequent responses (Figure 2A). The data shown in Figure 2A were, therefore, normalized by taking the baseline and the maximal shortening of each cell as 0 and 100%, respectively (Figure 2B). Threshold responses to Ca^{2+} were reduced to 0.2 μM from 0.6 μM in the presence of ACh (10 μM) (Figures 2 and 3). The normalized concentration-response relationships to Ca^{2+} in the presence of ACh were identical in repeated experiments despite incomplete relaxation between cycles (Mita & Uchida, 1987).

Addition of 1 mM GDP to the perfusion solution blocked the sensitization to Ca^{2+} induced by ACh (10 μM) (Figure 3). In order to determine if this effect was evoked as a result of

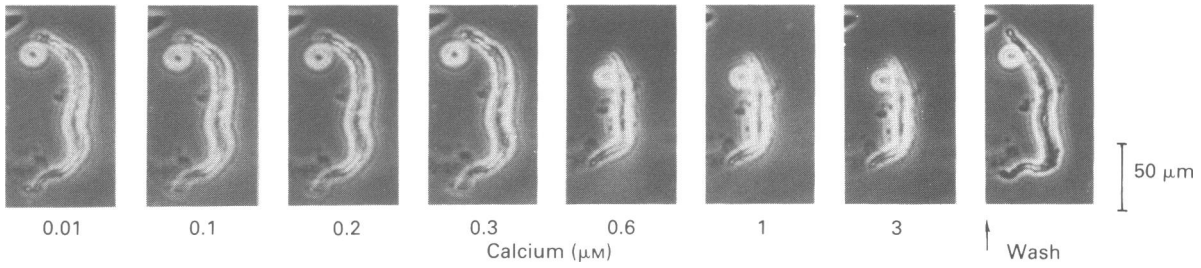

Figure 1 Phase contrast photomicrographs showing the typical shortening of an α-toxin-permeabilized single smooth muscle cell from the fundus of guinea-pig stomach in response to increasing free Ca^{2+}. After permeabilization and extensive washing with the Ca^{2+}-free cytosolic substitution solution for 20 min, cell shortening was evoked by perfusion with the cytosolic substitution solution containing an ascending concentration of free Ca^{2+} buffered at 10 nM to 3 μM. The cell was re-extended after washing with the Ca^{2+}-free cytosolic substitution solution for 20 min. The bar represents 50 μm.

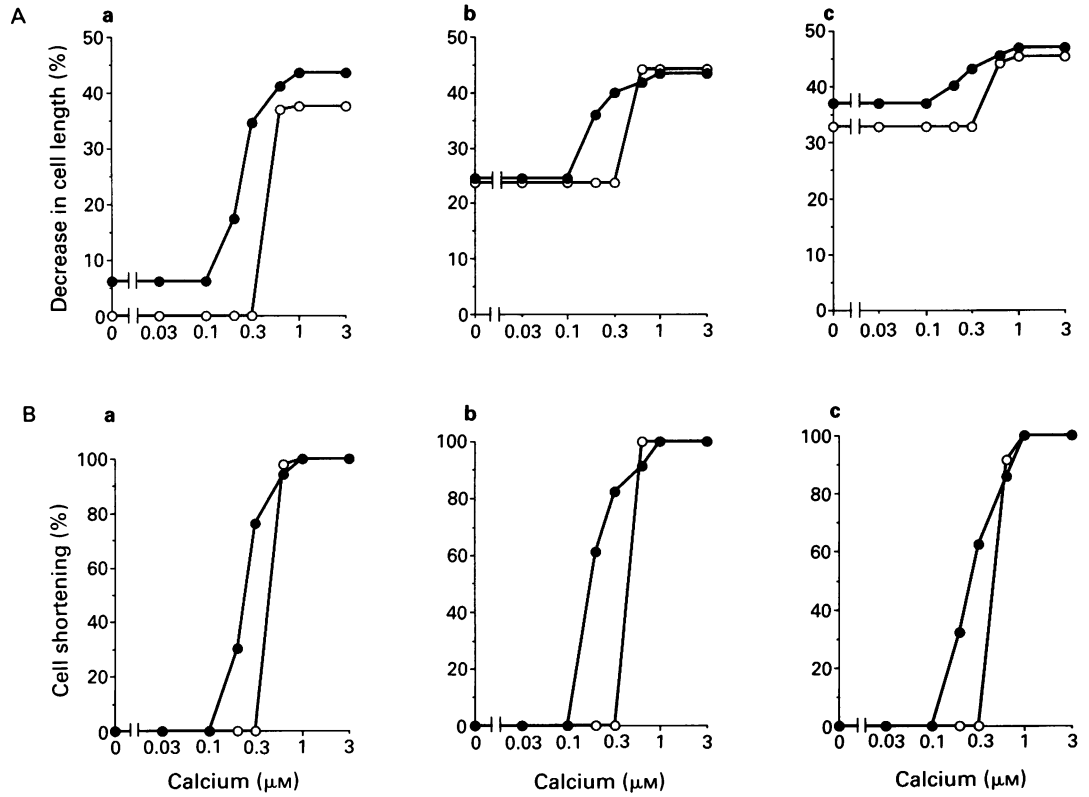

Figure 2 Responses of an α-toxin-permeabilized smooth muscle cell to repeated addition of free Ca^{2+} in the presence (●) and absence (○) of acetylcholine (ACh, 10 μM). (A) After washing the α-toxin-permeabilized smooth muscle cell with the Ca^{2+}-free cytosolic substitution solution for 20 min, the cell was perfused with the cytosolic substitution solution containing an ascending concentration of free Ca^{2+} buffered at 10 nM to 3 μM. The cell was allowed to re-extend by washing with the Ca^{2+}-free cytosolic substitution solution for 20 min, and then perfused with the cytosolic substitution solution containing an ascending concentration of free Ca^{2+} in the presence of ACh (a). This procedure was repeated twice more (b, 2nd; c, 3rd). The ordinate scale in A represents the changes in cell length as a percentage of the original cell length. (B) The data shown in (A) normalized by taking the baseline and the maximal shortening as 0 and 100%, respectively, in each case.

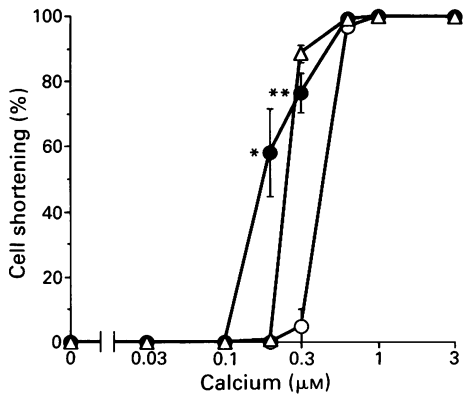

Figure 3 Effect of acetylcholine (ACh) on Ca^{2+}-induced shortening of α-toxin-permeabilized single smooth muscle cells and its blockade by guanosine 5'-diphosphate (GDP). After washing the α-toxin-permeabilized smooth muscle cell with the Ca^{2+}-free cytosolic substitution solution for 20 min, the first shortening was evoked by perfusion with the cytosolic substitution solution containing an ascending concentration of free Ca^{2+} buffered at 10 nM to 3 μM (○). The cells were allowed to re-extend by washing with the Ca^{2+}-free cytosolic substitution solution for 20 min, and a second shortening was evoked as before but in the presence of 10 μM ACh (●). After washing for 20 min, the next shortening was evoked in the presence of 10 μM ACh plus 1 mM GDP (△). The values were plotted by taking the baseline and the maximal shortening of each cell as 0 and 100%, respectively. Points and vertical bars represent means ± s.e.means from five independent experiments. Statistical significance was determined by Student's *t* test (paired): $*P<0.02$; $**P<0.01$.

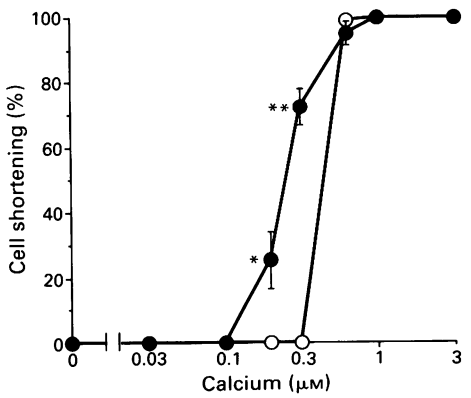

Figure 4 Effect of guanosine 5'-triphosphate (GTP) on Ca^{2+}-induced shortening of α-toxin-permeabilized single smooth muscle cells. After washing the α-toxin-permeabilized smooth muscle cell with the Ca^{2+}-free cytosolic substitution solution for 20 min, the first shortening was evoked by perfusion with the cytosolic substitution solution containing an ascending concentration of free Ca^{2+} buffered at 10 nM to 3 μM (○). The cells were allowed to re-extend by washing with the Ca^{2+}-free cytosolic substitution solution for 20 min, and the next shortening was evoked by an ascending concentration of Ca^{2+} in the presence of 100 μM GTP (●). GTP alone without Ca^{2+} did not influence cell length. The values were plotted by taking the baseline and the maximal shortening of each cell as 0 and 100%, respectively. Points and vertical bars represent means ± s.e.means from six independent experiments. Statistical significance was determined by Student's *t* test (paired): $*P<0.05$; $**P<0.001$.

activation of a GTP-binding protein(s), the effect of GTP was investigated. As shown in Figure 4, 100 μM GTP decreased the threshold concentration for Ca^{2+} from 0.6 μM to 0.2 μM.

Discussion

To date, there have been no reports of isolated single smooth muscle cells being permeabilized with α-toxin. The present study indicates for the first time that α-toxin is a useful tool to permeabilize isolated smooth muscle cells and still retain receptor and signal transduction systems. Detergents such as saponin and Triton X-100 have been widely used for the permeabilization of intact smooth muscle strips and isolated smooth muscle cells (Endo *et al.*, 1977; Gordon, 1978; Obara & Yamada, 1984). A major disadvantage of these chemically skinned muscles is a loss of receptor function (Itoh *et al.*, 1983; Somlyo *et al.*, 1985). Furthermore, detergents destroy the membranes of intracellular organelles (Ahnert-Hilger *et al.*, 1985; Knight & Scrutton, 1986) and interfere with proteins involved in stimulus-contraction coupling.

α-Toxin is a cytolytic exotoxin secreted by *Staphylococcus aureus* that selectively permeabilizes the plasma membranes of eucaryotic cells to small molecules such as ions and nucleotides (Füssle *et al.*, 1981; Ahnert-Hilger *et al.*, 1985; Hohman, 1988). The concentration of ions and small molecules in the cell cytosol can therefore be controlled precisely and specific molecules can be introduced directly.

Addition of 0.6 μM free Ca^{2+} resulted in cell shortening and the removal of Ca^{2+} resulted in relaxation, directly supporting the general idea that contractile activity is determined by increasing the level of intracellular free Ca^{2+} (Bolton, 1979). Our results reported here are in agreement with the calcium sensitivity (half-maximal contraction in the range from 0.3 to 1 μM) reported by others using α-toxin-permeabilized smooth muscle tissues (Nishimura *et al.*, 1988; Kitazawa *et al.*, 1989; 1991). However, one of the obvious discrepancies is that the concentration-response relationship to free Ca^{2+} was very steep in the present study, showing an all-or-none rather than a graded response (Mita & Uchida, 1991).

Augmentation of Ca^{2+}-sensitivity in receptor-operated contraction has been documented in studies using intact smooth muscles (Karaki *et al.*, 1988) and intact α-toxin-permeabilized smooth muscles (Nishimura *et al.*, 1988; Kitazawa *et al.*, 1989), and this was shown to be mediated by GTP-binding protein(s). In our present study, muscarinic receptor stimulation by ACh decreased the concentration of Ca^{2+} required for the threshold response and consequently, converted it to a graded rather than an all-or-none response. Furthermore, addition of GTP mimicked the ability of ACh to enhance sensitivity to Ca^{2+}. These findings suggest that a GTP-binding protein(s) regulates the sensitivity of the contractile proteins to Ca^{2+}. Nonhydrolyzable GTP analogues such as GTPγS are commonly used to activate GTP-binding proteins because GTP is promptly hydrolyzed by endogenous GTPase activity. However, in the present system, GTP itself was sufficient for activation, probably because it was supplied continuously in the perfusate. The increase in sensitivity to Ca^{2+} reported here has also been observed in α-toxin-permeabilized intact smooth muscles (Nishimura *et al.*, 1988; Kitazawa *et al.*, 1989; 1991).

The heterotrimeric signal transducing GTP-binding proteins are now well known to couple cell surface receptors to target enzymes such as phospholipase C and adenylate cyclase (Verghese *et al.*, 1987; Freissmuth *et al.*, 1989). It has been shown that stimulation of various cell surface receptors leads to an activation of phospholipase C via a GTP-binding protein (Cockcroft & Gomperts, 1985; Ashkenazi *et al.*, 1989). The degradation of phosphatidylinositol 4,5-bisphosphate by phospholipase C leads to the production of two second messengers $InsP_3$ and diacylglycerol. $InsP_3$ releases Ca^{2+} from intracellular Ca^{2+} storage sites in various types of smooth muscle (Suematsu *et al.*, 1984; Bitar *et al.*, 1986), whereas diacylglycerol activates protein kinase C in a concerted manner with membrane phospholipids and Ca^{2+}. We found that addition of 100 μM $InsP_3$ in the presence of 0.2 μM free Ca^{2+} did not cause cell shortening (data not shown) although 10 μM ACh in the presence of 0.2 μM free Ca^{2+} did (Figure 2). These results suggest that $InsP_3$-induced Ca^{2+} release is not involved in the receptor-coupled shortening of the permeabilized cells. Our observation is therefore different from those obtained with rabbit permeabilized pulmonary and mesenteric arteries and pig portal vein, where $InsP_3$ in the range 0.5–30 μM caused tension development (Somlyo *et al.*, 1985; Itoh *et al.*, 1985; Kitazawa *et al.*, 1989). The phasic contractions of these smooth muscles were reported to be dependent on Ca^{2+} release from intracellular Ca^{2+} stores (Itoh *et al.*, 1985; Iino *et al.*, 1988). Therefore, there is some dispute as to the contribution of intracellular stored Ca^{2+} to contraction. However, at present, we cannot eliminate an alternative possibility that the lack of response to $InsP_3$ is simply due to the inability to produce a significant rise in the Ca^{2+} level because of the diffusion of Ca^{2+} out of permeabilized cells.

In conclusion, our present study using α-toxin-permeabilized single smooth muscle cells provides direct evidence that receptor-operated augmentation of Ca^{2+} sensitivity is a cellular event. This preparation may prove valuable in investigating further the mechanisms underlying receptor-operated augmentation of Ca^{2+} sensitivity.

References

AHNERT-HILGER, G., BHAKDI, S. & GRATZL, M. (1985). Minimal requirements for exocytosis: a study using PC 12 cells permeabilized with *Staphylococcal* α-toxin. *J. Biol. Chem.*, **260**, 12730–12734.

ASHKENAZI, A., PERALTA, E.G., WINSLOW, J.W., RAMACHANDRON, J. & CAPON, D.J. (1989). Functionally distinct G proteins selectively couple different receptors to PI hydrolysis in the same cell. *Cell*, **57**, 487–493.

BITAR, K.N., BRADFORD, P.G., PUTNEY, J.W. Jr. & MAKHLOUF, G.B. (1986). Stoichiometry of contraction and Ca^{2+} mobilization by inositol, 1,4,5-trisphosphate in isolated gastric smooth muscle cells. *J. Biol. Chem.*, **261**, 16591–16596.

BOLTON, T.B. (1979). Mechanisms of action of transmitters and other substances on smooth muscle. *Physiol. Rev.*, **59**, 606–718.

COCKCROFT, S. & GOMPERTS, B.D. (1985). Role of guanine nucleotide binding protein in the activation of polyphosphoinositide phosphodiesterase. *Nature*, **314**, 534–536.

ENDO, M., KITAZAWA, T., YAGI, S., IINO, M. & KAKUTA, Y. (1977). Some properties of chemically skinned smooth muscle fibers. In *Excitation-Contraction Coupling in Smooth Muscle*. ed. Casteels, R., Godfraind, T. & Rüegg, J.C. pp. 199–209. New York: Elsevier/North-Holland.

FREISSMUTH, M., CASEY, P.J. & GILMAN, A.G. (1989). G proteins control diverse pathways of transmembrane signaling. *FASEB J.*, **3**, 2125–2131.

FÜSSLE, R., BHAKDI, S., SZIEGOLEIT, A., TRANUM-JENSEN, J., KRANZ, T. & WELLENSIEK, H.-J. (1981). On the mechanism of membrane damage by *Staphylococcus aureus* α-toxin. *J. Cell Biol.*, **91**, 83–94.

GORDON, A.R. (1978). Contraction of detergent-treated smooth muscle. *Proc. Natl. Acad. Sci. U.S.A.*, **75**, 3527–3530.

HARAFUJI, H. & OGAWA, Y. (1980). Re-examination of the apparent binding constant of ethylene glycol *bis*(β-aminoethyl ether)-N,N,N′,N′-tetraacetic acid with calcium around neutral pH. *J. Biochem.*, **87,** 1305–1312.

HOHMAN, R.J. (1988). Aggregation of IgE receptors induces degranulation in rat basophilic leukemia cells permeabilized with α-toxin from *Staphylococcus aureus*. *Proc. Natl. Acad. Sci. U.S.A.*, **85,** 1624–1628.

IINO, M., KOBAYASHI, T. & ENDO, M. (1988). Use of ryanodine for functional removal of the calcium store in smooth muscle cells of the guinea-pig. *Biochem. Biophys. Res. Commun.*, **152,** 417–422.

ITOH, T., KANMURA, Y. & KURIYAMA, H. (1985). A23187 increases calcium permeability of store sites more than of surface membranes in the rabbit mesenteric artery. *J. Physiol.*, **359,** 467–484.

ITOH, T., KURIYAMA, H. & SUZUKI, H. (1983). Differences and similarities in the noradrenaline- and caffeine-induced mechanical responses in the rabbit mesenteric artery. *J. Physiol.*, **337,** 609–629.

KARAKI, H., SATO, K. & OZAKI, H. (1988). Different effects of norepinephrine and KCl on the cytosolic Ca^{2+}-tension relationship in vascular smooth muscle of rat aorta. *Eur. J. Pharmacol.*, **151,** 325–328.

KITAZAWA, T., GAYLINN, B.D., DENNEY, G.H. & SOMLYO, A.P. (1991). G-protein-mediated Ca^{2+} sensitization of smooth muscle contraction through myosin light chain phosphorylation. *J. Biol. Chem.*, **266,** 1708–1715.

KITAZAWA, T., KOBAYASHI, S., HORIUTI, K., SOMLYO, A.V. & SOMLYO, A.P. (1989). Receptor-coupled, permeabilized smooth muscle: role of the phosphatidylinositol cascade, G-proteins, and modulation of the contractile response to Ca^{2+}. *J. Biol. Chem.*, **264,** 5339–5342.

KNIGHT, D. & SCRUTTON, M. (1986). Gaining access to the cytosol: the technique and some applications of electropermeabilization. *Biochem. J.*, **234,** 497–506.

LOWRY, O.H., ROSEBROUGH, N.J., FARR, A.L. & RANDALL, R.J. (1951). Protein measurement with the Folin phenol reagent. *J. Biol. Chem.*, **193,** 265–275.

MITA, M. & UCHIDA, M.K. (1987). Desensitization of isolated smooth muscle cells from guinea pig taenia caecum to acetylcholine. *Can. J. Physiol. Pharmacol.*, **65,** 293–297.

MITA, M. & UCHIDA, M.K. (1991). The change in the threshold for short-term desensitization in isolated smooth muscle cells showing an all-or-none response to acetylcholine. *Br. J. Pharmacol.*, **104,** 603–608.

NISHIMURA, J., KOLBER, M. & VAN BREEMEN, C. (1988). Norepinephrine and GTP-γ-S increase myofilament Ca^{2+} sensitivity in α-toxin permeabilized arterial smooth muscle. *Biochem. Biophys. Res. Commun.*, **157,** 677–683.

OBARA, K. & YAMADA, T. (1984). Some properties of chemically skinned single smooth muscle cells. *Jpn. J. Physiol.*, **34,** 1089–1104.

SOMLYO, A.V., BOND, M., SOMLYO, A.P. & SCARPA, A. (1985). Inositol trisphosphate-induced calcium release and contraction in vascular smooth muscle. *Proc. Natl. Acad. Sci. U.S.A.*, **82,** 5231–5235.

SUEMATSU, E., HIRATA, M., HASHIMOTO, T. & KURIYAMA, H. (1984). Inositol 1,4,5-trisphosphate releases Ca^{2+} from intracellular store sites in skinned single cells of porcine coronary artery. *Biochem. Biophys. Res. Commun.*, **120,** 481–485.

VERGHESE, M.W., CHARLES, L., JAKOI, L., DILLON, S.B. & SNYDERMAN, R. (1987). Role of a guanine nucleotide regulatory protein in the activation of phospholipase C by different chemoattractants. *J. Immunol.*, **138,** 4374–4380.

(Received January 2, 1992
Revised February 10, 1992
Accepted February 28, 1992)

Br. J. Pharmacol. (1992), **106**, 544–549

Pharmacological characterization of 5-hydroxytryptamine-induced excitation of afferent cervical vagus nerve in anaesthetized rats

[1]Mitsuhiro Yoshioka, Toshiya Ikeda, Masayuki Abe, Hiroko Togashi, *Masaru Minami & Hideya Saito

First Department of Pharmacology, Hokkaido University School of Medicine, Sapporo 060, Japan and *Department of Pharmacology, Higashi-Nippon-Gakuen University Faculty of Pharmaceutical Sciences, Ishikari-Tobetsu, Hokkaido 061-02, Japan

1 An excitatory response to 5-hydroxytryptamine (5-HT) was measured from the afferent vagus nerve of anaesthetized rats. Measurements were determined by an extracellular recording from the whole nerve.

2 Intravenous bolus injection of 5-HT (1.56–100 $\mu g\,kg^{-1}$) evoked a dose-dependent excitation of afferent vagus nerve activity. This response was blocked not only by a selective 5-HT_3 receptor antagonist, GR38032F (10 and 100 $\mu g\,kg^{-1}$), but also by a 5-HT_2 receptor antagonist, ketanserin (10 and 100 $\mu g\,kg^{-1}$).

3 Both a 5-HT_3 receptor agonist, 2-methyl-5-HT (3.12–100 $\mu g\,kg^{-1}$), and a 5-HT_2 receptor agonist, α-methyl-5-HT (3.12–50 $\mu g\,kg^{-1}$), produced a dose-dependent excitation of afferent vagus nerve activity. These excitatory effects were antagonized by GR38032F (10 $\mu g\,kg^{-1}$) and ketanserin (10 $\mu g\,kg^{-1}$), respectively.

4 A 5-HT_1 like receptor agonist, 5-carboxamidotryptamine (50 $\mu g\,kg^{-1}$), and a putative 5-HT_4 receptor agonist, 5-methoxytryptamine (100 $\mu g\,kg^{-1}$), failed to produce excitatory effects on the afferent vagus nerve.

5 These results suggest that the 5-HT-induced excitatory response of the afferent vagus nerve might be mediated not only via 5-HT_3 receptors but also via 5-HT_2 receptors in anaesthetized rats. It is unlikely, however, that either 5-HT_1-like or putative 5-HT_4 receptors are involved in the excitatory response of the afferent vagus nerve to 5-HT.

Keywords: 5-Hydroxytryptamine; sensory neurone; vagus nerve activity; 5-HT receptors

Introduction

The excitatory action of 5-hydroxytryptamine (5-HT) is seen in a variety of neurones in the mammalian peripheral nervous system (Fozard, 1984). In particular, 5-HT has a potent depolarizing action on the vagal afferent nerve (Round & Wallis, 1986; Ireland & Tyers, 1987). Most previous reports have concerned *in vitro* experiments, i.e., isolated vagus nerve, nodose ganglion or superior cervical ganglion without nerve endings. The depolarization of these neurones and ganglia by 5-HT *in vitro* is blocked by 5-HT_3 receptor antagonists but not by the cholinoceptor antagonists, atropine, hexamethonium or the 5-HT_2 receptor antagonists, methysergide or ketanserin (Neto, 1978; Higashi & Nishi, 1982; Ireland *et al.*, 1982; Wallis *et al.*, 1982; Bradly *et al.*, 1986; Round & Wallis, 1986; Ireland & Tyers, 1987). However, many peripheral sensory nerve endings are potently excited by 5-HT and this elicits prominent reflex effects on the cardiopulmonary system (Wallis, 1989). Kirby & McQueen (1984) reported that intracarotid injection of 5-HT in cats produces a triphasic chemoexcitation of the carotid sinus nerve. Both the initial transient chemoexcitation and the subsequent depression are virtually abolished by a 5-HT_3 receptor antagonist, MDL 72222. On the other hand, the delayed excitation is substantially reduced by a 5-HT_2 receptor antagonist, ketanserin. These findings suggest that *in vivo* responses cannot be extrapolated from *in vitro* responses because 5-HT_2 receptors as well as 5-HT_3 receptors may be involved in the excitatory response to 5-HT *in vivo*. To date, there is no literature concerning the pharmacological characteristics of the effects of 5-HT on afferent vagus nerve activity *in vivo*. In this study, therefore, direct extracellular recordings of the afferent cervical vagus nerve of anaesthetized rats were made in order to elucidate the pharmacological characteristics of the receptors mediating this 5-HT-induced excitatory effect *in vivo*.

Methods

General

Male Wistar rats (320–400 g b.w. and 8–12 weeks old) were used (Shizuoka Laboratory Animal Center, Hamamatsu, Japan). Rats were anaesthetized i.p. with 500 $mg\,kg^{-1}$ of urethane and 50 $mg\,kg^{-1}$ of α-chloralose. After immobilization with gallamine triethiodide (10 $mg\,kg^{-1}$, i.v.), respiration was maintained through a tracheal cannula connected to a rodent respirator (Harvard apparatus, model 683). End tidal O_2 and CO_2 concentrations were measured with an expired gas monitor (Nippondenki San-ei, Tokyo, Japan, IH26). Ventilation was adjusted to maintain an end tidal O_2 and CO_2 at approximately 15% to 16% and 4.5% to 5.0%, respectively. Drugs were administered i.v. through a catheter inserted into the femoral vein. Rectal temperature was maintained between 37 and 38°C with a heating pad.

[1] Author for correspondence.

Nerve recording

The right cervical vagus nerve was exposed and sectioned at its junction with the superior laryngeal nerve under an operating microscope. Afferent cervical vagus nerve activity was recorded from the peripheral cut end of the nerve with bipolar platinum-iridium wire electrodes. This portion of the nerve was immersed in a pool of warm paraffin oil. The nerve activity was amplified, passed through a filter (time constant of 0.001 s, and high cut filter of 1000 Hz) and displayed with a thermal array recorder (Nihon Kohden, WS-682G). The discharge rate of this nerve was counted every 1 or 2 s by a real-time data analyzer (Nihon Kohden, Tokyo, Japan, ATAC-450).

Drugs and statistics

The following drugs were used: 5-hydroxytryptamine (5-HT) creatinine sulphate (Sigma Chemical Co., St Louis, MO, U.S.A.); 2-methyl-5-hydroxytryptamine maleate (2-methyl-5-HT, Nippon Glaxo Ltd., Tokyo, Japan); α-methyl-5-hydroxytryptamine maleate (α-methyl-5-HT, Sandoz Ltd., Basel, Switzerland); 5-carboxamidotryptamine maleate (5-CT, Glaxo); 5-methoxytryptamine hydrochloride (Sigma); GR38032F (1,2,3,9-tetrahydro-9-methyl-3[(2-methyl-1H-imidazol-l-yl) methyl]-4H-carbazol-4-one, hydrochloride, dihydrate, Glaxo); methoxamine hydrochloride (Nihon Shinyaku, Tokyo, Japan). The agonists were dissolved in the Locke solution; antagonists were dissolved in normal saline. The composition of the Locke solution was (in mM): NaCl 157, KCl 1.88, $CaCl_2$ 1.08, $NaHCO_3$ 7.98 and glucose 5.55 (pH = 7.3). The volume injected was kept constant at 500 μl kg^{-1}. Dose-response curves for 5-HT, 2-methyl-5-HT and α-methyl-5-HT were constructed noncumulatively with a dose-cycle greater than 10 min to avoid tachyphylaxis (Ginzel & Kattegoda, 1954). The antagonists were administered intravenously 5 min before the injection of the agonists throughout the study. Lateral displacements of agonist dose-response curves were measured at the control half-maximum response level (ED_{50}). Data were expressed as the mean ± s.e.mean. Analysis of variance followed by the Student's *t* test was used for statistical comparison.

Results

Effects of GR38032F on the 5-hydroxytryptamine-induced increase in cervical vagus nerve activity

Intravenous bolus injection of 5-HT (3.12–100 μg kg^{-1}) produced a dose-dependent increase in afferent cervical vagus nerve activity (Figure 1). The ED_{50} was 28.0 ± 2.1 μg kg^{-1} ($n = 36$). Vehicle (saline) did not affect the 5-HT dose-response curve and the ED_{50} value was 28.9 ± 4.8 μg kg^{-1} ($n = 6$, Figure 2a). The maximum response induced by 5-HT was estimated to be 146.4 ± 8.2% of the pre-injection level. A selective 5-HT_3 receptor antagonist, GR38032F (10 and 100 μg kg^{-1}), caused a rightward shift in the 5-HT dose-response curve. The ED_{50}s were 50.4 ± 7.8 ($P<0.05$ vs saline, $n = 11$) and 63.5 ± 13.4 μg kg^{-1} ($P<0.05$ vs saline, $n = 6$), respectively (Figure 2a). However, GR38032F itself did not alter the discharge of the nerves significantly.

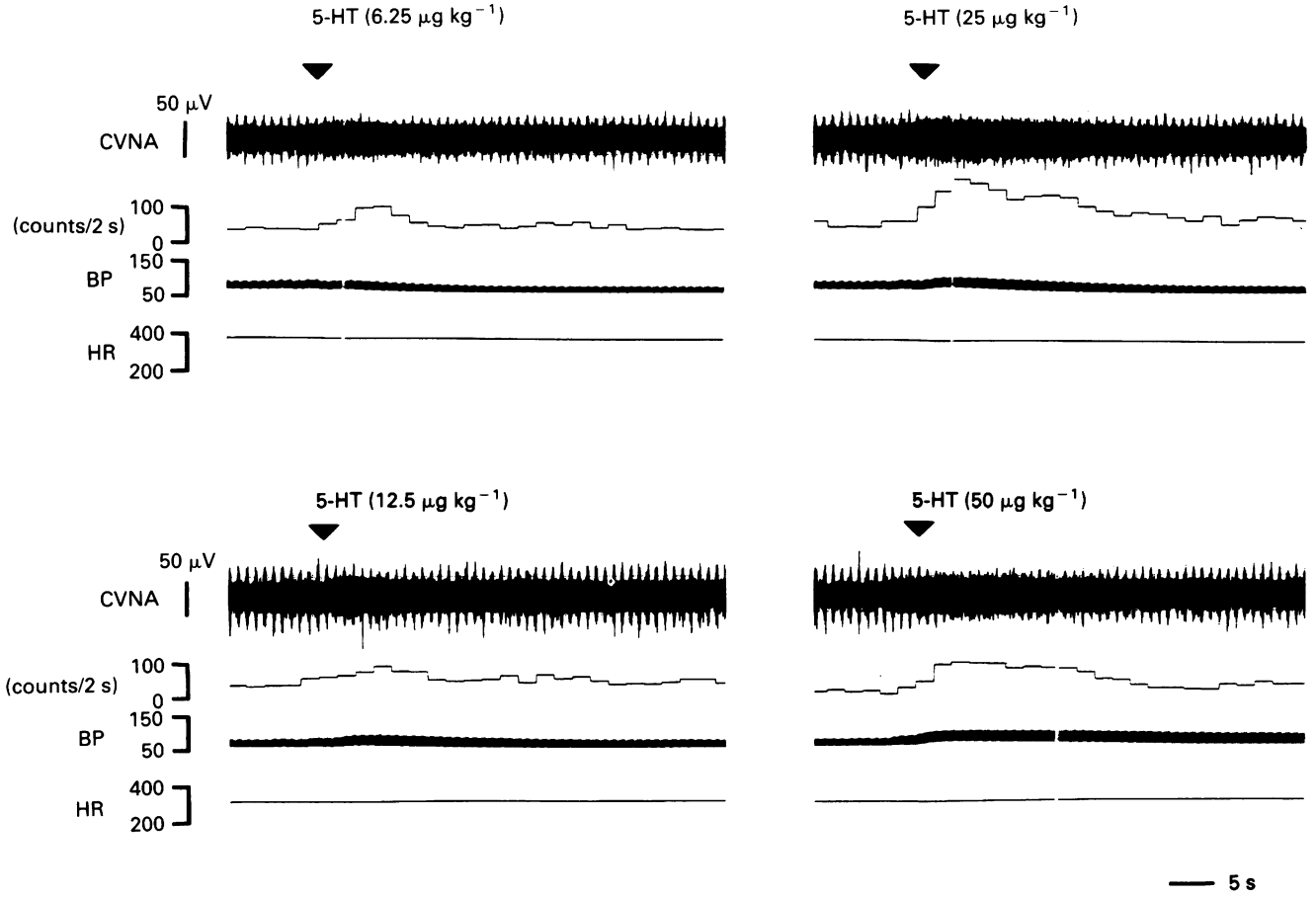

Figure 1 Effect of intravenous injection of 5-hydroxytryptamine (5-HT) on cervical vagus nerve activity in an anaesthetized rat. Top two panels, control experiment; lower two panels, pretreatment with GR38032F 10 μg kg^{-1}, 5 min before the next injection regime of 5-HT. A minimum of 10 min was allowed between the injection of each dose of 5-HT to avoid tachyphylaxis and allow for blood pressure recovery. Traces are the actual records of cervical vagus nerve activity (CVNA), pulse counts per 2 s, blood pressure (BP, mmHg) and heart rate (HR, b.p.m.). All records are from the same animal.

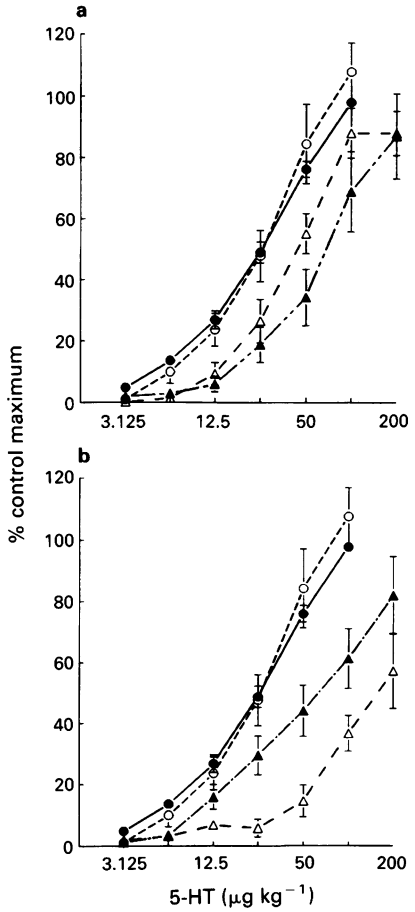

Figure 2 (a) Effect of GR38032F on the 5-hydroxytryptamine (5-HT)-induced increase in cervical vagus nerve activity. Symbols indicate control response (●); saline (○); GR38032F 10 μg kg^{-1} (△) and 100 μg kg^{-1} (▲). (b) Effect of ketanserin on the 5-HT-induced increase in cervical vagus nerve activity. Symbols indicate control response (●); saline (○); ketanserin 10 μg kg^{-1} (▲) and 100 μg kg^{-1} (△).

Effects of ketanserin on the 5-hydroxytryptamine-induced increase in cervical vagus nerve activity

A 5-HT$_2$ receptor antagonist, ketanserin (10 and 100 μg kg^{-1}), caused a rightward shift in the 5-HT dose-response curve. The ED$_{50}$s were 88.2 ± 26.4 μg kg^{-1} ($P<0.05$ *vs* saline, $n=6$) and 163.9 ± 32.6 μg kg^{-1} ($P<0.001$ *vs* saline, $n=4$), respectively (Figure 2b and 3). However, ketanserin itself did not alter the discharge of the nerves significantly.

Effects of 5-hydroxytryptamine agonists on cervical vagus nerve activity

A 5-HT$_3$ receptor agonist, 2-methyl-5-HT (3.12–100 μg kg^{-1}), also produced a dose-dependent but not marked increase in cervical vagus nerve activity. The ED$_{50}$ was 18.3 ± 2.4 μg kg^{-1} ($n=5$, Figure 4a and 5a). Although the maximum response induced by 2-methyl-5-HT reached only 107.4 ± 2.3% of the pre-injection level, GR38032F (10 μg kg^{-1}) caused a significant rightward shift in the 2-methyl-5-HT dose-response curve. The ED$_{50}$ was 50.7 ± 11.3 μg kg^{-1} ($P<0.05$, Figure 5a).

A 5-HT$_2$ receptor agonist, α-methyl-5-HT (3.12–50 μg kg^{-1}), produced a marked and dose-dependent increase in cervical vagus nerve activity (Figure 4b). The ED$_{50}$ was 13.6 ± 2.9 μg kg^{-1} ($n=5$, Figure 5b). The maximum response to α-methyl-5-HT reached 162.8 ± 5.4% as compared with the pre-injection level. Ketanserin (10 μg kg^{-1}) caused a significant rightward shift in the α-methyl-5-HT dose-response curve. The ED$_{50}$ was 41.2 ± 9.0 μg kg^{-1} ($P<0.05$ *vs* saline, Figure 5b).

Both a 5-HT$_1$ receptor agonist, 5-carboxamidotryptamine (50 μg kg^{-1}), and a putative 5-HT$_4$ receptor agonist, 5-methoxytryptamine (100 μg kg^{-1}), failed to increase cervical vagus nerve activity (Figure 6a and b).

In addition to being a potent 5-HT$_2$ receptor antagonist, ketanserin also has α$_1$-adrenoceptor blocking effects (Fozard, 1982; McCall & Schuette, 1984). In order to exclude the involvement of the α$_1$-adrenoceptor mechanism, we have examined the effect of the α$_1$-agonist, methoxamine, on cervical vagus nerve activity. Methoxamine (100 μg kg^{-1}) failed to produce an increase in cervical vagus nerve activity in spite of its effective pressor response (Figure 6c).

Discussion

In the present study, intravenous bolus injection of 5-HT produced a dose-dependent increase in mass discharges of cervical vagus nerve activity in anaesthetized rats. Treatment with a potent and selective 5-HT$_3$ receptor antagonist, GR38032F (Butler *et al.*, 1988), and a 5-HT$_2$ receptor antagonist, ketanserin (Van Nueten *et al.*, 1981), caused a significant rightward shift in the 5-HT dose-response curve. A selective 5-HT$_3$ receptor agonist, 2-methyl-5-HT (Hoyer & Neijt, 1988), and a selective 5-HT$_2$ receptor agonist, α-methyl-5-HT (Richardson *et al.*, 1985), also elicited dose-dependent increases in cervical vagus nerve activity. GR-38032F and ketanserin caused rightward displacement of the 2-methyl-5-HT and α-methyl-5-HT dose-response curves, respectively. These results suggest that not only 5-HT$_3$ receptors but also 5-HT$_2$ receptors might play an important role in the excitatory effect of 5-HT on the afferent vagus nerve *in vivo*. In terms of 5-HT$_3$ receptors, our results were in agreement with previous *in vitro* reports (Round & Wallis, 1986; Ireland & Tyers, 1987). Thus, the 5-HT-induced excitation of the afferent vagus nerves in anaesthetized rats has been shown to involve the 5-HT$_3$ receptor as well as the rat isolated vagus nerve.

It is also of interest to note that 5-HT$_2$ receptors were involved in the 5-HT-induced excitatory effect on cervical vagus nerve activity. In the present study, α-methyl-5-HT was found to produce activation closely resembling that induced by 5-HT. Thus, α-methyl-5-HT was similar to 5-HT in terms of the duration and pattern of evoked discharges of cervical vagus nerve activity (Figures 1 and 4b). The maximum response to α-methyl-5-HT reached 162.8 ± 5.4% and to 5-HT was 146.4 ± 8.2% as compared with their respective pre-injection levels. In contrast, 2-methyl-5-HT had a weak agonist action on cervical vagus nerve activity since the maximum response to this agent was only 107.4 ± 2.3% of the pre-injection level (Figure 4a). Dissimilarity of the agonisms produced by 2-methyl-5-HT and α-methyl-5-HT suggests that 5-HT-induced activation of afferent cervical vagus nerve activity might be mediated mainly by 5-HT$_2$ receptors rather than the 5-HT$_3$ receptors in anaesthetized rats. On the other hand, Butler *et al.* (1988) reported that 5-HT and 2-methyl-5-HT produced almost the same fall in heart rate, which is the Bezold-Jarisch reflex. A possible explanation for the difference in efficacy is that we measured the activities of the peripheral cut end of the cervical nerve without the nodose ganglion which is rich in 5-HT$_3$ receptors (Hoyer *et al.*, 1989), whereas Butler *et al.* used the intact afferent vagus nerve system. In other words, not only the vagus nerve trunk but also the nodose ganglion may be responsible for the initiation of the reflex. This speculation may be supported by a recent observation that 5-HT$_3$ receptor-mediated apnoea was abolished by vagotomy above, but not below, the nodose ganglia (Yoshioka *et al.*, 1992).

The location of the responsible 5-HT$_2$ receptor is still unknown; however, 5-HT$_2$ receptors generally exist in vas-

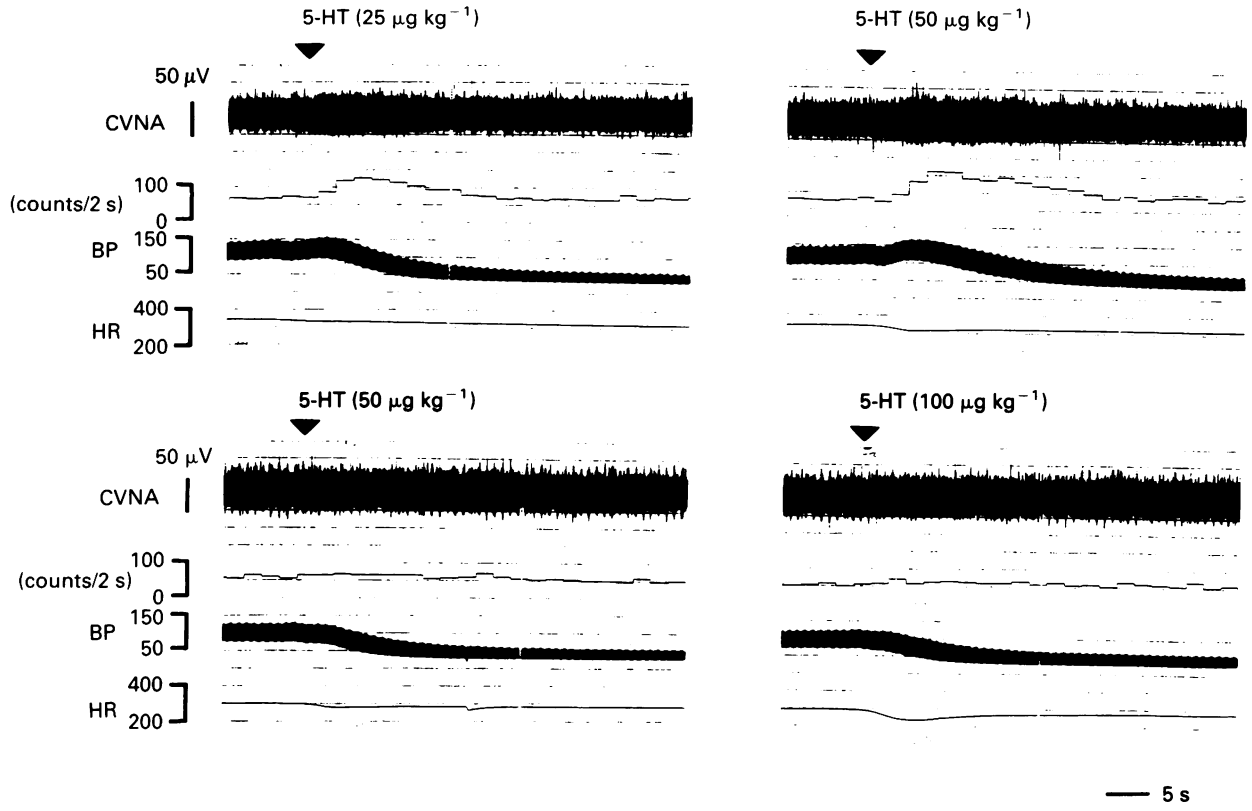

Figure 3 Effect of ketanserin on the 5-hydroxytryptamine (5-HT)-induced increase in cervical vagus nerve activity in an anaesthetized rat. Top two panels, control experiment; lower two panels, pretreatment with ketanserin 100 μg kg^{-1}, 5 min before the next injection regime of 5-HT. A minimum of 10 min was allowed between the injection of each dose of 5-HT to avoid tachyphylaxis and allow for blood pressure recovery. Traces are the actual records of cervical vagus nerve activity (CVNA), pulse counts per 2 s, blood pressure (BP, mmHg) and heart rate (HR, b.p.m.). All records are from the same animal.

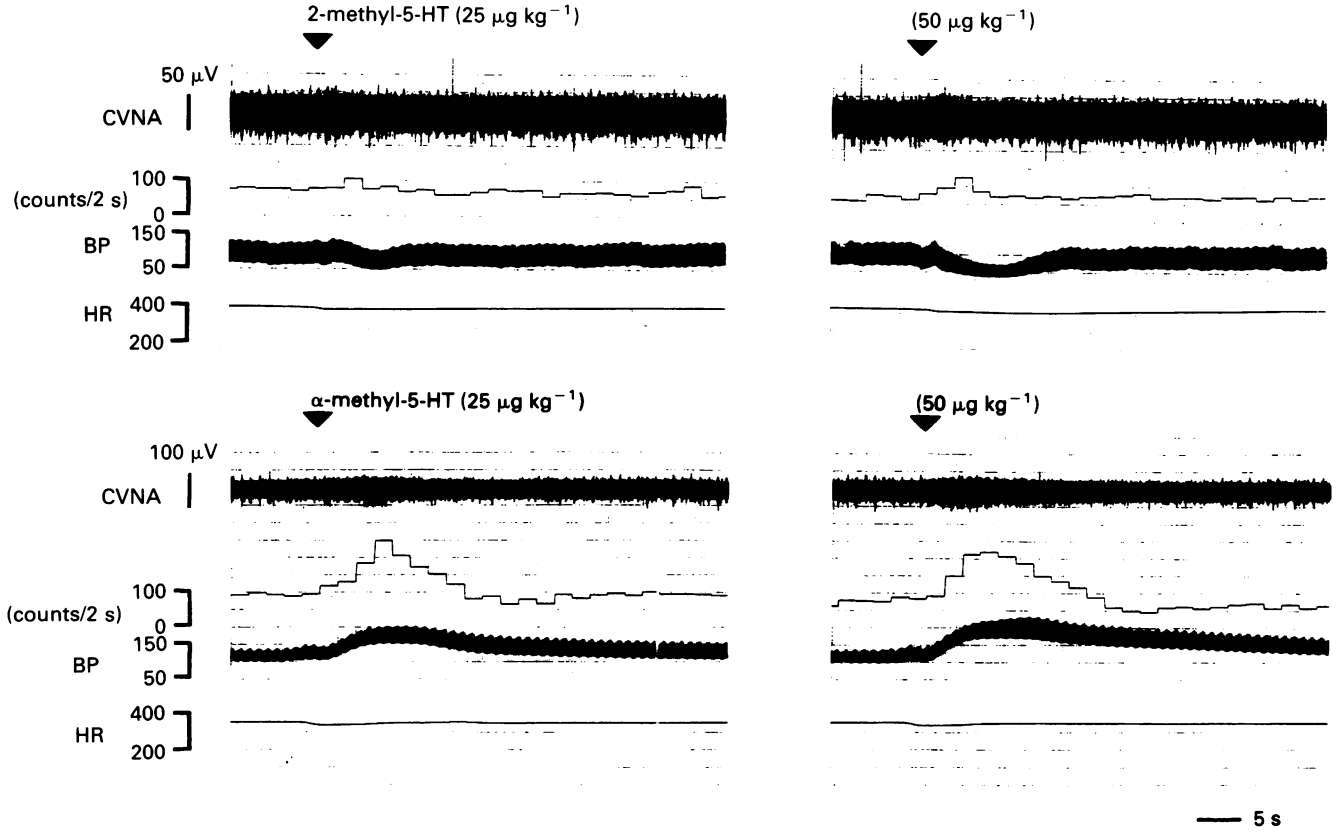

Figure 4 Effects of intravenous administration of 2-methyl-5-hydroxytryptamine (2-methyl-5-HT) (top 2 panels) and α-methyl-5-HT (lower 2 panels) on cervical vagus nerve activity. Traces are the actual records of cervical vagus nerve activity (CVNA), pulse counts per 2 s, blood pressure (BP, mmHg) and heart rate (HR, b.p.m.).

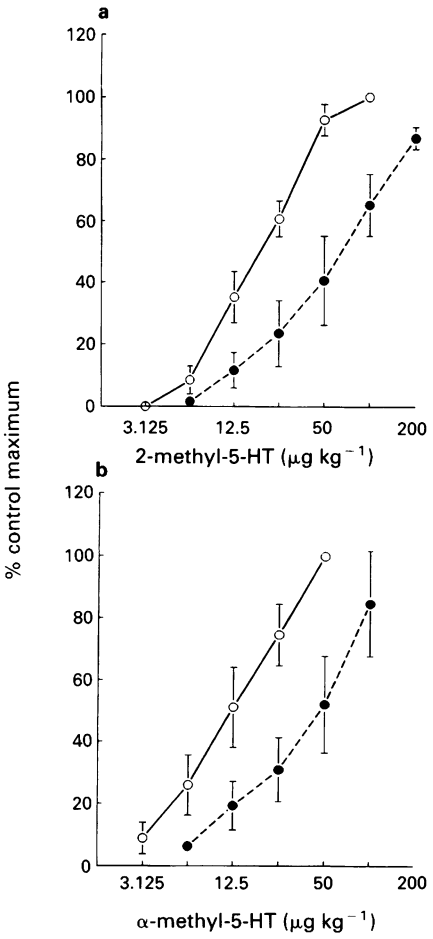

Figure 5 (a) Effect of GR38032F 10 μg kg^{-1} on the 2-methyl-5-hydroxytryptamine (2-methyl-5-HT)-induced increase in cervical vagus nerve activity. Symbols indicate control response (○) and presence of GR38032F (●). (b) Effect of ketanserin 10 μg kg^{-1} on the α-methyl-5-HT-induced increase in cervical vagus nerve activity. Symbols indicate control response (○) and ketanserin (●).

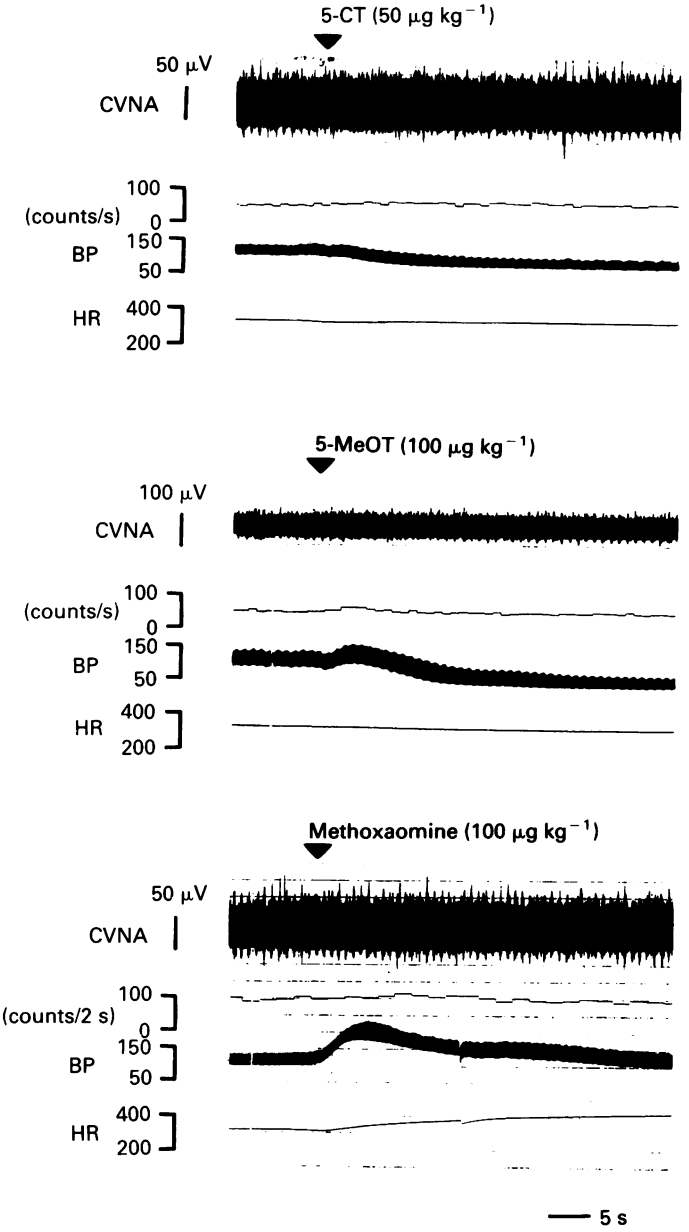

Figure 6 Effects of intravenous administration of (a) 5-carboxamidotryptamine (5-CT), (b) 5-methoxytryptamine (5-MeOT) and (c) methoxamine on cervical vagus nerve activity. Traces are the actual records of cervical vagus nerve activity (CVNA), pulse counts per 1 or 2 s, blood pressure (BP, mmHg) and heart rate (HR, b.p.m.). Each record is from a different animal.

cular and nonvascular smooth muscles such as the rat caudal artery, jugular vein, uterine and tracheal tissue etc. (Cohen *et al.*, 1985). The 5-HT$_2$ receptor is primarily responsible for 5-HT-induced contraction of smooth muscle. Anatomically, the cervical afferent vagus nerve is, in part, a visceral afferent sensory nerve (Hebel & Stromberg, 1986) and spontaneous activity of this nerve might also originate from the sensory nerve endings in the thoracic and abdominal viscera. However, after bilaterally cutting the vagus nerve below the diaphragm, no significant alteration of ongoing cervical vagus nerve activity was observed (data not shown). Furthermore, this surgical denervation did not significantly alter the 5-HT-induced excitation of cervical vagus nerve activity; the dose-ratio for the agonist before and after the surgical denervation was 1.17 ± 0.22 ($n = 4$). Taking these facts into account, the cardiopulmonary afferent nerve might play a much more important role than the abdominal afferents in terms of 5-HT-induced excitatory action of the cervical vagal afferents *in vivo*. A definitive conclusion on the receptor site(s) mediating the excitatory effect via 5-HT$_2$ receptors requires further investigation.

Excitation of cervical vagus nerve activity by 5-HT was not mimicked by 5-CT, a compound known to be a 5-HT$_1$-like receptor agonist (Saxena & Verdouw, 1985), or by 5-methoxytryptamine, a putative 5-HT$_4$ receptor agonist (Hoyer & Neijt, 1988), in the present study. In this context, neither a 5-CT-sensitive 5-HT$_1$-like receptor nor a putative 5-HT$_4$ receptor is likely to be involved in 5-HT-induced excitation of cervical vagus nerve activity *in vivo*.

Ketanserin inhibited both 5-HT- and α-methyl-5-HT-induced excitatory effects on cervical vagus nerve activity, however, it also has an α$_1$-adrenoceptor blocking property (Fozard, 1982; McCall & Schuette, 1984). In order to exclude the possibility of involvement of the α$_1$-adrenoceptor-mediated mechanism, we have examined the effect of α$_1$-agonist, methoxamine, on cervical vagus nerve activity. A high dose of methoxamine failed to produce an increase in nerve activity in spite of its effective pressor response via the α$_1$-adrenoceptor. This result may exclude the possibility that the α$_1$-blocking property of ketanserin inhibited the 5-HT induced excitatory effect on cervical vagus nerve activity.

It has been previously mentioned that 5-HT and α-methyl-5-HT have almost the same efficacy but 2-methyl-5-HT has less efficacy than 5-HT or α-methyl-5-HT, according to the percentage changes of pre-injection values. Although this was an *in vivo* experiment in which the ED$_{50}$ values of agonists were calculated from the dose-response curve, it is interesting

to note that the nature of the antagonism produced by GR38032F against 5-HT and 2-methyl-5-HT was different. With GR38032F (10 $\mu g\,kg^{-1}$), the dose-ratio (the means of the quotients: ED_{50} in the absence of antagonist/ED_{50} in the presence of antagonist) against 5-HT was 1.9 ± 0.3 ($n = 11$) and that against 2-methyl-5-HT was 2.7 ± 0.5 ($n = 5$). Similarly, with ketanserin (10 $\mu g\,kg^{-1}$), the ratio against 5-HT was 3.1 ± 0.8 ($n = 6$) and that against α-methyl-5-HT was 3.6 ± 0.5 ($n = 5$). A possible explanation for the differences in the dose-ratios between 5-HT and the agonists is that 5-HT is a substrate for uptake and the agonists are not. However, the ED_{50} against 5-HT is always smaller than that against selective agonists. These results might support the possibility that more than one receptor is responsible for the 5-HT-induced excitatory effect on cervical vagus nerve activity *in vivo*.

The most noteworthy conclusion of this investigation is that the 5-HT-induced excitatory effect on the afferent vagus nerve *in vivo* may be mediated not only by the $5\text{-}HT_3$ receptor mechanism but also by the $5\text{-}HT_2$-receptor mechanism.

References

BRADLEY, P.B., ENGEL, G., FENUIK, W., FOZARD, J.R., HUMPHREY, P.P.A., MIDDLEMISS, D.N., MYLECHARANE, E.J., RICHARDSON, B.P. & SAXENA, P.R. (1986). Proposals for the classification and nomenclature of functional receptors for 5-hydroxytryptamine. *Neuropharmacol.*, **25**, 563–576.

BUTLER, A., HILL, J.M., IRELAND, S.J., JORDAN, C.C. & TYERS, M.B. (1988). Pharmacological properties of GR38032F, a novel antagonist at $5\text{-}HT_3$ receptors. *Br. J. Pharmacol.*, **94**, 397–412.

COHEN, M.L., SCHENCK, K.W., COLBERT, W. & WITTENNAUER, L. (1985). Role of $5\text{-}HT_2$ receptors in serotonin-induced contractions of nonvascular smooth muscle. *J. Pharmacol. Exp. Ther.*, **232**, 770–774.

FOZARD, J.R. (1982). Mechanism of hypotensive effect of ketanserin. *J. Cardiovasc. Pharmacol.*, **4**, 829–838.

FOZARD, J.R. (1984). Neuronal 5-HT receptors in the periphery. *Neuropharmacol.*, **23**, 1473–1486.

GINZEL, K.H. & KATTEGODA, S.R. (1954). The action of 5-hydroxytryptamine and tryptamine on aortic and carotid sinus receptors in the cat. *J. Physiol.*, **123**, 277–228.

HEBEL, R. & STROMBERG, M.W. (1986). *Anatomy and Embryology of the Laboratory Rat*. pp. 188–189. Wörthsee: BioMed Verlag.

HIGASHI, H. & NISHI, S. (1982). 5-Hydroxytryptamine receptors of visceral primary afferent neurons on rabbit nodose ganglia. *J. Physiol.*, **323**, 543–567.

HOYER, D. & NEIJT, H.C. (1988). Identification of serotonin 5-HT3 recognition sites in membranes of N1E-115 neuroblastoma cells by radioligand binding. *Mol. Pharmacol.*, **33**, 303–309.

HOYER, D., WAEBER, C., KARPF, A., NEIJT, H. & PALACIOS, J.M. (1989). [^{3}H]ICS 205–930 labels 5-HT3 recognition sites in membranes of cat and rabbit vagus nerve and superior cervical ganglion. *Naunyn-Schmiedebergs Arch. Pharmacol.*, **340**, 396–402.

IRELAND, S.J., STRAUGHAN, D.W. & TYERS, M.B. (1982). Antagonism by metoclopramide and quipazine of 5-hydroxytryptamine-induced depolarizations of the rat isolated vagus nerve. *Br. J. Pharmacol.*, **75**, 16P.

IRELAND, S.J. & TYERS, M.B. (1987). Pharmacological characterization of 5-hydroxytryptamine-induced depolarization of the rat isolated vagus nerve. *Br. J. Pharmacol.*, **90**, 229–238.

KIRBY, G.C. & MCQUEEN, D.S. (1984). Effects of the antagonists MDL72222 and ketanserin on responses of cat carotid body chemoreceptors to 5-hydroxytryptamine. *Br. J. Pharmacol.*, **83**, 259–269.

MCCALL, R.B. & SCHUETTE, M.R. (1984). Evidence for an *alpha*-1 receptor-mediated central sympathoinhibitory action of ketanserin. *J. Pharmacol. Exp. Ther.*, **228**, 704–710.

NETO, F.R. (1978). The depolarizing action of 5-HT on mammalian non-myelinated nerve fibers. *Eur. J. Pharmacol.*, **49**, 351–356.

RICHARDSON, B.P., ENGEL, G., DONATSCH, P. & STADLER, P.A. (1985). Identification of serotonin M-receptor subtypes and their specific blockade by a new class of drugs. *Nature*, **316**, 126–131.

ROUND, A. & WALLIS, D.I. (1986). The depolarizing action of 5-hydroxytryptamine on rabbit vagal afferent and sympathetic neurones in vitro and its selective blockade by ICS 205–930. *Br. J. Pharmacol.*, **88**, 485–494.

SAXENA, P.R. & VERDOUW, P.D. (1985). 5-Carboxamidotryptamine, a compound with high affinity for $5\text{-hydroxytryptamine}_1$ binding sites, dilates arterioles and constricts arteriovenous anastomoses. *Br. J. Pharmacol.*, **84**, 533–544.

VAN NUETEN, J.M., JANSSEN, P.A.J., VAN BEEK, J., XHONNEUX, R., VERBEUREN, T.J. & VANHOUTTE, P.M. (1981). Vascular effects of ketanserin (R 41 468), a novel antagonist of $5\text{-}HT_2$ serotonergic receptors. *J. Pharmacol. Exp. Ther.*, **218**, 217–230.

WALLIS, D.I. (1989). Interaction of 5-hydroxytryptamine with autonomic and sensory neurones. In *The Peripheral Actions of 5-Hydroxytryptamine*. ed. Fozard, J.R. pp. 220–246. Oxford: Oxford Medical Publications.

WALLIS, D.I., STANSFELD, C.E. & NASH, H.L. (1982). Depolarising responses recorded from nodose ganglion cells of the rabbit evoked by 5-hydroxytryptamine and other substances. *Neuropharmacology*, **21**, 31–40.

YOSHIOKA, M., GODA, Y., TOGASHI, H., MATSUMOTO, M. & SAITO, H. (1992). Pharmacological characterization of 5-hydroxytryptamine-induced apnea in the rat. *J. Pharmacol. Exp. Ther.*, **260**, 917–924.

(Received November 25, 1991
Revised February 24, 1992
Accepted March 4, 1992)

Br. J. Pharmacol. (1992), **106**, 550–555

Evidence for a 5-HT_1-like receptor mediating the amplifying action of 5-HT in the rabbit ear artery

I.S. de la Lande

Department of Clinical and Experimental Pharmacology, University of Adelaide, G.P.O., Box 498, Adelaide, South Australia 5001

1 The nature of the 5-hydroxytryptamine (5-HT) receptors which amplify the vasoconstrictor effect of methoxamine was examined in the rabbit isolated perfused ear artery with intact endothelium. Indices of amplification were leftward shifts of methoxamine dose-response (DR) curves produced by 5-HT (0.3 μM) (Method I), and the appearance of vasoconstrictor responses to 5-HT receptor agonists when methoxamine was present in a near-threshold concentration (Method II).

2 The amplifying effect of 5-HT (Method I) was unaffected by prazosin (0.08 μM), was partly depressed by 5-HT_2-receptor antagonists in high concentrations (ketanserin 0.5 μM, LY53857, 1.0 μM), and was abolished by a non-selective antagonist of 5-HT_1 and 5-HT_2 receptors (methiothepin, 0.01 μM).

3 Amplifying potencies of agonists assessed by both Methods I and II were in the order 5-carboxamidotryptamine (5-CT) > 5-HT > α-methyl 5-HT. The potency of sumatriptan (assessed by Method II only) was intermediate between those of 5-HT and α-methyl 5-HT.

4 Ketanserin and LY53857 inhibited the amplifying action of 5-CT to about the same extent as that of 5-HT.

5 The amplifying potencies of the agonists are in marked contrast to the reported contractile potencies in the rabbit aorta where the receptor is 5-HT_2, but are almost identical with reported contractile potencies in the dog saphenous vein where the receptor is 5-HT_1-like.

6 It is concluded that a 5-HT_1-like receptor mediates the amplifying interaction between 5-HT and methoxamine in the rabbit ear artery which can be weakly blocked by ketanserin and LY53857.

7 Since 5-CT was equipotent when applied separately to the intimal and adventitial surfaces of the artery, it is suggested that the 5-HT_1-like receptors are distributed uniformly across the artery wall.

Keywords: Rabbit ear artery; amplifying interactions; 5-hydroxytryptamine$_1$-like receptors; 5-carboxamidotryptamine; sumatriptan

Introduction

In concentrations that are sub-threshold for contraction, 5-hydroxytryptamine (5-HT) exerts an excitatory effect in arteries *in vitro* which is manifested either by an increased response to a second contractile agent or by the appearance of a contractile response to 5-HT in the presence of the second agent. This synergistic interaction, which is commonly termed the amplifying action of 5-HT, is prominent in the rabbit ear artery where it was first documented (de la Lande *et al.*, 1966). The nature of the receptor mediating this amplifying action of 5-HT in the rabbit ear artery has been explored in the present study.

Previous attempts to identify the receptor have focussed on the possibility that amplification is simply a sub-threshold manifestation of excitability changes associated with the contractile response to 5-HT. The latter response, in the absence of other treatment, appears to be mediated only by the α-adrenoceptor (Apperley *et al.*, 1976); sensitivity to prazosin (Purdy *et al.*, 1981) implies that the receptor is of the α_1-subtype. However a 5-HT_2-receptor appears to play a contributory role in artery strips from reserpinized rabbits (de la Lande & Kennedy, 1985) and in artery rings exposed to ouabain (Xu *et al.*, 1990). So far, attempts to establish the role of these receptors in amplification have yielded results which are not easy to interpret. In reserpinized-strip preparations, both prazosin and ketanserin depressed amplification in the interaction between 5-HT and noradrenaline (NA) (see de la Lande, 1989), but had much less effect on the interaction between 5-HT and methoxamine (de la Lande & Kennedy, 1985). Nevertheless, Meehan *et al.* (1986), using the perfused segment preparation from untreated rabbits, noted that the 5-HT interaction with NA was unaffected by prazosin but was depressed by ketanserin in a concentration (0.03 μM) that was considered to be indicative of a role for the 5-HT_2 receptor.

The present study was confined to experiments on perfused segments from untreated rabbits, with methoxamine as the reference contractile agent. In order to characterize the amplifying receptor, two approaches were adopted. In one, the effects on the 5-HT-methoxamine interaction of α_1-adrenoceptor blockade by prazosin, of 5-HT_2 receptor blockade by ketanserin and LY53857 (for references see Mylecharane, 1990), and of non-selective 5-HT_1 and 5-HT_2 receptor blockade by methiotepin, were examined. In the other, the amplifying actions of 5-HT were compared with those of a 5-HT_2 selective agonist (α-methyl 5-HT) and two agonists with selectivity for receptors within the 5-HT_1 group, namely, 5-carboxamidotryptamine (5-CT) and sumatriptan. The agonists were selected in view of evidence that they are of value in distinguishing between effects mediated by 5-HT_1-like and 5-HT_2 receptors (e.g. Feniuk & Humphrey, 1989; Summer *et al.*, 1989).

A preliminary account of the present findings was presented to the Australasian Society for Clinical and Experimental Pharmacologists (de la Lande, 1990).

Methods

Preparation

Semi-lop eared rabbits, bred at the Central Animal House, University of Adelaide from the Belgian Lop-Eared strain,

were used in all experiments. Ear artery segments (1–2 cm long) were removed from rabbits which had been killed under pentobarbitone anaesthesia. The segments were perfused by the method of de la Lande *et al.* (1966). The segment was cannulated at both ends, placed in an organ bath containing Krebs solution (vol. 15 ml), and perfused intraluminally with Krebs solution (3.0 ml min^{-1}). After passing through the lumen, the perfusate escaped without mixing with the solution in the organ bath (termed 'extraluminal'). Intraluminal perfusion pressure was measured by a Statham Pressure Transducer; vasoconstriction was manifested by an increase in perfusion pressure. The perfusion pressure in the absence of vasoactive agents was usually between 5 and 10 mmHg and did not vary within an experiment. Note: Higher base-line pressures (10–20 mmHg) in the earlier experiments of de la Lande *et al.* (1966) reflected higher flow rates (6–8 ml min^{-1}).

Effects of 5-hydroxytryptamine on responses to methoxamine

Vasoconstrictor responses to methoxamine (administered as an intraluminal bolus in 0.1 ml) were measured in the absence and presence of 5-HT (0.03 μM). The 5-HT was present in both the intraluminal and extraluminal solutions. Responses to methoxamine were elicited in duplicate at three dose levels (most commonly 0.03, 0.10, and 0.30 μmol). The 5-HT was added 5–10 min before starting a second dose-response (DR) curve. Its amplifying effect was quantitated in terms of the ratio (termed sensitivity ratio) of doses of methoxamine which were equipotent in eliciting a response of 60 mmHg in the absence (numerator) and presence (denominator) of 5-HT.

In experiments where 5-HT was applied for a second time to the artery, a period of approximately 60 min after the preceding wash-out of 5-HT was allowed to enable sensitivity to methoxamine to return to its pre-5-HT level. Although recovery from the amplifying effect of 5-HT was extremely rapid (less than 5 min), it was followed by a period of depressed sensitivity to methoxamine which lasted about 30 min.

In all experiments, two or more arteries from the same animal were used. When effects of antagonists were studied, one of the arteries served as the control, the other (test artery) being exposed to the antagonist 60 min prior to commencing the first DR curve to methoxamine. The same time interval was allowed in the control artery. 5-HT sensitivity ratios were compared in the control and test arteries. Antagonists tested comprised prazosin, ketanserin, LY53857 and methiothepin.

The only departure from the above procedure was that in some experiments 5-HT was replaced by 5-CT (0.03 μM).

Interactions between 5-hydroxytryptamine receptor agonists and methoxamine

The agonists comprised 5-HT, α-methyl 5-HT, 5-CT and sumatriptan. With the exception of sumatriptan their effects were measured in two ways. In one, the agonist was present in the infusion and bathing media and its effects on the vasoconstrictor responses to intraluminally-injected methoxamine were measured. The concentration of the agonist was progressively increased in multiples of ten between 0.001 and 1.0 μM. The sensitivity ratio was measured at each concentration.

The second method used the constrictor response to the 5-HT-receptor agonist in the presence of methoxamine, as the index of amplification. Methoxamine was added to the extraluminal solution in a concentration (usually 0.3 μM) which resulted in a steady-state constrictor response between 15 and 40 mmHg. The agonist was then added cumulatively to the same solution in concentrations which, in the absence of methoxamine, did not constrict the artery. The concentration of agonist which elicited a constrictor response of 60 mmHg in the presence of methoxamine was estimated from the agonist concentration-response (CR) curve. When the second method was used, cocaine (3 μM) was present in both the intraluminal and extraluminal solutions to minimize any loss of the 5-HT agonists resulting from uptake into the sympathetic nerves.

Comparison of intraluminal and extraluminal amplifying potencies of 5-carboxamidotryptamine

Methoxamine was added to the extraluminal solution in a concentration that elicited a steady-state constrictor response of between 15 and 40 mmHg. Constrictor responses to 5-CT applied extraluminally were then compared with those to 5-CT perfused intraluminally. Concentrations which were equipotent in eliciting a response of 60 mmHg were estimated from the 5-CT CR curves. Cocaine (3 μM) was present in both the intraluminal and extraluminal solutions.

Endothelial function

Towards the end of each experiment, the vasodilator response to intraluminally-infused acetylcholine (ACh, 0.5 μM) was measured after the perfusion pressure had been elevated to between 100 and 200 mmHg by extraluminal methoxamine.

Maximum constriction

Before terminating an experiment, an indication of the maximum response to methoxamine was obtained. Depending on the nature of the experiment, methoxamine was either injected intraluminally in a large dose (3 or 10 μmol) or was applied extra-luminally in a high concentration (30 μM). The resultant response was usually in the 300 to 400 mmHg range but was often difficult to quantify due to a tendency for the perfusion pressure to fluctuate erratically as it reached this range. In view of this tendency, which was noted earlier (de la Lande, 1975), the response in mmHg rather than the response as a percentage of maximum was used in plotting dose-response relationships.

Statistics

Effects of drugs on constrictor responses and on sensitivity ratios, the latter converted to log units, were assessed for significance by the paired t test. Significance refers to $P<0.05$; except where otherwise stated n refers to the number of rabbits.

Drugs

The following compounds were purchased: cocaine hydrochloride (MacFarlane-Smith); 5-hydroxytryptamine creatinine sulphate (Sigma), methoxamine hydrochloride (Sigma); α-methyl 5-hydroxytryptamine maleate (Research Biochemicals); physostigmine salicylate (Sigma), prazosin hydrochloride (Sigma).

The following were gifts: methiothepin maleate (Roche); ketanserin hydrochloride (Janssen Pharmaceuticals); 5-carboxamidotryptamine maleate, sumatriptan (Glaxo); LY53857 (Lilly Research Laboratories).

LY53857 is 4-isopropyl-7-methyl-9-(2-hydroxy-1-methyl-propoxy-carbonyl) -4, 6, 6A, 7, 8, 9, 10, 10A-octahydro-indolol [4.3-FG] quinoline.

Results

Effects of antagonists on the amplifying action of 5-hydroxytryptamine

5-HT (0.03 μM) did not affect the perfusion pressure but caused an approximately four fold leftward shift of the

methoxamine DR curve (Figure 1a). The action of 5-HT was unchanged when sensitivity to methoxamine was depressed by prazosin (0.08 μM); the depression was manifested as a twenty fold rightward shift of the methoxamine DR curve (Figure 1a).

Ketanserin (0.05 μM and 0.5 μM) also shifted the methoxamine DR curve to the right by factors of 3 and 21 respectively. However, unlike prazosin, it also decreased the amplifying action of 5-HT (Table 1). Although not significant at the lower concentration of ketanserin, the effect of amplification was unequivocal at the higher concentration and is illustrated in Figure 1b.

LY53857 decreased the amplifying action of 5-HT but did not decrease the sensitivity of methoxamine. In the two concentrations tested, namely 0.1 and 1.0 μM, the inhibitory effects of LY53857 on amplification were comparable with those of ketanserin 0.05 and 0.5 μM respectively (Table 1, Figure 1b).

Methiothepin (0.01 μM) caused an approximately forty fold rightward shift of the methoxamine DR curve and abolished the action of 5-HT (Table 1).

Amplifying actions of 5-hydroxytryptamine receptor agonists

The agonists were 5-HT, 5-CT (5-HT_1 selective) and α-methyl 5-HT (5-HT_2 selective). Each increased the vasoconstrictor activity of methoxamine. Leftward shifts of methoxamine DR curves, measured at three subconstrictor concentrations of each agonist, indicated that 5-HT was less potent than 5-CT, but considerably more potent than α-methyl 5-HT (Figure 2). From the concentration-amplifying effect curves, it was estimated that concentrations eliciting a leftward shft of 0.5 log units (in nM with 95% confidence limits, $n = 4$) were 5-CT (3.4, 1.3–8.7), 5-HT (15, 3.5–64) and α-methyl 5-HT (300, 87–1040).

Since the above experiments revealed that 5-CT was a highly potent amplifying agent, the effects of ketanserin (0.5 μM) and of LY53857 (1.0 μM) on the 5-CT-methoxamine interaction were examined. As shown in Table 1, both agents inhibited the amplifying action of 5-CT to about the same extent as that of 5-HT.

Effect of methoxamine on vasoconstrictor activities of 5-hydroxytryptamine receptor agonists

In these experiments the vasoconstrictor response to the 5-HT receptor agonist in the presence of methoxamine (both applied extraluminally), was used as the index of amplification. The agonists included sumatriptan.

In the absence of methoxamine, none of the four agonists displayed vasoconstrictor activity when tested in concentrations ranging up to 0.4 μM (for 5-HT and 5-CT) and 1.4 μM (for α-methyl 5-HT and sumatriptan). However, when applied in much lower concentrations during a steady-state constriction of between 10 and 50 mmHg induced by methoxamine, the agonists displayed marked constrictor activity (Figure 3).

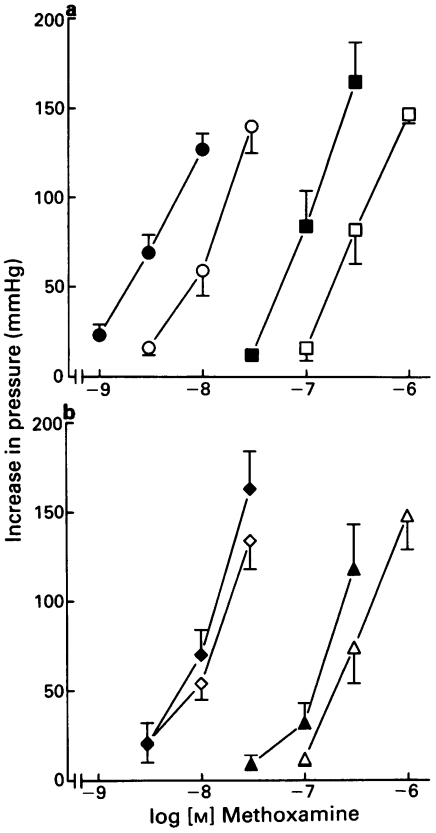

Figure 1 Effects of antagonists on the amplifying action of 5-hydroxytryptamine (5-HT). Shown are effects of prazosin (a), LY53857 and ketanserin (b) on dose-response (DR) curves to methoxamine in the absence and presence of 5-HT (0.03 μM): (○) Control ($n = 17$); (□) prazosin (0.08 μM, $n = 5$); (◇) LY53857 (1.0 μM, $n = 6$); (△) ketanserin (0.5 μM, $n = 6$). DR curves elicited in the presence of 5-HT are indicated by the closed symbols. Values shown are means with s.e.mean (vertical bars) from n experiments.

Table 1 Effects of 5-hydroxytryptamine (5-HT) receptor antagonists on amplifying actions of 5-HT and 5-carboxytryptamine (5-CT) on responses to methoxamine

Antagonist (μM)	*5-HT-receptor agonist*	n	*Sensitivity ratio geometric mean (with 95% confidence limits)* *Control*	*Antagonist present*
Ketanserin (0.05)	5-HT (0.03 μM)	5	4.6 (3.8–5.5)	2.8 (2.0–3.9)[a]
Ketanserin (0.5)	5-HT (0.03 μM)	6	3.6 (3.0–4.3)	1.8 (1.3–2.4)*
LY53857 (0.1)	5-HT (0.03 μM)	5	4.6 (3.7–5.6)	2.8 (1.7–4.6)[a]
LY53857 (1.0)	5-HT (0.03 μM)	6	3.7 (2.9–4.8)	1.3 (0.9–1.9)*
Methiothepin (0.01)	5-HT (0.03 μM)	4	4.5 (2.3–8.7)	1.1 (0.7–1.7)*
Ketanserin (0.5)	5-CT (0.03 μM)	5	4.8 (3.5–6.6)	2.3 (1.2–3.4)*
LY53857 (1.0)	5-CT (0.03 μM)	5	5.2 (3.2–8.7)	1.8 (1.1–3.0)*

* $P < 0.05$. [a] $0.1 > P > 0.05$.

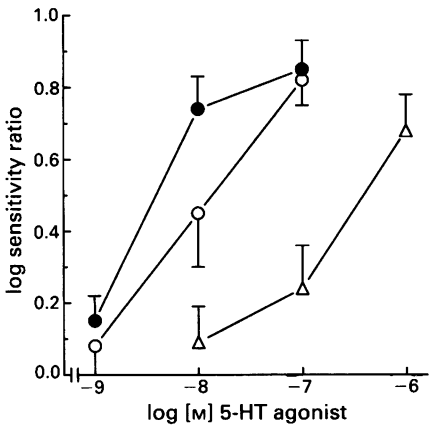

Figure 2 Amplifying potencies of 5-hydroxytryptamine (5-HT), 5-carboxamidotryptamine (5-CT) and α-methyl 5-HT: (●) 5-CT; (○) 5-HT; (△) α-methyl 5-HT. The graphs show leftward shifts of methoxamine dose-response curves (expressed as log sensitivity ratios) at three concentrations of each agonist ($n = 4$). Values shown are means with s.e.mean indicated by vertical bars.

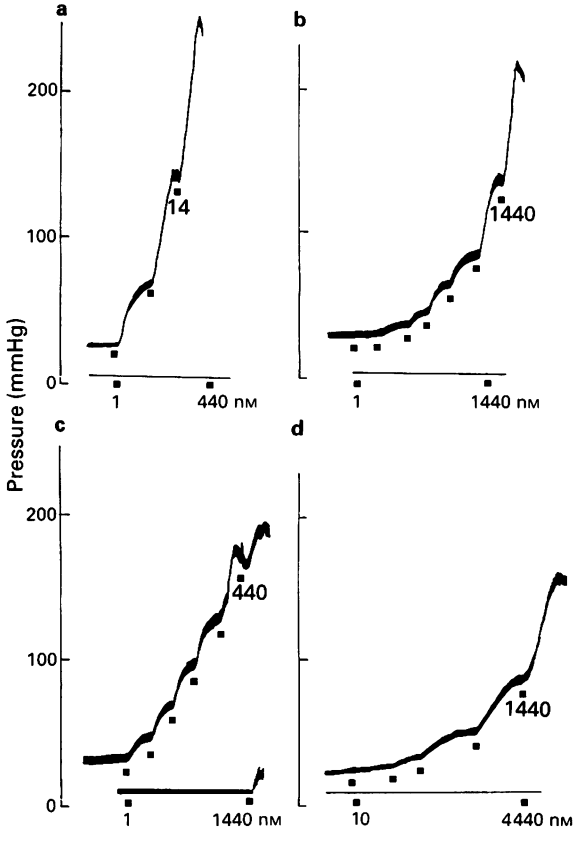

Figure 3 Effect of methoxamine on the contractile activities of 5-hydroxytryptamine (5-HT) receptor agonists: (a) 5-carboxamidotryptamine (5-CT); (b) sumatriptan; (c) 5-HT; (d) α-methyl 5-HT. The agonist concentration was cumulated by factors of 3.2–4.0 between the lowest and highest concentrations (shown in μM). The lower (horizontal) trace is the perfusion pressure in the absence of methoxamine and shows that the agonists were without constrictor effect, except for 5-HT at the highest concentration. The superimposed trace shows that, in the same arteries, the agonists became potent constrictor agents when methoxamine was present in a concentration which elevated the perfusion pressure by 15–30 mmHg.

Responses below 100–150 mmHg increase in pressure were well sustained, but above this range they displayed a pronounced tendency to fade. Comparison of concentration-constrictor response curves (Figure 4) indicated an order of amplifying potency: 5-CT > 5-HT > sumatriptan > α-methyl 5-HT. Concentrations which elicited a response of 60 mmHg (in nM, with 95% confidence limits in parentheses, $n = 4–6$) were: 5-CT (2.3, 0.8–6.6), 5-HT (6.2, 3.5–11), sumatriptan (76, 35–257), and α-methyl 5-HT (186, 62–562). Ratios of concentrations (with 95% confidence limits in parentheses) which were equipotent with 5-HT were: 5-CT, 0.4 (0.3–0.7, $n = 6$), sumatriptan, 11 (5–25, $n = 5$) and α-methyl 5-HT, 28 (13–58, $n = 4$).)

In the preceding experiments, the 5-HT receptor agonists were present only in the extraluminal solution. However experiments in which the effects of intraluminal and extraluminal 5-CT were compared, failed to reveal any difference in amplifying potencies. Thus concentrations of intraluminal and of extraluminal 5-CT which elicited a response of 60 mmHg in six arteries (in nM, with 95% confidence limits) were 1.6 (0.52–4.8) and 2.2 (0.74–6.8) respectively.

Vasodilator effect of acetylcholine

To assess the functional state of the endothelium, the vasodilator response to ACh (0.5 μM, applied intraluminally) was measured before terminating each experiment; the artery was constricted to between 100 and 200 mmHg by methoxamine. The ACh caused a decrease in perfusion pressure of 50 mmHg or greater in most (82 of 97) artery segments. In six pairs of arteries, responses to extraluminally-applied ACh (0.5 μM) were compared with those to intraluminal ACh (0.5 μM); physostigmine (3.0 μM) was present to minimize hydrolysis of the ACh. The response to the extraluminal ACh (a decrease in pressure of 48 ± 5%) was considerably less than to the intraluminal ACh (a decrease of 93 ± 4%).

Discussion

Effects of the 5-HT receptor agonists are discussed first since they provide a clearer insight into the nature of the receptors mediating amplification than do the effects of the agonists.

When assessed in terms of increases in the contractile activity of methoxamine, the amplifying potency of 5-HT was

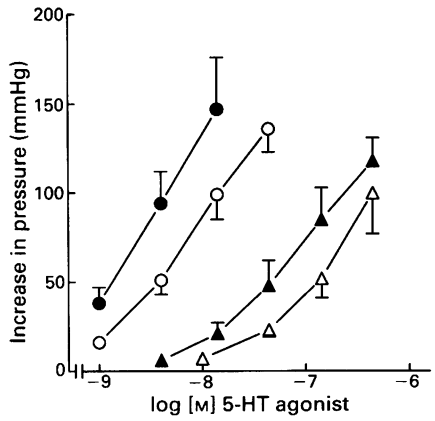

Figure 4 Concentration-response (CR) curves to 5-hydroxytryptamine (5-HT) receptor agonists in the presence of methoxamine. The increased steady-state levels of perfusion pressure due to methoxamine (0.2–0.4 μM) at the time the agonists were added were (in mmHg): 5-HT (27 ± 3, $n = 6$), 5-carboxamidotryptamine (5-CT, 31 ± 5, $n = 6$), sumatriptan (28 ± 5, $n = 5$), α-methyl 5-HT (20 ± 7, $n = 4$). Symbols: (●) 5-CT; (○) 5-HT, (▲) sumatriptan; (△) α-methyl 5-HT. Values shown are means with s.e.mean (vertical bars) from n experiments.

greater than that of α-methyl 5-HT but less than that of 5-CT. A similar rank order of potencies prevailed when the constrictor response to the 5-HT agonist in the presence of methoxamine was used as the index of amplification. The latter method indicated also an amplifying potency of sumatriptan between that of α-methyl 5-HT and 5-CT. As indicated in Table 2, the relative potencies agree closely with those for contractile activity in the dog saphenous vein, and are not too dissimilar from those for endothelium-dependent relaxation in the pig coronary artery; in both these vessels the effects of 5-HT are believed to be mediated by 5-HT_1-like receptors (Feniuk & Humphrey, 1989; Schoeffter & Hoyer, 1990). On the other hand, the relative amplifying potencies contrast markedly with those for 5-HT_2 receptor-mediated contraction in the rabbit aorta, where the rank order is 5-HT > α-methyl 5-HT > 5-CT > sumatriptan (inactive) (Feniuk *et al.*, 1985; Humphrey *et al.*, 1988).

In view of evidence that the 5-HT_1-like receptor in the pig coronary artery is very similar to the 5-HT_{1D} receptor (Shoeffter & Hoyer, 1990) it is noteworthy that the absolute amplifying potencies when assessed in terms of the concentrations eliciting a response of 60 mmHg in the methoxamine-exposed artery, are in the same rank order as IC_{50}s for binding to 5-HT_{1D} recognition sites in brain. The respective values (amplifying potency followed by binding affinity, in nM) on which the comparison of rank order is based are: 5-CT (2.3, 2.5), 5-HT (6.2, 4.0), sumatriptan (76, 17–68) and α-methyl 5-HT (186, 158). The data on binding are from the studies of Engel *et al.* (1986), Hoyer (1989), Shoeffter & Hoyer (1990), Peroutka & McCarthy (1989) and Van Wijngaarden *et al.* (1990).

It follows from the above considerations that there are reasonable grounds for placing the amplifying receptor in the rabbit ear artery in the 5-HT_1-like category.

Effects of antagonists

Criteria for the presence of a 5-HT_1-like receptor include insensitivity to 5-HT_2 selective antagonists (e.g. ketanserin) and sensitivity to antagonists which do not discriminate beween 5-HT_1 and 5-HT_2 receptors e.g. methysergide, methiothepin (Bradley *et al.*, 1986).

At first sight, the ability of the 5-HT_2 receptor antagonists, LY53857 and ketanserin, to inhibit amplification implies a departure from the above criteria. However, the following factors must be taken into account. Firstly, the effect of ketanserin was not impressive in the sense that 50 nM appeared to be close to the inhibitory threshold, yet this concentration is considerably greater than the pA_2 for the 5-HT_2 receptor, namely 0.4–8 nM (Mylecharane, 1990). Similarly, the inhibitory threshold for LY53857, which was in the vicinity of 100 nM, also seems high when compared with its pA_2 for the 5-HT_2 receptor namely 0.4–40 nM (Fenuik & Humphrey, 1989; Mylecharane, 1990). Secondly, the finding that both ketanserin (0.5 μM) and LY53857 (1.0 μM) inhibited the amplifying action of 5-CT to about the same extent as that of 5-HT suggests that these antagonists possess sufficient affinity for the 5-HT_1-like receptor to account for their effects on the action of 5-HT.

Methysergide was not used in the present study, since it is known to behave like an agonist of the amplifying receptor in the rabbit ear artery (de la Lande *et al.*, 1966; Fozard, 1976). However methiothepin proved to be a potent inhibitor of the amplifying action of 5-HT, abolishing the action in a concentration of 0.01 μM. The effects of these antagonists again emphasise the similarity between the actions of 5-HT in the rabbit ear artery and dog saphenous vein, since in the latter vessel methysergide also is a partial agonist and methiothepin a potent antagonist of the 5-HT_1-like receptor mediating the contractile response (Fenuik *et al.*, 1985; Fenuik & Humphrey, 1989).

Distribution of the amplifying receptor

In view of evidence that a 5-HT_1-like receptor is associated with the endothelium in pig coronary artery (see Table 2), an indication of the distribution of the amplifying receptor in the wall of the rabbit ear artery was sought by comparing the potencies of intraluminal and extraluminal 5-CT. The finding that the potencies did not differ is interpreted as evidence that the receptors are fairly evenly distributed between the inner and outer regions of the artery wall, and hence are probably associated with the smooth muscle cells. That this interpretation is valid is supported by the finding that the vasodilator effect of intraluminal ACh is considerably greater than that of extraluminal ACh. This finding accords with the substantial evidence that the cholinoceptors mediating vasodilatation are located on endothelial cells (Furchgott & Zawadski, 1980).

Relationship between amplifying and contractile actions of 5-hydroxytryptamine

In accord with evidence that the amplifying effect of 5-HT is manifested in concentrations below those eliciting constriction (de la Lande *et al.*, 1966), there was no indication of constrictor activity on the part of any of the 5-HT receptor agonists in concentrations of up to 100 fold greater than those eliciting detectable amplification. Earlier studies on the perfused artery from the untreated rabbit are in agreement that the constrictor activity is due to α-adrenoceptor activation (Apperley *et al.*, 1976; Fozard, 1976; see also Introduction). 5-HT_2 receptor-mediated contraction has also been demonstrated although only under certain conditions e.g. in reserpine-treated artery strips (de la Lande & Kennedy, 1985) and in oubain-exposed artery rings (Xu *et al.*, 1990). Nevertheless, the present results argue against a role for either of these receptors in the amplifying interaction between 5-HT and methoxamine. It is suggested therefore that the 5-HT_1-like receptor functions primarily as an amplifying receptor. Whether it simply facilitates constrictor activity of other agonists, or whether it requires the presence of a second excitatory agonist for expression of its own constrictor function, are complex questions which remain to be addressed.

Table 2 Relative potencies† of 5-hydroxytryptamine (5-HT) receptor agonists

				Agonist		
Receptor	*Tissue*	*Response*	*5-CT*	*5-HT*	*Sumatr*	*α-Me 5-HT*
?	Rabbit ear art	amplifn.	2.5	1.0	0.09	0.04
5-HT_1-like	Dog saph. vein	contrn.	3.3	1.0	0.20	0.08
5-HT_1-like	Pig cor. art.	relaxn*	1.0	1.0	0.03	0.06
5-HT_2	Rabbit aorta	contrn.	0.04	1.0	nil	0.5

†Concentration of 5-HT divided by equipotent concentrations of the agonist. *Endothelium-dependent. Data on dog saphenous vein from Humphrey *et al.* (1988), on pig coronary artery from Schoeffter & Hoyer (1989) and on rabbit aorta from Feniuk *et al.* (1985).

In conclusion, it is emphasised that the present evidence refers only to the interaction between 5-HT and methoxamine. It remains to be established whether amplifying interactions between 5-HT and other agonists such as NA and histamine also involve the 5-HT$_1$-like receptor. That these interactions may be more complex than the one between 5-HT and methoxamine is suggested by findings that amplification in the 5-HT interaction with NA is inhibited by prazosin and ketanserin (see de la Lande, 1989), while amplification in the 5-HT interaction with histamine is potentiated by histamine H_2-receptor activation (de la Lande *et al.*, 1989).

The author wishes to thank Sarah Wing and Maureen Newlyn for skilled technical assistance.

References

APPERLEY, A., HUMPHREY, P.P.A. & LEVY, G.P. (1976). Receptors for 5-hydroxytryptamine and noradrenaline in rabbit isolated ear artery and aorta. *Br. J. Pharmacol.*, **58,** 211–221.

BRADLEY, P.B., ENGEL, G., FENIUK, W., FOZARD, J.R., HUMPHREY, P.P.A., MIDDLEMISS, D.N., MYLECHARANE, E.J., RICHARDSON, B.P. & SAXENA, P.R. (1986). Proposals for the classification and nomenclature of functional receptors for 5-hyroxytryptamine. *Neuropharmacology*, **25,** 563–575.

DE LA LANDE, I.S. (1975). Adrenergic mechanisms in the rabbit ear artery. *Blood Vessels*, **12,** 137–160.

DE LA LANDE, I.S. (1989). Amplification mechanisms in peripheral tissues. In *Peripheral Actions of 5-Hydroxytryptamine*. ed. Fozard, J.R. pp. 123–141. Oxford: Oxford University Press.

DE LA LANDE, I.S. (1990). Amplifying effect of 5-HT in the rabbit ear artery is mediated by a 5-HT$_1$-like receptor. *Clin. Exp. Pharm. Physiol.* Supp. 17, 16.

DE LA LANDE, I.S., CANNELL, V.A. & WATERSON, J.G. (1966). The interaction of serotonin and noradrenaline on the perfused artery. *Br. J. Pharmacol. Chemother.*, **28,** 255–272.

DE LA LANDE, I.S. & KENNEDY, J.A. (1985). Receptors mediating the vasoconstrictor and amplifying actions of 5-hydroxytryptamine on the rabbit ear artery. *Clin. Exp. Pharmacol. Physiol.*, Suppl. **9,** 6–7.

DE LA LANDE, I.S., KENNEDY, J.A. & STANTON, B.J. (1989). Amplifying actions of 5-hydroxytryptamine in the rabbit ear artery. In *Serotonin, Actions, Receptors, Pathophysiology*. ed. Mylecharane, E.J., Angus, J.A., de la Lande, I.S. & Humphrey, P.P.A. pp. 123–129. London: MacMillan Press Ltd.

ENGEL, D., GOTHERT, M., HOYER, D., SCHLICKER, E. & HILLENBRAND, K. (1986). Identity of inhibitory pre-synaptic 5-hydroxytryptamine (5-HT) receptors in the rat brain cortex with 5-HT binding sites. *Naunyn Schmiederbergs Arch. Pharmacol.*, **332,** 1–7.

FENIUK, W. & HUMPHREY, P.P.A. (1989). Mechanisms of 5-hydroxytryptamine-induced vasoconstriction. In *Peripheral Actions of 5-Hydroxytryptamine*. ed. Fozard, J.R. pp. 100–114. Oxford: Oxford University Press.

FENIUK, W., HUMPHREY, P.P.A., PERREN, M.J. & WATTS, A.D. (1985). A comparison of 5-hydroxytryptamine receptors mediating contraction in rabbit aorta and dog saphenous vein: evidence for different receptor types obtained by use of selective agonists and antagonists. *Br. J. Pharmacol.*, **86,** 697–704.

FOZARD, J.R. (1976). Comparative effects of four migraine prophylactic drugs on an extracranial artery. *Eur. J. Pharmacol.*, **36,** 127–139.

FURCHGOTT, R. & ZAWADZKI, J. (1980). The obligatory role of the endothelial cells in the relaxation of arterial smooth muscle by acetylcholine. *Nature*, **288,** 373–376.

HOYER, D. (1989). 5-hydroxytryptamine receptors and effector coupling mechanism in peripheral tissues. In *The Peripheral Actions of 5-Hydroxytryptamine*. ed. Fozard, J.R. pp. 72–88. Oxford: Oxford University Press.

HUMPHREY, P.P.A., FENIUK, W., PERREN, M.J., CONNOR, H.E., OXFORD, A.W., COATES, I.H. & BUTINA, D. (1988). GR43175, a selective agonist for the 5-HT$_1$-like receptor in dog isolated saphenous vein. *Br. J. Pharmacol.*, **94,** 1123–1132.

MEEHAN, A.G., RAND, M.J. & MEDGETT, I.C. (1986). Effects of serotonin on sympathetic noradrenergic transmission in rabbit isolated ear artery. *J. Cardiovasc. Pharmacol.*, **8,** 114–153.

MYLECHARANE, E.J. (1990). Agonists and antagonists of 5-HT$_2$ receptors. In *Cardiovascular Pharmacology of 5-Hydroxytryptamine: Prospective Therapeutics Applications*. ed. Saxena, P.R., Bevan, P., Wallis, D.I. & Wouters, W. pp. 81–100. Dordrecht: Kluwer.

PEROUTKA, S.J. & MCCARTHY, B.G. (1989). Sumatriptan (GR43175) interacts selectively with 5-HT$_{1B}$ and 5-HT$_{1D}$ binding sites. *Eur. J. Pharmacol.*, **163,** 133–136.

PURDY, R.E., HURLBUT, D.E. & RAINS, L.A. (1981). Receptors for 5-hydroxytryptamine in rabbit isolated ear artery and aorta. *Blood Vessels*, **19,** 16–27.

SHOEFFTER, P. & HOYER, D. (1990). 5-Hydroxy-tryptamine (5-HT)-induced endothelium-dependent relaxation of pig coronary arteries is mediated by 5-HT receptors similar to the 5-HT$_{1D}$ receptor subtype. *J. Pharmacol. Exp. Ther.*, **252,** 387–394.

SUMMER, M.J., FENIUK, W. & HUMPHREY, P.P.A. (1989). Further characterization of the 5-HT receptor mediating vascular relaxation and elevation of cyclic AMP in porcine isolated vena cava. *Br. J. Pharmacol.*, **97,** 292–300.

VAN WIJNGAARDEN, I., TULP, M.Th.M. & SOUDIJN, W. (1990). The concept of selectivity in 5-HT receptor research. *Eur. J. Clin. Pharmacol.*, **188,** 301–312.

XU, Z., MONDAL, J.P., SONG, J.P. & PURDY, R.E. (1990). Effect of ouabain on the rabbit ear artery contraction to serotonin: enhanced response mediated by serotonergic rather than alpha adrenergic receptors. *J. Pharmacol. Exp. Ther.*, **253,** 668–675.

(Received October 31, 1991
Revised February 21, 1992
Accepted March 4, 1992)

Br. J. Pharmacol. (1992), **106**, 556–562

The effect of epithelium removal on leukotriene E_4-induced histamine hyperresponsiveness in guinea-pig tracheal smooth muscle

Crawford A.J. Jacques, Bernd W. Spur, *Malcolm Johnson & [1]Tak H. Lee

Department of Allergy and Allied Respiratory Disorders, Guy's Hospital, London SE1 9RT and *Dept. of Peripheral Pharmacology, Glaxo Group Research, Ware, Herts

1 Removal of the epithelium resulted in a threefold increase in guinea-pig tracheal sensitivity to histamine without increasing the maximal response.

2 Preincubation of epithelially-denuded guinea-pig tracheal smooth muscle with leukotriene E_4 (LTE_4) *in vitro* increased the subsequent maximal response of the tissues to histamine. The sensitivity of the tissues to histamine was unaffected by LTE_4 pretreatment.

3 Pretreatment of the epithelially-denuded tissues with the LTE_4-analogue, 20-COOH LTE_4, did not affect the maximal response to histamine.

4 LTE_4 pretreatment increased the maximal response of the epithelially-denuded tissues to substance P (SP) but did not affect the maximal response to carbachol, KCl nor to the β-adrenoceptor agonist, isoprenaline.

5 LTE_4-induced airway histamine hyperresponsiveness was blocked by indomethacin (5 μM), GR32191 (3 μM) and atropine (1 μM).

6 Both LTE_4 and U46619 pretreatment increased the contractile response of tracheal smooth muscle to electrical field stimulation.

7 It is proposed that LTE_4 induces an increased maximal response of epithelially-denuded guinea-pig airway smooth muscle to both histamine and substance P via a facilitation of cholinergic neurotransmission, which is dependent upon the secondary generaton of prostanoid mediator(s) acting on TP-receptors situated on cholinergic nerve terminals. Further, it is suggested that the increased maximal response of the epithelially-intact tissues to both histamine and substance P, after LTE_4 pretreatment, may be suppressed by an epithelially-derived factor.

Keywords: Leukotriene; asthma; histamine; substance P; hyperresponsiveness; epithelium; nerves; acetylcholine; neurotransmission; prostaglandin; EpDRF

Introduction

The sulphidopeptide leukotrienes, LTC_4, LTD_4 and LTE_4, comprise the activity previously recognised as slow-reacting substance of anaphylaxis. LTC_4, LTD_4 and LTE_4 are potent bronchoconstrictors of respiratory smooth muscle (Dahlen *et al.*, 1980), and may play a role in the pathophysiology of bronchial asthma.

In vitro studies have demonstrated that LTE_4 induces a specific hyperresponsiveness of guinea-pig epithelially-intact tracheal strips to histamine (Lee *et al.*, 1984; Jacques *et al.*, 1991). Responsiveness of parenchymal strips to histamine was unaffected by LTE_4 (Lee *et al.*,1984). The enchancement of histamine responsiveness was dependent upon both the concentration of LTE_4 and the time of preincubation with the smooth muscle. It was inhibited by the cyclo-oxygenase inhibitor, indomethacin, suggesting the secondary generation of prostanoids. The finding that the selective thromboxane A_2 antagonist, GR32191, also blocked LTE_4-induced histamine hyperresponsiveness suggested that the TP-receptor was involved (Jacques *et al.*, 1991). Finally, the production of histamine hyperresponsiveness by LTE_4 was critically dependent upon the structural integrity of the carboxyl group at C-1 and the nature of the peptide side-chain (Lee *et al.*, 1987).

Removal of the epithelium enhances the sensitivity but not the maximal response of respiratory smooth muscle to a wide variety of agonists, including acetylcholine and histamine, in the dog (Flavahan *et al.*, 1985), guinea-pig (Holroyde, 1986) and man (Aizawa *et al.*, 1988). This increase in sensitivity may be due to the loss of a functional barrier (Laitinen *et al.*, 1985) or to the loss of an epithelium-derived relaxant factor (Hay *et al.*, 1988). Many groups have demonstrated that epithelium removal can be mimicked by the addition of indomethacin (Aizawa *et al.*, 1988; Hay *et al.*, 1987).

We have now extended our previous work (Jacques *et al.*, 1991) on the effect of LTE_4 on epithelially-intact tracheal strips, by studying the capacity of LTE_4 to enhance the smooth muscle response in guinea-pig airways that have been denuded of epithelium.

Methods

Guinea-pig tracheal strips

Strips that were three cartilage rings thick, were prepared from Dunkin-Hartley male guinea-pigs (Charles River, UK. 300–350 g) for *in vitro* recording of isometric contraction using Grass FTO3D transducers. In all experiments the epithelium of the strips was removed with cotton wool. Histological sections of tissues treated in this way demonstrated no apparent damage to the underlying smooth muscle layer. The strips were suspended in 5 ml organ baths containing modified Krebs solution (composition, mM: NaCl 118, KH_2PO_4 1.2, KCl 4.7, $NaHCO_3$ 15.4, glucose 5.5, $MgCl_2$ 1.2 and $CaCl_2$ 1.3). The tissues were aerated with 95% O_2; 5%CO_2 and maintained at 37°C. Each tissue was loaded with

[1] Author for correspondence.

an initial tension of 2 g. The tissues were allowed to equilibrate for 1 h and were washed every 15 min over this period of time.

Once a stable baseline tension had been established (approximately 1.5 g), each tissue was exposed to logarithmically increasing concentrations of histamine over the range 1 nM to 100 μM in order to construct a cumulative histamine dose-response curve. The degree of contraction elicited by 100 μM histamine was assigned the value of 100% and all the subsequent contractile responses on each tissue were expressed as a percentage of this reference value. After completion of the initial histamine dose-response curve, the tissues were washed with Krebs solution every 15 min, for 1 h. During this time, the tension of the tissues returned to that recorded before histamine exposure.

Determination of the reproducibility of histamine dose-response curves

After the washout period and the re-establishment of the initial baseline tension, a second histamine dose-response curve was constructed. First and second histamine dose-response curves, on the same tissue, were compared in order to determine the within-tissue reproducibility of the response to histamine. The second histamine curves, on paired preparations from the same trachea, were compared in order to determine the between-tissues reproducibility of the histamine response.

The effect of leukotriene E_4 pretreatment on histamine responsiveness

In selected experiments, after completion of the first histamine curve, paired tissues were washed with Krebs solution every 15 min, for 1 h, until the tension had returned to initial baseline values. Test tissues were then exposed to either 4 nM or 15 nM leukotriene (LT) E_4, and control tissues to buffer, for an incubation time of 15 min, an incubation time shown to be optimal in a preliminary study of the kinetics of the effect of LTE_4 on histamine responsiveness. The concentrations of LTE_4 were selected as representing 10% and 30% respectively of the contractile response seen with 100 μM histamine. After incubation, the tissues were washed every 15 min for 60 min, in order to re-establish initial baseline tension values. A second histamine dose-response curve was then established.

In other experiments, the non-contractile analogue of LTE_4, 20-COOH LTE_4 (Samhoun *et al.*, 1989), was used in place of LTE_4.

Synthetic LTE_4 was prepared as previously described (Lewis *et al.*, 1980). Concentrations of leukotrienes were determined by ultraviolet absorbance at 280 nm assuming a molar extinction coefficient of 40,000 cm^{-1} M^{-1}.

Agonist selectivity of leukotriene E_4-induced hyperresponsiveness

LTE_4-induced hyperresponsiveness of guinea-pig tracheal smooth muscle to agonists other than histamine was investigated. The effect of a 15 min preincubation with 4 nM or 15 nM LTE_4 on the responsiveness of tracheal smooth muscle to either the muscarinic agonist, carbachol, substance P, or to potassium chloride (KCl), was investigated. Concentration-effect curves were constructed to carbachol over the range of 0.1 nM to 10 μM, substance P (0.1 nM to 10 μM) and to KCl (1 mM to 60 mM). In the experiments using substance P, phosphoramidon (1 μM), a metallopeptidase inhibitor, was added to all tissues.

In addition, the ability of LTE_4 to influence tracheal responsiveness to a relaxant agonist was studied. After pretreatment with LTE_4, tracheal strips were contracted with 100 μM histamine and dose-response curves to isoprenaline were then constructed over the concentration range 0.1 nM to 10 μM. Control tissues were used to determine the decay of the histamine contraction with time.

Pharmacological modulation of the effect of LTE_4 pretreatment on histamine responsiveness

The ability of various inhibitors or antagonists to block the effect of LTE_4 pretreatment on histamine responsiveness was investigated in separate experiments.

Indomethacin (5 μM), atropine (1 μM) or the TP-receptor antagonist, GR32191 (3 μM) (Humphrey *et al.*, 1990), were added to the Krebs solution at the beginning of the experiment for both the test (LTE_4-treated) and the control (buffer-treated) tissues. Neither atropine nor GR32191 caused any change in the smooth muscle baseline tension.

Electrical field stimulation

Tracheal strips were set up for electrical field stimulation (EFS) as described by Belvisi *et al.* (1990) and a Grass S88 stimulator was used to construct frequency-response curves over the range 1–50 Hz for each tissue. The following parameters were used: voltage, 20 V; pulse width, 0.1 ms and the length of stimulation was 10 s with a 2 min rest period. At least three EFS responses were obtained and the mean of these values was taken. The degree of contraction produced by 50 Hz stimulation, on the first curve, was assigned the value of 100%. All tissues were treated with propranolol (1 μM) in order to antagonize the effect of released sympathetic neurotransmitters. The contractions to EFS were blocked by tetrodotoxin (1 μM), showing that the response was of neural origin.

LTE_4 (4 nM) was incubated with the test tissues for 15 min and then the tissues were washed. Control tissues were treated with buffer. After the preparations had been washed for 1 h and regained initial basal tone, a second frequency-response curve was constructed. In separate experiments, in the presence of indomethacin (5 μM), tissues were pretreated with the thromboxane A_2-mimetic, U46619 {11, 9α -epoxymethano-PGH_2}. Test tissues were exposed to U46619 (4 nM – a non-contractile concentration) and control tissues to buffer for 30 min before constructing a second frequency-response curve.

Materials

Histamine, carbachol, substance P, isoprenaline, indomethacin, propranolol, tetrodotoxin, phosphoramidon and atropine were all obtained from Sigma, Poole, Dorset. GR32191 ([1-R-[1α(z), 2β,3β,5δ]]-(+)-7-[5-([1,1'-biphenyl]-4-ylmethoxy)-3-3-hydroxy-2- (1-piperidinyl) cyclopentyl -4-heptenoic acid, hydrochloride) and U46619 were gifts from Glaxo Group Research, Ware, Herts. All substances were diluted in 9 g $litre^{-1}$ saline.

Statistics

The concentration of histamine that elicited a 50% maximum contraction (EC_{50}) was interpolated from the second histamine dose-response curve for each tissue. The degree of contraction elicited by the highest concentration of any applied agonist is termed the maximal response (T_{max}). For the analysis of data, Student's *t* test for paired data was used. Values are given as mean ± s.d.

Results

Effect of epithelium removal on responsiveness to histamine of guinea-pig airway smooth muscle

Following removal of the epithelium, the histamine dose-response curve was displaced approximately 2–4 fold to the left (Figure 1). The histamine EC_{50} values for the intact and

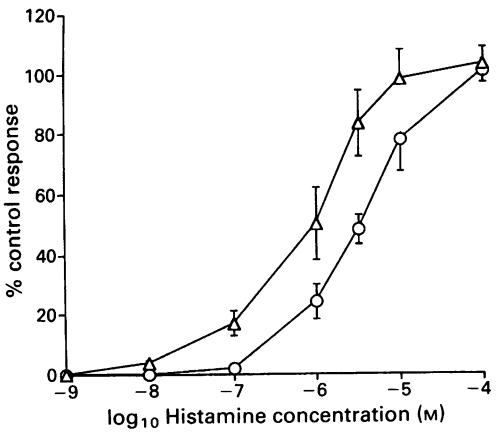

Figure 1 The effect of epithelium removal on tissue response to histamine. Intact tissues (○) and epithelially-denuded tissues (△), (mean with s.d. as vertical bars, $n = 4$).

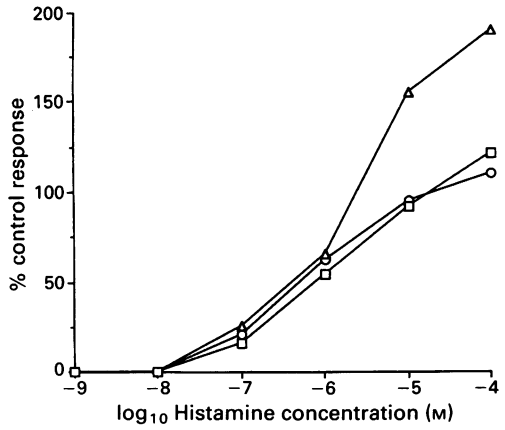

Figure 2 A single representative experiment (from $n = 5$) showing histamine dose-response curves constructed on guinea-pig epithelially-denuded tracheal smooth muscle pretreated with buffer (○), 4 nM leukotriene E_4 (LTE_4, △) or 15 nM LTE_4 (□), for 15 min.

denuded tissues were 3.2 ± 1.4 μM and 0.9 ± 1.1 μM, respectively (mean ± s.d., $n = 4$). The threshold concentrations of histamine eliciting contraction of intact and denuded tissues were 100 nM and 10 nM, respectively. There was no significant difference between intact and denuded tissues in terms of the maximal response to 100 μM histamine.

Reproducibility of histamine dose-response curves

Reproducibility of histamine dose-response curves was assessed both within and between tissues over the concentration range 1 nM to 100 μM. The threshold concentration for eliciting contraction was found to be approximately 10 nM for both the first and second dose-effect curves to histamine. The concentrations of histamine eliciting 50% contraction (EC_{50}) on the first and second histamine curves in the same tissues were 1.0 ± 0.8 μM and 1.2 ± 0.9 μM ($n = 25$), respectively. Randomly selected, paired tissues, taken from the same trachea, had EC_{50} values derived from the second histamine dose-response curves of 0.9 ± 1.1 μM and 1.0 ± 1.5 μM ($n = 12$), respectively.

The effect of leukotriene E_4 pretreatment on histamine responsiveness

LTE_4 dose-response curves were constructed on epithelially-intact guinea-pig tracheal strips over the concentration range 1 nM to 1 μM. Concentrations of LTE_4 eliciting 10%, 30% and 50% contraction were 4 ± 2.1 nM, 15 ± 3.8 nM and 29 ± 7 nM ($n = 4$), respectively. Concentrations of LTE_4 of 4 nM and 15 nM were used for the incubation on epithelially-denuded strips. The degree of contraction produced by these concentrations on epithelially-denuded tissue was $13.7 \pm 4\%$ and $34.5 \pm 2\%$ ($n = 4$), respectively.

The threshold concentration of histamine (10 nM) that elicited contraction of the epithelially-denuded tracheal smooth muscle (Figure 2) was unaffected by pretreatment with LTE_4. The histamine EC_{50} values of tissues treated with either buffer or LTE_4 (4 nM or 15 nM), for 15 min, were 0.6 ± 0.3 μM, 0.3 ± 0.2 μM and 0.5 ± 0.2 μM ($n = 5$), respectively (Figure 2). Thus there was no significant difference between control and test tissues in terms of tissue sensitivity (EC_{50}) to histamine after incubation with LTE_4.

There was a significant ($P < 0.01$) 60% increase in the maximal response to 100 μM histamine of denuded tissues treated with LTE_4 (4 nM), for 15 min, when compared with control tissues. These values were $197 \pm 15\%$ for the LTE_4-treated tissues and $137 \pm 25\%$ for the control tissues ($n = 5$), respectively. There was no significant difference between control tissues and those tissues treated with LTE_4 (15 nM) ($144 \pm 13\%$, $n = 5$) (Figure 2).

Kinetics of leukotriene E_4 incubation on the histamine maximal response (T_{max})

There was no significant difference between buffer-treated and LTE_4 (4 nM)-treated tissues in terms of sensitivity (EC_{50}) to histamine after incubation of tissues for 10, 15 or 20 min. There was also no difference between test and control tissues in terms of maximal response (T_{max}) to histamine (100 μM) after 10 min preincubation with 4 nM LTE_4 (Figure 3). However, when tissues were pretreated with LTE_4 (4 nM) for 15 min, there was a significant ($P < 0.01$) increase of 60% in T_{max}. When compared with controls, the corresponding increase in T_{max} after 20 min incubation was 35%, which was also statistically significant ($P < 0.05$) (Figure 3).

Effect of the 20-COOH LTE_4-analogue on histamine responsiveness

There was no significant difference between buffer- and 20-COOH LTE_4 (4 nM and 4 μM)-treated tissues, in terms of sensitivity to histamine (Figure 4), the EC_{50} values being 1.9 ± 0.6 μM, 1.7 ± 0.6 μM and 2.6 ± 1.7 μM ($n = 4$), respectively.

After pretreatment of test tissues with either 4 nM or 4 μM 20-COOH LTE_4, for 15 min, the corresponding T_{max} values were $78 \pm 26\%$ and $93 \pm 20\%$ ($n = 4$), respectively. These values were not significantly different from the control results of $103 \pm 12\%$.

Agonist selectivity of leukotriene E_4-induced hyperresponsiveness

Carbachol The EC_{50} values for carbachol in control tissues and tissues treated with either 4 nM or 15 nM LTE_4 were 34 ± 13 nM, 39 ± 17 nM and 39 ± 17 nM ($n = 4$), respectively. Similarly, LTE_4 pretreatment of tracheal strips was without effect on the maximal response to carbachol (10 μM); the maximal responses of control tissues and tissues treated with LTE_4 were $166 \pm 61\%$, $141 \pm 13\%$ and $149 \pm 13\%$ ($n = 4$), respectively, of the initial response to histamine (100 μM).

Potassium chloride The EC_{50} values for KCl in control tissues and in those tissues preincubated with either 4 nM or 15 nM LTE_4 were 20 ± 4 mM, 14 ± 10 mM and 15 ± 10 mM ($n = 4$), respectively. Additionally, preincubation of tracheal strips with LTE_4 did not affect the maximal response to KCl (60 mM), the maximal responses of control tissues and tissues treated with LTE_4 being $87 \pm 19\%$, $103 \pm 17\%$ and $105 \pm 33\%$ ($n = 4$) of the initial response to histamine (100 μM).

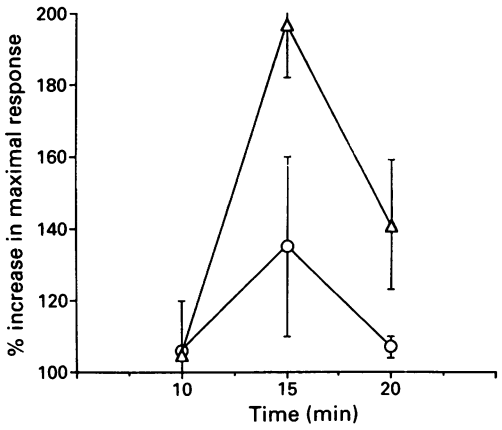

Figure 3 Plot of the maximal response to 100 μM histamine versus incubation time for tissues treated with either buffer (○) or 4 nM leukotriene E_4 (△). (Mean with s.d. as vertical bars, $n = 5$).

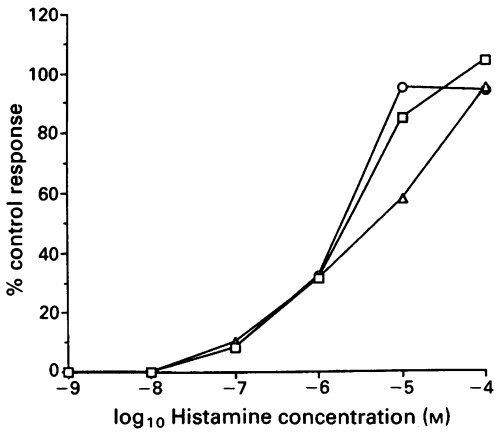

Figure 4 A single representative experiment (from $n = 4$) showing histamine dose-response curves constructed on guinea-pig epithelially-denuded tracheal smooth muscle pretreated with buffer (○), 4 nM 20-COOH LTE_4 (△) or 4 μM 20-COOH LTE_4 (□), for 15 min.

Substance P The EC_{50} values for SP in 4 nM- and 15 nM LTE_4-treated tissues were 13 ± 16 nM, 11 ± 8 nM ($n = 4$), respectively; these did not differ significantly from the EC_{50} of 15 ± 18 nM ($n = 4$) in the controls. However, there was a significant ($P < 0.05$) increase of 40% in the T_{max} value of 4 nM LTE_4-treated tissues (169 ± 23%, $n = 4$) compared with control tissues (131 ± 1%, $n = 4$). Those tissues pretreated with 15 nM LTE_4 did not differ significantly (122 ± 11%, $n = 4$) from control values in terms of the maximal response to 10 μM SP.

Isoprenaline LTE_4 pretreatment did not affect epithelially-denuded tracheal smooth muscle responsiveness to isoprenaline. The concentrations of isoprenaline producing 50% inhibition (IC_{50}) of histamine-induced contraction of control tissues and tissues pretreated with either 4 nM or 15 nM LTE_4 were 16 ± 22 nM, 12 ± 13 nM and 38 ± 23 nM ($n = 4$), respectively. Similarly, there was no significant difference between control tissues and those pretreated with LTE_4 in terms of the maximal response; T_{max} values for control and LTE_4-treated tissues were 93 ± 12%, 94 ± 6% and 91 ± 10% ($n = 4$), respectively. These results were corrected for decay of contraction with time.

Pharmacological modulation of the effect of leukotriene E_4 on histamine responsiveness

The enhanced maximal response to histamine after pretreatment with LTE_4 (4 nM) was inhibited by the presence of either the cyclo-oxygenase inhibitor, indomethacin; the TP-receptor antagonist, GR32191 or atropine.

Indomethacin Addition of indomethacin (5 μM) to tissues caused a decrease in baseline tension of approximately 500 ± 175 mg ($n = 4$), which was compensated for by raising the tension to the initial value. The histamine EC_{50} values obtained in the absence or presence of indomethacin were 0.7 ± 0.3 μM and 2.0 ± 0.9 μM ($n = 4$), respectively. This reflected a significant ($P < 0.05$) 3 fold rightward shift in the histamine dose-response curves. Indomethacin did not significantly affect the T_{max}, with values for buffer- and indomethacin-treated tissues being 110 ± 14% and 104 ± 20% ($n = 4$), respectively, of the initial response to histamine (100 μM).

However, preincubation of tissues with indomethacin (5 μM) inhibited the increased maximal response to histamine elicited by LTE_4 (Figure 5). The histamine EC_{50} for control tissues and tissues treated with 4 nM and 15 nM LTE_4 was 1.3 ± 0.5 μM, 1.0 ± 0.3 μM and 1.5 ± 0.7 μM ($n = 4$). The corresponding maximal contractile responses to 100 μM histamine were 106 ± 6%, 112 ± 14% and 111 ± 5% ($n = 4$), respectively. There was no significant difference between these values.

GR32191 In separate experiments, GR32191 (3 μM) was shown to inhibit the TP-receptor-mediated contraction of epithelially-denuded guinea-pig tracheal smooth muscle induced by the thromboxane A_2-mimetic, U46619 (results not shown). Addition of GR32191 (3 μM) did not affect tissue sensitivity to histamine; the histamine EC_{50} values for buffer and GR32191-treated tissues were 0.52 ± 0.4 μM and 0.78 ± 0.6 μM ($n = 4$), respectively. However, incubation of tissues with GR32191 (3 μM) inhibited LTE_4-induced increase in the maximal response to 100 μM histamine. Histamine EC_{50} values for control preparations and tissues treated with 4 nM LTE_4 were 0.47 ± 0.1 μM and 0.27 ± 0.2 μM ($n = 4$), respectively. The equivalent T_{max} values, in the presence of GR32191 (3 μM), were 128 ± 27% and 155 ± 32% ($n = 4$), respectively. None of these values showed significant difference.

Atropine Histamine dose-response curves were constructed on tracheal strips after pretreatment with either 4 nM LTE_4 or buffer, and in the presence or absence of atropine (1 μM). The incubation time was 15 min (Figure 6). Histamine curves, in the absence of atropine, were located with EC_{50}

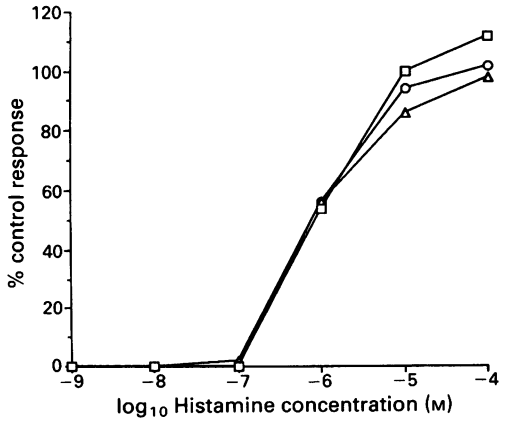

Figure 5 A single representative experiment (from $n = 4$) showing histamine dose-response curves constructed, in the presence of 5 μM indomethacin, on guinea-pig epithelially-denuded tracheal smooth muscle pretreated with buffer (○), 4 nM leukotriene E_4 (LTE_4, △) or 15 nM LTE_4 (□), for 15 min.

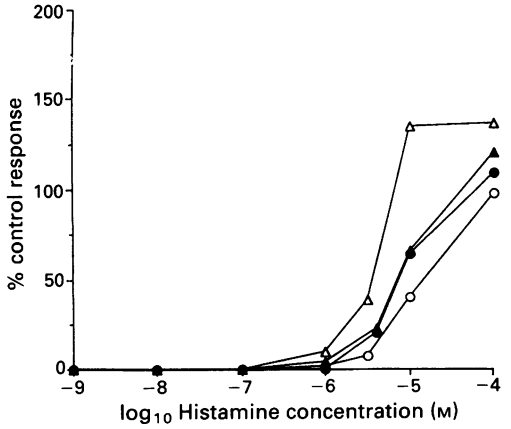

Figure 6 A single representative experiment (from $n = 4$) showing histamine dose-response curves constructed, either in the absence (○) or presence (●) of 1 μM atropine, on guinea-pig epithelially-denuded tracheal smooth muscle pretreated with either buffer (○,●) or 4 nM leukotriene E_4 (△,▲), for 15 min.

values of 9.8 ± 4.4 μM and 3.4 ± 3.3 μM ($n = 4$) with and without treatment with LTE_4 (4 nM). The locations of these curves were not significantly different. The T_{max} values for control and test tissues were $97 \pm 13\%$ and $138 \pm 8\%$ ($n = 4$), representing a significant ($P < 0.05$) increase of 40% in response in epithelially-denuded tracheal strips, which had been exposed to LTE_4 (4 nM).

Addition of atropine (1 μM) to tissues did not affect their sensitivity to histamine, with EC_{50} values for buffer and atropine-treated tissues being 9.8 ± 4.4 μM and 6.1 ± 4.2 μM ($n = 4$), respectively. Similarly, there was no significant difference between control and atropine-treated tissues in terms of maximal response to histamine; the T_{max} values were $97 \pm 13\%$ and $112 \pm 22\%$ ($n = 4$), respectively. In the presence of atropine (1 μM), preincubation of tissues with LTE_4 (4 nM) for 15 min did not alter either sensitivity or maximal responses to histamine, when compared with control tissues; the histamine EC_{50} for control tissues and tissues treated with LTE_4 (4 nM) were 6.1 ± 2.4 μM and 5.2 ± 3.1 μM ($n = 4$) and the T_{max} values for control and LTE_4-treated tissues were $112 \pm 22\%$ and $124 \pm 13\%$ ($n = 4$), respectively. There was no significant difference between these values.

The effects of leukotriene E_4 or U46619 pretreatment on electrical field stimulation (EFS)

The capacity of LTE_4 to influence guinea-pig tracheal response to EFS was investigated. Pretreatment of tissues with LTE_4 (4 nM), for 15 min, significantly ($P < 0.05$) increased the contractile response to EFS over the frequency-range 1–20 Hz when compared with control curves (Figure 7a). The frequencies producing 50% contraction of control and test tissues were approximately 8 ± 3 Hz and 4 ± 2 Hz ($n = 4$).

Since GR32191, the TP-receptor antagonist, had been previously shown to block the increase in T_{max} to histamine, the effect of the thromboxane A_2-mimetic, U46619, on electrically-stimulated tracheal strips was investigated. The concentration of U46619 used (4 nM) had no direct contractile effect and had no significant effect on responses to EFS at low frequencies (1–5 Hz). However, with EFS at frequencies of 10–40 Hz, U46619 caused a significant ($P < 0.05$) increase in the contractile response (Figure 7b). There was no significant difference between the two curves at the highest frequency of 50 Hz. The frequencies producing 50% contraction of control and test tissues were approximately 6 ± 3 Hz and 4 ± 3 Hz ($n = 4$), respectively.

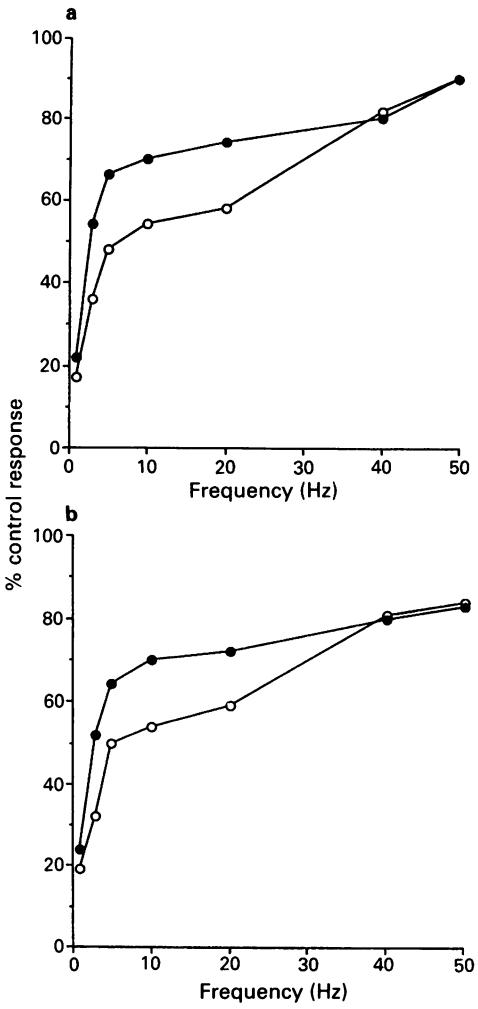

Figure 7 (a) A single representative experiment (from $n = 4$) showing frequency-response curves constructed on guinea-pig epithelially-denuded tracheal smooth muscle pretreated with either buffer (○) or 4 nM leukotriene E_4 (●), for 15 min and then subjected to electrical field stimulation. (b) A single representative experiment (from $n = 4$) showing frequency-response curves constructed on guinea-pig epithelially-denuded tracheal smooth muscle pretreated with either buffer (○) or 4 nM U46619 (●), for 15 min and then subjected to electrical field stimulation.

Discussion

Previous work has established that preincubation of guinea-pig epithelially-intact tracheal smooth muscle with LTE_4 enhances the subsequent contractile response to histamine. The effect was dose- and time-related (Lee *et al.*, 1984; Jacques *et al.*, 1991). In contrast to these findings, pretreatment of epithelially-denuded tissue with LTE_4 elicited a significant increase in the maximal response, without significantly affecting tissue sensitivity. The increase in the maximal response was again both time- and dose-related.

Removal of the respiratory epithelium produced an approximate 3 fold increase in tissue sensitivity to histamine without affecting the maximal response. This is in agreement with earlier reports (Holroyde, 1986).

The incubation concentrations of LTE_4 that were used in these studies were 4 nM and 15 nM. These concentrations elicited approximately the same degree of contraction in epithelially-denuded tracheal smooth muscle as in epithelially-intact tissue. This confirms the reports published by Hay *et al.* (1987) that epithelium removal had no effect on LTE_4-induced contractions.

LTE_4 pretreatment of denuded tissues did not modify sensitivity to histamine, in contrast to intact tissues where a significant increase in smooth muscle sensitivity to histamine of approximately 10 fold was observed (Jacques *et al.*, 1991). This would suggest that the epithelium is necessary for eliciting increased tissue sensitivity after LTE_4 exposure. Alternatively, having removed the epithelium and consequently enhanced sensitivity of the tissue to histamine, no further increase in sensitivity may be possible. Indeed, increasing the concentration of LTE_4 from 4 nM to 15 nM had no effect on tracheal smooth muscle sensitivity to histamine in epithelially-denuded tissues. Similarly, 20-COOH LTE_4, a structural analogue of LTE_4, which is without contractile activity on guinea-pig airway smooth muscle, did not affect tissue sensitivity to histamine.

Whereas in tissues with an intact epithelium pretreatment with either 4 nM or 15 nM LTE_4 did not significantly affect the maximal response to histamine, exposure of epithelially-denuded tissues to LTE_4 (4 nM) elicited significant increases in the T_{max}, with the optimal incubation time being 15 min. After 15 and 20 min incubation, there were significant increases of approximately 60% ($P < 0.01$) and 35% ($P < 0.05$), respectively. The increase in T_{max} in the absence of epithelium might be explained by the loss of an epithelium-derived relaxant factor (EpDRF) (Flavahan *et al.*, 1985; Tschirhart & Landry, 1986; Aizawa *et al.*, 1988; Hay *et al.*, 1988; Fernandes *et al.*, 1989; Raeburn *et al.*, 1990). The loss of increase of maximal response with time may be due to a variety of factors including the breakdown of the leukotriene or the production of a substance counteracting the increase. The lack of effect of tissue pretreatment with the higher concentration of LTE_4 (15 nM) might possibly be explained by the stimulated production of a suppressive factor (clearly not EpDRF as the epithelium has been removed) or, alternatively, the higher concentration may be interacting with receptors distinct from those activated by the lower concentration (4 nM). LTE_4 (15 nM) was only investigated for a 15 min incubation time, the optimal incubation time for LTE_4 (4 nM) to elicit an increase in maximal response, and further investigation with a variety of incubation times may show that the higher LTE_4 concentration is capable of enhancing the maximal response to histamine.

Actions of LTE_4 on epithelially-intact tissues were specific to histamine and did not modify carbachol, KCl, substance P (SP) or isoprenaline responses (Jacques *et al.*, 1991). Similarly, LTE_4, at concentrations of 4 nM and 15 nM, was unable to alter the sensitivity of epithelially-denuded tissues to any of these agonists. In addition, LTE_4 did not influence the maximal response of epithelially-denuded tissue to carbachol (10 μM). However, in the presence of a metalloendopeptidase inhibitor, pretreatment of epithelially-denuded tissues with LTE_4 (4 nM), for 15 min, significantly increased the maximal response to SP (10 μM). However, raising the concentration of LTE_4 to 15 nM produced no increase in the T_{max} in the test tissues. The lack of effect of LTE_4 treatment on 'denuded' tissue responsiveness to KCl may be due to the fact that contraction to KCl, in contrast to both histamine and SP, is not a receptor-mediated event.

The maximal relaxation to isoprenaline, in epithelially-denuded tissue previously exposed to LTE_4, remained unaltered. This suggests that the effect of LTE_4 pretreatment on epithelially-denuded tissue is selective for contractile agents.

The cyclo-oxygenase inhibitor, indomethacin, blocked the LTE_4-induced increase in maximal response to histamine in epithelially-denuded tracheal smooth muscle. Hay *et al.* (1987) have reported that indomethacin treatment of epithelially-denuded tracheal strips decreased LTE_4 sensitivity. This was not observed in our study. Hay *et al.* (1987)

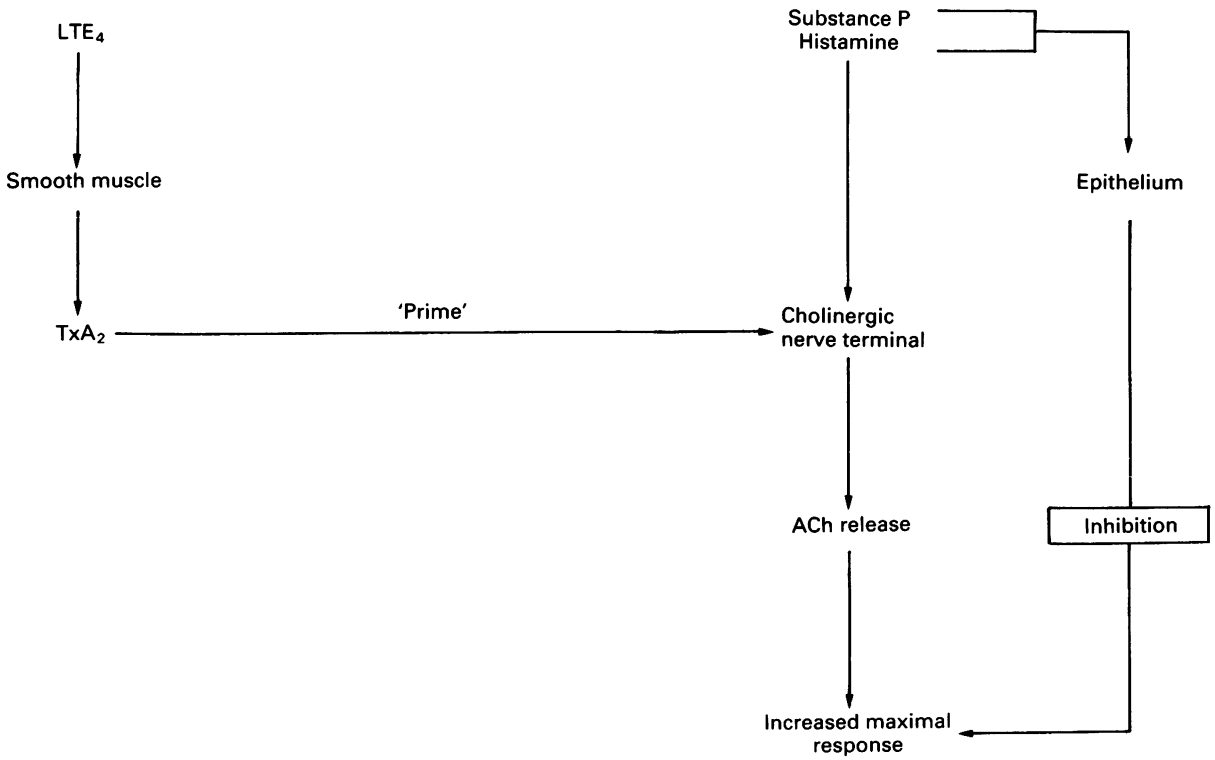

Figure 8 A proposed mechanism for leukotriene E_4 (LTE_4)-induced increase in the maximal response of guinea-pig central airway smooth muscle denuded of epithelium. It is suggested that LTE_4 stimulates the production of a prostanoid mediator that interacts with the TP-receptor, which is located on the cholinergic nerve terminal, to 'prime' neuronal activity. This action can be blocked by either indomethacin or GR32191. High concentrations of histamine or substance P interact with neuronal receptors to elicit the release of acetylcholine (ACh). Released ACh then interacts with postjunctional muscarinic M_3 receptors. This action can be blocked by atropine. A factor released from the epithelium could inhibit the increase in maximal response in epithelially-intact smooth muscle.

constructed cumulative dose-response curves to LTE_4, in the presence of indomethacin, whereas in the present experiments, only single concentrations of LTE_4 were used.

Various authors have reported that indomethacin is without effect on the maximal contractile response of epithelially-denuded guinea-pig trachea (Raeburn, 1990). Our results confirm this for histamine. Indomethacin was able to block completely the increase in maximal response to histamine of epithelially-denuded tissue, after pretreatment with LTE_4. This suggests that prostanoids are involved in the mechanism eliciting this phenomenon. The TP-receptor antagonist, GR32191, was also able to block the increase in the maximal response to histamine after exposure of epithelially-denuded tissues to LTE_4. Thus, the LTE_4-induced increase in T_{max} of epithelially-denuded tissues may be mediated by a TP-receptor-dependent mechanism.

Similarly, atropine, the muscarinic antagonist, was capable of completely blocking a 40% increase in the maximal response to histamine, after previous exposure to 4 nM LTE_4, for 15 min. This suggests that the increased T_{max} elicited by LTE_4 is via a cholinergic mechanism.

The contractile response of epithelially-denuded tissue to electrical field stimulation (EFS) was increased by prior exposure to LTE_4. The receptors that lead to an increased cholinergic response to EFS may be TP-receptors, as shown by the studies using the TP-receptor agonist, U46619. Pretreatment of 'denuded' tissues with a non-contractile concentration of U46619, potentiated the contractile response of tracheal strips to EFS. All of the observations were identical to those seen in the previous EFS studies on epithelially-intact tracheal smooth muscle (Jacques *et al.*, 1991). This suggests that epithelium removal is without effect on EFS in the guinea-pig trachea and confirms previous findings (Barnes *et al.*, 1985; Holroyde, 1986).

In conclusion, LTE_4 pretreatment of epithelially-denuded tracheal muscle increased the maximal contractile responses obtained with histamine and SP. This increase was blocked by both atropine and indomethacin, suggesting the involvement of both cholinergic and prostanoid mechanisms. A possible explanation for these findings is shown in Figure 8. LTE_4 acts on the epithelially-denuded smooth muscle to provoke release of a prostanoid, possibly TxA_2 or $PGF_{2\alpha}$, which then activates TP-receptors located on cholinergic nerve terminals. Activation of these receptors partially depolarizes or 'primes' the nerves without firing them. Low affinity receptors for histamine and SP could similarly be located on the nerve terminals and their activation might lead to the release of acetylcholine, which then acts postjunctionally to increase the maximal response (Figure 8).

In epithelially-intact tissues, the epithelium may release a relaxant factor that counteracts the increased T_{max} and as a result an increased maximal response is not observed. The inability of the LTE_4 analogue, 20-COOH-LTE_4, to increase the maximal response indicates the necessity of structural integrity of the LTE_4 molecule in order to produce this effect.

This work was supported by Glaxo Group Research, Ware, Herts.

References

AIZAWA, H., MIYAZAKI, N., SHIGEMATSU, N. & TOMOOKA, M. (1988). A possible role of airway epithelium in modulating hyperresponsiveness. *Br. J. Pharmacol.*, **93**, 139–145.

BARNES, P.J., CUSS, F.M.C. & PALMER, J.B.D. (1985). The effect of airway epithelium on smooth muscle contractility in bovine trachea. *Br. J. Pharmacol.*, **86**, 685–691.

BELVISI, M.G., STRETTON, C.D. & BARNES, P.J. (1990). Modulation of cholinergic neurotransmission in guinea-pig airways by opiods. *Br. J. Pharmacol.*, **100**, 131–137.

DAHLEN, S.-E., HEDQVIST, P., HAMMERSTROM, B. & SAMUELSSON, B. (1980). Leukotrienes are potent constrictors of human bronchi. *Nature*, **288**, 484–486.

FERNANDES, L.B., PATERSON, J.W. & GOLDIE, R.G. (1989). Co-axial bioassay of a smooth muscle relaxant factor released from guinea-pig tracheal epithelium. *Br. J. Pharmacol.*, **96**, 117–124.

FLAVAHAN, N.A., AARHUS, L.L., RIMELE, T.J. & VANHOUTTE, P.M. (1985). Respiratory epithelium inhibits bronchial smooth muscle tone. *J. Appl. Physiol.*, **58**, 834–838.

HAY, D.W.P., FARMER, S.G., RAEBURN, D., MUCCITELLI, R.M., WILSON, K.A. & FEDAN, F.S. (1987). Differential effects of epithelium removal on the responsiveness of guinea-pig tracheal smooth muscle to bronchoconstrictors. *Br. J. Pharmacol.*, **92**, 381–388.

HAY, D.W.P., MUCCITELLI, R.M., HORSTEMEYER, D.L. & RAEBURN, D. (1988). Is the epithelium-derived inhibitory factor in guinea-pig trachea a prostanoid? *Prostaglandins*, **35**, 625–637.

HOLROYDE, M.C. (1986). The influence of epithelium on responsiveness of guinea-pig isolated trachea. *Br. J. Pharmacol.*, **87**, 501–507.

HUMPHREY, P.P.A., HALLET, P., HORNBY, E.J., WALLIS, C.J., COLLINGTON, E.W. & LUMLEY, P. (1990). Pathophysiological actions of TxA_2 and their pharmacological antagonism by thromboxane-receptor blockade with GR32191. *Circulation*, **81**(suppl), 142–152.

JACQUES, C.A.J., SPUR, B.W., JOHNSON, M. & LEE, T.H. (1991). The mechanism of LTE_4-induced histamine hyperresonsiveness in guinea-pig tracheal and human bronchial smooth muscle, *in vitro*. *Br. J. Pharmacol.*, **104**, 859–866.

LAITINEN, L.A., HEINO, M., LAITINEN, A., KAVA, T. & HAAHTELA, T. (1985). Damage of the airway epithelium and bronchial reactivity in patients with asthma. *Am. Rev. Resp. Dis.*, **131**, 599–606.

LEE, T.H., ARM, J.P. & SPUR, B.W. (1987). Leukotrienes and bronchial hyperreactivity. In *Allergy and Inflation*. ed. Kay, A.B. Chapter 16. New York: Academic Press.

LEE, T.H., AUSTEN, K.F., COREY, E.J. & DRAZEN, J.M. (1984). LTE_4-induced airway hyperresponsiveness of guinea pig tracheal smooth muscle to histamine and evidence for 3 separate sulfidopeptide leukotriene receptors. *Proc. Natl. Acad. Sci, U.S.A.*, **81**, 4922–4925.

LEWIS, R.A., DRAZEN, J.M., AUSTEN, K.F., CLARK, D.A. & COREY, E.J. (1980). Identification of the C-(6)-S conjugate of leukotriene A with cysteine as a naturally occurring slow-reacting substance of anaphylaxis (SRS-A): importance of the 11-cis-geometry for biological activity. *Biochem. Biophys. Res. Commun.*, **96**, 271–277.

RAEBURN, D. (1990). Eicosanoids, epithelium and airway reactivity. *Gen. Pharmacol.*, **21**, 11–16.

SAMHOUN, M.N., COUROY, D.M. & PIPER, P.J. (1989). Pharmacological profile of leukotrienes E_4, N-acetyl LTE_4 and of four of their novel Ω- and β-oxidative metabolites in airways of guinea-pig and man, *in vitro*. *Br. J. Pharmacol.*, **98**, 1406–1412.

TSCHIRHART, E. & LANDRY, Y. (1986). Airway epithelium releases a relaxant factor: demonstration with substance P. *Eur. J. Pharmacol.*, **132**, 103–104.

(Received January 24, 1992
Revised March 2, 1992
Accepted March 4, 1992)

Br. J. Pharmacol. (1992), **106**, 563–567

Effects of nitric oxide synthesis inhibition on the goat coronary circulation under basal conditions and after vasodilator stimulation

J.L. García, N. Fernández, A.L. García-Villalón, L. Monge, B. Gómez & [1]G. Diéguez

Departamento de Fisiología, Facultad de Medicina, Universidad Autónoma, Arzobispo Morcillo 1, 28029 Madrid, Spain

1 The role of nitric oxide in the coronary circulation under basal conditions and when exposed to various vasodilator stimuli was studied in instrumented, anaesthetized goats, by examining the action of inhibiting endogenous nitric oxide production with N^G-nitro-L-arginine methyl ester (L-NAME).

2 In 12 goats, left circumflex coronary blood flow (electromagnetically measured), systemic arterial blood pressure and heart rate were continuously recorded. L-NAME (3–4, or 8–10 mg kg^{-1} injected i.v.) decreased resting coronary blood flow by 20 and 28%, increased mean arterial pressure by 23 and 30% and increased coronary vascular resistance by 47 and 65%, respectively, without affecting heart rate, or blood gases or pH. These haemodynamic effects were reversed by L-arginine (200– 300 mg kg^{-1} by i.v. injection, 5 goats).

3 Acetylcholine (0.001–0.1 μg), sodium nitroprusside (0.01–0.3 mg), and diazoxide (0.1–3 mg), injected intracoronarily in 6 goats, produced dose-dependent increases in coronary blood flow; sodium nitroprusside (0.1–0.3 mg) also caused hypotension and tachycardia.

4 During the effects of L-NAME, the coronary vasodilatation to acetylcholine was attenuated, to sodium nitroprusside was increased, and to diazoxide was unaffected, in comparison with control conditions. The hypotensive effects of sodium nitroprusside were also increased during treatment with L-NAME.

5 Graded coronary hyperaemic responses occurred after 5, 10 or 20 s of coronary occlusion. The magnitude of hyerpaemia for each occlusion duration was increased during treatment with L-NAME, in comparison to control.

6 The results suggest: (a) endogenous nitric oxide is involved in regulation of coronary circulation by producing a basal vasodilator tone, (b) acetylcholine-induced coronary vasodilatation is mediated, in part, by nitric oxide, and (c) inhibition of basal endogenous nitric oxide production induces supersensitivity of coronary vessels to nitrovasodilators and enhances hyperaemic responses after short periods of ischaemia of the myocardium.

Keywords: Endothelium; N^G-nitro-L-arginine methyl ester (L-NAME); vasodilator tone; reactive hyperaemia; acetylcholine; nitrovasodilators; supersensitivity

Introduction

Since the original observation by Furchgott & Zawadzki (1980) it is now recognized that the endothelium plays a major role in regulating vascular tone by releasing vasoactive factors and by modulating vascular responses to various stimuli (Furchgott & Vanhoutte, 1989). Experimental evidence indicates that nitric oxide, or a closely related compound, is at least one type of endothelium-derived relaxing factor that is synthesized from L-arginine (Palmer *et al.*, 1987; 1988; Ignarro *et al.*, 1987) and relaxes vascular smooth musculature via the stimulation of guanylate cyclase (Rapoport & Murad, 1983; Ignarro *et al.*, 1986). The synthesis of endothelial nitric oxide can be inhibited by several L-arginine analogues, and this inhibition induces vascular contraction *in vitro* and *in vivo* (Moncada & Higgs, 1990), increases resistance in several vascular beds (Gardiner *et al.*, 1990a; 1991) and reduces blood flow in the brachial artery of man (Vallance *et al.*, 1989). Thus, the basal release of nitric oxide (Martin *et al.*, 1986; Rees *et al.*, 1989a) appears to be responsible for maintaining a vasodilator tone in the cardiovascular system (Rees *et al.*, 1989b; Gardiner *et al.*, 1990a).

Endothelial function has been regarded as an important factor in the regulation of the coronary circulation and it may be of pathophysiological significance in several disease states (Harrison, 1989). However, many questions remain to be answered regarding the mechanisms by which the endothelium achieves this function. Endothelium-dependent vasodilatation has been found in coronary vessels from dogs (Rubanyi *et al.*, 1986; Hayashi *et al.*, 1988; Myers *et al.*, 1989) and man (Hodgson & Marshall, 1989). More recently it has been reported that human coronary vessels *in vitro* release nitric oxide, which is cleaved from L-arginine (Chester *et al.*, 1990) and that nitric oxide plays a significant role in modulating basal vasomotion and endothelial-dependent dilatation in the coronary circulation of dogs (Chu *et al.*, 1991).

The present experiments were performed to study the role of nitric oxide in basal vascular tone and in vasodilatation of the coronary circulation of anaesthetized goats. To this end, the animals were instrumented and the effects of a potent inhibitor of the nitric oxide synthesis, N^G-nitro-L-arginine methyl ester (L-NAME) (Moore *et al.*, 1990; Rees *et al.*, 1990), were investigated both on the basal coronary blood flow and on coronary vasodilator responses to acetylcholine, sodium nitroprusside, diazoxide and ischaemia.

[1] Author for correspondence.

Methods

Twelve female goats (32–49 kg) were anaesthetized with an intramuscular injection of 10 mg kg^{-1} ketamine hydrochloride and i.v. administration of 2% thiopentone sodium; supplemental doses were given as necessary for maintenance. After orotracheal intubation, artificial respiration with room air was instituted by use of a Harvard respirator. Adjustments in tidal volume or respiratory rate were used to maintain blood gases and pH within the following range: P_{O_2} = 85–110 mmHg; P_{CO_2} = 26–40 mmHg; pH = 7.35–7.45.

A polyethylene catheter was placed in one temporal artery to measure arterial blood pressure (Statham transducer), and to obtain blood samples for gas and pH analysis (Radiometer ABL, Copenhagen, Denmark).

A thoracotomy was performed through the fourth left intercostal space, and the pericardium opened to gain access to the left aspect of the heart. The proximal segment of the left circumflex coronary artery was dissected and an electromagnetic flow transducer (Biotronex) was placed on this artery to measure blood flow. A snare type occluder was also placed around this artery, just distal to the flow probe, to obtain zero flow baseline and to produce transient coronary ischaemias.

Coronary blood flow, systemic arterial pressure and heart rate were continuously recorded on a Beckman recorder throughout the experiments.

In this work the following experiments were performed: (1) after resting control measurements were recorded, 12 animals received an i.v. bolus of L-NAME (3–4 mg kg^{-1} within 5 min), and 5 min after the haemodynamic variables had reached a new steady state, animals received an additional i.v. infusion of L-NAME (0.05–0.08 mg kg^{-1} min^{-1} over 70–90 min). L-NAME was dissolved in isotonic saline (5 mg ml^{-1}), and each animal received in total 8–10 mg kg^{-1}. In five of these goats 200–300 mg kg^{-1} of L-arginine was given via i.v. route when the i.v. infusion of L-NAME was stopped. L-Arginine, dissolved in isotonic saline (50 mg ml^{-1}), was administered over 10–20 min; (2) the effects of acetylcholine (0.001, 0.003, 0.01, 0.03 and 0.1 μg), sodium nitroprusside (0.01, 0.03, 0.1 and 0.3 mg), and diazoxide (0.1, 0.3, 1 and 3 mg) were recorded in 6 animals before and during the i.v. infusion of L-NAME. All these substances were dissolved in isotonic saline and given in volumes of 0.3 ml directly into the left circumflex coronary artery through a 27G needle; these substances were injected in random sequence, and the administration of each dose was separated at least by 5 min, and (3) in 5 animals hyperaemic responses following occlusions of the left circumflex coronary artery lasting 5, 10 and 20 s were recorded before and during the i.v. infusion of L-NAME. The order of occlusions was randomized, and each observation was the average of 2 occlusions for each occlusion duration. To determine hyperaemic responses, the following measurements and calculations were made (Marcus *et al.*, 1981): (a) the control (basal) and the peak hyperaemic coronary blood flows were measured and then the peak hyperaemic flow to control flow ratio was calculated, and (b) the repayment-to-debt ratio was calculated as reactive hyperaemia blood flow divided by theoretical debt of blood flow. Reactive hyperaemia blood flow is the blood flow in ml during the total hyperaemic response over the control blood flow and was determined planimetrically on the recordings. The debt of blood flow is the blood flow in ml that theoretically would have occurred during arterial occlusion and was calculated as the control flow × the occlusion duration.

Resistance to blood flow through the left circumflex coronary artery was calculated before and during the effects of L-NAME as mean systemic arterial pressure in mmHg divided by the coronary blood flow in ml min^{-1}.

Drugs used were: N^G-nitro-L-arginine methyl ester (L-NAME, Sigma), acetylcholine chloride (Sigma), sodium nitroprusside (Sigma) and diazoxide (Hyperstat, Schering). Administration of isotonic saline alone intravenously or intracoronarily at the volumes employed in the present study had no systemic or coronary vascular effects.

Statistics: all haemodynamic measurements before and during treatment with L-NAME were compared using the same animal as its own control. Statistical analyses were performed using an analysis of variance for repeated measures, followed by an individual Student's t test for paired data.

Results

Effects of N^G-nitro-L-arginine methyl ester

Mean values for the circumflex coronary blood flow, mean systemic arterial pressure, coronary vascular resistance and heart rate obtained in 12 goats before and after treatment with L-NAME are summarized in Table 1. The i.v. bolus of L-NAME (3–4 mg kg^{-1} within 5 min) increased systemic arterial pressure by about 23% ($P<0.001$), decreased coronary blood flow by about 20% ($P<0.001$), increased coronary vascular resistance by about 47% ($P<0.001$), but did not change heart rate significantly ($P>0.05$). These effects occurred in all the animals except one in which coronary blood flow did not change; they were evident before completion of L-NAME injection. These haemodynamic changes were slightly accentuated during the additional i.v. infusion of L-NAME (0.05–0.08 mg kg^{-1} over 70–90 min); under these conditions, mean arterial pressure increased about 30%, coronary blood flow decreased about 28% and coronary vascular resistance increased about 65% with respect to control values. In these circumstances only the changes in coronary vascular resistance were significantly ($P<0.05$) different from the haemodynamic changes obtained after the i.v. bolus of L-NAME. Blood gases and pH during the effects of L-NAME were not significantly different from those obtained under control conditions. In 7 of these animals, the haemodynamic effects induced by L-NAME remained, at least, for 1 h after stopping its administration.

In 5 goats, administration of L-arginine, after stopping the i.v. infusion of L-NAME, decreased systemic arterial pressure, increased coronary blood flow, decreased coronary vascular resistance but did not change heart rate. The haemodynamic changes induced by L-NAME returned to control values within 5–10 min after stopping the i.v. administration of L-arginine (Table 1). This contrasted with the haemodynamics in the 7 goats treated with L-NAME, but not with L-arginine.

Effects of acetylcholine

Acetylcholine (0.001–0.1 μg), injected into the left circumflex coronary artery, produced dose-dependent increases in coronary blood flow, but did not change systemic arterial pressure significantly; the doses of 0.03 and 0.1 μg also caused bradycardia. However, the increments in coronary blood flow produced by acetylcholine during i.v. infusion of L-NAME were significantly lower than under control conditions (Figure 1).

Effects of sodium nitroprusside

Sodium nitroprusside (0.01–0.3 mg), injected into the left circumflex coronary artery, induced marked dose-dependent increases in coronary blood blood flow; these effects were significantly greater during treatment with L-NAME than under control conditions. The doses of 0.1 and 0.3 mg of sodium nitroprusside also induced decreases in systemic arterial pressure and caused tachycardia, and during treatment with L-NAME the doses of 0.03, 0.1 and 0.3 mg of sodium nitroprusside induced systemic hypotension and tachycardia. The hypotensive effects of each dose of sodium nitroprusside during L-NAME were significantly greater than

Table 1 Values (mean ± s.e.mean) for the left circumflex coronary blood flow (CBF), coronary vascular resistance (CVR), mean systemic arterial blood pressure (MAP), and heart rate (HR) obtained before (control), immediately (12 goats) or 1 h (7 goats) after i.v. administration of N^G-nitro-L-arginine methyl ester (L-NAME) and after i.v. administration of L-arginine following L-NAME (5 goats)

	Control	L-NAME 3–4 mg kg^{-1}	L-NAME 8–10 mg kg^{-1}	1 h later	L-Arginine (200–300 mg kg^{-1})
CBF (ml min^{-1})	39 ± 3.1	31 ± 2.5*	28 ± 1.5*	27 ± 1.8*	36 ± 2.2#
CVR (mmHg ml^{-1} min^{-1})	2.3 ± 0.2	3.4 ± 0.2*	3.8 ± 0.2*,†	3.9 ± 0.3*	2.2 ± 0.2#
MAP (mmHg)	84 ± 3.4	103 ± 4.9*	109 ± 3.7*	105 ± 3.2*	80 ± 7.4#
HR (beats min^{-1})	84 ± 4.7	87 ± 4.9	90 ± 6.2	88 ± 5.7	80 ± 10.8

*$P<0.001$ compared with the control; †$P<0.05$ compared with 3–4 mg kg^{-1} of L-NAME; #$P<0.01$ compared with L-NAME alone.

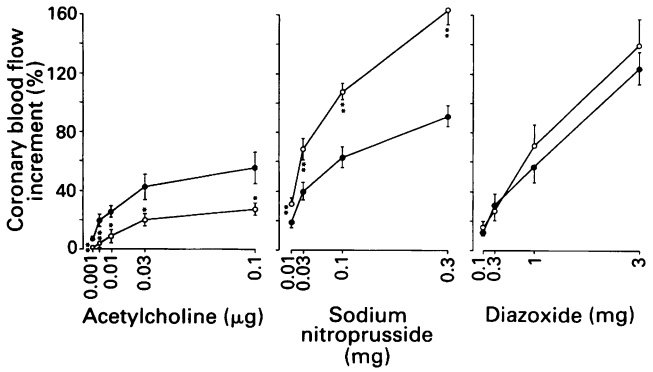

Figure 1 Effects of intracoronary injections of acetylcholine, sodium nitroprusside and diazoxide on coronary blood flow obtained in 6 goats in the absence (●) and in the presence (○) of N^G-nitro-L-arginine methyl ester (L-NAME). Values are mean and bars show s.e. mean.
*$P<0.05$; **$P<0.01$.

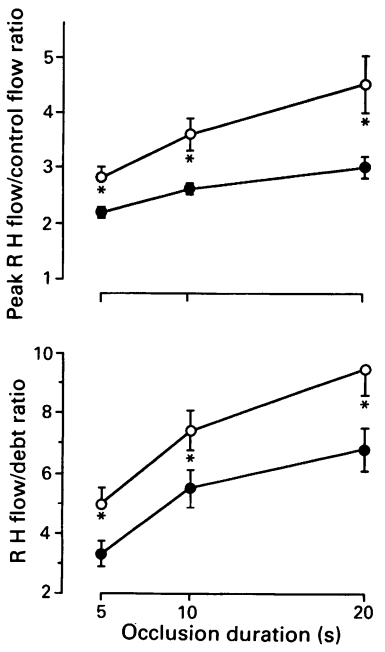

Figure 2 Reactive hyperemia (RH) in the coronary circulation of 5 goats obtained after coronary occlusions of 5, 10 and 20 s duration in the absence (●) and in the presence (○) of N^G-nitro-L-arginine-methyl ester (L-NAME). Values are mean and bars show s.e. mean.
*$P<0.05$.

the control responses; the average decrements in mean arterial pressure (mmHg) for each dose were (mean ± s.e.mean): 0 ± 0 vs. 9 ± 2 (0.03 mg), 10 ± 3 vs. 19 ± 3 (0.1 mg) and 22 ± 4 vs. 40 ± 6 (0.3 mg).

The coronary effects of sodium nitroprusside were evident, and were measured, before the systemic effects; they are summarized in Figure 1.

Effects of diazoxide

Diazoxide (0.1–3 mg), injected into the left circumflex coronary artery, produced marked, dose-dependent increases in the coronary blood flow without affecting significantly the systemic variables. The coronary effects of this drug were similar ($P>0.05$) under control conditions and during treatment with L-NAME (Figure 1).

Hyperaemic responses

After releasing the coronary arterial occlusion, a marked hyperaemic response was recorded, and the magnitude of the hyperaemic response (peak hyperaemic flow to control flow ratio, and repayment-to-debt ratio) increased significantly as occlusion duration increased from 5 to 20 s. This feature occurred under control conditions and during i.v. infusion of L-NAME. However, the magnitude of the hyperaemic responses (peak hyperaemic flow to control flow ration and repayment-to-debt ratio) for each occlusion duration was significantly higher during treatment with L-NAME than under control conditions (Figure 2).

In both circumstances, coronary occlusion of 20 s duration, but not of 5 and 10 s duration, was often accompanied by moderate decreases (5–10 mmHg for mean arterial pressure) in systemic arterial blood pressure. This hypotension coincided with the coronary occlusion and recovered within 15 s after releasing the occlusion.

Discussion

The present results show that i.v. administration of L-NAME, but not of the vehicle, produced reduction in resting coronary blood flow by increasing coronary vascular resistance. These coronary vascular effects were accompanied by a moderate increase in systemic arterial blood pressure, and changes in coronary blood flow and systemic arterial blood pressure by L-NAME were reversed with L-arginine. As L-NAME has proved to be a potent inhibitor of nitric oxide synthesis (Moore *et al.*, 1990; Rees *et al.*, 1990), our results suggest that the decreased coronary blood flow by this subs-

tance is related to reduction in basal nitric oxide production, and consequently with inhibition of nitric oxide-mediated basal vasodilator tone in the coronary vasculature *in vivo*. This agrees with observations in the dog coronary circulation (Chu *et al.*, 1991) and supports the suggestion that a basal vasodilator tone mediated by nitric oxide is present in the coronary circulation, as occurs in other vascular beds (Aisaka *et al.*, 1989; Rees *et al.*, 1989a; Gardiner *et al.*, 1990b). In awake dogs N^G-monomethyl-L-arginine (L-NMMA), another inhibitor of nitric oxide synthesis, induced reductions in resting coronary blood flow of about 19% and increases in systemic arterial blood pressure, without affecting left ventricular contractility (Chu *et al.*, 1991). Our study shows that lower concentrations of L-NAME were necessary to produce a reduction in coronary blood flow, comparable in magnitude to that found with L-NMMA (Chu *et al.*, 1991). Heart rate decreases are frequently observed when inhibitors of nitric oxide are administered (Aisaka *et al.*, 1989; Rees *et al.*, 1989b; Gardiner *et al.*, 1990b) but we did not find this phenomenon, probably because anaesthesia may block the baroreflex response (Widdop *et al.*, 1992). Systemic hypertension to L-NAME has also been found by others (Gardiner *et al.*, 1990a; Moncada *et al.*, 1991), and the haemodynamic responses to this substance seems to differ between vascular beds (Gardiner *et al.*, 1991; Van Gelderen *et al.*, 1991) and species (Van Gelderen *et al.*, 1991).

Intracoronary administration of acetylcholine produced coronary vasodilatation in anaesthetized goats, a feature also observed in dogs (Cox *et al.*, 1983; Reid *et al.*, 1985; Chu *et al.*, 1991) and man (Hodgson & Marshal, 1989). It appears that acetylcholine produces vasorelaxation by releasing endothelium-derived nitric oxide (Furchgott & Vanhoutte, 1989; Moore *et al.*, 1990; Rees *et al.*, 1990; Gardiner *et al.*, 1991) and we found that the acetylcholine-induced coronary vasodilatation was attenuated during treatment with L-NAME. As the coronary vasodilator response to diazoxide was preserved and those to sodium nitroprusside and ischaemia were enhanced, the reduction in acetylcholine-induced vasodilatation after L-NAME was probably a consequence of inhibition of nitric oxide formation and not secondary to a loss of ability of coronary vessels to dilate. This agrees with the observations in conscious dogs by Chu *et al.* (1991) and supports the idea that the coronary vasodilatation by acetylcholine is mediated, at least in part, by release of endothelial nitric oxide.

Both sodium nitroprusside and diazoxide produced increases in coronary blood flow, and the effects of sodium nitroprusside were increased, whereas those of diazoxide were not modified, during the action of L-NAME. Sodium nitroprusside has been used as a donor of exogenous nitric oxide and produces vasodilatation in a similar way to nitric oxide (Ignarro & Kadowitz, 1985). Enhanced vasorelaxant responses to sodium nitroprusside and other nitrous compounds have been found in the absence of a functional endothelium or in the presence of L-arginine analogues (Shirasaki & Su, 1985; Lüscher *et al.*, 1989; Forster *et al.*, 1990; Gardiner *et al.*, 1991; Moncada *et al.*, 1991) and this has been related to an increased sensitivity of guanylate cyclase in vascular musculature to exogenous nitric oxide when production of endogenous nitric oxide is reduced (Gardiner *et al.*, 1991; Moncada *et al.*, 1991). Therefore, it appears that the removal of endogenous nitric oxide in the vasculature could lead to increases in sensitivity to vasodilators that act by stimulating soluble guanylate cyclase (Gardiner *et al.*, 1991; Moncada *et al.*, 1991) and this phenomenon might also occur in the coronary circulation as suggested from our study. Supersensitivity to exogenous nitric oxide also seems to develop in the systemic circulation of the goat as indicated by the increased hypotensive effects to sodium nitroprusside during treatment with L-NAME.

Reactive hyperaemia after short ischaemias of the myocardium is known to occur in the coronary circulation, and metabolic and haemodynamic factors that contribute to the hyperaemic response have been explored (Feigl, 1983). However, very little is yet known of the role of the endothelium in the coronary hyperaemic response (Hayashi *et al.*, 1988; Ueeda *et al.*, 1990; Chu *et al.*, 1991). Using guinea-pig heart Langendorff preparations, it was observed that N^G-nitro-L-arginine (an inhibitor of nitric oxide synthesis) reduces coronary blood flow by 40%, but did not affect the peak hyperaemic response, although the duration of reactive hyperaemia to 30 s coronary occlusion was shortened (Ueeda *et al.*, 1990). In dogs, endothelium denudation (Hayashi *et al.*, 1988) or treatment with L-NMMA (Chu *et al.*, 1991) did not affect peak reactive hyperaemic flow, but reduced the flow-mediated vasodilatation after ischaemia following 20 s coronary occlusion. Our observations show that in the presence of L-NAME the hyperaemic responses (peak hyperaemic flow to control flow ratio, and repayment-to-debt ratio) to 5, 10, and 20 s of coronary occlusion were increased compared to those found before administration of L-NAME. We have no immediate explanation for the differences between our results and those of the above mentioned studies (Hayashi *et al.*, 1988; Ueeda *et al.*, 1990; Chu *et al.*, 1991). The possibility that coronary vasodilator reserve to transient ischaemias is augmented by an increased vascular tone during treatment with L-NAME may be excluded since an increased vasodilator reserve was not observed to diazoxide in those conditions. Thus, inhibition of basal nitric oxide production with L-NAME augments the hyperaemic responses after short ischaemias in the coronary circulation as seen with the vasodilator responses to sodium nitroprusside. This issue raises several questions that may deserve to be investigated, for example (1) is the increased hyperaemic response of the same nature as supersensitivity to nitrovasodilators, and (2) are the coronary vessels supersensitive to factors released from the myocardium and/or the endothelium during ischaemia when endothelial nitric oxide production is reduced?

In conclusion, the results presented herein support the idea that endogenous nitric oxide is involved in the regulation of the coronary circulation under basal conditions by producing a vasodilator tone. They also suggest that inhibition of basal endogenous nitric oxide production reduces the acetylcholine-induced coronary vasodilatation, induces supersensitivity of coronary vessels to nitrovasodilators, and enhances hyperaemic responses after short ischaemias of the myocardium. These findings could be of relevance for understanding pathophysiology and for treatment of some coronary diseases in which the endothelium is damaged.

The authors are grateful to Mrs H. Fernánez-Lomana and E. Martínez for technical assistance.

This work was supported, in part, by DGICYT (88/0058) and FIS (89/0639).

References

AISAKA, K., GROSS, S.S., GRIFFITH, O.W. & LEVI, R. (1989). N^G-methylarginine, an inhibitor of endothelium-derived nitric oxide synthesis, is a potent pressor agent in the guinea-pig: does nitric oxide regulate blood pressure *in vitro*? *Biochem. Biophys. Res. Commun.*, **160**, 881–886.

CHESTER, A.H., O'NEIL, G.S., TADJKARIMI, S., PALMER, R.M.J., MONCADA, S. & YACOUB, M.H. (1990). The role of nitric oxide in mediating endothelium dependent relaxations in the human epicardial coronary artery. *Int. J. Cardiol.*, **29**, 305–309.

CHU, A., CHAMBERS, D.E., LIN, C.-C., KUEHL, W.D., PALMER, R.M.J., MONCADA, S. & COBB, F.R. (1991). Effects of inhibition of nitric oxide formation on basal vasomotion and endothelium-dependent responses of the coronary arteries in awake dogs. *J. Clin. Invest.*, **87**, 1964–1968.

COX, D.A., HINTZE, T.H. & VATNER, S.F. (1983). Effects of acetylcholine on large and small coronary arteries in conscious dogs. *J. Pharmacol. Exp. Ther.*, **225**, 764–769.

FEIGL, E.O. (1983). Coronary physiology. *Physiol. Reg.*, **63**, 1–205.

FORSTER, C., MAIN, J.S. & ARMSTRONG, P.W. (1990). Endothelium modulation of the effects of nitroglycerin on blood vessels from dogs with pacing-induced heart failure. *Br. J. Pharmacol.*, **101**, 109–114.

FURCHGOTT, R.E. & VANHOUTTE, P.M. (1989). Endothelium-derived relaxing and contracting factors. *FASEB J.*, **3**, 2007–2018.

FURCHGOTT, R.F. & ZAWADSKI, J.V. (1980). The obligatory role of endothelial cells in the relaxation of arterial smooth muscle by acetylcholine. *Nature*, **228**, 373–376.

GARDINER, S.M., COMPTON, A.M., BENNETT, T., PALMER, R.M.J. & MONCADA, S. (1990a). Control of regional blood flow by endothelium-derived nitric oxide. *Hypertension*, **15**, 486–492.

GARDINER, S.M., COMPTON, A.M., KEMP, P.A. & BENNETT, T. (1990b). Regional and cardiac haemodynamic effects of N^G-nitro-L-arginine methyl ester in conscious, Long Evans rats. *Br. J. Pharmacol.*, **101**, 625–631.

GARDINER, S.M., KEMP, P.A. & BENNETT, T. (1991). Effects of N^G-nitro-L-arginine methyl ester on vasodilator responses to acetylcholine. 5-N-ethylcarboxamidoadenosine or salbutamol in conscious rats. *Br. J. Pharmacol.*, **103**, 1725–1732.

HARRISON, D.G. (1989). From isolated vessels to the catheterization laboratory. Studies of endothelial function in the coronary circulation of humans. *Circulation*, **80**, 703–706.

HAYASHI, Y., TOMOIKE, H., NAGASAWA, K., YAMADA, A., NISHIJIMA, H., ADACHI, H. & NAKAMURA, M. (1988). Functional and anatomical recovery of endothelium after denudation of coronary artery. *Am. J. Physiol.*, **254**, H1081–H1090.

HODGSON, J.MCB. & MARSHALL, J.J. (1989). Direct vasoconstriction and endothelium-dependent vasodilation. Mechanisms of acetylcholine effects on coronary flow and arterial diameter in patients with nonstenotic coronary arteries. *Circulation*, **79**, 1043–1051.

IGNARRO, L.J. & KADOWITZ, P.J. (1985). The pharmacological and physiological role of cyclic GMP in vascular smooth muscle relaxation. *Annu. Rev. Pharmacol. Toxicol.*, **25**, 171–191.

IGNARRO, L.J., BUGA, G.M., WOOD, K.S., BYRNS, R.E. & CHAUDHURI, G. (1987). Endothelium-derived relaxing factor produced and released from artery and vein is nitric oxide. *Proc. Natl. Acad. Sci. U.S.A.*, **84**, 9265–9269.

IGNARRO, L.J., HARBISON, R.G., WOOD, K.S. & KADOWITZ, P.J. (1986). Activation of purified soluble guanylate cyclase by endothelium-derived relaxing factor from intrapulmonary artery and vein: stimulation by acetylcholine, bradykinin and arachidonic acid. *J. Pharmacol. Exp. Ther.*, **237**, 893–900.

LÜSCHER, T.F., RICHARD, V. & YANG, Z. (1989). Interaction between endothelium-derived nitric oxide and SIN-1 in human and porcine blood vessels. *J. Cardiovasc. Pharmacol.*, **14**, Suppl. 11, S76–S80.

MARCUS, M., WRIGHT, C., DOTY, D., EASTHAM, C., LAUGHLIN, D., KRUMM, P., FASTENOW, C. & BRODY, M. (1981). Measurements of coronary velocity and reactive hyperemia in the coronary circulation of humans. *Circ. Res.*, **49**, 877–891.

MARTIN, W., FURCHGOTT, R.F., VILLANI, G.M. & JOTHIANANDAN, D. (1986). Depression of contractile responses in rat aorta by spontaneously released endothelium-derived relaxing factor. *J. Pharmacol. Exp. Ther.*, **237**, 529–538.

MONCADA, S. & HIGGS, E.A. (1990). *Nitric Oxide from L-arginine: A Bioregulatory System.* Amsterdam: Excepta Medica.

MONCADA, S., REES, D.D., SCHULZ, R. & PALMER, R.M.J. (1991). Development and mechanism of a specific supersensitivity to nitrovasodilators after inhibition of vascular nitric oxide synthesis in vivo. *Proc. Natl. Acad. Sci. U.S.A.*, **88**, 2166–2170.

MOORE, P.K., AL-SWAYEH, O.A., CHONG, N.W.S., EVANS, R.A. & GIBSON, A. (1990). L-N^G-nitro arginine (L-NOARG), a novel L-arginine-reversible inhibitor of endothelium-dependent vasodilatation in vitro. *Br. J. Pharmacol.*, **99**, 408–412.

MYERS, P.R., BANITT, P.F., GUERRA, F. Jr. & HARRISON, G. (1989). Characteristics of canine coronary resistance arteries: importance of endothelium. *Am. J. Physiol.*, **257**, H603–H610.

PALMER, R.M.J., FERRIGE, A.G. & MONCADA, S. (1987). Nitric oxide release accounts for the biological activity of endothelium-derived relaxing factor. *Nature*, **327**, 524–526.

PALMER, R.M.J., ASHTON, D.S. & MONCADA, S. (1988). Vascular endothelial cells synthesize nitric oxide from L-arginine. *Nature*, **333**, 664–666.

RAPOPORT, R.M. & MURAD, F. (1983). Agonist-induced endothelium dependent relaxation in rat thoraci aorta may be mediated through cGMP. *Circ. Res.*, **52**, 352–357.

REES, D.D., PALMER, R.M.J., HODSON, H.F. & MONCADA, S. (1989a). A specific inhibitor of nitric oxide formation from L-arginine attenuates endothelium-dependent relaxation. *Br. J. Pharmacol.*, **96**, 418–424.

REES, D.D., PALMER, R.M.J. & MONCADA, S. (1989b). Role of endothelium-derived nitric oxide in the regulation of blood pressure. *Proc. Natl. Acad. Sci. U.S.A.*, **86**, 3375–3378.

REES, D.D., PALMER, R.M.J., SCHULZ, R., HODSON, H.R. & MONCADA, S. (1990). Characterization of three inhibitors of endothelial nitric oxide synthase *in vitro* and *in vivo*. *Br. J. Pharmacol.*, **101**, 746–752.

REID, J.V.O., ITO, B.R., HUANG, A.H., BUFFINGTON, C.W. & FEIGL, E.O. (1985). Parasympathetic control of transmural coronary blood flow in dogs. *Am. J. Physiol.*, **249**, H337–H343.

RUBANYI, G.M., ROMERO, J.C. & VANHOUTTE, P.M. (1986). Flow-induced release of endothelium-derived relaxing factor. *Am. J. Physiol.*, **250**, H1145–H1149.

SHIRASAKI, Y. & SU, C. (1985). Endothelium removal augments vasodilatation by sodium nitroprusside and sodium nitrite. *Eur. J. Pharmacol.*, **114**, 93–96.

UEEDA, M., ARROYO, L.H. & OLSSON, R.A. (1990). Role of nitric oxide (N = O) in coronary reactive hyperemia (RH) and the active hyperemic response to pacing (AG). (Abstract). *The Physiologist*, **33**, A-78.

VALLANCE, P., COLLIER, J. & MONCADA, S. (1989). Effects of endothelium-derived nitric oxide on peripheral arteriolar tone in man. *Lancet*, **ii**, 997–1000.

VAN GELDEREN, E.M., HEILIGERS, J.P.C. & SAXENA, P.R. (1991). Haemodynamic changes and acetylcholine-induced hypotensive responses after N^G-nitro-L-arginine methyl ester in rats and cats. *Br. J. Pharmacol.*, **103**, 1899–1904.

WIDOPP, R.E., GARDINER, S.M., KEMP, P.A. & BENNETT, T. (1992). The influence of atropine and atenolol on the cardiac haemodynamic effects of N^G-nitro-L-arginine methyl ester in conscious, Long Evans rats. *Br. J. Pharmacol.*, **105**, 653–656.

(Received February 7, 1992
Revised March 2, 1992
Accepted March 4, 1992)

Br. J. Pharmacol. (1992), **106**, 568–573

Neurally evoked responses of human isolated resistance arteries are mediated by both α_1- and α_2-adrenoceptors

N.A. Parkinson, S.McG. Thom, A.D. Hughes, P.S. Sever, *M.J. Mulvany & *[1]H. Nielsen

Department of Clinical Pharmacology, St. Mary's Hospital Medical School, London W2 1NY and *Institute of Pharmacology & Danish Biomembrane Research Centre, Bartholin Building, University of Aarhus, DK-8000 C, Denmark

1 Human subcutaneous resistance arteries (internal diameter 113–626 μm) were mounted in an isometric myograph. Electrical field stimulation was applied either continuously in the form of a frequency-response curve or intermittently at 16 Hz. The magnitude of the maximum contraction induced by continuous stimulation expressed as a percentage of the response to a supramaximal concentration of noradrenaline (10 μM) was highly variable but unrelated to vessel calibre. Contractile responses to both continuous and intermittent stimulation were abolished by 1 μM tetrodotoxin.

2 Prazosin (100 nM and 1 μM, α_1-adrenoceptor antagonist) inhibited responses to continuous stimulation over a range of frequencies (2–8 Hz). The response to continuous stimulation at 8 Hz was inhibited by 78 ± 6% by 1 μM prazosin. Rauwolscine (100 nM, α_2-adrenoceptor antagonist) had a smaller effect on contractions induced by continuous stimulation. Rauwolscine inhibited the response at 8 Hz by 36 ± 6%. Rauwolscine at a higher concentration (1 μM) caused further inhibition of the response to continuous stimulation. Prazosin and rauwolscine in combination almost completely inhibited the response to continuous stimulation at concentrations of 1 μM.

3 Prazosin and rauwolscine inhibited responses to intermittent stimulation in a concentration-dependent manner. The IC_{50} for this action of prazosin was 3.7 ± 1.6 nM and the maximum inhibition induced by 100 nM prazosin was 78 ± 6%. The IC_{50} of rauwolscine was 12.0 ± 1.3 nM and 100 nM rauwolscine caused a 86 ± 7% reduction in the response to intermittent stimulation. Prazosin and rauwolscine in combination (each at 100 nM) caused marked inhibition of the response to intermittent stimulation leaving only 7.0 ± 2.6% of the response.

4 These data suggest that neurally released noradrenaline evokes contractions of human resistance arteries by activation of both α_1- and α_2-adrenoceptors postjunctionally.

Keywords: Prazosin-pharmacology; peripheral-nerves-drug-effects; peripheral-vascular; rauwolscine; α-adrenoceptors; resistance-vessel

Introduction

Studies using exogenously applied agonists and antagonists have demonstrated functional postjunctional α_1- and α_2-adrenoceptors in human arteries. Moulds & Jauernig (1977) were the first to describe *in vitro* a 'prazosin-resistant' component of the response to noradrenaline in human isolated digital arteries, and subsequently, responses mediated by arterial postjunctional α_2-adrenoceptors have been demonstrated both *in vivo* (Elliott & Reid, 1983; Jie *et al.*, 1984) and *in vitro* (Stevens & Moulds, 1981; Nielsen *et al.*, 1989).

The contribution of postjunctional α_2-adrenoceptors to neurally evoked responses is not yet clarified. It was originally proposed that the α_2-adrenoceptors would only be activated by circulating catecholamines and not by neuronally released noradrenaline; i.e. an extra-synaptic location of the α_2-adrenoceptor (Timmermans & Van Zwieten, 1982; Jie *et al.*, 1987). Studies using terminal arterioles of the rat cremaster muscle, however, have suggested that the α-adenoceptor being stimulated postjunctionally by neurally-released noradrenaline is mainly of the α_2-subtype (Ohyanagi *et al.*, 1991) and results from investigations on human isolated digital arteries indicate that both α_1- and α_2-adrenoceptors are activated postjunctionally by neurally released noradrenaline (Stevens & Moulds, 1985).

Responses to exogenously applied noradrenaline in human subcutaneous resistance arteries are mediated by both α_1- and α_2-adrenoceptors (Nielsen *et al.*, 1990). The objective of this study was to assess the possible contributions of the postjunctional α_1- and α_2-adrenoceptors to neurally-evoked contractions of these vessels. The normal pattern of nerve firing is highly irregular under *in vivo* conditions (Adrian *et al.*, 1982; Nilsson *et al.*, 1985) with impulses occurring in bursts separated by periods of quiescence. We therefore chose to activate perivascular nerves both continuously in a frequency-dependent manner and intermittently at high frequency (16 Hz) in bursts of 5 s duration. Some of the data have been presented previously as an abstract (Parkinson *et al.*, 1991).

[1] Author for correspondence.

Methods

Subjects and preparations

Biopsies of subcutaneous fat (approximately 2 × 1 × 1 cm) were obtained from patients undergoing surgery. This was approved by local ethics committees. Under the microscope, two small arteries (113–626 μm internal diameter) were dissected out from each biopsy and mounted as ring segments (approximately 2 mm long) in a microvascular isometric myograph by threading the vessels onto two 40 μm stainless steel wires and securing the wires across two mounting supports (Mulvany & Halpern, 1977). After a 1 h equilibration period at 37°C, the vessels were set to a normalised internal circumference, estimated to be 0.9 times L_{100}, where L_{100} is the circumference they would maintain when relaxed and exposed to a transmural pressure of 100 mmHg (Mulvany & Halpern, 1977). At 0.9 L_{100}, the contraction produced is close to maximal (Mulvany & Warshaw, 1979), and internal diameters of the arteries were calculated as $l_{100} = L_{100}/\pi$. After

normalisation, the arteries were initially exposed three times to 10 μM noradrenaline for 2 min at 5 min intervals to determined vessel viability and maximal noradrenergic response. Any vessel which was not able to produce an active pressure equivalent to at least 100 mmHg (approximately 10% of all vessels mounted) was discarded.

Electrical field stimulation

The mounting supports contained two 200 μm thick platinum electrodes. Each electrode had dimensions of approximately 1 × 2 mm and was fixed in a plane perpendicular to the plane containing the wires and about 800 μm from the nearest wire (Angus *et al.*, 1988). Square wave field pulses were passed between the electrodes in a monophasic manner, either continuously or intermittently.

Continuous field stimulation studies were carried out at the Institute of Pharmacology, University of Aarhus, Denmark. The current was controlled with a battery driven, low-output-resistance stimulator (Biophysics Institute, University of Aarhus, Denmark) and the pulses were monitored with a two-channel oscilloscope. Two frequency-response curves (FRCs) were generated at 12 V and a pulse width of 0.3 ms, starting at 0.5 Hz, and increasing the frequency until a plateau was reached. In preliminary studies it was found that the response to 8 Hz was near to maximal. Stimulation at frequencies in excess of 8 Hz decreased responses of subsequent frequency-response curves and so was not used. In the 1 h interval between the two FRCs, the vessels were challenged three times, once every 15 min with 10 μM noradrenaline for 2 min. The first FRC was always generated in the absence of drugs, whereas the second FRC was performed either (a) in the presence of prazosin alone (α_1-adrenoceptor antagonist), (b) in the presence of rauwolscine alone (α_2-adrenoceptor antagonist), (c) in the presence of the two antagonists in combination, (d) in the presence of tetrodotoxin (1 μM), or (e) in the absence of any drugs (i.e. time-control curves). When antagonists were used, the arteries were preincubated for 15 min with the drugs which remained in the solution during generation of the second FRC; for TTX, however, preincubation lasted for 1 h. Vessels failing in the first FRC to produce more than 10% of the response to exogenously applied noradrenaline were excluded from the study (12% of the arteries exposed to continuous field stimulation).

Intermittent field stimulation studies were carried out at the Department of Clinical Pharmacology, St. Mary's Hospital, London. The stimulation parameters were controlled with a Grass S48 stimulator and the pulses monitored on an oscilloscope (Solartron). Complete sensitivity of field stimulation-evoked responses to TTX was ensured in each vessel prior to stimulation: after 10 min preincubation with 1 μM TTX, the voltage was adjusted for each artery to the highest value (5–9 V) where contractile responses due to direct stimulation were absent. TTX added at the start of each experiment had no effect on the ability of the vessels to contract to exogenously applied noradrenaline. TTX was then washed out over 1 h whilst exposing the vessels three times to noradrenaline every 15 min to determine viability and maximal adrenergic activity. Following washout, field stimulation (pulse width 0.3 ms) was applied intermittently at 16 Hz for 5 s every 2 min for 50 min. Stable responses were obtained within 10 min and, unless time-control experiments were performed, three cumulative concentrations of either an α_2-adrenoceptor agonist (rauwolscine or yohimbine) or an α_1-adrenoceptor antagonist (prazosin or doxazosin) were then introduced into the bath 20, 30 and 40 min, respectively, after starting intermittent stimulation. In five arteries stimulation was continued for an extra 10 min to enable prazosin and rauwolscine to be introduced into the bath in combination.

Statistics

Values are expressed as mean ± s.e.mean. Based on results from the intermittent stimulation studies, IC_{50} values, i.e. the antagonist concentration needed to inhibit 50% of the responses, were calculated by linear interpolation. Statistical differences between two means were determined by a two-tailed, paired Student's *t* test and, when multiple comparisons were made, the Bonferroni procedure. The nominal level of significance was set at $P = 0.05$.

Drugs and solutions

The composition of the physiological saline solution (PSS) was (mM): NaCl 119, KCl 4.7, $CaCl_2.2H_2O$ 2.5, $MgSO_4.7H_2O$ 1.17, $NaHCO_3$ 25, KH_2PO_4 1.18, Na_2EDTA 0.026 and glucose 5.5, bubbled with 95% O_2 and 5% CO_2. Noradrenaline bitartrate, prazosin HCl, and tetrodotoxin were obtained from Sigma Chemical Co. (U.S.A.). Doxazosin-HCl was a gift from Pfizer, U.K. Rauwolscine HCl was obtained from Research Biochemical Inc. (U.S.A.).

Results

Continuous stimulation

A sample trace is shown in Figure 1a. In the absence of any drugs, stable tone in response to stimulation was observed to occur more rapidly at higher than at lower frequencies. The maximum response obtained with the first control FRC (usually at 8 Hz) was equivalent to 47 ± 5% (78 vessels) of the response to 10 μM noradrenaline applied exogenously. The size of the maximum response to continuous stimulation was quite variable, however, and no relationship with artery calibre was found (Figure 1b).

In the absence of any drugs, the maximum response of the

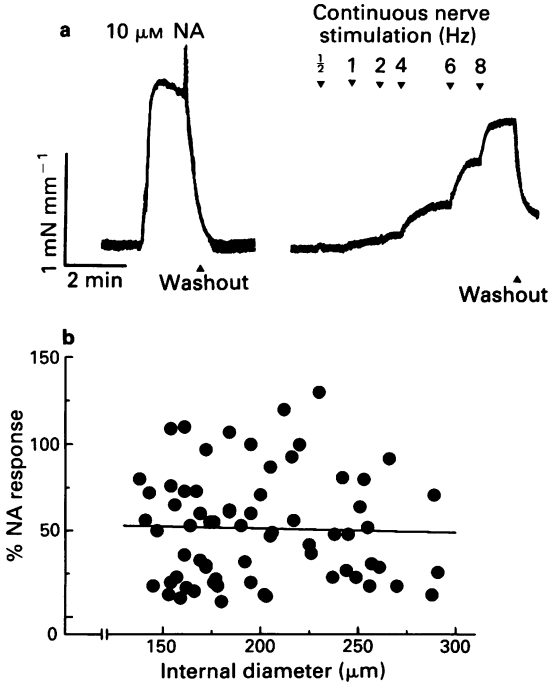

Figure 1 The upper panel (a) shows the response to exogenously applied noradrenaline (NA, 10 μM) and to continuous nerve stimulation at increasing frequencies (0.5–8 Hz). The lower panel (b) shows the individual points and regression line of the maximum response to continuous nerve stimulation as a percentage of the response to exogenously applied noradrenaline (10 μM) plotted against normalised internal diameter (l_{100}, see Methods).

second FRC was 108 ± 12% ($n = 8$) of the maximum response of the first FRC (Figure 2a). This response was almost totally inhibited by 1 μM TTX (Figure 2b).

Preincubation of vessels with prazosin (100 nM) reduced responses over the frequency range 4–8 Hz and significantly inhibited the maximum response to continuous stimulation by 63 ± 7% (Figure 3a). At a higher concentration, prazosin markedly reduced responses over the frequency range 2–8 Hz and significantly inhibited the response to continuous stimulation at 8 Hz by 74 ± 7% (Figure 3b).

The effect of rauwolscine (100 nM) on the frequency-response relationship was less marked; rauwolscine caused a small reduction in the response to continuous stimulation over the range 4–8 Hz (Figure 3d). Only the inhibition of response to stimulation at 8 Hz (36 ± 6%) differed significantly from control. A higher concentration of rauwolscine (1 μM) produced more pronounced inhibition of responses across the range of frequencies used (Figure 3e), reducing the response to stimulation at 8 Hz by 68 ± 5% ($P < 0.05$).

Prazosin (100 nM) and rauwolscine (100 nM) in combination significantly, but not completely, inhibited the neurogenic response (Figure 3c), leaving 48 ± 8% of the first FRC at 8 Hz. At higher concentrations, rauwolscine (1 μM) and prazosin (1 μM) in combination caused near complete inhibition of the neurogenic response (Figure 3f).

Intermittent stimulation

Figure 4 shows a sample trace of contractile responses to intermittent stimulation and the effect of adding increasing concentrations of rauwolscine to the bath. Both prazosin alone and rauwolscine alone caused significant inhibition of the contractile responses to intermittent stimulation in a concentration-dependent manner (Figure 5). The IC_{50} values for prazosin (5 vessels) and rauwolscine (5 vessels) were 3.7 ± 1.5 nM and 12 ± 1.3 nM, respectively. Prazosin (100 nM) inhibited the response to intermittent stimulation by 78 ± 6% and rauwolscine (100 nM) inhibited the response to intermittent stimulation by 86 ± 7%. Similar results were also obtained in other studies using yohimbine, ($IC_{50} = 12 \pm 1$ nM, 11 vessels) and doxazosin ($IC_{50} = 5 \pm 2$ nM, 9 vessels) as selective α_2- and α_1-adrenoceptor antagonists respectively (Parkinson *et al.*, 1991). Prazosin and rauwolscine in combination (each at 100 nM) caused marked inhibition of the response to intermittent stimulation leaving only 7.0 ± 2.6% of the response.

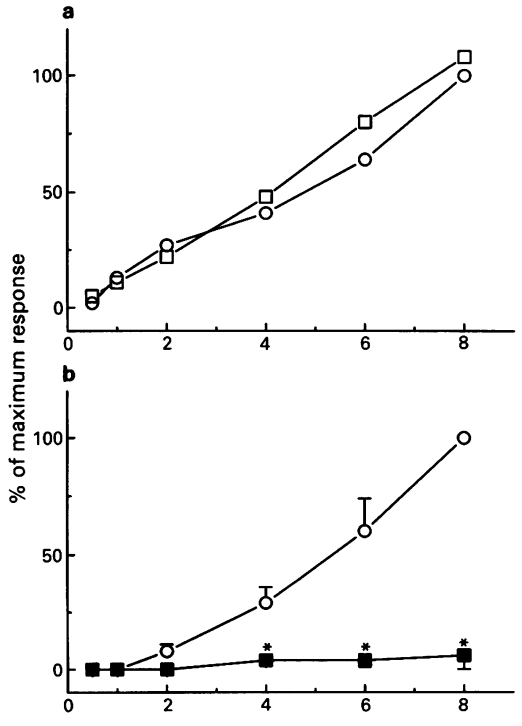

Figure 2 (a) Two consecutive frequency response curves (FRCs) in response to continuous field stimulation and in the absence of drugs (12 vessels), (○) first FRC; (□) second FRC. Error bars have been omitted for clarity in this panel, but did not exceed 9% of the maximum response. In (b), the effect of tetrodotoxin (TTX 1 μM) on the second FRC (■, 8 vessels) is shown. All responses are expressed relative to the response at 8 Hz of the first FRC as arithmetic means (± s.e.mean, vertical bars); *response of second FRC significantly different from response of first FRC.

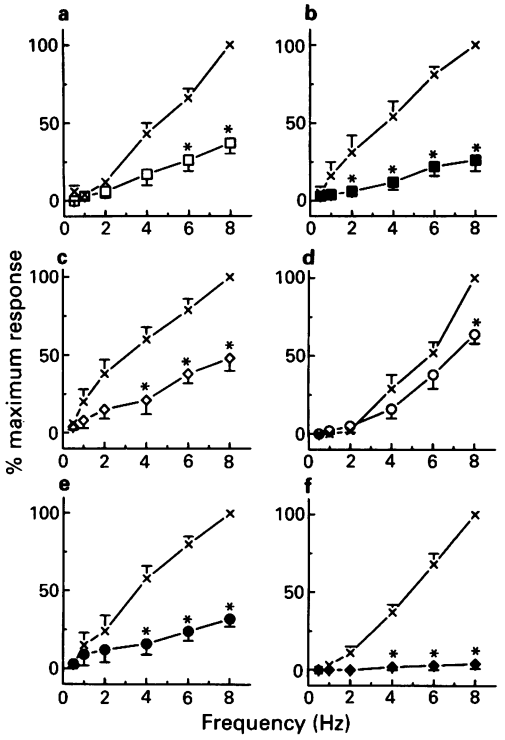

Figure 3 The effects of prazosin (Prz) and rauwolscine (Rwl) alone and in combination on responses to continuous nerve stimulation. The panel shows contractile responses of the first frequency response curve (FRC) (×) and the effects on the second FRC of: (a) 100 nM prazosin alone (□, 6 vessels), (b) 1 μM prazosin alone (■, 10 vessels), (c) 100 nM prazosin and 100 nM rauwolscine in combination (◇, 10 vessels), (d) 100 nM rauwolscine alone (○, 8 vessels), (e) 1 μM rauwolscine alone (●, 12 vessels), and (f) 1 μM prazosin and 1 μM rauwolscine in combination (◆, 14 vessels). All responses are expressed relative to the maximum response at 8 Hz of the first FRC as arithmetic mean (± s.e.mean, vertical bars); *response of second FRC significantly different from response of first FRC.

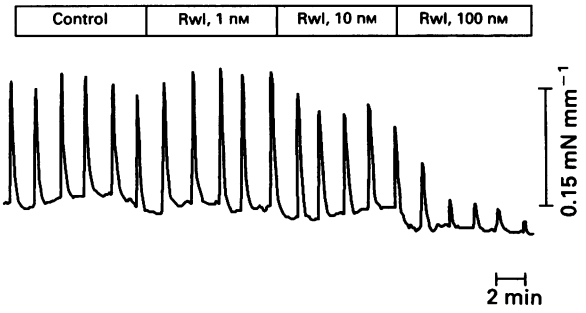

Figure 4 Trace showing contractile responses of human isolated resistance arteries to intermittent field stimulation and the effect of cumulatively adding increasing concentrations of rauwolscine (Rwl).

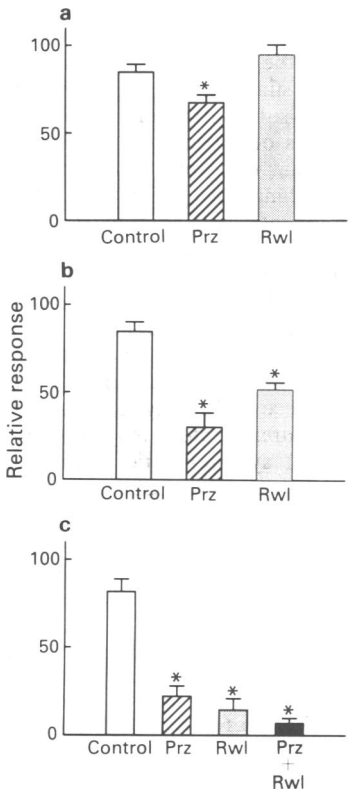

Figure 5 The inhibition of the responses to intermittent field stimulation produced by prazosin (Prz) and rauwolscine (Rwl). The panels show the effects of antagonists at concentrations of (a) 1 nM, (b) 10 nM, and (c) 100 nM. All responses are expressed relative to the responses obtained in the 10 min stimulation period preceding the addition of drugs as arithmetic mean (± s.e.mean, vertical bars). Time-control responses are shown by open columns . *Significant reductions in relative response.

Discussion

These studies demonstrate that electrical field stimulation causes contraction of isolated subcutaneous resistance arteries. The sensitivity to TTX and the near total inhibition of the responses to field stimulation by prazosin and rauwolscine in combination imply that the responses to field stimulation were due to activation of perivascular sympathetic nerves.

Previous studies *in situ* of resistance arteries from rat skeletal muscle (Boegehold & Johnson, 1988; Ohyanagi *et al.*, 1991) have shown inverse relationships between resistance artery diameter and sensitivity to sympathetic nerve stimulation, and the large variability in the maximum response to continuous nerve stimulation (Figure 1b) could be due to differences in innervation density of the vessels. This variation was apparently not dependent on vessel calibre (Figure 1b) and alternatively, the variability may be due to different degrees of degeneration of nerve terminals during transportation, dissection and mounting, since responses to exogenously applied noradrenaline did not show noticeable variation.

The sensitivity of the neurally evoked contractile responses of human subcutaneous resistance arteries to prazosin and rauwolscine suggests that the responses are mediated by both α_1- and α_2-adrenoceptors. This conclusion depends, however, on the selectivities of prazosin and rauwolscine for α-adrenoceptor subtypes in this tissue. Prazosin has a much higher affinity for α_1- than for α_2-adrenoceptors (Cubeddu, 1988) and earlier work in the same arteries from the same source as used in this study has shown that responses to the α_1-adrenoceptor agonist, phenylephrine, are antagonized competitively by prazosin (Nielsen *et al.*, 1990) and that responses to the selective α_2-adrenoceptor agonist B-HT 933 (Timmermans & Van Zwieten, 1980) are unaffected by 1 μM prazosin. These findings indicate that prazosin at concentrations up to 1 μM is selective for α_1-adrenoceptors in human subcutaneous resistance arteries. Rauwolscine is generally accepted to be a selective antagonist for α_2-adrenoceptors (Weitzell *et al.*, 1979) and rauwolscine competitively antagonizes responses to B-HT 933 in human subcutaneous resistance arteries with a potency similar to that described in other preparations (pA_2 7.6, Nielsen unpublished data). We have no data regarding the α_1-antagonist properties of rauwolscine in human resistance arteries, but in other species these are generally seen at concentrations above or around 1 μM (Wilson *et al.*, 1991). At the lower concentrations used in this study, prazosin (100 nM) and rauwolscine (100 nM) can probably be considered selective for α_1- and α_2-adrenoceptors, respectively. However, although the higher concentration of prazosin used in these studies can also probably be regarded as selectively antagonizing α_1-adrenoceptor-mediated responses, 1 μM rauwolscine is likely to show significant α_1-adrenoceptor antagonist properties and the effects of the drug at this higher concentration should not be attributed solely to α_2-adrenoceptor antagonism. Bearing this in mind it is noticeable that the effects of prazosin and rauwolscine appear to differ when continuous and intermittent stimulations are compared. Prazosin (100 nM and 1 μM) produced marked inhibition of contraction induced by continuous stimulation across the range of frequencies used in this study. In contrast, 100 nM rauwolscine had a much less marked effect on tone induced by continuous stimulation and only significantly reduced the response at the highest frequency. Although 100 nM rauwolscine may not be sufficient to abolish α_2-adrenoceptor-mediated responses completely, we would suggest that the more profound effect of 1 μM rauwolscine may represent α_1-adrenoceptor antagonism by this drug. This seems to be borne out when these results are compared with the findings using intermittent stimulation. In this case both prazosin and rauwolscine (10 and 100 nM) caused marked inhibition of the response to field stimulation at concentrations that are probably selective for α_1- and α_2-adrenoceptors, respectively. These findings appear to indicate that the response to intermittent stimulation involves postjunctional α_2-adrenoceptors to a greater extent than does the response to continuous stimulation. Others, on the basis of studies in various species, including man (Timmermans & Van Zwieten, 1982; Jie *et al.*, 1984) have suggested that α_2-adrenoceptors may be largely located extrajunctionally. We do not know whether the stimulation modes used in our studies activate extra- or intrajunctional α-adrenoceptors predominantly, not to mention possible preferential activation of prejunctional vs. postjunctional α_2-adrenoceptors. Clearly further work is needed in this context, possibly using uptake-1 blockers, such as cocaine to increase extrajunctional 'spillover', antagonists selective for pre- vs. postjunctional adrenoceptors, or future highly selective α_2-adrenoceptor antagonists.

It is not possible to estimate the relative contributions of these receptors to neurally evoked responses accurately, since concurrent blockade of presynaptic α_2-adrenoceptors by rauwolscine may enhance neuronal release of noradrenaline. This action will, if anything, lead to an underestimation of the contribution by postjunctional α_2-adrenoceptors. Even if the impact of prazosin and rauwolscine were attributed solely to postjunctional effects, estimation of the relative contribution of each receptor to the response is difficult as we have no information on the receptor-occupancy relationships for the interaction of noradrenaline with either receptor subtype, or the affinity of noradrenaline for either receptor subtype in this tissue. Although the relative importance of postjunctional α_1- and α_2-adrenoceptors to neurally evoked responses in human subcutaneous resistance arteries cannot be deduced from our data, the substantial inhibition by both α-adrenoceptor antagonists individually suggests an important contribution of both subtypes to neurally evoked responses in these arteries.

The innervation of vascular postjunctional α_1- and α_2-adrenoceptors varies, as indicated in the Introduction, from one arterial preparation to another. The postjunctional α-adrenoceptor stimulated by neurally released noradrenaline is of the α_1-subtype in canine aorta (Bobik & Anderson, 1983), in large arterioles of cremaster skeletal muscle (Ohyanagi *et al.*, 1991) and in femoral skeletal muscle arteries of the rat (Medgett & Ruffolo, 1988). In contrast, the predominant contractile effect of nerve stimulation is mediated by postjunctional α_2-adrenoceptors in terminal arterioles in rat cremaster skeletal muscle (Ohyanagi *et al.*, 1991) and in the cutaneous microcirculation of cats (Koss *et al.*, 1991) and rats (Wilette *et al.*, 1991). These findings suggest that the importance of postjunctional α_2-adrenoceptors as mediators of nerve stimulation may increase as arteries get smaller. Although the suggestion is still speculative, these considerations emphasise the problems associated with uncritical extrapolation of the results from this study to other vascular beds, in particular to arteries with calibres different from those examined in the present study. If is of note, however, that postjunctional α_2-adrenoceptors mediate in part responses to exogenously applied noradrenaline not only in human subcutaneous resistance arteries (Nielsen *et al.*, 1990) but also in human resistance arteries isolated from a variety of other vascular beds (Nielsen *et al.*, 1991).

Purinergic transmission has been demonstrated in a variety of animal blood vessels *in vitro* (Sneddon & Burnstock, 1984) and *in vivo* (Bulloch & McGrath, 1988). In man it has been suggested that ATP may account for a non-adrenergic component of sympathetic transmission in the forearm (Taddei *et al.*, 1989; 1990). Lower body negative pressure, the stimulus to sympathetic activation used in these studies, produces an increase in sympathetic nerve firing similar to the pattern of intermittent perivascular nerve stimulation (Sundlof & Wallin, 1978). Although our study has addressed noradrenergic neurotransmission, the near total abolition of the responses to perivascular field stimulation by α-adrenoceptor antagonists does not support a substantial role for purines in mediating contractile responses of subcutaneous resistance arteries. On the other hand, our data on the effect of prazosin and rauwolscine in combination do not totally exclude a modest non-α-adrenoceptor-mediated contractile response of human resistance arteries to nerve stimulation.

In conclusion, the data from this study strongly suggest that neurally evoked responses of human isolated subcutaneous resistance arteries are mediated postjunctionally not only by α_1- but also by α_2-adrenoceptors. Arteries of the size examined in this study contribute substantially to precapillary resistance (Mulvany & Aalkjaer, 1990). The postjunctional α_2-adrenoceptor may consequently be an important target for sympatholytic therapy in the management of essential hypertension, particularly in view of recent observations suggesting that postjunctional α_2-adrenoceptors can be differentiated pharmacologically from those located prejunctionally (Ruffolo *et al.*, 1987; Akers *et al.*, 1991).

We are grateful to the surgeons and the theatre staff at St. Mary's Hospital (London), Aarhus County Hospital, Aarhus Kommune Hospital, and Skejby Sygehus (Aarhus) for their co-operation. We thank Ms Tina Frederiksen for expert technical assistance. We also thank Boehringer Ingelheim for the gift of B-HT 933. This work was supported by the British Heart Foundation, the Danish Medical Research Council, the Danish Heart Foundation, P. Carl Petersens Fond, Lægeforeningens Forskningsfond, and P.A. Messerschmidt og Hustrus Fond. A.D.H. is a British Heart Foundation Intermediate Fellow. H.N. was in receipt of a Pfizer Fellowship conferred by the International Society of Hypertension.

References

ADRIAN, E.D., BRONK, D.W. & PHILIPS, G. (1932). Discharges in mammalian sympathetic nerves. *J. Physiol.*, **74**, 115–133.

AKERS, I., COATES, J., DREW, G.M. & SULLIVAN, A.T. (1991). β_2-Adrenoceptor blocking profile of SK&F-104078 – further evidence for receptor subtypes. *Br. J. Pharmacol.*, **102**, 943–949.

ANGUS, J.A., BROUGHTON, A. & MULVANY, M.J. (1988). Role of α-adrenoceptors in constrictor responses of rat, guinea-pig and rabbit small arteries to neural activation. *J. Physiol.*, **403**, 495–510.

BOBIK, A. & ANDERSON, W.P. (1983). Influence of sympathectomy on alpha 2 adrenoceptor binding sites in canine blood vessels. *Life Sci.*, **33**, 331–336.

BOEGEHOLD, M.A. & JOHNSON, P.C. (1988). Response of arteriolar network of skeletal muscle to sympathetic nerve stimulation. *Am. J. Physiol.*, **254**, H919–H928.

BULLOCH, J.M. & MCGRATH, J.C. (1988). Blockade of vasopressor and vas deferens responses by α,β-methylene ATP in the pithed rat. *Br. J. Pharmacol.*, **94**, 103–108.

CUBEDDU, L.X. (1988). New alpha1-adrenergic receptor antagonists for the treatment of hypertension: role of vascular alpha receptors in the control of peripheral resistance. *Am. Heart J.*, **116**, 133–162.

ELLIOTT, H.L. & REID, J.L. (1983). Evidence for postjunctional vascular alpha 2-adrenoceptors in peripheral vascular regulation in man. *Clin. Sci.*, **65**, 237–241.

JIE, K., VAN BRUMMELEN, P., VERMEY, P., TIMMERMANS, P.B. & VAN ZWIETEN, P.A. (1984). Identification of vascular postsynaptic alpha 1- and alpha 2-adrenoceptors in man. *Circ. Res.*, **54**, 447–452.

JIE, K., VAN BRUMMELEN, P., VERMEY, P., TIMMERMANS, P.B.M.W.M. & VAN ZWIETEN, P.A. (1987). Postsynaptic alpha1- and alpha2-adrenoceptors in human blood vessels: interaction with exogenous and endogenous catecholamines. *Eur. J. Clin. Invest.*, **17**, 174–181.

KOSS, M.C., KAWARAI, M. & ITO, T. (1991). Neural activation of alpha-2 adrenoceptors in cat cutaneous vasculature. *J. Pharmacol. Exp. Ther.*, **256**, 1126–1131.

MEDGETT, I.C. & RUFFOLO, R.R.J. (1988). Alpha adrenoceptor-mediated vasoconstriction in rat hindlimb: innervated alpha-2 adrenoceptors in the saphenous arterial bed. *J. Pharmacol. Exp. Ther.*, **246**, 249–254.

MOULDS, R.F.W. & JAUERNIG, R.A. (1977). Mechanism of prazosin collapse. *Lancet*, **i**, 200–201.

MULVANY, M.J. & AALKJÆR, C. (1990). Structure and function of small arteries. *Physiol. Rev.*, **70**, 921–961.

MULVANY, M.J. & HALPERN, W. (1977). Contractile properties of small arterial resistance vessels in spontaneously hypertensive and normotensive rats. *Circ. Res.*, **41**, 19–26.

MULVANY, M.J. & WARSHAW, D.M. (1979). The active tension-length curve of vascular smooth muscle related to its cellular components. *J. Gen. Physiol.*, **74**, 85–104.

NIELSEN, H., HASENKAM, J.M., PILEGAARD, H.K., MORTENSEN, F.V. & MULVANY, M.J. (1991). alpha-Adrenoceptors in human resistance arteries from colon, pericardial fat, and skeletal muscle. *Am. J. Physiol.*, **261**, H762–H767.

NIELSEN, H., MORTENSEN, F.V. & MULVANY, M.J. (1990). Responses to noradrenaline in human subcutaneous resistance arteries are mediated by both α_1- and α_2-adrenoceptors. *Br. J. Pharmacol.*, **99**, 31–34.

NIELSEN, H., THOM, S.M., HUGHES, A.D., MARTIN, G.N., MULVANY, M.J. & SEVER, P.S. (1989). Postjunctional α_2-adrenoceptors mediate vasoconstriction in human subcutaneous resistance vessels. *Br. J. Pharmacol.*, **97**, 829–834.

NILSSON, H., LJUNG, B., SJOBLOM, N. & WALLIN, B.G. (1985). The influence of the sympathetic impulse pattern on contractile responses of rat mesenteric arteries and veins. *Acta Physiol. Scand.*, **123**, 303–309.

OHYANAGI, M., FABER, J.E. & NISHIGAKI, K. (1991). Differential activation of alpha 1- and alpha 2-adrenoceptors on microvascular smooth muscle during sympathetic nerve stimulation. *Circ. Res.*, **68**, 232–244.

PARKINSON, N.A., NIELSEN, H., THOM, S.M., MULVANY, M.J. & SEVER, P.S. (1991). Electrical stimulation of α_1- and α_2-adrenoceptors. *Blood Vessels*, **28**, 327. (Abstract).

RUFFOLO, R.R.J., SULPIZIO, A.C., NICHOLS, A.J., DEMARINIS, R.M. & HIEBLE, J.P. (1987). Pharmacologic differentiation between pre- and postjunctional alpha 2-adrenoceptors by SK&F 104078. *Naunyn Schmiedebergs Arch. Pharmacol.*, **336**, 415–418.

SNEDDON, P. & BURNSTOCK, G. (1984). ATP as co-transmitter in the motor nerves of the guinea pig vas deferens: electrophysiological evidence. *Eur. J. Pharmacol.*, **106**, 149–152.

STEVENS, M.J. & MOULDS, R.F.W. (1981). Heterogeneity of postjunctional alpha-adrenoceptors in human vascular smooth muscle. *Arch. Int. Pharmacodyn. Ther.*, **254**, 43–57.

STEVENS, M.J. & MOULDS, R.F.W. (1985). Neuronally released norepinephrine does not preferentially activate postjunctional alpha 1-adrenoceptors in human blood vessels *in vitro*. *Circ. Res.*, **57**, 399–405.

SUNDLÖF, G. & WALLIN, B.G. (1978). Effect of lower body negative pressure on human muscle nerve sympathetic activity. *J. Physiol.*, **278**, 525–532.

TADDEI, S., SALVETTI, A. & PEDRINELLI, R. (1989). Persistence of sympathetic-mediated forearm vasoconstriction after α-blockade in hypertensive patients. *Circulation*, **80**, 485–490.

TADDEI, S., PEDRINELLI, R. & SALVETTI, A. (1990). Sympathetic nervous system-dependent vasoconstriction in humans. Evidence for mechanistic role of endogenous purine compounds. *Circulation*, **82**, 2061–2067.

TIMMERMANS, P.B.M.W.M. & VAN ZWIETEN, P.A. (1980). Postsynaptic alpha1- and alpha2- adrenceptors in the circulatory system of the pithed rat: selective stimulation of the alpha2-subtype by B-HT 933. *Eur. J. Pharmacol.*, **63**, 199–202.

TIMMERMANS, P.B.M.W.M. & VAN ZWIETEN, P.A. (1982). Alpha2-adrenoceptors: classification, localization, mechanisms, and target for drugs. *J. Med. Chem.*, **25**, 1389–1401.

WEITZELL, R., TANAKA, T. & STARKE, K. (1979). Pre- and postsynaptic effects of yohimbine stereoisomers on noradrenaline transmission in the pulmonary artery of the rabbit. *Naunyn-Schmiedebergs Arch. Pharmacol.*, **308**, 127–136.

WILETTE, R.N., HIEBLE, J.P. & SAUERMELCH, C.F. (1991). The role of alpha adrenoceptor subtypes in sympathetic control of the acral-cutaneous microcirculation. *J. Pharmacol. Exp. Ther.*, **256**, 599–605.

WILSON, V.G., BROWN, C.M. & MCGRATH, J.C. (1991). Are there more than two types of α-adrenoceptors involved in physiological responses? *Exp. Physiol.*, **76**, 317–346.

(Received December 16, 1991
Revised February 24, 1992
Accepted March 4, 1992)

Br. J. Pharmacol. (1992), **106**, 574–578

Phenytoin potentiates interleukin-1-induced prostaglandin biosynthesis in human gingival fibroblasts

[1,]*Thomas Modéer, *Gustaf Brunius, *,†Mitsuo Iinuma & **Ulf H. Lerner

*Department of Pedodontics, Faculty of Odontology, Karolinska Institute, Box 4064, S-141 04 Huddinge, Sweden; **Department of Oral Cell Biology, University of Umeå, S-901 87 Umeå, Sweden and †Department of Pediatric Dentistry, School of Dentistry, Asahi University, Hozumi, Gifu 501-02, Japan

1 The effect of phenytoin (PHT) on prostaglandin E_2 (PGE_2) biosynthesis in human gingival fibroblasts stimulated by interleukin-1 (IL-1α, IL-1β) or by tumour necrosis factor α (TNFα) was studied.

2 IL-1α (1.5–6.0 ng ml^{-1}) and IL-1β (30–300 pg ml^{-1}), dose-dependently, stimulated PGE_2 formation, in 24 h cultures, with IL-β being the most potent agonist.

3 PHT (2.5–20 μg ml^{-1}) did not induce PGE_2 formation itself but potentiated IL-1α- and IL-1β-induced PGE_2 formation in the gingival fibroblasts in a manner dependent on the concentrations of both IL-1 and PHT.

4 IL-1β (0.1–1.0 ng ml^{-1}) induced release of [^{3}H]-arachidonic acid ([^{3}H]-AA) from prelabelled fibroblasts that was potentiated by PHT (20 μg ml^{-1}).

5 TNF-α ($\geqslant$ 0.01 μg ml^{-1}) significantly stimulated the biosynthesis of PGE_2 by a process that was potentiated by PHT.

6 Addition of exogenous arachidonic acid (AA) ($\geqslant$ 1 μM) caused an increase of PGE_2 formation in the fibroblasts that was not potentiated by PHT (20 μg ml^{-1}).

7 The results indicate that treatment with PHT results in upregulation of prostaglandin biosynthesis in gingival fibroblasts challenged with IL-1 or TNFα, at least partly due to enhanced level of phospholipase A_2 activity.

Keywords: Interleukin-1; tumour necrosis factor; phenytoin; gingival fibroblasts; prostaglandin E_2

Introduction

Phenytoin (PHT) is an anticonvulsant drug causing a number of side effects including skeletal, endocrine, immunological and connective tissue disturbances (Reynolds, 1975; Hassell, 1981; Yaari *et al.*, 1986). One of these, gingival overgrowth, is characterized by an increased amount of non-collagenous extracellular matrix associated with gingival inflammation (Nuki & Cooper, 1972; Dahllöf *et al.*, 1986). Gingival fibroblasts derived from PHT-induced gingival overgrowth are characterized by an increased synthesis of glycosaminoglycans (GAGs) compared to fibroblasts derived from normal gingiva (Dahllöf & Hjerpe, 1987). However, the mechanism(s) by which PHT treatment results in gingival overgrowth is still unclear.

Interleukin-1α (IL-1α) and IL-1β are closely related pleitropic cytokines produced in inflammatory lesions, mainly by macrophages (Dinarello, 1988). IL-1α and IL-1β have been found to stimulate bone resorption as well as prostaglandin E_2 (PGE_2) formation in bone cells (Gowen & Mundy, 1986; Lerner *et al.*, 1991) and in several other cells including gingival fibroblasts (Akahoshi *et al.*, 1988; Richards & Rutherford, 1990; Lerner & Modéer, 1991). IL-1β has also been reported to stimulate the biosynthesis of hyaluronic acid and proteoglycans in human gingival fibroblasts (Bartold, 1988a,b).

Recently, we demonstrated that gingival fibroblasts isolated after 9 months of PHT therapy produce much larger amounts of PGE_2 and PGI_2 *in vitro* when the cells were challenged with IL-1, as compared to the amounts produced by cells isolated before the start of the anticonvulsant therapy (Modéer *et al.*, 1992). The present investigation was undertaken to study whether addition of PHT to gingival fibroblasts *in vitro* results in a similar upregulation of IL-1-induced prostaglandin biosynthesis.

[1] Author for correspondence.

Methods

Fibroblast cultures

Cultures of fibroblast cells were established from gingival biopsies obtained from three individuals (N-21, N-28, N-34), 9 to 11 years of age with no periodontal disease. The plan to take gingival biopsies was accepted by the Ethical Committee of Karolinska Institute. Minced pieces of the tissue were explanted to 25 cm^2 Falcon tissue culture flasks containing 5 ml of Eagle's basal medium (BME) medium. The fibroblasts were obtained by trypsinisation of the primary outgrowth of cells as previously described (Modéer *et al.*, 1982). The cells were grown in BME medium supplemented with sodium-glutamine (4 mmol l^{-1}), foetal calf serum (5%), penicillin (100 iu ml^{-1}) and streptomycin (100 μg ml^{-1}). The fibroblasts were incubated at 37°C in a humidified incubator gassed with 5% CO_2 in air and routinely passaged using 0.025% trypsin in phosphate-buffered saline (PBS) containing 0.02% EDTA. The cells used for the experiments proliferated in logarithmic phase between the 8th and 15th passage.

Prostaglandin production

Fibroblasts (2×10^4 cells) were seeded in Linbro multiwell dishes (24-well plate) in the presence of 5% foetal calf serum and grown for 48 h at 37°C. Then the cell layers were rinsed three times with BME medium without serum (37°C). Thereafter serum-free BME medium and the test substances recombinant human IL-1 (α;β) or tumour necrosis factor α (TNFα) were added in the presence or absence of phenytoin, 5.5-diphenylhydantoin (PHT). At different time points media were withdrawn, acidified to pH 3.5, frozen and stored at −20°C. In one series of experiments, the effect of addition of exogenous unlabelled arachidonic acid (AA) on PGE_2 bio-

synthesis was tested. In these experiments, the medium was withdrawn for analysis of PGE_2 after 24 h.

The amounts of PGE_2 in the media were determined by radioimmunoassays with a commercially available kit with [^{125}I]-PGE_2 as tracer (Gustafson *et al.*, 1986). After the experiments, the cells were detached with trypsin-EDTA in PBS and counted in a haemocytometer.

Analysis of [^{3}H]-arachidonic acid release

Fibroblasts (2×10^4 cells) were seeded in Linbro multiwell dishes (24-well plate) in medium containing 5% foetal calf serum and grown for 24 h at 37°C. Then the cell layers were rinsed once with serum-free medium and incubated in 0.5 ml serum-free medium per well containing 1 μCi ml^{-1} [^{3}H]-arachidonic acid ([^{3}H]-AA). After 24 h, the medium was withdrawn and the cells washed three times with serum-free medium (37°C). Subsequently, 0.5 ml HEPES-buffered (20 mmol l^{-1}) media, with different concentrations of IL-1β in the presence or absence of PHT, was added and the cells were further incubated for 24 h at 37°C. Samples of the media were withdrawn and analysed for ^{3}H in a scintillation counter. The ^{3}H-activity found in the supernatant represents free [^{3}H]-AA as well as ^{3}H-labelled metabolites.

Statistics

Student's *t* test (two-tailed) was used in the statistical analysis.

Chemicals

Eagle's basal medium, sodium-glutamine, foetal calf serum, penicillin and streptomycin were obtained from Flow laboratories, Irvine, Scotland; EDTA, 5.5-diphenylhydantoin and arachidonic acid from Sigma Chemical Co., St. Louis, U.S.A.; recombinant human interleukin-1α and β (specific activity 1.0×10^7 u mg^{-1}) from Boehringer, Mannheim, Germany; recombinant human tumour necrosis factor α (specific activity 2×10^7 u mg^{-1}) from Genzyme, Boston, U.S.A.; PGE_2 radioimmunoassay kit and [^{3}H]-arachidonic acid (specific activity 79.9 Ci mmol^{-1}) from Du Pont/New England Nuclear Chemicals, Germany.

Results

IL-1β, in 24 h cultures, dose-dependently stimulated PGE_2 formation in human gingival fibroblasts (Figure 1). Treatment of the cells with PHT (20 μg ml^{-1}) did not affect PGE_2 formation. When PHT (20 μg ml^{-1}) was added simultaneously with IL-1β, the stimulatory effect of IL-1β on PGE_2 formation was potentiated ($P < 0.07$) (Figure 1). The synergistic interaction between PHT and IL-1β (300 pg ml^{-1}) on PGE_2 formation in gingival fibroblasts was dependent on the concentration of the anticonvulsant drug (2.5– 20 μg ml^{-1}) (Figure 2). IL-1α ($\geq$ 1.5 ng ml^{-1}), in 24 h cultures, dose-dependently stimulated PGE_2 formation but was considerably less potent than IL-1β (Figure 3). When the fibroblasts were treated with IL-1α (1.5–6.0 ng ml^{-1}) together with PHT (20 μg ml^{-1}), the stimulatory effect of IL-1α on PGE_2 formation was potentiated ($P < 0.01$) by the anticonvulsant drug (Figure 3). All these experiments were performed with cells isolated from patient N-21. A similar upregulation of IL-1 (α, β)-induced PGE_2 formation by PHT was also observed in fibroblasts isolated from patients N-28 and N-34 (data not shown).

We have previously reported that the capacity to produce prostanoids is cell density-dependent (Lerner *et al.*, 1989). The effect of IL-1β on PGE_2 formation in fibroblasts was therefore tested at different cell densities ($7.5–30 \times 10^3$ cells cm^{-2}). At all cell densities tested, PHT potentiated IL-1β induced PGE_2 formation in the gingival fibroblasts (data not shown).

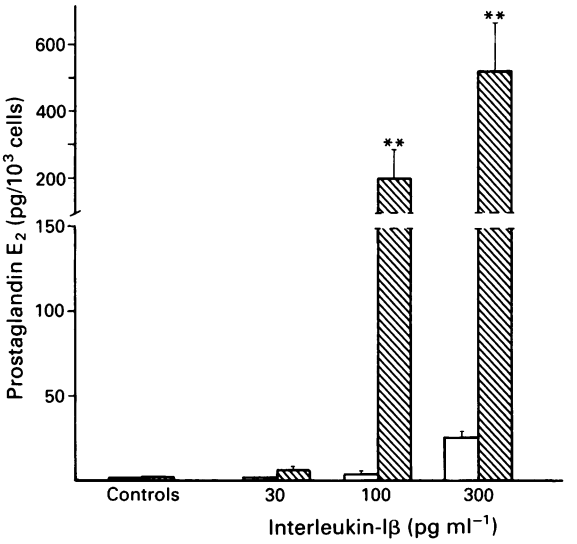

Figure 1 Effect of IL-1β (24 h) at different concentrations, in the absence (open columns) or presence of phenytoin (20 μg ml^{-1}) (hatched columns) on prostaglandin E_2 formation in human gingival fibroblasts (N-21). Cell density was 1.3×10^4 cells cm^{-2}. Mean value of triplicates with s.d. shown by vertical bars.

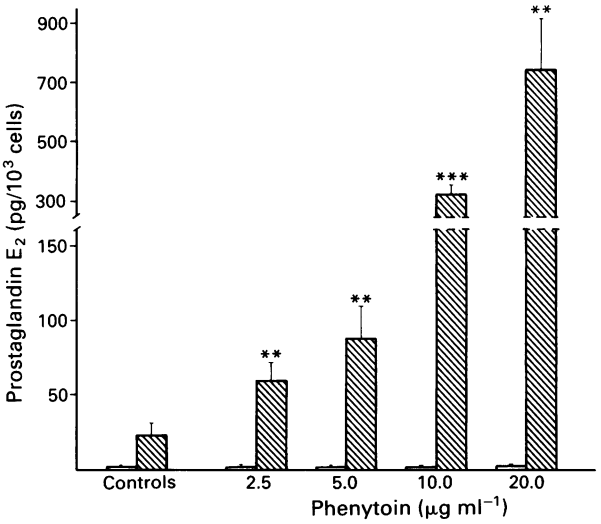

Figure 2 Effect of phenytoin (24 h) at different concentrations on prostaglandin E_2 formation in gingival fibroblasts (N-21), in the absence (open columns) or presence of (interleukin-1β) (IL-1β, 300 pg ml^{-1}) (hatched columns). Cell density was 1.2×10^4 cells cm^{-2}. Mean value of triplicates with s.d. shown by vertical bars.

In another series of experiments, the fibroblasts (N-21) were treated with TNFα (0.01–0.1 μg ml^{-1}) for 24 h, in the presence or absence of PHT (20 μg ml^{-1}). The TNFα-induced PGE_2 formation in fibroblasts was also potentiated ($P < 0.01$) by the anticonvulsant drug (Figure 4).

In a previous paper, we have shown that the capacity of IL-1β to stimulate PGE_2 formation in human gingival fibroblasts may, at least partially, be due to an enhanced release of arachidonic acid (Lerner & Modéer, 1991). We therefore studied whether PHT may potentiate IL-1β-induced release of [^{3}H]-AA from prelabelled fibroblasts. The cytokine IL-1β ($\geq$ 0.1 ng ml^{-1}), in agreement with previous findings (Modéer *et al.*, 1992) caused a dose-dependent, significant ($P < 0.05$) increase in the release of [^{3}H]-AA (Figure 5). When PHT (20 μg ml^{-1}) was added simultaneously with IL-1β ($\geq$ 0.3 ng ml^{-1}) the anticonvulsant drug potentiated ($P < 0.05$) the IL-1β-induced release of [^{3}H]-AA (Figure 5). When PHT was added in the absence of IL-1β, the drug itself did not increase the release of [^{3}H]-AA from the prelabelled fibroblasts.

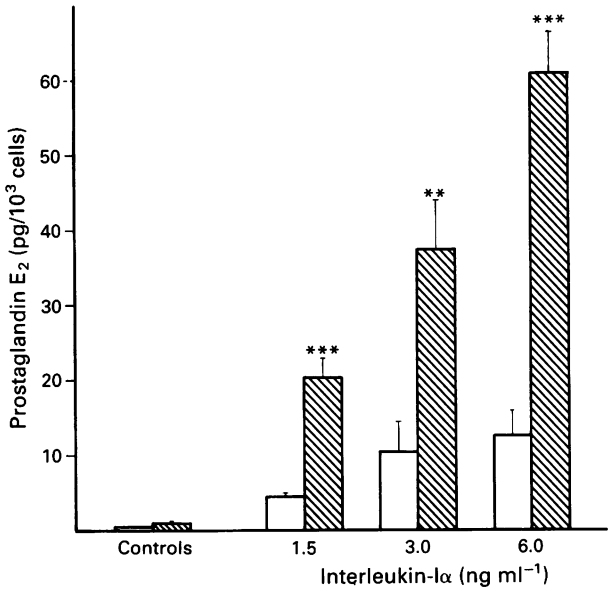

Figure 3 Effect of interleukin-1α (IL-1α; 24 h) at different concentrations, in the absence (open columns) or presence of phenytoin (20 μg ml^{-1}) (hatched columns), on prostaglandin E_2 formation in human gingival fibroblasts (N-21). Cell density was 1.3×10^4 cells cm^{-2}. Mean value of triplicates with s.d. shown by vertical bars.

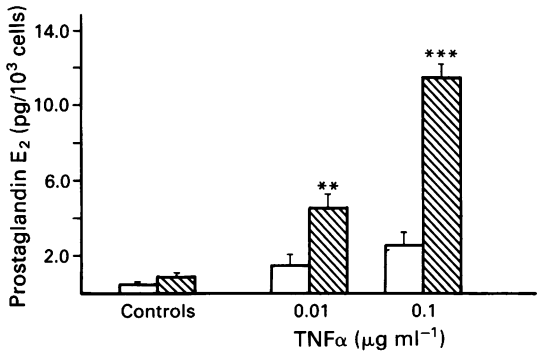

Figure 4 Effect of tumour necrosis factor α (TNFα; 24 h) at different concentrations, in the absence (open columns) or presence of phenytoin (20 μg ml^{-1}) (hatched columns), on prostglandin E_2 formation in human gingival fibroblasts (N-21). Cell density was 1.3×10^4 cells cm^{-2}. Mean value of triplicates with s.d. shown by vertical bars.

In one series of experiments we also examined the effect of addition of different concentrations of exogenous non-labelled AA upon the biosynthesis of PGE_2 in gingival fibroblasts in the presence or absence of PHT. In the absence of PHT, exogenous AA (> 1.0 μM) caused a dose-dependent increase in PGE_2 formation (Figure 6). Addition of AA in the presence of PHT (20 μg ml^{-1}) did not result in an increased PGE_2 formation in 24 h cultures of fibroblasts compared to the cultures not treated with PHT (Figure 6).

Discussion

In agreement with previous observations (Lerner & Modéer, 1991; Modéer *et al.*, 1992) we have found that IL-1α and IL-1β, in 24 h cultures, dose-dependently stimulate PGE_2 formation in human gingival fibroblasts, with IL-1β being the more potent agonist. The novel finding in the present study is that the anticonvulsant drug PHT, which by itself does not affect prostanoid biosynthesis, potentiates IL-1α- and IL-1β-induced PGE_2 biosynthesis in human gingival fibroblasts *in vitro*. The PHT-induced upregulation of PGE_2 formation was seen in cells challenged not only with IL-1α and IL-1β but also with TNFα indicating that the level of upregulation of prostaglandin biosynthesis is not related to receptor number or receptor affinity of IL-1 but rather a step distal to receptor ligand interaction.

Recently we have shown that gingival fibroblasts isolated after 9 months of PHT therapy produce much larger amounts of PGE_2 and PGI_2 *in vitro* as compared to the amounts produced by fibroblasts isolated before the treatment with the anticonvulsant drug (Modéer *et al.*, 1992). The data in the present paper demonstrate that the effect on fibroblast prostaglandin production caused by treatment with the anticonvulsant drug also can be seen by direct addition of PHT to fibroblasts isolated from untreated subjects.

The upregulation of PGE_2 formation in gingival fibroblast in the presence of PHT is probably, at least to some extent,

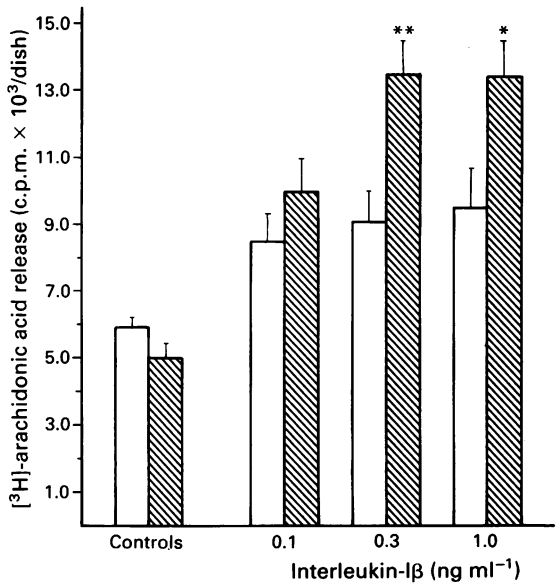

Figure 5 Effect of interleukin-1β (IL-1β; 24 h) at different concentrations, in the absence (open columns) or presence of phenytoin (20 μg ml^{-1}) (hatched columns), on the release of [^{3}H]-arachidonic acid ([^{3}H]-AA) and ^{3}H-labelled metabolites from gingival fibroblasts (N-21) prelabelled with [^{3}H]-AA (1 μCi ml^{-1}). Cell density was 1.2×10^4 cells cm^{-2}. Mean value of triplicates with s.d. shown by vertical bars.

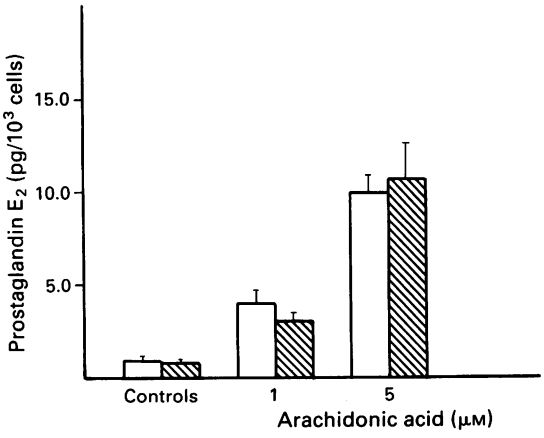

Figure 6 Effect of different concentrations of exogenous unlabelled arachidonic acid added to the cells (24 h) in the absence (open columns) or presence of phenytoin (20 μg ml^{-1}) (hatched column), on the prostglandin E_2 formation in human gingival fibroblasts (N-28). Cell density was 1.0×10^4 cells cm^{-2}. Mean value of triplicates with s.d. shown by vertical bars.

due to an increased phospholipase A_2 (PLA_2) activity, resulting in increased release of arachidonic acid. This assumption is based on the findings that IL-1-induced significantly higher release of [^{3}H]-AA in the presence of PHT. The enhancement of PLA_2 activity also seems to occur as a consequence of PHT medication since we earlier demonstrated that the release of [^{3}H]-AA was significantly higher in fibroblasts isolated during PHT medication in comparison to the level in gingival fibroblasts isolated before the start of the PHT therapy (Modéer *et al.*, 1992). The enzyme PLA_2 is calcium ion-dependent and may be influenced by the anticonvulsant drug, since we have reported that PHT affects the intracellular calcium ion level in gingival fibroblasts *in vitro* (Modéer *et al.*, 1991).

Addition of exogenous AA to the gingival fibroblasts results in enhanced PGE_2 formation. When the cells were treated with exogenous AA and PHT simultaneously, the PHT-treated cells did not produce larger amounts of PGE_2 than the fibroblasts in the absence of PHT. This finding indicates that the upregulation of the IL-1-induced PGE_2 formation seen in the presence of PHT is not due to upregulation of cyclo-oxygenase activity but to enhancement of PLA_2 activity.

However, we found earlier that an enhanced level of cyclo-oxygenase activity also contributes to the upregulation of PGE_2 formation, found in fibroblasts isolated during PHT medication (Modéer *et al.*, 1992). This indicates that upregulation of cyclo-oxygenase activity by PHT may require long term exposure to the drug or that a metabolite of PHT rather than the drug itself may be involved in the stimulation of cyclo-oxygenase.

The PHT-induced potentiation of IL-1 induced release of [^{3}H]-AA in the fibroblasts is less than would be expected compared to the large degree of PHT-induced enhancement of IL-1-stimulated PGE_2 biosynthesis. This discrepancy may indicate that PHT also affects the metabolism of other metabolites of arachidonic acid (thus favouring PGE_2 biosynthesis) or that the drug may inhibit the degradation of PGE_2. Another possibility could be that PHT affects the reacylation of arachidonic acid. The fact that PHT did not potentiate TNFα-induced PGE_2 formation as much as IL-1-induced PGE_2 biosynthesis argues against the view that PHT affects arachidonic acid metabolism at several levels. Rather, the preferential large degree of upregulation of IL-1-induced PGE_2 biosynthesis indicates that PHT specifically potentiates the mechanism of action for IL-1-induced PGE_2 formation.

Our observations in the present study are in contrast to a report by Katsumata and co-workers who showed that PHT inhibits the production of 6-keto-$PGF_{1\alpha}$, the stable metabolite of prostacyclin, in mice thymocytes (Katsumata *et al.*, 1982). We do not have any simple explanation for the conflicting results although the discrepancy may be due to species or cell type differences.

Whether the upregulation of prostaglandin synthesis induced by PHT plays an important role in the pathogenesis of the drug-induced gingival overgrowth is so far unclear. The consequence of the upregulation of prostaglandin formation in gingival fibroblasts due to PHT on extracellular matrix synthesis should be further studied, since it has been reported that hyaluronic acid synthesis as well as GAGs synthesis in fibroblasts may be regulated by PGE_2 (Bartold, 1988a; Karlinsky & Goldstein, 1989). This is specially relevant in light of earlier reports showing that PHT-induced gingival overgrowth represents a tissue with an increased amount of hyaluronic acid as well as of GAGs as compared to normal gingival tissue (Dahllöf *et al.*, 1986).

It has been reported that the cyclo-oxygenase inhibitor, acetylsalicylic acid, reduces the incidence of foetal cleft palate in CD-1 mice treated with PHT (Wells *et al.*, 1989). In animals treated with both PHT and 12-O-tetradecanoylphorbol-13-acetate (TPA) the anticonvulsant drug-induced embryopathy was enhanced, indicating that protein kinase C may be involved in the potentiation (Wells & Vo, 1989).

In conclusion, this study demonstrates that PHT potentiates the prostaglandin biosynthesis in gingival fibroblasts, challenged with IL-1 or TNFα, partly due to enhanced PLA_2 activity.

This study was supported by grants from the Swedish Medical Research Council (Projects No. 7211 and 7525), the Swedish Association Against Rheumatic Diseases, the Royal 80 Year Fund of King Gustav V and A-L Craaford Foundation.

References

AKAHOSHI, T., OPPENHEIM, J.J. & MATSUSHIMA, K. (1988). Interleukin 1 stimulates its own receptor expression on human fibroblasts through the endogenous production of prostaglandin(s). *J. Clin. Invest.*, **82**, 1219–1224.

BARTOLD, P.M. (1988a). The effect of interleukin-1β on hyaluronic acid synthesized by adult human gingival fibroblasts in vitro. *J. Periodont. Res.*, **23**, 139–147.

BARTOLD, P.M. (1988b). The effect of interleukin 1β on proteoglycans synthesized by human gingival fibroblasts in vitro. *Connect. Tissue Res.*, **23**, 287–304.

DAHLLÖF, G., MODÉER, T., REINHOLT, F.B., WIKSTRÖM, B. & HJERPE, A. (1986). Proteoglycans and glycosaminoglycans in phenytoin-induced gingival overgrowth. *J. Periodont. Res.*, **21**, 13–21.

DAHLLÖF, G. & HJERPE, A. (1987). Synthesis of sulfated glycosaminoglycans by human gingival fibroblasts from phenytoin-induced gingival overgrowth in vitro. *Scand. J. Dent. Res.*, **95**, 250–255.

DINARELLO, C.A. (1988). Biology of interleukin-1. *FASEB J.*, **2**, 108–115.

GOWEN, M. & MUNDY, G.R. (1986). Actions of recombinant interleukin 1, interleukin 2, and interferon on bone resorption in vitro. *J. Immunol.*, **136**, 2478–2482.

GUSTAFSON, G.T., LJUNGGREN, Ö., BOONEKAMP, P. & LERNER, U. (1986). Stimulation of bone resorption in cultured mouse calvaria by Lys-bradykinin (kallidin), a potential mediator of bone resorption linking anaphylaxis processes to rarefying osteitis. *Bone Miner.*, **1**, 267–277.

HASSELL, T.M. (1981). Phenytoin: gingival overgrowth. In *Epilepsy and the Oral Manifestations of Phenytoin Therapy*. ed. Hassell, T.M. pp. 116–205. Basel: Karger.

KARLINKSY, J.B. & GOLDSTEIN, R.H. (1989). Regulation of sulfated glycosaminoglycan production by prostaglandin E_2 in cultured lung fibroblasts. *J. Lab. Clin. Med.*, **114**, 176–184.

KATSUMATA, M., GUPTA, C., BAKER, M.K., SUSSDORF, C.E. & GOLDMAN, A.S. (1982). Diphenylhydantoin: an alternative ligand of a glucocorticoid receptor affecting prostaglandin generation in A/J Mice. *Science*, **218**, 1313–1315.

LERNER, U.H., LJUNGGREN, Ö., DEWHIRST, F.E. & BORASCHI, O. (1991). Comparison of human interleukin-1β and its 163-171 peptide in bone resorption and the immune response. *Cytokine*, **3**, 141–148.

LERNER, U.H. & MODÉER, T. (1991). Bradykinin B_1 and B_2 receptor agonists synergistically potentiate interleukin-1 induced prostaglandin biosynthesis in human gingival fibroblasts. *Inflammation*, **15**, 427–435.

LERNER, U.H., RANSJÖ, M. & LJUNGGREN, Ö. (1989). Bradykinin stimulates production of prostaglandin E_2 and prostacyclin in murine osteoblasts. *Bone Miner.*, **5**, 139–154.

MODÉER, T., BRUNIUS, G., MENDEZ, C., JUNTTI-BERGGREN, L. & BERRGREN, P.-O. (1991). Influence of phenytoin on cytoplasmic free Ca^{2+} level in human gingival fibroblasts. *Scand. J. Dent. Res.*, **99**, 310–315.

MODÉER, T., DAHLLÖF, G. & OTTESKOG, P. (1982). The effect of the phenytoin metabolite p-HPPH on proliferation of gingival fibroblasts in vitro. *Acta Ondontol. Scand.*, **40**, 353–357.

MODÉER, T., ANDURÉN, I. & LERNER, U.H. (1992). Enhanced prostaglandin biosynthesis in human gingival fibroblasts isolated from patients treated with phenytoin. *J. Oral Pathol. Med.*, (in press).

NUKI, K. & COOPER, S.H. (1972). The role of inflammation in the pathogenesis of gingival enlargement during the administration of diphenylhydantoin to cats. *J. Periodont. Res.*, **7**, 102–110.

REYNOLDS, E.H. (1975). Chronic antiepileptic toxicity. A review. *Epilepsia*, **16**, 319–352.

RICHARDS, D. & RUTHERFORD, R.B. (1990). The effects of interleukin 1 on collagenolytic activity and prostaglandin-E secretion by human periodontal-ligament and gingival fibroblasts. *Archs Oral Biol.*, **33**, 237–243.

WELLS, P.G. & VO, H.P.N. (1989). Effects of the tumour promoter 12-0-Tetradecanoylphorbol-13-acetate on phenytoin-induced embryopathy in mice. *Toxicol. Appl. Pharmacol.*, **97**, 398–405.

WELLS, P.G., ZUBOVITS, J.T., WONG, S.T., MOLINARI, L.M. & ALL, S. (1989). Modulation of phenytoin teratogenicity and embryonic covalent binding by acetylsalicylic acid, caffeic acid and α-phenyl-N-t-butylnitrone: implications for bioactivation by prostaglandin synthetase. *Toxicol. Appl. Pharmacol.*, **97**, 192–202.

YAARI, Y., SELZER, M.E. & PINCUS, J.H. (1986). Phenytoin: mechanisms of its anticonvulsant action. *Ann. Neurol.*, **20**, 171–184.

(Received December 23, 1991
Revised March 2, 1992
Accepted March 9, 1992)

Br. J. Pharmacol. (1992), **106**, 579–582

Endothelin-1 inhibits PAF-induced paw oedema and pleurisy in the mouse

[1]Maria G.M.O. Henriques, *Giles A. Rae, Renato S.B. Cordeiro & **Timothy J. Williams

Department of Physiology and Pharmacodynamics, Fundação Oswaldo Cruz, Av. Brasil, 4365, Cx Postal 926, Rio de Janeiro, 20010, Brazil; *Department of Pharmacology, CCB, Universidade Federal de Santa Catarina, Florianópolis, 88000, Brazil and **Department of Applied Pharmacology, National Heart and Lung Institute, London, U.K.

1 The current study analyses the effects of endothelin-1 (ET-1) on paw oedema and pleurisy induced by platelet activating factor (PAF) and other inflammatory agents in the mouse.

2 Combined subplantar injection of ET-1 (0.5 pmol/paw) did not modify oedema caused by histamine (1 to 100 μmol/paw), 5-hydroxytryptamine (1 to 100 μmol/paw) or bradykinin (1 to 100 nmol/paw) but markedly inhibited the response to PAF (0.95 to 3.8 nmol/paw). The selective action of ET-1 against PAF-induced (1.9 nmol/paw) oedema was dose-dependent, reaching a maximum at 0.5 pmol/paw and lasted up to 2 h.

3 ET-1 (0.5 pmol/paw) also inhibited paw oedema (3–4 h) caused by zymosan (500 μg/paw). In contrast, it did not modify either the early (1–4 h) or late (48–72 h) phases of the oedematogenic response to carrageenin (300 μg/paw), when given either together with or 24 h after the carrageenin.

4 Intrathoracic injection of PAF (1.9 nmol/cavity) induced pleurisy characterized by an increase in pleural exudate volume, and in accumulation of Evans Blue which was maximal at 30 min and lasted up to 4 h. When injected together with PAF, ET-1 (0.5 pmol/cavity) virtually abolished PAF-induced pleurisy.

5 It is concluded that ET-1 is a potent inhibitor of PAF-induced inflammation in the mouse. Its mechanism of anti-inflammatory action in this species, in contrast to what has been found in other species, does not appear to derive from its potent vasoconstrictor properties as ET-1, at the doses used, failed to affect oedematogenic responses to other inflammatory mediators.

Keywords: Endothelin-1; mouse, paw oedema; pleurisy; inflammation; zymosan; carrageenin; histamine; 5-hydroxytryptamine; bradykinin

Introduction

The vascular endothelium can exert an important modulatory role on blood vessel tone by releasing vasoactive substances, such as prostacyclin (Moncada & Vane, 1979) and endothelium-derived relaxing factor (Furchgott & Zawadski, 1980), the latter recently identified as nitric oxide (Palmer *et al.*, 1987). Production of endothelium-derived contracting factors (EDCFs) has also been detected in response to certain stimuli (Rubanyi, 1988). One such EDCF, endothelin-1 (ET-1), has been isolated from the culture supernatant of porcine aortic endothelial cells and characterized as a 21-residue peptide with potent and sustained pressor and vasoconstrictor activities (Yanagisawa *et al.*, 1988). On a molar basis, ET-1 is at least 10 fold more potent than other known vasoconstrictors in constricting isolated rings of porcine coronary artery. It is now clear that ET-1 belongs to a family of peptides which also includes ET-2, ET-3 (Inoue *et al.*, 1989), 'vasoactive intestinal contractor' (Ishida *et al.*, 1989) and the sarafotoxins present in venom of *Atractaspis engaddensis* (Kloog *et al.*, 1988).

Besides its potent vasoconstrictor action on both arterial and venous conductance vessels (Yanagisawa *et al.*, 1988; De Nucci *et al.*, 1988), ET-1 can also affect smooth muscle tone in the microvasculature. It is a powerful constrictor of rat mesenteric arterioles and venules *in vitro* (Warner, 1990) and *in vivo* (Fortes *et al.*, 1989a) and of arterioles of the hamster cheek pouch (Öhlén *et al.*, 1989), rabbit tenuissimus muscle (Öhlén *et al.*, 1989) and skin (Brain *et al.*, 1988), porcine pia matter (Armstead *et al.*, 1989) and human skin (Brain *et al.*, 1989) *in vivo*. Moreover, ET-1 was found to constrict mesenteric lymphatic vessels in the anaesthetized rats (Fortes *et al.*, 1989b). Hence, ET-1 may be an important regulator of systemic blood pressure and of local haemodynamics.

Possibly because of its vasoconstrictor properties, ET-1 also inhibits plasma extravasation induced in rat skin by intradermal injection of the inflammatory mediators 5-hydroxytryptamine (5-HT), histamine, bradykinin (BK), and platelet activating factor (PAF) and of the vasodilatation induced by nitric oxide and nitroprusside (Chander *et al.*, 1988). When given intradermally together with BK or the chemotactic peptide N-formyl-methionyl-leucyl-phenylalanine (FMLP) into rabbit dorsal skin, ET-1 dose-dependently reverses the increased extravascular accumulation of radiolabelled albumin potentiated by calcitonin gene-related peptide (CGRP; Brain *et al.*, 1989). The current study reassesses the potential anti-inflammatory properties of ET-1 in another species, the mouse, by analysing the effects of the peptide on paw oedema and pleurisy induced by several mediators and phlogistic agents. We have found that, in contrast to the results obtained in other species, ET-1 exhibits a selective action against PAF-induced vascular leakage in the mouse.

Methods

Mice (20–25 g) of either sex from our own colony of the Swiss 44 strain were used.

Production of paw oedema

The subplantar surface of one hind paw of mice was injected with 50 μl NaCl solutions containing one of the following substances bradykinin (1–100 nmol/paw), 5-HT (1–100 μmol/paw), histamine (1–100 μmol/paw), PAF (0.9–3.8 nmol/paw), and zymosan (500 μg/paw) or carrageenin (300 μg/paw). The

[1] Author for correspondence.

contralateral paw received the same volume of saline (50 μl) and was used as control.

To assess the anti-oedematogenic activity of ET-1, the peptide (0.1, 0.25, 0.5 pmol/paw) was given together with each inflammatory stimulus. The volumes of both hindpaws were measured with a plethysmograph and oedema was calculated as the volume difference (μl) between control and mediator-injected paws. Oedema induced by the mediators was evaluated at the time of peak responses (30 min for PAF; 1 h for 5-HT, BK or histamine), whereas that caused by the phlogistic agents was determined at several times after injection (1, 2, 3 and 4 h for zymosan; 2, 4, 24, 48 and 72 h for carrageenin). Another set of experiments was performed to determine the time course of the anti-inflammatory effect of ET-1 against PAF-induced paw oedema. In such experiments, ET-1 (0.5 pmol/paw) was injected into the footpad at various times before PAF (1.9 nmol/paw) injection. The contralateral paws were treated simultaneously with an equal volume of saline (50 μl) to serve as controls.

Induction of pleurisy

Pleurisy was induced by the technique of Spector (1956) as modified for mice by Henriques *et al.* (1990). Briefly, an adapted needle (13 × 5 gauge) was inserted carefully 2 mm through the parietal pleura into the right side of the thoracic cavity of mice to enable injection of PAF (1.9 nmol/cavity), either alone or in combination with ET-1 (0.5 pmol/cavity). Control animals received an equal volume (50 μl) of sterile saline only.

Exudate quantification

Mice were injected intravenously with Evans blue 25 mg kg^{-1} solution 24 h before receiving the intrathoracic injection of saline, PAF or PAF plus ET-1. The animals were killed at different times (15–240 min) after injection and their thoracic cavities were washed with 1 ml saline containing heparin (10 iu ml^{-1}). The fluid was collected, its volume was measured and the lipids were extracted by the addition of 1 ml chloroform. After removal of the dye-free pleural wash, absorbance was read at 600 nm with a Beckman DU-8 spectrophotometer. The results on exudate accumulation are expressed either as the volume of pleural wash or as total Evans blue (μg) recovered per cavity.

Materials

The following substances were used: ET-1 (porcine endothelin, Peptide Institute Inc., Japan), heparin (Liquemine Roche, Brazil), Evans blue dye (Merck, Germany), 5-hydroxytryptamine, histamine hydrochloride, zymosan, bradykinin (all from Sigma, St. Louis, U.S.A.) and hexadecyl PAF (Bachen, Switzerland).

Statistical analysis

All results are presented as the mean ± s.e.mean. The data were anlaysed statistically by means of Student's t test for unpaired samples (Snedecor, 1953) with $P \leq 0.05$ considered significant.

Results

Paw oedema induced by inflammatory mediators

As shown in Figure 1, histamine, 5-HT, BK and PAF each produced significant dose-related oedema when injected into the mouse hindpaw. The oedematogenic responses to these agonists peaked either at 30 (PAF) or at 60 min (5-HT, BK and histamine) after administration. Simultaneous subplantar injection of ET-1 (0.5 pmol/paw, which corresponds to 1.25 ng/paw) failed to affect the development of oedema in response to histamine, 5-HT or BK (Figure 1a, b and c, respectively). In marked contrast, the same dose of ET-1 caused substantial inhibition of PAF-induced oedema (Figure 1d). To ensure that these findings were reproducible, the effects of ET-1 against paw oedema induced by each of the four mediators were reassessed in two other experiments ($n = 6$ for each dose of mediator) and comparable data were obtained (results not shown).

This selective action of ET-1 against PAF was dose-dependent as, in another set of mice, ET-1 at 0.1 pmol/paw was ineffective and at 0.25 and 0.5 pmol/paw the peptide diminished the oedematogenic response to 1.9 nmol/paw of PAF from 55.6 ± 5.0 μl to 42.6 ± 7.8 μl (23.4% of inhibition; $P < 0.05$) and 22.5 ± 6.2 μl (60.4% of inhibition; $P \leq 0.05$), respectively ($n = 7$ in each group). Responses to PAF measured 1 h after its injection were also effectively suppressed when the lipid was mixed with ET-1 (results not shown).

Figure 2 illustrates the long-lasting effect of ET-1 against PAF-induced paw oedema. It is clear that, when injected 2 h or less before PAF, ET-1 caused significant interval-dependent attenuation of oedema. However, no detectable anti-inflammatory effect was seen in mice given ET-1 4 h or 8 h before PAF.

Paw oedema induced by zymosan and carrageenin

Zymosan (500 μg/paw) produced an oedematogenic response which reached a maximum 4 h after injection. Given simultaneously with the phlogistic agent, ET-1 (0.5 pmol/paw) did not change the magnitude of oedema measured 1 or 2 h later. However, the inflammatory reaction observed at 3 and 4 h after the stimulus was markedly inhibited in ET-1-treated mice ($P \leq 0.05$) as compared to control animals (Figure 3).

As described previously (Henriques *et al.*, 1987), subplantar injection of carrageenin (300 μg/paw) caused a typical biphasic oedematogenic response in mice, characterized by a initial peak of low magnitude within 4 h followed by a more substantial raise in paw volume at 48 and 72 h after administration. The response to carrageenin was not influenced by treatment with ET-1 (0.5 pmol/paw) either together with or 24 h after injecting carrageenin ($n = 7$; results not shown).

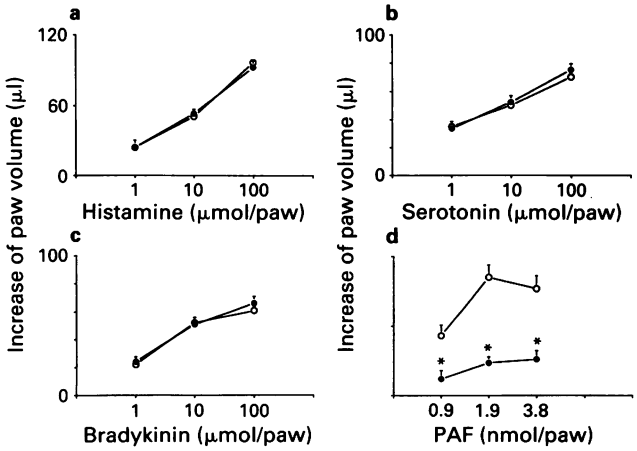

Figure 1 Paw oedema produced in mice by subplantar injection of histamine (a), 5-hydroxytryptamine (b), bradykinin (c) or PAF (d), either alone (○) or mixed with 0.5 pmol/paw of endothelin-1 (●). Only peak oedematogenic responses are shown, which occurred either 1 h (a, b and c) or 30 min (d) after injection. Oedema is expressed as the difference between mediator-injected and saline-injected (control) paws. Each value represents the mean of 7 mice and vertical lines indicate the s.e.means. *$P \leq 0.05$ when compared to PAF alone (Student's t test).

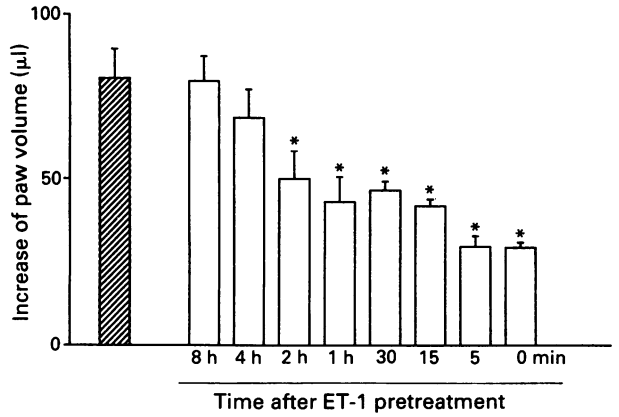

Figure 2 Time course of the inhibitory effect of endothelin-1 (ET-1) against PAF-induced mouse paw oedema. PAF (1.9 nmol/paw) was injected 5 min to 8 h after pretreatment of paws with either saline (hatched column) or ET-1 (0.5 pmol/paw; open columns). The amount of oedema caused by simultaneous treatment of PAF plus ET-1 (0 min) is also shown. Oedema is expressed as the difference between ET-1-injected and saline-injected paw volumes 30 min after PAF. Each value represents the mean of 7 mice and vertical lines indicate the s.e.means. $*P \leqslant 0.05$ when compared to PAF plus saline (Student's t test).

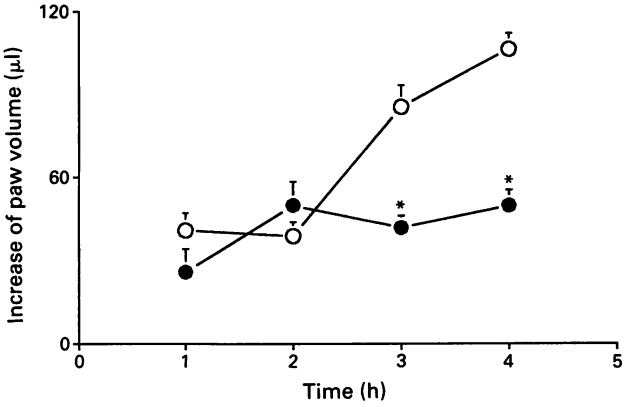

Figure 3 Paw oedema induced in mice by subplantar injection of zymosan (500 µg/paw) either alone (○) or together with (0.5 pmol/cavity) endothelin-1 (●). Oedema is expressed as the difference between volumes of drug-injected and saline-injected paws. Each value represents the mean of 7 mice and vertical lines indicate the s.e.means. $*P \leqslant 0.05$ when compared to corresponding value obtained with zymosan alone (Student's t test).

Pleural exudation induced by PAF

Intrathoracic injection of PAF (1.9 nmol/cavity) caused a pronounced increase in pleural exudate volume and in Evans blue pleural accumulation. This response remained relatively constant between 15 and 60 min after PAF administration and decreased thereafter (Figure 4). Mice receiving combined treatment with PAF plus ET-1 (0.5 pmol/cavity) exhibited significantly less pleural exudation and Evans blue accumulation at 15, 30 and 60 min than animals injected only with PAF ($P \leqslant 0.05$, Figure 4).

Discussion

The main finding of this study was that, in the mouse, ET-1 caused a prolonged dose-dependent and reproducible inhibition of paw oedema induced by PAF, without affecting that induced by 5-HT, BK or histamine. This selective anti-inflammatory action of ET-1 contrasts markedly with the reported nonselective inhibition by the peptide of vascular leakage induced by all four inflammatory mediators in the

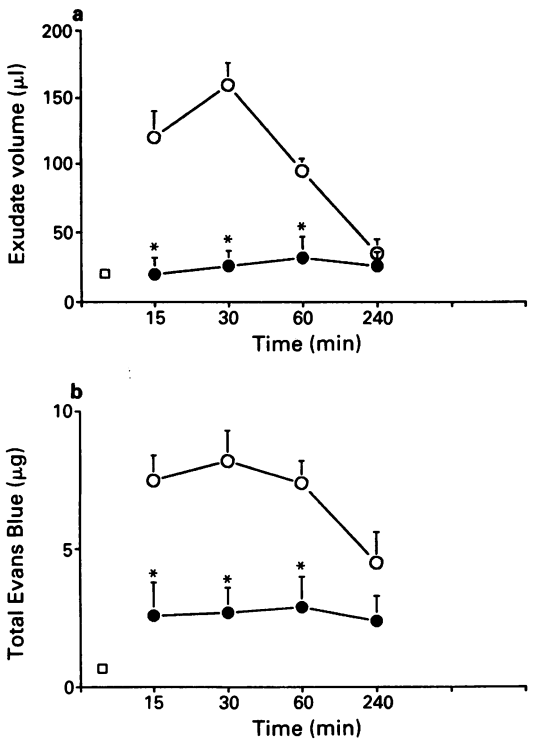

Figure 4 Pleural exudation stimulated by intrathoracic injection of PAF (1.9 nmol/paw) either alone (○) or together with (0.5 pmol/cavity) endothelin-1 (●) in mice. The volume of exudate was quantified either as µl of pleural wash (a) or by total Evans blue leakage (µg/cavity) into the pleura (b). The basal values found in control mice treated only with saline are also shown (□). Each value represents the mean of 7 mice and vertical lines indicate the s.e.means. $*P \leqslant 0.05$ when compared to corresponding value obtained with PAF alone (Student's t test).

rat skin (Chander *et al.*, 1988; 1990). It is also in contrast to the report of Brain *et al.* (1989) showing that, in rabbit skin, ET-1 suppressed plasma exudation induced by CGRP in combination with BK or FMLP. Thus, the selectivity of the anti-inflammatory actions of ET-1 appears to exhibit considerable species variation.

The mechanism(s) involved in the attenuation by ET-1 of PAF-induced mouse paw oedema is as yet unclear. However, it is possible to rule out that such an effect was mediated solely by microvascular vasoconstriction, as this should have also affected oedema caused by the other inflammatory mediators. Moreover, the substantial evidence accumulated from functional, binding and autoradiographic studies, showing that ET-1 interacts with specific ET-receptors or binding sites in many tissues (Yanagisawa *et al.*, 1988; Gu *et al.*, 1989; Davenport *et al.*, 1989) argues against a possible blockade of PAF receptors by the peptide.

Because PAF has been proposed as an important mediator of inflammation induced by zymosan in the rat (Martins *et al.*, 1989) we also tested whether ET-1 could affect paw oedema triggered by this agent in the mouse. Though the peptide did not modify the early stages of the oedematogenic response (up to 2 h), it significantly depressed the later stages of the inflammation (3 and 4 h). This result correlates well with the long-lasting effect of ET-1 against PAF-induced oedema detected in the time course experiments, and its sustained pressor action in rats (Yanagisawa *et al.*, 1988).

In contrast, ET-1 failed to affect both the early and late components of oedema caused by carrageenin. This was a rather unexpected finding, as paw oedema induced by this agent in mice has been shown to be sensitive to blockade by WEB 2170, a selective PAF receptor antagonist (Henriques *et al.*, 1990). Carrageenin-induced paw oedema in the rat, which develops much faster (peaking 3 to 4 h of injection) than in

mice and is mediated to a large extent by generation of eicosanoids and BK (Crunkhorn & Meacok, 1971; Hargreaves *et al.*, 1989) but not by PAF (Cordeiro *et al.*, 1986), has been shown to be inhibited, or at least postponed, by simultaneous injection of ET-1 (Chander *et al.*, 1990). The lack of effect of ET-1 against carrageenin-induced oedema in the mouse may reflect the fact that the biological effect of ET-1, given at 0 or 24 h, will have declined before full development of inflammation (48–72 h). Further experiments should help clarify this issue.

In line with its actions on mouse paw oedema, ET-1 also caused marked, sustained and dose-dependent suppression of PAF-induced pleural exudation. Though again the mechanism(s) underlying this effect remains to be established, the results indicate that the inhibitory effect of ET-1 against PAF-induced effects is not restricted to the paw oedema model of inflammation.

The results of the current study demonstrate that, in addition to its previously reported profound effects on vasomotor tone, ET-1 can modulate selectively microvascular leakage triggered by PAF in the mouse. The mechanism(s) involved in this selective anti-inflammatory effect of ET-1 is possibly unrelated to its vasoconstrictor action, but remains to be full characterized.

The present study was supported by FINEP, FAPERJ and CNPq (Brazil).

References

ARMSTEAD, W.M., MIRRO, R., LEFFER, C.W. & BUSIJA, D.W. (1989). Influence of endothelin on piglet cerebral microcirculation. *Am. J. Physiol.*, **257**, H707–H710.

BRAIN, S.D., TIPPINS, J.R. & WILLIAMS, T.J. (1988). Endothelin induces potent microvascular constriction. *Br. J. Pharmacol.*, **95**, 1005–1007.

BRAIN, S.D., CROSSMAN, D.C., BUCKLEY, T.L. & WILLIAMS, T.J. (1989). Endothelin-1: demonstration of potent effects on the microcirculation of humans and other species. *J. Cardiovasc. Pharmacol.*, **13** (suppl. 5), S147–S149.

CHANDER, C.L., MOORE, A.R., DESA, F.M., HOWAT, D. & WILLOUGHBY, D.A. (1988). The local modulation of vascular permeability by endothelial cell derived products. *J. Pharm. Pharmacol.*, **40**, 745–746.

CHANDER, C.L., HOWAT, D.W., MOORE, A.R., COLVILLE-NASH, P.R., DESA, F.M., BRAQUET, P. & WILLOUGHBY, D.A. (1990). Comparison of endothelin-1 and -3 on models of inflammation. *Agents Actions*, **29**, 27–29.

CODEIRO, R.S.B., MARTINS, M.A., RODRIGUES-E-SILVA, P.M., HENRIQUES, M.G.M.O., WEG, V.B., CASTRO-FARIA-NETO, H.C. & LIMA, M.C.R. (1986). Interference of BN 52021 with carrageenan-induced inflammatory response: is the effect due to PAF-acether antagonism? In *The Ginkolides: Chemistry, Biology, Pharmacology and Clinical Perspectives*. ed. Braquet, P. & Prous, J.R. pp. 261–270. Barcelona: Methods and Findings.

CRUNKHORN, P. & MEACOK, S.C.R. (1971). Mediators of the inflammation induced in the rat paw by carrageenin. *Br. J. Pharmacol.*, **42**, 392–402.

DAVENPORT, A.P., NUNEZ, D.J., HALL, J.A., KAUMANN, A.J. & BROWN, M.J. (1989). Autoradiographical localization of binding sites for porcine [^{125}I]endothelin in humans, pigs and rats: functional relevance in humans. *J. Cardiovasc. Pharmacol.*, **13** (suppl. 5), S166–S170.

DE NUCCI, G., THOMAS, R., D'ORLEANS-JUSTE, P., ANTUNES, E., WALDER, C., WARNER, T.D. & VANE, J.R. (1988). Pressor effects of circulating endothelin are limited by its removal in the pulmonary circulation and by release of prostacyclin and endothelium-derived relaxing factor. *Proc. Natl. Acad. Sci. U.S.A.*, **85**, 9797–9800.

FORTES, Z.B., DE NUCCI, G. & GARCIA-LEME, J. (1989a). Effect of endothelin-1 on arterioles and venules in vivo. *J. Cardiovasc. Pharmacol.*, **13** (suppl. 5), S200–S201.

FORTES, Z.B., SCIVOLETO, R. & GARCIA-LEME, J. (1989b). Endothelin-1 induces potent constriction of lymphatic vessels in situ. *Eur. J. Pharmacol.*, **170**, 69–73.

FURCHGGOT, R.F. & ZAWADSKI, J.V. (1980). The obligatory role of endothelial cells in the relaxation of arterial smooth muscle by acetylcholine. *Nature*, **288**, 373–376.

GU, X.H., LIU, J.J., DILON, J.J. & NAYLER, W.G. (1989). The failure of endothelin to displace bound, radioactively-labelled calcium antagonists (PN 200/110, D888 and diltiazem). *Br. J. Pharmacol.*, **96**, 262–264.

HARGREAVES, K.M., TROULLOS, E., DIONNE, R., SCHMIDT, E., SCHAFFER, S. & JORIS, J. (1989). Suppression of carrageenan-induced hyperalgesia, hyperthermia and edema by a bradykinin antagonist. *Eur. J. Pharmacol.*, **171**, 259–263.

HENRIQUES, M.G.M.O., SILVA, P.M.R., MARTINS, M.A., FLORES, C.A., CUNHA, F.Q., ASSREUY-FILHO, J. & CORDEIRO, R.S.B. (1987). Mouse paw oedema. A new model for inflammation. *Brazil. J. Med. Biol. Res.*, **20**, 243–249.

HENRIQUES, M.G.M.O., WEG, V., MARTINS, M.A., SILVA, P.M.R., FERNANDES, P.D., CORDEIRO, R.S.B. & VARGAFTIG, B.B. (1990). Differential inhibition by two hetrazepine PAF antagonists of acute inflammation in the mouse. *Br. J. Pharmacol.*, **99**, 164–168.

INOUE, A., YANAGISAWA, M., KIMURA, S., KASUYA, Y., MIYAUICHI, T., GOTO, K. & MASAKI, T. (1989). The human endothelin family: three separate genes. *Proc. Natl. Acad. Sci. U.S.A.*, **86**, 2863–2867.

ISHIDA, N., TSUJIOKA, K., TOMOI, M., SAIDA, K. & MITSUI, Y. (1989). Differential activities of two distinct endothelin family peptides on ileum and coronary artery. *FEBS Lett.*, **247**, 337–340.

KLOOG, Y., AMBAR, I., SOKOLOVSKY, M., KOCHVA, E., WOLLBERG, Z. & BDOLAH, A. (1988). Sarafotoxin, a novel vasoconstrictor peptide: phosphoinositide hydrolysis in rat heart and brain. *Science*, **242**, 268–270.

MARTINS, M.A., SILVA, P.M.R., CASTRO FARIA NETO, H.C., BOZZA, P.T., DIAS, P.M.L.F., LIMA, M.C.R., CORDEIRO, R.S.B. & VARGATFIG, B.B. (1989). Pharmacological modulation of PAF-acether-induced pleurisy in rats and its relevance for inflammation by zymosan. *Br. J. Pharmacol.*, **96**, 363–371.

MONCADA, S. & VANE, J.R. (1979). Pharmacology and endogenous roles of prostaglandin endoperoxides, thromboxane A_2 and prostacyclin. *Pharmacol. Rev.*, **30**, 293–331.

ÖHLÉN, A., RAUD, J., HEDQVIST, P. & WIKLUND, N.P. (1989). Microvascular effects of endothelin in the rabbit tenuissimus muscle and hamster cheek pouch. *Microvasc. Res.*, **37**, 115–118.

PALMER, R.M.J., FERRIGE, A.G. & MONCADA, S. (1987). Nitric oxide release accounts for the biological activity of endothelium-derived relaxing factor. *Nature*, **333**, 524–526.

RUBANYI, G.M. (1988). Endothelium-derived vasoconstrictor factors. In *Endothelial Cells*, ed. Ryan, U.S. Vol. 3, pp. 61–74. Boca Raton: CRC Press.

SNEDECOR, G.W. (1953). Statistical methods applied to experiments in agriculture and biology. p. 482. Ames Iowa: Iowa University Press.

SPECTOR, W.G. (1956). The mediation of altered capillary permeability in acute inflammation. *J. Pathol. Bact.*, **72**, 367–380.

WARNER, T.D. (1990). Simultaneous perfusion of rat isolated superior mesenteric arterial and venous beds – comparison of their vasoconstrictor and vasodilator responses to agonists. *Br. J. Pharmacol.*, **99**, 427–436.

YANAGISAWA, M., KURIHARA, H., KIMURA, S., TOMOBE, Y., KOBAYASHI, M., MITSUI, Y., YASAKI, Y., GOTO, K. & MASAKI, T. (1988). A novel potent vasoconstrictor peptide produced by vascular endothelial cells. *Nature*, **332**, 411–415.

(Received May 17, 1991
Revised February 20, 1992
Accepted March 9, 1992)

Br. J. Pharmacol. (1992), **106**, 583–586

β-Adrenoceptor agonist stimulation of acid secretion by rat stomach *in vitro* is mediated by 'atypical' β-adrenoceptors

[1]Paul Canfield & Paraskevas Paraskeva

Department of Physiology & Biophysics, St Mary's Hospital Medical School, Norfolk Place, London W2 1PG

1 A previous study showed β-adrenoceptor agonists stimulated acid secretion by rat stomach *in vitro*. The receptors could not be classed as either the β_1- or β_2-subtype. This study examines the effect of 2 'atypical' β-agonists on acid secretion.

2 Basal and isoprenaline-stimulated acid secretion were compared in tissues bathed either in HEPES/O_2- or HCO_3^-/CO_2-buffer. Basal secretion was underestimated in HCO_3^- by an amount equal to the rate of base section. Tissues responded well in HEPES buffer and there was no base secretion following acid inhibition with SCH 28080. HEPES was used for the study.

3 SR 58611A stimulated acid in a concentration-related way (0.1–5 μM). Maximum response at 1 μM was equal to the response to a maximal concentration of isoprenaline. BRL 37344 (1 μM) also stimulated to the same extent.

4 Responses to isoprenaline (5 μM) and SR 58611A (1 μM) were reduced by propranolol (10 μM) but not by alprenolol (10 μM) or by practolol (12.5 μM) plus ICI 118551 (1 μM).

5 Exposure to SR 58611A (1 μM) led to desensitization to isoprenaline but not to bethanechol (1 μM) or histamine (50 μM).

6 We conclude that a HEPES/O_2-buffer is advantageous when measuring gastric acid secretion *in vitro* and the stimulatory effect of β-adrenoceptor agonists is mediated by 'atypical' receptors.

Keywords: Gastric acid secretion; 'atypical' β-adrenoceptors; stomach *in vitro*; 'atypical' β-agonists; SR 58611A; BRL 37344; propranolol; alprenolol; SCH 28080

Introduction

Isoprenaline stimulates acid secretion in the rat stomach *in vitro* by an action at β-adrenoceptors. These responses were antagonized by non-selective but not by selective β-antagonists (Canfield & Price, 1981) suggesting that the receptors could not be designated as belonging to either the β_1- or β_2-subtypes. A similar lack of effect of selective β-receptor antagonists has been reported in some adipocytes (Hollenga & Zaagsma, 1989; Hollenga *et al.*, 1991; Carpene *et al.*, 1991) and in various gastrointestinal muscle preparations (Coleman *et al.*, 1987; Bianchetti & Manara, 1990; MacDonald *et al.*, 1990) and ascribed to the presence of 'atypical' β-adrenoceptors. These responded to selective 'atypical' agonists such as BRL 37344 and SR 58611A (Guidice *et al.*, 1989; McLaughlin & MacDonald, 1990). We now report the effects of these two 'atypical' agonists on acid secretion by rat isolated stomach.

Methods

Preparation

Stomachs were taken from male Wistar rats (30–50 g) which had been kept with a lactating female and set up as a flat sheet tied over a plastic tube with the mucosa facing the tube lumen as described previously (Canfield & Price, 1981). The mucosal surface was bathed with 5 ml of solution containing (in mM): NaCl 136, KCl 5, $MgSO_4$ 1.2, $CaCl_2$ 2.4 and glucose 11.7, gassed with 100% O_2. The tube was suspended in a bath containing 30 ml of a similar solution in which either 26 mM $NaHCO_3$ or 10 mM HEPES replaced an equivalent amount of NaCl and maintained at 36°C. The HCO_3^--containing saline was gassed with 95% O_2/5% CO_2 and the HEPES with 100% O_2; both having a pH of 7.4.

Measurement of secretion

The mucosal saline was changed every 15 min throughout the experiment and acid secretion assessed by back-titration with 5 mM NaOH by use of an autotitrator system (ABU 80, Radiometer, Copenhagen). During titration at room temperature the solution was continually gassed with 95% O_2/5% CO_2. The titration end point was determined as that pH obtained when a sample of mucosal saline taken directly from the stock reservoir was similarly gassed and was rechecked several times during the experiment. The method was validated by adding known amounts of HCl to 5 ml of mucosal saline, equivalent to the amounts produced by the tissues. A linear regression of the amount of HCl estimated by titration on the amount added gave a correlation coefficient of 0.9952 ($n = 6$) with a slope of 0.860. This technique is analogous to that used previously to measure bicarbonate secretion (Canfield, 1991) and was adopted because some parts of the study required sequential measurement of both acid and base secretion in the same tissues (with 5 ml HCl titrant).

Expression of results

Acid secretion is expressed either as $\mu mol\ cm^{-2}\ h^{-1}$ or as the secretory ratio = (plateau response to drug/preceeding basal secretion) as used in the earlier study (Canfield & Price, 1981) and values are mean ± s.e.mean with n as the number of tissues. Means were compared by either the paired or unpaired t test as appropriate and values of $P < 0.05$ were taken as indicating a significant difference between means.

Materials

The following were obtained from Sigma (Poole, Dorset); isoprenaline, propranolol and alprenolol. Other compounds were supplied as gifts for which we are grateful: practolol, ICI 118551 (erythro-(±)-1-(7-methylindan-4-yloxy)-3-isopro-

[1] Author for correspondence.

pylaminobutan-2-ol; ICI Pharmaceuticals, Cheshire), BRL 37344 (sodium-4[2[2-hydroxy-2(3-chlorphenyl)ethylamino] propyl]phenoxyacetate; SmithKline Beecham, Great Burgh), SR 58611A (N-[(2R)-7-hydroxy-1,2,3,4-tetrahydronapth-2-yl]-(2R)-2-hydroxy-2-(3-chlorphenyl) ethanol hydrochloride; Sanofi Recherche, Milan, Italy), SCH 28080 (2-methyl-8-(phenylmethoxy)imidazol[1,2-a]pyridine-3-acetonitrile; Kirby-Warrick Pharmaceuticals, Bury St Edmunds, Suffolk). Drugs were made up freshly in saline (except SCH 28080 which was dissolved in ethanol) as required and added to the serosal side of the preparation.

Results

Choice of serosal buffer

In previous studies from this laboratory using this preparation the serosal solution was always buffered with HCO_3^-/CO_2. It is likely that acid output was underestimated as a result of being partly neutralised by bicarbonate secreted by surface cells of the stomach (Flemström, 1987). To avoid this possibility we have used a HEPES/O_2 buffered serosal saline in the present study. It was therefore necessary to compare the preparation in this buffer with previous work in HCO_3^-/CO_2. Basal secretion of acid in the HEPES-buffered tissues was well maintained; 1 h into the experiment it was 1.70 ± 0.80 and at 6 h 1.9 ± 0.13 $\mu mol\ cm^{-2}\ h^{-1}$ ($n = 6$). Addition of the proton pump inhibitor SCH 28080 (50 μM) at the peak of response to isoprenaline (5 μM; 3.75 ± 0.25 $\mu mol\ cm^{-2}\ h^{-1}$) abolished acid secretion in all 6 tissues after 75 min. With HEPES as serosal buffer, there was no net alkaline secretion following complete inhibition of acid output which contrasts with the effect of SCH 28080 in HCO_3^--buffered serosal saline shown in Figure 1 described below. We made the following predictions for the HEPES-buffered tissue compared with HCO_3^--buffered; basal secretion would be higher, the increase in secretion in response to isoprenaline would be the same and consequently the response expressed as secretory ratio would be less. The change in basal acid secretion going from HEPES to HCO_3^- buffer should be the same as the measured rate of alkalinisation following total inhibition of acid output with SCH 28080. These predictions were tested experimentally and the results are shown in Figure 1. Basal acid in HEPES was significantly greater than in HCO_3^- (1.98 ± 0.23 and 0.76 ± 0.07 $\mu mol\ cm^{-2}\ h^{-1}$, $n = 6$). Response to isoprenaline (5 μM) in HEPES was not different from HCO_3^- (1.21 ± 0.15 and 1.57 ± 0.16 $\mu mol\ cm^{-2}\ h^{-1}$) but expressed as the secretory ratio, the HEPES value was lower (1.44 ± 0.17 and 1.95 ± 0.1) due to the greater rate of basal secretion in HEPES.

The change in basal secretion going from HEPES to HCO_3^- (1.22 ± 0.28 $\mu mol\ cm^{-2}\ h^{-1}$) was not different from the rate of alkalinisation measured in the presence of SCH 28080 (1.12 ± 0.12 $\mu mol\ cm^{-2}\ h^{-1}$). Responses to repeated stimulation with isoprenaline were well maintained in the HEPES buffer as shown in Figure 2. All subsequent results refer to studies using the HEPES/O_2-buffered saline.

Effect of SR 58611A

Each stomach was first exposed to isoprenaline (5 μM) for 60 min; this was washed out and when acid had returned to a steady rate (usually 60 min), SR 58611A was added at one of the selected concentrations (0.1–5 μM). When the peak response had been obtained (60–75 min) SR 58611A was washed out and isoprenaline (5 μM) was added again. The concentration-response data for SR 58611A is shown in Figure 3. The maximum response was at 1 μM and the secretory ratio was 1.47 ± 0.03 ($n = 4$) whilst the response to the initial isoprenaline for all tissues used in the curve was 1.46 ± 0.07 ($n = 24$).

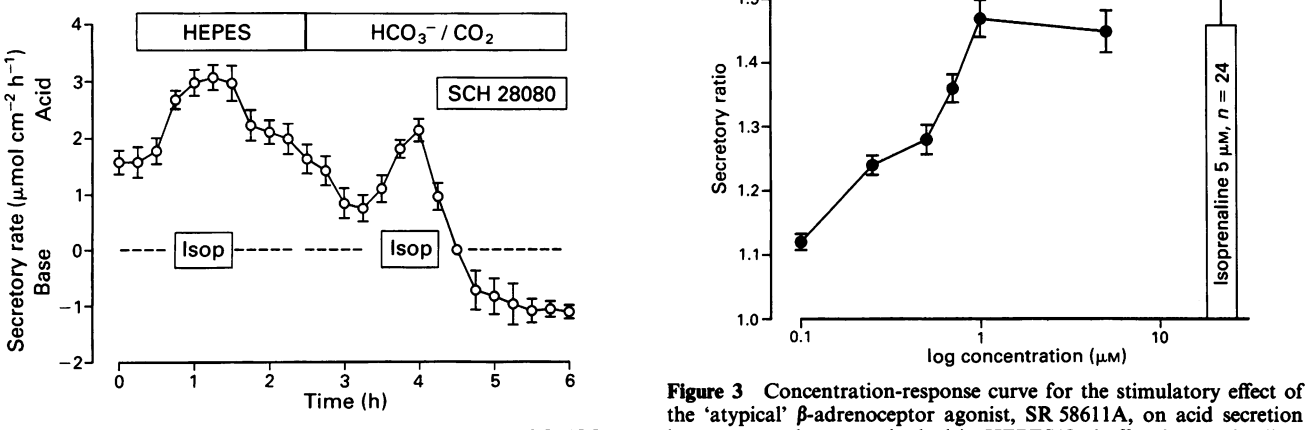

Figure 1 Effect of changing from a HEPES/O_2- to a HCO_3^-/CO_2-buffered (both pH 7.4) serosal saline on basal and isoprenaline (Isop)-stimulated (5 μM) acid secretion by rat stomach *in vitro*. Subsequent addition of the proton pump inhibitor SCH 28080 (50 μM) abolished acid secretion and revealed a net secretion of base (shown as – ve scale). Values are mean with s.e.mean shown by vertical bars, $n = 6$.

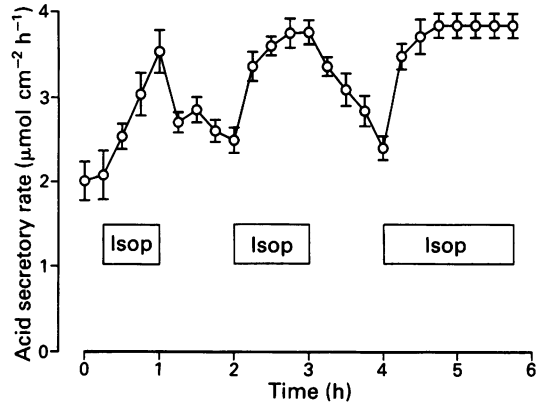

Figure 2 Repeated stimulation of acid secretion with isoprenaline (5 μM) (Isop) in rat stomach bathed with HEPES/O_2 buffered serosal saline *in vitro*. Values are mean with s.e.mean shown by vertical bars, $n = 6$.

Figure 3 Concentration-response curve for the stimulatory effect of the 'atypical' β-adrenoceptor agonist, SR 58611A, on acid secretion by rat stomach *in vitro* bathed in HEPES/O_2 buffered serosal saline. Data shown as secretory ratio (plateau response to drug/preceding basal secretion). Each tissue was first exposed to isoprenaline (5 μM) (Isop) for 60 min and, after washout, to one concentration of SR 58611A (60–75 min). Values are mean with s.e.mean shown by vertical bars, $n = 4$. The mean value for all the initial isoprenaline responses is also shown ($n = 24$) for comparison.

In a separate experiment in HCO_3^-/CO_2-buffered serosal solution containing SCH 28080 (50 μM), the rate of bicarbonate secretion was 1.31 ± 0.09 and, following exposure to SR 58611A (1 μM), was 1.38 ± 0.14 μmol cm^{-2} h^{-1} ($n = 6$) showing that there was no effect of SR 58611A on alkaline secretion. Similar results were obtained with isoprenaline (5 μM, data not shown).

Effect of β-antagonists

The effects of pretreatment of tissues with either propranolol (10 μM), alprenolol (10 μM) or a combination of ICI 118551 (1 μM) plus practolol (12.5 μM) for 60 min was compared with control tissues that had not received antagonist. Tissues were exposed first to isoprenaline (5 μM) and subseqeuntly to SR 58611A (1 μM) as above and the results are shown in Table 1. Only propranolol resulted in a significant inhibition of response to either agonist.

Desensitization following SR 58611A

It was apparent from the initial concentration-response studies that the response to isoprenaline following SR 58611A was much lower than the initial isoprenaline response, a situation not seen with repeated isoprenaline stimulation (Figure 2). We therefore carried out an experiment where all tissues were first exposed to isoprenaline (5 μM), then to SR 58611A (1 μM) as before and finally to either isoprenaline again, bethanechol (1 μM) or histamine (50 μM). The results are shown in Figure 4; SR 58611A significantly reduced the response to the second exposure to isoprenaline but tissues responded well to both histamine and bethanechol.

Discussion

HEPES/O_2-buffered preparations

When the serosal saline was buffered with HCO_3^-/CO_2 in the present study, the maximum response to isoprenaline was the same as in the earlier study (Canfield & Price, 1981). However, the present study differed from the earlier in the introduction of HEPES/O_2 as serosal buffer. HEPES is the preferred buffer as it permits acid secretion to be measured without the complication of serosal bicarbonate being secreted by the surface cells and neutralising part of the acid. With the HCO_3^--buffered system, drug-induced changes in measured acid secretion could be due to either changes in proton pump activity, changes in HCO_3^- flux or a mixture of both. Although an exhaustive comparison of the preparation in the two buffers has not been made, the results suggest that the lack of an exogenous source of CO_2 in the HEPES-buffered tissues does not impair the acid-secretory activity or responsiveness of the tissue. Preparations responded to histamine and bethanechol (Figure 4) as well as the β-adrenoceptor agonists and responses to isoprenaline were well maintained (Figure 1). Additionally, changing from HEPES/O_2 to HCO_3^-/CO_2 buffer containing the proton pump inhibitor SCH 28080 allows easy measurement of both acid and base secretion by the same preparation. The rate of bicarbonate secretion obtained in this way was similar to the value reported with SCH 28080 in guinea-pig stomach (Chiu *et al.*, 1983).

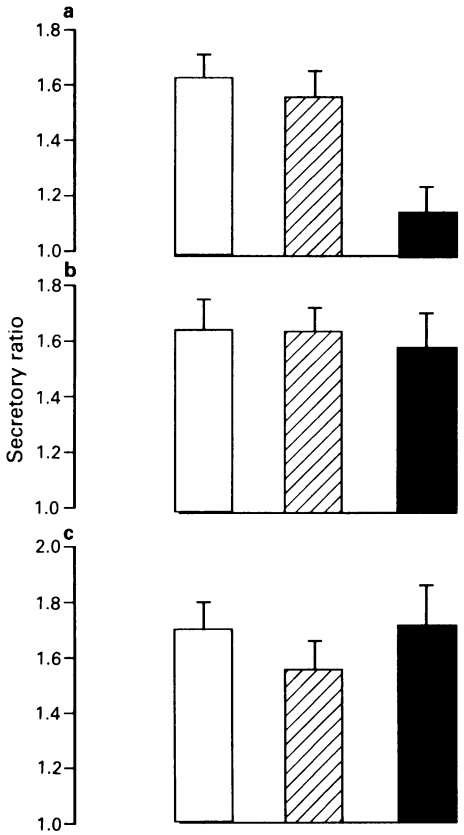

Figure 4 This shows the secretory response as secretory ratio (plateau response to drug/preceding basal secretion) of rat stomach *in vitro* bathed with a HEPES/O_2 buffered serosal saline in response to drug treatments. Three experiments are shown (a, b and c); all tissues were first exposed to isoprenaline for 60 min (5 μM, open columns). This was washed out and all were exposed to the 'atypical' β-adrenoceptor agonist SR 58611A for 60 min (1 μM, hatched columns). Following washout of SR 58611A, tissues were exposed as follows; (a) isoprenaline (5 μM); (b) histamine (50 μM) and (c) bethanechol (1 μM) for 60 min in each case. All values are mean with s.e.mean shown by vertical bars and $n = 6$ in each experiment. The second response to isoprenaline in (a) was significantly lower than the first ($P < 0.05$) in contrast to the situation in Figure 2.

Table 1 Effect of β-adrenoceptor antagonists on acid secretory response to isoprenaline and SR 58611A in rat stomach *in vitro*

Treatment	*Isoprenaline* (5 μM)	*SR 58611A* (1 μM)
Control	1.50 ± 0.02	1.53 ± 0.07
+ Propranolol (10 μM)	1.18 ± 0.03*	1.22 ± 0.06*
+ Alprenolol (10 μM)	1.49 ± 0.08	1.58 ± 0.04
+ Practolol (12.5 μM) + ICI 118551 (1 μM)	1.56 ± 0.05	1.60 ± 0.08

Tissues were preincubated with antagonist (except control) for 60 min before addition of isoprenaline. When response had plateaued, isoprenaline was washed out and when secretion was steady, SR 58611A was added. Values are mean ± s.e.mean of secretory ratio (plateau response/initial basal secretion) and $n = 4$ in each treatment.
*$P < 0.05$ compared with control.

Effects of 'atypical' β-adrenoceptor agonists

The 'atypical' β-adrenoceptor agonists SR 58611A and BRL 37344 were able to stimulate acid secretion to the same maximum extent as isoprenaline. Responses to SR 58611A and isoprenaline were unaffected by the selective β-antagonists but were inhibited by propranolol as expected. The lack of effect of alprenolol was surprising. This has been reported to be particularly effective (but not selective for) 'atypical' β-receptors (Blue *et al.*, 1988; 1990). In addition, in another study in this laboratory in the *in vitro* stimulation of bicarbonate secretion in rat caecum by isoprenaline and SR 58611A, the same alprenolol stock solution inhibited the responses at 10 μM (Canfield & Abdul-Ghaffar, 1992). This may indicate that the 'atypical' β-adrenoceptors in the two tissues are not identical but further studies will be necessary to substantiate this, preferably with a selective antagonist.

The lack of effect of either isoprenaline or SR 58611A on gastric bicarbonate secretion is consistent with the reported lack of effect of β-adrenoceptor agonists on this activity (Flemström, 1987) and contrasts with their stimulation of bicarbonate secretion in rat duodenum (White & Canfield, 1985) and caecum (Abdul-Ghaffar & Canfield, 1990) and bullfrog duodenum (Garner *et al.*, 1984).

Desensitization following SR 58611A

Following the first application of SR 58611A, tissues subsequently showed a very reduced response to either a second application or to isoprenaline but did respond to bethanechol or histamine. It is not possible to say that responses to bethanechol or histamine were totally unaffected by the previous exposure SR 58611A as we do not have repeat control data for these drugs in HEPES/O_2 but the size of responses was comparable with the earlier study (Canfield & Price, 1981). These findings suggest that homologous desensitization of the adrenoceptors may be occurring (Lefkowitz *et al.*, 1990). BRL 37344 also reduced the response to subsequent application of isoprenaline (data not shown). BRL 37344 has been reported to cause desensitization in gastro-intestinal muscle preparations (Coleman *et al.*, 1987; McLaughlin & MacDonald, 1990) and SR 58611A has been used only as a single concentration in each tissue (Guidice *et al.*, 1989). We have also found similar results indicating desensitization following application of these 'atypical' agonists on bicarbonate secretion in rat caecum (Canfield & Abdul-Ghaffar, 1992). Desensitization may thus be a feature of the action of currently available 'atypical' β-agonists.

In summary, the previously reported *in vitro* stimulation of rat gastric acid secretion by β-adrenoceptor agonists (Canfield & Price, 1981) appears to be mediated by so called 'atypical' β-receptors.

References

ABDUL-GHAFFAR, T. & CANFIELD, S.P. (1990). Cholinergic inhibition and adrenergic stimulation of bicarbonate secretion in rat cecum in vitro. *Gastroenterol*, **98**, A535.

BIANCHETTI, A. & MANARA, L. (1990). *In vitro* inhibition of intestinal motility by phenylethanolaminotetralines: evidence of atypical β-adrenoceptors in rat colon. *Br. J. Pharmacol.*, **100**, 831–839.

BLUE, D.R., BOND, R.A. & CLARKE, D.E. (1988). Blockade of putative adrenoceptor in guinea pig ileum by alprenolol. *Br. J. Pharmacol.*, **95**, 541P.

BLUE, D.R., BOND, R.A., ADHAM, N., DELMENDO, R., MICHEL, A.D., EGLEN, R.M., WHITING, R.L. & CLARKE, D.E. (1990). Antagonist characterisation of atypical beta adrenoceptors in guinea pig ileum: blockade by alprenolol and dihydroalprenolol. *J. Pharmacol. Exp. Ther.*, **252**, 1034–1042.

CANFIELD, P. (1991). Characteristics of luminal bicarbonate secretion by rat cecum in vitro. *Am. J. Physiol. Gastrointest. Liver Physiol.*, **260**, G464–G470.

CANFIELD, S.P. & ABDUL-GHAFFAR, T. (1992). Stimulation of bicarbonate secretion by atypical β-receptor agonists in rat cecum in vitro. *Eur. J. Pharmacol.*, (in press).

CANFIELD, S.P. & PRICE, C.A. (1981). A comparison of the effects of sympathomimetic agents on gastric acid secretion in the rat. *J. Physiol.*, **316**, 11–21.

CARPENE, C., GALITZKY, J., ESCLAPEZ, G., AMBID, L. & LAFONTAN, M. (1991). Atypical beta-adrenergic stimulation of lipolysis in rodent adipocytes: comparison of the lipolytic and the intrinsic sympathomimetic activities of various beta-blockers. *Fund. Clin. Pharmacol.*, **5**, 459.

CHIU, P.J.S., CASCIANO, C., TETZLOFF, G., LONG, J.F. & BARNETT, A. (1983). Studies on the mechanisms of the antisecretory and cytoprotective actions of SCH 28080. *Pharmacol. Res. Commun.*, **226**, 121–125.

COLEMAN, R.A., DENYER, L.H. & SHELDRICK, K.E. (1987). β-Adrenoceptors on guinea pig gastric fundus – are they the same as the 'atypical' β-adrenoceptors in rat adipocytes? *Br. J. Pharmacol.*, **90**, 40P.

FLEMSTROM, G. (1987). Gastric and duodenal mucosal bicarbonate secretion. In *Physiol of the Gastrointestinal Tract.* ed. Johnson, L.R. pp. 1011–1029. New York: Raven Press, 2nd Edition.

GARNER, A., HEYLINGS, J.R., PETERS, T.J. & WILKES, J.M. (1984). Adrenergic agonists stimulate bicarbonate secretion by amphibian duodenum in vitro via an action on beta-2 receptors. *J. Physiol.*, **354**, 34P.

GUIDICE., A., CROCI, T., BIANCHETTI, A. & MANARA, L. (1989). Inhibition of rat colonic motility and cardio-vascular effects of new gut-specific beta-adrenergic phenylethanolaminotetralines. *Life Sci.*, **44**, 1411–1417.

HOLLENGA, C., BROUWER, F. & ZAAGSMA, J. (1991). Relationship between lipolysis and cyclic AMP generation mediated by atypical β-adrenoceptors in rat adipocytes. *Br. J. Pharmacol.*, **102**, 577–580.

HOLLENGA, C.H. & ZAAGSMA, J. (1989). Direct evidence for the atypical nature of functional β-adrenoceptors in rat adipocytes. *Br. J. Pharmacol.*, **98**, 1420–1424.

LEFKOWITZ, R.J., HAUSDORFF, W.P. & CARON, M.G. (1990). Role of phosphorylation in desensitisation of the β-adrenoceptor. *Trends Pharmacol. Sci.*, **11**, 190–194.

MACDONALD, A., FORBES, I.J., GALLACHER, D., HEEPS, G. & MCLAUGHLIN, D.P. (1990). Beta adrenoceptors mediating relaxation in rat small intestine are atypical in nature. *Br. J. Pharmacol.*, **102**, 167P.

MCLAUGHLIN, D.P. & MACDONALD, A. (1990). Evidence for the existence of 'atypical' β-adrenoceptors (β_3-adrenoceptors) mediating relaxation in the rat distal colon *in vitro*. *Br. J. Pharmacol.*, **101**, 569–574.

WHITE, J.P.N. & CANFIELD, S.P. (1985). Effect of isoproterenol and IBMX on acid disposal by rat duodenum in vitro. *Dig. Dis. Sci.*, **30**, A41.

(Received August 28, 1991
Revised January 29, 1992
Accepted March 9, 1992)

Br. J. Pharmacol. (1992), **106**, 587–592

Analysis of the depressant effect of the endothelium on contractions of rabbit isolated basilar artery to 5-hydroxytryptamine

[1]D.J. Trezise, *G.M. Drew & A.H. Weston

Smooth Muscle Research Group, Department of Physiological Sciences, University of Manchester Medical School, Oxford Road, Manchester M13 9PT and *Department of Peripheral Pharmacology, Glaxo Group Research Ltd, Ware, Hertfordshire, SG12 0DP

1 The effects of endothelium removal and of a number of pharmacological agents known to modify endothelial cell function on the contractile response of rabbit isolated basilar arteries to 5-hydroxytryptamine (5-HT) and other vasoconstrictors were studied.

2 Endothelium removal slightly reduced the contractile response to potassium chloride (40 mM) but markedly augmented and potentiated contractions to 5-HT (1 nM–10 μM).

3 L-N^G-nitro-arginine (L-NOARG, 1–30 μM), an inhibitor of nitric oxide formation in vascular endothelial cells, evoked endothelium-dependent contraction, and augmented and potentiated contractions to 5-HT in endothelium-intact but not endothelium-denuded tissues. Prior incubation with L-arginine (1 mM), but not D-arginine (1 mM), abolished these effects of L-NOARG (1 μM). L-NOARG (30 μM) also augmented contractions of endothelium-intact tissues to noradrenaline, prostaglandin $F_{2\alpha}$, and to a lesser degree endothelin-1.

4 Neither glibenclamide (3 μM) nor N-ethylmaleimide (1 μM), putative inhibitors of the effects of endothelium-derived hyperpolarizing factor (EDHF) and of agonist-stimulated endothelium-derived relaxing factor (EDRF) release respectively, had any effect on either resting tension or the contractile response to 5-HT. In some tissues indomethacin (3 μM), a cyclo-oxygenase inhibitor, produced a small contraction and augmented the contractile response to 5-HT, but in most cases indomethacin was without effect.

5 In endothelium-intact tissues precontracted with uridine 5'-triphosphate (UTP; 100 μM), 5-HT did not evoke relaxation but rather caused further contraction. Under the same conditions acetylcholine (0.01–10 μM) evoked endothelium-dependent relaxation.

6 These data demonstrate that the endothelium profoundly depresses contractions of rabbit isolated basilar artery to 5-HT, and that this phenomenon can be fully accounted for by the release of an L-NOARG-sensitive relaxing factor. Neither glibenclamide-sensitive EDHF nor cyclo-oxygenase products plays a major role. As we could find no evidence that 5-HT stimulates the production of EDRF *per se*, and L-NOARG caused endothelium-dependent contraction and augmented contractions to other vasoconstrictor agents, it seems likely that a basal release of EDRF underlies this phenomenon.

Keywords: 5-Hydroxytryptamine; rabbit basilar artery; endothelium; nitric oxide; L-N^G-nitro-arginine (L-NOARG); endothelin; endothelium-derived hyperpolarizing factor (EDHF); glibenclamide; N-ethylmaleimide; indomethacin

Introduction

Several studies have shown that the presence of an intact endothelial cell layer can profoundly depress the contractility of certain isolated blood vessels to exogenous vasoconstrictor agents. For example, Martin *et al.* (1986) demonstrated that removal of the endothelium augmented the contractile response of rat aorta to α-adrenoceptor agonists. Primarily on the basis that haemoglobin, an inhibitor of the effects of endothelium-derived relaxing factor (EDRF), caused endothelium-dependent contraction, and augmented contractions to α-adrenoceptor agonists in endothelium-intact tissues, Martin *et al.* (1986) proposed that a spontaneous release of EDRF accounted for this depressent effect of the endothelium. A similar conclusion was made by Connor & Feniuk (1989) who showed that addition of methylene blue (another inhibitor of the effects of EDRF) or removal of the endothelium markedly augmented contractions of dog isolated basilar arteries to 5-hydroxytryptamine (5-HT) and other vasoconstrictors. The mechanisms underlying these phenomena are, however, not yet fully understood.

Recent evidence strongly suggests that the chemical identity of EDRF is nitric oxide, or a related nitric oxide-containing moiety (Palmer *et al.*, 1987), and is formed by the action of the enzyme nitric oxide synthase on the precursor amino acid L-arginine (Palmer *et al.*, 1988a). Importantly, several close structural analogues of L-arginine are selective inhibitors of the relaxant effects of EDRF and of vascular endothelial cell nitric oxide synthesis, e.g. L-N^G-monomethyl arginine (L-NMMA) and L-N^G-nitro arginine (L-NOARG) (Palmer *et al.*, 1988b; Moore *et al.*, 1990; Mulsch & Busse, 1990). Both L-NMMA and L-NOARG evoke endothelium-dependent contraction of vascular smooth muscle (Gold *et al.*, 1990; Moore *et al.*, 1990; Mulsch & Busse, 1990) providing further evidence that blood vessels spontaneously release EDRF. The detailed effects of these agents on contractile responses of isolated blood vessels to exogenous vasoconstrictors have not, however, been studied. Interestingly, the sulphydryl alkylating agent, N-ethylmaleimide (NEM), is reported to inhibit agonist-stimulated but not spontaneously-liberated EDRF from cultured vascular endothelial cells (Siegle *et al.*, 1991), suggesting either that there may be more than one EDRF, or that the cellular mechanisms responsible for its formation and release are

[1] Author for correspondence.

different. Finally, it has become clear that the endothelium can also release another entity, considered chemically distinct from nitric oxide, that hyperpolarizes vascular smooth muscle, and which has been termed 'endothelium-derived hyperpolarizing factor' (EDHF) (Taylor & Weston, 1988; Chen & Suzuki, 1989). In rabbit cerebral arteries the hyperpolarizing actions of acetylcholine-liberated EDHF are inhibited by the potassium (K) channel blocker glibenclamide (Brayden, 1990), suggesting that EDHF may open glibenclamide-sensitive K channels. The contribution (if any) that spontaneously liberated EDHF may make to the depressant effect of the endothelium on contractions of blood vessels has yet to be studied.

In preliminary experiments we observed that removal of the endothelium markedly augmented contractions of rabbit isolated basilar artery to 5-HT, as previously described by Garland (1987). Using the currently commercially available modulators of endothelial cell function (i.e. L-NOARG, L-arginine, glibenclamide, NEM, indomethacin), we evaluated the mechanisms underlying this phenomenon. In particular, we examined the various contributions made by L-NOARG-sensitive EDRF, EDHF and cyclo-oxygenase products, and attempted to demonstrate whether such factors were released as a direct result of an action of 5-HT on the endothelial cell, or liberated spontaneously.

A preliminary account of some of this work has been presented to the British Pharmacological Society (Trezise & Weston, 1991).

Methods

Tissue preparation

New Zealand White and half-lop rabbits of either sex (2–4.5 kg), obtained from the Manchester University Animal Unit, were killed by injection of sodium pentobarbitone (300 mg kg^{-1}) into an ear vein. The brain was removed, placed in Krebs physiological salt solution (PSS; for the composition see below), and the basilar artery dissected out with the aid of a low power dissecting microscope. The artery was then cleared of extraneous connective tissue and cut into four ring sections of equal length (approximately 2 mm). In some experiments the endothelium was removed mechanically by inserting a fine steel needle into the lumen of the artery. Vascular rings were then mounted for the recording of isometric force.

Force recordings

Each vascular ring was placed in a tissue bath of 8 ml volume and suspended between two fine L-shaped wires inserted into the lumen of the vessel. One wire was firmly attached to the tissue bath and the other suspended on a sensitive force transducer (Ether UF1), whose signal was amplified (Grass 7P1) and recorded on a Grass Polygraph (model 79C). Tissues were continually bathed in Krebs-PSS, maintained at 37 ± 0.1°C by a Grant water circulator (model W6), and gassed with 95% O_2/5% CO_2. In all studies tissues were placed under a resting force of 3 mN, and after an equilibration period of 45 min, tension was readjusted to 2.9 mN. Fifteen min later 40 mM KCl was added to the bath in order to assess the tissue viability. Once the contractile response to KCl had reached a plateau, tissues were washed by overflow with fresh PSS every 5 min until responses returned to baseline. After a further 30 min equilibration period the integrity of the endothelium was assessed by precontracting the tissue with either prostaglandin $F_{2\alpha}$ (3 μM) or uridine 5'-triphosphate (UTP, 100 μM) and examining the relaxant response to the endothelium-dependent vasodilator acetylcholine (10 μM). Tissues which relaxed by more than 40% or less than 10% to acetylcholine were considered endothelium-intact and endothelium-denuded respectively. Other tissues were discarded. Preparations were then washed for 30 min or until the original baseline was reestablished. Cumulative concentration-response curves to 5-HT were then constructed in the presence of either L-NOARG (1 or 30 μM), glibenclamide (3 μM), indomethacin (3 μM) or N-ethylmaleimide (1–10 μM) following previous incubation with these agents for 25 min. In some experiments tissues were exposed to either L-arginine (1 mM) or D-arginine (1 mM) 10 min before L-NOARG (1 μM). One vascular ring from each animal received only the respective drug vehicle prior to 5-HT, thus acting as a control. Similar experiments were performed with L-NOARG (30 μM) using the vasoconstrictor agents prostaglandin $F_{2\alpha}$, noradrenaline and endothelin-1. One vasoconstrictor concentration-response curve only was constructed in each tissue.

Statistical analysis

To minimize variation between tissues, vasoconstrictor-evoked responses are expressed as a percentage of the contraction induced by KCl (40 mM). Data are expressed as arithmetic mean ± s.e.mean, or geometric mean with 95% confidence limits (in parentheses) where appropriate. EC_{50} values were calculated as the concentration of drug required to elicit 50% of the maximal response, and E_{max} values as the maximal response of a tissue to a given drug. Statistical comparisons were made either by Student's t test where two groups were concerned, or an analysis of variance using Duncan's test for the case of multiple comparisons. Differences between data were considered of significance when $P<0.05$.

Drugs and solutions

The composition of the PSS was as follows (mM): NaCl 115, KCl 4.6, KH_2PO_4 1.2, $MgSO_4$ 1.2, $CaCl_2$ 2.5, $NaHCO_3$ 25 and glucose 11.1. The following drugs were used: endothelin-1 (Cambridge Research Biochemicals, Cambridge U.K.), 5-hydroxytryptamine creatinine sulphate (5-HT), acetylcholine chloride, prostaglandin $F_{2\alpha}$ tris salt, noradrenaline bitartrate, L-N^G-nitro-arginine (L-NOARG), L-arginine, D-arginine, N-ethylmaleimide (NEM), glibenclamide, uridine 5'-triphosphate sodium salt (UTP) and indomethacin (all Sigma Chemical Co., Poole, Dorset). All drugs were freshly prepared each day. Drugs were dissolved and diluted in twice distilled water, with the following exceptions: prostaglandin $F_{2\alpha}$ and glibenclamide (10 mM in 100% ethanol), L-NOARG (10 mM in 0.01 M HCl), NEM (10 mM in dimethylsulphoxide) and indomethacin (10 mM in 0.5 M sodium hydrogen carbonate solution). Drugs were administered to the organ bath in volumes of between 5–80 μl to provide the required final bath concentrations.

Results

The contractile response of rings of rabbit isolated basilar artery to 40 mM KCl was smaller in endothelium-denuded compared to endothelium-intact preparations (8.1 ± 1.1 mN ($n = 20$) compared to 11.8 ± 1.1 mN ($n = 42$); $P<0.05$), suggesting that the technique used to denude the endothelium causes a small degree of damage to the smooth muscle. The absolute magnitude of the contractile response to 5-HT was, however, significantly larger in endothelium-denuded compared to endothelium-intact preparations (9.0 ± 1.6 mN compared to 4.1 ± 0.8 mN; $P<0.05$) and thus we do not think that expression of the data as a percentage of the response to KCl gives rise to any undue artefacts.

Pharmacological modulation of 5-hydroxytryptamine-induced contraction

5-HT-evoked concentration-related contractions of endothelium-intact rings of rabbit isolated basilar artery with an

EC_{50} value of 126 nM (74–216, $n = 12$), and a maximal contractile response of 34.7 ± 5.4%. Removal of the endothelium both potentiated and augmented the contraction to 5-HT as shown by the respective significant leftward shift in the response curve yielding an EC_{50} value of 21.9 nM (16.2–29.5, $n = 8$; $P<0.05$), and increase in the maximal response to 108.4 ± 7.1% ($P<0.05$, Figure 1).

In endothelium-intact tissues L-NOARG (30 μM)-evoked a slowly developing contractile response (1.5 ± 0.4 mN, $n = 22$), and augmented and potentiated the contractile response to 5-HT (EC_{50} 26.3 nM (15.8–43.6) and E_{max} 111.8 ± 5.5%, $P<0.05$ compared to the endothelium-intact control curve; Figure 1). The effects of incubation with L-NOARG and removal of the endothelium on the 5-HT concentration-response curve were very similar. In endothelium-denuded tissues L-NOARG (30 μM) was without effect on either resting tone or the contractile response to 5-HT (EC_{50} 14.8 nM (10.7–20.4) and E_{max} 102.7 ± 8.9%; not significantly different from endothelium-denuded control curve values; Figure 1). At a lower concentration (1 μM) L-NOARG also evoked contraction (0.5 ± 0.2 mN, $n = 12$), and potentiated and augmented the contractile response to 5-HT in endothelium-intact tissues (EC_{50} 43.9 nM (29.5–65.0) and E_{max} 112.2 ± 6.6%). These effects were abolished by prior incubation with L-arginine (1 mM; EC_{50} 203 nM (118–348) and E_{max} 32.0 ± 7.3%, $P<0.05$ compared to endothelium-intact curve in the presence of L-NOARG (1 μM); Figure 2). The stereospecific nature of this effect was revealed by the fact that D-arginine (1 mM) had no effect on the action of L-NOARG (EC_{50} 75.8 nM (32.0–177) and E_{max} 125.0 ± 16.0%; Figure 2).

Neither glibenclamide (3 μM) nor NEM (1 μM) altered resting tone or the contractile response to 5-HT in endothelium-intact tissues (respective EC_{50} values of 56.2 nM (24.9–126) and 56.5 nM (29.8–107) and E_{max} values of 47.7 ± 15.0% and 42.3 ± 11.6%; not significantly different from endothelium-intact control curve; Figure 3). At a higher concentration (10 μM) NEM abolished the contractile response to 5-HT. In most cases indomethacin (3 μM) had no effect on the resting tone of endothelium-intact preparations, and the subsequent 5-HT concentration-response curves were similar to the respective controls. However, in 2 out of 9 experiments indomethacin caused contraction (1.8 mN, mean of $n = 2$), and markedly enhanced the contractile response to 5-HT. When taken together indomethacin had no overall significant effect on the 5-HT concentration-response curve (EC_{50} 75.1 nM (31.3–171) and E_{max} 46.3 ± 16.3%, not significantly different from endothelium-intact control curve; Figure 3).

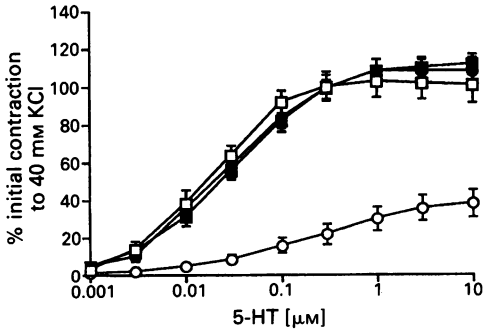

Figure 1 Effect of L-N^G-nitro-arginine (L-NOARG, 30 μM) on the contractile response of rabbit isolated basilar artery to 5-hydroxytryptamine (5-HT). Control responses to 5-HT in endothelium-intact and endothelium-denuded tissues shown by (○) and (●) respectively. Responses to 5-HT in the presence of L-NOARG shown by (□) in endothelium-intact tissues and (■) in endothelium-denuded tissues. L-NOARG was added to the organ bath 25 min before construction of the 5-HT concentration-response curve. Abscissa scale: 5-HT concentration expressed as micromolar concentration. Ordinate scale: contractile response to 5-HT expressed as a percentage of the initial contractile response of the tissue to 40 nM KCl. Each point represents the arithmetic mean value and the vertical bars the s.e.mean, $n = 9-12$.

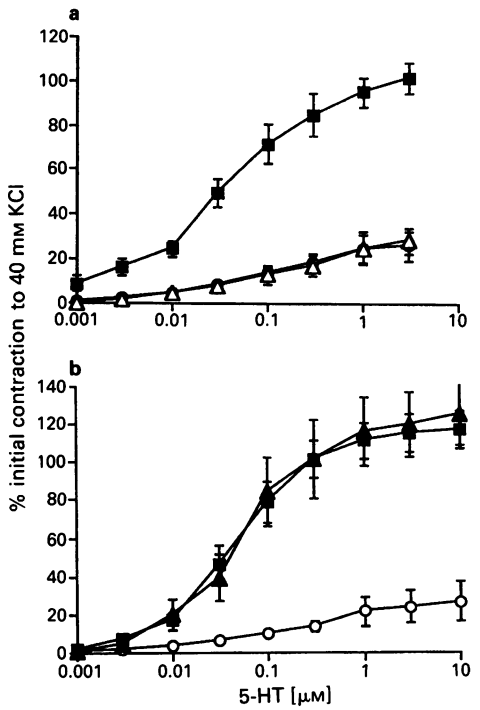

Figure 2 Inhibition of the effects of L-N^G-nitro-arginine (L-NOARG, 1 μM) on the 5-hydroxytryptamine (5-HT) concentration-response curve in endothelium-intact rabbit isolated basilar arteries by (a) L-arginine (1 mM), but not by (b) D-arginine (1 mM). The responses to 5-HT in the presence of either L-NOARG alone (■), L-NOARG and L-arginine (△), L-NOARG and D-arginine (▲) are compared with the control (○). Either L- or D-arginine was given 10 min before L-NOARG, which itself was given 25 min before construction of the 5-HT concentration-response curve. Abscissa scale: 5-HT concentration expressed as micromolar concentration. Ordinate scale: contractile response to 5-HT expressed as a percentage of the initial contractile response of the tissue to 40 mM KCl. Each point represents the arithmetic mean value and the vertical bars the s.e.mean, $n = 9-12$.

In an attempt to reveal a possible direct relaxant effect of 5-HT, endothelium-intact vascular rings were precontracted with UTP (100 μM) and then exposed to 5-HT (1 nM–10 μM) which only evoked further increases in tension. Under the same experimental conditions acetylcholine (0.01–10 μM) produced endothelium-dependent relaxation.

Effect of L-N^G-nitro-arginine on responses to other vasoconstrictor agents

Noradrenaline, prostaglandin $F_{2\alpha}$ and endothelin-1 all evoked concentration-related contraction of rabbit isolated basilar artery. The responses to noradrenaline and prostaglandin $F_{2\alpha}$ were small compared with that of 40 mM KCl (respective E_{max} values of 31.7 ± 6.7% and 25.3 ± 8.5%) whilst the responses to endothelin-1 were larger than that of KCl, although an E_{max} value could not be calculated due to limited availability of the peptide. In the presence of L-NOARG (30 μM) responses to all three vasoconstrictors were augmented (see Figure 4); the effect on the endothelin-1 contraction was much less marked than that on the noradrenaline and prostaglandin $F_{2\alpha}$ contractions.

Discussion

5-HT evoked concentration-related contractions of endothelium-intact rabbit isolated basilar artery, with a threshold

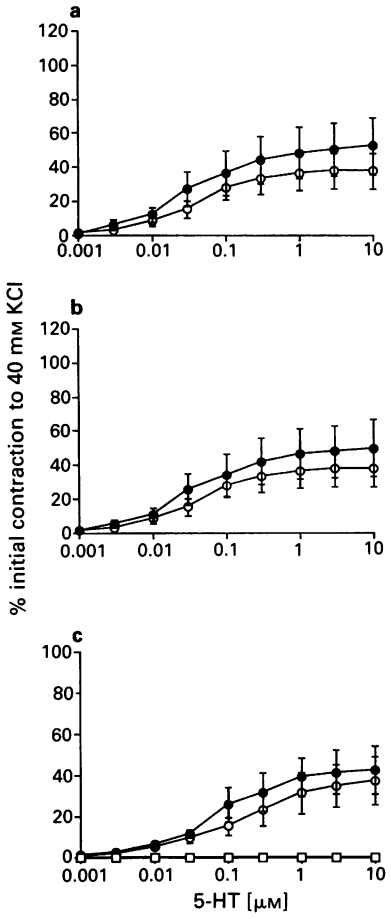

Figure 3 Lack of effect of (a) glibenclamide (3 μM), (b) indomethacin (3 μM) and (c) N-ethylmaleimide (NEM, 1–10 μM) on the contractile concentration-response curve to 5-hydroxytryptamine (5-HT) in endothelium-intact rabbit isolated basilar artery. Control responses shown by (○) and in the presence of drug by (●). In (c) the effect of 10 μM NEM is represented by (□). The test drug was administered 25 min before construction of the 5-HT concentration-response curve. Abscissa scale: 5-HT concentration expressed as micromolar concentration. Ordinate scale: contractile response to 5-HT expressed as a percentage of the initial contractile response of the tissue to 40 mM KCl. Each point represents the arithmetic mean value and the vertical bars the s.e.mean, $n = 4-8$.

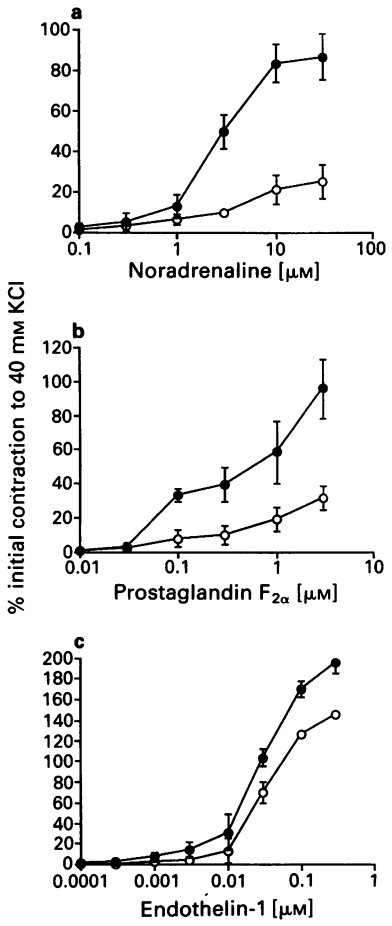

Figure 4 Augmentation by L-N^G-nitro-arginine (L-NOARG, 30 μM) of the contractile responses of endothelium-intact rabbit isolated basilar artery to (a) noradrenaline, (b) prostaglandin $F_{2\alpha}$ and (c) endothelin-1. Control responses shown by (○) and in the presence of L-NOARG (●). L-NOARG was added to the organ bath 25 min before construction of the concentration-response curve to the respective vasoconstrictor. Abscissa scale: vasoconstrictor concentration expressed as micromolar concentration. Ordinate scale: contractile response to the vasoconstrictor expressed as a percentage of the initial contractile response of the tissue to 40 mM KCl. Each point represents the arithmetic mean value and the vertical bars the s.e.mean, $n = 9-12$.

concentration and potency very similar to values previously reported (Parsons & Whalley, 1987; Cain & Nicholson, 1988). Removal of the endothelium reduced the size of the contraction to 40 mM KCl, but increased the absolute magnitude of the contractile response to 5-HT. The smaller contractile response to 40 mM KCl in endothelium-denuded tissues is probably the result of a degree of smooth muscle damage produced by the method of endothelium removal. We have tried other methods to remove the endothelium from these small arteries without damaging the smooth muscle (e.g. Triton-X detergent perfusion, air perfusion) but found the simple mechanical technique described here to cause the least reduction of KCl-induced responses. The augmentation of the contractile response to 5-HT by endothelium removal is very similar to that described in basilar arteries of the dog (Connor & Feniuk, 1989) and indicates that the endothelium exerts a depressant effect on the contractility of these vessels to 5-HT. In the present study endothelium-removal also potentiated the response to 5-HT, as shown by the significant difference in the EC_{50} values between endothelium-intact and endothelium-denuded tissues; such a phenomenon was not observed in the dog basilar artery (Connor & Feniuk, 1989). Using pharmacological agents known to modify endothelial cell function, we examined in detail the mechanisms underlying this depressant effect of the endothelium on contractile responses of rabbit isolated basilar artery to 5-HT.

L-NOARG, at a concentration previously shown to inhibit endothelium-dependent vasodilatation maximally (30 μM; Moore *et al.*, 1990) both augmented and potentiated the contractile response of endothelium-intact arterial rings to 5-HT. Interestingly, the concentration-response curve to 5-HT in the presence of the endothelium and the presence of L-NOARG was superimposable on the curve to 5-HT in the absence of the endothelium and absence of L-NOARG. Thus, removal of the endothelium or incubation with L-NOARG had almost identical effects on the response to 5-HT. L-NOARG had no further effect on the 5-HT concentration-response curve in endothelium-denuded tissues. These data collectively suggest that the depressant effect of the endothelium can be fully accounted for by the release of an L-NOARG-sensitive EDRF. Since L-NOARG inhibits the formation of nitric oxide from its precursor L-arginine in vascular endothelial cells (Mulsch & Busse, 1990), it seemed

probable that the nitric oxide/L-arginine pathway was involved. Such a conclusion is based on the assumption that L-NOARG and related compounds are specific inhibitors of nitric oxide synthase. Although this has yet to be unequivocally demonstrated, such a view seems reasonable in the absence of data to the contrary.

To test further the involvement of the nitric oxide/L-arginine pathway, we studied the effect of prior incubation with L-arginine on the action of L-NOARG. Addition of excess L-arginine to the system generally prevents the actions of nitric oxide synthase inhibitors by competing for the same enzyme (Palmer *et al.*, 1988b; Mulsch & Busse, 1990), provided that the concentration of inhibitor is not too high (Amezcua *et al.*, 1989; Moore *et al.*, 1990). Thus, we reduced the concentration of L-NOARG to 1 μM for these experiments. At this concentration L-NOARG still markedly augmented and potentiated the contractile response of endothelium-intact tissues to 5-HT. This action was completely prevented by a 1000 fold excess of L-arginine, but unaffected by a similar excess of the stereoisomer, D-arginine. Taken together these observations strongly suggest that endothelium-derived nitric oxide formed from L-arginine fully accounts for the depression of 5-HT-induced contractions in this vessel.

In accordance with this are the observations that both glibenclamide and indomethacin were without significant effect on either resting tone or the response to 5-HT. These data demonstrate that neither glibenclamide-sensitive EDHF nor cyclo-oxygenase products play a major role in this depressant phenomenon. In rabbit cerebral arteries, acetylcholine-evoked endothelium-dependent hyperpolarization together with part of the associated relaxation, is reportedly attenuated by glibenclamide (Brayden, 1990; but see Parsons *et al.*, 1991). If, in the present study, there was a release of EDHF either spontaneously or in response to 5-HT, a glibenclamide-induced contraction or augmentation of the response to 5-HT could have been anticipated. This was clearly not the case. Interestingly, we have previously shown that glibenclamide depolarizes endothelium-intact rabbit basilar arteries (Trezise & Weston, 1992), and thus it remains a possibility that there is an ongoing release of EDHF. However, this seems of little importance with respect to maintenance of resting vascular tone. The most likely explanation of this finding is that the glibenclamide-sensitive smooth muscle K channel is open under the experimental conditions irrespective of the presence or absence of the endothelium (see McPherson & Angus, 1991). The overall lack of effect of indomethacin is in support of the findings of Connor & Feniuk (1989) who showed that flurbiprofen, another inhibitor of cyclo-oxygenase, was similarly inactive in the dog isolated basilar artery. The reason for the apparent sensitivity of 2 out of 9 animals to indomethacin is presently unclear.

Having identified the primary mediator, we attempted to determine whether the depression of contractions to 5-HT was a consequence of a basal or a 5-HT-stimulated production of endothelium-derived nitric oxide. Several lines of circumstantial evidence suggest that the former is true. Firstly, L-NOARG (1–30 μM) evoked concentration-dependent contractions of endothelium-intact, but not endothelium-denuded basilar arterial rings, as has previously been described in bovine pulmonary artery (Gold *et al.*, 1990) and rabbit femoral artery (Mulsch & Busse, 1990). Such contractions were prevented by L-arginine but not by D-arginine, again implying the involvement of the nitric oxide/L-arginine pathway. It seems probable that the contractile response to L-NOARG reflects the inhibition of an on-going, basal release of nitric oxide from the endothelium which permits the contractile effects of an endogenously liberated mediator, or possibly the development of a spontaneous 'myogenic' tone. Such a basal release of nitric oxide might play an important role, under the experimental conditions, in maintaining the artery in a dilated state, and also serve generally to depress contractility to exogenous vasoconstrictor agents.

In support of this proposal is the fact that the augmentation of contractile responses by L-NOARG was not restricted to 5-HT; L-NOARG also augmented contractions to prostaglandin $F_{2\alpha}$, noradrenaline and endothelin-1. Our findings of differential modification of vasoconstrictor-evoked responses by L-NOARG parallel those of others that endothelium removal differentially modifies the response to various vasoconstrictor drugs (Martin *et al.*, 1986; Connor & Feniuk, 1989). In both rat aorta and dog basilar artery, removal of the endothelium markedly enhanced contractions to agonists of relatively low intrinsic activity, but had less effect on agonists with high intrinsic efficacy. In the present study contractions to prostaglandin $F_{2\alpha}$ and to noradrenaline were markedly enhanced by L-NOARG, whilst responses to endothelin-1 were little affected. We have discussed earlier the similarity between the effects of L-NOARG and endothelium removal on the 5-HT concentration-response curve. Taken together these data add weight to the argument that nitric oxide release underlies the general depressant effect of the endothelium.

Secondly, we could find no evidence that 5-HT stimulates the production of endothelium-derived nitric oxide *per se*. In endothelium-intact preparations precontracted with UTP, 5-HT did not evoke relaxation but rather caused further contraction. Under these experimental conditions acetylcholine still evoked relaxation, demonstrating that endothelium-dependent relaxation was possible. In several other isolated blood vessels 5-HT induces endothelium-dependent relaxation, via activation of 5-HT_1-like receptors that bear some similarities to the 5-HT_{1C} binding site (see Mylecharane, 1990 for review). These observations, however, do not disprove that 5-HT does not release EDRF in the rabbit basilar artery; it is possible that any relaxant action was simply masked by the accompanying contractile response. We could have attempted to discriminate between the contractile and possible relaxant effects of 5-HT using selective agonists and antagonists for 5-HT receptor subtypes. Connor & Feniuk (1989) adopted this approach in dog basilar arteries and even after abolition of the contractile component, could demonstrate no inhibitory effects of 5-HT, or of selective 5-HT receptor agonists. Indeed, similar studies have recently been performed in rabbit isolated basilar arteries and only a small endothelium-dependent, indomethacin-sensitive contraction to 5-HT and related 5-HT receptor agonists in partially contracted vessels was apparent (Seager *et al.*, 1992).

Finally, NEM (1 μM), a sulphydryl alkylating agent, failed to increase resting tone or to augment the contractile responses to 5-HT in rabbit basilar arteries with a functionally intact endothelium. This is consistent with the hypothesis that 5-HT does not release EDRF directly, since, in cultured vascular endothelial cells, NEM inhibits agonist-stimulated but not basally released EDRF (Siegle *et al.*, 1991). In the present study we used lower concentrations of NEM (1 μM) than Siegle and coworkers since at higher concentrations NEM (10–30 μM) abolished the contractile response to 5-HT, and to subsequently administered KCl (data not shown). The reason for this remains unclear, but possibly reflects a nonspecific effect of alkylation of cell sulphydryl moieties by NEM.

In summary, the strength of evidence suggests that the endothelial cell layer of rabbit basilar artery supresses contractions of the underlying smooth muscle to 5-HT, and probably other vasoconstrictors, by spontaneously liberating nitric oxide formed from L-arginine. Inhibitors of nitric oxide synthesis (e.g. L-NOARG, haemoglobin) may sensitize the cerebrovasculature to the actions of circulating or locally released vasoconstrictor agents.

We would like to thank Mr M. Miller for expert technical assistance and Mrs C. Ironmonger for help in preparation of the manuscript. D.J.T. is in receipt of a Glaxo Group Research Scholarship.

References

AMEZCUA, J.L., PALMER, R.M.J., DE SOUZA, B.M. & MONCADA, S. (1989). Nitric oxide synthesised from L-arginine regulates vascular tone in the coronary circulation of the rabbit. *Br. J. Pharmacol.*, **97**, 1119–1124.

BRAYDEN, J.E. (1990). Membrane hyperpolarisation is a mechanism of endothelium-dependent cerebral vasodilation. *Am. J. Physiol.*, **259**, H668–H673.

CAIN, C.R. & NICHOLSON, C.D. (1989). Comparison of the effects of cromakalim, a potassium conductance enhancer, and nimodipine, a calcium antagonist, on 5-hydroxytryptamine responses in a variety of vascular smooth muscle preparations. *Naunyn-Schmiedebergs Arch. Pharmacol.*, **340**, 293–299.

CHEN, G. & SUZUKI, H. (1989). Some electrical properties of the endothelium-dependent hyperpolarisation recorded from rat arterial smooth muscle cells. *J. Physiol.*, **410**, 91–106.

CONNOR, H.E. & FENIUK, W. (1989). Influence of the endothelium on contractile effects of 5-hydroxytryptamine and selective 5-HT agonists in canine basilar artery. *Br. J. Pharmacol.*, **96**, 170–178.

GARLAND, C.J. (1987). The role of membrane depolarisation in the contractile response of the rabbit basilar artery to 5-hydroxytryptamine. *J. Physiol.*, **392**, 333–348.

GOLD, M.E., FUKOTO, J.M. & IGNARRO, L.J. (1990). Structural analogs of L-arginine cause endothelium-dependent and endothelium-independent, nitric oxide-mediated cyclic GMP formation and vasodilation, and cause vasoconstriction associated with decreased cyclic GMP formation. *Eur. J. Pharmacol.*, **183**, 1610–1611.

MARTIN, W., FURCHGOTT, R.F., VILLANI, G.M. & JOTHIANANDAN, D. (1986). Depression of contractile responses in rat aorta by spontaneously released endothelium-derived relaxing factor. *J. Pharmacol. Exp. Ther.*, **237**, 529–538.

MCPHERSON, G.A. & ANGUS, J.A. (1991). Evidence that acetylcholine-mediated hyperpolarisation of the rat small mesenteric artery does not involve the K^+-channel opened by cromakalim. *Br. J. Pharmacol.*, **103**, 1184–1190.

MOORE, P.K., AL-SWAYEH, O.A., CHONG, N.W.S., EVANS, R.A. & GIBSON, A. (1990). L-N^G-nitro arginine (L-NOARG), a novel L-arginine-reversible inhibitor of endothelium-dependent vasodilatation *in vitro*. *Br. J. Pharmacol.*, **99**, 408–412.

MULSCH, A. & BUSSE, R. (1990). N^G-nitro-L-arginine (N^5-[imino-(nitroamino)methyl]-L-ornithine) impairs endothelium-dependent dilations by inhibiting cytosolic nitric oxide synthesis from L-arginine. *Naunyn-Schmiedebergs Arch. Pharmacol.*, **341**, 143–147.

MYLECHARANE, E.J. (1990). Mechanisms involved in serotonin-induced vasodilatation. *Blood Vessels*, **27**, 116–126.

PALMER, R.M.J., ASHTON, D.S. & MONCADA, S. (1988a). Vascular endothelial cells synthesise nitric oxide from L-arginine. *Nature*, **333**, 664–666.

PALMER, R.M.J., FERRIGE, A.G. & MONCADA, S. (1987). Nitric oxide release accounts for the biological activity of endothelium-derived relaxing factor. *Nature*, **327**, 524–526.

PALMER, R.M.J., REES, D.D., ASHTON, D.S. & MONCADA, S. (1988b). L-arginine is the physiological precursor for the formation of nitric oxide in endothelium-dependent relaxation. *Biochem. Biophys. Res. Commun.*, **153**, 1251–1256.

PARSONS, A.A., SCHILLING, L. & WAHL, M. (1991). Analysis of the acetylcholine-induced relaxation of rabbit isolated middle cerebral artery – effects of inhibitors of nitric oxide synthesis, Na,K-ATPase, and ATP-sensitive K^+-channels. *J. Cereb. Blood Flow Metab.*, **11**, 700–704.

PARSONS, A.A. & WHALLEY, E.T. (1989). Evidence for the presence of 5-HT_1-like receptors in rabbit isolated basilar arteries. *Eur. J. Pharmacol.*, **174**, 189–196.

SEAGER, J.M., CLARK, A.H. & GARLAND, C.J. (1991). Endothelium-dependent contractile response to 5-hydroxytryptamine in the rabbit basilar artery. *Br. J. Pharmacol.*, **105**, 424–428.

SIEGLE, I., HECKER, M., SESSA, W.C. & VANE, J.R. (1991). Sulfhydryl reagents inhibit stimulated but not basal EDRF release from cultured endothelial cells. *Br. J. Pharmacol.*, **102**, 119P.

TAYLOR, S.G. & WESTON, A.H. (1988). Endothelium-derived hyperpolarising factor: a new endogenous inhibitor from the vascular endothelium. *Trends Pharmacol. Sci.*, **9**, 272–274.

TREZISE, D.J. & WESTON, A.H. (1991). EDRF release accounts for the depressant effect of the endothelium on contractions of rabbit isolated basilar artery to 5-HT. *Br. J. Pharmacol.*, **104**, 12P.

TREZISE, D.J. & WESTON, A.H. (1992b). Comparison of the relaxant and hyperpolarising actions of calcitonin gene-related peptide (CGRP) and BRL38227 in rabbit isolated basilar artery; studies using glibenclamide. *Br. J. Pharmacol.*, **105**, 75P.

(Received November 21, 1991
Revised March 3, 1992
Accepted March 10, 1992)

Br. J. Pharmacol. (1992), **106**, 593–602

Calcium-activated currents in cultured neurones from rat dorsal root ganglia

[1]Kevin P.M. Currie & Roderick H. Scott

Department of Physiology, St. George's Hospital Medical School, London SW17 0RE

1 Voltage-activated Ca^{2+} currents and caffeine (1 to 10 mM) were used to increase intracellular Ca^{2+} in rat cultured dorsal root ganglia (DRG) neurones. Elevation of intracellular Ca^{2+} resulted in activation of inward currents which were attenuated by increasing the Ca^{2+} buffering capacity of cells by raising the concentration of EGTA in the patch solution to 10 mM. Low and high voltage-activated Ca^{2+} currents gave rise to Cl^- tail currents in cells loaded with CsCl patch solution. Outward Ca^{2+} channel currents activated at very depolarized potentials (V_c + 60 mV to +100 mV) also activated Cl^- tail currents, which were enhanced when extracellular Ca^{2+} was elevated from 2 mM to 4 mM.

2 The Ca^{2+}-activated Cl^- tail currents were identified by estimation of tail current reversal potential by use of a double pulse protocol and by sensitivity to the Cl^- channel blocker 5-nitro 2-(3-phenylpropylamino) benzoic acid (NPPB) applied at a concentration of 10 μM.

3 Cells loaded with Cs acetate patch solution and bathed in medium containing 4 mM Ca^{2+} also had prolonged Ca^{2+}-dependent tail currents, however these smaller tail currents were insensitive to NPPB. Release of Ca^{2+} from intracellular stores by caffeine gave rise to sustained inward currents in cells loaded with Cs acetate. Both Ca^{2+}-activated tail currents and caffeine-induced inward currents recorded from cells loaded with Cs acetate were attenuated by Tris based recording media, and had reversal potentials positive to 0 mV suggesting activity of Ca^{2+}-activated cation channels.

4 Our data may reflect (a) different degrees of association between Ca^{2+}-activated channels with voltage-gated Ca^{2+} channels, (b) distinct relationships between channels and intracellular Ca^{2+} stores and Ca^{2+} homeostatic mechanisms, (c) regulation of Ca^{2+}-activated channels by second messengers, and (d) varying channel sensitivity to Ca^{2+}, in the cell body of DRG neurones.

Keywords: Chloride currents; cation currents; caffeine; voltage-activated calcium currents

Introduction

Ca^{2+}-activated Cl^- currents ($I_{Cl(Ca)}$) have been recorded from a number of cell types including a variety of different neuronal preparations. In cells loaded with Cl^-, $I_{Cl(Ca)}$ can be observed as slowly decaying inward tail currents following activation of Ca^{2+} currents (I_{Ca}) by step depolarization. These Cl^- tail currents have been recorded in cultured spinal neurones of the mouse (Owen *et al.*, 1984), cultured dorsal root ganglion (DRG) neurones of the rat (Mayer, 1985; Scott *et al.*, 1988), quail cultured sensory and parasympathetic neurones (Bader *et al.*, 1987) and rabbit pelvic parasympathetic ganglia neurones (Akasu *et al.*, 1990), amongst other cells.

In addition to being activated by Ca^{2+} entry, $I_{Cl(Ca)}$ can be activated in *xenopus* oocytes (Barish, 1983), exocrine gland cells (Evans & Marty, 1986), hepatocytes (Ogden *et al.*, 1990) and ear artery cells (Amédée *et al.*, 1990) by liberation of Ca^{2+} from intracellular stores. Both Ca^{2+}-induced Ca^{2+} release (Barish, 1983; Miledi & Parker, 1984) and inositol (1,4,5) trisphosphate-induced Ca^{2+} release (Evans & Marty, 1986; Dascal *et al.*, 1986; Nomura *et al.*, 1987; Oosawa & Yamagishi, 1989; Ogden *et al.*, 1990) can give rise to activation of $I_{Cl(Ca)}$. In DRG neurones Ba^{2+}-induced Cl^- tail currents were found to depend on Ba^{2+}-induced Ca^{2+} release from caffeine-sensitive stores (Scott *et al.*, 1988). Furthermore in GH_3 pituitary cells (Rogawski *et al.*, 1988) and DRG neurones (Scott *et al.*, 1988) intracellular guanosine 5'-0(3-thio) triphosphate (GTP-γ-S) promotes $I_{Cl(Ca)}$ suggesting roles for both intracellular Ca^{2+} stores and second messengers in the regulation of neuronal $I_{Cl(Ca)}$. It remains to be determined if GTP-γ-S has its effect by direct action on the Ca^{2+}-activated Cl^- channels, an indirect action involving release of Ca^{2+} from stores, or by attenuating Ca^{2+} homeostatic mechanisms.

In addition to $I_{Cl(Ca)}$, other Ca^{2+}-activated conductances have been identified including Ca^{2+}-activated K^+ conductances (Blatz & Magleby, 1987) and Ca^{2+}-activated non-selective cation currents (I_{CAN}) (Partridge & Swandulla, 1988). In this study to simplify the situation we have inhibited Ca^{2+}-activated K^+ currents and other K^+ currents by using Cs^+ based patch solution and including tetraethylammonium (TEA) in the extracellular recording medium. I_{CAN} has been studied in molluscan neurones where it is involved in the depolarizing phase of bursting pace-maker activity. In DRG neurones, Ca^{2+}-activated non-selective cation channels have been identified. These cation channels have a unitary conductance of around 20 pS and are permeant to Na^+, K^+, Cs^+ and TEA (Simonneau *et al.*, 1987). In this study we have compared $I_{Cl(Ca)}$ and I_{CAN} activated in DRG cell bodies by both Ca^{2+} entry through voltage-activated channels and caffeine-induced release of Ca^{2+} from intracellular stores.

Methods

One or 2 day-old rats were killed by decapitation, the dorsal root ganglia were dissected out and the neurones dissociated and plated on polyornithine-laminin coated cover slips. The DRG neurones were maintained in culture at 37°C in humidified air containing 5% CO_2 for between 2 days and 3 weeks before being studied. For some experiments cells which had been in culture for up to 1 week were replated. This involved the removal of DRG neurones from the coverslips by careful washing with culture medium and then replating on other polyornithine coated coverslips (Dolphin & Menon-Johanssen, personal communication). The replated cells

[1] Author for correspondence.

attached to the substrate and recordings were made from 2 to 4 h later. The freshly replated cells have the advantage that they have no processes extending from the cell body which can present space clamp problems. Furthermore replated cells offer another approach to isolating currents generated solely and unequivocally in the cell body.

The whole-cell recording variant of the patch clamp technique (Hamill *et al.*, 1981) was used to examine voltage-activated and Ca^{2+}-activated currents. Experiments were carried out at room temperature (~23°C) and inward Ca^{2+} currents were evoked at a frequency of 0.03 Hz. Low resistance patch pipettes (3–7 MΩ) were used, and cells were voltage-clamped with an Axoclamp-2A switching amplifier, operated at a sampling rate of 25–35 kHz. The recording medium contained (mM): choline chloride 130, KCl 3.0, $MgCl_2$ 0.6, $NaHCO_3$ 1.0, HEPES 10, glucose 4.0, tetraethylammonium bromide (TEA) 25, tetrodotoxin (TTX, Sigma) 0.0025 and $CaCl_2$ 2.0 or 4.0. The pH and osmolarity were adjusted to 7.4 and 320 mOsm with NaOH and sucrose respectively. Patch electrodes were filled with a solution containing (mM): either CsCl or Cs acetate 140, $MgCl_2$ 2.0, ATP-Na 2.0, HEPES 10, $CaCl_2$ 0.1 and EGTA 0.1, 1.1 or 10. The pH was adjusted to 7.2 with Tris and osmolarity to 310 mOsm with sucrose. The pCa of these patch solutions were calculated by use of a computer programme supplied by Dr A. Hughes, the values were 1.32×10^{-6} M, 1.6×10^{-8} M and 1.6×10^{-9} M for the solutions containing 0.1 mM, 1.1 mM and 10 mM EGTA respectively. To study the cation current some experiments were carried out with a Tris-based recording medium which contained in (mM): Tris-Cl 145, $CaCl_2$ 4.0, $MgCl_2$ 0.6, glucose 5.0, HEPES 10.0, TTX 0.0025 and Tris/sucrose based recording medium which contained in (mM): Tris-Cl 72.5, sucrose 154, $CaCl_2$ 4.0, $MgCl_2$ 0.3, glucose 2.5, HEPES 5.0 and TTX 0.0025. The pH of these solutions was adjusted to 7.4 with HCl. Drugs (caffeine, Sigma; dimethylsulphoxide (DMSO), Sigma; and 5-nitro 2-(3-phenylpropylamino) benzoic acid (NPPB) SmithKline and French), were applied by low-pressure ejection (~7 kPa) from micropipettes (tip diameter of about 10 μm) placed about 100 μm from the cell. The Cl^- channel blocker NPPB (Wangemann *et al.*, 1986) was dissolved in DMSO to give a 100 mM stock solution. The NPPB stock solution was diluted in recording medium to give a test solution containing 10 μM NPPB and 0.01% (or 1.41 mM) DMSO. Although 0.01% DMSO had no significant action on the peak voltage-activated Ca^{2+} current, 0.1% DMSO produced a varied but significant increase of 19 ± 6% ($n = 7$). The DMSO effect on Ca^{2+} currents did not readily reverse over 10 min and subsequent decline in current may reflect rundown rather than recovery. Preliminary experiments with KCl rather than CsCl based patch solution revealed that 0.1% DMSO inhibited outward TEA-insensitive K^+ current, suggesting that at least in part, DMSO enhancement of Ca^{2+} currents involves a reduction in residual K^+ conductance. These findings led us to limit the concentration of NPPB used in this study to 10 μM.

Electrophysiological data were stored on a digital audio tape recorder (Biologic) and analysis was performed with a Tandon personal computer and Cambridge Electronic Design (CED) voltage clamp software, or a PDP 11/23 computer. All Ca^{2+} channel current data are shown following subtraction of scaled linear leakage and capacitance currents (unless stated otherwise), and all data are given as mean ± standard error of the mean (s.e.mean). The significance of the difference in data observed in this study was determined by paired or independent Student's t test, where appropriate.

Results

$I_{Cl(Ca)}$ tail currents

Prolonged tail currents activated by Ca^{2+} entry through voltage-activated Ca^{2+} channels were not observed in all cultured sensory neurones studied. As previously reported (Mayer, 1985; Scott *et al.*, 1988; Schlichter *et al.*, 1989) only a percentage of cells expressed prolonged tail currents. The expression of tail currents was not only dependent on the type of DRG neurones, but also the stage of cell development (Bernheim *et al.*, 1989). In this study we found that the time spent in culture altered the percentage of cells expressing tail currents with a chloride component following high voltage-activated Ca^{2+} currents: 50% (30 out of 60 cells) of rat DRG neurones loaded with CsCl patch solution and maintained in culture for up to 1 week had Ca^{2+}-activated tail currents. The percentage of cells expressing Ca^{2+}-activated tail currents increased to 64% (54 out of 84 cells) when recordings were made from cells in culture for between 1 and 2 weeks.

In some cells low threshold T-type Ca^{2+} currents activated from a holding potential (V_h) of −90 mV by step depolarization to a clamp potential (V_c) of −30 mV supported prolonged tail currents (Scott *et al.*, 1992). The mean T-type current amplitudes were −0.30 ± 0.1 nA ($n = 4$) and −1.16 ± 0.49 ($n = 5$) for extracellular Ca^{2+} concentrations of 2 mM and 4 mM respectively. Inspite of the difference in Ca^{2+} current amplitude the mean amplitude of the tail currents measured 20 ms after the end of voltage step were not significantly different with values of −0.21 ± 0.07 nA ($n = 4$) and −0.29 ± 0.04 nA ($n = 5$) following elevation of extracellular Ca^{2+}. The tail currents activated by T-type I_{Ca} and recorded from cells bathed with recording medium containing 2 mM Ca^{2+} all deactivated with a single exponential decay, which had a mean time constant (τdeact) of 114 ± 13 ms ($n = 4$). In contrast the tail currents which followed the larger T-type currents (with 4 mM extracellular Ca^{2+}) had more complex deactivation kinetics with several exponentials, and decayed by 69% of maximum in 348 ± 185 ms ($n = 5$). However, even with 4 mM extracellular Ca^{2+} in 6 out of 11 cells T-type Ca^{2+} current did not support tail currents although high voltage-activated Ca^{2+} currents in the same cells were followed by prolonged tail currents.

Similar results were obtained studying high voltage-activated Ca^{2+} currents evoked at a V_c of 0 mV (Figure 1a,b). In 2 mM Ca^{2+}, the mean peak Ca^{2+} current and tail current were −1.13 ± 0.10 nA and −0.89 ± 0.13 nA ($n = 19$), and in higher Ca^{2+} (4 mM) the Ca^{2+} currents were significantly larger with a mean amplitide of −1.96 ± 0.21 nA ($P < 0.005$), but the tail current amplitude was not increased and had a mean value of −0.86 ± 0.12 nA ($n = 29$). In recording medium containing either 2 mM or 4 mM Ca^{2+} the tail currents following high voltage-activated Ca^{2+} currents deactivated with 2 or more expontentials the mean times to decay by 69% of maximum were 726 ± 247 ms ($n = 19$) and 1201 ± 317 ms ($n = 28$) respectively.

In contrast a different relationship between outward Ca^{2+} channel currents and tail currents was observed. Outward Ca^{2+} channel currents are carried by K^+ and Cs^+ leaving the cell through Ca^{2+} channels at very depolarized clamp potentials (Bean, 1989; Dolphin & Scott, 1990). Ca^{2+}-dependent tail curents were observed following outward Ca^{2+} channel currents (Figure 1a,b) suggesting that significant Ca^{2+} entry occurs even at a V_c of 100 mV, although the resultant current is masked by the dominant outward movement of monovalent cations (the equilibrium potential for Ca^{2+} was 149 mV and 158 mV for 2 mM and 4 mM extracellular Ca^{2+} respectively). In recording medium containing 2 mM or 4 mM Ca^{2+} the outward Ca^{2+} channel currents were not significantly different with values of +1.14 ± 0.16 nA ($n = 12$) and +1.35 ± 0.31 nA ($n = 24$). However, increasing extracellular Ca^{2+} concentration significantly enhanced tail current amplitude, without significantly changing the rate of tail current deactivation. With 2 mM and 4 mM external Ca^{2+}, the mean tail current amplitudes were −0.26 ± 0.07 nA ($n = 12$) and −0.50 ± 0.09 nA ($n = 24$; $P < 0.05$) and corresponding times to decay by 69% were 370 ± 195 ms ($n = 10$) and 305 ± 108 ms ($n = 23$).

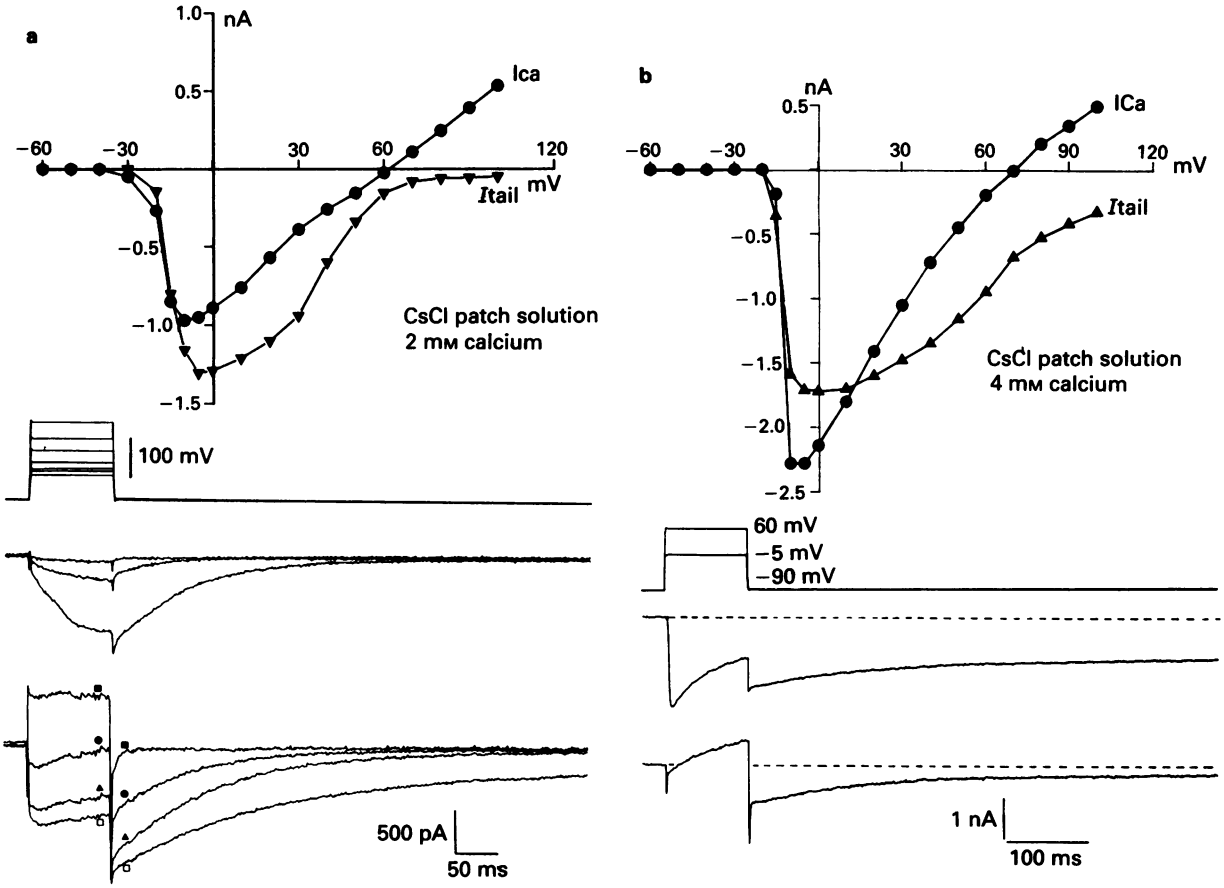

Figure 1 Current-voltage relationships for Ca^{2+} currents (I_{Ca}) and accompanying tail currents (I tail) in 2 cells loaded with CsCl based patch solution. Cells were held at a V_h of -90 mV and peak Ca^{2+} channel current (●) and tail current (▼, ▲) measured 20 ms after the end of the voltage step are plotted. (a) The current-voltage relationship for a cell bathed in medium containing 2 mM Ca^{2+}. Inset traces show voltage steps, Ca^{2+} currents and accompanying tail currents. The Ca^{2+} currents associated with each tail current are indicated by symbols (■ ● ▲ □). (b) Current-voltage relationship for a cell bathed in medium containing 4 mM Ca^{2+}. Below are traces of two voltage step commands and resultant Ca^{2+} currents and associated tail currents.

The tail currents recorded from cells loaded with CsCl patch solution were predominantly due to activation of $I_{Cl(Ca)}$. Two lines of evidence support this conclusion: firstly, double pulse experiments have revealed that the mean estimated reversal potential for the tail currents is the same as the chloride equilibrium potential (E_{Cl}). The double pulse experimental protocol involved primary test voltage step commands to activate Ca^{2+} and leak currents, these were followed by second steps to clamp potentials between -180 mV and -40 mV (Figure 2). The current-voltage relationship of the tail current was linear between V_c -180 mV and -40 mV, and could be extrapolated to give an estimation of the tail current reversal potential. Potentials positive to -40 mV activated Ca^{2+} currents and therefore could not be used to calculate reversal potentials. From 3 experiments the mean apparent reversal potential was -1 ± 6 mV, compared with E_{Cl} of -1 mV calculated using the Nernst equation. Because E_{Cl} under our conditions was close to the reversal potential for the non-selective cation current (see below) we shifted E_{Cl} to -32 mV, by combining CsCl and Cs acetate based patch solutions in a ratio of 1:3. Double pulse experiments showed that using this modified patch solution the apparent reversal potential of the tail current shifted to -14 ± 4 mV ($n = 4$). We limited our voltage steps to clamp potentials between -90 mV and -30 mV. Hyperpolarizing steps from a V_h of -90 mV gave currents which did not have a linear current-voltage relationship, possibly because at increasingly negative potentials, impermeant acetate ions block the Cl^- channels to a gradually greater extent. This may also be a factor which reduced the predicted shift in tail current reversal potential. The second approach to determining $I_{Cl(Ca)}$ involvement in the tail currents was to use the Cl^- channel blocker NPPB. Application of 10 μM NPPB did not significantly reduce the mean tail current amplitude measured 20 ms after the voltage step command. With 2 mM extracellular Ca^{2+} the mean control tail current amplitude was -0.75 ± 0.2 nA and in the presence of 10 μM NPPB the mean tail current amplitude was -0.57 ± 0.13 nA ($n = 13$). In spite of this result substantial reductions in tail current amplitude up to 54% were observed (Figure 3a) although 4 of 13 cells showed no change or an increase in tail current amplitude. These data suggest that a Cl^--independent component contributes to some tail currents, this component is a cation conductance (see below). However NPPB did significantly reduce the duration of the Cl^- tail currents. Two to 5 min applications of NPPB (10 μM) reduced the time for the tail currents to decay by 69% from 1769 ± 532 ms to 479 ± 133 ms ($n = 13$, $P < 0.03$). These results indicate that NPPB may act as a slow open channel blocker. In all 13 cells NPPB reduced the mean integrated tail current by 33 ± 12.5%. Analysis of the 9 cells which were sensitive to NPPB showed that the mean integrated tail current was reduced from 3.83 ± 1.84 nA.s to 0.82 ± 0.52 nA.s (nC) (mean ± s.e.mean). Although this is not statistically significant ($P = 0.13$) we feel that this reflects the problem of variation in the amplitude of the integrated tail currents (range 15.3–0.03 nA.s (nC)). However, the reduction of tail current is readily seen in the mean percentage reduction, which was 57 ± 10%. The actions of NPPB were partially reversible, 5 to 10 min after removal of the drug pipette. Additionally, $I_{Cl(Ca)}$ gives rise to

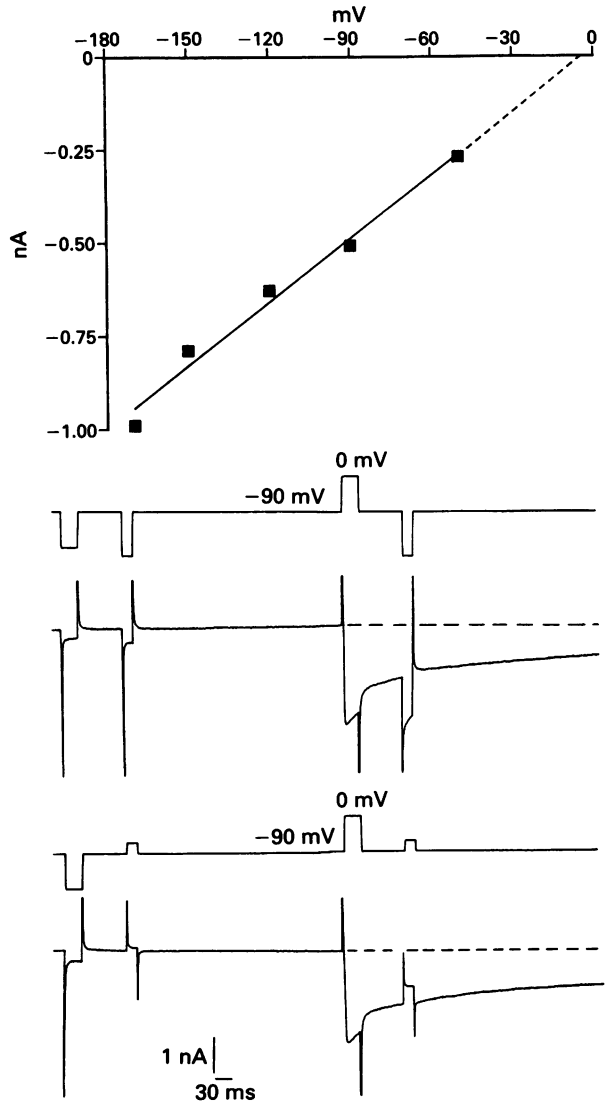

Figure 2 Current voltage relationship for the Ca^{2+}-activated tail current. The net tail current amplitudes are plotted against the voltage amplitude at steps applied during the initial decay of the tail current. This current-voltage relationship is linear (regression analysis $r = 0.991$), and has been extrapolated (dotted line) to show the estimated reversal potential of -3.6 mV for this cell. Below are traces showing the voltage protocols and current responses. Leak currents on the left were subtracted from I_{Ca} and currents activated on top of the tail current (right) to give net currents.

the after depolarization which follows a prolonged action potential (Dichter & Fischbach, 1977). The mean after depolarization was markedly reduced by 10 μM NPPB. The mean amplitude measured 20 ms after the end of the plateau Ca^{2+} component of the prolonged action potential was reduced from 22 ± 3 mV to 13 ± 3 mV ($n = 4$) and duration by about 77% (Figure 3b). The prolonged action potentials were not significantly altered by NPPB and had a mean duration of 861 ± 240 ms ($n = 5$). NPPB was not applied at concentrations greater than 10 μM because of effects on voltage-activated Ca^{2+} currents.

Caffeine-induced $I_{Cl(Ca)}$

Only in cells in which a Cl^- tail current was observed did caffeine produce a rapid transient $I_{Cl(Ca)}$ (Figure 4a,b). This caffeine activated $I_{Cl(Ca)}$ deactivated by 69% of maximum in 6.4 ± 2.7 s ($n = 8$). The caffeine (10 mM) induced $I_{Cl(Ca)}$ was activated with a delay of less than 30 s following the start of caffeine application. There was good correlation (0.94, using Pearson's product moment correlation (r) matrix) between tail and caffeine-induced peak current amplitudes, with mean values of -1.01 ± 0.13 nA and -0.84 ± 0.14 nA ($n = 8$) respectively. Repeated applications of caffeine gave progressively smaller but longer lasting currents, so the action of NPPB was studied in different cells from controls. It was not possible to refill caffeine-sensitive Ca^{2+} stores (Neering & McBurney, 1984) by repeatedly activating voltage-activated Ca^{2+} currents because the tail currents were enormously prolonged after application of caffeine in some cases lasting tens of seconds. Repeated activation of I_{Ca} therefore increased holding current and Ca^{2+} channel inactivation. When caffeine was applied in the presence of NPPB the mean amplitude of the transient $I_{Cl(Ca)}$ was attenuated by 60% to -0.34 ± 0.08 nA ($n = 9$, $P < 0.01$) (Figure 4b). Continuous application of NPPB to reduce the Cl^- tail current prior to simultaneous application of NPPB and caffeine ensured identification of $I_{Cl(Ca)}$. Furthermore the relatively slow activation of these transient caffeine responses which under control conditions had a mean time to peak of 2.4 ± 0.5 s, improved the efficiency of NPPB block of the Cl^- channels.

Ca^{2+}-activated cation tail currents

Ca^{2+}-activated tail currents were also observed when Cs acetate patch solution was used. These smaller tail currents were more easily observed when the extracellular Ca^{2+} concentration was increased to 4 mM. As with $I_{Cl(Ca)}$ these Cl^- independent tail currents were not seen in all cells, but were more prevalent in cells maintained in culture for more than 7 days. In the first week of being cultured 59% (30 out of 51) of cells had tails. In the second week in culture the proportion of cells with tail currents increased to 80% (82 out of 102) of cells. These tail currents were small and had a mean amplitude of -0.31 ± 0.03 nA ($n = 57$) measured 20 ms after the end of the 100 ms voltage step command, inspite of the large Ca^{2+} loads, as reflected by large Ca^{2+} currents. The current-voltage relationships for I_{Ca} revealed that the tail current was supported by I_{Ca}-activated over a wide voltage range (Figure 5). In several cases low voltage-activated T-type currents were followed by tail currents. The tail current deactivation was slow and variable and composed of two or more exponentials, the mean time taken for the current to decay by 69% of the maximum was 856 ± 104 ms ($n = 55$). Unlike $I_{Cl(Ca)}$ the tail currents recorded with Cs acetate patch solution were very sensitive to changes in Ca^{2+} current amplitude. Microperfusion of recording medium containing 2 mM rather than 4 mM Ca^{2+} resulted in a $27 \pm 5\%$ and $23 \pm 7\%$ reduction in I_{Ca} measured at the peak and end of the voltage step command respectively, but a larger $50 \pm 4\%$ ($n = 4$) reduction in tail current amplitude. The Cl^--independent tail currents were not due to acetate leaving the cell through Ca^{2+}-activated Cl^- channels because these currents were completely insensitive to 10 μM NPPB ($n = 6$), applied for 1 to 3 min or included in the bath solution (Figure 6a). Two lines of evidence point to this Ca^{2+}-activated tail current being a non-selective cation current (I_{CAN}). Firstly, double pulse experiments revealed that the tail current had an estimated (extrapolated from -40 mV) reversal potential of 14 ± 6 mV ($n = 6$). Secondly low pressure ejection of Tris/sucrose or Tris based recording media, which contained only very low levels of monovalent cations, attenuated these tail currents (Figure 6b). The mean tail current amplitudes measured 20 ms after the end of the voltage step command were reduced by $53 \pm 7\%$ ($n = 9$) and $37 \pm 5\%$ ($n = 9$) for Tris/sucrose and Tris based recording media respectively. The residual tail currents were not still present due to inefficient applications of the modified recording media, because small tail currents were also observed when Tris/sucrose (3 out of 7 cells) or Tris (6 out of 8 cells) recording media were bath applied. These data suggest that the tail currents are supported by cations including choline and that Tris does to

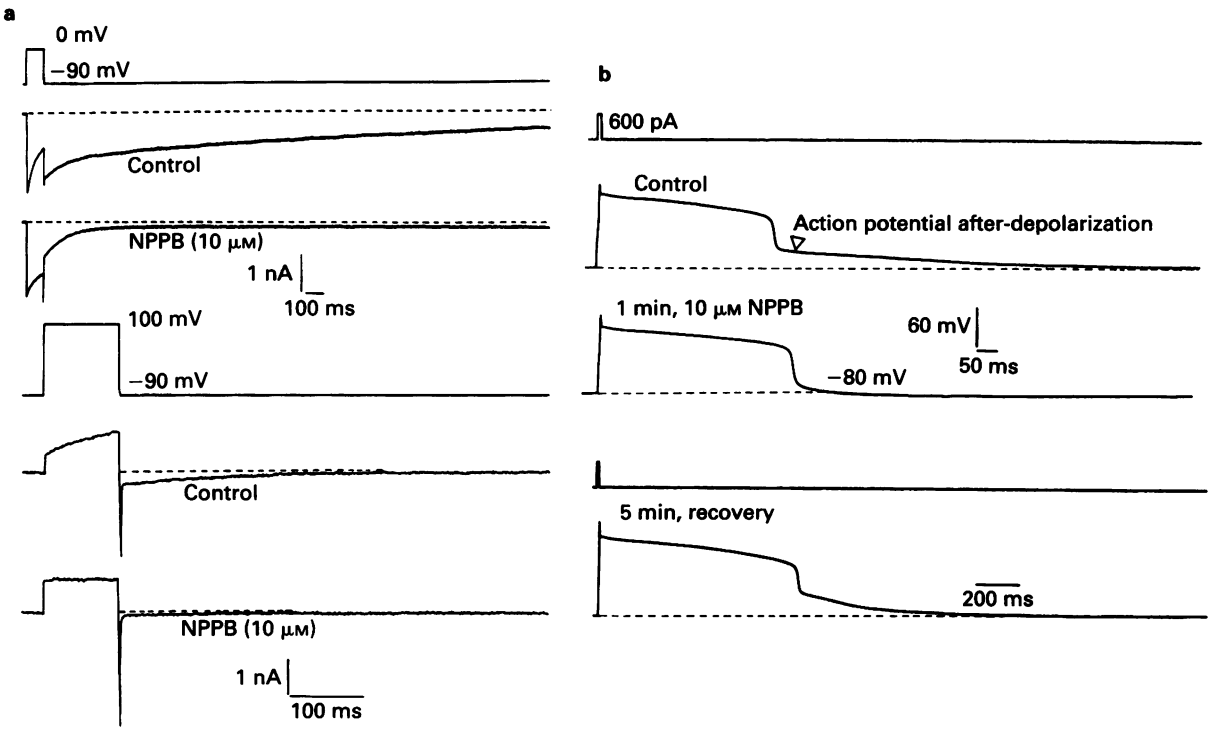

Figure 3 The Cl^- channel blocker 5-nitro-2-(3-phenylpropylamino) benzoic acid (NPPB) attenuated Ca^{2+} activated tail currents and action potential after depolarizations. (a) Shows $I_{Cl(Ca)}$, following inward and outward Ca^{2+} channel currents, inhibited by 3 min application of NPPB (10 μM). The cell was held at a V_h of −90 mV and Ca^{2+} channel currents activated at 0 mV and 100 mV. The change in outward current produced by NPPB may reflect inhibition of outward Cl^- current flowing during the voltage step to +100 mV. At this very depolarized potential there is a large driving force for Cl^- to enter the cell, through Ca^{2+}-activated Cl^- channels. (b) Prolonged action potentials evoked by 10 ms, 600 pA depolarizing current steps, had action potential after depolarizations in some cells loaded with CsCl patch solution. Cells were current clamped at −80 mV and action potentials activated at a constant frequency of 1 min^{-1}. Application of 10 μM NPPB for 1 min markedly inhibited the action potential after depolarization. Five minutes after removal of the pipette containing NPPB, partial recovery was observed, although in this cell the action potential was more prolonged, this was not significant (note the change in time scale).

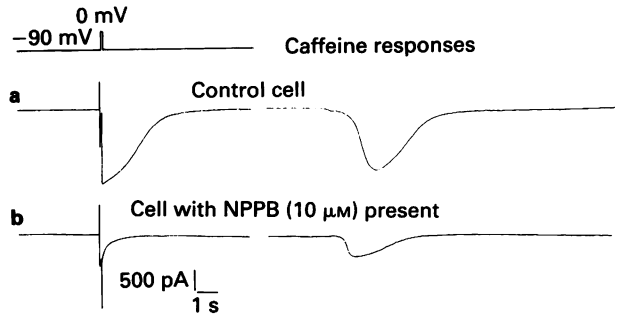

Figure 4 5-Nitro-2- (3-phenylpropylamino) benzoic acid (NPPB) inhibits $I_{Cl(Ca)}$ activated by I_{Ca} and caffeine induced release of Ca^{2+} from intracellular stores. (a) Traces from a control cell illustrating the $I_{Cl(Ca)}$ activated by I_{Ca} and 10 mM caffeine. (b) Traces from a cell bathed in 10 μM NPPB with $I_{Cl(Ca)}$ activated by I_{Ca} and 10 mM caffeine. Cells were held at a V_h of −90 mV. Note: leak subtraction has not been performed on these currents.

some degree pass through some of these channels. We found in some cells that application of Tris recording media shifted the voltage-dependence of I_{Ca} to the right and reduced the leak current, however the peak I_{Ca} amplitudes were similar to controls. The contribution of Ca^{2+} influx to I_{CAN} could not be studied using Ca^{2+} dependent tail currents, but was investigated using caffeine to release Ca^{2+} from intracellular stores and thus activate I_{CAN} (see below).

Caffeine-activated I_{CAN}

Application of 1 to 10 mM caffeine produced large inward currents when pipettes containing Cs acetate patch solution were used. The reversal potential of the caffeine evoked current was estimated from difference currents measured between −160 mV and −30 mV. Families of 30 ms voltage step commands were activated prior to application of caffeine and during the caffeine response (Figure 7a,b). The difference current, current-voltage relationship was linear and could be extrapolated to give an estimated reversal potential of +8.3 ± 1.8 mV ($n = 7$). Improving the Ca^{2+} buffering capacity of the cell by increasing the intracellular EGTA concentration from 1.1 mM to 10 mM markedly attenuated the caffeine-evoked current and delayed its onset (Figure 7c). This suggests that the caffeine-evoked currents were activated by Ca^{2+} release from intracellular caffeine-sensitive stores. In addition to the reversal potential, the action of Tris and Tris/sucrose recording media suggests that the caffeine evoked current was I_{CAN}. Tris/sucrose recording medium (Tris, 72.5 mM) reduced I_{CAN} to a greater extent than Tris recording medium (Tris, 145 mM). However Tris based recording with no added Ca^{2+} or Mg^{2+} did not attenuate I_{CAN} to any greater degree than Tris based recording medium with normal levels of Ca^{2+} and Mg^{2+}. These data suggest that Tris but not Ca^{2+} passes through some cation channels activated by Ca^{2+} released from stores by caffeine. Tris has previously been found to permeate through Ca^{2+}-activated non-selective cation channels in *Helix* neurones (Partridge & Swandulla, 1987).

The nature of caffeine-activated I_{CAN} was dependent on the intracellular anion. With Cs acetate patch solution the caffeine responses were very long lasting (Figure 7b). Sometimes transient responses were observed and these were subsequently dominated by the development of the sustained current. It was noted in some cells that considerable delay occurred (10 min) between applying caffeine (10 mM) and activation of transient currents greater than 100 pA when Cs

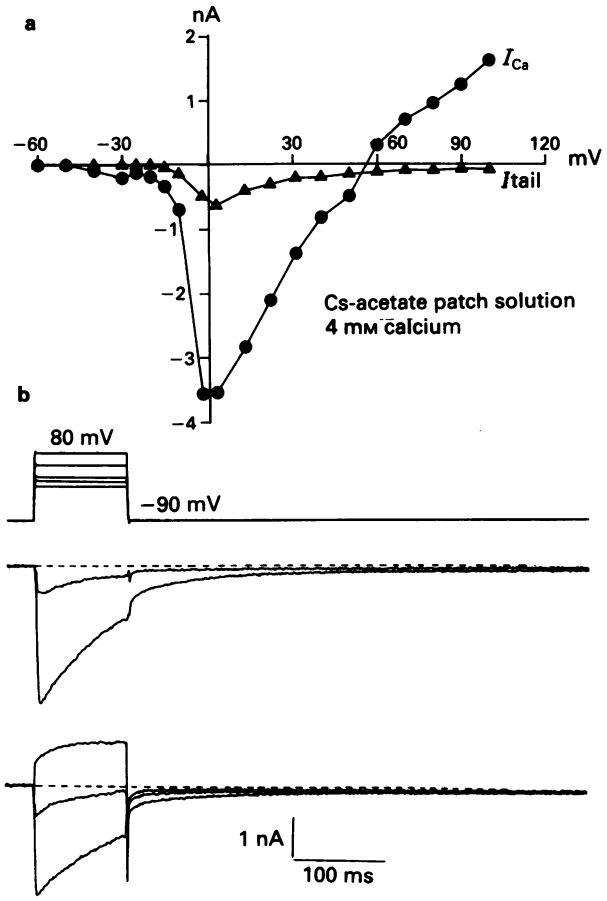

Figure 5 (a) Current-voltage relationship for I_{Ca} and accompanying tail currents activated in a cell loaded with Cs acetate patch solution and bathed in a recording medium containing 4 mM Ca^{2+}. The cell was held at a V_h of −90 mV and peak Ca^{2+} channel current (●) and tail current (▲) measured 20 ms after the end of the voltage step are plotted. (b) Traces of some of the voltage steps and resultant Ca^{2+}-channel currents and cation tail currents used to produce the current-voltage plot shown above (a).

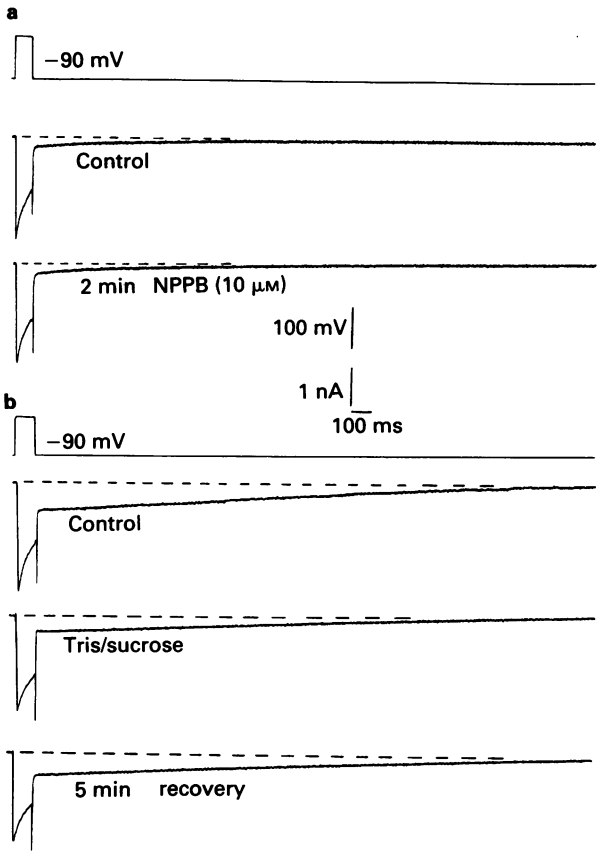

Figure 6 Action of 5-nitro-2-(3-phenylproylamino) benzoic acid (NPPB) and Tris/sucrose recording medium on tail currents recorded from cells loaded with Cs acetate patch solution. (a) Traces show that 2 min application of NPPB (10 μM) had no effect on I_{Ca} or tail current. (b) Replacement of choline chloride recording medium by microperfusion of Tris/sucrose recording medium attenuated the Ca^{2+}-activated tail current. Partial recovery was observed 5 min after removal of the pressure ejection pipette containing Tris/sucrose recording medium. Cells were held at a V_h of −90 mV and bathed in recording medium containing 4 mM Ca^{2+}.

acetate patch solution was used. In contrast when CsCl patch solution was used only transient oscillating inward cation currents were activated (Figure 7d), these currents were insensitive to the Cl^- channel blocker NPPB. Two minutes application of caffeine (10 mM) also reduced the peak I_{Ca} activated at a V_c of 0 mV by 26 ± 6% ($n = 4$) and increased inactivation, furthermore activating I_{Ca} greatly enhanced the subsequent inward I_{CAN} (Figure 7d). This is consistent with previous studies which have linked Ca^{2+} entry through voltage-activated channels and caffeine-sensitive Ca^{2+} stores with the control of intracellular Ca^{2+} transients (Lipscombe *et al.*, 1988). The oscillating I_{CAN} activated by Ca^{2+} released from intracellular stores were also attenuated by Tris recording medium (Figure 7e).

Freshly replated cells

Both $I_{Cl(Ca)}$ and I_{CAN} tail currents were observed in freshly replated DRG neurones which did not have processes. These observations support the contention that Ca^{2+}-activated Cl^- and cation channels are present in the cell body membrane, and that the tail currents are not primarily due to spread of current from neuronal processes. However, we cannot discount the possibility that in cells which have not been freshly plated, Ca^{2+}-activated channels could also be expressed on neurites.

Increasing the concentration of EGTA in the patch solution attentuated $I_{Cl(Ca)}$ *and* I_{CAN}

$I_{Cl(Ca)}$ and I_{CAN} activated either as tail currents following voltage-activated I_{Ca}, or by release of Ca^{2+} from caffeine sensitive intracellular stores, were attenuated by increasing the concentration of the Ca^{2+} chelator EGTA in the patch solution. I_{Ca} and accompanying tail currents were activated immediately (within 10 s) upon entering the whole cell recording configuration. These initial currents were compared with the currents activated 3 to 10 min later, which allowed time for the patch solution to equilibrate with the cell cytoplasm. Increasing intracellular EGTA to 10 mM in conjunction with actions of K^+ channel blockers resulted in marked enhancement of I_{Ca} but also significant reduction in both $I_{Cl(Ca)}$ and I_{CAN} tail currents (Table 1, Figure 8a,b). Both $I_{Cl(Ca)}$ ($n = 3$) and I_{CAN} ($n = 3$) activated following outward Ca^{2+} channel currents evoked by strong depolarizations were abolished within 5 min in cells containing patch solutions with 10 mM EGTA present. I_{CAN} activated by caffeine (1 to 10 mM) induced release of Ca^{2+} from stores was also attenuated by increasing intracellular EGTA. Both transient and sustained responses to caffeine were significantly attenuated by increasing the concentration of intracellular EGTA (Table 2, Figure 7c).

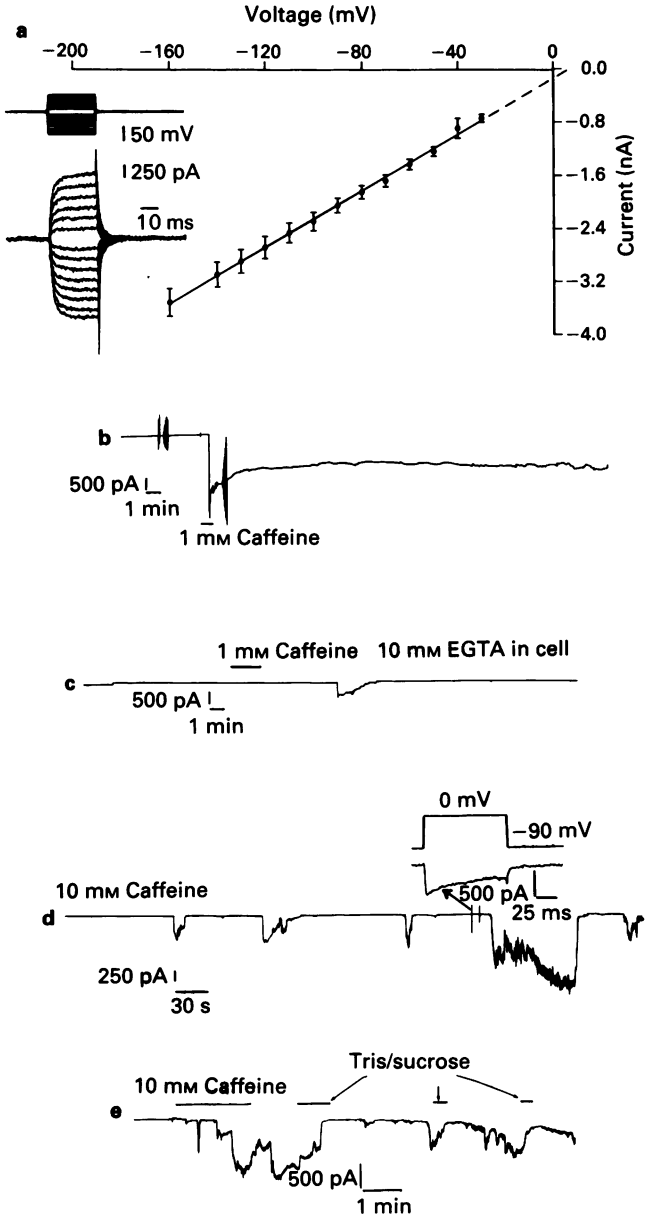

Figure 7 Sustained and oscillating caffeine responses recorded from cells loaded with Cs acetate or CsCl patch solutions respectively. All cells were held at a V_h of -90 mV. (a) Difference current I/V relationship for caffeine ($n = 7$). The linear relationship extrapolated (dotted line) to give an estimated reversal potential of $+8$ mV. The inset traces show a family of difference currents generated in the cell illustrated below (b). (b) A sustained response to 1 mM caffeine in a cell loaded with Cs acetate patch solution. A family of 30 ms voltage step commands were activated before application of caffeine and during the sustained response. The patch solution contained 1.1 mM EGTA. (c) The caffeine (1 mM) response was delayed and attenuated by increasing the EGTA (10 mM) concentration in the Cs acetate patch solution. (d) Trace from a cell recorded with a patch pipette containing CsCl patch solution, and bathed in choline chloride medium. Caffeine (10 mM) was applied for 1.5 min and there was a 1 min delay before the first inward oscillating current was generated. Activation of I_{Ca} (shown in the inset as a leak subtracted current on an expanded time base and marked with an arrow), after the third inward current, greatly enhanced the subsequent oscillation. (e) Trace from a cell recorded with a pipette containing CsCl patch solution and bathed in Tris based recording medium. The first fast transient current activated after the start of caffeine application is typical of $I_{Cl(Ca)}$. Oscillating inward currents were then observed and attenuated by microejection of Tris/sucrose recording medium, suggesting the involvement of I_{CAN}. Tris/sucrose only partially inhibits I_{CAN} and no further reduction was observed when Tris/sucrose medium was bath applied. These findings are consistent with those for the I_{CAN} tail currents.

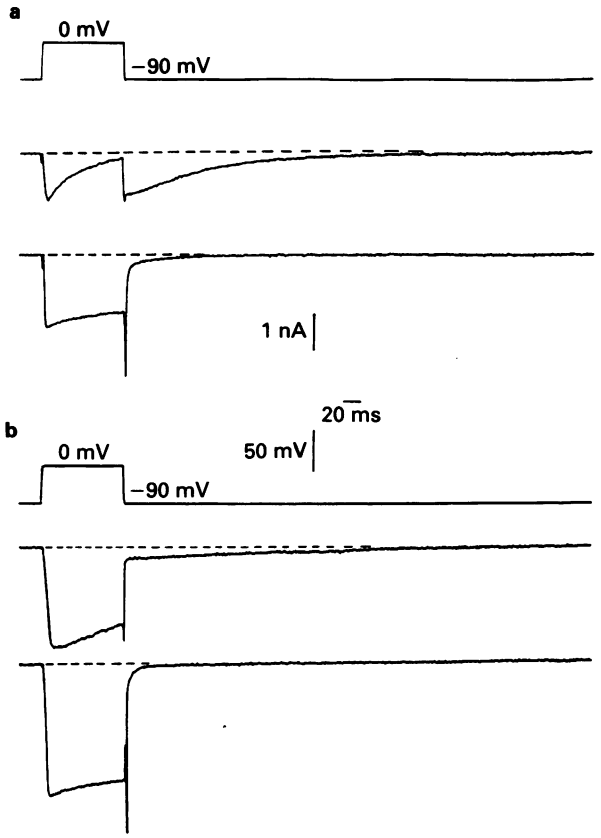

Figure 8 Intracellular EGTA (10 mM) attentuated $I_{Cl(Ca)}$ and I_{CAN} tail currents. (a) Cell recorded with a pipette containing CsCl patch solution. Initial I_{Ca} and $I_{Cl(Ca)}$ recorded within 10 s of entering the whole cell configuration and currents activated after 5 min are illustrated. (b) Cell recorded with a pipette containing Cs acetate patch solution. Initial I_{Ca} and I_{CAN} and currents activated 5 min later are shown. Note that in both cells I_{Ca} increases after 5 min recording but the tail currents are reduced.

The effect of replacing extracellular Ca^{2+} with Ba^{2+} on $I_{Cl(Ca)}$ and I_{CAN}

We observed that replacing extracellular Ca^{2+} with Ba^{2+} by low pressure ejection reversibly abolished Cl^- and cation tail currents following both inward and outward voltage-activated Ca^{2+} channel currents in 4 out of 5 cells and 3 out of 4 cells respectively. Ba^{2+} does not directly activate Ca^{2+}-activated Cl^- currents and cells bathed with recording medium containing Ba^{2+} do not have I_{CAN} tail currents following I_{Ba}. However Cl^- tail currents have previously been observed in cells bathed in recording medium containing Ba^{2+}, but this activation of $I_{Cl(Ca)}$ involves release of Ca^{2+} from a caffeine sensitive intracellular store (Scott *et al.*, 1988). It appears that different results are obtained studying Cl^- tail currents when Ca^{2+} is replaced by Ba^{2+} compared with when Ba^{2+} is replaced by Ca^{2+} (Mayer, 1985; Scott *et al.*, 1988; Akasu *et al.*, 1990). This may reflect sensitization of the Ca^{2+}-induced Ca^{2+} release store, with prolonged exposure to different extracellular divalent cations.

Discussion

In this study we have shown that an increase in intracellular Ca^{2+} can activate Cl^- currents and Cl^--independent non-selective cation currents. The Cl^- channel blocker NPPB (Wangemann *et al.*, 1986) inhibited $I_{Cl(Ca)}$ but did not reduce I_{CAN} activated by Ca^{2+} entering through voltage-gated channels or by release from a caffeine-sensitive store. The insen-

Table 1 Actions of intracellular EGTA (10 mM) on I_{Ca} and $I_{Cl(Ca)}$, I_{CAN} tail currents

Current	*Patch solution*	*Current amplitude* (nA)	
		Initial	3 to 10 min
Peak I_{Ca}	CsCl	-1.66 ± 0.19	-2.33 ± 0.41 $(n = 7)$*
End I_{Ca}	CsCl	-0.77 ± 0.23	-1.67 ± 0.32 $(n = 7)$**
$I_{Cl(Ca)}$	CsCl	-0.62 ± 0.15	-0.22 ± 0.05 $(n = 4)$*
Peak I_{Ca}	Cs acetate	-2.06 ± 0.23	-3.05 ± 0.31 $(n = 6)$*
End I_{Ca}	Cs acetate	-0.86 ± 0.38	-2.29 ± 0.5 $(n = 6)$†
I_{CAN}	Cs acetate	-0.24 ± 0.03	-0.10 ± 0.02 $(n = 6)$†

Peak and end I_{Ca} were the maximum I_{Ca} and the I_{Ca} measured at the end of a 100 ms voltage step command to a clamp potential of 0 mV respectively. Significance of the difference compared to initial current determined by Student's t test.
*$P < 0.05$; †$P < 0.01$; **$P < 0.005$.

Table 2 Actions of intracellular EGTA on caffeine-induced I_{CAN}

	0.1 mM EGTA	1.1 mM EGTA	10 mM EGTA
CsCl	-0.64 ± 0.13 $(n = 6)$	—	-0.23 ± 0.05 $(n = 10)$**
Cs acetate	—	-2.73 ± 0.35 $(n = 9)$	-0.67 ± 0.10 $(n = 9)$*

The CsCl data were calculated from the maximum transient I_{CAN} produced by caffeine in each cell. The significance of the difference was determined by Student's t test: *$P < 0.005$; **$P < 0.001$.

sitivity of I_{CAN} evoked by caffeine, indicates that NPPB did not effect Ca^{2+} release from intracellular stores and that its action was restricted to the Cl^- channel. $I_{Cl(Ca)}$ was particularly sensitive to entry of Ca^{2+} through voltage-activated Ca^{2+} channels. We found that Cl^- tail currents were supported by outward Ca^{2+} channel currents at very depolarized potentials, and as previously described in vascular smooth muscle cells (Pacaud *et al.*, 1989), this was more apparent when the extracellular Ca^{2+} concentration was increased. These findings suggest that $I_{Cl(Ca)}$ is a good physiological indicator of Ca^{2+} levels close to the cell membrane and reveals Ca^{2+} entry which had been masked by other conductances under very depolarized conditions. This Ca^{2+} entry did not arise from voltage-mediated reversal of the Na^+/Ca^{2+} exchanger which has a minor role on DRG cell bodies (Benham *et al.*, 1989) because choline chloride based recording medium was used in these experiments. Two other possibilities need to be considered: Cl^- tail currents activated following very strong depolarization ($V_c + 100$ mV), could be contaminated by a Ca^{2+} tail current, or a voltage-activated Cl^- current. However the Cl^- tail currents described here were not observed in all cells, were attenuated by NPPB, abolished by increasing the Ca^{2+} buffering capacity of the cell with EGTA, and were dependent on extracellular Ca^{2+} concentration. The combination of these results suggests that when a Cl^- tail current is identified following an inward Ca^{2+} current, $I_{Cl(Ca)}$ is also activated following outward Ca^{2+} channel currents evoked by stronger depolarizations. Raising the extracellular Ca^{2+} concentration (2 to 4 mM) increases the driving force for Ca^{2+} entry. As a result there is an increase in activation of $I_{Cl(Ca)}$ which follows outward Ca^{2+} channel currents. This does not occur at all potentials because following the maximum inward I_{Ca}, $I_{Cl(Ca)}$ is already fully activated in cells bathed in medium containing 2 mM Ca^{2+}. Ca^{2+} entry through T-type Ca^{2+} channels was also able in some cells to activate $I_{Cl(Ca)}$. However the T-type I_{Ca} only activated a modest $I_{Cl(Ca)}$, the total available population of Ca^{2+}-activated Cl^- channels were only fully activated by high voltage-activated Ca^{2+} currents, or release of Ca^{2+} from caffeine-sensitive intracellular stores. Doubling the extracellular Ca^{2+} concentration (2 mM to 4 mM) markedly increased the T-type I_{Ca} but did not increase the amplitude of $I_{Cl(Ca)}$, suggesting no recruitment of Cl^- channels to increase the peak current occured. However, increasing the T-type current did slow the deactivation of $I_{Cl(Ca)}$, with greater Ca^{2+} entry the deactivation of Cl^- tail currents no longer following a single exponential. This is similar to what is observed when the duration of high voltage-activated I_{Ca} is reduced, less Ca^{2+} entry results in Cl^- tail currents which decay with a single exponential (Mayer, 1985). Researchers in a previous study failed to show $I_{Cl(Ca)}$ activated by T-type I_{Ca} (Akasu *et al.*, 1990) and in some cells in this investigation similar results were obtained. Therefore not all Ca^{2+} channels are associated with functional Ca^{2+}-activated Cl^- channels, in cells which express $I_{Cl(Ca)}$. The relationship between Cl^- tail currents and inward low and high voltage-activated I_{Ca} data may be due to the close association between Ca^{2+} and Cl^- channels. If colocalization occurs between Ca^{2+} and Cl^- channels this may ensure rapid and complete activation of the Cl^- channels when the increases in intracellular Ca^{2+} are restricted to microscopic 'domains' round the Ca^{2+} channels (Chad & Eckert, 1984; Simon & Llinás, 1985). Ca^{2+}-activated Cl^- channels have also been shown in a number of preparations to be highly sensitive to changes in Ca^{2+} concentration (Evans & Marty, 1986; Taleb *et al.*, 1988).

The deactivation of $I_{Cl(Ca)}$ tail currents also provides information on how cells handle Ca^{2+} loads. The slowing and changes in kinetics of $I_{Cl(Ca)}$ deactivation resulting from increasing Ca^{2+} (Mayer, 1985), changing the extracellular divalent cation (Scott *et al.*, 1988), or reduced regulation of intracellular Ca^{2+} due to impaired metabolism (Duchen, 1990), have previously been described. In this study changes in $I_{Cl(Ca)}$ deactivation were found even when small tail currents were activated by T-type I_{Ca} of different amplitudes. However, interpretation of $I_{Cl(Ca)}$ deactivation has recently been made more complex by observations in *Xenopus* oocytes which suggest Ca^{2+}-dependent inactivation may possibly involve protein kinase C (Boton *et al.*, 1990). This form of $I_{Cl(Ca)}$ inactivation involves very large Ca^{2+} loads and awaits study in neurones.

The second type of tail current investigated, I_{CAN}, was small but long lasting and only easily studied following large Ca^{2+} currents. This may be because Ca^{2+}-activated non-selective cation channels are diffusely distributed on the DRG neurone cell bodies, and that DRG neurones efficiently buffer Ca^{2+} and restrict I_{CAN} activation. However, differences in channel sensitivity to Ca^{2+} and possibly regulation of Ca^{2+}-activated channels by second messengers may account for our observations.

Caffeine induced Ca^{2+} mobilization can activate a variety of Ca^{2+}-dependent conductances in neurones (Smith *et al.*, 1983; Neering & McBurney, 1984; Lipscombe *et al.*, 1988;

Akaike & Sadoshima, 1989), including $I_{Cl(Ca)}$ and I_{CAN}. In contrast to activation of I_{CAN} by voltage-activated I_{Ca}, caffeine-evoked currents were large suggesting more widespread elevation of Ca^{2+} round the cell membrane and so more efficient activation of the non-selective cation channels. Ca^{2+} imaging studies have shown that caffeine produces transient increases in intracellular Ca^{2+} throughout neuronal cell bodies (Lipscombe *et al.*, 1988; Hernadez-Cruz *et al.*, 1990). The time course of the single transient $I_{Cl(Ca)}$ activated by caffeine, was similar to the duration of Ca^{2+} transients (6 to 8 s) measured with Ca^{2+} dyes (Hernandez-Cruz *et al.*, 1990). The duration of I_{CAN} evoked by caffeine was in part determined by the intracellular anion, with transient oscillating currents being recorded with intracellular Cl^- and more sustained currents dominating when cells were loaded with Cs acetate. Transient rather than sustained Ca^{2+} responses have been more usually observed when Ca^{2+} sensitive dyes were used to study caffeine responses (Lipscombe *et al.*, 1988; Thayer *et al.*, 1988). However, different anions affect inositol triphosphate evoked Ca^{2+}-activated K^+ currents (Cloues & Robbins, 1991). A number of factors may contribute to the different anion effects, these include: (1) anions effecting the Ca^{2+} release process; (2) anions altering Ca^{2+} homeostatic mechanisms; (3) anions acting as Ca^{2+} buffers; (4) anions acting on the Ca^{2+} – activated non-selective cation channels, to alter their activity or responsiveness to Ca^{2+}.

In conclusion our data suggest that $I_{Cl(Ca)}$ is efficiently activated by I_{Ca} and that I_{CAN} is more dependent on Ca^{2+} release from intracellular stores which may give more wide spread elevation in Ca^{2+}. I_{CAN} can generate large currents in response to Ca^{2+} release from intracellular stores and in some cases cell swelling and damage may occur. This raises the possibility that I_{CAN} may play a role in Ca^{2+}-mediated cell injury. The physiological role of $I_{Cl(Ca)}$ remains to be determined in neurones but both voltage-activated I_{Ca} and Ca^{2+} release from stores may be involved.

We thank the Medical Research Council and the Nuffield Foundation for supporting our work. We also thank Dr A. Hughes for the computer programme for calculating free Ca^{2+} levels.

References

AKAIKE, N. & SADOSHIMA, J.-I. (1989). Caffeine affects four different ionic currents in the bull-frog sympathetic neurone. *J. Physiol.*, **412**, 221–244.

AKASU, T., NISHIMURA, T. & TOKIMASA, T. (1990). Calcium-dependent chloride current in neurones of the rabbit pelvic parasympathetic ganglia. *J. Physiol.*, **422**, 303–320.

AMÉDÉE, T., LARGE, W.A. & WANG, Q. (1990). Characteristics of chloride currents activated by noradrenaline in rabbit ear artery cells. *J. Physiol.*, **428**, 501–516.

BADER, C.R., BERTRAND, D. & SCHLICHTER, R. (1987). Calcium-activated chloride current in cultured sensory and parasympathetic quail neurones. *J. Physiol.*, **394**, 125–148.

BARISH, M.E. (1983). A transient calcium-dependent chloride current in the immature xenopus oocyte. *J. Physiol.*, **342**, 309–325.

BEAN, B.P. (1989). Neurotransmitter inhibition of neuronal calcium currents by changes in channel voltage dependence. *Nature*, **340**, 153–155.

BENHAM, C.D., EVANS, M.L. & MCBAIN, C.J. (1989). Inhibition of Ca-ATPase slows recovery from voltage-gated Ca_i load in cultured neurones from rat dorsal root ganglia. *J. Physiol.*, **415**, 21P.

BERNHEIM, L., BADER, C.R., BERTRAND, D. & SCHLICHTER, R. (1989). Transient expression of a Ca^{2+}-activated Cl^- current during development of quail sensory neurones. *Devel. Biol.*, **136**, 129–139.

BLATZ, A.L. & MAGLEBY, K.L. (1987). Calcium-activated potassium channels. *Trends Neurosci.*, **10**, 463–467.

BOTON, R., SINGER, D. & DASCAL, N. (1990). Inactivation of calcium-activated chloride conductance in *Xenopus* oocytes: roles of calcium and protein kinase C. *Pflügers Arch.*, **416**, 1–6.

CHAD, J.E. & ECKERT, R. (1984). Calcium domains associated with individual channels can account for anomalous voltage relations of Ca-dependent responses. *Biophys. J.*, **45**, 993–999.

CLOUES, R. & ROBBINS, J. (1991). Dependence of the inositol triphosphate evoked potassium current on anions in whole cell recordings from rodent neuroblastoma x glioma hybrid cells. *J. Physiol.*, **438**, 222P.

DASCAL, N., IFUNE, C., HOPKINS, R., SNUTCH, T.P., LUBBERT, H., DAVIDSON, N., SIMON, M.I. & LESTER, H.A. (1986). Involvement of a GTP-binding protein in mediation of serotonin and acetylcholine responses in *Xenopus* ococytes injected with rat brain messenger RNA. *Mol. Brain Res.*, **1**, 201–209.

DICHTER, M.A. & FISCHBACH, G.D. (1977). The action potential of chick dorsal root ganglion neurones maintained in culture. *J. Physiol.*, **267**, 281–298.

DOLPHIN, A.C. & SCOTT, R.H. (1990). Activation of calcium channel currents in rat sensory neurones by large depolarizations: effect of guanine nucleotides and (−)-baclofen. *Eur. J. Neurosci.*, **2**, 104–108.

DUCHEN, M.R. (1990). Effects of metabolic inhibition on the membrane properties of isolated mouse primary sensory neurones. *J. Physiol.*, **424**, 387–409.

EVANS, M.G. & MARTY, A. (1986). Potentiation of muscarinic and α-adrenergic responses by an analogue of guanosine 5′-triphosphate. *Proc. Natl. Acad. Sci. U.S.A.*, **83**, 4099–4103.

HAMILL, O.P., MARTY, A., NEHER, E., SAKMANN, B. & SIGWORTH, F.J. (1981). Improved patch-clamp techniques for high-resolution current recording from cells and cell-free membrane patches. *Pflügers Arch.*, **391**, 85–100.

HERNANDEZ-CRUZ, A., SALA, F. & ADAMS, P.R. (1990). Subcellular calcium transients visualized by confocal microscopy in a voltage-clamped vertebrate neurone. *Science*, **247**, 858–862.

LIPSCOMBE, D., MADISON, D.V., POENIE, M., REUTER, H., TSIEN, R.W. & TSIEN, R.Y. (1988). Imaging of cytosolic Ca^{2+} transients arising from Ca^{2+} stores and Ca^{2+} channels in sympathetic neurones. *Neuron*, **1**, 355–365.

MAYER, M.L. (1985). A calcium-activated chloride current generates the after-depolarization of rat sensory neurones in culture. *J. Physiol.*, **364**, 217–239.

MILEDI, R. & PARKER, I. (1984). Chloride current induced by injection of calcium into *Xenopus* oocytes. *J. Physiol.*, **357**, 173–183.

NEERING, I.R. & MCBURNEY, R.N. (1984). Role of microsomal Ca storage in mammalian neurones? *Nature*, **309**, 158–160.

NOMURA, Y., KANEKO, S., KATO, K.-I., YAMAGISHI, S.-I. & SUGIYAMA, H. (1987). Inositol phosphate formation and chloride current responses induced by acetylcholine and serotonin through GTP-binding proteins in *Xenopus* oocyte after injection of rat brain messenger RNA. *Mol. Brain Res.*, **2**, 113–123.

OGDEN, D.C., CAPIOD, T., WALKER, J.W. & TRENTHAM, D.R. (1990). Kinetics of the conductance evoked by noradrenaline, inositol triphosphate or Ca^{2+} in guinea-pig isolated hepatocytes. *J. Physiol.*, **422**, 585–602.

OOSAWA, Y. & YAMAGISHI, S. (1989). Rat brain glutamate receptors activate chloride channels in *Xenopus* oocytes coupled by inositol triphosphate and Ca^{2+}. *J. Physiol.*, **408**, 223–232.

OWEN, D.G., SEGAL, M. & BARKER, J.L. (1984). A Ca-dependent Cl^- conductance in cultured mouse spinal neurones. *Nature*, **311**, 567–570.

PACAUD, P., LOIRAND, G., LAVIE, J.L., MIRONNEAU, C. & MIRONNEAU, J. (1989). Calcium-activated chloride current in rat vascular smooth muscle cells in short-term primary culture. *Pflügers Arch.*, **413**, 629–636.

PARTRIDGE, L.D. & SWANDULLA, D. (1987). Single Ca-activated cation channels in bursting neurons of Helix. *Pflügers Arch.*, **410**, 627–631.

PARTRIDGE, L.D. & SWANDULLA, D. (1988). Calcium-activated non-specific cation channels. *Trends Neurosci.*, **11**, 69–72.

ROGAWSKI, M.A., INOUE, K., SUZUKI, S. & BARKER, J.L. (1988). A slow calcium-dependent chloride conductance in clonal anterior pituitary cells. *J. Neurophys.*, **59**, 1854–1870.

SCHLICHTER, R., BADER, C.R., BERTRAND, D., DUBOIS-DAUPHIN, M. & BERNHEIM, L. (1989). Expression of substance P and of a Ca^{2+}-activated Cl^- current in quail sensory trigeminal neurones. *Neurosci*, **30**, 585–594.

SCOTT, R.H., CURRIE, K.P.M., SUTTON, K.G. & DOLPHIN, A.C. (1992). Modulation of neuronal Ca^{2+}-dependent currents by neurotransmitters, G-proteins and toxins. *Biochem. Soc. Trans.*, **20**, 443–449.

SCOTT, R.H., MCGUIRK, S.M. & DOLPHIN, A.C. (1988). Modulation of divalent cation-activated chloride ion currents. *Br. J. Pharmacol.*, **94**, 653–662.

SIMON, S.M. & LLINÁS, R.R. (1985). Compartmentalization of the submembrane calcium activity during calcium influx and its significance in transmitter release. *Biophys. J.*, **48**, 485–496.

SIMONNEAU, M., DISTASI, C., TAUC, L. & BARBIN, G. (1987). Potassium channels in mouse neonate dorsal root ganglion cells: a patch-clamp study. *Brain. Res.*, **412**, 224–232.

SMITH, S.J., MACDERMOTT, A.B. & WEIGHT, F.F. (1983). Detection of intracellular Ca^{2+} transients in sympathetic neurones using arsenazo III. *Nature*, **304**, 350–352.

TALEB, O., FELTZ, P., BOSSU, J.-L. & FELTZ, A. (1988). Small-conductance chloride channels activated by calcium on cultured endocrine cells from mammalian pars intermedia. *Pflügers Arch.*, **412**, 641–646.

THAYER, S.A., PERNEY, T.M. & MILLER, R.J. (1988). Regulation of calcium homeostasis in sensory neurones by bradykinin. *J. Neurosci.*, **8**, 4089–4097.

WANGEMANN, P., WITTNER, M., DISTEFANO, A., ENGLERT, H.C., LANG, H.J., SCHLATTER, E. & GREGER, R. (1986). Cl^--channel blockers in the thick ascending limb of the loop of Henle, structure activity relationship? *Pflügers Arch.*, **407**, S128–S141.

(Received November 14, 1991
Revised March 9, 1992
Accepted March 11, 1992)

Br. J. Pharmacol. (1992), **106**, 603–609

Evidence for postsynaptic mediation of the hypothermic effect of 5-HT_{1A} receptor activation

[1]M.T. O'Connell, [2]G.S. Sarna & [3]G. Curzon

Department of Neurochemistry, Institute of Neurology, Queen Square, London WC1N 3BG

1 The 5-HT_{1A} ligand BMY 7378 (8-[2[4-(2-methoxyphenyl)-1-piperazinyl]ethyl]8-azaspirol [4,5]-decane-7,9-dione dihydrochloride, 0.032–2 mg kg^{-1}, s.c.) caused hyperphagia, a response to the activation of presynaptic 5-HT_{1A} receptors.

2 BMY 7378 (8 mg kg^{-1}, s.c.) and the 5-HT_{1A} agonist (8-hydroxy-2-(di-n-propylamino) tetralin (8-OH-DPAT), 0.10 and 0.25 mg kg^{-1} s.c.) also caused hypothermia. This was inhibited by (−)-pindolol (1 mg kg^{-1}, i.p.) and not prevented by pretreatments with *p*-chlorophenylalanine which grossly depleted 5-hydroxytryptamine (5-HT) from terminal regions. The hypothermic effects are explicable by activation of postsynaptic 5-HT_{1A} receptors. Infusion of BMY 7378 (8–64 μg) into the dorsal raphe was without convincing hypothermic effect.

3 BMY 7378 (8 mg kg^{-1}, s.c.) inhibited another effect of activation of postsynaptic 5-HT_{1A} receptors, i.e., the induction of components of the 5-HT syndrome by 8-OH-DPAT (0.5, 1.0 mg kg^{-1}, s.c.) which suggests that BMY 7378 has antagonistic as well as agonistic effects at these sites.

4 Partial agonist properties of BMY 7378 at postsynaptic sites were also indicated by doses for hypothermia being much greater than those for hyperphagia i.e., ED_{50} (hypothermia) > 2 mg kg^{-1}, ED_{50} (hyperphagia) = 0.010 mg kg^{-1}. This contrasts with the similar ED_{50} values for both the hypothermic (ED_{50} = 0.08–0.10 mg kg^{-1}) and hyperphagic (ED_{50} = 0.06–0.10 mg kg^{-1}) effects of 8-OH-DPAT.

5 The evidence obtained for mediation of the hypothermic response to 5-HT_{1A} agonists by postsynaptic sites is relevant to the interpretation of the effects on it of antidepressant treatments and depressive illness.

Keywords: Feeding; 5-HT_{1A} agonists; 5-HT_{1A} antagonists; 5-HT behaviour; temperature

Introduction

The rat brain contains both pre- and postsynaptic 5-HT_{1A} binding sites (Gozlan *et al.*, 1983). The presynaptic sites mostly occur in the dorsal and median raphe nuclei (Verge *et al.*, 1985; Weissman-Nanopoulos *et al.*, 1985). They act as somatodendritic autoreceptors which on activation by 5-HT_{1A} agonists (e.g. 8-hydroxy-2-(di-n-propylamino) tetralin (8-OH-DPAT)) decrease the release of 5-hydroxytryptamine (5-HT) at terminals (Hjorth & Magnusson, 1988; Hutson *et al.*, 1989; Sharp *et al.*, 1989). Behavioural consequences occur including hyperphagia in freely feeding rats (Dourish *et al.*, 1985; 1986a; Hutson *et al.*, 1986) and altered motor activity (Hillegaart, 1990). Activation of postsynaptic 5-HT_{1A} receptors causes at least two components of the 5-HT behavioural syndrome, reciprocal forepaw padding and flat body posture (Tricklebank *et al.*, 1984).

5-HT_{1A} agonists also cause hypothermia but, as reviewed by Martin & Heal (1991), evidence on whether this occurs via a pre- or postsynaptic mechanism is conflicting. Thus, Goodwin *et al.* (1987a) reported that the hypothermic effect of 8-OH-DPAT was mediated presynaptically as it was attenuated when 5-HT was depleted by repeated i.p. administration of *p*-chlorophenylalanine (pCPA) or by injection of 5,7-dihydroxytryptamine (5,7-DHT) into the third ventricle. Similar results were obtained in mice (Goodwin *et al.*, 1985; Heal *et al.*, 1989). However, other workers found that pCPA tended to increase the hypothermic effect of 8-OH-DPAT in both rats (Hjorth, 1985; Hutson *et al.*, 1987) and mice (Matsuda *et al.*, 1990). Similar effects occurred when rats were pretreated with either pCPA or 5,7-DHT and given the 5-HT_{1A} agonist LY 165163 (Hutson *et al.*, 1987) and a very recent paper reported the above pretreatments opposed the hypothermic response to 8-OH-DPAT in mice but not in rats (Bill *et al.*, 1991). These findings suggest that 5-HT_{1A} agonists cause hypothermia in the rat by activating not presynaptic but postsynaptic receptors. On the other hand, Higgins *et al.* (1988) and Hillegaart (1991) induced hypothermia by injecting 8-OH-DPAT into the dorsal raphe, which is consistent with the data of Goodwin *et al.* (1985, 1987a).

This discrepancy is of some importance, especially as 8-OH-DPAT induced hypothermia has been taken as a model of presynaptic 5-HT_{1A} function (Goodwin *et al.*, 1985; Lesch *et al.*, 1990a). We have therefore attempted to elucidate it by use of the buspirone analogue BMY 7378, (8-[2-[4-(2-methoxyphenyl) -1-piperazinyl] ethyl]-8-azaspirol [4,5] -decane-7, 9-dione dihydrochloride which is an agonist at 5-HT_{1A} receptors in the dorsal raphe (VanderMaelen *et al.*, 1987; Sharp *et al.*, 1990) but has mainly antagonist properties at postsynaptic 5-HT_{1A} sites and relatively weak affinity for 5-HT receptors of other types (Yocca *et al.*, 1987; Chaput & De Montigny, 1988; Sharp *et al.*, 1990). The above dual action of BMY 7378 was confirmed by determining its effects on feeding and on the 5-HT behavioural syndrome. Its effects on temperature were then used to investigate the mechanism of the hypothermia.

Methods

Animals

Male Sprague-Dawley rats (Charles River, U.K., weight 200–250 g) were housed individually under a 12 h light-dark cycle (lights on 06 h 00 min) at 22 ± 1°C for 5 days before experimentation. Rat diet (Labsure, Poole, Dorset) and water were freely available.

[1] Present address: Department of Clinical Neurology, Institute of Neurology, Queen Square, London WC1N 3BG.
[2] MRC Cyclotron Unit, Hammersmith Hospital, 150 DuCane Road, London W12 0HS.
[3] Author for correspondence.

Food intake

BMY 7378 (0.002, 0.008, 0.032, 0.125, 0.5 and 2.0 mg kg^{-1}) or 0.9% NaCl vehicle (1.0 ml kg^{-1}, s.c.) was given s.c. between 12 h 00 min and 13 h 00 min to freely feeding rats in their home cages. A weighed amount of food was placed in the hopper, the amount of food remaining at 2, 4 and 24 h weighed and food intakes calculated.

5-Hydroxytryptamine syndrome

Animals were tested in their home cages but after the removal of most of their bedding in order to facilitate the observation of behaviour. BMY 7378 (8 mg kg^{-1}) or 0.9% NaCl vehicle was administered s.c. into the right flank 30 min prior to injecting 8-OH-DPAT or 0.9% NaCl s.c. into the left flank. Behaviour was recorded on video tape from 10 to 70 min after the final drug injection and subsequently analysed by use of a micro-computer as described by Dourish *et al.* (1986a).

Temperature measurements

The rectal temperature of rats briefly retained in a 6 cm i.d. perspex tube was measured with a lubricated digital thermometer probe (Philip Harris Scientific, London) inserted 3 cm into the rectum. Readings were taken 15 min before and 30, 60, 120 and 300 min after giving BMY 7378 (2, 8 or 32 mg kg^{-1}, s.c., $n = 6$ or 7 per group) or 0.9% NaCl vehicle ($n = 13$).

p-*Chlorophenylalanine pretreatment*

In view of disagreements in the literature on the effect of pretreatment with pCPA on the hypothermic responses of rats to 5-HT_{1A} agonists (Hjorth, 1985; Goodwin *et al.*, 1987a; Hutson *et al.*, 1987) three different pCPA procedures were used. Initially the method of Hutson *et al.* (1987) was applied. Rats were injected i.p. with pCPA (150 mg kg^{-1}) on three consecutive days and 24 h later given BMY 7378 (8 mg kg^{-1}, $n = 6$) or 0.9% NaCl vehicle ($n = 6$). Control groups were given 0.9% NaCl instead of pCPA but otherwise treated as above. Rectal temperature was measured 15 min before and 30 and 60 min after final drug administration. The rats were then immediately killed by decapitation and their brains rapidly removed, dissected into regions (see later) and stored at −70°C for subsequent determination of 5-HT.

In a second experiment, the pCPA treatment of Goodwin *et al.* (1987a) was used in which the doses were larger than those used by Hutson *et al.* (1987) and the drug was given 4 times instead of 3. Effects on the hypothermic responses to BMY 7378 and 8-OH-DPAT were determined. pCPA (200 mg kg^{-1}, i.p.) was given on days 1, 2, 6 and 12. Twenty-four h after the final injection, BMY 7378 (8 mg kg^{-1}), 8-OH-DPAT (0.1, 0.75 mg kg^{-1}) or 0.9% NaCl was given s.c. ($n = 5$–6 per group) and temperature measured as before. Control animals were given 0.9% NaCl instead of pCPA. The rats were killed and their brains removed, dissected, stored and analysed as before.

Finally rats were pretreated with pCPA as in the previous experiments but, following the procedure of Goodwin *et al.* (1987a) exactly, 8-OH-DPAT (0.1 and 0.75 mg kg^{-1}) were given twice (days 4 and 14) and rectal temperature recorded on both days. This experiment was performed to determine whether the first treated with 8-OH-DPAT used by these authors affected the hypothermic response to the second treatment (see discussion). Brain 5-HT was not determined.

(−)-Pindolol pretreatment

Rectal temperatures were measured immediately before i.p. injection of (−)-pindolol (1 mg kg^{-1}) or 0.9% NaCl. The rats were injected 15 min later with 8-OH-DPAT (0.25 mg kg^{-1}), BMY 7278 (8 mg kg^{-1}) or 0.9% NaCl ($n = 5$–7 per group). Temperatures were measured again 30 min after the second injection.

Infusion of BMY 7378 into the dorsal raphe

Rats were anaesthetized with Sagatal (sodium pentobarbitone B.P., RMB Animal Health Ltd., U.K., 20–30 mg kg^{-1}, i.p.) and stereotactically implanted at coordinates: AP −7.8 mm, L 0.0 mm and V 5.0 mm, relative to bregma (Paxinos & Watson, 1982), with guide cannulae (26 G, Plastics One Inc., Virginia, U.S.A.) so that the tip of the indwelling stylet was flush with the guide which terminated 1 mm superior to the dorsal raphe and just before the cerebral aqueduct. Dental acrylic and two screws firmly secured the guide cannula. The rats were allowed to recover for five days with daily handling and rotation of the stylet.

On the sixth day the rectal temperature was measured and 15 min later the stylet was replaced by a stainless steel infusion needle that protruded 1 mm beyond the guide: 0.9% NaCl or BMY 7378 (8, 32 or 64 μg) were infused in 1 μl 0.9% NaCl over 1 min with the needle remaining *in situ* for an additional 1 min, to allow for diffusion from the tip. Rectal temperature measurements were made after 15, 30, 45, 60, 90 and 120 min.

The rats were then overdosed with Sagatal and cardiac perfusion performed with 10% formalin in 0.9% NaCl as a brain tissue fixative. The brains were removed and stored refrigerated before histological determination of the injection site.

Biochemical analysis

Brains were placed in an ice-cold rat brain slicer (Henry & Yashpal, 1984) and dissected as follows with Paxinos & Watson (1982) as a guide. Frontal cortex material was obtained by use of a 2 mm anterior transverse cut with subsequent removal of the olfactory lobes. Further cuts made 2.5 mm anterior to and on the interaural line gave a slice from which a 3 mm i.d. punch was taken with the cerebral aqueduct and the pontine nuclei as upper and lower limits. This contained the dorsal and medial raphe nuclei, some of the caudal linear raphe nucleus and also some extraneous material. The hippocampus, hypothalamus and 'rest of brain' (minus the cerebellum) were then dissected out freehand.

Tissue samples were treated and 5-HT and 5-hydroxyindoleacetic acid (5-HIAA) determined by high performance liquid chromatography (h.p.l.c.) as described by Adell *et al.* (1989) except that the mobile phase was 0.1 M KH_2PO_4, 0.16 mM octyl sodium sulphate, 0.4 mM Na-EDTA, (adjusted to pH 3.6 with phosphoric acid) and 15% methanol. Typical retention times (min) were: 5-HT, 2.45; 5-HIAA, 3.25. Protein was determined in the raphe samples by the method of Lowry *et al.* (1951).

Drugs

Drugs used were as follows: 8-[2-[4-(2-methoxyphenyl)-1-piperazinyl]ethyl]8-azaspirol[4,5]-decane-7,9-dione 2HCl (BMY 7378), Bristol-Myers Co., Evansvill, IN, U.S.A.; 8-hydroxy-2-(di-n-propylamino)tetralin HBr (8-OH-DPAT), Research Biochemicals Inc., Semat, St. Albans, U.K.; DL-*p*-chlorophenylalanine methyl ester HCl (pCPA) (Sigma Chemical Co., Poole, Dorset); (−)-pindolol (Sandoz, Basle, Switzerland). All drugs except (−)-pindolol were freshly dissolved in 0.9% NaCl and injected (s.c. for 8-OH-DPAT or BMY 7378, i.p. for pCPA) in a volume of 1.0 ml kg^{-1} between 12 h 00 min and 14 h 00 min. (−)-Pindolol was dissolved in a few drops of 0.1 M HCl, brought to neutrality with 0.1 M NaOH and made to volume with 0.9% NaCl.

Data analysis

Differences between the effects of various doses of BMY 7378 on food intake were evaluated by Mann-Whitney U-test after significant Kruskal-Wallis ANOVA. The ED_{50} value was calculated by linear regression. Effects of BMY 7378 on 8-OH-DPAT–induced behaviour were also assessed by this method. Effects of BMY 7378 at different dosage on temperature were assessed by Duncan's test after significant parametric one way ANOVA. The effects of pCPA and (−)-pindolol pretreatment on the temperature response to BMY 7378 and the effects of pCPA on brain 5-HT and 5-HIAA were analysed by Student's *t* test.

Results

Effect of BMY 7378 on feeding

Food intake over 2 h by freely feeding animals was increased by BMY 7378 (Figure 1) in a dose-related manner with significant effects at 0.032 mg kg^{-1}, s.c. and above. Maximum response occurred at 0.5 mg kg^{-1}. The dose-response curves for 2 and 4 h intakes were parallel i.e. BMY 7378 caused hyperphagia during the first but not the second 2 h after injection. Food intake over 24 h was unaffected (results not shown).

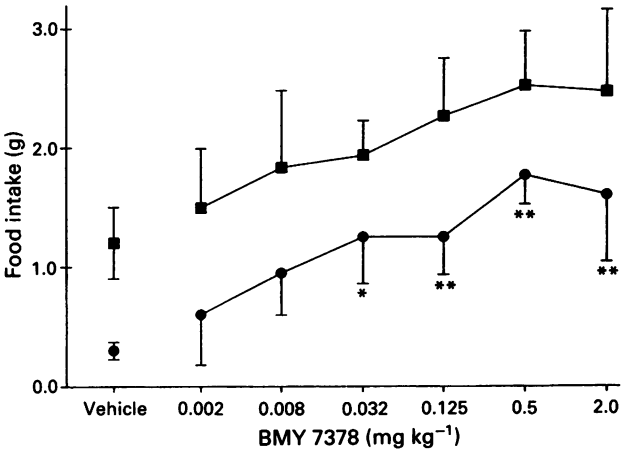

Figure 1 The effect of BMY 7378 on feeding in rats. Intakes are shown as means (s.e.mean shown by vertical bars) over 2 h (●) and 4 h (■) after injection s.c. ($n = 6$/group). Differences from rats treated with 0.9% NaCl vehicle: $*P<0.05$; $**P<0.02$ (Mann-Whitney U-test after Kruskal-Wallis ANOVA).

Effect of BMY 7378 on the 5-HT syndrome induced by 8-OH-DPAT

Table 1 shows that BMY 7378 (8 mg kg^{-1}, s.c.) did not elicit any components of the 5-HT syndrome and almost completely prevented its induction by 8-OH-DPAT (0.5 and 1.0 mg kg^{-1}, s.c.). 8-OH-DPAT at the higher dose increased walking but this was suppressed in rats pretreated with BMY 7378. None of the groups of rats showed significant differences of grooming frequency but the duration of grooming episodes was much decreased in all groups given 8-OH-DPAT (not shown).

Effects of BMY 7378 and 8-OH-DPAT on body temperature

BMY 7378 (8, 32 mg kg^{-1} s.c.) caused significant and comparable hypothermia 30 min after giving either dose (Figure 2). The response to the 8 mg kg^{-1} dose then declined while the effect of the larger dose was somewhat more prolonged. BMY (2 mg kg^{-1}) did not decrease temperature but prevented the initial slight transient hyperthermia of animals injected with vehicle.

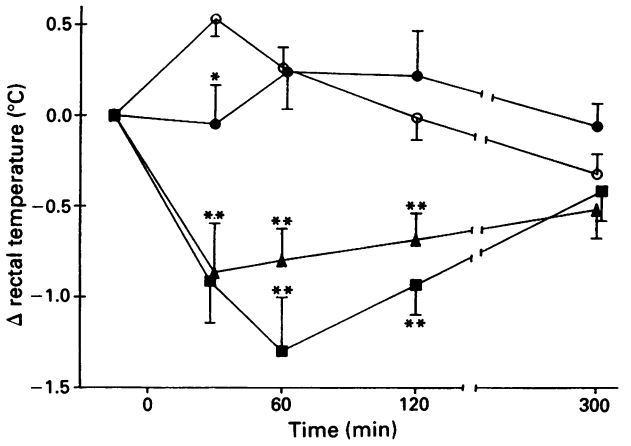

Figure 2 The effect of BMY 7378 on rectal temperature. Rats were given BMY 7378 s.c.; 2 mg kg^{-1} (●), 8 mg kg^{-1} (▲), 32 mg kg^{-1} (■), $n = 6$/group. Temperatures are differences from values 15 min before drug injection and are shown as means with s.e.mean shown by vertical bars. Differences from rats given 0.9% NaCl (○, $n = 13$); $*P<0.05$; $**P<0.01$ (Duncan's test after significant one way ANOVA).

Table 1 Effect of BMY 7378 on motor activity and components of the 5-hydroxytryptamine (5-HT) syndrome induced by 8-hydroxy-2-(di-n-propylamino) tetralin (8-OH-DPAT)

First injection	*0.9% NaCl*			*BMY 7378* (8 mg kg^{-1})		
Second injection	*0.9% NaCl*	*8-OH-DPAT* (0.5 mg kg^{-1})	*8-OH-DPAT* (1.0 mg kg^{-1})	*0.9% NaCl*	*8-OH-DPAT* (0.5 mg kg^{-1})	*8-OH-DPAT* (1.0 mg kg^{-1})
n	4	5	4	4	4	4
Forepaw treading (FRQ)	0	15.2 ± 2.3	12.3 ± 0.2	0	0	0
Wet-dog shakes (FRQ)	0	1.8 ± 0.4	4.8 ± 3.3	0	0	0.3 ± 0.3
Hindlimb abduction (FRQ)	0	8.4 ± 1.6	9.3 ± 1.9	0	0	0.3 ± 0.3
Flat body posture (DUR)	0	24.7 ± 2.9	29.9 ± 1.6	0	0	0
Walking (DUR)	3.4 ± 1.7	3.3 ± 0.7	9.0 ± 0.6†	0.4 ± 0.1	0.4 ± 0.2*	1.2 ± 0.4*
Grooming (FRQ)	6.8 ± 2.5	2.4 ± 1.2	3.7 ± 1.2	2.8 ± 0.6	3.0 ± 1.5	1.5 ± 0.9

Values are means ± s.e.mean. DUR = duration in min. FRQ = frequency. Observation over 1 h (see 'Methods'). Differences from rats given 0.9% NaCl instead of BMY 7378: $*P<0.05$. Differences from rats given 0.9% NaCl instead of 8-OH-DPAT: $†P<0.05$. Mann-Whitney U-test after significant Kruskal-Wallis ANOVA.

pCPA pretreatments Rats depleted of 5-HT by pretreatment with pCPA (150 mg kg^{-1}, i.p.) on days 1, 2 and 3 showed a hypothermic response to BMY 7378 (8 mg kg^{-1}, s.c.) on day 4 which was essentially identical to that of animals pretreated with 0.9% NaCl (Table 2, experiment 1).

Pretreatment with pCPA (200 mg kg^{-1}, i.p.) on days 1, 2, 6 and 12 led to an essentially unaltered hypothermic response to BMY 7378 (8 mg kg^{-1}, s.c.) at 30 min after injection and a moderately but not significantly increased hypothermia at 60 min (Table 2, experiment 2). The response to 8-OH-DPAT (0.1 mg kg^{-1}, s.c.) was however substantially and significantly increased by the pCPA pretreatment.

In experiment 3, the same pCPA treatment was used but 8-OH-DPAT was given on day 4 and then on day 14. The hypothermic response to 8-OH-DPAT (0.10 mg kg^{-1}) was the same on both days but less marked on day 14 than in experiment 2. The response to 8-OH-DPAT (0.75 mg kg^{-1}) at 30 min after injection was somewhat lower on day 14 than on day 4 but the response at 60 min was somewhat higher.

Temperatures 15 min before final drug treatments of rats pretreated with pCPA were marginally higher than those of animals pretreated with 0.9% NaCl.

Effect of (−)-pindolol The decreases of temperature 30 min after injection of BMY 7378 (8 mg kg^{-1}, s.c.) or 8-OH-DPAT (0.25 mg kg^{-1}, s.c.) were substantially attenuated when (−)-pindolol (1 mg kg^{-1}, i.p.) was given 15 min before the above drug treatments (Table 3). (−)-Pindolol pretreatment had negligible effects on temperature in the absence of BMY 7378 or 0.9% NaCl.

Infusion of BMY 7378 into the dorsal raphe Infusion of 0.9% NaCl vehicle into the dorsal raphe caused a rise in temperature which was maximal at 30 min (Table 4). BMY 7378 (8 μg) caused a marginally smaller rise and BMY 7378 (32 μg) caused slight hypothermia at 15 min so that the temperature was significantly below that of rats infused with 0.9% NaCl. A higher dose (64 μg) had an effect which was slightly less than that of 32 μg and did not attain significance.

Table 2 Effect of *p*-chlorophenylalanine (pCPA) pretreatment on hypothermic responses to BMY 7378 and 8-hydroxy-2-(di-n-propylamino) tetralin (8-OH-DPAT)

n	*Pretreatment*	*Temperature 15 min before treatment*	*Treatment*	*Change of temperature* 30 min after treatment	60 min after treatment
Expt. 1					
	Days 1,2,3		*Day 4*		
5	0.9% NaCl	37.6 ± 0.2	0.9% NaCl	+0.3 ± 0.2	+0.1 ± 0.2
5	0.9% NaCl	37.4 ± 0.2	BMY 7378 (8 mg kg^{-1})	−0.8 ± 0.3**	−0.7 ± 0.2*
				Δ −1.1	Δ −0.8
5	pCPA (150 mg kg^{-1})	37.6 ± 0.3	0.9% NaCl	+0.3 ± 0.1	+0.2 ± 0.1
6	pCPA (150 mg kg^{-1})	38.1 ± 0.2	BMY 7378 (8 mg kg^{-1})	−0.8 ± 0.4*	−0.8 ± 0.3*
				Δ −1.1	Δ −1.0
Expt. 2					
	Days 1,2,6,12		*Day 14*		
6	0.9% NaCl	37.5 ± 0.1	0.9% NaCl	+0.7 ± 0.1	+0.6 ± 0.2
5	0.9% NaCl	37.7 ± 0.2	BMY 7378 (8 mg kg^{-1})	−0.5 ± 0.3**	−0.4 ± 0.3*
				Δ −1.2	Δ −1.0
6	0.9% NaCl	37.6 ± 0.2	8-OH-DPAT (0.1 mg kg^{-1})	−0.6 ± 0.3**	−0.2 ± 0.2*
				Δ −1.3	Δ −0.8
4	pCPA (200 mg kg^{-1})	37.6 ± 0.2	0.9% NaCl	+0.6 ± 0.2	+0.6 ± 0.3
5	pCPA (200 mg kg^{-1})	38.1 ± 0.2	BMY 7328 (8 mg kg^{-1})	−0.7 ± 0.2**	−0.8 ± 0.1**
				Δ −1.3	Δ −1.4
5	pCPA (200 mg kg^{-1})	38.2 ± 0.2	8-OH-DPAT (0.1 mg kg^{-1})	−1.8 ± 0.3**†	−1.1 ± 0.4**
				Δ −2.4	Δ −1.7
Expt. 3					
	Days 1,2		*Day 4*		
8	pCPA (200 mg kg^{-1})	38.1 ± 0.2	0.9% NaCl	+0.2 ± 0.2	−0.1 ± 0.2
8	pCPA (200 mg kg^{-1})	38.1 ± 0.1	8-OH-DPAT (0.1 mg kg^{-1})	−0.7 ± 0.2*	−0.1 ± 0.1
				Δ −0.9	Δ −0.0
8	pCPA (200 mg kg^{-1})	38.1 ± 0.2	8-OH-DPAT (0.75 mg kg^{-1})	−2.4 ± 0.4**	−1.0 ± 0.3**
				Δ −2.6	Δ −0.9
	Day 6,12		*Day 14*		
	Continued experiment on above three groups				
8	pCPA (200 mg kg^{-1})	37.9 ± 0.2	0.9% NaCl	+0.1 ± 0.1	−0.1 ± 0.1
8	pCPA (200 mg kg^{-1})	37.8 ± 0.2	8-OH-DPAT (0.1 mg kg^{-1})	−0.8 ± 0.2**	−0.2 ± 0.2
				Δ −0.9	Δ −0.1
8	pCPA (200 mg kg^{-1})	37.9 ± 0.1	8-OH-DPAT (0.75 mg kg^{-1})	−1.8 ± 0.1**	−1.5 ± 0.3**
				Δ −1.9	Δ −1.4

Values are means ± s.e.mean.
Mean differences from rats treated with 0.9% NaCl instead of BMY 7378 or 8-OH-DPAT is indicated by Δ. Significance of differences from rats treated with 0.9% NaCl. *$P<0.05$; **$P<0.01$ by Duncan's multiple group comparison after significant one-way ANOVA. Significances of difference from rats pretreated with 0.9% NaCl instead of pCPA: †$P<0.02$ (Student's *t* test).

Depletion of brain 5-HT by pCPA treatments

Both pCPA treatments (see Table 2, experiments 1 and 2) grossly reduced 5-HT concentrations in brain regions with the exception of the raphe where considerable amounts of 5-HT were detectable (Table 5) especially in experiment 2, i.e., when the conditions of Goodwin *et al.* (1987a) were used. Relative decreases of 5-HIAA were consistently somewhat greater than those of 5-HT.

Table 3 Effect of (−)-pindolol (1 mg kg^{-1}) on hypothermic effects of BMY 7378 (8 mg kg^{-1}) and 8-hydroxy-2-(di-n-propylamino) tetralin (8-OH-DPAT, 0.25 mg kg^{-1})

n	*Pretreatment*	*Treatment*	*Changes of temperature* (30 min after treatment)
5	0.9% NaCl	0.9% NaCl	+0.1 ± 0.1
7	(−)-Pindolol	0.9% NaCl	+0.1 ± 0.2
5	0.9% NaCl	BMY 7378	−1.2 ± 0.3
6	(−)-Pindolol	BMY 7378	−0.3 ± 0.15**
6	0.9% NaCl	8-OH-DPAT	−1.8 ± 0.1
6	(−)-Pindolol	8-OH-DPAT	−0.8 ± 0.3*

Changes of temperature are from values determined immediately before pretreatment i.e., 15 min before treatment. Values are means ± s.e.mean. Differences from rats not given (−)-pindolol: *$P<0.05$; **$P<0.01$ (t test).

Table 4 Effect of infusing BMY 7378 into the dorsal raphe on temperature

n	*BMY 7378* (μg)	*Change of temperature* *15 min*	*30 min*	*45 min*
6	0	+0.7 ± 0.1	+0.9 ± 0.2	+0.8 ± 0.2
6	8	+0.4 ± 0.1	+0.6 ± 0.1	+0.6 ± 0.1
5	32	−0.2 ± 0.2*	+0.2 ± 0.1	+0.5 ± 0.1
5	64	+0.2 ± 0.2	+0.6 ± 0.2	+0.8 ± 0.2

Changes of temperature are from values determined 15 min before infusing the drug. Values are means ± s.e.mean. Difference from rats given vehicle: *$P<0.05$ (Duncan's test after significant one way ANOVA).

Discussion

BMY 7378 caused both hypothermia and hyperphagia in the rat. The hyperphagic response, a well authenticated effect of activation of presynaptic 5-HT$_{1A}$ receptors (Dourish *et al.*, 1985; 1986a; Hutson *et al.*, 1986); had an ED$_{50}$ value of 0.010 mg kg^{-1}. The hypothermic potency of BMY 7378 is more than two orders of magnitude weaker as a dose of 2 mg kg^{-1} had only marginal effect. Unlike BMY 7378, the 5-HT$_{1A}$ agonist 8-OH-DPAT, has comparable potencies for both hyperphagia (ED$_{50}$ values calculated from Dourish *et al.* (1985) and Pregalinski *et al.* (1990) = 0.06 and 0.10 mg kg^{-1} respectively) and hypothermia (ED$_{50}$ values calculated from Aulakh *et al.* (1988) and Bill *et al.* (1991) = 0.08 and 0.10 mg kg^{-1} respectively).

These findings are consistent with evidence that 8-OH-DPAT has strongly agonistic properties at both presynaptic and postsynaptic 5-HT$_{1A}$ receptors but that while BMY 7378 has comparably agonistic properties at presynaptic sites it is mainly an antagonist with no more than weak agonist properties at the postsynaptic sites (VanderMaelen *et al.*, 1987; Yocca *et al.*, 1987; Chaput & De Montigny, 1988; Sharp *et al.*, 1990). This suggests that 5-HT$_{1A}$ agonists cause hypothermia by activating 5-HT$_{1A}$ receptors at which BMY is, at most weakly effective i.e., at postsynaptic sites. That 5-HT$_{1A}$ sites mediate this response to BMY 7378 is consistent with its blockade by (−)-pindolol (Table 3). The hypothermic effect of 8-OH-DPAT in both man (Lesch *et al.*, 1990a) and rats (Millan, 1991) is also blocked by pindolol. In the latter species, blockade by a range of other antagonists strongly indicates the involvement of 5-HT$_{1A}$ sites (Millan, 1991). Whether the weakly hypothermic effect of BMY 7378 is due to action at these or at other sites e.g. DA$_2$ receptors for which it has some affinity (Yocca *et al.*, 1987) would not affect the main argument of the present paper, i.e., that when activation of 5-HT$_{1A}$ receptors mediates hypothermia, the responsible sites are located postsynaptically.

Antagonistic effects of BMY 7378 at postsynaptic 5-HT$_{1A}$ receptors explain its inhibition of the hypothermic effect of 8-OH-DPAT (Moser, 1991). They also may explain why it inhibits the 5-HT behavioural syndrome induced by 8-OH-DPAT (Table 1) as some components of the latter (i.e., forepaw treading and flat body posture) result from activation of postsynaptic 5-HT$_{1A}$ sites (Tricklebank *et al.*, 1984). It is also conceivable that the syndrome was inhibited due to

Table 5 Effect of *p*-chlorophenylalanine (pCPA) on brain regional 5-hydroxytryptamine (5-HT) and 5-hydroxyindoleacetic acid (5-HIAA) concentrations

	Injected i.p. days 1,2,3; killed day 4 0.9% NaCl $n=10$	pCPA (150 mg kg^{-1}) $n=9$	% decrease	*Injected i.p. days 1,2,6,12; killed day 14* 0.9% NaCl $n=10$	pCPA (200 mg kg^{-1}) $n=8$	% decrease
Frontal cortex						
5-HT	471 ± 39	44 ± 4	91	445 ± 39	56 ± 6	87
5-HIAA	336 ± 36	18 ± 1	95	330 ± 27	27 ± 5	92
Hippocampus						
5-HT	215 ± 24	16 ± 1	93	162 ± 7	28 ± 3	83
5-HIAA	576 ± 68	27 ± 6	95	503 ± 18	34 ± 4	93
Hypothalamus						
5-HT	1529 ± 129	145 ± 29	91	1544 ± 172	150 ± 24	90
5-HIAA	572 ± 33	40 ± 5	93	546 ± 41	38 ± 4	93
Raphe						
5-HT	47.0 ± 2.7	20.6 ± 2.4	56	47.3 ± 3.0	30.5 ± 1.7	36
5-HIAA	38.9 ± 1.0	15.2 ± 1.4	61	38.2 ± 3.1	20.4 ± 1.4	47
Rest of brain						
5-HT	751 ± 69	67 ± 8	91	896 ± 64	161 ± 16	82
5-HIAA	392 ± 21	26 ± 1	93	439 ± 14	49 ± 4	89

Values are means ± s.e.mean in ng g^{-1} of wet weight tissue except for the raphe where results are given as ng mg^{-1} protein. Difference from rats treated with 0.9% NaCl: $P<0.001$ in all cases (Student's t test).

sedation as Table 1 suggests that BMY 7378 may have suppressed walking (albeit not to a statistically significant extent). However, the lack of effect of BMY 7378 on frequency of grooming and the resistance of the *p*-chloroamphetamine-induced 5-HT syndrome to the sedative reserpine (Adell *et al.*, 1989) suggest otherwise. In our hands, BMY 7378 (8 mg kg^{-1}) did not elicit the syndrome though Sharp *et al.* (1990) report that a dose of 5 mg kg^{-1} weakly induced two components of it i.e. hindlinb abduction and flat body posture.

Our results, and those of Moser (1991) show that BMY 7378 is hypothermic only at high dosage when its agonist properties presumably become manifest. The finding that depletion of brain 5-HT by either pCPA or 5,7-DHT did not decrease the hypothermic effects of the 5-HT_{1A} agonists 8-OH-DPAT and LY 165163 in the rat (Hjorth, 1985; Hutson *et al.*, 1987; Bill *et al.*, 1991) agree with the involvement of a postsynaptic site. Similarly, the present results show that hypothermias induced by 8-OH-DPAT and BMY 7378 were largely unaffected by pretreatments with pCPA according to dosage schedules used by Hutson *et al.* (1987) and Goodwin *et al.* (1987a) which depleted 5-HT in regions rich in 5-HT axon terminals by about 90% (Table 5).

As availability of 5-HT for release falls in proportion with its depletion by pCPA (O'Connell *et al.*, 1991), a hypothermic effect of 5-HT_{1A} agonists due to decreased release at axon terminals following activation of presynaptic receptors would be unlikely to survive the above pCPA treatments. Incidentally, Satinoff *et al.* (1991) found that pCPA was acutely hypothermic but, in agreement with our findings, temperature was normal on the day after injection. As 5-HT would have still been depleted, this suggests that compensatory changes opposed the hypothermia. It is relevant that Larsson *et al.* (1990) found that the hypothermia effect of 8-OH-DPAT was readily attenuated on repeated injection of the drug.

Although as previously shown (Aghajanian *et al.*, 1973; Deguchi *et al.*, 1973; Steinman *et al.*, 1987), raphe 5-HT largely survived pCPA treatment (Table 5) a presynaptic mechanism of 5-HT_{1A} hypothermia mediated by a decrease of raphe 5-HT release is improbable as Artigas *et al.* (1991) report that 8-OH-DPAT did not decrease extracellular 5-HT in the raphe. Furthermore, although 5-HT also resists depletion by pCPA in a few small terminal regions (Tohyama *et al.*, 1988), these do not include the anterior hypothalamus, where 5-HT has been implicated in temperature control (Myers, 1975; Cox *et al.*, 1980). Another indication that 5-HT_{1A} hypothermia is mediated postsynaptically is that 5-hydroxytryptophan and fenfluramine did not decrease 8-OH-DPAT-induced hypothermia (Bill *et al.*, 1991). As these drugs increase 5-HT at postsynaptic sites they would be expected to oppose the hypothermia if it was due to activation of presynaptic receptors and resultant decreased release of 5-HT.

A possible explanation of why Goodwin *et al.* (1985; 1987a) and Heal *et al.* (1989) but not Hjorth *et al.* (1985), Hutson *et al.* (1987), Bill *et al.* (1991) and the present authors, prevented the hypothermic effects of 5-HT_{1A} agonists in rats with pCPA and 5,7-DHT is suggested by the downregulation of 8-OH-DPAT hypothermia by a single pretreatment with the drug (Larsson *et al.*, 1990) as when Goodwin *et al.* (1987a) reported that pCPA prevented the hypothermia, the rats had already been given a previous dose of 8-OH-DPAT. However, pCPA did not prevent the hypothermic effect of a second dose of 8-OH-DPAT in the present study (Table 2, Experiment 3). Lecci *et al.* (1990) suggest an alternative explanation i.e., that the results of Goodwin *et al.* were due to pCPA preventing a presynaptically mediated anxiolytic effect of 8-OH-DPAT which opposed a hyperthermic response to the stress of removal from group housing. However, Bill *et al.* (1991) used group housing and obtained similar results to those of the present study in which individual caging was used.

Another problem is posed by the hypothermia on injecting 8-OH-DPAT into the rat dorsal raphe (Higgins *et al.*, 1988; Hillegaart, 1991). BMY 7378 was not convincingly hypothermic when given by this route as although it decreased the slightly hyperthermic effect of injecting vehicle into the raphe (Table 4) the decrease was marginally significant and lacked clear dose-dependence. Diffusion of the drug to postsynaptic receptors may well have been responsible as Higgins *et al.* (1988) reported appreciable diffusion of 8-OH-DPAT to adjacent tissue and noted that hypothermic doses of 8-OH-DPAT were subsequently greater than those needed for a response thought to involve activation of presynaptic 5-HT_{1A} sites i.e. anxiolysis (Dourish *et al.*, 1986b). Injection into the median raphe did not affect temperature (Hillegart, 1991).

The present findings and earlier work suggest that, despite some conflicting data, the balance of evidence favours a postsynaptic mechanism for the hypothermic effects of 5-HT_{1A} agonists in the rat. This is relevant to the interpretation of reports that the hypothermic response of rats to 8-OH-DPAT was attenuated by repeated electroconvulsive shock (Goodwin *et al.*, 1987b) and by some chronic antidepressant drug treatments (Goodwin *et al.*, 1987b; Wozniak *et al.*, 1988; Martin & Heal, 1991)) and that the hypothermic effect of the 5-HT_{1A} agonist ipsapirone was low in depression and decreased further after chronic amitriptyline treatment (Lesch *et al.*, 1990b). What these findings indicate about the role of 5-HT in depression is critically dependent on whether the hypothermia is due to activation of presynaptic or postsynaptic 5-HT_{1A} sites with resultant decrease or increase of postsynaptic 5-hydroxytryptaminergic activity respectively.

We thank the MRC for financial support and Bristol-Myers and Sandoz for samples of BMY 7378 and (−)-pindolol respectively.

References

ADELL, A., SARNA, G.S., HUTSON, P.H. & CURZON, G. (1989). An in vivo dialysis and behavioural study of the release of 5-HT by p-chloroamphetamine in reserpine-treated rats. *Br. J. Pharmacol.*, **97**, 206–212.

AGHAJANIAN, G.K., KUHAR, M.J. & ROTH, R.H. (1973). Serotonin – containing neuronal perikarya and terminals: differential effects of p-chlorophenylalanine. *Brain Res.*, **54**, 85–101.

ARTIGAS, F., ADELL, A. & CELADA, P. (1991). Extracellular 5-hydroxytryptamine in the raphe nuclei: basal values and the effects of ions and drugs. In *Monitoring Molecules in Neuroscience*. ed. Rollema, H., Westerink, B.H.L. & Drijfhout, W.J. Groningen: University Centre for Pharmacy. pp. 232–234.

AULAKH, C.S., WOZNIAK, K.M., HAAS, M., HILL, J.L., ZOHAR, J. & MURPHY, D.L. (1988). Food intake, neuroendocrine and temperature effects of 8-OH-DPAT in the rat. *Eur. J. Pharmacol.*, **146**, 253–259.

BILL, A., KNIGHT, M., FORSTER, E.A. & FLETCHER, A. (1991). Direct evidence for an important species difference in the mechanism of 8-OH-DPAT-induced hypothermia. *Br. J. Pharmacol.*, **103**, 1857–1864.

CHAPUT, Y. & DE MONTIGNY, C. (1988). Effects of the 5-hydroxytryptamine receptor antagonist, BMY 7378, on 5-hydroxytryptamine neurotransmission: electrophysiological studies in the rat central nervous system. *J. Pharmacol. Exp. Ther.*, **246**, 359–370.

COX, B., KERWIN, R.W., LEE, T.F. & PYCOCK, C.J. (1980). A dopamine-5-hydroxytryptamine link in the hypothalamic pathways which mediate heat loss in the rat. *J. Physiol.*, **303**, 9–21.

DEGUCHI, T., SINHA, A.K. & BARCHAS, J.D. (1973). Biosynthesis of serotonin in raphe nuclei of rat brain: effect of p-chlorophenylalanine. *J. Neurochem.*, **20**, 1329–1336.

DOURISH, C.T., HUTSON, P.H. & CURZON, G. (1985). Low doses of the putative serotonin agonist 8-hydroxy-2-(di-n-propylamino) tetralin (8-OH-DPAT) elicit feeding in the rat. *Psychopharmacology*, **86**, 197–204.

DOURISH, C.T., HUTSON, P.H. & CURZON, G. (1986a). Para-chlorophenylalanine prevents feeding induced by the serotonin agonist 8-hydroxy-2-(di-n-propylamino) tetralin (8-OH-DPAT). *Psychopharmacology*, **89**, 467–471.

DOURISH, C.T., HUTSON, P.H. & CURZON, G. (1986b). Putative anxiolytics 8-OH-DPAT, buspirone and TVX Q. 7821 are agonists at 5-HT$_{1A}$ autoreceptors in the raphe nuclei. *Trends Pharmacol. Sci.*, **7**, 212–214.

GOODWIN, G.M., DE SOUZA, R.J. & GREEN, A.R. (1985). The pharmacology of the hypothermic response in mice to 8-hydroxy-2-(di-n-propylamino) tetralin (8-OH-DPAT): a model of presynaptic 5-HT$_1$ function. *Neuropharmacology*, **24**, 1187–1194.

GOODWIN, G.M., DE SOUZA, R.J., GREEN, A.R. & HEAL, D.J. (1987a). The pharmacology of the behavioural and hypothermic responses of rats to 8-hydroxy-2-(di-n-propylamino)-tetralin (8-OH-DPAT). *Psychopharmacology*, **91**, 506–511.

GOODWIN, G.M., DE SOUZA, R.J. & GREEN, A.R. (1987b). Attenuation by electroconvulsive shock and antidepressant drugs of the 5-HT$_{1A}$ receptor mediated hypothermia and serotonin syndrome produced by 8-OH-DPAT in the rat. *Psychopharmacology*, **91**, 500–505.

GOZLAN, H., EL MESTIKAWY, S., PICHAT, L., GLOWINSKI, J. & HAMON, M. (1983). Identification of presynaptic serotonin autoreceptors using a new ligand: ^{3}H-PAT. *Nature*, **305**, 140–142.

HEAL, D.J., PROW, M.R., MARTIN, K.F. & BUCKETT, W.R. (1989). Effects of lesioning central 5-HT and noradrenaline containing neurones on 8-OH-DPAT hypothermia mydriasis and hypoactivity. *Br. J. Pharmacol.*, **97**, 406P.

HENRY, J.L. & YASHPAL, K. (1984). Rat brain slicer, a simple device for rapidly obtaining serial slabs of fresh brain. *Brain Res. Bull.*, **13**, 195–197.

HIGGINS, G.A., BRADBURY, A.J., JONES, B.J. & OAKLEY, N.R. (1988). Behavioural and biochemical consequences following activation of 5-HT$_1$-like and GABA receptors in the dorsal raphe nucleus of the rat. *Neuropharmacology*, **27**, 993–1001.

HILLEGART, V. (1990). Effects of local application of 5-HT and 8-OH-DPAT into the dorsal and median raphe nuclei on motor activity in the rat. *Physiol. Behav.*, **48**, 143–148.

HILLEGART, V. (1991). Effects of local application of 5-HT and 8-OH-DPAT into the dorsal and median raphe nuclei on core temperature in the rat. *Psychopharmacology*, **103**, 291–296.

HJORTH, S. (1985). Hypothermia in the rat induced by the potent serotoninergic agent 8-OH-DPAT. *J. Neural Transm.*, **61**, 131–135.

HJORTH, S. & MAGNUSSON, T. (1988). The 5-HT$_{1A}$ receptor agonist, 8-OH-DPAT, preferentially activates cell body 5-HT autoreceptors in the rat brain in vivo. *Naunyn-Schmiedebergs Arch. Pharmacol.*, **338**, 463–471.

HUTSON, P.H., DONOHOE, T.P. & CURZON, G. (1987). Hypothermia induced by the putative 5-HT$_{1A}$ agonists LY 165163 and 8-OH-DPAT is not prevented by 5-HT depletion. *Eur. J. Pharmacol.*, **143**, 221–228.

HUTSON, P.H., DOURISH, C.T. & CURZON, G. (1986). Neurochemical and behavioural evidence for mediation of the hyperphagic action of 8-OH-DPAT by 5-HT cell body autoreceptors. *Eur. J. Pharmacol.*, **129**, 347–352.

HUTSON, P.H., SARNA, G.S., O'CONNELL, M.T. & CURZON, G. (1989). Hippocampal 5-HT synthesis and release in vivo is decreased by infusion of 8-OH-DPAT into the nucleus raphe dorsalis. *Neurosci. Lett.*, **100**, 276–280.

LARSSON, L.G., RENYI, L., ROSS, S.B., SVENSSON, B. & ANGEBY-MOLLER, K. (1990). Different effects on the responses of functional pre- and postsynaptic 5-HT$_{1A}$ receptors by repeated treatment of rats with the 5-HT$_{1A}$ receptor agonist 8-OH-DPAT. *Neuropharmacology*, **29**, 85–91.

LECCI, A., BORSINI, F., MANCINELLI, A., D'ARANNO, V., STASI, M.A., VOLTERRA, G. & MELI, A. (1990). Effect of serotonergic drugs on stress-induced hyperthermia (SIH) in mice. *J. Neurol Transm. [Gen Sect.]*, **82**, 219–230.

LESCH, K.P., POTEN, B., SOHNLE, K. & SCHULTE, H.M. (1990a). Pharmacology of the hypothermic response to 5-HT$_{1A}$ receptor activation in humans. *Eur. J. Clin. Pharmacol.*, **39**, 17–19.

LESCH, K.P., DISSELKAMP-TIETZE, J. & SCHULTE, H.M. (1990b). 5-HT$_{1A}$ receptor function in depression: effect of chronic amitriptyline treatment. *J. Neural Transm (Gen. Sect.)*, **80**, 157–161.

LOWRY, O.H., ROSEBROUGH, N.J., FARR, S.L. & RANDALL, R.J. (1951). Protein measurement with the Folin phenol reagent. *J. Biol. Chem.*, **193**, 265–275.

MARTIN, K.F. & HEAL, D.J. (1991). 8-OH-DPAT-induced hypothermia in rodents. A specific model of 5-HT$_{1A}$ autoreceptor function? In *Serotonin: Molecular Biology, Receptors and Functional Effects*. ed. Fozard, J.R. & Saxena, P.R. pp. 483–490. Basle: Birkhauser.

MATSUDA, T., KANDA, T., SEONG, Y.H., BABA, A. & ITAWA, H. (1990). p-Chlorophenylalanine attenuates the pituitary – adrenocortical responses to 5-HT$_{1A}$ receptor agonist in mice. *Eur. J. Pharmacol.*, **181**, 295–297.

MILLAN, M.J. (1991). Induction of hypothermia in the rat as a model of 5-HT$_{1A}$ receptor-mediated activity: a pharmacological characterization. Abstr. *5-HT 1991*. p. 62. Birmingham.

MOSER, P.C. (1991). The effect of putative 5-HT$_{1A}$ receptor antagonists on 8-OH-DPAT – induced hypothermia in rats and mice. *Eur. J. Pharmacol.*, **193**, 165–172.

MYERS, R.D. (1975). Impairment of thermoregulation, food and water intakes in the rat after hypothalamic injection of 5,6-dihydroxytryptamine. *Brain Res.*, **94**, 491–506.

O'CONNELL, M.T., PORTAS, C.M., SARNA, G.S. & CURZON, G. (1991). Effect of p-chlorophenylalanine on release of 5-HT from the rat frontal cortex in vivo. *Br. J. Pharmacol.*, **102**, 832–836.

PAXINOS, G. & WATSON, C. (1982). *The Rat Brain in Stereotaxic Coordinates*. New York: Academic Press.

PREGALINSKI, E., BARAN, L. & SIWANOWICZ, J. (1990). Repeated treatment with imipramine, amitriptyline or electroconvulsive shock does not affect the 8-OH-DPAT induced increase in food intake in free feeding rats. *Pol. J. Pharmacol. Pharm.*, **42**, 327–332.

SATINOFF, E., KENT, S., LI, H., MEGIRIAN, D.C. & TOMKOWIAK, J.M. (1991). Circadian rhythms of body temperature and drinking and response to thermal challenge in rats after pCPA. *Pharmacol. Biochem. Behav.*, **38**, 253–257.

SHARP, T., BRAMWELL, S.R. & GRAHAME-SMITH, D.G. (1989). 5-HT$_1$ agonists reduce 5-hydroxytryptamine release in rat hippocampus in vivo as determined by brain microdialysis. *Br. J. Pharmacol.* **96**, 283–290.

SHARP, T., BACKUS, L.I., HJORTH, S., BRAMWELL, S.R. & GRAHAME-SMITH, D.G. (1990). Further investigation of the in vivo antagonist, BMY 7378. *Eur. J. Pharmacol.*, **176**, 331–340.

STEINMAN, J.L., CARLTON, S.M., HABER, B. & WILLIS, W.D. (1987). Differential effects of p-chlorophenylalanine on indoleamines in brainstem nuclei and spinal cord of rats I. Biochemical and behavioural analysis. *Brain Res.*, **426**, 297–309.

TOHYAMA, I., KAMEYAMA, M. & KIMURA, H. (1988). Quantitative morphometric analysis of two types of serotonin – immunoreactive nerve fibres differentially responding to p-chlorophenylalanine treatment in the rat brain. *Neuroscience*, **26**, 971–991.

TRICKLEBANK, M.D., FORLER, C. & FOZARD, J.R. (1984). The involvement of subtypes of the 5-HT$_1$ receptor and of catecholaminergic systems in the behavioural response to 8-hydroxy-2-(di-n-propylamino) tetralin in the rat. *Eur. J. Pharmacol.*, **106**, 271–282.

VANDERMAELEN, C.P., BRASELTON, J.P. & GEHLBACH, G. (1987). In vivo and in vitro electrophysiological studies indicate that BMY 7378 is a partial agonist at 5-HT$_{1A}$ receptors in the rat dorsal raphe nucleus. *Neurosci. Abstr.*, **13**, 459.5.

VERGE, D., DAVAL, G., PATEY, A., GOZLAN, H., EL MESTIKAWY, S. & HAMON, M. (1985). Presynaptic 5-HT autoreceptors on serotonergic cell bodies and/or dendrites but not terminals are of the 5-HT$_{1A}$ subtype. *Eur. J. Pharmacol.*, **113**, 463–464.

WEISSMAN-NANOPOULOS, D., MACH, E., MAGRE, J., DEMASSEY, Y. & PUJOL, J.F. (1985). Evidence for the localization of 5-HT$_{1A}$ binding sites on serotonin containing neurones in the raphe dorsalis and raphe centralis nuclei of the rat brain. *Neurochem. Int.*, **7**, 1061–1072.

WOZNIAK, K.M., AULAKH, C.S., HILL, J.L. & MURPHY, D.L. (1988). The effect of 8-OH-DPAT on temperature in the rat and its modification by chronic antidepressant treatments. *Pharmacol. Biochem. Behav.*, **30**, 451–456.

YOCCA, F.D., HYSLOP, D.K., SMITH, D.W. & MAAYANI, S. (1987). BMY 7378, a buspirone analogue with high affinity, selectivity and low intrinsic activity at the 5-HT$_{1A}$ receptor in rat and guinea pig hippocampal membranes. *Eur. J. Pharmacol.*, **137**, 293–294.

(Received November 27, 1991
Revised February 26, 1992
Accepted March 11, 1992)

Br. J. Pharmacol. (1992), **106**, 610–615

P_{2y} purinoceptor responses of β cells and vascular bed are preserved in diabetic rat pancreas

[1]D. Hillaire-Buys, R. Gross, J. Chapal, G. Ribes & M.M. Loubatières-Mariani

Faculté de Médecine, Laboratoire de Pharmacologie, CNRS, URA 599, Montpellier Cedex, France

1 To investigate the effect of experimental diabetes on the P_{2y} purinoceptor responses of pancreatic β-cells and vascular bed, we used adenosine-5'-O-(2-thiodiphosphate) (ADPβS), a potent and stable P_{2y} agonist. This work was performed in the isolated perfused pancreas of the rat.

2 Diabetes was induced by streptozotocin (66 mg kg^{-1}, i.p.). Five weeks after the induction of diabetes, on the day of pancreas isolation, the animals displayed marked hyperglycaemia (37.6 ± 2.7 mM). Age-matched rats were used as controls.

3 Insulin response to a glucose stimulation from 5 to 10 mM was completely lost and stimulation of insulin release by the sulphonylurea, tolbutamide (185 μM), was drastically impaired in the diabetic pancreas (maximum responses were 1.5 ± 0.4 and 7.0 ± 1.4 ng min^{-1} for diabetic and age-matched rats respectively).

4 In contrast, in the diabetic pancreas ADPβS (15 μM), infused in the presence of glucose 5 mM, elicited an immediate and significant insulin release similar to that observed in the age-matched pancreas (maximum responses were 7.6 ± 1.5 and 6.7 ± 1.3 ng min^{-1} respectively). This ADPβS stimulating effect occurred independently of the glucose concentration (5, 8.3 and 28 mM) in the diabetic pancreas. On pancreatic vascular resistance, ADPβS induced a similar vasodilatation in diabetic and age-matched rats.

5 In conclusion, ADPβS retains its insulin stimulatory and vasodilator effects in experimental diabetes; P_{2y} purinoceptors could therefore be considered as a new target for the development of antidiabetic drugs.

Keywords: P_{2y} purinoceptors; adenosine-5'-O-(2-thiodiphosphate) (ADPβS); streptozotocin; diabetic rats; insulin; pancreatic vessels

Introduction

The impairment of insulin secretion in non insulin-dependent diabetes mellitus has been extensively studied; in various models of experimental diabetes, insulin response to glucose is lost whereas that to other secretagogues, such as arginine and carbachol, appears to be less affected, preserved or even increased depending on the experimental conditions (Weir *et al.*, 1981; Giroix *et al.*, 1983; Okabayashi *et al.*, 1989). In addition, vascular dysfunctions altering the responses to various vasodilator or vasoconstrictor agents develop during the diabetic state (Kamata *et al.*, 1989a,b; Mulhern & Docherty, 1989).

Purine nucleotides or nucleosides are widely known to affect many cellular processes via two types of purinoceptors: P_1 receptors for adenosine and P_2 receptors for ATP and/or ADP (Burnstock, 1978; Gordon, 1986; White, 1988). Concerning pancreatic endocrine function, we have shown that A cells possess P_1 and β cells P_2 receptors, the stimulation of which evokes glucagon and insulin secretion respectively (Loubatières-Mariani & Chapal, 1988). Adenosine receptors on A cells were shown to belong to the A_2 subtype. P_2 purinoceptors have also been subclassified into P_{2x} and P_{2y} subtypes (Burnstock & Kennedy, 1985). A previous study has demonstrated that the purinoceptors of the pancreatic β cells were of the P_{2y} subtype (Bertrand *et al.*, 1987). In addition, it has been recently shown in rat isolated perfused pancreas that adenosine-5'-O-(2-thiodiphosphate) (ADPβS), a stable P_{2y} purinoceptor agonist, elicited both insulin release and vasodilatation (Bertrand *et al.*, 1991) via the activation of P_{2y} receptors on β cells and vessels; this substance was about 100 times more potent than ATP. In pancreas from rats with streptozotocin-induced diabetes (STZ-D), we have shown that P_1-mediated glucagon secretion and blood vessel dilatation responses to adenosine were abolished and strongly reduced respectively (Gross *et al.*, 1989). In the present study we wished to obtain further insight into possible other diabetes-induced disturbances of the purinergic control of pancreatic endocrine and vascular functions. We therefore investigated whether STZ-D could modify the insulin response as well as the vasodilatation evoked by the stable agonist ADPβS via activation of P_{2y} purinoceptors.

Methods

Animals

Our study was carried out with adult male Wistar rats that had free access to food and water. All rats were housed in individual cages; a 10-day acclimatization period was allowed before the experiments began; the rats weighed from 320 to 350 g. Diabetes was induced by an i.p. injection of streptozotocin (66 mg kg^{-1}). A group of normal rats served as age-matched controls. Thereafter, daily glucosuria measurements were made to ensure the diabetic state of the animals over 5 wk; their glucosuria was higher than 10 g per 24 h. On the day of the experiment, just before the pancreas was removed, blood was sampled by intracardiac puncture for measurement of glycaemia and plasma insulin and glucagon concentrations.

Pancreas isolation

Animals were anaesthetized with 60 mg kg^{-1} i.p. pentobartitone sodium. The procedure of Loubatières *et al.* (1969) was used to isolate the pancreas completely from all neighbouring tissues. The pancreas was then transferred into a

[1] Author for correspondence at: Laboratoire de Pharmacologie, Faculté de Médecine, Institut de Biologie, Boulevard Henri IV, 34060 Montpellier Cedex, France.

plastic chamber maintained at 37.5°C. The perfusion medium, which was not allowed to recirculate, was Krebs-Ringer buffer containing 2 g l^{-1} bovine serum albumin (fraction V, Sigma, St. Louis, MO, U.S.A.) and 5 mM glucose, and was continuously bubbled with 95% O_2/5% CO_2 to maintain the pH between 7.35 and 7.40.

A peristaltic pump was used for the circulation of the perfusion medium. Perfusion pressure was maintained constant, and the excess of medium not accepted by the organ at the given pressure, returned to the origin reservoir. The pressure was selected to provide a basal vascular flow rate of about 2.5 ml min^{-1} at the beginning of the experiment. Any change in pancreatic vascular bed resistance due to drug administration resulted in changes in outflow rate; the latter was measured by collecting outflow samples in graduated tubes during 1 min.

For determination of insulin concentration, a 1 ml aliquot of pancreatic effluent was immediately frozen. For determination of glucagon concentration, a 500 µl aliquot of pancreatic outflow was collected in chilled tubes containing 50 µl of a mixture of 32 mM EDTA and 10,000 KIU ml^{-1} aprotinin (Antagosan, Hoechst, Puteaux) and immediately frozen.

Experimental protocol

The first sample was taken after a 30 min equilibration period (time measured from beginning of pancreas perfusion). Another sample was collected 15 min later. Drugs, ADPβS (Boehringer, Mannheim, FRG) or tolbutamide (Sigma, St. Louis, MO, U.S.A.), were then administered for 30 min, and samples were collected every min for 5 min and then, 8, 10, 15 and 30 min after the beginning of drug infusion. The effects were studied simultaneously in age-matched and diabetic rats.

In a separate set of experiments, we investigated the effect of 5-wk diabetes on glucagon and insulin contents in islets. Batches of 10 islets were prepared, from normal and diabetic rat pancreas, according to the isolation technique of Lacy & Kostianowski (1967); for the extraction of peptides, they were incubated for 24 h at 4°C in 1 ml acid ethanol (pure HCl and 75% ethanol (1:65 vol/vol)).

Assay methods

Blood glucose and glucosuria were measured by the potassium ferricyanide method with a Technicon autoanalyser (Alric *et al.*, 1965). Insulin concentration was determined according to the method of Herbert *et al.* (1965). We used rat insulin as a standard and the anti-insulin serum supplied by Miles Laboratories (Paris). The sensitivity of the method was 0.1 ng ml^{-1}. Glucagon concentration was measured according to the radioimmunological method described by Unger *et al.* (1970). We used the BR 124 antiglucagon serum supplied by the Institut de Biochimie Clinique of Geneva. The sensitivity of the method was 15 pg ml^{-1}. Results are given as picogram equivalents of porcine glucagon.

Data analysis

Results are given as mean ± s.e.mean. Insulin and glucagon outputs were calculated by multiplying the hormone concentration (ng ml^{-1} or pg ml^{-1}) by the vascular flow rate (ml min^{-1}). Insulin and glucagon outputs are expressed as absolute values; vascular outflow rate is expressed as a percentage of the 45 min value (100%). Kinetic data were submitted to analysis of variance with the multiple-comparison test (Zar, 1974).

Results

Characteristics of diabetic state

In Table 1 are shown various parameters recorded just before removal of the pancreas, 5 wk after STZ injection. Diabetic animals were markedly hyperglycaemic and glucosuric and their mean body weight had not increased. They were strongly hypoinsulinaemic and the determination of islet insulin storage showed that insulin content was drastically decreased.

Insulin response

We first tested the effect of a glucose infusion and of an insulin secretory agent, tolbutamide. Basal insulin secretion with a non-stimulatory glucose concentration (5 mM) was similar in normal and diabetic rats (0.8 ± 0.1 and 0.7 ± 0.1 ng min^{-1} respectively). Increasing glucose concentration from 5 to 10 mM elicited an immediate and biphasic insulin response in age-matched rats ($P<0.001$), whereas the insulin response was totally abolished in diabetic rats (Figure 1). The insulin response to the sulphonylurea, tolbutamide (185 µM), in the presence of 5 mM glucose was drastically impaired in diabetic rats (Figure 2). The maximum insulin release observed was 7.0 ± 1.4 ($P<0.001$) and 1.5 ± 0.4 ng min^{-1} ($P<0.05$) for age-matched and diabetic rats respectively (respective basal values being 1.0 ± 0.3 and 0.6 ± 0.2 ng min^{-1}). Insulin output was stable throughout the experiment in the presence of glucose (5 mM) alone in age-matched and diabetic rats (Figure 3).

ADPβS (15 µM) infused in the presence of 5 mM glucose increased insulin secretion both in age-matched and diabetic animals (Figure 3). The insulin stimulating effect of ADPβS occurred immediately and insulin release peaked at 6.7 ± 1.3 ($P<0.001$) and 7.6 ± 1.5 ng min^{-1} ($P<0.001$) in age-matched and diabetic rats respectively (basal values being 1.0 ± 0.1 and 0.8 ± 0.2 ng min^{-1}). Thereafter insulin secretion remained slightly higher than the basal values in both groups. The kinetics of insulin output was similar in age-matched and diabetic rats. In the diabetic pancreas, ADPβS was then tested in the presence of different glucose concentrations: 8.3 and 28 mM. The stimulatory effects on insulin secretion were comparable to those obtained in the presence

Table 1 Various parameters recorded in non-fasting diabetic or normal rats just before pancreas extirpation: islet insulin and glucagon contents obtained in a separate set of experiments are given

	Body weight (g)	*Glucosuria* (g per 24 h)	*Glycaemia* (mM)	*Plasma insulin* (ng ml^{-1})	*Plasma glucagon* (pg ml^{-1})	*Islet insulin content* (ng per islet)	*Islet glucagon content* (pg per islet)
Age-matched rats	471	0	9.6	2.80	144	27.7	1217
	± 8		± 0.3	± 0.30	± 7	± 5.8	± 266
Diabetic rats	309	14.1	37.6	0.30	297	3.0	1609
	± 10	± 1.0	± 2.7	± 0.05	± 15	± 0.5	± 447

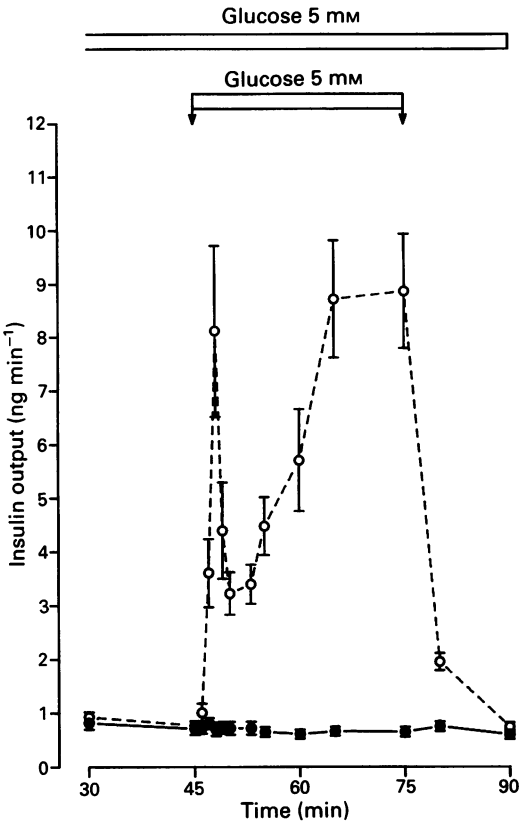

Figure 1 Insulin secretion in response to an increasing glucose concentration (5 to 10 mM), from the isolated perfused pancreas from 5-wk streptozotocin-induced diabetic (●) and age-matched (○) rats. Each point represents the mean with s.e.mean shown by vertical bars from 6 experiments.

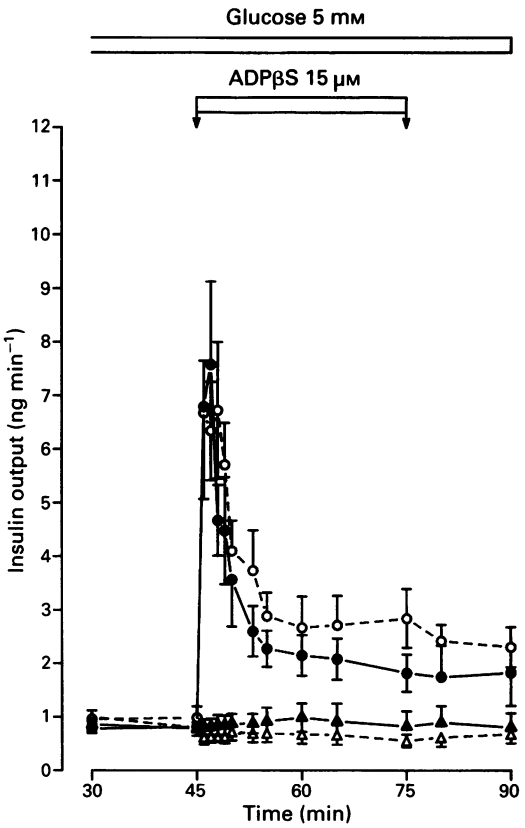

Figure 3 Insulin secretion in response to adenosine-5'-O-(2-thiodiphosphate) (ADPβS, 15 μM) from isolated perfused pancreas from 5-wk streptozotocin-induced diabetic (●) and age-matched (○) rats. Controls perfused with glucose 5 mM alone are shown: age-matched (△) and diabetic (▲) rats. Each point represents the mean with s.e.mean shown by vertical bars from 6 experiments.

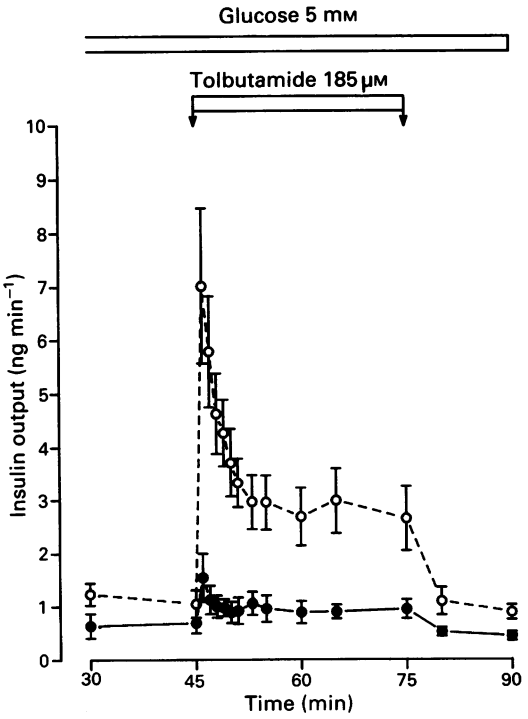

Figure 2 Insulin secretion in response to tolbutamide (185 μM) from isolated perfused pancreas from 5-wk streptozotocin-induced diabetic (●) and age-matched (○) rats. Each point represents the mean with s.e.mean shown by vertical bars from 6 experiments.

of 5 mM glucose (Figure 4) (the maximum insulin release being 6.1 ± 1.6 and 9.1 ± 1.2 ng min^{-1} respectively for diabetic pancreas perfused with 8.3 or 28 mM glucose).

Glucagon response (Figure 5)

Under basal conditions, in the presence of glucose 5 mM, glucagon output was stable during the whole experiment in normal as well as in diabetic rats. However, it was observed that the basal glucagon release was lower in diabetic than in normal rats. ADPβS (15 μM) caused an immediate but slight and transient rise in glucagon output ($P < 0.01$ versus 45 min value within 2 min of infusion) in age-matched rat pancreas. This effect of ADPβS was not observed in 5 wk diabetic rats.

Vascular response

In control experiments performed in the presence of glucose 5 mM alone, the vascular flow rate was not significantly modified during the entire 90 min experiment, although there was a very slight and progressive but not significant decrease to 97 ± 2 and 96 ± 4% of the 45 min values, which were 2.43 ± 0.04 and 2.49 ± 0.03 ml min^{-1} for age-matched and diabetic rats respectively. ADPβS (15 μM) induced a dual effect on pancreatic vascular flow rate in age-matched rats: a first transient vasoconstriction, significant only at the second min, ($P < 0.01$ versus 45 min value) followed by a long lasting and sustained vasodilatation (Figure 6). In the diabetic rat pancreas, an immediate and significant vasodilatation was observed which persisted throughout the ADPβS infusion ($P < 0.001$ versus 45 min value). From 65 min on, the maximum vasodilator effect was similar in age-matched and diabetic rats (+ 16 ± 4 and + 16 ± 3% respectively).

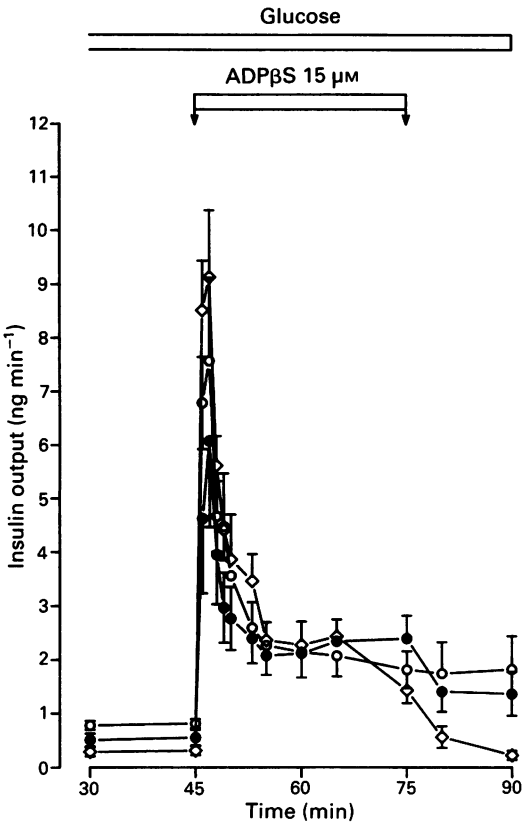

Figure 4 Effects of adenosine-5'-O-(2-thiodiphosphate) (ADPβS, 15 μM) on insulin secretion from isolated perfused pancreas from 5-wk streptozotocin-induced diabetic rats in presence of different glucose concentrations: (○) 5 mM; (●) 8.3 mM; and (◇) 28 mM glucose. Each point represents the mean with s.e.mean shown by vertical bars from 6 experiments.

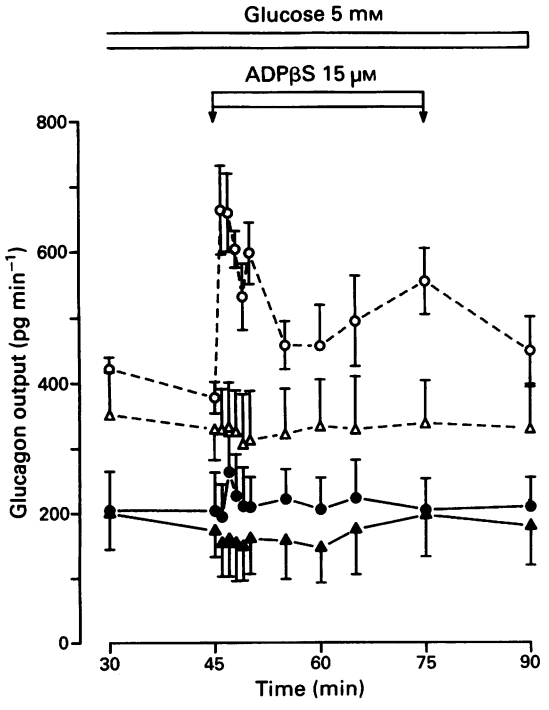

Figure 5 Glucagon secretion in response to adenosine-5'-O-(2-thiodiphosphate) (ADPβS, 15 μM) from isolated perfused pancreas from 5-wk streptozotocin-induced diabetic (●) and age-matched (○) rats. Controls perfused with glucose 5 mM alone are shown: age-matched (△) and diabetic (▲) rats. Each point represents the mean with s.e.mean shown by vertical bars from 6 experiments.

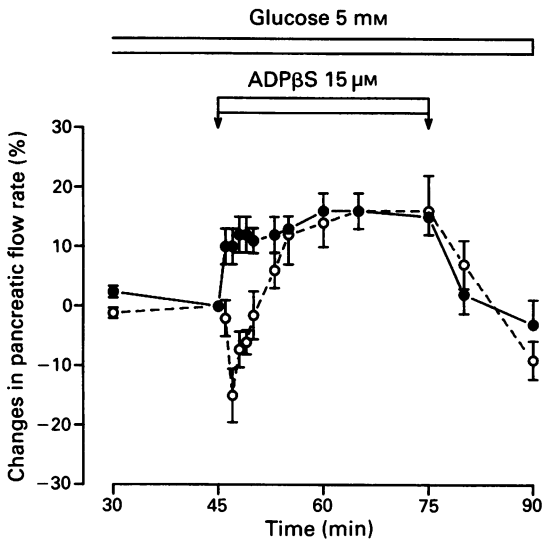

Figure 6 Effects of adenosine-5'-O-(2-thiodiphosphate) (ADPβS, 15 μM) on vascular flow rate in isolated perfused pancreas from 5-wk streptozotocin-induced diabetic (●) and age-matched (○) rats in presence of 5 mM glucose. Each point represents the mean with s.e.mean shown by vertical bars from 6 experiments.

Discussion

Our results show that (1) the pancreas from adult STZ-diabetic rats with impaired responses to glucose and tolbutamide, retain their ability to secrete insulin under ADPβS stimulation; (2) ADPβS remains fully active in inducing vasodilatation in diabetic rats.

The glucose insensitivity of the diabetic pancreas that we observed in our model of STZ-D rats, is in total agreement with other data obtained with animals rendered diabetic by STZ in lower dosage (Okabayashi *et al.*, 1989) or as neonates (Weir *et al.*, 1981; Giroix *et al.*, 1983). The same results were reported in spontaneously diabetic BB rats (Grill & Herberg, 1983) where the β cells were not destroyed by diabetogenic substances like STZ or alloxan, but by immunological factors (Marliss *et al.*, 1982). In another model with reduced β cell mass by partial pancreatectomy (pancreatic remnant being approximately 12% of the whole pancreas), a poor but significant response to glucose was preserved (Leahy *et al.*, 1984).

The most striking observation of the present study is that the remaining β cells of this diabetic rat model are extremely sensitive to ADPβS, since we obtained a comparable response in the age-matched and diabetic pancreas, despite a 10 times lower pancreatic insulin content in the latter. In our study, this P_{2y} purinoceptor agonist evoked a similar pattern of insulin response in the presence of higher glucose concentrations, 8.3 and 28 mM (the latter concentration mimicking glycaemia observed in these diabetic rats), thereby confirming β cell insensitivity to glucose in the diabetic pancreas. The results obtained with ADPβS contrast with those obtained with the antidiabetic sulphonylurea, tolbutamide, the insulin secretory effect of which was drastically decreased in our diabetic model. This finding is in agreement with the work of Weir *et al.* (1981) showing that tolbutamide, at the same concentration, was ineffective in eliciting an insulin response in neonatal STZ-D rats in the presence of glucose 7.8 mM; however, it is at variance with other data obtained in the same diabetic model, but in the absence of glucose (Giroix *et al.*, 1983; Serradas *et al.*, 1989). It is noteworthy that, in addition to their responsiveness to cholinergic, β-adrenergic and amino acid stimulation (Weir *et al.*, 1981; Giroix *et al.*, 1983; Grill & Herberg, 1983; Okabayashi *et al.*, 1989), diabetic β cells retain their ability to respond to purinergic stimulation.

Confirming our previous study (Gross *et al.*, 1989) basal *in vitro* glucagon output was found reduced in diabetic pancreas; this contrasted with the marked hyperglucagonaemia that occurred *in vivo*, suggesting that the high plasma glucagon levels measured originate from extrapancreatic sources. ADPβS elicited a slight and transient response of A cells in the age-matched rat. The rapidity of onset and transient nature of the glucagon response to ADPβS is in favour of an action via a P_1 site (on A cells) rather than a breakdown of this stable compound into adenosine. Such an action of ADPβS on a P_1 site has been described in rabbit jugular vein (Wood *et al.*, 1989). This glucagon response to ADPβS was completely suppressed in 5-wk-diabetic rats and is in agreement with our previous study showing that the A cell response to P_1 receptor activation was abolished in the diabetic state (Gross *et al.*, 1989).

Concerning our data on pancreatic vascular resistance in the diabetic state, ADPβS induced only a relaxing effect which contrasts with the biphasic response observed in age-matched rats: a transient vasoconstriction followed by a vasodilatation. The biphasic pattern of pancreatic vascular bed response obtained in our control group, could be explained by the existence of 2 types of receptors previously shown to regulate pancreatic tone (Hillaire-Buys *et al.*, 1991): P_{2y} and P_{2x} purinoceptors inducing vasodilator and vasoconstrictor effects respectively. As the contractile properties of rat aorta and mesenteric artery are in part dependent upon the smooth muscle mass of the preparation (Cohen & Berkowitz, 1974), ADPβS failure to induce vasoconstriction in diabetic rats could be ascribed to diabetes-induced reduction of the mass of smooth muscle. With this in mind, we performed a set of experiments with weight-matched (but not age-matched) rats, and the vasoconstrictor effect of ADPβS could no longer be observed (data not shown) confirming previous results obtained in normal rats weighing about 330–350 g (Bertrand *et al.*, 1991). In this regard, it has been reported that the adrenergic contractile response of aortic and mesenteric artery strips is age-dependent (Cohen & Berkowitz, 1974); our results with ADPβS in normal rats may suggest that the purinoceptor-induced constrictor effect in pancreatic vascular bed could also be age-dependent. An alternative explanation for the failure of ADPβS to induce vasoconstriction in diabetic rats could be the impairment of P_{2x} receptors by experimental diabetes. This is unlikely since the P_{2x} selective agonist, α,β-methylene ATP, induced similar transient vasoconstrictor responses both in diabetic and age-matched rats (respective maximal decrease of vascular flow rate reaching -60 ± 8 and $-69 \pm 5\%$ at 2 min with 0.5 μM α, β-methylene ATP). Whatever it may be, it is noteworthy that, the vasodilator effect due to P_{2y} purinoceptors is preserved and prevails in diabetic rats. These data are interesting when compared with our previous studies which showed that in diabetic rats, vasodilator responses to adenosine, isoprenaline and forskolin were decreased (Gross *et al.*, 1989; 1991), suggesting an impairment of the adenylate cyclase pathway. Thus the retained ability of ADPβS to induce a vasodilator response in diabetic rats suggests that the mechanisms underlying the effect of the P_{2y} agonist are unaffected by the diabetic state.

In conclusion, ADPβS retains its insulin stimulatory and vasodilator effects in experimental diabetes; P_{2y} purinoceptors should therefore be considered as a new target for the development of antidiabetic drugs.

The expert technical assistance of M. Tournier, M.F. Courty, R. Puech, M. Roye and V. Montesinos is gratefully acknowledged. This study was supported by Grant N 882008 from INSERM.

References

ALRIC, R., MARIANI, M.M. & LOUBATIERES, A.L. (1965). Importance de l'état des éléments figurés du sang et en particulier de celui des gobules rouges sur les valeurs du glucose sanguin mesuré par l'auto-analyseur Technicon. *Pathol. Biol.*, **13**, 506–511.

BERTRAND, G., CHAPAL, J., LOUBATIERES-MARIANI, M.M. & ROYE, M. (1987). Evidence for two different P_2-purinoceptors on β cell and pancreatic vascular bed. *Br. J. Pharmacol.*, **91**, 783–787.

BERTRAND, G., CHAPAL, J., PUECH, R. & LOUBATIERES-MARIANI, M.M. (1991). Adenosine-5'-O-(2-thiodiphosphate) is a potent agonist at P_2 purinoceptors mediating insulin secretion from perfused rat pancreas. *Br. J. Pharmacol.*, **102**, 627–630.

BURNSTOCK, G. (1978). A basis for distinguishing two types of purinergic receptors. In *Cell Membrane Receptors for Drugs and Hormones: A Multidisciplinary Approach.* ed. Straub, R.W. & Bolis, L. pp. 107–118. New York: Raven Press.

BURNSTOCK, G. & KENNEDY, C. (1985). Is there a basis for distinguishing two types of P_2-purinoceptor ? *Gen. Pharmacol.*, **16**, 433–440.

COHEN, M.L. & BERKOWITZ, B.A. (1974). Age-related changes in vascular responsiveness to cyclic nucleotides and contractile agonists. *J. Pharmacol. Exp. Ther.*, **191**, 147–155.

GIROIX, M.H., PORTHA, B., KERGOAT, M., BAILBE, D. & PICON, L. (1983). Glucose insensitivity and amino-acid hypersensitivity of insulin release in rats with non-insulin-dependent diabetes. *Diabetes*, **32**, 445–451.

GORDON, J.L. (1986). Extracellular ATP; effects, sources and fate. *Biochem. J.*, **233**, 309–319.

GRILL, V. & HERBERG, L. (1983). Glucose- and arginine-induced insulin and glucagon responses from the isolated perfused pancreas of the BB-Wistar diabetic rat. Evidence for selective impairment of glucose regulation. *Acta Endocrinol.*, **102**, 561–566.

GROSS, R., HILLAIRE-BUYS, D., RIBES, G. & LOUBATIERES-MARIANI, M.M. (1989). Diabetes and impaired response of glucagon cells and vascular bed to adenosine in rat pancreas. *Diabetes*, **38**, 1291–1295.

GROSS, R., HILLAIRE-BUYS, D., RIBES, G. & LOUBATIERES-MARIANI, M.M. (1991). Diabetes alters the responses of glucagon secreting cells and vascular bed to isoprenaline and forskolin in vitro in rat pancreas. *Life Sci.*, **48**, 2349–2358.

HERBERT, V., LAW, K.S., GOTLIEB, C.W. & BLEICHER, S.J. (1965). Coated charcoal immunoassay of insulin. *J. Clin. Endocrinol. Metab.*, **25**, 1375–1384.

HILLAIRE-BUYS, D., CHAPAL, J., PETIT, P. & LOUBATIERES-MARIANI, M.M. (1991). Dual regulation of pancreatic vascular tone by P_{2x} and P_{2y} purinoceptor subtypes. *Eur. J. Pharmacol.*, **199**, 309–314.

KAMATA, K., MIYATA, N. & KASUYA, Y. (1989a). Impairment of endothelium-dependent relaxation and changes in levels of cyclic GMP in aorta from streptozotocin-induced diabetic rats. *Br. J. Pharmacol.*, **97**, 614–618.

KAMATA, K., MIYATA, N. & KASUYA, Y. (1989b). Involvement of endothelial cells in relaxation and contraction responses of the aorta to isoproterenol in naive and streptozotoxin-induced diabetic rats. *J. Pharmacol. Exp. Ther.*, **249**, 890–894.

LACY, P. & KOSTIANOWSKI, M. (1967). Method for the isolation of intact islets of Langerhans from the rat pancreas. *Diabetes*, **16**, 35–39.

LEAHY, J.L., BONNER-WEIR, S. & WEIR, G.C. (1984). Abnormal glucose regulation of insulin secretion in models of reduced B-cell mass. *Diabetes*, **33**, 667–673.

LOUBATIERES, A.L., MARIANI, M.M., DE MALBOSC, H., RIBES, G. & CHAPAL, J. (1969). Etude expérimentale d'un nouveau sulfamide hypoglycémiant particulièrement actif, le HB 419 ou glibenclamide. I. Action bêtacytotrope et insulino-sécrétrice. *Diabetologia*, **5**, 1–10.

LOUBATIERES-MARIANI, M.M. & CHAPAL, J. (1988). Purinergic receptors involved in the stimulation of insulin and glucagon secretion. *Diabète Métabol.*, **14**, 119–126.

MARLISS, E.B., NAKHOODA, A.F., POUSSIER, P. & SIMA, A.A.F. (1982). The diabetic syndrome of the 'BB' Wistar rat: possible relevance to type 1 (insulin-dependent) diabetes in man. *Diabetologia*, **22**, 225–232.

MULHERN, M. & DOCHERTY, J.R. (1989). Effects of experimental diabetes on the responsiveness of rat aorta. *Br. J. Pharmacol.*, **97**, 1007–1012.

OKABAYASHI, Y., OTSUKI, M., OHKI, A., TANI, S. & BABA, S. (1989). Increased β-cell secretory responsiveness to ceruletide and TPA in streptozocin-induced mildly diabetic rats. *Diabetes*, **38**, 1042–1047.

SERRADAS, P., BAILBE, D. & PORTHA, B. (1989). Long-term gliclazide-treatment improves the in vitro glucose-induced insulin release in rats with Type 2 (non-insulin-dependent) diabetes induced by neonatal streptozotocin. *Diabetologia*, **32**, 577–584.

UNGER, R.H., AGUILAR-PARADA, E., MULLER, W. & EISENTRAUT, A.M. (1970). Studies of pancreatic alpha cell function in normal and diabetic subjects. *J. Clin. Invest.*, **49**, 837–848.

WEIR, G.C., CLORE, E.T., ZMACHINSKI, C.J. & BONNER-WEIR, S. (1981). Islet secretion in a new experimental model for non-insulin-dependent diabetes. *Diabetes*, **30**, 590–595.

WHITE, T.D. (1988). Role of adenine compounds in autonomic neurotransmission. *Pharmacol. Ther.*, **38**, 129–168.

WOOD, B.E., SQUIRE, A., O'CONNOR, S.E. & LEFF, P. (1989). ADP-β-F is not a selective P_{2y}-receptor agonist in rabbit jugular vein. *Br. J. Pharmacol.*, **98**, 794P.

ZAR, J.H. (1974). *Biostatistical Analysis*. Englewood Cliffs, N.J.: Prentice-Hall.

(Received November 25, 1991
Revised March 6, 1992
Accepted March 11, 1992)

Br. J. Pharmacol. (1992), **106**, 616–622

The non-adrenergic, non-cholinergic response counteracts changes in guinea-pig airway tone with and without sympathetic activation

[1]A. Lindén, *A. Ullman, B.-E. Skoogh & C.-G. Löfdahl

Divisions of Pulmonary Medicine, Renströmska Hospital, University of Göteborg, PO Box 17301, S-40264 Gothenburg and *Clinical Pharmacology, Sahlgrenska Hospital, University of Göteborg, S-413 45 Gothenburg, Sweden

1 We examined whether the non-adrenergic, non-cholinergic (NANC) neural response can counteract changes in smooth-muscle tone with and without simultaneous sympathetic activation in guinea-pig airways.

2 Isolated airway preparations were pretreated with indomethacin (10 μM) and incubated with either atropine (1 μM) and guanethidine (10 μM) or atropine (1 μM) alone. The response to electrical field stimulation (EFS: 1200 mA, 0.5 ms, 3 Hz for 240 s) was studied at various levels of tone prior to EFS: first without induced tone, then at a moderate tone induced by histamine (0.3 μM) and finally at a high tone induced by histamine (6 μM).

3 The response to EFS was a contraction when the tone prior to EFS was low and a relaxation when the tone prior to EFS was high. These responses converged towards a similar level of tone, in the distal trachea and in the main bronchus, with and without guanethidine.

4 The mean (s.e.mean) level of tone towards which the responses to EFS converged was lower after incubation with atropine alone compared with incubation with atropine and guanethidine, both in the distal trachea [8 (1)% compared with 30 (6)% of maximum tone] and in the main bronchus [28 (4)% compared with 57 (2)% of maximum tone]. In separate experiments, the guanethidine-induced effect on the responses to EFS was imitated by propranolol (1 μM) but not by prazosin (0.3 μM) and yohimbine (1 μM).

5 These findings indicate that the NANC neural response can counteract changes in airway smooth-muscle tone via a contraction or via a relaxation, depending on the tone prior to activation. This stabilizing effect on tone does not appear to depend upon adrenergic activation *per se*. The level of tone towards which the NANC responses converge can, however, be reduced by β-adrenoceptor activation, thus suggesting an interaction which provides protection from severe airway smooth-muscle contraction.

Keywords: Guinea-pig; airway tone; *in vitro*; neural regulation; non-adrenergic, non-cholinergic neural responses; smooth-muscle tone; sympathetic

Introduction

In contrast to the extensive documentation of non-adrenergic, non-cholinergic (NANC) neural responses in the airways of several species including man, there is still a limited understanding of the role played by these responses (Barnes, 1986; 1991; Andersson & Grundström, 1987). Recent data on guinea-pig airways do, however, demonstrate that contractile and relaxant NANC neural responses can change smooth-muscle tone by as much as 40% of maximum tone (Lindén *et al.*, 1991a), thereby suggesting that NANC activation can produce a significant regulatory power.

The point of having both contractile and relaxant NANC responses may be illustrated by the observation that, in guinea-pig isolated airways, contractile and relaxant NANC responses converge towards a similar level of airway smooth-muscle tone (Lindén *et al.*, 1990; 1991b). A NANC 'convergence effect' is thus exerted by either a contraction or a relaxation, depending on the level of tone prior to NANC activation, thereby indicating that the direction of the NANC response is determined by the level of tone prior to activation. These findings are also compatible with the idea that the role of contractile and relaxant NANC responses is to counteract changes in airway smooth-muscle tone. It is not known, however, how the NANC convergence effect relates to the activation of the adrenergic, sympathetic system in guinea-pig airways (Kamikawa & Shimo, 1976).

In the present study, we examined the ability of contractile and relaxant NANC responses to counteract changes in smooth-muscle tone prior to NANC activation, with and without simultaneous sympathetic activation, in guinea-pig isolated airways. We also characterized the interaction between NANC and sympathetic responses.

Methods

Airway preparation

Twenty-eight female Dunkin-Hartley guinea pigs (300–500 g) were killed by cervical dislocation and exsanguination. The thoracic contents were removed and placed in a 200 ml dissection bath filled with oxygenated (94% O_2:6% CO_2) Krebs-Ringer solution (mM: NaCl 118, KCl 5.9, $CaCl_2$ 2.5, $MgSO_4$ 1.2, NaH_2PO_4 1.2, $NaHCO_3$ 25.5 and glucose 5.6) at room temperature. The intermediate (cervical) trachea, the distal (intrathoracic) trachea and the main bronchi were dissected free and two airway rings were cut transversely from each airway segment, each ring containing four to five cartilaginous rings. The airway rings were opened longitudinally along the anterior, cartilaginous part and connected to steel hooks as isolated strips. These preparations were mounted vertically in warmed (37°C) and oxygenated 8 ml organ baths, which were continuously flushed with fresh Krebs-Ringer solution (0.4 ml min^{-1}). The histological evalu-

[1] Author for correspondence.

ation of the mounted preparations showed intact epithelial and smooth-muscle cells (Lindén *et al.*, 1991a).

Tension recordings

The isometric tension was continuously recorded by connecting the preparations to Grass force transducers (FT03). The signals from these transducers were transformed in an NB-MIO-16 analogue/digital converting board and registered in a Macintosh II computer with the signal-processing software LabVIEW (National Instruments, Austin, Texas, U.S.A.) (Ullman *et al.*, 1990).

Electrical field stimulation

Constant current generators provided electrical field stimulation (EFS) via rectangular platinum electrodes (5 × 30 mm) mounted in parallel (10 mm apart), with the airway preparations in between. For all responses, square biphasic electrical impulses of 0.5 ms pulse duration were delivered at a current of 1200 mA (Lindén *et al.*, 1991a;b). Control contractions were evoked at a stimulation frequency of 12 Hz with a total duration of 20 s. Selective NANC activation was performed with a frequency of 3 Hz and a total duration of 240 s with cholinergic blockade by atropine (1 μM) and adrenergic depletion by guanethidine (10 μM) (Kamikawa & Shimo, 1976; Andersson & Grundström, 1983; Brock & Cunnane, 1988) which produces pronounced tetrodotoxin-sensitive responses (Lindén *et al.*, 1991a). Simultaneous NANC and sympathetic activation was performed with the same stimulation parameters but with cholinergic blockade by atropine (1 μM) alone. When atropine and guanethidine were added, they were present continuously throughout the experiments.

Protocols

General procedures In all experiments, the spontaneous airway tone was abolished by indomethacin (10 μM) (Lindén *et al.*, 1991c) which was present continuously in the Krebs-Ringer solution. A passive tension of 1.2 g was applied to the preparation, followed by 25 min of initial equilibration and a control contraction induced by EFS. A wash-out was performed and the applied passive tension was re-adjusted to 1.2 g, which is near the optimum level for contractile responses to EFS (12 Hz for 20 s), in both the trachea and the main bronchus (data not shown). After this adjustment of passive tension, the protocols differed (see below). All the experiments ended, however, with a flushing period of 25 min followed by a maximum histamine-induced (0.1 mM) contraction without flushing.

Frequency-response characteristics for the NANC relaxant response with and without simultaneous sympathetic activation In these experiments only, the responses were related to and expressed as the percentage of the maximum response to EFS in each airway preparation. The additional relaxant effect induced by simultaneous sympathetic activation did thus not affect the results.

Preparations from the intermediate trachea were used. We did this because the intermediate trachea has a very weak contractile NANC response (data not shown) and this contractile response, with its slightly different frequency-response characteristics, could have confused the results (Lindén *et al.*, 1991a). After the initial control contraction, atropine and guanethidine or atropine alone was added; 70 min of drug incubation followed. A histamine-induced (6 μM) tone (approximately EC_{90}) was established during the last 20 min of the incubation period. After this increased level of tone had stabilized, a series of EFS (240 s) was performed in the following order: 0.3, 1, 3, 10, 30 Hz in two experiments and 30, 10, 3, 1, 0.3 Hz in two experiments. A wash-out followed each EFS and the tone was allowed to return to the pre-stimulatory level during a period of 60 min prior to the subsequent EFS.

Effects induced by the NANC response with and without simultaneous sympathetic activation In these experiments, we examined the effect of simultaneous sympathetic activation on the ability of the NANC response to counteract changes in tone prior to activation.

Preparations from the distal trachea and the main bronchi were used (Lindén *et al.*, 1990; 1991a,b). After the initial control contraction, atropine and guanethidine or atropine alone was added; 70 min of drug incubation followed, after which the first EFS (3 Hz for 240 s) was performed without any induced tone prior to activation. This EFS was followed by a wash-out and 25 min of flushing. A moderate level of tone was then induced (approximately EC_{40}) by histamine (0.3 μM) prior to EFS. The tone stabilized over a period of 20 min and a second EFS (3 Hz for 240 s) was performed. Another wash-out and 25 min of flushing followed and a high level of tone was then induced (approximately EC_{90}) by histamine (6 μM) prior to EFS. The tone stabilized over a period of 20 min and a third EFS (3 Hz for 240 s) with subsequent wash-out followed.

Interactions between sympathetic and NANC responses mediated by α-adrenoceptors These experiments were performed in order to determine whether there is an interaction between sympathetic and NANC responses which is mediated via α-adrenoceptors.

The protocol was identical to the previous one on the convergence effect (above) with one exception: after the initial control contraction and adjustment of the applied passive tension, atropine and prazosin (0.3 μM) and yohimbine (1 μM) or atropine alone was added. Prazosin and yohimbine were present continuously in order to establish α_1- and α_2-adrenoceptor blockade (Starke *et al.*, 1975; Cambridge *et al.*, 1977).

Interactions between sympathetic and NANC responses mediated by β-adrenoceptors In these experiments, we determined whether there is an interaction between sympathetic and NANC responses which is mediated via β-adrenoceptors.

The protocol was identical to the one on the convergence effect (above) with one exception: after the initial control contraction and adjustment of the applied passive tension, atropine and propranolol (1 μM) or atropine alone was added. Propranolol was present continuously in order to establish β-adrenoceptor blockade (Bilski *et al.*, 1983; Ellis & Farmer, 1989).

Data analysis

Tone levels For all but the frequency-response experiments, the tone levels were presented as follows. The total (active plus passive) tension (Lindén *et al.*, 1991c) was measured immediately before and at the end of each EFS and, in some experiments, 25 min after each EFS. The tension level before the first EFS, and thus before any addition of histamine, was regarded as purely passive tension (Lindén *et al.*, 1991c). Separate experiments demonstrated that the level of this passive tension was stable after the initial drug incubation period (data not shown). Within each airway preparation, the difference in tension between the level before the first EFS (240 s) and the peak level during the maximum histamine-induced contraction (0.1 mM) was regarded as the maximum active tension. Within each preparation, all the levels of active tension (tone) were then related to and expressed as the mean percentage (s.e.mean) of this maximum active tension (% of maximum tone).

Convergence effect This term describes the added magnitude of the converging contractile and relaxant responses to EFS

(Lindén et al., 1991b). The convergence effect was defined on the basis of the difference between the lowest level of tone (no histamine) and the highest level of tone (histamine 6 μM) which were established prior to EFS. The convergence effect was calculated as the decrease of this difference in tone induced by the converging contractile and relaxant responses to EFS.

Tonus equilibrium This estimation of the level of tone towards which the responses to EFS converged (Lindén et al., 1991b) reflects the balance between the contractile and relaxant responses to EFS. The tonus equilibrium was calculated within each preparation as the mean of the tone levels at the end of the three EFS evoked at different levels of tone.

Statistical evaluation The data are presented as the arithmetic mean (s.e.mean). Differences between the means of paired data were evaluated by Student's t distribution (two-tailed) determined at 95% confidence intervals (Colton, 1974). These confidence intervals are presented immediately after each comparison in the text (95% confidence interval for difference). n equals the number of guinea-pigs (independent observations).

Drugs

Atropine sulphate (Sigma), guanethidine sulphate (Ciba-Geigy), histamine dichloride (E. Merck) and (±)-propranolol hydrochloride (Sigma) were dissolved directly in Krebs-Ringer solution. Prazosin hydrochloride (Pfizer) and yohimbine hydrochloride (Sigma) were initially dissolved in ethanol (50%) producing less than 0.08% of ethanol in the organs baths after dilution. Indomethacin (Dumex, Confortid, 5 mg ml^{-1}) was diluted in Krebs-Ringer solution. All the concentrations (mM) refer to the final organ bath concentration.

Results

Characteristics of responses to electrical field stimulation

Without induced tone prior to EFS, in the presence of indomethacin, atropine and guanethidine, a contractile NANC response with one dominant phase was demonstrated in the main bronchus (Figure 1a). An increase in the tone prior to EFS, as a result of the addition of histamine (0.3 μM), reduced the magnitude of this NANC contraction. A further increase in the tone prior to EFS, produced by the addition of more histamine (6 μM), reversed the NANC contraction into a relaxation in 8/8 preparations. The configuration of the response to EFS was similar for the selective NANC activation and for the simultaneous NANC and sympathetic activation (Figures 1a and b). The simultaneous sympathetic activation did, however, modify the response to EFS towards more relaxation and less contraction. The distal trachea demonstrated a pattern similar to the main bronchus but tended to relax more (tracings not shown).

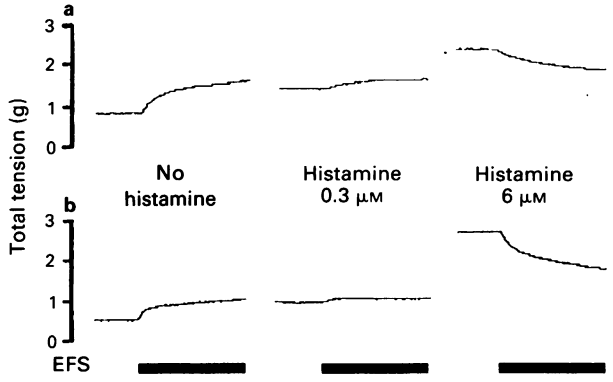

Figure 1 Original tracings from the guinea-pig isolated main bronchus showing the monophasic response to electrical field stimulation (EFS; 1200 mA, 0.5 ms, 3 Hz for 240 s) in the presence of atropine (1 μM), at a gradually increased histamine-induced (0–0.3–6 μM) tone prior to EFS within two airway preparations from the same guinea-pig, with (a) and without (b) adrenergic depletion by guanethidine (10 μM). Indomethacin (10 μM) was continuously present.

Frequency-response characteristics for the NANC relaxant response with and without simultaneous sympathetic activation

At 3 Hz, the added NANC and sympathetic relaxant response demonstrated a slightly higher degree of activation than the NANC response but this difference was not statistically significant (95% confidence interval for difference: −21–38% of maximum response to EFS, $n = 4$) (Figure 2). At the frequencies lower than 3 Hz, the corresponding difference tended to be more pronounced.

Effects induced by the NANC response with and without simultaneous sympathetic activation

Convergence effect During the selective NANC activation, a contractile response was evoked when the tone prior to EFS was low and a relaxant response was evoked when the tone prior to EFS was high. These NANC responses converged and this pattern was observed both with and without simultaneous sympathetic activation (Figure 3). In both these groups, the difference between the lowest and the highest level of tone prior to EFS was approximately 90% of maximum. The converging contractile and relaxant responses markedly reduced this difference in tone – a 'convergence effect'. The selective NANC activation and the simultaneous NANC and sympathetic activation did not display any pronounced difference in the magnitude of this convergence effect (Table 1). The small difference between the two treatment groups was not statistically significant in either the distal trachea (95% confidence interval for difference: −12–11% of maximum tone, $n = 8$) or the main bronchus (95% confidence interval for difference: −14–19% of maximum tone, $n = 8$). After EFS, the tone returned to a level similar to that prior to EFS (Figure 3).

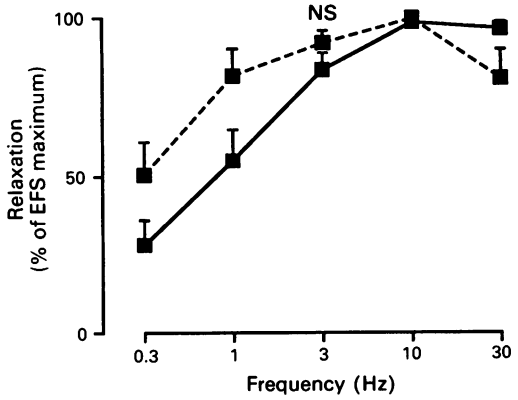

Figure 2 Frequency-response characteristics for the relaxant NANC response alone (continuous line) and with (dashed line) simultaneous sympathetic activation in the guinea-pig isolated intermediate trachea. Responses to electrical field stimulation (EFS; 1200 mA, 0.5 ms, for 240 s) were evoked at a histamine-induced (6 μM) tone in the presence of atropine (1 μM) with (continuous line) and without (dashed line) guanethidine (10 μM). Indomethacin (10 μM) was continuously present. The responses are presented as the mean (with bars indicating s.e.mean) percentage of the maximum relaxation induced by EFS in each airway preparation. NS = $P > 0.05$. $n = 4$.

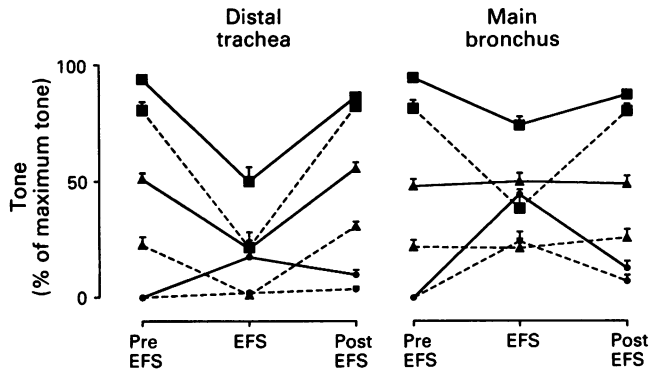

Figure 3 The effect on guinea-pig airway smooth-muscle tone induced by NANC activation only (continuous lines) and with (dashed lines) simultaneous sympathetic activation at various levels of tone prior to activation by electrical field stimulation (EFS; 1200 mA, 0.5 ms, 3 Hz for 240 s). The various tone levels prior to EFS were established by indomethacin (10 μM) only (●), histamine (0.3 μM) (▲) and histamine (6 μM) (■). EFS was performed in the presence of atropine (1 μM) with (continuous lines) and without (dashed lines) guanethidine (10 μM). The tone levels prior to (Pre EFS), at the end of (EFS) and after (Post EFS) electrical field stimulation are presented as the mean (with bars indicating s.e.mean) percentage of the maximum histamine-induced (0.1 mM) tone (% of maximum tone). $n = 8$.

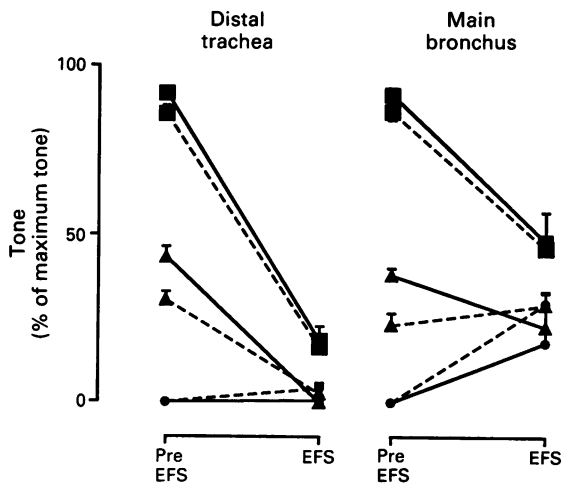

Figure 4 The effect of guinea-pig airway smooth-muscle tone induced by NANC and β-adrenoceptor activation only (continuous lines) and with (dashed lines) simultaneous α-adrenoceptor activation at various tone levels prior to electrical field stimulation (EFS – see Figure 3). EFS was performed in the presence of atropine (1 μM) with (continuous lines) and without (dashed lines) prazosin (0.3 μM) and yohimbine (1 μM). The tone prior to (PreEFS) and at the end of (EFS) electrical field stimulation is presented as in Figure 3. $n = 8$.

Tonus equilibrium The mean (s.e.mean) level of tone towards which the contractile and relaxant NANC responses converged, the 'tonus equilibrium', was lower with simultaneous sympathetic activation than without it: 8 (1)% compared with 30 (6)% in the distal trachea and 28 (4)% compared with 57 (2)% in the main bronchus (% of maximum tone). This difference was statistically significant in the distal trachea (95% confidence interval for difference: 9–34% of maximum tone, $n = 8$) and in the main bronchus (95% confidence interval for difference: 21–36% of maximum tone, $n = 8$).

Interactions between sympathetic and NANC responses mediated by α-adrenoceptors

Convergence effect During the simultaneous NANC and β-adrenoceptor activation, a contractile response was evoked when the tone prior to EFS was low and a relaxant response was evoked when the tone prior to EFS was high (Figure 4). These contractile and relaxant responses converged and this pattern was observed both with and without simultaneous α-adrenoceptor activation. In both these treatment groups, the convergence effect thus markedly reduced the difference in tone established prior to EFS, without any pronounced difference in the magnitude (Table 1). The small difference between the two treatment groups was not statistically significant in either the distal trachea (95% confidence interval for difference: −11–9% of maximum tone, $n = 8$) or the main bronchus (95% confidence interval for difference: −8–26% of maximum tone, $n = 8$).

Tonus equilibrium The mean level of the tonus equilibrium towards which the contractile and relaxant responses to EFS converged did not display any pronounced difference with and without α-adrenoceptor activation: 8 (2)% compared with 6 (1)% in the distal trachea and 35 (3)% compared with 30 (5)% in the main bronchus (% of maximum tone). The small differences between the two treatment groups were not statistically significant in either the distal trachea (95% confidence interval for difference: −6–3% of maximum tone, $n = 8$) or the main bronchus (95% confidence interval for difference: −10–20% of maximum tone, $n = 8$).

Interactions between sympathetic and NANC responses mediated by β-adrenoceptors

Convergence effect During the simultaneous NANC and α-adrenoceptor activation, a contractile response was evoked when the tone prior to EFS was low and a relaxant response was evoked when the tone prior to EFS was high (Figure 5). These contractile and relaxant responses converged and this pattern was observed both with and without simultaneous β-adrenoceptor activation. In both these treatment groups, the convergence effect thus markedly reduced the difference

Table I Convergence effect [mean (s.e.mean) % of maximum tone] induced by contractile and relaxant responses to electrical field stimulation in guinea-pig isolated airways

	n	Atropine plus guanethidine	Atropine	Atropine prazosin & yohimbine	Atropine	Atropine plus propranolol	Atropine
Distal trachea	8	62 (3)%	61 (4)%	74 (4)%	73 (2)%	49 (5)%	62 (4)%
Main bronchus	8	65 (3)%	68 (6)%	61 (7)%	70 (4)%	61 (4)%	66 (7)%

Convergence effect: the difference (70–90% of maximum tone) between the highest and lowest level of tone prior to electrical field stimulation was reduced by the converging contractile and relaxant responses to electrical field stimulation (1200 mA, 0.5 ms, 3 Hz for 240 s). Maximum tone: induced by histamine (0.1 mM). Drug concentrations: atropine (1 μM), guanethidine (10 μM), prazosin (0.3 μM), yohimbine (1 μM) and propranolol (1 μM). Treatment by atropine alone represents the paired control group.

in tone established prior to EFS, without any pronounced difference in the magnitude (Table 1). The small difference between the two treatment groups was not statistically significant in either the disal trachea (95% confidence interval for difference: −4–30% of maximum tone, $n = 8$) or the main bronchus (95% confidence interval for difference: −6–17% of maximum tone, $n = 8$).

Tonus equilibrium The mean level of the tonus equilibrium towards which the contractile and relaxant responses to EFS converged was lower with β-adrenoceptor activation than without it: 2 (1)% compared with 20 (4)% in the distal trachea and 25 (4)% compared with 46 (3)% in the main bronchus (% of maximum tone). This difference was statistically signifiant in the distal trachea (95% confidence interval for difference: 7–29% of maximum tone, $n = 8$) and in the main bronchus (95% confidence interval for difference: 11–30% of maximum tone, $n = 8$).

Effects on the tone before electrical field stimulation

The histamine-induced (0.3 μM) tone prior to EFS tended to be increased by treatment with guanethidine (Figure 3). A similar effect was produced by prazosin and yohimbine (Figure 4) but not by propranolol (Figure 5).

Maximum tension levels in experiments on the convergence effect

For all the treatment groups, the maximum active tension induced by histamine (0.1 mM) were within a limited range, both in the distal trachea and the main bronchus (Table 2).

Discussion

Our previous studies on the role of NANC responses in the regulation of airway smooth-muscle tone have demonstrated that contractile and relaxant NANC neural responses converge and thus tend to adjust tone towards a similar level, a tonus equilibrium (Lindén *et al.*, 1990; 1991b). The present data on guinea-pig airways extend the previous findings and indicate that simultaneous sympathetic activation does not significantly alter the magnitude of the convergence effect induced by contractile and relaxant NANC responses. The level of tone towards which the NANC responses converge appears, however, to be reduced by simultaneous sympathetic activation via a β-adrenoceptor mechanism.

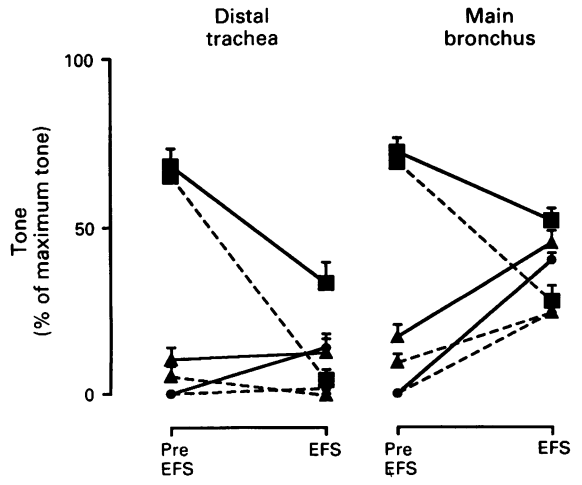

Figure 5 The effect on guinea-pig airway smooth-muscle tone induced by NANC and α-adrenoceptor activation only (continuous lines) and with (dashed lines) simultaneous β-adrenoceptor activation at various tone levels prior to electrical field stimulation (EFS – see Figure 3). EFS was performed in the presence of atropine (1 μM) with (continuous lines) and without (dashed lines) propranolol (1 μM). The tone prior to (PreEFS) and at the end of (EFS) electrical field stimulation is presented as in Figure 3. $n = 8$.

The magnitude of the NANC convergence effect was not significantly altered by simultaneous sympathetic activation. This lack of a significant sympathetic effect could not be attributed to an inadequate stimulation frequency for the sympathetic system as indicated by the frequency response experiments. These experiments demonstrated that 3 Hz, the stimulation frequency which was used in the convergence experiments, tended to favour slightly sympathetic activation rather than NANC activation although there was no statistically significant difference in the degree of activation. Separate experiments (data not shown) did not reveal any tachyphylaxis for contractile and relaxant NANC responses or sympathetic responses that could explain the constancy of the NANC convergence effect. Thus the lack of sympathetic effect on the magnitude of the NANC convergence effect cannot be attributed to methodological errors. The present finding therefore indicates that the ability of NANC responses to counteract changes in tone is not *per se* dependent upon sympathetic mechanisms. The stabilizing effect on tone might therefore be exclusive for the NANC neural response, at least in relation to sympathetic activation in guinea-pig airways.

The NANC convergence effect abolished the major part of the difference between the lowest and the highest level of tone established before electrical field stimulation. This means that the NANC responses counteracted variations in tone ranging from 0% of maximum to approximately 70 to 90% of maximum. NANC neural activation can thus produce a significant regulatory power and in this respect, the present study confirms our previous studies on NANC responses in guinea-pig airways (Lindén *et al.*, 1990; 1991b).

The level of the tonus equilibrium towards which the contractile and relaxant NANC responses converged was significantly reduced by sympathetic activation and this modulation of the NANC responses towards more relaxation was mediated by β-adrenoceptors. The sympathetic response thus appears to interact functionally with the NANC response which might provide additional protection from severe airway smooth-muscle contraction. According to another study on guinea-pig airways (Verleden *et al.*, 1991a), the site of this type of β-adrenoceptor interaction is both pre- and postjunctional and also offers a pathway accessible for exogenous β_2-agonists.

Prejunctional α_2-adrenoceptor activation can inhibit the contractile NANC response in guinea-pig airways (Grundström *et al.*, 1984). We therefore examined whether α-adrenoceptor blockade alters the level of the tonus equilibrium towards which the NANC responses converge. The lack of a significant α-adrenergic effect on the tonus equilibrium does, however, militate against prejunctional α_2-adrenoceptors having any functional importance in the modulation of the contractile NANC airway response.

The histamine-induced tone prior to electrical field stimulation tended to be increased by adrenergic depletion with guanethidine. It could therefore be argued that the increase of the tonus equilibrium seen after treatment by guanethidine was not directly related to its sympatholytic effects. This seems unlikely, however, since both guanethidine and the β-adrenoceptor blocker, propranolol, significantly increased the tonus equilibrium but propranolol induced only a very small increase of the histamine-induced tone prior to electrical field stimulation. Further evidence against an indirect effect of guanethidine is provided by the observation that α-adrenoceptor blockade by prazosin and yohimbine markedly increased the histamine-induced tone but tended to decrease the tonus equilibrium slightly.

Relaxant responses to sympathetic neural activation by electrical field stimulation have previously been demonstrated in the trachea but not in the main bronchus of the guinea-pig (Kamikawa & Shimo, 1976; Taylor *et al.*, 1984; Ellis &

Table 2 Maximum histamine-induced active tension [mean (s.e.mean) in g] in guinea-pig isolated airways

	n	Atropine plus guanethidine	Atropine	Atropine, prazosin & yohimbine	Atropine	Atropine plus propranolol	Atropine
Distal trachea	8	2.56 (0.19)	3.00 (0.23)	3.13 (0.31)	2.52 (0.22)	2.65 (0.30)	2.98 (0.30)
Main bronchus	8	2.51 (0.25)	2.62 (0.31)	2.79 (0.39)	2.97 (0.32)	3.50 (0.24)	3.02 (0.28)

Active tension: the difference in tension between the recorded level and the level of passive tension. Drug concentrations: atropine (1 μM), guanethidine (10 μM), histamine (0.1 mM), prazosin (0.3 μM), yohimbine (1 μM) and propranolol (1 μM). Treatment by atropine alone represents the paired control group.

Farmer, 1989). Souhrada *et al.* (1980) did, however, find a relaxant response to electrical field stimulation in the guinea-pig main bronchus but did not determine whether or not this response was adrenergic. The present finding of a β-adrenergic relaxant response in the guinea-pig main bronchus therefore provides new information which is consistent with sympathetic nerves being present in the more peripheral airways of the guinea-pig. This finding has methodological implications and indicates that studies on drug-induced modulation of the contractile NANC response should be conducted using adrenergic depletion or β-adrenoceptor blockade. If adrenergic depletion or β-adreoceptor blockade is not established, a drug-induced alteration of the sympathetic response might confuse the interpretation of the results (compare Kamikawa & Shimo, 1989; Verleden *et al.*, 1991b).

In man, there is little evidence of a significant neural sympathetic effect on airway smooth-muscle tone and the adrenergic effect on tone is most probably exerted primarily by circulating catecholamines (Partanen *et al.*, 1982; Laitinen *et al.*, 1985; Taylor *et al.*, 1984; Palmer *et al.*, 1986). The present demonstration of a sympathetic modulation of NANC responses is therefore not directly applicable to the conditions in human airways. Nevertheless, the sympathetic response in guinea-pig airways is an endogenous, adrenergic and relaxant response which, as in human airways, is mediated primarily via β_2-adrenoceptors (Kamikawa & Shimo, 1976; Johansson & Waldeck, 1981; Zaagsma *et al.*, 1984). The sympathetic modulation of NANC responses might therefore constitute an example of an interaction between β_2-adrenergic and NANC responses which could contribute to the physiological control of airway smooth-muscle tone.

In line with our previous data on guinea-pig airways (Lindén *et al.*, 1991b), functional studies on human isolated airways have demonstrated NANC responses which are tetrodotoxin-sensitive and stimulation-frequency-dependent (Lundberg *et al.*, 1983; Taylor *et al.*, 1984; Palmer *et al.*, 1986). There is also evidence of contractile and relaxant NANC responses in human airways *in vivo* as there is in the guinea-pig (Fuller *et al.*, 1985; Ichinose *et al.*, 1988; Lammers *et al.*, 1988; Venugopalan *et al.*, 1991). Further, the present pattern, with a contractile NANC response evoked at a low tone prior to activation and of the relaxant NANC response at a high tone prior to activation is similar to the pattern seen after sensory nerve activation by capsaicin in human subjects. In man and without induced tone prior to inhalation, inhaled capsaicin produces non-cholinergic bronchoconstriction (Fuller *et al.*, 1985), whereas, when an induced tone is present prior to inhalation, inhaled capsaicin produces NANC bronchodilatation (Ichinose *et al.*, 1988; Lammers *et al.*, 1988). If these findings reflect the same mechanisms, then NANC neural responses may stabilize human airway smooth-muscle tone as well. At the present state of knowledge, it thus seems possible that the NANC convergence effect is present in human airways and that it can be modulated by β-adrenoceptor activation, since β-agonists readily relax human bronchial smooth-muscle (Palmer *et al.*, 1986).

In conclusion, the present study indicates that the NANC neural response can counteract pronounced changes in airway smooth-muscle tone with and without sympathetic activation in the guinea-pig. This stabilizing effect on tone might *per se* be exclusive for the NANC response in relation to adrenergic activation. β-Adrenoceptor activation can, however, reduce the level of tone towards which the contractile and relaxant NANC responses converge, thereby suggesting an interaction which provides protection from severe airway smooth-muscle contraction.

This study was approved by the Experimental Ethics Committee of the Medical Faculty of the University of Göteborg (Dno 92/89). The authors wish to thank the Swedish Medical Research Council, the Swedish Heart-Lung Fund and Hermann Krefting's Foundation for financial support.

References

ANDERSSON, R.G.G. & GRUNDSTRÖM, N. (1983). The excitatory non-cholinergic, non-adrenergic nervous system of the guinea-pig airways. *Eur. J. Respir. Dis.*, **131**, 141–157.

ANDERSSON, R.G.G. & GRUNDSTRÖM, N. (1987). Innervation of airway smooth muscle. Efferent mechanisms. *Pharmacol. Ther.*, **32**, 107–130.

BARNES, P.J. (1986). Neural control of human airways in health and disease. *Am. Rev. Respir. Dis.*, **134**, 1289–1314.

BARNES, P.J. (1991). Neuropeptides and asthma. *Am. Rev. Respir. Dis.*, **143**, S28–S32.

BILSKI, A.J., HALLIDAY, S.E., FITZGERALD, J.D. & WALE, J.L. (1983). The pharmacology of a selective β2-selective adrenoceptor antagonist (ICI 118,551). *J. Cardiovasc. Pharmacol.*, **5**, 430–437.

BROCK, J.R. & CUNNANE, T.C. (1988). Studies on the mode of action of bretylium and guanethidine in post-ganglionic sympathetic nerve fibres. *Naunyn-Schmidebergs Arch. Pharmacol.*, **338**, 504–509.

CAMBRIDGE, D., DAVEY, M.J. & MASSINGHAM, R. (1977). Prazosin, a selective antagonist of post-synaptic α-adrenoceptors. *Br. J. Pharmacol.*, **59**, 514–515.

COLTON, T. (1974). *Statistics in Medicine*. 1st ed. Boston, USA: Little, Brown and Company.

ELLIS, J.L. & FARMER, S.G. (1989). The effects of vasoactive intestinal peptide (VIP) antagonists, and VIP and peptide histidine isoleucine antisera on non-adrenergic, non-cholinergic relaxations of tracheal smooth muscle. *Br. J. Pharmacol.*, **96**, 513–520.

FULLER, R.W., DIXON, C.M.S. & BARNES, P.J. (1985). Bronchoconstrictor response to inhaled capsaicin in humans. *J. Appl. Physiol.*, **85**, 1080–1084.

GRUNDSTRÖM, N., ANDERSSON, R.G.G & WIKBERG, J.E.S. (1984). Inhibition of the excitatory non-adrenergic, non-cholinergic neurotransmission in the guinea pig tracheo-bronchial tree mediated by alpha-2-adrenoceptors. *Acta Pharmacol. Toxicol.*, **54**, 8–14.

ICHINOSE, M., INOUE, H., MIURA, M. & TAKISHIMA, T. (1988). Non-adrenergic bronchodilation in normal subjects. *Am. Rev. Respir. Dis.*, **138**, 31–34.

JOHANSSON, U. & WALDECK, B. (1981). β-Adrenoceptors mediating relaxation of the guinea pig trachea: experiments with prenalterol, a β1-selective adrenoceptor agonist. *J. Pharm. Pharmacol.*, **33**, 353–356.

KAMIKAWA, Y. & SHIMO, Y. (1976). Pharmacological differences of non-adrenergic inhibitory response and of ATP-induced relaxation in guinea-pig tracheal strip-chains. *J. Pharm. Pharmacol.*, **28**, 854–855.

KAMIKAWA, Y. & SHIMO, Y. (1989). Adenosine selectively inhibits noncholinergic transmission in guinea pig bronchi. *J. Appl. Physiol.*, **66**, 2084–2091.

LAITINEN, A., PARTANEN, M., HERVONEN, A. & LAITINEN, L.A. (1985). Electron microscopic study on the innervation of the human lower respiratory tract: evidence of adrenergic nerves. *Eur. J. Respir. Dis.*, **67**, 209–215.

LAMMERS, J.-W.J., MINETTE, P., MCCUSKER, M.T., CHUNG, K.F. & BARNES, P.J. (1988). Nonadrenergic bronchodilator mechanisms in normal human subjects in vivo. *J. Appl. Physiol.*, **64**, 1817–1822.

LINDÉN, A., LÖFDAHL, C.-G., ULLMAN, A. & SKOOGH, B.-E. (1990). The non-adrenergic, non-cholinergic nervous system stabilizes airway tone altered by indomethacin and histamine in the guinea-pig. *Eur. J. Respir. Dis.*, **3**, 69, A61.

LINDÉN, A., ULLMAN, A., SKOOGH, B.-E. & LÖFDAHL, C.-G. (1991a). Non-adrenergic, non-cholinergic regulation of guinea pig airway smooth-muscle – indomethacin-induced changes and segmental differences. *Pulm. Pharmacol.*, **4**, 170–176.

LINDÉN, A., ULLMAN, A., LÖFDAHL, C.-G. & SKOOGH, B.-E. (1991b). Non-adrenergic, non-cholinergic neural activation stabilizes smooth muscle tone independently of eicosanoid factors in guinea-pig isolated airways. *Br. J. Pharmacol.*, **104**, 509–513.

LINDÉN, A., LÖFDAHL, C.-G., ULLMAN, A. & SKOOGH, B.-E. (1991c). In vitro characteristics of spontaneous airway tone in the guinea pig. *Acta Physiol. Scand.*, **142**, 351–357.

LUNDBERG, J.M., MARTLING, C.-R. & SARIA, A. (1983). Substance P and capsaicin-induced contraction of human bronchi. *Acta Physiol. Scand.*, **119**, 49–53.

PALMER, J.B.D., CUSS, F.M.C. & BARNES, P.J. (1986). VIP and PHM and their role in non-adrenergic inhibitory responses in isolated human airways. *J. Appl. Physiol.*, **61**, 1322–1328.

PARTANEN, M., LAITINEN, A., HERVONEN, A., TOIVANEN, M. & LAITINEN, L.A. (1982). Catecholamine- and acetylcholinesterase-containing nerves in human lower respiratory tract. *Histochemistry*, **76**, 175–188.

SOUHRADA, J.F., MELZER, E. & GRANTHAM, P. (1980). Some characteristics of the purinergic nervous system in normal and sensitized airway smooth muscle. *Respir. Physiol.*, **40**, 199–209.

STARKE, K., BOROWSKI, E. & ENDO, T. (1975). Preferential blockade of presynaptic alpha-adrenoceptors by yohimbine. *Eur. J. Pharmacol.*, **34**, 385–388.

TAYLOR, S.M., PARÉ, P.D. & SCHELLENBERG, R.R. (1984). Cholinergic and non-adrenergic mechanisms in human and guinea pig airways. *J. Appl. Physiol.*, **56**, 958–965.

ULLMAN, A., CIABATTONI, G., LÖFDAHL, C-G., LINDÉN, A., SVEDMYR, N. & SKOOGH, B.-E. (1990). Epithelium-derived PGE2 inhibits the contractile response to cholinergic stimulation in isolated ferret trachea. *Pulm. Pharmacol.*, **3**, 155–160.

VENUGOPALAN, C.S., HOLMES, E.P., FUCCI, V. & GUTHRIE, A.J. (1991). Stimulation frequency-dependent nonadrenergic, noncholinergic airway responses of the guinea-pig. *J. Appl. Physiol.*, **70**, 1006–1010.

VERLEDEN, G.M., BELVISI, M.G., RABE, K. & BARNES, P.J. (1991a). Inhibition of non-adrenergic, non-cholinergic neural bronchoconstriction in guinea-pig airways in vitro by β2-adrenoceptors. *Am. Rev. Respir. Dis.*, **143**, A357.

VERLEDEN, G.M., BELVISI, M.G., STRETTON, C.D. & BARNES, P.J. (1991b). Nedocromil sodium modulates non-adrenergic, non-cholinergic bronchoconstrictor nerves in guinea-pig airways in vitro. *Am. Rev. Respir. Dis.*, **143**, 114–118.

ZAAGSMA, J., VAN DER HEIJDEN, P.J.C.M., VAN DER SCHAAR, M.W.G. & BANK, C.M.C. (1984). Differentiation of functional adrenoceptors in human and guinea-pig airways. *Eur. J. Respir. Dis.*, **64**, (S135), 16–33.

(Received December 20, 1991
Revised February 20, 1992
Accepted March 12, 1992)

Br. J. Pharmacol. (1992), **106**, 623–627

Kinetics of nicotinic acetylcholine ion channels in the presence of intravenous anaesthetics and induction agents

[1]Ruth E. Wachtel & Edward S. Wegrzynowicz

Department of Veterans Affairs Medical Center, Iowa City, IA 52246 and Department of Anesthesia, College of Medicine, University of Iowa, Iowa City, IA 52242, U.S.A.

1 Single channel currents activated by 250 nM acetylcholine were recorded from cell-attached patches of BC3H1 mouse tumour cells grown in culture. Channels were recorded in the absence and presence of alphaxalone, diazepam, etomidate, fentanyl, ketamine, meperidine, or propofol.

2 All of the anaesthetics tested shortened channel open time but did not alter single channel current amplitude. Drug concentrations calculated to reduce the time constant of open-time distributions by 50% were 99 μM alphaxalone, 66 μM diazepam, 57 μM etomidate, 26 μM fentanyl, 15 μM ketamine, 16 μM meperidine, or 81 μM propofol.

3 Ketamine, meperidine, and propofol reduced channel open time at concentrations comparable to plasma levels attained during therapeutic use of these agents, while alphaxalone, diazepam, etomidate, and fentanyl reduced channel open time only at levels higher than those encountered clinically.

4 The potency of these drugs in decreasing channel open time appears to be directly correlated with their octanol/buffer partition coefficients. In contrast to expectations, however, agents with higher partition coefficients were less potent in altering channel open time.

5 Ketamine and meperidine produced a prominent third component in closed-time distributions, which were otherwise well described by the sum of two exponential components. Alphaxalone, diazepam, and etomidate also produced a small third component, while no additional component was seen with propofol or fentanyl. These additional components probably arise from creation of an additional closed state of the channel.

6 We conclude that these agents are not altering channel properties merely by exerting non-specific effects via the lipid bilayer and that they are probably not all acting by similar mechanisms.

Keywords: Acetylcholine: receptor channels; analgesics: opioid: fentanyl, meperidine; anaesthetics: intravenous: etomidate, fentanyl, ketamine, meperidine, propofol; anaesthetics: steroid: alphaxalone; electrophysiology: flickering blockade; patch clamp; hypnotics: diazepam; etomidate; receptors: acetylcholine

Introduction

A wide variety of general anaesthetic compounds depress responses to acetylcholine (ACh). At the motor endplate, the decay rate of endplate currents is increased by potent volatile agents, long chain aliphatic alcohols, and barbiturates (Gage & Hamill, 1976; Torda & Gage, 1977; Gage *et al.*, 1978). Single channel recordings have confirmed that all of these agents decrease the open time of ACh-activated ion channels (Lechleiter & Gruener, 1984; Gate & McKinnon, 1985; Murrell *et al.*, 1991; Wachtel & Wegrzynowicz, 1991).

The mechanisms by which pharmacological agents decrease the open time of ACh-activated channels is not well understood. Some agents, such as barbiturates, are thought to enter the open channel to block it (Adams, 1976). Other drugs are thought to partition into the lipid phase of the membrane and alter fluidity in the vicinity of the channel (see reviews by Trudell, 1991; Ueda, 1991). For compounds with general anaesthetic properties, clinical potency in inducing general anaesthesia appears to be directly related to lipid solubility, usually measured as oil/water or octanol/buffer partition coefficient. This suggests that non-specific interactions with hydrophobic moieties may underlie some of the clinical effects of these drugs, and that anaesthetic solubility in the membrane may determine effectiveness.

At the single channel level, the potency of compounds with general anaesthetic properties may also be a function of lipid solubility. Alternatively, these agents may each be interacting with the channel in a unique fashion unrelated to lipid solubility.

The purpose of this study was to compare the effects of a variety of anaesthetic compounds and induction agents, with widely differing structures, in order to determine whether their potency in reducing the open time of ACh-activated channels is a non-specific function of lipid solubility, or whether their effects on ACh-activated channels exhibit structural specificity.

Methods

The methods used in these experiments have been described previously (Wachtel, 1988a; 1990). Patch clamp techniques were used to record single channel currents activated by ACh from cell-attached patches of BC3H1 mouse tumour cells grown in culture. BC3H1 is a muscle-like clonal cell line derived from a mouse cerebrovascular tumour. Cells express nicotinic receptors for ACh when allowed to differentiate in serum-free medium (Munson *et al.*, 1982; Olson *et al.*, 1983). ACh-activated channels in BC3H1 cells have been studied extensively by Sine & Steinbach (1984; 1986).

Cells were bathed in a Ringer solution containing (mM): NaCl 100, KCl 4, $CaCl_2$ 2, $MgCl_2$ 5 and HEPES 10, pH 7.4. Electrodes had resistances of 2–5 Mohm. They were filled with bathing solution containing 250 nM ACh plus anaesthetic agent. Experiments were performed at controlled room temperature (18–22°C).

Dilutions of diazepam (Valium, Roche), etomidate (Amidate, Abbott Laboratories), fentanyl citrate (Sublimaze,

[1] Author for correspondence at: Research Service (151), VA Medical Center, Iowa City, IA 52246, U.S.A.

Janssen Pharmaceutica), ketamine (Ketaset, Aveco), and meperidine (pethidine; Demerol, Winthrop-Breon) were prepared daily. A 10 mM alphaxalone stock was prepared weekly by dissolving the powder (courtesy of Glaxo, Inc) in propylene glycol (1:10), and this stock was diluted daily to yield final concentrations of 20–500 μM in Ringer. The maximum concentration of propylene glycol in the final dilution was 1:200. A propofol (Aldrich) stock of approximately 500 μM was prepared by carefully adding 2 μl to 21 ml Ringer solution. The mixture was gently warmed and sonicated until the propofol was fully dispersed, then diluted daily. The exact concentration of this stock solution was determined by gas chromatography to be 493 μM.

Single channel opening events were recorded with the patch pipette hyperpolarized + 75 mV relative to cell resting potential, which was estimated to be − 59 mV based on a null potential of 0 mV for ACh-activated currents. Thus the potential across the membrane patch was − 134 mV. Signals were low pass filtered at 5 kHz, digitized at 20 μs per point and stored on an AST Premium 286 computer. Single channel events were analyzed to determine channel amplitude and open and closed durations with pCLAMP software package (Axon Instruments). Events containing more than one channel open at a time were not included in the analysis. Average channel amplitude was calculated from the mean amplitude of events > 500 μs in duration. Channel open-time and closed-time distributions were described as sums of exponential components. Parameters were estimated by the method of maximum likelihood (Wachtel, 1988b; 1991). Open-time distributions were corrected for missed openings less than 0.1 ms in duration, but were not corrected for undetected closed times. Similarly, closed-time distributions were corrected for missed closings less than 0.1 ms in duration, but were not corrected for undetected opening events.

Octanol/buffer partition coefficients of ketamine and alphaxalone were measured by gas chromatography because values could not be found in the literature. Aliquots of 10 mM ketamine (10 ml) or 50 mM alphaxalone (4 ml) in 0.1 mM phosphate buffer were mixed with equal volumes of octanol and shaken vigorously. The two phases were separated by centrifugation and the pH of the aqueous phase after centrifugation was 7.4. Samples of the aqueous phase (4 μl for ketamine, 10 μl for alphaxalone) were injected onto a gas chromatograph equipped with a 6-foot column packed with 3% OV-101 on 120/140 gas-chrom Q at 250°C and a flame ionization detector. Similar volumes of standard solutions of known concentrations were also injected. Retention times were 7.5 min for ketamine and 5.4 min for alphaxalone. The octanol/buffer partition coefficient was defined as the ratio of drug concentration remaining in the octanol phase, assumed to be 10 mM ketamine or 50 mM alphaxalone, to the concentration in the aqueous phase. Calculated partition coefficients were 60 for ketamine and 1900 for alphaxalone.

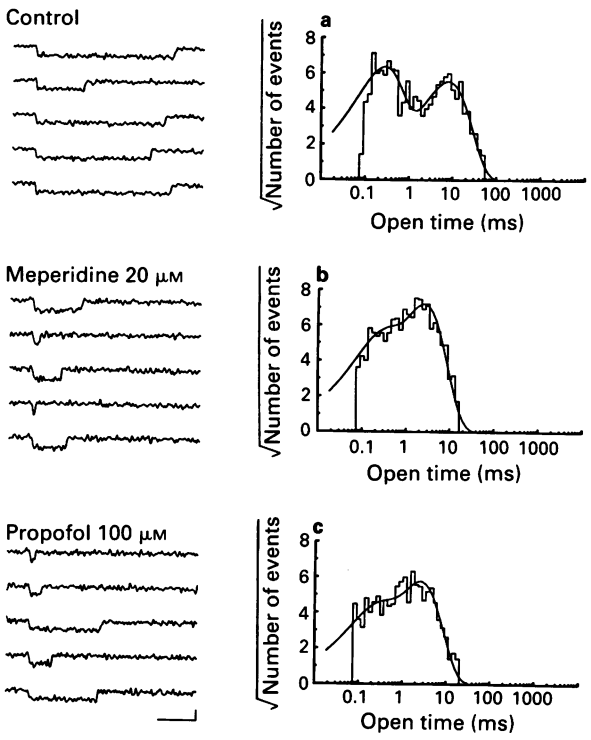

Figure 1 *Left panel*: representative single channel currents activated by 250 nM acetylcholine (ACh) from cell attached patches of BC3H1 cells. Opening events are shown as downward deflections. Channels were recorded in the absence of anaesthetic (control), or with meperidine (20 μM) or propofol (100 μM) in the recording electrode. In the presence of anaesthetic, opening events appeared much briefer in duration. Similar results were obtained with alphaxalone, diazepam, etomidate, fentanyl, and ketamine. Patch potential + 75 mV. Calibration marks 2 ms and 3 pA. *Right panel*: representative open-time histograms. Note logarithmic abscissa and square root ordinate scales. Each smooth curve is the square root of the probability density function corresponding to the sum of 2 exponential components, with time constants τ_f and τ_s ($\tau_f < \tau_s$) and fast component amplitude A_f. The probability density function for each component is exp {ln(t) − ln(τ) − exp [ln(t) − ln(τ)]} multiplied by the number of events in that component times the bin width (Sigworth & Sine, 1987). (a) ACh 250 nM. $\tau_f = 0.26$ ms, $\tau_s = 7.91$ ms, and $A_f = 0.55$. N = 770 events. (b) ACh 250 nM plus meperidine 20 μM. $\tau_f = 0.22$ ms, $\tau_s = 2.50$ ms, and $A_f = 0.27$. N = 852 events. (c) ACh 250 nM plus propofol 100 μM. $\tau_f = 0.21$ ms, $\tau_s = 2.43$ ms, and $A_f = 0.27$. N = 540 events. All of the anaesthetics tested shifted channel open-time distributions toward faster times.

Results

Figure 1 (left panel) shows examples of representative single channel currents activated by 250 nM ACh in the absence and presence of meperidine or propofol. With anaesthetic in the recording electrode, individual opening events appear briefer in duration. All of the agents tested produced qualitatively similar results and decreased the open duration of ACh-activated channels.

Amplitudes

None of the drugs tested altered mean single channel current amplitude, which was 2.68 ± 0.19 pA (mean ± s.d. from n = 49 patches) in the absence of anaesthetic. Channels were either non-conducting or fully-conducting, indicating that channel conductance was altered in an all or none fashion. This lack of effect on single channel amplitude suggests that the anaesthetics were not inducing a rapid flickering block of the open state that was not resolved by the recording system. An extremely rapid flickering block that was low-pass filtered would appear as an apparent reduction in single channel amplitude.

Open times

The distribution of open times from patches exposed to either 250 nM ACh or 250 nM ACh plus 20 μM meperidine or 100 μM propofol are shown in the right panel of Figure 1. Individual open times have been sorted into logarithmically spaced bins to form a histogram. For each of these patches the distribution of open times is well described by the sum of 2 exponential components, $A_f \exp(-t/\tau_f) + (1-A_f) \exp(-t/\tau_s)$, where t is open time and τ_f and τ_s are time constants ($\tau_f < \tau_s$). Similar distributions were obtained with the other agents. For these patches in which both components of open-time distributions could be clearly resolved, $\tau_f = 0.39 \pm 0.20$ (mean ± s.d. from $n = 26$ out of 39 patches) in the absence of anaesthetic and was not altered in any consistent manner by the agents tested.

For patches exposed to higher concentrations of anaesthetic, the faster component was not always apparent and a single time constant was adequate to describe the data. τ (or τ_s for 2-component distributions) was 6.92 ± 1.39 ms ($n = 39$) in the absence of anaesthetic and was decreased in a dose-dependent manner by all of the agents tested (Figure 2).

Based on these dose-response relationships, an EC_{50} was calculated for each anaesthetic (Table 1), where EC_{50} is the concentration that reduced τ_s, or τ, by 50%. EC_{50}s range from a low of 15 μM for ketamine to a high of 99 μM for alphaxalone, a difference of approximately 6 fold.

If the potency of a compound in reducing the open time of ACh-activated channels were solely a function of its concentration in the membrane, then drug potency should be directly correlated with lipid solubility. Figure 3 shows the relationship between EC_{50} and octanol/buffer partition coefficient, used as a measure of lipid solubility, for all of the agents tested. Indeed, the potency of these drugs in decreasing channel open time appears to be directly correlated with their partition coefficients. However, those agents with higher partition coefficients were actually less potent in altering channel open time. This is exactly the opposite of what would be predicted if the potency of a substance were determined merely by its tendency to partition into the membrane. Thus factors other than simple lipid solubility must underlie drug effects on these channels. In order to look for some evidence of a specific interaction between the anaesthetics and ACh-activated channels, as opposed to an interaction based on the colligative properties of drug molecules in the membrane, closed-time distributions were also examined.

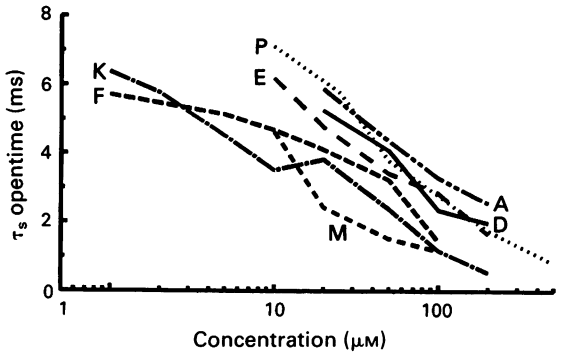

Figure 2 All of the agents tested decreased channel open time in a concentration-dependent manner. τ_s has been used as an indication of channel open time for those patches in which two exponential components were required to describe open-time distributions. Lines are labelled A = alphaxalone; D = diazepam, E = etomidate; F = fentanyl; K = ketamine; M = meperidine; P = propofol. Data points and error bars have been omitted for clarity. In the absence of anaesthetic, τ_s was 6.92 ± 1.39 ms ($n = 39$ patches). Drug concentrations that reduced τ_s by 50% are shown in Table 1.

Table 1 Comparison between EC_{50} values and peak blood levels usually attained after intravenous administration of therapeutic doses

	EC_{50} (μM)	*Peak plasma level (μM)*	*Intravenous dose*
Alphaxalone	99	12	0.4 mg kg^{-1}
Diazepam	66	70	20 mg
Etomidate	57	4.0	0.3 mg kg^{-1}
Fentanyl	26	0.06	50 μg kg^{-1}
Ketamine	15	8.4	2.5 mg kg^{-1}
Meperidine	16	3.6	50 mg
Propofol	81	34	2.5 mg kg^{-1}

Alphaxalone: Hillestad *et al.*, 1974; Sear & Prys-Roberts, 1979; diazepam: Reidenberg *et al.*, 1978; etomidate: Van Hamme *et al.*, 1978; Schuttler *et al.*, 1980; De Ruiter *et al.*, 1981; fentanyl: Hug, 1984; ketamine: Johnston *et al.*, 1974; Wieber *et al.*, 1975; meperidine: Mather *et al.*, 1974; propofol: Cockshott, 1985; Schuttler *et al.*, 1985; Kirkpatrick *et al.*, 1988; Shafer *et al.*, 1988.

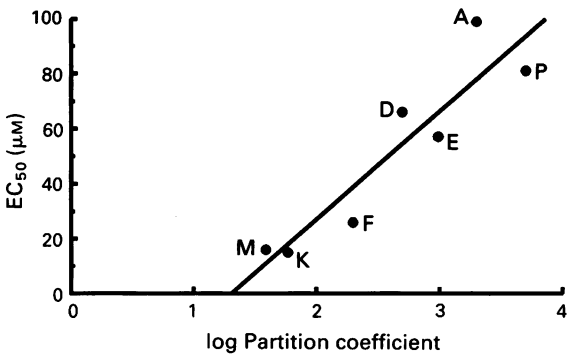

Figure 3 Relationship between the octanol/buffer partition coefficient of a drug and its EC_{50}, the concentration that reduces channel open time by 50% (listed in Table 1). Partition coefficients for alphaxalone (1900) and ketamine (60) were measured; values for diazepam (500), etomidate (1000), fentanyl (200), meperidine (40), and propofol (5000) are from the literature (Leo *et al.*, 1971; Heykants *et al.*, 1975; Hug, 1984; James & Glen, 1980). The EC_{50} for ketamine is from Wachtel (1988). Line is a least squares fit with correlation coefficient 0.92. In contrast to predictions, drugs with higher partition coefficients were less potent in decreasing channel open time.

Closed times

Figure 4 shows typical closed-time distributions for patches exposed to either 250 nM ACh or 250 nM ACh plus 20 μM meperidine or 100 μM propofol. Closed-time distributions for channels activated by ACh typically have 2 distinct components, a rapid closed time τ_f representing gaps within a burst, and a slower closed time τ_s representing gaps between bursts.

Channel closed-time distributions obtained in the presence of meperidine contained an additional intermediate component with time constant τ_i and relative amplitude A_i. At 20 μM meperidine, τ_i = 21.5 ± 9.1 ms and A_i = 0.39 ± 0.05 ($n = 5$). A similar new intermediate component was also observed with ketamine. Apparent differences in τ_s between patches do not necessarily reflect drug-induced changes in channel opening rate, but may simply be due to differences in the number of active channels in each patch.

No additional component in closed-time distributions was observed with propofol ($n = 34$) or fentanyl ($n = 29$). Alphaxalone, diazepam, and etomidate sometimes generated a small third component with amplitude less than 10%, although these findings have not yet been analyzed in detail.

Discussion

All of the agents tested decreased the open time of ion channels activated by ACh. Table 1 shows plasma levels normally attained during therapeutic use of these drugs. Ketamine, meperidine, and propofol altered channel properties at concentrations similar to those encountered clinically. Reductions in the open time of ACh-activated channels may be significant during use of ketamine, meperidine, and propofol, and may contribute to some of the clinical properties and side effects of these agents.

Alphaxalone, diazepam, etomidate, and fentanyl significantly reduced channel open time only at concentrations at least 8 times higher than clinical levels. Fentanyl, a potent synthetic opiate, altered channel properties at concentrations similar to those required for the other agents, but at

concentration 400 times greater than plasma levels. The lack of effect of alphaxalone, diazepam, and fentanyl at clinical concentrations is consistent with theories that these compounds exert their clinical effects by binding to specific receptor sites in the central nervous system. Alterations in the properties of ACh-activated ion channels are most probably unrelated to the clinical properties of these agents.

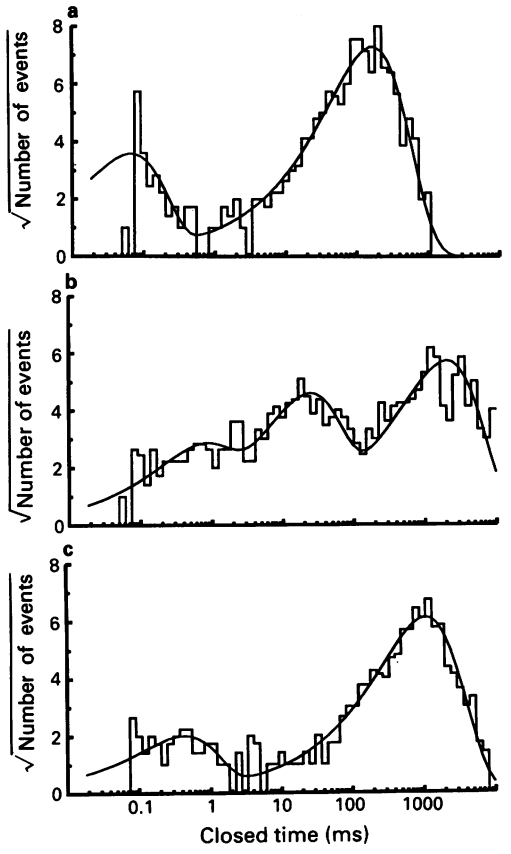

Figure 4 Representative closed-time histograms. Meperidine produces a prominent third component in the distributions, while propofol does not. (a) ACh 250 nM. The distribution of channel open times is described by a function that is the sum of two exponential components, with $\tau_f = 0.07$ ms, $\tau_s = 166$ ms, and $A_f = 0.19$. N = 763 events. (b) ACh 250 nM plus meperidine 20 μM. Three exponential components are required to describe the closed-time distribution, with $A_f = 0.11$, $\tau_f = 0.67$ ms, $A_i = 0.34$, $\tau_i = 23.6$ ms, and $\tau_s = 2032$ ms. N = 801 events. (c) ACh 250 nM plus propofol 100 μM. Two components are adequate, with $\tau_f = 0.43$ ms, $\tau_s = 1116$ ms, and $A_f = 0.10$. N = 545 events. Patch potential + 75 mV.

Lipid solubility, measured in terms of octanol/buffer partition coefficient, does not seem to be an important factor that determines the ability of a drug to decrease the open time of ACh-activated channels in these cells. This finding suggests that it is unlikely these drugs are acting merely by exerting non-specific effects via hydrophobic interactions.

The finding that ketamine and meperidine cause the appearance of a new, intermediate component in channel closed-time distributions suggests the appearance of a new closed state of the channel. Additional experiments are in progress to determine whether this new closed state may arise from block of the open channel by molecules of drug, and also to describe in more detail the changes in closed-time distributions produced by alphaxalone, diazepam, and etomidate.

Propofol and fentanyl, however, did not cause the appearance of an additional component in closed-time distributions, suggesting that a different mechanism may underlie their effects. Although it is possible that these agents were producing a third component in closed time distributions that was not resolved, this component would have to have represented less than 2–3% of events to remain undetected (Wachtel, 1991). The observed constancy of single channel amplitude indicates that these drugs were not inducing an extremely fast flickering type block of the open state that was unresolved due to bandwidth limitations. Upon filtering, a flickering block would appear as a single opening event with reduced amplitude. Such reduced amplitude events were not observed, even at higher drug concentrations that reduced channel open time by ten fold.

It is probably reasonable to conclude that the drugs tested here are not all acting by the same mechanism. In addition, some structural specificity is apparent, since lipid solubility alone is not an important factor in determining drug potency.

This work was supported in part by a grant from the Department of Veterans Affairs and by an allocation of computing funds from the College of Medicine, University of Iowa. Alphaxalone was a gift of Glaxo, Inc., U.K.

References

ADAMS, P.R. (1976). Drug blockade of open end-plate channels. *J. Physiol.*, **260**, 531–552.

COCKSHOTT, I.D. (1985). Propofol ('Diprivan') pharmacokinetics and metabolism – an overview. *Postgrad. Med. J.*, **61**, 45–50.

DE RUITER, G., POPESCU, D.T., DE BOER, A.G., SMEEKENS, J.B. & BREIMER, D.D. (1981). Pharmacokinetics of etomidate in surgical patients. *Arch. Int. Pharmacodyn.*, **249**, 180–188.

GAGE, P.W. & HAMILL, O.P. (1976). Effects of several inhalation anaesthetics on the kinetics of postsynaptic conductance changes in mouse diaphragm. *Br. J. Pharmacol.*, **57**, 263–272.

GAGE, P.W., MCBURNEY, R.N. & VAN HELDEN, D. (1978). Octanol reduces end-plate channel lifetime. *J. Physiol.*, **274**, 279–298.

GAGE, P.W. & MCKINNON, D. (1985). Effects of pentobarbitone on acetylcholine-activated channels in mammalian muscle. *Br. J. Pharmacol.*, **85**, 229–235.

HEYKANTS, J.J.P., MEULDERMANS, W.E.G., MICHIELS, L.J.M., LEWI, P.J. & JANSSEN, P.A.J. (1975). Distribution, metabolism and excretion of etomidate, a short-acting hypnotic drug, in the rat. Comparative study of (R)-(+) and (S)-(−)-etomidate. *Arch. Int. Pharmacodyn.*, **216**, 113–129.

HILLESTAD, L., HANSEN, T., PHARM, B., MELSOM, H. & DRIVENES, A. (1974). Diazepam metabolism in normal man. *Clin. Pharmacol. Ther.*, **16**, 479–484.

HUG, C.C. (1984). Pharmacokinetics and dynamics of narcotic analgesics. In *Pharmacokinetics of Anaesthesia*, ed. Prys-Roberts, C. & Hug, C.C. pp. 187–234. London: Blackwell Scientific Publications.

JAMES, R. & GLEN, J.B. (1980). Synthesis, biological evaluation, and preliminary structure-activity considerations of a series of alkyphenols as intravenous anesthetic agents. *J. Med. Chem.*, **23**, 1350–1357.

JOHNSTON, R.R., MILLER, R.D. & WAY, W.L. (1974). The interaction of ketamine with d-tubocurarine, pancuronium, and succinylcholine in man. *Anesth. Analg.*, **53**, 496–501.

KIRKPATRICK, T., COCKSHOTT, I.D., DOUGLAS, E.J. & NIMMO, W.S. (1988). Pharmacokinetics of propofol (Diprivan) in elderly patients. *Br. J. Anaesth.*, **60**, 140–150.

LECHLEITER, J. & GRUENER, R. (1984). Halothane shortens acetylcholine receptor channel kinetics without affecting conductance. *Proc. Natl. Acad. Sci. U.S.A.*, **81**, 2929–2933.

LEO, A., HANSCH, C. & ELKINS, D. (1971). Partition coefficients and their uses. *Chem. Rev.*, **71**, 525–604.

MATHER, L.E., TUCKER, G.T., PFLUG, A.E., LINDOP, M.J. & WILKERSON, C. (1974). Meperidine kinetics in man: Intravenous injection in surgical patients and volunteers. *Clin. Pharmacol. Ther.*, **17**, 21–30.

MUNSON, R., CALDWELL, K.L. & GLASER, L. (1982). Multiple controls for the synthesis of muscle-specific proteins in BC_3H1 cells. *J. Cell Biol.*, **92**, 350–356.

MURRELL, R.D., BRAUN, M.S. & HAYDON, D.A. (1991). Actions of n-alcohols on nicotinic acetylcholine receptor channels in cultured rat myotubes. *J. Physiol.*, **437**, 431–448.

OLSON, E.N., GLASER, L., MERLIE, J.P., SEBBANE, R. & LINDSTROM, J. (1983). Regulation of surface expression of acetylcholine receptors in response to serum and cell growth in the BC_3H1 muscle cell line. *J. Biol. Chem.*, **258**, 13946–13953.

REIDENBERG, M.M., LEVY, M., WARNER, H., COUTINHO, C.B., SCHWARTZ, M.A., YU, G. & CHERIPKO, J. (1978). Relationship between diazepam dose, plasma level, age, and central nervous system depression. *Clin. Pharmacol. Ther.*, **23**, 371–374.

SCHUTTLER, J., STOECKEL, H. & SCHWILDEN, H. (1985). Pharmacokinetic and pharmacodynamic modelling of propofol ('Diprivan') in volunteers and surgical patients. *Postgrad. Med. J.*, **61**, 53–54.

SCHUTTLER, J., WILMS, M., LAUVEN, P.M., STOECKEL, H. & KOENIG, A. (1980). Pharmakokinetische untersuchungen uber etomidat beim menschen. *Anaesthesist*, **29**, 658–661.

SEAR, J.W. & PRYS-ROBERTS, C. (1979). Plasma concentrations of alphaxalone during continuous infusion of althesin. *Br. J. Anaesth.*, **51**, 861–865.

SHAFER, A., DOZE, V.A., SHAFER, S.L. & WHITE, P.F. (1988). Pharmacokinetics and pharmacodynamics of propofol infusions during general anesthesia. *Anesthesiol.*, **69**, 348–356.

SIGWORTH, F.J. & SINE, S.M. (1987). Data transformations for improved display and fitting of single-channel dwell time histograms. *Biophys. J*, **52**, 1047–1054.

SINE, S.M. & STEINBACH, J.H. (1984). Activation of a nicotinic acetylcholine receptor. *Biophys. J*, **45**, 175–185.

SINE, S.M. & STEINBACH, J.H. (1986). Activation of acetylcholine receptors on clonal mammalian BC3H-1 cells by low concentrations of agonist. *J. Physiol.*, **373**, 129–162.

TORDA, T.A. & GAGE, P.W. (1977). Postsynaptic effect of I.V. anaesthetic agents at the neuromuscular junction. *Br. J. Anaesth.*, **49**, 771–776.

TRUDELL, J.R. (1991). Role of membrane fluidity in anesthetic action. In *Drug and Anesthetic Effects on Membrane Structure and Function*. ed. Aloia, R.C., Curtain, C.C. & Gordon, L.M. pp. 1–14. New York: Wiley-Liss, Inc.

UEDA, I. (1991). Interfacial effects of anesthetics on membrane fluidity. In *Drug and Anesthetic Effects on Membrane Structure and Function*. ed. Aloia, R.C., Curtain, C.C. & Gordon, L.M. pp. 15–33. New York: Wiley-Liss, Inc.

VAN HAMME, M.J., GHONEIM, M.M. & AMBRE, J.J. (1978). Pharmacokinetics of etomidate, a new intravenous anesthetic. *Anesthesiol.*, **49**, 274–277.

WACHTEL, R.E. (1988a). Ketamine decreases the open time of single-channel currents activated by acetylcholine. *Anesthesiol.*, **68**, 563–570.

WACHTEL, R.E. (1988b). Use of BMDP statistical package to generate maximum likelihood estimates for single channel data. *J. Neurosci. Methods*, **25**, 121–128.

WACHTEL, R.E. (1990). Comparison of anticholinesterases and their effects on acetylcholine-activated ion channels. *Anesthesiol.*, **72**, 496–503.

WACHTEL, R.E. (1991). Fitting of single-channel dwell time distributions. In *Methods in Neurosciences*, Vol. 4, ed. Conn, P.M. pp. 410–428. San Diego: Academic Press Inc.

WACHTEL, R.E. & WEGRZYNOWICZ, E.S. (1991). Mechanism of volatile anesthetic action on ion channels. In *Molecular and Cellular Mechanisms of Alcohol and Anesthetics*, ed. Rubin, E., Miller, K.W. & Roth, S.H. pp. 116–128. New York: Annals of the New York Academy of Sciences, Volume 625.

WIEBER, J., GUGLER, R., HENGSTMANN, J.H. & DENGLER, H.J. (1975). Pharmacokinetics of ketamine in man. *Anaesthesist*, **24**, 260–263.

(Received November 11, 1991
Revised March 10, 1992
Accepted March 12, 1992)

Br. J. Pharmacol. (1992), **106**, 628–631

Steroid inhibition of oedema formation in the rat skin

[1]A. Ahluwalia, S.H. Peers & R.J. Flower

Department of Biochemical Pharmacology, The William Harvey Research Institute, St. Bartholomew's Hospital Medical College, Charterhouse Square, London, EC1M 6BQ

1 A model has been developed to compare the inhibitory effects of the topical steroid, betamethasone-17-valerate, to those of systemically administered betamethasone upon oedema responses induced by 5-hydroxytryptamine (5-HT), platelet activating factor (PAF) and zymosan-activated serum (ZAS) ± prostaglandin E_1 (PGE_1), measured in the rat skin by use of ^{125}I-labelled human serum albumin.

2 Systemic betamethasone had a selective, time- and dose-dependent inhibitory effect upon oedema treatment, with 1 mg kg^{-1} and a 3 h pretreatment having the greatest effect of the doses and times employed.

3 Topical betamethasone inhibited the oedema responses to all of the stimuli showing no apparent selectivity.

4 Topical betamethasone inhibits inflammatory stimuli in a different manner from systemic betamethasone. The broad spectrum of inhibition suggests that topical betamethasone acts by affecting a fundamental feature of the inflammatory response common to all of the stimuli.

Keywords: Topical steroid; anti-inflammatory; oedema; rat skin; betamethasone

Introduction

Glucocorticosteroids represent one of the most widely used forms of drug treatment today with several million prescriptions per year, the majority of which are for topical steroids. Although these drugs are used extensively it is unclear as to exactly how these beneficial, anti-inflammatory effects of the topical steroids are produced. There now exist several different potency assays utilising different properties inherent to the topical steroids, such as the atrophogenic and the anti-mitotic properties (described by Fritz & Weston, 1983), the development of which have provided further insight into an understanding of the multifarious actions of the topical steroids.

In the early 1960's McKenzie & Stoughton designed an effective assay for the anti-inflammatory potency of the topical steroids on human skin, exploiting the vasoconstrictor properties of these drugs. Today, this test system remains the assay of choice when assessing topical steroid potency. The precision and moreover, the simplicity of this assay has probably been the major contributory factor in the lack of interest prevalent in gaining a full understanding of the mechanism of action of the topical steroids. Although these assays exploit a range of different properties of the topical steroids, they provide no distinctive explanation for the anti-inflammatory effects of these drugs.

Many of the studies investigating the effects of topical treatments upon the skin have used biopsy techniques such as that carrried out by Norris and associates (1984); however, the ideal situation in which a comprehensive understanding of the effects of the topical steroids could be gained must be via the investigation of the effects of these drugs upon induced inflammatory responses in the skin *in vivo*.

In 1973 Williams & Morley described a technique which measured oedema formation in animal skin developed in response to certain inflammatory mediators. It was with this technique that the inhibitory effects of the steroid dexamethasone, given systemically, upon the development of inflammatory oedema was demonstrated. Dexamethasone was shown to inhibit the formation of oedema in response to certain 'direct-acting stimuli' (Peers & Flower, 1991) and also 'neutrophil-dependent stimuli' (Yarwood *et al.*, 1988, Peers & Flower, 1991).

In light of the effectiveness of systemic dexamethasone in the rabbit skin oedema model, we have extended and further developed the oedema model to the rat, to provide a system whereby the anti-inflammatory effects of the topical steroids, in comparison to systemically administered steroids, may be assessed.

Methods

The formation of local oedema in the skin was measured in male wistar rats (250–350 g) by use of a technique similar to that described by Williams (1979), in the rabbit. Rats were anaesthetized with a cocktail of Hypnorm:Hypnovel:water (1:1:2), the backs of the rats shaved and 2 μCi kg^{-1} of body weight ^{125}I-labelled human serum albumin in 1% Evans blue solution injected intravenously. Following this 8 agents were injected intradermally (0.1 ml) in duplicate and were comprised of: 5-hydroxytryptamine (5-HT) (2.5×10^{-8} mol/site), platelet activating factor (PAF) (5×10^{-8} mol/site), 50% zymosan-activated serum (ZAS), in the presence or absence of prostaglandin E_1 (PGE_1) (3×10^{-10} mol/site) and saline controls. Thirty minutes later blood samples were taken by intracardiac puncture and the animals killed. Following this the injection sites were removed and plasma exudation calculated as described by Williams (1979).

To investigate the effect of systemic betamethasone, rats were given betamethasone sodium phosphate (0.1 or 1.0 mg kg^{-1}) or saline s.c., either 1 or 3 h prior to the administration of the stimuli described above.

To look at the effects of topical steroid, rats were anaesthetized, their backs shaved and 2 g of 0.1% w/w betamethasone-17-valerate (Betnovate), or vehicle cream, rubbed evenly into a measured area of the skin (11 cm by 10 cm), bifurcated by the mid-line of the rat back, for approximately 2–3 min, 18 h before the intradermal injections. Both of the topical treatments were compared to untreated controls.

Materials

Betamethasone sodium phosphate was produced by Glaxo. Topical preparations of betamethasone-17-valerate and vehi-

[1] Author for correspondence.

cle cream were generous gifts from Glaxo, UK, Evans blue, 5-HT, PAF, PGE_1 and zymosan were all obtained from Sigma, UK and ^{125}I-labelled human serum albumin was obtained from Amersham International PLC, UK.

5-HT was dissolved in 0.9% NaCl (saline), stock solutions of PAF and PGE_1 were prepared in absolute ethanol and all were stored at − 20°C. 1% Evans blue solution was made in saline and stored at room temperature.

ZAS was prepared as described by Williams & Jose, (1981) and was stored at − 20°C.

Dilutions of all agents were made in saline.

Data and statistical analysis

All results are expressed as means ± s.e.mean. The effects of steroid treatment, given systemically or topically, upon the oedema inducing capacity of each stimulus is expressed as a percentage i.e.

$$\frac{\text{Mean oedema (µl of plasma) in steroid treated rats}}{\text{Mean oedema (µl of plasma) in control rats}} \times 100\%$$

Control rats are those given saline in the case of systemic steroid treatment and no topical treatment in the case of topical steroid treatment.

Where required Student's *t* test (two-tailed) analysis was used.

Results

Figure 1 shows the oedema inducing effects of all of the intradermal stimuli in absolute values of plasma volume. These stimuli were used as they were found to be the most effective, of a selection of known inflammatory mediators including bradykinin and fMLP (N-formyl-methionyl-leucyl-phenylalamine), both of which when given alone or in combination with a vasodilator produced no more than 10 µl of oedema, whereas all of the stimuli used in this assay gave at least 20 µl of oedema. The effects of arachidonic acid, PGE_2, adenosine and PGE_1 upon the oedema induced by the chosen stimuli were tested to determine which vasodilator had the greatest potentiating effect. PGE_1 was the most effective agent at enhancing the induction of oedema formation in the rat back skin by increasing the oedema response to PAF by 114.0% ($n = 5$), with adenosine having no potentiating effect at all ($n = 5$), PGE_2 potentiating the response by 10.0% ($n = 5$), and arachidonic acid increasing the response by only 34.0% ($n = 5$).

Saline controls alone produced little oedema (4.3 ± 0.9 µl of plasma). PGE_1 induced a small oedema which was significantly different ($P < 0.05$) from that shown by saline above. Both PAF and ZAS caused substantial oedema and were significantly potentiated in the presence of PGE_1, with $P < 0.001$ and $P < 0.01$ respectively. However, this was not the case for 5-HT, which also produced substantial oedema, where PGE_1 had no significant potentiating or inhibitory effect upon the oedema response.

Figure 2 shows the effect of systemically administered betamethasone upon responses to each of the intradermal stimuli. The lower dose of 0.1 mg kg^{-1} with a 3 h pretreatment had no significant inhibitory effect upon any of the responses. Increasing the dose 10 fold with a 1 h pretreatment period appeared to have a low level of inhibition across most of the stimuli but was only significant upon the oedema response induced by ZAS in the presence of PGE_1. An increase in the duration of the pretreatment period to 3 h with this dose of 1 mg kg^{-1} resulted in a wider range of inhibition (77–15%), significantly affecting the responses to all of the stimuli except for that of PAF in the presence of PGE_1 and ZAS alone.

For topical betamethasone a treatment of 2 g betamethasone-17-valerate was used as this dose produced approximately the same extent of inhibition of the oedema response to ZAS ± PGE_1, the only stimulus which appears to incorporate both direct-acting and neutrophil-dependent mechanisms of oedema formation, as that seen with the systemic treatment of 1 mg kg^{-1} betamethasone with a 3 h pretreatment period. Also the inhibitory effects seen with this topical treatment were produced purely in a local manner, with no systemic component. This was demonstrated by treating only half of the rat back and comparing the oedema responses on each side ($n = 3$). The degree of oedema produced on the steroid treated side was visibly lower than that of the untreated side in each case, indicating that the inhibitory activity observed with this topical treatment was due to a local effect upon the skin and was not the result of penetration into the systemic circulation. An 18 h pretreat-

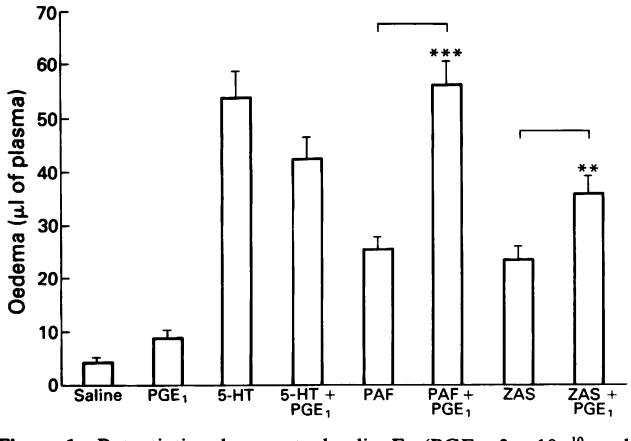

Figure 1 Potentiation by prostaglandin E_1 (PGE_1, 3×10^{-10} mol/site) of the oedema (µl of plasma) induced by 5-hydroxytryptamine (5-HT, 2.5×10^{-8} mol/site), platelet activating factor (PAF, 5×10^{-8} mol/site) and 50% zymosan-activated serum (ZAS) per site. Results are expressed as mean (with s.e.mean shown by the vertical bars) of $n = 17$ rats. Significant differences between oedema induced by the agents alone and in the presence of PGE_1 are indicated by $^{**}P < 0.01$ and $^{***}P < 0.001$.

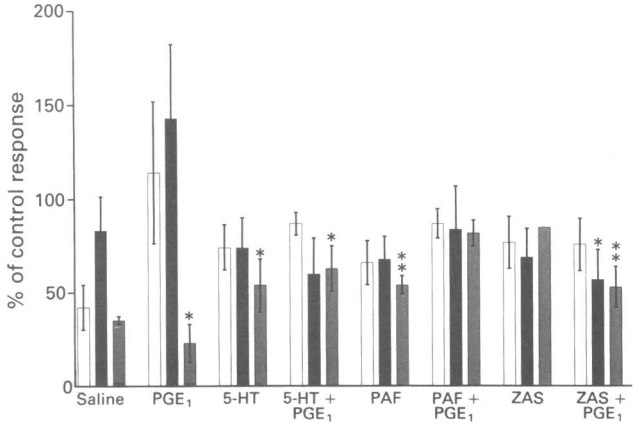

Figure 2 The effect of betamethasone, administered systemically, upon the oedema induced by 5-hydroxytryptamine (5-HT, 2.5×10^{-8} mol/site), platelet activating factor (PAF, 5×10^{-8} mol/site) and 50% zymosan-activated serum (ZAS) per site given alone or in the presence of prostaglandin E_1 (PGE_1, 3×10^{-10} mol/site). Oedema responses presented after a 3 h pretreatment of betamethasone (0.1 mg kg^{-1}) are shown by the open columns, a 1 h pretreatment of betamethasone (1 mg kg^{-1}) by solid columns and a 3 h pretreatment of betamethasone (1 mg kg^{-1}) by stippled columns. Results are expressed as mean (with s.e.mean represented by vertical bars) of $n = 5$-6. Significant inhibition of oedema formation are indicated by $^{*}P < 0.05$ and $^{**}P < 0.001$.

ment period was chosen for these experiments as both 3 h and 6 h pretreatment periods were shown to be insufficient to produce significant inhibitory effects upon the inflammatory stimuli and thus an overnight treatment had to be used ($n = 3$ in each case). This is in agreement with treatment periods used in a variety of studies investigating other properties of the topical steroids, such as that of Barry & Brace (1975), where the maximum effects of the steroids were seen after a period ranging between (12–24 h).

Unlike the systemically administered betamethasone, topical betamethasone had a more general inhibitory action as can be seen in Figure 3, significantly inhibiting the inflammatory oedema responses to all of the stimuli including the saline control, the inhibition ranging from between 33–58%. The vehicle alone was without any net effect (3 experiments, 9 animals) except in the case of PAF in the presence of PGF_1 where a mean inhibition of 23%, which reached significance at the 1% level, was achieved. This inhibitory effect, however was not as great as that seen with the steroid cream ($P<0.01$).

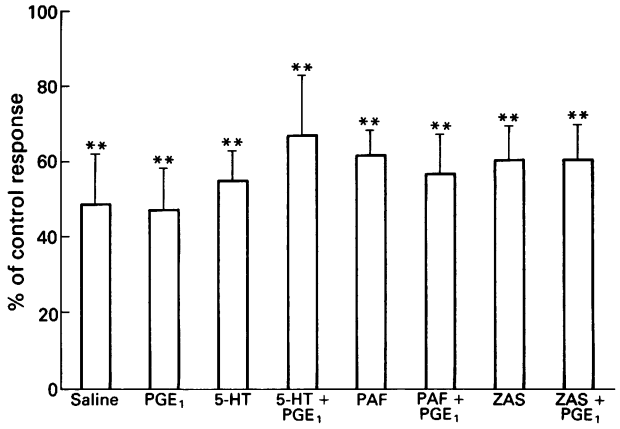

Figure 3 Effect of topical betamethasone-17-valerate, 2 g with an 18 h pretreatment, upon the oedema induced by the stimuli 5-hydroxytryptamine (5-HT, 2.5×10^{-8} mol/site), platelet activating factor (PAF, 5×10^{-8} mol/site) and 50% zymosan-activated serum (ZAS) per site in the presence or absence of prostaglandin E_1 (PGE_1, 3×10^{-10} mol/site). Results are expressed as mean (with s.e.mean represented by vertical bars) of $n = 6$. Significant inhibition of oedema formation is indicated by $^{**}P<0.01$.

Discussion

The aim of our present study was to try and gain some insight into how the anti-inflammatory topical steroids work, and how these mechanisms or modes of action may differ from those of systemically administered steroids; and for this purpose we have developed the rat skin oedema model.

Both PAF and ZAS induced greater oedema when injected in combination with PGE_1, a phenomenon explained by the two-mediator hypothesis (Wedmore & Williams, 1981; Williams *et al.*, 1983). PAF is a direct acting stimulus such that an increased vascular permeability is produced when gaps are formed between endothelial cells in response to their contraction. PGE_1, in the microvasculature, is a vasodilator and as such induces an increase in blood flow and will act synergistically with inflammatory agents, such as PAF, to produce a greater net oedema. ZAS, which is a source of C5a desArg enhances plasma exudation via a neutrophil-dependent manner in the rabbit (Williams & Jose, 1981). However, in the rat after treatment with the 5-HT receptor blocker, methysergide, and the $histamine_1$ receptor blocker, mepyramine, the oedema response to ZAS was only $40.0 \pm 2\%$ ($n = 3$) of the response shown in untreated rats. This suggests that the response shown to ZAS, here, is mediated in part by mechanisms independent of the neutrophil, and probably involves mast cell degranulation. The oedema-inducing capacity of 5-HT remained unaffected in the presence of PGE_1, perhaps 5-HT here is acting as a vasodilator as well as directly inducing plasma exudation.

The inhibitory action of betamethasone administered systemically was shown to be a time- and dose-dependent effect which is in agreement with the findings of Peers & Flower (1991). In addition, systemic betamethasone appears to exert some selectivity in its inhibitory effects, inhibiting the actions of 5-HT and PAF when given alone, with no greater inhibition when given in combination with PGE_1, suggesting that the steroid is perhaps affecting the permeability portion of the response. This, however is not consistently the case for all the stimuli, as with ZAS. It is only when ZAS is given in combination with PGE_1 that betamethasone exerts any inhibitory effects. There have been suggestions that steroids can directly affect prostanoid receptor numbers resulting in down-regulation of the receptor (Sessa *et al.*, 1990a,b). This down-regulation may well explain some of the effects seen here.

Topically administered betamethasone appears to act in a manner quite different from that of the sytemically administered betamethasone, inhibiting the oedema induced by all stimuli. It is difficult to assess how the local steroid concentrations would compare when using the different routes of administration. However, the results would suggest that the mechanism of action of betamethasone, and perhaps other steroids, varies with the mode of application. The broad spectrum of inhibition intimates that topical betamethasone is acting by affecting a fundamental feature of the inflammatory response. An immediate thought that comes to mind is that this inhibitory effect may be at the level of the endothelial cell, although further studies are necessary before we can verify this. Finally with the aid of this rat skin oedema model we hope to dissect further and ultimately gain an understanding of the mechanism of action of the topical steroids.

References

BARRY, B.W. & BRACE, A.R. (1975). Vasoconstrictor activities of some novel synthetic steroids in alcoholic solution. *J. Invest. Dermatol.*, **64**, 418–422.

FRITZ, K.A. & WESTON, W.L. (1983). Topical glucocorticosteroids. *Ann. Allergy*, **50**, 68.

MCKENZIE, A.W. & STOUGHTON, R.B. (1962). Method for comparing percutaneous absorption of steroids. *Arch. Dermatol.*, **86**, 608–610.

NORRIS, J.F.B., ILDERTON, E., YARDLEY, H.J., SUMMERLY, R. & FORSTER, S. (1984). Utilization of epidermal phospholipase A_2 inhibition to monitor topical steroid action. *Br. J. Dermatol.*, **III** (suppl 27), 195–203.

PEERS, S.H. & FLOWER, R.J. (1991). Site of anti-inflammatory action of dexamethasone in rabbit skin. *Eur. J. Pharmacol.*, **196**, 37–41.

SESSA, W.C. & NASJJLETTI, A. (1990a). Dexamethasone selectively attenuates prostanoid-induced vasoconstrictor responses in vitro. *Circ. Res.*, **66**, 383–388.

SESSA, W.C., LIN, L. & NASJJLETTI, A. (1990b). Reciprocal effects of dexamethasone on vasodilatory responses to arachidonic acid and prostanoids in the isolated perfused rabbit kidney. *Hypertension*, **15** (suppl I), 93–96.

WEDMORE, C.V. & WILLIAMS, T.J. (1981). Control of vascular permeability by polymorphonuclear leukocytes in inflammation. *Nature*, **289**, 646–650.

WILLIAMS, T.J. (1979). Prostaglandin E_2, prostaglandin I_2 and the vascular changes of inflammation. *Br. J. Pharmacol.*, **65**, 517–524.

WILLIAMS, T.J. & JOSE, P.J. (1981). Mediation of increased vascular permeability after complement activation. *J. Exp. Med.*, **153,** 136–153.

WILLIAMS, T.J., JOSE, P.J., WEDMORE, C.V., PECK, M.J. & FORREST, M.J. (1983). *Adv. Prost. Thromb. Leuk. Res.*, **11,** 33–37.

WILLIAMS, T.J. & MORLEY, J. (1973). Prostaglandins as potentiators of increased vascular permeability in inflammation. *Nature*, **246,** 215–217.

YARWOOD, H., NOURSHARGH, S., BRAIN, S.D. & WILLIAMS, T.J. (1988). Suppression of neutrophil accumulation and neutrophil-dependent oedema by dexamethasone in rabbit skin. *Br. J. Pharmacol.*, **95,** 726P.

(Received October 8, 1991
Accepted March 12, 1992)

Br. J. Pharmacol. (1992), **106**, 632–638

Release of endogenous adenosine and its metabolites by the activation of NMDA receptors in the rat hippocampus *in vivo*

[1]Ying Chen, *D.I. Graham & T.W. Stone

Department of Pharmacology and *Neuropathology, University of Glasgow, Glasgow G12 8QQ

1 The effects of N-methyl-D-aspartate (NMDA), KCl, and veratridine on the release of endogenous adenosine and its metabolites, inosine and hypoxanthine, from the rat hippocampus have been studied by *in vivo* microdialysis.

2 In the hippocampus of rats anaesthetized with urethane the adenosine level reached a stable state estimated at 0.93 μM during the first 2 h after the implantation of the dialysis probe. NMDA (50 μM to 25 mM) in the perfusate evoked a concentration-dependent release of adenosine, inosine and hypoxanthine with an EC_{50} of 180 μM. The release was reduced by 93% by the specific NMDA receptor antagonist 2-amino-5-phosphonopentanoic acid (2-AP5) at 200 μM, indicating an NMDA receptor-mediated process. In addition, the 100 mM KCl-evoked release of adenosine was also substantially reduced by 77% by 2-AP5, suggesting that a large component of the K^+-evoked release is NMDA-receptor-mediated.

3 Perfusion with zero-Ca^{2+} artificial cerebrospinal fluid attenuated the NMDA-evoked release of adenosine only by 16% (not signficant) but depressed the K^+-evoked release by 62%, indicating that most of the NMDA-evoked release is directly receptor-mediated, whereas a large component of the K^+-evoked release could be via the release of an excitatory amino acid acting at the NMDA receptors.

Keywords: Adenosine; inosine; hypoxanthine; NMDA (N-methyl-D-aspartate); 2-AP5 (2-amino-5-phosphonopentanoic acid); hippocampus; microdialysis; release *in vivo*

Introduction

Adenosine is an inhibitory modulator of synaptic transmission and neuronal activity (for recent reviews see Stone, 1989; Williams, 1990; Phillis, 1991; Stone & Simmonds, 1991). In the central nervous system this regulation is achieved partly by a suppression of the release of neurotransmitters, especially those with a predominantly excitatory function such as glutamate (Corradetti *et al.*, 1984; Fastbom & Fredholm, 1985; Burke & Nadler, 1988) and acetylcholine (Jackisch *et al.*, 1984; Spignoli *et al.*, 1984). There is much less effect on the release of inhibitory agents such as noradrenaline (Fredholm *et al.*, 1983) or 4-aminobutyric acid (GABA) (Hollins & Stone, 1980). Adenosine also acts directly upon neuronal postsynaptic membranes to increase potassium or decrease calcium conductances so as to depress excitability (Dunwiddie, 1985; Trussell & Jackson, 1985; Haas & Green, 1988).

In order to act upon the purine receptors mediating these effects, adenosine must be released from the cytoplasm into the extracellular space. Although there is a continuing debate as to whether adenosine itself is transported out of cells or whether it is largely formed extracellularly by the catabolism of adenosine 5'-monophosphate (AMP) and other nucleotides, there is no doubt that circumstances which increase the metabolic demand of a tissue or which restrict the availability of oxygen induce a substantial rise in the extracellular concentration of adenosine and its metabolites (Stone *et al.*, 1990).

In the CNS, hypoxia or ischaemia thus elevate the extracellular level of adenosine in the striatum (Zetterstrom *et al.*, 1982; van Wylen *et al.*, 1986; Hagberg *et al.*, 1987), the hippocampus (Andine *et al.*, 1990) and the cerebral cortex (Phillis *et al.*, 1987; 1988; 1991). It is also known, for example, that excitatory amino acids (EAA) such as glutamate and aspartate are released from neurones into extracellular space by hypoxic or ischaemic insults (Benveniste *et al.*, 1984; Hagberg *et al.*, 1985; Globus *et al.*, 1988; Phillis *et al.*, 1991), and the excessive release of excitatory amino acids is thought to mediate cell death. Although the precise mechanisms underlying the releasing sequence of the excitatory amino acids (EAA) and adenosine during ischaemia remain unclear, adenosine and its analogues decrease the release of endogenous EAA neurotransmitters glutamate and aspartate (Andine *et al.*, 1990; Phillis *et al.*, 1991). Thus, if adenosine is elevated in the extracellular space in conjunction with the activation of EAA receptors, it may act to diminish further neuronal damage caused by EAA excitation. So far, there is substantial evidence that adenosine analogues (Evans *et al.*, 1987; Connick & Stone, 1989; Januszewicz von Lubitz *et al.*, 1989; Arvin *et al.*, 1989), adenosine uptake inhibitors (DeLeo *et al.*, 1987; 1988; Andine *et al.*, 1990) and deaminase inhibitors (Phillis & O'Regan, 1989) protect against ischaemic and excitotoxic cell loss *in vivo*.

In the hippocampus, a high density of EAA receptors has been found (Cotman & Iversen, 1987), with NMDA (N-methyl-D-aspartate) and quisqualate receptors located primarily on the CA1 pyramidal cell layer and kainate receptors on the CA3 cell layer. The distribution corresponds to the vulnerability of the hippocampal pyramidal cells during excitotoxicity or ischaemia. The hippocampus also possesses a high density of adenosine A1 receptors, particularly on the CA1 pyramidal cells (Reddington & Lee, 1991). In addition, the rise of the extracellular adenosine level after electrical stimulation in hippocampal slices is higher than in slices of striatum or cerebal cortex (Pedata *et al.*, 1990). The present project was designed to investigate the ability of the activation of NMDA receptors *in vivo* to induce the release of endogenous adenosine and its metabolites, inosine, hypoxanthine and xanthine, from the hippocampus of anaesthetized rats by use of the microdialysis technique. The time course of the release of adenosine and its metabolites and the nature of the receptors involved were studied. Preliminary results have been presented in an earlier abstract (Chen & Stone, 1991).

[1] Author for correspondence at present address: Dept. of Physiology and Pharmacology, University of Southampton, Southampton SO9 3TU.

Methods

Male Wistar rats weighing 270–310 g were anaesthetized with urethane (1.25 g kg^{-1}, i.p.) and placed in a stereotaxic head frame arranged for use with the coordinates of Paxinos & Watson (1986). The body temperature of the animal was monitored and maintained by a heating pad at 36–37°C. Concentric microdialysis probes made with 4 mm polyacrylonitrile membrane (HOSPAL) 0.3 mm in diameter were implanted into the ventral hippocampus at 5.6 mm posterior, 5 mm lateral and 8 mm ventral relative to the bregma such that the dialysis membrane lay along the pyramidal cell layer of the hippocampus (Figure 1). Following the completion of each experiment, pontamine sky blue (10% solution) was perfused through the probes for 5 min. The brain was removed into 10% formaldehyde solution (pH 7.4) to fix overnight, and then sectioned to locate the dye to confirm the placement of the probes.

Immediately after the implantation, perfusion with artificial cerebrospinal fluid (ACSF) of composition (mM: NaCl 125, $NaHCO_3$ 27, KCl 2.5, KH_2PO_4 0.5, $MgSO_4$ 1.2, $CaCl_2$ 1.2, glucose 10, pH 7.2) was started at a flow rate of 2 μl min^{-1} (Harvard Apparatus, infusion pump 22). Drugs, e.g. N-methyl-D-aspartate (NMDA) (Sigma) and 2-amino-5-phosphonopentanoic acid (2-AP5) (Research Biochemicals) were dissolved in ACSF, and the pH was adjusted to 7.2. When the concentration of KCl was increased, the same amount of NaCl was removed from the perfusate to maintain osmolarity. Test and control solutions were changed by means of a liquid switch, which caused little disturbance to the flow.

Purine contents in the samples were analyzed by a high performance liquid chromatography (h.p.l.c.) system (Severn Analytical, SA6410B) with u.v. detection at 254 nm (Severn Analytical, SA6500). This employed a Techsphere C18 3 μm microsphere column and the mobile phase was NaH_2PO_4 0.01 M with 6% methanol (pH 6.1) at a flow rate of 0.8 ml min^{-1}. The amount (in pmol) of adenosine (Ado), inosine (Ino), hypoxanthine (Hyp) and xanthine (Xan) in 20 μl dialysate samples was analyzed and is presented in the figures. The limit of sensitivity of the system for adenosine was 0.5 pmol. Identification and quantification of the compounds was achieved by parallel chromatography of standards.

In our preliminary experiments, it was established that the efflux of the purines was high initially and had declined to a steady baseline within 1 h after the implantation of the dialysis probes (Figure 2). This is in agreement with Zetterström *et al.* (1982) and van Wylen *et al.* (1986) who found that the initial trauma caused by the implantation of the dialysis probes subsides within 1 h. Subsequent samples were collected over successive 20 min periods and 2 h were allowed for the tissue to recover from the probe insertion. Samples were collected in Eppendorf tubes and either analyzed immediately or snap frozen in liquid nitrogen for later analysis. After the recovery period, two further control samples were taken to establish the basal levels. Following this, stimulation with a 5 min pulse of NMDA or KCl was introduced. To determine the effects of receptor antagonists and ionic changes, two pulses (S1 and S2) with an interval of 3 h were used. Changes were made in the ACSF 2 h before S2. The net increments of purines in two samples following stimulation were calculated and assigned to the values for S1 or S2 correspondingly. The control ratio of S2 over S1 (S2/S1), and the test ratio were obtained.

Statistical comparisons were made between the control and the test experiments. For the sample populations having equal variances, which was checked by F test, t test was used. For the few extreme cases which violated the equal variance, the Mann-Whitney U test was applied. Paired t test was also applied where it was appropriate.

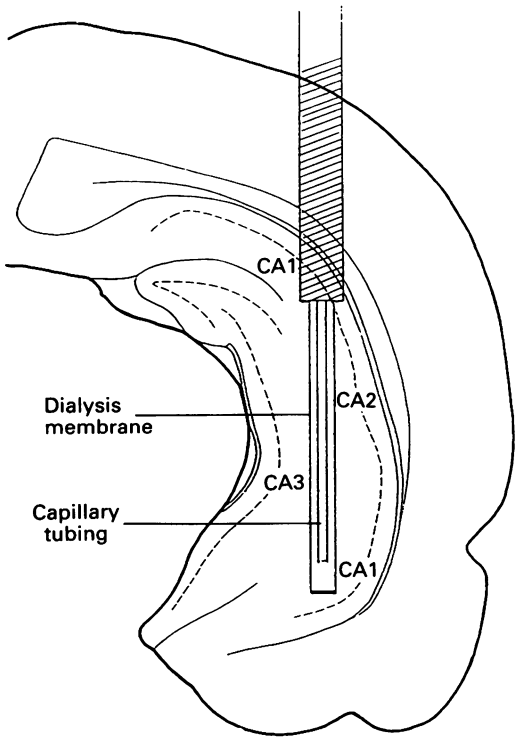

Figure 1 An illustration of the position of the dialysis probe in parallel to the pyramidal cell layers in the rat hippocampus.

Results

Endogenous release of adenosine evoked by NMDA, KCl and veratridine

Two hours after the implantation of the dialysis probes, two 20 min samples were collected and the basal levels of purines in the dialysate were determined. In order to estimate the concentrations of the purines in the extracellular space of the hippocampus, the relative recoveries of the compounds at a 2.0 μl min^{-1} perfusion rate by the probe were calibrated *in vitro* by use of standard purine solutions in the concentration range of 1.0 to 20.0 μM. Constant relative recoveries for the four purine compounds were found at around 10%. The individual ratios for adenosine, inosine, hypoxanthine and xanthine are shown in Table 1. Using the relative recoveries

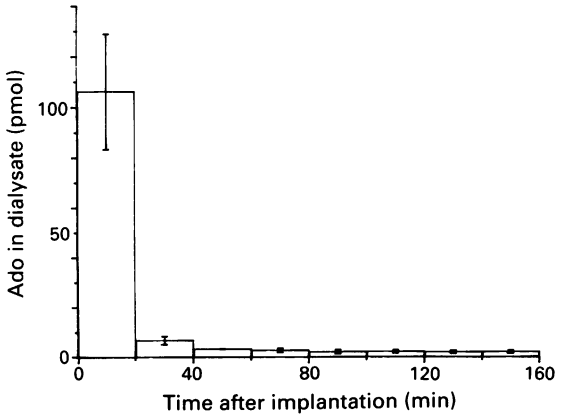

Figure 2 Total amount of adenosine (Ado) (mean with s.e.mean shown by vertical bars, in pmol, $n = 4$) in 20 μl dialysate samples during the first 2 h after the implantation of the dialysis probes. Rate of the perfusion was 2.0 μl min^{-1}.

Table 1 Basal levels of adenosine (Ado), inosine (Ino), hypoxanthine (Hyp) and xanthine (Xan) in the hippocampal extracellular medium were estimated from the basal concentrations of the compounds in hippocampal dialysate, by the relative recoveries calibrated in purine solutions *in vitro*

	Relative recovery (n)	*Measured level in dialysate* (n)	*Estimated level in hippocampus*
Ado	10.7 ± 1.1% (7)	0.10 ± 0.01 (63)	0.93 ± 0.09
Ino	10.2 ± 1.2% (7)	0.14 ± 0.01 (61)	1.37 ± 0.10
Hyp	11.1 ± 0.9% (3)	0.27 ± 0.01 (52)	2.43 ± 0.09
Xan	8.5 ± 0.7% (3)	0.65 ± 0.03 (53)	7.65 ± 0.35

Concentration values are expressed as μM (mean ± s.e.mean) (number of experiments)

the approximate basal concentrations of the purines in the hippocampus can be estimated according to the basal concentrations of the purines measured in hippocampal dialysate (Table 1).

The presence of NMDA, 100 mM KCl or 100 μM veratridine in the perfusing ACSF released endogenous adenosine, inosine, hypoxanthine and xanthine from the rat hippocampus. A 5 min pulse of NMDA from 50 μM to 20 mM evoked a dose-dependent release of adenosine expressed as the total amount evoked above the basal (Figure 3). The EC_{50} was 180 μM NMDA. When the NMDA concentrations were above 1 mM, the total evoked release of adenosine saturated at 13–15 pmol in 20 μl dialysate samples.

The release patterns of adenosine, inosine, hypoxanthine and xanthine evoked by the perfusion of 200 μM NMDA are shown in Figure 4. A 5 min pulse of NMDA significantly elevated the levels of adenosine, inosine and hypoxanthine 2–4 fold above the basal level. The level of xanthine was only slightly increased although it was significant. The levels of adenosine, inosine and hypoxanthine in the two 20 min samples collected immediately after the 5 min pulse of NMDA were all significantly higher than the basal level, whereas the percentage increase of adenosine (252 ± 50%) in the first sample is significantly ($P < 0.01$, paired t test) higher than those of inosine (135 ± 12%) and hypoxanthine (137 ± 99%), suggesting that inosine and hypoxanthine are the probable products of adenosine which was directly released by the application of NMDA.

KCl at 100 mM also released adenosine, inosine and hypoxanthine 2–5 fold over basal in a similar pattern to the NMDA-evoked release (Figure 5). None of the corresponding values between NMDA-evoked release and K^+-evoked release are significantly different. A small but significant release of xanthine was also seen. Veratridine at 100 μM evoked the release of adenosine to a peak about three fold above basal, similar to the evoked release described above.

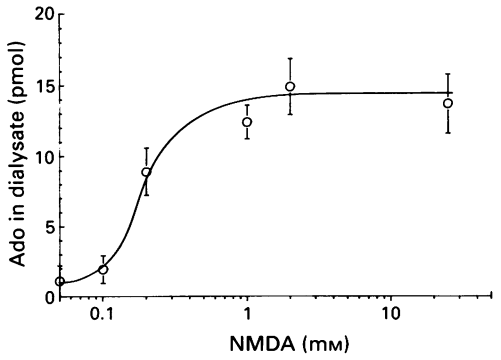

Figure 3 Concentration-dependent total net release of adenosine (Ado, pmol) in 20 μl dialysate samples evoked by a 5 min pulse of N-methyl-D-aspartate (NMDA, 50 μM–20 mM) in perfusate ($n = 3$–8). A sharp increase in the amount of adenosine released is shown in the NMDA concentration range between 50 μM to 1 mM. The EC_{50} is 180 μM NMDA. At a higher concentration range, the total release reached a plateau at about 14 pmol.

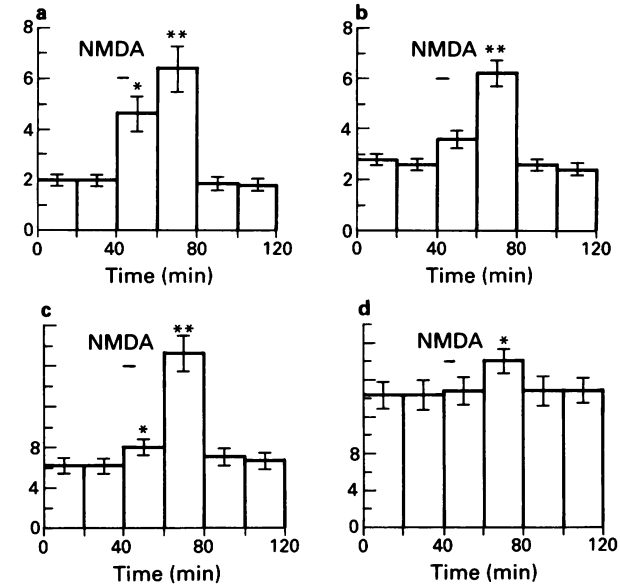

Figure 4 The release profiles for adenosine (Ado), (a), inosine (Ino) (b), hypoxanthine (Hyp) (c) and xanthine (Xan) (d) evoked by 5 min pulse of 200 μM N-methyl-D-aspartate ($n = 14$). Levels of Ado, Ino and Hyp in both of the two samples following the stimulation were elevated significantly, while the level of Xan was only increased slightly in the second sample after stimulation. Paired t test was employed to determine the significance level (*$P < 0.05$; **$P < 0.001$).

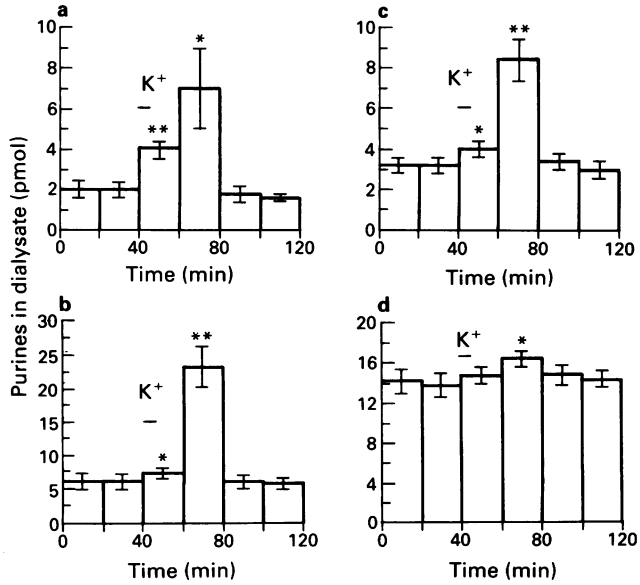

Figure 5 The release profiles for adenosine (Ado) (a), inosine (ino) (b), hypoxanthine (Hyp) (c) and xanthine (Xan) (d) evoked by 5 min pulse of 100 mM K^+ ($n = 10$). Levels of Ado, Ino and Hyp in both of the two samples following the stimulation were elevated significantly, while the level of Xan was only increased slightly in the second sample after stimulation. Paired t test was employed to determine the significance level (*$P < 0.05$; **$P < 0.001$).

NMDA receptor-mediated release of adenosine

To determine whether the NMDA-evoked release of adenosine was mediated by specific NMDA receptors, the effects of the competitive NMDA receptor antagonist, 2-AP5 (200 μM), on the NMDA-evoked release and the K^+-evoked release were examined. Twin pulses of 200 μM NMDA or 100 mM KCl 3 h apart without the introduction of the antagonist were used to obtain control ratios of the amount of purines evoked by the second stimulus relative to the first (S2/S1). To determine the effects of the antagonist, 200 μM 2-AP5 was incorporated in the ACSF 1 h after the first stimulus (S1), and maintained throughout the second stimulus (S2).

In the five experiments using twin pulses of 200 μM NMDA, both S1 and S2 evoked a net release of the purines, and the release of adenosine is shown in Figure 6a, with a S2/S1 of 45 ± 10% ($n = 5$) (Figure 6d, open column). The application of 2-AP5 before and during the second stimulus in the test experiments (Figure 6c) abolished the release of adenosine, and thus reduced the S2/S1 value (Figure 6d) to only 3 ± 2% ($n = 4$) which is significantly ($P < 0.05$, Mann-Whitney U test) smaller than the control. The basal release of the purines was not affected by 200 μM 2-AP5 (Figure 6c).

The control S2/S1 for 100 mM KCl evoked release of adenosine (Figure 7a) was also obtained, which is 45 ± 9% ($n = 5$) (Figure 7d, open column), similar to that for NMDA. The incorporation of 200 μM 2-AP5 also reduced the S2 (Figure 7c), leaving the S2/S1 value as 11 ± 4% ($n = 6$) (Figure 7d). This reduction is statistically significant ($P < 0.01$, t test).

The effects of 2-AP5 on the release of inosine and hypoxanthine followed the same trend as for adenosine. The control S2/S1 values for inosine and hypoxanthine are slightly higher and the percentage changes in S2/S1 slightly different following the treatments with 2-AP5 (Table 2). The second release of xanthine was generally very little, so the S2/S1 for xanthine was not studied.

Calcium dependence of the NMDA-evoked release of adenosine

For stimulation-induced release by two pulses of 200 μM NMDA, perfusion with zero-Ca^{2+} (Figure 6b) produced a slight reduction in the second release of adenosine, and the S2/S1 ($n = 5$) (Figure 6d, crosshatched column) was not significantly different from the control. However, in the case of 100 mM KCl (Figure 7b), the S2/S1 value (Figure 7d,

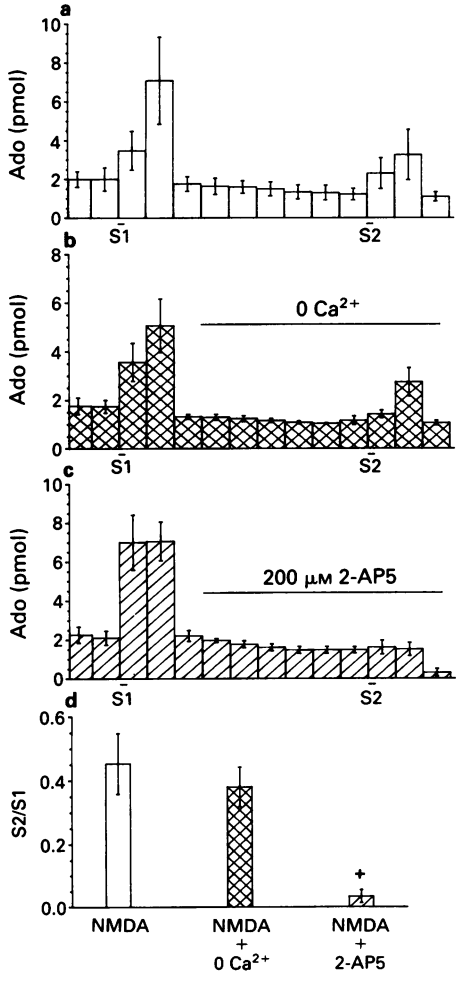

Figure 6 Twin pulses of 200 μM N-methyl-D-aspartate (NMDA) with a 3 h interval were used to study the release of adenosine in the control condition (a) ($n = 5$), with the perfusion of zero-Ca^{2+} solution (b) ($n = 5$) and the incorporation of 2-amino-5-phosphonopentanoic acid (2-AP5) (c) ($n = 4$). The perfusion of zero-Ca^{2+} and 200 μM 2-AP5 started 1 h after the first stimulus (S1) and are indicated by the horizontal bar over each histogram. The average S2 over S1 ratios (S2/S1) (d) in each condition were used to indicate the blockade of the release by 2-AP5 (hatched column, $*P < 0.05$, Mann-Whitney U test) and the insignificant effect of zero-Ca^{2+} (crosshatched column).

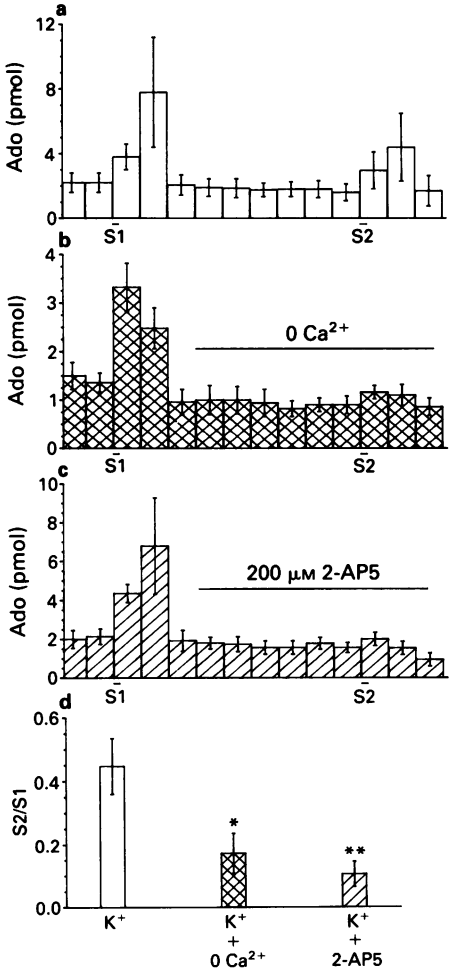

Figure 7 Twin pulses of 100 mM K^+ with a 3 h interval were used to study the release of adenosine in the control condition (a) ($n = 5$), with the perfusion of zero-Ca^{2+} solution (b) ($n = 4$) and the incorporation of 2-amino-5-phosphonopentanoic acid (2-AP5) (c) ($n = 6$). The perfusion periods of zero-Ca^{2+} and 200 μM 2-AP5 started 1 h after the first stimulus (S1) and are indicated by the horizontal bar over each histogram. The average S2 over S1 ratios (S2/S1) (d) in each condition were used to indicate the reduced release following the application of zero-Ca^{2+} (crosshatched column, $*P < 0.05$, t test) and 2-AP5 (hatched column, $**P < 0.01$, t test).

crosshatched column) was markedly ($P < 0.05$, t test) reduced to 17 ± 6%, 38% of the control. Perfusion without Ca^{2+} did not affect the basal release of adenosine either. The effects of zero-Ca^{2+} on the release of inosine and hypoxanthine, which are similar to that on adenosine, are presented in Table 2.

Discussion

Purine release

The key finding described here is that the activation of NMDA receptors increased the extracellular concentrations of endogenous purines, adenosine, inosine, hypoxanthine and xanthine, in the rat hippocampus *in vivo* detected by h.p.l.c. following microdialysis.

Microdialysis is a convenient method for investigation of the factors affecting extracellular concentrations of compounds *in vivo*. It does, however, carry the disadvantage that the drug concentration within the extracellular fluid cannot be known with certainty and the inevitable variations in location of the probe relative to the release sites lead to large variations in the concentration of active materials within the perfusion medium. In order to compensate for this variability, the S2/S1 was employed as a reliable means of comparing data in different experiments. Compared with release studies on classical neurotransmitters (Young & Bradford, 1991), the release evoked by S2, 3 h after S1, was relatively small for the purines (about 45%). A similar decline in release was noted in studies of cortical slides (Hoehn & White, 1990b) and explained as being due to desensitization of NMDA receptors (Krishtal *et al.*, 1988). In the present experiments, however, depolarizing agents were administered only as 5 min pulses, 3 h apart, and such a prolonged desensitization would seem unlikely. Another explanation, that a degree of neuronal toxicity leads to a reduced pool of viable cells also seems unlikely since similar or even higher NMDA concentrations have been used to obtain the repeated release of aspartate and glutamate (Young & Bradford, 1991). As indicated in Table 2, the ratios of S2/S1 were higher for inosine and, particularly, for hypoxanthine than for adenosine itself. The reason for this is unclear but may indicate a change of purine metabolism or compartmentation initiated by the first depolarizing stimulus, a possibility which might merit further investigation with *in vitro* systems.

The estimated basal interstitial concentrations of adenosine and other purines in the hippocampus were consistent with previous findings that the adenosine concentration in the extracellular space of brain tissue is of the order of 0.1–2 μM (Winn *et al.*, 1979; Zetterström *et al.*, 1982; van Wylen *et al.*, 1986; Hagberg *et al.*, 1987; Ballarin *et al.*, 1991). Although the microdialysis technique provides a close reflection of the extracellular concentrations of the compounds of interest in the brain *in vivo*, evaluation based solely on the relative recovery of the compound in standard solutions may underestimate the interstitial concentrations (Benveniste *et al.*, 1989), due to the complex diffusion medium of brain tissue.

The initial trauma by the penetration of the dialysis probes into the brain tissue was indicated by the high levels of adenosine in the first 20 min to 1 h of the experiment, after which the levels of adenosine were stable. This could indicate that the tissue recovered from the initial damage in 1 h, a suggestion consistent with the demonstration that the cannula produces only a narrow track through the tissue, leaving the surrounding cells relatively intact (Lehmann *et al.*, 1983; Jacobson & Hamberger, 1984). However a recent study by Ballarin *et al.* (1991) revealed that a further decline of purine levels occurred up to 24 h following insertion of the microdialysis probe. It remains possible, therefore, that the basal levels reported here are still higher than the physiological value. Alternatively the 24 h decline might reflect the presence of gliosis or dead cells surrounding the probe.

Although the physiological role of adenosine as an inhibitory neuromodulator in the mammalian CNS has been well established, the physiological factors controlling the release of adenosine to the extracellular space are less clear (Stone *et al.*, 1990). Adenosine can be derived from energy-related compounds such as ATP and is released in distress states such as hypoxia, ischaemia and epileptic fits. Adenosine release may occur via a nucleoside transport system from a non-vesicular cytoplasmic pool and the direct release from such an intracellular source of adenosine independently of nucleotides has been demonstrated by several groups (Pons *et al.*, 1980; Barberis *et al.*, 1984; MacDonald & White, 1985; Jonzon & Fredholm, 1985; Meghji *et al.*, 1989).

The net pool of released adenosine, having escaped reuptake, will be subject to attack by adenosine deaminase in the extracellular fluid. This will lead to the formation of inosine and hypoxanthine and it is of great interest that the recovered levels of both these substances are increased following depolarization, but with a delayed time course relative to adenosine itself. This is a reassuring observation, suggesting strongly that the anticipated physiological deamination sequence is operating in the experimental paradigm employed here. If the production of hypoxanthine and inosine had paralleled or even preceded adenosine, then this would have presented great difficulties for interpretation, possibly implying some non-selective destruction or breakdown of tissue, with substantial intracellular deamination of adenosine.

NMDA and K^+ evoked release

In the present experiments both NMDA and potassium were able to release endogenous adenosine and its metabolites from the rat hippocampus *in vivo*. The effectiveness of

Table 2 Effects of 2-amino-5-phosphonopentanoic acid (2-AP5) and zero-Ca^{2+} on the release of adenosine, inosine and hypoxanthine evoked by either N-methyl-D-aspartate (NMDA) or KCl

	Adenosine		*Iosine*		*Hypoxanthine*	
	S2/S1 (%) (n)	% Con	S2/S1 (%) (*n*)	% Con	S2/S1 (%) (*n*)	% Con
NMDA						
Con	45 ± 10 (5)	–	56 ± 8 (5)	–	70 ± 14 (5)	–
2-AP5	3 ± 2* (4)	7.5	8 ± 5** (4)	14.2	4 ± 4* (4)	5.2
0Ca^{2+}	38 ± 6 (5)	83.9	43 ± 8 (5)	76.3	76 ± 27 (5)	108.4
K^+						
Con	45 ± 9 (5)	–	54 ± 12 (5)	–	76 ± 20 (5)	–
2-AP5	11 ± 4** (6)	23.5	16 ± 7* (5)	28.6	15 ± 13* (5)	19.3
0Ca^{2+}	17 ± 7* (4)	38.5	14 ± 8* (4)	26.4	18 ± 13* (4)	23.6

The significant changes in the S2/S1 values following the administration of 2-AP5 or zero-Ca^{2+} (0Ca^{2+}) compared to their controls (Con) are given (*$P < 0.05$; **$P < 0.01$). The test S2/S1 values in their controls in percentage (% Con) are also given to mark the changes.

NMDA was abolished, and that of potassium was substantially reduced by 2-AP5, yielding the important conclusion that the effects of both were mediated largely by NMDA-selective receptors. While this is not surprising in the case of NMDA itself, it was unexpected in the case of potassium. About 80% of the potassium-evoked release was inhibited by 200 μM 2-AP5, a concentration that is much lower than that used in brain slices to block the release evoked by L-glutamate or NMDA (Hoehn & White, 1990a). This is in marked contrast to the results of Hoehn & White (1990a) using cortical slices, where the application of 1 mM 2-AP5 reduced potassium-evoked release by only 30%. It is not easy to explain the difference between that study and the present one, but it may be related to the degree of tissue damage inflicted during the preparation of cortical slices. This may have severely reduced the capacity of the slice for action potential generation in feedback circuits, which are likely to remain functional *in vivo*.

The largely calcium-independent nature of the NMDA-evoked release may indicate that part of the adenosine was not from a transmitter-like vesicular pool in nerve terminals. However, the release could have occurred from a cytoplasmic pool located either in nerve terminals or cell bodies (neurones or glia), and resulting directly from depolarization induced by NMDA. It is interesting to note here recent reports suggesting the existence of NMDA receptors on striatal nerve terminals releasing dopamine (Chowdhury & Fillenz, 1991; Krebs *et al.*, 1991) and glutamate (Young & Bradford, 1991), and on noradrenergic terminals in cortex (Fink *et al.*, 1990) and hippocampus (Pittaluga & Raiteri, 1990). However such receptors may not be able to induce any release of adenosine from the terminals, since amino acids were not able to induce adenosine release from cortical or hippocampal synaptosomes (Hoehn & White, 1990b; Poli *et al.*, 1991).

In contrast to NMDA, potassium-induced purine release was significantly reduced in the absence of perfused calcium. It is very likely that potassium depolarization induced action potentials which in turn released glutamate and other excitatory amino acids able to evoke adenosine release by activating NMDA receptors. As noted above, this may be limited in slices of neocortex, accounting for the low efficiency of 2-AP5 on K^+-evoked release in that preparation (Hoehn & White, 1990b).

The ability of adenosine to suppress the release of excitatory neurotransmitters such as glutamate (Corradetti *et al.*, 1984; Fastbom & Fredholm, 1985; Burke & Nadler, 1988) and acetylcholine (Spignoli *et al.*, 1984; Jackisch *et al.*, 1984) makes it a potentially important agent in limiting the increase of excitatory neurotransmitter release and thus neurotoxicity, which follows cerebral hypoxia or ischaemia. Analogues of adenosine have indeed been shown to reduce substantially the cell damage produced by ischaemia (Januszewicz von Lubowitz *et al.*, 1989) and excitotoxins (Connick & Stone, 1989; Arvin *et al.*, 1989). Since depolarizing stimuli as diverse as NMDA and potassium ions appear to elevate readily adenosine concentration into the physiologically effective range, it may be that the endogenous purine can act as a critical brake at least in the early stages of excitotoxic phenomena. It should also be emphasized that the elevated concentration of adenosine may not be due only to its release evoked by NMDA or KCl, since adenosine and its metabolites are subject to uptake and further metabolism, which have not been inhibited in this study. It is also therefore possible that the changes of extracellular concentration of adenosine produced by NMDA or KCl could result from changes in uptake and metabolism.

This work was supported by the Scottish Home and Health Department. The authors are grateful to Professor C.A. Marsden for help and advice and Miss P. Feely for technical assistance.

References

ANDINE, P., RUDOLPHI., K.A., FREDHOLM, B.B. & HAGBERG, H. (1990). Effect of propentofylline (HWA 285) on extracellular purines and excitatory amino acids in CA1 of rat hippocampus during transient ischaemia. *Br. J. Pharmacol.*, **100**, 814–818.

ARVIN, B., NEVELLE, L.F., PAN, J. & ROBERTS, P.J. (1989). 2-Chloroadenosine attenuates kainic acid-induced toxicity within the rat striatum: relationship to release of glutamate and Ca^{2+} influx. *Br. J. Pharmacol.*, **98**, 225–235.

BALLARIN, M., FREDHOLM, B.B., AMBROSIO, S. & MAHY, N. (1991). Extracellular levels of adenosine and its metabolites in the striatum of awake rats: inhibition of uptake and metabolism. *Acta Physiol. Scand.*, **142**, 97–103.

BARBERIS, C., GUILBERT, B., DAUDET, F., CHARRIERE, B. & LEVIEL, V. (1984). In vivo release of adenosine from cat basal ganglia-studies with a push pull cannula. *Neurochem. Int.*, **6**, 545–551.

BENVENISTE, H., DREJER J., SCHOUSBOE, A. & DIEMER, N.H. (1984). Elevation of the extracellular concentrations of glutamate and aspartate in rat hippocampus during transient cerebral ischaemia monitored by intracerebral microdialysis. *J. Neurochem.*, **43**, 1369–1374.

BENVENISTE, H., HANSEN, A.J. & OTTOSEN, N.S. (1989). Determination of brain interstitial concentrations by microdialysis. *J. Neurochem.*, **52**, 1741–1750.

BURKE, S.P. & NADLER, J.V. (1988). Regulation of glutamate and aspartate release from slices of the hippocampal CA1 area: effects of adenosine and baclofen. *J. Neurochem.*, **51**, 1541–1551.

CHEN, Y. & STONE, T.W. (1991). Release of endogenous adenosine and related purines from the rat hippocampus *in vivo*. *Br. J. Pharmacol.*, **104**, 76P.

CHOWDHURY, M. & FILLENZ, M. (1991). Presynaptic adenosine-A2 and N-methyl-D-aspartate receptors regulate dopamine synthesis in rat striatal synaptosomes. *J. Neurochem.*, **56**, 1783–1788.

CONNICK, J.H. & STONE, T.W. (1989). Quinolinic acid neurotoxicity: protection by intracerebral phenylisopropyladenosine (PIA) and potentiation by hypotension. *Neurosci. Lett.*, **101**, 191–196.

CORRADETTI, R., LO CONTE, G., MORONI, F., PASSANI, B. & PEPEU, G. (1984). Adenosine decreases aspartate and glutamate release from rat hippocampal slices. *Eur. J. Pharmacol.*, **104**, 19–26.

COTMAN, C.W. & IVERSEN, L.L. (1987). Excitatory amino acids in the brain: focus on NMDA receptors. *Trends Pharmacol. Sci.*, **10**, 263–265.

DELEO, J., SCHUBERT, P. & KREUTZBERG, G.W. (1988). Propentofylline (HWA 285) protects hippocampal neurons of Mongolian gerbils against ischemic damage in the presence of an adenosine antagonist. *Neurosci. Lett.*, **84**, 301–311.

DELEO, J., TOTH, L., SCHUBERT, P., RUDOPHI, K. & KREUTZBERG, G.W. (1987). Ischemia-induced neuronal cell death, calcium accumulation, and glial response in the hippocampus of the mongolian gerbil and protection by propentofylline (HWA 285). *J. Cereb. Blood Flow Metab.*, **7**, 745–751.

DUNWIDDIE, T.V. (1985). The physiological role of adenosine in the central nervous system. *Int. Rev. Biochem.*, **27**, 63–139.

EVANS, M.C., SWAN, J.H. & MELDRUM, B.S. (1987). An adenosine analogue, 2-chloroadenosine, protects against long term development of ischaemic cell loss in the rat hippocampus. *Neurosci. Lett.*, **83**, 287–292.

FASTBOM, J. & FREDHOLM, B.B. (1985). Inhibition of [^{3}H]glutamate release from rat hippocampal slices by 1-phenylisopropyladenosine. *Acta Physiol. Scand.*, **125**, 121–123.

FINK, K., BONISCH, H. & GOTHERT, M. (1990). Presynaptic NMDA receptors stimulate noradrenaline release in the cerebral cortex. *Eur. J. Pharmacol.*, **185**, 115–117.

FOSTER, A.C. & FAFF, G.E. (1987). Taking apart NMDA receptors. *Nature*, **239**, 395–396.

FREDHOLM, B.B., JONZON, B. & LINDGREN, E. (1983). Inhibition of NA release from hippocampal slices by a stable analogue. *Acta Physiol. Scand. Suppl.*, **515**, 7–10.

GLOBUS, M.Y.-T., BUSTO, R., DIETRICH, W.D., MARTINEZ, E., VALDES, I. & GINSBERG, M.D. (1988). Effect of ischaemia on the in vivo release of striatal dopamine, glutamate, and gamma-aminobutyric acid studied with intracerebral microdialysis. *J. Neurochem.*, **51**, 1455–1464.

HAAS, H.L. & GREEN, R.W. (1988). Endogenous adenosine inhibits hippocampal CA1 neurones: further evidence from extra- and intracellular recording. *Naunyn Schmiedebergs Arch. Pharmacol.*, **337**, 561–565.

HAGBERG, H., LEHMANN, A., SANDBERG, M., NYSTROM, B., JACOBSON, I. & HAMBERGER, A. (1985). Ischaemia-induced shift of inhibitory and excitatory amino acids from intra- to extracellular compartments. *J. Cereb. Blood Flow Metab.*, **5**, 413–419.

HAGBERG, H., ANDERSSON, P., LKACAREWICZ, J., JACOBSON, I., BUTCHER, S. & SANDBERG, M. (1987). Extacellular adenosine, inosine, hypoxanthine and xanthine in relation to tissue nucleotides and purines in rat striatum during transient ischemia. *J. Neurochem.*, **49**, 227–231.

HOEHN, K. & WHITE, T.D. (1990a). Role of excitatory amino acid receptors in K^+- and glutamate-evoked release of endogenous adenosine from rat cortical slices. *J. Neurochem.*, **54**, 256–265.

HOEHN, K. & WHITE, T.D. (1990b). N-methyl-D-aspartate, kainate and quisqualate release endogenous adenosine from rat cortical slices. *Neurosci.*, **39**, 441–450.

HOLLINS, C. & STONE, T.W. (1980). Characteristics of the release of adenosine from slices of rats cerebral cortex. *J. Physiol.*, **303**, 73–82.

JACKISCH, R., STRITTMATTER, H., LKASAKOV, T. & HERTTING, G. (1984). Endogenous adenosine as a modulator of hippocampal Ach release. *Arch. Pharmacol.*, **327**, 319–325.

JACOBSON, I. & HAMBERGER, A. (1984). Veratridine-induced release in vivo and in vitro of amino acids in the rabbit olfactory bulb. *Brain Res.*, **299**, 103–112.

JANUSZEWICZ VON LUBITZ, D.K.E., DAMBROSIA, J.M. & REDMOND, D.J. (1989). Protective effect of cyclohexyl adenosine in treatment of cerebral ischemia in gerbils. *Neurosci.*, **30**, 451–462.

JONZON, B. & FREDHOLM, B.B. (1985). Release of purines, noradrenaline and GABA from rat hippocampal slices by field stimulation. *J. Neurochem.*, **44**, 217–224.

KREBS, M.O., DESCE, J.M., KEMEL, M.L., GAUCHY, C., GODEHEU, G., CHERAMY, A. & GLOWINSKI, J. (1991). Glutamatergic control of dopamine release in the rat striatum – evidence for presynaptic N-methyl-D-aspartate receptors on dopaminergic nerve terminals. *J. Neurochem.*, **56**, 81–85.

KRISHTAL, O.A., SMIRNOV, S.V. & OSIPCHUK, YU.V. (1988). Changes in the state of the excitatory synaptic system in the hippocampus on prolonged exposure to excitatory amino acids and antagonists. *Neurosci. Lett.*, **85**, 82–88.

LEHMANN, A., ISACSSON, H. & HAMBERGER, A. (1983). Effects of in vivo administration of kainic acid on the extracellular amino acid pool in the rabbit hippocampus. *J. Neurochem.*, **40**, 1314–1320.

MACDONALD, W.F. & WHITE, T.D. (1985). Nature of extrasynaptosomal accumulation of endogenous adenosine evoked by K^+ and veratridine. *J. Neurochem.*, **45**, 791–797.

MEGHJI, P., TUTTLE, J.J. & RUBIO. R. (1989). Adenosine formation and release by embryonic chick neurons and glia in cell culture. *J. Neurochem.*, **53**, 1852–1860.

PAXINOS, G. & WATSON, C. (1986). *The Rat Brain in Stereotaxic Coordinates.* New York: Academic Press.

PEDATA, F., PAZZAGLI, M., TILLI, S. & PEPEU, G. (1990). Regional differences in the electrically stimulated release of endogenous and radioactive adenosine and purine derivatives from rat brain slices. *Naunyn-Schmiedebergs Arch Pharmacol.*, **342**, 447–453.

PHILLIS, J.W. (ed.) (1991). *Adenosine and Adenine Nucleotides as Regulators of Cell Function.* Boca Raton: CRC Press.

PHILLIS, J.W. & O'REGAN, M.H. (1989). Deoxycoformycin antagonizes ischaemia-induced neuronal degeneration. *Brain Res. Bull.*, **22**, 537–540.

PHILLIS, J.W., WALTER, G.A., O'REGAN, M.H. & STAIR, R.E. (1987). Increases in cerebral cortical perfusate adenosine and inosine concentrations during hypoxia and ischaemia. *J. Cereb. Blood Flow Metab.*, **7**, 679–686.

PHILLIS, J.W., O'REGAN, M.H. & WALTER, G.A. (1988). Effects of deoxycoformycin on adenosine, inosine, hypoxanthine, xanthine and uric acid release from the hypoxic rat cerebral cortex. *J. Cereb. Blood Flow Metab.*, **8**, 733–741.

PHILLIS, J.W., WALTER, G.A. & SIMPSON, R.E. (1991). Brain adenosine and transmitter amino acid release from the ischemic rat cerebral cortex: effects of the adenosine deaminase inhibitor deoxycoformycin. *J. Neurochem.*, **56**, 644–650.

PITTALUGA, A. & RAITERI, M. (1990). Release-enhancing glycine-dependent presynaptic NMDA receptors exist on noradrenergic terminals of hippocampus. *Eur. J. Pharmacol.*, **191**, 231–234.

POLI, A., LUCCHI, R., VIBIO, M. & BARNABEI, O. (1991). Adenosine and glutamate modulate each other's release from rat hippocampal synaptosomes. *J. Neurochem.*, **57**, 298–306.

PONS, F., BRUNS, R.F. & DALY, J.W. (1980). Depolarization-evoked accumulation of cyclic AMP in brain slices: the requisite intermediate adenosine is not derived from hydrolysis of released ATP. *J. Neurochem.*, **34**, 1319–1323.

REDDINGTON, M. & LEE, K.S. (1991). Adenosine receptor subtypes: classification and distribution. In *Adenosine in the Nervous System* ed. Stone, T.W. London: Academic Press. (in press).

SPIGNOLI, G., PEDATA, F. & PEPEU, G. (1984). A_1 and A_2 adenosine receptors modulate acetylcholine release from brain slices. *Eur. J. Pharmacol.*, **97**, 341–343.

STONE, T.W. (1989). Purine receptors and their pharmacological potential. *Adv. Drug Res.*, **18**, 292–429.

STONE, T.W., NEWBY, A.F. & LLOYD, H.G.E. (1990). Adenosine release. In *Adenosine and Adenosine Receptors* ed. Williams, M. New Jersey: Humana Press. pp. 173–224.

STONE, T.W. & SIMMONDS, H.A. (1991). *Purines: Basic and Clinical Aspects.* London: Kluwer Academic Press.

TRUSSEL, L.D. & JACKSON, M.B. (1985). Adenosine activated K^+ conductance in cultured striatal neurons. *PANS*, **82**, 4857–4861.

WILLIAMS, M. (1990). (ed.) *Adenosine and Adenosine Receptors.* New Jersey: The Humana Press.

WINN, H.R., RUBIO, R. & BERNE, R.M. (1979). Brain adenosine production in the rat during 60 seconds of ischemia. *Circ. Res.*, **45**, 486–492.

VAN WYLEN, D.G.L., PARK, T.S., RUBIO, R. & BERNE, R.M. (1986). Increases in cerebral interstitial fluid adenosine concentrations during hypoxia, local potassium infusion and ischemia. *J. Cereb. Blood Flow Metab.*, **6**, 522–528.

YOUNG, A.M.J. & BRADFORD, H.F. (1991). N-Methyl-D-aspartate releases excitatory amino acids in rat corpus striatum *in vivo*. *J. Neurochem.*, **56**, 1677–1683.

ZETTERSTRÖM, T., VERNET, L., UNGERSTEDT, U., TOSSMAN, U., JONZON, B. & FREDHOLM, B.B. (1982). Purine levels in the intact brain, studied with an implanted perfused hollow fibre. *Neurosci. Lett.*, **29**, 111–115.

(Received December 5, 1991
Revised March 5, 1992
Accepted March 13, 1992)

Br. J. Pharmacol. (1992), **106**, 639–643

The M_3 muscarinic receptor links to three different transduction mechanisms with different efficacies in circular muscle of guinea-pig stomach

[1]Anant B. Parekh & Alison F. Brading

University Department of Pharmacology, Mansfield Road, Oxford OX1 3QT

1 In a previous publication, we showed that 10 μM carbachol induced contraction by activating three independent transduction mechanisms in circular smooth muscle of guinea-pig gastric fundus (Parekh & Brading, 1991). These were: inositol trisphosphate-mediated intracellular Ca^{2+} release, Ca^{2+} influx through a nifedipine-sensitive route and Ca^{2+} influx through a receptor operated nifedipine-insensitive pathway. The former two processes contribute to the phasic contraction and the latter two to the tonic contraction. In this paper, we have studied the effects of muscarinic receptor antagonists with known selectivity for different muscarinic receptor subtypes, on the contraction evoked by 10 μM carbachol.

2 Low concentrations of pirenzepine (M_1 selective) had little effect on the contraction initiated by carbachol. Higher concentrations (> 1 μM) reduced only the phasic component. This concentration of pirenzepine greatly reduced the contraction evoked by 10 μM carbachol in Ca^{2+}-free solution, indicating inhibition of intracellular Ca^{2+} release.

3 In the presence of 10 μM nifedipine, the tonic contraction evoked by 10 μM carbachol (reflecting the receptor-operated nifedipine-insensitive route) was abolished by 10 μM pirenzepine. In the absence of nifedipine pretreatment, however, 10 μM pirenzepine did not abolish the contraction to 10 μM carbachol. This contraction was subsequently abolished by nifedipine.

4 Only high concentrations (> 10 μM) of the M_2-selective antagonist, gallamine, inhibited the contraction to 10 μM carbachol. Like pirenzepine, gallamine preferentially inhibited the phasic component of the contraction, indicating an effect on intracellular Ca^{2+} release.

5 The non-selective muscarinic receptor antagonist, atropine, abolished all components of the contraction. At low concentrations, atropine also reduced the phasic component without affecting the tonic one, indicating preferential inhibition of intracellular Ca^{2+} release.

6 It is concluded that (i) the different transduction mechanisms have different sensitivities to the antagonists used and (ii) an M_3 receptor activates the three transduction mechanisms with different efficacies.

Keywords: Carbachol; stomach; pirenzepine; efficacy; muscarinic receptors

Introduction

Muscarinic receptor activation can regulate several different postsynaptic transduction mechanisms within the same tissue. In the heart, for example, acetylcholine regulates an atrial potassium channel through a pertussis toxin-sensitive G protein (Yatani *et al.*, 1987) and reduces the positive ionotropic and chronotropic effects of adenosine 3′:5′-cyclic monophosphate (cyclic AMP) by activating a guanosine 3′:5′-cyclic monophosphate (cyclic GMP)-dependent cyclic AMP phosphodiesterase (Hartzell & Fischmeister, 1986). Similarly, in smooth muscle, several transduction mechanisms are affected by muscarinic receptor activation. In longitudinal muscle of guinea-pig ileum, muscarinic receptor stimulation can (1) depolarize the plasma membrane through a pertussis toxin-sensitive G protein that links to a non-selective cation channel (Inoue & Isenberg, 1990), (2) increase inositol trisphosphate (IP_3) levels (Best *et al.*, 1985) and (3) increase cyclic GMP levels (Lee *et al.*, 1972). It is not clear, however, whether these effects are independent or related causally such that activation of one transduction system secondarily activates the others.

Muscarinic receptor stimulation contracts circular muscle of guinea-pig gastric fundus through nifedipine-sensitive and nifedipine-insensitive calcium influx and IP_3-induced calcium release (Parekh & Brading, 1991). This diversity could arise either through the presence of three different muscarinic receptor subtypes (each preferentially linked to one transduction mechanism) or one subtype linked to the three transduction mechanisms with different efficacies. The aim of this study was to distinguish between these two alternatives by use of muscarinic receptor antagonists of known pharmacological selectivity. The results suggest that, in guinea-pig gastric fundus, one receptor subtype (M_3) links to the three transduction mechanisms with different efficacies.

Methods

Tissue preparation and solutions

Guinea-pigs of either sex were killed by stunning and bleeding. Stomachs were removed, and circularly oriented smooth muscle strips (about 1 mm wide and 10 mm long) were dissected from the fundus and mounted for isometric tension recording as previously described (Parekh & Brading, 1991). The composition of the physiological saline solution was (mM): NaCl 130, KCl 5.9, $MgCl_2$ 1.2, $CaCl_2$ 2.4, $NaHCO_3$ 5, glucose 11, HEPES 5. pH was adjusted to 7.35–7.40 with Tris base. The solutions were gassed with 100% oxygen and warmed to 35–38°C. Drugs used were carbachol chloride, nifedipine, atropine sulphate, pirenzepine

[1] Author for correspondence.

dihydrochloride and gallamine triethyliodide (all from Sigma).

Experimental protocol and rationale

Carbachol (10 μM) activates all three muscarinic receptor transduction mechanisms involved in the contractile response of the circular smooth muscle of the gastric fundus (Parekh & Brading, 1991), resulting in a response consisting of a transient phasic contraction followed by a tonic contraction. The phasic contraction (measured at 2 min) reflects both intracellular calcium release and calcium influx through a nifedipine-sensitive route, whereas the tonic contraction (measured at 15 min) reflects calcium influx through both nifedipine-sensitive and nifedipine-insensitive routes. We therefore examined the effects of increasing concentrations of muscarinic antagonists with different subtype selectivities on the contractile response to a 15 min application of 10 μM carbachol, supposing that if an antagonist reduced the phasic but not the tonic contraction, it would preferentially be inhibiting receptor-mediated intracellular calcium release. The effects of antagonists on the tonic contractions were also studied in the absence or presence of nifedipine to enable a distinction to be made between the nifedipine-sensitive and insensitive pathways. Antagonists and nifedipine were applied for 15 min before and during the tissue exposure to carbachol.

Results are expressed as means ± s.e.mean. Significance was assessed by a paired t test when responses were compared in the same strip. Values of P less than 0.05 are taken as significant and shown with a single *.

Results

Effects of pirenzepine

After a reproducible control contraction had been obtained to a 15 min application of 10 μM carbachol (usually after the third carbachol exposure), preparations were exposed to the M_1 selective antagonist pirenzepine (0.01–10 μM) for 15 min before, and during the application of carbachol. Typical results are shown in Figure 1. Only at pirenzepine concentrations of ⩾ 1 μM was an effect clearly seen (Figure 1b and 1f). The phasic response was reduced in both rate of rise and amplitude but the tonic component was not affected. Indeed, a small increase in this latter component was generally observed. In the presence of 10 μM pirenzepine, only a small, slowly developing contraction occurred (Figure 1c, g). This contraction was abolished by 10 μM nifedipine (Figure 1g; 8 strips from 3 animals). If preparations were first exposed to 10 μM nifedipine, a slowly developing tonic contraction developed on carbachol application as previously described (Figure 1b in Parekh & Brading, 1991). This contraction (in the maintained presence of nifedipine) was abolished after 10 μM pirenzepine pretreatment (Figure 1d; 9 strips from 3 animals). The effects of pirenzepine were not the result of either a gradual rundown of the response of the tissue or of a specific loss of contraction to carbachol because contractions in control strips taken from the same animal were highly reproducible over a time-course of hours. The effects of pirenzepine are summarised in Figure 2 (16 strips from 4 animals).

In another set of experiments, the effects of pirenzepine on the contraction arising from intracellular Ca^{2+} release were studied. The approach was as previously described (Parekh & Brading, 1991). In brief, preparations were exposed to 40 mM K^+-containing physiological saline solution for 4 min (to load the intracellular stores via depolarization-induced Ca^{2+} entry). Tissues were then washed in Ca^{2+}-free solution (containing 1 mM EGTA) for 4 min to remove extracellular Ca^{2+}. A 2 min application of carbachol in Ca^{2+}-free solution resulted in a contraction which was not significantly affected by 0.1 μM pirenzepine (the response being 87 ± 12% of the control), but which was reduced to 37 ± 6% by 1 μM pirenzepine and abolished by 10 μM pirenzepine.

Effects of gallamine

The effects of this non-competitive M_2 antagonist were studied by the same approach as that for pirenzepine de-

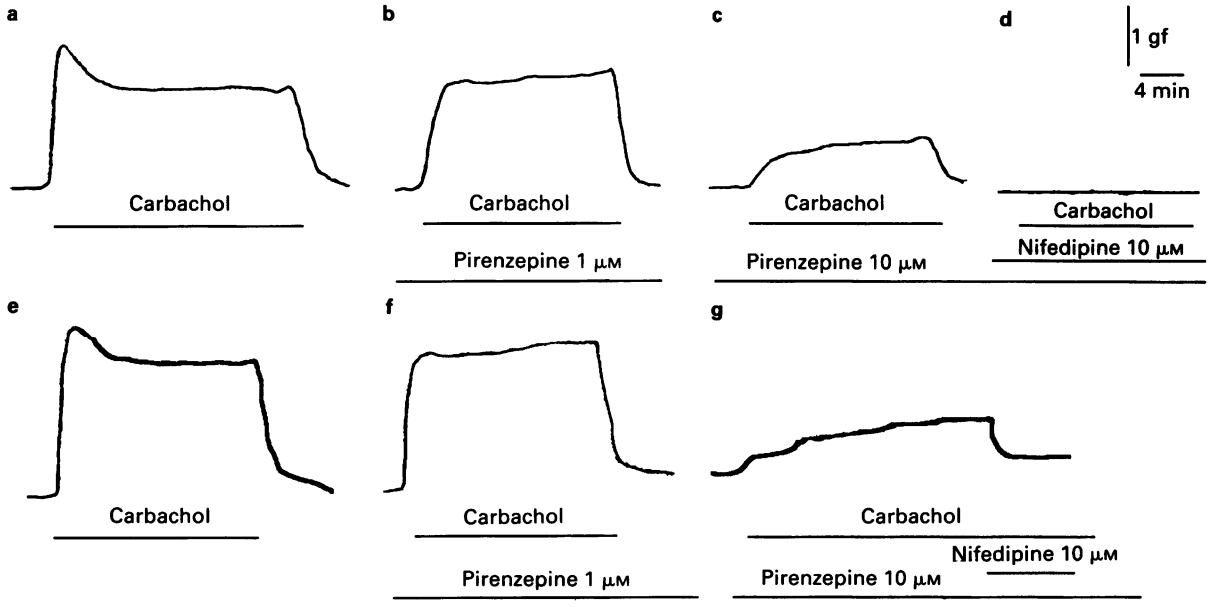

Figure 1 Effects of pirenzepine on the contractions of the circular smooth muscle of the guinea-pig stomach evoked by 10 μM carbachol: (a) and (e) control responses to carbachol; (b) and (f) responses to carbachol in the presence of 1 μM pirenzepine; (c) (d) and (g) responses to carbachol in the presence of 10 μM pirenzepine. In (d) the preparation had been exposed to 10 μM nifedipine for 15 min before application of carbachol. In (g) carbachol was applied for 15 min, and then in the continuous presence of carbachol, 10 μM nifedipine was applied. Tissues were pretreated with pirenzepine for 15 min before, and during exposure to carbachol. (a–d) are from one preparation and (e–g) are from another preparation.

scribed above. Results are summarised in Figure 3. Only at a concentration of 10 μM did gallamine have any effect. At this concentration, the phasic contraction was reduced in both rate of rise and amplitude but the tonic component was not affected. During the tonic contraction, application of 30 μM gallamine only slightly reduced the contraction further (result not shown).

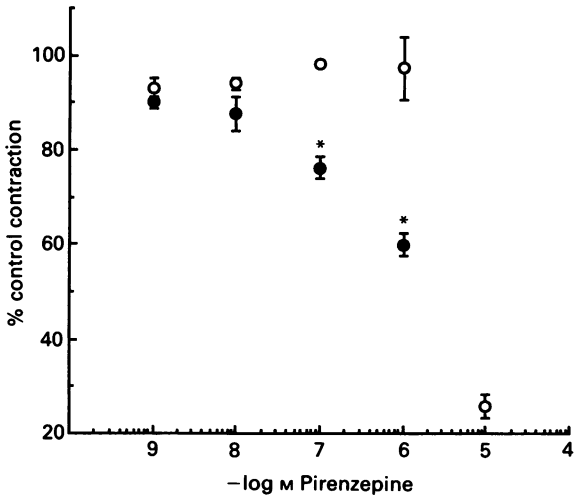

Figure 2 Effects of pirenzepine on the contractions of the circular smooth muscle of the guinea-pig stomach evoked by 10 μM carbachol: (●) phasic contractions (after 2 min carbachol); (○) tonic contractions (after 15 min carbachol). In all experiments pirenzepine was applied for 15 min before, and during the carbachol exposure. The carbachol contracture was recorded in the presence of all five concentrations of pirenzepine for each strip, and preparations were perfused with pirenzepine-free physiological saline for 10 min between pirenzepine exposures. The response evoked by 10 μM carbachol in the absence of pirenzepine was taken as 100%. Means with s.e.mean shown by vertical bars (where larger than symbol). $n = 16$ strips from 3 animals. *Denotes significant difference between phasic and tonic contractions ($P < 0.01$).

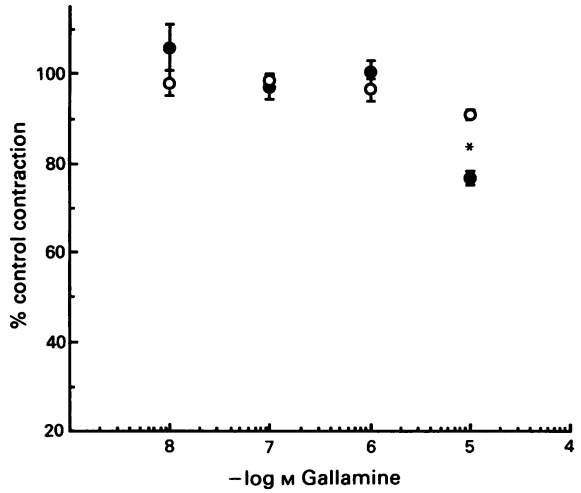

Figure 3 Effects of gallamine on the contractions of the circular smooth muscle of the guinea-pig stomach evoked by 10 μM carbachol: (●) phasic contractions (after 2 min carbachol); (○) tonic contractions (after 15 min carbachol). In all experiments gallamine was applied for 15 min before, and during the carbachol exposure. The carbachol contracture was recorded in the presence of all four concentrations of gallamine for each strip, and preparations were perfused with gallamine-free physiological saline for 10 min between gallamine exposures. The response evoked by 10 μM carbachol in the absence of gallamine was taken as 100%. Means with s.e.mean shown by vertical bars (where larger than symbol). $n = 10$ strips from 2 animals. *Denotes significant difference between phasic and tonic contractions ($P < 0.01$).

Effects of atropine

The same protocol as above was used to study the effects of the non-selective competitive muscarinic antagonist, atropine. Results are summarised in Figures 4 and 5. Atropine 0.01 μM significantly reduced the phasic contraction but had only a slight inhibitory effect on the tonic contraction. At 0.1 μM, atropine greatly reduced both phasic and tonic components (Figure 4c), leaving a small, slowly developing contraction; 1 μM atropine abolished the contraction altogether.

Discussion

The two main findings of this study are first, that the different transduction mechanisms involved in muscarinic receptor activation have different sensitivities to the antagonists used and second, that none of these transduction mechanisms is mediated by pharmacologically defined M_1 or M_2 muscarinic receptor subtypes.

Pirenzepine is considered to be a relatively specific M_1 competitive antagonist with an IC_{50} of approximately 80 nM (Buckley *et al.*, 1989). As an effect was seen only with a high pirenzepine concentration (IC_{50} approximately 3 μM), it would appear that the responses to carbachol are not mediated by an M_1 subtype. Similar conclusions have been drawn from results in some other types of smooth muscle. Thus in rabbit gastric antrum, pirenzepine inhibited contractions to acetylcholine with an IC_{50} of approximately 1 μM (Moummi *et al.*, 1988), an IC_{50} of 450 nM was found for pirenzepine inhibition of muscarinic receptor stimulation of inositol phosphate accumulation in guinea-pig taenia caeci (Gardner *et al.*, 1988), an IC_{50} of 3 μM was found for pirenzepine inhibition of phospho-inositide turnover in bovine tracheal smooth muscle (Grandordy *et al.*, 1986) and pirenzepine inhibited the binding of [^{3}H]-quinuclidinyl benzilate (a non-selective muscarinic antagonist) with an IC_{50} of 870 nM in rabbit colonic smooth muscle (Ringer *et al.*, 1987). In each of these studies, it was also concluded that an M_1 receptor was not involved. We also observed that atropine was about 100 times more potent than pirenzepine in inhibiting contraction to carbachol. Similar observation has been made in rabbit saphenous vein (Komori & Suzuki, 1987) and human urinary bladder (Zappia *et al.*, 1986).

In our experiments the initial phasic component of the carbachol contraction was reduced by 1 μM pirenzepine wheras the tonic component was unchanged. As we have previously shown that the tonic contraction is a function of Ca^{2+} influx through both nifedipine-sensitive and receptor-operated pathways, whereas the phasic component reflects Ca^{2+} release via IP_3 as well as nifedipine-sensitive Ca^{2+} influx (Parekh & Brading, 1991), it seems reasonable to conclude that intracellular Ca^{2+} release is more sensitive to pirenzepine than are the other two transduction mechanisms. Consistent with this, was the finding that the contraction to carbachol in Ca^{2+}-free solution (reflecting only intracellular Ca^{2+} release) was significantly reduced by 1 μM pirenzepine. These observations lead to another conclusion: as the tonic contraction (in the presence of extracellular Ca^{2+}) was not affected by 1 μM pirenzepine, it seems that Ca^{2+} influx through both the nifedipine-sensitive and receptor-operated pathways does not enter the intracellular store first (otherwise block of intracellular Ca^{2+} release should prevent contraction). Hence it seems that Ca^{2+} influx and intracellular release pathways are in parallel and not in series, as is also the case for avian nasal gland (Shuttleworth, 1990).

In the presence of 10 μM pirenzepine, a small contraction occurred on exposure to carbachol and this was abolished by nifedipine. This suggests that inhibition of the transduction mechanism linking the muscarinic receptor to the voltage-

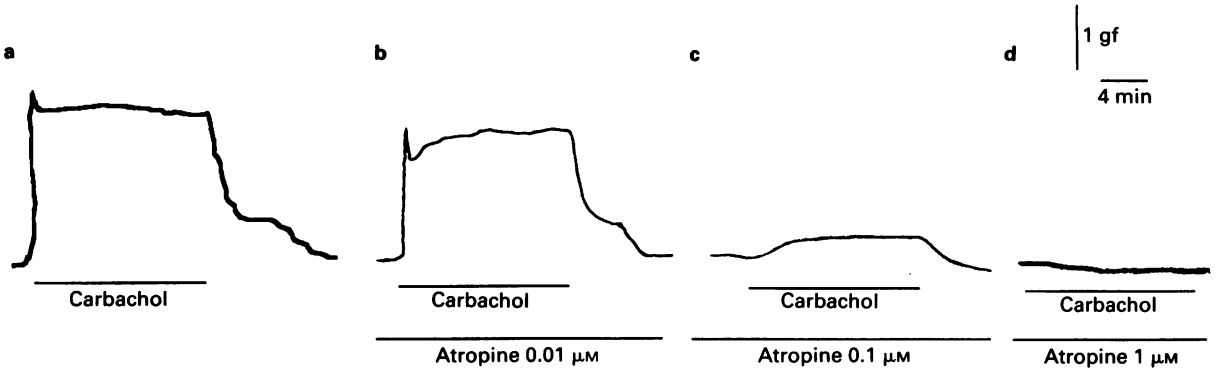

Figure 4 Effects of atropine on the contractions of the circular smooth muscle of the guinea-pig stomach evoked by 10 μM carbachol. (a) Control response to carbachol; (b–d) responses to carbachol in the presence of increasing concentrations of atropine. Tissues were pretreated with atropine for 15 min before, and during exposure to carbachol.

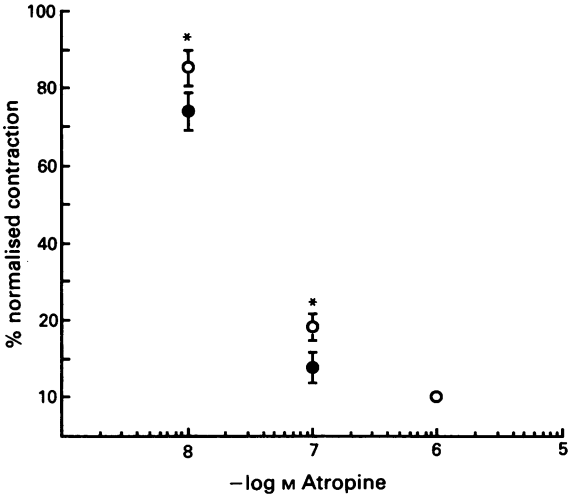

Figure 5 Effects of atropine on the contractions of the circular smooth muscle of the guinea-pig stomach evoked by 10 μM carbachol: (●) phasic contractions (after 2 min carbachol); (○) tonic contractions (after 15 min carbachol). In all experiments atropine was applied for 15 min before, and during the carbachol exposure. The carbachol contracture was recorded in the presence of all three concentrations of atropine for each strip, and preparations were perfused with atropine-free physiological saline for 10 min between atropine exposures. The response evoked by 10 μM carbachol in the absence of atropine was taken as 100%. Means with s.e.mean shown by vertical bars (where larger than symbol). $n = 12$ strips from 2 animals. *Denotes significant difference between phasic and tonic contractions ($P < 0.01$).

gated (nifedipine-sensitive) Ca^{2+} influx pathway is less sensitive to pirenzepine than the mechanism linking the receptor operated (nifedipine-insensitive) Ca^{2+} influx pathway. A corollary of this is that activation of the receptor-operated Ca^{2+} influx pathway is not secondarily activating the voltage-gated Ca^{2+} entry mechanism as the latter is present (albeit reduced) when the former is lost. This substantiates our previous conclusion that the transduction mechanisms are independent (Parekh & Brading, 1991).

The greater sensitivity of the phasic component of the carbachol contraction to pirenzepine, is also seen with gallamine, an M_2-selective antagonist (Watson & Abbott, 1990; Pedder *et al.*, 1991) and atropine, a non-selective muscarinic receptor antagonist. All three reduced the phasic contraction at concentrations that did not affect the tonic component. As gallamine only had this effect at high concentrations (10 μM), it seems that an M_2 muscarinic receptor subtype is not significantly involved in the contraction to carbachol. If neither the M_1 nor the M_2 receptors are involved, and since the responses to carbachol are more sensitive to the non-selective muscarinic receptor antagonist atropine, than to pirenzepine and gallamine, then it seems probable that the receptors involved are M_3 muscarinic receptors.

Taken together, these results suggest that the intracellular Ca^{2+} release mechanism is the most sensitive to muscarinic receptor blockade, whereas the nifedipine-sensitive Ca^{2+} influx pathway is the least sensitive.

The answer to the key question of whether one muscarinic receptor subtype is linked to more than one transduction mechanism (i.e. with different efficacies) or the different transduction mechanisms are linked to different muscarinic receptor subtypes in the circular, muscle of the guinea-pig stomach, seems to be the former. The results suggest that the pharmacologically defined M_3 subtype is involved in all three signal transduction mechanisms. The M_3 subtype has been shown to be expressed postsynaptically in several types of mammalian smooth muscle (guinea-pig ileum, Giraldo *et al.*, 1988; trachea, Barnes *et al.*, 1988) as well as toad stomach (Lucchesi *et al.*, 1989). We would conjecture that the M_3 subtype in the guinea-pig gastric fundus links to the different, independent transduction mechanisms with different efficacies In support of this are the results of Ashkenazi *et al.* (1987) who concluded that a transfected muscarinic receptor (in this case the M_2 subtype) could link to two different transduction mechanisms.

References

ASHKENAZI, A., WINSLOW, J.W., PERALTA, E.G., PETERSON, G.L., SCHIMERLIK, M.I., CAPON, D.J. & RAMACHANDRAN, J. (1987). An M_2 muscarinic receptor subtype coupled to both adenylyl cyclase and to phosphatidyl inositol turnover. *Science*, **238**, p. 672–675.

BARNES, P.J., MINETTE, P. & MACLAGAN, J. (1988). Muscarinic receptor subtypes in airways. *Trends Pharmacol. Sci.*, **9**, 412–416.

BEST, L., BROOKS, K.J. & BOLTON, T.B. (1985). Relationship between stimulated inositol lipid hydrolysis and contractility in guinea-pig visceral longitudinal smooth muscle. *Biochem. Pharmacol.*, **34**, 2297–2301.

BUCKLEY, N.J., BONNER, T.I., BUCKLEY, C.M. & BRANN, M.R. (1989). Antagonist binding properties of five cloned muscarinic receptors expressed in CHO-K1 cells. *Molec. Pharmacol.*, **35**, 469–476.

GARDNER, A.L., CHOO, L.K. & MITCHELSON, F. (1988). Comparison of the effects of some muscarinic agonists on smooth muscle function and phosphatidylinositol turnover in the guinea-pig taenia caeci. *Br. J. Pharmacol.*, **94**, 199–211.

GIRALDO, E., VIGANO, M.A., HAMMER, R. & LADINSKY, H. (1988). Characterisation of muscarinic receptors in guinea pig ileum longitudinal smooth muscle. *Molec. Pharmacol.*, **33**, 617–625.

GRANDORDY, B.M., CUSS, F.M., SAMPSON, A.S., PALMER, J.B. & BARNES, P.J. (1986). Phosphatidylinositol response to cholinergic agonists in airway smooth muscle: relationship to contraction and muscarinic receptor occupancy. *J. Pharmacol. Exp. Ther.*, **238**, 273–279.

HARTZELL, H.C. & FISCHMEISTER, R. (1986). Opposite effects of cyclic GMP and cyclic AMP on Ca^{2+} current in single heart cells. *Nature*, **323**, 273–275.

INOUE, R. & ISENBERG, G. (1990). Acetylcholine activates nonselective cation channels in guinea-pig ileum through a G protein. *Am. J. Physiol.*, **27**, C1173–C1178..

KOMORI, K. & SUZUKI, H. (1987). Heterogenous distribution of muscarinic receptors in the rabbit saphenous artery. *Br. J. Pharmacol.*, **92**, 657–664.

LEE, T.-P., KUO, J.F. & GREENGARD, P. (1972). Role of muscarinic cholinergic receptors in regulation of guanosine 3:5-cyclic monophosphate content in mammalian brain, heart muscle and intestinal smooth muscle. *Proc. Natl. Acad. Sci. U.S.A.*, **69**, 3287–3291.

LUCCHESI, P.A., ROMANO, F.D., SCHEID, C.R., YAMAGUCHI, H. & HONEYMAN, T.W. (1989). Interaction of agonists and selective antagonists with gastric smooth muscle muscarinic receptors. *Naunyn-Schmiedebergs Arch. Pharmacol.*, **339**, 145–151.

MOUMMI, C., MAGOUS, R., STROSBERG, D. & BALI, J.P. (1988). Muscarinic receptors in isolated smooth muscle cells from gastric antrum. *Biochem. Pharmacol.*, **37**, 1363–1369.

PAREKH, A.B. & BRADING, A.F. (1991). The sources of calcium for carbachol-induced contraction in the circular smooth muscle of guinea-pig stomach. *Br. J. Pharmacol.*, **104**, 412–418.

PEDDER, E.K., EVELEIGH, P., POYNER, D., HULME, E.C. & BIRDSALL, N.J.M. (1991). Modulation of the structure-binding relationships of antagonists for muscarinic acetylcholine receptor subtypes. *Br. J. Pharmacol.*, **103**, 1561–1567.

RINGER, A.J., HYMAN, P.E., KAO, H.W., HSU, C.T., TOMOMASA, T. & SNAPE, W.J. Jr. (1987). [3H] QNB binding and contraction of rabbit colonic smooth muscle cells. *Am. J. Physiol.*, **253**, G656–661.

SHUTTLEWORTH, T. (1990). Receptor-activated calcium entry in exocrine cells does not occur via agonist-sensitive intracellular pools. *Biochem. J.*, **266**, 719–726.

WATSON, S.P. & ABBOTT, A. (1990). Receptor nomenclature. *Trends Pharmacol. Sci.*, **11**, (suppl.) 18.

YATANI, A., CODINA, J., BROWN, A.M. & BIRNBAUMER, L. (1987). Direct activation of mammalian atrial muscarinic potassium channels by GTP regulatory protein. G_k. *Science*, **235**, 207–211.

ZAPPIA, L., CARTELLA, A., POTENZONI, D. & BERTACCINI, G. (1986). Action of pirenzepine on the human urinary bladder in vitro. *J. Urol.*, **136**, 739–742.

(Received November 11, 1991
Revised January 21, 1992
Accepted March 16, 1992)

Br. J. Pharmacol. (1992), **106**, 644–649

Effects of glucose, insulin or aldose reductase inhibition on responses to endothelin-1 of aortic rings from streptozotocin-induced diabetic rats

[1]W.C. Hodgson & R.G. King

Department of Pharmacology, Monash University, Clayton, Victoria, Australia, 3168

1 This study investigated the constrictor responsiveness to endothelin-1 (ET-1, 0.1 nM–0.1 μM) of aortic rings (under 10 g resting tension in Krebs solution) from 2- and 6-week streptozotocin (STZ, 60 mg kg^{-1}, i.v.)-induced diabetic rats and vehicle-treated control rats.

2 In aortae from 2- and 6-week STZ-treated rats, and their corresponding controls, removal of endothelium caused leftward shifts of ET-1 concentration-response curves without affecting maximum responses.

3 Maximum responses to ET-1 were reduced in aortae from both 2- and 6-week STZ-treated rats compared to those from control rats. Such reductions were still evident after removal of the endothelium.

4 Decreased responsiveness to ET-1 of aortae from 2-week STZ-treated rats was still evident after chronic treatment with the aldose reductase inhibitor epalrestat, but not after chronic insulin treatment or in aortae bathed in high glucose (30 mM) Krebs solution.

5 Decreased responsiveness to ET-1 of aortae from 6-week STZ-treated rats (compared with those from controls) was still evident after chronic epalrestat treatment and in high glucose Krebs solution.

6 These data suggest that the decreased responsiveness to ET-1 observed in aortae from 2- and 6-week STZ-induced diabetic rats is not due to abnormal activity of the polyol pathway. The altered responsiveness in aortae from 2-week diabetic rats (compared with those from control rats) may possibly be a manifestation of changes (adaptive or otherwise) which occur as a result of high glucose concentrations *in vivo*. However, in aortae from rats with diabetes of longer duration, other mechanisms may also play a role in the altered responsiveness, since it was no longer reversible by bathing in high glucose Krebs solution.

Keywords: Diabetes mellitus; rat aortae; endothelial cells; endothelin; aldose reductase inhibitor; insulin

Introduction

Elevated glucose levels can trigger the release of the potent vasoconstrictor peptide endothelin (ET) from endothelial cells (Yamauchi *et al.*, 1990). Changes in endothelial cell function have been found to occur in various cardiovascular disorders (Luscher *et al.*, 1989), some of which are associated with diabetes mellitus. We have previously reported that maximum responsiveness to ET-1 of aortic rings from 2-week streptozotocin (STZ)-induced diabetic rats was significantly reduced compared to that of rings from control rats (Fulton *et al.*, 1990; 1991). Such reduced responsiveness was also evident in the presence of the cyclo-oxygenase inhibitor indomethacin, or in the absence of extracellular calcium. The present study was designed to determine whether aortae from 6-week STZ-treated rats were less responsive to ET-1. The effect of insulin treatment on the altered responsiveness of aortae from 2-week STZ-treated rats was examined. Also, the effects of *in vitro* changes in extracellular glucose concentration, as well as the effect of aldose reductase inhibition, on responsiveness to ET-1 was examined in aortae from both 2- and 6-week STZ-treated rats.

Methods

Male Wistar rats (290–385 g) were treated with STZ (60 mg kg^{-1}, i.v.) or vehicle (50 mM citrate buffer) under 4% halothane anaesthesia (O_2/N_2O 2:1) as previously described (Fulton *et al.*, 1991). The animals were then housed in treatment pairs, being allowed free access to food and water at all times. Rat body weights and blood glucose levels were measured on the day of STZ or citrate buffer administration and again after either 2 or 6 weeks. Only rats displaying elevated blood glucose levels (> 16 mM, Ames Minilab 1) after 2 or 6 weeks were considered to be diabetic. Vehicle control rats had normal blood glucose levels when tested at the same times. After 2 or 6 weeks, a STZ-induced diabetic and a control animal were killed, and two 5 mm rings cut from each descending thoracic aorta (Fulton *et al.*, 1991). Endothelial cells were removed from one ring from each treatment group by rubbing (Fulton *et al.*, 1991). Rings were placed in 15 ml organ baths containing Krebs solution of the following composition (mM): NaCl 118.4, KCl 4.7, $CaCl_2$ 2.5, $NaHCO_3$ 25.0, KH_2PO_4 1.2, $MgSO_4.7H_2O$ 1.2, glucose 11.1. Where indicated, high-glucose Krebs consisted of Krebs solution with 30 mM glucose. Physiological solutions were maintained at 37°C, and bubbled with 5% CO_2 in O_2. Rings were placed under 10 g resting tension throughout the experiment, as this approximates more to the physiological wall tension than does the more commonly used *in vitro* tension of 1–2 g (Fulton *et al.*, 1991). Apart from the area of tissue directly in contact with the wire within the lumen, effective transmural pressure is assumed to apply uniformly when a blood vessel ring is stretched between two fixed points (Mulvany & Halpern, 1977). After 1 h equilibration at 10 g tension, a submaximal concentration of phenylephrine (0.3 μM) was added to the bath. At the plateau of contraction, acetylcholine

[1] Author for correspondence.

(10 μM) was added. The presence of functional endothelial cells was indicated by subsequent relaxation (Fulton *et al.*, 1991). A cumulative concentration-response (CR) curve to ET-1 was then obtained. ET-1 was added at intervals of between 5–20 min depending on the time taken for the previous response to reach a plateau. Contractions were recorded with a Grass FTO3 tension transducer connected to a Grass polygraph (Model 79E).

After each experiment, aortic rings were oven dried (50°C) and then weighed. The order of killing STZ-treated and control rats and the arrangement of tissues in organ baths were randomized.

Epalrestat treatment

Where indicated the aldose reductase inhibitor (ARI) epalrestat (40 mg kg^{-1} daily, p.o. by gavage), in 0.5% carboxymethyl-cellulose, was administered for 2 or 6 weeks, starting on the day of STZ or citrate buffer treatment.

Insulin treatment

Where indicated STZ-treated rats were injected with a single daily dose of Lente MC insulin zinc suspension (5 units day^{-1}). This treatment commenced on the second day after the STZ injection, and was continued until the rats were killed. Insulin treatment was started on the second day after STZ administration, since STZ-induced diabetes is characterized by the following pattern of blood glucose levels. After an initial delay of approximately 45–60 min there is a short period of hyperglycaemia (up to 6 h duration; Dulin *et al.*, 1967) followed by a severe hypoglycaemia lasting up to 48 h, and then chronic hyperglycaemia (Rerup, 1970).

Drugs

The following drugs were used: acetylcholine chloride (Sigma), carboxymethyl-cellulose (Sigma), endothelin-1 (Auspep; Batch no. CP36), epalrestat (ONO Pharmaceuticals), insulin (Lente MC zinc suspension, CSL-Novo), (−)-phenylephrine HCl (ICN Pharmaceutical), streptozotocin (Sigma).

Phenylephrine was dissolved in catecholamine diluent (0.312 g NaH_2PO_4 and 0.08 g ascorbic acid per litre of 0.9% (w/v) saline). Acetylcholine was dissolved in distilled water. Endothelin stock was dissolved in distilled water, divided into aliquots and frozen. On the day of use it was thawed and diluted in 0.9% saline.

Statistics

Single comparisons between responses in aortae from STZ-treated and control rats were made by Student's unpaired *t* test. Paired *t* tests were used for comparison of values from the same animal. Multiple comparisons were analysed by two way analysis of variance (ANOVA) and Tukey tests on the CLR ANOVA package (Apple Macintosh). Values shown are means ± s.e.mean. In all cases, statistical significance is indicated by $P<0.05$. EC_{50} values were determined from the E_{max} of each individual curve and the geometric mean (i.e. mean of the log values) determined.

Results

As shown in Table 1, dry weights of aortic rings from 2-week STZ-treated rats were not significantly different from those of 2-week controls. However weights of rings from 6-week STZ-treated rats were significantly reduced. Rats with diabetes of both 2 and 6 weeks duration displayed significantly reduced body weights compared to their pre-injection weights. However, 2- and 6-week control rats displayed significantly increased body weights compared to their corresponding pre-injection weights. The reduction in body weight observed in 2-week STZ-treated rats was not observed in 2-week diabetic rats treated with insulin. Increased blood glucose levels in 2-week STZ-treated rats were evident in rats chronically-treated with epalrestat, but were normalized (i.e. were between 4–8 mM) by chronic insulin treatment (Table 1).

Cumulative CR curves were obtained to ET-1 (0.1 nM–0.1 μM) in aortic rings from 2-week (Figure 1a,b) and 6-week (Figure 2a,b) STZ-treated rats and their corresponding controls, with and without endothelial cells. As shown in these Figures and Table 2, maximum responses of aortae from 2- and 6-week STZ-treated rats, with or without endothelial cells, were significantly reduced compared with those of aortae from controls. This decrease in responsiveness observed in aortae from 2-week STZ-treated rats was no longer significant in aortae from insulin-treated diabetic rats (Figure 1a,b). As shown in Figure 3a and b and Table 2, the reduction in maximum responsiveness to ET-1 in 2-week STZ-treated rats (compared to those from control rats) was not prevented by chronic treatment of diabetic rats with the aldose reductase inhibitor (ARI) epalrestat.

When experiments were performed in high glucose (30 mM) Krebs solution, there was no significant difference in responses to ET-1 between rings obtained from 2-week STZ-

Table 1 Body weights, blood glucose levels and aortic ring dry weights of control and streptozotocin (STZ)-treated rats

		Body weights (g)		*Blood glucose levels* (mM)		*Aortic ring dry weights* (mg)	
	(n)	*Initial*	*Final*	*Initial*	*Final*	*With E*	*Without E*
Control (2-week)	11	326 ± 8	379 ± 11†	6.3 ± 0.2	6.3 ± 0.2	1.67 ± 0.03	1.64 ± 0.03
Control (6-week)	12	330 ± 7	431 ± 10†	5.7 ± 0.3	6.0 ± 0.1	1.90 ± 0.08	1.83 ± 0.05
STZ (2-week)	11	332 ± 4	310 ± 9†*	5.8 ± 0.3	20.4 ± 0.6*†	1.60 ± 0.04	1.66 ± 0.04
STZ (6-week)	12	334 ± 5	281 ± 12*†	6.1 ± 0.2	21.1 ± 1.3*†	1.61 ± 0.04*	1.57 ± 0.04*
Control (2-week) /epalrestat	5	345 ± 11	390 ± 15†	6.8 ± 0.4	6.4 ± 0.3	1.69 ± 0.03	1.68 ± 0.04
STZ (2-week) /epalrestat	5	336 ± 13	321 ± 13*	5.7 ± 0.4	19.4 ± 0.9*†	1.56 ± 0.02	1.54 ± 0.06
Control (6-week) /epalrestat	6	335 ± 8	416 ± 12†	6.0 ± 0.5	5.6 ± 0.2	1.64 ± 0.06	1.62 ± 0.04
STZ (6-week) /epalrestat	6	349 ± 4	283 ± 13*†	6.8 ± 0.5	21.2 ± 1.1*†	1.40 ± 0.03*	1.42 ± 0.02*
STZ (2-week) /insulin	5	309 ± 7	359 ± 8†	5.5 ± 0.3	6.1 ± 0.8	1.47 ± 0.05	1.49 ± 0.07

Initial measurements were made at the time of STZ or vehicle injection, and final measurements made 2 or 6 weeks later.
E = endothelial cells.
*Significantly different from corresponding control group, $P<0.05$, unpaired *t* test.
†Significantly different from initial value in same treatment group, $P<0.05$, paired *t* test.

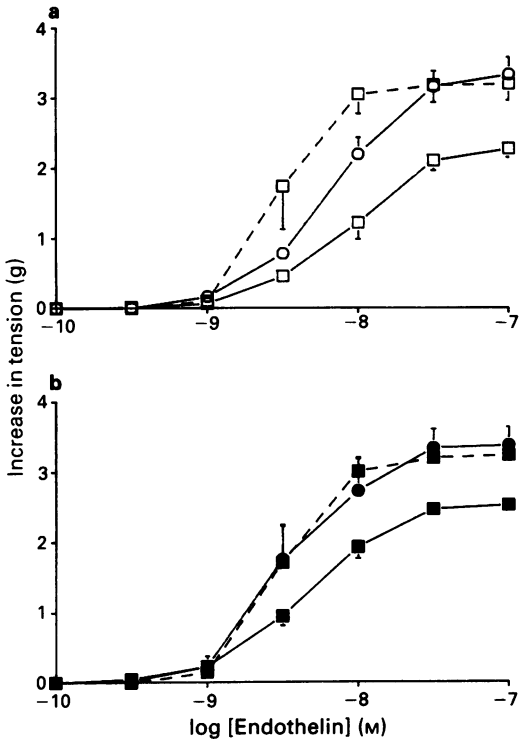

Figure 1 Responses to endothelin-1 of aortic rings from 2-week streptozotocin (STZ)-treated rats. (a) With endothelium: STZ-treated (□—□, $n = 6$), control (○—○, $n = 6$) and STZ-treated with insulin (□--□, $n = 5$). (b) Without endothelium: STZ-treated (■—■, $n = 6$), control (●—●, $n = 6$) and STZ-treated with insulin (■--■, $n = 5$).

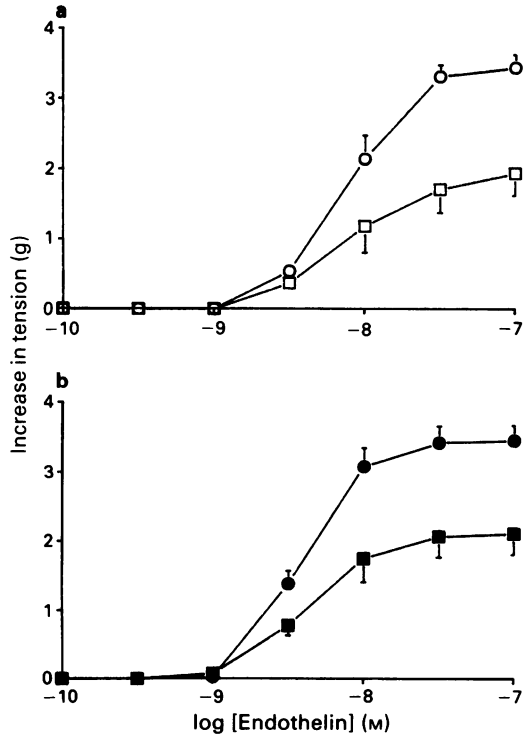

Figure 2 Responses to endothelin-1 of aortic rings from 6-week streptozotocin (STZ)-treated rats ($n = 6$). (a) With endothelium: STZ-treated (□) and control (○). (b) Without endothelium: STZ-treated (■) and control (●).

treated versus those from control rats (Figure 3a,b). There was also no significant difference when responses of aortic rings from 2-week control rats bathed in normal Krebs solution were compared to those from 2-week diabetic rats bathed in 30 mM glucose Krebs solution (Table 2, ANOVA). However, in high glucose Krebs solution there was a significant difference between responses of aortae from 6-week diabetic versus those from control rats (Figure 4a,b). There was also a significant difference in responsiveness to ET-1 of aortae bathed in normal Krebs solution from control rats, compared to that of aortae bathed in 30 mM glucose Krebs solution from diabetic rats (Table 2, ANOVA, $P < 0.05$). As shown in Figure 4a and b and Table 2, the reduction in maximum responsiveness to ET-1 in 6-week STZ-treated rats (compared to those from control rats) was not prevented by chronic treatment of diabetic rats with the ARI epalrestat. In all cases (except for endothelium-intact rings from 6-week diabetic rats bathed in 30 mM glucose Krebs solution) there was no significant effect of diabetes on EC_{50}s for ET-1 (Table 2).

Discussion

Results of the present study indicate that the previously reported reduced maximum responsiveness to ET-1 of aortic rings from 2-week STZ-treated rats (compared with 2-week controls; Fulton *et al.*, 1991) also occurs in aortae of 6-week diabetic rats. In the case of endothelium-intact or -denuded aortic rings from 2-week diabetic rats, the difference in maximum responses in the presence of normal glucose versus 30 mM glucose was not significant. However, the difference in responsiveness of aortae from 2-week diabetic versus control rats was not observed in physiological bathing solution containing 30 mM glucose. Thus it is possible that the high glucose concentrations which occur *in vivo* during diabetes may affect responsiveness to ET-1. Indeed, it is possible that the reduced responsiveness to ET-1 of aortae from 2-week diabetic rats (compared with controls), observed in normal Krebs solution, may be a manifestation of an adaption of the vasculature to high levels of circulating blood glucose. However, normalization of ET-1 responses in high glucose Krebs solution was not observed in aortae from 6-week rats. One conceivable explanation for this observation could be that with a longer duration of diabetes (6 weeks), changes and/or damage occurs to the vasculature which hinder the adaptive responses to high glucose levels postulated above. In addition to causing a change in responsiveness to ET-1, high glucose levels may also affect ET-1 release. Yamauchi *et al.* (1990) found that increasing the glucose concentration from 5.5 to 11.1 mM or 22.2 mM significantly stimulated ET-1 release from cultured bovine aortic endothelial cells. However, Hattori *et al.* (1991) found that hyperglycaemia caused inhibition of ET-1 release from cultured porcine aortic endothelial cells: under hyperglycaemic conditions (27.5 and 55 mM glucose) ET-1 release was inhibited by greater than 50%.

Results of the present study indicate that streptozotocin *per se* was not responsible for the changed responsiveness to ET-1 of aortae from 2-week diabetic rats, since insulin treatment prevented this changed responsiveness.

Some cells, including endothelial cells of blood vessels (Dvornik, 1978), do not require insulin to enable glucose entry, and are consequently susceptible to the fluctuating plasma levels of glucose associated with diabetes. During periods of hyperglycaemia the glycolytic pathway in these cells may become saturated and the polyol pathway activated. It has been postulated that this increased activity leads to many of the complications of diabetes (Beyer & Hutson, 1986). Inhibition of the rate-limiting enzyme of the polyol pathway, aldose reductase, has been shown to restore normal biochemical and functional parameters in some of these affected tissues (Beyer & Hutson, 1986). Indeed, Williamson *et al.* (1990) have reported that 30 mM glucose caused micro-

Table 2 Maximum responses and EC_{50} values for endothelin-1 (ET-1) of aortae from streptozotocin (STZ)-treated and control (C) rats with (+) and without (−) endothelial cells (E)

	(n)		*C + E*	*STZ + E*	*C − E*	*STZ − E*
2-week	6	Maximum (g)	3.33 ± 0.25	2.28 ± 0.13*	3.38 ± 0.26	2.53 ± 0.12*
		EC_{50} (-log M)	8.17 ± 0.08	8.06 ± 0.10	8.41 ± 0.13	8.34 ± 0.05‡
		Slope	2.38 ± 0.61	1.65 ± 0.45*	2.06 ± 0.81	1.54 ± 0.29
6-week	6	Maximum (g)	3.44 ± 0.19	1.94 ± 0.32*	3.45 ± 0.22	2.11 ± 0.31*
		EC_{50} (-log M)	8.11 ± 0.07	8.03 ± 0.10	8.42 ± 0.04‡	8.37 ± 0.05‡
		Slope	2.77 ± 0.68	1.34 ± 0.87*	3.04 ± 0.57	1.68 ± 0.65*
2-week/Epalrestat	5	Maximum (g)	3.51 ± 0.16	2.29 ± 0.19*	3.81 ± 0.25	2.45 ± 0.23*
		EC_{50} (-log M)	8.22 ± 0.06	8.28 ± 0.05	8.69 ± 0.01‡	8.53 ± 0.09‡
		Slope	2.62 ± 0.63	1.59 ± 0.49*	3.40 ± 0.81	1.94 ± 0.53*
6-week/Epalrestat	6	Maximum (g)	3.91 ± 0.14	2.49 ± 0.18*	3.94 ± 0.11	2.36 ± 0.17*
		EC_{50} (-log M)	8.03 ± 0.09	7.87 ± 0.06	8.38 ± 0.03‡	8.30 ± 0.08‡
		Slope	3.17 ± 0.72	1.73 ± 0.52*	3.64 ± 0.49	1.77 ± 0.53*
2-week/Insulin	5	Maximum (g)	NA	3.20 ± 0.24	NA	3.24 ± 0.19
		EC_{50} (-log M)		8.51 ± 0.10		8.51 ± 0.11
		Slope		2.94 ± 1.19		2.86 ± 0.98
2-week/30 mM Glucose	5	Maximum (g)	2.84 ± 0.30	2.76 ± 0.15	3.04 ± 0.24	2.80 ± 0.07
		EC_{50} (-log M)	8.33 ± 0.02	8.13 ± 0.10	8.45 ± 0.11	8.37 ± 0.06
		Slope	1.94 ± 0.54	1.68 ± 0.40†	2.43 ± 0.83	2.14 ± 0.51
6-week/30 mM Glucose	6	Maximum (g)	3.23 ± 0.12	2.11 ± 0.20*†	3.46 ± 0.18	2.26 ± 0.32*†
		EC_{50} (-log M)	8.25 ± 0.01	7.95 ± 0.07*	8.13 ± 0.18	8.13 ± 0.20
		Slope	2.58 ± 0.58	1.43 ± 0.47*†	2.79 ± 0.63	1.30 ± 0.92*†

Values are given ± s.e.mean (except for slopes, which are ± 95% confidence limits).
*Significantly different from corresponding control group, $P<0.05$ unpaired t test.
‡Significantly different from same treatment group with endothelial cells, $P<0.05$ unpaired t test.
†Significantly different from corresponding control group in normal Krebs solution, $P<0.05$ ANOVA and Tukey test.
NA = not applicable.

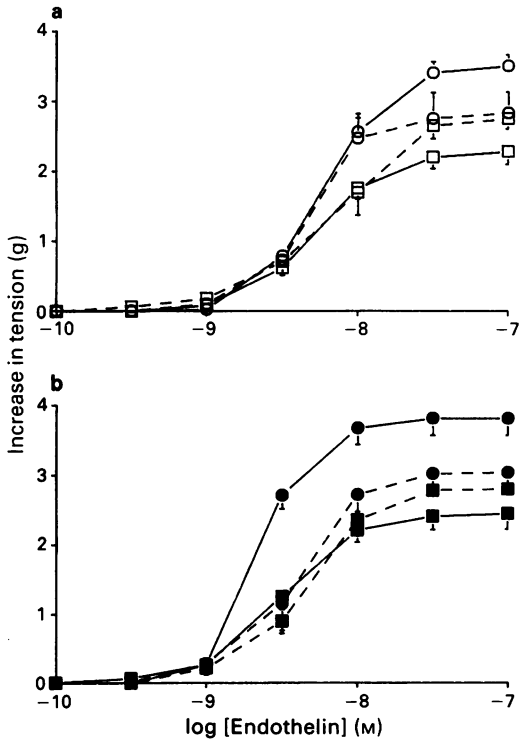

Figure 3 Responses to endothelin-1 of aortic rings from 2-week streptozotocin (STZ)-treated rats. (a) With endothelium: STZ/epalrestat-treated (□—□, $n = 5$), control/epalrestat-treated (○—○, $n = 5$), STZ-treated in 30 mM glucose Krebs solution (□- -□, $n = 5$) and control in 30 mM glucose Krebs solution (○- -○, $n = 5$). (b) Without endothelium: STZ/epalrestat-treated (■—■, $n = 5$), control/epalrestat-treated (●—●, $n = 5$), STZ-treated in 30 mM glucose Krebs solution (■- -■, $n = 5$) and control in 30 mM glucose Krebs solution (●- -●, $n = 5$).

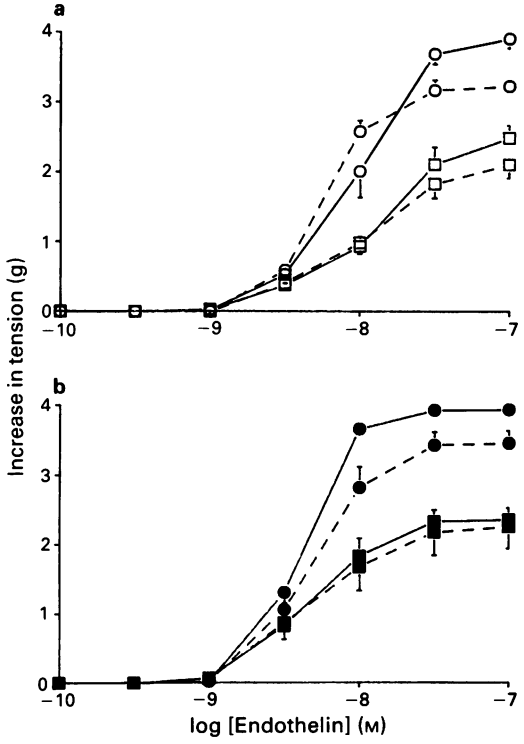

Figure 4 Responses to endothelin-1 of aortic rings from 6-week streptozotocin (STZ)-treated rats. (a) With endothelium: STZ/epalrestat-treated (□—□, $n = 6$), control/epalrestat-treated (○—○, $n = 6$), STZ-treated in 30 mM glucose Krebs solution (□- -□, $n = 6$) and control in 30 mM glucose Krebs solution (○- -○, $n = 6$). (b) Without endothelium: STZ/epalrestat-treated (■—■, $n = 6$), control/epalrestat-treated (●—●, $n = 6$), STZ-treated in 30 mM glucose Krebs solution (■- -■, $n = 6$) and control in 30 mM glucose Krebs solution (●- -●, $n = 6$).

vascular functional changes in non-diabetic rats (indicating that such changes were the consequence of hyperglycaemia *per se*) and that these changes were prevented by the aldose reductase inhibitor (ARI) tolrestat.

Aldose reductase has been detected in human aortae (Srivastava *et al.*, 1986). It was therefore of interest to determine whether the reduced maximum responsiveness to ET-1 of aortae from diabetic rats was prevented by chronic treatment with an ARI. Yorek & Dunlap (1989) showed that incubation of cultured bovine aortic endothelial cells in high ambient glucose (30 mM) led to a reduction in intracellular myo-inositol and an accumulation of sorbitol. This occurred after a minimum incubation period of one week. Therefore these changes could possibly occur in the time-frame of the present study. However, in the present study, reduced responsiveness to ET-1 was still observed in aortae from diabetic rats chronically treated with the ARI, epalrestat. The dose of epalrestat used was greater than that which had been previously shown to prevent peripheral nerve dysfunction in STZ-treated rats (Kikkawa *et al.*, 1984). The same dose as used in the present study has also been shown to improve responsiveness to nerve stimulation in isolated atria of STZ-treated rats, but to have no significant effect on postsynaptic stimulation (by exogenous noradrenaline) (Hashimoto *et al.*, 1990). It is therefore possible that the inability of epalrestat to normalize responses to ET-1 in the present study may be because altered polyol pathway activity is not the chief cause of the abnormality occurring in 2- or 6-week STZ-induced diabetic rats.

Previous workers have shown that in isolated aortic rings from non-diabetic rats, removal of endothelial cells shifted the CR curve to ET-1 to the right with no significant change in maximum responses (Topouzis *et al.*, 1991). This has been confirmed in the present study in aortae from both control and STZ-treated rats. However, this is in contrast to the observations of Rodman *et al.* (1989) who reported that removal of endothelial cells from non-diabetic rat aortic rings enhanced maximum responses to ET-1 but did not significantly affect EC_{50} values.

As has been reported previously (Fulton *et al.*, 1991), in the present study the dry weights of aortic rings were not significantly affected by 2 weeks of diabetes. However, dry weights of aortae from 6-week STZ-treated rats were significantly reduced. A reduction in wet weight of aortic rings from 8-week STZ-treated rats has been previously reported by Head *et al.* (1987), indicating that these changes may be dependent on the duration of diabetes.

A comparison of the potency of ET-1, in aortae from 2-week diabetic and control rats (both with and without endothelium), between the present study and a previous study (Fulton *et al.*, 1991) shows a mean difference in EC_{50} values of 0.52 log (M) units. This discrepancy may be due to the different batches of ET-1 used in each study, as an examination of the amino acid analysis from each batch indicates a slight variation.

In summary, results of the present study suggest that the decreased responsiveness to ET-1 of aortae from 2-week diabetic rats may not be due to abnormal activity of the polyol pathway. Similarly, it was probably not due to streptozotocin *per se* as responses were normalized by insulin treatment. The results of our previous study (Fulton *et al.*, 1991) did not indicate a role for cyclo-oxygenase products or extracellular Ca^{2+} in the change in ET-1 responsiveness observed during diabetes. In both the earlier study and in the present study, decreased responsiveness to ET-1 has still been observed in denuded aortae, indicating that changes in endothelium-derived relaxing factor/NO are probably not responsible for this change. However, Nayler *et al.* (1989) have reported a reduction in the density of [^{125}I]-ET binding sites in cardiac membrane fragments from STZ-treated rats. If a similar change occurs in rat aortae then this may explain the reduced responsiveness to ET-1 observed in the present study.

It is conceivable that the altered responsiveness following 2 weeks of diabetes (compared with controls) was a manifestation of an adaptive change to hyperglycaemia occurring *in vivo*, since it was not observed when aortae were bathed in high glucose Krebs solution. The finding that responsiveness to ET-1 of aortae from 6-week diabetic rats was still reduced in the presence of high glucose Krebs solution suggests that in longer term diabetes, other factors may play a role in the altered responsiveness to ET-1.

We thank ONO Pharmaceuticals Co Ltd (Japan) for the generous gift of ONO2235 (epalrestat). We thank Bogdan Sikorski and Richard Booth for animal tissues.

This work was supported in part by an Australasian Society of Clinical and Experimental Pharmacologists small equipment grant.

References

BEYER, T.A. & HUTSON, N.J. (1986). Introduction: Evidence for the role of the polyol pathway in the pathophysiology of diabetic complications. *Metabolism*, **35**, 1–3.

DULIN, W.E., LUND, G.H. & GERRITSEN, G.C. (1967). Streptozotocin-induced diabetes in the rat. *Diabetes*, **16**, 23.

DVORNIK, D. (1978). Chronic complications of diabetes. *Annu. Rep. Med. Chem.*, **13**, 159–166.

FULTON, D.J.R., HODGSON, W.C., KING, R.G. & BOURA, A.L.A. (1990). Attenuated endothelin-1 responses in streptozotocin-diabetic rat aorta. *Clin. Exp. Pharmacol. Physiol.*, (Suppl) **17**, 24.

FULTON, D.J.R., HODGSON, W.C., SIKORSKI, B.W. & KING, R.G. (1991). Attenuated responses to endothelin-1, KCl and $CaCl_2$, but not noradrenaline, of aortae from rats with streptozotocin-induced diabetes mellitus. *Br. J. Pharmacol.*, **104**, 928–932.

HASHIMOTO, H., SATOH, N., TAKIGUCHI, Y. & NAKASHIMA, M. (1990). Effects of an aldose reductase inhibitor, ONO-2235, insulin and their combination on the altered responsiveness to the nerve stimulation and agonists of the isolated atria of diabetic rats. *J. Pharmacol. Exp. Ther.*, **253**, 552–557.

HATTORI, Y., KASAI, K., NAKAMURA, T., EMOTO, T. & SHIMODA, S.-I. (1991). Effect of glucose and insulin on immunoreactive endothelium-1 release from cultured porcine aortic endothelial cells. *Metabolism*, **40**, 165–169.

HEAD, R.J., LONGHURST, P.A., PANEK, R.L. & STITZEL, R.E. (1987). A contrasting effect of the diabetic state upon the contractile responses of aortic preparations from the rat and rabbit. *Br. J. Pharmacol.*, **91**, 275–286.

KIKKAWA, R., HATANAKA, I., YASUDA, H., KOBAYASHI, N. & SHIGETA, Y. (1984). Prevention of peripheral nerve dysfunction by an aldose reductase inhibitor in streptozotocin-diabetic rats. *Metabolism*, **33**, 212–214.

LUSCHER, T.F., YANG, Z., DIEDERICH, D. & BUHLER, F.R. (1989). Endothelium-derived vasoactive substances: Potential role in hypertension, atherosclerosis, and vascular occlusion. *J. Cardiovasc. Pharmacol.*, **14**, S63–S69.

MULVANY, M.J. & HALPERN, W. (1977). Contractile properties of small arterial resistance vessels in spontaneously hypertensive and normotensive rats. *Circ. Res.*, **41**, 19–26.

NAYLER, W.G., LIU, J., PANAGIOTOPOULOS, S. & CASLEY, D.J. (1989). Streptozotocin-induced diabetes reduces the density of [^{125}I]-endothelin-binding sites in rat cardiac membranes. *Br. J. Pharmacol.*, **97**, 993–995.

RERUP, C.C. (1970). Drugs producing diabetes through damage of the insulin secreting cells. *Pharmacol. Rev.*, **2**, 485–518.

RODMAN, D.M., MCMURTRY, I.F., PEACH, J.L. & O'BRIEN, R.F. (1989). Comparative pharmacology of rat and porcine endothelin in rat aorta and pulmonary artery. *Eur. J. Pharmacol.*, **165**, 297–300.

SRIVASTAVA, S.K., ANSARI, N.H., HAIR, G.A., AWASTHI, S. & DAS, B. (1986). Activation of human erythrocyte, brain, aorta, muscle, and ocular tissue aldose reductase. *Metabolism*, **35**, 114–118.

TOPOUZIS, S., HUGGINS, J.P., PELTON, J.T. & MILLER, R.C. (1991). Modulation by endothelium of the responses induced by endothelin-1 and by some of its analogues in rat isolated aorta. *Br. J. Pharmacol.*, **102**, 545–549.

WILLIAMSON, J.R., OSTROW, E., EADES, D., CHANG, K., ALLISON, W., KILO, C. & SHERMAN, W.R. (1990). Glucose-induced microvascular functional changes in nondiabetic rats are stereospecific and are prevented by an aldose reductase inhibitor. *J. Clin. Invest.*, **85**, 1167–1172.

YAMAUCHI, T., OHNAKA, K., TAKAYANAGI, R., UMEDA, F. & NAWATA, H. (1990). Enhanced secretion of endothelin-1 by elevated glucose levels from cultured bovine aortic endothelial cells. *FEBS Lett.*, **267**, 16–18.

YOREK, M.A. & DUNLAP, J.A. (1989). The effect of elevated glucose levels on myo-inositol metabolism in cultured bovine endothelial cells. *Metabolism*, **38**, 16–22.

(Received December 5, 1991
Revised March 10, 1992
Accepted March 16, 1992)

Br. J. Pharmacol. (1992), **106**, 650–655

Nitric oxide and sensory nerves are involved in the vasodilator response to acetylcholine but not calcitonin gene-related peptide in rat skin microvasculature

[1]V. Ralevic, Z. Khalil, *G.J. Dusting & R.D. Helme

National Research Institute of Gerontology & Geriatric Medicine, North West Hospital (Mount Royal Campus), Parkville, Australia and *Department of Physiology, University of Melbourne, Parkville, Victoria 3052, Australia

1 The contributions of sensory nerves and nitric oxide (NO) to vasodilator responses to acetylcholine (ACh) and calcitonin gene-related peptide (CGRP) were examined in rat skin microvasculature with a laser Doppler flowmeter to monitor relative blood flow.

2 Perfusion of ACh (100 μM; for 30 min) over a blister base on the rat hind footpad elicited microvascular vasodilatation and this response was not sustained. CGRP (1 μM; 10 min perfusion) also elicited vasodilatation and this response was maintained even when CGRP was no longer in contact with the blister base.

3 The vasodilator response to ACh was significantly smaller in rats pretreated as neonates with capsaicin to destroy primary sensory afferents than it was in age-matched controls. The vasodilator response to CGRP was unaffected by capsaicin pretreatment.

4 Selective inhibitors of NO synthase, N^G-nitro-L-arginine (L-NOARG) and N^G-monomethyl-L-arginine (L-NMMA) (both at 100 μM) attenuated the vasodilator response to ACh in control rats, but had no effect on the vasodilator response to CGRP. There was a significant L-NOARG-resistant component in control rats while in capsaicin-treated rats the vasodilator response to ACh was virtually abolished by L-NOARG. The inactive stereoisomer N^G-monomethyl-D-arginine (100 μM) did not affect the vasodilator response to ACh.

5 The efficacy of L-NOARG and L-NMMA as inhibitors of endothelium-dependent responses was confirmed by use of an endothelium-dependent vasodilator, the calcium ionophore A23187 (100 μM; 10 min perfusion). Vasodilatation to A23187 was strongly attenuated by both L-NOARG and L-NMMA.

6 These results suggest that sensory nerves and NO are both involved in the dilatation produced by ACh in rat skin microvasculature. A component of the vasodilator response elicited by ACh involves a direct action on the microvascular endothelium with subsequent generation of NO, while an additional component is elicited via activation of sensory nerves. The vasodilator mediator(s) released by ACh from sensory nerves acts largely independently of NO.

7 The vasodilator response to CGRP is independent of a prejunctional action on sensory nerves and of NO.

Keywords: Nitric oxide; endothelium; microvasculature; sensory nerves; acetylcholine; calcitonin gene-related peptide; neurogenic inflammation

Introduction

Neurogenic inflammation constitutes a complex series of events involving the release of peptide neurotransmitters, particularly substance P and calcitonin gene-related peptide (CGRP), from sensory nerve endings in the skin. CGRP is a potent vasodilator in human and animal skin (Brain *et al.*, 1985; Thom *et al.*, 1987). In rat skin, CGRP may potentiate the oedema induced by substance P and other tachykinins, while substance P causes vasodilatation and an increase in vascular permeability and may modulate the vasodilatation induced by CGRP (Brain & Williams, 1985). Neurogenic inflammation additionally involves the release of mediators from mast cells and activation of sensory nerves (Lembeck & Holzer, 1979; Foreman *et al.*, 1983; Barnes *et al.*, 1986). Nitric oxide (NO) acts as a transduction molecule in many biological systems (Moncada & Higgs, 1990) and is also likely to be involved in neurogenic inflammation since it may be released from mast cells (Salvemini *et al.*, 1990) as well as from the endothelium and has been shown to have a role in the inflammatory response to substance P (Hughes *et al.*, 1990; Ralevic *et al.*, 1991).

Acetylcholine (ACh) causes pain when applied to blister bases in man (Armstrong *et al.*, 1953). It has been suggested that ACh released from postganglionic sympathetic nerve fibres contributes to the inflammatory response since antidromic vasodilatation and neurogenic plasma extravasation are reduced by atropine (Couture *et al.*, 1985; Couture & Kerouac, 1987; Low & Westerman, 1989). In large blood vessels it is well established that vasodilatation due to ACh is largely mediated through an action on the vascular endothelium with subsequent release of endothelium-derived relaxing factor or NO (Furchgott, 1983; Palmer *et al.*, 1988). In cutaneous microvasculature, sensory nerves may also be involved, since ACh has been shown to excite perivascular nociceptive C-fibres in man (Westerman *et al.*, 1987; Parkhouse & LeQuesne, 1988), rabbit (Juan, 1982) and cat (Fjallbrandt & Iggo, 1961).

It was the aim of the present study to examine the contribution of sensory nerves and of NO to ACh- and CGRP-induced inflammatory responses in rat skin microvasculature. The role of sensory nerves was examined in rats pretreated as neonates with capsaicin to destroy selectively these nerves,

[1] Author for correspondence at present address: Department of Anatomy & Developmental Biology, University College London, Gower St., London WC1E 6BT.

while the involvement of NO was examined with two selective inhibitors of NO synthase, N^G-nitro-L-arginine (L-NOARG) and N^G-monomethyl-L-arginine (L-NMMA) (Palmer *et al.*, 1988; Rees *et al.*, 1989; Dubbin *et al.*, 1990; Moore *et al.*, 1990). Some of these results have been published in preliminary form (Ralevic *et al.*, 1991).

Methods

Sprague-Dawley rats of either sex with an average weight of 200–250 g were used. Anaesthesia was induced with pentobarbitone sodium (60 mg kg^{-1}, i.p.). Further doses of 15 mg kg^{-1} anaesthetic were administered intermittently to ensure that rats were kept under a constant state of anaesthesia. This method of anaesthesia was previously shown not to alter the basal plasma extravasation or sympathetic tone (Khalil & Helme, 1989). Body temperature of the rats was maintained at 37°C. At the end of the experiment animals were killed by barbiturate overdose.

Blister induction and experimental protocol

A blister was induced in the right hind footpad of the rat by applying a vacuum pressure of − 40 kPA for approximately 30 min, with a metal suction cap heated to 40°C. The surface epithelium was removed and the foot of the rat secured in a perspex chamber with inlet and outlet ports. Ringer solution was perfused over the surface of the blister at 4 ml h^{-1} by means of a peristaltic pump (Microperpex S, LKB, Sweden) (Khalil & Helme, 1989). Relative blood flow was monitored over time with a laser Doppler flowmeter (Periflux, PF2B, Perimed, Sweden) via a probe placed in a central port immediately above the blister base; blood flux (volt; V) was recorded on a chart recorder.

An initial equilibration period of 30 min was allowed, during which time a stable baseline was achieved. In control experiments ACh (100 μM) was perfused for 30 min over the blister base. In experiments with L-NOARG, L-NMMA or the inactive stereoisomer N^G-monomethyl-D-arginine (D-NMMA) (all at 100 μM) these agents were perfused for 14 min before and during ACh perfusion. (The concentration of L-arginine analogues used was predetermined to cause an attenuation of vasodilator responses to endothelium-dependent agents without a significant change in the baseline). CGRP (1 μM) was perfused for 10 min at the end of each experiment (20 min after cessation of ACh perfusion). Concentration-response curves for ACh (10, 100 and 1000 μM) and CGRP (0.1, 1 and 10 μM) were produced by perfusing these agents over the surface of the blister base; because of the effects of desensitization, responses to single concentrations were established in separate animals. In a separate series of experiments A23187 (100 μM) was perfused for 10 min over the blister base. All agonists were used at submaximal concentrations; the time of perfusion used was based on the vasodilator characteristics of these agents. Experiments with L-NOARG were repeated in rats having undergone destruction of primary sensory afferents by neonatal capsaicin treatment (Jancso *et al.*, 1977).

Capsaicin pretreatment

Animals were given a single dose of capsaicin, 50 mg kg^{-1}, subcutaneously, on the fourth day of life. The effectiveness of the neonatal capsaicin treatment was tested prior to each experiment by the eye-wiping response to topical application of capsaicin to the cornea (0.1% capsaicin in alcohol) (Khalil & Helme, 1990).

Drugs

Calcitonin gene-related peptide was obtained from Auspep, Melbourne, Australia. Acetylcholine perchlorate, capsaicin (8-methyl-N-vanillyl-6-nonenamide), and N^G-nitro-L-arginine were from Sigma Chemical Company, U.S.A. A23187 (free acid) and N^G-monomethyl-L-arginine acetate were from Calbiochem, U.S.A. N^G-monomethyl-D-arginine acetate was from the Institute of Drug Technology (Boronia, Victoria). Capsaicin was dissolved in a saline solution containing 10% Tween 80 and 10% alcohol. A23187 was initially dissolved in dimethylsulphoxide (DMSO) and then diluted in Ringer solution. The appropriate solvent controls were carried out with DMSO. All other drugs were dissolved in Ringer solution.

Statistics and expression of data

Relative blood flow responses were measured as the area under the response curve (cm^2) with a digital planimeter (Tamaya, Japan). For ACh and A23187 this was the area during the entire perfusion; for CGRP this was the area during 8 min of perfusion since the response was maintained. Maximum height of responses was also measured. Small non-specific solvent effects were accounted for in experiments using A23187 by performing controls with DMSO at the appropriate concentration. Results were expressed as mean ± s.e.mean. Statistical analyses were performed by analysis of variance with *post hoc* Student-Newman-Keuls pairwise comparisons where necessary. Type 1 error rate was set at $\alpha = 0.05$ for all tests.

Results

Effect of L-NOARG, L-NMMA and D-NMMA on the vasodilator response to ACh

In control rats, ACh (100 μM; perfused for 30 min) produced an initial rapid vasodilator response in the rat skin microvasculature which reached a maximum and then gradually subsided (Figure 1). L-NOARG (100 μM) and L-NMMA (100 μM) but not D-NMMA (100 μM) caused a significant reduction in the area of the vasodilator response to ACh (Figure 2). This inhibition was manifested primarily as a reduction in the time-dependent maintenance of the response; in the presence of L-NOARG or L-NMMA the vasodilator response to ACh returned to baseline (Figure 1). There was no significant difference between the inhibitory effects of L-NOARG or L-NMMA (both at 100 μM) on the area of the vasodilator response to ACh. Only L-NMMA significantly attenuated the maximum height of the vasodilator response to 100 μM ACh (6.98 ± 1.12 ($n = 6$), 4.8 ± 0.36 ($n = 5$) and 2.95 ± 0.64 ($n = 4$) cm in control, L-NOARG- and L-NMMA-

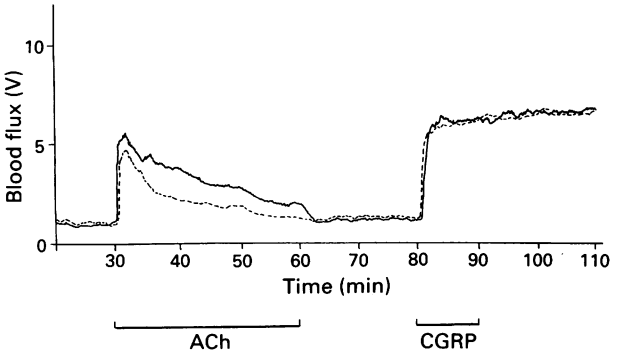

Figure 1 Representative trace showing the effect of N^G-nitro-L-arginine (L-NOARG, 100 μM) on vasodilator responses (blood flux, V) of the rat skin microvasculature to acetylcholine (ACh; 100 μM perfused for 30 min) and calcitonin gene-related peptide (CGRP, 1 μM perfused for 10 min). Unbroken line indicates control responses; broken line indicates responses in the presence of L-NOARG, introduced 14 min prior to and during challenge with ACh and CGRP.

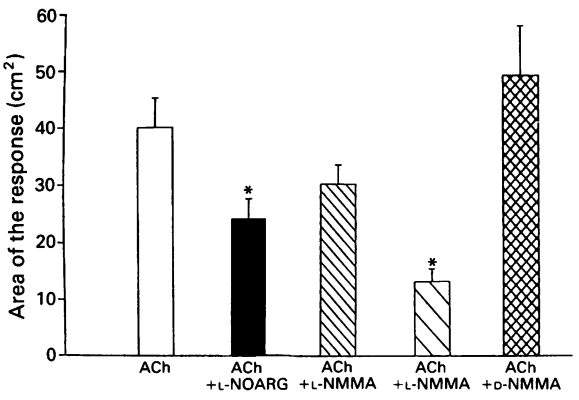

Figure 2 Effect of N^G-nitro-L-arginine (L-NOARG), N^G-monomethyl-L-arginine (L-NMMA) or D-NMMA on the dilatation response of the rat skin microvasculature to acetylcholine (ACh; 100 μM). Open column = ACh alone; solid column = ACh + L-NOARG (100 μM); narrow hatched column = ACh + L-NMMA (10 μM); wide hatched column = ACh + L-NMMA (100 μM); cross hatched column = ACh + D-NMMA (100 μM). Columns represent the means of 4–7 separate experiments with vertical bars indicating s.e.mean. *Indicates significant difference from control response.

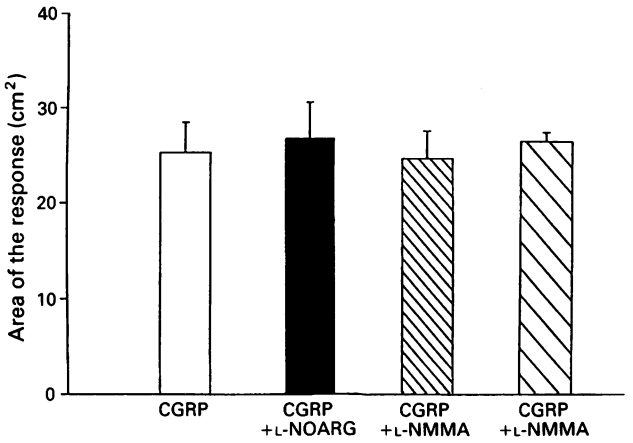

Figure 3 Effect of N^G-nitro-L-arginine (L-NOARG), or N^G-monomethyl-L-arginine (L-NMMA) on the dilatation response of the rat skin microvasculature to calcitonin gene-related peptide (CGRP, 1 μM). Open column = CGRP alone; solid column = CGRP + L-NOARG (100 μM); narrow hatched column = CGRP + L-NMMA (10 μM); wide hatched column = CGRP + L-NMMA (100 μM). Columns represent the means of 4–6 separate experiments with vertical bars indicating s.e.mean.

treated rats respectively). The maximum height of the vasodilator response to ACh at a concentration of 1 mM was significantly attenuated by L-NOARG (Figure 4). A lower concentration (10 μM) of either L-NOARG or L-NMMA (Figure 2) had no significant effect on the vasodilator response to ACh.

Effect of L-NOARG and L-NMMA on the vasodilator response to CGRP

The vasodilator response to CGRP (1 μM, 10 min perfusion) was characterized by an initial rapid vasodilatation which reached a maximum and was maintained even after CGRP was removed from the perfusate (Figure 1). Previous studies in our laboratory have shown that this vasodilator response can be maintained for several hours after cessation of perfusion with CGRP. L-NOARG (100 μM) or L-NMMA (100 μM) had no significant effect on the vasodilator response to CGRP (Figure 3). A concentration-response curve showed that L-NOARG had no effect on CGRP at concentrations of 0.1, 1 or 10 μM (Figure 4).

Effect of L-NOARG and L-NMMA on the vasodilator response to A23187

The vasodilator response to A23187 (100 μM) was slow in onset (Figure 5). L-NOARG and L-NMMA (both at 100 μM) markedly inhibited the area of the response (Figure 6). In all but one of the five animals L-NOARG abolished the vasodilator response due to A23187. L-NOARG, but not L-NMMA significantly inhibited the maximum height of the vasodilator response (2.5 ± 0.41, 0.36 ± 0.29 and 1.72 ± 0.62 cm (n = 5) in control, L-NOARG- and L-NMMA-treated rats respectively).

Effect of capsaicin pretreatment on vasodilator responses to ACh and CGRP

In rats pretreated with capsaicin there was a significant reduction in the area of the vasodilator response to ACh (Figure 7). There was also a significant reduction in the maximum height of the response between these groups (6.98 ± 1.12 and 3.97 ± 0.37 cm (n = 6) in control and capsaicin treated rats respectively). Capsaicin pretreatment had no significant effect on vasodilator responses to CGRP (Figure 8).

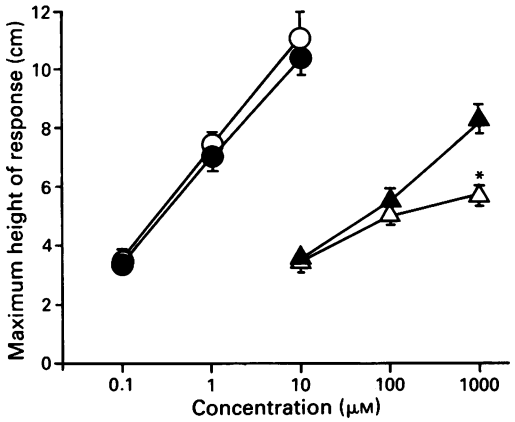

Figure 4 Concentration-response curves showing vasodilator responses (maximum height of response) of rat skin microvasculature to calcitonin gene-related peptide (circles) and acetylcholine (triangles) in the absence (closed symbols) and presence (open symbols) of N^G-nitro-L-arginine. Each symbol represents the mean of 5 separate experiments. *Denotes a significant difference from control.

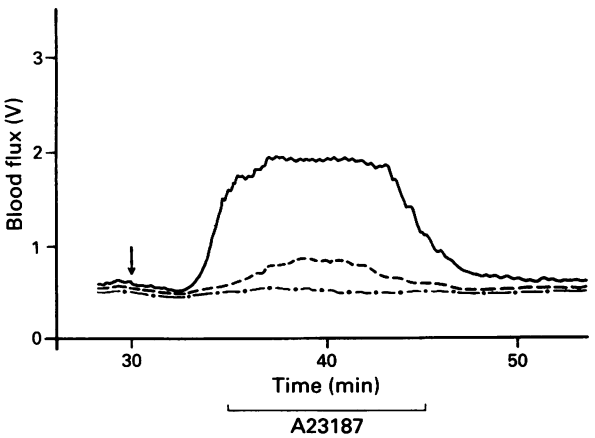

Figure 5 Representative trace showing the effect of N^G-nitro-L-arginine (L-NOARG) or N^G-monomethyl-L-arginine (L-NMMA) (both at 100 μM) on the vasodilator response to A23187 (100 μM perfused for 10 min). Unbroken line = A23187 alone; dashed line = A23187 + L-NMMA; dashed-dotted line = A23187 + L-NOARG. L-NOARG or L-NMMA was introduced 14 min before and during perfusion with A23187. Point of addition of A23187 indicated by arrow.

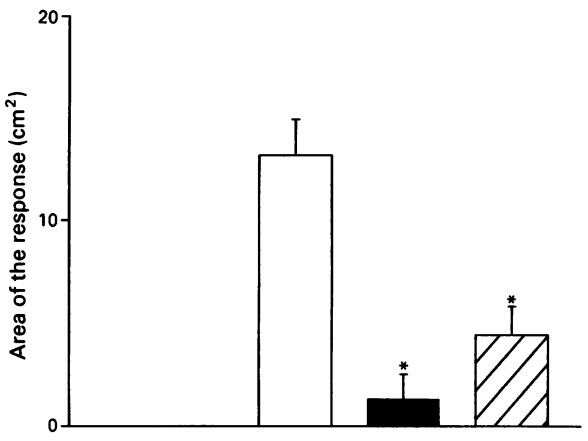

Figure 6 Effect of N^G-nitro-L-arginine (L-NOARG) or N^G-monomethyl-L-arginine (L-NMMA) (both at 100 μM) on the dilatation response of the rat skin microvasculature to A23187 (100 μM). Open column = A23187 alone; solid column = A23187 + L-NOARG; hatched column = A23187 + L-NMMA. Columns represent the means of 5–6 separate experiments with vertical bars indicating s.e.mean. *Indicates significant difference from control.

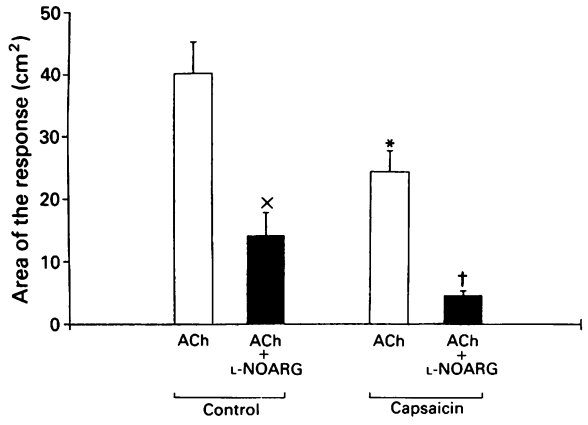

Figure 7 Effect of capsaicin pretreatment and N^G-nitro-L-arginine (L-NOARG, 100 μM) on the dilatation response of rat skin microvasculature to acetylcholine (ACh; 100 μM). Open columns = ACh alone; solid columns = ACh + L-NOARG. Columns represent the means of 6–7 separate experiments with vertical bars indicating s.e.mean. *Indicates significant difference between responses obtained to ACh in capsaicin-treated rats and control rats. Control group: ×indicates significant difference from control. Capsaicin-treated group: †indicates significant difference from capsaicin-control.

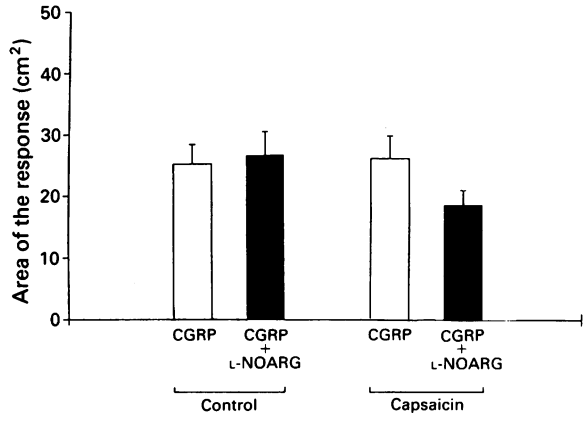

Figure 8 Effect of capsaicin pretreatment and N^G-nitro-L-arginine (L-NOARG, 100 μM) on the dilatation response to calcitonin gene-related peptide (CGRP; 1 μM). Open columns = CGRP alone; solid columns = CGRP + L-NOARG. Columns represent the means of 5–7 separate experiments with vertical bars indicating s.e.mean.

Effect of L-NOARG on vasodilator responses to ACh and CGRP in capsaicin pretreated rats

L-NOARG (100 μM) significantly reduced the vasodilator response to ACh in capsaicin pretreated rats (Figure 7). This was primarily a reflection of a reduction in the time-dependent maintenance of the response since the maximum height of the response was not significantly affected.

L-NOARG had no significant effect on the vasodilator response to CGRP in capsaicin pretreated animals (Figure 8).

Discussion

In this study we have shown that in blister bases raised in rat skin, part of the vasodilator action of ACh is mediated via the generation of NO. A further component of the vasodilator response to ACh results following excitation of capsaicin-sensitive C-fibres which release a transmitter(s) that acts largely through NO-independent mechanisms. The vasodilator action of CGRP proceeds independently of both NO and primary sensory afferents.

In man, iontophoresed ACh can stimulate peripheral nociceptive C-fibres to produce flare (neurogenic vasodilatation) which is abolished by anaesthetic and is absent in denervated skin (Westerman *et al.*, 1987; Parkhouse & LeQuesne, 1988). A direct action of ACh on non-myelinated C-fibres has also been demonstrated in the saphenous nerve (Douglas & Ritchie, 1960) and cutaneous afferent nerves (Fjallbrandt & Iggo, 1961) of the cat. In the rabbit, nociceptive effects of acetylcholine have been shown to be mediated through nicotinic receptors present on perivascular sensory nerve endings (Juan, 1982). In the present study, capsaicin pretreatment was used to destroy selectively sensory nerves (Jancso *et al.*, 1977) and this significantly reduced ACh-induced vasodilator responses of the skin microvasculature. To our knowledge this is the first demonstration that ACh has an excitatory action on peripheral nociceptive C-fibres in the rat. Non-specific effects of capsaicin treatment were not likely to contribute since vasodilator responses to CGRP were unaffected.

Neurogenic inflammation may involve cholinergic nerves since atropine reduces axon reflex vasodilatation and plasma extravasation in rat skin (Couture *et al.*, 1985; Low & Westerman, 1989) and these nerves are likely to be of sympathetic postganglionic origin (Lembeck & Holzer, 1979; Couture *et al.*, 1985). In a previous study (Ralevic *et al.*, 1991) we suggested that NO may be involved in microvascular inflammatory responses, since L-NOARG attenuated substance P-induced vasodilatation and plasma extravasation. The present study provides further evidence to support this since L-NOARG and L-NMMA attenuated the vasodilator response to ACh. That the action of these inhibitors was specific was confirmed by the fact that the inactive stereoisomer, D-NMMA, was ineffective as an inhibitor of ACh-induced vasodilatation. Furthermore, neither L-NOARG nor L-NMMA inhibited the vasodilator response to CGRP, which is consistent with previous findings that CGRP generally does not activate the endothelium. Endothelium-dependent relaxations to CGRP have been demonstrated in some human vessels (Thom *et al.*, 1987) and in the rat aorta (Brain *et al.*, 1985; Grace *et al.*, 1987; Gray & Marshall, 1990).

The major source of NO in our system is probably the microvascular endothelium. However, it is also possible that NO may derive partly from mast cells (Salvemini *et al.*, 1990) since both A23187 and ACh have been shown to act on isolated mast cells, causing the release of histamine which is known to have potent effects on vascular permeability (Blandina *et al.*, 1980; Khalil & Helme, 1989). If an ACh- or A23187-induced release of NO from mast cells does occur in our system, this is likely to occur at concentrations of these agents below those required to induce the release of hista-

mine, since neither ACh nor A23187 elicited plasma extravasation (unpublished observations).

A comparison of concentration-response curves to CGRP and ACh showed the rat skin microvasculature to be approximately 100 fold more sensitive to CGRP than to ACh. While our results demonstrate an action of ACh on sensory nerves the largest proportion of its effects are mediated postjunctionally. Smooth muscle cells acting as a barrier to diffusion of ACh to receptors on endothelial cells and rapid hydrolysis of ACh could account for much of its lower potency compared with CGRP which, in our preparation, acts directly on receptors on the smooth muscle. In this respect it has been shown that in large blood vessels ACh is approximately 100 fold less sensitive when applied abluminally (Angus *et al.*, 1983). The implication of this is that sensory nerves releasing CGRP (together with substance P and other tachykinins) are comparatively more important than cholinergic fibres in neurogenic inflammation. The latter may have a role when relatively high local concentrations of ACh are achieved, possibly in severe cases of neurogenic trauma.

The most marked inhibitory effect of L-NOARG and L-NMMA on the vasodilator response to ACh was an attenuation of the time-dependent maintenance of the response. Similar effects have been observed in rats and guinea-pigs *in vivo* where L-NMMA (Aisaka *et al.*, 1989) and NOLA (synonymous with L-NOARG) (Zambetis *et al.*, 1991) attenuated the duration but not the amplitude of the hypotensive response to ACh. These workers suggested that the immediate vasodilatation of resistance vessels to ACh occurs by a mechanism which does not involve *de novo* synthesis of endothelially-derived NO, while the succeeding longer-lasting vasodilatation does depend on NO biosynthesis and the availability of L-arginine. Substantial components of the vasodilator response to ACh have also been shown to be resistant to inhibition by L-NMMA and L-NAME (the methyl ester of L-NOARG) in rabbit muscle microvasculature *in vivo* (Persson *et al.*, 1991), and human subcutaneous resistance arteries (Woolfson & Poston, 1990), while the vasodilator response to ACh was unaffected by L-NAME in conscious rats (Gardiner *et al.*, 1990). It is possible that hyperpolarization might be involved in the vasodilator action of ACh (Feletou & Vanhoutte, 1988; Chen & Suzuki, 1990) although it is not likely to be via the ATP-sensitive K^+ channel since dilatation to ACh in the rat *in vivo* was not attenuated by glibenclamide (Zambetis *et al.*, 1991). A direct action on the vascular smooth muscle as has been observed in some vessels (Brayden & Bevan, 1985) also cannot be excluded. At the highest concentration of ACh used (1 mM) the attenuation of the maximum height of the vasodilatation to ACh by L-NOARG indicates a significant contribution of NO to this part of the response. If multiple mechanisms are involved in the vasodilator response to ACh it is likely that their relative contributions vary with the concentration of agonist.

In capsaicin-treated rats, L-NOARG virtually abolished ACh-induced vasodilatation in contrast to control animals where the L-NOARG-resistant component constituted about 40% of the total ACh response. Since a substantial L-NOARG-resistant component was not observed after destruction of sensory nerves it is likely that the NO-independent component of the vasodilator response to ACh is largely due to the action of a mediator released from capsaicin-sensitive C-fibres. This mediator would not be expected to affect vascular permeability, since ACh did not elicit plasma extravasation. Further studies are warranted to identify the mediator released by ACh from sensory nerves which appears to act independently of NO. One of many possible candidates is CGRP which is localized in and released from sensory nerves (Gulbenkian *et al.*, 1986; Manzini *et al.*, 1991) and our experiments using L-NOARG confirmed the endothelium-independent nature of CGRP-induced vasodilatation in rat skin microvasculature.

In conclusion, we have shown that in rat skin microvasculature, the vasodilator response to ACh is comprised of two distinct components; one part of the response is mediated through NO probably arising following direct stimulation of the microvascular endothelium, and the other part of the response is mediated through an excitatory action on peripheral nociceptive C-fibres with release of a sensory transmitter which causes vasodilatation independently of NO. The vasodilator response to CGRP is independent of NO and sensory nerves. It has previously been shown that plasma protein extravasation induced by substance P in rat skin is reduced by atropine suggesting cholinergic modulation of this response (Couture & Kerouac, 1987). These data, together with the present results, suggests that reciprocal interactions between cholinergic and sensory nerve fibres may contribute to the rapid spread of the inflammatory response.

We are grateful to Dr Steve Gibson for help with the statistical analyses. V.R. was the recipient of an Anglo-Australian travel fellowship from The Royal Society to visit Dusting's laboratory in Melbourne.

References

AISAKA, K., GROSS, S.S., GRIFFITH, O.W. & LEVI, R. (1989). L-Arginine availability determines the duration of acetylcholine-induced systemic vasodilatation in vivo. *Biochem. Biophys. Res. Commun.*, **163**, 710–717.

ANGUS, J.A., CAMPBELL, G.R., COCKS, T.M. & MANDERSON, J.A. (1983). Vasodilatation by acetylcholine is endothelium-dependent: a study by sonomicrometry in canine femoral artery in vivo. *J. Physiol.*, **344**, 209–222.

ARMSTRONG, D.R.M.L., KEELE, C.A. & MARKHAM, J.W. (1953). Observations on chemical excitants of cutaneous pain in man. *J. Physiol.*, **120**, 326–351.

BARNES, P.J., BROWN, M.J., DOLLERY, C.T., FULLER, R.W., HEAVEY, D.J. & IND, P.W. (1986). Histamine is released from skin by substance P but does not act as the final vasodilator in the axon reflex. *Br. J. Pharmacol.*, **88**, 741–745.

BLANDINA, P., FANTOZZI, R., MANNAIONI, P.F. & MASINI, E. (1980). Characteristics of histamine release evoked by acetylcholine in isolated rat mast cells. *J. Physiol.*, **301**, 281–293.

BRAIN, S.D. & WILLIAMS, T.J. (1985). Inflammatory oedema induced by synergism between calcitonin gene-related peptide (CGRP) and mediators of increased vascular permeability. *Br. J. Pharmacol.*, **86**, 855–860.

BRAIN, S.D., WILLIAMS, T.J., TIPPINS, J.R., MORRIS, J.R. & MACINTYRE, I. (1985). Calcitonin gene-related peptide is a potent vasodilator. *Nature*, **313**, 54–56.

BRAYDEN, J.E. & BEVAN, J.A. (1985). Neurogenic muscarinic vasodilatation in the cat. An example of endothelial cell-independent cholinergic relaxation. *Circ. Res.*, **56**, 205–211.

CHEN, G. & SUZUKI, H. (1990). Ca-dependency of endothelium-dependent hyperpolarization in smooth muscle cells of the rabbit carotid artery. *J. Physiol.*, **421**, 521–534.

COUTURE, R., CUELLO, A.C. & HENRY, J.L. (1985). Trigeminal antidromic vasodilatation and plasma extravasation in the rat: effects of sensory, autonomic and motor denervation. *Brain Res.*, **346**, 108–114.

COUTURE, R. & KEROUAC, R. (1987). Plasma protein extravasation induced by mammalian tachykinins in rat skin: influence of anaesthetic agents and an acetylcholine antagonist. *Br. J. Pharmacol.*, **91**, 265–273.

DOUGLAS, W.W. & RITCHIE, J.M. (1960). The excitatory action of acetylcholine on cutaneous non-myelinated fibres. *J. Physiol.*, **150**, 501–514.

DUBBIN, P.N., ZAMBETIS, M. & DUSTING, G.J. (1990). Inhibition of endothelial nitric oxide biosynthesis by N-nitro-L-arginine. *Clin. Exp. Pharmacol. Physiol.*, **17**, 281–286.

FELETOU, M. & VANHOUTTE, P.M. (1988). Endothelium-dependent hyperpolarization of canine coronary smooth muscle. *Br. J. Pharmacol.*, **93**, 515–524.

FJALLBRANDT, N. & IGGO, A. (1961). The effect of histamine, 5-hydroxytryptamine and acetylcholine on cutaneous afferent nerve fibres. *J. Physiol.*, **156,** 578–590.

FOREMAN, J.C., JORDAN, C.C., OEHME, P. & RENNER, H. (1983). Structure-activity relationships for some substance P-related peptides that cause wheal and flare reactions in human skin. *J. Physiol.*, **335,** 449–465.

FURCHGOTT, R.F. (1983). Role of endothelium in responses of vascular smooth muscle. *Circ. Res.*, **53,** 557–573.

GARDINER, S.M., COMPTON, A.M., KEMP, P.A. & BENNETT, T. (1990). Regional and cardiac haemodynamic responses to glyceryl trinitrate, acetylcholine, bradykinin and endothelin-1 in conscious rats: effects of N^G-nitro-L-arginine methyl ester. *Br. J. Pharmacol.*, **101,** 632–639.

GRACE, G.C., DUSTING, G.J., KEMP, B.E. & MARTIN, T.J. (1987). Endothelium and the vasodilator action of rat CGRP. *Br. J. Pharmacol.*, **91,** 729–733.

GRAY, D.W. & MARSHALL, I. (1990). Calcitonin gene-related peptide (CGRP) endothelium-dependent relaxation in rat aorta is inhibited by L-NMMA. *Br. J. Pharmacol.*, **99,** 104P.

GULBENKIAN, S., MERIGHI, A., WHARTON, J., VARNDELL, I.M. & POLAK, J.M. (1986). Ultrastructural evidence for the co-existence of CGRP and SP in secretory vesicles in the peripheral nervous system of guinea-pig. *J. Neurocytol.*, **15,** 535–542.

HUGHES, S.R., WILLIAMS, T.J. & BRAIN, S.D. (1990). Evidence that endogenous nitric oxide modulates oedema formation induced by substance P. *Eur. J. Pharmacol.*, **191,** 481–484.

JANCSO, G., KIRALY, E. & JANCSO-GABOR, A. (1977). Pharmacologically induced selective degeneration of chemosensitive primary sensory neurons. *Nature*, **270,** 741–743.

JUAN, H. (1982). Nicotinic nociceptors on perivascular sensory nerve endings. *Pain*, **12,** 259–264.

KHALIL, Z. & HELME, R.D. (1989). Involvement of capsaicin-sensitive afferent nerve fibres in serotonin-induced plasma extravasation and vasodilatation in rat skin. *Neurosci. Lett.*, **104,** 105–109.

KHALIL, Z. & HELME, R.D. (1990). Serotonin modulates substance P-induced plasma extravasation and vasodilatation in rat skin by an action through capsaicin-sensitive primary afferent nerves. *Brain Res.*, **527,** 292–298.

LEMBECK, F. & HOLZER, P. (1979). Substance P as neurogenic mediator of antidromic vasodilatation and neurogenic plasma extravasation. *Naunyn-Schmiedebergs Arch. Pharmacol.*, **310,** 175–183.

LOW, A. & WESTERMAN, R.A. (1989). Neurogenic vasodilatation in the rat hairy skin measured using a laser Doppler flowmeter. *Life Sci.*, **45,** 49–57.

MANZINI, S., PERRETTI, F., TRAMONTANA, M., DEL BIANCO, E., SANTICIOLI, P., MAGGI, C.A. & GEPPETTI, P. (1991). Neurochemical evidence of calcitonin gene-related peptide-like immunoreactivity (CGRP-LI) release from capsaicin-sensitive nerves in rat mesenteric veins and arteries. *Gen. Pharmacol.*, **22,** 275–278.

MONCADA, S. & HIGGS, E.A. (1990). (Eds.) *Nitric Oxide from L-Arginine: a Bioregulatory System.* Amsterdam: Excerpta Medica.

MOORE, P.K., AL-SWAYEH, O.A., CHONG, N.W.S., EVANS, R.A. & GIBSON, A. (1990). L-N^G-nitro arginine (L-NOARG), a novel L-arginine-reversible inhibitor of endothelium-dependent vasodilatation in vitro. *Br. J. Pharmacol.*, **99,** 408–412.

PALMER, R.M.J., REES, D.D., ASHTON, D.S. & MONCADA, S. (1988). L-arginine is the physiological precursor for formation of nitric oxide in endothelium-dependent relaxation. *Biochem. Biophys. Res. Commun.*, **153,** 1251–1256.

PARKHOUSE, N. & LEQUESNE, P.M. (1988). Quantitative objective assessment of peripheral nociceptive C fibre function. *J. Neurol. Neurosurg. Psychiatry.*, **51,** 28–34.

PERSSON, M.G., WIKLUND, N.P. & GUSTAFSSON, L.E. (1991). Nitric oxide requirement for vasomotor nerve-induced vasodilatation and modulation of resting blood flow in muscle microcirculation. *Acta Physiol. Scand.*, **141,** 49–56.

RALEVIC, V., KHALIL, Z., DUSTING, G.J. & HELME, R.D. (1991). Nitric oxide contributes to substance P-induced inflammation in rat blisters. *Prog. Microcirc. Res.* Proceedings of the Sixth Australian & New Zealand Symposium Printing Unit, The University of South Wales. pp. 99–100.

REES, D.D., PALMER, R.M.J., HODSON, H.F. & MONCADA, S. (1989). A specific inhibitor of nitric oxide formation from L-arginine attenuates endothelium-dependent relaxation. *Br. J. Pharmacol.*, **96,** 418–424.

SALVEMINI, D., MASINI, E., ANGGARD, E., MANNAIONI, P.F. & VANE, J. (1990). Synthesis of a nitric oxide-like factor from L-arginine by rat serosal mast cells: stimulation of guanylate cyclase and inhibition of platelet aggregation. *Biochem. Biophys. Res. Commun.*, **169,** 596–601.

THOM, S., McG., HUGHES, A.D., GOLDBERG, P., MARTIN, G., SCHACHTER, M. & LEVER, P.S. (1987). The actions of calcitonin gene-related peptide and vasoactive intestinal peptide as vasodilators in man in vivo and in vitro. *Br. J. Clin. Pharmacol.*, **24,** 139–144.

WESTERMAN, R.A., WIDDOP, R.E., HOGAN, C. & ZIMMET, P. (1987). Non-invasive tests of neurovascular function: reduced responses in diabetes mellitus. *Neurosci. Lett.*, **81,** 177–182.

WOOLFSON, R.G. & POSTON, L. (1990). Effect of N^G-monomethyl-L-arginine on endothelium-dependent relaxation of human subcutaneous resistance arteries. *Clin. Sci.*, **79,** 273–278.

ZAMBETIS, M., DUSTING, G.J., RAJANAYAGAM, S. & WOODMAN, O.L. (1991). Mechanism of the hypertension produced by inhibition of nitric oxide biosynthesis in rats. *J. Cardiovasc. Pharmacol.*, **17,** Suppl. 3, 191–197.

(Received December 13, 1991
Revised March 3, 1992
Accepted March 16, 1992)

Br. J. Pharmacol. (1992), **106**, 656–664

Inhibition of human neutrophil responses by α-cyano-3,4-dihydroxythiocinnamamide; a protein-tyrosine kinase inhibitor

Peter Dryden, Vincent Duronio, Liana Martin, *Alan T. Hudson & [1]Hassan Salari

Department of Medicine, University of British Columbia, Vancouver, B.C., Canada and *The Wellcome Research Laboratories, Beckenham, Kent BR3 3BS

1 Activation of neutrophils results in increased tyrosine phosphorylation of several proteins that may have important roles in receptor/effector coupling. In this study, the effect of a protein tyrosine kinase inhibitor on receptor-mediated neutrophil activation by platelet-activating factor (PAF), leukotriene, B_4 (LTB_4) and N-formylmethionylleucylphenylalanine (FMLP) is investigated.

2 α-Cyano-3,4-dihydroxythiocinnamamide dose-dependently inhibited intracellular calcium release and superoxide generation from human neutrophils activated by 1 μM LTB_4, PAF, and FMLP.

3 In the presence of cytochalasin B, FMLP stimulated elastase release from neutrophils was also inhibited to unstimulated levels by 5 min pretreatment with α-cyano,3,4-dihydroxythiocinnamamide.

4 The inhibitory action of α-cyano-3,4-dihydroxythiocinnamamide was found to be at or upstream of phospholipase C activation, blocking both phosphatidylinositol hydrolysis and protein kinase C activation. α-Cyano-3,4-dihydroxythiocinnamamide did not affect agonist receptor binding sites or receptor affinity in neutrophils.

5 Immunoblot analysis demonstrated the tyrosine phosphorylation of proteins of 41, 56, 66, and 104 kDa in neutrophils treated with agonists. Treatment of neutrophils with α-cyano-3,4-dihydroxythiocinnamamide prior to stimulation with chemoattractants reduced tyrosine phosphorylation of the above phosphoproteins.

6 These results indicate that α-cyano-3,4-dihydroxythiocinnamamide might be a useful agent in characterizing the essential proteins and biochemical pathways that regulate neutrophil activation.

Keywords: Neutrophil; protein-tyrosine kinase; tryphostins; protein kinase C; inositol phosphates; elastase; superoxide anion

Introduction

Neutrophils respond to various chemotactic factors such as N-formylmethionylleucylphenylalanine (FMLP), leukotriene B_4 (LTB_4) and platelet-activating factor (PAF) by releasing their granule contents, generating oxygen free radicals, and undergoing directional migration towards the stimuli (Sha'afi & Molski, 1988). Activation of neutrophils by these agonists involves a pertussis toxin-sensitive G-protein (G_i) that activates phospholipase C (PLC) (Snyderman *et al.*, 1986; Sha'afi & Molsi, 1988). An initial step in the activation of neutrophils is the PLC catalyzed hydrolysis of phosphatidylinositol-4,5-bisphophate (PIP_2), producing two second messengers, inositol trisphosphate (IP_3) and 1,2-dioleoyl-sn-glycerol (DAG). IP_3 causes calcium release from intracellular stores (Berridge & Irvine, 1984) and acts synergistically with DAG to activate protein kinase C (PKC) (Nishizuka, 1988).

The signal transduction events involved in neutrophil activation are largely unknown. It has been reported that activation of neutrophils by various agonists involves phosphorylation on tyrosine residues of several proteins. Gomez-Cambronero *et al.* (1989a) reported tyrosine phosphorylation of five proteins with molecular masses of 118, 92, 78, 54, and 40 kDa in neutrophils stimulated with granulocyte-macrophage colony stimulating factor (GM-CSF). Cytosolic and particulate substrates have been shown to be tyrosine phosphorylated in neutrophils stimulated with FMLP, LTB_4, a phorbol ester, and a calcium ionophore suggesting receptor-dependent and receptor-independent tyrosine kinase activation (Berkow & Dodson, 1990). Proteins of similar molecular weight have also been shown to be tyrosine phosphorylated in neutrophils stimulated with chemotactic peptide FMLP (Gomez-Cambronero *et al.*, 1989b). In addition, similarities in the patterns of protein tyrosine phosphorylation are also evident in neutrophils activated with PAF and LTB_4 (Huang *et al.*, 1990; Gomez-Cambronero *et al.*, 1991). Attempts have been made to identify these phosphoproteins and to characterize their roles in neutrophil activation. In contrast to some growth factors such as epidermal growth factor and insulin (Ullrich *et al.*, 1984; Shechter *et al.*, 1989), the receptors for inflammatory agonists such as PAF, LTB_4, and FMLP have not been shown to have a kinase domain. In fact, the PAF receptor that was recently cloned (Honda *et al.*, 1991) contains seven transmembrane domains and guanine nucleotide binding protein (G-protein) binding sites, but no indication of how a tyrosine kinase might be activated. This suggests that the stimulation of tyrosine kinases by receptors for inflammatory mediators might be occurring as a consequence of other second messenger systems downstream of G-proteins.

Stimulation of protein tyrosine phosphorylation in electroporated human neutrophils treated with GTPγS suggests that the activated G-proteins can stimulate tyrosine kinases (Nasmith *et al.*, 1989). Similarily, receptor-mediated tyrosine phosphorylation has been shown to be mediated in part by a pertussis toxin-sensitive guanine nucleotide regulatory protein (Gomez-Cambronero *et al.*, 1989a). Various studies have demonstrated tyrosine phosphorylation of PLCγ- following interaction with ligand-activated PDGF or EGF receptors (Wahl *et al.*, 1989; Margolis *et al.*, 1989; Meisenhelder *et al.*, 1989). Unlike PLC α, β, and δ, which are coupled to a G-protein, PLCγ activity increases following tyrosine phosphorylation (Taylor *et al.*, 1991). Therefore, the precise relationship between tyrosine kinase activation and activation via G-proteins remains unclear.

In neutrophils, the role of tyrosine phosphorylation in response to agonist stimulation has not been clearly defined. When neutrophils were treated with erbstatin, a protein-

[1] Author for correspondence at: The Jack Bell Research Centre, 2660 Oak St., Vancouver, B.C. V6H 3Z6, Canada.

tyrosine kinase inhibitor, the superoxide generation elicited by FMLP was dose-dependently inhibited (Naccache *et al.*, 1990). Erbstatin also blocked the change in cytosolic pH caused by PAF and LTB_4, but not by FMLP. However, erbstatin was unable to inhibit the lysosomal enzyme release or elastase release in response to stimulation with FMLP in the presence of cytochalasin B (Naccache *et al.*, 1990). Due to the partial inhibitory activity of erbstatin, the effect of α-cyano,-3,4-dihydroxythiocinnamamide on neutrophil biochemical and physiological responses to chemoattractants were studied. The results of this study suggest that tyrosine phosphorylation is required for neutrophil activation in response to chemotactic factors. Although the precise role of tyrosine phosphorylation in neutrophil activation is unclear, inhibition of tyrosine kinase activity was associated with decreases in Ca^{2+} release, PLC activity, and PKC activity. In addition, we demonstrate that physiologically and pathologically related responses including superoxide anion production and elastase release are diminished. Thus, tyrosine kinase activity plays a major role in signal transduction and stimulus response coupling in neutrophils and inhibition of this class of enzymes decreases cellular responses.

Methods

Preparation of neutrophils

Human blood from normal volunteers was obtained in heparin. Blood was diluted with Tyrode buffer (pH 6.5) (5:1, v/v) and red cells were sedimented for 30 min after mixing blood with Dextran as described by Salari *et al.* (1985). Neutrophils were isolated following Ficoll-hypaque gradient centrifugation and the remaining erythrocytes were removed by Tris-NH_4Cl haemolysis (Boyle, 1968). Neutrophils at greater than 97% purity and greater than 95% viability as assessed by trypan blue dye exclusion were collected in an appropriate buffer.

Fura-2 loading and measurement of Ca^{2+}

Neutrophils were suspended in PBS (no Ca^{2+} or Mg^{2+}) with 1 μM Fura-2AM for 60 min, at 37°C. Free Fura-2AM was removed by washing the cells three times with PBS. Cells (5×10^6 cells ml^{-1}) were warmed to 37°C in a 1 cm^2 quartz cuvette in a volume of 2.5 ml. Changes in Ca^{2+}-dependent Fura-2 fluorescence were measured with a Perkin-Elmer (Norwalk, CT) LS-50 luminescence spectrophotometer with excitation wavelengths of 340 and 380 nm and an emission wavelength of 510 nm. The baseline level of fluorescence before addition of agonists was subtracted from agonist-induced fluorescence in the presence and absence of drug. Values described are arbitrary units taken from ratios between the absorbances at 340 nm and 380 nm.

Polyphosphoinositide hydrolysis

Neutrophils (2.5×10^7 cells ml^{-1}) were incubated with 100 μCi ml^{-1} of *myo*-[2-^{3}H]-inositol in Tyrode buffer (no Ca^{2+}), for 90 min at 37°C. Cells were washed twice and resuspended in Tyrode buffer containing 12 mM LiCl, 1.3 mM $CaCl_2$ and 0.6 mM $MgCl_2$. Cells in 0.5 ml volumes were incubated with or without α-cyano-3,4-dihydroxythiocinnamamide for 5 min and then treated with agonists for a further 5 min. The reaction was terminated by addition of 1.5 ml methanol/chloroform/HCl (200:100:2) as described by Watson *et al.* (1984). Following overnight storage at 4°C, water (0.6 ml) was added to each sample to extract water-soluble inositol phosphates; 1.8 ml of the upper phase was diluted with 2.5 ml of water and layered onto 1 ml Dowex anion exchange resin (Bio-Rad) columns, pre-equilibrated with water. Inositol phosphates were isolated and quantified as described earlier (Salari *et al.*, 1990b).

Protein kinase C assay

Neutrophils (10^7 cells ml^{-1}) in Tyrode buffer containing 1.4 mM $CaCl_2$ were stimulated with or without pretreatment with α-cyano-3,4-dihydroxythiocinnamamide and chemotactic factors at 37°C. Treatments were terminated by quick centrifugation in a microfuge. Pellets were resuspended on ice in a homogenizing buffer and sonicated for 30 s as reported earlier (Pelech *et al.*, 1990). The particulate and cytosolic fractions were isolated by centrifugation at 200,000 *g* in a Beckman TL-100 ultracentrifuge; 500 μg of cytosolic and NP-40 solubilized particulate extracts were fractionated on a 1 ml anion exchange Mono Q column coupled to a FPLC system (Pharmacia). Fractions were eluted at a flow rate of 0.8 ml min^{-1} using a linear gradient of 0–0.8 M NaCl. PKC activity of column fractions were assayed as described previously (Pelech *et al.*, 1990). Reactions were carried out at 30°C in a volume of 25 μl with 50 μM [γ-^{32}P]-ATP (1500 c.p.m. $pmol^{-1}$), 25 mM β-glycerophosphate, 10 mM MOPS (pH 7.2), 15 mM $MgCl_2$, 2 mM EGTA, 2 mM EDTA, 1 mM dithiothreitol, 500 nM PKIP, and 1 mM sodium orthovanadate, with 1 mg ml^{-1} histone H1 or protamine chloride as the substrate. Where stated, incubations included 4.5 mM $CaCl_2$ 60 μg^{-1} ml^{-1} phosphatidylserine and 6 μg ml DAG. Reactions were terminated by spotting 20 μl aliquots on 2 cm^2 pieces of Whatman P81 phosphocellulose paper, dried 30 s, and washed with several changes of 1% (v/v) phosphoric acid. Filter papers were counted for radioactivity in a Beckman model LS5000 scintillation counter.

Tyrosine phosphorylation

Neutrophils (10^7 cells ml^{-1}) in Tyrode solution containing 1.4 mM $CaCl_2$ were treated at 37°C for 1 min with each agonist or pretreated with α-cyano-3,4-dihydroxythiocinnamamide prior to stimulation for 5 min at 37°C. After stimulation, cells were rapidly pelleted by microcentrifugation (14,000 r.p.m. for 5 s), pellets were solubilized with 3% Triton or sonicated in buffer composed of 50 mM Tris-HCl, pH 7.7, 5 mM β-methylaspartate, 150 mM NaCl, 0.2 mM Na_3VO_4, 10 mM NaF, 1 mM $NaMoO_4$, 5 mM EDTA, 10 μg ml^{-1} leupeptin, 10 μg ml^{-1} soybean trypsin inhibitor, 1 μM pepstatin, 1 mM PMSF, and 1 mM diisopropylfluorophosphate. Insoluble cellular debris were removed by microcentrifugation (14,000 r.p.m. for 1 min) and soluble cell supernatants were combined with SDS-PAGE sample buffer, boiled, and electrophoresed by discontinuous SDS-PAGE. Separated proteins were transferred to nitrocellulose sheets and blocked overnight in Tris-buffered saline (TBS) (0.02 M Tris-HCl, pH 7.5, 0.05 M NaCl) containing 5% BSA and 1% ovalbumin. Blots were washed with TBS and probed with antiphosphotyrosine specific antibody PY-20 in TBS with 1% BSA and 0.02% sodium azide. After washing, blots were incubated with alkaline phosphatase conjugated goat anti-mouse IgG in TBS + 0.05% NP-40 for 2 h at room temperature before colour development with 5-bromo-4-chloro-3-indolyphosphate (BCIP) and nitro blue tetrazolium (NBT). The specificity of antibody PY-20 has been demonstrated by competition with phosphotyrosine or phenylphosphate but not phosphoserine, phosphothreonine, or free phosphate (Glenny *et al.*, 1988).

Elastase release

[^{3}H]-elastin substrate was prepared as previously described with [^{3}H]-$NaBH_4$ used as the radioactive source (Takahashi *et al.*, 1973). The [^{3}H]-elastin suspension (specific activity = 3168 c.p.m. μg^{-1}) was sonicated, agitated, and 20 μl suspensions were evenly spread on 16 mm wells (Costar plates). The plates were dried at 45°C overnight, washed with phosphate buffered saline (PBS), and stored at 4°C until use (usually 1–7 weeks). 10^6 cells in 500 μl DMEM were added to each well, stimuli or inhibitors diluted in DMEM were added, and

plates were incubated at 37°C in an atmosphere of 5% CO_2. To monitor elastase release by the cells into the media, after 1 h incubation, 100 µl of media was removed, microcentrifuged (14,000 r.p.m. for 2 min) to remove contaminating cells, and the soluble phase was counted for radioactivity. Tritium counts from control wells incubated with DMEM in the absence of cells were subtracted from wells with cells and µg elastin degraded by 10^6 cells in 1 h was calculated.

Superoxide anion generation

Continuous spectrophotometric measurement of a superoxide dismutase inhibitable reduction of ferricytochrome C at 549 nm was measured in cuvettes as described (Robinson *et al.*, 1985). Reaction mixtures containing 500 units ml^{-1} catalase and 1.24 mg ml^{-1} cytochrome C in HBSS supplemented with 5.5 mM glucose, 0.1% gelatin and $1.5-2.5 \times 10^6$ cells ml^{-1}. Prior to stimulation, mixtures were warmed to 37°C, agonists diluted in HBSS + 0.1% gelatin were added, and absorbance at 549 nm was scanned every 10 s with a Beckman DU-65 spectrophotometer and plotted manually.

PAF binding

Competition binding studies were performed at room temperature as described previously (Duronio *et al.*, 1990). Neutrophils and reagents were suspended in binding buffer (10 mM Tris-HCl, pH 7.5, 10 mM KCl, 5 mM $MgCl_2$, and 2.5 mg ml^{-1} BSA) and 5×10^6 cells were added to start the reaction in tubes containing 0.25 nM [^{3}H]-PAF and 0 to 500 fold excess of unlabelled PAF for 30 min at room temperature. Reactions were terminated by filtration through prewetted GF/C filters and washed with 5 ml binding buffer and counted for radioactivity. Nonspecific binding was referred to as the radioactivity associated with cells in the presence of a 500 fold excess of unlabelled ligand.

Chemicals and drugs

Histone H1, bovine serum albumin (BSA), ovalbumin, L-α-phosphatidyl-L-serine, DAG, phenylmethyl sulphonyl fluoride (PMSF), leupeptin, pepstatin, β-methylaspartate, diisopropylfluorophosphate (DFP), pepstatin, PAF, LTB_4, FMLP, Ficoll-Hypaque, cytochalasin B, cyclic AMP-dependent protein kinase inhibitor peptide (amino acids 5-24) (PKIP), and other chemicals, unless stated, were purchased from Sigma Chemical Co. (St. Louis, Mo, U.S.A.). Fura-2AM was purchased from Molecular Probes (Eugene, OR, U.S.A.). Dextran T500 was purchased from Pharmacia (Montreal, Canada). Electrophoresis reagents, nitrocellulose sheets, and alkaline phosphatase conjugated goat anti-mouse antibody were purchased from Bio-Rad Laboratories (Richmond, CA, U.S.A.). [γ-^{32}P]-ATP (~3000 Ci $mmol^{-1}$), *myo*-[2-^{3}H]-inositol (18.3 Ci $mmol^{-1}$), and [^{3}H]-PAF (80 Ci $mmol^{-1}$) were purchased from Amersham (Arlington Heights, IL, U.S.A.). Scintillation fluid, 3-(N-morpholino) propanesulphonic acid (MOPS), and antibody PY-20 were purchased from ICN Biomedicals, Inc (Costa Mesa, CA, U.S.A.). GF/C filters and P81 phosphocellulose paper were purchased from Whatman (Mandel Scientific, Toronto, Canada). Dulbecco's modified Eagle's medium (DMEM) was purchased from GIBCO (Grand Island, NY, U.S.A.). α-Cyano-3,4-dihydroxythiocinnamamide was synthesized as described by Gazit *et al.* (1989) and stored in a stock solution of dimethylsulphoxide (DMSO) before serial dilution in an appropriate buffer for each experiment. DMSO concentrations were below 0.2% in all experiments.

Statistical analysis

Data are expressed as mean ± s.d. Elastase data were analysed by a two-way analysis of variance using the Systat programme version 5.1 (Evanston, IL, U.S.A.). Cellular inositol phosphate measurements were compared by Student's *t* test with correction for multiple comparisons.

Results

The effect of the α-cyano-3,4-dihydroxythiocinnamamide on ligand-induced increases in cytosolic free Ca^{2+} concentration

Since a rapid increase in intracellular free Ca^{2+} is required for neutrophil activation, the effect of this tyrosine kinase inhibitor on Ca^{2+} release was analysed. In all cases, a calcium ionophore was used as a positive control and addition of buffer alone served as a baseline. An increase in intracellular Ca^{2+} levels were observed in Fura-2 AM loaded cells stimulated with PAF, FMLP, or LTB_4. Maximum release of calcium with the three agonists were in the order $LTB_4 > FMLP > PAF$ at a concentration of 1 µM. Pretreatment of neutrophils for 5 min with α-cyano-3,4-dihydroxythiocinnamamide caused a dose-dependent decrease in Ca^{2+} mobilization in response to PAF, LTB_4 and FMLP by agonist stimulation of 10^{-5}, 10^{-7}, and 10^{-6} M, respectively (Figure 1b). α-Cyano-3,4-dihydroxythiocinnamamide was effective when added as little as 1 min before the stimulus (data not shown). α-Cyano-3,4-dihydroxythiocinnamamide did not cause neutrophil toxicity as neutrophils washed with buffer after incubation with α-cyano-3,4-dihydroxythiocinnamamide for 5 min were fully responsive to stimulation with the three agonists (data not shown).

Inhibition of human neutrophil physiological responses

It has been reported that FMLP (Lehmeyer *et al.*, 1979) and PAF (Dewald & Baggiolini, 1986) are capable of increasing superoxide production in human neutrophils. We evaluated the effect of α-cyano-3,4-dihdyroxythiocinnamamide on the generation of superoxide anion by neutrophils treated with 1 µM FMLP or PAF. When neutrophils were treated with FMLP and cytochalasin B (1 µM) a rapid generation of superoxide (O_2^-) was observed. The O_2^- generation reached a plateau at about 5 min after agonist treatment. Similarly, PAF in the presence of cytochalasin B caused a rapid generation of O_2^- from neutrophils. FMLP was a more potent stimulus for O_2^- production (Figure 2). FMLP and PAF alone caused O_2^- release, although the presence of cytochalasin B potentiated O_2^- release as reported (Dewald & Baggiolini, 1986). When cells were pretreated with 0.2 mM α-cyano-3,4-dihydroxythiocinnamamide (50 µg ml^{-1}) 5 min before the addition of FMLP or PAF, a potent inhibition of O_2^- generation was observed. The drug was able to inhibit O_2^- release by PAF or FMLP by more than 70% in several independent experiments (Figure 2).

Neutrophil degranulation leads to the production of lysosomal enzymes and oxygen radicals. One component of lysosomal enzyme contents is elastase, a serine protease that has been implicated in various disease states (Sandberg *et al.*, 1981). In the present investigation, the effect of α-cyano-3,4-dihydroxythiocinnamamide on the release of elastase from neutrophils was evaluated. As has been reported (Styrt *et al.*, 1987), cytochalasin B appreciably augments neutrophil degranulation. In the absence of cytochalasin B, no significant increases in elastase release was detected in cells stimulated with FMLP, PAF, or LTB_4 (data not shown). In the presence of 1 µM cytochalasin B, a concentration previously shown to stimulate human polymorphonuclear leukocyte functions (Salari *et al.*, 1985), 1 µM FMLP significantly stimulated elastase release from neutrophils (Figure 3a). Although cytochalasin B potentiated FMLP-induced elastase release, the presence of cytochalasin B did not significantly enhance PAF or LTB_4-induced elastase release. Pretreatment of neutrophils with α-cyano-3,4-dihydroxythiocinnamamide for 5 min before the addition of FMLP inhibited FMLP-

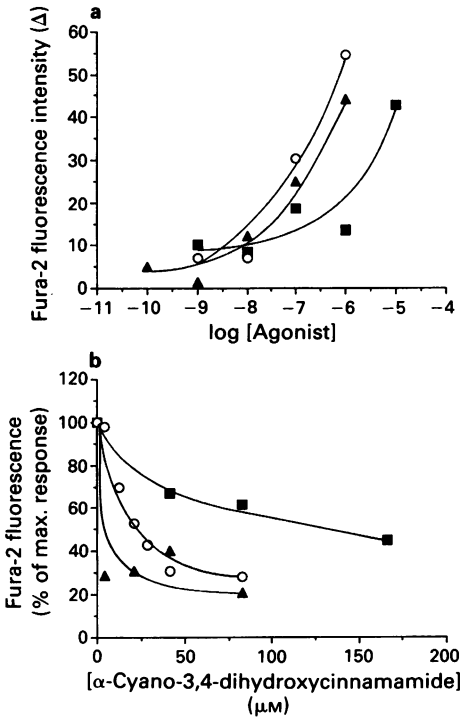

Figure 1 Effect of α-cyano-3,4-dihydroxythiocinnamamide on intracellular calcium release. (a) Effect of agonist concentration on intracellular Ca^{2+} release. Neutrophils were loaded with Fura-2AM (1 μM) and free dye was washed from cells with PBS. Cells were warmed to 37°C and stimulated with various concentrations of PAF (■), leukotriene B_4 (LTB_4) (○), and fMet-Leu-Phe (▲) and the change in fluorescence is plotted. Changes in fluorescence are reported as the difference in fluorescence before stimulation and at maximal fluorescence after stimulation. (b) Concentration-dependent dose-response curve of inhibition of intracellular Ca^{2+} release in human neutrophils by α-cyano-3,4-dihydroxythiocinnamamide in response to 10 μM PAF (■), 0.1 μM LTB_4 (○), and 1 μM FMLP (▲). Fluorescence is reported as the ratio between the absorbances at 340 nm and 380 nm. Results are illustrated by drawing curves by visual inspection and a representative of three similar experiments is illustrated.

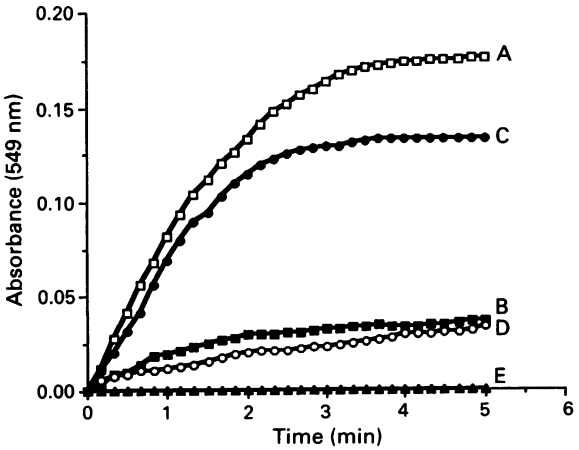

Figure 2 Effect of α-cyano-3,4-dihydroxythiocinnamamide on stimulation of superoxide generation from human neutrophils. Spectrophotometric analysis of agonist-induced reduction of ferricytochrome C was monitored at 549 nm. Cells were either stimulated with 1 μM PAF or fMet-Leu-Phe in the presence of 1 μM cytochalasin B or cells were exposed to 0.2 mM α-cyano-3,4-dihydroxythiocinnamamide for 5 min before addition of agonists: (A) FMLP, (B) α-cyano-3,4-dihydroxythiocinnamamide and FMLP, (C) PAF, (D) α-cyano-3,4-dihydroxythiocinnamamide and PAF, and (E) untreated cells or cells stimulated in the presence of superoxide dismutase. Representative data of 3 independent experiments are shown.

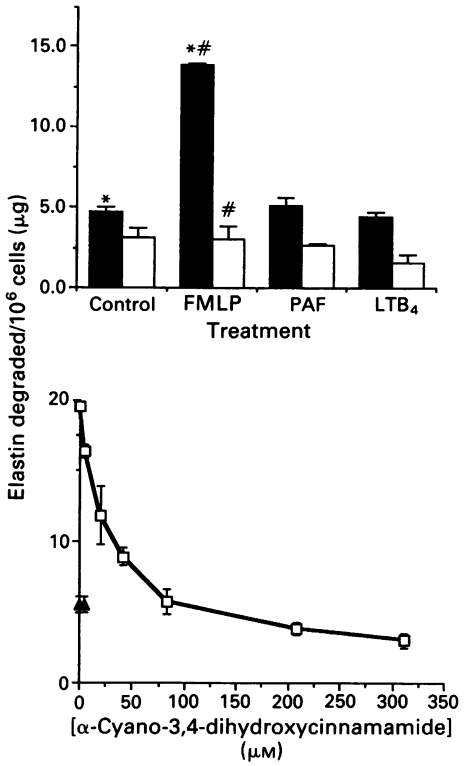

Figure 3 Inhibition of elastase release in human neutrophils by α-cyano-3,4-dihydroxythiocinnamamide. (a) Neutrophils were preincubated with buffer alone (solid columns) or 0.2 mM α-cyano-3,4-dihydroxythiocinnamamide (open columns) for 5 min at 37°C. Elastase release in the presence of 1 μM cytochalasin B was stimulated by 1 μM of each agonist used. Vertical bars span the standard deviation. The values obtained indicate that fMet-Leu-Phe (FMLP) significantly stimulates elastase release from neutrophils in the presence of cytochalasin B ($*P \leq .001$, $n = 3$) and that α-cyano-3,4-dihydroxythiocinnamamide significantly inhibits FMLP-stimulated elastase release ($\#P \leq 0.001$, $n = 3$). (b) Dose-response curve of inhibition of FMLP-stimulated elastase release by α-cyano-3,4-dihydroxythiocinnamamide. Increasing amounts of α-cyano-3,4-dihydroxythiocinnamamide were incubated for 5 min at 37°C with 10^5–10^6 neutrophils prior to 1 mM FMLP stimulation (□) or untreated cells (△). Solubilized [^{3}H]elastin released into the culture medium was counted for radioactivity after a 1 h incubation.

stimulated elastase release. The effect of α-cyano-3,4-dihydroxythiocinnamamide was dose-dependent (Figure 3b) and total inhibition of FMLP-induced elastase release to control levels was seen at a drug concentration 83 μM. The IC_{50} for inhibition of elastase release was calculated to be about 35 μM. It was observed that higher concentrations of α-cyano-3,4-dihydroxythiocinnamamide reduced non-specific elastase release, presumably due to stabilization of cellular activation processes. The basal release of elastase and the minimal effects of PAF and LTB_4 on elastase secretion were also reduced below unstimulated levels by α-cyano-3,4-dihydroxythiocinnamamide (Figure 3a). Cells pretreated with the drug were viable after 1 h incubation as determined by a trypan blue exclusion dye assay.

Effect of α-cyano-3,4-dihydroxythiocinnamamide on ligand-receptor interactions

Studies with calcium release and O_2^- generation indicated that the action of α-cyano-3,4-dihydroxythiocinnamamide is directed against receptor-mediated responses in neutrophils, perhaps due to inhibition of agonist-receptor interactions. To investigate this possibility, we tested the effect of α-cyano-3,4-dihydroxythiocinnamamide on one of the agonists that binds to neutrophil membranes to initiate cellular responses. PAF

was selected for this study as a result of our previous experience with PAF receptor binding (Duronio *et al.*, 1990). Specific PAF receptor binding was unaffected by the presence of 0.2 mM α-cyano-3,4-dihydroxythiocinnamamide (510 ± 119 d.p.m., 511 ± 105 d.p.m. ($n = 3$); α-cyano-3,4-dihydroxythiocinnamamide absent, α-cyano-3,4-dihydroxythiocinnamamide present). In a single experiment, Scatchard plot analysis of data showed that human neutrophils possess ~6000 receptors/cell with a K_d of ~2.3 nM when neutrophils were incubated with 0.2 mM α-cyano-3,4-dihydroxythiocinnamamide for 5 min before PAF binding. In the absence of the drug, the K_d remained 2.5 ± 0.2 nM with a B_{max} of about 6000 receptors/cell (data not shown). The affinity constant and number of receptor sites per neutrophil reported in this study are comparable to previously determined values for high affinity PAF binding sites on peripheral blood neutrophils (O'Flaherty *et al.*, 1986). These results suggest that α-cyano,3,4-dihydroxythiocinnamamide is not inhibiting PAF-induced responses at the receptor. Previous studies have demonstrated that erbstatin does not inhibit FMLP binding (Naccache *et al.*, 1990).

Inhibition of protein kinase C activation

PKC has been shown to play a major role in neutrophil activation as demonstrated by the inhibition of neutrophil oxidative burst and degranulation by PKC inhibitors (Berkow *et al.*, 1987). In an attempt to characterize the site of action of α-cyano-3,4-dihydroxythiocinnamamide in neutrophils, the effect of this drug on PKC activity was investigated. The effect of 5 min pretreatment of cells with α-cyano-3,4-dihydroxythiocinnamamide on agonist-induced PKC activity was analysed. A rapid extraction of kinase activity was required to prevent proteolytic degradation of PKC during enzyme preparations. Neutrophils were treated with PAF (1 μM) for 1 min and extracts were isolated and separated by Mono Q FPLC chromatography. This fractionation was required since PKC inhibitors have been found in cytosolic sources that may be removed by anion exchange chromatography (Lang & Vallotton, 1987). Fractions were assayed for PKC activity by monitoring Ca^{2+} and phospholipid-dependent phosphorylation of histone H1 as well as the Ca^{2+}/DAG/PS-independent phosphorylation of protamine, a PKC substrate in the absence of activators (Bazzi & Nelsestuen, 1987). Most of the Ca^{2+}/PS/DAG-dependent PKC activity (~60%) was present in the cytosolic fraction and PKC was only slightly translocated to the microsomal fraction by PAF stimulation (data not shown). The phosphorylation of protamine chloride was observed in the same fractions as those that phosphorylated histone H1. Basal levels of PKC activity were associated with both cytosolic and microsomal fractions of control cells (Table 1). Microsomal fractions contained two peaks of PKC activity eluting at 0.33 M and 0.5 M NaCl. Ca^{2+}/PS/DAG-dependent PKC activity in particulate derived fractions eluting at 0.33 M was stimulated ~1.5 fold by PAF. After α-cyano-3,4-dihydroxythiocinnamamide pretreatment, PKC activity stimulated by PAF treatment was reduced below control levels (Table 1). α-Cyano-3,4-dihydroxythiocinnamamide entirely abolished the activity associated with the 0.5 M NaCl peak in the particulate fraction, which was the major peak of PAF-induced activation. Cytosolic extracts of untreated neutrophils contained a single peak of PKC activity eluting at 0.33 M NaCl as separated by MonoQ chromatography. PAF also stimulated the cytosolic PKC activity by approximately 1.5 fold. As with microsomal PKC activity, α-cyano-3,4-dihydroxythiocinnamamide also inhibited the cytosolic PKC activity to levels below baseline. The Ca^{2+} and phospholipid-dependence of phosphorylating activity eluting at 0.33 M NaCl in both cytosolic and microsomal fractions is exemplified by its inability to phosphorylate histone H1 in the absence of Ca^{2+}, DAG, and PS. Similar results were observed with cells stimulated with FMLP and LTB_4 (data not shown). To confirm further the inhibitory action of α-cyano-3,4-dihydroxythiocinnamamide on PKC, neutrophils were labelled with ^{32}Pi. Cells were then stimulated with PAF, FMLP, and LTB_4. Cytosolic fractions were analysed by SDS-PAGE and phosphorylated proteins were detected by autoradiography. All agonists stimulated phosphorylation of a 47 kD protein, previously identified as a major PKC substrate in neutrophils (Kramer *et al.*, 1988). Phosphorylation of this 47 kD protein was decreased when neutrophils were treated with 0.2 mM α-cyano-3,4-dihydroxythiocinnamamide (data not shown), correlating with the PKC *in vitro* assay results.

Effect of α-cyano-3,4-dihydroxythiocinnamamide on polyphosphoinositide hydrolysis

Receptor-induced activation of PLC catalyzes the hydrolysis of PIP_2, leading to an accumulation of inositol trisphospate (IP_3), inositol bisphosphate (IP_2) and inositol monophosphate (IP). As an index of PLC activity, PLC products including inositol mono, di, and triphosphates were monitored. Addition of 1 μM PAF and 1 μM FMLP were effective stimuli, increasing the production of all inositol phosphates above control levels (Figure 4; I, II, and III, treatments c and g). Although PAF was a more potent stimulus, the effects of both agonists were inhibited by pretreatment of cells with α-cyano-3,4-dihydroxythiocinnamamide (Figure 4; I, II, and III, d and h). LTB_4 (1 μM) slightly stimulated PIP_2 hydrolysis with IP_1 the only metabolite appreciably detectable above control whereas the levels of IP_2 and IP_3 were similar to unstimulated controls (Figure 4; I, II, III, e). PI hydrolysis in

Table 1 Effect of α-cyano-3,4-dihydroxythiocinnamamide (DHC) on PAF-induced protein kinase C (PKC) activation in human neutrophils

Treatment (fraction)	*Protein phosphorylation* (pmol min^{-1} ml^{-1})		
	Histone		*Protamine*
	No addition	+ Ca^{2+}, + ,PS, + DG	
Control (cytosol)	67 ± 12	1534 ± 401	1231 ± 317
Control (particulate)	726 ± 110	1073 ± 87	273 ± 46
PAF (cytosol)	91 ± 38	2524 ± 305	2419 ± 392
PAF (particulate)	1073 ± 186	1714 ± 162	294 ± 63
PAF + DHC (cytosol)	65 ± 44	1511 ± 287	1078 ± 401
PAF + DHC (particulate)	463 ± 94	563 ± 106	264 ± 71

Histone H1 phosphorylation was assayed in the presence and absence of activators including Ca^{2+}, phosphatidylserine (PS), and diacylglycerol (DG). Cells were untreated, exposed to 1 μM PAF for 1 min or preincubated with 0.2 mM α-cyano-3,4- dihydroxythiocinnamamide for 5 min before 1 μM PAF stimulation for 1 min. Mean and s.d. are given from three independent experiments.

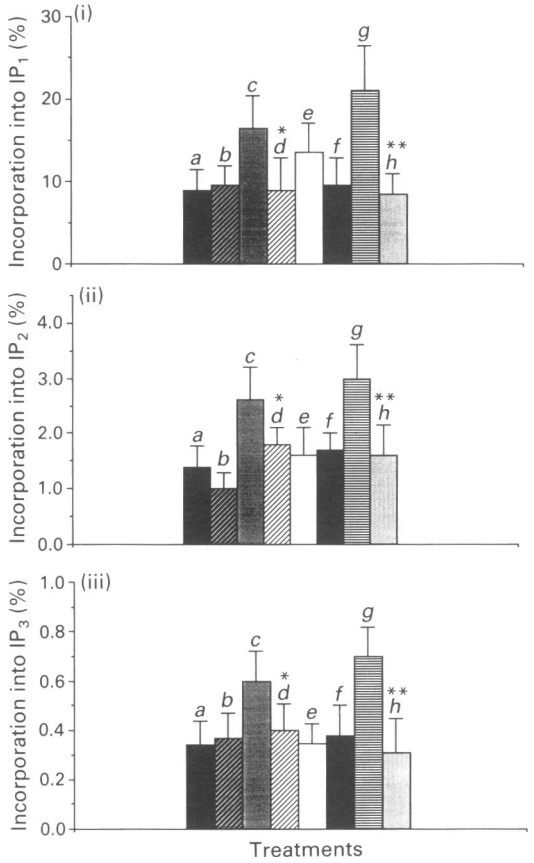

Figure 4 Effect of α-cyano-3,4-dihydroxythiocinnamamide on agonist-induced polyphosphoinositide hydrolysis. Human neutrophils prelabelled with *myo*-[2-^{3}H]-inositol were stimulated for 5 min with 1 μM leukotriene B_4 (LTB_4), PAF, or fMet-Leu-Phe (FMLP) and the effect of a 5 min preincubation with 0.2 mM α-cyano-3,4-dihydroxythiocinnamamide was analysed for stimulation of inositol phosphate incorporation into (i) IP_1 (ii) IP_2 and (iii) IP_3. Prior to harvesting and chromatography of inositol phosphates, cells were treated as follows: (a) untreated, (b) α-cyano-3,4-dihydroxythiocinnamamide; (c) FMLP; (d) α-cyano-3,4-dihydroxythiocinnamamide + FMLP; (e) LTB_4; (f) α-cyano-3,4-dihydroxythiocinnamamide + LTB_4; (g) PAF; (h) α-cyano-3,4-dihydroxythiocinnamamide + PAF. The incorporation of radioactivity into the various polyphosphatidylinositide metabolites was expressed as a percentage of the total radioactivity associated with free inositol, IP, IP_2, and IP_3 together. Results are mean of 6 samples with s.d. shown by vertical bars. Significantly inhibited compared to agonist-stimulated at $^{**}P < 0.05$; $^{*}P < 0.1$

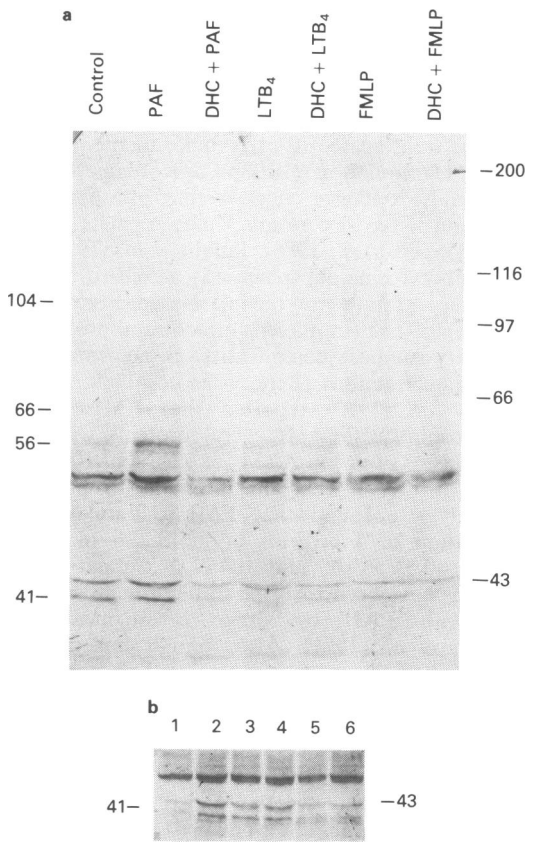

Figure 5 Inhibition of tyrosine phosphorylation in neutrophils stimulated with PAF, leukotriene B_4 (LTB_4) and fMet-Leu-Phe (FMLP) by α-cyano-3,4-dihydroxythiocinnamamide. Human neutrophils (10^7 cells ml^{-1}) in buffer containing Ca^{2+} were preincubated with 0.2 μM α-cyano-3,4-dihydroxythiocinnamamide (DHC) for 5 min prior to the addition of agonists (1 μM) at 37°C for 1 min. Cell extracts were separated by SDS-PAGE, transferred to nitrocellulose, and probed with antiphosphotyrosine antibodies. (a) Effect of various agonists and inhibition by α-cyano-3,4-dihydroxythiocinnamamide treated as indicated. (b) Dose response of inhibition of PAF-induced protein-tyrosine phosphorylation of p41 by α-cyano-3,4-dihydroxythiocinnamamide. Cells were untreated (lane 1), treated with 1 μM PAF (lane 2), or pretreated with 4.16 μM, 20.8 μM, 41.6 μM and 104 μM α-cyano-3,4-dihydroxythiocinnamamide (lanes 3–6) prior to 1 μM PAF treatment. Molecular mass markers (in kDa) are shown to the right and molecular masses of tyrosine phosphorylated substrates are shown on the left of the figure.

all cases was reduced to levels obtained with untreated cells by drug treatment. Incorporation of [^{3}H]-inositol into these water soluble phosphates was not significantly affected by treatment with α-cyano-3,4-dihydroxythiocinnamamide (Figure 4; I, II, and III, b) as compared with untreated control cells.

Inhibition of human neutrophil protein-tyrosine phosphorylation

The ability of PAF, LTB_4 and FMLP to stimulate tyrosine phosphorylation in human neutrophils was investigated. As seen by visual inspection of Figure 5 (a), unstimulated cells contained tyrosine phosphorylated proteins, although agonist stimulation caused an increase in the tyrosine phosphorylation of proteins of 41, 56, 66, and 104 kDa. Preincubation of cells for 5 min with 0.2 mM α-cyano-3,4-dihydroxythiocinnamamide inhibited ligand-stimulated tyrosine phosphorylation of the proteins that were tyrosine phosphorylated in response to the agonists used. Tyrosine phosphorylation was reduced by drug treatment to the base line level seen in control, unstimulated neutrophils. A dose-dependent inhibition of PAF-induced tyrosine phosphorylation was observed from 0–0.1 mM α-cyano-3,4-dihydroxythiocinnamamide (Figure 5b). Complete inhibition of PAF-induced tyrosine phosphorylation was observed at 10 μg ml^{-1} (42 μM) in comparison with unstimulated neutrophils.

Discussion

Tyrosine kinases and their substrates have been associated primarily with growth factors and are believed to play important roles in the onset of oncogenes (Heldin *et al.*, 1987). We have demonstrated protein tyrosine phosphorylation in platelets in response to PAF and showed that a protein tyrosine kinase inhibitor (erbstatin) can inhibit platelet activation (Salari *et al.*, 1990a). The effect of this inhibitor was also investigated in neutrophils (Naccache *et al.*, 1990). Another tyrosine kinase inhibitor, genistein, was found to inhibit PAF-induced rabbit platelet aggregation and PLC activation at doses greater than 0.5 mM (Dhar *et al.*, 1990). Genistein was also found to inhibit human platelet responses to stimulation with thromboxane A_2 and collagen, but not thrombin (Nakashima *et al.*, 1991). In leukocytes, various

forms of protein tyrosine kinases such as c-*fgr* (Gutkind & Robbins, 1989), c-*fes/fps* (Smithgall *et al.*, 1988), c-*hck* (Ziegler *et al.*, 1988) and c-*src* (Gee *et al.*, 1986) have been identified. The mechanism of stimulation of these kinases is unknown. Recent work suggests that c-*fgr* in human neutrophils may be translocated from granules to the plasma membrane upon degranulation (Gutkind & Robbins, 1989). In the *src* gene family, evidence suggests that phosphorylation of carboxy-terminal tyrosine residues may regulate their kinase activities (Cooper *et al.*, 1986). Pulido *et al.* (1989) reported that a phosphotyrosine phosphatase is mobilized from specific and/or tertiary granules to the plasma membrane fractions when neutrophils are stimulated. In addition, protein tyrosine kinase activity has been demonstrated in neutrophil cytosolic and particulate fractions (Berkow *et al.*, 1989; 1990).

Huang *et al.* (1990) reported that FMLP stimulated tyrosine phosphorylation of several proteins with apparent molecular masses of group A (54–58 kDa and 100–125 kDa) and group B (36–41 kDa) in rabbit neutrophils. In the present study, we found that FMLP stimulated tyrosine phosphorylation of 4 proteins of molecular masses of approximately 40.5, 56, 66 and 104 kDa. Similar phosphorylated proteins have been reported to be present in neutrophils activated with PAF by other investigators (Gomez-Cambronero *et al.*, 1991). Also, similar but not identical proteins were found to be phosporylated in human neutrophils stimulated with GM-CSF (Gomez-Cambronero *et al.*, 1989a) although GM-CSF also stimulates tyrosine phosphorylation of proteins of 78 and 92 kD that may be the GM-CSF receptor (Gomez-Cambronero *et al.*, 1989b). The major human neutrophil tyrosine phosphorylated proteins as a result of PAF stimulation were pp41, pp66, pp54, pp104 and pp116 (Gomez-Cambronero *et al.*, 1991).

By using inhibitors of protein tyrosine kinases or phosphatases, several investigators have suggested that tyrosine phosphorylation may be a central process controlling neutrophil activation through receptor-mediated processes (Kraft & Berkow, 1987; Grinstein *et al.*, 1989). Although erbstatin was able to inhibit superoxide production in human neutrophils stimulated by FMLP (Naccache *et al.*, 1990), this inhibitor failed to inhibit elastase release and intracellular calcium release. Since the inhibitor used in this study is more potent than erbstatin, this may account for its ability to inhibit Ca^{2+} release. In addition, for erbstatin to inhibit O_2^- production, it required at least 1 h of exposure for effective inhibition. These data suggest that the action of erbstatin on O_2^- production may not be specific and it is possible that erbstatin was interfering with some other components of the superoxide generating system as well as tyrosine phosphorylation. Several analogues of erbstatin have been synthesized (Isshiki *et al.*, 1987; Gazit *et al.*, 1989) in an attempt to produce selective, non-toxic and potent inhibitors of tyrosine kinases. Another class of protein-tyrosine kinase inhibitors having a cinnamamide structure was tested for their ability to inhibit tyrosine kinase activity in response to growth factors. The most potent of this class of compounds was reported to inhibit EGF-dependent cell proliferation (Lyall *et al.*, 1989) with a K_i of 0.85 μM (Yaish *et al.*, 1988), about six times more potent than erbstatin (Imoto *et al.*, 1987). In the present study, the effect of α-cyano-3,4-dihydroxythiocinnamamide on human neutrophil responses was investigated. This work stems from the observation that this inhibitor was the most potent tyrosine kinase inhibitor as reported in a previous study (Yaish *et al.*, 1988).

We demonstrated in this paper that α-cyano-3,4-dihydroxythiocinnamamide is capable of inhibiting agonist-induced neutrophil activation. Responses such as O_2^- generation and elastase release as well as components of intracellular signalling pathways were inhibited. α-Cyano-3,4-dihydroxythiocinnamamide partially inhibited TPA and zymosan-induced O_2^- generation when used at 0.2 mM (data not shown). To elucidate the site of action of α-cyano-3,4-dihydroxythiocinnamamide, a series of biochemical assays was used to investigate the effect on calcium mobilization, polyphosphoinositide hydrolysis and PKC activation. It is well documented that the increase in intracellular free calcium is associated with agonist-induced neutrophil activation (Lew *et al.*, 1984; Korchak *et al.*, 1984). The ability of α-cyano-3,4-dihydroxythiocinnamamide to inhibit agonist-induced intracellular Ca^{2+} accumulation suggests that the drug is acting by inhibiting PLC, possibly the substrate for an activated tyrosine kinase. The inhibition of Ca^{2+} release was inhibited by short (5 min) preincubation with the drug and inhibition was reversible. When the drug was washed from the neutrophils, agonists were capable of inducing Ca^{2+} release from the neutrophils suggesting that the drug did not cause cell toxicity. Since the agonist-induced rise in cytosolic free Ca^{2+} was inhibited by α-cyano,3,4-dihydroxythiocinnamamide, other parameters of neutrophil activation were analysed.

We discovered that the activities of PKC and PLC were decreased by this drug suggesting that α-cyano-3,4-dihydroxythiocinnamamide was probably acting at a signal transduction process above or at the level of PLC. Therefore, the inhibition of PKC is the consequence of inhibition of DAG and IP_3-induced Ca^{2+} generation from PIP_2 hydrolysis, and may not be the direct effect of the drug on this kinase. In this study, PKC was activated in both the particulate and cytosolic fractions, although a significant translocation of PKC to the membrane fraction did not accompany PKC stimulation. Since cytochalasin B was not present during stimulation, this correlates with reports that cytochalasin B is necessary for induction of particulate protein kinase activity (Pike *et al.*, 1986). PKC inhibition below baseline levels may be due to a direct inhibitory effect on PKC as well as inhibiting upstream signals. A nonspecific inhibition of signal transduction processes may account for inhibition of all responses tested. A previous study correlates tyrosine phosphorylation and G-protein activation with the respiratory burst, indicating that kinases other than PKC are involved in this agonist-stimulated response (Nasmith *et al.*, 1989). Our results support the claim that tyrosine phosphorylation may play an important role in neutrophil activation. The ability of α-cyano-3,4-dihydroxythiocinnamamide to decrease PI hydrolysis to baseline levels indicates that this inhibitor is capable of decreasing neutrophil stimulated activity initiated via PLC. α-Cyano-3,4-dihydroxythiocinnamamide pretreatment of cells does not decrease PI hydrolysis below baseline levels, suggesting that metabolism of unstimulated cells are not affected by this inhibitor.

In conclusion, the present study demonstrates that an increase in protein tyrosine phosphorylation in neutrophils in response to chemotactic factors has an important role in neutrophil activation and α-cyano-3,4-dihydroxythiocinnamamide can specifically inhibit neutrophil activation with relevance to inflammatory reactions. In addition, we show that α-cyano-3,4-dihydroxythiocinnamamide can inhibit neutrophil activation by interrupting tyrosine phosphorylation of proteins that may have a key role in neutrophil function.

The authors thank Dr Felix Ofulue for advice on the elastase assays as well as Sandra Howard and Sandra Wong for assisting with the protein kinase C assays. We thank Barry R. Wiggs for statistical analysis. These studies were supported by a grant in aid from the B.C. and Yukon Heart and Stroke Foundation.

References

BAZZI, M.D. & BELSESTUEN, G.L. (1987). Substrate-specific stimulation of protein kinase C by polyvalent anions. *Biochem. Biophys. Res. Commun.*, **147,** 248–253.

BERKOW, R.L., DODSON, R.W. & KRAFT, A.S. (1987). The effect of protein kinase C inhibitor, H-7, on human neutrophil oxidative burst and degranulation. *J. Leuk. Biol.*, **41,** 411–446.

BERKOW, R.L., DODSON, R.W. & KRAFT, A.S. (1989). Human neutrophils contain distinct cytosolic and particulate tyrosine kinase activities: possible role in neutrophil activation. *Biochim. Biophys. Acta*, **997,** 292–301.

BERKOW, R.L. & DODSON, R.W. (1990). Tyrosine-specific protein phosphorylation during activation of human neutrophils. *Blood*, **75,** 2445–2452.

BERRIDGE, M.J. & IRVINE, R.F. (1984). Inositol trisphosphate, a novel second messenger in cellular signal transduction. *Nature*, **312,** 315–321.

BOYLE, W. (1968). An extension of the ^{51}Cr-release assay for the estimation of mouse cytotoxins. *Transplantation*, **6,** 761–764.

COOPER, J.A., GOULD, K.L., CARTWRIGHT, C.A. & HUNTER, T. (1986). Tyr527 is phosphorylated in pp60$^{c\text{-}src}$: implications for regulation. *Science*, **231,** 1431–1434.

DEWALD, B. & BAGGIOLINI, M. (1986). Platelet-activating factor as a stimulus of exocytosis in human neutrophils. *Biochem. Biophys. Acta*, **888,** 42–48.

DHAR, A., PAUL, A.K. & SHUKLA, S.D. (1990). Platelet-activating factor stimulation of tyrosine kinase and its relationship to phospholipase C in rabbit platelets: studies with genistein and monoclonal antibody to phosphotyrosine. *Mol. Pharmacol.*, **37,** 519–525.

DURONIO, V., REANY, A., WONG, S., BIGRAS, C. & SALARI, H. (1990). Characterization of platelet-activating factor receptors in porcine platelets. *Can. J. Physiol. Pharmacol.*, **68,** 1514–1519.

GAZIT, A., YAISH, P., GILON, C. & LEVITZSKI, A. (1989). Tyrphostins I: synthesis and biological activity of protein tyrosine kinase inhibitors. *J. Med. Chem.*, **32,** 2344–2352.

GEE, C.E., GRIFFIN, J., SASTRE, L., MILLER, L.J., SPRINGER, T.A., PIWNICA-WORMS, H. & ROBERTS, T.M. (1986). Differentiation of myeloid cells is accompanied by increased levels of pp60$^{c\text{-}src}$ protein and kinase activity. *Proc. Natl. Acad. Sci. U.S.A.*, **83,** 5131–5135.

GLENNY, J.,R., ZOKAS, L. & KAMPS, M.P. (1988). Monoclonal antibodies to phosphotyrosine. *J. Immunol. Meth.*, **109,** 277–285.

GOMEZ-CAMBRONERO, J., YAMAZAKI, M., METWALLY, F., MOLSKI, T.F.P., BONAK, V.A., HUANG, C.-K., BECKER, E.L. & SHA'AFI, R.I. (1989a). Granulocyte-macrophage colony-stimulating factor and human neutrophils: role of guanine nucleotide regulatory proteins. *Proc. Natl. Acad. Sci. U.S.A.*, **86,** 3569–3573.

GOMEZ-CAMBRONERO, J., HUANG, C.-K., BONAK, V.A., WANG, E., CASNELLIE, J.E., SHIRAISHI, T. & SHA'AFI, R.I. (1989b). Tyrosine phosphorylation in human neutrophil. *Biochem. Biophys. Res. Commun.*, **162,** 1478–1485.

GOMEZ-CAMBRONERO, J., WANG, E., JOHNSON, G., HUANG, C.-K. & SHA'AFI, R.I. (1991). Platelet-activating factor induces tyrosine phosphorylation in human neutrophils. *J. Biol. Chem.*, **266,** 6240–6245.

GRINSTEIN, S., FURUYA, W., LU, D.J. & MILLS, G.B. (1989). Vanadate stimulates oxygen consumption and tyrosine phosphorylation in electropermeabilized human neutrophils. *J. Biol. Chem.*, **265,** 318–327.

GUTKIND, J.S. & ROBBINS, K.C. (1989). Translocation of the FGR protein-tyrosine kinase as a consequence of neutrophil activation. *Proc. Natl. Acad. Sci. U.S.A.*, **86,** 8783–8787.

HELDIN, C.-H., BETSHOLTZ, C., CLAESSAN-WELSH, L. & WESTERMARK, B. (1987). Subversion of growth regulatory pathways in malignant transformation. *Biochim. Biophys. Acta*, **907,** 219–244.

HONDA, Z., NAKAMURA, M., MIKI, I., MINAMI, M., WATANABE, T., SEYAMA, Y., OKADO, H., TOH, H., ITO, K., MIYAMOTO, T. & SHIMIZU, T. (1991). Cloning by functional expression of platelet-activating factor receptor from guinea-pig lung. *Nature*, **349,** 342–346.

HUANG, C.-K., BONAK, V., LARAMEE, G.R. & CASNELLIE, J.E. (1990). Protein tyrosine phosphorylation in rabbit peritoneal neutrophils. *Biochem. J.*, **269,** 431–436.

IMOTO, M., UMEZAWA, K., ISSHIKI, K., KUNIMOTO, S., SAWA, T., TAKEUCHI, T. & UMEZAWA, H. (1987). Kinetic studies of tyrosine kinase inhibition by erbstatin. *J. Antibiotics*, **40,** 1471–1473.

ISSHIKI, K., IMOTO, M., SAWA, T., UMEZAWA, K., TAKEUCHI, T., UMEZAWA, H., TSUCHIDA, T., YOSHIOKA, T. & TATSUTA, K. (1987). Inhibition of tyrosine protein kinase by synthetic erbstatin analogs. *J. Antibiotics*, **40,** 1209–1210.

KORCHAK, H.M., VIENNE, K., RUTHERFORD, L.E., WELKENFELD, C., FINKELSTEIN, M.C. & WEISSMANN, G. (1984). Stimulus response coupling in the human neutrophil. II. Temporal analysis of changes in cytosolic calcium and calcium efflux. *J. Biol. Chem.*, **259,** 4076–4082.

KRAFT, A.S. & BERKOW, R.L. (1987). Tyrosine kinase and phosphotyrosine phosphatase activity in human promyelocytic leukemia cells and human polymorphonuclear leukocytes. *Blood*, **70,** 356–362.

KRAMER, I.M., VERHOEVEN, A.J., VAN DER BEND, R.L., WEENING, R.S. & ROOS, D. (1988). Purified protein kinase C phosphorylates a 47 kDa protein in control neutrophil cytoplasts but not in neutrophil cytoplasts from patients with the autosomal form of chronic granulomatous disease. *J. Biol. Chem.*, **263,** 2352–2357.

LANG, U. & VALLOTTON, M.B. (1987). Angiotensin II but not potassium induces subcellular redistribution of protein kinase C in bovine adrenal glomerulosa cells. *J. Biol. Chem.*, **262,** 8047–8050.

LEHMEYER, J.E., SNYDERMAN, R. & JOHNSON, R.B. (1979). Stimulation of neutrophil oxidative metabolism by chemotactic peptides: influence of calcium concentration and cytochalasin B and comparison with stimulation by phorbol myristate acetate. *Blood*, **54,** 35–45.

LEW, D.P., WOLLHEIM, C.B., WALDVOGEL, F.A. & POZZAN, T. (1984). Modulation of cytosolic-free calcium transients by changes in intracellular calcium-buffering capacity: correlation with exocytosis and O_2^- production in human neutrophils. *J. Cell. Biol.*, **99,** 1212–1220.

LYALL, R.M., ZILBERSTEIN, A., GAZIT, A., GILON, C., LEVITSKI, A. & SCHLESSINGER, J. (1989). Tyrphostins inhibit epidermal growth factor (EGF)-receptor tyrosine kinase activity in living cells and EGF-stimulated cell proliferation. *J. Biol. Chem.*, **264,** 14503–14509.

MARGOLIS, B.,, RHEE, S.G., FELDER, S., MERVIC, M., LYALL, R., LEVITZKI, A., ULLRICH, A., ZILBERSTEIN, A. & SCHLESSINGER, J. (1989). EGF induces tyrosine phosphorylation of phospholipase C-II: a potential mechanism for EGF receptor signaling. *Cell*, **57,** 1101–1107.

MEISENHELDER, J., SUH, P.-G., RHEE, S.G. & HUNTER, T. (1989). Phospholipase C-γ is a substrate for the PDGF and EGF receptor protein-tyrosine kinases *in vivo* and *in vitro*. *Cell*, **57,** 1109–1122.

NACCACHE, P.H., GILBERT, C., CAON, A.C., GAUDRY, M., HUANG, C.-K., BONAK, V.A., UMEZAWA, K. & MCCOLLS, S.R. (1990). Selective inhibition of human neutrophil functional responsiveness by erbstatin, an inhibitor of tyrosine protein kinase. *Blood*, **76,** 2098–2104.

NAKASHIMA, S., KOIKE, T. & NOZAWA, Y. (1991). Genistein, a protein tyrosine kinase inhibitor, inhibits thromboxane A_2 mediated human platelet responses. *Mol. Pharmacol.*, **39,** 475–480.

NASMITH, P.E., MILLS, J.B. & GRINSTEIN, S. (1989). Guanine nucleotides induce tyrosine phosporylation and activation of the respiratory burst in neutrophils. *Biochem. J.*, **257,** 893–897.

NISHIZUKA, Y. (1988). The molecular heterogeneity of protein kinase C and its implications for cellular regulation. *Nature*, **334,** 661–665.

O'FLAHERTY, J.T., SURLES, J.R., REDMAN, J., JACOBSON, D., PIANTADOSI, C. & WYKLE, R.L. (1986). Binding and metabolism of platelet-activating factor by human neutrophils. *J. Clin. Invest.*, **78,** 381–388.

PELECH, S.L., CHAREST, D.L., HOWARD, S.L., PADDON, H.B. & SALARI, H. (1990). Protein kinase C activation by platelet-activating factor is independent of enzyme translocation. *Biochim. Biophys. Acta*, **1051,** 100–107.

PIKE, M.C., JAKOI, M., MCPHAIL, L.C. & SNYDERMAN, R. (1986). Chemoattractant-mediated stimulation of the respiratory burst in human polymorphonuclear leukocytes may require appearance of protein kinase activity in the cells' particulate fraction. *Blood*, **67,** 909–913.

PULIDO, R., LACAL, P., MOLLINEDO, F. & SANCHEZ-MADRID, F. (1989). Biochemical and antigenic characterization of CD45 polypeptide expressed on plasma membrane and internal granules of human neutrophils. *FEBS Lett.*, **249,** 337–342.

ROBINSON, J.M., BADWEY, J.A., KARNOVSKY, M.L. & KARNOVSKY, M.J. (1985). Release of superoxide and change in morphology by neutrophils in response to phorbol esters: antagonism by inhibitors of calcium-binding proteins. *J. Cell. Biol.*, **101,** 1052–1058.

SALARI, H., BRAQUET, P., NACCACHE, P. & BORGEAT, P. (1985). Characterization of effect of N-formyl-methionyl-leucyl-phenylalanine on leukotriene synthesis in human polymorphonuclear leukocytes. *Inflammation*, **9,** 127–138.

SALARI, H., DURONIO, V., HOWARD, S.L., DEMOS, M., JONES, K., REANY, A., HUDSON, A.T. & PELECH, S.L. (1990a). Erbstatin blocks platelet-activating factor-induced protein-tyrosine phosphorylation, polyphosphoinositide hydrolysis, protein kinase C activation, serotonin secretion and aggregation of rabbit platelets. *FEBS Lett.*, **263,** 104–108.

SALARI, H., DURONIO, V., HOWARD, S., DEMOS, M. & PELECH, S.L. (1990b). Translocation-independent activation of protein kinase C by platelet-activating factor, thrombin and prostacyclin. *Biochem. J.*, **267,** 689–696.

SANDBERG, L.B., SOSKEL, N.T. & LESLIE, J.G. (1981). Elastin structure, biosynthesis, and relation to disease states. *N. Engl. J. Med.*, **304,** 566–579.

SHA'AFI, R.I. & MOLSKI, T.F.P. (1988). Activation of the neutrophil. *Prog. Allergy.*, **42,** 1–64.

SHECHTER, Y., YAISH, P., CHOREV, M., GILON, C., BRAUN, S. & LEVITZKI, A. (1989). Inhibition of insulin-dependent lipogenesis and anti-lipolysis by protein tyrosine kinase inhibitors. *EMBO J.*, **8,** 1671–1676.

SMITHGALL, T.E., YU, G. & GLAZER, R.I. (1988). Identification of the differentiation-associated p93 tyrosine protein kinase of HL-60 leukemic cells as the product of the human *c-fes* locus and its expression in myelomonocytic cells. *J. Biol. Chem.*, **263,** 15050–15055.

SNYDERMAN, R., SMITH, C.D. & VERGHES, E.M.W. (1986). Model for leukocyte regulation by chemoattractant receptors: roles of a guanine nucleotide regulatory protein and polyphosphoinositide metabolism. *J. Leuk. Biol.*, **40,** 785–800.

STYRT, B., SCHWARTZ, M.A. & KLEMPNER, M.S. (1987). Linkage between neutrophil degranulation and calcium discharge. *Biochem. Biophys. Res. Commun.*, **146,** 1386–1391.

TAKAHASKI, S., SEIFTER, S. & YANG, F.C. (1973). A new radioactive assay for enzymes with elastolytic activity using reduced tritiated elastin. The effect of sodium dodecyl sulfate on elastolysis. *Biochim. Biophys. Acta*, **327,** 138–145.

TAYLOR, S.J., CHAE, H.Z., RHEE, S.G. & EXTON, J.H. (1991). Activation of the β1 isozyme of phospholipase C by α subunits of the G_q class of G proteins. *Nature*, **350,** 516–518.

ULLRICH, A., COUSSENS, L., HAYFLICK, J.S., DULL, T.J., GRAY, A., TAM, A.W., LEE, J., YARDEN, Y., LIBERMANN, T.A., SCHLESSING,R J., DOWNWARD, J., MAYES, E.L.V., WHITTLE, N., WATERFIELD, M.D. & SEEBURG, P.H. (1984). Human epidermal growth factor receptor cDNA sequence and aberrant expression of the amplified gene in A431 epidermoid carcinoma cells. *Nature*, **309,** 418–425.

WAHL, M.I., OLASHAW, N.E., NISHIBE, S., RHEE, S.G., PLEDGER, W.J. & CARPENTER, G. (1989). Platelet-derived growth factor induces rapid and sustained tyrosine phosphorylation of phospholipase C-γ in quiescent BALB/c 3T3 cells. *Mol. Cell. Biol.*, **9,** 2934–2943.

WATSON, S.P., McCONNELL, R.T. & LAPETINA, E.G. (1984). The rapid formation of inositol phosphates in human platelets by thrombin is inhibited by prostacyclin. *J. Biol. Chem.*, **259,** 13199–13203.

YAISH, P., GAZIT, A., GILON, C. & LEVITZKI, A. (1988). Blocking of EGF-dependent cell proliferation by EGF receptor kinase inhibitors. *Science*, **242,** 933–935.

ZIEGLER, S.F., WILSON, C.B. & PERLMUTTER, R.M. (1988). Augmented expression of a myeloid-specific protein tyrosine kinase gene (*hck*) after macrophage activation. *J. Exp. Med.*, **168,** 1801–1810.

(Received January 30, 1992
Revised March 13, 1992
Accepted March 16, 1992)

Br. J. Pharmacol. (1992), **106**, 665–671

Prevention of intimal thickening after endothelial removal by a nonpeptide angiotensin II receptor antagonist, losartan

[1]Hiroshi Azuma, *Yasunari Niimi & Hidehisa Hamasaki

Department of Medicinal Chemistry, Institute for Medical and Dental Engineering and *Department of Neurosurgery, Faculty of Medicine, Tokyo Medical and Dental University, 2-3-10 Surugadai, Kanda, Chiyoda-ku, Tokyo 101, Japan

1 The present experiments were designed to investigate the role of local angiotensin II receptors in the myointimal proliferative response of the vascular wall after endothelial removal, by use of a novel, nonpeptide, angiotensin II receptor antagonist, losartan.

2 When administered 1 week before endothelial removal from the rabbit carotid artery and then continuously until animals were killed 6 weeks later, losartan in a dose of 10 mg kg^{-1} daily, p.o. had no significant effects on the carotid blood flow (CBF), mean arterial blood pressure (MBP) and heart rate (HR).

3 A full endothelial lining with increased density of regenerated endothelial cells was observed 6 weeks after the endothelial removal. These changes were unaffected by treatment with losartan.

4 Six weeks after endothelial removal, acetylcholine (ACh)- and adenosine diphosphate (ADP)-induced relaxations were greatly reduced though endothelial cells had regenerated. The reduction of the relaxations to these agonists were significantly restored by chronic treatment with losartan. The endothelial-independent, sodium nitroprusside (SNP)-induced relaxation remained unaffected in all groups.

5 There were no differences in the noradrenaline (NA)- and endothelin-1 (ET-1)-induced contractions of the carotid artery strips between vehicle and losartan-treated groups. In contrast, the contractile response of the strips to angiotensin II was significantly decreased in the losartan group, indicating the specific antagonism by chronic losartan against the angiotensin II receptor.

6 Six weeks after endothelial removal, marked myointimal proliferation resulting from new accumulation of proliferating smooth muscle cells and connective tissue was observed in the vehicle group. Losartan treatment greatly suppressed the myointimal proliferative response.

7 These results suggest that the local angiotensin II receptors play a role in the myointimal proliferative response of the vascular wall to removal of the endothelium.

Keywords: Intimal thickening; endothelial removal; nonpeptide angiotensin II receptor antagonist; losartan; endothelial-derived relaxing factor (EDRF); regrowth of endothelial cells

Introduction

The mechanisms causing the myointimal proliferative response of the vascular wall to removal of the endothelium are complex and poorly understood, but initially quiescent smooth muscle cells must be activated either directly by the injury or indirectly by a variety of factors. Recently, Powell *et al.* (1989) have reported that the local angiotensin system may participate in modulating the proliferation of the vascular wall after arterial injury, since inhibitors of angiotensin-converting enzyme prevent the myointimal proliferation. There has been evidence indicating that angiotensin-converting enzyme (Nakamura *et al.*, 1988), angiotensinogen mRNA (Cassis *et al.*, 1988) and angiotensin II receptors (Penit *et al.*, 1983) are involved in the vascular wall.

On the other hand, we have demonstrated that the myointimal proliferative response after endothelial removal may be brought about partly by the decreased release/production of the endothelium-derived relaxing factor (EDRF, Furchgott & Zawadzki, 1980) by the regenerated endothelial cells (Azuma *et al.*, 1990). According to Garg & Hassid (1989), the endogenous EDRF (nitric oxide, Palmer *et al.*, 1987) may function as an inhibitory modulator of vascular smooth muscle cell mitogenesis and proliferation. In addition, EDRF is an antiaggregating substance (Azuma *et al.*, 1986b; Furlong *et al.*, 1987; Radomski *et al.*, 1987) which may also modulate the release of platelet-derived growth factor.

The present experiments were designed to investigate the role of local angiotensin II receptors and endothelial cells in the vascular response to endothelial removal by use of a newly developed, orally active, nonpeptide angiotensin II receptor antagonist, losartan {2-n-butyl-4-chloro-1-[(2′-(tetrazol-5-yl)-1,1′-biphenyl-4-yl)methyl]-1H-imidazole-5-methanol, potassium salt} (Chiu *et al.*, 1990; Wong *et al.*, 1990). The agent was chronically administered p.o. to rabbits in which the right carotid artery was subjected to removal of the endothelium.

Methods

Animals

Japanese White male rabbits, 10 weeks of age, were used. These rabbits were purchased at 8 weeks of age and housed individually for 2 weeks before the experiments in a temperature (23 ± 1°C)- and humidity (50 ± 20%)-controlled room and were fed regular chow (CE-2, Japan Clea) throughout the experimental periods.

Seventeen rabbits were divided randomly into two groups consisting of 8 and 9. The body weight changes (Table 1) and general behaviour of all rabbits before and after the endothelial removal and during the administration of losartan appeared to be normal.

Administration of losartan

Losartan was dissolved in distilled water at a concentration of 0.05 mg ml^{-1} and given as a drinking water in a dose of

[1] Author for correspondence.

10 mg 200 ml^{-1} kg^{-1} daily for 7 weeks (1 week before and 6 weeks after the endothelial removal). Losartan did not influence drinking behaviour; 200 ml kg^{-1} of water was sufficient for intake of the drug and was completely consumed in a day. Rabbits given distilled water without losartan served as controls.

Endothelial removal of the carotid artery

Rabbits were anaesthetized with 25 mg kg^{-1}, i.v. of sodium pentobarbitone. An arterial embolectomy catheter (12-040-3F/40 cm/3F, American Edwards Laboratories, Santa Ana, California, U.S.A.) was inserted into the right common carotid artery through the incision made on the vessel wall, as described elsewhere (Azuma *et al.*, 1990). The intraluminal surface of the artery was then gently rubbed by means of one stroke of a balloon (filled with 0.15 ml air and approximately 2.5 mm in diameter) so as not to damage underlying smooth muscle cells and other tissues. Complete denudation of the endothelium was achieved throughout the common carotid artery as assessed by the morphological examination (scanning electron microscopy) of random controls (4 rabbits) at 2 h after the procedure. For the left carotid artery, a sham operation without the balloon was carried out and the artery of this side served as a control.

Measurement of carotid blood flow (CBF), mean arterial blood pressure (MBP) and heart rate (HR)

At 6 weeks after endothelial removal, rabbits were anaesthetized with sodium pentobarbitone (25 mg kg^{-1}, i.v.). After a midline incision in the ventral cervical region, the common carotid arteries of both sides were exposed; special care was taken not to disturb the vascular wall and the CBF was measured by means of a FR-015T probe (Nihon Kohden Kogyo Co., Tokyo) and an electromagnetic flow meter (MFV-1200, Nihon Kohden Kogyo Co.). In order to measure MBP, the right femoral artery was exposed and cannulated with polyethylene tubing filled with saline containing heparin. The other end of the tubing was connected to a pressure transducer (TP-400T, Nihon Kohden Kogyo Co.). MBP was recorded on a pen-writing oscillograph (CP-642G, Nihon Kohden Kogyo Co.) via an amplifier (AP-620G, Nihon Kohden Kogyo Co.). HR was measured with an ECG pulse counter (AC-611G, Nihon Kohden Kogyo Co.) and bioelectric amplifier (AB-620G, Nihon Kohden Kogyo Co.).

Organ chamber experiments

After measurement of CBF, MBP and HR, rabbits were exsanguinated from the femoral arteries. The common carotid arteries were rapidly excised and kept in modified Krebs solution. After removal of fat and connective tissue, a 2-mm wide transverse ring was cut off with a razor blade, and a transverse strip was made and mounted vertically in an organ bath containing 20 ml of modified Krebs solution continuously bubbled with 95% O_2 and 5% CO_2 at 37°C. Special care was taken to avoid unintentional rubbing of the intraluminal surface. Mechanical responses were measured according to the method described previously (Azuma *et al.*, 1986a,b; 1989; 1990). The composition of modified Krebs solution was as follows (mM): NaCl 115.0, KCl 4.7, $MgSO_4 \cdot 7H_2O$ 1.2, $CaCl_2 \cdot 2H_2O$ 2.5, KH_2PO_4 1.2, $NaHCO_3$ 25.0 and glucose 10.0. After 60 min of equilibration, 10^{-6} M ACh was given to all strips during contraction caused by 10^{-6} M NA to test for the presence or absence of the functional endothelial cells. After this, relaxations to ACh ($10^{-8} \sim 10^{-5}$ M), ADP ($3 \times 10^{-8} \sim 10^{-5}$ M) and sodium nitroprusside (SNP, $10^{-9} \sim 3 \times 10^{-5}$ M) were examined during a contraction caused by 10^{-6} M NA as follows: In groups a and c, responses of the control left and the previously denuded right carotid arteries prepared from rabbits given vehicle were tested, respectively. In groups b and d, responses of the control left and the previously denuded right carotid arteries prepared from rabbits given losartan were tested, respectively. Relaxations caused by ACh, ADP and SNP were given as a percentage of the 10^{-6} M NA-induced contraction. Contractions to NA ($10^{-9} \sim 3 \times 10^{-5}$ M), ET-1 ($10^{-10} \sim 3 \times 10^{-8}$ M) and angiotensin II ($10^{-10} \sim 10^{-7}$ M) in the quiescent left and the right carotid arteries prepared from rabbits which had been treated with vehicle or losartan were examined in different experiments. The E_{max} (the maximum response) and ED_{50} (the concentration producing 50% of the E_{max}) were obtained from the log concentration-response curves.

Electron microscopy

Scanning electron microscopic examinations were performed according to the methods described in a previous paper (Azuma *et al.*, 1990). The ultrastructure of the intraluminal surface was observed by means of a scanning electron microscope (ESM-3200, Elionix).

Light microscopy

Left and right carotid arteries were isolated and fixed in a 10% neutral solution of formaldehyde. The transverse specimen was embedded in paraffin after dehydration with ethanol. Thin sections were stained with haematoxylin-eosin (HE), Elastica-Van Gieson method (Weigert, 1898) or Sudan III for light microscopic analysis. The initimal thickness of the cross-sections was evaluated by measuring the area of intima and media on the picture at final magnification × 40 by means of a KP-90N planimeter (Uchida Co.). Results are expressed as a percentage of intimal area to that of medial one.

Chemicals

The following chemicals were used: acetylcholine chloride (ACh, Ovisot for injection, Daiichi Pharmaceutical Co.), indomethacin (Merck-Banyu), N^G-nitro-L-arginine (L-NNA), angiotensin II (human) and endothelin-1 (ET-1, human) (all from Protein Research Foundation), (−)-noradrenaline bitartrate (NA), adenosine 5′-diphosphate sodium salt (ADP), methylene blue and sodium nitroprusside (SNP) (all from Sigma), 2-n-butyl-4-chloro-1-[(2′-(tetrazol-5-yl)-1,1′-biphenyl-4-yl)methyl]-1H-imidazole-5-methanol, potassium salt (losartan, generous gift from Banyu Pharmaceutical Co.), which is a specific antagonist of angiotensin II receptors and is orally active (Chiu *et al.*, 1990; Wong *et al.*, 1990). All chemicals were dissolved in distilled water immediately before use except for indomethacin and L-NNA which were dissolved in dimethylsulphoxide (DMSO) and kept frozen at −20°C until use (10^{-2} M stock solution). DMSO was present in a final concentration of 0.5% in the experiments with these agents, and this concentration had no effect on any parameters tested.

Statistical analysis

All data are expressed as the mean ± s.e.mean. The statistical significance between two means was determined by Student's *t* test.

Results

Baseline data

Carotid blood flow (CBF) was not significantly different in the control left and the previously denuded right carotid arteries both in the vehicle- and the losartan-treated groups. The chronic administration of losartan in a dose of 10 mg kg^{-1} daily for 7 weeks did not affect the CBF in the arteries

of either sides. The mean arterial blood pressure (MBP) was slightly lower (approximately 10 mmHg) in the losartan group, but not significantly different from the vehicle group. There was no difference in the heart rate (HR) between the two groups. These results are shown in Table 1. Wong *et al.* (1990) have reported that a bolus oral dosing at 10 mg kg^{-1} of losartan produced marked inhibition of the angiotensin II pressor response in conscious normotensive rats, although it did not alter basal MBP and HR.

Electron microscopic findings

In the sham-operated left carotid arteries from both groups, scanning electron microscopy revealed that the endothelial cells were regularly arranged parallel to the direction of the blood stream. A representative micrograph is shown in Figure 1a. Six weeks after endothelial removal, a full endothelial lining on the intraluminal surface was observed in the previously denuded right carotid arteries both in vehicle- and losartan-treated groups. The shape, direction and type of junctions of the regenerated endothelial cells were, however, different from control arteries (Figure 1b and c).

The cell density was determined by means of scanning electron microscopy. Results are shown in Table 2. The density of regenerated endothelial cells in the right carotid artery was significantly increased compared with that of the corresponding controls, and was unaffected by the administration of losartan.

Influence of losartan on the relaxation responses

In the control left and the previously denuded right carotid artery strips, 10^{-6} M ACh and 10^{-6} M ADP produced relaxation in arteries precontracted with 10^{-6} M NA. Relaxation was abolished after deliberate denudation of the endothelial cells (complete endothelial removal without damage of the smooth muscle layer was confirmed morphologically), or greatly reduced by pretreatment with 10^{-5} M methylene blue and 10^{-5} M L-NNA, an inhibitor of EDRF synthesis (Kobayashi & Hattori, 1990), but unaffected by 10^{-5} M indomethacin (data not shown), indicating that the ACh- and ADP-induced relaxations are mediated by EDRF (Furchgott & Zawadzki, 1980), but not by prostaglandin I_2.

The concentration-dependent relaxation induced by ACh in the control left carotid artery of the vehicle-treated group did not significantly differ from that of losartan-treated group (Figure 2). The E_{max} values were estimated to be 74.4 ± 7.5% ($n = 6$) in the former and 81.8 ± 4.9% ($n = 7$) in the latter. In the right carotid artery of the vehicle-treated group 6 weeks after endothelial removal, the ACh-induced relaxation was greatly reduced although endothelial cells had regenerated. It should be noted that this reduced relaxation was significantly restored toward the control level by the chronic treatment with losartan. Similar results were obtained for ADP-induced relaxation (data not shown).

In contrast, the SNP-induced relaxation in arteries precontracted with NA remained unaffected by chronic losartan

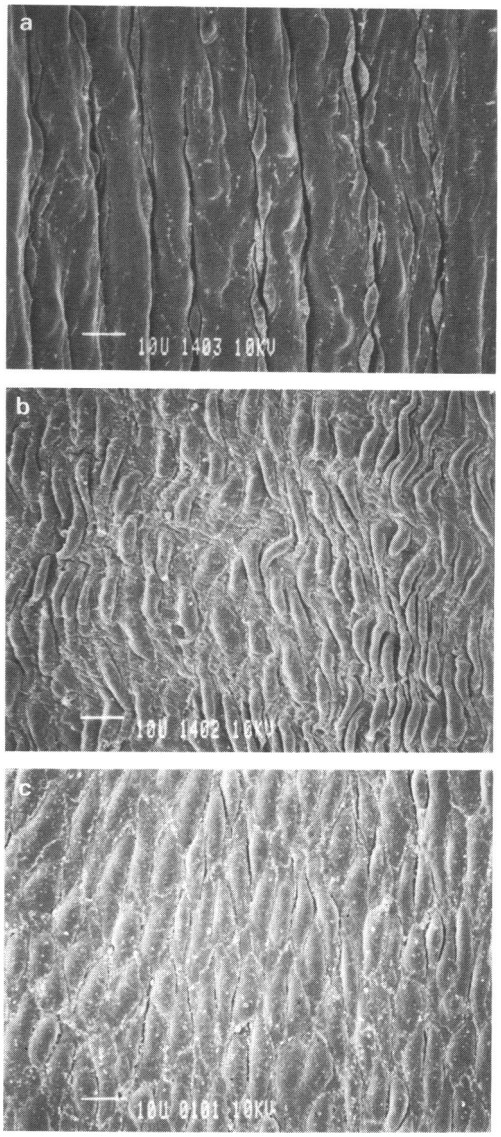

Figure 1 Scanning electron microscopic findings on the intraluminal surface of rabbit carotid arteries. (a) Normal appearance of endothelial cells in the sham-operated left carotid artery (vehicle group). The endothelial cells were regularly arranged, parallel to the direction of the blood stream. (b) (Vehicle group) and (c) (losartan group): 6 weeks after endothelial removal, the luminal surface was entirely covered with the regenerated endothelial cells, which were morphologically different from native ones and irregularly oriented. Scale bar: 10 μm.

Table 1 Baseline data on body weight (BW), carotid blood flow (CBF), mean arterial blood pressure (MBP) and heart rate (HR) of rabbits

	BW (kg)		*CBF* (ml min^{-1})			
Treatment	*1w before surgery*	*6w after surgery*	*Control side*	*Denuded side*	*MBP* (mmHg)	*HR* (beats min^{-1})
Vehicle	1.82 ± 0.08 (8)	2.61 ± 0.06 (6)	23.9 ± 2.8 (6)	20.5 ± 2.3 (6)	114.7 ± 7.0 (6)	276 ± 13 (5)
Losartan	1.85 ± 0.08 (9)	2.60 ± 0.05 (7)	21.9 ± 1.0 (6)	21.2 ± 2.2 (6)	104.0 ± 3.4 (6)	279 ± 26 (5)

Results are given as mean ± s.e.mean. Losartan was dissolved in distilled water and given as a drinking water at a dose of 10 mg 200 ml^{-1} kg^{-1} daily for 7 weeks (1 week before and 6 weeks after endothelial removal) (see text). Measurements of CBF, MBP and HR were performed under sodium pentobarbitone anaesthesia 6 weeks after the endothelial removal (immediately before the rabbits were killed) (see text). Figures in parentheses indicate the number of rabbits. In order to assess morphologically the completeness of endothelial removal, 2 rabbits each in vehicle and losartan groups were killed 2 h after the operation at week 0.

Table 2 Influence of losartan on regeneration of endothelial cells

Vessel	Treatment	Number of endothelial cells ($\times 10^3$ mm^{-2})	
Control artery	Vehicle	8.5 ± 0.7 (5)	***
	Losartan	8.1 ± 0.8 (7)	
Denuded artery	Vehicle	12.5 ± 0.2 (5)	**
	Losartan	12.0 ± 0.5 (5)	

Number of endothelial cells was determined by means of scanning electron microscopy 6 weeks after removal of endothelium from the rabbit carotid artery (see text). Six weeks after the endothelial removal, the luminal surface was entirely covered with regenerated endothelium. Results are given as mean ± s.e.mean.
*$P<0.01$ and **$P<0.005$. Figures in parentheses indicate the number of rabbits.

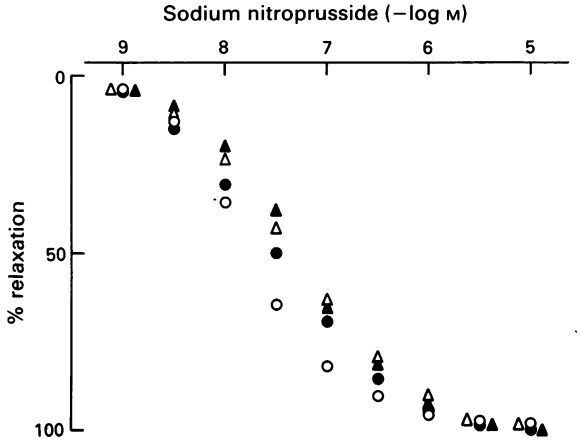

Figure 3 Comparison of endothelium-independent relaxation response of control left (△, ▲) and the prevously denuded right carotid arteries (○, ●) to sodium nitroprusside between vehicle (open symbols) and losartan (closed symbols) groups. Each point represents the mean of 5 to 7 experiments. Relaxation is given as a percentage (percent relaxation) of the 10^{-6} M noradrenaline-induced contraction.

treatment both in the control left and the previously denuded right carotid arteries (Figure 3).

Influence of losartan on contractile responses

In the control left carotid artery and the previously denuded right carotid artery, NA, ET-1 and angiotensin II produced a concentration-dependent contraction. The concentration-response curves and contraction parameters (E_{max} and ED_{50}) for each agonist, and influence of losartan administration are shown in Figure 4 and Table 3. As can be seen in Figure 4, there were no differences in the NA- and ET-1-induced contractions of the previously denuded right carotid arteries between vehicle and losartan groups. In contrast, the contractile response of the strips to angiotensin II was significantly decreased in the losartan group.

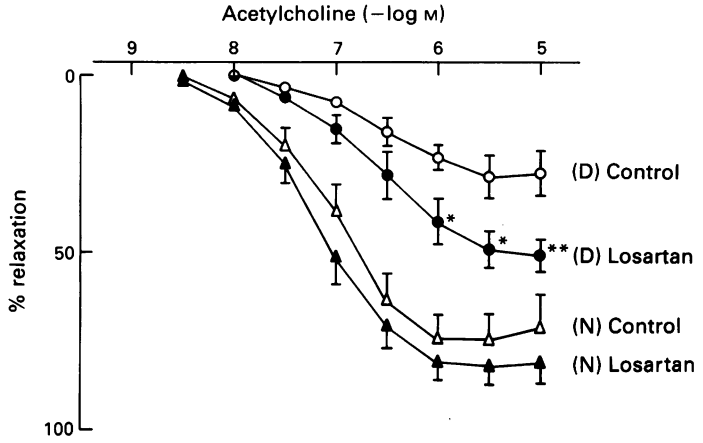

Figure 2 Comparison of endothelium-dependent relaxation response of control left (N) and previously denuded right (D) carotid arteries to acetylcholine between vehicle and losartan groups. Each point represents the mean of 6 to 7 experiments. Vertical bars show s.e.mean. Significant difference at *$P<0.05$ and **$P<0.01$ vs. the corresponding value in the denuded right carotid artery of vehicle group. Relaxation is given as a percentage (percent relaxation) of the 10^{-6} M noradrenaline-induced contraction.

Table 3 Comparison of the contractile responses of control and denuded carotid artery strips to noradrenaline, endothelin-1 and angiotensin II in vehicle and losartan-treated groups

		Noradrenaline		Endothelin-1		Angiotensin II	
Vessel	Treatment	E_{max} (mg)	ED_{50} ($\times 10^{-8}$ M)	E_{max} (mg)	ED_{50} ($\times 10^{-9}$ M)	E_{max} (mg)	ED_{50} ($\times 10^{-9}$ M)
Control artery	Vehicle	821 ± 43 (5)	2.3 ± 0.1 (5)	622 ± 26 (5)	1.8 ± 0.2 (5)	308 ± 15 (5) ***	2.0 ± 0.4 (5)
	Losartan	864 ± 97 (7) **	2.0 ± 0.2 (7)	586 ± 89 (7)	1.5 ± 0.1 (7)	* 109 ± 36 (7) ***	2.8 ± 1.2 (5)
Denuded artery	Vehicle	1108 ± 75 (5)	3.6 ± 0.8 (5)	645 ± 34 (6)	2.0 ± 0.3 (6)	450 ± 64 (6) **	2.5 ± 0.4 (6)
	Losartan	1013 ± 102 (6)	2.4 ± 0.2 (5)	649 ± 97 (7)	1.8 ± 0.2 (7)	181 ± 53 (7) **	3.2 ± 0.5 (5)

Results are given as mean ± s.e.mean. The E_{max} (maximum response) and ED_{50} (concentration to produce 50% of E_{max}) values were obtained from concentration-response curves. Figures in parentheses indicate the number of rabbits. Losartan was dissolved in distilled water and given as a drinking water at a concentration of 10 mg 200 ml^{-1} kg^{-1} daily for 7 weeks (1 week before and 6 weeks after endothelial removal) (see text). Rabbits were killed 6 weeks after the operation and carotid artery strips were prepared to analyze the mechanical responses (see text).
*$P<0.05$; **$P<0.01$ and ***$P<0.005$, respectively.

The E_{max} values for NA, ET-1 and angiotensin II were significantly higher or tended to be higher in the previously denuded right carotid artery strips than those values in the corresponding controls. The ED_{50} values, however, remained unchanged in all groups (Table 3).

Histological findings

In the sham-operated left carotid artery of the vehicle and the losartan groups, no noticiable changes could be detected (Figure 5a). Six weeks after endothelial removal, marked myointimal proliferative response resulting from new accumulation of proliferating smooth muscle cells and connective tissue was observed in the vehicle group (Figure 5b and Table 4). Losartan significantly suppressed the myointimal proliferative response to ballooning (Figure 5c and Table 4). The decreased amount of neointima appeared to reflect a reduction in all components of the intimal thickening, with fewer smooth muscle cells and less matrix formation (Figure 5c).

Discussion

Six weeks after removal of the endothelium from the rabbit carotid artery, the endothelial lining was reestablished with significantly increased density of the regenerated endothelial cells. Significant impairment of the endothelium-dependent relaxation was accompanied by myointimal proliferation. All these findings were similar to those in our previous paper (Azuma *et al.*, 1990). The exact level at which the impairment occurs is not known. It has been suggested that the site of the impairment occurs beyond the level of the receptors (Azuma *et al.*, 1990; Flavahan & Vanhoutte, 1990), but may also be due to reduction in the synthesis/release of EDRF by the regenerated endothelial cells and that the capacity to synthesize/release EDRF per cell greatly reduces, since the cell density had significantly increased over the normal (Azuma *et al.*, 1990). In addition, it is well established that EDRF is an anti-aggregating substance (Azuma *et al.*, 1986b; Furlong *et al.*, 1987; Radomski *et al.*, 1987) and it has been suggested by Garg & Hassid (1989) that endogenous EDRF (NO, Palmer *et al.*, 1987) may act as an inhibitory modulator of vascular smooth muscle cell mitogenesis and proliferation. These findings support the hypothesis that the injury or dysfunction of endothelial cells, together with resultant platelet aggregation and release of platelet products, is one of the important mechanisms of myointimal proliferative res-

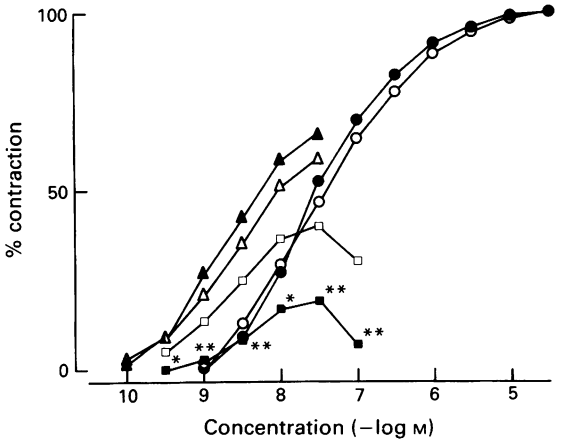

Figure 4 Comparison of contractile responses of the previously denuded right carotid artery to noradrenaline (○, ●), endothelin-1 (△, ▲) and angiotensin II (□, ■) between vehicle- (open symbols) and losartan-treated (closed symbols) groups. Each point represents the mean of 6 to 7 experiments. Significant difference at $*P<0.05$ and $**P<0.01$, respectively vs. corresponding controls. The maximum contraction (E_{max}) to 3×10^{-5} M noradrenaline was taken as 100% and determined to be 1108 ± 75 mg ($n = 6$) in the vehicle group and 1013 ± 102 mg ($n = 7$) in the losartan group.

Table 4 Influence of losartan on myointimal proliferative response to endothelial removal of right carotid artery

Treatment	*Intima/Media* (%)
Vehicle	59.4 ± 5.9 (6)
Losartan	24.9 ± 3.7 (7)***

Results are given as mean ± s.e.mean. Figures in parentheses indicate the number of rabbits. Intima/Media (%) in the sham-operated left carotid artery was estimated to be 4.7 ± 0.4 ($n = 6$).
Significantly different from vehicle group at $***P<0.005$.

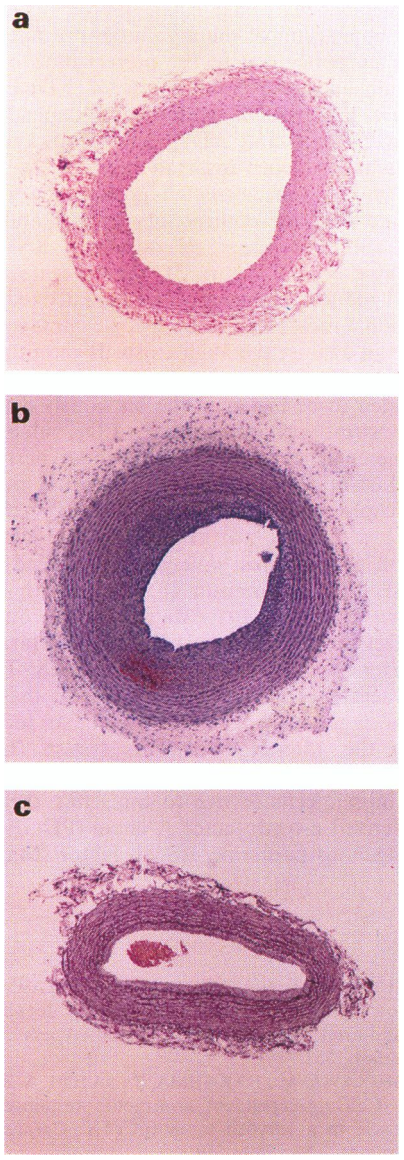

Figure 5 Light microscopic findings in rabbit carotid arteries. (a) Almost normal appearance of the cross-section of control left carotid artery (vehicle group). HE-staining (× 40). (b) Six weeks after endothelial removal, myointimal proliferation resulting from new accumulation of smooth muscle cells and connective tissue, and a slight accumulation of lipid can be observed. Sudan III -staining (× 40). (c) Less myointimal proliferation can be observed in losartan-treated group. Elastica-Van Gieson-staining (× 40).

ponse (Schwartz *et al.*, 1981; Ross, 1986).

Thus, the suppression of the myointimal proliferation with losartan may be partly due to the preservation of the endothelial function in the release/action of EDRF with this agent, because the reduced endothelium-dependent relaxations induced by ACh and ADP were significantly restored by chronic treatment with losartan (Figure 2).

Although, in the vehicle-treated group as well as in the losartan-treated one, the contractility to NA and ET-1 and the endothelium-independent relaxation to SNP remained unaltered (Table 3 and Figure 3), the exogenously applied angiotensin II-induced contraction was greatly reduced in the losartan group, indicating the specific antagonism with chronic losartan against the angiotensin II receptor. The E_{max} values for NA, ET-1 and angiotensin II were significantly higher or tended to be higher in the previously denuded right carotid artery strips without change in ED_{50} values (Table 3). We have some evidence indicating that the hyperreactivity of the thickened carotid artery may be due to the increased and sustained phosphorylation of the myosin light chain in the neointima. These results will be published elsewhere.

Studies with cell cultures have generally failed to support the hypothesis that angiotensin II is a smooth muscle cell mitogen. However, the *in vitro* data do not rule out an *in vivo* mitogenic effect for angiotensin II (Emmet & Harris-Hooker, 1986; Geisterfer *et al.*, 1988; Lyall *et al.*, 1988; Taubman *et al.*, 1989). Daemen *et al.* (1991) have shown that the mitogenic effect of angiotensin II *in vivo* may be an indirect result of activating the adrenergic nervous system (Luft *et al.*, 1989), since the α_1-adrenoceptor agonists can directly stimulate smooth muscle cells *in vivo* to transcribe the mRNA of the platelet-derived growth factor A-chain (PDGF-A) gene, a possible endogenous paracrine growth factor (Majeski *et al.*, 1990). It has also been demonstrated that angiotensin II increases the induction of ET mRNA expression and synthesis of functional ET peptide in cultured human vascular smooth muscle cells and these effects of angiotensin II are blocked by a specific receptor antagonist, [Sar^1,Ala^8]-angiotensin II (Resink *et al.*, 1990). ET is a potent mitogen and may play a potential role in the development of vascular diseases (Hirata *et al.*, 1989). Thus losartan may prevent the myointimal proliferative response through blocking angiotensin II receptors which mediate direct and indirect mitogenic effects of angiotensin II. In support of this hypothesis, Powell *et al.* (1989) have provided evidence showing that inhibitors of angiotensin-converting enzyme prevent the myointimal proliferation after vascular injury. Therefore, the present observations, taken together with observations demonstrating angiotensin-converting enzyme (Nakamura *et al.*, 1988), angiotensinogen mRNA (Cassis *et al.*, 1988) and angiotensin II receptors (Penit *et al.*, 1983) in the vascular wall, lead us to suggest that local angiotensin II receptors may play a role in the myointimal proliferative response of the vascular wall to endothelial removal.

In conclusion, the nonpeptide and specific angiotensin II receptor antagonist, losartan, may be a useful tool for investigation of the mechanisms of myointimal thickening after endothelial removal and may have therapeutic applications in preventing the proliferative response occurring after coronary angioplasty and vascular surgery.

The authors thank Dr A. Saito for light microscopy, H. Masuda for technical assistance and Banyu Pharmaceutical Co. for the generous gift of losartan.

This work was supported in part by the Suzuken Memorial Foundation and by the Smoking Research Foundation.

References

AZUMA, H., FUNAYAMA, N., KUBOTA, T. & ISHIKAWA, M. (1990). Regeneration of endothelial cells after balloon denudation of the rabbit carotid artery and changes in responsiveness. *Jpn. J. Pharmacol.*, **52**, 541–552.

AZUMA, H., ISHIKAWA, M., NAKAJIMA, T., SATOH, A. & SEKIZAKI, S. (1986a). Calcium-dependent contractile response of arterial smooth muscle to a jellyfish toxin (pCrTX: *Carybdea rastonii*). *Br. J. Pharmacol.*, **88**, 549–559.

AZUMA, H., ISHIKAWA, M. & SEKIZAKI, S. (1986b). Endothelium-dependent inhibition of platelet aggregation. *Br. J. Pharmacol.*, **88**, 411–414.

AZUMA, H., SUGIMOTO-TOKUSHIMA, M., TANAKA, K., IKENOUE, Y., ITO, S. & ISHIKAWA, M. (1989). α_1-Adrenoceptor antagonist activity of novel pyrimidine derivatives (SHI437 and IK29) in rabbit aorta and trigone of the bladder. *Br. J. Pharmacol.*, **96**, 1000–1006.

CASSIS, L.A., SAYE, J. & PEACH, M.J. (1988). Location and regulation of rat angiotensinogen messenger RNA. *Hypertension*, **11**, 591–596.

CHIU, A.T., MCCALL, D.E., PRICE, W.A., WONG, P.C., CARINI, D.J., DUNCIA, J.V., WEXLER, R.R., YOO, S.E., JOHNSON, A.L. & TIMMERMANS, P.B.M.W.M. (1990). Nonpeptide angiotensin II receptor antagonists. VII. Cellular and biochemical pharmacology of DuP753, an orally active antihypertensive agent. *J. Pharmacol. Exp. Ther.*, **252**, 711–718.

DAEMEN, M.J.A.P., LOMBARDI, D.M., BOSMAN, F.T. & SCHWARTZ, S.M. (1991). Angiotensin II induces smooth muscle cell proliferation in the normal and injured rat arterial wall. *Circ. Res.*, **68**, 450–456.

EMMET, N. & HARRIS-HOOKER, S. (1986). The inhibition of cultured smooth muscle cell growth by saralasin (abstract). *Fed. Proc.*, **45**, 58.

FLAVAHAN, N.A. & VANHOUTTE, P.M. (1990). G-proteins and endothelial response. *Blood Vessels*, **27**, 218–229.

FURCHGOTT, R.F. (1983). Role of endothelium in responses of vascular smooth muscle. *Circ. Res.*, **53**, 557–573.

FURCHGOTT, R.F. & ZAWADZKI, J.V. (1980). The obligatory role of endothelial cells in the relaxation of arterial smooth muscle by acetylcholine. *Nature*, **288**, 373–376.

FURLONG, B., HENDERSON, A.H., LEWIS, M.J. & SMITH, J.A. (1987). Endothelium-derived relaxing factor inhibits *in vitro* platelet aggregation. *Br. J. Pharmacol.*, **90**, 687–692.

GARG, U.C. & HASSID, A. (1989). Nitric oxide-generating vasodilators and 8-bromo-cyclic guanosine monophosphate inhibit mitogenesis and proliferation of cultured rat vascular smooth muscle cells. *J. Clin. Invest.*, **83**, 1774–1777.

GEISTERFER, A.T.T., PEACH, M.J. & OWENCE, G.K. (1988). Angiotensin II induces hypertrophy, not hyperplasia, of cultured smooth muscle cells. *Circ. Res.*, **62**, 749–756.

HIRATA, Y., TAKAGI, Y., FUKUDA, Y. & MARUMO, F. (1989). Endothelin is a potent mitogen for rat vascular smooth muscle cells. *Arteriosclerosis*, **78**, 225–228.

KOBAYASHI, Y. & HATTORI, K. (1990). Nitroaginine inhibits endothelium-derived relaxation. *Jpn. J. Pharmacol.*, **52**, 167–169.

LUFT, F.C., WILCOX, C.S., UNGER, T., KUEHN, R., DEMMERT, G., ROHMEISS, P., GANTEN, D. & STERZEL, R.B. (1989). Angiotensin-induced hypertension in the rat. *Hypertension*, **14**, 396–403.

LYALL, F., MORTON, J.J., LEVER, A.F. & GRAGOE, E.J. (1988). Angiotensin II activates Na^+-H^+ exchange and stimulates growth in cultured vascular smooth muscle cells. *J. Hypertens.*, **6**, S348–S441.

MAJESKI, M.W., DAEMEN, M.J.A.P. & SCHWARTZ, S.M. (1990). Alpha-one adrenergic stimulation of platelet-derived growth factor A-chain (PDGF-A) gene expression in rat aorta. *J. Biol. Chem.*, **265**, 1082–1088.

NAKAMURA, Y., NAKAMURA, K., MATSUKURA, T. & NAKAMURA, K. (1988). Vascular angiotensin converting enzyme activity in spontaneously hypertensive rats and its inhibition with cilazapril. *J. Hypertens.*, **6**, 105–110.

PALMER, R.M.J., FERRIGE, A.G. & MONCADA, S. (1987). Nitric oxide accounts for the biological activity of endothelium-derived relaxing factor. *Nature*, **327**, 524–526.

PENIT, J., FAURE, M. & JARD, S. (1983). Vasopressin and angiotensin II receptors in rat aortic smooth muscle cells in culture. *Am. J. Physiol.*, **244**, E72–E82.

POWELL, J.S., CLOZEL, J.-P., MULLER, R.K.M., KUHN, H., HEFTI, F., HOSANG, M. & BAUMGARTNER, H.R. (1989). Inhibitors of angiotensin-converting enzyme prevent myointimal proliferation after vascular injury. *Science*, **245**, 186–188.

RADOMSKI, M.W., PALMER, R.M.J. & MONCADA, S. (1987). The antiaggregating properties of vascular endothelium: interaction between prostacyclin and nitric oxide. *Br. J. Pharmacol.*, **92**, 639–646.

RESINK, T.J., HAHN, A.W.A., SCOTT-BURDEN, T., POWELL, J., WEBER, E. & BUHLER, F. (1990). Inducible endothelin mRNA expression and peptide secretion in cultured human vascular smooth muscle cells. *Biochem. Biophys. Res. Commun.*, **168**, 1303–1310.

ROSS, R. (1986). The pathogenesis of atherosclerosis – an update. *N. Engl. J. Med.*, **314**, 488–500.

SCHWARTZ, S.M., GAJDUSEK, C.M. & SELDEN, S.C. (1981). Vascular wall growth control: The role of the endothelium. *Arteriosclerosis*, **1**, 107–171.

TAUBMAN, M.B., BERK, B.C., IZUMO, S., TSUDA, T., ALEXANDER, W. & NADAL-GINARD, B. (1989). Angiotensin II induces c-fos mRNA in aortic smooth muscle. *J. Biol. Chem.*, **264**, 526–530.

WEIGERT, C. (1898). Uber eine Methode zur Farbung elastischer Fasern. *Zbl. Allg. Path. Anat.*, **9**, 289–292.

WONG, P.C., PRICE, W.A., CHIU, A.T., DUNCIA, J.V., CARINI, D.J., WEXLER, R.R., JOHNSON, A.L. & TIMMERMANS, P.B.M.W.M. (1990). Nonpeptide angiotensin II receptor antagonist. VIII. Characterization of functional antagonism displayed by DuP 753, an orally active anithypertensive agent. *J. Pharmacol. Exp. Ther.*, **252**, 719–725.

(Received December 16, 1991
Revised February 7, 1992
Accepted March 19, 1992)

Br. J. Pharmacol. (1992), **106**, 672–676

Characterization of muscarinic receptors that mediate contraction of guinea-pig isolated trachea to choline esters: effect of removing epithelium

[1]Keith J. Morrison & Paul M. Vanhoutte

Center for Experimental Therapeutics, Baylor College of Medicine, One Baylor Plaza, Houston TX 77030, U.S.A.

1 The muscarinic receptor subtype that mediates contraction of guinea-pig trachea, in the presence and absence of epithelium, to acetic and carbamic acid choline esters was determined by use of preferential muscarinic receptor antagonists: pirenzepine (M_1 receptor), methoctramine (M_2 receptor) and 4-diphenylacetoxy-N-methylpiperidine (4-DAMP) (M_3 receptor).

2 Acetylcholine (ACh), methacholine (MeCh), carbachol (CCh), bethanechol (BeCh) and oxotremorine induced concentration-dependent contraction of guinea-pig isolated tracheal strips in the presence and absence of epithelium. Contraction to acetic choline esters (ACh and MeCh) was augmented by removal of the epithelium, whereas contraction to carbamic acid choline esters (CCh and BeCh) and oxotremorine was not influenced by removal of the epithelium.

3 Pirenzepine, methoctramine and 4-DAMP caused parallel rightward displacements of the concentration-contraction curves to the muscarinic agonists. The pA_2 values (determined from Arunlakshana-Schild graphs) for pirenzepine and 4-DAMP in guinea-pig trachea in the presence of epithelium were: ACh as the agonist, 7.6 and 9.0, respectively; CCh as the agonist, 7.6 and 9.1, respectively. The apparent pK_B values for methoctramine with the same system were: ACh as the agonist, 5.6; CCh as the agonist, 5.6. Similar values were obtained with MeCh, BeCh and oxotremorine as the agonists. These values were agonist- and epithelium-independent.

4 It is concluded from the pA_2 and apparent pK_B values obtained for the muscarinic receptor antagonists used in this study that contraction of guinea-pig isolated trachea, with and without epithelium, to both acetic and carbamic acid choline esters is mediated via the muscarinic M_3 receptor subtype. Differential contractile responses of guinea-pig trachea to acetic and carbamic acid choline esters upon the mechanical removal of the epithelium may not be explained by activation of different muscarinic receptor subtypes by these agonists.

Keywords: Trachea; choline esters; epithelium; muscarinic receptors

Introduction

The responsiveness of airway smooth muscle preparations to various stimuli *in vitro*, may be modulated by the presence of a functional epithelium (Barnes *et al.*, 1985; Flavahan *et al.*, 1985; for reviews see Fedan *et al.*, 1988; Goldie *et al.*, 1990; Morrison *et al.*, 1990). Contraction of guinea-pig trachea to acetic choline esters, e.g. acetylcholine (ACh), which is the endogenous cholinergic transmitter, and methacholine (MeCh), but not to the carbamic acid derivatives, e.g. carbachol (CCh) and bethanechol (BeCh), is augmented by the mechanical removal of the epithelium (Goldie *et al.*, 1986; Hay *et al.*, 1986; Holroyde, 1986; Tschirhart *et al.*, 1987; Small *et al.*, 1990). This has suggested that acetic, but not carbamic acid choline esters, may stimulate the release of epithelium-derived relaxing factor (s) (EpDRF (s)) that depress tracheal tone (Goldie *et al.*, 1990). However, both ACh and CCh stimulate the release of a substance (s) from tracheal epithelium that relaxes vascular smooth muscle in the co-axial bioassay preparation (Ilhan & Sahin, 1986; Fernandes & Goldie, 1990). Furthermore, contraction of guinea-pig tracheal strips, denuded of epithelium, to CCh is diminished when this tissue is surrounded by an intact tracheal segment (Guc *et al.*, 1988a). Therefore, the differential contractile responses of guinea-pig trachea, in the presence and absence of epithelium, to acetic and carbamic acid choline esters may be due to a mechanism (s) other than differences in the abilities of these cholinoceptor agonists to stimulate the release of a relaxing substance (s) from the epithelium.

Choline esters induce contraction of the guinea-pig trachea and the release of a relaxing substance (s) from the epithelium via the stimulation of muscarinic receptors since these responses are sensitive to atropine (Eglen & Whiting, 1988; Guc *et al.*, 1988b; Fernandes *et al.*, 1989). Muscarinic receptors have been classified, from functional studies, into three major subtypes which are present in the airways: M_1, M_2 and M_3 receptors (Barnes *et al.*, 1988). Both M_1 and M_2 muscarinic receptors may be involved in the epithelial control of smooth muscle tone in response to cholinoceptor agonists in the rabbit trachea (Lev *et al.*, 1990). The aim of the present study was to determine the role of muscarinic receptors in the modulation of smooth muscle reactivity to choline esters by the epithelium in guinea-pig trachea. This study used preferential receptor antagonists to characterize the muscarinic receptor subtypes in this preparation.

Methods

Preparation of tracheal strips

Male, Hartley guinea-pigs (350–500 g) were anaesthetized with sodium pentobarbitone (60 mg kg^{-1}, i.p.) and killed by exsanguination. The trachea was excised and placed in cold physiological salt solution of the following composition (mM): NaCl 118.3, KCl 4.7, $CaCl_2$ 2.5, $MgSO_4$ 1.2, KH_2PO_4 1.2, $NaHCO_3$ 25.0, calcium disodium edetate 0.026, and glucose 11.1 Fat and connective tissue were cleaned from the trachea and paired rings (2 cartilage rings wide) were prepared. In one ring of each pair, the epithelium was removed

[1] Author for correspondence.

by inserting the tips of a watchmaker's forceps into the lumen and rolling the tissue gently over a saline-soaked filter paper. Transverse strips were then prepared from each ring by making a longitudinal cut along the ventral surface of the cartilage. The successful removal of the epithelium was confirmed by histological examination of the luminal surfaces of the tissues at the end of preliminary experiments (e.g. Flavahan *et al.*, 1988). Tracheal strips were suspended between two stainless steel wire hooks, under a resting load of 500 mg (e.g. Tucker *et al.*, 1990), in organ chambers containing 25 ml of physiological salt solution, maintained at 37°C, and gassed with a mixture of 95% O_2:5% CO_2 (pH 7.4). Tissues were connected to a strain gauge (Statham Gould UC2) for recording isometric tension and allowed to equilibrate for 45 min with regular washing before the start of experiments.

Materials

The following drugs were used: acetylcholine chloride; acetyl-β-methyl choline chloride (methacholine); carbamylcholine chloride (carbachol); carbamyl-β-methylcholine chloride (bethanechol); eserine sulphate (physostigmine); indomethacin; oxotremorine sesquifumarate and pirenzepine dihydrochloride (Sigma Chemical Company, St Louis, MO, U.S.A.); hexamethonium bromide (K & K Laboratories, Incorporated, Plainview, NY, U.S.A.); 4-diphenylacetoxy-N-methylpiperidine methiodide (4-DAMP) and methoctramine 4-hydrochloride (Research Biochemicals Incorporated, Natick, MA, U.S.A.). Most drugs were prepared daily in distilled water, kept on ice and added to organ chambers in volumes not exceeding 250 μl. Indomethacin was prepared with an equimolar concentration of Na_2CO_3. Concentrations of drugs were expressed as the final organ chamber concentrations (M).

Experimental protocol

All experiments were conducted in the presence of physostigmine (0.1 μM; an inhibitor of acetylcholinesterase) and hexamethonium (1 mM; a ganglionic nicotinic receptor antagonist). Tissues, with and without epithelium, were contracted with ACh (100 μM), followed by a washout period of 30 min. Absolute contraction to ACh was not affected significantly by removal of the epithelium (e.g. with epithelium: 483.3 ± 35.3 mg; without epithelium: 440.0 ± 42.5 mg; $n = 6$). Subsequent contraction to agonists was expressed as a percent of the contraction to ACh (100 μM) since this concentration of ACh was equi-effective in the presence or absence of epithelium. Tracheal strips were then incubated with either pirenzepine (0.03–1 μM), methoctramine (3 and 30 μM), or 4-DAMP (1–30 nM) for 30 min. Control and treated tissues were studied in parallel. Cumulative concentration-response curves for ACh, CCh, MeCh (0.01–100 μM), BeCh (0.01 μM–1 mM) and oxotremorine (1 nM–30 μM) were then obtained. One concentration-response curve was obtained from each tissue.

pA_2 values (estimates of the equilibrium dissociation constants) for pirenzepine and 4-DAMP were determined from graphs of log concentration-ratios minus 1 (CR-1) versus log concentration of antagonist (Arunlakshana & Schild, 1959). The concentration-ratio is defined as the concentration of agonist required to induce a 50% maximal contraction (EC_{50}) in the presence of the antagonist, divided by the agonist EC_{50} value in the absence of antagonist. The slopes and intercepts on the abscissae of the Arunlakshana-Schild graphs were determined by linear regression (Statview II, Berkeley, CA, U.S.A.). Since only 2 concentrations of methoctramine were used, pA_2 values for this antagonist could not be determined from Arunlakshana-Schild graphs. Apparent pK_B values (equivalent to the negative logarithm of the dissociation constant) for methoctramine at each concentration were calculated by single point analysis using the formulae:

$$K_B = \frac{\text{Concentration of methoctramine}}{\text{Concentration ratio-1}}$$

$$pK_B = -\log K_B$$

(Furchgott, 1972)

Analysis of data

Results are expressed as mean ± s.e.mean. All n values refer to the number of animals. For single comparisons within or between groups, Student's paired or unpaired t test was used. For multiple comparisons between groups, one-way analysis of variance was used and where significance was indicated, Scheffe's test (Scheffe, 1959) was applied. Statistical significance was accepted at P values of less than 0.05.

Results

ACh, MeCh, CCh (0.01–100 μM), BeCh (0.01 μM–1 mM) and oxotremorine (1 nM–30 μM) induced concentration-dependent contraction of guinea-pig tracheal strips. Contraction induced by ACh (Figure 1a) and MeCh was augmented by removal of the epithelium whereas contraction to CCh (Figure 1b), BeCh and oxotremorine was not influenced by the presence or absence of the epithelium (Table 1). The maximal responses to each agonist, in the presence and absence of epithelium, were not significantly different (Table 1).

Indomethacin (5 μM) caused a small, leftward and parallel displacement of the concentration-response curves for ACh and CCh both in the presence and absence of epithelium. There was no significant change in the maximal responses induced by these agonists. Indomethacin did not abolish the augmentation of contraction to ACh upon denudation of the epithelium (Table 1).

Pirenzepine (0.03–1 μM), methoctramine (3 and 30 μM), and 4-DAMP (1–30 nM) caused parallel rightward displacements of the concentration-response curves (at the linear portion of the curves) to ACh, MeCh, CCh, BeCh and oxotremorine with no significant changes in the maximal contraction of the tissues, both in the presence and absence of epithelium. The effects of 4-DAMP on contraction induced by ACh or CCh, in the presence and absence of epithelium, are shown in Figures 2 and 3, respectively. 4-DAMP caused concentration-dependent parallel rightward displacements of the concentration-response curves for ACh and CCh. The concentration-ratio shifts (CR) induced by 4-DAMP (1 nM, 10 nM and 30 nM) were, respectively: ACh as the agonist, 2, 8 and 20 with epithelium and 2, 14 and 22 without epithelium; CCh as the agonist, 2, 10 and 19 with epithelium and 2, 7 and 16 without epithelium.

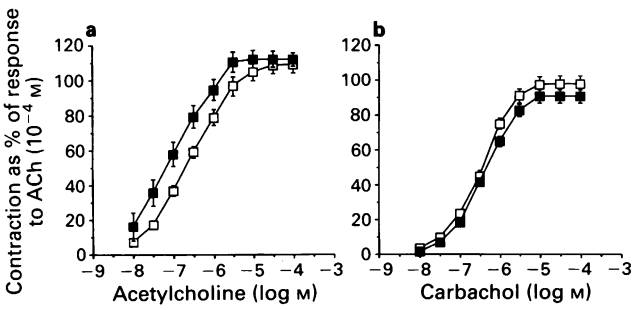

Figure 1 Concentration-response curves for acetylcholine (ACh, a) and carbachol (b) in guinea-pig trachea in the presence (□) and absence (■) of epithelium. Results are shown as mean values (with s.e.mean indicated by vertical bars) and are expressed as a percentage of the contraction to ACh (100 μM). $n = 6$.

Table 1 Responses of guinea-pig trachea to muscarinic agonists

Agonist	$-\log$ M EC_{50} with epithelium	$-\log$ M EC_{50} without epithelium	Maximal response with epithelium	Maximal response without epithelium
ACh	6.61 ± 0.05	7.04 ± 0.06*	109.2 ± 4.7	110 ± 6.2
ACh + indomethacin	6.88 ± 0.05	7.17 ± 0.05*	105.8 ± 3.3	120.5 ± 10.6
MeCh	6.49 ± 0.04	6.75 ± 0.05*	98.3 ± 5.2	96.3 ± 6.3
CCh	6.38 ± 0.05	6.41 ± 0.07	97.0 ± 7.1	94.0 ± 4.5
CCh + indomethacin	6.55 ± 0.09	6.76 ± 0.06	129.8 ± 12.6	118.3 ± 8.8
BeCh	5.05 ± 0.15	5.09 ± 0.12	106.3 ± 6.1	113.9 ± 7.5
Oxotremorine	6.85 ± 0.06	6.91 ± 0.03	102.5 ± 7.3	97.9 ± 7.1

Results are expressed as mean ± s.e.mean. $n = 5$–6. ACh: acetylcholine; MeCh: methacholine; CCh: carbachol; BeCh: bethanechol. *Values are significantly different from tissues with epithelium.
Maximal response is expressed as percentage of the contraction to ACh (100 μM).

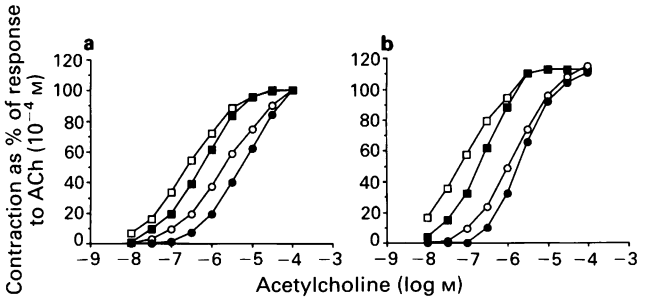

Figure 2 Effect of 4-diphenylacetoxy-N-methylpiperidine (4-DAMP, 1–30 nM) on contraction to acetylcholine (ACh) in guinea-pig trachea in the presence (a) and absence (b) of epithelium. Responses of control tissues (□) and effects of 4-DAMP 1 nM (■), 10 nM (○), and 30 nM (●) are shown. Results are shown as mean values and are expressed as a percentage of the contraction to ACh (100 μM). Error bars (s.e.mean) are omitted for clarity but did not exceed 10%. $n = 5$.

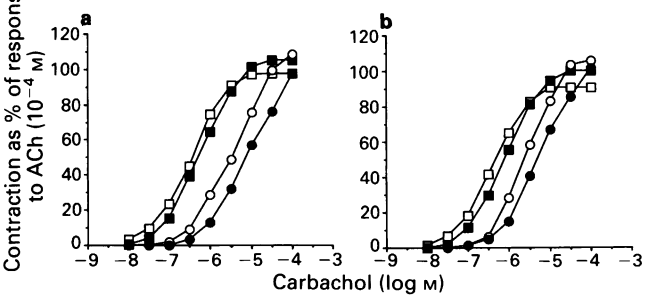

Figure 3 Effect of 4-diphenylacetoxy-N-methylpiperidine (4-DAMP, 1–30 nM) on contraction to carbachol in guinea-pig trachea in the presence (a) and absence (b) of epithelium. Responses of control tissues (□) and effects of 4-DAMP 1 nM (■), 10 nM (○), and 30 nM (●) are shown. Results are shown as mean values and are expressed as a percentage of the contraction to ACh (100 μM). Error bars (s.e.mean) are omitted for clarity but did not exceed 10%. $n = 5$.

The pA_2 values for pirenzepine and 4-DAMP (Table 2) and the apparent pK_B values for methoctramine (Table 3) did not differ significantly with the muscarinic agonist chosen for study, nor by removal of the epithelium. The values of log (CR − 1) plotted on the Arunlakshana-Schild graphs for 4-DAMP versus ACh or CCh, in the presence and absence of epithelium, were not significantly different (Figure 4). Furthermore, the slopes of the Arunlakshana-Schild plots for pirenzepine and 4-DAMP versus each agonist did not differ significantly from unity (Table 2).

Table 2 Summary of pA_2 values for muscarinic antagonists in guinea-pig trachea

Agonist	Antagonist: Pirenzepine	Antagonist: 4-DAMP
Acetylcholine with epithelium	7.6 ± 0.09 (0.84)	9.0 ± 0.06 (0.80)
Acetylcholine without epithelium	7.5 ± 0.08 (0.83)	9.0 ± 0.05 (0.90)
Methacholine with epithelium	7.4 ± 0.07 (0.84)	8.8 ± 0.05 (0.98)
Methacholine without epithelium	7.5 ± 0.06 (0.91)	9.0 ± 0.08 (0.89)
Carbachol with epithelium	7.6 ± 0.05 (0.91)	9.1 ± 0.06 (0.89)
Carbachol without epithelium	7.6 ± 0.10 (0.80)	9.1 ± 0.07 (0.79)
Bethanechol with epithelium	7.4 ± 0.06 (0.77)	8.9 ± 0.05 (0.90)
Bethanechol without epithelium	7.6 ± 0.09 (1.18)	8.8 ± 0.07 (0.88)
Oxotremorine with epithelium	7.7 ± 0.07 (0.97)	8.9 ± 0.04 (0.88)
Oxotremorine without epithelium	7.8 ± 0.04 (0.75)	9.0 ± 0.03 (0.80)

Results are shown as mean ± s.e.mean. $n = 4$–6. 4-DAMP: 4-diphenylacetoxy-N-methylpiperidine.
Values in parentheses are the slopes of the Arunlakshana-Schild graphs, and are not significantly different from unity.

Discussion

This study used preferential muscarinic receptor antagonists to characterize the muscarinic receptor subtypes that mediate contraction of guinea-pig tracheal strips to acetic and carbamic acid choline esters in the presence and absence of epithelium.

In guinea-pig trachea, muscarinic M_3 receptors are located on the smooth muscle cells (Mak & Barnes, 1990). However, muscarinic receptors may also be present on epithelial cells since atropine prevents the release of a relaxing substance (s) from the epithelium in response to choline esters in the co-axial bioassay assembly (Ilhan & Sahin, 1986; Guc *et al.*, 1988b; Fernandes *et al.*, 1989).

Contraction of tracheal strips to the cholinergic transmitter, ACh and its methyl derivative, MeCh, was augmented by removal of the epithelium. However, contraction to the carbamic acid choline esters CCh and BeCh, was not altered by the presence of the epithelium. This confirms previous findings and demonstrates that contraction of guinea-pig trachea to acetic, but not carbamic acid choline esters is

Table 3 Summary of apparent pK_B values for methoctramine in guinea-pig trachea

Agonist	*pK_B methoctramine 3 μM*	*pK_B methoctramine 30 μM*
ACh	5.5 ± 0.12	5.7 ± 0.10
with epithelium		
without epithelium	5.2 ± 0.11	5.2 ± 0.12
MeCh	4.9 ± 0.11	5.3 ± 0.07
with epithelium		
without epithelium	5.0 ± 0.14	5.5 ± 0.05
CCh	5.7 ± 0.08	5.6 ± 0.06
with epithelium		
without epithelium	5.6 ± 0.04	5.4 ± 0.06
BeCh	5.8 ± 0.05	5.5 ± 0.06
with epithelium		
without epithelium	5.6 ± 0.04	5.4 ± 0.06
Oxotremorine	5.7 ± 0.03	5.7 ± 0.04
with epithelium		
without epithelium	5.5 ± 0.06	5.6 ± 0.03

ACh: acetylcholine; MeCh: methacholine; CCh: carbachol; BeCh: bethanechol.
Results are shown as − log M and are expressed as mean ± s.e.mean. $n = 4-6$.

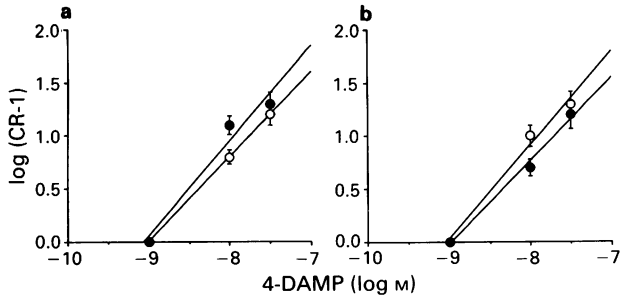

Figure 4 Arunlakshana-Schild graphs for 4-diphenylacetoxy-N-methylpiperidine (4-DAMP) versus acetylcholine (a) or carbachol, (b) in guinea-pig trachea in the presence (○) and absence (●) of epithelium. Results are shown as mean with s.e.mean indicated by vertical bars. $n = 5$.

modulated by the presence of a functional epithelium (Goldie *et al.*, 1986; Hay *et al.*, 1986; Holroyde 1986; Tschirhart *et al.*, 1987; Small *et al.*, 1990).

Pirenzepine, methoctramine and 4-DAMP caused concentration-dependent parallel rightward displacements of the concentration-contraction curves for each cholinoceptor agonist that was studied, suggesting competitive antagonism at the muscarinic receptors. This is emphasized by the facts that: (a) the slopes of the Arunlakshana-Schild graphs for pirenzepine and 4-DAMP were not significantly different from unity (Arunlakshana & Schild, 1959); and (b) the apparent pK_B values for methoctramine were not significantly different from each other at the two concentrations used (Kenakin, 1984). The pA_2 values obtained for pirenzepine and 4-DAMP, and the apparent pK_B values calculated for methoctramine are consistent with muscarinic M_3 receptors mediating contraction of guinea-pig trachea to choline esters, in the presence and absence of epithelium (Eglen & Whiting, 1988). The apparent affinities of the receptor antagonists for muscarinic receptors were not influenced by the cholinoceptor agonist chosen for study. Furthermore, these affinity values were not altered significantly by removal of the epithelium. It appears from these results, therefore, that contraction of guinea-pig trachea in the presence and absence of epithelium in response to acetic and carbamic acid choline esters and oxotremorine is mediated via muscarinic M_3 receptors. This is consistent with other findings (Eglen *et al.*, 1991).

The augmentation of contraction of airway smooth muscle preparations to various agonists upon removal of the epithelium has suggested that it is stimulated release of a non-prostanoid EpDRF (s) that depresses muscle tone (Barnes *et al.*, 1985; Flavahan *et al.*, 1985). The evaluation of antagonist potency in the present experiments was conducted in the absence of indomethacin and therefore, the involvement of epithelium-derived relaxant prostanoids in the modulation of smooth muscle tone cannot be excluded. The effect of removing the epithelium on contraction to ACh may be mimicked by indomethacin in intact guinea-pig tracheal strips (Hay *et al.*, 1986). Also, indomethacin can impair the augmentation of contraction to acetic choline esters in this preparation (Eglen *et al.*, 1991). In contrast, several studies have demonstrated that augmentation of contraction of guinea-pig trachea to ACh and MCh upon removal of the epithelium is not impaired by indomethacin (e.g. Holroyde, 1986; Murlas, 1986). Furthermore, in the present study, inhibition of cyclooxygenase by indomethacin caused a small parallel leftward displacement of the concentration-response curves to both ACh and CCh in the presence and absence of epithelium. However, the augmentation of contraction to ACh upon denudation of the epithelium was not inhibited by indomethacin. These results suggest that the putative EpDRF(s) may not be a prostanoid. The release of EpDRF(s) from the same tissue induced by muscarinic receptor agonists in the co-axial bioassay system is insensitive to indomethacin (Guc *et al.*, 1988b; Fernandes *et al.*, 1989; Eglen *et al.*, 1991). Although the release of prostanoid and non-prostanoid epithelium-derived relaxing substances was not measured in this study, the results obtained are consistent with the proposal that the release of EpDRF(s) induced by both acetic and carbamic acid choline esters from the epithelium of guinea-pig trachea is mediated via muscarinic M_3 receptors (Eglen *et al.*, 1991). However, it must be recognised that the relaxing substance (s) that is detected in the co-axial bioassay assembly, may be distinct from the putative EpDRF(s) that may modulate airway smooth muscle tone (Goldie *et al.*, 1990). Failure to observe a modulatory effect of the epithelium on contraction to carbamic acid choline esters in tracheal strips suspended in conventional organ chambers does not imply that CCh cannot stimulate the release of EpDRF(s). CCh may induce the release of EpDRF(s) that is detected by tracheal strips denuded of epithelium in the co-axial bioassay preparation (Guc *et al.*, 1988a).

The differential contractile responses of guinea-pig trachea to acetic and carbamic acid choline esters upon removal of the epithelium may be explained by differences in the abilities of these choline esters to diffuse to the muscarinic receptor sites in the tracheal model used in this and other studies. It is clear that the epithelium functions as a barrier to the diffusion of various bronchoactive agents (Boucher *et al.*, 1978; 1981; Nadel *et al.*, 1985; Weibel, 1985; Holroyde, 1986; Undem *et al.*, 1988). Indeed, contraction of perfused tracheal segments to CCh was augmented by removal of the epithelium when this agonist was applied exclusively to the luminal surface (Small *et al.*, 1990). The present experiments were performed under apparent equilibrium conditions since the slopes of the Arunlakshana-Schild graphs were not significantly different from unity, and similar pA_2 and apparent pK_B values were calculated for the receptor antagonists in the presence and absence of epithelium (Arunlakshana & Schild, 1959). This suggests that the two classes of choline ester had equal access to the muscarinic receptor population in the guinea-pig tracheal strip preparation (Kenakin, 1984). Alternatively, if the epithelium functioned as a non-saturable barrier over the full range of agonist concentrations, then parallel rightward shifts in the agonist concentration-effect curves would be obtained in response to the muscarinic antagonists. Thus, these antagonists would exhibit competitive antagonism and the Arunlakshana-Schild plots

would yield slopes of unity. However, if the barrier capability of the epithelium became saturated at higher concentrations of agonists, then the equilibrium state of the agonist, antagonist and receptor population would be changed and the slope of the Arunlakshana-Schild plot would be less than unity (Kenakin, 1984). Therefore, the present results are consistent with the epithelium behaving as a non-saturable diffusion barrier. The relative contributions of the epithelium as a diffusion barrier and source of EpDRF(s) to the regulation of tracheal smooth muscle tone, cannot be determined from the results of this study.

Differences in the susceptibilities of cholinoceptor agonists to hydrolysis by cholinesterase may also explain the differential contractile responses to acetic and carbamic acid choline esters in guinea-pig trachea. However, cholinesterase activity does not account for the augmented contractions to cholinoceptor agonists upon removal of the epithelium in this tissue (Small *et al.*, 1990). Furthermore, the present experiments were conducted in the presence of physostigmine (0.1 μM), an inhibitor of cholinesterase, and augmentation of contraction to acetic choline esters was still observed.

The present study demonstrates that contraction of guinea-pig trachea, in the presence and absence of epithelium, to both acetic and carbamic acid choline esters is mediated by muscarinic M_3 receptors. This suggests that the differential contractile responses of guinea-pig trachea to acetic and carbamic acid choline esters upon removal of the epithelium, may not be explained by activation of different muscarinic receptor subtypes.

This work was supported in part by National Institutes of Health Grant HL-39423. The authors thank Mr Barnabas Desta and Mr Gregory Green for their technical assistance, and Mrs Kay Shaw for her secretarial skills.

References

ARUNLAKSHANA, O. & SCHILD, H.O. (1959). Some quantitative uses of drug antagonists. *Br. J. Pharmacol. Chemother.*, **14**, 48–58.

BARNES, P.J., CUSS, F.M. & PALMER, J.B. (1985). The effect of airway epithelium on smooth muscle contractility in bovine trachea. *Br. J. Pharmacol.*, **86**, 685–691.

BARNES, P.J., MINETTE, P. & MACLAGAN, J. (1988). Muscarinic receptor subtypes in airways. *Trends Pharmacol. Sci.*, **9**, 412–416.

BOUCHER, R.C., RANGA, V., PARE, P.D., INOUE, S., MOROZ, L.A. & HOGG, J.C. (1978). Effect of histamine and methacholine on guinea pig tracheal permeability to HRP. *J. Appl. Physiol.*, **45**, 939–948.

BOUCHER, R.C., STUTTS, M.J. & GATZY, J.T. (1981). Regional differences in bioelectric properties and ion flow in excised canine airways. *J. Appl. Physiol.*, **51**, 706–714.

EGLEN, R.M. & WHITING, R.L. (1988). Comparison of the muscarinic receptors of the guinea-pig oesophageal muscularis mucosae and trachea in vitro. *J. Autonom. Pharmacol.*, **8**, 181–189.

EGLEN, R.M., HARRIS, G.C., TAYLOR, M., PFISTER, J.R. & WHITING, R.L. (1991). Characterization of muscarinic receptors mediating release of epithelial derived relaxant factor (EpDRF) in guinea-pig isolated trachea. *Naunyn-Schmiedebergs Arch. Pharmacol.*, **344**, 29–35.

FEDAN, J.S., HAY, D.W.P., FARMER, S.G. & RAEBURN, D. (1988). Epithelial cells: production of airway smooth muscle reactivity. In *Asthma: Basic Mechanisms and Clinical Management* ed. Barnes, P.J., Rodger, I.W. & Thompson, N.C. pp. 143–162. London: Academic Press.

FERNANDES, L.B., PATERSON, J.W. & GOLDIE, R.G. (1989). Co-axial bioassay of a smooth muscle relaxant factor released from guinea-pig tracheal epithelium. *Br. J. Pharmacol.*, **96**, 117–124.

FERNANDES, L.B. & GOLDIE, R.G. (1990). Pharmacological evaluation of a guinea-pig tracheal epithelium-derived inhibitory factor (EpDIF). *Br. J. Pharmacol.*, **100**, 614–618.

FLAVAHAN, N.A., AARHUS, L.L., RIMELE, T.J. & VANHOUTTE, P.M. (1985). Respiratory epithelium inhibits bronchial smooth muscle tone. *J. Appl. Physiol.*, **58**, 834–838.

FLAVAHAN, N.A., SLIFMAN, N.R., GLEICH, G.J. & VANHOUTTE, P.M. (1988). Human eosinophil major basic protein causes hyperreactivity of respiratory smooth muscle. *Am. Rev. Respir. Dis.*, **138**, 685–688.

FURCHGOTT, R.F. (1972). The classification of adrenoceptors (adrenergic receptors). An evaluation from the standpoint of receptor theory. In *Handbook of Experimental Pharmacology, Catecholamines*, vol 33. ed. Blaschko, H. & Muscholl, E. pp. 283–335. New York: Springer-Verlag.

GOLDIE, R.G., PAPADIMITRIOU, J.M., PATERSON, J.W., RIGBY, P.J., SELF, H.M. & SPINA, D. (1986). Influence of the epithelium on responsiveness of guinea-pig isolated trachea to contractile and relaxant agonists. *Br. J. Pharmacol.*, **87**, 5–14.

GOLDIE, R.G., FERNANDES, L.B., FARMER, S.G. & HAY, D.W.P. (1990). Airway epithelium-derived inhibitory factor. *Trends Pharmacol. Sci.*, **11**, 67–70.

GUC, M.O., ILHAN, M. & KAYAALP, S.O. (1988a). Epithelium-dependent relaxation of guinea-pig tracheal smooth muscle by carbachol. *Arch. Int. Pharmacodyn.*, **294**, 241–247.

GUC, M.O., ILHAN, M. & KAYAALP, S.O. (1988b). The rat anococcygeus muscle is a convenient bioassay organ for the airway epithelium-derived relaxant factor. *Eur. J. Pharmacol.*, **148**, 405–409.

HAY, D.W.P., FARMER, S.G., RAEBURN, D., ROBINSON, V.A., FLEMING, W.W. & FEDAN, J.S. (1986). Airway epithelium modulates the reactivity of guinea-pig respiratory smooth muscle. *Eur. J. Pharmacol.*, **129**, 11–18.

HOLROYDE, M.C. (1986). The influence of epithelium on the responsiveness of guinea-pig isolated trachea. *Br. J. Pharmacol.*, **87**, 501–507.

ILHAN, M. & SAHIN, I. (1986). Tracheal epithelium releases a vascular smooth muscle relaxant factor: demonstration by bioassay. *Eur. J. Pharmacol.*, **131**, 293–296.

KENAKIN, T.P. (1984). The classification of drugs and drug receptors in isolated tissues. *Pharmacol. Rev.*, **36**, 165–222.

LEV, A., CHRISTENSEN, G.C., ZHANG, R. & KELSEN, S.G. (1990). Epithelial effects on tracheal smooth muscle tone: influence of muscarinic antagonists. *Am. J. Physiol.*, **258** (*Lung Cell. Mol. Physiol.*, **2**): L52–L56.

MAK, J.C.W. & BARNES, P.J. (1990). Autoradiographic visualization of muscarinic receptor subtypes in human and guinea pig lung. *Am. Rev. Respir. Dis.*, **141**, 1559–1568.

MORRISON, K.J., GAO, Y. & VANHOUTTE, P.M. (1990). Epithelial modulation of airway smooth muscle. *Am. J. Physiol.*, **258** (*Lung Cell. Mol. Physiol.*, **2**), L254–L262.

MURLAS, C. (1986). Effects of mucosal removal on guinea-pig airway smooth muscle responsiveness. *Clin. Sci.*, **70**, 571–575.

NADEL, J.A., WIDDICOMBE, J.H. & PEATFIELD, A.C. (1985). Regulation of airway secretion, ion transport, and water movement. In *Handbook of Physiology. The Respiratory System. Circulation and Nonrespiratory Functions.* sect. 3, vol I, pp. 419–445. Bethesda, MD: Am. Physiol. Soc.

SCHEFFE, H. (1959). *The Analysis of Variance.* New York: John Wiley & Sons.

SMALL, R.C., GOOD, D.M., DIXON, J.S. & KENNEDY, I. (1990). The effects of epithelium removal on the actions of cholinomimetic drugs in opened segments and perfused tubular preparations of guinea-pig trachea. *Br. J. Pharmacol.*, **100**, 516–522.

TSCHIRHART, E., FROSSARD, N., BERTRAND, C. & LANDRY, Y. (1987). Arachidonic acid metabolites and airway epithelium-dependent relaxant factor. *J. Pharmacol. Exp. Ther.*, **243**, 310–316.

TUCKER, J.F., BRAVE, S.R., CHARALAMBOUS, L., HOBBS, A.J. & GIBSON, A. (1990). L-N^G-nitro arginine inhibits non-adrenergic, non-cholinergic relaxations of guinea-pig isolated tracheal smooth muscle. *Br. J. Pharmacol.*, **100**, 663–664.

UNDEM, B.J., RAIBLE, D.G., ADKINSON, N.F. & ADAMS, G.K. (1988). Effect of removal of epithelium on antigen-induced smooth muscle contraction and mediator release from guinea pig isolated trachea. *J. Pharmacol. Exp. Ther.*, **244**, 659–665.

WEIBEL, E.R. (1985). Lung cell biology. In *Handbook of Physiology. The Respiratory System. Circulation and Nonrespiratory Functions.* sect. 3, vol I, pp. 47–91. Bethesda, MD: Am. Physiol. Soc.

(Received January 15, 1992
Revised March 4, 1992
Accepted March 16, 1992)

Br. J. Pharmacol. (1992), **106**, 677–684

Effect of human recombinant interleukin-5 on *in vitro* responsiveness to PAF of lung from actively sensitized guinea-pigs

[1]Marina Pretolani, Jean Lefort, Dominique Leduc & B. Boris Vargaftig

Unité de Pharmacologie Cellulaire, Unité Associée Institut Pasteur/INSERM n° 285, 25, rue du Dr. Roux, 75015, Paris, France

1 The intra-tracheal (i.t.) administration of human recombinant interleukin-5 (rhIL-5; 100 or 300 ng) to isolated perfused lungs from guinea-pigs actively sensitized to ovalbumin induced an increased bronchoconstriction and release of thromboxane A_2 (TXA_2) and histamine into the lung effluent following the subsequent (10 min) intra-arterial injection of platelet-activating factor (PAF). Lung responses to 5-hydroxytryptamine were unaffected by rhIL-5.

2 Hyperresponsiveness to PAF was observed when the lungs were obtained from guinea-pigs used 2 or 7 days after a booster injection of the antigen and, to a lower extent, when they were from animals sensitized by a single antigen administration. By contrast, rhIL-5 did not modify the responses to PAF of lungs from passively sensitized or from adjuvant-treated guinea-pigs, suggesting that immunological stimulation is required to allow the expression of synergism between rhIL-5 and PAF.

3 Guinea-pigs killed 2 and 7 days after the booster injection of the antigen exhibited a marked increase in the number of eosinophils in the bronchoalveolar lavage fluid (BAL), as compared to non-sensitized animals.

4 Our results demonstrate that rhIL-5 and PAF act synergistically to induce enhanced bronchoconstriction and mediator release exclusively when lungs are obtained from guinea-pigs sensitized once to ovalbumin and then boosted. Since recruitment of eosinophils into the airways and the development of hyperresponsiveness to PAF are concomitant, it is suggested that eosinophils are the target cells for interaction between rhIL-5 and PAF.

Keywords: Interleukin-5; lung hyperresponsiveness; PAF; isolated lung; eosinophils; bronchoalveolar lavage

Introduction

Non-specific bronchial hyperreactivity, an increased sensitivity to inhaled irritants which characterizes some forms of intrinsic or allergic asthma and lung inflammation are related (Boushey *et al.*, 1980). Inflammation is thought to follow the activation of resident cells which triggers the migration of eosinophils, neutrophils and lymphocytes into the lung tissue (Djukanovic *et al.*, 1990). These invading cells may in turn release cytotoxic enzymes and pro-inflammatory mediators which contribute to the amplification and perpetuation of the disease.

We have previously demonstrated that isolated lungs from actively sensitized guinea-pigs exhibit a long-lasting bronchopulmonary hyperresponsiveness to various mediators including platelet activating factor (PAF) (Pretolani *et al.*, 1988). This phenomenon, which is expressed as a reduced threshold for bronchoconstriction and an enhanced release of the secondary mediators thromboxane A_2 (TXA_2), leukotriene C_4 (LTC_4), prostacyclin and histamine, is triggered by the booster injection of the antigen. Acting as an immune provocation, the booster injection may start changes in the reactivity of resident cells and/or promote lung invasion by inflammatory cells. In confirmation, the development of lung hyperresponsiveness is accompanied by an increased number of eosinophils in the bronchoalveolar lavage fluid (BAL) (Pretolani *et al.*, 1990), as demonstrated in other experimental situations (Kallos & Kallos, 1984; Hutson *et al.*, 1988; Coyle *et al.*, 1989).

More recently, it became apparent that cytokines, secreted by T cells in response to antigen stimulation, may play a role in pulmonary eosinophilia and lung inflammation and in the consequent hyperresponsiveness (Gonzalez *et al.*, 1987; Frew *et al.*, 1990), although the precise relationship between these phenomena is not yet established. The main cytokines involved are interleukin-5 (IL-5), IL-3 and granulocyte-macrophage colony stimulating factor (GM-CSF), which support eosinophil proliferation and differentiation from their bone marrow precursors (Coffman *et al.*, 1988; Miyajima *et al.*, 1988) and prime target cells to express enhanced responses to exogenous stimuli (Silberstein *et al.*, 1986; Dahinden *et al.*, 1989; Bischoff *et al.*, 1990a,b). However, administration of very large doses of rhIL-3, rhGM-CSF or tumour necrosis factor-α to non-sensitized guinea-pigs induces an increased eosinophilia in the BAL (Kings *et al.*, 1990; Sanjar *et al.*, 1990), but does not lead to lung hyperresponsiveness. These results indicate that eosinophilia *per se* does not necessarily correlate to hyperresponsiveness.

In the present study we show that the exposure of guinea-pigs to antigen results in lung eosinophilia and in a small increase in bronchoconstriction and mediator release in response to PAF. However, *in vitro* administration of rhIL-5 to lungs prior to challenge with PAF, leads to a marked increase in these parameters. This suggests that priming of a pulmonary target cell, probably the eosinophil, by rhIL-5 is followed by an increased mediator release from other cell types, which in turn accounts for the enhanced bronchoconstriction.

Methods

Sensitization procedures

Male Hartley guinea-pigs (400–600 g) were actively sensitized by two s.c. injections, 2 weeks apart, of 0.5 ml of 0.9% NaCl (saline) containing 10 μg of ovalbumin dispersed in 1 mg $Al(OH)_3$. The animals were used either 2 or 7 days after the

[1] Author for correspondence.

second injection (booster injection). This procedure promotes the production of high titers of specific homocytotropic antibodies (Ovary, 1964), estimated to be approximately 1/800 by passive cutaneous anaphylaxis in serum from animals killed 7 days after the booster injection of antigen (Pretolani *et al.*, 1988). In a separate set of experiments, guinea-pigs received the first sensitizing injection of ovalbumin, but on the day of the booster injection, they were injected with the adjuvant alone, i.e. 1 mg $Al(OH)_3$, to be used 2 days thereafter. In control experiments, guinea-pigs were injected twice, 2 weeks apart, with 1 mg $Al(OH)_3$ alone and killed 2 or 7 days after the second injection.

In another series of experiments, guinea-pigs were passively sensitized with 1 ml of homologous serum obtained from actively sensitized animals and used after 10 days (Lagente *et al.*, 1987).

Lung perfusion experiments

Guinea-pigs were anaesthetized with sodium pentobarbitone (30 mg kg^{-1}, i.p.), tracheae were cannulated, and the animals were ventilated (60 strokes min^{-1}; 1 ml 100 g^{-1} body weight) with Palmer miniature respiratory pumps. A thoracotomy was performed, and the lungs were removed, as described (Lefort *et al.*, 1984). Each organ was placed in a plastic chamber, immediately ventilated (60 strokes min^{-1}, 1 ml 100 g^{-1} body weight) and perfused via the pulmonary artery (10 ml min^{-1}, 37°C) with gassed (95% O_2 5% CO_2) Krebs solution containing 0.25% (w/v) bovine serum albumin (BSA). The changes in resistance to inflation were continuously recorded. After a 10 min equilibration period, 100 or 300 ng rhIL-5 were injected intratracheally (i.t.) in a volume of 100 µl. In control experiments, the lungs received the vehicle of rhIL-5, i.e. 100 µl saline. Ten min after the injection of rhIL-5 or of saline, PAF (0.01, or 1 and 10 ng in 100 µl saline containing 0.25% BSA) or 5-hydroxytryptamine (5-HT, 10 to 3000 ng in 100 µl saline) were successively administered into the pulmonary artery (i.a.), at 10 min intervals for PAF, or every 5 min, for 5-HT.

In a separate series of experiments, lungs from actively sensitized guinea-pigs used 2 days after the booster injection of the antigen were injected i.t. with 100 µg lipopolysaccharide (LPS) and then challenged with 1 and 10 ng PAF, as described above.

Bronchoconstriction was estimated from airways resistance tracings, measured as the area under the curve during a 10 min period. Results are expressed as a percentage of the maximal value obtained by clamping the tracheal cannula. Bronchoconstriction to 5-HT was calculated as % of the peak-intensity of the response.

One ml fractions of the lung effluent were collected before and during the first 6 min after the injection of the various agonists for the determination of TXB_2 and histamine, as described (Sors *et al.*, 1978; Lebel, 1983).

Measurement of thromboxane B_2 and histamine in the lung effluent

Before storage at −20°C, aliquots (1 ml) of the lung perfusate were maintained at room temperature for 30 min to allow the conversion of TXA_2 into its stable metabolite, TXB_2 which approaches 100% under these experimental conditions (Charpentier *et al.*, 1986). The radioimmunoassay for TXB_2 was performed as described (Pretolani *et al.*, 1988), using a monoclonal antibody with less than 0.2% cross-reactivity with prostaglandin D_2 (PGD_2), PGE_2, $PGF_{2\alpha}$, 6-keto-$PGF_{1\alpha}$ and archidonic acid. The sensitivity of the assay was approximately 2 pg of immunoreactive TXB_2 in 100 µl sample.

For the histamine assay, 1 ml of each fraction was mixed with 1 ml of a 0.8 N solution of perchloric acid, centrifuged for 10 min (1,200 *g* at 4°C), and supernatants were stored at 4°C. Histamine content of supernatants was measured by an automatic spectro-fluorometric assay method (Lebel, 1983).

Harvest of bronchoalveolar cells

Four groups of animals were used: (i) non sensitized, (ii) actively sensitized non-boosted, and actively sensitized guinea-pigs killed either (iii) 2, or (iv) 7 days after the booster injection of the antigen. The animals were anaesthetized as above and bronchoalveolar cells were collected in 10 successive lavages with 5 ml aliquots of sterile saline at room temperature injected and recovered through a polyethylene tracheal cannula. The lavage fluid was stored on ice and total cell counts made. The suspension was then diluted to reach a final concentration of 1.5×10^5 cell ml^{-1} and, after cytocentrifugation, differential cell counts were performed after staining with May-Grünwald Giemsa dye. Since the yield of the injected fluid was equivalent in all groups of animals (around 90%), the results are expressed as a concentration of each cell population ml^{-1}.

Materials

The composition of the Krebs solution was (in mM): NaCl 118, KCl 4.7, $CaCl_2 \cdot 2H_2O$ 2.5, $MgSO_4 \cdot 7H_2O$ 1.2, KH_2PO_4 1.2, $NaHCO_3$ 25 and glucose 5.6. Suppliers of the reagents were as follows: rhIL-5 (Mony's International Imports, Beverly Hills, CA, U.S.A.); PAF (1-O-hexadecyl-2-acetyl-sn-glycero-3-phosphocholine), BSA fraction V, bovine γ-globulins fraction II, TXB_2, 5-HT (serotonin) (Sigma, St. Louis, MO, U.S.A.); $Al(OH)_3$, perchloric acid, polyethyleneglycol 6000 (Merck, Darmstadt, Germany); pentobarbitone (sodium pentobarbital, Clin-Midy, Montpellier, France); chicken ovalbumin (Miles, Napterville, IL, U.S.A.); LPS W *E. coli* 0.55:B5 (Difco Laboratories, Detroit, MI, U.S.A.); the antibody and radiolabelled ligand for radioimmunoassay of TXB_2 were from the URIA, Institut Pasteur/INSERM U 207, Paris, France.

Data analysis

The results are expressed as means ± s.e.mean of the indicated number of experiments. Statistical significance was assessed by two-way analysis of variance (ANOVA). If significance was determined, comparisons were made by Student's *t* test for unpaired values. A value of $P \leqslant 0.05$ was considered significant.

Results

Effect of rhIL-5 on bronchial resistance to inflation and mediator release

The i.t. instillation of 100 µl saline or 300 ng rhIL-5 into isolated lungs from adjuvant-treated guinea-pigs or from actively sensitized animals used either 16 days after the first sensitizing injection, or 2 or 7 days after the booster injection of the antigen, induced a slight bronchoconstriction ranging between 6.5 ± 3.3% and 12.9 ± 4.4% ($n = 5-6$ per group) and no statistically significant difference was observed between the groups. Similarly, TXB_2 and histamine release following the i.t. administration of 100 µl saline or 300 ng rhIL-5 ranged between 0.8 ± 0.2 and 2.1 ± 0.9 ng ml^{-1} ($n = 5-6$ per group) and 1.4 ± 0.4 ng ml^{-1} and 6.0 ± 1.6 ng ml^{-1} ($n = 5-6$ per group), respectively. Again, no statistically significant difference was observed between the groups.

Effect of rhIL-5 on PAF-induced bronchoconstriction

The i.a. injection of 10 ng PAF into lungs from adjuvant-treated guinea-pigs 10 min after *in vitro* i.t. instillation of 100 µl saline or 300 ng rhIL-5 induced a slight bronchoconstriction (approximately 10% of the maximum), whereas

no response followed 1 ng of the agonist (Figure 1a). Administration of 1 and 10 ng PAF to lungs from single-sensitized (non-boosted) (Figure 1b) or from passively sensitized guinea-pigs induced a moderate and dose-dependent bronchoconstriction (Table 1). As previously shown (Pretolani *et al.*, 1988), the response to 1 ng PAF was significantly enhanced in lungs from actively sensitized guinea-pigs killed 2 or 7 days after the booster injection of the antigen (Figure 1c and d). Such an enhanced response was not observed following the subsequent administration of 10 ng of PAF. Lungs from adjuvant-treated (Figure 1a) or from passively sensitized (Table 1) guinea-pigs instilled i.t. with 300 ng rhIL-5, responded to PAF as intensively as vehicle-treated preparations. By contrast, a slight increase in the extent of bronchoconstriction by 1 ng of PAF was observed in lungs from single sensitized animals, i.e., those which received no booster injection of the antigen (Figure 1b). This increased response to PAF after rhIL-5 administration was more pronounced when the lungs were obtained from guinea-pigs which had been boosted with antigen and were used 2 or 7 days thereafter (Figure 1c and d). Under these conditions, no further increase in the bronchoconstrictor response following challenge of the organs with 10 ng PAF was noted (Figure 1c).

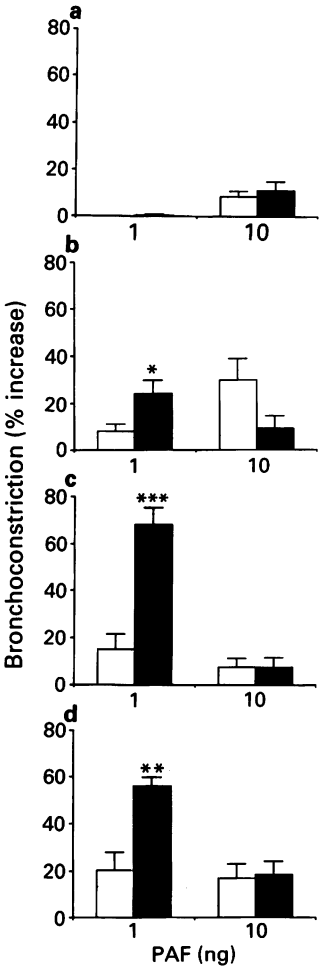

Figure 1 Bronchoconstriction induced by the i.a. administration of 1 and 10 ng PAF into guinea-pig isolated lungs 10 min after an i.t. injection of 100 µl saline (open columns) or 300 ng rhIL-5 (solid columns). Lungs were obtained from adjuvant-treated guinea-pigs (a), or from actively sensitized animals used either 16 days after the first sensitizing injection (b), or 2 (c) or 7 (d) days after the booster injection of the antigen. Bronchoconstrictions were calculated as areas under the curve of increased airways resistance measured for 10 min. Results (mean with s.e.mean of 5–6 experiments) are expressed as % maximal bronchoconstriction obtained by clamping the tracheal cannula.
$^{*}P<0.05$; $^{**}P<0.01$; $^{***}P<0.001$.

The instillation of 100–300 ng of rhIL-5 to lungs from actively sensitized guinea-pigs used 2 days after the booster injection of antigen induced a dose-related increase in bronchoconstriction in response to 1 ng of PAF (Figure 2a, left panel). By contrast, when 300 ng of rhIL-5 was instilled, the bronchoconstrictor response to 1 ng of PAF was so intense as to desensitize the lungs to a subsequent administration of 10 ng of PAF (Figure 2a, right panel). Such a desensitization was also observed with respect to TXB_2 and histamine release (see below).

In a separate series of experiments, the administration of 0.01 ng PAF to lungs from guinea-pigs killed 2 days after the booster injection of the antigen, also induced a moderate bronchoconstriction, which was markedly increased when preceded by the i.t. instillation of 300 ng of rhIL-5. Indeed, bronchoconstrictions amounting to 3.3 ± 1.1% and 40.2 ± 5.9% ($n = 5–6$, $P<0.001$) were measured in vehicle- and rhIL-5-treated lungs, respectively.

Effect of rhIL-5 on PAF-induced mediator release

No release of TXB_2 or histamine above basal values was detected following the administration of 1 and 10 ng PAF to lungs from adjuvant-injected guinea-pigs, irrespective of prior instillation of either rhIL-5 or its vehicle (Figures 3a and 4a). Higher amounts of TXB_2 were released after injection of 1 ng PAF to lungs obtained from actively sensitized guinea-pigs killed at various intervals following the booster injection of antigen, as compared to those from adjuvant-treated or actively sensitized and non-boosted guinea-pigs (Figure 3). Following the injection of 300 ng rhIL-5, the production of TXB_2 in response to 1 ng PAF was markedly increased in lungs from guinea-pigs used 2 days after the booster injection of antigen (Figure 3c) and, to a lesser extent, in those from animals used after 7 days (Figure 3d). In both groups, the increased TXB_2 production was also observed after the injection of 10 ng PAF, although the difference was less marked (Figure 3c and d).

As previously described (Pretolani *et al.*, 1988), histamine was secreted by PAF-stimulated lungs in amounts above basal values only when the organs were obtained from guinea-pigs used 2 or 7 days after the booster injection of antigen (Figure 4). Under these conditions, the administration of 300 ng rhIL-5 significantly increased histamine release in re-

Table 1 Bronchoconstriction and release of thromboxane B_2 (TXB_2) and of histamine induced by the i.a. injection of 1 and 10 ng of PAF 10 min after the i.t. administration of 100 µl saline (vehicle) or 300 ng rhIL-5 into isolated lungs of passively sensitized guinea-pigs

	Vehicle		*rhIL-5 (300 ng)*	
PAF (ng)	1	10	1	10
Bronchoconstriction (%)	3.2 ± 1.6	16.9 ± 3.1	3.0 ± 1.9	14.2 ± 3.0
Thromboxane B_2 (ng ml^{-1})	0.7 ± 0.3	3.3 ± 1.4	0.8 ± 0.3	3.2 ± 0.6
Histamine (ng ml^{-1})	1.3 ± 0.3	2.4 ± 0.2	1.3 ± 0.1	2.9 ± 0.1

Bronchoconstriction was calculated and expressed as described in the legend of Figure 1. Thromboxane B_2 and histamine release were measured in the lung effluent over a 6 min period following the injection of PAF. Results are expressed in ng ml^{-1} (mean ± s.e.mean of 5–6 experiments).

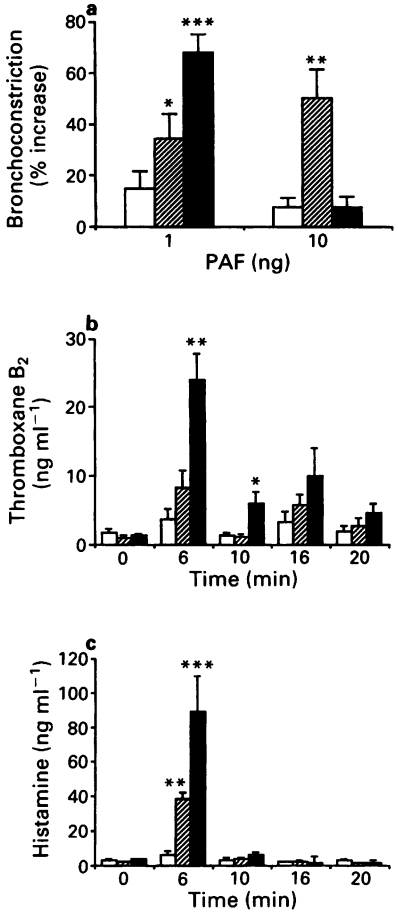

Figure 2 Bronchoconstriction (a) and kinetics of the release of thromboxane B_2 (TXB_2) (b) and of histamine (c) induced by the i.a. injection of 1 and 10 ng PAF 10 min after the i.t. administration of 100 µl saline (open columns), or 100 ng (hatched columns) or 300 ng (solid columns) rhIL-5 into isolated lungs from actively sensitized guinea-pigs used 2 days after the booster injection of antigen. Bronchoconstriction was calculated as described in the legend of Figure 1. Release of TXB_2 and histamine were measured in 1 ml fractions of lung effluent collected before and during the first 6 min after injection of 1 and 10 ng PAF. Results are expressed as mean with s.e.mean (vertical bars) of 5 experiments.
*$P<0.05$; **$P<0.01$; ***$P<0.001$.

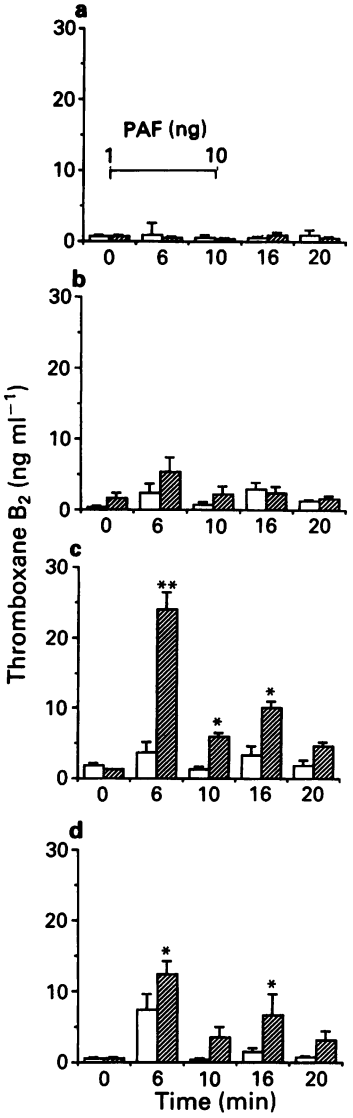

Figure 3 Kinetics of thromboxane B_2 (TXB_2) release induced by the i.a. administration of 1 and 10 ng PAF 10 min after an i.t. injection of 100 µl saline (open columns) or 300 ng rhIL-5 (hatched columns) into guinea-pig isolated lungs. Lungs were obtained from adjuvant-treated guinea-pigs (a), or from actively sensitized animals used either 16 days after the first sensitizing injection (b), or 2 (c) or 7 (d) days after the booster injection of antigen. Results were calculated and expressed as described in the legend of Figure 2 (mean with s.e. mean [vertical bars] of 5–6 experiments).
*$P<0.05$; **$P<0.01$.

sponse to the injection of 1 ng PAF (Figure 4). This increase was more pronounced in lungs from animals killed 2 days after the booster injection of antigen (Figure 4c), as compared to those used 7 days thereafter (Figure 4d). However, no histamine release was noted following the second challenge with 10 ng PAF.

As in case of bronchoconstriction, the effect of rhIL-5 was dose-dependent, since lungs from actively sensitized guinea-pigs used 2 days after the booster injection of the antigen and injected i.t. with 100 ng rhIL-5 also released more TXB_2 and histamine in response to 1 ng PAF, but this increase was less than when 300 ng of the cytokine was used (Figure 2b and c).

The administration of 0.01 ng PAF to lungs from actively sensitized guinea-pigs used 2 days after the booster injection of antigen, induced the release of low quantities of TXB_2 and histamine into the effluent. Pretreatment of the lungs with 300 ng rhIL-5 significantly increased these amounts, since 2.3 ± 1.3 and 8.1 ± 1.3 ng ml^{-1} TXB_2 ($n = 5-7$; $P<0.05$) and 2.3 ± 0.4 and 28.2 ± 4.0 ng ml^{-1} histamine ($n = 5-7$, $P<0.001$) were measured in vehicle- and in rhIL-5-treated lungs, respectively.

Kinetics of rhIL-5-induced lung hyperresponsiveness to PAF

The i.a. injection of 1 ng of PAF 2 min after the i.t. administration of 300 ng rhIL-5 to lungs from guinea-pigs killed 2 days after the booster injection of antigen triggered slight bronchoconstriction and the release of small amounts of TXB_2 and histamine, responses similar to those observed in saline-injected preparations (Figure 5). In contrast, the pulmonary response was increased markedly when PAF was injected 10 min after rhIL-5 and this increase persisted for at least 30 min (Figure 5).

Effect of rhIL-5 on 5-HT-induced bronchoconstriction

Regardless of the previous administration of 300 ng rhIL-5 or of its vehicle, i.a. injections of 5-HT (10 to 3000 ng) to

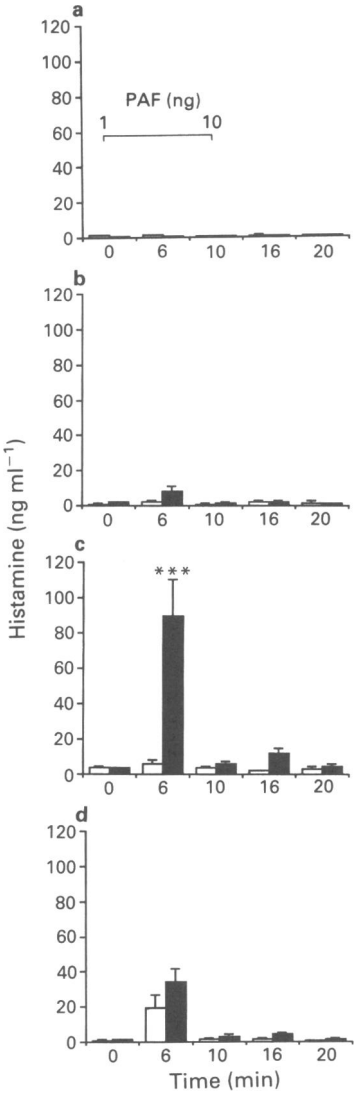

Figure 4 Kinetics of histamine release induced by the i.a. administration of 1 and 10 ng PAF 10 min after an i.t. injection of 100 µl saline (open columns) or 300 ng rhIL-5 (solid columns) into guinea-pig isolated lungs. Lungs were obtained from adjuvant-treated guinea-pigs (a), or from actively sensitized animals used either 16 days after the first sensitizing injection (b), or 2 (c) or 7 (d) days after the booster injection of antigen. Results were calculated and expressed as described in the legend of Figure 2 (mean with s.e.mean [vertical bars] of 5–6 experiments).
***$P<0.01$.

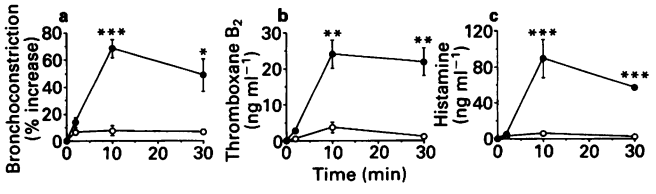

Figure 5 Kinetics of rhIL-5-induced lung hyperresponsiveness to PAF in isolated lungs from actively sensitized guinea-pigs used 2 days after the booster injection of antigen. PAF (1 ng) was administered i.a. at different time intervals (2, 10 and 30 min) after the i.t. injection of 100 µl saline (○) or 300 ng rhIL-5 (●). Bronchoconstriction (a) was calculated as described in the legend to Figure 1. Thromboxane B_2 (b) and histamine release (c) were measured in the lung effluent collected for 6 min after the injection of PAF and results are expressed in ng ml^{-1} (mean with s.e.mean [vertical bars] of 4–6 experiments).
*$P<0.05$; **$P<0.01$; ***$P<0.001$.

lungs from actively sensitized guinea-pigs used 2 days after the booster injection of antigen evoked a similar dose-dependent bronchoconstriction (Figure 6). No significant release of TXB_2 or histamine in response to 5-HT was measured in the effluent of vehicle- or rhIL-5-treated lungs (not shown).

Effect of lipopolysaccharide on PAF-induced bronchoconstriction and mediator release

The possibility that rhIL-5 was contaminated with LPS led us to study whether the lung response to PAF would be modified by LPS alone. The i.t. administration of 100 µg LPS neither induced bronchoconstriction nor mediator release from lungs of actively sensitized guinea-pigs used 2 days after the booster injection of antigen (not shown). In addition, bronchoconstriction and release of TXB_2 and histamine in response to the i.a. injections of 1 and 10 ng PAF were similar in LPS-treated, as compared to saline-injected lungs. Indeed, bronchoconstrictor responses of $15.1 \pm 3.5\%$ and $7.6 \pm 3.7\%$ were measured after 1 and 10 ng PAF, respectively in lungs previously injected i.t. with 100 µl saline, and $13.5 \pm 2.9\%$ and $8.4 \pm 3.0\%$ ($n = 4$; not significant) in LPS-treated lungs. PAF at 1 and 10 ng triggered the release of 3.7 ± 1.4 ng ml^{-1} and 3.3 ± 1.4 ng ml^{-1} TXB_2 after 100 µl saline and of 3.2 ± 0.2 ng ml^{-1} and 3.2 ± 0.6 ng ml^{-1} TXB_2 after the injection of LPS ($n = 4$; not significant). Similarly, 6.1 ± 2.1 ng ml^{-1} and 2.2 ± 0.4 ng ml^{-1} and 5.6 ± 1.4 ng ml^{-1} and 3.0 ± 1.2 ng ml^{-1} histamine ($n = 4$; not significant) were measured in the effluent of saline- and LPS-treated lungs.

Effect of active sensitization on the cell composition of bronchoalveolar lavage fluid

The average number of cells recovered was $3.3 \pm 0.8 \times 10^5$ cells ml^{-1} ($n = 8$), $4.1 \pm 0.4 \times 10^5$ cells ml^{-1} ($n = 10$), $4.9 \pm 0.4 \times 10^5$ cells ml^{-1} ($n = 10$) and $7.1 \pm 0.4 \times 10^5$ cells ml^{-1} ($n = 10$) in BAL from non-immunized, actively sensitized non boosted and actively sensitized guinea-pigs used 2 or 7 days after the booster injection of the antigen, respectively. The number of cells recovered in BAL from actively sensitized guinea-pigs used 7 days after the booster injection of antigen was significantly higher ($P<0.01$) when compared to that evaluated in the other groups of animals. As seen in Figure 7, non boosted or boosted guinea-pigs showed a significant increase in the number of eosinophils in BAL, as compared

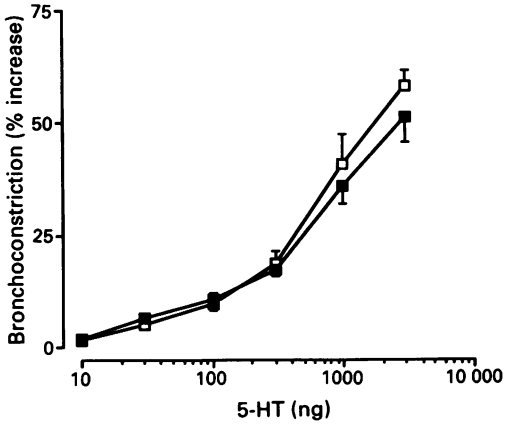

Figure 6 Bronchoconstriction induced by the i.a. administration of 10 to 3000 ng 5-hydroxytryptamine (5-HT) into isolated lungs from actively sensitized guinea-pigs killed 2 days after the booster injection of antigen and pretreated by an i.t. injection of 100 µl saline (□) or 300 ng rhIL-5 (■) 10 min before-hand. Bronchoconstriction was expressed as % of the peak-intensity of the response (mean with s.e.mean [vertical bars] of 4 experiments).

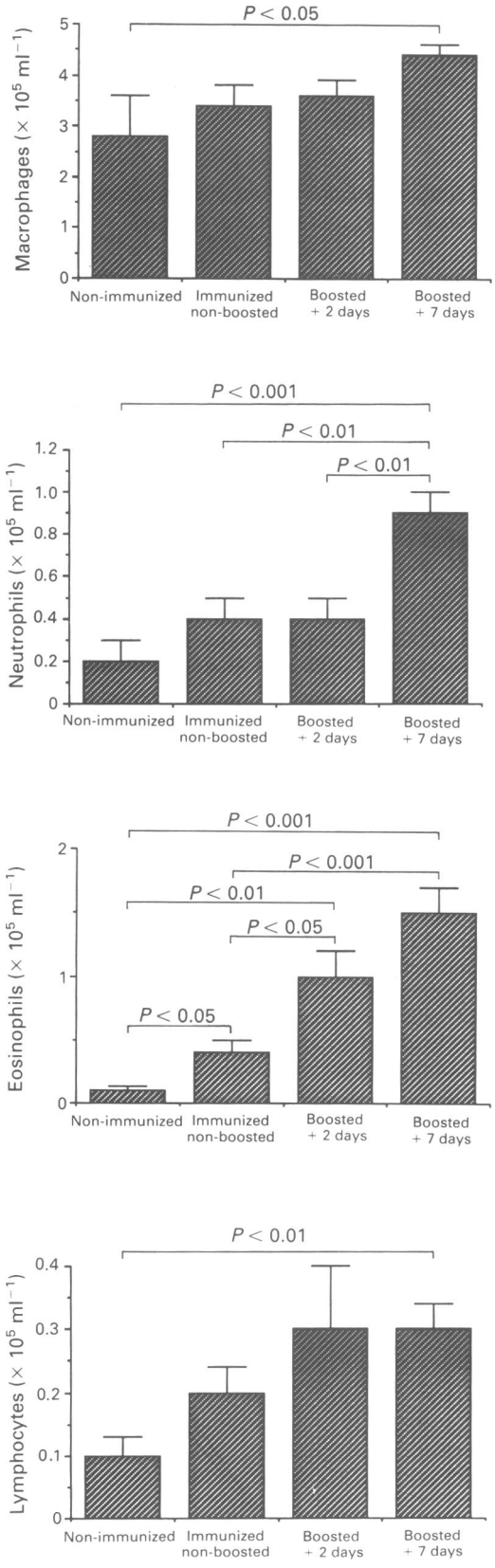

Figure 7 Cell content of bronchoalveolar lavage fluid (BAL) obtained from non-immunized guinea-pigs or from animals actively sensitized by a first s.c. injection of 10 μg ovalbumin in 1 mg of the adjuvant, i.e. $Al(OH)_3$ and used either 2 days after a s.c. injection of the adjuvant alone (group 'Immunized non-boosted'), or 2 or 7 days after a booster injection of antigen (groups 'Boosted + 2 days' and 'Boosted + 7 days', respectively). Bronchoalveolar cells were collected in 10 successive lavages and differentiated by May-Grünwald-Giemsa stain. Results are expressed as concentration of each cell population ml^{-1}. Data are expressed as mean with s.e.mean (vertical bars) of 8–10 experiments.

to non immunized animals. This increase reached a maximum 7 days after the booster injection, even though no significant difference was observed when compared to the animals killed 2 days after the booster injection. A significant increase in the number of the other cell types, i.e., alveolar macrophages, polymorphonuclear neutrophils and lymphocytes was detected only in BAL obtained from guinea-pigs used 7 days after the booster injection of antigen (Figure 7).

Discussion

In this study, the *in vitro* administration of rhIL-5 into lungs from actively sensitized guinea-pigs is shown to trigger a marked time-dependent hyperresponsiveness to PAF. The observation that a human cytokine affects the reactivity of an animal tissue is not an exception, since rhGM-CSF, rhIL-3 and rhIL-5 share antigenic and functional activities with cytokines from other species (Metcalf, 1986; Yamaguchi *et al.*, 1988). Hyperresponsiveness to PAF following i.t. administration of rhIL-5 was intense in lungs obtained from immunized and boosted animals and was present, even though to a much lower extent, in those from guinea-pigs actively sensitized but not boosted. This agrees with our previous results showing that the booster injection of the antigen is followed within a few days by an increased lung responsiveness to PAF (Pretolani *et al.*, 1988). The key role of active sensitization was confirmed by the failure of rhIL-5 to enhance bronchoconstriction and mediator release in response to PAF in lungs from non-immunized or passively sensitized animals. This parallels our previous finding showing that passively sensitized animals do not exhibit lung hyperresponsiveness to PAF (Pretolani *et al.*, 1988), indicating that the presence of homocytotropic antibodies in the lung (Lagente *et al.*, 1987) cannot account alone for the observed modifications of its reactivity.

In the present experiments, rhIL-5 was given i.t., because we assumed that in allergic situations, it is produced by stimulated mast cells (Plaut *et al.*, 1989) and by T lymphocytes (Coffman *et al.*, 1988), located in the airways. T lymphocytes are found in increased numbers in the BAL (this manuscript) and in the bronchial submucosa of sensitized guinea-pigs (Frew *et al.*, 1990; Lapa e Silva *et al.*, 1992). PAF, on the other hand, was given i.a., since this route has allowed us to demonstrate that lungs from sensitized and boosted, as compared to non-boosted guinea-pigs, show an enhanced responsiveness to PAF (Pretolani *et al.*, 1988).

Two min after the administration of rhIL-5, no significant increase in the responsiveness to PAF was observed, indicating that a delay of a few minutes is required to allow the diffusion of rhIL-5 throughout the lung tissue or to exert its effect. By contrast, hyperresponsiveness to PAF reached a peak by 10 min and remained at a plateau for at least 30 min, despite the continuous lung perfusion and wash-off of the cytokine. In this case, rhIL-5 can neither operate as a differentiating/maturing substance nor via cell recruitment, since the enhancement of the effects of PAF occurred in the isolated lungs and over a short period of time, i.e. within 10 min.

To verify whether the enhancing effect of rhIL-5 was restricted to PAF, the lungs were challenged with 5-HT, which induces a smooth muscle contraction, attributable mostly to a direct effect. Since the administration of rhIL-5 failed to induce hyperresponsiveness to 5-HT, the smooth muscle is probably not the direct target for rhIL-5. Most likely, active immunization and rhIL-5 promote hyperresponsiveness which is revealed by agonists such as PAF, interacting with inflammatory cells (Braquet *et al.*, 1987).

Among the various cytokines, IL-3, IL-5 and GM-CSF are major candidates for playing a role in the inflammatory component of immediate hypersensitivity reactions. At low concentrations, they increase eosinophil (Fujisawa *et al.*, 1990), basophil (Bischoff *et al.*, 1990a,b) and neutrophil

(Dahinden *et al.*, 1988) response to exogenous stimuli. Interestingly, this increase involves the release of arachidonic acid metabolites including LTC_4, which is produced in larger amounts upon stimulation with various agonists after pretreatment of the cells with these cytokines (Dahinden *et al.*, 1988; 1989; Kurimoto *et al.*, 1989; Bischoff *et al.*, 1990a,b). Since peptido-leukotrienes are potent smooth muscle-contracting agents released during allergic or non-allergic inflammatory reactions (Piper, 1984), a link between the regulatory role of haematopoietic growth factors and lipid mediators appears likely.

Our results on isolated lung preparations raise the question of the target(s) for IL-5 present only in lungs from actively sensitized guinea-pigs and not in those from normal animals. Our previous observation that actively sensitized and boosted guinea-pigs exhibit an increased number of eosinophils in the BAL fluid, as compared to non-immunized animals (Pretolani *et al.*, 1990) and the evidences that IL-5 stimulates selectively mature eosinophils (Lopez *et al.*, 1988; Wang *et al.*, 1989), may explain the increase in lung response to PAF brought about by this cytokine. Indeed, in the present work the number of eosinophils was markedly increased in BAL obtained from guinea-pigs killed after the booster injection of antigen, suggesting that the development of lung hyperresponsiveness to PAF induced by rhIL-5 follows a profile similar to that of eosinophil invasion into the airways. Since a significant ($P<0.05$) augmentation of the number of eosinophils was also observed in BAL from unboosted sensitized guinea-pigs, it is likely that inflammatory mechanisms, which are markedly enhanced by the booster administration of the antigen, are already operative in its absence. This may explain the increased response to PAF after the acute instillation of rhIL-5 which is already observed, although to a lower extent, in lungs from sensitized and non-boosted animals.

A similar increase in the effects of PAF induced by rhIL-5 has been observed in purified peritoneal guinea-pig eosinophils (Coëffier *et al.*, 1991). Indeed, incubation of these cells with this cytokine is followed by an increased PAF-induced chemotactic activity and superoxide anion generation. This phenomenon is restricted to PAF, since no priming of the LTB_4-induced effects by rhIL-5 was observed.

A pulmonary eosinophilia following s.c. or i.p. injections of factors which promote eosinophil differentiation and activation, such as GM-CSF and IL-3, has been demonstrated in normal guinea-pigs (Kings *et al.*, 1990; Sanjar *et al.*, 1990). In those cases, however, eosinophilia was not accompanied by bronchial hyperresponsiveness to PAF or to histamine (Sanjar *et al.*, 1990), indicating that the lung invasion by eosinophils alone does not account for its development. These results and ours do not conflict, since those experiments were performed on non-immunized guinea-pigs which, according to our hypothesis, lack the specific target(s) for IL-5 that are only present in the lungs after the booster injection of the antigen.

Even though eosinophils recruited into the lungs by the booster injection of antigen are a likely target for rhIL-5, other mechanisms may account for the increased responsiveness induced by rhIL-5 observed in the lung from boosted guinea-pigs. Indeed, following a second immune challenge, the release from T lymphocytes of cytokines other than IL-5 may influence the activation of lung cells and thus play a role in the priming effect induced by rhIL-5. In addition, it has been shown that, besides eosinophils, basophils are also a target for IL-5 and may thus participate in the development of lung hyperresponsiveness observed under our conditions. Indeed, rhIL-5 primes human basophils (Bischoff *et al.*, 1990a) which are involved in cutaneous hypersensitivity reaction in the guinea-pig (Golden *et al.*, 1986), a situation that is reminiscent of our observations in lungs.

In conclusion, our data indicate that IL-5 may be implicated in bronchopulmonary allergic reactions in the guinea-pig, particularly in the expression of lung hyperresponsiveness and the underlying airway inflammation. These results should be considered in the light of recent observations (Hamid *et al.*, 1991) showing an increased messenger RNA expression of the IL-5 gene in mucosal bronchial biopsies from asthmatic subjects.

The ability of rhIL-5 to increase the lung response to PAF suggests that an interaction between cytokines and lipid mediators may contribute to the bronchopulmonary hyperresponsiveness that accompanies airway inflammation.

The authors thank Mrs A. Leroy (Unité d'Immunoallergie, Institut Pasteur) for histamine determination and Ms M.-A. Nahori, Mrs D. Joseph and Dr E. Coëffier for help and discussion.

References

BISCHOFF, S.C., BRUNNER, T., DE WECK, A.L. & DAHINDEN, C.A. (1990a). Interleukin 5 modifies histamine release and leukotriene generation by human basophils in response to diverse agonists. *J. Exp. Med.*, **172,** 1577–1582.

BISCHOFF, S.C., DE WECK, A.L. & DAHINDEN, C.A. (1990b). Interleukin 3 and GM-CSF render human basophils responsive to low concentrations of the complement component C3a. *Proc. Natl. Acad. Sci. U.S.A.*, **87,** 6813–6817.

BOUSHEY, H.A., HOLTZMANN, M.J., SHELLER, J.R. & NADEL, J.A. (1980). Bronchial hyperreactivity. *Am. Rev. Respir. Dis.*, **121,** 389–413.

BRAQUET, P., TOUQUI, L., SHEN, T.Y. & VARGAFTIG, B.B. (1987). Perspectives in platelet-activating factor research. *Pharmacol. Rev.*, **39,** 97–145.

CHARPENTIER, M.C., LECOMPTE, T., NICHOLAS, P. & DRAY, F. (1986). Validation of radioimmunoassay for eicosanoids. In *Advances in Inflammation Research.* ed. Russo-Marie, F., Chignard, M. & Mencia-Huerta, J.M. Vol. 10, pp. 150–153. New York: Raven Press.

COËFFIER, E., JOSEPH, D. & VARGAFTIG, B.B. (1991). Activation by human recombinant IL-5 of guinea pig eosinophils. Selective priming to PAF and interference of its antagonists. *J. Immunol.*, **147,** 2595–2602.

COFFMAN, R.L., SEYMOUR, B.W.P., LEBMAN, D.A., HIRAKI, D.D., CHRISTIANSEN, J.A., SHRADER, B., CHERWINSKI, H.M., SAVELKOUL, H.F.J., FINKELMAN, F.D., BOND, M.W. & MOSMANN, T.R. (1988). The role of helper T cell products in mouse B cell differentiation and isotype regulation. *Immunol. Rev.*, **102,** 5–28.

COYLE, A.J., URWIN, S.C., PAGE, C.P., TOUVAY, C., VILAIN, B. & BRAQUET, P. (1989). The effect of the selective PAF antagonist, BN 52021, on PAF- and antigen-induced bronchial hyperreactivity and eosinophil accumulation. *Eur. J. Pharmacol.*, **148,** 51–58.

DAHINDEN,C.A., KURIMOTO, Y., DE WECK, A.L., LINDLEY, B., DEWALD, B. & BAGGIOLINI, M. (1989). The neutrophil-activating peptide NAF/NAP-1 induces histamine and leukotriene release by interleukin 3-primed basophils. *J. Exp. Med.*, **170,** 1787–1792.

DAHINDEN, C.A., ZINGG, J., MALY, F.E. & DE WECK, A.L. (1988). Leukotriene production in human neutrophils primed by recombinant human granulocyte/ macrophage colony-stimulating factor and stimulated with the complement component C5a and FMLP as second signals. *J. Exp. Med.*, **167,** 1281–1286.

DJUKANOVIC, R., ROCHE, R., WILSON, J.W., BEASLEY, C.R.W., TWENTYMAN, O.P., HOWARTH, P.H. & HOLGATE, S.T. (1990). Mucosal inflammation and asthma. *Am. Rev. Respir. Dis.*, **142,** 434–457.

FREW, A.J., MOQBEL, R., AZZAWI, M., HARTNELL, A., BARKANS, J., JEFFERY, P.K., KAY, A.B., SCHEPER, R.J., VARLEY, J., CHURCH, M.K. & HOLGATE, S.T. (1990). Lymphocytes and eosinophils in allergen-induced late-phase asthmatic reactions in the guinea pig. *Am. Rev. Respir. Dis.*, **141,** 407–413.

FUJISAWA, T., ABU-GHAZALEH, R., KITA, H., SANDERSON, C.J. & GLEICH, G.J. (1990). Regulatory effect of cytokines on eosinophil degranulation. *J. Immunol.*, **144,** 642–646.

GOLDEN, H.W., CREAN, G.L., IACUZIO, D.A. & OTTERNESS, I.G. (1986). Effect of disodium cromoglycate on cutaneous basophil anaphylaxis. *J. Immunol.*, **137,** 1495–1503.

GONZALEZ, M.C., DIAZ, P., GALLEGUILLOS, F.R., ANCIC, P., CROMWELL, O. & KAY, A.B. (1987). Allergen-induced recruitment of bronchoalveolar helper (OKT4) and suppressor (OKT8) T-cells in asthma. *Am. Rev. Respir. Dis.*, **136,** 600–604.

HAMID, Q., AZZAWI, M., YING, S., MOQBEL, R., VARNEY, V., WARDLAW, A.J., CORRIGAN, C.J., BRADLEY, B., DURHAM, S.R., GAGA, M. & KAY, A.B. (1991). Expression of mRNA for interleukin-5 in mucosal bronchial biopsies from asthma. *J. Clin. Invest.*, **87,** 1541–1546.

HUTSON, P.A., HOLGATE, S.T. & CHURCH, M.K. (1988). Effect of cromonyl sodium and albuterol on early and late phase bronchoconstriction and airway leukocyte infiltration after allergen challenge of nonanesthetized guinea-pigs. *Am. Rev. Respir. Dis.*, **138,** 1157–1163.

KALLOS, P. & KALLOS, L. (1984). Experimental asthma in guinea pigs revisited. *Int. Arch. Allergy Appl. Immunol.*, **73,** 77–85.

KINGS, M.A., CHAPMAN, I., KRISTERSSON, A., SANJAR, S. & MORLEY, J. (1990). Human recombinant lymphokines and cytokines induce pulmonary eosinophilia in the guinea-pig which is modified by ketotifen and AH 21-132. *Int. Arch. Allergy Appl. Immunol.*, **91,** 354–361.

KURIMOTO, Y., DE WECK, A.L. & DAHINDEN, C.A. (1989). Interleukin-3-dependent mediator release in basophils triggered by C5a. *J. Exp. Med.*, **170,** 467–479.

LAGENTE, V., TOUVAY, C., RANDON, J., DESQUAND, S., CIRINO, M., VILAIN, B., LEFORT, J., BRAQUET, P. & VARGAFTIG, B.B. (1987). Interference of the PAF antagonist BN 52021 with the passive anaphylaxis in the guinea-pig. *Prostaglandins*, **33,** 265–274.

LAPA E SILVA, J.R., PRETOLANI, M., BACHELET, C.M., BAKER, D. & VARGAFTIG, B.B. (1992). Changes in T-lymphocytes subsets in bronchial wall of actively sensitized guinea-pigs. *Am. Rev. Respir. Dis.*, abstract (in press).

LEBEL, B. (1983). A high sampling rate automated continuous flow fluorimetric technique for the analysis of nanogram levels of histamine in biological samples. *Analyt. Biochem.*, **133,** 16.

LEFORT, J., ROTILIO, D. & VARGAFTIG, B.B. (1984). The platelet-independent release of thromboxane A2 by PAF from guinea-pig lungs involves mechanisms distinct from those of leukotrienes. *Br. J. Pharmacol.*, **82,** 565–575.

LOPEZ, A.L., SANDERSON, C.J., GAMBLE, J.R., CAMPBELL, H.D., YOUNG, I.G. & VADAS, M.A. (1988). Recombinant human interleukin 5 is a selective activator of human eosinophil function. *J. Exp. Med.*, **167,** 219–225.

METCALF, D. (1986). The molecular biology and functions of the granulocyte-macrophage colony-stimulating factors. *Blood*, **67,** 257–267.

MIYAJIMA, A., MIYATAKE, S., SCHREURS, J., DE VRIES, J., ARAI, N., YOKOTA, T. & ARAI, K. (1988). Coordinate regulation of immune and inflammatory responses by T cell-derived lymphokines. *FASEB J.*, **2,** 2462–2473.

OVARY, Z. (1964). Passive cutaneous anaphylaxis. In *Immunological Methods.* ed. Ackroyd, J.F. pp. 259–301. Oxford: Blackwell Scientific Publications Ltd.

PIPER, P. (1984). Formation and action of leukotrienes. *Physiol. Rev.*, **64,** 744–761.

PLAUT, M., PIERCE, J.H., WATSON, C.J., HANLEY-HYDE, J., NARDAN, R.P. & PAUL, W.E. (1989). Mast cell lines produce lymphokines in response to cross-linkage of FcεRI or to calcium ionophores. *Nature*, **339,** 64–67.

PRETOLANI, M., LEFORT, J., SILVA, P., MALANCHÈRE, E., DUMAREY, C., BACHELET, M. & VARGAFTIG, B.B. (1990). Protection by nedocromil sodium of active immunization-induced bronchopulmonary alterations in the guinea pig. *Am. Rev. Respir. Dis.*, **141,** 1259–1265.

PRETOLANI, M., LEFORT, J. & VARGAFTIG, B.B. (1988). Active immunization induces lung hyperresponsiveness in the guinea pig. Pharmacological modulation and triggering role of the booster injection. *Am. Rev. Respir. Dis.*, **138,** 1572–1578.

SANJAR, S., SMITH, D., KINGS, M.A. & MORLEY, J. (1990). Pretreatment with rh-GM-CSF, but not rh-IL-3, enhances PAF-induced eosinophil accumulation in guinea-pig airways. *Br. J. Pharmacol.*, **100,** 399–400.

SILBERSTEIN, D.S., OWEN, W.F., GASSON, J.C., DIPERSIO, J.F., GOLDE, D.W., BINA, J.C., SOBERMAN, R., AUSTEN, K.F. & DAVID, J.R. (1986). Enhancement of human eosinophil cytotoxicity and leukotriene synthesis by biosynthetic (recombinant) granulocyte-macrophage colony-stimulating factor. *J. Immunol.*, **137,** 3290–3294.

SORS, H., PRADELLES, P. & DRAY, F. (1978). Analytical methods for thromboxane B_2 measurement and validation on radioimmunoassay by gas liquid chromatography-mass spectrometry. *Prostaglandins*, **16,** 277–290.

WANG, J.M., RAMBALDI, A., BIONDI, A., GUO CHEN, Z., SANDERSON, C.J. & MANTOVANI, A. (1989). Recombinant human interleukin 5 is a selective eosinophil chemoattractant. *Eur. J. Immunol.*, **19,** 701–705.

YAMAGUCHI, Y., SUDA, T., SUDA, J., EGUCHI, M., MIURA, Y., HARADA, N., TOMINAGA, A. & TAKATSU, K. (1988). Purified interleukin 5 (IL-5) supports the terminal differentiation proliferation of murine eosinophilic precursors. *J. Exp. Med.*, **167,** 43–48.

(Received January 30, 1992
Revised March 11, 1992
Accepted March 16, 1992)

Br. J. Pharmacol. (1992), **106**, 685–692

The effect of neosurugatoxin on the release of neurohypophysial hormones by nicotine, hypotension and an osmotic stimulus in the rat

[1]G.W. Bisset, K.M. Fairhall & *K. Tsuji

Division of Neurophysiology & Neuropharmacology, National Institute for Medical Research, Mill Hill, London NW7 1AA and *School of Pharmaceutical Science, University of Shizuoka, 395 Yada, Shizuoka shi, Shizuoka-ken, 422, Japan

1 Experiments were carried out to test whether neosurugatoxin (NSTX) which blocks autonomic ganglia also acts centrally, like hexamethonium, on nicotinic cholinoceptors involved in the neural control of release of vasopressin and oxytocin from the neurohypophysis.

2 In the water-loaded rat under ethanol anaesthesia, nicotine 100 μg i.v. produced a pressor and an antidiuretic response accompanied by an increase in the urinary excretion of vasopressin and of oxytocin-like radioimmunoreactivity (OLRI). This indicates release of both vasopressin and oxytocin.

3 Under conditions in which tachyphylaxis was avoided, NSTX, 80 ng i.c.v., caused a prolonged inhibition of the release of both hormones by nicotine.

4 NSTX i.c.v. caused some reduction in the pressor response to nicotine. It is suggested that this response involves both central and peripheral stimulation of the sympathetic nervous system and that the central component is blocked by neosurugatoxin.

5 Muscarine, 40 ng i.c.v., produced a pressor and an antidiuretic response with increased urinary excretion of vasopressin and OLRI. All these effects were blocked by atropine but were not inhibited by NSTX.

6 Sodium nitroprusside (SN), 200 μg i.v., and hypertonic saline (HS; 1.54 M NaCl solution) 4 μl i.c.v., both produced antidiuretic responses accompanied by increased urinary excretion of vasopressin and OLRI. The ratio of the excretion of vasopressin to that of OLRI was 5.1 ± 1.3 (mean ± s.e.: $n = 8$) for SN and 1.2 ± 0.24 (mean ± s.e.: $n = 6$) for HS. NSTX 80 ng i.c.v., caused a significant reduction in the antidiuretic response to the hypotension induced with SN: the increased urinary excretion of vasopressin was also significantly reduced but not that of OLRI. NSTX had no effect on the response to HS.

7 We conclude that NSTX acts centrally on nicotinic cholinoceptors to block the release of vasopressin and oxytocin by nicotine and the release of vasopressin, but not that of oxytocin, by hypotension. It does not inhibit the release of either hormone by a central osmotic stimulus.

Keywords: Neosurugatoxin; vasopressin; oxytocin; nicotinic receptors; muscarinic receptors; hypertonic saline

Introduction

Two outbreaks of food poisoning which occurred in Japan in 1957 and 1965 after ingestion of the Japanese Ivory mollusc, *Babylonia japonica*, produced a pattern of symptoms, including hypotension, mydriasis and constipation, reminiscent of the side-effects of ganglion blocking agents in man (Hirayama *et al.*, 1974). A toxin, IS-toxin, contained in a crude extract of the mollusc was found to block the ciliary ganglia in mice and the superior cervical ganglia in cats (Hirayama *et al.*, 1970). Kosuge *et al.* (1972) isolated a pure crystalline substance which they named surugatoxin. It was reported that this toxin caused selective block of nicotinic cholinoceptors in sympathetic and parasympathetic ganglia and on adrenal chromaffin cells, without any action on muscarinic receptors in smooth muscle or on nicotinic cholinoceptors at the neuromuscular junction (Hirayama *et al.*, 1974; Hayashi & Yamada, 1975; Brown *et al.*, 1976; Ascher *et al.*, 1979). It now appears that the mydriatic activity which was used in the isolation of surugatoxin is due to contamination with two other toxins (Kosuge *et al.*, 1982). A new toxin, neosurugatoxin, NSTX, has been isolated (Kosuge *et al.*, 1981; 1982) which possesses the same functional groups, myo-inositol, bromo-oxindole and dioxopyrimidine, as surugatoxin but differs from it in having a 6–7 rather than 6–6 heterocyclic ring system. NSTX evokes mydriasis in mice and has an anti-nicotinic action on the guinea-pig ileum about 100 times as potent as that reported for surugatoxin with a pA_2 of 9.07 compared with 5.46 for hexamethonium (Kosuge *et al.*, 1982; Hayashi *et al.*, 1983; 1984). It also inhibits the secretion of catecholamines from cultured bovine adrenal medullary cells in response to nicotine (Bourke *et al.*, 1988) and carbachol (Wada *et al.*, 1989).

There has been considerable interest in the possibility that NSTX might block nicotinic cholinoceptors in the CNS. This would be useful for identifying sub-types of receptors and for investigating cholinergic transmission in physiological systems. Specific binding of the toxin to brain membranes and inhibition of nicotine binding has been demonstrated (Hayashi *et al.*, 1983; 1984; Rapier *et al.*, 1985; Yamada *et al.*, 1985; 1988a; Billiar *et al.*, 1988). NSTX blocked the presynaptic nicotinic facilitation of [^{3}H]-dopamine release from striatal nerve terminals (Rapier *et al.*, 1985). *In vivo* studies have demonstrated an inhibition of nicotine-induced antinociception in mice (Yamada *et al.*, 1988b) and a decrease in the frequency, although not the amplitude, of pulses of luteinizing hormone (LH) secretion in rats (Billiar *et al.*, 1988).

A well-established central action of nicotine discovered by Burn *et al.* (1945) is the release of vasopressin from the neurohypophysis. Hexamethonium i.c.v. blocks the release of vasopressin by nicotine and by hypotension (Bisset & Feldberg, 1977; Bisset & Chowdrey, 1984). It also blocks the release of vasopressin by application of hypertonic saline

[1] Author for correspondence.

(HS) to the rat hypothalamo-neurohypophyseal explant (Sladek & Joynt, 1979) but not by i.c.v. injection in the rat (Bisset et al., 1988; 1989). To test whether NSTX has a central as well as a peripheral action like that of hexamethonium, we have investigated the effect of i.c.v. NSTX on the release of vasopressin by nicotine, hypotension and i.c.v. HS. Release of vasopressin was measured by antidiuretic responses and increased urinary excretion of vasopressin in water-loaded rats under ethanol anaesthesia. In the same experiments, the excretion of oxytocin-like radioimmunoreactivity (OLRI) was also measured as an indicator of oxytocin release (Bisset et al., 1989; 1990b).

Methods

The experiments were carried out on Wistar rats under ethanol anaesthesia in which a constant fluid load equivalent to 8% body weight (220–230 g) was maintained. This produced a sustained diuresis. Drugs were injected i.v. (0.1–0.4 ml) into an external jugular vein or i.c.v. (1–4 μl) into a lateral cerebral ventricle. Blood pressure was recorded from a femoral artery. The hypotensive response to sodium nitroprusside was integrated to provide a count comprising both amplitude and duration. The trachea was cannulated to maintain a free airway but artificial ventilation was not applied; amyl nitrite was administered by inhalation through the tracheal cannula. Urine flow was recorded from the cannulated bladder with a drop counter set to a 1 min time base. Samples of urine (5 ml) were collected during a control period at the start of each experiment, as soon as a steady diuresis had been achieved, and immediately after each drug injection. The antidiuretic response to nicotine, muscarine and HS, all of which produced a pressor response, was calculated as the percentage reduction in urine flow from the expression 100 (A – B) ÷ A, where A is the control rate of flow immediately before the injection and B the mean rate of flow during the period in which the 5 ml urine sample was collected after the injection. In calculating the antidiuretic response to sodium nitroprusside, the initial antidiuresis resulting from the renal vascular reponse to hypotension (Bisset & Chowdrey, 1984) was discounted. At the end of the collection, each sample of urine was acidified by the addition of 0.5 ml 1 M formic acid and stored at 4°C until extracted. Extracts were prepared with octadecasilyl silica (La Rochelle et al., 1980) for estimation by radioimmunoassay of the content of vasopressin (AVP) and oxytocin-like radioimmunoreactivity (OLRI). Urinary excretion of vasopressin and OLRI is expressed as the total amount (pg) contained in a 5 ml sample of urine. Full experimental details have been published (Bisset & Chowdrey, 1984; Bisset et al., 1990b). In all experiments with nicotine, except those illustrated in Figure 9, atropine 200 μg was given i.v. at the start of the experiment to prevent hypotension resulting from stimulation of parasympathetic ganglia which might have caused reflex release of vasopressin.

Drugs

Drugs used were nicotine hydrogen tartrate and sodium nitroprusside (BDH), atropine sulphate, hexamethonium bromide, muscarine chloride and noradrenaline hydrochloride (Sigma), doses of which are expressed in terms of the salts; amyl nitrite vitrellae BPC (Evans); arginine vasopressin (1st International Standard for Arginine Vasopressin for Bioassay); the synthetic vasopressin antagonist, (+)-$[CH_2]_5$ D-Tyr(Et) valyl arginine vasopressin (VAVP) (Manning et al., 1982) and neosurugatoxin (NSTX). The vasopressin antagonist was a generous gift from Dr Manning of the Department of Biochemistry & Molecular Biology, Medical College of Ohio, U.S.A. NSTX was isolated in the School of Pharmaceutical Science, University of Shizuoka by the method of Kosuge et al. (1982). A 100 μg sample of toxin was dissolved in 1 ml of phosphate buffered saline at pH 6.5 and dispensed into 10 aliquots of 100 μl each containing 10 μg which were stored at −20°C until use. All further dilutions were made with phosphate buffered saline.

Statistics

Results are expressed as mean ± s.e.mean. Significance of differences between means was determined by Student's t test, using a paired (Figures 3, 8 and 9) or unpaired (Figure 6) test as appropriate. A level of $P<0.05$ was taken to be significant.

Results

Nicotine i.v. produced an antidiuretic and a pressor response with increased urinary excretion of both vasopressin and OLRI. The threshold dose for an antidiuretic response (ADR) was 50 μg: a dose of 200 μg frequently caused apnoea. A standard dose of 100 μg was adopted which did not cause apnoea in any experiment. Figure 1 compares the antidiuretic and pressor responses to 100 μg nicotine i.v. and 0.5 and 1.0 ng vasopressin i.v before (a) and after (b) the injection i.v. of a synthetic vasopressin antagonist, (+)-$[CH_2]_5$ D-Tyr(Et) VAVP, which blocks both the V_1 (vascular) and V_2 (renal) receptors. In (a) the ADR to nicotine was similar to that produced by 1 ng vasopressin but the pressor response to nicotine was much larger and more prolonged. In (b) the antagonist blocked the antidiuretic and pressor responses to vasopressin but the pressor response to nicotine was unchanged and accompanied by a pronounced diuresis.

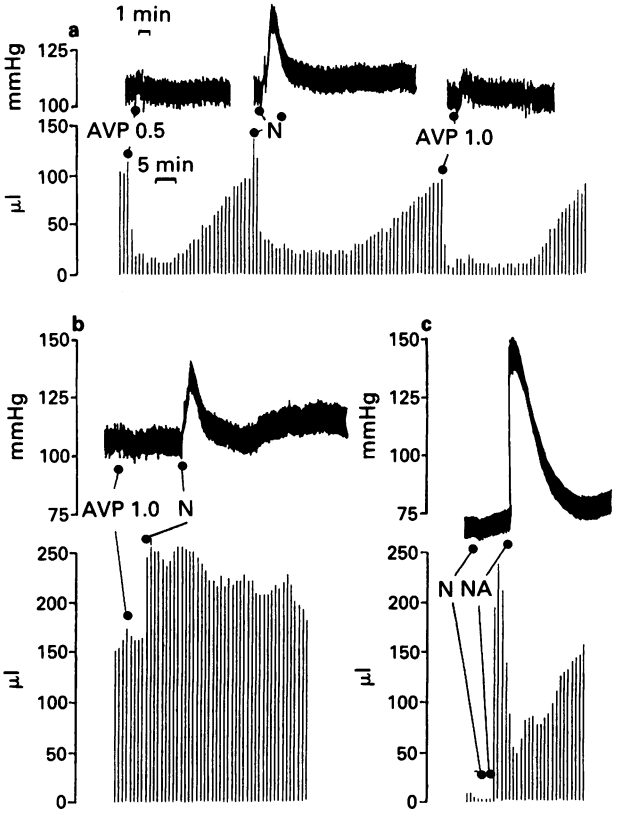

Figure 1 Blood pressure (upper traces) and urine flow (lower traces) in a water-loaded rat under ethanol anaesthesia. Each vertical line in the lower traces indicates the urine flow (μl) in 1 min. AVP = arginine vasopressin, 0.5 and 1.0 ng; N = nicotine, 100 μg; NA = noradrenaline, 1 μg. Between (a) and (b), 4 μg (+)-$[CH_2]_5$ D-Tyr (Et) VAVP was injected, and, between (b) and (c) 4 mg hexamethonium. All injections i.v.

Between (b) and (c), hexamethonium 4 mg was injected i.v.; this caused a large and sustained fall of blood pressure and antidiuresis. The pressor response to nicotine was abolished; the i.v. injection of 1 μg noradrenaline then produced a rise of blood pressure and diuresis. In similar experiments the threshold dose of NSTX i.v. for producing a fall of blood pressure was 200 ng; a dose of 8 μg i.v. blocked the pressor response to nicotine. The vasopressin antagonist was tested in five experiments and there was no significant difference between the pressor responses to nicotine before (41 mmHg ± 7.05) and after (38 mmHg ± 7.05) the antagonist.

Three series of experiments were carried out to test for an inhibitory effect of NSTX i.c.v. on the responses to nicotine. In the first series, three successive injections of nicotine i.v. were given to each of five rats. Four responded to 100 μg; in the fifth the dose was increased to 200 μg without causing apnoea. The first injection served as a control; 5 min before the second injection a single dose of 40 ng NSTX was injected i.c.v. One of these experiments is illustrated in Figure 2. The second injection of nicotine, N2, produced a smaller pressor response than the first injection, N1, a greatly reduced urinary excretion of vasopressin and only a small ADR. The pressor response to the third injection, N3, was considerably less than that to N2 and accompanied by a diuresis with a urinary excretion of vasopressin less than in a control sample of urine, C, collected at the beginning of the experiment before the first injection of nicotine. The urinary excretion of OLRI, in contrast with that of vasopressin showed little change. The mean values for the five experiments are shown in Figure 3. There was a significant difference in both the antidiuretic and pressor responses between N1 and N2 and between N2 and N3; N2 produced a significantly smaller urinary excretion of vasopressin than N1 and N3 did not differ significantly from the control. Although the urinary excretion of OLRI showed some decline from N1 to N2 and from N2 to N3, the differences were not significant.

Control experiments were carried out to test whether the diminished response to successive injections of nicotine could have been due to tachyphylaxis rather than an inhibitory effect of NSTX. Figure 4 illustrates an experiment in which two injections of nicotine at an interval of 60 min produced almost identical responses. However, tachyphylaxis was observed in three experiments in which the first injection of

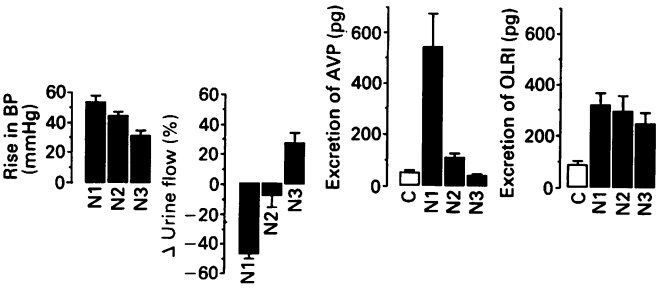

Figure 3 Summary of results of 5 experiments including that illustrated in Figure 2 and with the same protocol and abbreviations. The mean interval between injections of nicotine N1 and N2 was 101 min and between N2 and N3, 82 min. The columns show mean responses with s.e. indicated by vertical bars.

nicotine produced an exceptionally prolonged ADR and subsequent injections were given after only a partial recovery. One of these experiments is illustrated in Figure 5. The first injection of 100 μg of nicotine produced an extremely large rise of blood pressure and a persistent ADR. Although an interval of 65–75 min was allowed between injections there was a progressive decline in the pressor and antidiuretic responses and in the urinary excretion of vasopressin. The fourth injection produced a diuresis although the urinary excretion of vasopressin was still increased compared with the control. In contrast with vasopressin, the increased urinary excretion of OLRI did not decline. In the experiments of Figure 3, nicotine was injected at intervals of 65–140 min and the urine flow recovered completely between injections. However, in three of these experiments, the first injection of nicotine resulted in a relatively prolonged ADR which might have induced tachyphylaxis. Therefore, in order to exclude any possibility of tachyphylaxis, a second series of experiments was carried out (Figure 6) in which a single injection of 100 μg nicotine was examined in two groups of rats. The first group served as a control. Each rat in the test

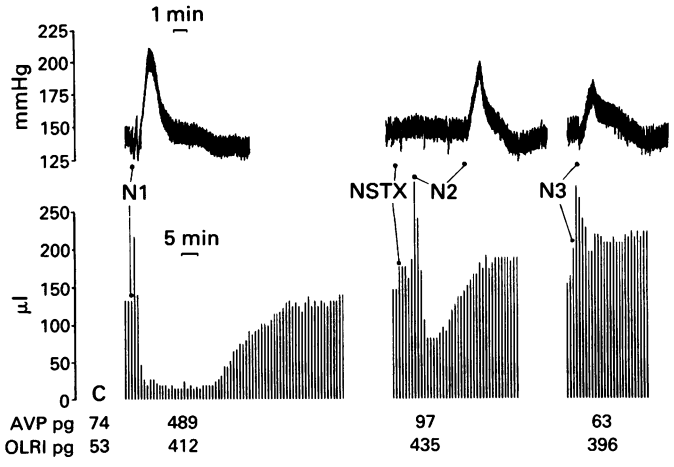

Figure 2 Blood pressure and urine flow in a water-loaded rat under ethanol anaesthesia, recorded as in legend to Figure 1. Three successive injections of nicotine, 100 μg i.v., (N1, N2 and N3) were given; the interval between N1 and N2 was 75 min; and between N2 and N3, 65 min. Neosurugatoxin (NSTX) 40 ng i.c.v. was injected 5 min before N2. Arginine vasopressin (AVP) and oxytocin-like radioimmunoreactivity (OLRI); total amount (pg) excreted in a 5 ml control sample of urine (C) collected at the start of the experiment, before N1, or in 5 ml samples collected after the injections of nicotine.

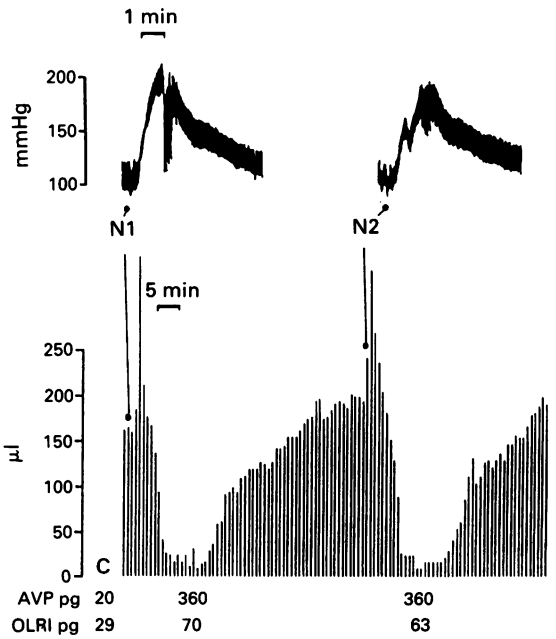

Figure 4 Water-loaded rat under ethanol anaesthesia. The effect of 2 injections of nicotine, 100 μg i.v. (N1 and N2), at an interval of 60 min, on urine flow and blood pressure recorded as in legend to Figure 1, and on urinary excretion of arginine vasopressin (AVP) and oxytocin-like immunoradioactivity (OLRI) in 5 ml samples of urine: C = control. Note the absence of tachyphylaxis.

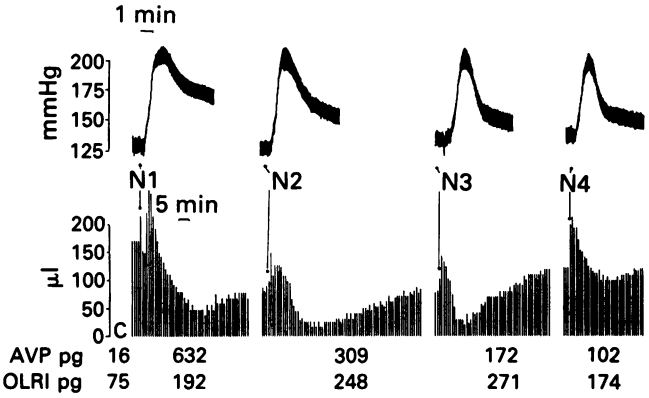

Figure 5 Similar experiment to that in Figure 4 with four successive injections of nicotine, 100 µg i.v. (N1, N2, N3 and N4) at intervals of 65–75 min. The antidiuretic response to N1 had not fully recovered when N2 was given. The pressor and antidiuretic responses and the urinary excretion of arginine vasopressin (AVP) exhibited tachyphylaxis but not the excretion of oxytocin-like immunoreactivity (OLRI): C = control.

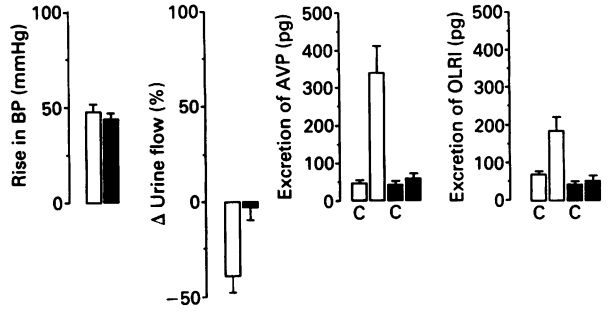

Figure 6 Results of experiments on 10 control (open columns) and 6 test (solid columns) rats water-loaded under ethanol anaesthesia. All received nicotine 100 µg i.v. The test rats were given 2 injections of neosurugatoxin (NSTX) 40 ng i.c.v., 20 min and 10 min before nicotine. Control samples of urine (C) were collected in each group. The columns show mean responses with s.e. indicated by vertical bars. Excretion of arginine vasopressin (AVP) and oxytocin-like immunoreactivity (OLRI) measured as total amount in 5 ml samples of urine.

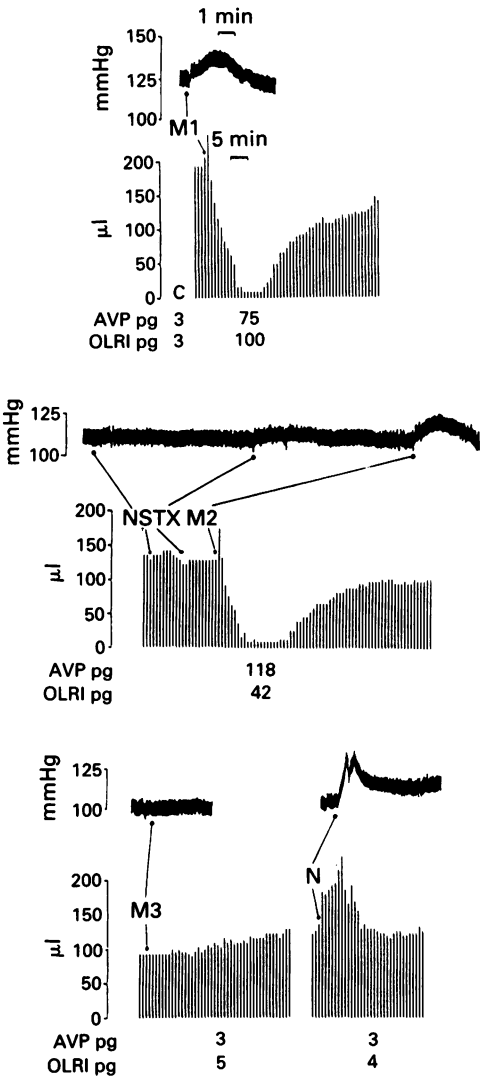

Figure 7 Blood pressure and urine flow in a water-loaded rat under ethanol anaesthesia, recorded as in legend to Figure 1. Three successive injections of muscarine, 20 ng i.c.v. (M1, M2 and M3) were given followed by nicotine (N), 100 µg i.v. Two injections of neosurugatoxin (NSTX) 40 ng i.c.v., were given 20 min and 10 min before M2 and 200 µg atropine i.v. was injected between M2 and M3. Control (C) sampes of urine were collected at the start of the experiment. Excretion of arginine vasopressin (AVP) and oxytocin-like immunoreactivity (OLRI) measured as total amount (pg) in 5 ml samples of urine.

group was given an injection of NSTX i.c.v. before nicotine. Since the response to nicotine was not completely inhibited 5 min after the injection of 40 ng NSTX in the first series of experiments, two injections of 40 ng NSTX were given in the present series, the first 20, and the second 10 min, before nicotine. Only one of the ten rats in the control group failed to respond to 100 µg nicotine. There was no significant difference between the pressor responses in the two groups, but the ADR was almost abolished in the test group. Nicotine increased the excretion of both vasopressin and OLRI significantly in the control group: after NSTX, there was no significant change in either vasopressin or OLRI in response to nicotine.

A third series of experiments was carried out in six rats to test whether NSTX acts selectively on nicotinic receptors. One of these experiments is illustrated in Figure 7, and the mean results of the six experiments are shown in Figure 8. Three injections of 20 ng muscarine i.c.v. (M1, M2 and M3) were given: M1 served as a control; two injections of 40 ng NSTX were given i.c.v. 20 and 10 min before M2 to conform with the procedure used in the second series of experiments and atropine, 200 µg i.v., was given between M2 and M3. Finally the response to nicotine, 100 µg i.v., was tested. Muscarine produced pressor and antidiuretic responses and a significant increase in the urinary excretion of both vasopressin and OLRI: none of these effects was significantly reduced by NSTX but all were abolished by atropine. Nicotine produced a pressor and diuretic response but no increase in the urinary excretion of vasopressin or OLRI; this confirmed that central nicotinic cholinoceptors had been effectively blocked by NSTX. At the end of each experiment an inhalation of amyl nitrite was given to produce hypotension; no antidiuretic response was observed. In contrast, the injection of hypertonic saline (HS; 1.54 M NaCl solution) 4 µl i.c.v. after nicotine in 2 experiments produced pressor and antidiuretic responses with an increase in the urinary excretion of vasopressin to 262 and 279 pg and that of OLRI to 813 and 781 pg. These preliminary results suggested that NSTX might have a differential effect on the release of vasopressin by hypotension and an osmotic stimulus. To investigate this, two further series of experiments were carried out, but using sodium nitroprusside (SN) in preference to amyl nitrite since the hypotensive responses to SN were more reproducible.

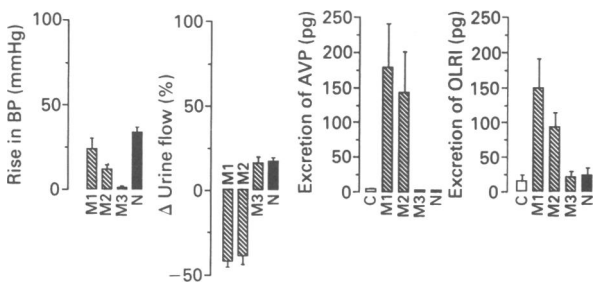

Figure 8 Summary of results of six experiments including that illustrated in Figure 7 and with the same protocol. The columns show mean responses with s.e. indicated by vertical bars.

Doses of 50, 100 and 200 μg SN in the same rat produced graded hypotensive and antidiuretic responses and increases in the urinary excretion of vasopressin. A dose of 200 μg was adopted as standard. Each rat was given two injections of either SN (8 experiments) or hypertonic saline (HS) (6 experiments). NSTX was given before the second injection, the first serving as a control. Two doses of toxin, 40 ng i.c.v. were given at an interval of 10 min, as in the experiments illustrated in Figures 6–8 but, in order to allow for the time to the maximum onset of action, the first NSTX injection was given 60 min before SN or HS. The results are shown in Figure 9. Both SN and HS increased the urinary excretion of OLRI as well as that of vasopressin but the mean vasopressin: OLRI ratio was 5.1 ± 1.3 for SN compared with 1.2 ± 0.24 for HS. After NSTX, SN produced a similar hypotensive response but there was a significant reduction in both the antidiuretic response and the increased urinary excretion of vasopressin. The reduction in the hypotension-induced vasopressin release we not due to tachyphylaxis since, in a control series of experiments in which two injections of SN were given at a similar time interval but without the intervention of NSTX, there was no significant difference in the responses. Interestingly, the increased urinary excretion of OLRI after SN was not reduced by NSTX. In contrast with the effects of a hypotensive stimulus, the responses to HS before and after NSTX were almost identical. Nicotine injected after SN or HS produced pressor and diuretic responses with no significant increase in the urinary excretion of vasopressin or OLRI compared with that in the controls. This demonstrated, as in the experiments illustrated in Figures 6 and 8, an effective block of central nicotinic cholinoceptors.

Discussion

The fact that the antidiuretic response to i.v. nicotine in the rat was accompanied by an increase in the urinary excretion of OLRI as well as vasopressin indicates that both vasopressin and oxytocin are released. This contrasts with the cat in which i.v. nicotine has been shown to release vasopressin alone (Bisset *et al.*, 1975; Bisset & Feldberg, 1977). Many of the actions of nicotine, including the release of vasopressin, exhibit tacahyphylaxis (Paton & Savini, 1968; Bisset & Feld-

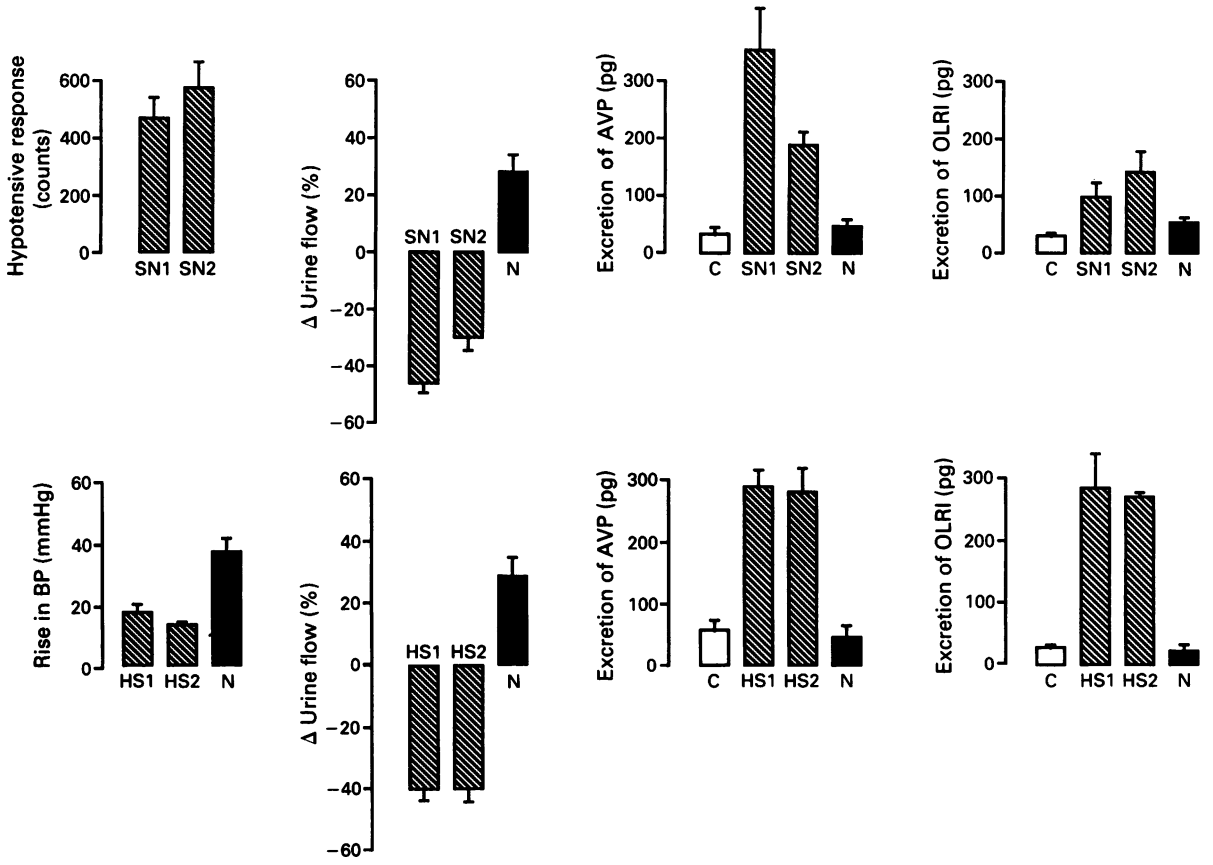

Figure 9 Results of two series of experiments in water-loaded rats under ethanol anaesthesia in which two i.v. injections (SN1 and SN2; $n = 8$) of 200 μg sodium nitroprusside, or two i.c.v. injections (HS1 and HS2; $n = 6$) of 4 μl hypertonic saline (1.54 M NaCl solution) were given in each rat. Two injections of neosurugatoxin (NSTX) 40 ng i.c.v., were given 60 and 50 min before SN2 and HS2. Nicotine, 100 μg i.v., was injected after SN2 and HS2 to test for the effectiveness of NSTX in blocking nicotinic cholinoceptors. A control sample of urine (C) was collected at the start of each experiment. Columns show mean responses with s.e. indicated by vertical bars. Excretion of arginine vasopressin (AVP) and oxytocin-like immunoreactivity (OLRI) measured as total amount in 5 ml samples of urine. The hypotensive response to SN is measured as an integrated count (see Methods).

berg, 1977; Wonnacott, 1990). In the present investigation, tachyphylaxis was observed in those control experiments in which the first injection of nicotine produced a relatively prolonged antidiuretic response with only partial recovery of the urine flow before the next injection. It is interesting to note however that, although the urinary excretion of vasopressin declined progressively with successive injections of nicotine in these experiments, the excretion of OLRI was unchanged. Also, in the first series of experiments in which three successive injections of nicotine were given in one rat, the second after 40 ng NSTX, the decline in the excretion of vasopressin with the second and third injections was not accompanied by any significant decrease in the excretion of OLRI. This dissociation emphasises the independence of the neural mechanisms which control the release of vasopressin and oxytocin. The possibility cannot be excluded that the results obtained in the first series of experiments were due at least in part to tachyphylaxis. However, the results obtained in the second and third series of experiments in which each rat received only one injection of nicotine and a larger dose of 80 ng NSTX was used, show unequivocally that this dose of NSTX blocks the release of both vasopressin and oxytocin by nicotine and that this inhibitory effect persists for at least 3 h. This prolonged block is consistent with a report that NSTX may irreversibly inactivate nicotine binding sites *in vitro* (Yamada *et al.*, 1985) and that inhibition of nicotine binding *in vivo* persists up to 7 days after i.c.v. injection of NSTX (Yamada *et al.*, 1988a).

Agonists acting on muscarinic cholinoceptors have been shown to release vasopressin and oxytocin in the rat and this release is blocked by atropine (Kühn & McCann, 1971; Kühn, 1974; Clarke & Merrick, 1978; Bisset & Chowdrey, 1984; Iitake *et al.*, 1986; Shoji *et al.*, 1989). In our experiments, NSTX acted selectively on nicotinic, and not on muscarinic, receptors. The antidiuretic response to muscarine and the increased urinary excretion of vasopressin and OLRI which were blocked by atropine were not inhibited by doses of NSTX which blocked the response to nicotine in the same experiments.

Since the pressor response which accompanied the antidiuretic response to i.v. nicotine was blocked by i.v. hexamethonium but not by a vasopressin antagonist, it is due not to release of vasopressin but to stimulation of the sympathetic nervous system. The partial inhibition of this response by only 80 ng NSTX i.c.v. could not have been caused by a peripheral sympathetic block since the minimum dose of NSTX i.v. to block the pressor response to i.v. nicotine was 8 μg. This suggests that the pressor response is mediated in part by central sympathetic stimulation which is blocked by NSTX. In many experiments in which NSTX blocked the release of vasopressin, the residual pressor response was accompanied by diuresis, probably caused by an effect on renal haemodynamics of catecholamines released by the peripheral component of sympathetic stimulation.

Hypotension induced with i.v. sodium nitroprusside (SN) and an osmotic stimulus consisting of i.c.v. hypertonic saline (HS) caused an increase in the urinary excretion of vasopressin and OLRI, although not in the same ratio. This implies release of both vasopressin and oxytocin. A species difference is again involved since, in the cat, hypotension, haemorrhage, carotid occlusion and i.c.v. HS have all been shown to release vasopressin without oxytocin (Bisset *et al.*, 1989). Changes in blood pressure are monitored by peripheral receptors in the cardiovascular system (for review see Bisset & Chowdrey, 1988) which have an afferent input to the nucleus of the tractus solitarius (NTS) on the dorsal surface of the medulla. The NTS projects to the A1 group of noradrenergic neurones on the ventral surface which, in turn, selectively innervate the vasopressin-secreting cells in the supraoptic and paraventricular nuclei (SON and PVN) either directly or indirectly through the lateral preoptic nucleus (LPN) (Banks & Harris, 1984). It is now thought that this group of neurones is coincident with the nicotine sensitive area which has been defined on the ventral surface of the medulla in the cat (Bisset *et al.*, 1975). Topical application of nicotine to this area causes a release of vasopressin without oxytocin which is blocked by hexamethonium (Bisset & Feldberg, 1977). The LPN, which is a part of the magnocellular basal nucleus lying dorsolateral to the SON provides the only known cholinergic input to this nucleus (Mason *et al.*, 1983; Hatton & Mason, 1985). Electrical stimulation in the region of the LPN causes an excitation of the vasopressin-secreting neurones in the SON which is blocked by hexamethonium (Hatton *et al.*, 1983). Intracellular recording from the neurones innervated by the LPN demonstrated depolarization after microperfusion with acetylcholine and this effect also was blocked by hexamethonium (Cobbett *et al.*, 1986). The SON was stained with a monoclonal antibody to the α sub-unit of the nicotinic receptor (Mason, 1985). However, a recent immunocytochemical study involving both light and electron microscopy failed to demonstrate a direct innervation of the cell bodies and dentrites in the SON and PVN by cholinergic synapses (Theodosis & Mason, 1988). This suggests the possibility of intervening neurones (Tribollet *et al.*, 1985; Raby & Renaud, 1989a; Pow & Morris, 1989; Jhamandas *et al.*, 1989; Renaud & Bourque, 1991) and is consistent with the finding that binding sites for nicotine and acetylcholine lie predominantly outside the SON and PVN (Clarke *et al.*, 1985; Sharp *et al.*, 1987; Härfstrand *et al.*, 1988). In previous work (Bisset & Chowdrey, 1984) we showed that i.c.v. hexamethonium blocked the antidiuretic response to amyl nitrite in the water-loaded rat preparation, although it has been reported not to inhibit the release of vasopressin by non-hypotensive or hypotensive haemorrhage (Iitake *et al.*, 1989). In the present experiments, i.c.v. NSTX, in the same dose which blocked the release of vasopressin and oxytocin by nicotine, blocked the antidiuretic response to amyl nitrite and caused a significant reduction in the antidiuretic response to SN and in the increased urinary excretion of vasopressin. This suggests that NSTX acts on the same or a similar type of receptor to that on which hexamethonium acts and confirms the existence of one or more cholinergic synapses in the central neural pathways controlling the release of vasopressin by hypotension. These synapses are probably the site of action of nicotine in releasing vasopressin and of NSTX in blocking this release. In contrast with vasopressin, the release of oxytocin by hypotension was not inhibited by NSTX. This is consistent with the absence of any direct cholinergic input to the oxytocin-secreting cells in the SON and PVN and with the recent suggestion that the release of oxytocin may be controlled by a direct projection from the NTS to the oxytocin-secreting cells in which the transmitter at the final synapse is not acetylcholine or noradrenaline but the peptide inhibin β (Sawchenko *et al.*, 1988; Raby & Renaud, 1989a,b,; Bourque & Renaud, 1990; Renaud & Bourque, 1991). It is conceivable that nicotine may cause release of oxytocin by stimulating this efferent projection from the NTS.

The osmotic control of vasopressin release is still controversial. The main issue is whether the SON itself functions as an osmoreceptor or receives an afferent neural input from extraneous osmoreceptors in the circumventricular organs (Bisset & Chowdrey, 1988; Bisset *et al.*, 1990a). The entire system may be integrated in an 'osmoreceptor complex' (Honda *et al.*, 1990). Sladek & Joynt (1979) produced evidence from *in vitro* work with hypothalamic explants for a cholinergic input to the vasopressin-secreting cells in the SON from the organum vasculosum laminae terminalis (OVLT). Excitation of neurosecretory cells in the PVN by intracarotid HS was inhibited by microionophoretic application of hexamethonium and atropine (Akaishi & Negoro, 1983). In the water-loaded rat preparation, both hexamethonium and atropine failed to block the release of vasopressin by i.c.v. HS (Bisset *et al.*, 1988) and, in the present experiments, NSTX, in a dose which effectively inhibited release by nicotine or hypotension, caused no reduction in the excretion of either vasopressin or OLRI after i.c.v. HS.

Similarly, Iitake *et al.* (1989) reported that doses of i.c.v. hexamethonium and atropine which blocked the release of vasopressin in response to i.c.v cholinoceptor agonists, did not block release by i.v. HS in conscious rats. There is, therefore, no evidence for a cholinergic link in osmotic control *in vivo*.

In conclusion, we have shown that NSTX, which is known to block peripheral nicotinic cholinoceptors in autonomic ganglia and the adrenal medulla, also acts centrally to block the release of vasopressin and oxytocin by nicotine. It inhibits the release of vasopressin but not that of oxytocin by hypotension and has no effect on the release of either hormone by an osmotic stimulus. Our experiments provide further evidence for a central action of NSTX on nicotinic cholinoceptors and illustrate its potential for elucidating cholinergic pathways in the CNS.

Part of this work was supported by an MRC project grant to G.W.B. We thank Miss A. Basham and Miss C. Gilsenan for typing the manuscipt.

References

AKAISHI, T. & NEGORO, H. (1983). Effects of microelectrophoretically applied acetylcholine- and angiotensin-antagonists on the paraventricular neurosecretory cells excited by osmotic stimuli. *Neurosci. Lett.*, **36**, 157–161.

ASCHER, P., LARGE, W.A. & RANG, H.P. (1979). Studies on the mechanism of acetylcholine antagonists on rat parasympathetic ganglion cells. *J. Physiol.*, **295**, 139–170.

BANKS, D. & HARRIS, M.C. (1984). Lesions of the locus coeruleus abolish baroreceptor-induced depression of supraoptic neurones in the rat. *J. Physiol.*, **355**, 383–398.

BILLIAR, R.B., KALASH, J., ROMITA, V., TSUJI, K. & KOSUGE, T. (1988). Neosurugatoxin: CNS acetylcholine receptors and luteinizing hormone secretion in ovariectomized rats. *Brain Res. Bull.*, **20**, 315–322.

BISSET, G.W. & CHOWDREY, H.S. (1984). A cholinergic link in the reflex release of vasopressin by hypotension in the rat. *J. Physiol.*, **354**, 523–545.

BISSET, G.W. & CHOWDREY, H.S. (1988). Control of release of vasopressin by neuroendocrine reflexes. *Q. J. Exp. Physiol.*, **73**, 811–872.

BISSET, G.W. & FELDBERG, W. (1977). Effect of hexamethonium on the release of vasopressin by nicotine and carotid occlusion. *J. Physiol.*, **267**, 30–31P.

BISSET, G.W., CHOWDREY, H.S. & FELDBERG, W. (1990a). The effect of an osmotic stimulus on the release of neurohypophysial hormones in the cat: preferential release of vasopressin with a possible involvement of the area postrema. *J. Neuroendocr.*, **2**, 201–207.

BISSET, G.W., CHOWDREY, H.S., FAIRHALL, K.M. & GUNN, L.K. (1988). Is there a cholinergic link in vivo mediating the osmotic release of vasopressin in the rat? *J. Physiol.*, **398**, 82P.

BISSET, G.W., CHOWDREY, H.S., FAIRHALL, K.M., FELDBERG, W. & GUNN, L.K. (1989). Osmotic control of release of vasopressin and oxytocin in the cat and rat. *Proceedings of the Fourth International Conferrence on the Neurohypophysis.* pp. 83–86. Oxford: Oxford Community Press.

BISSET, G.W., CHOWDREY, H.S., FAIRHALL, K.M. & GUNN, L.K. (1990b). Central inhibition of γ-aminobutyric acid and muscimol of the release of vasopressin and oxytocin by an osmotic stimulus in the rat. *Br. J. Pharmacol.*, **99**, 529–535.

BISSET, G.W., FELDBERG, W., GUERTZENSTEIN, P.G. & ROCHA E SILVA, JR (1975). Vasopressin release by nicotine: the site of action. *Br. J. Pharmacol.*, **54**, 463–474.

BOURKE, J.A., BUNN, S.J., MARLEY, P.D. & LIVETT, B.G. (1988). The effects of neosurugatoxin on evoked catecholamine secretion from bovine adrenal chromaffin cells. *Br. J. Pharmacol.*, **93**, 275–280.

BOURQUE, C.W. & RENAUD, L.P. (1990). Electrophysiology of mammalian magnocellular vasopressin and oxytocin neurosecretory neurons. *Frontiers in Neuroendocrinology*, **11**, 183–212.

BROWN, D.A., GARTHWAITE, J., HAYASHI, E. & YAMADA, S. (1976). Action of surugatoxin on nicotine receptors in the superior cervical ganglion of the rat. *Br. J. Pharmacol.*, **58**, 157–159.

BURN, J.H., TRUELOVE, L.H. & BURN, I. (1945). Antidiuretic action of nicotine and of smoking. *Br. Med. J.*, **i**, 403–406.

CLARKE, G. & MERRICK, L.P. (1978). Tentative identification of the synaptic transmitters involved in the neural regulation of oxytocin release. *J. Physiol.*, **277**, 19–20P.

CLARKE, P., SCHWARTZ, R., PAUL, S., PERT, C. & PERT, A. (1985). Nicotinic binding in rat brain: autoradiographic comparison of [^{3}H] acetylcholine, [^{3}H] nicotine and [^{125}I] alpha-bungarotoxin. *J. Neurosci.*, **5**, 1307–1315.

COBBETT, P.J.R., MASON, W.T. & POULAIN, D.A. (1986). Intracellular analysis of control of rat supraoptic neurone (SON) activity in vitro by acetylcholine (ACh). *J. Physiol.*, **371**, 216P.

HÄRFSTRAND, A., ADEM, A., FUXE, K., AGNATI, L. ANDERSSON, K. & NORDBERG, A. (1988). Distribution of nicotinic cholinergic receptors in the rat tel- and diencephalon: a quantitative receptor autoradiographical study using [^{3}H]- acetylcholine, [α-^{125}] bungarotoxin and [^{3}H]nicotine. *Acta Physiol. Scand.*, **132**, 1–14.

HATTON, G.I. & MASON, W.T. (1985). Acetylcholine input to vasopressin neurones in the hypothalamus. In *Vasopressin.* ed. Schrier, R.W. pp. 361–366. New York: Raven Press.

HATTON, G.I., HO, Y.W. & MASON, W.T. (1983). Synaptic activation of phasic bursting in rat supraoptic nucleus neurones recorded in hypothalamic slices. *J. Physiol.*, **345**, 297–317.

HAYASHI, E., ISOGAI, M., KAGAWA, Y. & YAMADA, S. (1983). Characterization of central nicotinic receptors by [^{3}H]-nicotine: effect of neosurugatoxin. *Jpn. J. Pharmacol.*, (Suppl.) **33**, 89P.

HAYASHI, E., ISOGAI, M., KAGAWA, Y., TAKAYANAGI, N. & YAMADA, S. (1984). Neosurugatoxin, a specific antagonist of nicotinic acetylcholine receptors. *J. Neurochem.*, **42**, 1491–1494.

HAYASHI, E. & YAMADA, S. (1975). Pharmacological studies on surugatoxin, the toxic principle from Japanese ivory mollusuc (*Babylonia japonica*). *Br. J. Pharmacol.*, **53**, 207–215.

HIRAYAMA, H., GOHGI, K., URAKAWA, N. & IKEDA, M. (1970). A ganglion-blocking action of the toxin isolated from Japanese ivory shell (*Babylonia japonica*) *Jpn. J. Pharmacol.*, **20**, 311–312.

HIRAYAMA, H., SUGIHARA, K., TSUYAMA, S., WAKIGAWA, K., OHKUMA, H. & GOHGI, K. (1974). A ganglion blocking action of toxic substances, IS-toxin and surugatoxin, from the Japanese ivory shell (*Babylonia japonica*). *Jpn. J. Pharmacol.*, **24**, 599–574.

HONDA, K., NEGORO, H., DYBALL, R.E.J., HIGUCHI, T. & TAKANO, S. (1990). The osmoreceptor complex in the rat: evidence for intersections between the supraoptic and other diencephalic nuclei. *J. Physiol.*, **431**, 225–241.

IITAKE, K., SHARE, L., OUCHI, Y., CROFTON, J.T. & BROOKS, D.P. (1986). Central cholinergic control of vasopressin release in conscious rats. *Am. Physiol. Soc.*, **251**, E146–E150.

IITAKE, K., SHARE, L., BROOKS, D.P., CROFTON, J.T. & OUCHI, Y. (1989). Role of brain acetylcholine in vasopressin release during osmotic stimulation and haemorrhage. *Exp. Brain. Res.*, **75**, 47–52.

JHAMANDAS, J.H.., RABY, W., ROGERS, J., BUIJS, R.M. & RENAUD, L.P. (1989). Diagonal band projection towards the hypothalamic supraoptic nucleus: light and electron microscopic observations in the rat. *J. Comp. Neurol.*, **282**, 15–23.

KOSUGE, T., ZENDA, H., OCHIAI, A., MASAKI, N., NOGUCHI, M., KIMURA, S. & NARITA, H. (1972). Isolation and structure determination of a new marine toxin, surugatoxin from the Japanese ivory shell, *Babylonia japonica. Tetrahedron Letts.*, **25**, 2545–2548.

KOSUGE, T., TSUJI, K., HIRAI, K., YAMAGUCHI, K., OKAMOTO, T. & IITAKA, Y. (1981). Isolation and structure determination of a new marine toxin, neosurugatoxin, from the Japanese ivory shell, *Babylonia japonica. Tetrahedron Letts.*, **35**, 3417–3420.

KOSUGE, T., TSUJI, K. & HIRAI, K. (1982). Isolation of neurosurugatoxin from the Japanese ivory shell, *Babylonia japonica. Chem. Pharmacol. Bull*, **30**, 3255–3259.

KÜHN, E.R. (1974). Cholinergic and adrenergic release mechanism for vasopressin in the male rat: a study with injections of neurotransmitters and blocking agents into the third ventricle. *Neuroendocrinol.*, **16**, 255–264.

KÜHN, E.R. & MCCANN, S.M. (1971). Release of oxytocin and vasopressin in laboratory rats after injection of carbachol into the third ventricle. *Neuroendocrinol.*, **8**, 48–58.

LA ROCHELLE, F.T., NORTH, W.G. JR & STERN, P. (1980). A new extraction of arginine vasopressin from blood. The use of octadecasilyl silica. *Pflügers Arch.*, **387**, 79–81.

MANNING, M., OLMA, A., KLIS, W.A., KOLODZIEJCZYK, M., SETO, J. & SAWYER, W.H. (1982). Design of more potent antagonists of the antidiuretic responses to arginine vasopressin. *J. Med. Chem.*, **25**, 45–50.

MASON, W.T. (1985). Staining of the magnocellular nuclei of the rat hypothalamus by a monoclonal antibody directed against the α-subunit of the nicotinic cholergic receptor. *Neurosci. Letts.*, **59**, 89–95.

MASON, W.T., HO, Y.W., ECKENSTEIN, F. & HATTON, G.I. (1983). Mapping of cholinergic neurones associated with rat supraoptic nucleus: combined immunocytochemical and histochemical identification. *Brain Res. Bull.*, **11**, 617–626.

PATON, W.D.M. & SAVINI, E.C. (1968). The action of nicotine on the motor endplate in the cat. *Br. J. Pharmacol. Chemother.*, **32**, 360–380.

POW, D.V. & MORRIS, J.F. (1989). Differential distribution of acetyl cholinesterase activity among vasopressin- and oxytocin-containing supraoptic magnocellular neurones. *Neuroscience*, **28**, 109–119.

RABY, W.N. & RENAUD, L.P. (1989a). Dorsomedial medulla stimulation activates rat supraoptic oxytocin and vasopressin neurones through different pathways. *J. Physiol.*, **417**, 279–294.

RABY, W.N. & RENAUD, L.P. (1989b). Nucleus tractus solitarius innervation of supraoptic nucleus: anatomical and electrophysiological studies in the cat suggest differential innervation of oxytocin and vasopressin neurones. *Prog. Brain Res.*, **81**, 319–332.

RAPIER, C., HARRISON, R., LUNT, G.G. & WONNACOTT, S. (1985). Neosurugatoxin blocks nicotinic acetylcholine receptors in the brain. *Neurochem. Int.* **7**, 389–396.

RENAUD, L.P. & BOURQUE, C.W. (1991). Neurophysiology and neuropharmacology of hypothalamic magnocellular neurones secreting vasopressin and oxytocin. *Prog. Neurobiol.*, **36**, 131–169.

SAWCHENKO, E., PLOTSKY, P.M., PFEIFFER, S.W., CUNNINGHAM, T. Jr., VAUGHAN, J., RIVIER, J. & VALE, W. (1988). Inhibit β in central neural pathways involved in control of oxytocin secretion. *Nature*, **334**, 615–617.

SHARP, B.M., NICOL, S., CUMMINGS, S. & SEYBOLD, V. (1987). Distribution of nicotinic binding sites with respect to CRF and neurophysin immunoreactive perikarya within the rat hypothalamus. *Brain Res.*, **422**, 361–366.

SHOJI, M., SHARE, L., CROFTON, J.T. & BROOKS, D.P. (1989). The effect on vasopressin release of microinjection of cholinergic agonists into the paraventricular nucleus of conscious rats. *J. Neuroendocrinol.*, **1**, 401–406.

SLADEK, C.D. & JOYNT, R.J. (1979). Characterization of cholinergic control of vasopressin release by the organ-cultured rat hypothalamo-neurohypophysial system. *Endocrinol.*, **104**, 659–663.

THEODOSIS, D.T. & MASON, W.T. (1988). Choline acetyltransferase immunocytochemical staining of the rat supraoptic nucleus and its surroundings: a light- and electron microscope study. *Cell Tissue Res.*, **254**, 119–124.

TRIBOLLET, E., ARMSTRONG, W.E., DUBOIS-DAUPHIN, M. & DREIFUSS, J.J. (1985). Extra-hypothalamic afferent inputs to the supraoptic nucleus area of the rat as determined by retrograde and anterograde straining techniques. *Neuroscience*, **15**, 135–148.

WADA, A., UEZONOA, Y., ARITA, M., TSUJI, K., YANAGIHARA, N., KOBAYASHI, H. & IZUMI, F. (1989). High-affinity and selectively of neosurugatoxin for the inhibition of ^{22}Na influx via nicotinic receptor-ion channel in cultured bovine adrenal medullary cells: comparative study with histrionicotoxin. *Neurosci.*, **2**, 333–339.

WONNACOTT, S. (1990). The paradox of nicotinic acetylcholine receptor upregulation by nicotine. *Trends Pharmacol. Sci.*, **11**, 216–219.

YAMADA, S., ISOGAI, M., KAGAWA, T., TAKAYANAGI, N., HAYASHI, E., TSUJI, K. & KOSUGE, T. (1985). Brain nicotinic acetylcholine receptors. Biochemical characterization by neosurugatoxin. *Mol. Pharmacol.*, **28**, 120–127.

YAMADA, S., USHIJIMA, H., NAKAYAMA, K., HAYASHI, E., TSUJI, K. & KOSUGE, T. (1988a). Intracellular injection of neosurugatoxin induces a prolonged blockade of brain nicotinic acetycholine receptors. *Eur. J. Pharmacol.*, **156**, 279–282.

YAMADA, S., KAGAWA, Y., TAKAYAMA, K., HAYASHI, E., TSUJI, K. & KOSUGE, T. (1988b). Inhibition by neosurugatoxin of nicotine-induced anti-nociception. *Brain Res.*, **375**, 360–362.

(Received December 20, 1991
Revised March 12, 1992
Accepted March 16, 1992)

Br. J. Pharmacol. (1992), **106**, 693–696

Identification and distribution of 5-HT_3 recognition sites in the rat gastrointestinal tract

[1]S. Champaneria, B. Costall, R.J. Naylor & *D.W. Robertson

Postgraduate Studies in Pharmacology, School of Pharmacy, University of Bradford, Bradford, West Yorkshire, BD7 1DP and *Lilly Research Laboratories, Eli Lilly and Company, Lilly Corporate Centre, Indianapolis, Indiana 46285, U.S.A.

1 Tritiated derivatives of the potent and selective 5-HT_3 receptor antagonists GR65630 and LY278584 were used to identify 5-HT_3 recognition sites in the rat gastrointestinal tract.

2 Binding studies were carried out in homogenates of the rat oesophagus, the cardia, fundus, body and antrum of the stomach, regions of the small intestine, caecum and large intestine. The specific binding of a single concentration of GR65630 (0.5 nM) defined by granisetron (10 μM) in these areas indicated that the density of 5-HT_3 recognition sites varied from 2.4 ± 1.0 to 10.1 ± 1.0 fmol mg^{-1} protein.

3 Saturable binding of [^{3}H]-GR65630 could only be demonstrated in the terminal regions of the small intestine (B_{max} in the range of 13.83 ± 4.54–21.19 ± 0.89 fmol mg^{-1} protein; mean ± s.e.mean) and of high affinity (K_d in the range of 0.42 ± 0.18–0.79 ± 0.24 nM). Use of [^{3}H]-LY278584 revealed a similar binding density (B_{max} 19.54 ± 0.26 fmol mg^{-1} protein) and affinity (K_d 1.04 ± 0.07 nM) in the terminal small intestine.

4 Binding of [^{3}H]-GR65630 and [^{3}H]-LY278584 to the terminal region of the small intestine was inhibited by 5-HT_3 receptor ligands ondansetron and S-zacopride (and 5-hydroxytryptamine), but not by 5-HT_1, 5-HT_2, catecholamine, γ-aminobutyric acid and opioid receptor ligands.

5 These data demonstrate that there are regional variations in the density of 5-HT_3 recognition sites within the rat gastrointestinal tract. Such data are relevant to the potential use of 5-HT_3 receptor ligands to modify secretory and contraction responses in the gastrointestinal system.

Keywords: 5-HT_3 recognition sites; [^{3}H]-GR65630; [^{3}H]-LY278584; rat intestine

Introduction

A neuronally located 5-hydroxytryptamine (5-HT) receptor mediating transmitter release was first identified in the guinea-pig ileum by Gaddum & Picarelli (1957). Subsequent studies established that 5-HT receptors are widely distributed on peripheral nerves (see review by Richardson & Engel, 1986), and the development of selective antagonists for the 5-HT receptor subtypes has allowed characterization and designation of this neuronal receptor as the 5-HT_3 receptor (see Bradley *et al.*, 1986). The characterization was based on an antagonism by 5-HT_3 receptor antagonists such as MDL72222, ICS205-930 and ondansetron of the effects of 5-HT to induce, for example, neuronal depolarization of the isolated vagus nerve, superior cervical ganglion and the von Bezold Jarisch reflex (Fozard, 1984; Richardson *et al.*, 1985; Butler *et al.*, 1988). This initial pharmacological characterization was achieved before these 5-HT_3 receptors could be defined by radioligand binding assays. However, with the development of radiolabelled ligands such as [^{3}H]-GR65630, [^{3}H]-ICS205-930 and [^{3}H]-zacopride, 5-HT_3 receptors were identified in the brains of many species including man (Kilpatrick *et al.*, 1987; Barnes *et al.*, 1988; 1989; Waeber *et al.*, 1988), the vagus nerve and superior cervical ganglion (Kilpatrick *et al.*, 1989; Hoyer *et al.*, 1989).

However, few studies have attempted to characterize 5-HT_3 receptors in the gastrointestinal tract via radioligand binding assays. [^{3}H]-zacopride has been used at a single concentration for the tentative identification of 5-HT_3 recognition sites in certain areas of the rabbit, rat and ferret gastrointestinal tract (Pinkus *et al.*, 1989), which are associated with enteric neuronal plasma membranes (Gordon *et al.*, 1990). Such sites may provide the sites of action for 5-HT and 5-HT_3 receptor ligands to modify contraction and secretory responses in the gastrointestinal tract (Donowitz *et al.*, 1977; Cooke & Cary, 1985; Baird & Cuthbert, 1987; Costall & Naylor, 1990).

There have been no attempts to investigate systematically the presence and density of 5-HT_3 receptors throughout the whole gastrointestinal tract. Such information would be particularly helpful for identification of those regions of the tract worthy of further investigation as sites of 5-HT_3 agonist-antagonist action. In the present study we determined the distribution of 5-HT_3 recognition sites in the gastrointestinal tract of the rat.

Methods

Preparation of tissue for radioligand binding

Female Hooded-Lister rats (250–300 g, Bradford bred) were killed by cervical dislocation, and the tissues removed over ice. The gastrointestinal tract was separated as follows: oesophagus, stomach (dissected into the fundus, cardia, body and antrum), small intestine (20 cm lengths measured from the stomach), caecum (complete) and large intestine (complete). The contents of the gastrointestinal tract were removed and the tissues rinsed with ice-cold 2-[4-(2-hydroxyethyl-1-piperazinyl)]-ethane sulphonic acid (HEPES) buffer (50 mM buffered to pH 7.4 with NaOH; final Na^+ concentration was 10 mM). For most experiments the tissues were stored frozen at −20°C.

For binding studies the tissue was finely chopped with scissors and homogenized (Polytron, full speed for 10 s) in 20 volumes of ice-cold HEPES buffer and centrifuged (48,000 *g*, 10 min, 4°C). The resulting supernatant was discarded and the pellet resuspended in HEPES buffer and recentrifuged. The supernatant was discarded and the pellet resuspended in HEPES buffer at a concentration of 50 mg original wet weight ml^{-1} and kept on ice until used.

[1] Author for correspondence.

Binding studies with [^{3}H]-GR65630

Homogenates (250 µl) of the gastrointestinal tract (or HEPES buffer for filter blanks) were added to pre-incubated (2 min, 37°C) test tubes in triplicate, containing 650 µl of competing drug or buffer (containing appropriate drug-vehicle) and 100 µl [^{3}H]-GR65630 (final concentration 0.47–0.93 nM for competition studies or a range of concentrations between 0.1–5 nM for saturation studies). The tubes were incubated for 30 min at 37°C, before termination by rapid filtration through pre-wet (0.01% v/v polyethyleneimine in HEPES buffer) Whatman GF/B filters. The filters were immediately washed twice with 9.6 ml of HEPES buffer at room temperature (wash time 8 s). Filter discs were placed in scintillation vials and covered with 10 ml of 'Ultima Gold' scintillant (Packard), and left for dark adaption for 6 h before liquid scintillation spectroscopy (efficiency approximately 47%). Protein in the homogenate was measured by the Bio-Rad Coomassie Blue method (Bradford, 1976), with bovine serum albumin used as standard.

Binding studies with [^{3}H]-LY278584

Binding studies with [^{3}H]-LY278584 were carried as described above for [^{3}H]-GR65630, except that the final concentration of [^{3}H]-LY278584 was 0.43–0.58 nM for competition studies, or a range of concentrations between 0.05–5 nM for saturation studies. Binding assays were terminated with rapid filtration as above, but ice-cold buffer was used for washing the filters.

Expression of results

Estimates of equilibrium binding parameters (K_d and B_{max}) were obtained by non-linear regression analysis from the equation $y = B_{max}\ (L/(L + K_d))$ and the KaleidoGraph programme (Synergy Software, 1990); where L = free ligand concentration.

Compounds

Atropine sulphate (Sigma), dopamine hydrochloride (Sigma), granisetron hydrochloride (Glaxo), GR65630 hydrochloride (3- (5-methyl-1H-imidazole-4-yl) -1- (1-methyl-1H-indol-3-yl) -1-propanone.HCl) (Glaxo), hexamethonium hydrobromide (Sigma), 5-hydroxytryptamine maleate (5-HT, Sigma), 5-methoxytrptamine hydrochloride (Sigma), methysergide maleate (Sandoz), ondansetron hydrochloride (Glaxo), nicotine hydrogen tartrate (British Drug Houses), prazosin hydrochloride (Pfizer), pentazocine hydrochloride (Sigma), spiperone (Janssen) and (S)-zacopride hydrochloride (A.H. Robins) were prepared in distilled water and diluted with HEPES buffer as required. γ-Amino-n-butyric acid (Sigma) and noradrenaline bitartrate (Sigma) were dissolved in the minimum quantity of glacial acetic acid and made up to volume with distilled water (pH adjusted to 6–7 with sodium bicarbonate). Ritanserin (Research Biochemicals Inc.) was dissolved in the minimum quantity of methanol and made up to volume with distilled water. [^{3}H]-GR65630 (79.9 Ci mmol^{-1}, NEN) and [^{3}H]-LY278584 maleate (1-methyl-*N*-(8-methyl-8-azabicylo[3.2.1]oct-3-yl)-1*H*-indazole-3-carboxamide) (84 Ci mmol^{-1}, Amersham) were supplied in ethanol and diluted in HEPES buffer.

Results

Determination of specific binding of [^{3}H]-GR65630 and [^{3}H]-LY278584 in the rat gastrointestinal tract

In preliminary experiments, granisetron (10 µM) was found to compete for [^{3}H]-GR65630 (0.5 nM) binding to regions of the gastrointestinal tract. However, the use of the single concentration of ligand revealed marked differences between regions in the percentage inhibition of [^{3}H]-GR65630 binding. For example, 10 µM granisetron inhibited 43–63% of the total binding of [^{3}H]-GR65630 in the small intestine, whereas lower inhibition values of 14 to 36% were recorded from preparations of the oesophagus, stomach and caecum (Table 1).

The preliminary indications of specific [^{3}H]-GR65630 binding to regions of the small intestine were confirmed in subsequent studies where [^{3}H]-GR65630 (0.1–5 nM) displayed saturable specific binding (defined by 10 µM granisetron) in homogenates prepared from the terminal regions (40–60, 60–80 and 80–100 cm segments) of the small intestines. Non-linear regression analysis of the data showed that [^{3}H]-GR65630 binding was of high affinity and to a single population of receptors (K_d in the range of 0.42 ± 0.18 to 0.79 ± 0.24 nM; mean ± s.e.mean; maximum binding density, B_{max} 13.83 ± 4.54 to 21.19 ± 0.89 fmol mg^{-1} protein with r values of 0.92–0.95, Table 2 and Figure 1a). The use of [^{3}H]-LY278584 revealed a similar binding density (B_{max} 19.54 ± 0.26 fmol mg^{-1} protein) and affinity (K_d 1.04 ± 0.07 nM, r = 0.98 ± 0.01) in the terminal 80–100 cm segment of the small intestine (Table 2).

However, with preparations of the oesophagus, the four regions of stomach, the first 40 cm of the small intestine, the caecum and large intestine, non-linear regression analysis indicated that the 'specific binding' of [^{3}H]-GR65630 was not saturable and did not give good curve fits (Table 2 and Figure 1b).

Specificity of the binding of [^{3}H]-GR65630 (0.47–0.93 nM) and [^{3}H]-LY278584 (0.43–0.58 nM) to rat small intestine

In the 80–100 cm section of small intestine which had the highest density of binding sites, the 5-HT$_3$ receptor antagonists granisetron, ondansetron and (S)-zacopride competed for the binding sites with p*Ki* values in the nanomolar range (Table 3). 5-Hydroxytryptamine also effectively competed for the binding site (p*Ki* 6.15–6.93), whereas methysergide, ritanserin and 5-methoxytryptamine influencing respectively 5-HT$_1$/5-HT$_2$, 5-HT$_2$ and the putative 5-HT$_4$ receptor were ineffective. Similarly, compounds affecting catecholamine, acetylcholine, opioid and GABA receptors were without significant effect (Table 3).

Table 1 The 'specific' binding of [^{3}H]-GR65630 (0.5 nM) and [^{3}H]-LY278584 (0.5 nM) to homogenates of the rat gastrointestinal tract

Region	*Specific binding* (fmol mg^{-1} protein)	*Specific binding × 100 / Total binding*
	[^{3}H]-GR65630	
Oesophagus	4.5 ± 1	35 ± 4
Stomach		
fundus	3.0 ± 0.4	14 ± 3
cardia	3.2 ± 1	26 ± 4
body	3.1 ± 1	36 ± 18
antrum	2.4 ± 1	17 ± 5
Small intestine		
0–20 cm	5.3 ± 1	43 ± 11
20–40 cm	5.9 ± 1	63 ± 9
40–60 cm	8.2 ± 1	62 ± 2
60–80 cm	8.9 ± 2	62 ± 4
80–100 cm	10.1 ± 1	61 ± 3
Caecum	7.6 ± 3	36 ± 6
Large intestine	6.5 ± 1	42 ± 2
	[^{3}H]-LY278584	
Small intestine		
80–100 cm	6.2 ± 0.3	100 ± 2

'Specific' binding was defined by 10 µM granisetron. Values represent the mean ± s.e.mean obtained from 3 experiments.

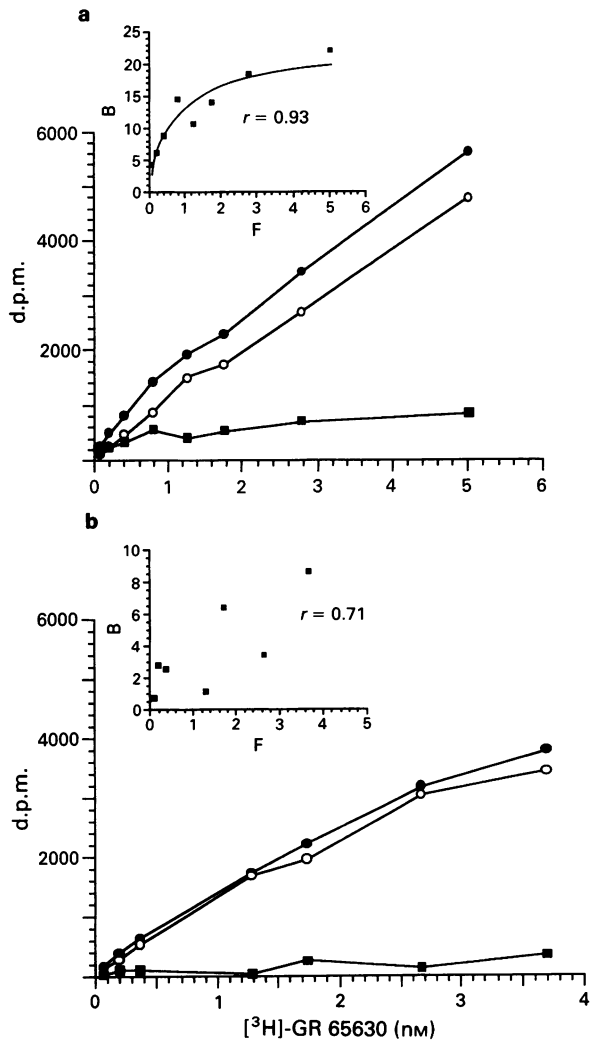

Figure 1 Representative saturation experiments with [^{3}H]-GR65630 in membranes of the rat gastrointestinal tract: (a) terminal section of small intestine and (b) oesophagus. Membranes were incubated with varying concentrations of [^{3}H]-GR65630 in the absence (● total binding) and the presence of granisetron (10 μM) (○ non-specific binding); specific binding (■). Points are means of triplicate determinations. The insets represent a non-linear regression analysis of the data; bound (B, fmol mg^{-1} protein) versus free (F, nM).

Discussion

The main purpose of this study was to determine the distribution of 5-HT$_3$ recognition sites in the gastrointestinal tract of the rat. The selective 5-HT$_3$ receptor antagonist [^{3}H]-GR65630 (Kilpatrick *et al.*, 1987) was used as the major pharmacological tool in radioligand binding studies; the 5-HT$_3$ receptor antagonist [^{3}H]-LY278584 (Robertson *et al.*, 1990) was used in more restricted experiments to provide supportive evidence for the data obtained with [^{3}H]-GR65630.

Specific binding sites defined by the use of the 5-HT$_3$ receptor antagonist, granisetron (Sanger & Nelson, 1989) were detected in the distal regions of the small intestine with both [^{3}H]-GR65630 and [^{3}H]-LY278584, the binding density being highest in the sections taken immediately before the ileo-caecal junction. The binding was most probably to a 5-HT$_3$ recognition site since the specific binding was defined by granisetron and other 5-HT$_3$ receptor antagonists, ondansetron and (S)-zacopride (Butler *et al.*, 1988; Smith *et al.*, 1988) and also 5-HT. The specificity and selectivity of the binding was further indicated by the failure of 5-HT$_1$ and 5-HT$_2$ receptor antagonists methysergide and ritanserin, and a variety of agonists and antagonists at cholinoceptor, catecholamine, opioid and GABA receptor sites to compete for the binding of [^{3}H]-GR65630 and [^{3}H]-LY278584. It is possible, if not probable, that the 5-HT$_3$ recognition sites identified in the present study may be the 5-HT$_3$ receptors that mediate changes in secretion in the rat ileum induced by 5-HT$_3$ receptor ligands (Ball *et al.*, 1988).

The presence of 5-HT$_3$ recognition sites in other parts of the rat gastrointestinal tract is less clear. Whilst the use of a single concentration of [^{3}H]-GR65630 identified 'specific' binding defined by the presence of granisetron in the oesophagus, regions of the stomach, proximal regions of the small intestine, colon and caecum, the use of a full range of concentrations and non-linear regression analysis failed to reveal saturable binding. Therefore it is difficult to demonstrate unequivocally the presence or absence of 5-HT$_3$ recognition sites in these areas of the rat gastrointestinal tract. Moreover, it is interesting that it has not been possible to characterize the 5-HT receptor mediating Cl^- secretory changes in the rat isolated colon as the 5-HT$_3$ receptor subtype (see Bunce *et al.*, 1991).

The location of 5-HT$_3$ recognition sites in different regions of the gastrointestinal tract is important to an understanding of how a pharmacological manipulation of 5-HT$_3$ receptor function might be expected to modify motility and secretion.

Table 2 Non-linear regression analysis of the specific binding of [^{3}H]-GR65630 and [^{3}H]-LY278584 to homogenates of discrete regions of the rat gastrointestinal tract

Region	B_{max} (fmol mg^{-1} protein)	K_d (nM)	r
	[^{3}H]-GR65630		
Oesophagus	NC	NC	0.81 ± 0.06
Stomach			
fundus	NC	NC	0.87 ± 0.05
cardia	NC	NC	0.87 ± 0.05
body	NC	NC	0.84 ± 0.05
antrum	NC	NC	0.71 ± 0.1
Small intestine			
0–20 cm	NC	NC	0.85 ± 0.07
20–40 cm	NC	NC	0.83 ± 0.07
40–60 cm	13.83 ± 4.54	0.42 ± 0.18	0.95 ± 0.01
60–80 cm	21.19 ± 0.89	0.79 ± 0.24	0.94 ± 0.01
80–100 cm	20.98 ± 0.97	0.47 ± 0.11	0.92 ± 0.02
Large intestine	NC	NC	0.82 ± 0.06
Caecum	NC	NC	0.68 ± 0.02
	[^{3}H]-LY278584		
Small intestine			
80–100 cm	19.54 ± 0.26	1.04 ± 0.07	0.98 ± 0.01

Values represent the mean ± s.e.mean of 3–4 separate experiments. Specific binding defined by 10 μM granisetron. NC, not calculable.

Table 3 The affinities of various compounds in competing for the binding of [^{3}H]-GR65630 (0.47–0.93 nM) and [^{3}H]-LY278584 (0.43–0.58 nM) to homogenates of the terimanl section of the rat small intestine

Compound	*[^{3}H]-GR65630* pKi	*[^{3}H]-LY278584* pKi
S-Zacopride	9.43 ± 0.21	9.52 ± 0.07
Granisetron	8.66 ± 0.11	8.54 ± 0.07
Ondansetron	8.05 ± 0.18	8.43 ± 0.09
5-Hydroxytryptamine	6.93 ± 0.07	6.15 ± 0.08
Hexamethonium	92 ± 3% TB at 0.1 μM	100 ± 5% TB at 0.1 μM
Noradrenalin	97 ± 2% TB at 0.1 μM	99 ± 3% TB at 0.1 μM
Nicotine	99 ± 5% TB at 0.1 μM	103 ± 5% TB at 0.1 μM
5-Methoxytryptamine	105 ± 3% TB at 0.1 μM	95 ± 2% TB at 0.1 μM
Pentazocine	83 ± 2% TB at 1 μM	96 ± 2% TB at 1 μM
Prazosin	87 ± 2% TB at 1 μM	105 ± 5% TB at 1 μM
Atropine	95 ± 1% TB at 1 μM	83 ± 5% TB at 1 μM
Dopamine	95 ± 6% TB at 1 μM	100 ± 6% TB at 1 μM
Spiperone	96 ± 1% TB at 1 μM	103 ± 5% TB at 1 μM
Methysergide	96 ± 6% TB at 1 μM	103 ± 6% TB at 1 μM
γ-Amino-n-butyric acid	97 ± 3% TB at 1 μM	106 ± 5% TB at 1 μM
Ritanserin	102 ± 3% TB at 1 μM	95 ± 8% TB at 1 μM

Values represent the mean ± s.e.mean of at least 3 separate experiments.
TB = total binding.

It is necessary to extend these studies to other species since 5-HT$_3$ receptor antagonists are reported to have varying effects in modifying motility and secretion in different species (see Costall & Naylor, 1990; Bunce *et al.*, 1991). Finally, the location of the 5-HT$_3$ receptors within the enteric neuronal system remains to be demonstrated.

References

BAIRD, A.W. & CUTHBERT, A.W. (1988). Neuronal involvement in type I hypersensitivity reactions in gut epithelia. *Br. J. Pharmacol.*, **92**, 647–655.

BALL, M.T., BUNCE, K.T. & SPRAGGS, C.F. (1988). Neuronal and non-neuronal 5-HT receptors control electrolyte secretion in isolated ileal mucosa. *Br. J. Pharmacol.*, **94**, 465P.

BARNES, J.M., BARNES, N.M., COSTALL, B., IRONSIDE, J.W. & NAYLOR, R.J. (1989). Identification and characterisation of 5-hydroxytryptamine recognition sites in human brain tissue. *J. Neurochem.*, **53**, 1787–1793.

BARNES, N.M., COSTALL, B. & NAYLOR, R.J. (1988). [^{3}H]-zacopride: ligand for the identification of 5-HT$_3$ recognition sites. *J. Pharm. Pharmacol.*, **40**, 548–551.

BRADFORD, M.M. (1976). A rapid and sensitive method for the quantitation of microgram quantities of protein utilising the principle of protein dye binding. *Analyt. Biochem.*, **172**, 248–254.

BRADLEY, P.B., ENGEL, G., FENIUK, W., FOZARD, J.R., HUMPHREY, P.P.A., MIDDLEMISS, D.N., MYLECHARANE, E.J., RICHARDSON, B.P. & SAXENA, P.R. (1986). Proposals for the classification and nomenclature of functional receptors for 5-hydroxytryptamine. *Neuropharmacology*, **25**, 563–576.

BUNCE, K.T., ELSWOOD, C.J. & BALL, M.T. (1991). Investigation of the 5-hydroxytryptamine receptor mechanism mediating the short-circuit current response in rat colon. *Br. J. Pharmacol.*, **102**, 811–816.

BUTLER, A., HILL, J.M., IRELAND, S.J., JORDAN, C.C. & TYERS, M.B. (1988). Pharmacological properties of GR38032F, a novel antagonist at 5-HT$_3$ receptors. *Br. J. Pharmacol.*, **94**, 397–412.

COOKE, H.J. & CAREY, H.V. (1985). Pharmacological analysis of 5-hydroxytryptamine actions on guinea-pig ileum mucosa. *Eur. J. Pharmacol.*, **111**, 329–337.

COSTALL, B. & NAYLOR, R.J. (1990). 5-Hydroxytryptamine: New receptors and novel drugs for gastrointestinal motor disorders. *Scand. J. Gastroenterol.*, **25**, 769–787.

DONOWITZ, M., CHARNEY, A.N. & HEFFERNAN, J.M. (1977). Effect of serotonin treatment on intestinal transport in the rabbit. *Am. J. Physiol.*, **232**, E85–E94.

FOZARD, J.R. (1984). MDL72222: a potent and highly selective antagonist at neuronal 5-hydroxytryptamine receptors. *Naunyn-Schmiedebergs Arch. Pharmacol.*, **326**, 36–44.

GADDUM, J.H. & PICARELLI, Z.P. (1957). Two kinds of tryptamine receptor. *Br. J. Pharmacol. Chemother.*, **12**, 323–328.

GORDON, J.C., SARBIN, N.S., BAREFOOT, D.S. & PINKUS, L.M. (1990). Solubilization of a 5-HT$_3$ binding site from rabbit small bowel muscularis membranes. *Eur. J. Pharmacol.*, **188**, 313–319.

HOYER, D., WAEBER, C., KARPF, A., NEIJT, H. & PALACIOS, J.M. (1989). [^{3}H]-ICS205-930 labels 5-HT$_3$ recognition sites in membranes of cat and rabbit vagus nerve and superior cervical ganglion. *Naunyn-Schmiedebergs Arch. Pharmacol.*, **340**, 396–402.

KILPATRICK, G.J., JONES, B.J. & TYERS, M.B. (1987). The identification and distribution of 5-HT$_3$ receptors in rat brain using radioligand binding. *Nature*, **330**, 746–748.

KILPATRICK, G.J., JONES, B.J. & TYERS, M.B. (1989). Binding of the 5-HT$_3$ ligand, [^{3}H]-GR65630, to rat postrema, vagus nerve and the brains of several species. *Eur. J. Pharmacol.*, **159**, 157–164.

PINKUS, L.M., SARBIN, N.S., BAREFOOT, D.S. & GORDON, J.C. (1989). Association of [^{3}H]-zacopride with 5-HT$_3$ binding sites. *Eur. J. Pharmacol.*, **168**, 355–362.

RICHARDSON, B.P. & ENGEL, G. (1986). The pharmacology and function of 5-HT$_3$ receptors. *Trends Neurosci.*, **9**, 424–428.

RICHARDSON, B.P., ENGEL, G., DONATSCH, P. & STADLER, P.A. (1985). Identification of serotonin M-receptor subtypes and their specific blockade by a new class of drugs. *Nature*, **316**, 126–131.

ROBERTSON, D.W., BLOOMQUIST, W., COHEN, M.L., REID, L.R., SCHENCK, K. & WONG, D.T. (1990). Synthesis and biochemical evaluation of tritium-labelled 1-methyl-N-(8-methyl-8-azabicyclo [3.2.1.]oct-3-yl)-1H-indazole-3-carboxamide, a useful radioligand for 5-HT$_3$ receptors. *J. Med. Chem.*, **33**, 3176–3181.

SANGER, G.J. & NELSON, D.R. (1989). Selective and functional 5-hydroxytryptamine$_3$ receptor antagonism by BRL43694 (granisetron). *Eur. J. Pharmacol.*, **159**, 113–124.

SMITH, W.L., SANCILIO, L.F., OWERA-ATEPO, J.B., NAYLOR, R.J. & LAMBERT, L. (1988). Zacopride: a potent 5-HT$_3$ antagonist. *J. Pharm. Pharmacol.*, **40**, 301–302.

WAEBER, C., DIXON, K., HOYER, D. & PALACIOS, J.M. (1988). Localization by autoradiography of neuronal 5-HT$_3$ receptors in the mouse CNS. *Eur. J. Pharmacol.*, **151**, 351–352.

(Received October 25, 1991
Revised January 22, 1992
Accepted March 17, 1992)

Br. J. Pharmacol. (1992), **106**, 697–702

Effects of almitrine on the release of catecholamines from the rabbit carotid body *in vitro*

L. Almaraz, R. Rigual, A. Obeso, *Y. Evrard & [1] C. Gonzalez

Departamento de Bioquimica y Biologia Molecular y Fisiologia, Facultad de Medicina, Universidad de Valladolid, 47005 Valladolid, Spain and *Institut de Recherches Internationales Servier, Neuilly-sur-Seine, France

1. Almitrine increases ventilation by stimulating the carotid body (CB) arterial chemoreceptors but neither its intraglomic target nor its mechanism of action have been elucidated.

2. We have tested the hypothesis that chemoreceptor cells are targets for almitrine by studying its effects on the release of ^{3}H-catecholamines in an *in vitro* rabbit CB preparation.

3. It was found that almitrine (0.3 and 1.5×10^{-6} M; i.e. 0.2 and $1\ mg\ l^{-1}$) increases the resting release of ^{3}H-catecholamines from CBs (previously loaded with [^{3}H]-tyrosine) incubated in a balanced 95% O_2/5% CO_2-equilibrated solution.

4. Almitrine at a concentration of 3×10^{-6} M ($2\ mg\ l^{-1}$) also augmented the release of ^{3}H-catecholamines elicited by incubating the CBs in a hypoxic solution (equilibrated with 7% O_2/5% CO_2 in N_2), by high external K^+ (35 mM) and by veratridine (2×10^{-5} M), but did not modify release induced by dinitrophenol (7.5×10^{-5} M).

5. At the same concentration (3×10^{-6} M), almitrine increased the rate of dopamine synthesis and was ineffective in modifying the cyclic AMP levels in either normoxic or hypoxic CBs.

6. It is concluded that chemoreceptor cells are the intraglomic targets for almitrine. The mechanisms of action of almitrine on chemoreceptor cells are discussed.

Keywords: Carotid body; arterial chemoreceptors; catecholamine; almitrine

Introduction

Almitrine bismesylate intravenously administered produces a potent and long-lasting stimulation of carotid body (CB) chemoreceptors leading to an equally long-lasting hyperventilatory response in different animal species including man (Laubie & Schmitt, 1980; Bisgard, 1981; O'Regan *et al.*, 1983; McQueen *et al.*, 1989; Lahiri *et al.*, 1989). In spite of the abundant literature on almitrine, not only its mechanism of action but even its intraglomic target(s) (chemoreceptor cells, sensory nerve endings or blood vessels) remain undefined.

On the other hand, it is well documented that all chemostimulants tested, including the natural stimuli low P_{O_2} and low pH/high P_{CO_2} and many pharmacological agents produce, in parallel, an increase in action potential frequency in the carotid sinus nerve (CSN) and in the release of catecholamines (CA) from chemoreceptor cells (see Fidone *et al.*, 1990, for a review). In the present study we have tested the hypothesis that almitrine also activates the release of CA from chemoreceptor cells. Our results show that almitrine produces a long-lasting increase in the release of ^{3}H-CA from chemoreceptor cells in resting normoxic conditions, augmenting also the release response evoked by low P_{O_2} and high external K^+. Almitrine was ineffective in modifying the release evoked by dinitrophenol (DNP) and did not alter adenosine 3':5'-cyclic monophosphate (cyclic AMP) levels in the CB in either normoxic or hypoxic conditions.

Methods

Carotid bodies were isolated from adult New Zealand rabbits (1.5–2.5 kg) under pentobarbitone anaesthesia as previously described (Fidone & Gonzalez, 1982). After CB removal the animals were killed with an overdose of pentobarbitone. The release of CA from the *in vitro* CBs was studied following the protocol and analytical procedures recently described by Rocher *et al.* (1991). In brief, the CA stores were labelled by incubating the organs for 2 h in a metabolic shaker at 37°C in 0.5 ml of 100% O_2-equilibrated Tyrode solution, containing 2×10^{-5} M of [^{3}H]-tyrosine (3,5-[^{3}H]-tyrosine, 30 Ci $mmol^{-1}$), 10^{-4} M DL-6-methyl-5,6,7,8-tetrahydropterine and 10^{-3} M ascorbic acid. Under these conditions the CBs synthesized an average of 20 pmol mg^{-1} tissue $2\ h^{-1}$, equivalent to 3.5×10^5 c.p.m. The ^{3}H-CA synthesized were [^{3}H]-dopamine and [^{3}H]-noradrenaline ([^{3}H]-NA) in a proportion near 10:1 (Fidone & Gonzalez, 1982; Rocher *et al.*, 1991). Individual CBs were then incubated for the rest of the experiment in 4 ml of [^{3}H]-tyrosine-free and CO_2/HCO_3^- -buffered Tyrode (pH = 7.42, 95% O_2:5% CO_2). During the first 2 h, the incubating solutions were renewed every 30 min and discarded; thereafter the solutions were renewed every 10 min and collected for subsequent analysis of their ^{3}H-catechol content. Test solutions were applied in this latter period of the experiments as indicated in the Results section. ^{3}H-catechols present in the collected samples were adsorbed onto alumina at a pH of 8.6, batch eluted with 1 N HCl (Weil-Malherbe, 1971) and counted in a scintillation spectrometer. In typical experiments from each series, the alumina eluates were subjected to thin layer chromatography and it was found that about 90% of all the ^{3}H-catechols present corresponded to [^{3}H]-dopamine plus its catabolite [^{3}H]-dihydroxyphenylacetic acid, the rest being [^{3}H]-NA and its catabolites (Rocher *et al.*, 1991). This indicates that the released material comes mostly from chemoreceptor cells (Fidone & Gonzalez, 1982).

The synthesis of ^{3}H-CA was studied by incubating the CBs with [^{3}H]-tyrosine as in the loading period of the release experiments, but the specific activity of the precursor was lower ($4\ Ci\ mmol^{-1}$) and the incubation lasted 1 h. At the end of the incubation period, and after 3 min of washing out in ice cold saline, the CBs were homogenized in 0.4 N perchloric acid and centrifuged. ^{3}H-CA and free [^{3}H]-tyrosine present in the supernatants were isolated by high performance liquid chromatography (h.p.l.c.) and quantified by

[1] Author for correspondence.

liquid scintillation spectrometry. [^{3}H]-tyrosine incorporated into proteins was measured in the pellet.

The protocols for the experiments in which cyclic AMP was determined have also been recently described (Perez-Garcia *et al.*, 1990). The nucleotide was assayed with a radioimmunoassay kit in pairs of CBs incubated in control (95% O_2:5% CO_2 equilibrated) and in hypoxic (7% O_2:5% CO_2:88% N_2 equilibrated) solutions, both, in the presence and in the absence of almitrine.

In all the experiments (except in the labelling periods for the release experiments; Rocher *et al.*, 1991) the incubating solution was a modified CO_2-bicarbonate Tyrode with the following composition (mM): NaCl 120, KCl 4.7, CaCl 2.2, MgCl 1.1, $NaHCO_3$ 24, HEPES 5 and glucose 5.5. The solutions were equilibrated with a 5% CO_2-containing gas mixture and adjusted to pH = 7.42 at 37°C. The control solution was equilibrated with 95% O_2:5% CO_2 to achieve true resting conditions for the CB chemoreceptors (Fidone *et al.*, 1982).

Statistical significance of the differences observed were assessed with Student's *t* test for paired and unpaired data according to the experimental design, except for those release experiments in which the time course of almitrine action was studied. In these later experiments the significance of the differences was determined by a one tail test of homogeneity of slopes model (General Lineal Models, 'GLM-SAS').

Drugs

Almitrine bismesylate was provided by Servier International. The rest of the chemicals used, including sodium pentobarbitone, were obtained from Sigma. The radioimmunoassay kit for cyclic AMP measurement and [^{3}H]-tyrosine were purchased from Amersham.

Results

Effects of almitrine on the basal release of ^{3}H-catecholamines

In previous studies (Rigual *et al.*, 1991; Rocher *et al.*, 1991) it has been established that weak acids, when applied alone, do not modify the release of ^{3}H-CA at concentrations below 1 mM. In spite of that, malic acid (used as solvent for almitrine) was added to the control CBs incubation media at the same concentrations used in almitrine-treated organs. Figure 1a shows that malic acid applied for 20 min (3 and 15×10^{-6} M) did not modify the typical slowly declining basal release of ^{3}H-CA (Almaraz *et al.*, 1986). In contrast, in the experimental group (contralateral CBs), the basal release of ^{3}H-CA showed a tendency to increase after the treatment with the same concentrations of malic acid plus 0.3 and 1.5×10^{-6} M of almitrine. This tendency to increase is long-lasting for both concentrations of almitrine, but is greatest with the higher concentration. The effect is more clearly shown in Figure 1b where the data have been normalized. In another group of experiments dimethyl sulphoxide (DMSO) was used as the solvent for almitrine (3×10^{-6} M) and we found that DMSO itself did not modify the release of ^{3}H-CA at concentrations below 0.2%; almitrine was also effective in augmenting basal release with this solvent (not shown).

Effects of almitrine on stimulus-induced release of ^{3}H-catecholamine

The effect of almitrine on the release of ^{3}H-CA induced by low P_{O_2}, DNP and high external K^+ was studied following the experimental protocol shown in Figure 2. Figure 2a and b show the release response obtained in a pair of CBs in

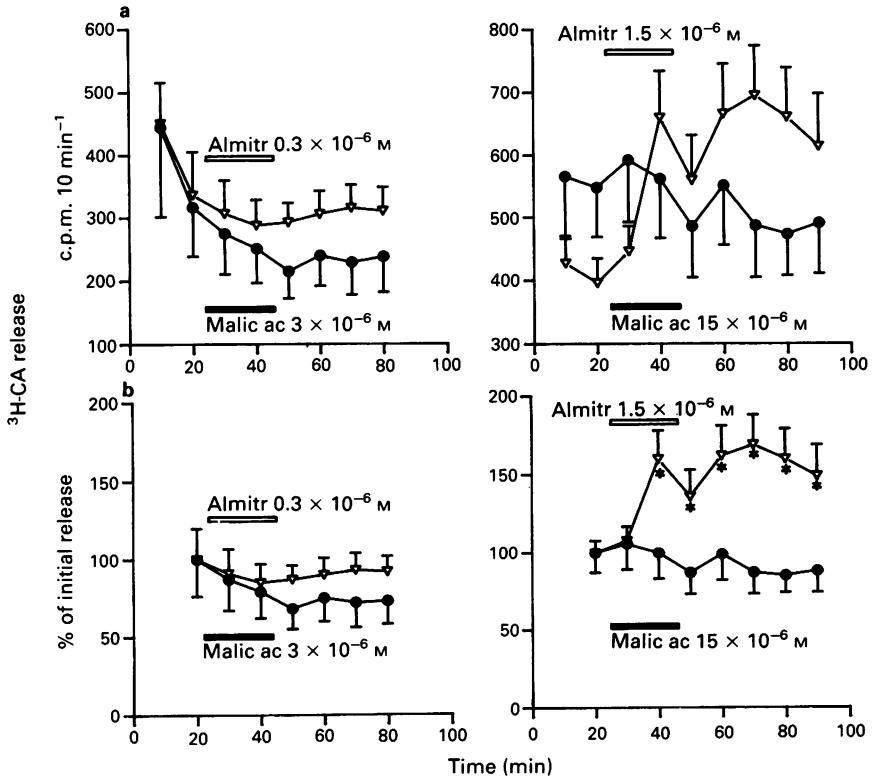

Figure 1 Effects of almitrine (Almitr, open bar) and malic acid (Malic ac, solid bar) on the basal release of ^{3}H-catecholamines (^{3}H-CA). (a) The data are expressed as c.p.m. present in each collected sample. (b) The data were normalized; the ^{3}H-CA present in the sample collected immediately prior to drug application was taken as 100%. (●) Malic acid-treated carotid bodies (CBs); (△) almitrine plus malic acid-treated CBs. Concentrations as shown in the figure. Data are means with s.e.mean (vertical bars) of $n = 5$ (left panels) and of $n = 9$ (right panels). *$P < 0.01$ (one tail test of homogeneity of slopes).

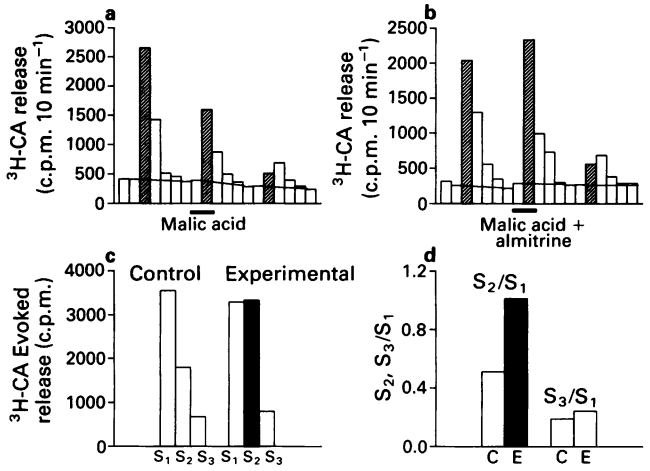

Figure 2 Effects of almitrine on low PO_2-induced release of ^{3}H-catecholamines (^{3}H-CA). Single experiment with two carotid bodies (CBs) to illustrate the general protocol followed to study the effects of almitrine on stimulus-induced release. (a) One CB (control) was subjected to three consecutive hypoxic stimulations (10 min each; hatched columns). Malic acid at a concentration of 30×10^{-6} M was present in the incubation solution during the 10 min period prior to and for the second presentation of the stimulus. (b) The contralateral CB was similarly stimulated, but during the second presentation of the stimulus $30 \times ^{-6}$ M malic acid and 3×10^{-6} M almitrine were present in the bathing solution. In both graphs each column represents the c.p.m. present in the incubation solutions that were collected every 10 min. Open columns: solution equilibrated with 95% O_2:5% CO_2; hatched columns: solutions equilibrated with 7% O_2:5% CO_2; in N_2. The horizontal lines through the columns in (a) and (b) separate the stimulus-induced release (above) from the basal release (below). (c) Shows the evoked release (c.p.m.) calculated as described for the three presentations of the stimulus (S_1, S_2 and S_3) in the control and in the experimental CB; (d) shows the ratios of the evoked release in the second (S_2) and third (S_3) presentation of the stimulus to that obtained in the first (S_1) for the control (C) and for the experimental (E) CB. Note that only at the second presentation of the hypoxic stimulus to the experimental CB was almitrine present in the incubation solution.

response to three consecutive applications of a hypoxic stimulus (incubation with a 7% O_2:5% CO_2:88% N_2-equilibrated solution for 10 min; dashed columns). In the control CB (a) the 10 min period prior to and during the presentation of the second stimulus, the incubating solution contained 30×10^{-6} M malic acid. At this concentration malic acid did not modify basal release. In the experimental CB (b), and also in relation to the second presentation of the stimulus, the incubation solution contained 3×10^{-6} M almitrine in addition to malic acid. It is evident that almitrine augmented the evoked release response, which corresponds to the c.p.m. above the horizontal lines in (a) and (b) and is represented in part (c) of the Figure. The evoked release in the first presentation of the stimulus, for both control and experimental CB, amounted to about 3000 c.p.m., which corresponds to approximately 2.5% of the total ^{3}H-CA stored in the organs (mean CB weight is 0.4 mg). As normally found, in the control CB the evoked release decreased on the second and third presentation of the stimulus (S_2 and S_3, respectively), while in the experimental CB in the second presentation of the stimulus carried out in the presence of almitrine, the evoked release was similar to that seen in the first stimulus. Figure 2d shows the ratios of the evoked release for control and experimental CBs in the second and third presentation of the stimulus to that obtained in the first one (S_2/S_1 and S_3/S_1, respectively). This form of presenting the data corrects for individual variations in the absolute amount of ^{3}H-CA released and allows a better dissection of the effects due to the treatment.

Average results obtained in 14 pairs of CBs for low PO_2 stimulation, 5 pairs for DNP and 9 for high external K^+ are shown in Figure 3. Left panels show mean evoked release responses in the successive presentations of the stimuli for control and experimental CBs and for the three different stimuli. The intensity of the different stimuli was chosen to produce similar absolute responses. Right panels show mean ratios of the evoked responses. Almitrine produced a 56% increase in the response evoked by low PO_2 ($P<0.02$), a 34% increase in release evoked by high K^+ ($P<0.05$) and a non significant (22%) tendency to augment DNP-induced release of ^{3}H-CA.

Figure 4 shows the effects of almitrine on the release of ^{3}H-CA induced by veratridine (2×10^{-5} M). Due to the slow wash out of veratridine and to the fact that on successive applications the release responses decrease very markedly (Rocher *et al.*, 1988), the protocol followed to study the effects of almitrine on veratridine-induced release was different: it was studied in single presentations of the stimulus in 5 pairs of CBs as shown in Figure 4. Almitrine produced over 100% increase in the release response evoked by veratridine ($P<0.02$).

Effects of almitrine on ^{3}H-catecholamine synthesis

Taking into consideration the mechanisms of the short-term control of tyrosine hydroxylase activity (Weiner *et al.*, 1972; Zigmond *et al.*, 1989), it would be expected from our release experiments that almitrine increases the rate of ^{3}H-CA synthesis. Figure 5 shows that this was indeed the case. In seven CBs incubated for 1 h with [^{3}H]-tyrosine (2×10^{-5} M) in the presence of 30×10^{-6} M malic acid plus almitrine (3×10^{-6} M) there was a small (15%) but significant ($P<0.05$) increase in the synthesis of [^{3}H]-dopamine in comparison to that obtained in the contralateral organs incubated in the absence of almitrine. No change was observed in the rate of

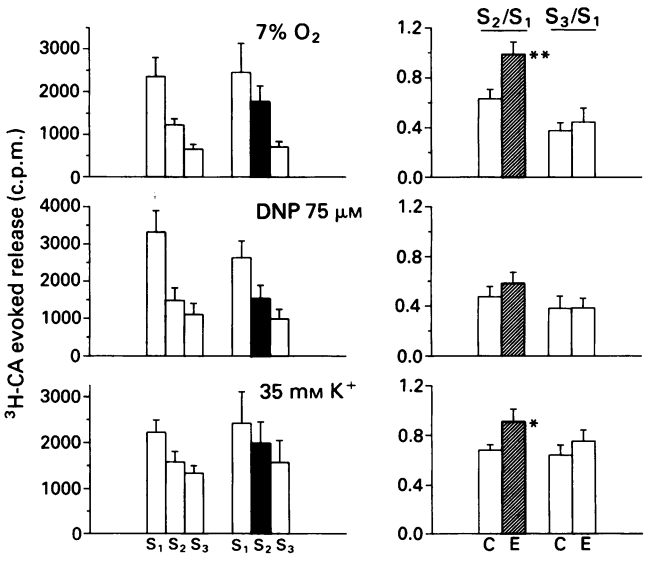

Figure 3 Effects of almitrine on low PO_2, dinitrophenol (DNP) and high external K^+ induced release of ^{3}H-catecholamines (^{3}H-CA). Protocols as in previous figure. Left panels show average evoked release for the three presentations of the stimulus (S_1, S_2 and S_3) and for the three stimuli; in S_2, 30×10^{-6} M malic acid (open columns) or malic acid plus 3×10^{-6} M almitrine (solid columns) were present 10 min before and during the stimulation period. Right panels show mean S_2/S_1 and S_3/S_1 ratios for the three stimuli. The intensity of the stimuli is indicated in the figure. Data are means with s.e.mean (vertical bars) of 14 values for low PO_2, 5 values for DNP and 9 values for K^+.
*$P<0.05$; **$P<0.02$; (two tailed Student's t test for unpaired observations).

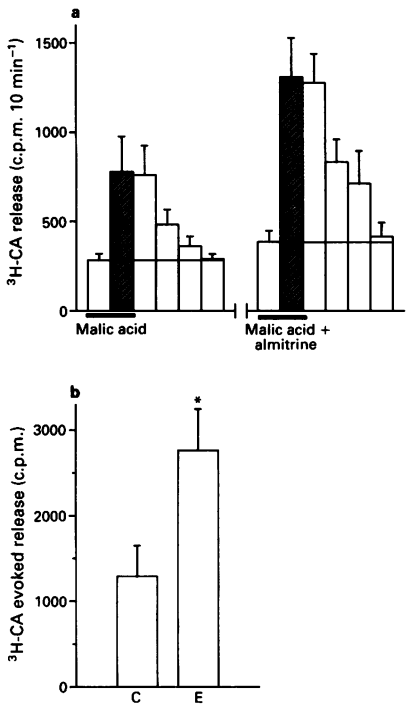

Figure 4 Effects of almitrine on veratridine-induced release of ^{3}H-catecholamines (^{3}H-CA). (a) The data are expressed as c.p.m. in the collected incubation solutions (means with s.e.mean shown by vertical bars). Veratridine (2×10^{-6} M) was applied during 10 min (hatched columns); malic acid (30×10^{-6} M) and malic acid plus almitrine (3×10^{-6} M) were applied as indicated in the figure. (b) Mean evoked release in control and experimental CBs ($n = 5$). *$P < 0.02$; (two tailed Student's t test for unpaired observations).

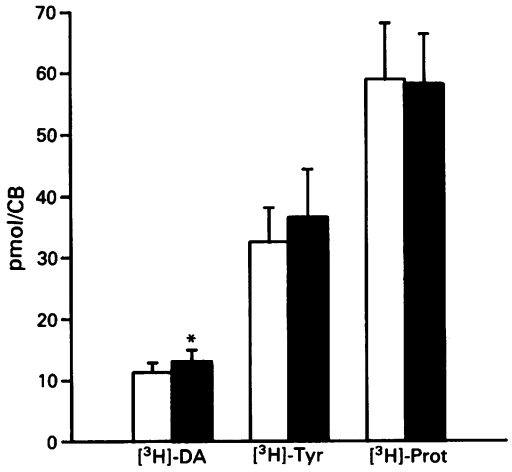

Figure 5 Effects of almitrine on catecholamine synthesis in the carotid body (CB). The organs were incubated for 1 h in a solution equilibrated with 95% O_2:5% CO_2 at a pH of 7.4 in the presence of 30×10^{-6} M malic acid (controls; open columns) or malic acid plus 3×10^{-6} M almitrine (experimentals; solid columns). [^{3}H]-noradrenaline synthesis, not shown in the figure, was not different in control and experimental CBs and amounted to 0.25 pmol/CB. *$P < 0.05$. (Student's t test for paired observations; $n = 7$).

[^{3}H]-NA synthesis (see Figure legend). There was neither a significant change in the accumulation of free [^{3}H]-tyrosine nor in the incorporation of [^{3}H]-tyrosine to proteins.

Effects of almitrine on cyclic AMP levels of the carotid body

Since low Po_2 increases cyclic AMP content in the CB (Perez-Garcia *et al.*, 1990) and, on the other hand, different manoeuvres that increase cyclic AMP levels in the CB also increase the release of ^{3}H-CA induced by low Po_2 (Perez-Garcia *et al.*, 1991; Wang *et al.*, 1991), we tested the possibility that almitrine increased the levels of this nucleotide as a ready explanation for its effect on the release of ^{3}H-CA. Two groups of 14 CBs were used. In the first one, 7 organs were incubated in control solution (95% O_2/5% CO_2-equilibrated) containing 0.5×10^{-3} M isobutylmethylxantine (a phophodiesterase inhibitor) and 30×10^{-6} M malic acid, and their contralaterals in the same solution that contained, in addition, 3×10^{-6} M almitrine. In the second group 7 CBs were incubated for 10 min in a 7% O_2:5% CO_2-equilibrated solution that contained isobutylmethylxantine and malic acid and their contralaterals were similarly incubated, but the solution also contained almitrine. As shown in Figure 6, almitrine did not modify cyclic AMP levels in either condition.

Discussion

The present results show that almitrine *in vitro*, at concentrations similar to those found in blood after administration of effective doses *in vivo* (Gordon *et al.*, 1987), augments the release of CA, mostly dopamine, from chemoreceptor cells in a preparation of the intact rabbit CB. Regardless of what the physiological role of the released CA is (see Fidone *et al.*, 1990 vs. Ponte & Sadler, 1989, for a discussion on this topic), the present results are consistent with previous studies in showing that almitrine, as any other chemostimulant agent tested, increases the release of CA from chemoreceptor cells (Fidone *et al.*, 1990). It should be pointed out also that the long-lasting effect of almitrine on the release of ^{3}H-CA, seen in the present study, accords with the well known long-lasting increases in ventilation (Laubie & Schmitt, 1980) and carotid sinus nerve (CSN) chemoreceptor potential frequency (Bisgard, 1981; O'Regan *et al.*, 1983; McQueen *et al.*, 1989; Lahiri *et al.*, 1989) observed when the drug is administered *in vivo*.

It has been reported (Pallot & Al Neamy, 1983) that almitrine causes a decrease in the content of CA in the CB, and the suggestion was made that almitrine increased the

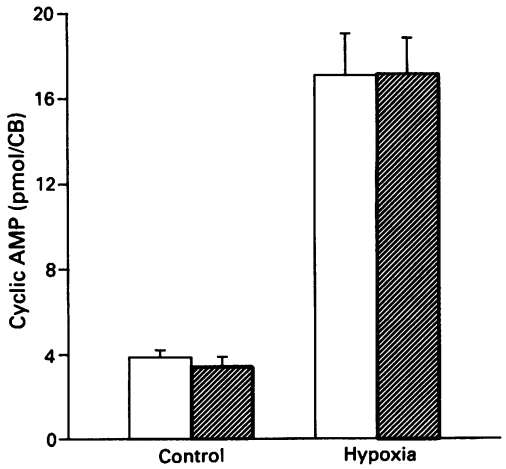

Figure 6 Effects of almitrine on cyclic AMP content in control and hypoxic carotid bodies (CBs). Control CBs were incubated in a solution equilibrated with 95% O_2:5% CO_2 and hypoxic ones in another equilibrated with 7% O_2:5% CO_2 in N_2. In both cases the incubation solutions contained 0.5×10^{-3} M isobutylmethylxanthine and 3×10^{-5} M malic acid; almitrine 3×10^{-6} M was present only in the experimental group (hatched columns). In all the cases the data are means with s.e.mean shown by vertical bars; $n = 7$. Means are not statistically different.

release of these biogenic amines. Pequignot *et al.* (1987) also found that almitrine (5 mg kg^{-1}) produced a decrease in the content of CA in the CB that was accompanied by a decrease in the turnover rate of these biogenic amines, the effect being greater in the case of dopamine than in the case of NA. No change in CA content was observed with lower doses of almitrine (1 and 3 mg kg^{-1}). In this later study, carried out for periods as long as 15 days, the possibility cannot be excluded that in the initial moments there was an increase in CA release because the turnover rates could not be assessed at intervals shorter than 2 h. In the present study the *in vitro* preparation allows an almost minute by minute analysis of the action of any experimental manoeuvre, and the results are clear in demonstrating that almitrine increases the release and synthesis of CA. In addition, in relation to previous studies and despite the observed modifications in dopamine metabolism, it was not possible in these studies to establish whether the action of almitrine was directly on chemoreceptor cells or, if it was reflexely mediated. It was also not possible to exclude the possibility that the observed effects on dopamine metabolism in the CB was produced by an efferent pathway present in the ganglioglomerular nerves which is known to be activated by almitrine (McQueen *et al.*, 1989). This uncertainty is eliminated in the present *in vitro* study where the CB is not subjected to reflex inputs. The possibility that almitrine is promoting the release of CA indirectly via retrograde influences on the nerve endings or via endothelial-derived factors is considered remote, for the following reasons. Almaraz & Fidone (1986) have shown that even supramaximal electrical stimulation of the carotid sinus nerve elicits a release of dopamine which is much lower than that observed here with almitrine treatment. The possibility that almitrine is acting on capillary endothelial cells promoting the genesis of a diffusible factor (e.g. NO), which in turn activates the release of dopamine from chemoreceptor cells, cannot be excluded. However, we have found (Obeso, unpublished) that inhibition of NO synthesis affects neither basal nor high external K^+-induced release of dopamine. We therefore conclude that almitrine augments the release of CA by a direct action on chemoreceptor cells.

The precise mechanism of action of almitrine remains elusive. We have found an increase in the release of ^{3}H-CA in all conditions tested except for DNP, a protonophore that at the concentration used, mimics acidic stimulus (Rocher *et al.*, 1991). Contrary to our observation on the lack of effect of almitrine on acidic (DNP)-induced release, it is well established that almitrine *in vivo* activates chemoreceptor activity in the CSN at any P_{O_2} and P_{CO_2}. It should be pointed out, however, that while the chemoreceptor discharge evoked by almitrine appears indistinguishable from that evoked by hypoxia, these do not resemble the response to hypercapnic stimulus (Nye *et al.*, 1990). Since the actions of almitrine on the CSN responses or on the hyperventilation elicited by protonophores have not been studied, the possibility remains that these agents interfere with the action of almitrine.

Our findings can be interpreted in the light of observations made by Peers & O'Donnell (1990) that almitrine produces a long lasting inhibition of K^+ currents in CB chemoreceptor cells. Thus, almitrine would be expected to cause a resting (normoxic) depolarization and would tend to increase low P_{O_2}, high external K^+ and veratridine-induced depolarization (Gonzalez *et al.*, 1990). As a consequence, an increase in the release of ^{3}H-CA would be anticipated in all these situations. Our interpretation of the mechanism of action of almitrine rests on this inhibition of the K^+ currents in chemoreceptor cells and it has the merit of unifying conceptually the mechanisms of action of almitrine as a chemostimulant and as potentiator of pulmonary hypoxic vasoconstriction (e.g. Naeije *et al.*, 1989). It has been found that chemoreceptor cells possess an oxygen-sensitive K^+ channel (Lopez-Barneo *et al.*, 1988; Lopez-Lopez *et al.*, 1989; Ganfornina & Lopez-Barneo, 1991) and the proposal has been made that the inhibition of this channel by low P_{O_2} leads to depolarization of chemoreceptor cells, Ca^{2+} entry and release of neurotransmitters (Gonzalez *et al.*, 1990). Quite recently it has been suggested (Rodman & Voelkel, 1991) that the same mechanism could be operating in the smooth muscle cells of the pulmonary vessels, in such a way that in response to pulmonary hypoxia the muscular cells would be depolarized and vasoconstriction would follow. Almitrine, by blocking K^+ channels in both cell types, would potentiate their natural responses.

Our results also suggest that contrary to the situation with the natural hypoxic stimulus (Perez-Garcia *et al.*, 1990), the adenylate cyclase system does not appear to participate in the acute responses elicited by almitrine in chemoreceptor cells. This finding could explain why some of the well known effects produced by long-term hypoxic stimulation (e.g. increase in the turnover rate of CA in the CB) are not seen during long term treatment with almitrine (Pequignot *et al.*, 1987).

In conclusion, we have studied the effects of almitrine on the synthesis and release of catecholamines in an *in vitro* preparation of rabbit CB and have found that almitrine, like any other chemostimulant agent tested, increases both parameters. This suggest that chemoreceptor cells are direct targets for the drug. In contrast to a natural stimulus (hypoxia), almitrine does not activate adenylate cyclase in the CB. It is suggested that the two pharmacologically important effects of almitrine, i.e. potentiation of the pulmonary hypoxic vasoconstriction and CB chemoreceptor activation, could be mediated via inhibition of O_2-sensitive K^+ currents present in pulmonary vessels smooth muscle and CB chemoreceptor cells.

The authors are indebted to J.-F. Martin for help in the statistical analysis. We also thank Maria Bravo for technical assistance. This work was supported by grants from the Institut de Recherches Internationales Servier, DGICYT PB89/0358 and Junta de Castilla y Leon 1101/89.

References

ALMARAZ, L. & FIDONE, S. (1986). Carotid sinus nerve C-fibers release catecholamines from the cat carotid body. *Neurosci. Lett.*, **67**, 153–158.

ALMARAZ, L., OBESO, A. & GONZALEZ, C. (1986). Effects of high potassium on the release of ^{3}H-dopamine from the cat carotid body in vitro. *J. Physiol.*, **379**, 293–307.

BISGARD, G.E. (1981). The response of few-fiber carotid chemoreceptor preparation to almitrine in the dog. *Can. J. Physiol. Pharmacol.*, **59**, 396–401.

FIDONE, S.J. & GONZALEZ, C. (1982). Catecholamine synthesis in rabbit carotid body *in vitro*. *J. Physiol.*, **333**, 69–79.

FIDONE, S.J., GONZALEZ, C., OBESO, A., GOMEZ-NINO, A. & DINGER, B. (1990). Biogenic amine and neuropeptide transmitters in carotid body chemotransmission: experimental findings and perspectives. In *Hypoxia: The Adaptations*. ed. Sutton, J.R., Coates, G. & Remmers, J.E. pp. 116–126. Philadelphia: B.C. Decker Inc.

FIDONE, S., GONZALEZ, C. & YOSHIZAKI, K. (1982). Effects of low oxygen on the release of dopamine from the rabbit carotid body in vitro. *J. Physiol.*, **333**, 93–110.

GANFORNINA, M.D. & LOPEZ-BARNEO, J. (1991). Single K^+ channels in membrane patches of arterial chemoreceptor cells are modulated by O_2 tension. *Proc. Natl. Acad. Sci. U.S.A.*, **88**, 2927–2930.

GONZALEZ, C., ROCHER, A., OBESO, A., LOPEZ-LOPEZ, J.R., LOPEZ-BARNEO, J. & HERREROS, B. (1990). Ionic mechanisms of the chemoreception process in type I cells of the carotid body. In *Arterial Chemoreception*. ed. Eyzaguirre, C., Fidone, S.J., Fitzgerald, R.S., Lahiri, S. & McDonald, D.M. pp. 44–57. New York: Springer Verlag.

GORDON, B.H., PALLOT, D., MIR, A., INGS, R.M.J., EVRARD, Y. & CAMPBELL, D.B. (1987). Kinetics of almitrine bismesylate and its metabolites in the carotid body and other tissues of the rat. In *Chemoreceptors in Respiratory Control.* ed. Ribeiro, J.A. & Pallot, D.J. pp. 394–407. London: Croom Helm Ltd.

LAHIRI, S., MOKASHI, A., HUANG, W., SHERPA, A.K. & DIGIULIO, C. (1989). Stimulus interaction between CO_2 and almitrine in the cat carotid chemoreceptors. *J. Appl. Physiol.*, **67,** 232–238.

LAUBIE, M. & SCHMITT, H. (1980). Long lasting hyperventilation induced by almitrine: evidence for a specific effect on carotid and thoracic chemoreceptors. *Eur. J. Pharmacol.*, **61,** 125–136.

LOPEZ-BARNEO, J., LOPEZ-LOPEZ, J.R., URENA, J. & GONZALEZ, C. (1988). Chemotransduction in the carotid body: K^+ current modulated by PO_2 in type I chemoreceptor cells. *Science*, **241,** 580–582.

LOPEZ-LOPEZ, J.R., GONZALEZ, C., URENA, J. & LOPEZ-BARNEO, J. (1989). Low PO_2 selectively inhibits K channel activity in chemoreceptor cells of the mammalian carotid body. *J. Gen. Physiol.*, **93,** 1001–1014.

MCQUEEN, D.S., EVRARD, Y., GORDON, B.H. & CAMPBELL, B.D. (1989). Ganglioglomerular nerves influence responsiveness of carotid body chemoreceptors to almitrine. *J. Auton. Nerv. Syst.*, **27,** 57–66.

NAEJIE, R., LEJEUNE, P., LEEMAN, M., MELOT, C. & CLOSSET, J. (1989). Pulmonary vascular responses to surgical chemodenervation and chemical sympathectomy in dogs. *J. Appl. Physiol.*, **66,** 42–50.

NYE, P.C.G., MAXWELL, D.L., QUIRK, P.G. & COOK, C. (1990). The carotid body and almitrine bismesylate. In *Arterial Chemoreception.* ed. Eyzaguirre, C., Fidone, S.J., Fitzgerald, R.S., Lahiri, S. & McDonald, D.M. pp. 199–206. New York: Springer Verlag.

O'REGAN, R.G., MAJCHERCZYK, S. & PRZYBYSZEWSKI, A. (1983). Effects of almitrine bismesylate on activities recorded from nerves supplying the carotid bifurcation in the cat. *Eur. J. Resp. Dis.*, **64, (126),** 197–202.

PALLOT, D.J. & AL NEAMY, K.W. (1983). The effects of hypoxia, hypercapnia and almitrine bismesylate on carotid body catecholamines. *Eur. J. Respir. Dis.*, **64** (126), 203–207.

PEERS, C. & O'DONELL, J. (1990). Effects of chemoexcitatory agents on K^+ currents of isolated type I cells from neonatal rat carotid body. In *Arterial Chemoreception.* ed. Eyzaguirre, C., Fidone, S.J., Fitzgerald, R.S., Lahiri, S. & McDonald, D.M. pp. 63–69. New York: Springer Verlag.

PEQUIGNOT, J.M., TAVITIAN, E., BOUDET, C., EVRARD, Y., CLAUSTRE, J. & PEYRIN, L. (1987). Inhibitory effect of almitrine on dopaminergic activity of the rat carotid body. *J. Appl. Physiol.*, **63,** 746–751.

PEREZ-GARCIA, M.T., ALMARAZ, L. & GONZALEZ, C. (1990). Effects of different types of stimulation on cyclic AMP content in the rabbit carotid body: functional significance. *J. Neurochem.*, **55,** 1287–1293.

PEREZ-GARCIA, M.T., ALMARAZ, L. & GONZALEZ, C. (1991). Cyclic AMP modulates differentially the release of dopamine induced by hypoxia and other stimuli and increases dopamine synthesis in the rabbit carotid body. *J. Neurochem.*, **57,** 1992–2000.

PONTE, J. & SADLER, C.L. (1989). Interactions between hypoxia, acetylcholine and dopamine in the carotid body of rabbit and cat. *J. Physiol.*, **410,** 395–410.

RIGUAL, R., LOPEZ-LOPEZ, J.R. & GONZALEZ, C. (1991). Release of dopamine and chemoreceptor discharge induced by low pH and high PCO_2 stimulation of the cat carotid body. *J. Physiol.*, **433,** 519–531.

ROCHER, A., OBESO, A., GONZALEZ, C. & HERREROS, B. (1991). Ionic mechanisms for the transduction of acidic stimuli in rabbit carotid body glomus cells. *J. Physiol.*, **433,** 533–548.

ROCHER, A., OBESO, A., HERREROS, B. & GONZALEZ, C. (1988). Activation of the release of dopamine in the carotid body by veratridine. Evidence for the presence of voltage dependent Na^+ channels in type I cells. *Neurosci. Lett.*, **94,** 274–278.

RODMAN, D.M. & VOELKEL, N.F. (1991). Regulation of vascular tone. In *The Lung: Scientific Foundations.* ed. Crystal, R.G. & West, J.B. pp. 1105–1120. New York: Raven Press.

WANG, W.-J., CHENG, G.-F., YOSHIZAKY, K., DINGER, B. & FIDONE, S. (1991). The role of cyclic AMP in chemoreception in the carotid body. *Brain Res.*, **540,** 96–104.

WEIL-MALHERBE, H. (1971). Determination of catecholamines. In *Analysis of Biogenic Amines and Their Related Enzymes.* ed. Glick, D. pp. 119–152. New York: Interscience Publishers.

WEINER, N., CLOUTIER, G., BJUR, R. & PFEFFER, R. (1972). Modification of norepinephrine synthesis in intact tissue by drugs and during short-term adrenergic nerve stimulation. *Pharmacol. Rev.*, **24,** 203–221.

ZIGMOND, R.E., SCHWARZSCHILD, M.A. & RITTENHOUSE, A.R. (1989). Acute regulation of tyrosine hydroxylase by nerve activity and by neurotransmitters via phosphorylation. *Annu. Rev. Neurosci.*, **12,** 415–461.

(Received December 10, 1991
Revised March 16, 1992
Accepted March 17, 1992)

Br. J. Pharmacol. (1992), **106**, 703–709

An endothelial 5-HT receptor that mediates relaxation in guinea-pig isolated jugular vein resembles the 5-HT_{1D} subtype

Paul Gupta

Department of Biomedical Research, Wyeth Research (UK) Ltd., Huntercombe Lane South, Taplow, Maidenhead, Berkshire, SL6 0PH

1 Endothelium-dependent and -independent, concentration-related, relaxations to 5-hydroxytryptamine (5-HT) are described in a preparation of guinea-pig isolated jugular vein.

2 An endothelial 5-HT receptor was studied in the presence of mesulergine (at 10.0 μM, a concentration sufficient to antagonize 5-HT_2 receptor-mediated contractions and endothelium-independent relaxations to 5-HT). Relaxations mediated by the endothelial 5-HT receptor were resistant to antagonism by mesulergine.

3 Several 5-HT receptor agonists activated the endothelial receptor with the following rank order of potency: 5-carboxamidotryptamine (5-CT) > 5-HT > methysergide ≥ α-methyl-5-HT > sumatriptan > 8-hydroxy-2-(di-n-propylamino)tetralin (8-OH-DPAT) > 2-methyl-5-HT.

4 Relaxations to 5-HT were not blocked by (±)-pindolol (1.0 μM), (−)-propranolol (1.0 μM), spiperone (1.0 μM), ondansetron (1.0 μM) or ICS 205-930 (10.0 μM).

5 Both 5-HT and sumatriptan evoked endothelium-dependent relaxations which were sensitive to antagonism (pA_2 and apparent pA_2 values respectively) by methiothepin (8.1 and 8.6), metergoline (7.4 and 7.5), PAPP (8.2 and 8.2), yohimbine (7.1 and 6.8), rauwolscine (6.8 and 6.7), but not by corynanthine (10.0 μM).

6 These observations are consistent with a 5-HT_{1D} receptor-mediated effect, and provide further support for the concept that differences exist between endothelial 5-HT receptors in different tissues and species.

Keywords: Endothelium; jugular vein; guinea-pig; 5-HT_{1D} receptor

Introduction

5-Hydroxytryptamine$_1$ (5-HT_1) binding sites were originally described in rat brain (Peroutka & Snyder, 1979), and on the basis of radioligand binding studies, these sites have been subdivided into subtypes termed 5-HT_{1A}, 5-HT_{1B}, 5-HT_{1C} and 5-HT_{1D} (Pedigo *et al.*, 1981; Pazos *et al.*, 1984; Hoyer *et al.*, 1985; Heuring & Peroutka, 1987). The functional receptors which correspond to these binding sites are now well established in brain tissue (De Vivo & Maayani, 1986; Engel *et al.*, 1986; Conn *et al.*, 1986; Schoeffter *et al.*, 1988).

However, in some peripheral tissues, 5-HT receptors with properties similar to the 5-HT_1 class have been described which do not fully correspond to any of the above 5-HT_1 receptor subtypes; some examples of preparations containing such 5-HT receptors include dog saphenous vein (Humphrey *et al.*, 1988), guinea-pig ileum (Kalkman *et al.*, 1986), rabbit jugular vein (Martin *et al.*, 1987), porcine vena cava (Sumner *et al.*, 1989), and rat kidney (Charlton *et al.*, 1986). These peripheral 5-HT receptors have been termed 5-HT_1-like in accordance with the proposals of Bradley *et al.* (1986), since they are activated by the 5-HT_1 receptor agonist 5-carboxamidotryptamine (5-CT), antagonized by 5-HT_1 receptor antagonists methiothepin and/or methysergide, but are resistant to 5-HT_2 and 5-HT_3 receptor antagonists.

It is well established that 5-HT can evoke endothelium-dependent relaxations of some isolated smooth muscle preparations by activation of a receptor(s) which resembles a 5-HT_1 receptor (reviewed by Angus & Cocks, 1989). Recent evidence now suggests that endothelium-dependent relaxations to 5-HT are mediated by a heterogeneous receptor population. In porcine coronary artery (Schoeffter & Hoyer, 1989; 1990), the endothelial receptor displays properties which are consistent with the 5-HT_{1D} receptor described in both rabbit saphenous vein (Martin *et al.*, 1991) and guinea-pig frontal cortex (Middlemiss *et al.*, 1988). In contrast, endothelial 5-HT receptors in both rabbit jugular vein (Leff *et al.*, 1987) and porcine vena cava (Sumner, 1991) display similar pharmacological properties, but do not appear to correspond to 5-HT receptor subtypes which are currently recognised.

The aim of the work described here was to investigate further the pharmacology of 5-HT receptors which can mediate endothelium-dependent relaxations. A species known to possess 5-HT_{1D} receptors was selected, and a preparation of guinea-pig isolated jugular vein was used since previous unpublished studies in this laboratory had demonstrated the existence of an endothelial 5-HT receptor in this tissue.

Methods

Experimental protocol

Male Dunkin-Hartley guinea-pigs (300–500 g) were killed by cervical dislocation. Right and left external jugular veins were excised and dissected free of adhering fat and connective tissue. Two rings, 2 mm in length, were prepared from each vein and suspended on parallel tungsten wires (125 μm in diameter) in isolated organ baths (20 ml) which contained Krebs solution gassed with 95% O_2 and 5% CO_2 at 37°C. The initial resting load was 0.5 g, the tissues being equilibrated for 30 min, during which time the bathing fluid was changed once. All tissues partially relaxed from the initial 0.5 g loading tension during the 30 min equilibration period. The tension in the preparations was measured with a Grass FT03C force-displacement transducer and displayed on a Servogor Type 220 potentiometric recorder. Preparations were then exposed to either three or four separate challenges with the stable thromboxane-A_2-mimetic, U-46619 (30 nM; contact time 5 min), until the magnitude of the peak contraction had become constant.

Measurement of agonist potency

Following a final exposure to U-46619 (30 nM), which was left in the bathing medium for the remainder of the experiment, preparations were left for up to 60 min, allowing the tension developed to stabilize. Agonist-evoked relaxant responses were then determined by constructing cumulative concentration-effect curves. Each successive agonist dose was administered after the response to the previous concentration had reached a plateau; this occurred generally after 2 to 4 min. Relaxant effects were expressed as a percentage value of the final U-46619 (30 nM)-evoked contraction, this representing the difference between resting and sustained tone.

Preliminary experiments demonstrated that 5-HT_2 receptors and 5-HT_1-like receptors present on the smooth muscle cells could mediate contraction and relaxation responses respectively to 5-HT. Consequently, agonist potencies were determined following a 30 min incubation with mesulergine (10.0 μM), a concentration of the drug which adequately blocked both 5-HT_2 and 5-HT_1-like effects on the smooth muscle (see Results section) prior to the final challenge with U-46619 (30 nM).

Measurement of antagonist potency

The conditions employed to determine agonist potencies were used to measure antagonist potencies. It was possible to study endothelium-dependent relaxations to 5-HT over a concentration range of 1 nM to 10.0 μM, thus allowing the measurement of a 100 fold rightward displacement of the control concentration-effect curve of the amine. At concentrations of 5-HT greater than 10.0 μM, the antagonist effect of mesulergine (10.0 μM) at the smooth muscle relaxant 5-HT receptor was overcome, and therefore such high 5-HT concentrations were not used.

A single concentration-effect curve for 5-HT was constructed in each tissue in either the absence or presence of antagonist since tachyphylaxis to 5-HT was observed with a second curve in the same tissue. Compounds which displayed antagonist activity were examined at a minimum of three different concentrations. Antagonists were equilibrated with tissues for at least 60 min before the construction of agonist concentration-effect curves. Agonist concentration-ratios obtained from individual experiments were plotted by the method of Arunlakshana & Schild (1959). Linear regression analysis was used to calculate the pA_2 value and the slope of the line from the pooled data for each antagonist. When sumatriptan was the agonist used, antagonist potency was determined, from the displacement of the sumatriptan concentration-effect curve observed at one antagonist concentration only, by applying the following relationship: $pA_2 = \log_{10}$ (concentration-ratio $-1) - \log_{10}$ (molar concentration of antagonist). This latter protocol avoided the problem of vehicle effects seen when using sumatriptan at high concentrations. Antagonist potencies determined by this procedure were expressed as apparent pA_2 values, rather than pK_B values, assuming that the Schild plot slope did not differ from unity. Since the K_B value reflects an estimate of antagonist binding affinity, and implies much assurance concerning the antagonist-receptor interaction, the term apparent pA_2 was preferred as it refers only to the negative logarithm_{10} of the antagonist concentration (M) that would result in an agonist concentration-ratio of 2 (Schild, 1947).

Determination of the role of vascular endothelial cells in mediating relaxant responses to agonists

Vessels were denuded by endothelium by a physical method which involved rubbing a matchstick (reduced in diameter to 0.75 mm) across the endothelial cell lining. Following this treatment, relaxations to acetylcholine (1 nM–1 μM), but not papaverine (100 μM), were abolished. The functional integrity of denuded preparations was tested by comparing concentration-effect curves to U-46619 (1 nM–1 μM) in intact and denuded vessels; no changes occurred following endothelium removal (mean pEC_{50} values ± s.e.mean: intact 7.91 ± 0.09, denuded 8.08 ± 0.06, both $n = 7$, $P > 0.05$; maximal contraction developed, intact 574 ± 68 mg tension, denuded 593 ± 65 mg tension, both $n = 7$, $P > 0.05$). The procedure employed to denude vessels of endothelium was not, therefore, considered to have compromised the functional integrity of the underlying smooth muscle cells.

Drugs and solutions

The composition of the Krebs solution used was as follows (mM): NaCl 118.4, KCl 4.8, $NaHCO_3$ 25.0, $MgSO_4$ 1.2, KH_2PO_4 1.2, glucose 11.1, $CaCl_2$ 1.25. The following compounds were either purchased or donated: acetylcholine chloride, (±)-pindolol, corynanthine hydrochloride, pargyline hydrochloride, imipramine hydrochloride, U-46619 (9,11-dideoxy-11α, 9α-epoxy-methanoprostaglandin $F_{2\alpha}$), yohimbine hydrochloride and tetrodotoxin (all purchased from the Sigma Chemical Company, St. Louis, MO, U.S.A.); rauwolscine hydrochloride (Roth, Germany); papaverine hydrochloride (Hopkin & Williams Ltd., U.K.); mianserin hydrochloride, PAPP (LY-165,163; 1-[-2-[4-aminophenyl] ethyl] -4-[3-trifluoromethylphenyl]piperazine) and 8-OH-DPAT (8-hydroxy-2(di-n-propylamino)tetralin hydrobromide); all purchased from Research Biochemicals Inc., U.S.A.; 5-hydroxytryptamine hydrochloride (Fluorochem Ltd., U.K.); mesulergine and methysergide maleate (gifts from Sandoz Pharma Ltd., Basle, Switzerland).

The following compounds were synthesized at Wyeth Laboratories (U.K.): 5-carboxamidotryptamine; sumatriptan; α-methyl-5-hydroxytryptamine; 2-methyl-5-hydroxytryptamine; ketanserin tartrate; (−)-propranolol hydrochloride; methiothepin maleate; spiperone; ondansetron; and ICS 205-930 ((3α-tropanyl)-1-H-indole-3-carboxylic acid ester).

Sumatriptan, spiperone, PAPP and methysergide were dissolved in 100% v/v dimethyl sulphoxide, and diluted in distilled H_2O. Metergoline was dissolved in 100% v/v ethanol, and diluted in distilled H_2O. U-46619 was dissolved in 5% w/v $NaHCO_3$. All other drugs were dissolved in distilled H_2O, and diluted in Krebs solution.

Statistical analysis and calculations

Agonist-evoked relaxant and contractile responses are expressed as the arithmetic mean ± s.e.mean for n separate experiments, using tissues from different animals. EC_{50} values were calculated as the concentration of agonist required to produce 50% of the maximum response attainable for that particular agonist; pEC_{50} values, where quoted, represent the negative logarithm_{10} of the EC_{50} value. Agonist concentration-ratios were determined by calculating the EC_{50} value of the agonist in the presence of antagonist, in the test preparation, divided by the EC_{50} value of the agonist in the control preparation; tissues were obtained from the same animal. EC_{50} values and agonist concentration-ratios were derived by the logistic curve-fitting programme ALLFIT (DeLean *et al.*, 1978), and are expressed as the arithmetic mean ± s.e.mean or the geometric mean with 95% confidence limits in parentheses. Where appropriate, differences between means were determined by a paired Student's t test, after checking the homogeneity of the variances. P values of less than 0.05 were considered to indicate a significant difference between the responses being compared.

Results

In both intact and endothelium-denuded preparations of jugular vein (precontracted with U-46619, 30 nM, and treated with ketanserin, 3 μM), 5-HT evoked concentration-dependent relaxations. The latter resulted in the production of

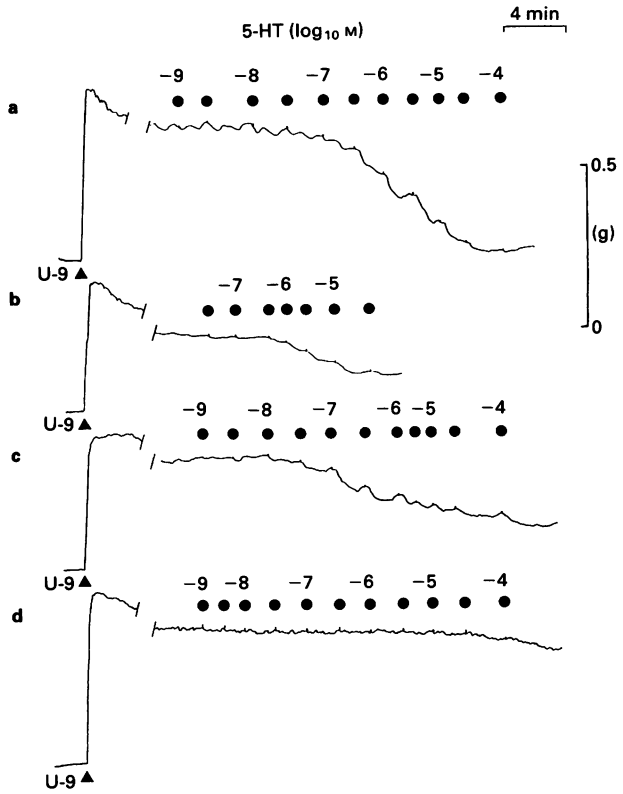

Figure 1 Cumulative concentration-effect curves to 5-hydroxytryptamine (5-HT) in preparations of guinea-pig isolated jugular vein, precontracted with U-46619 (30 nM; U-9), under the following conditions: (a) intact, and (b) endothelium-denuded preparations, in the presence of ketanserin (3 μM): (c) intact and (d) endothelium-denuded preparations in the presence of a combination of ketanserin (3 μM) and mesulergine (3 μM).

monophasic concentration-effect curves (Figures 1a and b). The relaxant responses to 5-HT in endothelium-denuded tissues were smaller in magnitude compared with the intact control. In intact preparations equilibrated with both ketanserin (3 μM) and mesulergine (3 μM), biphasic concentration-effect curves were obtained (Figure 1c). However, in preparations denuded of endothelium, in the presence of mesulergine (3 μM; ketanserin present), relaxant responses to 5-HT (10 nM–10 μM) were absent and relaxations were seen only with concentrations in excess of 30 μM (Figure 1d). These observations suggested that the biphasic concentration-effect curves observed for 5-HT in intact preparations in the presence of mesulergine consisted of an initial high affinity endothelium-dependent, and mesulergine-resistant, relaxant phase. The subsequent relaxant phase occurring to higher concentrations of 5-HT was due to an endothelium-independent, and mesulergine-sensitive, relaxant mechanism which occurred as the antagonist effect of mesulergine was surmounted.

From these studies, a high concentration of mesulergine (10 μM) was considered to be suitable for studying agonist and antagonist potencies at the endothelial 5-HT receptor, without the complication of activating either the smooth muscle relaxant 5-HT receptor or contractile 5-HT_2 receptors. Ketanserin (3 μM) could not be used to provide an antagonist effect at the 5-HT_2 receptors present, since extensive studies with ketanserin (3 μM) showed that it produced a 10 fold rightward displacement of the concentration-effect curve for all of the endothelial 5-HT receptor agonists examined.

Agonist studies

Preliminary experiments in groups of four tissues demonstrated that in the presence of the monoamine oxidase inhibitor, pargyline (50 μM) or the 5-HT uptake inhibitor imipramine (10 μM), geometric mean 5-HT concentration-ratios were 1.26 [0.39–4.06] and 0.96 [0.31–2.98] respectively. The maximal relaxations observed to 5-HT were also unchanged by either treatment (maximal relaxation developed, expressed as % change in precontracted tone ± s.e.mean, $n = 4$: control tissue 34.1 ± 8.3, pargyline-treated tissue 26.0 ± 2.9, $P > 0.05$; control tissue 32.6 ± 7.0, imipramine-treated tissue 28.6 ± 2.1, $P > 0.05$). Consequently, neither ligand was used during the agonist potency determinations.

5-CT was similar to 5-HT and produced a biphasic concentration-effect curve in the presence of mesulergine (10 μM). Only the first relaxant phase to 5-CT (0.1 nM –1.0 μM) was demonstrated to be endothelium-dependent and, therefore, analysed quantitatively. The second relaxant phase observed to 5-CT occurred at concentrations greater than 1.0 μM. Both sumatriptan (30 nM–10 μM) and α-methyl-5-HT (30 nM–3 μM) produced only monophasic, endothelium-dependent, concentration-effect curves. In endothelium-denuded preparations, both ligands were inactive at the smooth muscle relaxant receptor when studied up to a concentration of 30 μM. Monophasic concentration-effect curves were also observed for methysergide (10 nM–1.0 μM), 8-OH-DPAT (100 nM–10 μM) and 2-methyl-5-HT (300 nM–30 μM) and since these effects were observed in the presence of mesulergine (10 μM), an action at the smooth muscle relaxant 5-HT receptor was considered unlikely. The agonist concentration-effect curves are shown in Figure 2. The following rank order of agonist potency was obtained on the basis of the calculated EC_{50} values: 5-CT > 5-HT > methysergide ≥ α-methyl-5-HT ≥ sumatriptan > 8-OH-DPAT > 2- methyl- 5-HT. Although sumatriptan was of similar potency to methysergide, α-methyl-5-HT and 8-OH-DPAT, the former exhibited a higher efficacy in evoking relaxations. Data obtained for the agonists tested are summarised in Table 1.

Sumatriptan (at concentrations up to 30 μM) was highly selective for the endothelial 5-HT receptor and, therefore, the presence of mesulergine was not a prerequisite for investigating endothelium-dependent relaxant responses. The possibility that mesulergine could interact with the endothelial 5-HT receptor, and thus alter agonist potency measurements, was therefore examined. Mesulergine (3.0–10.0 μM) produced no change in the EC_{50} of the concentration-effect curve to sumatriptan (pEC_{50} values ± s.e.mean; mesulergine absent, 6.26 ± 0.16, $n = 5$; mesulergine 3.0 μM, 6.14 ± 0.11, $n = 5$; mesulergine 10.0 μM, 6.58 ± 0.04, $n = 21$).

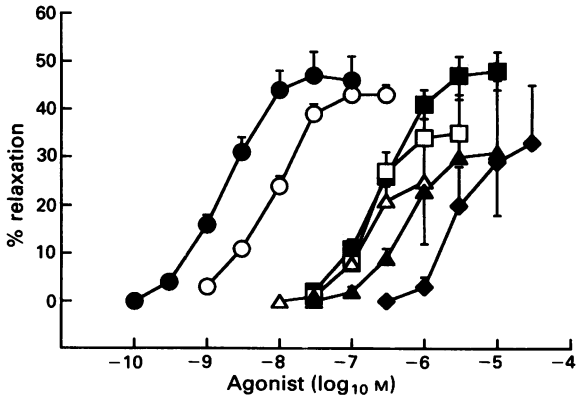

Figure 2 Endothelium-dependent relaxation of intact guinea-pig isolated jugular vein to 5-hydroxytryptamine (5-HT, ○), 5-carboxamidotryptamine (5-CT, ●), sumatriptan (■), α-methyl-5-HT (□), methysergide (△), 8-hydroxy-2-(di-n-propylamino)tetralin (8-OH-DPAT, ▲) and 2-methyl-5-HT (◆). Preparations were precontracted with U-46619 (30 nM) in the presence of mesulergine (10.0 μM), and cumulative concentration-effect curves were constructed from data obtained after the tone evoked had stabilized. Data represent the arithmetic mean for between 3–58 separate experiments, with s.e. mean values shown by the vertical bars.

Table 1 Potencies of agonists for the endothelial 5-HT receptor mediating relaxation of guinea-pig isolated jugular vein

Agonist tested	pEC_{50}	E_{max} (%)	n
5-HT	8.07 ± 0.04	44.2 ± 1.9	58
5-CT	8.74 ± 0.05	48.2 ± 4.8	8
Sumatriptan	6.58 ± 0.04	48.4 ± 3.7	21
Methysergide	6.89 ± 0.12	25.9 ± 7.9	3
α-methyl-5-HT	6.75 ± 0.01	34.9 ± 6.7	4
8-OH-DPAT	6.37 ± 0.12	31.1 ± 14.3	3
2-methyl-5-HT	5.59 ± 0.04	31.8 ± 11.7	4

pEC_{50} values represent the negative $\log_{10}$ of the molar concentration of agonist which produced 50% of the maximum relaxation developed to that particular agonist. E_{max} (%) values represent maximal relaxation developed to an agonist, expressed as a percentage of the sustained tone evoked to U-46619 (30 nM). Data are expressed as the arithmetic mean ± s.e.mean for n separate experiments. Abbreviations as in text.

Antagonist studies

A series of antagonists with known selectivity towards various 5-HT receptor subtypes, were tested against relaxations evoked by 5-HT. Several of these compounds (spiperone 1.0 μM, (±)-pindolol 1.0 μM, (−)-propranolol 1.0 μM, ondansetron 1.0 μM, ICS 205-930 10.0 μM) were inactive when used at high concentrations (Table 2). Furthermore, inhibition of neuronal activity by tetrodotoxin (100 nM) did not antagonize the relaxations evoked by 5-HT (geometric mean agonist concentration-ratio 1.64, $n = 2$).

However, relaxations to 5-HT and sumatriptan were sensitive to antagonism by ligands which have an affinity for the 5-HT_{1D} binding site. Methiothepin (30–300 nM), metergoline (100–1000 nM) and PAPP (30–300 nM; a 5-HT_{1A} receptor agonist) behaved as competitive antagonists against 5-HT (pA_2 [95% confidence limits], methiothepin 8.1 [7.7–8.9] $n = 7$, metergoline 7.4 [7.1–8.2] $n = 5$, PAPP 8.2 [7.9–8.8] $n = 4$; Schild slope [95% confidence limits], methiothepin 1.20 [0.69–1.71] $n = 7$, metergoline 1.36 [0.76–1.96] $n = 5$, PAPP 1.02 [0.72–1.33] $n = 4$: Figure 3 a–c). Using sumatriptan as an agonist, apparent pA_2 values estimated at single concentrations of methiothepin (30 nM), metergoline (100 nM) and PAPP (30 nM) were found to be similar (apparent pA_2 value [95% confidence limits], methiothepin 8.6 [7.7–9.5] $n = 4$, metergoline 7.5 [7.3–7.8] $n = 5$, PAPP 8.2 [7.9–8.4] $n = 4$) to the values determined previously with 5-HT.

In further studies, relaxations to 5-HT were also found to be antagonized by compounds with recognised affinity toward both α-adrenoceptors and 5-HT_{1D} receptors such as yohimbine (1.0–10.0 μM) and rauwolscine (0.3–10.0 μM) (pA_2 value [95% confidence limits], yohimbine 7.1 [6.8–7.7] $n = 4$, rauwolscine 6.8 [6.5–7.2] $n = 4$: Schild slope [95% confidence limits], yohimbine 0.90 [0.69–1.12] $n = 4$, rauwolscine 1.11 [0.81–1.42] $n = 4$: Figure 4a–b). In contrast, however, the yohimbine stereoisomer, corynanthine (10.0 μM) did not exhibit this effect (geometric mean 5-HT concentration-ratio [95% confidence limits], 1.47 [1.13–1.92], $n = 3$; Figure 4c). Both yohimbine (1.0 μM) and rauwolscine (1.0 μM) also antagonized relaxations to sumatriptan (apparent pA_2 value [95% confidence limits], yohimbine 6.8 [6.6–7.0], $n = 4$, rauwolscine, 6.7 [6.1–7.4], $n = 3$) although corynanthine (10.0 μM) showed no antagonist effect (geometric mean sumatriptan concentration-ratio [95% confidence limits], 1.48 [1.01–2.17], $n = 3$). The similarity between the antagonist potency estimates suggested that both 5-HT and sumatriptan activated the same receptor population.

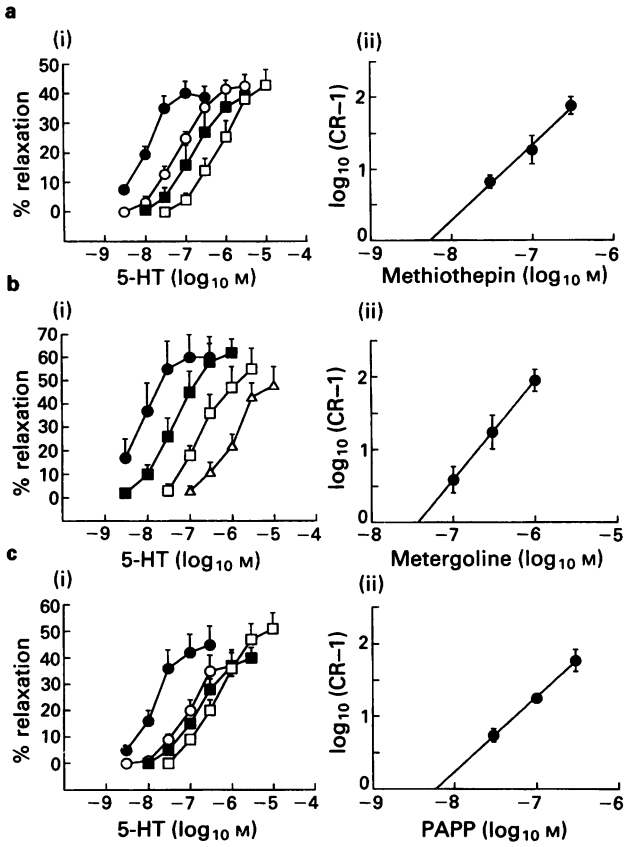

Figure 3 (i) Cumulative concentration-effect curves to 5-hydroxytryptamine (5-HT) of intact guinea-pig isolated jugular vein in the absence and presence of antagonist; (ii) Schild plot for the antagonism of 5-HT-evoked relaxant responses. The data shown are in panels: (a) methiothepin (30–300 nM, $n = 7$); (b) metergoline (100–1000 nM, $n = 5$) and (c) PAPP (30–300 nM, $n = 4$). The antagonist concentrations used are represented by the symbols (●) control, (○) 30 nM, (■) 100 nM, (□) 300 nM, and (△) 1000 nM. All experiments were performed in preparations precontracted with U-46619 (30 nM) in the presence of mesulergine (10 μM). The data are expressed as the mean ± s.e.mean (vertical bars) values for n separate experiments.

Table 2 Summary of antagonists which are inactive at the endothelial 5-HT receptor in guinea-pig isolated jugular vein

Antagonist (μM)	*Receptor selectivity*	*Agonist concentration-ratio* [95% confidence limits]	n
(±)-Pindolol (1.0)	$5\text{-HT}_{1A/1B}$	0.91 [0.28–2.94]	4
(−)-Propranolol (1.0)	$5\text{-HT}_{1A/1B}$	1.02 [0.38–2.69]	3
Spiperone (1.0)	$5\text{-HT}_{1A/2}$	0.96 [0.56–1.64]	4
Ondansetron (1.0)	5-HT_3	1.11 [0.39–3.20]	4
ICS 205-930 (10.0)	$5\text{-HT}_{3/4}$	0.84 [0.42–1.69]	4

5-HT concentration-ratio values are expressed as the geometric mean, with 95% confidence limits given in parentheses; n refers to the number of separate experiments.

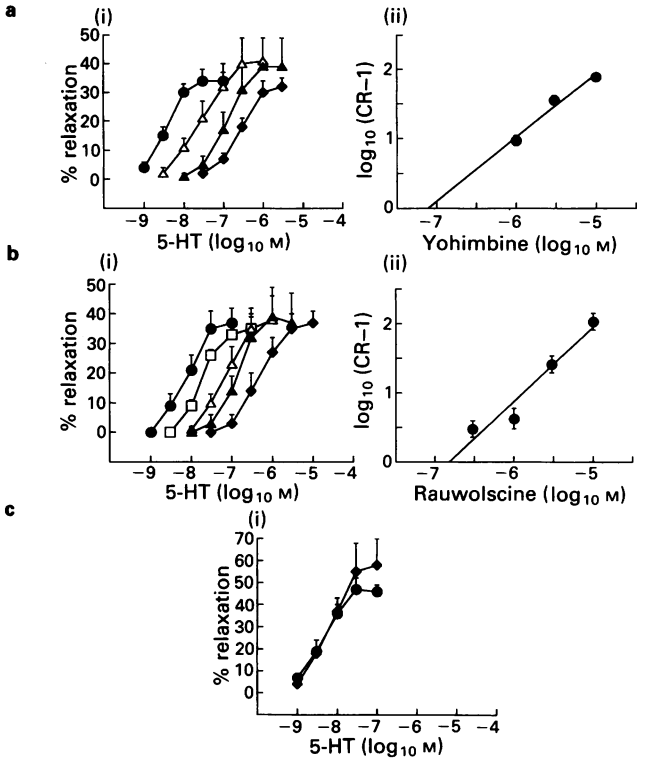

Figure 4 (i) Cumulative concentration-effect curves to 5-hydroxytryptamine (5-HT) of intact guinea-pig isolated jugular vein in the absence and presence of antagonist; (ii) Schild plot for the antagonism of 5-HT-evoked relaxant responses. The data shown are in panels: (a) yohimbine (1–10 μM, $n = 4$); (b) rauwolscine (0.3–10 μM, $n = 4$) and (c) corynanthine (10 μM, $n = 3$). The antagonist concentrations used are represented by the symbols (●) control, (□) 0.3 μM, (△) 1.0 μM, (▲) 3.0 μM, and (◆) 10.0 μM. All experiments were performed on preparations precontracted with U-46619 (30 nM) in the presence of mesulergine (10 μM). The data are expressed as the mean ± s.e.mean (vertical bars) values for n separate experiments.

Discussion

The identity of the 5-HT receptors which mediate endothelium-dependent relaxations to 5-HT in smooth muscle preparations may differ between tissues and species. In porcine coronary artery for example, the receptor is similar to the 5-HT_{1D} subtype (Schoeffter & Hoyer, 1989; 1990), whereas in rabbit jugular vein (Leff *et al.*, 1987) and porcine vena cava (Sumner, 1991) the receptors are atypical, in that they do not satisfy the criteria for any of the currently recognised 5-HT receptor types (see Bradley *et al.*, 1986). This paper examines the characteristics of an endothelial 5-HT receptor which mediates relaxation of guinea-pig isolated jugular vein.

By use of mesulergine (10 μM), it was possible to isolate endothelium-dependent relaxations to 5-HT (1 nM–10 μM) from an endothelium-independent component (which is blocked by this concentration of mesulergine). The activity of antagonists with affinities for a range of 5-HT receptor subtypes could thus be investigated. Concentration-dependent relaxations to 5-HT were resistant to antagonism by high concentrations of (±)-pindolol (5-$HT_{1A/1B}$), (−)-propranolol (5-$HT_{1A/1B}$), spiperone (5-$HT_{1A/2}$) and ondansetron (5-HT_3) respectively. In the presence of ICS 205–930 (10 μM), which has been used previously to study the putative 5-HT_4 receptor (Dumuis *et al.*, 1988; Craig *et al.*, 1990; Elswood *et al.*, 1991), 5-HT-evoked relaxations were unaltered. Moreover, relaxations to sumatriptan (which appeared to activate the same receptor as 5-HT) were also resistant to mesulergine (10.0 μM; 5-$HT_{1C/2}$). Thus the relative lack of activity of these compounds suggests that neither 5-HT_{1A}, 5-HT_{1B}, 5-HT_{1C}, 5-HT_2, 5-HT_3 nor the putative 5-HT_4 receptors are involved in the endothelium-dependent relaxation to 5-HT observed in this preparation.

Is the endothelial 5-HT receptor in guinea-pig isolated jugular vein a 5-HT_{1D} receptor as proposed in porcine coronary artery, or is it similar to those described in other venous preparations? The rank order of agonist potencies in the present study (5-CT > 5-HT > α-methyl-5-HT > sumatriptan > 8-hydroxy-DPAT > 2-methyl-5-HT) is similar to that described in porcine coronary artery (Schoeffter & Hoyer, 1990), but contrasted with that described in rabbit jugular vein (Leff *et al.*, 1987) and porcine vena cava preparations (α-methyl-5-HT > 2-methyl- 5-HT >> 5-CT; Sumner, 1991). Furthermore, no agonism or antagonism was observed with sumatriptan or 8-OH-DPAT when they were tested on the porcine vena cava preparation. Considering the 5 fold higher potency of 5-CT compared with 5-HT, the sensitivity to methiothepin, and the lack of activity of ligands with affinities toward 5-HT_2, 5-HT_3 and the putative 5-HT_4 receptors, a 5-HT_1-like classification of the endothelial receptor in guinea-pig isolated jugular vein would seem appropriate (see Bradley *et al.*, 1986). When compared with peripheral and central 5-HT_{1D} receptor models, the antagonist potencies determined in this study were consistent with a 5-HT_{1D} effect (see Table 3). In previous studies, emphasis has been placed upon the demonstration of antagonist activity of metergoline, yohimbine and rauwolscine when positively identifying functional 5-HT_{1D} receptors (Middlemiss *et al.*, 1988; Schoeffter & Hoyer, 1990; Limberger *et al.*, 1991; Martin *et al.*, 1991). Conversely, in dog saphenous vein the rank order of agonist potencies are similar, if not identical, to those described in the present study as well as in other proposed 5-HT_{1D} receptor models (5-HT > sumatriptan > 8-OH-DPAT; Perren *et al.*, 1991). However, Humphrey and co-workers were unable to demonstrate antagonist activity to either metergoline (0.1 μM), yohimbine (1.0 μM) or rauwolscine (1.0 μM) in dog saphenous vein, observations which were considered to preclude a 5-HT_{1D} receptor classification (Humphrey *et al.*, 1988; Perren *et al.*, 1991). Since the relaxations to 5-HT (and also

Table 3 Comparison of antagonist potencies in peripheral and central putative 5-HT_{1D} receptor models

Antagonist	*GPJV*	*PCA*	*RSV*	*HPA*	*PBC*	*GPFC*	*CSN*	*GPSN*
Methiothepin	8.1	7.3	9.5	8.6	7.5	8.2	7.0	8.9
Metergoline	7.4	6.9	7.8	6.9	7.1	7.0	–*	6.9
Yohimbine	7.1	6.4	6.6	–	–*	6.5	–*	–
Rauwolscine	6.8	6.0	6.8	–	–	–	–	–
PAPP	8.2	7.0	–	–	–	–	–	–

Data represent either pA_2 or pK_B values obtained with 5-HT as the agonist, taken from: GPJV, guinea-pig jugular vein, present study; PCA, pig coronary artery, Schoeffter & Hoyer, (1990); RSV, rabbit saphenous vein, Martin *et al.* (1991); HPA, human pial arterioles, Hamel & Bouchard, (1991), PBC, pig brain cortex, Schlicker *et al.* (1989); GPFC, guinea-pig frontal cortex, Middlemiss *et al.* (1988); CSN, calf substantia nigra, Schoeffter *et al.* (1988); GPSN, guinea-pig substantia nigra, Stanton *et al.* (1991).
*Indicates presence of agonist activity.

to sumatriptan) in guinea-pig isolated jugular vein were sensitive to metergoline (100–1000 nM), yohimbine (1.0–10.0 μM) and rauwolscine (0.3–10.0 μM), as well as to methiothepin (30–300 nM) and PAPP (30–300 nM), and also mimicked by agonists displaying high affinity toward the 5-HT_{1D} binding site, it is appropriate to consider a 5-HT_{1D} classification for this receptor.

In conclusion, the receptor which mediates an endothelium-dependent relaxation to 5-HT, and other 5-HT receptor agonists, in guinea-pig isolated jugular vein is similar to that described in porcine coronary artery (Schoeffter & Hoyer, 1990) but differs from the endothelial 5-HT receptor(s) reported in other venous preparations (Leff *et al.*, 1987; Sumner, 1991). A 5-HT_{1D} classification is proposed for the receptor described in this study, but clearly a definitive classification is only possible following the development of selective 5-HT_{1D} receptor antagonists. The results obtained in this study provide further evidence for the existence of endothelial 5-HT receptor heterogeneity.

I would like to express my thanks to Dr K.F. Rhodes and Mrs S.J. Bill for their advice given during the preparation of this manuscript. Thanks also to Mrs Debbie McCreanney for excellent secretarial skills.

Methysergide and mesulergine were gifts from Sandoz Pharma Ltd., Switzerland.

References

ANGUS, J.A. & COCKS, T.M. (1989). Endothelium-derived relaxing factor. *Pharmacol. Ther.*, **41**, 303–351.

ARUNLAKSHANA, O. & SCHILD, H.O. (1959). Some quantitative uses of drug antagonists. *Br. J. Pharmacol. Chemother.*, **14**, 48–58.

BRADLEY, P.B., ENGEL, G., FENIUK, W., FOZARD, J.R., HUMPHREY, P.P.A., MIDDLEMISS, D.N., MYLECHARANE, E.J., RICHARDSON, B.P. & SAXENA, P.R. (1986). Proposals for the classification and nomenclature of functional receptors for 5-hydroxytryptamine. *Neuropharmacology*, **25**, 563–76.

CHARLTON, K.G., BOND, R.A. & CLARKE, D.E. (1986). An inhibitory prejunctional 5-HT_1-receptor in the isolated perfused rat kidney. Apparent distinction from 5-HT_{1A}, 5-HT_{1B} and 5-HT_{1C} subtypes. *Naunyn-Schmiedebergs Arch. Pharmacol.*, **332**, 8–15.

CONN, P.J., SANDERS-BUSH, E., HOFFMAN, B.J. & HARTIG, P.R. (1986). A unique serotonin receptor in choroid plexus is linked to phosphatidylinositol turnover. *Proc. Natl. Acad. Sci. U.S.A.*, **83**, 4086–4088.

CRAIG, D.A., EGLEN, R.M., WALSH, L.K.M., PERKINS, L.A., WHITING, R.L. & CLARKE, D.E. (1990). 5-Methoxytryptamine and 2-methyl-5-hydroxytryptamine-induced desensitization as a discriminative tool for the 5-HT_3 and putative 5-HT_4 receptors in guinea-pig ileum. *Naunyn-Schmiedebergs Arch. Pharmacol.*, **342**, 9–16.

DELEAN, A., MUNSON, P.J. & RODBARD, D. (1978). Simultaneous analysis of families of sigmoidal curves: application to bioassay, radioligand assay and physiological dose curves. *Am. J. Physiol.*, **235**, E97–E102.

DE VIVO, M. & MAAYANI, S. (1986). Characterisation of 5-hydroxytryptamine$_{1A}$ receptor-mediated inhibition of adenylate cyclase activity in guinea-pig and rat hippocampal membranes. *J. Pharmacol. Exp. Ther.*, **238**, 248–253.

DUMUIS, A., BOUHELAL, R., SEBBEN, M. & BROCKAERT, J. (1988). A 5-HT receptor in the central nervous system positively coupled with adenylate cyclase is antagonised with ICS 205-930. *Eur. J. Pharmacol.*, **146**, 187–188.

ELSWOOD, C.J., BUNCE, K.T. & HUMPHREY, P.P.A. (1991). Identification of putative 5-HT_4 receptors in guinea-pig ascending colon. *Eur. J. Pharmacol.*, **196**, 149–155.

ENGEL, G., GOTHERT, M., HOYER, D., SCHLICKER, E. & HILLENBRAND, K. (1986). Identity of inhibitory presynaptic 5-hydroxytryptamine (5-HT) autoreceptors in the brain cortex with 5-HT_{1B} sites. *Naunyn-Schmiedebergs Arch. Pharmacol.*, **332**, 1–7.

HAMEL, E. & BOUCHARD, D. (1991). Contractile 5-HT_1 receptors in human isolated pial arterioles: correlation with 5-HT_{1D} binding sites. *Br. J. Pharmacol.*, **102**, 227–233.

HEURING, R.E. & PEROUTKA, S.J. (1987). Characterisation of a novel [^{3}H]-5-hydroxytryptamine binding site subtype in bovine brain membranes. *J. Neurosci.*, **7**, 894–903.

HOYER, D., ENGEL, G. & KALKMAN, H.O. (1985). Characterisation of the 5-HT_{1B} recognition site in rat brain: binding studies with [^{125}I]iodocyanopindolol. *Eur. J. Pharmacol.*, **118**, 1–12.

HUMPHREY, P.P.A., FENIUK, W., PERREN, M.J., CONNOR, H.E., OXFORD, A.W., COATES, I.H. & BUTINA, D. (1988). GR 43175, a selective agonist for the 5-HT_1-like receptor in dog isolated saphenous vein. *Br. J. Pharmacol.*, **94**, 1123–1132.

KALKMAN, H.O., ENGEL, G. & HOYER, D. (1986). Inhibition of 5-carboxamidotryptamine-induced relaxation of guinea-pig ileum correlates with [^{125}I]LSD binding. *Eur. J. Pharmacol.*, **129**, 139–145.

LEFF, P., MARTIN, G.R. & MORSE, J.M. (1987). Differential classification of vascular smooth muscle and endothelial cell 5-HT receptors by use of tryptamine analogues. *Br. J. Pharmacol.*, **91**, 321–331.

LIMBERGER, N., DEICHER, R. & STARKE, K. (1991). Species differences in presynaptic serotonin autoreceptors: mainly 5-HT_{1B} but possibly in addition 5-HT_{1D} in the rat, 5-HT_{1D} in the rabbit and guinea-pig brain cortex. *Naunyn-Schmiedebergs Arch. Pharmacol.*, **343**, 353–364.

MARTIN, G.R., LEFF, P., CAMBRIDGE, D. & BARRETT, V.J. (1987). Comparative analysis of two types of 5-hydroxytryptamine receptor mediating vasorelaxation: differential classification using tryptamines. *Naunyn-Schmiedebergs Arch. Pharmacol.*, **336**, 365–373.

MARTIN, G.R., PRENTICE, D.J. & MACLENNAN, S.J. (1991). The 5-HT receptor in rabbit saphenous vein. Pharmacological identity with the 5-HT_{1D} recognition site? *Fund. Clin. Pharmacol.*, **5**, 417.

MIDDLEMISS, D.N., BREMER, M.E. & SMITH, S.M. (1988). A pharmacological analysis of the 5-HT receptor mediating inhibition of 5-HT release in the guinea-pig frontal cortex. *Eur. J. Pharmacol.*, **157**, 101–107.

PAZOS, A., HOYER, D. & PALACIOS, J.M. (1984). The binding of serotonergic ligands to the porcine choroid plexus: characterisation of a new type of serotonin recognition site. *Eur. J. Pharmacol.*, **106**, 539–546.

PEDIGO, N.W., YAMAMURA, H.I. & NELSON, D.L. (1981). Discrimination of multiple [^{3}H]-5-hydroxytryptamine binding sites by the neuroleptic spiperone in rat brain. *J. Neurochem.*, **36**, 220–226.

PEROUTKA, S.J. & SNYDER, S.H. (1979). Multiple serotonin receptors: differential binding of [^{3}H]5-hydroxytryptamine, [^{3}H]lysergic acid diethylamide and [^{3}H]spiroperidol. *Mol. Pharmacol.*, **16**, 687–699.

PERREN, M.J., FENIUK, W. & HUMPHREY, P.P.A. (1991). Vascular 5-HT_1-like receptors that mediate contraction of the dog isolated saphenous vein and carotid arterial vasoconstriction in anaesthetised dogs are not of the 5-HT_{1A} or 5-HT_{1D} subtype. *Br. J. Pharmacol.*, **102**, 191–197.

SCHILD, H.O. (1947). pA, a new scale for the measurement of drug antagonism. *Br. J. Pharmacol. Chemother.*, **2**, 189–206.

SCHLICKER, E., FINK, K., GOTHERT, M., HOYER, D., MOULDERINGS, G., ROSCHKE, I. & SCHOEFFTER, P. (1989). The pharmacological properties of the presynaptic autoreceptor in the pig brain cortex conform to the 5-HT_{1D} receptor subtype. *Naunyn-Schmiedebergs Arch. Pharmacol.*, **340**, 45–51.

SCHOEFFTER, P. & HOYER, D. (1989). Is the sumatriptan (GR 43175)-induced endothelium-dependent relaxation of pig coronary arteries mediated by 5-HT_{1D} receptors? *Eur. J. Pharmacol.*, **166**, 117–119.

SCHOEFFTER, P. & HOYER, D. (1990). 5-Hydroxytryptamine (5-HT)-induced endothelium-dependent relaxation of pig coronary arteries is mediated by 5-HT receptors similar to the 5-HT_{1D} receptor subtype. *J. Pharmacol. Exp. Ther.*, **252**, 387–395.

SCHOEFFTER, P., WAEBER, C., PALACIOS, J.M. & HOYER, D. (1988). The 5-hydroxytryptamine 5-HT_{1D} receptor subtype is negatively coupled to adenylate cyclase in calf substantia nigra. *Naunyn-Schmiedebergs Arch. Pharmacol.*, **337**, 602–608.

STANTON, J.A., SCHOLEY, K.S., BEER, M.S., HARGREAVES, R.J. & MIDDLEMISS, D.N. (1991). Antagonist actions of methiothepin and metergoline in guinea pig substantia nigra and rabbit saphenous vein. *Serotonin 1991: 5-Hydroxytryptamine-CNS Receptors and Brain Function.* International Conference, Birmingham, U.K., 79.

SUMNER, M.J. (1991). Characterisation of the 5-HT receptor mediating endothelium-dependent relaxation in porcine vena cava. *Br. J. Pharmacol.*, **102**, 938–942.

SUMNER, M.J., FENIUK, W. & HUMPHREY, P.P.A. (1989). Further characterisation of the 5-HT receptor mediating vascular relaxation and elevation of cyclic AMP in porcine isolated vena cava. *Br. J. Pharmacol.*, **97**, 292–300.

(Received February 19, 1992
Accepted March 17, 1992)

Br. J. Pharmacol. (1992), **106**, 710–716

Construction of antagonist dose-response curves for estimation of pA_2-values by Schild-plot analysis and detection of allosteric interactions

[1]Gerald Pöch, Friedrich Brunner & Elisabeth Kühberger

Institut für Pharmakologie und Toxikologie, Universität Graz, Univ. pl. 2, A-8010 Graz, Austria

1 One aim of this paper is to show an alternative approach for the determination of antagonist affinity estimates, K_B and pA_2, by construction and evaluation of antagonist dose-response curves (DRCs), using the curve-fitting programme, ALLFIT.

2 Parallel antagonist DRCs were derived by vertical analysis of families of conventional agonist DRCs in the presence and absence of an antagonist at a certain agonist concentration above its ED_{50}. The latter represents a chosen, i.e. fixed dose-ratio (DR). The antagonist concentration that reduces an agonist effect to its $E_{max}/2$ was termed B_x. It corresponds to B, the fixed antagonist concentration, tested to obtain DR − 1, conventionally.

3 The dissociation constant was calculated as $K_B = B_x/DR - 1$, analogous to the conventional approach ($K_B = B/DR - 1$). Likewise, pA_2-values were estimated by plotting log B_x, obtained by the alternative approach, vs log (DR − 1) in an 'alternative Schild plot'.

4 Experimental agonist DRCs from our laboratory and from the literature were analysed and K_B- and pA_2-values obtained by the alternative approach were compared with those obtained by the conventional method. The results showed a very good agreement (correlation) between the pA_2-values obtained by either method (slope = 1.02, $r = 0.99$, $n = 9$), in agreement with theoretical DRCs.

5 Besides estimation of K_B and pA_2, antagonist DRCs were also evaluated qualitatively. The most important finding was that allosteric antagonists or competitive antagonists with an allosteric component, such as gallamine, showed a significant reduction in the maximum of the antagonist DRCs (I_{max}). The evaluation of antagonist DRCs appears to be a sensitive procedure to detect allosteric interactions.

6 This alternative approach can supplement or replace the conventional approach for the evaluation of antagonists on a quantitative and qualitative basis. The alternative approach appears of special advantage where the supply and/or the solubility of the agonist is limited, resulting in incomplete agonist DRCs.

7 For rapid screening of potential antagonists, a single antagonist DRC at the maximum effective agonist concentration may be constructed to calculate K_B reliably.

Keywords: Antagonists; dose-response curves; K_B; pA_2; competitive; allosteric

Introduction

The dissociation constant K_B of a competitive antagonist is derived from the shift of an agonist dose-response curve (DRC), i.e. the dose-ratio (DR) of equieffective agonist concentrations at a fixed antagonist concentration of B. A plot of log (DR − 1) vs log B (Schild plot), gives a straight line and allows calculation of $-\log K_B = pA_2$ for a dose-ratio x = 2 (Arunlakshana & Schild, 1959). If the regression of log (DR − 1) vs log B is linear and has a slope of unity, a competitive antagonism between agonist and antagonist at the receptor is inferred. More than 40 years after Schild's formulation, the Schild regression is still a powerful tool in experimental pharmacology and provides a cornerstone of receptor classification (Tallarida *et al.*, 1979; Kenakin, 1987).

The present paper, while adhering to the derivation of the model by Schild (1947, 1957) and the pA_2-analysis by Schild regression (Arunlakshana & Schild, 1959), describes an alternative approach by estimating the antagonist concentration B_x which reduces the agonist response to its $E_{max}/2$ at a fixed agonist concentration, i.e. at a fixed DR, rather than estimating values of DR − 1 at a fixed antagonist concentration B. This procedure requires the conventional testing of an agonist in the absence and presence of a fixed concentration of an antagonist. Also, the (chosen) fixed dose-ratio corresponds to the agonist concentration in the absence and presence of an antagonist, routinely determined at the 50% effect level of the agonist. In order to differentiate between the fixed concentration of the antagonist B and the antagonist concentration which reduces an agonist effect to its $E_{max}/2$, to be determined from antagonist DRCs, the latter was termed B_x.

As a major advantage, this procedure is also applicable to incomplete agonist DRCs, which may be due to limited agonist availability and/or solubility. Besides this practical aspect, it was hoped that the direct presentation of antagonist effects in form of DRCs might provide better information as to the type of antagonism exerted by a particular blocker in a given test tissue. Thus, purely competitive antagonists as well as antagonists with a competitive and an allosteric component were selected and tested in a simple experimental set-up. In addition, published data of several authors were analysed to give DRCs of various antagonists at different receptors, obtained in different laboratories. The inclusion of literature data for this paper served the purpose of examining our new approach for a variety of different receptors with different agonists and antagonists to exclude a possible biased interpretation derived only from interactions at muscarinic and β-adrenoceptors of the bovine heart and tracheal muscle, respectively.

[1] Author for correspondence.

The results provide evidence that this new approach is advantageous both from a practical and theoretical point of view: even incomplete dose-response curves give reliable affinity estimates. In some cases, the type of antagonism that is operative in a given experiment, is clearly more easily discerned than in the conventional approach of agonist DRCs.

In this paper we use the expressions 'conventional Schild plot' and 'alternative Schild plot' to indicate that the values for the antagonist concentrations and for DR − 1 were obtained by the conventional and by the present alternative approach, respectively.

A preliminary account of this work has appeared in abstract form (Pöch *et al.*, 1990).

Methods

Isolated organ preparations used in our laboratory

Trabecular muscles Left bovine atria were obtained from the local slaughterhouse. Trabeculae (length 4–5 mm, diameter 1–2 mm) were rapidly excised from the auricular appendix and suspended in 5 ml organ baths filled with a modified Tyrode solution of the following composition (mmol l^{-1}): NaCl 137, KCl 5.4, $CaCl_2$ 4.8, $MgCl_2$ 1.1, NaH_2PO_4 0.4, $NaHCO_3$ 11.9 and glucose 10.1, gassed with carbogen and kept under constant temperature of 32°C. Muscles were electrically stimulated (frequency 1 Hz; duration 5 ms; 5 fold threshold voltage) at a resting tension of 1.5 g by means of a HSE 215/I-stimulator (Hugo Sachs Elektronik, Freiburg, Germany). Contractile force was recorded isometrically with Gould transducers connected to a Watanabe multichannel recorder.

Preparations were allowed to stabilize for 45 min. DRCs for the negative inotropic effect of the muscarinic agonist methacholine were established by adding the drug cumulatively to the organ bath. After 30 min equilibration, the trabeculae were pretreated with antagonists for 45 min and cumulative DRCs to methacholine were repeated (10 nmol l^{-1} to 30 mmol l^{-1}). For a given antagonist, each muscle was exposed to all three or four antagonist concentrations in ascending order. Each concentration was tested on three to four different trabeculae derived from one heart, and for each antagonist, three to four hearts were used. The negative inotropic effect was quantitated as percentage of the control contraction, i.e. after tissue equilibration and before administration of methacholine.

Bovine tracheal muscle strips were prepared and treated as described earlier (Pöch & Zimmermann, 1988). The muscles were precontracted by 27 mmol l^{-1} KCl in order to study the relaxant effects of the β-adrenoceptor agonist orciprenaline in the absence and in the presence of 0.075, 0.375, and 3.75 μmol l^{-1} propranolol.

Drugs

Orciprenaline sulphate was a gift of Boehringer Ingelheim, Germany, propranolol was kindly supplied by ICI, Wilmslow, Cheshire, England. Methacholine bromide and gallamine triethiodide were purchased from Sigma Chemical Co., Munich, Germany. Pirenzepine dihydrochloride was a generous gift from Dr R. Hammer, di Angeli, Milano, Italy, and AF-DX 116 (11-[[2-[(diethylamino) methyl]-1-piperidinyl] acetyl]-5,11-dihydro-6H-pyrido [2,3-b][1,4] benzodiazepine-6-one) from Dr Thomae GmbH, Biberach, Germany.

Construction of agonist- and antagonist dose-response curves

The construction of antagonist DRCs is illustrated in Figure 1, which shows the basic difference between the conventional and the alternative approach, exemplified with idealized curves. First, agonist DRCs were constructed as usual (Figure 1a,1c); second, in the submaximum to maximum dose-range of the agonist, vertical lines were drawn at fixed dose-ratios, exemplified for DR = 10 (Figure 1a) and for DR = 300 (Figure 1c). The inhibitory effects of the antagonist B were then calculated as indicated in Figure 1a and Figure 1b. They were determined by using experimental points of the agonist DRCs, rather than points of the fitted DRCs, when possible. With the values of inhibition obtained graphically, antagonist DRCs were constructed, shown in Figure 1b and Figure 1d, by the ALLFIT programme package (De Lean *et al.*, 1988), analogously to the agonist DRCs. B_x, the concentration which reduced the effect of the agonist to its $E_{max}/2$, corresponds to an inhibitory effect of 44.7% in Figure 1a and to 50% in Figure 1c. Hence, Figure 1 shows that if B_x is determined from antagonist DRCs at submaximum effective agonist concentrations (Figure 1a,b), it corresponds to a value lower than B_{50}, i.e. to a value $< IC_{50}$. When B_x is determined at E_{max} of the agonist, it equals the half maximum effective antagonist concentration, termed B_{50} in the present paper (Figure 1d); it corresponds to the IC_{50} of B.

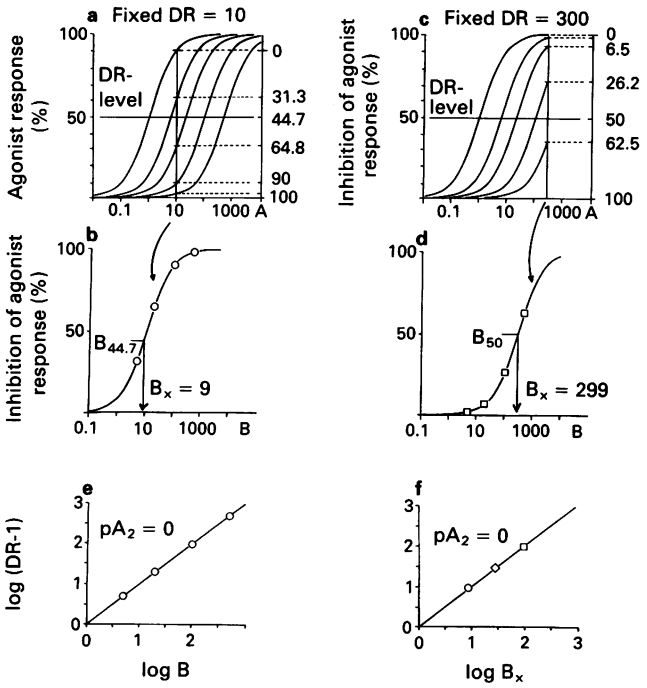

Figure 1 Theoretical dose-response curves (DRCs) of an agonist A alone and in the presence of a competitive antagonist B at concentrations of 5, 20, 100 and 300 (a,c). DRCs of inhibitory effects of the antagonist in the presence of agonist concentrations of 10 (b) and 300(d). The antagonist DRC in (b) was derived from (a) by vertical evaluation of inhibition of agonist response (right scale) at the agonist concentration of 10, corresponding to a fixed DR = 10. The antagonist DRC in (d) was derived analogously by vertical evaluation at the agonist concentration of 300, corresponding to DR = 300. Schild plots derived from the agonist DRCs in the upper panel are shown in (e), from antagonist DRCs in the lower panel in (f), supplemented by values obtained at DR = 30 (◇).

An important feature of the ALLFIT programme is the possibility of doing more than one fit with and without forcing fitting of data points to curves with the same slope and/or the same maximum. The results of various fits are then compared statistically, whereby $P<0.05$ indicates a significant deterioration of the respective fit. We took advantage of this possibility in the analysis of experimental agonist or antagonist DRCs in the present investigation by performing a first fit without and a second with the constraints of the

same slope and the same maximum, and checked whether these constraints were acceptable statistically, as expected in the case of competitive antagonists. Where a reduction of the maximum response appeared, we checked whether or not it was statistically significant by comparing the fits with and without the constraint of unaffected maximum.

Construction of Schild plots

Antagonist concentrations were plotted versus values of DR − 1 as usual. B indicates the antagonist concentrations chosen in the conventional approach, B_x the antagonist concentration derived by the alternative approach. As described above, B_x was derived from antagonist DRCs at a fixed dose-ratio. The estimation of DR − 1 in both procedures is in principle determined at the dose-ratio level, i.e. the effect level which represents $E_{max}/2$ of the agonist control curve, in accordance with general practice.

Statistical analyses

The slopes of Schild plots were tested for difference from unity by the partial *F*-test (Rodbard, 1974) as follows: The data points log (DR − 1) were regressed against log B (or B_x) and the sum of squared deviations (SSQ) determined. In a second step, the slope for the regression line was fixed as 1 and SSQ determined as before. Naturally, the second procedure gave a larger sum of squared deviations. Using the two SSQ values, the partial *F*-test was performed with the first regression as the more complex and the second regression (unity slope) as the less complex condition. Slopes were considered significantly different from unity in case of $P<0.05$.

Calculation of K_B

In addition to the graphical estimation of pA_2-values, described above, K_B was calculated according to the equation

$$K_B = B/DR - 1 \text{ and } K_B = B_x/DR - 1,$$

respectively. The same values can be obtained from a Schild plot with the constraint of a slope of 1. Mean values of K_B were calculated in this paper from individual values of B and DR − 1 and B_x and DR − 1, respectively. These are listed and compared in Table 1.

Results

Theory

Competitive antagonism DRCs of an agonist A are shown in the absence and presence of a competitive antagonist B in the arbitrary concentrations of 5, 20, 100 and 300 with a slope of 1 (Figure 1a,c), constructed according to the theory. An antagonist affinity corresponding to $K_B = 1$ ($pA_2 = 0$) and equal values for B and DR − 1 were assumed. Hence, antagonist concentrations of B = 5, 20, 100 and 300 correspond to values of DR − 1 of 5, 20, 100 and 300, derived from Figure 1a. The logarithms of these values are plotted in the conventional Schild plot in Figure 1e, yielding a pA_2-value of 0 with a slope of 1.

In the lower panel of Figure 1, DRCs of the inhibitory effects of this antagonist B are shown and the corresponding alternative Schild plot was derived from these results. Two antagonist DRCs are shown in Figure 1b and d, namely DRCs of inhibitory effects against A at the fixed DR = 10 and 300, respectively. The antagonist DRCs had a slope close to 1 (0.997 and 0.97, respectively) and were anticipated to reach the same maximum, i.e. 100% inhibition of the control response to the agonist, when completely displaced; the control response to the undisplaced agonist represents 0% inhibition. Two additional antagonist DRCs were constructed at DR = 30 and DR = 100 (not shown in Figure 1) which gave slope-values of 0.991 and 0.996. All four antagonist DRCs thus had a slope very close to 1 and a forced shared slope-value was accepted statistically ($P = 0.17$). Hence, antagonist DRCs derived from theoretical, i.e. parallel agonist DRCs with a slope of 1 were also parallel with a slope of 1.

The B_x-values in the example correspond to antagonist concentrations which caused 44.7 (Figure 1b) and 50% inhibition of the agonist response (Figure 1d). These inhibitory concentrations reduced the agonist effects to the effect level where the dose-ratio was determined in the conventional approach (Figure 1a and c: DR-level). B_x correspond to concentrations of 9 and 299 of B. They were observed at fixed agonist concentrations of 10 and 300, which correspond to values of DR − 1 = 9 and 299. Of necessity, the alternative Schild plot (Figure 1f) gives the same value of $pA_2 = 0$ at a slope 1 as the conventional approach (Figure 1e).

Allosteric interactions A parallel shift of agonist DRCs by an antagonist can also be caused by allosteric antagonists. However, these shifts do not follow the mass action law. We here show theoretical curves of an agonist A in the absence and presence of an allosteric antagonist, that were published by Ehlert (1988a), in Figure 2a. The corresponding Schild plot is shown in Figure 2c. From this plot it is clear that there is a pronounced deviation of the curve from a straight line with the slope of 1. A close inspection of the agonist DRCs also shows deviations from a competitive type of interaction, the shift of the DRCs is much less than would be expected from the respective concentrations of a competitive antagonist, namely 3, 10, 100 and 1000 B.

Antagonist DRCs in Figure 2b, derived from Figure 2a, show a pronounced reduction in the maximum of the DRCs of inhibitory effects (I_{max}), progressively increasing with the

Table 1 Comparison of experimental, calculated K_B-values obtained by the conventional and the alternative approach

	K_B			
Antagonist/Agonist	*Conventional*	*Alternative*	P	*Reference*
Propranolol/Orciprenaline	0.017 ± 0.005	0.017 ± 0.003	–	This paper
AF-DX 116/MeCh	0.13 ± 0.05	0.09 ± 0.01	0.39	Not shown
Butoxamine/Tazolol	0.26 ± 0.11	0.16 ± 0.04	0.19	Kenakin (1982)
Butoxamine/Terbutaline	0.27 ± 0.11	0.24 ± 0.05	0.72	Kenakin (1982)
Pirenzepine/MeCh	0.27 ± 0.06	0.25 ± 0.006	0.56	This paper
Pirenzepine/MeCh	1.34 ± 0.58	1.35 ± 0.33	0.98	This paper
Gallamine/MeCh	1.60 ± 0.69	0.89 ± 0.10	0.13	This paper
C 6/BuNMe$_3$Br	31 ± 2.95	32.6 ± 0.57	0.52	Ariëns *et al.* (1956)
Theophylline/Adenosine	31.1 ± 6.23	32.8 ± 5.24	0.72	Persson *et al.* (1982)

K_B-values are expressed as $\mu mol\ l^{-1}$. Mean values ± s.d. of 3–5 pairs of B or B_x and DR − 1, derived from the 9 independent series of experiments listed. Statistical comparison by *t* test.
MeCh, methacholin; C6, lexamethonium.

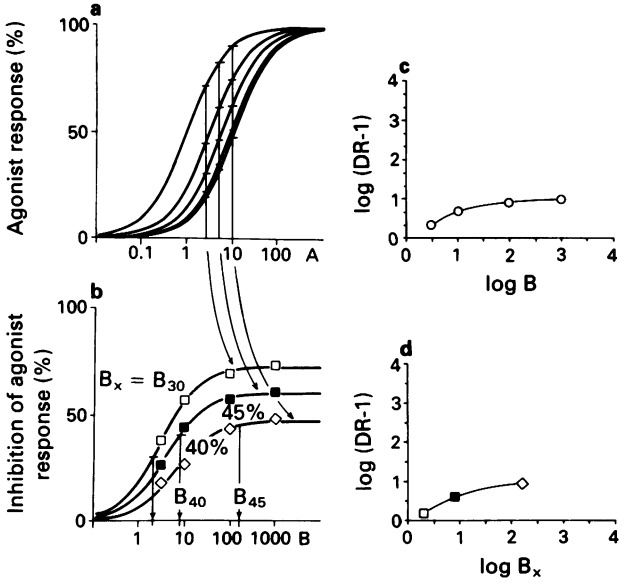

Figure 2 Theoretical dose-response curves (DRCs) of an agonist A in the absence and presence of an allosteric inhibitor in the concentrations of 3, 10, 100 and 1000 (a), according to Ehlert (1988a), which shifted the DRCs by DR − 1 = 2.2, 5, 8.5 and 10. Antagonist DRCs (b) at agonist concentrations of 2.5 (□), 5 (■) and 10 (◇) were derived analogously to Figure 1. These agonist concentrations correspond to DR − 1 = 1.5, 2 and 18. The antagonist DRCs show increasing depression of the maximum with increasing agonist concentrations. The B_x-values, calculated analogously to Figure 1, were 2, 8 and 160. Accordingly, a non-linear relationship between the concentrations of B and B_x, respectively, and DR − 1 was obtained from both graphs, the agonist DRCs and the antagonist DRCs in the respective Schild plots (c,d).

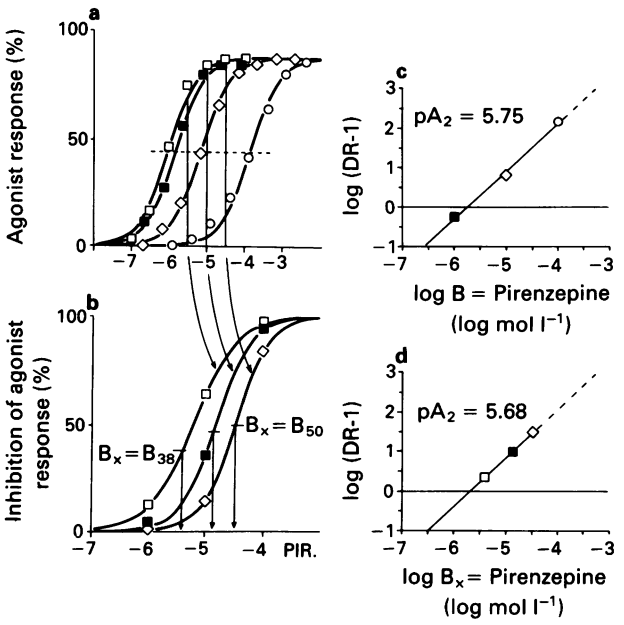

Figure 3 Experimental dose-response curves (DRCs) of methacholine (MeCh) and pirenzepine, presented as in Figure 1 together with the Schild plots. Agonist response: negative inotropy of trabecular muscle. The symbols indicate mean values from 3 experiments. The DRCs in (a) show the control curve (□) and the DRCs in the presence of 1 (■), 10 (◇) and 100 (○) μmol l^{-1} pirenzepine; they were fitted with the constraints of common slope and E_{max}, yielding a slope of 1.1. The DRCs in (b) represent antagonist DRCs in the presence of 3 (□), 10 (■) and 30 (◇) μmol l^{-1} MeCh; they were fitted with the constraint of common I_{max}. The slopes of the 3 curves were 1.1, 1.4 and 1.5, respectively. The slopes in the Schild plots were 1.21 (c) and 1.23 (d), not significantly different from 1.

agonist concentrations from 2.5 to 10 A, at which the inhibitory effects of B have been assessed. The corresponding alternative Schild plot in Figure 2d shows the same deviation, i.e. from a straight line with slope = 1 as the conventional Schild plot in Figure 2c.

Experiments

Competitive interaction: complete dose-response curves As an example of a competitive interaction with complete agonist DRCs, we here show DRCs of the agonist, methacholine (MeCh), in the absence and presence of the M_1-receptor antagonist, pirenzepine, in a cardiac preparation (Figure 3). The DRCs of methacholine are shifted to the right in a parallel fashion up to DR − 1 = 145.

The pA_2-value derived from these agonist DRCs was found to be 5.75 at a slope of 1.21 (Figure 3c). The mean value of calculated K_B was 1.34 μmol l^{-1} (Table 1), corresponding to $-\log K_B = pA_2 = 5.87$. The latter value was calculated according to the equation $K_B = B/DR - 1$, which assumes a slope of 1.

From the results of Figure 3a, three antagonist DRCs were obtained at concentrations of the agonist of 3, 10 and 30 μmol l^{-1}. The alternative Schild plot, shown in Figure 3d, gave a pA_2-value of 5.68 at a slope of 1.23, very close to the values obtained by the conventional approach. The calculated mean pA_2-value was 5.87 ($K_B = 1.35$ μmol l^{-1} in Table 1).

Competitive interaction: incomplete dose-response curves To illustrate the usefulness of the alternative approach to estimate pA_2-values of competitive antagonists from incomplete agonist DRCs, we show DRCs of the agonist BuN_3MeBr in the absence and presence of the competitive antagonist hexamethionium (C6) obtained with the isolated rectus muscle of the frog. These curves have been taken from Ariëns *et al.* (1956) and are shown in Figure 4a as incomplete DRCs by cutting the DRCs at concentrations >200 μmol l^{-1}.

Figure 4a shows fitted agonist DRCs of the incomplete data with the constraints of shared and constant parameters of $E_{max} = 100$ and identical slope for the 4 curves. This fit was not significantly worse than the fit without these constraints ($P = 0.33$). Thereby, a common slope of 1.58 was obtained. The Schild-plot analysis in Figure 4c gave $pA_2 = 4.49$ at a slope = 1.0.

Figure 4b shows two curves for the inhibitory effects of C6, assessed at 100 and 200 μmol l^{-1} of BuN of Figure 4a, at concentrations of the agonist which were in the range of experimental points. The curves were parallel and showed the same maximum ($P = 0.14$), and a (common) slope = 1.52. The alternative Schild plot in Figure 4d with two points gave $pA_2 = 4.51$, practically identical with the value of 4.49 in Figure 4c.

Allosteric antagonist or competitive antagonist with allosteric component Figure 5 shows the results of antagonism between gallamine and methacholine (MeCh) in bovine atrial muscle strips in the same presentation as in the foregoing figures. According to several reports, e.g. Michel *et al.* (1990), gallamine is probably a competitive antagonist with an allosteric component.

The agonist DRCs were shifted in parallel to the right up to a DR − 1 = 358 in Figure 5a. The inhibitory effects of gallamine at 10, 50 and 200 μmol l^{-1} methacholine are shown in Figure 5b, from which it can be seen that I_{max} of the antagonist DRC at 200 μmol l^{-1} MeCh was markedly, and significantly ($P = 0$), reduced, a phenomenon which has been observed with a pure allosteric antagonist in Figure 2b.

The corresponding conventional Schild plot is shown in

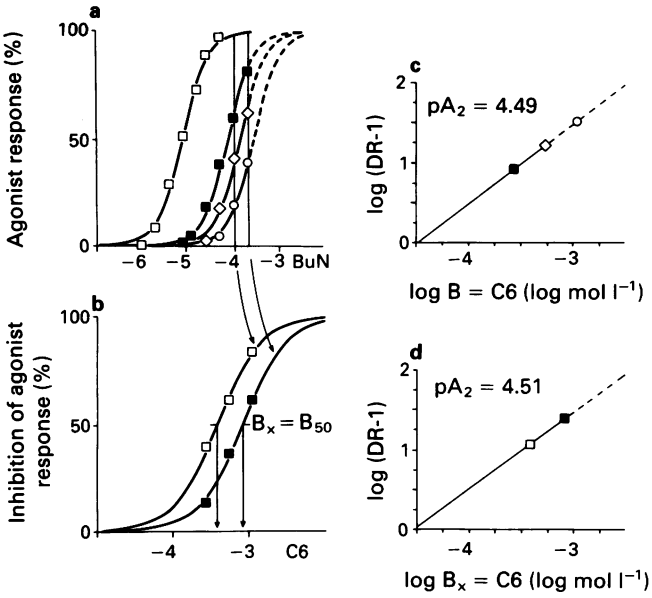

Figure 4 Incomplete agonist dose-response curves (DRCs) of $BuNMe_3Br$ (BuN) in the absence (□) and presence of 270 (■), 540 (◇), and 1080 (○) μmol l^{-1} (C6) (a). Agonist response: contraction of rectus muscle of frog. Incomplete DRCs were derived from complete DRCs from Ariëns *et al.* (1956) and antagonist DRCs of hexamethonium (C_6) at 100 and 200 μmol l^{-1} of $BuNMe_3Br$ (b), with Schild plots (c,d), analogously to Figure 1. The agonist DRCs had a common slope of 1.6 (a), similar (1.5) to the antagonist DRCs in (b). The slopes of the Schild plots were 1.00 (c) and 0.97 (d).

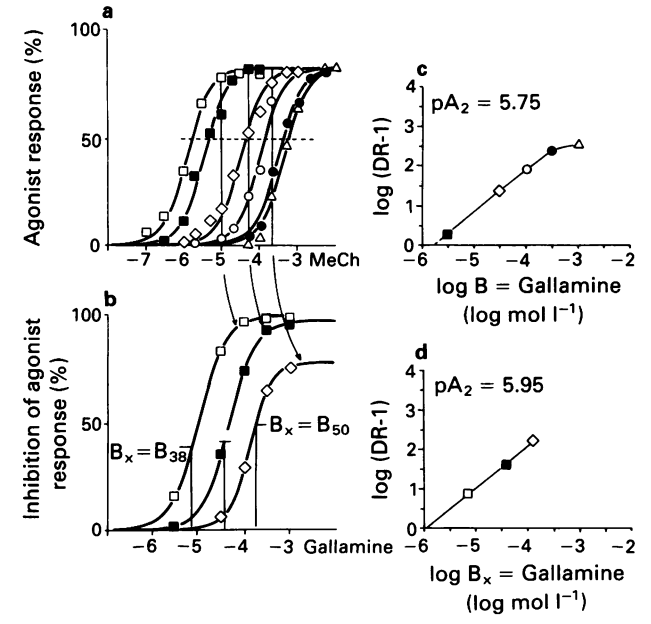

Figure 5 Experimental dose-response curves (DRCs) of methacholine (MeCh) in the absence and presence of 3, 30, 100, 300 and 1000 μmol l^{-1} gallamine, presented as in Figure 1. Agonist response: negative inotropy of trabecular muscle. Antagonist DRCs of gallamine in the presence of 10 (□), 50 (■) and 200 (◇) μmol l^{-1} MeCh (b). The reduction of I_{max} of the antagonist DRCs in (b) was significant. The symbols indicate mean values of 3 experiments. The agonist DRCs had a slope of 1.4 (a), the antagonist DRCs had slopes of 1.5, 1.5 and 2.0, respectively (d).

Figure 5c. Extrapolation of the linear part of the curve yields a pA_2-value of 5.75. The calculated value for K_B = 1.60 μmol l^{-1}, corresponding to pA_2 = 5.80. At the highest antagonist concentration of 1 mmol l^{-1} gallamine, the point in the plot deviates from a straight line, indicating an allosteric mechanism or a possible negative allosteric component of the inhibitory action of gallamine. We cannot differentiate between these two possibilities by analysis of the experimental DRCs and Schild plots.

The analysis of the alternative Schild plot (Figure 5d) does not show a deviation from linearity up to about 100 μmol l^{-1} gallamine. The pA_2-value was estimated to be 5.95. By calculation of $K_B = B/DR - 1$, the pA_2-value was found to be 6.05 (K_B = 0.89 μmol l^{-1}). The finding of a straight line is not surprising in view of the fact that the points for the conventional Schild plot up to about 100 μmol l^{-1} gallamine could obviously also be fitted to a straight line (Figure 5c).

Comparison of methods From the foregoing results it appears that similar pA_2-values can be obtained by the conventional and alternative approach. Figure 6 compares the results of Figures 3–5 but also includes results, obtained in the same way, not shown as figures. There is a very good agreement between the pA_2-values obtained by the two methods. The regression line in Figure 6 has a slope near 1 (1.02), the correlation coefficient is 0.99, $r^2 = 0.98$. The pA_2-values were obtained by Schild-plot analysis as shown in Figures 3–5 without constraint to slope = 1.

Table 1 gives a comparison of K_B-values calculated according to the equation $K_B = B/DR - 1$, and $K_B = B_x/DR - 1$, respectively, for the individual pairs of antagonist concentrations, B or B_x, and the shift of agonist DRCs, DR − 1. These calculations are based on the mass action law and, in principle, assume a slope of 1 in the Schild plot. As is evident from Table 1, the K_B-values calculated from B_x-values are comparable with the corresponding K_B-values derived from B-values. The differences were in no case significant. It is interesting that the K_B-values calculated as mean values from the B_x-values of the antagonist DRCs in many cases showed a lower standard deviation (s.d.) than those obtained by the conventional approach. One possible reason might be that the antagonist DRCs were always assessed at submaximum to maximum effective agonist concentrations, avoiding possible deviations from competitive interaction, which are more likely to occur at higher agonist concentrations. For example, an allosteric component of the action of gallamine was

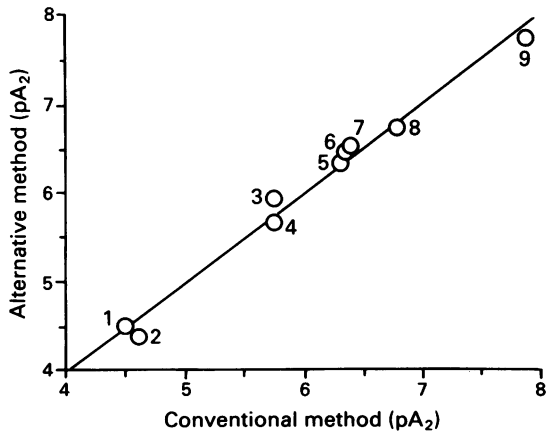

Figure 6 Correlation of pA_2-values of antagonism, evaluated from Schild plots by the conventional and alternative approach, respectively: slope = 1.02, r = 0.99, n = 9. The numbers refer to the following interactions of agonists/antagonists: (1) = BuNMeBr/C6 (Ariëns *et al.*, 1956); (2) = adenosine/theophylline (Persson *et al.*, 1982); (3) = MeCh/gallamine (Figure 5); (4) = MeCh/pirenzepine (Figure 3); (5) = terbutaline/butoxamine (Kenakin, 1982); (6) = MeCh/pirenzepine (tested analogously to Figure 3); (7) = tazolol/butoxamine (Kenakin, 1982); (8) = MeCh/AF-DX 116 (tested analogously to Figure 3); (9) = orciprenaline/propranolol in bovine trachea (exp. conditions: Pöch & Zimmerman, 1988).

obviously not yet clearly evident in the Schild plot, although the antagonist DRCs showed a pronounced reduction in I_{max} (Figure 5).

The statistical analysis of the slope factors obtained by both methods for the drugs listed in Table 1 gave no evidence for a significant deviation from unity ($P > 0.05$). The observed deviations ranged from 0.87 to 1.27 and 0.89 to 1.26, respectively.

Discussion

An alternative method for the evaluation of agonist-antagonist interactions is described in this paper. It is based on the usual DRCs of an agonist in the absence and in the presence of fixed concentrations of an antagonist.

Antagonist DRCs were constructed at a submaximum to maximum effective control response to the agonist by expressing the inhibitory effects as a percentage of the maximum possible inhibitory effect. The antagonist concentration which reduced the control effect of the agonist to its $E_{max}/2$ was termed B_x in order to differentiate it from the fixed antagonist concentration B used for testing the agonist in its presence. As can be seen from Figure 1, B_x equals $B_{50} = IC_{50}$ of the antagonist at the maximum effect of the agonist, only. At submaximum effective concentrations of the agonist, B_x corresponds to values lower than IC_{50}. Hence, the antagonist concentration was determined at fixed agonist concentrations, and hence at fixed DR, by 'vertical examination' of agonist DRCs, rather than the DR − 1 at fixed antagonist concentrations.

The procedure outlined in this paper has in part been used by others. In an attempt to measure the potency with which muscarinic antagonists inhibit muscarinic agonist-stimulated phosphoinositol breakdown, Lazareno & Roberts (1987) have calculated $K_B = IC_{50}/[(\text{fixed agonist concentration}/EC_{50})-1]$, with [(fixed agonist concentration/EC_{50})-1] corresponding to DR − 1. The approach of these authors was to test the responses to a fixed concentration of agonist in the presence of various concentrations of antagonist. In addition, in each experiment a concentration-effect curve to the agonist alone was obtained. The authors pointed out in their paper (Lazareno & Roberts, 1987) that using the principles of dose ratio analysis, it need only be assumed that equieffective agonist concentrations correspond to equal receptor occupancy of agonist. Since they measured the IC_{50}- and EC_{50}-values at the same effect level, their mathematical treatment is identical to the one used in this paper. The experimental procedure of Lazareno & Roberts (1987) is, however, limited to a single fixed agonist concentration and thus does not extend to Schild plots.

Another attempt at quantifying functional inhibition data was presented by Eglen & Whiting (1989), who tested the dose response of inhibitory effects of the antagonist in the presence of a maximum effective concentration of an agonist, and calculated dissociation constants by inappropriately applying (Lazareno & Roberts, 1987; Lazareno, in preparation) the Cheng-Prusoff equation for the determination of enzyme inhibitor constants (K_i) (Cheng & Prusoff, 1973).

Our approach allowed antagonist DRCs to be derived from experimental data points of incomplete agonist DRCs, as exemplified in Figure 4, as an alternative to an estimation of DR-1 which then yields only a few or extrapolated points for a conventional Schild plot (Figure 4c). Although dose ratios may be estimated at the 50% or lower effect level, estimated values are likely to have a higher variation at low compared with the half maximum effect level. Antagonist DRCs can be determined from experimental data points of incomplete agonist curves, as in Figure 4, in the same way as from complete agonist curves (e.g. Figure 4). In this example, as in others not shown, the pA_2- or K_B-values derived by the present procedure were in good agreement with those obtained from incomplete agonist DRCs (Figure 4c vs d) which were complemented, i.e. extrapolated by fitting the experimental points to complete DRCs by ALLFIT. The procedure of assessment of antagonist DRCs can thus meaningfully supplement an investigation or can be chosen as an attractive alternative.

It is noteworthy that even in the case of complete experimental agonist DRCs, the antagonist DRCs were determined as if they were incomplete. Where possible, as in Figures 3 and 5, antagonist DRCs were assessed up to concentrations of the agonist exhibiting effects lower than 50% in the presence of the antagonist, in order to obtain rather complete DRCs for the inhibition of agonist response.

The antagonist DRCs also allow a qualitative evaluation of various aspects of DRCs, e.g. with respect to slope and I_{max}. In theory, DRCs of competitive antagonists give parallel DRCs with a common slope and $I_{max} = 100\%$ inhibition of agonist effects, independent of agonist concentrations. The experimental DRCs shown in Figures 3 and 4 are in accordance with the theory.

Allosteric antagonists or competitive antagonists with an allosteric component exhibit antagonist DRCs with reduced I_{max}. Experimental results with gallamine (Figure 5) share this phenomenon with theoretical antagonist DRCs of an allosteric antagonist (Figure 2). As a matter of fact, the depression of I_{max} of the antagonist DRCs appears to be a sensitive indicator of allosteric interaction. The results obtained with gallamine support this view, since deviations from a straight line in the conventional Schild plot were hardly detectable (Figure 5c) while the reduction in I_{max} of the DRC of the inhibitory effects of gallamine against methacholine was clearly seen (Figure 5b). In the literature, allosteric interaction by gallamine with binding of agonists or antagonists to muscarinic receptors has been described by various groups, either as the sole mechanism or as an additional property of this muscarinic antagonist at higher concentrations (Ehlert, 1988b; Lee & El-Fakahany, 1988; Roffel *et al.*, 1989; Michel *et al.*, 1990).

A drawback of the alternative Schild plot is that deviations from linearity at high antagonist concentrations are more difficult to detect since the highest antagonist concentrations B_x plotted are somewhat lower than B in conventional Schild plots. This disadvantage appears to be more than compensated for by the sensitive depression of I_{max} of antagonist DRCs since deviation from linearity in the respective Schild plots with gallamine was barely seen while I_{max} was significantly reduced from 100 to 78% (Figure 5).

A comparison between K_B and pA_2-values obtained by either method showed an excellent agreement (Figure 6, Table 1). The values for DR − 1 and B by the conventional approach were determined from more or less complete experimental agonist DRCs. B_x-values at a fixed DR were obtained from antagonist DRCs which in principle were assessed from incomplete DRCs. For example, the agonist response above 50 μmol l^{-1} methacholine in Figure 3 was not taken into consideration for the determination of antagonist DRCs. However, it appears that the alternative approach leads to K_B and pA_2-values which are at least as precisely estimated as by the conventional approach. This means that accurate affinity estimates can be obtained from incomplete DRCs. This finding appears of practical importance where incomplete experimental agonist DRCs have to be evaluated, e.g. due to limited supply and/or solubility of the agonist.

The K_B-values determined by the alternative approach showed small differences between those obtained at the submaximum to maximum effective range of agonist concentrations (Table 1). Hence, it appears reasonable to estimate rapidly K_B-values of antagonists in screening experiments by the assessment of a single antagonist DRC at a maximum effective agonist concentration. This procedure is applicable irrespective of whether or not the experimental data points correspond to complete or incomplete agonist DRCs.

The excellent technical assistance of Mrs Heike Stessel and Mrs Betty Oberer is gratefully acknowledged. We thank Dr Sebastian Lazareno for showing us his manuscript in preparation, referred to in the Discussion.

References

ARIËNS, E.J., VAN ROSSUM, J.M. & SIMONIS, A.M. (1956). A theoretical basis of molecular pharmacology. Part I: Interaction of one or two compounds with one receptor system. *Arzneim.-Forsch. (Drug Res.)*, **6**, 282–293.

ARUNLAKSHANA, O. & SCHILD, H.O. (1959). Some quantitative uses of drug antagonists. *Br. J. Pharmacol. Chemother.*, **14**, 48–58.

CHENG, Y.-C. & PRUSOFF, W.H. (1973). Relationship between the inhibition constant (K_i) and the concentration of inhibitor which causes 50 per cent inhibition (I_{50}) of an enzymatic reaction. *Biochem. Pharmacol.*, **22**, 3099–3108.

DE LEAN, A., MUNSON, P.J., GUARDABASSO, V. & RODBARD, D. (1988). A *User's Guide to ALLFIT*. Lab. Theoret. Physical Biol., Nat'l Inst. Child Hlth, NIH, Bethesda, MD 20892, USA.

EGLEN, R.M. & WHITING, R.L. (1989). Problems associated with the application of the Cheng-Prusoff relationship to estimate atropine affinity constants using functional tissue responses. *Life Sci.*, **44**, 81–94.

EHLERT, F.J. (1988a). Estimation of the affinities of allosteric ligands using radioligand binding and pharmacological null methods. *Mol. Pharmacol.*, **33**, 187–194.

EHLERT, F.J. (1988b). Gallamine allosterically antagonizes muscarinic receptor-mediated inhibition of adenylate cyclase activity in the rat myocardium. *J. Pharmacol. Exp. Ther.*, **247**, 596–602.

KENAKIN, T.P. (1982). Theoretical and practical problems with the assessment of intrinsic efficacy of agonists: efficacy of reputed beta-1 selective adrenoceptor agonists for beta-2 adrenoceptors. *J. Pharmacol. Exp. Ther.*, **223**, 416–423.

KENAKIN, T.P. (1987). *Pharmacologic Analysis of Drug-Receptor Interaction*. New York: Raven Press.

LAZARENO, S. & ROBERTS, F.F. (1987). Measuring the potency with which muscarinic antagonists inhibit muscarinic agonist stimulated phosphoinositide breakdown in rat cortical slices. In *International Symposium on Muscarinic Cholinergic Mechanisms*. ed. Cohen, S. & Sokolovsky, M. pp. 272–277. London: Freund Publ. House Ltd.

LEE, N.H. & EL-FAKAHANY, E.E. (1988). Influence of ligand choice on the apparent binding profile of gallamine to cardiac muscarinic receptors. Identification of three main types of gallamine-muscarinic receptor interactions. *J. Pharmacol. Exp. Ther.*, **246**, 829–838.

MICHEL, A.D., DELMENDO, R.E., LOPEZ, M. & WHITING, R.L. (1990). On the interaction of gallamine with muscarinic receptor subtypes. *Eur. J. Pharmacol.*, **182**, 335–345.

PERSSON, C.G.A., KARLSON, J.-A. & ERJEFÄLT, I. (1982). Differentiation between bronchodilation and universal adenosine antagonism among xanthine derivatives. *Life Sci.*, **30**, 2181–2189.

PÖCH, G., BRUNNER, F. & KÜHBERGER, E. (1990). Alternative approach to the Schild plot analysis. *Eur. J. Pharmacol.*, **183**, 2135.

PÖCH, G. & ZIMMERMANN, I. (1988). Simple pA_2 estimation of partial agonists: comparison with the Kaumann-Blinks method. *J. Pharmacol. Methods*, **19**, 47–56.

RODBARD, D. (1974). Statistical quality control and routine data processing for radioimmunoassays and immunoradiometric assays. *Clin. Chem.*, **20**, 1255–1270.

ROFFEL, A.F., ELZINGA, C.R.S., MEURS, H. & ZAAGSMA, J. (1989). Allosteric interactions of three muscarine antagonists at bovine tracheal smooth muscle and cardiac M_2 receptors. *Eur. J. Pharmacol.*, **172**, 61–70.

SCHILD, H.O. (1947). pA, a new scale for the measurement of drug antagonism. *Br. J. Pharmacol. Chemother.*, **2**, 189–206.

SCHILD, H.O. (1957). Drug antagonism and pA_x. *Pharmacol. Rev.*, **9**, 242–256.

TALLARIDA, R.J., COWAN, A. & ADLER, M.W. (1979). pA_2 and receptor differentiation: A statistical analysis of competitive antagonism. *Life Sci.*, **25**, 635–654.

(Received December 11, 1991
Revised January 17, 1992
Accepted March 17, 1992)

Br. J. Pharmacol. (1992), **106**, 717–726

Characterization of potassium currents modulated by BRL 38227 in rat portal vein

[1]Thomas Noack, Petra Deitmer, *Gillian Edwards & *Arthur H. Weston

Department of Physiology, Philipps University, Deutschhausstrasse 2, W-3550 Marburg, Germany and *Smooth Muscle Research Group, Department of Physiological Sciences, University of Manchester, Manchester, M13 9PT

1 Smooth muscle cells of the rat portal vein were dispersed by enzymatic treatment and recordings of whole-cell membrane potassium currents were made by the voltage-clamp technique. In isolated cells by use of combined voltage- and current-clamp the effect of BRL 38227 on membrane potential and ionic currents was also studied.

2 BRL 38227 (0.1 to 10 μM) induced a non-inactivating potassium current (I_{KCO}) which developed slowly (900 s to 300 s, respectively) to its full size. These effects of BRL 38227 were reversible.

3 In addition to its K-channel opening properties, BRL 38227 (1 to 10 μM) inhibited the amplitude and changed the activation and inactivation characteristics of a slowly-inactivating, calcium influx-independent, outward potassium current (I_{TO}).

4 Application of stationary fluctuation analysis to I_{KCO}, showed a mean single channel current of 0.65 pA at − 10 mV under a quasi-physiological potassium gradient.

5 In a combined voltage-clamp/current-clamp configuration, BRL 38227 (1 μM) induced a mean hyperpolarization of 22 mV.

6 The induction of I_{KCO} by BRL 38227 and the associated hyperpolarization were suppressed by glibenclamide (1 to 10 μM) in a concentration-dependent manner. Glibenclamide (1 μM) had no effect on the inhibition of I_{TO} by BRL 38227 (1 μM).

Keywords: BRL 38227; glibenclamide; voltage-clamp; current-clamp; rat portal vein; K-channel; K-current

Introduction

BRL 38227, the active enantiomer of the racemate cromakalim (BRL 34915), is a smooth muscle relaxant classified as a potassium channel opener (KCO) (Edwards & Weston, 1990). Although the effects of KCOs on potassium (K) currents in smooth muscle have been widely studied (Standen *et al.*, 1989; Beech & Bolton, 1989b; Klöckner *et al.*, 1989; Gelband *et al.*, 1990; Kajioka *et al.*, 1990; 1991; Okabe *et al.*, 1990; Clapp & Gurney, 1991; Lindeman *et al.*, 1991; Nakao & Bolton, 1991; Noack *et al.*, 1991; Pavenstädt *et al.*, 1991) the K-channel responsible for the characteristic hypotensive and vasorelaxant effects of these agents has not been unequivocally identified.

In rat mesenteric artery it was reported that KCOs opened a K-channel with a relatively large single channel conductance (Standen *et al.*,1989) and in human mesenteric artery an increased open probability of the large conductance calcium-activated K-channel (BK_{Ca}) was detected (Klöckner *et al.*, 1989). In contrast to these findings, a variety of studies in vascular smooth muscle has indicated that BK_{Ca} is not opened by KCOs (Beech & Bolton, 1989b; Okabe *et al.*, 1990; Lindeman *et al.*, 1991; Pavenstädt *et al.*, 1991). Furthermore, investigations on rat and rabbit portal vein have shown that the KCOs open a K-channel with a unitary conductance of approximately 10 pS (Kajioka *et al.*, 1990; Nakao & Bolton, 1991).

To date, the majority of studies on the detailed smooth muscle single cell electrophysiology of the KCOs have involved isolated membrane patches but no clear picture of the target K-channel has emerged. For this reason we decided to characterize the electrophysiological effects of the KCOs using BRL 38227 and whole-cell voltage-clamp techniques. In the present study in rat portal vein we now show that BRL 38227 induces a non-inactivating, calcium influx-independent K-current that is glibenclamide-sensitive. The results, some of which were previously presented to the German Physiological Society (Noack *et al.*, 1991) indicate that a small conductance K-channel is the site of action of the KCOs.

[1] Author for correspondence.

Methods

All experiments were performed on single smooth muscle cells isolated from portal veins which were removed from male Spague-Dawley rats, previously killed by stunning and bleeding.

Production of isolated cells

Each portal vein (about 20 mm length) was carefully cleaned of fat and connective tissue with fine scissors in conjuction with a dissecting microscope. The vein was cut into small pieces and then incubated in a nominally Ca^{2+}-free physiological salt solution (PSS) for 30 min. The cell dispersion consisted of a consecutive treatment of the tissue with a high K^+ PSS (1 ml) containing purified collagenase (100 units ml^{-1}; Sigma) and a high K^+ PSS containing papain (20 units ml^{-1}; Sigma) and collagenase inhibitor (phosphoramidon, 200 μg ml^{-1}; Sigma) (for details see Lammel *et al.*, 1991). The cells were used for experiments within 12 h of separation, during which time they were stored at 4°C in Kraftbrühe (KB-medium; Klöckner & Isenberg, 1985). All experiments were performed at 26°C.

Single-cell electrophysiology

The whole-cell configuration of the patch-clamp technique (Hamill *et al.*, 1981) using a clamp system designed in our laboratory which was functionally similar to the commercially-available EPC 7 (List, Germany), was used in

all experiments. The settling time of this system was less than 500 μs. Patch pipettes were pulled from Pyrex glass (H15/10, Jencons, UK) and had resistances of 3–4 MΩ when filled with the internal (intracellular) solution.

Voltage commands and data acquisition were performed on-line with an AT-compatible computer equipped with an appropriate interface (Axolab 1100 or Axon TL-1, Axon Instruments, U.S.A.). For cell stimulation and for recording and analyzing data the pCLAMP 5.5 programme was used (Axon Instruments, U.S.A.). A video recorder in conjunction with a pulse code modulator was used to store data. Voltage protocols and evoked membrane currents were monitored continuously on a chart pen recorder (Series 2400, Gould, U.S.A.). Currents were displayed on the computer monitor and hard copies were obtained using a plotter (Taxan, U.S.A.). Leakage current was estimated at the end of an experiment by addition of 5 mM $CdCl_2$ to the extracellular solution (Noack *et al.*, 1992). The leak resistance ranged from 3 to 5 GΩ and the experimental values were used to estimate errors of potential measurement under whole-cell current-clamp. The cadmium (5 mM) resistant current (leakage current) was not subtracted from either current traces or from current-voltage relationships in this paper. Recordings were evaluated from a total of 30 cells from which continuous measurements of at least 20 min were made. The effects of BRL 38227 were investigated by adding the appropriate amount of this agent to the main reservoir containing the external solution to ensure that responses were obtained under steady-state conditions. The bath (volume: 1 ml) was continuously perfused (1 ml min^{-1}) with fresh external solution using a pump (Microperpex, Pharmacia LKB, Freiburg, Germany); a second identical pump was used to remove excess solution from the recording chamber.

To determine the effects of BRL 38227 and glibenclamide on membrane potential, a series of measurements was performed with a voltage-clamp amplifier which permitted fast (< 1 ms) switching to current-clamp conditions. The properties of this combined voltage/current-clamp amplifier were similar to those described by Clark & Giles (1987).

Drugs and solutions

The nominally Ca^{2+}-free PSS used for the cell separation comprised (mM): NaCl 137, KCl 2.7, $MgCl_2$ 1.0, glucose 5.6, HEPES 4.2; buffered with NaOH to pH 7.3. High K^+ PSS contained (mM): KCl 140, $MgCl_2$ 1.0, glucose 5.6, HEPES 4.2, buffered with KOH to pH 7.3. The PSS in the bath had the following composition (mM): NaCl 125, KCl 4.8, $MgCl_2$ 3.7, KH_2PO_4 1.2, glucose 11, HEPES 10, EGTA 1.0 buffered with NaOH to pH 7.3; aerated with O_2. The pipette (internal) solution contained (mM): NaCl 5, KCl 120, $MgCl_2$ 1.2, K_2HPO_4 1.2, glucose 11, HEPES 10, EGTA 1.2, oxalacetic acid 5, sodium pyruvate 2, sodium succinate 5, buffered with KOH to pH 7.3. After buffering, the pipette solution contained a total of 152 mM K^+. Assuming a contaminant concentration of 10 μM calcium in the external and in the pipette solutions, the addition of 1 mM and 1.2 mM EGTA (ethylene glycol-*bis* (β-aminoethyl ether) tetra-acetic acid; Sigma) to the bath and pipette solutions, respectively, should have produced an average free calcium concentration in these solutions of less than 1 nM.

To minimize solvent effects on membrane currents, BRL 38227 (SmithKline Beecham, UK) was first dissolved in dimethyl sulphoxide (DMSO; Sigma) to produce a concentrated stock solution (250 mM). Glibenclamide (Hoechst, FRG) was prepared as 10 mM stock solution in DMSO. From such stocks, dilutions were prepared with distilled water immediately before they were required.

Results

Whole-cell currents in calcium-free PSS

When a rat portal vein cell was depolarized from a holding potential of − 90 mV to a test potential of − 30 mV in the calcium-free PSS (free calcium lower than 1 nM), a current with fast activation kinetics which inactivated to a steady current level within less than 20 ms was observed (Figure 1a(i), 6th and 7th trace from bottom). On depolarization to test potentials positive to − 30 mV (Figure 1a(i), 8th to 10th trace from bottom) an additional outward current component became activated. This component also inactivated but exhibited slower kinetics than the current previously described. Both of these time-dependent outward current components declined to a steady current level. The complete inactivation of the slower component is not shown in Figure 1a(i) because of the relatively short test pulse duration. The faster outward current showed some similarity to the A-like K-current which has previously been described in rabbit portal vein (Beech & Bolton, 1989a). The more slowly-inactivating current was comparable to I_{TO}, a K-current recently characterized in guinea-pig portal vein (Noack *et al.*, 1990) and the designation I_{TO} will also be used to describe the slowly-inactivating current in the present study. The steady current level observed after complete inactivation of I_{TO} (deviation from zero current; zero current indicated by arrows in Figure 1) could also be obtained when the membrane potential was stepped from a holding potential of − 10 mV to the same test potentials as those used when the holding potential was − 90 mV (Figure 1a(ii)). Thus the magnitude of I_{TO} is given by the difference between the peak outward current elicited from a holding potential of − 90 mV and that current elicited from a holding potential of − 10 mV. The difference between the non-inactivating current and zero current was designated I_{NI}.

Effects of BRL 38227 on whole-cell currents

When portal vein cells were held at a potential of − 10 mV and BRL 38227 (10 μM) was added to the bathing solution, the current slowly increased in an outward direction (Figure 2a). In contrast, when the cells were exposed to BRL 38227 (1 to 10 μM) at a holding potential of − 90 mV (close to the calculated potassium equilibrium potential, E_K = − 83 mV) BRL 38227 had no effect or induced a small inward current indicating that a K-current was induced by this substance (compare holding currents in Figure 1a(i) and b(i) and holding currents in Figure 1a(ii) and b(ii)). The time-course of action of BRL 38227 (10 μM) on membrane currents (I_{KCO}) was relatively slow and was essentially complete after 300 s. Such a slow effect cannot be explained by the time-course of the increase in the bath concentration of BRL 38227. For example, on perfusing with 10 μM BRL 38227, a concentration of 1 μM was achieved within the first 10 s. At a steady-state concentration of BRL 38227 (1 μM), a very marked enhancement of evoked membrane currents was observed at all test voltages (positive to E_K) on stepping from holding potentials of either − 90 mV or − 10 mV (Figure 1b). At a concentration of 1 μM, BRL 38227 produced near-maximal effects. Increasing the concentration of BRL 38227 to 10 μM did not produce significantly larger effects but the onset of I_{KCO} was somewhat faster. When BRL was used in a concentration of 0.1 μM, I_{KCO} reached approximately 20% of the magnitude produced by 1 μM BRL 38227. From this the EC_{50} value of BRL 38227 for generation of I_{KCO} can be estimated to be approximately 0.5 μM.

A more detailed analysis of the interaction of BRL 38227 with the different K-currents in rat portal vein was derived from the construction of the current-voltage relationships (I–V curves) under control conditions and in the presence of BRL 38227 with holding potentials of − 90 mV and − 10 mV (Figure 3a and b). In Figure 3a the peak

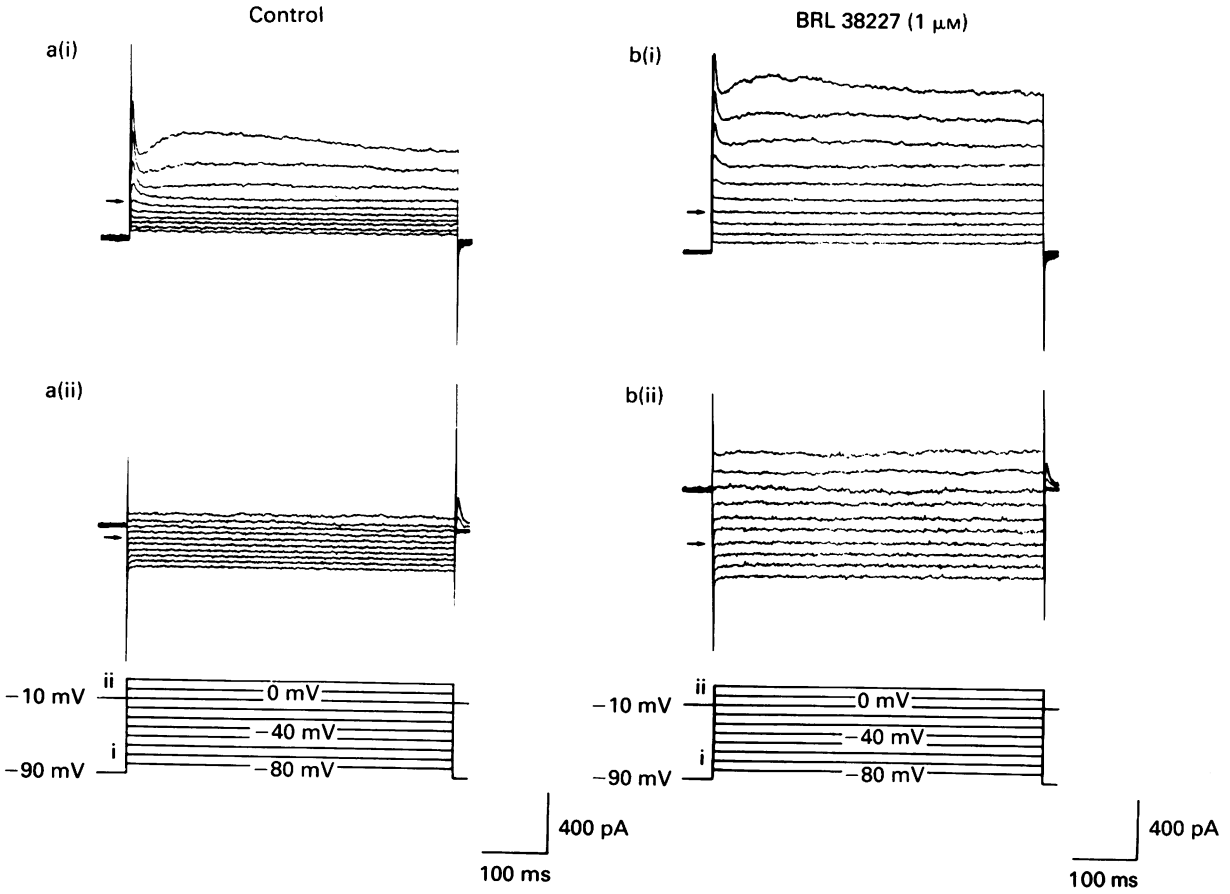

Figure 1 Effect of BRL 38227 on whole-cell currents in a smooth muscle cell from rat portal vein bathed in a calcium-free physiological salt solution (containing 1 mM EGTA). (a) The cell was held either at − 90 mV (i) or − 10 mV (ii) and stepped for 500 ms to the different test potentials as indicated. Note the fast inactivating outward current shortly after the capacitive transient in (i). (b) Conditions as in (a) but after exposure to BRL 38227 (1 μM) for 5 min. The arrows indicate the zero current. Note that the current associated with a holding potential of − 90 mV was virtually unchanged in the presence of BRL 38227.

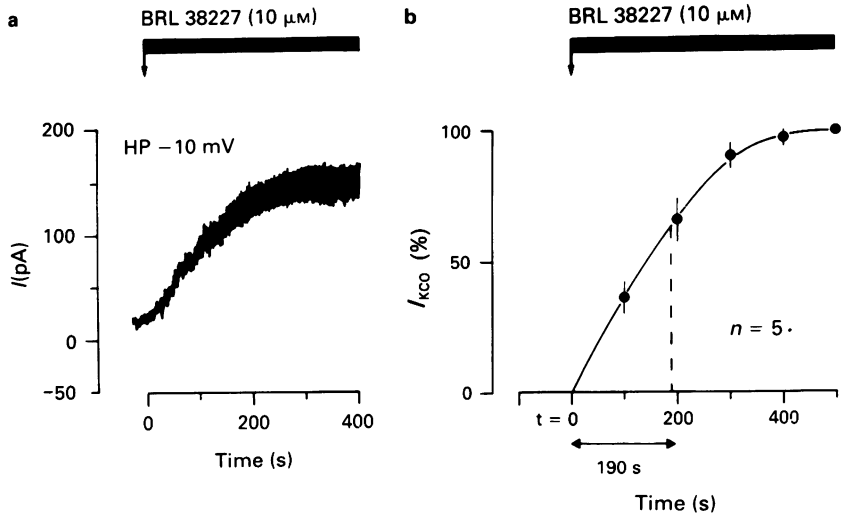

Figure 2 Effect of BRL 38227 (10 μM) on the current associated with a holding potential of − 10 mV. (a) The onset of the BRL 38227-induced current I_{KCO} was accompanied by increased current noise. (b) Time-course of the onset of I_{KCO} (curve fitted by eye). The results are expressed as a percentage of the maximum current induced by BRL 38227 (10 μM) in each cell ($n = 5$ cells). The vertical bars indicate s.e.mean. Assuming an exponential time-course for the development of I_{KCO}, the mean activation time constant (time taken to achieve 63% of the maximum current produced by BRL 38227) was 190 s (dashed line in b).

outwardly-directed current was measured between 100 ms and 300 ms after the start of the depolarizing pulse from a holding potential of − 90 mV. This peak current in the absence of BRL 38227 represents the sum of the components I_{TO} and I_{NI}. On exposure to BRL 38227 (1 μM) the current reflects the sum of I_{TO} and I_{NI}, together with the effects of BRL 38227 on one or both of these components, plus any new current (I_{KCO}) induced by BRL 38227 and which was not present under control conditions.

From a holding potential of − 90 mV, the I–V curve in

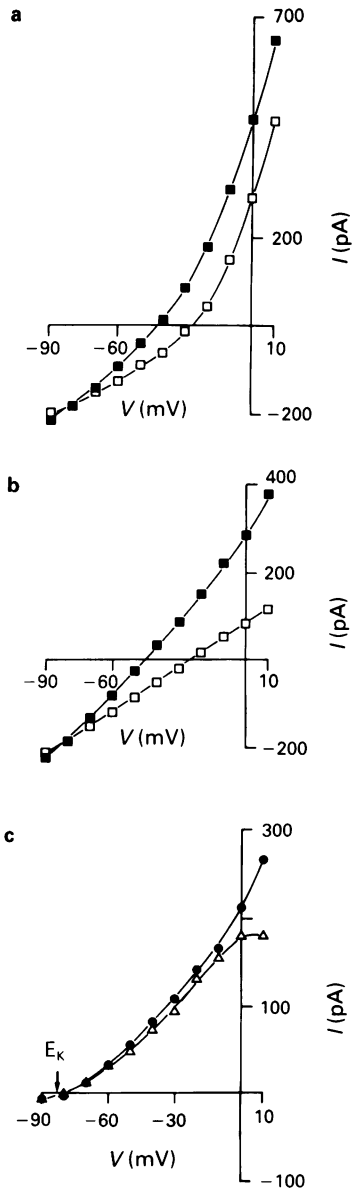

Figure 3 Current-voltage relationships of the currents in rat portal vein and the effect of BRL 38227. (a) Current-voltage relationship of the peak total current (peak of I_{TO}) under control conditions (□) and in the presence of BRL 38227 (1 μM) (■). The holding potential was − 90 mV to ensure full activation of I_{TO}. (b) Current-voltage relationship of the non-inactivating currents under control conditions (□) and in the presence of 1 μM BRL 38227 (■) obtained from the same cells as in (a). The holding potential was − 10 mV which ensured complete inactivation of the time-dependent current components. (c) Current-voltage relationships of the net current induced by BRL (difference between currents in the presence and absence of BRL 38227: $I_{BRL} - I_{control}$) for the two holding potentials (Δ, − 90 mV; ●, − 10 mV). The data were obtained from three different cells. In all cells, the current induced by BRL 38227 had a reversal potential of − 80 mV and showed a significant flattening at potentials positive to − 10 mV when the holding potential was − 90 mV.

the presence of BRL 38227 lies above the control curve and crosses it at approximately − 80 mV. The difference between the control and test curves, which represents the net effect of BRL 38227 (1 μM) on I_{TO} and I_{NI} is shown in Figure 3c and exhibits a conspicuous flattening at potentials positive to − 10 mV. The current-voltage relationship for I_{NI} alone was constructed by plotting the steady current under control conditions against the test potentials at which it was activated from a holding potential of − 10 mV (Figure 3b). Compared with the control $I-V$ curve obtained at the same test potentials elicited from a holding potential of − 90 mV, the curve derived from a holding potential of − 10 mV exhibited very little or no outward rectification (Figure 3b). In the presence of BRL 38227 (1 μM) the steady current-voltage relationship ran above the control curve, crossed it near − 80 mV and showed outward rectification (Figure 3b).

The effects of BRL 38227 can be seen more clearly in Figure 3c in which the current difference curves (obtained by subtracting control currents from currents in the presence of BRL 38227) for the two holding potentials of − 90 mV and − 10 mV are illustrated. In the potential range up to − 10 mV both curves are nearly identical. However, at potentials more positive than − 10 mV, the currents induced by BRL 38227 and observed on stepping from a holding potential of − 90 mV were smaller than those elicited from a holding potential of − 10 mV. Since the inactivating current I_{TO} was only available on stepping from − 90 mV and at potentials positive to − 30 mV, these data suggest that BRL 38227 inhibits I_{TO}.

To determine the effects of BRL 38227 on I_{TO} alone, this current was separated from total current by subtracting the current which was available on stepping to test potentials from a holding potential of − 10 mV from that current which was achieved at the same test potentials but by stepping from a holding potential of − 90 mV (i.e. $I_{TO} = I_{HP-90} - I_{HP-10}$). The fast inactivating A-like current was digitally subtracted from current traces and thus did not contaminate re-fitting to zero time.

Under control conditions the activation time constant for I_{TO} was about 20 ms and the inactivation could be described by a single exponential process with a time constant of 990 ms at + 10 mV (Figure 4). As indicated by the $I-V$ curves in Figure 3a and 3b and shown in Figure 3c, I_{TO} was reduced in magnitude (by 21%) by 1 μM BRL 38227. However, BRL 38227 reduced the activation and inactivation time constants of I_{TO} by approximately 50% (assuming a single exponential process for each), both of which would independently reduce the magnitude of I_{TO}. Thus the BRL 38227-induced reduction of I_{TO}, which was independent

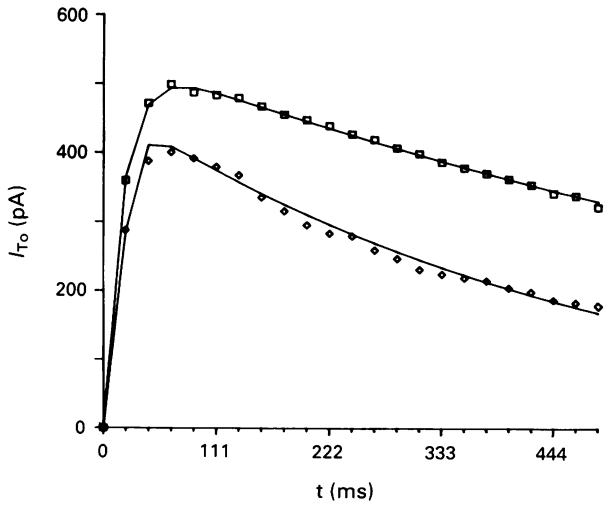

Figure 4 Time course of I_{TO} and effect of BRL 38227. The current values of I_{TO} were sampled in steps of 22 ms under control conditions (□) and in the presence of BRL 38227 (1 μM, ◇). Both sets of data were fitted with a single exponential process of activation and inactivation according to the equation: $I = I_o \times (1\text{-}e^{-t/\tau a}) \times e^{-t/\tau i}$, where I_o is the maximum current, t the time and τa and τi the activation and inactivation time constants, respectively. The continuous lines give the least square fits for control and BRL 38227 time courses. Note, that I_{TO} changed its inactivation in the presence of BRL 38227 so that it could no longer be described by a single exponential inactivation process. A second exponential power could not improve the fit.

of changes in the kinetics of I_{TO} activation and inactivation, was in the order of 14%. It should be noted that the inactivation phase of I_{TO} in the presence of BRL 38227 was not well-fitted by a single or double exponential process (Figure 4).

Single channel conductance underlying I_{KCO}

As can be seen from Figure 2b the increase of outward current induced by BRL 38227 was always accompanied by an increase in current noise. To derive information about the conductance of the channels associated with this effect of BRL 38227, we used the stationary fluctuation analysis technique (Neher & Stevens, 1977). Amplitude histograms of the level of total current at a constant holding potential were fitted by Gaussian normal distributions to provide the mean current (μ) and the standard deviation (σ) of the mean value. To determine single channel conductance from μ and σ, three general assumptions were made concerning the channels activated by BRL 38227. Firstly, they were assumed to exist only in either conducting or non-conducting states, with a probability p_o of being in the conducting state. Secondly, the gating of each channel was assumed to be statistically independent of other channels and thirdly, the population of channels was assumed to be homogeneous (for details see Noack *et al.*, 1992). Thus, the current (i) flowing through one channel is given by:

$$i = \sigma^2/(\mu \times (1\text{-}p_o)) \quad (1)$$

It can be seen from this equation that i is described by three variables of which only two (μ and σ) can be measured. However, for a low open probability, this expression can be simplified to $i = \sigma^2/\mu$ but the use of this simple equation leads to a significant error in the estimation of i if p_o is large.

As shown in Figures 2a and 2b, the increase of BRL 38227-induced current was very slow and required more than 300 s to become completely established. Thus the open probability for the channels influenced by BRL 38227 increased very slowly with time and this feature of I_{KCO} was used to determine the variable p_o. For this quasi-stationary fluctuation analysis, the time course of current was divided into segments, each of 2 s duration. Such a period was long enough to describe current fluctuation with a Gaussian normal distribution and short enough to ensure that the increase of mean current over this 2 s period was negligible compared with the current noise associated with I_{KCO}. Figure 5a shows amplitude histograms and fitted normal distributions obtained from such 2 s intervals of current recording at a holding potential of − 10 mV both under control conditions and in the presence of BRL 38227. In the case depicted, the mean control holding current was 6.62 pA with a standard deviation of 3.38 pA. The mean current had increased to 90.48 pA, with a standard deviation of 7.12 pA, 300 s after exposure to BRL 38227. As mentioned above, the current (I_{KCO}) generated by BRL 38227 showed outward rectification and was selective for K^+. Both these features of I_{KCO} are different from those of I_{NI} (see Figure 3b and 3c) and it thus seems likely that the current noise generated under control conditions and in the presence of BRL 38227 arose from independent sources (i.e. I_{NI} and I_{KCO}). Therefore, the mean current values (μ) quoted above and shown in Figure 5a and the associated variances (σ^2) are additive.

Thus the difference between the mean currents (μ) and the differences between the variances (σ^2) determined under control conditions and in the presence of BRL 38227 (10 μM) were calculated. These pairs of μ and σ^2 were grouped according to increasing values of μ. Observations where the difference between μ-values was smaller than 2 pA were summed. These values for mean current and variance were transferred to a graph (Figure 5b) and represent the pure membrane current and current noise associated with the presence of BRL 38227. The mean current can be expressed as a function of the number of channels involved (N), the current flowing through a single channel (i) and the channel open probability (p_o).

Thus:

$$\mu = N \times i \times p_o \quad (2)$$

or

$$p_o = \mu/(N \times i)$$

Substituting p_o in equation (1) gives the variance, σ^2 as a function of i, μ and N.

$$\sigma^2 = i \times \mu - \mu^2/N \quad (3)$$

This equation predicts a parabolic shape of the current variance - mean current plot; with increasing N the maximum of the curve increases and the right-hand intercept with the μ-axis shifts to the right. Fitting equation 3 to the experimental data points (criterion: weighted least squares) by variation of i and N produced a value of 500 for N with a corresponding single channel current (i) of 0.6 pA (Figure 5b). Data from six cells gave a mean single channel current of 0.65 pA ± 0.06 pA (mean ± s.e.mean). Although the experimental values in Figure 5b tend to deviate from a straight line, we never observed the opening of all the channels which carried I_{KCO} (which would have been indicated by a reduction of current noise to control values). The calculated number for N (500) gives the minimum number of channels involved in the observed BRL 38227-induced effects. From the rising phase of the parabola in Figure 5b the unitary current (i) could have been calculated from the simpler equation ($i = \sigma^2/\mu$). However, using this over the whole range of experimental points would have produced an error (a reduction of about 10%) in the calculated value of i.

If the mean single channel current (0.65 pA) is simply divided by the driving force [holding potential E_K: (10 mV − (− 83 mV) = 73 mV)], a single channel conductance of 8.9 pS ± 0.82 pS (mean ± s.e.mean) results. When the single channel conductance was calculated according to the Goldman-Hodgkin-Katz equation a value of 16.6 pS at 0 mV was the result. Under symmetrical potassium concentrations $[K_i] = [K_o] = 152$ mM this value would be approximately 34 pS.

Effect of BRL 38227 on membrane potential

The above calculations suggest that in a single cell, BRL 38227 (1 μM) induces a current (I_{KCO}) carried by a few hundred channels each with a relatively small single channel conductance. To what extent this current can induce hyperpolarization can be approximately determined from the shift in the zero current potentials of the I–V curves in Figure 3b. A more precise way to determine the hyperpolarization induced by BRL 38227 was to measure the membrane potential and the ionic currents in the same cells. This was performed with an amplifier which provided fast switching between voltage-clamp and current-clamp. The upper traces of Figure 6 show the mean ionic currents generated by stepping to 0 mV from a holding potential of − 50 mV under control conditions and in the presence of BRL 38227 (1 μM). Data from three different cells, each subjected to 10 identical voltage/current-clamp protocols have been averaged. After 600 ms, the system was switched to current-clamp at 0 pA and the corresponding lower traces show the measured membrane potentials. BRL 38227 (1 μM) induced an average hyperpolarization of 22 mV in the investigated cells. An injection of a positive-going current pulse (10 pA) gave information about the input resistance of the cell under each condition. The marked deviation of membrane potential which was achieved immediately after switching into current-clamp from that potential achieved after 3000 ms at the end of the current-clamp was due to the deactivation of I_{TO}. The absolute value of membrane potential measured using whole-cell current-clamp is always influenced by the leakage current between membrane and pipette. Although the leakage current

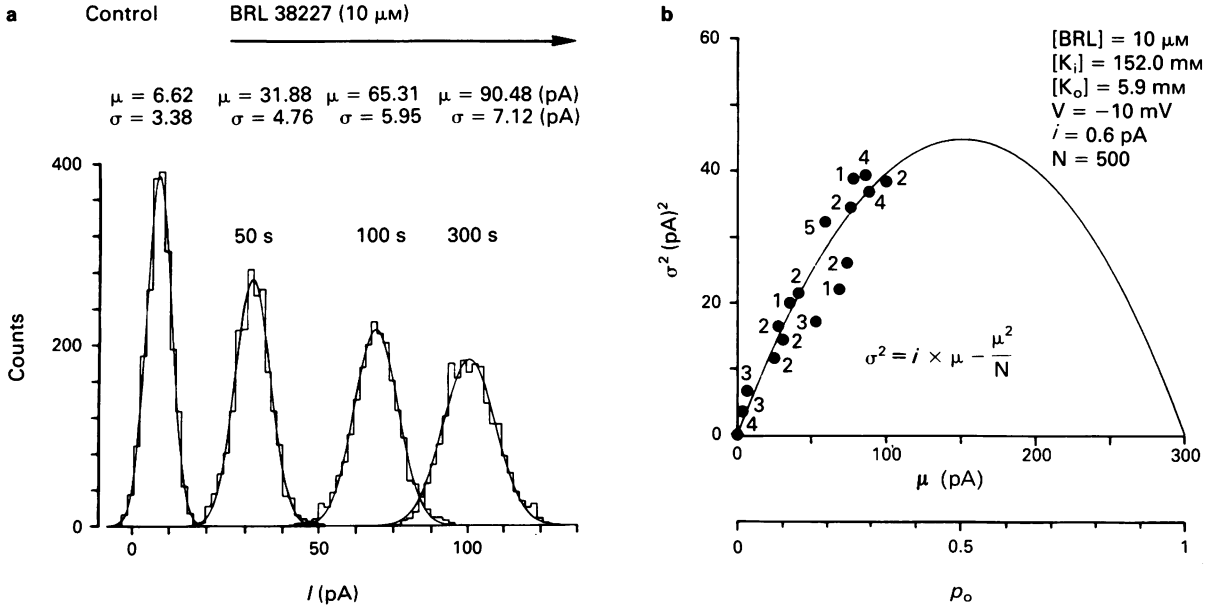

Figure 5 Determination using stationary fluctuation analysis of the single channel current associated with I_{KCO}. (a) Typical amplitude histograms of the current and accompanying current noise under control conditions (first peak) and in the presence of 10 μM BRL 38227 (peaks 2–4) in a single cell. The control reading was taken immediately prior to exposure to BRL 38227 and the effects of this agent were assessed at three different times, chosen to reflect the time-course of action of BRL 38227 in that particular cell. The numbers in (a) show the mean current (μ) after 50 s, 100 s and 300 s exposure to 10 μM BRL 38227 with the associated standard deviation (σ) of the current. Each histogram was constructed from 2048 data points. (b) Current variance (σ^2) — mean current (μ) plot for I_{KCO}. The numbers near each data point indicate the number of histograms and thus observations from which the points were derived. The data points were best fitted with a single channel current of 0.6 pA and with N (number of channels) = 500 channels. The open probability of the channels was calculated according to these values (lower scale in b).

was small because of the high leakage resistance (3 to 5 GΩ), the measured membrane potential was nevertheless shifted 10 to 20 mV in a positive direction (see Methods for an estimation of leakage current). However, the relative hyperpolarization measured with the present experimental configuration was little affected by such leakage.

Effect of glibenclamide on membrane currents and potential in the presence of BRL 38227

To study the effect of glibenclamide on the currents induced (I_{KCO}) and inhibited (I_{TO}) by BRL 38227, the same voltage/current-clamp protocol was used as described above. At a concentration of 1 μM, nearly 600 s was required to produce a steady-state response to BRL 38227, and thus the recording conditions of these long-lasting experiments (usually more than 45 min) had to be extremely stable. Figure 7 shows an experiment in which it was possible to determine the effects of glibenclamide at two different concentrations (1 and 10 μM). The results clearly demonstrate that the large hyperpolarizations induced by BRL 38227 (1 μM) were substantially reversed by glibenclamide (1 μM). Almost complete reversal of the BRL 38227-induced hyperpolarization was established at a concentration of 10 μM glibenclamide.

The ability of glibenclamide to oppose BRL 38227-induced membrane hyperpolarization has been described above. However, this does not indicate which current components were influenced by glibenclamide. We therefore performed a series of voltage-clamp protocols in which the initial control run was followed by a second sequence in the presence of 1 μM BRL 38227 and a third in the presence of both 1 μM BRL 38227 and 1 μM glibenclamide. Current traces obtained on stepping to test potentials from holding potentials of − 90 mV and − 10 mV under each of the three conditions were analysed and current-voltage relationships were constructed (Figure 8). Stepping from a holding potential of − 90 mV under control conditions elicited I_{NI} and I_{TO} (Figure 8a). The addition of BRL 38227 induced I_{KCO} and inhibited a fraction (designated β) of I_{TO}. This dual effect of BRL 38227 (also evident in Figure 3) is clearly demonstrated in Figure 8c, in which the current induced by BRL 38227 was less under conditions in which I_{TO} was activated than when there was no current contribution from I_{TO}. The current-voltage relationship for the current induced by BRL 38227 (Figure 8c) was similar to that shown in Figure 3c which was obtained in a cell from a different animal. Glibenclamide (1 μM) added to the bathing fluid in the continuous presence of BRL 38227, inhibited I_{KCO} in a concentration-dependent manner. The fraction of I_{KCO} inhibited by glibenclamide is designated α in Figure 8. It is clear from Figure 8c that glibenclamide (1 μM) did not inhibit I_{TO} since the currents which were available from holding potentials of − 90 mV or − 10 mV were inhibited by glibenclamide to the same extent. Any inhibition of I_{TO} by glibenclamide would have produced a larger suppression of current when stepping from a holding potential of − 90 mV than when stepping from − 10 mV. Thus the current I_{KCO} was always reversed by glibenclamide (with an EC_{50} value of approximately 3 μM; $n = 5$) but no significant reduction of I_{TO} by glibenclamide (1 μM) was detected.

Discussion

The results described in this paper demonstrate that BRL 38227 (100 nM to 10 μM) opens K-channels in the plasma membrane of isolated smooth muscle cells from the rat portal vein. The time taken for K-channel opening to reach steady-state (several minutes) was dependent on the concentration of BRL 38227. In those experiments in which a low concentration of BRL 38227 (100 nM) was used, it took nearly 15 min to produce such a response. A slow onset of the action of cromakalim was also observed in cells from rat and rabbit portal veins (Beech & Bolton, 1989b; Okabe *et al.*, 1990).

The current induced by BRL 38227 was non-inactivating

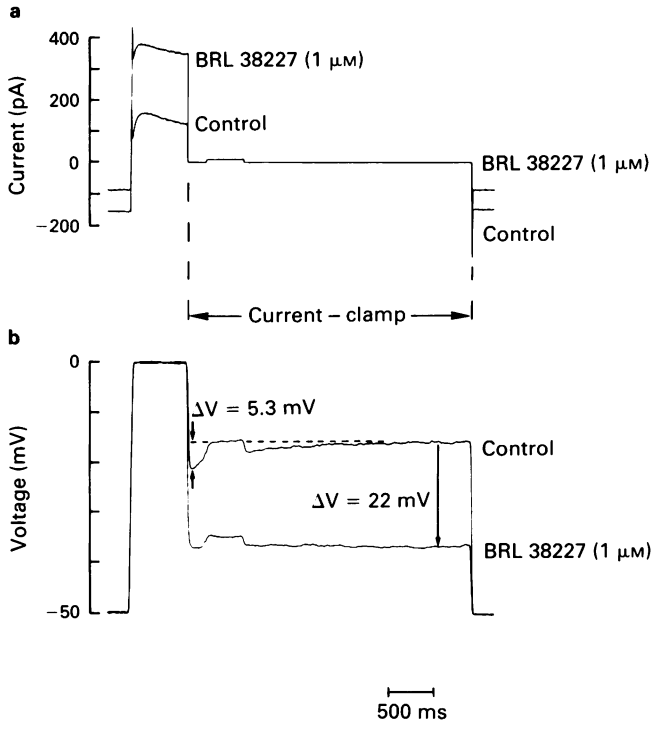

Figure 6 Mean effect of BRL 38227 (1 μM) on membrane currents and membrane potential using the voltage-clamp/current-clamp protocol. (a) The superimposed current traces show the effect of BRL 38227 on membrane currents when the potential was stepped from a holding potential of − 50 mV to 0 mV. Under current-clamp the membrane current was held at 0 pA apart from a current pulse of + 10 pA injected to give an indication of membrane input resistance. (b) Voltage protocol and membrane potential which corresponds to the current traces above. The size of the BRL 38227-induced hyperpolarization at the end of the 3000 ms current-clamp protocol (V = 22 mV) is given by the vertical arrow. The slow decay of membrane potential immediately after switching into current-clamp (V = 5.3 mV) is due to deactivation of I_{TO}. From the electrotonic potential, following current injection of 10 pA it can be deduced that I_{TO} contributed about 20 pA to the total current immediately after switching into current-clamp. Data are the mean of 10 identical successive voltage/current-clamp protocols in each of three different cells (i.e. a total of 30 episodes).

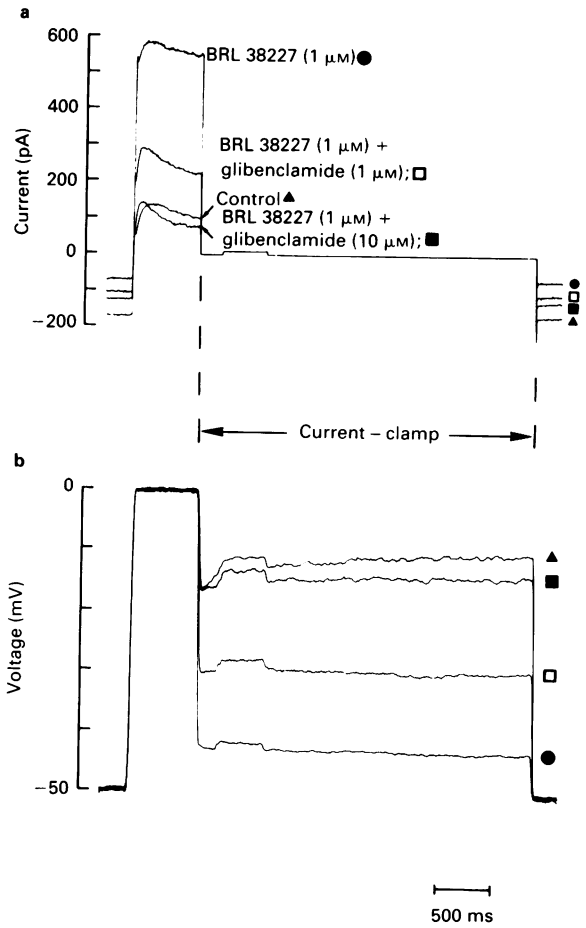

Figure 7 Effect of glibenclamide on membrane currents in the presence of BRL 38227 (1 μM). The experimental protocol was the same as that used in Figure 6. After the first trial (control, ▲) the cell was exposed to BRL 38227 (1 μM, ●). The outward current induced by depolarization to 0 mV was markedly increased by BRL application and the membrane potential hyperpolarized by more than 30 mV. The addition of glibenclamide (1 μM, □ or 10 μM, ■) in the continuous presence of 1 μM BRL reversed BRL 38227-induced current increase and shifted the membrane potential towards control values in a concentration-dependent manner. Each current and voltage trace is the average derived from 10 identical successive voltage/current-clamp protocols.

and was associated with an increase of current noise density. Analysis of this noise indicated that the channel involved in this response had a quite small single channel conductance and the single channel current associated with I_{KCO} was 0.65 pA at − 10 mV. The macroscopic current induced by BRL 38227 was well-described by the Goldman-Hodgkin-Katz equation and using this, the unitary conductance of the channel which underlies I_{KCO} was calculated to be close to 17 pS. Importantly, this current was inhibited in a concentration-dependent manner by glibenclamide, a compound which blocks all the effects of the KCOs both *in vivo* and *in vitro* (Buckingham *et al.*, 1989; Newgreen *et al.*, 1990). In experiments using isolated patches, the KCOs have been demonstrated to increase the open probability of a large variety of K-channels, ranging from small conductance (7.5 pS) K-channels (Nakao & Bolton, 1991) to very large (251 pS) K-channels (BK_{Ca}; Hu *et al.*, 1990) and from small conductance (30 pS) K-channels sensitive to extracellular calcium (Inoue *et al.*, 1989) to small conductance calcium-dependent K-channels sensitive to intracellular ATP (Kajioka *et al.*, 1990). In the present study, the whole-cell current induced by BRL 38227 was associated with a small (17 pS) K-channel. The involvement of a small conductance K-channel in the whole-cell current was also reported by Beech & Bolton (1989b).

This contrasts with data obtained from isolated patches, or from planar lipid bilayers into which several KCOs were found to increase the open probability of a large conductance Ca-sensitive K-channel which was identified as BK_{Ca} by its sensitivity to charybdotoxin (Gelband *et al.*, 1990; Hu *et al.*, 1990). However, purified charybdotoxin (which blocks BK_{Ca}) has no effect *in vitro* on the mechano-inhibitory response to either cromakalim or the structurally dissimilar KCO, minoxidil sulphate, in rat portal vein or rabbit aorta (Winquist *et al.*, 1989; Wickenden *et al.*, 1991). In addition, charybdotoxin has no effect on cromakalim-induced $^{86}Rb^+$ efflux from rabbit aorta (Strong *et al.*, 1989).

Furthermore, the whole-cell current induced by cromakalim in the rabbit portal vein was unaffected by charybdotoxin (Beech & Bolton, 1989b). Thus, the observations that KCOs are capable of increasing the open probability of large conductance Ca-sensitive K-channels in isolated patches or after incorporation into lipid bilayers (Gelband *et al.*, 1990; Hu *et al.*, 1990) may have little physiological relevance.

Since the effects of the KCOs are inhibited by glibenclamide (Buckingham *et al.*, 1989; Newgreen *et al.*, 1990), a selective blocker of the ATP-sensitive K-channel (K_{ATP}) in insulin-secreting cells (Sturgess *et al.*, 1988) and cardiac cells

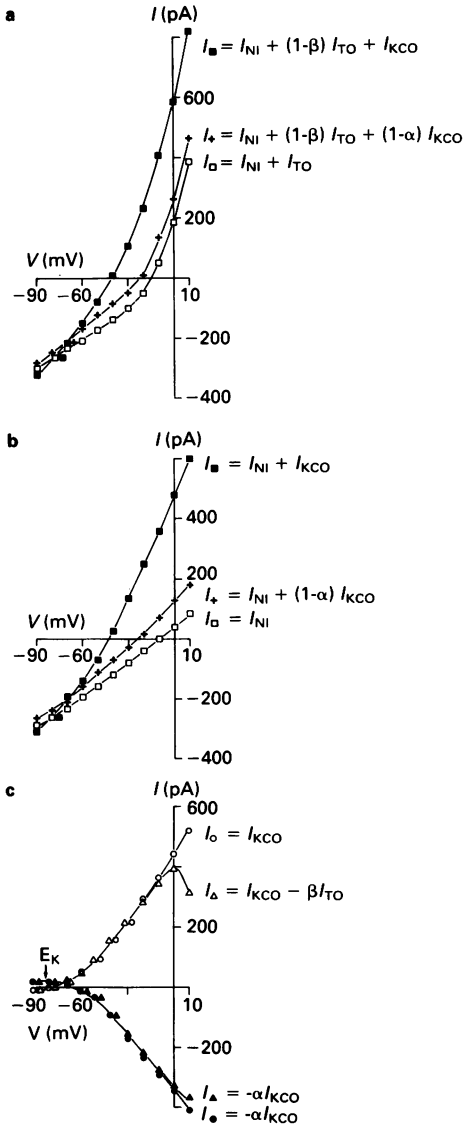

Figure 8 Current-voltage relationships of the currents in rat portal vein and effects of BRL 38227 and glibenclamide. (a) Current-voltage relationship of the peak of total current (peak of I_{TO}) under control conditions (□), in the presence of BRL 38227 (1 μM) (■) and in the presence of both 1 μM BRL 38227 and 1 μM glibenclamide (+). The holding potential was − 90 mV to ensure full activation of I_{TO}. (b) Current-voltage relationship of the non-inactivating currents under control conditions (□) and in the presence of 1 μM BRL (■), obtained from the same cell as in (a). The holding potential was − 10 mV which ensured complete inactivation of the time-dependent current components. (c) Current-voltage relationships of the net current induced by BRL 38227 (difference between currents in the presence and absence of BRL 38227) for the two holding potentials (△, − 90 mV; ○, − 10 mV). Also shown is the effect of glibenclamide (difference between currents in the presence of BRL 38227 and those in the presence of both BRL 38227 and glibenclamide) for the two holding potentials (▲, − 90 mV; ●, − 10 mV).

(Escande *et al.*, 1988) it has been suggested that this channel might be involved in the effects of the KCOs in smooth muscle (Quast & Cook, 1989). However, the relative sensitivity of the heart and pancreatic β-cell to KCOs and glibenclamide differs from that of smooth muscle (see Weston & Edwards, 1991), suggesting that the channel activated by the KCOs in smooth muscle differs from that at which they exert their effect in the heart or pancreas. Indeed, a channel similar to K_{ATP} in the pancreatic β-cell or the heart has not been found in smooth muscle. A brief report has described an ATP-sensitive K-channel in rat and rabbit mesenteric artery which was opened by cromakalim and inhibited by glibenclamide (Standen *et al.*, 1989). Whether ATP *per se* or whether magnesium released from the ATP salt was responsible for the channel inhibition (Kajioka *et al.*, 1991) is not certain. Further evidence that an ATP-sensitive K-channel exists in vascular smooth muscle is still awaited. Nevertheless, the suggestion (Standen *et al.*, 1989) that this relatively large conductance channel (135 pS under asymmetrical K^+ conditions, 60 mM extracellular K^+; 120 mM intracellular K^+) might be the main carrier of the K-current induced by BRL 38227 would be inconsistent with the findings of the present study.

Although single channel recordings are useful to indicate the properties of identified channels, it is impossible to extrapolate to what extent changes in single channel parameters influence membrane potential. The experimental conditions used in the present study (whole-cell voltage-clamp; whole-cell current-clamp; stationary fluctuation analysis) provide information about whole-cell currents, single channel current and membrane potential in the same cell. Using this approach the observed single channel responses and associated whole-cell currents are the determinants of the change in membrane potential. Having concluded that, under our experimental conditions, the main channel responsible for the actions of BRL 38227 is a non-inactivating channel with a conductance of 17 pS, future single channel experiments can now be performed in which patches which do not possess this channel will be excluded. In the present experiments I_{KCO} was recorded under conditions of very low intra- and extracellular calcium (free calcium lower than 1 nM). This suggests that the calcium-dependency of the channel is very low, especially in comparison to BK_{Ca}. However, it is not possible to conclude that the current is totally Ca-independent since the intracellular Ca^{2+} distribution might not be homogeneous. Under similar experimental voltage-clamp conditions, I_{KCO} was described as a non-inactivating current with a small single channel conductance by Okabe *et al.* (1990) and Kajioka *et al.* (1990). However, these workers concluded that I_{KCO} was calcium-dependent from the observation that I_{KCO} decreased when manganese was substituted for extracellular calcium. In our experiments extracellular calcium was replaced with magnesium and EGTA was added (see Methods) which should have provided a much lower concentration of extracellular calcium in our experiments than in those of Okabe *et al.* (1990) and Kajioka *et al.* (1990). The most likely explanation for the discrepancy is that manganese can act as a K-channel blocker.

In the present study, BRL 38227 inhibited a transient outward current which activated and inactivated relatively slowly (I_{TO}) and which is probably identical to the delayed rectifier current (I_{dK}) described by Beech & Bolton (1989b). Although we have already briefly described this effect (Noack *et al.*, 1991), the finding that a K-channel opener can also inhibit a K-current is essentially novel. A similar inhibition of K-current by nicorandil or cromakalim was not described in the papers by Kajioka *et al.* (1990) or Okabe *et al.* (1990), respectively, although this inhibitory effect appears to be evident in many of the figures which illustrate current-voltage relationships in the presence of these KCOs. A suppression of I_{TO} and an induction of I_{KCO} by the KCOs can lead to a net current which exhibits two reversal potentials. Such $I-V$ relationships were usually obtained when positive test potentials (up to + 50 mV) were applied. One reversal potential corresponded to the potassium equilibrium potential, indicating that both I_{KCO} and I_{TO} were K^+ currents. The other reversal potential varied between + 10 mV and + 50 mV in different cells and was dependent on the magnitude of I_{KCO} and the degree of suppression of I_{TO}. The variability in this second reversal potential was evidence that the induction of I_{KCO} and the inhibition of I_{TO} were independent processes. The suppression of I_{TO} by BRL 38227 led to a reduction in the outward current which was quite marked at

very depolarized potentials. However, such potentials (+ 10 mV to + 50 mV) are unlikely to be achieved physiologically and it is unlikely that inhibition of I_{TO} would diminish the hyperpolarizing effect of BRL 38227 *in vivo*. Nevertheless, it will be interesting to determine whether such an effect on I_{TO} is shared by other structurally-dissimilar KCOs.

Based on the relative potencies of a variety of compounds to inhibit the K-channels present in the rabbit portal vein, Beech & Bolton (1989b) concluded that cromakalim exerted a stimulatory effect on the delayed rectifier current, I_{dK} (I_{TO}). Although cromakalim apparently induced a non-inactivating current (in contrast to I_{dK} itself), Beech & Bolton (1989b) concluded that the voltage sensitivity of the channel underlying I_{dK} had been modified by cromakalim. In our study, the total K-current (compare Figures 3c and 8c) in the presence of BRL 38227 showed a pronounced point of inflection at potentials over which I_{TO} was strongly activated. This cannot be explained by modification of the voltage-dependent activation and inactivation parameters of I_{TO} (I_{dK}) by BRL 38227, such that I_{TO} is always activated but that the underlying single channel conductance is unchanged. Moreover, noxiustoxin, a blocker of the delayed rectifier current (Carbone *et al.*, 1982), did not inhibit the mechano-inhibitory response to either cromakalim or minoxidil sulphate in rabbit aorta (Wickenden *et al.*, 1991). In the study performed by Beech & Bolton (1989b), glibenclamide (50 μM) blocked only the current induced by cromakalim but apparently not I_{dK} which was of a similar magnitude in the presence of glibenclamide and cromakalim as before exposure to these two agents (which would mean that cromakalim both changes the voltage-dependency of I_{dK}-channels and induces glibenclamide-sensitivity to the channels). In the present study, glibenclamide inhibited the current induced by BRL 38227 but had no relevant effect on the inhibition of I_{TO} by BRL 38227. This is illustrated in Figure 8c but is clearly evident in Figure 7, in which the current suppressed by glibenclamide was not influenced by changing the holding potential from − 90 mV to − 10mV. Since glibenclamide neither modified the effect of BRL 38227 on I_{TO} significantly nor reduced the non-inactivating current component which could not be attributed to BRL 38227, it appears that glibenclamide is a selective blocker of I_{KCO}. This is consistent with the finding *in vitro* that glibenclamide only inhibits BRL 38227-induced efflux of $^{42}K^+$ but has no effect on the basal $^{42}K^+$ efflux from rat portal vein (Edwards *et al.*, 1991).

Using the fast-switching voltage-clamp/current-clamp amplifier, a very large hyperpolarization was induced by 1 μM BRL 38227. Such a large hyperpolarization, produced by activation of I_{KCO} alone, would be sufficient to reduce calcium influx through voltage-operated calcium channels and to account for the observed effects of BRL 38227 in whole tissues. This observation, together with the inability of charybdotoxin to modify the response to BRL 38227 *in vitro* (see earlier) questions the possible role of other K-channel types (e.g. BK_{Ca}; Gelband *et al.*, 1989; Hu *et al.*, 1989) in the action of the KCOs.

The present study strongly suggests that the effects of BRL 38227 in whole tissues can be fully explained by the generation of a K-current which we have designated I_{KCO}. Based on stationary fluctuation analysis, the channel underlying I_{KCO} has a unitary conductance of 17 pS. Some of the characteristics of I_{KCO} are apparently different from those of the KCO-induced current and KCO-activated K-channel described by Kajioka *et al.* (1990, nicorandil; 1991, pinacidil), Xiong *et al.* (1991, pinacidil) and Nakao & Bolton (1991, cromakalim). However, it seems possible that all these recent investigations (present study; Nakao & Bolton,1991; Kajioka *et al.*, 1990; 1991; Xiong *et al.*, 1991) describe an identical channel, the properties of which are modified by the different cell separation procedures and/or detailed recording conditions in the various laboratories. In particular there are close similarities between our raw data and those of Beech & Bolton (1989b); the more detailed analysis in the present study strongly suggests that the K-current activated by KCOs is indeed a separate current (I_{KCO}) rather than a modified I_{dK} (I_{TO}) as suggested by Beech & Bolton (1989b). Studies are now in progress to characterize I_{KCO} further and to establish its ATP-sensitivity and unitary conductance in isolated patches.

This study was supported by grants from the Deutsche Forschungsgemeinschaft (Th.N. and P.D.) and by Pfizer Central Research (G.E.). Generous gifts of BRL 38227 (SmithKline Beecham) are gratefully acknowledged.

References

BEECH, D.J. & BOLTON, T.B. (1989a). Two components of potassium current activated by depolarization of single smooth muscle cells from the rabbit portal vein. *J. Physiol.*, **418**, 293–309.

BEECH, D.J. & BOLTON, T.B. (1989b). Properties of the cromakalim-induced potassium conductance in smooth muscle cells isolated from the rabbit portal vein. *Br. J. Pharmacol.*, **98**, 851–864.

BUCKINGHAM, R.E., HAMILTON, T.C., MOOTOO, S. & WILSON, C. (1989). Inhibition by glibenclamide of the vasorelaxant action of cromakalim in the rat. *Br. J. Pharmacol.*, **97**, 57–64.

CARBONE, E., WANKE, E., PRESTIPINO, G., POSSANI, L.D. & MAELICKE, A. (1982). Selective blockade of voltage-dependent K^+ channels by a novel scorpion toxin. *Nature*, **296**, 90–91.

CLAPP, L.H. & GURNEY, A.M. (1991). ATP modulates the resting potential of isolated rabbit pulmonary arterial cells via a cromakalim- and glibenclamide-sensitive K^+ current. *J. Physiol.*, **438**, 373P.

CLARK, R.B. & GILES, W. (1987). Sodium current in single cells from bullfrog atrium: voltage dependence and ion transfer properties. *J. Physiol.*, **391**, 235–265.

EDWARDS, G., HENSHAW, M., MILLER, M. & WESTON, A.H. (1991). Comparison of the effects of several potassium-channel openers on rat bladder and rat portal vein in vitro. *Br. J. Pharmacol.*, **102**, 679–686.

EDWARDS, G. & WESTON, A.H. (1990). Potassium channel openers and vascular smooth muscle relaxation. *Pharmacol. Ther.*, **48**, 237–258.

ESCANDE, D., THURINGER, D., LEGUERN, S. & CAVERO, I. (1988). The potassium channel opener cromakalim (BRL 34915) activates ATP-dependent K^+ channels in isolated cardiac myocytes. *Biochem. Biophys. Res. Commun.*, **154**, 620–625.

GELBAND, C.H., SILBERBERG, S.D., GROSCHNER, K. & VAN BREEMEN, C. (1990). ATP inhibits smooth muscle Ca^{2+} activated K^+ channels. *Proc. R. Soc. L. Ser. B.*, **242**, 23–28.

HAMILL, O.P., MARTY, A., NEHER, E., SAKMANN, B. & SIGWORTH, F.J. (1981). Improved patch-clamp techniques for high-resolution current recording from cells and cell-free membrane patches. *Pflügers Arch.*, **391**, 85–100.

HU, S., KIM, H.S., OKOLLE, P. & WEISS, G.B. (1990). Alterations by glyburide of effects of BRL 34915 and P1060 on contraction, $^{86}Rb^+$ efflux and maxi-K^+ channel in rat portal vein. *J. Pharmacol. Exp. Ther.*, **253**, 771–777.

INOUE, I., NAKAYA, Y., NAKAYA, S. & MORI, H. (1989). Extracellular Ca^{2+}-activated K channel in coronary artery smooth muscle cells and its role in vasodilation. *FEBS Lett.*, **255**, 281–284.

KAJIOKA, S., KITAMURA, K. & KURIYAMA, H. (1991). Guanosine diphosphate activates an adenosine 5'-triphosphate-sensitive K+ channel in the rabbit portal vein. *J. Physiol.*, **444**, 397–418.

KAJIOKA, S., OIKE, M. & KITAMURA, K. (1990). Nicorandil opens a calcium-dependent potassium channel in smooth muscle cells of the rat portal vein. *J. Pharmacol. Exp. Ther.*, **254**, 905–913.

KLÖCKNER, U. & ISENBERG, G. (1985). Action potentials and net membrane currents of isolated smooth muscle cells (urinary bladder of the rat). *Pflügers Arch.*, **405,** 329–339.

KLÖCKNER, U., TRIESCHMANN, U. & ISENBERG, G. (1989). Pharmacological modulation of calcium and potassium channels in isolated vascular smooth muscle cells. *Arzneim.-Forsch.*, **39,** 120–126.

LAMMEL, E., DEITMER, P. & NOACK, TH. (1991). Suppression of steady membrane currents by acetylcholine in single smooth muscle cells of the guinea-pig gastric fundus. *J. Physiol.*, **432,** 259–282.

LINDEMAN, V., PAVENSTÄDT, H., KUNZELMANN, K., SCHOLLMEYER, P. & GREGER, R. (1991). Cromakalim increases K^+-conductance of vascular smooth muscle cells (VSMC) of rabbit aorta: nystatin patch and whole-cell clamp studies. *Pflügers Arch.*, **418,** (suppl. 1), R50.

NAKAO, K. & BOLTON, T.B. (1991). Cromakalim-induced potassium currents in single dispersed smooth muscle cells of rabbit artery and vein. *Br. J. Pharmacol.*, **102,** 155P.

NEHER, E. & STEVENS, C.F. (1977). Conductance fluctuations and ionic pores in membranes. *Annu. Rev. Biophys. Bioeng.*, **6,** 345–381.

NEWGREEN, D.T., BRAY, K.M., MCHARG, A.D., WESTON, A.H., DUTY, S., BROWN, B.S., KAY, P.B., EDWARDS, G. & LONGMORE, J. (1990). The action of diazoxide and minoxidil sulphate on rat blood vessels–a comparison with cromakalim. *Br. J. Pharmacol.*, **100,** 605–613.

NOACK, TH., DEITMER, P., EDWARDS, G., WESTON, A.H. & GOLENHOFEN, K. (1991). Effects of BRL 38227 on whole-cell currents in vascular smooth muscle. *Pflügers Arch.*, **419,** (suppl. 1) R85.

NOACK, TH., DEITMER, P. & GOLENHOFEN, K. (1990). Features of a calcium-independent, caffeine sensitive outward current in single smooth muscle cells from guinea-pig portal vein. *Pflügers Arch.*, **416,** 467–469.

NOACK, TH., DEITMER, P. & LAMMEL, E. (1992). Characterization of membrane currents in single smooth muscle cells from the guinea-pig gastric antrum. *J. Physiol.*, **451,** 387–417.

OKABE, K., KAJIOKA, S., NAKAO, K., KITAMURA, K., KURIYAMA, H. & WESTON, A.H. (1990). Actions of cromakalim on ionic currents recorded from single smooth muscle cells of the rat portal vein. *J. Pharmacol. Exp. Ther.*, **252,** 832–839.

PAVENSTÄDT, H., LINDEMAN, V., LINDEMAN, S., KUNZELMANN, K., SPÄTH, M. & GREGER, R. (1991). Effect of depolarizing and hyperpolarizing agents on the membrane potential difference of primary cultures of rabbit aorta vascular smooth muscle cells. *Pflügers Arch.*, **419,** 69–75.

QUAST, U. & COOK, N.S. (1989). Moving together: K^+ channel openers and ATP-sensitive K^+ channels. *Trends Pharmacol. Sci.*, **10,** 431–435.

STANDEN, N.B., QUAYLE, J.M., DAVIES, N.W., BRAYDEN, J.E., HUANG, Y. & NELSON, M.T. (1989). Hyperpolarizing vasodilators activate ATP-sensitive K^+ channels in arterial smooth muscle. *Science*, **245,** 177–180.

STRONG, P.N., WEIR, S.W., BEECH, D.J., HIESTAND, P. & KOCHER, H.P. (1989). Effects of potassium channel toxins from *Leiurus quinquestriatus hebraeus* venom on responses to cromakalim in rabbit blood vessels. *Br. J. Pharmacol.*, **98,** 817–826.

STURGESS, N.C., KOZLOWSKI, R.Z., CARRINGTON, C.A., HALES, C.N. & ASHFORD, M.L.J. (1988). Effects of sulphonylureas and diazoxide on insulin secretion and nucleotide-sensitive channels in an insulin-secreting cell line. *Br. J. Pharmacol.*, **95,** 83–94.

WESTON, A.H. & EDWARDS, G. (1991). Latest developments in K-channel modulator pharmacology. *Z. Kardiol.*, (suppl. 7), **80,** 1–8.

WICKENDEN, A.D., GRIMWOOD, S., GRANT, T.L. & TODD, M.H. (1991). Comparison of the effects of the K^+-channel openers cromakalim and minoxidil sulphate on vascular smooth muscle. *Br. J. Pharmacol.*, **103,** 1148–1152.

WINQUIST, R.J., HEANEY, L.A., WALLACE, A.A., BASKIN, E.P., STEIN, R.B., GARCIA, M.L. & KACZOROWSKI, G.J. (1989). Glyburide blocks the relaxation response to BRL 34915 (cromakalim), minoxidil sulphate and diazoxide in vascular smooth muscle. *J. Pharmacol. Exp. Ther.*, **248,** 149–156.

XIONG, Z., KAJIOKA, S., SAKAI, T., KITAMURA, K. & KURIYAMA, H. (1991). Pinacidil inhibits the ryanodine-sensitive outward current and glibenclamide antagonizes action in cells from the rabbit portal vein. *Br. J. Pharmacol.*, **102,** 788–790.

(Received February 5, 1992
Revised March 10, 1992
Accepted March 19, 1992)

Br. J. Pharmacol. (1992), **106**, 727–732

Cooling and response to adrenoceptor agonists of rabbit ear and femoral artery: role of the endothelium

A.L. García-Villalón, L. Monge, J.J. Montoya, J.L. García, N. Fernández, B. Gómez & [1] G. Diéguez

Departamento de Fisiologia, Facultad de Medicina, Universidad Autónoma, Arzobispo Morcillo 1, 28029 Madrid, Spain

1 The effects of cooling on the response of the rabbit central ear (cutaneous) and femoral (non-cutaneous) arteries to stimulation of adrenoceptors and the role of the endothelium in these effects, were studied in 2 mm long cylindrical segments.

2 Concentration-response curves for noradrenaline (10^{-9}–3×10^{-4} M), phenylephrine (α_1-adrenoceptor agonist, 10^{-9}–3×10^{-4} M) and B-HT 920 (α_2-adrenoceptor agonist, 10^{-7}–10^{-3} M) were recorded isometrically in arteries with and without endothelium at 37°C and at 24°C (cooling). To analyze further the endothelial mechanisms in the responses to adrenoceptor stimulation during cooling, the effects of the adrenoceptor agonists on ear arteries in the presence of N^G-nitro-L-arginine methyl esther (L-NAME) (10^{-5} M) were also determined.

3 In every condition tested, the three adrenoceptor agonists produced a concentration-dependent arterial contraction and the order of potency in ear and femoral arteries was noradrenaline ≥ phenylephrine > B-HT 920. The response of ear and femoral arteries to phenylephrine or B-HT 920 was blocked by prazosin (10^{-6} M). Yohimbine (10^{-6} M) decreased slightly the response of ear arteries and increased that of femoral arteries to B-HT 920.

4 The sensitivity of both ear and femoral arteries to the three adrenoceptor agonists was significantly lower at 24°C than at 37°C.

5 In ear arteries, endothelium removal or treatment with L-NAME did not influence the response at 37°C, but did increase it during cooling to adrenoceptor stimulation. In femoral arteries, endothelium removal increased the sensitivity to noradrenaline and, especially, to B-HT 920 at 37°C, but did not affect the response at 24°C.

6 The results suggest that: (a) rabbit ear and femoral arteries are equipped mainly with α_1-adrenoceptors; (b) at 37°C, the contraction of the ear artery to adrenoceptor agonists is mostly endothelium-independent, and in the femoral artery the contraction to α_2-adrenoceptor activation is endothelium-dependent; (c) cooling inhibits the contraction to adrenoceptor agonists in both ear and femoral arteries: in the ear artery probably by increasing the availability of endothelial nitric oxide, but in the femoral artery by depressing the sensitivity of α-adrenoceptors in the smooth musculature.

7 The results suggest that the endothelium may modulate the adrenoceptor response of cutaneous arteries during changes in temperature.

Keywords: Skin arteries; temperature; nitric oxide; noradrenaline; phenylephrine; B-HT 920; adrenoceptors

Introduction

The endothelium appears to play a major role in the regulation of vascular tone by releasing relaxing and contracting factors (Furchgott & Vanhoutte, 1989). As vascular relaxants, the endothelium can produce nitric oxide from L-arginine (Palmer *et al.*, 1987; 1988), which acts via the stimulation of the soluble guanylate cyclase in the vascular smooth muscle (Rapoport & Murad, 1983). The synthesis of endothelial nitric oxide can be inhibited by arginine analogues such as N^G-nitro-L-arginine methyl ester (L-NAME) (Moore *et al.*, 1990; Rees *et al.*, 1990).

At present very little is known about the role of the endothelium in the effects of temperature on vascular reactivity (Karaki & Nagase, 1987; Bodelsson *et al.*, 1989). This could be of relevance in blood vessels such as cutaneous ones that have thermoregulatory functions. Experimental evidence shows that cutaneous vessels of several species, including man, are equipped with a mixed population of postjunctional α_1- and α_2-adrenoceptors, frequently with a predominance of the α_2-adrenoceptor subtypes (Vanhoutte & Flavahan, 1986; Borbujo *et al.*, 1989; Harker *et al.*, 1991), and that cooling augments the constrictor response of these vessels to adrenergic activation by an increased α_2-adrenoceptor responsiveness (Flavahan *et al.*, 1985) or by an increased responsiveness of both α_1- and α_2-adrenoceptors (Gómez *et al.*, 1991). The role of the endothelium in these cooling-induced effects has not been studied.

The present experiments were designed to study the effects of moderate cooling on the response of cutaneous and non-cutaneous arteries to α-adrenoceptor activation with analysis of the role of the endothelium in these effects. To achieve this, central ear and femoral arteries from rabbits were mounted in an organ bath at 37°C and 24°C (cooling), and the effects of α-adrenoceptor activation were recorded isometrically in intact arteries and in arteries without endothelium or treated with an inhibitor of nitric oxide synthesis. The central ear artery was selected because this vessel is easily accessible and used as a model of cutaneous blood vessels (Patton & Wallace, 1978; Roberts & Zygmunt, 1984; Harker & Vanhoutte, 1988).

Methods

Seventeen male New Zealand White rabbits, weighing 2–2.5 kg, were killed by intraperitoneal injection of sodium

[1] Author for correspondence.

pentobarbitone, 100 mg kg^{-1}. Central ear and femoral arteries were dissected free and cut into cylindrical segments 2 mm in length. Each segment was prepared for isometric tension recording in a 6-ml organ bath containing modified Krebs-Henseleit solution of the following composition (millimolar): NaCl 115, KCl 4.6, KH_2PO_4 1.2, $MgSO_4$ 1.2, $CaCl_2$ 2.5, $NaHCO_3$ 25 and glucose 11.1. The solution was equilibrated with 95% O_2 and 5% CO_2 to give a pH of 7.3–7.4. Briefly, the method consists of passing two fine, stainless steel pins, 150 μm in diameter, through the lumen of the vascular segment. One pin is fixed to the organ bath wall while the other is connected to a strain gauge for isometric tension recording, thus permitting the application of passive tension in a plane perpendicular to the long axis of the vascular cylinder. The recording system included a Universal Transducing Cell UC3 (Statham Instruments, Inc.), a Statham Microscale Accessory UL5 (Statham Instruments, Inc.) and a Beckman Type RS Recorder (model R-411, Beckman Instruments, Inc.). A resting tension of 0.5 g was applied to the tissue and the segments were allowed to equilibrate for 60–90 min before any drug was added.

Part of the ear and femoral arteries were kept in the bath at a temperature of 37°C throughout the experiment, and the others were kept at 24°C (cooling). In some of the arterial segments, at 37°C or 24°C, the endothelium was removed prior to mounting the vessels in the organ bath. The removal of the endothelium was accomplished by gently rubbing the lumen of the vessel with a roughened steel rod. The presence of the endothelium in non-rubbed arteries as well as the adequacy of endothelium removal in rubbed arteries was functionally tested by recording the response to acetylcholine (10^{-6} M) in arteries precontracted with 5-hydroxytryptamine (10^{-6} M), and at the end of the experiments by morphological observation after 'en face' silver staining. In non-rubbed, intact arteries acetylcholine produced relaxation and more than 60–70% of the luminal surface was covered by endothelium. In rubbed arteries acetylcholine did not cause any reponse and less than 5% of the luminal surface was covered by endothelium.

Cumulative concentration-response curves were determined in central ear and femoral arteries with and without endothelium for noradrenaline (10^{-9}–3×10^{-4} M), the specific α_1-adrenoceptor agonist, phenylephrine (10^{-9}–3×10^{-4} M) and the α_2-adrenoceptor agonist, B-HT 920 (10^{-7}–10^{-3} M) at 37°C and at 24°C. Propranolol (10^{-6} M) was added to the bath 10 min before adding the agonists to block a possible β-adrenoceptor effect of the drugs. To test the specificity of B-HT 920 for α_2-adrenoceptors and phenylephrine for α_1-adrenoceptors, experiments with these drugs were also done in presence of the α_1-adrenoceptor antagonist, prazosin (10^{-6} M) or the α_2-adrenoceptor antagonist, yohimbine (10^{-6} M), at 37°C and at 24°C.

In order to analyze the role of endothelial nitric oxide in the vascular response, concentration-response curves to each adrenoceptor agonist were obtained in ear arteries in the presence of N^G-nitro-L-arginine methyl esther (L-NAME, 10^{-5} M), a nitric oxide-synthase inhibitor (Moore *et al.*, 1990; Rees *et al.*, 1990) at 37°C and 24°C. This drug was added to the bath 30 min before beginning the experiments. These types of experiments were not performed in femoral arteries because in these vessels endothelial removal did not affect the response to the α-adrenoceptor agonists used.

Concentrations of the α-adrenoceptor drugs causing 50% of the maximal response (EC_{50}) were calculated from each individual concentration-response curve. The geometric mean of EC_{50} and its 95% confidence interval were obtained for each group of experiments. At 37°C and 24°C the logarithms of the EC_{50} obtained in vascular segments with or without endothelium, and in the presence of L-NAME or the α-adrenoceptor antagonists were compared statistically. The data expressed as means ± s.e.mean, were evaluated by Student's *t* test, considering as significant a probability value of less than 0.05.

Drugs used were: (−)-noradrenaline bitartrate (Sigma), (−)-phenylephrine hydrochloride (Sigma), B-HT 920 (5-allyl- 2- amino- 5,6,7,8- tetrahydro- 4H-thiazolo- [4,5]-dazepin dihydrochloride, Boehringer Ingelheim), L-NAME (N^G-nitro-L-arginine methyl ester hydrochloride, Sigma), prazosin (1- [4- amino- 6,7- dimethoxy -2- quinazolinyl] -4- [furanyl - carbonyl] piperazine hydrochloride, Sigma) and yohimbine hydrochloride (Sigma).

Results

Ear arteries

Noradrenaline The effects of noradrenaline on ear arteries with and without endothelium obtained at 37°C and 24°C are summarized in Figure 1. At 37°C, noradrenaline (10^{-9}–3×10^{-4} M) produced a concentration-dependent contraction of intact ear arteries ($EC_{50} = 1.3 \times 10^{-7}$ M, 95% confidence interval = 7×10^{-8}–1.6×10^{-7} M), and after endothelium removal the sensitivity was not significantly ($P > 0.05$) affected and the maximal contraction was decreased ($P < 0.001$) to noradrenaline.

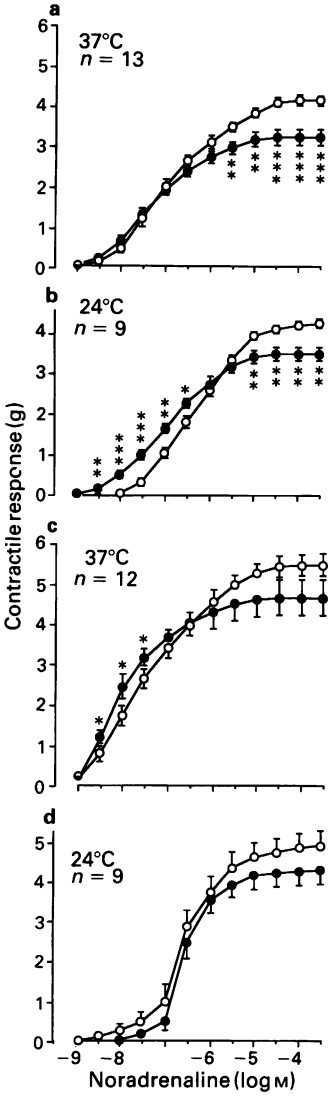

Figure 1 Contractile response of rabbit central ear (a,b) and femoral (c,d) arteries to noradrenaline at 37°C and 24°C in segments with (○) and without (●) endothelium. Values are means with s.e.mean shown by vertical bars. Statistically significant difference $^*P < 0.05$; $^{**}P < 0.01$; $^{***}P < 0.001$; n = number of animals.

During cooling (24°C), the sensitivity ($EC_{50} = 5.6 \times 10^{-7}$ M, 95% confidence interval = 3.4×10^{-7} M), but not the maximal response, of intact ear arteries to noradrenaline was lower (4 times, $P<0.001$) than at 37°C. At 24°C, ear arteries without endothelium showed an increased sensitivity (4 times, $P<0.001$) and lower maximal contraction with respect to intact arteries to noradrenaline.

At 37°C ear arteries treated with L-NAME (10^{-5} M) exhibited a comparable sensitivity ($P<0.05$) and a lower maximal contraction ($P<0.05$) than non-treated arteries, whereas at 24°C treatment with L-NAME induced a parallel leftward shift (2.5 times, $P<0.01$) of the concentration-response curve to noradrenaline (Table 1).

Phenylephrine The effects of phenylephrine on ear arteries with and without endothelium at 37°C and 24°C are summarized in Figure 2. At 37°C, phenylephrine (10^{-9}–3×10^{-4} M) induced a concentration-dependent contraction of intact arteries ($EC_{50} = 1.7 \times 10^{-7}$ M, 95% confidence interval = 1.2×10^{-7}–2.4×10^{-7} M), and after endothelium removal the sensitivity was comparable ($P>0.05$) and the maximal contraction was significantly reduced ($P<0.001$) to this α_1-adrenoceptor agonist.

During cooling the sensitivity ($EC_{50} = 3.4 \times 10^{-7}$ M, 95% confidence interval = 2.2×10^{-7}–5.1×10^{-7} M), but not the maximal contraction, of intact arteries to phenylephrine was reduced about 2 times ($P<0.001$) as compared to that obtained at 37°C. At 24°C, in arteries without endothelium the concentration-response curves for phenylephrine ($EC_{50} = 1.0 \times 10^{-7}$ M, 95% confidence interval = 7.5×10^{-8}–1.4×10^{-7} M) were shifted to the left in a parallel way about 3.4 times ($P<0.001$) in comparison to intact arteries.

Treatment with L-NAME (10^{-5} M) did not significantly affect the response of ear arteries at 37°C, and tended to induce a parallel leftward shift of the response at 24°C to phenylephrine (Table 1) although this was not significant.

Prazosin (10^{-6} M) induced a parallel rightward shift of the concentration-response curve to phenylephrine in intact arteries at 37°C and at 24°C. The displacement at 37°C was about 82 times ($P<0.001$), and at 24°C was about 132 times ($P<0.001$). Yohimbine (10^{-6} M) did not significantly modify the response of intact ear arteries to phenylephrine at either temperature.

B-HT 920 The effects of B-HT 920 on ear arteries with and without endothelium at 37°C and at 24°C are summarized in Figure 3. At 37°C this substance contracted the intact ear arteries in a concentration-dependent manner ($EC_{50} = 2.1 \times 10^{-6}$ M, 95% confidence interval = 1.4×10^{-6}–2.7×10^{-6} M) and the response was not significantly affected by endothelium removal.

During cooling a rightward shift ($EC_{50} = 5.7 \times 10^{-5}$ M, 95% confidence interval = 3.3×10^{-5}–7.1×10^{-5} M; 27 times, $P<0.001$) was found in the response of the intact ear arteries to B-HT 920 with respect to that obtained at 37°C. At 24°C, arteries without endothelium showed a response to B-HT 920 that was shifted to the left in a parallel way (5 times, $P<0.001$) in comparison to that recorded in intact arteries.

Yohimbine (10^{-6} M) produced a rightward shift of the response at 37°C (3 times, $P<0.001$), but it did not significantly affect the response at 24°C ($P>0.05$) of intact arteries to B-HT 920. Prazosin (10^{-6} M) also shifted to the right in a parallel way the response of intact ear arteries at 37°C (124 times, $P<0.001$), and it markedly reduced the response at 24°C to B-HT 920.

Treatment with L-NAME (10^{-5} M) did not modify significantly the concentration-response curve at 37°C, but it did produce a parallel leftward shift (3.5 times, $P<0.001$) of the response at 24°C to B-HT 920 (Table 1).

Femoral arteries

Noradrenaline (10^{-9}–3×10^{-4} M) produced a concentration-dependent contraction of intact femoral arteries at 37°C, and the sensitivity ($EC_{50} = 3.1 \times 10^{-8}$ M, 95% confidence interval = 1.8×10^{-8}–4.4×10^{-8} M) and maximal contraction (5.5 ± 0.27 g) exhibited by these arteries were significantly ($P<0.001$) higher than with intact ear arteries ($EC_{50} = 1.3 \times 10^{-7}$ M, 95% confidence interval = 7×10^{-8}–1.6×10^{-7} M; maximal contraction = 4.1 ± 0.13 g) (Figure 1). At 37°C the response of femoral arteries without endothelium to noradrenaline was shifted to the left (2.4 times, $P<0.05$) as compared with the intact arteries.

During cooling, the sensitivity ($EC_{50} = 2.5 \times 10^{-7}$ M, 95% confidence interval = 1.4×10^{-7}–4.6×10^{-7} M), but not the maximal response, of the intact femoral arteries was significantly lower (8 times, $P<0.001$) than at 37°C. At 24°C, endothelium removal did not affect significantly the arterial response to noradrenaline with respect to intact arteries (Figure 1).

Phenylephrine (10^{-9}–3×10^{-4} M) caused a concentration-dependent contraction of intact femoral arteries, the sensitivity being similar (EC_{50} 2.4×10^{-7} M, 95% confidence interval = 1.2×10^{-7}–4.8×10^{-7} M vs. 1.7×10^{-7} M, 95% confidence interval = 1.2×10^{-7}–2.4×10^{-7} M, $P>0.05$) and the maximal response being higher (5.5 ± 0.15 vs. 3.9 ± 0.02 g, $P<0.001$) than in ear arteries at 37°C (Figure 2).

Table 1 EC_{50} values with 95% confidence intervals and maximal contraction for the adrenoceptor agonists used in rabbit central ear arteries in absence (control) and in the presence of N^G-nitro-L-arginine methyl ester (L-NAME, 10^{-5} M) at 37°C and at 24°C

	EC_{50} (M)		*Maximal contraction (g)*	
	37°C	*24°C*	*37°C*	*24°C*
Noradrenaline				
Control	1.3×10^{-7} (7.0×10^{-8}–1.6×10^{-7})	5.6×10^{-7} (3.4×10^{-7}–7.0×10^{-7})	4.1 ± 0.13 ($n = 13$)	4.3 ± 0.11 ($n = 12$)
With L-NAME	1.6×10^{-7} (1.0×10^{-7}–2.3×10^{-7})	2.3×10^{-7}** (1.3×10^{-7}–3.9×10^{-7})	3.0 ± 0.56* ($n = 6$)	3.8 ± 0.33 ($n = 6$)
Phenylephrine				
Control	1.7×10^{-7} (1.2×10^{-7}–2.4×10^{-7})	3.4×10^{-7} (2.2×10^{-7}–5.1×10^{-7})	3.9 ± 0.09 ($n = 16$)	4.1 ± 0.15 ($n = 17$)
With L-NAME	1.1×10^{-7} (6.3×10^{-8}–1.8×10^{-7})	1.7×10^{-7} (1.0×10^{-7}–3.5×10^{-6})	3.8 ± 0.42 ($n = 8$)	4.2 ± 0.32 ($n = 8$)
B-HT 920				
Control	2.1×10^{-6} (1.4×10^{-6}–2.7×10^{-6})	5.7×10^{-5} (3.3×10^{-5}–7.1×10^{-5})	3.2 ± 0.35 ($n = 8$)	2.1 ± 0.18 ($n = 14$)
With L-NAME	1.1×10^{-6} (5.8×10^{-7}–1.8×10^{-6})	1.6×10^{-5}*** (9.1×10^{-6}–2.1×10^{-5})	3.7 ± 0.43 ($n = 5$)	3.0 ± 0.20*** ($n = 10$)

Statistically different with respect to its control at the same temperature. *$P<0.05$; **$P<0.01$; ***$P<0.001$. n = number of animals.

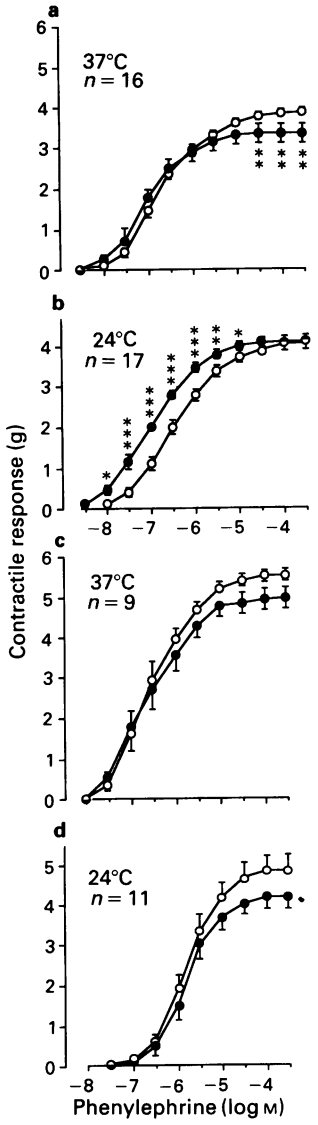

Figure 2 Contractile response of rabbit central ear (a,b) and femoral (c,d) arteries to phenylephrine at 37°C and 24°C in segments with (○) and without (●) endothelium. Values are means with s.e.mean shown by vertical bars. Statistically significant difference $*P<0.05$; $**P<0.01$; $***P<0.001$; n = number of animals.

During cooling, the sensitivity ($EC_{50} = 1.5 \times 10^{-6}$ M, 95% confidence interval = 9.6×10^{-7}–2.3×10^{-6} M), but not the maximal response, of intact femoral arteries to phenylephrine was lower (6 times, $P<0.001$) than at 37°C (Figure 2).

At 37°C and 24°C endothelium removal did not significantly influence the response of femoral arteries with respect to intact arteries to phenylephrine.

Prazosin (10^{-6} M) induced a parallel rightward shift of the response of femoral arteries to phenylephrine at 37°C (207 times, $P<0.001$) and at 24°C (80 times, $P<0.001$). Yohimbine (10^{-6} M) also produced a small parallel rightward shift of the response of these arteries to phenylephrine at 37°C and 24°C, these displacements being only about 2 times ($P<0.05$) in both cases.

B-HT 920 (10^{-7}–10^{-3} M) contracted intact femoral arteries in a concentration-dependent manner, the sensitivity ($EC_{50} = 6.8 \times 10^{-5}$ M, 95% confidence interval = 4.7×10^{-5}–9×10^{-5} M vs. 2.1×10^{-6} M, 95% confidence interval = 1.4×10^{-6}–2.7×10^{-6} M, $P<0.001$) and maximal response (2.1 ± 0.43 vs. 3.2 ± 0.35 g, $P<0.05$) being significantly lower than in intact ear arteries at 37°C (Figure 3).

During cooling the response of intact femoral arteries to B-HT 920 was markedly depressed, and this response was very small so that reliable values of EC_{50} for these responses could not be obtained (Figure 3).

At 37°C femoral arteries without endothelium showed a response to B-HT 920 ($EC_{50} = 2.3 \times 10^{-5}$ M, 95% confidence interval = 1.1×10^{-5}–3.6×10^{-5} M) that was significantly shifted to the left (2 times, $P<0.05$) in comparison with intact arteries. At 24°C the response to this agonist was very small and similar in endothelium-denuded and intact arteries (Figure 3).

Yohimbine (10^{-6} M) produced, paradoxically, a parallel leftward shift (2 times, $P<0.05$) of the response of femoral arteries to B-HT at 37°C. The response to B-HT 920 in the presence of yohimbine (10^{-6} M) at 24°C was very small and difficult to evaluate. Prazosin (10^{-6} M) abolished completely the response of intact arteries to this agonist at 37°C and at 24°C.

Discussion

In the present work we have studied the effects of moderate cooling on the response of the ear (cutaneous) artery of the rabbit to α-adrenoceptor stimulation, paying special attention to the influence of the endothelium in these effects. The ear artery was used because this superficial vessel has been used as a model of cutaneous blood vessels (Patton & Wallace,

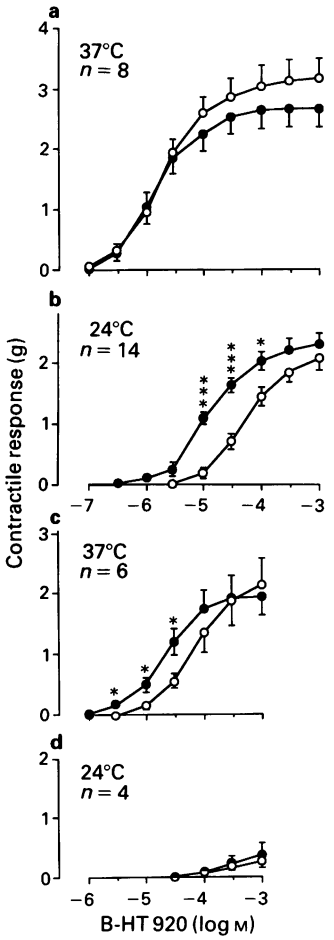

Figure 3 Contractile response of rabbit central ear (a,b) and femoral (c,d) arteries to BH-T 920 at 37°C and 24°C in segments with (○) and without (●) endothelium. Values are means with s.e.mean shown by vertical bars. Statistically significant difference $*P<0.05$; $**P<0.01$; $***P<0.001$; n = number of animals.

1978; Roberts & Zygmunt, 1984; Harker & Vanhoutte, 1988). Cooling to 24°C was chosen because it represents a modest tissue cooling that is likely to occur in skin surface exposed to ambient temperature under certain circumstance and comparable data are available in the literature for blood vessels. The results in this cutaneous artery are compared with those obtained in the femoral artery of the rabbit, which is a deep, non-cutaneous vessel.

Our results indicate that at 37°C the α-adrenoceptor agonists used produce contraction in rabbit ear and femoral arteries by stimulating postjunctional α-adrenoceptors located probably on the smooth muscle cells. In both types of arteries the sensitivity to noradrenaline and to the α_1-adrenoceptor agonist phenylephrine was similar, but the sensitivity to the α_2-adrenoceptor agonist, B-HT 920, was much lower than to noradrenaline or phenylephrine, this being more evident for femoral arteries. The response of both types of arteries to phenylephrine was blocked, as expected, by prazosin but not by yohimbine, indicating that this adrenoceptor agonist indeed acts on these arteries by activating α_1-adrenoceptors. The α_1-adrenoceptor antagonist prazosin, paradoxically, also blocked in a competitive manner the response to B-HT 920 in both femoral and ear arteries, whereas the α_2-adrenoceptor antagonist, yohimbine, produced a very small blockade of the response in ear arteries, or increased the sensitivity of femoral arteries to B-HT 920. This suggests that at the concentrations producing arterial contraction in these arteries, B-HT 920 produces contraction by acting mainly on α_1-adrenoceptors in ear and femoral arteries. Therefore, our results suggest that in the ear and femoral arteries of the rabbit α_1-adrenoceptors predominate over α_2-adrenoceptors to mediate vasoconstriction, probably by a higher concentration and/or sensitivity of the α_1-adrenoceptor subtype. The α_2-adrenoceptor subtype would have a relatively small importance for inducing constriction, especially in femoral arteries. Our data for the ear artery agree with those found in this artery by others (Harker & Vanhoutte, 1988). The ear artery, a cutaneous thermoregulatory vessel, seems to differ from other cutaneous vessels in which a predominance of the α_2-adrenoceptor over the α_1-adrenoceptor subtype has frequently been observed (Vanhoutte & Flavahan, 1986; Borbujo *et al.*, 1989; Harker *et al.*, 1991). The observations in the femoral artery correlate with those found in deep, non-cutaneous vessels (Vanhoutte & Flavahan, 1986).

At 37°C the sensitivity of the ear artery to the three adrenoceptor agonists used was not affected by removing the endothelium, thus suggesting that the adrenergic contraction of this artery is mostly caused by activation of the α-adrenoceptors located in the smooth musculature. The maximal contraction to noradrenaline and phenylephrine was found to be significantly reduced and tended to be lower to B-HT 920 in the ear arterial segments without endothelium. This feature could be related to some damage of the smooth muscle of these particular arteries when rubbed for removing the endothelium. This procedure, however, did not apparently affect the sensitivity of ear arteries to the adrenoceptor agonists used. In the femoral artery at 37°C, endothelium removal did not affect the effects by phenylephrine, but increased the response to noradrenaline and, especially, to B-HT 920. This suggests that α_2-adrenoceptors are also present in the endothelial cells of the femoral artery, and the activation of these particular receptors would induce the release of relaxant factors to oppose the adrenergic vasoconstriction mediated by activation of α-adrenoceptors of smooth musculature. This correlates with the paradoxical facilitating effect of yohimbine on the response to B-HT 920 found in intact femoral arteries. Yohimbine, by blocking the α_2-adrenoceptors in the endothelium, could reduce the release of relaxant factors from the endothelium, and thus unmask the direct effects of B-HT 920 on α-adrenoceptors located on smooth musculature. The influence of the endothelium on the adrenergic vasoconstriction has been observed in some vessels (Cocks & Angus, 1983; Carrier & Shite, 1985; Miller & Vanhoutte, 1985) but not in others (Rimele & Vanhoutte, 1983; Singer & Peach, 1983; Nava-Hernández *et al.*, 1991). α_2-Adrenoceptor activation seems to be very sensitive to the endothelium modulatory effect, because activation of α_2-adrenoceptors in the endothelium strongly stimulates nitric oxide release (Vanhoutte & Miller, 1989).

It is accepted that cooling depresses the contractile response of both cutaneous and non cutaneous blood vessels by direct activation of vascular smooth muscle with KCl or $BaCl_2$, an effect that has been considered to be due mainly to a decrease in permeability of vascular smooth muscle membrane for calcium ions (Vanhoutte, 1980). The inhibitory effect of cooling on the response of ear arteries to KCl has been described previously (Monge *et al.*, 1991) and was also observed in ear and femoral arteries (not shown). The present results also show that cooling inhibits the contraction of the ear and femoral arteries to α-adrenergic activation. Most of the results indicate that cooling potentiates the adrenergic contraction of cutaneous blood vessels and this has been related to the relative predominance of the α_2-adrenoceptors in these vessels (Vanhoutte & Flavahan, 1986; Borbujo *et al.*, 1989; Harker *et al.*, 1991). The lack of a potentiating effect of cooling on adrenergically induced contraction in the ear artery could be related to the relative paucity of the α_2-adrenoceptor subtype in this artery, a feature also observed by Harker & Vanhoutte (1988). The reduction of the adrenergic contraction by cooling found in the femoral artery is in accordance with that described in deep, non-cutaneous blood vessels (Vanhoutte & Flavahan, 1986).

Our results suggest that mechanisms underlying the inhibitory effects of cooling on the adrenergic response differ in the ear and femoral arteries. In femoral arteries endothelium removal did not affect the action of cooling, whereas in ear arteries endothelium removal reversed the inhibitory effects of cooling on the α-adrenoceptor response. This suggests that the inhibitory action of cooling on the adrenergic constriction in the femoral artery is the result of the reduced sensitivity of the α-adrenoceptors located in the smooth musculature, whereas in the ear artery it is mediated by an endothelium-dependent mechanism. In the ear artery the endothelium inhibits the contraction to α-adrenoceptor activation during cooling as derived from the results in this artery with and without endothelium. Treatment with L-NAME, an inhibitor of the nitric oxide synthesis (Moore *et al.*, 1990; Rees *et al.*, 1990), also increased the sensitivity of ear arteries to noradrenaline and B-HY 920 at 24°C, but not at 37°C, as occurred in the endothelium-denuded ear arteries. This suggests that the inhibitory effect of cooling on the response of the ear artery to α-adrenergic activation is probably due to the increased effects of endothelium-released nitric oxide at a low temperature. These increased effects of nitric oxide may counteract the response of cutaneous arteries to direct adrenergic activation during cooling. Under resting conditions L-NAME at the concentration used (10^{-5} M) did not modify the basal tension of the arteries. This feature was also observed when higher concentrations of L-NAME (10^{-4} M) were used (Monge *et al.*, 1991), and both of them suggest that the endothelium of these arteries does not release or releases insufficient nitric oxide to produce a vasodilator tone under resting conditions after applying a passive tension of 0.5 g. With regard to the observation that L-NAME reduced the maximal contraction of ear arteries to noradrenaline, but not to phenylephrine or B-HT 920 we have no explanation for this feature. Recently we have found that the contraction of the rabbit ear artery to endothelin-1 is also inhibited, probably by an augmented production in the endothelium or an increased half-life of nitric oxide, during cooling (Monge *et al.*, 1991). In that study (Monge *et al.*, 1991) it was found that the relaxation of the ear artery to nitroprusside, a compound that relaxes vascular smooth muscle in a similar way to nitric oxide (Ignarro & Kadowitz, 1985), was independent of the endothelium and was

decreased during cooling. Thus, cooling may increase the availability of endothelial nitric oxide not only when the ear artery is activated with endothelin-1, but also when it is adrenergically stimulated. These effects of cooling on the endothelial nitric oxide might be specific for cutaneous blood vessels as a cooling-induced inhibitory effect of the endothelium on the adrenergic contraction was not observed in femoral arteries. It is remarkable that in the study of Monge et al. (1991) 10^{-4} M concentrations of L-NAME were needed to increase the reactivity of the rabbit ear artery to endothelin-1 during cooling, whereas in the present study 10^{-5} M concentrations of this inhibitor of nitric oxide production were sufficient to increase the reactivity of this artery to noradrenaline or B-HT 920. This lower concentration of L-NAME was found to be capable of reducing the relaxation of precontracted ear arteries to acetylcholine at 37°C and 24°C (unpublished observations), thus suggesting that 10^{-5} M concentration of L-NAME is sufficient for blocking the production of endothelial nitric oxide. It can be suggested, therefore, that the inhibitory effect of cooling on the response of the ear artery by increasing the effects of endothelial nitric oxide may be more sensitive to adrenergic stimulation than to endothelin-1.

In conclusion, the main observation of the present study indicates that cooling inhibits the contraction of the ear and femoral arteries of the rabbit to adrenergic activation by different mechanisms. In the ear artery cooling inhibits this contraction, probably by increasing the availability of endothelial nitric oxide, whereas in the femoral artery by decreasing the sensitivity of α-adrenoceptors of smooth musculature. If the results in the ear artery could be extended to other cutaneous vessels, the endothelial function might be of relevance to thermoregulatory function of the cutaneous circulation as well as to the physiopathology of some pathological situations. Patients with Raynaud's phenomenon, which is in part characterized by intense cold-induced cutaneous vasospasm (Harper & LeRoy, 1987), present alterations in the endothelium of finger arteries (Rodnan et al., 1980). Thus, we can speculate that damage of the cutaneous vascular endothelium in these patients may underlie the augmented response of cutaneous vessels by lack of the inhibitory function of the endothelium during cooling.

The authors are grateful to Mrs M.E. Martínez and H. Fernández-Lomana for technical assistance. B-HT 920 was kindly provided by Europharma S.A.

This work was supported, in part, by DGICYT (88/0058) and Universidad Autónoma (Madrid, Spain).

References

BODELSSON, M., ARNEKLO-NOBIN, B. & TORNEBRANDT, K. (1989). Cooling augments contractile response to 5-hydroxytryptamine via an endothelium-dependent mechanism. *Blood Vessels*, **26**, 347–359.

BORBUJO, J., GARCIA-VILLALON, A.L., VALLE, J., GOMEZ, B. & DIEGUEZ, G. (1989). Postjunctional alpha-1 and alpha-2 adrenoceptors in human skin arteries. An in vitro study. *J. Pharmacol. Exp. Ther.*, **249**, 284–287.

CARRIER, G.O. & WHITE, R.E. (1985). Enhancement of $alpha_1$- and $alpha_2$ adrenergic agonists by removal of endothelium in rat aorta. *J. Pharmacol. Exp. Ther.*, **232**, 682–687.

COCKS, T.M. & ANGUS, J.A. (1983). Endothelium dependent relaxation of coronary arteries by noradrenaline and serotonin. *Nature*, **1305**, 627–630.

FLAVAHAN, N.A., LINDBLAD, L.E., VERBEUREN, T.J., SHEPHERD, J.T. & VANHOUTTE, P.M. (1985). Cooling and $alpha_1$- and $alpha_2$-adrenergic responses in cutaneous veins: role of receptor reserve. *Am. J. Physiol.*, **249**, H950–H955.

FURCHGOTT, R.F. & VANHOUTTE, P.M. (1989). Endothelium-derived relaxing and contracting factors. *FASEB J.*, **3**, 2007–2018.

GOMEZ, B., BORBUJO, J., GARCIA-VILLALON, A.L., NAVA-HERNANDEZ, E., VALLE, J., GARCIA, J.L. & DIEGUEZ, G. (1991). $Alpha_1$- and $alpha_2$-adrenergic response in human isolated skin arteries during cooling. *Gen Pharmacol.*, **221**, 341–346.

HARKER, C.T., OUSLEY, P.J., BOWMAN, C.J. & PORTER, J.M. (1991). Cooling augments $alpha_2$-adrenoceptor-mediated contractions in rat tail artery. *Am. J. Physiol.*, **260**, H1166–H1171.

HARKER, C.T. & VANHOUTTE, P.M. (1988). Cooling the central ear artery of the rabbit: Myogenic and adrenergic responses. *J. Pharmacol. Exp. Ther.*, **245**, 89–93.

HARPER, F.E. & LEROY, E.C. (1987). Raynaud's Phenomenon. In *Clinical Dermatology*, Vol. II. ed. Demis, D.J., Unit 7-36, pp. 1–9. Philadelphia: J.B. Lippincott.

IGNARRO, L.J. & KADOWITZ, P.J. (1985). The pharmacological and physiological role of cyclic GMP in vascular smooth muscle relaxation. *Annu. Rev. Pharmacol. Toxicol.*, **25**, 171–191.

KARAKI, H. & NAGASE, H. (1987). Low temperature augments the endothelium-dependent relaxation in isolated rat aorta. *Eur. J. Pharmacol.*, **142**, 129–132.

MILLER, V.M. & VANHOUTTE, P.M. (1985). Endothelial $alpha_2$-adrenoceptors in canine pulmonary and systemic blood vessels. *Eur. J. Pharmacol.*, **118**, 123–129.

MONGE, L., GARCIA-VILLALON, A.L., MONTOYA, J.J., GARCIA, J.L., GOMEZ, B. & DIEGUEZ, G. (1991). Response of rabbit ear artery to endothelin-1 during cooling. *Br. J. Pharmacol.*, **104**, 609–612.

MOORE, P.K., AL-SWAYEH, O.A., CHONG, N.W.S., EVANS, R.A. & GIBSON, A. (1990). L-N^G-nitro arginine (L-NOARG), a novel, L-arginine-reversible inhibitor of endothelium-dependent vasodilatation *in vitro*. *Br. J. Pharmacol.*, **99**, 408–412.

NAVA-HERNANDEZ, E., VALLE, J., GARCIA-VILLALON, A.L., GARCIA, J.L., MONGE, L., GOMEZ, B. & DIEGUEZ, G. (1992). The canine internal carotid system: Regional differences in reactivity to nerve stimulation, noradrenaline and 5-hydroxytryptamine. *Acta Physiol. Scand.*, **144**, 000–000.

PALMER, R.M.J., FERRIGE, A.G. & MONCADA, S. (1987). Nitric oxide release accounts for the biological activity of endothelium-derived relaxing factor. *Nature*, **327**, 524–526.

PALMER, R.M.J., ASHON, D.S. & MONCADA, S. (1988). Vascular endothelial cells synthesize nitric oxide from L-arginine. *Nature*, **333**, 664–666.

PATTON, J.N. & WALLACE, W.F.M. (1978). Responses of isolated rabbit ear arteries to intra- and extraluminal L- and D-noradrenaline and histamine in the temperature range 37–3°C. *Ir. J. Med. Sci.*, **147**, 313–317.

RAPOPORT, R.M. & MURAD, F. (1983). Agonist-induced endothelium dependent relaxation in rat thoracic aorta may be mediated through cGMP. *Circ. Res.*, **52**, 352–357.

REES, D.D., PALMER, R.M.J., SCHULZ, R., HODSON, H.F. & MONCADA, S. (1990). Characterization of three inhibitors of endothelial nitric oxide synthase *in vitro* and *in vivo*. *Br. J. Pharmacol.*, **101**, 146–152.

RIMELE, T.J. & VANHOUTTE, P.M. (1983). Effects of inhibitors of arachidonic acid metabolism and calcium entry on responses to acetylcholine, potassium and norepinephrine in the isolated canine saphenous vein. *J. Pharmacol. Exp. Ther.*, **225**, 720–726.

ROBERTS, M.F. & ZYGMUNT, A.C. (1984). Reflex and local thermal control of rabbit ear blood flow. *Am. J. Physiol.*, **246**, R979–R984.

RODNAN, G.P., MYEROWITZ, R.L. & JUSTH, G.O. (1980). Morphologic changes in the digital arteries of patients with progressive systemic sclerosis (scleroderma) and Raynaud phenomenon. *Medicine*, **59**, 393–408.

SINGER, H.A. & PEACH, M.J. (1983). Endothelium dependent relaxations of rabbit aorta I: relaxation stimulated by arachidonic acid. *J. Pharmacol. Exp. Ther.*, **226**, 790–795.

VANHOUTTE, P.M. (1980). Physical factors of regulation. In *Handbook of Physiology*, Section 2, Circulation, Vol. II, Vascular Smooth Muscle, ed. Bohr, D.F., Somlyo, A.P. & Sparks, H.V. pp. 443–474. Bethesda, Maryland: American Physiological Society.

VANHOUTTE, P.M. & FLAVAHAN, N.A. (1986). Effects of temperature on alpha-adrenoceptors in limb veins: role of receptor reserve. *Fed. Proc.*, **45**, 2347–2354.

VANHOUTTE, P.M. & MILLER, V.M. (1989). $Alpha_2$-adrenoceptors and endothelium-derived relaxing factor. *Am. J. Med.*, **87**, (Suppl. 3C), 1S–5S.

(Received November 27, 1991
Revised February 18, 1992
Accepted March 19, 1992)

Br. J. Pharmacol. (1992), **106**, 733–738

Responses to endothelins in the rat cutaneous microvasculature: a modulatory role of locally-produced nitric oxide

Elizabeth Lawrence & [1]Susan D. Brain

Pharmacology Group, Biomedical Sciences Division, King's College, Manresa Road, London SW3 6LX

1 The response of the cutaneous microvasculature to intradermal injection of the endothelins (ET-1, ET-2 and ET-3) and the modulatory effect of endogenously produced nitric oxide (NO) have been determined in the rat.

2 Intradermal injection of endothelins (0.1– 10 pmol/site) induced dose-dependent local reductions in blood flow, measured by ^{133}xenon clearance, with the following potency order; ET-1 = ET-2 > ET-3.

3 Laser Doppler blood flowmetry established that ET-1 (10 pmol/site) significantly ($P<0.05$) reduced microvascular blood flow for 3 h after injection. Over a wide dose-range, the response to the endothelins did not include any vasodilatation or visible flare.

4 A possible modulatory role of locally-produced NO was investigated by the intradermal injection of the potent inhibitor of NO generation N^G-nitro-L-arginine methyl ester (L-NAME). L-NAME (100 nmol/site) injected alone induced a significant decrease in blood flow. The vasoconstriction induced by L-NAME was partially reversed by L-arginine ($P<0.05$) but not observed with N^G-nitro-D-arginine methyl ester (D-NAME).

5 L-NAME significantly ($P<0.05$) enhanced the decrease in blood flow induced by submaximal doses of ET-1, ET-2 and ET-3 and vasopressin, although the results do not suggest that any of the vasoconstrictors stimulate NO release. The response to L-NAME was still observed 3.5 h after inducing a prolonged constriction with ET-1 (10 pmol/site).

6 These results indicate that locally produced NO maintains a dilator tone in the cutaneous microvasculature of the rat and acts to modulate the effect of vasoconstrictors such as endothelins. Hence, it is suggested that in conditions where endogenous NO release is reduced, vasoconstrictor agents such as the endothelins could induce a dangerous decrease in blood flow possibly leading to ischaemia and tissue necrosis.

Keywords: Nitric oxide; skin; endothelins; blood flow; microvascular vasoconstrictors

Introduction

Endothelin-1 was originally described as a potent and long-lasting vasoconstrictor derived from porcine endothelial cells (Yanagisawa *et al.*, 1988b). It is a member of a small mammalian family of highly homologous vasoconstrictor peptides which includes ET-2 and ET-3 (Yanagisawa *et al.*, 1988a; Inoue *et al.*, 1989). The *in vivo* actions of ET-1 on microvessels in the skin of several species (Brain *et al.*, 1989) and in the rat mesenteric preparation (Fortes *et al.*, 1989) have been characterized. Intradermal injection of ET-1 induces a potent, long-lasting vasoconstriction in rabbit and human skin (Brain *et al.*, 1988; 1989). It is equipotent with angiotensin II and vasopressin and more potent as a vasoconstrictor than noradrenaline in rabbit skin (Brain *et al.*, 1988). ET-1 inhibits oedema formation and neutrophil accumulation in rabbit skin (Brain *et al.*, 1988), these anti-inflammatory actions are a consequence of the intense vasoconstriction induced in this microvascular bed by ET-1.

Although ET-1, ET-2 and ET-3 have a high degree of structural homology (Inoue *et al.*, 1989), they vary in potency and biological activity. ET-2 is equipotent with ET-1 as a vasoconstrictor of macrovessels and as a pressor agent when given intravenously to rats, but ET-3 is less potent with respect to both these activities (Yanagisawa *et al.*, 1988a; Inoue *et al.*, 1989). Systemic administration of low doses of endothelins to anaesthetised rats induces a biphasic response consisting of an initial transient fall in blood pressure followed by a long-lasting pressor effect. The initial depressor response is greater in response to ET-3 than ET-1, (Inoue *et al.*, 1989) and at low doses ET-3 is a vasodilator in the preconstricted rat isolated perfused mesentery (Warner *et al.*, 1989). It has been reported that both ET-1 and ET-3 induce regional vasodilatations *in vivo* when administered intravenously at doses lower than those causing vasoconstrictions (Wright & Fozard 1988; Gardiner *et al.*, 1990a). The mechanisms underlying the vasodilator responses induced by systemic ET-1 and ET-3 are not clear, although the vasoconstriction is thought to be a direct effect on vascular smooth muscle receptors. The vasodilatation may be an indirect effect of the endothelins acting via endothelial cell receptors to stimulate release of vasodilators including prostanoids (Rakugi *et al.*, 1989) and/or endothelium-derived relaxing factor (EDRF) (De Nucci *et al.*, 1988; Warner *et al.*, 1989). NO derived from L-arginine is a mediator of endothelium-derived vasodilatation (Palmer *et al.*, 1987; 1988). The biosynthesis of NO by endothelial cells can be inhibited by several L-arginine analogues, one of the most potent described is N^G-nitro-L-arginine methyl ester (L-NAME) (Moore *et al.*, 1990). The development of NO synthase inhibitors has revealed the importance of basal NO production for the maintenance of blood pressure (Rees *et al.*, 1989). It is evident that a basal level of NO synthesis occurs at the microvascular level in the gastric mucosa (Whittle *et al.*, 1990) and rat skin, where it can act to modulate inflammatory oedema induced by substance P (Hughes *et al.*, 1990).

The aims of the present study were initially to compare activities of the endothelin isotypes on cutaneous microvas-

[1] Author for correspondence.

cular blood flow in the rat, and then to investigate the possible modulatory role of endogenous NO on the cutaneous responses to the endothelins. This work has been presented as a preliminary communication to the British Pharmacological Society (Lawrence & Brain, 1991).

Methods

Male adult Wistar rats (Bantin and Kingman, Hull, U.K.) weighing between 150 and 250 g were used. Animals had free access to food (SDS RM1E) and tap water; they were housed in a room maintained at a temperature of 20–22°C, with lights on from 07 h 00 min to 19 h 00 min.

Blood flow measured by ^{133}xenon clearance

Rats were anaesthetized by an intraperitoneal injection of pentobarbitone sodium (50 mg kg^{-1}, plus maintenance doses as necessary) and the dorsal skin was shaved. Blood flow changes produced by intradermal injections of agents were calculated as percentage increase or decrease of ^{133}Xe washout over that in the control, Tyrode-injected sites. Measurements were made at multiple sites in the dorsal skin using a ^{133}Xe clearance technique described in the rabbit (Williams 1979), modified for use in the rat. Endothelins and other test agents were made up in a balanced salt solution (Tyrode) and kept on ice until use. Equal quantities of ^{133}Xe (3.6 MBq) were mixed with each 1 ml sample of test agent for each experiment. The solutions were drawn up into 1 ml syringes fitted with 27 gauge needles. The samples were then given rapidly by intradermal injection in 100 µl volumes. The samples were randomised in each experiment and then injected in random order according to a predetermined site pattern. Three rats were used on each study day. The injection pattern was designed as follows: the dorsal skin was separated into two halves by drawing a central line in a neck to tail direction. Either eight or nine sites were marked on each half. The sites were allocated with one duplicate on each half, according to a balanced site pattern in order to minimize inter-site variations in basal blood flow. The site pattern was then rotated in the second and third rats. The order of injection was changed in the second and third rats. On completion of injections, 100 µl of each sample was put into counting vials, covered with 2 ml paraffin oil and capped immediately. These samples provide the total ^{133}Xe activity in each 100 µl injection. Fifteen minutes after completion of the first half of duplicate injections on the first rat, the animal was killed by pentobarbitone overdose. The second and third rats were similarly killed 15 min after completion of the first set of duplicate injections. The area of dorsal skin encompassing all the skin sites was removed from the lumbar muscles and any subcutaneous and connective tissue was dissected away. The sites were then punched out with a 16 mm diameter steel punch. The discs of skin were placed in counting vials and covered with 2 ml of paraffin oil before capping. The radioactivity in the samples was immediately counted in fixed order in an automatic gamma-counter (LKB 1282 commpugamma CF).

Percentage blood flow change was calculated from the following equation:

$$[\ln Xe_T - \ln Xe_A]/[\ln Xe_i - \ln Xe_T],$$

where Xe_T = count min^{-1} Tyrode-injected skin
Xe_A = count min^{-1} agent-injected skin
Xe_i = count min^{-1} in 100 µl volume of injection fluid

A 15 min clearance period was used in the experiments. The clearance process is treated as mono-exponential if a short clearance period is used, as described by Williams (1976; 1979). If the clearance period is 15 min, as in the present study, the experimental variation caused by the time taken for intradermal injections is reduced and there is sufficient time to inject up to nine samples in duplicate in a rat.

Modifications to ^{133}xenon clearance technique

In one set of experiments it was necessary to inject test agents in volumes other than the standard 100 µl. In these experiments changes in blood flow induced by the test agents were always compared with that induced by an equivalent volume of Tyrode solution, injected at other sites in the same rat. Volumes used are indicated in the results.

In other experiments local and systemic pretreatments were given. When the skin sites were pretreated, pretreatment agents were given by intradermal injection (100 µl volume) and then at a specific time point (indicated in the results) the second intradermal injections were made. ^{133}Xenon clearance was then measured over 15 min as above.

Systemic pretreatment of agents was given via a 25 gauge butterfly needle inserted into the tail vein, as a bolus injection make up in isotonic saline (0.9% w/v NaCl solution, 0.25 ml injection volume) and flushed through with 0.25 ml of saline. Intradermal injections were then made as above and ^{133}xenon clearance measured over 15 min.

Blood flow measured with laser Doppler blood flow meter

In separate experiments the time course of the constrictor activity of ET-1 on microvascular blood cell flow in rat skin was determined through the use of a dual channel laser Doppler blood flow meter (Moor Instruments, Devon, U.K.). The technique used was similar to that described previously (Brain & Williams 1989). The rats were anaesthetized with pentobarbitone sodium (50 mg kg^{-1}) the dorsal skin was shaved and depilated with a commercial depilatory cream (Immac). Throughout the experiments the rats were kept on a heating pad at 37°C. The Moor laser Doppler blood flow meter was set at a band width of 14.9 kHz with a time constant of 0.1 s and 0.5 s for flux and concentration respectively. Skin sites with equal basal blood cell flux were located and numbered in random order. The agents under test were made up in Tyrode solution and given by intradermal injection (100 µl volume) to each of a pair of predetermined sites, the laser Doppler blood flow meter used was equipped with dual channels thereby allowing simultaneous measurement at a test and a control site. A second pair of sites located on the opposite side and end of the dorsal skin (therefore a balanced site pattern) were injected 5 min later. Measurements were taken at each of the duplicate sites. Three readings of 1 min each were taken sequentially at both pairs of sites at the following time points after intradermal injection: 3, 15, 30 min and then every 30 min until 4.5 h after the intradermal injections. The mean of the 3 readings at each time point was calculated and results expressed as percentage change in blood cell flux compared with flux at the sites prior to injection. The flux value is a measure of the number of red blood cells moving in the path of the laser beam multiplied by the mean cell velocity. This value is used as an index of blood flow. The technique is based on the assumption that an increase in blood flux is linear with an increase in skin blood flow provided that the haematocrit is constant. The laser Doppler flowmeter records blood cell flux in a 1–2 mm^3 area of skin observed by the laser probe.

Materials

The following drugs were used: human endothelins 1, 2 and 3, were purchased from Bachem (U.K.) Ltd. (Essex). These peptides were all stored in aliquots at −30°C until just before use. L-NAME, the enantiomer N^G-nitro-D-arginine methyl ester (D-NAME), L-arginine, vasopressin and (−)-phenylephrine were all purchased from Sigma Chemical Company Ltd. (Dorset). L-N^G-monomethyl-arginine (L-NMMA) was a gift from Wellcome Research Laboratories (Kent). All of these agents were made up immediately before use. ^{133}Xe was obtained from Amersham International

(Amersham, Bucks). Sagatal was bought from May and Baker Ltd. (Kent). In all the experiments test agents were made up in Tyrode solution of the following composition (mM): NaCl 137, KCl 2.7, $MgCl_2$ 1.1, NaH_2PO_4 0.4, $NaHCO_3$ 11.9 and glucose 5.6.

Statistical treatment of results

The significance of differences between treatments was assessed by Bonferroni's modified t test; the standard error estimate for the analysis of variance was used to allow comparison of multiple sites. $P<0.05$ was accepted as statistically significant.

Results

The effect of endothelin-1, -2 and -3, phenylephrine and vasopressin in rat skin

ET-1, ET-2 and ET-3 all induced concentration-dependent decreases in rat skin microvascular blood flow as measured by ^{133}xenon clearance over 15 min (Figure 1). The three endothelins caused a similar range of blood flow changes, however ET-1 and ET-2 were approximately 3 times more potent on a molar basis than ET-3 and 100 times more potent than phenylephrine; vasopressin was 100 times more potent that ET-1 and ET-2. Very low doses of the endothelins (0.0001 −100 fmol/site) did not exhibit any activity, suggesting that at these doses neither a vasoconstriction nor a vasodilatation is observed.

The laser Doppler blood flow meter was used to measure the length of the reponse to vasopressin (0.1 pmol/site) and ET-1 (10 pmol/site). Both induced a similar decrease in blood cell flux 3 min after injections, vasopressin 28.1 ± 2.6% and ET-1 20.6 ± 5.7% decrease in flux compared with Tyrode-injected sites, but by 15 min the blood cell flux at vasopressin-injected sites had returned to the levels at Tyrode-injected sites while blood cell flux at the ET-1 injected-sites was still significantly depressed ($P<0.05$) mean ± s.e.mean, $n=6$.

The effect of nitric oxide synthase inhibitors on blood flow and endothelin responses

We have previously shown that the nitric oxide inhibitor L-NAME inhibits, in a dose-dependent manner, oedema formation induced by substance P (Hughes *et al.*, 1990). A dose effective in decreasing oedema formation (100 nmol/site) was chosen for this study. L-NAME but not the enantiomer D-NAME, inhibited microvascular blood flow in rat skin as measured by ^{133}xenon clearance. The blood flow was significantly lower at L-NAME-injected sites than at D-NAME-injected sites ($P<0.01$, Figure 2). Pretreatment with intravenous L-arginine attenuated this inhibitory action of L-NAME ($P<0.05$, Figure 2), indicating that intradermal L-NAME inhibits the local generation of vasodilator quantities of NO in the cutaneous microvasculature. L-arginine was given intravenously because, at the required doses, intradermal L-arginine alone induced inconsistent vascular changes. Further evidence for NO generation was obtained with a second inhibitor of nitric oxide synthase. L-NMMA (100 nmol/site), had a similar inhibitory effect (23.9 ± 6.8% decrease, $n=11$ rats) on blood flow in experiments using an identical protocol to that described for L-NAME. The possibility that local generation of NO was stimulated by the trauma of a 100 µl injection into rat skin was examined by investigating effects of the same concentration of L-NAME, injected in different volumes of Tyrode solution, on local blood flow. Blood flow was measured at sites receiving 20, 50, 100 and 200 µl Tyrode solution and the effect of these different volumes of L-NAME (100 nmol/100 µl) determined in each case. L-NAME inhibited blood flow by 38.5 ± 2.0% when 20 µl was injected, by 46.3 ± 5.9% when 50 µl was injected, by 37.5 ± 2.4% when 100 µl was injected and by 37.4 ± 4.4% when 200 µl was injected. Results are expressed as the mean ± s.e.mean of $n=6$ rats and as a percentage decrease in blood flow when compared with Tyrode-injected sites. Thus, a similar inhibitory effect of L-NAME was observed over a range of injection volumes suggesting that the pressure increase caused by injecting fluid into rat skin does not itself stimulate release of NO.

Effect of N^G-nitro-L-arginine methyl ester on endothelin responses

The results in Figure 3 show that L-NAME alone caused a mean inhibition of blood flow of between 30 and 40% in

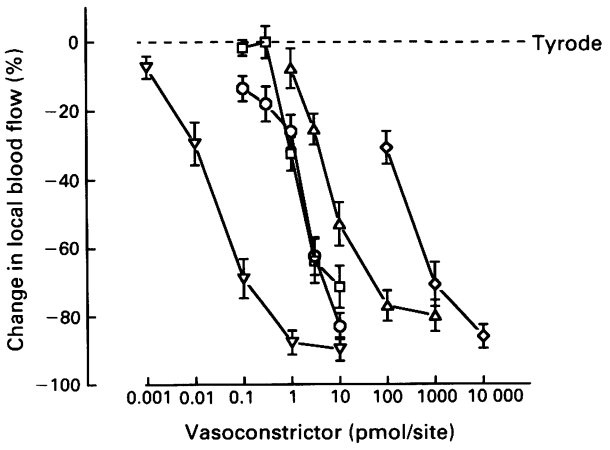

Figure 1 The effect of endothelins and other vasoconstrictors on blood flow in rat skin. Results are expressed as percentage change in local blood flow at test sites compared with at Tyrode solution-injected sites in the same rat. The dashed line represents blood flow at control sites injected with Tyrode solution alone. Responses to endothelin-1 (○), endothelin-2 (□), endothelin-3 (△), vasopressin (▽) and phenylephrine (◇) are shown. The results are expressed as the mean of 5–12 rats in each group; s.e.mean shown by vertical bars.

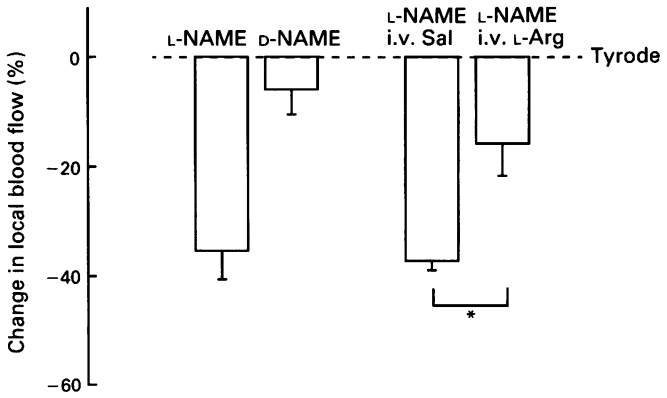

Figure 2 The effect of a nitric oxide synthase inhibitor on blood flow in rat skin. The first and second columns represent the response to N^G-nitro-L-arginine methyl ester (L-NAME, 100 nmol/site) and the enantiomer D-NAME (100 nmol/site) respectively. The third and fourth columns represent the effect of intradermal L-NAME (100 nmol/site) following a 1 min pretreatment with either intravenous saline (Sal) or L-arginine (L-Arg, 600 µmol kg^{-1}). A significant effect of L-arginine on the action of L-NAME is shown by $*P<0.05$. The dashed line represents blood flow at control sites injected with Tyrode solution alone. Each column is the mean from 6–8 rats; s.e.mean shown by vertical bars.

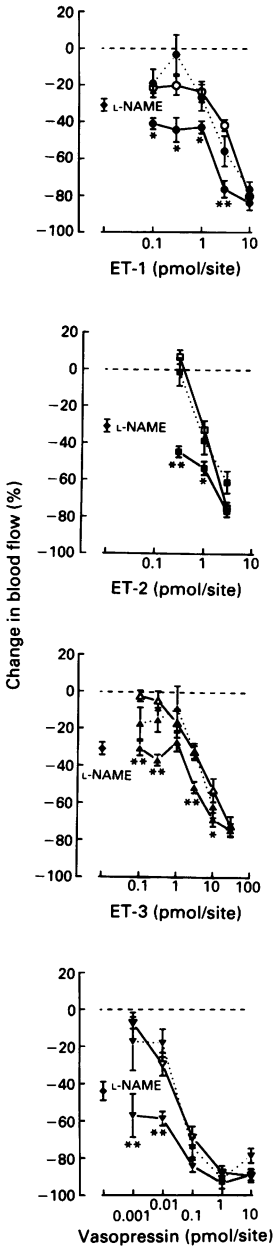

Figure 3 The effect of N^G-nitro-L-arginine methyl ester (L-NAME) on the vasoconstrictor responses induced by endothelins and vasopressin in rat skin. The change in blood flow when each was injected alone is shown by the open symbols and when co-injected with L-NAME (10 nmol/site) by the closed symbols. The solid line indicates results expressed as % change compared with Tyrode injected sites and the dotted line indicates results recalculated as percentage change in blood flow compared with sites which received L-NAME alone. The response to L-NAME (100 nmol/site) injected alone is indicated by (◆) in each group. A significant effect of L-NAME on the action of the vasoconstrictors when compared with Tyrode-injected sites is indicated as follows: $*P<0.05$; $**P<0.01$. The dashed line in each graph represents blood flow at Tyrode-injected sites. Each point is the mean of 3–18 rats with vertical bars showing s.e.mean.

each case, compared with Tyrode-injected sites. L-NAME enhanced the vasoconstrictor effects of submaximal doses of all the endothelins and vasopressin as shown in Figure 3, when all results were calculated by comparison with Tyrode-injected sites. Similar results were obtained with phenylephrine (not shown). We wanted to determine whether the effect of L-NAME was due to the vasoconstrictors stimulating NO release. Therefore, to attempt this, results were recalculated so that the decrease in blood flow induced by the vasoconstrictors in the presence of L-NAME was compared with that at sites injected with L-NAME alone (Figure 3). When the results are expressed in this way it is clear that the dose-response curves to ET-1 in the presence and absence of L-NAME coincide almost exactly, suggesting that ET-1 does not stimulate release of NO. The same lack of additional vasoconstriction by L-NAME can be seen for ET-2, ET-3 and vasopressin (Figure 3), also for phenylephrine (not shown).

Effect of pretreatment with high doses of endothelin-1 on subsequent effect of N^G-nitro-L-arginine methyl ester on blood flow

The laser Doppler blood flow meter was used to measure blood cell flux just before injection of either Tyrode solution or ET-1 (10 pmol/site) and at 3, 15 and 30 min, and then every 30 min until 4.5 h after the injection. The results shown in Figure 4 demonstrate that a high dose of ET-1 (10 pmol/site) caused a reduction in blood flow which was significantly different from that at Tyrode-injected sites ($P<0.05$) for 3 h after injections.

Having established that the vasoconstriction induced by ET-1 is so long-lasting, we designed experiments to determine whether NO could still be released in dilator quantities from the skin following long term constriction by a high dose of ET-1. The results in Figure 5 show that ET-1 (10 pmol/site) still caused a significant vasoconstriction at sites where blood flow was measured for 15 min by ^{133}xenon clearance after a 3.5 h pretreatment with a constricting dose of ET-1. L-NAME potentiated this vasoconstrictor response suggesting that the local generation of vasodilator quantities of NO still occurs after prolonged and intense constriction of the cutaneous microvasculature.

Discussion

The results clearly show that ET-1, ET-2 and ET-3 are potent vasoconstrictors in the cutaneous microvasculature, acting to inhibit unstimulated blood flow in rat skin. The techniques used in the present study do not allow accurate localization of the endothelin binding sites within the cutaneous microvasculature. However, our previous studies using intravital microscopy in the hamster check pouch

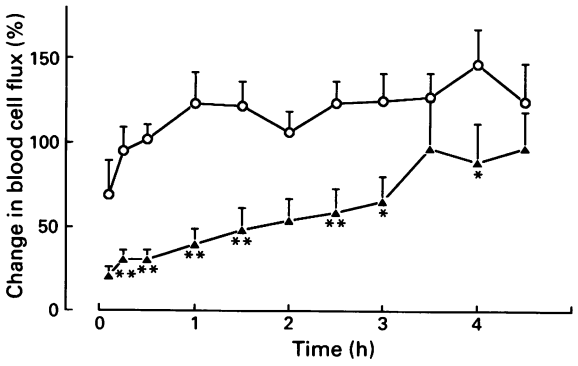

Figure 4 The duration of the vasoconstrictor response to endothelin-1 (ET-1) in rat skin measured by the laser Doppler blood flow meter. Either ET-1 (10 pmol/site, ▲) or the vehicle Tyrode solution (○) was injected at time 0 h. Measurements were initially taken at 3, 15 and 30 min after the injections and then at 30 min intervals for the next 4.5 h. The results are expressed as the percentage change in blood cell flux compared with the initial flux at the uninjected sites (100%), and as the mean of 3 readings at each site and time point in 4 rats; s.e.mean shown by vertical bars. A significant difference from Tyrode-injected sites is indicated by $*P<0.05$ and $**P<0.01$.

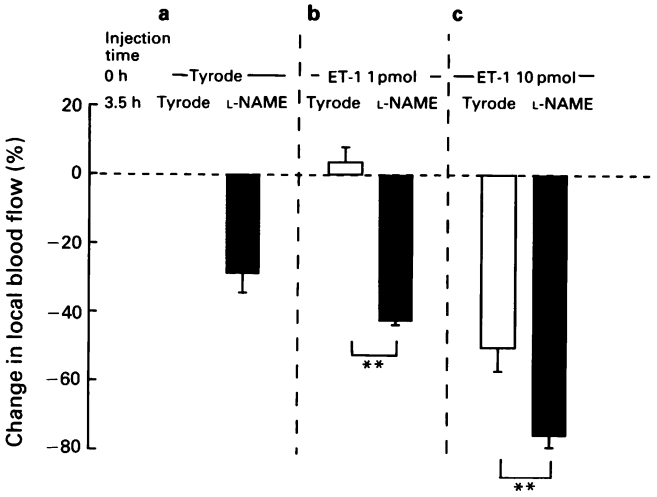

Figure 5 The effect of N^G-nitro-L-arginine methyl ester (L-NAME) on blood flow at sites preconstricted by endothelin-1 (ET-1). Sites were pretreated with Tyrode solution (a), ET-1 (1 pmol/site, b) or ET-1 (10 pmol/site, c); 3.5 h later the ^{133}xenon was mixed with either Tyrode solution (open column) or L-NAME (100 nmol/site, solid columns) and injected as normal. A significant difference between the response to Tyrode and to L-NAME preinjection is indicated by $^{**}P < 0.01$. The horizontal dashed line represents the blood flow at Tyrode-injected sites. Each column is the mean of 6 rats; s.e.mean shown by vertical bars.

established that ET-1, applied topically, has a direct and selective effect on arterioles (Brain, 1989). Subsequent studies suggest that larger venules are equally sensitive to ET-1 in the same preparation (Boric *et al.*, 1990). Autoradiographical studies in porcine skin have shown that ET-1 binding sites are located on both arterioles and venules, (Zhao *et al.*, 1991) further supporting the findings that both types of microvessel are responsive to ET-1.

In the present study, ET-1 is equipotent with ET-2 as a vasoconstrictor, whereas ET-3 is significantly less potent. This rank order of vasoconstrictor potency is in accordance with that observed on isolated macrovessels, (Inoue *et al.*, 1989), and may be due to different selectivities of the endothelin receptor subtypes. Two endothelin receptor subtypes have been cloned to date. One receptor has been located in many vascular and non-vascular tissues and has a high selectivity for ET-1 (Arai *et al.*, 1990). The other subtype binds with similar affinities to all the endothelins and is not located on vascular smooth muscle cells, (Sakurai *et al.*, 1990). It has been suggested that this is the endothelial cell receptor responsible for endothelin-induced release of vasodilators in some tissues. In the present study, intradermal injections of endothelins, including ET-3, induced only vasoconstriction in rat skin and no vasodilatation was observed, even at very low doses. This is in contrast to the studies which showed that low doses of the endothelins, ET-3 in particular, when administered intravascularly to rats induce an initial hypotensive response and regional increases in perfusion (Yanagisawa *et al.*, 1988a; Wright & Fozard 1988; Inoue *et al.*, 1989; Gardiner *et al.*, 1990a). The route of administration may well be an important factor for the mediation of vasodilator effects in response to the endothelins. In the cerebral microvasculature, systemic treatment of rats with low doses of ET-1 induced an increase in cortical microvascular perfusion (Willette *et al.*, 1990) while intraparenchymal application induced a dose-related decrease in perfusion, with a transient increase at only the highest dose of ET-1 (Willette & Sauermelch, 1990). These authors concluded that ET-1 mediates vasoconstriction at the adventitia while any vasodilatation is mediated by an intraluminal action. Our results, obtained by the intradermal injection of endothelin, support this concept. Further, a recent study by Ohlstein and co-workers (1990) has shown that intra-arterial administration of ET-1 increased hindquarters blood flow in the rat without causing a significant increase in cutaneous microvascular perfusion as measured by laser Doppler blood flowmetery. In human skin, intradermal ET-1 produces pallor, due to decreased blood flow at the injection site, accompanied by a surrounding axon-reflex flare. It is suggested that in human skin ET-1 could directly activate C-fibre nerves, (Crossman *et al.*, 1991); however, from the present study we have no evidence of a neurogenic component in the response to any endothelin in rat skin.

We consider that intradermal injection of vasoactive agents mimics the action of locally produced endothelins in skin more closely than the systemic administration of the endothelins. The obvious source of endogenous ET-1 is endothelial cells, and the precursor preproendothelin-1 is expressed in cultured microvascular endothelial cells, (MacCumber *et al.*, 1989); however, ET-2 and ET-3 are not derived from endothelial cells (Inoue *et al.*, 1989). The best evidence of a source for ET-2 and ET-3 comes from studies carried out with nervous tissue (MacCumber *et al.*, 1989; Shinmi *et al.*, 1989). It has been shown that endothelins, and related molecules are found in the brain and dorsal root ganglia in man (Giaid *et al.*, 1989) as well as in animal species including the rat (Matsumoto *et al.*, 1989). Thus, it is possible that endothelins are released from extravascular sites in skin.

Our results demonstrate that L-NAME, an inhibitor of NO synthase, given intradermally reduces blood flow in the rat cutaneous microcirculation. This supports previous results in rat skin (Hughes *et al.*, 1990). Thus, local constitutive release of NO may play an important role in maintaining microvascular blood flow in rat skin. The vasoconstriction to L-NAME is consistent with findings of a recent study on the regional haemodynamic effects of intravenous L-NAME in conscious rats, (Gardiner *et al.*, 1990b), where similar vasoconstriction to L-NAME occurred in the mesenteric and hindquarters vascular beds and at a higher dose in the renal vascular bed. Our results suggest a continuous release of NO occurs at rest in rat skin; also that this basal level of NO acts to antagonize in a functional manner the constrictor actions of endothelins, phenylephrine and vasopressin.

These studies provide no evidence that ET-1, ET-2 and ET-3 act to stimulate additional NO release. Agents which are known to stimulate NO release in major blood vessels are weak vasodilators in rat skin, e.g. acetylcholine (Lawrence & Brain, unpublished observation) and substance P (Brain & Williams, 1989). Thus, although it is suggested that the constitutive release of NO is important in skin, it is unknown whether further NO release can be stimulated.

In conclusion, we have shown that the endothelins are potent constrictors in rat skin. Basal release of NO could have an important role maintaining basal blood flow as well as opposing the vasoconstrictor effects of endothelins. We suggest that in conditions where damage to, or loss of endothelial cells, leads to a reduced generation of nitric oxide in the periphery, vasoconstrictors such as endothelin can act to cause a potentially damaging decrease in blood flow.

E.L. is the recipient of a British Heart Foundation Ph.D. studentship.

References

ARAI, H., HORI, S., ARAMORI, I., OHKUBO, H. & NAKANISHI, S. (1990). Cloning and expression of a cDNA encoding an endothelin receptor. *Nature*, **348**, 730–732.

BORIC, M.P., DONOSO, V., FOURNIER, A., ST. PIERRE, S. & HUIDOBRO-TORO, J.P. (1990). Endothelin reduces microvascular blood flow by acting on arterioles and venules of the hamster cheek pouch. *Eur. J. Pharmacol.*, **190**, 123–133.

BRAIN, S.D. (1989). The direct observation of arteriolar constriction induced by endothelin in vivo. *Eur. J. Pharmacol.*, **160**, 401–403.

BRAIN, S.D., CROSSMAN, D.C., BUCKLEY, T.L. & WILLIAMS, T.J. (1989). Endothelin-1: demonstration of potent effects on the microcirculation of humans and other species. *J. Cardiovasc. Pharmacol.*, **13** (Suppl 5), S147–S149.

BRAIN, S.D., TIPPINS, J.R. & WILLIAMS, T.J. (1988). Endothelin induces potent microvascular constriction. *Br. J. Pharmacol.*, **95**, 1005–1007.

BRAIN, S.D. & WILLIAMS, T.J. (1989). Interactions between the tachykinins and calcitonin gene-related peptide lead to the modulation of oedema formation and blood flow in rat skin. *Br. J. Pharmacol.*, **97**, 77–82.

CROSSMAN, D.C., BRAIN, S.D. & FULLER, R.W. (1991). Potent vasoactive properties of endothelin in human skin. *J. Appl. Physiol.*, **70**, 260–266.

DE NUCCI, G., THOMAS, R., D'ORLEANS-JUSTE, P., ANTUNES, E., WALDER, C., WARNER, T. & VANE, J.R. (1988). Pressor effects of circulating endothelin are limited by its removal in the pulmonary circulation and by the release of prostacyclin and endothelium-derived relaxing factor. *Proc. Natl. Acad. Sci. U.S.A.*, **85**, 9797–9800.

FORTES, Z.B., DE NUCCI, G. & GARCIA-LEME, J. (1989). Effect of endothelin-1 on arterioles and venules in vivo. *J. Cardiovasc. Pharmacol.*, **13** (Suppl 5), S200–S201.

GARDINER, S.M., COMPTON, A.M. & BENNETT, T. (1990a). Effects of indomethacin on the regional haemodynamic responses to low doses of endothelins and safarotoxin. *Br J. Pharmacol.*, **100**, 158–162.

GARDINER, S.M., COMPTON, A.M., KEMP, P.A. & BENNETT, T. (1990b). Regional and cardiac haemodynamic effects of N^G-nitro-L-arginine methyl ester in conscious Long Evans rats. *Br. J. Pharmacol.*, **101**, 625–631.

GIAID, A., GIBSON, S.J., IBRAHIM, N.B.N., LEGON, S., BLOOM, S.R., YANAGISAWA, M., MASAKI, T., VARNDELL, I.M. & POLAK, J.M. (1989). Endothelin-1, and endothelium-derived peptide, is expressed in neurons of the human spinal cord and dorsal root ganglia. *Proc. Natl. Acad. Sci. U.S.A.*, **86**, 7634–7638.

HUGHES, S.R., WILLIAMS, T.J. & BRAIN, S.D. (1990). Evidence that endogenous nitric oxide modulates oedema formation induced by substance P. *Eur. J. Pharmacol.*, **191**, 481–484.

INOUE, A., YANAGISAWA, M., KIMURA, S., KASUYA, Y., MIYAUCHI, T., GOTO, K. & MASAKI, T. (1989). The human endothelin family: three structurally and pharmacologically distinct isopeptides predicted by three separate genes. *Proc. Natl. Acad. Sci. U.S.A.*, **86**, 2863–2867.

LAWRENCE, E. & BRAIN, S.D. (1991). Evidence that locally-generated nitric oxide has a modulatory role in the control of microvascular blood flow in rat dorsal skin. *Br. J. Pharmacol.*, **102**, 323P.

MACCUMBER, M.W., ROSS, C., GLASER, B.M. & SNYDER, S.H. (1989). Endothelin: visualization of mRNAs by in situ hybridization provides evidence for local action. *Proc. Natl. Acad. Sci. U.S.A.*, **86**, 7285–7289.

MATSUMOTO, H., SUZUKI, N., ONDA, G. & FUJINO, M. (1989). Abundance of endothelin-3 in rat intestine, pituitary gland and brain. *Biochem. Biophys. Res. Commun.*, **164**, 74–80.

MOORE, P.K., AL-SWAYEH, O.A., CHONG, N.W.S., EVANS, R.A. & GIBSON, A. (1990). L-N^G-nitro arginine (L-NOARG), a novel L-arginine-reversible inhibitor of endothelium-dependent vasodilatation *in vitro*. *Br. J. Pharmacol.*, **99**, 408–412.

OHLSTEIN, E.H., VICKERY, L., SAUERMELCH, C. & WILLETTE, R.N. (1990). Vasodilatation induced by endothelin: role of EDRF and prostanoids in rat hindquarters. *Am. J. Physiol.*, **259**, H1835–H1841.

PALMER, R.M.J., FERRIGE, A.G. & MONCADA, S. (1987). Nitric oxide release accounts for the biological activity of endothelium-derived relaxing factor. *Nature*, **327**, 524–526.

PALMER, R.M.J., ASHTON, D.S. & MONCADA, S. (1988). Vascular endothelial cells synthesise nitric oxide from L-arginine. *Nature*, **333**, 664–666.

RAKUGI, H., NAKAMARU, M., TABUCHI, Y,. NAGANO, M., MIKAMI, H. & OGIHARA, T. (1989). Endothelin stimulates the release of prostacyclin from rat mesenteric arteries. *Biochem. Biophys. Res. Commun.*, **160**, 924–928.

REES, D.D., PALMER, R.M.J., MONCADA, S. (1989). Role of endothelium-derived nitric oxide in the regulation of blood pressure. *Proc. Natl. Acad. Sci. U.S.A.*, **86**, 3375–3378.

SAKURAI, T., YANAGISAWA, M., TAKUWA, Y., MIYAZAKI, H., KIMURA, S., GOTO, K. & MASAKI, T. (1990). Cloning of a cDNA encoding a non-isopeptide-selective subtype of the endothelin receptor. *Nature*, **348**, 732–735.

SHINMI, O., KUMURA, S., SAWAMURA, T., SUGITA, Y., YOSHIZAWA, T., UCHIYAMA, Y., YANAGISAWA, M., GOTO, K., MASAKI, T. & KANAZAWA, I. (1989). Endothelin-3 is a novel neuropeptide: isolation and sequence determination of ET-1 and ET-3 in porcine brain. *Biochem. Biophys. Res. Commun.*, **164**, 587–593.

WARNER, T.D., DE NUCCI, G. & VANE, J.R. (1989). Rat endothelin is a vasodilator in the isolated perfused mesentery of the rat. *Eur. J. Pharmacol.*, **159**, 325–326.

WHITTLE, B.J.R., LOPEZ-BELMONTE, J. & MONCADA, S. (1990). Regulation of gastric mucosal integrity by endogenous nitric oxide: interactions with prostanoids and sensory neuropeptides in the rat. *Br. J. Pharmacol.*, **99**, 607–611.

WILLETTE, R.N. & SAUERMELCH, C.F. (1990). Abluminal effects of endothelin in cerebral microvasculature assessed by laser-Doppler flowmetry. *Am. J. Physiol.*, **259**, H1688–H1693.

WILLETTE, R.N., SAUERMELCH, C.F., EZEKIEL, M., FEUERSTEIN, G. & OHLSTEIN, E.H. (1990). Effect of endothelin on cortical microvascular perfusion in rats. *Stroke*, **21**, 451–458.

WILLIAMS, T.J. (1976). Simultaneous measurement of local plasma exudation and blood flow changes induced by intradermal injection of vasoactive substances, using [^{131}I]albumen and ^{133}Xe. *J. Physiol.*, **254**, 4–5P.

WILLIAMS, T.J. (1979). Prostaglandin E_2, prostaglandin I_2 and the vascular changes in inflammation. *Br. J. Pharmacol.*, **65**, 517–524.

WRIGHT, C.E. & FOZARD, J.R. (1988). Regional vasodilatation is a prominent feature of the haemodynamic response to endothelin in anaesthetized, spontaneously hypertensive rats. *Eur. J. Pharmacol.*, **155**, 201–203.

YANAGISAWA, M., INOUE, A., ISHIKAWA, T., KASUYA, Y., KIMURA, S., KUMAGAYE, S.I., NAKAJIMA, K., WATANABE, T.X., SAKAKIBARA, S., GOTO, K. & MASAKI, T. (1988a). Primary structure, synthesis and biological activity of rat endothelin, an endothelium-derived vasoconstrictor peptide. *Proc. Natl. Acad. Sci. U.S.A.*, **85**, 6964–6967.

YANAGISAWA, M., KIRIHARA, H., KIMURU, S., TOMOBE, Y., KOBAYASHI, M., MITSUI, Y., YAZAKI, Y., GOTO, K. & MASAKI, T. (1988b). A novel potent vasoconstrictor peptide produced by vascular endothelial cells. *Nature*, **332**, 411–415.

ZHAO, Y.D., SPRINGALL, D.R., WHARTON, J. & POLAK, J.M. (1991). Autoradiographic localization of endothelin-1 binding sites in porcine skin. *J. Invest. Dermatol.*, **96**, 152–154.

(Received November 18, 1991
Revised March 6, 1992
Accepted March 20, 1992)

Br. J. Pharmacol. (1992), **106**, 739–745

Effect of 17β-oestradiol on contraction, Ca^{2+} current and intracellular free Ca^{2+} in guinea-pig isolated cardiac myocytes

Canwen Jiang, Philip A. Poole-Wilson, *Philip M. Sarrel, Seibu Mochizuki, Peter Collins & [1]Kenneth T. MacLeod

Department of Cardiac Medicine, National Heart and Lung Institute, Dovehouse Street, London SW3 6LY and *Department of Obstetrics, Gynecology and Psychiatry, Yale University School of Medicine, 333 Cedar Street, New Haven, CT 06510, U.S.A.

1 The effect of 17β-oestradiol on cardiac cell contraction, inward Ca^{2+} current and intracellular free Ca^{2+} ([free Ca^{2+}]$_i$) was investigated in guinea-pig single, isolated ventricular myocytes. The changes of cell length were measured by use of a photodiode array, the voltage-clamp experiments were performed with a switch clamp system and [free Ca^{2+}]$_i$ was measured with the Ca^{2+} indicator, Fura-2.

2 17β-Oestradiol (10, 30 μM) caused a decrease in cell shortening at both 22 and 35°C. This negative inotropic effect was accompanied by a decrease in action potential duration mainly brought about by a shortening of the plateau region of the action potential. 17β-Oestradiol (10, 30 μM) induced a similar decrease in cell shortening in voltage-clamped and current-clamped cells.

3 In Fura-2 loaded cells, 17β-oestradiol (10 and 30 μM) decreased systolic Fura-2 fluorescence to 72 ± 7% and 47 ± 4% ($n = 6$, $P < 0.001$) of control respectively. 17β-Oestradiol (10 μM) had no significant effect on diastolic Fura-2 fluorescence, but at higher concentration (30 μM) induced a slight decrease in resting Fura-2 fluorescence. The effect of 17β-oestradiol was reversible after 1–2 min of washout of the steroid.

4 17β-Oestradiol (10 and 30 μM) decreased the peak inward Ca^{2+} current (I_{Ca}), which was sensitive to $[Ca^{2+}]_o$, dihydropyridines and isoprenaline, to 59 ± 3% and 39 ± 5% ($n = 7 \sim 9$, $P < 0.01$) respectively, without producing any significant change in the shape of the current-voltage relationship.

5 The recovery time of I_{Ca} from inactivation was delayed by 17β-oestradiol (10 μM). The inhibitory effect of 17β-oestradiol on I_{Ca} was less at a holding potential of −80 mV than at −40 mV.

6 We conclude that 17β-oestradiol has a negative inotropic effect on guinea-pig single ventricular myocytes by inhibiting I_{Ca} and so reducing systolic $[Ca^{2+}]_i$. 17β-Oestradiol may therefore have a Ca^{2+} channel blocking property in guinea-pig isolated ventricular myocytes.

Keywords: Calcium current; intracellular free calcium; Fura-2; 17β-oestradiol; hormone; cardiac muscle

Introduction

The direct effects of oestrogen on heart muscle are largely unknown though there are oestrogen receptors present in the tissue (Stumpf *et al.*, 1977). Recently, it has been demonstrated that at micromolar concentrations, 17β-oestradiol decreases the contraction of perfused rabbit hearts (Raddino *et al.*, 1986), but the mechanism was not understood. It was uncertain whether this effect was due to alterations in the contractility of the myocardium or in the coronary circulation. In order to investigate the mechanism underlying the effects of those concentrations of 17β-oestradiol on cardiac muscle, we have assessed the *in vitro* effect of 17β-oestradiol on contraction, Ca^{2+} current (I_{Ca}) and intracellular free Ca^{2+} ([free Ca^{2+}]$_i$) in single ventricular myocytes isolated from guinea-pig hearts. Thus, we can observe changes at the single cell level, independent of any effect of coronary circulation.

Methods

Preparation of guinea-pig ventricular myocytes

Single ventricular myocytes from male guinea-pigs (450–600 g) were prepared by enzymatic dissociation as previously described (MacLeod & Harding, 1991). Briefly, animals were heparinised and after killing by cervical dislocation, the heart was rapidly removed and placed in Krebs-Henseleit solution (composition see below). The aorta was cannulated and the heart retrogradely perfused on a Langendorff apparatus with fresh Krebs-Henseleit solution, then with low-Ca^{2+} ($Ca^{2+} \approx 12$ μM) Tyrode solution (composition see below). Protease (4 u ml^{-1}, Sigma type) XXIV and then a mixture of 1.0 mg ml^{-1} collagenase (Worthington) and 1.0 mg ml^{-1} hyaluronidase (Sigma) was added to the low-Ca^{2+} Tyrode solution and perfused through the heart for 2 and 10 min respectively. The ventricular muscle was chopped and incubated for two periods of 5 min in fresh low-Ca^{2+} Tyrode solution containing enzymes (for the second period of digestion, free Ca^{2+} was increased to ≈200 μM and nitrolotriacetic acid (NTA, Sigma) was absent). The medium was shaken gently and the dispersed cells were then strained through a gauze and centrifuged. The pellet was resuspended and stored in Dulbecco's medium (Gibco) buffered with hydroxyethylpipirazine-ethanesulphonic acid (HEPES) at room temperature.

Solutions

The Krebs-Henseleit solution contained (mM): NaCl 119; KCl 4.2, $CaCl_2$ 1.0, $MgSO_4$ 0.9, KH_2PO_4 1.2, $NaHCO_3$ 25 and glucose 11.5, and was vigorously bubbled with 95% O_2 and 5% CO_2 to obtain a pH = 7.4 at room temperature. Low-Ca^{2+} Tyrode solution contained (mM): NaCl 120, KCl 5.4, $MgSO_4$ 5.0, pyruvate (Sigma) 5, glucose 20, taurine (Sigma) 20, HEPES 10; NTA 5 and free $Ca^{2+} \approx 12$ μM.

[1] Author for correspondence.

Normal Tyrode solution contained (mM): NaCl 140, KCl 6, $CaCl_2$ 1 or 2.5, $MgCl_2$ 1, HEPES 10, glucose 10, pH = 7.4 at 22°C or 35°C. 17β-Oestradiol was dissolved in ethanol to give a stock solution of 10^{-2} M. Ethanol (1:2000 v/v) was usually added to Normal Tyrode for control purposes.

Potential and current recording

Myocytes were placed in a perspex superfusion chamber (volume = 60 μl), mounted on the stage of an epifluorescence microscope (Nikon Diaphot). Solutions were carried to the chamber via gas-impermeable tubing. Cells were superfused (1.5 ml min^{-1}) with either Normal Tyrode at room temperature (about 22°C) or 35°C. The exchange of solution in the superfusion chamber was complete within 20 s. Microelectrodes were filled with either 3 M KCl or 2.1 M K-citrate plus 60 mM KCl and had resistances from 10–25 MΩ. No differences in effects of 17β-oestradiol were observed with different filling solutions. Action potentials were recorded with an Axoclamp-2A system (Axon Instruments, Foster City, California, U.S.A.) and were elicited by passing a pulse of current up to 1 nA for 10 ms in duration down the microelectrodes at 0.5 Hz or 1 Hz. Action potential duration (APD) was measured at 90% repolarization with a circuit described by Kentish & Boyett (1983). Voltage-clamp experiments were performed with the Axoclamp-2A in switch-clamp mode (discontinuous single microelectrode voltage-clamp), switching at 5–8 kHz at gains $\geqslant$ 1 nA mV^{-1}. Voltage-clamp software for data acquisition, analysis and control was kindly provided by John Dempster, University of Strathclyde.

Cell length and Fura-2 measurements

The methods for recording cell length and changes in [free $Ca^{2+}]_i$ with Fura-2 have been described previously (MacLeod & Harding, 1991). Briefly, cells were loaded with Fura-2 using the acetoxymethyl ester form of the indicator (Fura-2 AM; Molecular Probes, Eugene, Oregon, U.S.A.). After 20 min incubation in 5 μM Fura-2 AM at 22°C, the cells were pelleted and resuspended in fresh Dulbeccos.

Effect of 17β-oestradiol on cell contraction, action potentials and [free $Ca^{2+}]_i$

Cell shortening, action potentials and APD were continually recorded in current-clamped conditions either at 22°C or 35°C. Normal Tyrode solution containing 1 mM Ca^{2+} was used in these experiments. The effects of 17β-oestradiol were studied in a non-cumulative manner. 17β-Oestradiol was washed out after a stable maximum effect was achieved at any one concentration. This usually took 2 min. Different concentrations of 17β-oestradiol were added after action potentials returned to control conditions 3–5 min after washout. Some cells were loaded with Fura-2 and the fluorescence ratio (340 mm/380 mm), action potentials and APD were continually recorded in control or in the presence of 17β-oestradiol at 22°C. The effects of testosterone (10 and 30 μM) on action potentials were performed in a similar manner.

Effect of 17β-oestradiol on I_{Ca}

Voltage-clamp experiments were carried out at 22°C. In different groups of cells, different voltage-clamp protocols were used to investigate the possible effects of 17β-oestradiol on I_{Ca}, the recovery time of I_{Ca} from inactivation and the voltage-dependency of the inhibitory effect of the hormone. The individual protocol was applied to cells in control conditions, 2 min after application and washout of 17β-oestradiol respectively.

Drugs

The following drugs and chemicals were used: 17β-oestradiol (Sigma or Fluka, dissolved in ethanol); testosterone (Sigma, dissolved in ethanol).

Statistical analysis

Data are expressed as mean ± standard error of mean (s.e.mean). Unpaired or paired Student's t tests were used to analyse the data. A probability value (P) less than 0.05 was considered significant.

Results

Effect of 17β-oestradiol on cell contraction

Figure 1 demonstrates the effect of 17β-oestradiol on cell contraction in current-clamped or voltage-clamped conditions at 22°C. The top trace of panel (a) shows that addition of 17β-oestradiol (30 μM) decreased cell shortening after 1 min in the current-clamped condition. The resting membrane potential was −86 mV. The effect was reversible after 1 min washout. We noted that the negative inotropic effect was accompanied by a decrease in APD mainly due to a shortening of the plateau of the action potential. The same cell was then voltage-clamped at −80 mV. The effect of

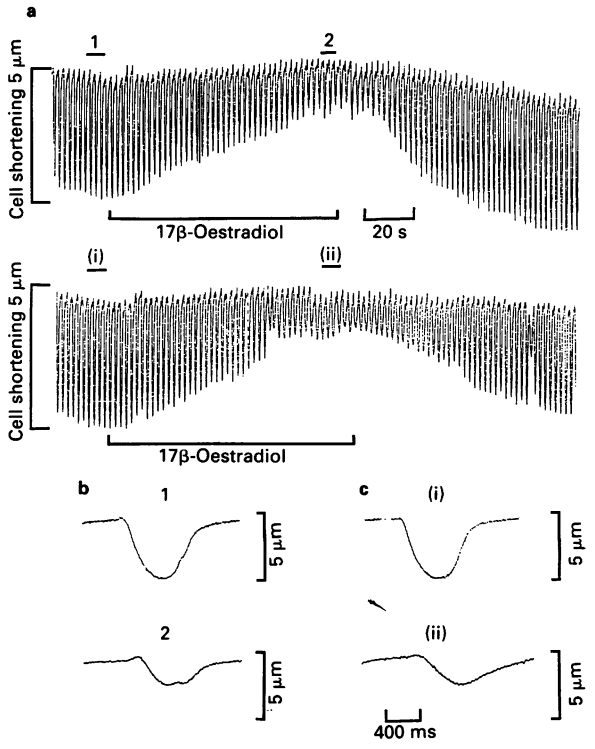

Figure 1 Effect of 17β-oestradiol (30 μM) on cell shortening. Top trace of (a) shows the time course over which 17β-oestradiol induced a reversible negative inotropic effect in a current-clamped cell. The resting potential was −86 mV. The bottom trace of (a) shows the effect 17β-oestradiol (30 μM) on cell shortening in the same cell now voltage clamped at −80 mV. Twitches were elicited by depolarizing voltage steps for 400 ms to 0 mV. These were applied at 0.5 Hz. (b) Shows the changes in cell shortening taken from parts 1 (before application of 17β-oestradiol) and 2 (in the presence of 17β-oestradiol) of the top trace respectively at a faster chart speed. These traces have been signal averaged to reduce noise (n = 8). In (c), the changes of cell shortening taken from parts (i) (before application of 17β-oestradiol) and (ii) (in the presence of 17β-oestradiol) respectively of the bottom trace of (a) are shown at a faster chart speed. These traces have also been signal averaged (n = 8).

17β-oestradiol (30 μM) on cell shortening, induced by a depolarizing step to 0 mV for 400 ms in duration, is shown in the bottom trace of Figure 1a. The time course and the magnitude of the effect of 17β-oestradiol on cell shortening was similar in current-clamped and voltage-clamped cells. 17β-Oestradiol (10, 30 μM) decreased cell shortening to 72 ± 6.2% and 56 ± 4.8% in current-clamped cells, and to 76 ± 7.5% and 59 ± 3.6% in voltage-clamped cells ($n \geqslant 6$) respectively. To assess the effects of 17β-oestradiol on cell shortening and action potentials at a more physiological temperature and higher stimulation frequency, we carried out experiments at 35°C with stimulation rate of 1 Hz. In these conditions, APD (584 ± 42 ms, $n = 6$) is much shorter than that at 22°C (795 ± 56 ms, $n = 10$) in the absence of 17β-oestradiol. At 35°C, 17β-oestradiol (10 and 30 μM) decreased cell shortening to 79 ± 5.4% and 63 ± 6.1% in current-clamped cells ($n = 6$), accompanied by a reduction in APD. Thus, the effects of 17β-oestradiol on cell shortening were similar at either temperature. In order to control for any possible effect of the solvent, ethanol (1:2000 v/v) was also present in the control solutions during this and subsequent experiments. In addition, testosterone (10 and 30 μM) had no effect on APD.

Effect of 17β-oestradiol on [free Ca^{2+}]$_i$

To understand the possible mechanism by which 17β-oestradiol induced a negative inotropic effect, we have examined the effect of 17β-oestradiol on [free Ca^{2+}]$_i$ as indicated by Fura-2. Because of the difficulties of the calibration of Fura-2 (Roe *et al.*, 1990), we have chosen to use the ratios of Fura-2 fluorescence as a qualitative indicator of changes in [free Ca^{2+}]$_i$ but not to quantify the absolute value of [free Ca^{2+}]$_i$. Figure 2a shows the time course over which 10 and 30 μM 17β-oestradiol decreased both the fluorescence ratio (340/380) and APD in a concentration-dependent manner without producing any signifcant effect on resting membrane potential. The decrease in both APD and Fura-2 fluorescence occurred within 1 min after the addition of 17β-oestradiol. The effects were reversible after washout. In Figure 2b, action potentials and Ca^{2+} transient taken from portions 1, 2 and 3 of Figure 2a trace are shown at faster chart speeds. These records have been signal averaged ($n = 8$). The decrease of Fura-2 fluorescence was accompanied by a reduction in APD. We note that 10 μM 17β-oestradiol had no effect on resting Fura-2 fluorescence, whilst 30 μM 17β-oestradiol slightly decreased the resting fluorescence. Figure 2c shows that 10 and 30 μM 17β-oestradiol decreased Fura-2 fluorescence ratio (340/380) to 72 ± 7% and 47 ± 4% ($P < 0.01$, $n = 6$) respectively. In order to compare the effects of 17β-oestradiol on Ca^{2+} transients with its action on I_{Ca} and APD, we carried out the experiments at 22°C. We noted that the time course over which the Ca^{2+} transient rose to a peak and then fell to diastolic levels was closely related to temperature. The Ca^{2+} transients at 22°C were greatly slowed in rise and fall compared with those at 35°C (data not shown).

Effect of 17β-oestradiol on I_{Ca}

The effect of 17β-oestradiol on I_{Ca} is shown in Figure 3. This I_{Ca} was typically increased by increasing extracellular Ca^{2+} concentration or in the presence of isoprenaline and decreased by addition of Co^{2+}, Cd^{2+} or nifedipine in cells from similar preparations (data not shown). In the experiments shown here, the initial holding potential was −40 mV to inactivate the fast inward sodium current. Depolarizing voltage steps of 200 ms in duration were applied to the cells at a frequency of 0.5 Hz. Figure 3a demonstrates that 10 and 30 μM 17β-oestradiol decreased I_{Ca} in a concentration-dependent manner. The maximal inhibition occurred within 2 min of application of 17β-oestradiol. Thus, the time course of effects induced by 17β-oestradiol on cell shortening, I_{Ca} and [free Ca^{2+}]$_i$ were similar. The inhibition of I_{Ca} was reversible

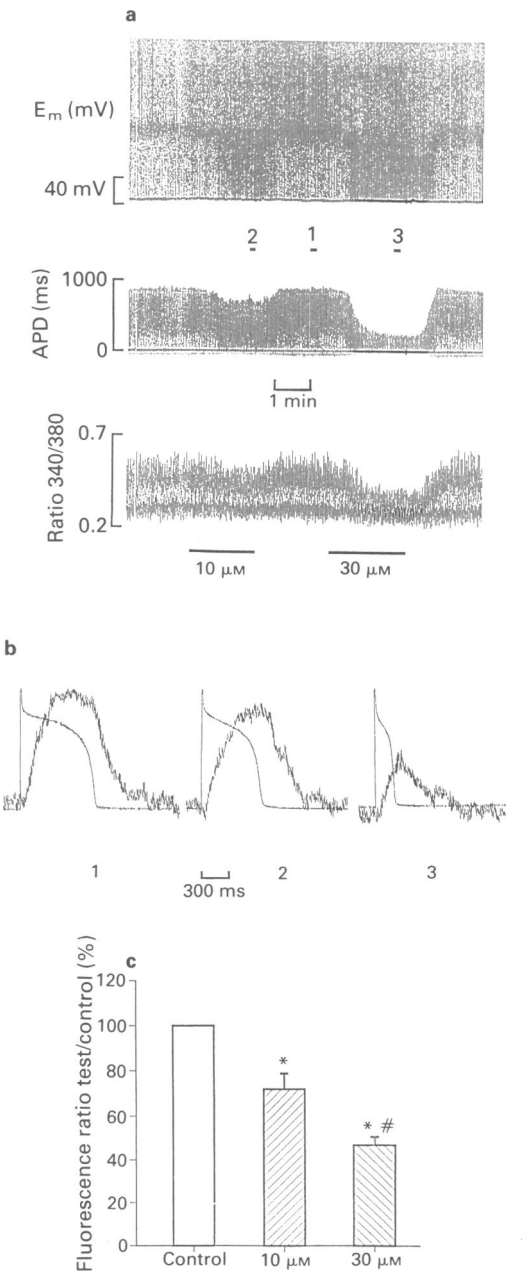

Figure 2 Effect of 17β-oestradiol (10 and 30 μM) on membrane potential (E_m), action potential duration (APD) and [free Ca^{2+}]$_i$ indicated by Fura-2. The fluorescence ratio was filtered at 10 Hz. (a) Shows the time course with which 17β-oestradiol induced a concentration-dependent and reversible decrease in systolic fluorescence ratio and APD. No significant alterations to resting membrane potential and diastolic fluorescence ratio were seen, although 17β-oestradiol at a concentration of 30 μM slightly decreased the diastolic fluorescence ratio; (b) shows specimen action potentials and fluorescence ratio transients taken from points 1 (control), 2 (in the prescence of 10 μM 17β-oestradiol) and 3 (in the presence of 30 μM 17β-oestradiol) in (a). These have been signal averaged ($n = 8$) and played at a faster chart speed. The vertical scale is increased by 85%. (c) Shows the average decreases in fluorescence ratio induced by 10 and 30 μM 17β-oestradiol in 6 cells. Data are expressed as mean (with s.e.mean, vertical bars) test/control. * indicates $P < 0.01$ in comparison with control; # indicates $P < 0.01$ in comparison between 10 and 30 μM 17β-oestradiol.

after 2 min washout indicating that the decrease is unlikely to be due to 'run-down' or use-dependence of I_{Ca} (Fedida *et al.*, 1988). We were able to hold this particular cell under voltage clamp for 1 h and over this time we did not see any decline in the size of I_{Ca}. In 84% of cells tested we did not see

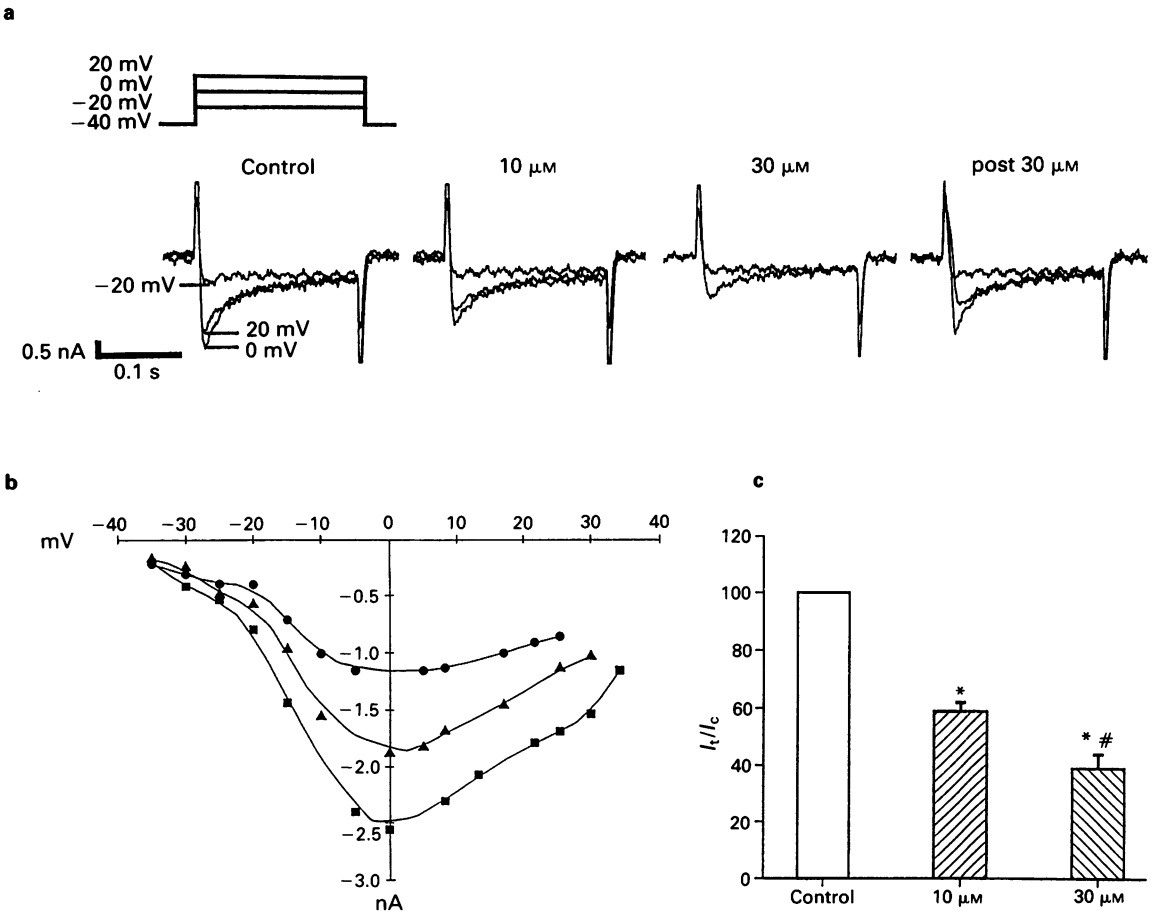

Figure 3 Effect of 17β-oestradiol on I_{Ca}: (a) shows I_{Ca} elicited by depolarizing voltage steps from a holding potential of −40 mV to −20, 0 and +20 mV in control and again 2 min after the addition of 17β-oestradiol (10 and 30 μM). 17β-Oestradiol induced a concentration-dependent decrease in I_{Ca}. Please note that I_{Ca} traces elicited by depolarizing steps to −20 mV and 20 mV are overlapped in the presence of 30 μM 17β-oestradiol. (b) Shows the current-voltage relationship in control (■) and in the presence of 17β-oestradiol (10 and 30 μM, ▲ and ● respectively) in the same cell of panel as in (a). (c) Shows the measured data in 7–9 cells. Data were expressed as mean with s.e.mean (vertical bars) of $I_{Test}/I_{Control}$. * indicates $P<0.01$ in comparison with control. # indicates $P<0.01$ in comparison between 10 and 30 μM 17β-oestradiol.

significant run-down of I_{Ca} after washout of the steroid. Figure 3b shows the current-voltage relationship in the absence and presence of 10 and 30 μM 17β-oestradiol. The shape of the relation is not significantly changed. Figure 3c demonstrates that I_{Ca} was decreased by 10 and 30 μM 17β-oestradiol to 59 ± 3% ($P<0.01$, $n=7$) and 39 ± 5% ($P<0.01$ compared with control and 10 μM, $n=9$) respectively. To ensure inactivation of the fast inward sodium current, we performed similar voltage-clamp experiments in the presence of tetrodotoxin (25 μM). In these experiments, 17β-oestradiol decreased I_{Ca} by the same percentage. In addition, testosterone (10 and 30 μM) had no effect on I_{Ca}.

In another group of experiments, we tested the effect of 17β-oestradiol on the recovery time of I_{Ca} from inactivation. The initial holding potential was −40 mV. A control depolarizing voltage step to 0 mV of 200 ms in duration was followed by an identical test step 100 ms later. The time between control and test steps was then increased in increments of 200 ms. Figure 4a shows that the recovery time of I_{Ca} was delayed by application of 10 μM 17β-oestradiol. 17β-Oestradiol (10 μM) shifted the relationship between the interpulse interval and I_{Ca} reactivation as shown in Figure 4b. At interpulse intervals of 300, 700 and 900 ms the values for test I_{Ca} (I_t) divided by control I_{Ca} (I_c) were significantly different ($P<0.02$, 0.05 and 0.01 respectively; $n=6$) in the presence of 10 μM 17β-oestradiol, whilst at the other interpulse intervals there was a trend of delay but no statistically significant differences. In order to increase the magnitude of the I_c and I_t 2.5 mM external Ca^{2+} was used in these experiments. When the inhibition of I_{Ca} by 17β-oestradiol was large we often had difficulty in calculating the value of I_t/I_c, so we have chosen experiments where the inhibition of I_{Ca} by 17β-oestradiol was small. We may therefore have underestimated the effect of 17β-oestradiol on the recovery of I_{Ca} from inactivation. The time of 63% of recovery for control cells was 403 ms (c.f. 300 ms measured by Hadley & Hume, 1987). This time increased to 730 ms in the presence of 10 μM 17β-oestradiol.

In 6 cells, the process of I_{Ca} inactivation during the clamp pulse (−40 mV to 0 mV and 200 ms in duration) was also analysed. The decay of I_{Ca} during the clamp step could be fitted by the following equation:

$$I_{Ca} = x \times \exp(-t/\tau) + y$$

where tau, τ = decay constant (ms), x = peak I_{Ca} (nA) and y = steady-state current at the end of the pulse (nA). τ = 36.3 ± 4.2, x = − 1.5 ± 0.5 and y = − 0.26 ± 0.08 in control and 48.2 ± 7.1, −0.68 ± 0.26 and −0.17 ± 0.07 respectively, in the presence of 17β-oestradiol (10 μM). 17β-Oestradiol (10 μM) increased τ by 31.3 ± 9.2% whilst x decreased by 54.4 ± 2.9%

We have also examined the voltage-dependency of the inhibitory effect of 17β-oestradiol on I_{Ca}. In this group of experiments, 10 μM 17β-oestradiol was applied to the preparation at a holding potential of −80 mV for 2 min. In

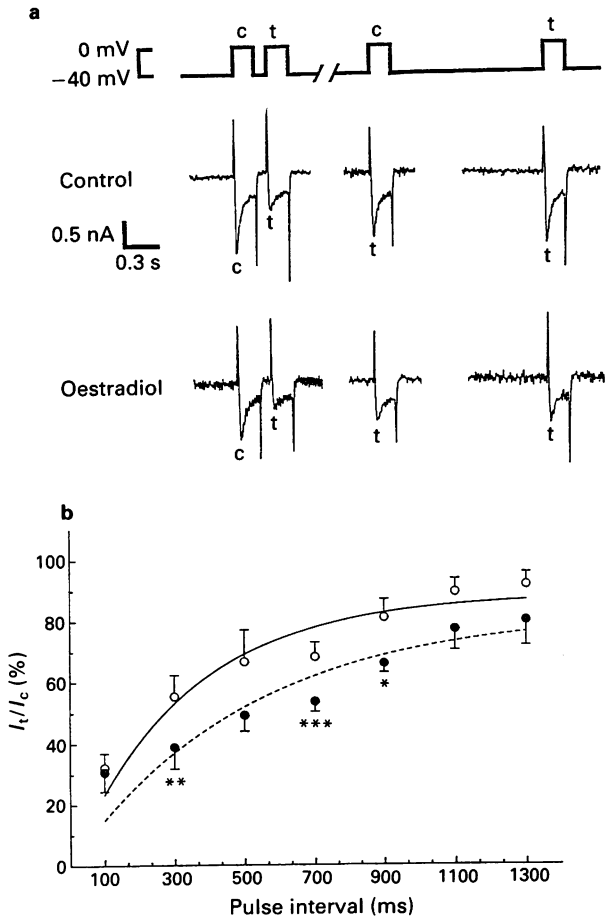

Figure 4 Effect of 17β-oestradiol (10 μM) on the recovery time of I_{Ca} from inactivation. Top trace of (a) shows the protocol. A control pulse (c) was followed by an identical test pulse (t) with an interpulse interval starting at 100 ms. The interpulse interval was increased in steps of 200 ms. The I_{Ca} induced by the test pulse and the control pulse (indicated as 'c' and 't' respectively) are shown in the other traces in (a). Note the tonic effect of 17β-oestradiol on I_c and its effect on I_t. (b) Shows the relationship between I_t/I_c (the I_{Ca} induced by the test pulse divided by the I_{Ca} induced by the control pulse) and interpulse interval in control (○) and in the presence of 10 μM 17β-oestradiol (●). Data were calculated from 6 cells and expressed as mean with s.e.mean of I_t/I_c. The curves were fitted to the equation $Y = A^*(1-X^{-k^*t})$, where A = 88.6 and k = 0.003 for control data (r = 0.825, ○) and A = 82.9 and k = 0.002 for 17β-oestradiol data ($r = 0.929$, ●). *, **, *** indicate a significant difference from control: $P<0.005$, 0.02, 0.01 respectively.

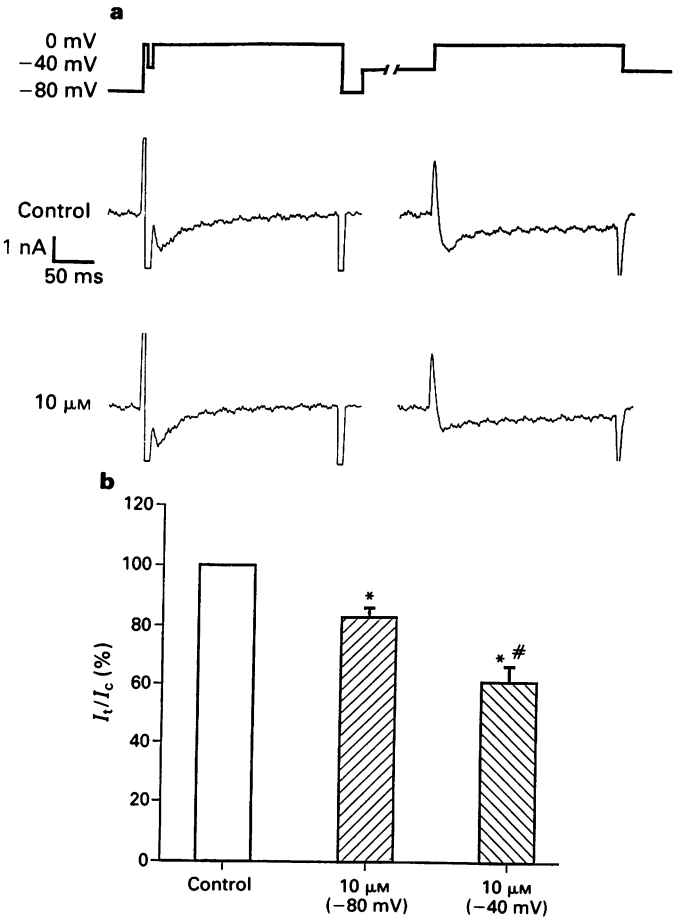

Figure 5 Effect of the initial holding potential on the inhibition of I_{Ca} induced by 10 μM 17β-oestradiol. The protocol is shown in the top trace of (a). After holding at −80 mV, a voltage step to 0 mV for 5 ms in duration was followed by a voltage step to −40 mV for 5 ms in duration. Then another voltage step to 0 mV for 200 ms was given to elicit the I_{Ca} in the absence or presence of 10 μM 17β-oestradiol. In the same cell, after 2 min holding at −40 mV, a voltage step of 200 ms in duration was repeated in the absence or presence of 10 μM 17β-oestradiol. From lower traces of (a) we see the different holding potentials did not significantly alter the control peak I_{Ca}. 17β-Oestradiol 10 μM, had little effect when the holding potential was −80 mV in this particular cell. (b) Shows the data calculated from 6 cells and expressed as mean with s.e.mean (vertical bars) percentage I_{Ca} in the control condition. Note that 17β-oestradiol (10 μM) induced a significant inhibition of I_{Ca} at either holding potential. However, 17β-oestradiol (10 μM) was less effective at a holding potential of −80 mV compared with its effects at −40 mV. * indicates $P<0.01$ in comparison with control; # indicates $P<0.01$, comparison between holding potentials of −80 mV and −40 mV.

order to inactivate fast inward sodium current, a depolarizing voltage step to 0 mV of 5 ms in duration was given. This was followed by another step of 5 ms in duration to −40 mV from where a depolarizing voltage step of 200 ms to 0 mV was applied to elicit I_{Ca}. The size of I_{Ca} so elicited was compared with that produced on a depolarizing step to 0 mV after 17β-oestradiol had been applied from 2 min at a holding potential of −40 mV. From Figure 5a, we noted that the initial holding potential did not significantly affect the size of I_{Ca} recorded using the above protocols in this particular cell. However, the effect of 17β-oestradiol on I_{Ca} was greater at the more depolarized holding potential of −40 mV. The statistical data from 6 cells are shown in Figure 5b. At a holding potential of −80 mV, 10 μM 17β-oestradiol significantly reduced I_{Ca} to 83 ± 3.1% of control. At a holding potential of −40 mV, however, the same concentration of 17β-oestradiol reduced I_{Ca} to 61 ± 5.4%. These results suggest that the inhibitory effect of 17β-oestradiol on I_{Ca} may be voltage-dependent.

Discussion

We have demonstrated that 17β-oestradiol induces a negative inotropic effect in guinea-pig single ventricular myocytes. 17β-Oestradiol inhibits I_{Ca} and decreases systolic [free Ca^{2+}]$_i$ in a concentration-dependent manner. 17β-Oestradiol delays the recovery time of I_{Ca} from inactivation and its inhibition of I_{Ca} appears to be voltage-dependent. In addition, testosterone had no effect on APD and I_{Ca}.

Effect of 17β-oestradiol on I_{Ca}

17β-Oestradiol has been shown to enhance the inhibitory effect of nifedipine, a Ca^{2+} channel antagonist, on arterial smooth muscle contraction and this enhancement can be reversed by increasing the external Ca^{2+} (Downing *et al.*, 1988). It has also been reported that 4-hydroxylated oestradiol reduced the Ca^{2+} uptake in uterine smooth muscle pos-

sibly by affecting the potential-sensitive Ca^{2+} channel (Stice *et al.*, 1987a,b). In the present study, we have examined the effect of 17β-oestradiol on I_{Ca} in guinea-pig ventricular myocytes. In order to maintain the myocytes in as normal a physiological state as possible with intact intracellular ionic and biochemical environments, we have used the switch clamp to record I_{Ca}. This technique allows adequate voltage control of the cell during the peak of I_{Ca} (Fedida *et al.*, 1988; Salata & Wasserstrom, 1988). In addition, we did not usually observe any decrease or 'run-down' in I_{Ca} (see Belles *et al.*, 1988) after washout of the steroid. We have demonstrated that 17β-oestradiol induces a reversible and concentration-dependent inhibition of I_{Ca}. The indications are that the inhibition of I_{Ca} is probably due to 17β-oestradiol inducing a modification of the Ca^{2+} channel which decreases the macroscopic Ca^{2+} current.

In general, the action of Ca^{2+} channel antagonists appears to be voltage-dependent (Bean, 1984; Sanguinetti & Kass, 1984). The compounds are more efficacious in heart if the cells are maintained in a depolarized condition (more positive than −50 mV) and exhibit less inhibitory activity if the cells are maintained near their resting membrane potential of around −80 mV. We tested the effect of initial holding potential on the inhibition of I_{Ca} induced by 17β-oestradiol. The inhibition of I_{Ca} was significantly greater when the initial holding potential was −40 mV rather than −80 mV. This finding is in keeping with observed mechanisms of Ca^{2+}-channel inhibition by dihydropyridines. This behaviour would be expected if 17β-oestradiol bound more effectively to the inactivated state of the Ca^{2+} channel. Thus, the concentration and voltage-dependent inhibition of I_{Ca} suggests that 17β-oestradiol has a Ca^{2+} channel antagonistic property in guinea-pig single ventricular myocytes. We note that 17β-oestradiol induced a decrease in cell shortening or Fura-2 fluorescence ratio in non voltage-clamped cells whilst the resting potential was about −80 mV. This decrease presumably results from at least some 17β-oestradiol binding at a holding potential of −80 mV. It is possible that there is significant binding of 17β-oestradiol during the long plateau phase of the action potential. Where cells were voltage-clamped, 17β-oestradiol induced a similar decrease in cell shortening at a holding potential of −80 mV. We assume that this inhibition is due to the same effect of 17β-oestradiol on I_{Ca} which is less at a holding potential of −80 mV than −40 mV, but still occurs.

One of the factors which will regulate how much Ca^{2+} enters the cell during excitation is Ca^{2+}-channel inactivation. It seems that, in heart, both voltage and intracellular Ca^{2+} can control the rate of inactivation (Sanguinetti & Kass, 1984; Lee *et al.*, 1985; Hadley & Hume, 1987) though changes in intracellular Ca^{2+} can account for many of the alterations in I_{Ca} observed during staircases, increasing $[Ca^{2+}]_o$ and in the presence of isoprenaline (Fedida *et al.*, 1988). We assessed the recovery time of I_{Ca} from inactivation in the presence and absence of 17β-oestradiol. We found that 17β-oestradiol induced a delay in the recovery time (Figure 4) and affected the process of I_{Ca} inactivation during the clamp pulse. If [free Ca^{2+}]$_i$ is important in controlling I_{Ca} inactivation then a reduction in [free Ca^{2+}]$_i$, presumably resulting from the tonic effect of 17β-oestradiol on I_{Ca}, should not induce a delay of I_{Ca} inactivation. Therefore, we presume that the effect of 17β-oestradiol on inactivation is likely to be due to its direct effect on a channel site rather than an indirect effect via I_{Ca} or [free Ca^{2+}]$_i$.

Effect of 17β-oestradiol on [free Ca^{2+}]$_i$

I_{Ca} and Ca^{2+}-induced Ca^{2+} release from sarcoplasmic reticulum (SR) are thought to be the main contributors to the transient increase in [free Ca^{2+}]$_i$ which produces contraction in cardiac muscle, though the relative contributions of SR Ca^{2+} and extracellular Ca^{2+} to the Ca^{2+} transient are not clear (Fabiato, 1989) and vary from species to species (Bers, 1985). In the present study, we have demonstrated that 17β-oestradiol decreased [free Ca^{2+}]$_i$ as indicated by Fura-2. This reduction was accompanied by a decrase in APD with a decreased and shortened plateau of the action potential. The time course of the effect of 17β-oestradiol on [free Ca^{2+}]$_i$ and I_{Ca} and the percentage decrease of the effect were similar. Since there is strong evidence that the release of Ca^{2+} from the SR is under the control of Ca^{2+} influx through the sarcolemmal Ca^{2+} channel (Fabiato, 1985a,b), our results suggest that the reduction of systolic [free Ca^{2+}]$_i$ can be mainly attributed to the inhibitory effect of 17β-oestradiol on I_{Ca}. While there may be a secondary effect of APD shortening producing a decrease in twitch, the primary effect is that of I_{Ca} inhibition.

A reduction in I_{Ca} during stimulation can reduce the duration of the action potential appreciably (Noble, 1984) and, indeed, the inverse relation between APD and contraction has been shown in guinea-pig single cardiac myocytes (Fedida *et al.*, 1988). This originates from alterations in the amount of Ca^{2+} entering the cell which may change the size of the [free Ca^{2+}]$_i$ transient and hence the strength of contraction either by affecting the myofilaments directly (Bers, 1985) or the Ca^{2+} load and subsequent release from SR (Fabiato, 1985a,b). In the present study, we have demonstrated that 17β-oestradiol induced a similar decrease in cell shortening in either current-clamped or voltage-clamped conditions. This provides evidence that the negative inotropic effect of 17β-oestradiol is mainly caused by its direct inhibition of Ca^{2+} influx rather than a secondary effect through the alterations of action potential duration. Thus, a possible Ca^{2+} channel blocking property mediating a reduction of systolic [free Ca^{2+}]$_i$ may be one of the mechanisms underlying the inotropic effect of 17β-oestradiol in guinea-pig ventricular myocytes. A shortening of the action potential could also be brought about by an alteration in Na^+/Ca^{2+} exchange. The decrease in systolic [free Ca^{2+}]$_i$ will mean there will be less depolarizing current through Na^+/Ca^{2+} exchange though the present experiments were not designed to look at this in detail. In addition, we cannot say if the Na^+/Ca^{2+} exchange mechanism is directly affected by the steroid.

The effect of 17β-oestradiol on the contraction of perfused rabbit hearts has been demonstrated but whether it is due to an effect on myocardium or on coronary circulation is uncertain (Raddino *et al.*, 1986). In the present study, we have demonstrated the negative inotropic effect of 17β-oestradiol in single ventricular myocytes of guinea-pigs. In this case we can observe the effect at the single cell level independent of any effect of circulating hormones, blood volume or coronary circulation. This effect occurs at concentrations that are above the normal plasma concentration of 17β-oestradiol which have been shown to be under 10 nM in various species including guinea-pig (Naftolin *et al.*, 1990). Thus, it is difficult to establish any relationship between the acute *in vitro* effects of the 17β-oestradiol and the *in vivo* effects over a long period of time.

The heart is also a target for androgens in female monkeys (McGill *et al.*, 1980), although their acute effects on myocardium are not well known. In this study, we did not observe any significant effect of testosterone, a most active androgen, on APD and I_{Ca}. Therefore we assume that the acute *in vitro* effect of 17β-oestradiol on I_{Ca} is not a common action of steroids.

In conclusion, 17β-oestradiol induces a negative inotropic effect in single ventricular myocytes isolated from guinea-pigs. This effect may be the mechanism underlying the inhibitory effect of 17β-oestradiol on the contraction of perfused rabbit heart. Inhibition by 17β-oestradiol of I_{Ca}, which results in a reduction of systolic [free Ca^{2+}]$_i$, may partially explain this negative inotropic effect.

We would like to thank Mr Peter O'Gara for expert technical assistance, John Dempster for electrophysiological software and the British Heart Foundation for financial support.

References

BEAN, B.P. (1984). Nitrendipine block of cardiac calcium channels: high-affinity binding to the inactivated state. *Proc. Natl. Acad. Sci. U.S.A.*, **81**, 6388–6392.

BELLES, B., MALECOT, C.O. & TRAUTWEIN, W. (1988). "Run-down" of the Ca current during long whole-cell recordings in guinea-pig heart cells: role of the phosphorylation and intracellular calcium. *Pflügers Arch.*, **411**, 353–360.

BERS, D.M. (1985). Ca influx and sarcoplasmic reticulum Ca release in cardiac muscle activation during post rest recovery. *Am. J. Physiol.*, **248**, 366–381.

DOWNING, S.J., HOLLINGSWORTH, M. & MILLER, M. (1988). The influence of oestrogen and progesterone on the action of two calcium entry blockers in the rat uterus. *J. Endocrinol.*, **118**, 251–258.

FABIATO, A. (1985a). Time and calcium dependence of activation and inactivation of calcium-induced release of calcium from the sarcoplasmic reticulum of a skinned canine cardiac Purkinje cell. *J. Gen. Physiol.*, **85**, 247–289.

FABIATO, A. (1985b). Simulated calcium current can cause both calcium loading in and trigger calcium release from the sarcoplasmic reticulum of a skinned canine cardiac Purkinje cell. *J. Gen. Physiol.*, **85**, 291–320.

FABIATO, A. (1989). Appraisal of the physiological relevance of two hypotheses for the mechanism of calcium release from the mammalian cardiac sarcoplasmic reticulum: calcium-induced release versus charge- coupled release. *Mol. Cell Biochem.*, **89**, 135–140.

FEDIDA, D., NOBLE, D. & SPINDLER, A.J. (1988). Use-dependent reduction and facilitation of Ca^{2+} current in guinea-pig myocytes. *J. Physiol.*, **405**, 439–460.

HADLEY, R.W. & HUME, J.R. (1987). An intrinsic potential-dependent inactivation mechanism associated with calcium channels in guinea pig myocytes. *J. Physiol.*, **389**, 205–222.

KENTISH, J.C. & BOYETT, M.R. (1983). A simple electronic circuit for monitoring changes in the duration of the action potential. *Pflügers Arch.*, **398**, 233–235.

LEE, K.S., MARBAN, E. & TSIEN, R.W. (1985). Inactivation of calcium channels in mammalian heart cells: joing dependence on membrane potential and intracellular calcium. *J. Physiol.*, **364**, 395–411.

MACLEOD, K.T. & HARDING, S.E. (1991). The effects of phorbol ester on contraction, intracellular pH and intracellular Ca^{++} in isolated mammalian ventricular myocytes. *J. Physiol.*, **444**, 481–498.

MCGILL, H.C.J., ANSELMO, V.C., BUCHANAN, J.M. & SHERIDAN, P.J. (1980). The heart is a target organ for androgen. *Science*, **207**, 775–777.

NAFTOLIN, F., CUTMANN, J.N., DECHERNEY, A.H. & SARREL, P.M. (1990). *Ovarian Secretions and Cardiovascular and Neurological Function*. New York: Raven Press.

NOBLE, D. (1984). The surprising heart: a review of recent progress in cardiac electrophysiology. *J. Physiol.*, **353**, 1–50.

RADDINO, R., MANCA, C., POLI, E., BOLOGNESI, R. & VISIOLI, ? (1986). Effects of 17β-estradiol on the isolated rabbit heart. *Arch. Int. Pharmacodyn. Ther.*, **281**, 57–65.

ROE, M.W., LEMASTERS, J.J. & HERMAN, B. (1990). Assessment of Fura-2 for measurements of cytosolic free calcium. *Cell Cal.*, **11**, 63–73.

SALATA, J.J. & WASSERSTROM, J.A. (1988). Effects of quinidine on action potentials and ionic currents in isolated canine ventricular myocytes. *Circ. Res.*, **62**, 324–337.

SANGUINETTI, M.C. & KASS, R.S. (1984). Voltage-dependent block of calcium channel current in the calf cardiac Purkinje fiber by dihydropyridine calcium channel antagonists. *Circ. Res.*, **55**, 336–348.

STICE, S.L., FORD, S.P., ROSAZZA, J.P. & VAN ORDEN, D.E. (1987a). Role of 4-hydroxylated estradiol in reducing Ca^{2+} uptake of uterine arterial smooth muscle cells through potential-sensitive channels. *Biol. Reproduct.*, **36**, 361–368.

STICE, S.L., FORD, S.P., ROSAZZA, J.P. & VAN ORDEN, D.E. (1987b). Interaction of 4-hydroxylated estradiol and potential-sensitive Ca^{2+} channels in altering uterine blood flow during the estrous cycle and early pregnancy in gilts. *Biol. Reprod.*, **36**, 369–375.

STUMPF, W.E., SAR, M. & AUMULLER, G. (1977a). The heart: a target organ for estradiol. *Science*, **196**, 319–321.

(Received March 16, 1992
Accepted March 20, 1992)

Br. J. Pharmacol. (1992), **106**, 746–750

Calcitonin gene-related peptide increases blood flow and potentiates plasma protein extravasation in the rat knee joint

H. Cambridge & S.D. Brain

Pharmacology Group, Biomedical Sciences Division, King's College, Manresa Road, London SW3 6LX

1 The effects of calcitonin gene-related peptide (CGRP) and other vasoactive mediators of inflammation on blood flow in the synovial vessels and plasma protein extravasation into the knee (femoro-tibial) joint of the pentobarbitone-anaesthetized rat were measured.

2 Changes in synovial blood flow were estimated by ^{133}xenon clearance from the synovial cavity. CGRP (0.1 pmol and 10 pmol) and prostaglandin E_1 (PGE_1; 3 pmol and 300 pmol) significantly increased clearance from the knee joint measured 5 min after intra-articular injection. Substance P (10 pmol) had no effect on synovial blood flow.

3 Intra-articular perfusion of the rat knee with CGRP at concentrations up to 0.1 mM, or PGE_1 at concentrations up to 10 μM, did not increase plasma extravasation into the synovial cavity measured by accumulation of intravenously injected ^{125}I-albumin in the perfusate.

4 Plasma extravasation into the knee was significantly increased by infusion of bradykinin (0.1 μM), 5-hydroxytryptamine (1 μM) and histamine (0.1 mM), compared with the contralateral joints in the same animals which were perfused with Tyrode solution.

5 Perfusion of the knee joint with substance P did not specifically induce ^{125}I-labelled albumin accumulation in the synovial cavity even at doses that had systemic effects as observed by marked plasma extravasation into other tissues.

6 The increase in plasma extravasation induced by histamine (0.1 mM) was potentiated by co-infusion with CGRP (0.1 μM) and PGE_1 (3 μM). However the response to a submaximal dose (0.1 μM) of bradykinin, which induced similar plasma extravasation to histamine (0.1 mM), was not increased by co-infusion with CGRP or PGE_1.

7 These results show that CGRP is a potent vasodilator in the rat knee. CGRP released from sensory nerves may act synergistically with mediators of increased vascular permeability to modify the inflammatory response in this site.

Keywords: CGRP; calcitonin gene-related peptide; knee joint, synovium; blood flow; plasma protein extravasation; substance P

Introduction

Small diameter primary afferent, or C-fibre, nerves containing the vasoactive peptides, calcitonin gene-related peptide (CGRP) and substance P, have been identified in rat synovium, (Konttinen *et al.*, 1990). Release of peptides by antidromic stimulation may contribute to inflammation by increasing blood flow and vascular permeability. The nerves also have a close anatomical relationship to mast cells in normal tissue (Hukkanen *et al.*, 1991) and may modulate mast cell function in this site.

Extravasation of plasma protein into the synovial cavity or joint capsule is a commonly used marker of acute inflammation in the joint although the neural mechanisms and mediators which control this process are not well defined and may be species-dependent. In the cat knee joint, Ferrell & Russell (1986) showed plasma extravasation was decreased by stimulation of sympathetic efferents and increased by stimulation of C-fibre afferent nerves. Based on intra-articular perfusion of mediators in surgically or chemically sympathectamised rats, the possibility of an interaction between the sympathetic nerves and C-fibre nerves has been proposed by Coderre *et al.* (1989). They consider C-fibre evoked plasma extravasation to be at least partly dependent on intact sympathetic postganglionic nerves and mast cells. Specific roles for individual neuropeptides in the joint have not been defined, but there is some evidence that substance P may exacerbate adjuvant arthritis (Colpaert *et al.*, 1983; Weihe *et al.*, 1988). Elevated levels of substance P have also been found in rabbit knee joints after injection of inflammatory cytokines (O'Byrne *et al.*, 1990). A recent study showed intra-articular injection of substance P at high doses increased vascular permeability in the rat joint by releasing histamine and 5-hydroxytryptamine (5-HT) from mast cells and possibly by acting on vascular receptors (Lam & Ferrell, 1990).

CGRP is established as a potent and long-lasting vasodilator in the skin (Brain *et al.*, 1985). In this tissue CGRP also potentiates oedema formation by mediators of increased vascular permeability (Brain & Williams, 1985; 1989). The activity of CGRP has not been extensively studied in the joint although Kidd *et al.* (1990) have demonstrated modulation of vascular permeability changes in this site and Lam & Ferrell (1991) have shown a prolonged vasodilator response following topical application to the rat knee.

The aim of this study was to establish the effects of CGRP and other mediators of inflammation on synovial blood flow and plasma extravasation in the rat knee joint. Interactive effects of CGRP and two mediators of vascular permeability, histamine and bradykinin were also investigated. We have adapted and validated a ^{133}xenon clearance method, previously described in skin (Williams, 1979), for measuring synovial blood flow. Plasma extravasation was studied by a modification of the joint perfusion method described by Coderre *et al.* (1989).

Methods

Blood flow and oedema formation were measured in the knee joint of male Wistar rats (300–400 g) anaesthetized with 50 mg kg^{-1} pentobarbitone by intraperitoneal injection.

Measurement of blood flow changes by ^{133}xenon clearance

One ml of test agent in Tyrode solution or Tyrode solution alone (for control) was mixed with 10 MBq of ^{133}Xe and then 100 µl rapidly injected into the synovial cavity with a 30 G needle. The animals received Tyrode solution in one knee and test agent in the opposite joint so that each acted as its own control. Five minutes after completion of the intra-articular injections the animals were killed by anaesthetic overdose and the knee joints removed and counted for radioactivity. Changes in blood flow were calculated by comparing ^{133}Xe clearance over 5 min from both knees in the same animal.

Measurement of plasma extravasation by ^{125}I-albumin accumulation

Each rat received a mixture of Evans Blue (25 mg kg^{-1}) and ^{125}I-labelled human serum albumin (50 kBq) by injection via the tail vein. A 1 cm incision was made in the skin over the anterior aspect of both femoro-tibial joints. Two 27 G needles were placed in the synovial cavity approximately 3 mm apart and connected via flexible cannulae to a roller pump (Watson-Marlow). Tyrode solution was infused and withdrawn at a constant rate of 100 µl min^{-1} into both joints for 30 min. Placement of the needles within the synovial space was verified by lack of swelling of peri-articular tissues and a clear perfusate which could be continuously withdrawn at 100 µl min^{-1}. Mediators were then perfused for 4 min into one joint whilst the opposite joint acted as a control and was perfused with Tyrode solution. The solutions were left in the joint for a further 10 min after which perfusion was recommenced and 1 ml of perfusate collected from each joint. At the end of the experiment, blood (1 ml) was withdrawn by cardiac puncture and then the animal killed by anaesthetic overdose. Radioactivity was counted in 100 µl of plasma and in the 1 ml perfusate samples to quantify extravasation into the joint as µl of plasma. To measure potentiation of oedema, histamine or bradykinin were perfused with CGRP or prostaglandin E_1 (PGE_1) into one joint whilst histamine or bradykinin alone was perfused into the opposite joint.

^{125}I-labelled albumin accumulation was also measured in the skin of the hind paws in some experiments to assess systemic effects of test agents on vascular permeability. Immediately after death, approximately 100 mg of skin was removed from the dorsal aspect of each of the hind paws, weighed, counted for radioactivity and extravasation calculated as for the joint perfusates.

The effect of cyclo-oxygenase inhibition on plasma extravasation was investigated in animals treated with indomethacin (20 mg kg^{-1}, subcutaneously) or vehicle 30 min before the start of joint perfusion.

Statistical analysis

Results are expressed as mean ± s.e.mean and each data point represents one rat. The significance of the blood flow data was analyzed by Bonferroni's modified t test using the s.e. estimate for the analysis of variance to account for multiple comparisons to the control value. Student's paired t test was used to compare the treated and control limbs in the plasma extravasation studies.

Materials

The following drugs were used: histamine, 5-hydroxytryptamine, bradykinin, indomethacin, substance P, prostaglandin E_1 (PGE_1), all from Sigma Chemical Company, Poole, Dorset; human alpha calcitonin gene-related peptide, a gift from Dr U. Ney, Celltech, Slough, Berks; human endothelin-1 (ET-1) from Bachem Ltd, Saffron Walden, Essex. Each was dissolved in Tyrode solution except for PGE_1 and bradykinin, which were initially prepared in stock solutions of 1 mg ml^{-1} in absolute ethanol, and indomethacin which was dissolved in 5% NaH_2CO_3. ^{133}Xenon and ^{125}I-labelled human serum albumin (^{125}I-HSA) were obtained from Amersham International, Aylesbury, Bucks. The composition of the Tyrode solution was as follows (mM): NaCl 136.89, KCl 2.68, NaH_2PO_4 0.42, $NaHCO_3$ 11.9, $MgCl_2$ 1.05, glucose 5.55.

Results

Blood flow

Changes in blood flow were calculated by comparing ^{133}Xe clearance in test joints with that observed in control joints of the same animal. In initial experiments (designed to test the validity of the assay) the difference in ^{133}Xe clearance between joints when both were injected with equal amounts of ^{133}Xe in 0.1 ml Tyrode solution was small (Figure 1). To establish whether a decrease in synovial blood flow could be detected, the response to the potent vasoconstrictor peptide endothelin-1 was measured. There was virtually no clearance (3.9 ± 6.0% of total radioactivity injected, mean ± s.d., $n = 3$) from the joint after injection of 100 pmol endothelin-1. In joints which received 10 pmol of endothelin-1 18.2 ± 22.7% of total radioactivity injected (mean ± s.d., $n = 3$) was cleared. CGRP and PGE_1 produced a dose-dependent increase in blood flow of up to 300% over the 5 min clearance period when compared with contralateral Tyrode injected knee (Figure 1). A significant effect was seen with a dose of 100 fmol CGRP but, by contrast, substance P did not increase blood flow at doses of 0.1 and 10 pmol.

Plasma extravasation

In animals where both joints were perfused with Tyrode solution there was minimal plasma extravasation into the synovial cavity (0.76 µl ± 0.22, mean ± s.e.mean, $n = 6$). Plasma extravasation into the treated joint was increased in a dose-dependent manner by bradykinin, histamine and 5-hydroxytryptamine (Figure 2a), but not by CGRP or PGE_1 (Figure 2b). Substance P induced plasma extravasation only at the highest dose tested (0.1 mM) when systemic effects, resulting in the death of 3 out of 8 animals, were also seen.

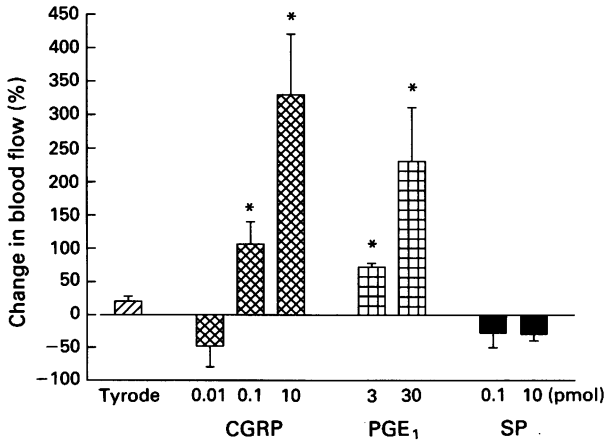

Figure 1 The effect of intra-articular injection of 0.1 ml of calcitonin gene-related peptide (CGRP), prostaglandin E_1 (PGE_1) or substance P (SP) on blood flow in the rat knee joint. Clearance of ^{133}Xe from test knees is compared, over 5 min, with the clearance of Tyrode alone (solid line at 0%) in the opposite knee of each rat ($n = 5$–8 animals). The hatched column represents the effect of Tyrode solution into the test joint. Results are mean values (s.e.mean indicated by vertical bars) and * indicates a significant change ($P < 0.05$, Bonferroni's t test) in blood flow compared with control.

At the highest doses of the mediators, plasma extravasation into the control joint was not increased by any mediator (Figure 3a). Infusion of 0.1 mM substance P, but none of the other mediators into the treated joint produced significant plasma extravasation into the skin of both the treated and control limbs (Figure 3b).

In further experiments interactions between the vasodilators (CGRP and PGE_1) and mediators of increased vascular permeability were studied. Plasma extravasation produced by submaximal doses of histamine and bradykinin is shown in Figure 4. The response to histamine was potentiated by co-perfusion with doses of CGRP and PGE_1 previously shown to have significant vasodilator activity in the ^{133}Xe clearance assay. Co-perfusion of the vasodilators with a submaximal dose of bradykinin, however, did not result in potentiation of oedema formation (Figure 4).

The response to a high dose of histamine (0.2 mM) appeared to be reduced in indomethacin-treated rats, presumably due to the inhibition of vasodilator prostaglandin production, but this was not significant ($P = 0.0593$, $n = 12$). Co-perfusion with CGRP (0.1 μM, $n = 7$) or PGE_1 (3 μM, $n = 4$) attenuated the inhibitory trend of indomethacin on histamine-induced plasma extravasation. Indomethacin pretreatment had no effect on the response to bradykinin (0.1 μM) or 5-HT (1 μM) in other experiments, (results not shown).

Discussion

These results show CGRP to be a potent vasodilator in the rat knee joint, as intra-articular injection of 100 fmol caused a significant increase in synovial blood flow. Although endogenous release of CGRP into rat joints has not been studied, our results show that physiological amounts of this peptide could modulate blood flow (a fundamental component of the inflammatory response), at this site. CGRP alone did not stimulate oedema formation in our model, however co-infusion of CGRP potentiated the effects of histamine, probably by increasing blood flow to leaky microvessels. Thus CGRP may be important in modulating oedema formation induced by amines released from activated mast cells. Synergy between CGRP and a range of mediators of increased vascular permeability have been demonstrated in skin (Brain & Williams, 1985; Gamse & Saria, 1985). There is also evidence that CGRP may also potentiate acute inflammation by increasing neutrophil accumulation induced by mediators that include interleukin-1, in skin (Buckley *et al.*, 1991a,b).

In our study bradykinin was the most potent mediator of plasma extravasation into the joint but the effects of a submaximal dose were not increased by the vasodilators, possibly because bradykinin alone was able to stimulate blood flow in addition to increasing vascular permeability. Interestingly, using a different protocol Kidd *et al.* (1990) were able to show potentiation of bradykinin by CGRP in the rat knee. In our study 5-HT was also a potent mediator of joint oedema and, if released in to the joint from mast cells, could contributed to acute inflammation in rodents. Sensory C-fibre

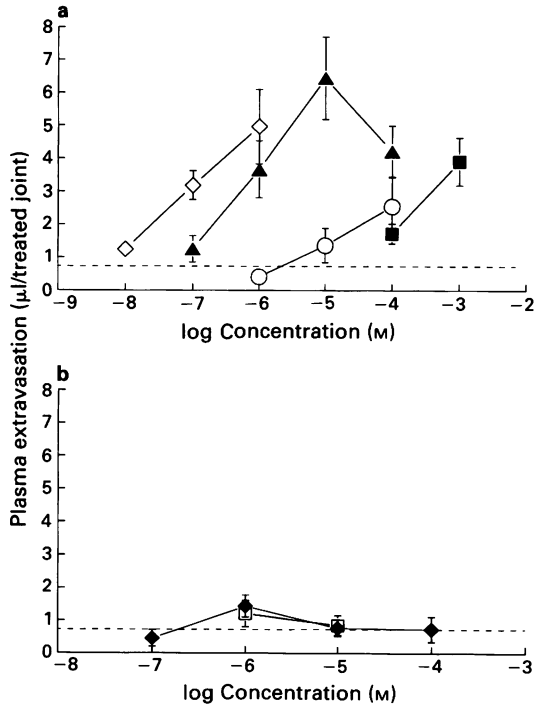

Figure 2 The effect of mediators on plasma extravasation into the rat knee. Plasma extravasation induced by increasing doses of bradykinin (◇), 5-hydroxytryptamine (▲), substance P (○) and histamine (■) is shown in (a) and by calcitonin gene-related peptide (◆) and prostaglandin E_1 (□) in (b) Plasma extravasation was measured by comparing the accumulation of intravenously injected ^{125}I-albumin in the joint perfusate to activity in plasma, as detailed in the methods section. The dashed line refers to plasma extravasation in joints infused with Tyrode solution alone. Results are mean values (s.e.mean indicted by vertical bars) of $n = 6-12$ rats.

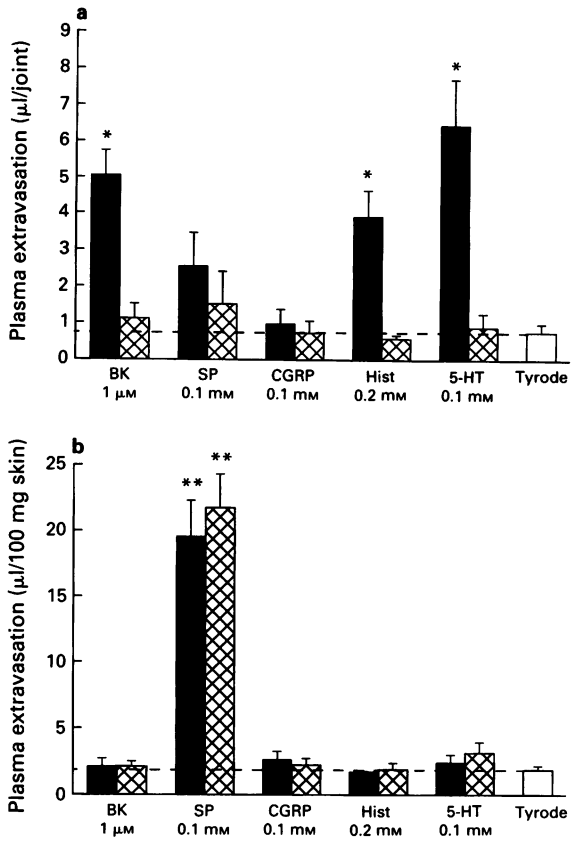

Figure 3 Effect of high doses of mediators on plasma extravasation into (a) knee joints and (b) skin of both hind paws. Results in (a) show plasma exudation induced by high doses of mediators infused into the treated knee (solid columns), whilst the control knee received Tyrode solution alone (cross-hatched columns). Plasma exudation into the skin in these experiments is shown in (b). The open column, and dashed line, refers to 3 rats which received Tyrode solution into both knees. BK: bradykinin; SP: substance P; CGRP: calcitonin gene-related peptide; Hist: histamine; 5-HT: 5-hydroxytryptamine. Results are the mean values (s.e.mean indicated by vertical bars) for $n = 6-10$ rats. A significant effect of mediator in injected knee compared to the opposite knee in the same animal is indicated *($P < 0.05$, paired t test). Significant extravasation into the skin compared to Tyrode solution is indicated **($P < 0.01$, unpaired t test).

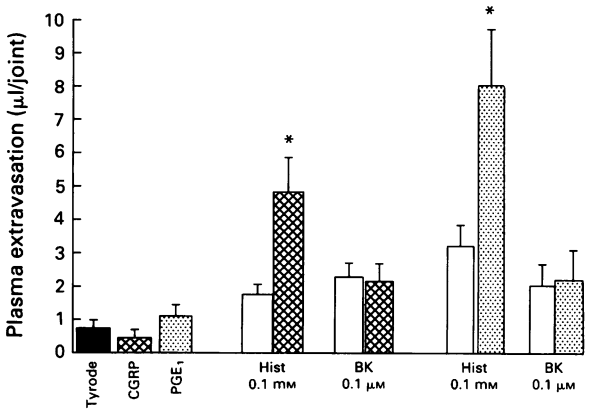

Figure 4 The effect of calcitonin gene-related peptide (CGRP) and prostaglandin E_1 (PGE_1) on plasma extravasation induced by histamine (Hist) and bradykinin (BK). Extravasation induced by Tyrode solution, CGRP (0.1 μM) and PGE_1 (3 μM) is shown by the solid, cross-hatched and stippled columns respectively. The response to histamine and BK alone is shown in the open columns. The effect of co-administration of CGRP and PGE_1 with histamine and BK is shown by the adjacent cross-hatched and striped columns. Results are mean values (s.e.mean indicated by vertical bars) for $n = 6-12$ rats. A significant potentiating effect of CGRP and PGE_1 compared to histamine alone in the opposite joint is indicated * ($P < 0.05$, paired t test.

nerves in the rat ankle are activated by 5-HT (Grubb *et al.*, 1988) and it is possible that some of the actions of both 5-HT and bradykinin may be related to release of neuropeptides, including CGRP. Alternatively it is possible that vasodilator prostanoids contribute to the responses, although this is not supported by the results of our study where indomethacin had no effect on bradykinin or 5-HT-induced plasma extravasation. Plasma extravasation induced by a high dose of histamine was attenuated by indomethacin (although this did not reach significance).

The importance of substance P in producing joint inflammation is difficult to assess. Lam & Ferrell (1989) showed that intra-articular injection of 20 μg substance P caused significant plasma extravasation into the joint capsule of the rat knee. In our study, minimal plasma extravasation was found in the joint even at doses sufficient to cause generalized plasma extravasation into most tissues, as demonstrated by accumulation of radioactivity in the skin. At lower concentrations, substance P had no significant effect on blood flow or plasma extravasation. O'Byrne and colleagues (1990) found levels of substance P up to 0.5 pmol in lavage fluid from rabbit knees after intra-articular injection of interleukin-1. Our results indicate that this amount would not contribute to oedema and we consider it unlikely that sufficient substance P can be released in the joint to cause local vasoactive effects. There is indirect evidence, however, for a pro-inflammatory role of capsaicin-sensitive nerves in chronic arthritis in the rat. Capsaicin selectively activates then desensitizes sensory nerves and systemic capsaicin pretreatment decreased substance P content of peripheral nerves in arthritic rats (Colpaert *et al.*, 1983). Paw swelling and degree of arthritis was also decreased in these animals although it is difficult to establish a direct relationship between these findings. Capsaicin also depletes CGRP and this may also contribute to its long-term anti-inflammatory effects. Levine *et al.* (1984) showed that intra-articular injections of substance P exacerbated arthritis in rats and more severe arthritis was found in joints, such as the ankle, which are densely innervated with substance P-containing fibres. Substance P may play a more important role in activating cellular rather than vascular mechanisms, as small doses of substance P stimulate proliferation of rheumatoid synoviocytes in culture and cause release of collagenase and PGE_2 (Lotz *et al.*, 1987). Recently, however, O'Byrne *et al.* (1991) have shown interleukin-1-induced cartilage degradation to be independent of substance P.

The specific contribution of CGRP to arthritis is not clear although the chronic stages of adjuvant arthritis in rats may be attentuated by immunization with CGRP prior to induction of disease (Louis *et al.*, 1990). Immunohistochemical methods have demonstrated substance P- and CGRP-containing nerves throughout the synovium of normal rats but inflammatory arthritis produces complex changes in peripheral innervation. In rats with chronic adjuvant arthritis there is increased staining for CGRP and substance P in the sciatic nerve, dorsal root ganglia and tissue overlying the joints (Weihe *et al.*, 1988) suggesting increased synthesis of these neuropeptides. In the proliferating synovium, however, the amount of nervous tissue is reduced and neuropeptide containing nerves are found only at the junction of the bone and the synovial membrane (Konttinenn *et al.*, 1990). This may be due to increased turnover and release of neuropeptides but it is also possible that release of CGRP is decreased in severe inflammatory arthritis. The relevance of these findings to disease progression is as yet unknown. Raud *et al.* (1991) have recently reported that pretreatment with either CGRP or capsaicin leads to an inhibition of oedema induced by inflammatory mediators in human skin, rat paw and hamster cheek pouch. These findings illustrate significant species differences but also raise the possibility that loss of sensory nerves in severe arthritis may contribute to, rather than inhibit, synovial inflammation. The role of neuropeptides may therefore differ in acute or chronic inflammation as the distribution of sensory nerves is altered by the ongoing inflammatory response.

In conclusion, our results show that CGRP is a potent vasodilator in the rat knee and can potentiate oedema formation induced by histamine. CGRP is significantly more potent as a vasodilator than substance P with which it is often co-localized in sensory nerves. We consider that CGRP may modulate blood flow in the synovium and hence contribute to the inflammatory response in the joint.

This study was supported by the Arthritis and Rheumatism Council.

References

BRAIN, S.D. & WILLIAMS, T.J. (1985). Inflammatory oedema induced by synergism between calcitonin gene-related peptide (CGRP) and mediators of increased vascular permeability. *Br. J. Pharmacol.*, **86**, 855–860.

BRAIN, S.D. & WILLIAMS, T.J. (1989). Interactions between the tachykinins and calcitonin gene-related peptide lead to the modulation of oedema formation and blood flow in rat skin. *Br. J. Pharmacol.*, **97**, 77–82.

BRAIN, S.D., WILLIAMS, T.J., TIPPINS, J.R., MORRIS, H.R. & MACINTYRE, I. (1985). Calcitonin gene-related peptide is a potent vasodilator. *Nature*, **313**, 54–56.

BUCKLEY, T.L., BRAIN, S.D., COLLINS, P.D. & WILLIAMS, T.J. (1991a). Inflammatory oedema induced by interactions between IL-1 and the neuropeptide calcitonin gene-related peptide. *J. Immunol.*, **146**, 3424–3430.

BUCKLEY, T.L., BRAIN, S.D., RAMPART, M. & WILLIAMS, T.J. (1991b). Time-dependent synergistic interactions between the vasodilator neuropeptide calcitonin gene-related peptide (CGRP) and mediators of inflammation. *Br. J. Pharmacol.*, **103**, 1515–1519.

CODERRE, T.J., BASBAUM, A.I. & LEVINE, J.D. (1989). Neural control of vascular permeability: interactions between primary afferents, mast cells, and sympathetic efferents. *J. Neurophysiol.*, **62,** 48–58.

COLPAERT, F.C., DONNERER, J. & LEMBECK, F. (1983). Effects of capsaicin on inflammation and on the substance P content of nervous tissue in rats with adjuvant arthritis. *Life Sci.*, **32,** 1827–1834.

FERRELL, W.R. & RUSSELL, N.J. (1986). Extravasation in the knee induced by antidromic stimulation at articular C-fibre afferents of the anaesthetised cat. *J. Physiol.*, **379,** 407–416.

GAMSE, R. & SARIA, A. (1985). Potentiation of tachykinin-induced plasma protein extravasation by calcitonin gene-related peptide. *Eur. J. Pharmacol.*, **114,** 61–66.

GRUBB, B.D., MCQUEEN, D.S., IGGO, A., BIRRELL, G.J. & DUTIA, M.B. (1988). A study of 5HT-receptors associated with afferent nerves located in normal and inflamed rat ankle joints. *Agents Actions*, **25,** 216–218.

HUKKANEN, M., GRONBLAD, M., REES, R., KONTTINEN, Y.T., GIBSON, S.J., HIETANEN, J., POLAK, J.M. & BREWERTON, D.A. (1991). Regional distribution of mast cells and peptide containing nerves in normal and adjuvant arthritic rat synovium. *J. Rheumatol.*, **18,** 177–183.

KIDD, B.L., MAPP, P.I. & BLAKE, D.R. (1990). Intra-articular CGRP potentiates oedema formation by inflammatory mediators. *Br. J. Rheumatol.*, **29,** Suppl.2, p 26.

KONTTINEN, Y.T., REES, R., HUKKANEN, M., GRONBLAD, M., TOLVANEN, E., GIBSON, S.J., POLAK, J.M. & BREWERTON, D.A. (1990). Nerves in inflammatory synovium: immunohistochemical observations on the adjuvant arthritic rat model. *J. Rheumatol.*, **17,** 1586–1591.

LAM, F.Y. & FERRELL, W.R. (1989). Capsaicin suppresses substance P-induced joint inflammation in the rat. *Neurosci. Lett.*, **105,** 155–158.

LAM, F.Y. & FERRELL, W.R. (1990). Mediators of substance P-induced inflammation in the rat knee joint. *Agents Actions*, **31,** 298–307.

LAM, F.Y. & FERRELL, W.R. (1991). CGRP modulates nerve-mediated vasoconstriction of rat knee joint blood vessels. *Regul. Pept.*, **34,** 118 (abstr.).

LEVINE, J.D., CLARK, R., DEVOR, M., HELMS, C., MOSKOWITZ, M.A. & BASBAUM, A.I. (1984). Intraneuronal substance P contributes to the severity of experimental arthritis. *Science*, **226,** 547–549.

LOTZ, M., CARSON, D.A. & VAUGHAN, J.H. (1987). Substance P activation of rheumatoid synoviocytes: neural pathway in pathogenesis of arthritis. *Science*, **235,** 893–895.

LOUIS, S.M., JOHNSTONE, D., MILLEST, A.J., RUSSELL, N.J.W. & DOCKRAY, G.J. (1990). Immunization with calcitonin gene-related peptide reduces the inflammatory response to adjuvant arthritis in the rat. *Neuroscience*, **39,** 727–731.

O'BYRNE, E.M., BLANCUZZI, V., WILSON, D.E., WONG, M. & JENG, A.Y. (1990). Elevated substance P and accelerated cartilage degradation in rabbit knees injected with interleukin-1 and tumor necrosis factor. *Arthritis Rheum.*, **33,** 1023–1028.

O'BYRNE, E.M., GOLDBERG, R.L., DOUGHTY, J.R., WONG, M., BLANCUZZI, V., WILSON, D. & JENG, A.Y. (1991). Interleukin-1-induced cartilage degradation is independent of substance P level in rabbit knees. *Agents Actions*, **34,** 232–234.

RAUD, J., LUNDEBERG, T., BRODDA-JANSEN, G., THEODORSSON, E. & HEDQVIST, P. (1991). Potent anti-inflammatory action of calcitonin gene-related peptide. *Biochem. Biophys. Res. Comm.*, **180,** 1429–1435.

WEIHE, E., NOHR, D., MILLAN, M.J., STEIN, C., MULLER, S., GRAMSCH, C. & HERZ, A. (1988). Peptide neuroanatomy of adjuvant-induced arthritic inflammation in the rat. *Agents Actions*, **25,** 255–259.

WILLIAMS, T.J. (1979). Prostaglandin E_2, prostaglandin I_2 and the vascular changes of inflammation. *Br. J. Pharmacol.*, **65,** 517–524.

(Received January 7, 1992
Revised March 16, 1992
Accepted March 20, 1992)

Br. J. Pharmacol. (1992), **106**, 751–755

The selective action of quinacrine on high-threshold calcium channels in rat hippocampal cells

S.L. Mironov & [1]H.D. Lux

Department of Neurophysiology, Max-Planck-Institute for Psychiatry, Am Klopferspitz 18a, 8033 Planegg-Martinsried, Germany

1 The whole-cell patch-clamp technique has been used to examine Ca channel currents carried by Ba (I_{Ba}) in rat hippocampal neurones.

2 Quinacrine selectivity decreased the high-threshold current activated by membrane depolarization from a holding potential of −70 mV. Neither the low-threshold Ca channel current nor the fast tetrodotoxin (TTX)-sensitive sodium current were affected by quinacrine.

3 Bath application of quinacrine caused a dose-dependent reduction of the peak amplitude of I_{Ba}. This effect was fast, voltage-independent, reversible and had a K_d of 30 ± 5 μM.

4 The quinacrine-induced block did not change the time-course and the voltage dependence of I_{Ba} activation and deactivation. The inhibition revealed no use-dependence, ruling out an open channel block by quinacrine.

5 *p*-Bromophenacyl bromide had no effect on I_{Ba} suggesting the lack of involvement of phospholipase A_2 in the action of quinacrine. In addition, the quinacrine-induced block was not related to the calmodulin pathway and internal quinacrine did not affect the peak amplitude of I_{Ba}.

6 The effect of quinacrine on the amplitude of I_{Ba} was dependent of the external pH, and suggested that only the single-protonated form of the drug can bind to the channel receptor with a K_d of 3 μM. Quinacrine and other substituted acridines can thus be useful for pharmacological and structure-activity studies of Ca channels.

Keywords: High-threshold calcium current; hippocampal neurones; quinacrine

Introduction

Quinacrine is used as an antihelmintic and antiprotozoan agent (Chou *et al.*, 1984). It has reported to bind to DNA (Darzynkiewicz *et al.*, 1984), to inhibit phospholipase A_2 (Schweitzer *et al.*, 1990) and calmodulin (Prozialeck & Weiss, 1982) and to block potassium channels in rat melanotrophs (Kehl, 1991). As part of the pharmacological characterization of neuronal Ca channels the effects of quinacrine were investigated. The results described in this paper show that the drug exerts a specific action on a high-threshold Ca channel current in neurones.

Methods

Acutely isolated pyramidal neurones from rat hippocampus were prepared by conventional techniques (Yaari *et al.*, 1987) with slight modifications. Briefly, following the dissection of one hippocampus from the brain of rat embryos (18–19 days gestation), tissue chunks (1 mm^3) were prepared and placed into Earle's saline containing 1% of antibiotic-antimycotic liquid, 0.4% glucose and $Mg_2SO_4 \cdot 7H_2O$ 1.5 mg ml^{-1}; they were then washed twice with serum-free BME medium with 1% L-glutamine, 0.44% glucose, 0.375% insulin and 0.25% penicillin-streptomycin. After dissociation by trituration, the cells were plated on poly-L-ornithine coated tissue-culture dishes, each containing 2 ml of incubation medium (BME medium enriched with 10% horse serum). The plates were kept in a humified incubator at 37°C. To suppress the proliferation of glial cells, on the 4th day of cultivation the cell culture medium was supplied with 1 μM cytosine-β-D-arabinofuranoside hydrochloride. The cells were used for the experiments 8–14 days after plating.

The whole-cell currents were recorded by conventional patch-clamp technique using the amplifier EPC-7 (List Electronics, Darmstadt-Eberhardt, Germany) with about 70% compensation of the series resistance. Patch pipettes were pulled in two steps from a soft Kimax glass (Witz Scientific, Maumee, Ohio, U.S.A.) and heat polished with a final inner tip diameter between 1 and 1.5 μm. Their resistance ranged from 1 to 3 MOhm when filled with the standard pipette solution and the seal resistance was from 1 to 10 GOhm. The holding potential was −70 to −60 mV, a potential at which the inactivation of low-threshold Ca channels is complete.

For recording of this current component, the holding potential was set to −100 or −110 mV; 3–5 min was allowed for equilibration of patch pipette contents with the cytoplasm before recording was begun, although interfering potassium currents usually washed out earlier. Data were stored and digitized at 10 kHz, for analysis with PC programme. Records were correlated for linear leak and capacitance currents. All mean data are given ± s.e.mean of the number of experiments given in parentheses. All the experiments were carried out at room temperature (18–22°C).

The standard recording solution contained (mM): $BaCl_2$ 5, NaCl 120, N-2-hydroxyethylpiperazine-N'-2-ethanesulphonic acid (HEPES) 20 (adjusted to pH 7.5 with NaOH), glucose 10, and tetrodotoxin (TTX) 0.001 to block the fast sodium current. In some experiments TTX was not added. The patch electrodes were filled with a solution containing (mM): CsCl 100, tetraethylammonium (TEA) chloride 40, glucose 10, ethyleneglycol-*bis*-(β-aminoethyl ether)-N,N,N',N'-tetraacetic acid (EGTA) 100, HEPES 10 (adjusted to pH 7.5 with CsOH). To record the sodium current through the Ca channel $BaCl_2$ was replaced by 5 μM EGTA.

All chemicals and drugs were obtained from Sigma and culture reagents were from Gibco. Solutions containing quinacrine dihydrochloride were prepared fresh from 10 mM stock solutions. Experiments were performed under dimmed

[1] Author for correspondence.

lights to prevent photoinactivation of the test drugs. Solution changes were carried out with the fast perfusion system (Konnerth *et al.*, 1987), consisting of a large bore six-barrelled pipette placed 30–60 μm from a patched cell.

Results

Reduction by quinacrine of the peak amplitude of high-threshold Ca channels

In each cell examined the Ba current decreased after the application of quinacrine (Figure 1). The effects of the drug were similar for both rat hippocampal and chick sensory neurones, but only the data obtained for the former cell type are shown. The block developed within several seconds and wash-out of quinacrine was accomplished in 10–20 s with complete removal of the block in most cases. The block of Ca channel current by quinacrine was concentration-dependent but it was independent of the test voltage.

With voltage steps from the holding potential of −100 mV, both high- and low-threshold Ba currents could be observed. Quinacrine blocked only the high-threshold current (Figure 1). Nowycky *et al.* (1985) suggested a division of high-threshold Ca channels into L- and N-type. N-type channels are largely inactivated at holding potentials more positive than −70 mV. Quinacrine always blocked the same amount of current elicited by test pulses from the holding potential of −100 and −70 mV. This result rules out the effect of the drug on N-type channels, if present in the cells examined.

The drug was equally effective in blocking the Na current through the Ca channel in Ca-free solutions (Figure 2). In cells exposed to 36 μM quinacrine the peak amplitude of the current carried by Ba, Ca and Na decreased by 49 ± 4% ($n = 12$), 45 ± 6% ($n = 10$), 47 ± 8% ($n = 8$), respectively, indicating that the drug blocks the Ca channel independently of its conductive mode. Quinacrine had no effect on TTX-sensitive Na current. As shown in Figure 3, the drug application selectivity suppressed the steady component of the total current while the amplitude of fast transients remained unchanged.

Lack of effect of quinacrine on Ca channel kinetics

Quinacrine did not change the time-course and the voltage-dependence of whole-cell Ca channel current. Inactivation kinetics was not changed by quinacrine (Figure 4a) and no shift in the voltage-dependence of the steady state inactivation was observed in 5 cells exposed to 36 μM quinacrine (data not shown).

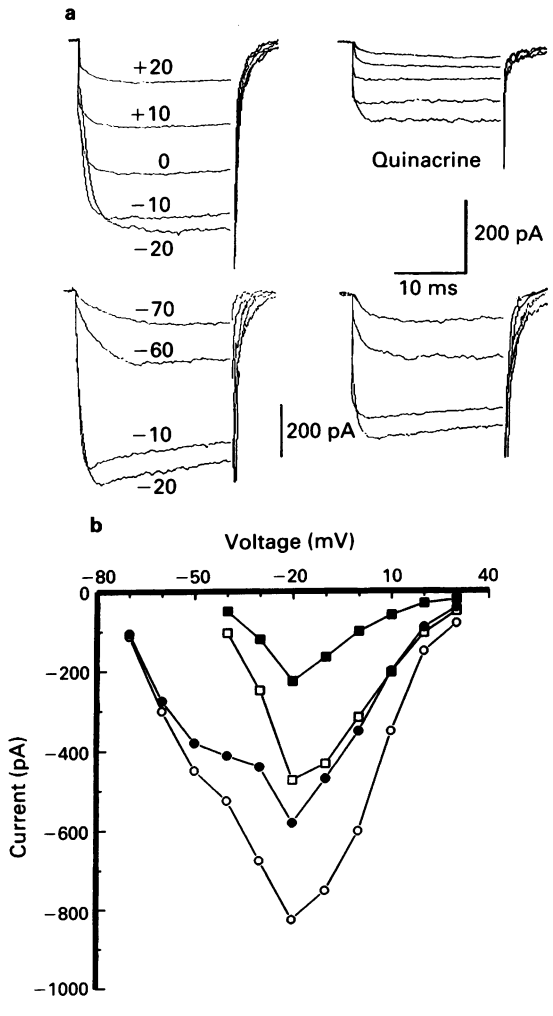

Figure 1 Quinacrine block of Ca channel current. (a) The traces show Ba currents recorded before and at equilibrium after 2 min application of 36 μM quinacrine in standard external solution. Recordings were made from holding potentials of −70 mV (top) and of −100 mV (bottom) for different depolarizing steps as indicated (in mV). (b) The dependence of peak currents on applied voltage for the same cell recorded before (open symbols) and after the application of quinacrine (solid symbols) for a holding potential of −100 mV (circles) and of −70 mV (squares). Note the unchanged peak current amplitudes between −70 and −50 mV which are attributable to low-threshold Ba currents.

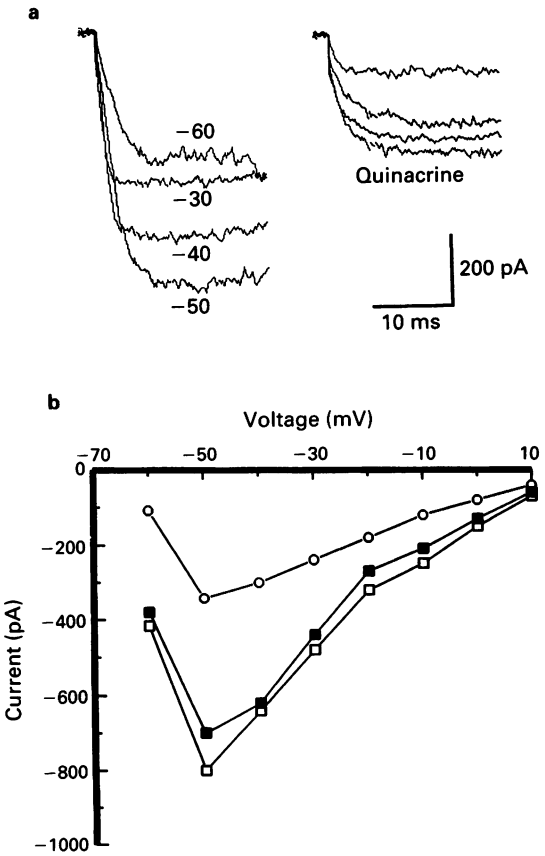

Figure 2 Quinacrine block of the sodium current through the Ca channel. (a) The traces show currents recorded before and 2 min after application of 36 μM quinacrine in Ca-free external solution. Recordings were made from the holding potential of −90 mV for different depolarizing steps in (mV) as indicated. The holding potential was made more negative regarding the shift of the activation curve of high-threshold Ca channels in solutions free of divalent cations. (b) The dependence of peak currents on the applied voltage for the same cell recorded before (□) 2 min after quinacrine application (○) and 2 min after wash-out of the drug (■).

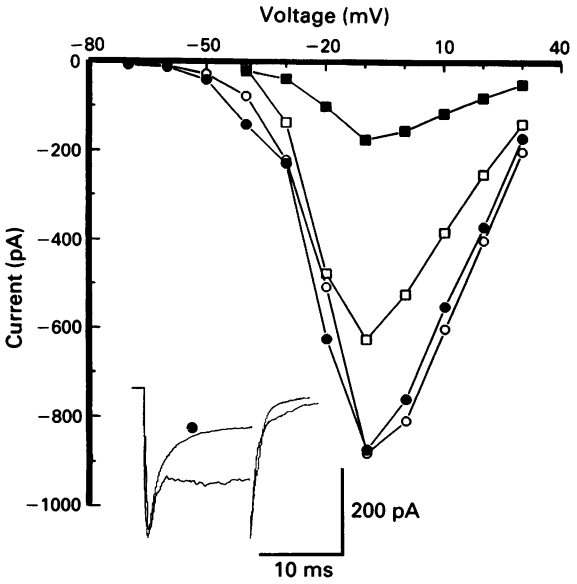

Figure 3 Quinacrine block of fast Na and slow Ba currents. The dependence of peak currents on applied voltage for the same cell recorded in tetrodotoxin TTX-free standard external solution before (open symbols) and at equilibrium after 2 min application of 50 μM quinacrine (solid symbols). Holding potential, −100 mV. Circles – peak current; squares – steady current measured at the end of 15 ms depolarizing steps. The inset shows two superimposed inward currents during test pulses from −100 to −30 mV, with and without the drug.

Like local anaesthetics acting on the fast sodium channels and some organic Ca antagonists, the quinacrine-induced block might possess use-dependence, originating from the block of open channels. Three lines of evidence, however, are against this possibility. First, the deactivation time constant was not affected by quinacrine (data not shown), although many drugs which block open channels alter tail current kinetics. Secondly, the time-course of the Ba current observed during long depolarizing pulses was unaffected by quinacrine (Figure 4a). Finally, no additional block was observed when the Ba current was evoked by a high-frequency train of depolarizing pulses. Quinacrine produced a fast decline of I_{Ba} and the block was still developing even when the stimulation was interrupted and the membrane was held at −70 mV (Figure 4b).

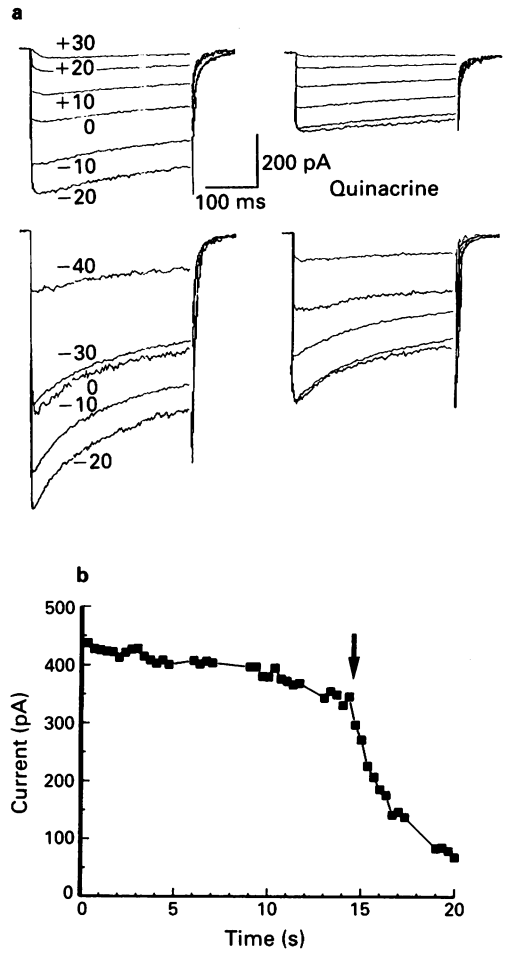

Figure 4 Absence of use-dependence in the quinacrine-induced block. (a) Ba currents recorded from the holding potential of −70 mV (upper row of records) and −100 mV (lower row of records), with voltage steps (in mV, as indicated near corresponding traces) before (left panel) and after 2 min application of 30 μM quinacrine (right panel). (b) Ba currents elicited by a train of 40 ms-long test pulses to 0 mV from holding potential of −70 mV delivered with a frequency of 3 s^{-1}. The pulse protocol was interrupted several times, indicated by the intervals between the experimental points. During these periods the cell membrane was held at −70 mV. Application of μM quinacrine is indicated by an arrow. Six other cells demonstrated similar behaviour.

pH-dependence of quinacrine block

The dose-response curve of the quinacrine block of the high-threshold Ba current is shown in Figure 5. The Hill coefficient was 0.97 ± 0.03 suggesting 1:1 quinacrine binding to the corresponding receptor in the channel. The dissociation constant was 30 ± 5 μM (confidence limits 19–41 μM). The drug can exist in several forms with different charge. One positive charge is located at the aminoacridine ring nitrogen, having a pK_a of 8.2, whereas the pK_a of the tertiary amine of the side chain is 10.2. Thus, at normal pH, quinacrine is mostly present as a single charged cation. Since the hydrophobicity of the ring might be an important determinant of binding, the pH-dependence of the quinacrine-induced block of the Ca channel current was studied.

Figure 6a shows that I_{Ba} was progressively reduced by successive applications of standard recording solution containing 36 μM quinacrine with increased external pH. Apppplication of acidic solutions produced brief transients in the current at holding potential due to the pH-activated non-selective conductance, $I_{Na(H)}$ (Krishtal & Pidoplichko, 1980; Konnerth *et al.*, 1987). In six out of ten cells examined, this current was absent but quinacrine revealed the same amount of I_{Ba} block. The quinacrine-induced block at different pH

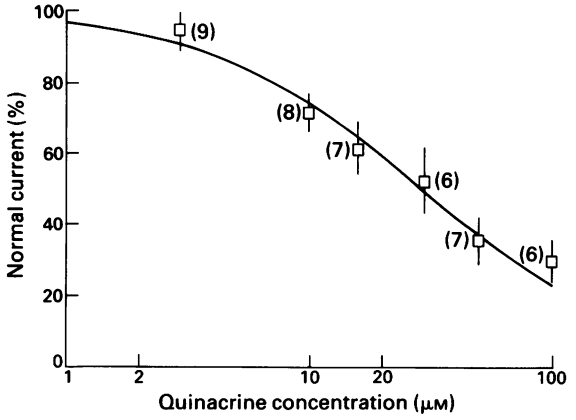

Figure 5 The dose-response curve of quinacrine block of high-threshold Ca channel current carried by Ba. For each cell examined the normalized amplitude ($I_{quinacrine}/I_{control}$) was measured for 2 to 3 different concentrations of quinacrine. All data are mean values with s.e.mean (vertical bars) and with number of cells given in parentheses. The solid line represents the least squares fit to a Michaelis-Menten equation with a K_d of 30 μM.

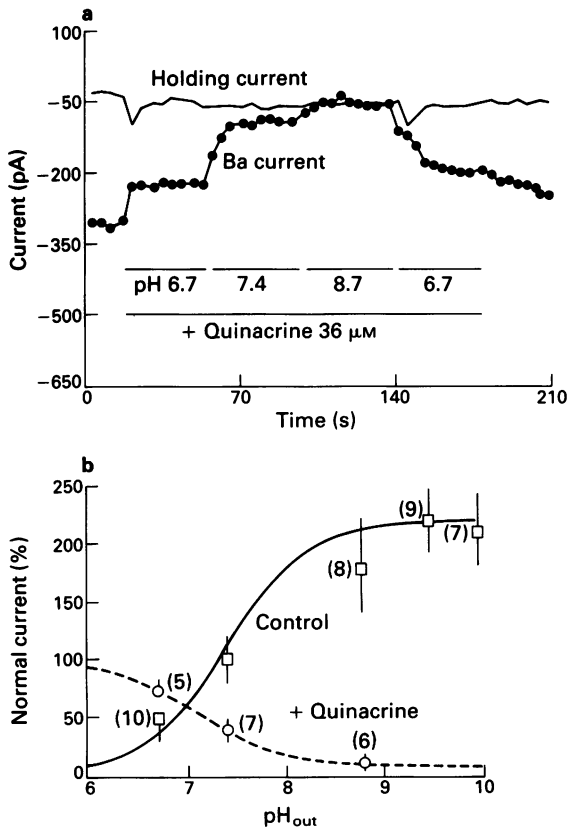

Figure 6 Dependence on pH of the block of Ca channel current by quinacrine. (a) Shown are the peak Ba currents (●) and the current at holding potential (solid line). The data were received after a transient current response which appears with fast application of acidic solutions. The test pulses to 0 mV from −70 mV holding potential lasted 40 ms and were delivered every 3 s. Horizontal bars indicate the periods of application of standard external solution containing 36 μM quinacrine at different pH. (b) The pH-dependence of peak Ba currents shown by (□). A new steady value of I_{Ba} was established within 1 min of cell perfusion with standard external solution of a different pH. The pH-dependence of the quinacrine block obtained as the ratio of peak currents at a given pH in the presence and in the absence of the drug shown by (○). All data are mean values with s.e.mean (bars) and number of cells denoted in parentheses. Curves represent the least squares fits to Michaelis-Menten equations. The solid curve was drawn according to $I_{Ba}(\%) = 220/(1 + 10^{7.4-pH})$ and the dotted line was drawn evaluated according to the equation $I_{Ba}(\%) = 100 \times K_Q/(K_Q + C_Q^+)$ with the concentration of single-protonated quinacrine given by $C_Q^+ = C_Q/(1 + 10^{pK-pH})$, where the total quinacrine concentration C_Q is 36 μM and $pK = 8.2$ for protonation of the nitrogen in the aminoacridine ring.

should be corrected for the pH-dependence of Ca channel current shown in Figure 6b. This effect is due to I_{Ba} increase with intracellular alkalinization as has recently been shown in sensory neurones (Mironov & Lux, 1991a). The block produced by quinacrine at different pH can be described as the binding of its single-protonated form to the channel with a dissociation constant of 3 μM, see the legend to Figure 6b.

External action of quinacrine

The voltage-independence of the quinacrine-induced block of the Ca current may indicate an intracellular target. Quinacrine has been reported to affect potassium current by inhibiting phospholipase A_2 (Schweitzer *et al.*, 1990). However, 10 μM *p*-bromophenacyl bromide, another inhibitor of this enzyme, was without effect either on Ca channel current or its block by quinacrine. An inhibition of calmodulin activity by quinacrine has also been demonstrated (Prozialeck & Weiss, 1982) but the Ca channel current was only increased after bath application of the calmodulin antagonists, trifluoperasine and W-13 (Mironov & Lux, 1991b). Thus, the mechanisms underlying this effect seem to be different from the quinacrine action on Ca channels observed in this study.

The results of experiments when quinacrine was included in the pipette solution are in line with data mentioned above. The persistence of the inward current at 0 mV with 36 μM internal quinacrine (−210 ± 60 pA, $n = 6$ vs. −285 ± 104 pA in 12 control cells and vs. −99 ± 31 pA in 36 μM external quinacrine, $n = 6$) indicated that there was little or no effect of quinacrine when it was applied internally.

Discussion

It has been shown that quinacrine blocks specifically high-threshold Ca channel currents blocked by quinacrine while no effect was observed on the low-threshold Ca channel and the fast Na channel. The fast transient potassium current I_K^f has been shown to be inhibited by quinacrine, 70% inhibition by 100 μM quinacrine at pH 8.5 (Figure 7 in Kehl, 1991). Our data show that Ca channels are more sensitive since a 90% block of I_{Ba} was produced by 36 μM quinacrine at pH 8.8 (cf. Figure 6).

Internal application of the drug had little if any effect on I_{Ba}. Inhibitors of phospholipase A_2 and calmodulin did not mimic the action of quinacrine which was reported to affect these two enzymes. These results speak against an intracellular action of quinacrine.

Amongst the possibilities that might explain the action of quinacrine observed in this study are a reduction of the probability of channel opening and/or a decrease of the single channel conductance. The absence of use-dependence rules out the modulated receptor-hypothesis suggested to describe the block of the fast Na current by local anaesthetics (Hille, 1977) and of the Ca channels by other organic antagonists (Lee & Tsien, 1983).

The effect of quinacrine was essentially similar for the two cell types examined, hippocampal neurones of the rat and peripheral sensory neurones of the chicken. For neuronal Ca channels the drug efficiency appears similar to that of other Ca antagonists (this only concerns the comparison of dissociation constants determined in electrophysiological studies). The data suggest that a quinacrine-binding site may be a distinct structural element common to neuronal high-threshold Ca channels.

The quinacrine molecule consists of a hydrophobic portion, the heterocyclic aminoacridine ring with the aliphatic side chain attached. The pH-dependence of the quinacrine-induced block indicates that only a single-protonated form can bind to the channel receptor. At pH 7.2 only about 10% of total quinacrine is active, resulting in a difference between the apparent and the putative dissociation constants of one order of magnitude. This information may provide a useful clue to increase the drug efficiency. Chemical modification in the aminoacridine ring can be made by introduction of nucleophylic substituents which will pump the electronic density on an aromatic nitrogen. The resulting shift of pK_a to the alkaline side should increase the percentage of single-charged drug molecules at normal pH: this will be evident as a decrease of the apparent dissociation constant for the block. A specific action of quinacrine on a high-threshold Ca channel, therefore, makes acridines suitable for biophysical and biochemical studies of this membrane protein.

We are grateful to Ms S. Engers and Ms H. Tyrlas for isolation and maintenance of cells and making the electrodes.

References

CHOU, S.-C., CONCLIN, K.A., LEVY, M.R. & WARHURST, D.C. (1984). Surrogate models for antimalarials. In *Antimalarial Drugs*, II, ed. Peters, W. & Richards, W.H.G. pp. 281–344. New York: Springer- Verlag.

DARZYNKIEWICZ, Z., TRAGANOS, F., KAPUSCINSKI, J., STAIANO-COICO, L. & MELAMED, M.R. (1984). Accessibility of DNA in situ to various fluorchromes. *Cytometry*, **5**, 355–363.

HILLE, B. (1977). Local anesthetics: hydrophylic and hydrophobic pathways for the drug receptor reaction. *J. Gen. Physiol.*, **69**, 497–515.

KEHL, S.J. (1991). Quinidine-induced inhibition of the fast transient outward K current in rat melanotrophs. *Br. J. Pharmacol.*, **103**, 1807–1813.

KONNERTH, A., LUX, H.D. & MORAD, M. (1987). Proton-induced transformation of calcium channel current in chick dorsal root ganglion cells. *J. Physiol.*, **386**, 603–633.

KRISHTAL, O.A. & PIDOPLICHKO, V.I. (1980). A receptor for protons in the nerve cell membrane. *Neuroscience*, **6**, 2325–2327.

LEE, K.S. & TSIEN, R.W. (1983). Mechanism of calcium channel blockade by verapamil, D 600, diltiazem and nitrendipine in single dialysed heart cells. *Nature*, **302**, 790–795.

MIRONOV, S.L. & LUX, H.D. (1991a). Cytoplasmic alkalinization increases high-threshold calcium current in chick sensory neurons. *Pflügers Arch.*, **419**, 138–143.

MIRONOV, S.L. & LUX, H.D. (1991b). Calmodulin antagonists and protein phosphatase inhibitor okadaic acid fasten the 'run-up' of high-voltage activated calcium current in rat hippocampal neurons. *Neurosci. Lett* (in press).

NOWYCKY, M.C., FOX, A.P. & TSIEN, R.W. (1985). Three types of neuronal calcium channels with different agonist sensitivity. *Nature*, **316**, 440–443.

PROZIALECK, W.C. & WEISS, B. (1982). Inhibition of calmodulin by phenotiazines and related drugs: structure-activity relationships. *J. Pharmacol. Exp. Ther.*, **222**, 509–515.

SCHWEITZER, P., MADAMBA, S. & SIGGINGS, G.R. (1990). Arachidonic acid metabolites as mediators of somatostatin induced increase of neuronal M-current. *Nature*, **346**, 464–467.

YAARI, Y., HAMON, B. & LUX, H.D. (1987). Development of two types of calcium channels in cultured mammalian hippocampal neurons. *Science*, **681**, 680–682.

(Received August 28, 1991
Revised March 19, 1992
Accepted March 24, 1992)

Erratum

Br. J. Pharmacol. (1992), **105**, 973–979

L. Fagni, A. Dumuis, M. Sebben & J. Bockaert. The 5-HT_4 receptor subtype inhibits K^+ current in colliculi neurones via activation of a cyclic AMP-dependent protein kinase.

In the above paper three lines were omitted from the final paragraph of column 1 on page 976. The complete paragraph is reproduced below.

Our results show that PKA was involved in 5-HT_4-mediated inhibition of K^+ current in colliculi neurones. However, we do not know, as is the case with other K^+ channels, whether the modulation is due to direct phosphorylation of the channel or to phosphorylation of some intermediate proteins. The final answer to this question must await specific experiments on purified or cloned K^+ channels.

British Journal of Pharmacology

VOLUME 106 (3) JULY 1992

ERRATUM

SPECIAL REPORTS

The purpose of *Special Reports* is to provide rapid publication for **new** and **important** results which the Editorial Board considers are likely to be of special pharmacological significance. (Please note that Short Communications are no longer acceptable for publication.) *Special Reports* will have publication priority over all other material and so authors are asked to consider carefully the status of their work before submission.

In order to speed publication there is normally no revision allowed beyond very minor typographical or grammatical corrections. If significant revision is required, the Board may either invite rapid re-submission or, more probably, propose that it be re-written as a Full Paper and be re-submitted for consideration. In order to reduce delays, proofs of *Special Reports* will be sent to authors but **essential corrections must reach the Production Office within 48 hours of receipt.** Authors should ensure that their submitted material conforms exactly to the following requirements.

Special Reports should normally occupy no more than two printed pages of the Journal; two illustrations (Figures or Tables, with legends) are permitted. As a guideline, with type face of 12 pitch and double-line spacing, a page of A4 paper could contain about 400 words. The absolute maximum length of the *Special Report* is 1700 words. For each Figure or Table, please deduct 200 words. The manuscript should comprise a Title page with key words (maximum of 10), a Summary consisting of a single short paragraph, followed by Introduction, Methods, Results, Discussion and References (maximum of 10). In all other respects, the requirements are the same as for Full Papers (see current 'Instructions to Authors').

Papers will be considered for publication on all aspects of pharmacology, including chemotherapy.

Manuscripts (two copies) should be sent to Editorial Office, British Journal of Pharmacology, St. George's Hospital Medical School, Cranmer Terrace, London SW17 0RE. Authors should consult the Instructions to Authors in Vol. 105, 245–251 (1992) and the Nomenclature Guidelines for Authors in Vol. 105, 252–254 (1992). These Instructions and Guidelines also appear with the journal Index for volumes 102–104, 1991.

The *British Journal of Pharmacology* is published monthly by the Scientific & Medical Division, Macmillan Press Ltd.

The journal is covered by *Current Contents*, *Excerpta Medica* and *Index Medicus*.

All business correspondence and reprint requests should be addressed to the Scientific & Medical Division, Macmillan Press Ltd., Houndmills, Basingstoke, Hampshire RG21 2XS, UK. Telephone: (0256) 29242; Fax: (0256) 810526.

Annual subscription prices for 1992 EEC £412, elsewhere £445/US$825 (sterling rate is definitive). Orders must be accompanied by remittance. Cheques should be made payable to Macmillan Press, and sent to: Macmillan Press Ltd., Subscription Department, Brunel Road, Houndmills, Basingstoke, Hampshire RG21 2XS, UK.

Overseas subscribers may make payments into UK Post Office Giro Account No. 5192455. Full details must accompany the payment.

Second Class postage paid at Rahway NJ. US Mailing Agent: Mercury Airfreight International Ltd, Inc., 2323 Randolph Avenue, Avenel, New Jersey, NJ 07001, USA.

Enquiries concerning advertising space or rates should be addressed to: Michael Rowley, Advertisement Manager, Macmillan Press Ltd., 4 Little Essex Street, London WC2R 3LF. Telephone: 071 836 6633; Fax: 071 379 4204.

ISSN 0007–1188

0007–1188/92 $3.50 + $0.00

ERRATUM

SPECIAL REPORTS

The purpose of *Special Reports* is to provide rapid publication for **new** and **important** results which the Editorial Board considers are likely to be of special pharmacological significance. (Please note that Short Communications are no longer acceptable for publication.) *Special Reports* will have publication priority over all other material and so authors are asked to consider carefully the status of their work before submission.

In order to speed publication there is normally no revision allowed beyond very minor typographical or grammatical corrections. If significant revision is required, the Board may either invite rapid re-submission or, more probably, propose that it be re-written as a Full Paper and be re-submitted for consideration. In order to reduce delays, proofs of *Special Reports* will be sent to authors but **essential corrections must reach the Production Office within 48 hours of receipt.** Authors should ensure that their submitted material conforms exactly to the following requirements.

Special Reports should normally occupy no more than two printed pages of the Journal; two illustrations (Figures or Tables, with legends) are permitted. As a guideline, with type face of 12 pitch and double-line spacing, a page of A4 paper could contain about 400 words. The absolute maximum length of the *Special Report* is 1700 words. For each Figure or Table, please deduct 200 words. The manuscript should comprise a Title page with key words (maximum of 10), a Summary consisting of a single short paragraph, followed by Introduction, Methods, Results, Discussion and References (maximum of 10). In all other respects, the requirements are the same as for Full Papers (see current 'Instructions to Authors').

PREPARATION OF MANUSCRIPTS

Authors are strongly recommended to read the full *Instructions to Authors* and *Nomenclature Guidelines for Authors* (*Br. J. Pharmacol.* 1992, **105,** 245–254) before submitting a manuscript for publication in the *British Journal of Pharmacology*. The manuscript and cover letter should be checked against the following list before mailing.

The original and one copy of the manuscript must be supplied. Manuscripts must be typed in double-line spacing on one side of A4 paper, in type not smaller than 12 characters per inch or 10 point. Both copies to include Tables and a set of labelled Figures. One set of Figures without numbers or letters is also to be included. The text to be arranged in the following subsections:

1. **Title**—To have no more than 150 characters on a separate page, which should also include a Short Title (50 characters maximum) and the name and address of the author for correspondence.

2. **Summary**—To be arranged in numbered paragraphs (Full Papers) or a single paragraph (Special Reports).
   —to include aims, principal results and conclusions.
   —to include Key words (10 maximum) at end of summary.

3. **Introduction**—To contain concise statements of the problem and the aims of the investigation.

4. **Methods**—To have brief but adequate account of the procedures; *full names of drugs* (*including those referred to by manufacturer's code*), sources of drugs and statistical tests to be stated.

5. **Results**—To have no repetition of data in Figures, Tables and text.

6. **Discussion**—Findings and conclusions to be placed in context of other relevant work.
   NB Simple repetition of results and unwarranted speculation are not acceptable.

7. **Acknowledgments**—Sources of support. Sources of drugs not widely available commercially.

8. **References**—All references in the text to be included in the Reference List and *vice versa*. References in alphabetical order with complete citations; Journals publishing 'in press' papers identified.
   References to manuscripts submitted to other journals but not yet accepted are not allowed.

9. **Tables**—Each on a separate page and prepared in accordance with current requirements of the Journal.

10. **Figures**—Both labelled and non-labelled Figures to be prepared in accordance with current requirements of the Journal (see *Instructions to Authors*, 1992, **105,** 245–251) and provided with Figure Number and Authors' names on back (*in pencil*).
    —each legend to be typed on a separate page and carrying keys to symbols.
    —keys to symbols and histograms must not appear on the figures themselves, but in the respective legends.
    —'box style' figures are not in keeping with the Journal style; line drawings etc must have only left-hand and bottom axes.

11. **Manuscripts**—To be accompanied by a declaration signed by each author that
    (a) results are original
    (b) approval of all persons concerned has been given to submit manuscripts for consideration (see also 12b)
    (c) the same material is neither 'in press' (i.e. is in proof or has definitely been accepted for publication) nor under consideration elsewhere. Furthermore it will not be submitted or published elsewhere before a decision has been reached by the Editorial Board of the *British Journal of Pharmacology* and will not be submitted elsewhere if accepted by the *British Journal of Pharmacology*.
    (d) Copyright assignment is included.

12. **Cover letter**—To state clearly
    (a) Corresponding author's full postal address, telephone, telex or Fax number
    (b) where appropriate, that *either* ethical approval has been given for investigation *or* Company or Institutional permission to publish work has been received.

13. **Reminder**—Packaging to be sufficiently robust to protect Figures and to withstand mailing.

Failure to comply with *Instructions to Authors* may lead to substantial delays in processing, review and publication and may even jeopardize acceptance of the manuscript.

NOMENCLATURE

Authors are reminded that accepted receptor and associated terminology is laid out in *Nomenclature Guidelines for Authors*, as published in the *British Journal of Pharmacology, Br. J. Pharmacol., 1992,* **105,** 245–254.

BRITISH JOURNAL OF PHARMACOLOGY VOLUME 106 (3) 1992

SPECIAL REPORTS

PAPERS

ERRATUM

Typeset by Elite Typesetting Techniques, Southampton, Hampshire
and printed in Great Britain by Unwin Brothers Ltd., The Gresham Press, Old Woking, Surrey